

T. Fransson 12

COMMUNICATION
DU LABORATOIRE DE THERMIQUE APPLIQUÉE ET DE TURBOMACHINES
DE L'ÉCOLE POLYTECHNIQUE FÉDÉRALE DE LAUSANNE
PROF. DR. A. BÖLCS

Nr. 13

**AEROELASTICITY IN TURBOMACHINES
COMPARISON OF THEORETICAL
AND EXPERIMENTAL CASCADE RESULTS**

par

DR. A. BÖLCS ET DR. T.H. FRANSSON

APPENDIX A5

All Experimental and Theoretical Results
for the 9 Standard Configurations

LAUSANNE, EPFL
1986

COMMUNICATIONS DE L'INSTITUT DE THERMIQUE APPLIQUÉE
DE L'ÉCOLE POLYTECHNIQUE FÉDÉRALE DE LAUSANNE
PROF. DR. A. BÖLCS

- Nr. 1 *Albin Bölcse*: Theoretische und experimentale Untersuchung der drallbehafteten Überschallströmung in einer Ringspaltdüse.
- Nr. 2 *Jean-Claude Mévillot*: Risques d'obstruction, par de petites particules, des orifices d'aubes de turbines à gaz refroidies par film.
- Nr. 3 *A. J. T. Horvath*: Der Pumpvorgang von Verdichtern und Kreiselpumpen als nicht-lineare Schwingung.
- Nr. 4 *Daniel Favrat*: Interaction entre une onde de choc oblique et une grille d'aubes fixes parcourues par un écoulement subsonique.
- Nr. 5 *A. Bölcse and T. Fransson*: Measuring Techniques in Transonic and Supersonic Cascades and Turbomachines (Proceedings of the Symposium held in Lausanne on November 18-19, 1976).
- Nr. 6 *Mohamed A. M. Abdelrahman*: Technical Evaluations of Gaseous Suspensions of Graphite for the Absorption of Concentrated Solar Radiation.
- Nr. 7 *Tashin Boyman*: Phénomènes de transport dans les garnitures à labyrinthes des turbomachines.
- Nr. 8 *Horst Stoff*: Calcul et mesure de la turbulence d'un écoulement incompressible dans le labyrinthe entre un arbre en rotation et un cylindre stationnaire.
- Nr. 9 *Herms Scheel*: Einfluss von dreidimensionalen Effekten auf die Vorderkantenströmung an Überschall-Turbomaschinen-Schaufeln.
- Nr. 10 *P. Suter*: Aeroelasticity in Turbomachines (Proceedings of the second international Symposium held in Lausanne, September 8-12, 1980).
- Nr. 11 *C. Durand*: Performances et limites de chaudières à gaz de centrales solaires.
- Nr. 12 *Torsten H. Fransson*: Numerical Investigation of Unsteady Subsonic Compressible Flows Through an Oscillating Cascade.

Contents

- I Nomenclature
- II Standard Configurations
- III Prediction Models
- 1. First Standard Configuration
 - 1.1 Definition
 - 1.2 Aeroelastic Test Cases
 - 1.3 Results
- 2. Second Standard Configuration
 - 2.1 Definition
 - 2.2 Aeroelastic Test Cases
 - 2.3 Results
- 3. Third Standard Configuration
 - 3.1 Definition
 - 3.2 Aeroelastic Test Cases
 - 3.3 Results
- 4. Fourth Standard Configuration
 - 4.1 Definition
 - 4.2 Aeroelastic Test Cases
 - 4.3 Results
- 5. Fifth Standard Configuration
 - 5.1 Definition
 - 5.2 Aeroelastic Test Cases
 - 5.3 Results
- 6. Sixth Standard Configuration
 - 6.1 Definition
 - 6.2 Aeroelastic Test Cases
 - 6.3 Results
- 7. Seventh Standard Configuration
 - 7.1 Definition
 - 7.2 Aeroelastic Test Cases
 - 7.3 Results
- 8. Eighth Standard Configuration
 - 8.1 Definition
 - 8.2 Aeroelastic Test Cases
 - 8.3 Results
- 9. Ninth Standard Configuration

- 9.1 Definition
- 9.2 Aeroelastic Test Cases
- 9.3 Results

IV. Nomenclature

Note:

- a) At the request of some participants, the nomenclature of the first report [4] has been slightly modified. A complete list of the changes is given in section V.
- b) Throughout this report, "standard configuration" will designate a cascade geometry and "aeroelastic case" or "aeroelastic test case" will indicate the different time-dependent (and, in some cases time-averaged) conditions within a standard configuration.
- c) The tables and figures will be numbered as the sections. For example, Figure 3.7-2 denotes the second figure in section 3.7.
- d) In order to be consistent with Appendix A5 in which all results obtained in the project are presented (in format A4), an identification is given in each figure as a plotnumber.

These plots are numbered according to the sections, with separation for the type of result presented such as plot K.L-M.N where

- K indicates the section (for example 7)
- L " standard configuration number (for example, 7.4 indicates results on the fourth standard configuration, given in section 7.)
- M indicates the type of result:
 - M=1 : time-averaged pressure coefficient ($=\bar{c}_p$)
and/or Mach number (M_{is})
 - M=2 : time-dependent pressure coefficient ($=\tilde{c}_p$)
 - M=3 : " " " difference coefficient ($=\Delta \tilde{c}_p$)
 - M=4 : lift, force coefficient ($= \tilde{c}_l, \tilde{c}_h, \tilde{c}_f$)
 - M=5 : moment coefficient ($=\tilde{c}_m$)
 - M=6 : aerodynamic damping coefficient ($=\Xi$)
- N : indicates the plot number of type K.L-M
(for example, Plot 7.1-6.2 indicates the second plot of type 6 of the 1st standard configuration in section 7)

e) The terms "controlled excitation", "forced excitation" and "flutter" tests will be extensively used throughout the report. In the present context, they are defined as follows:

- Controlled excitation test:

When the blades are vibrated with a force (mechanical, electro magnetic,...) external to the flow.

- Forced excitation test:

The blades are excited by the flow, but in a known way (for example blade passing frequency from upstream blades).

- Flutter test:

Self excited vibrations, i.e. the blades vibrate even though there is no controlled or forced excitation in the experiment.

Symbol	Explanation	Dimension
--------	-------------	-----------

Latin Alphabet

A	amplitude ($A=h$ for pure sinusoidal bending) ($A=\alpha$ for pure sinusoidal pitching)	-
A	Fourier coefficient	-
c	chord length	m
$\tilde{c}_f(t)$	unsteady perturbation force coefficient vector per unit amplitude, positive in positive coordinate directions (Eq. 5): $\tilde{c}_f(t) = \tilde{c}_f e^{i\{\omega t + \Phi_f\}} \hat{e}_f$	-
\tilde{c}_f	real amplitude of the unsteady perturbation force coefficient per unit amplitude (Eq. 5)	-
$\tilde{c}_l(t)$	unsteady perturbation lift coefficient per unit amplitude, positive in positive y-direction (Eq. 4): $\tilde{c}_l(t) = \tilde{c}_l e^{i\{\omega t + \Phi_l\}} \hat{e}_y$	-
Note: In the present study, the lift coefficient is defined as the force component perpendicular to the chord!		
\tilde{c}_l	real amplitude of the unsteady perturbation lift coefficient per unit amplitude (Eq. 4)	-
$\tilde{c}_m(t)$	unsteady perturbation moment coefficient per-unit amplitude, positive in clockwise direction (Eq. 6): $\tilde{c}_m(t) = \tilde{c}_m e^{i\{\omega t + \Phi_m\}} \hat{e}_z$	-
\tilde{c}_m	real amplitude of the unsteady perturbation moment coefficient per unit amplitude (Eq. 6)	-
$\tilde{c}_p(x,t)$	unsteady perturbation blade surface pressure coefficient per unit amplitude (Eq. 3): $\tilde{c}_p(x,t) = \tilde{c}_p(x) e^{i\{\omega t + \Phi_p(x)\}}$	-

$\tilde{c}_p(x)$	real amplitude of the unsteady perturbation	-
	pressure coefficient per unit amplitude (Eq. 3)	
\bar{c}_p	time-averaged pressure coefficient = $[p - \bar{p}_{\infty}] / [\bar{p}_{w-\infty} - \bar{p}_{\infty}]$	-
c_w	coefficient of aerodynamic work done on the airfoil during the oscillation cycle (Eq. 12, 13)	-
d	maximum blade thickness (dimensionless with chord)	-
e_f	unit vector in force direction	
\hat{e}_h	unit vector in bending direction	-
\hat{e}_n	unit vector normal to blade surface, positive inwards)	-
\hat{e}_s	unit vector tangent to blade surface, positive in positive coordinate directions	-
\hat{e}_x	unit vector in x-direction	-
\hat{e}_y	unit vector in y-direction	-
f	vibration frequency	Hz
f	function	-
$h(x,y,t)$	dimensionless (with chord) bending vibration, positive in positive coordinate directions	-
h	dimensionless (with chord) bending amplitude	-
i	complex notation = $(-1)^{0.5}$	-
i	incidence angle, from mean camberline at leading edge	deg
k	reduced frequency	-

$$k = [c \cdot \omega] / [2 \cdot v_{ref}]$$

M	Mach number	-
$p(x,y,t)$	pressure	N/m ²
	(with superscript \sim : time-dependent perturbation)	
	(with superscript $\bar{-}$: time averaged)	
\vec{R}	dimensionless vector from mean pivot axis to an arbitrary point on the mean blade surface	-
Re	real part of complex value	-
Re	Reynolds number = $(v_{ref} c) / \nu$	-
T	dimensionless time: $T = t/T_0$	-
T_0	period of a cycle	s
t	time	s
v	velocity	m/s
v_{ref}	reference velocity for reduced frequency	m/s
	$v_{ref} = v_1$ for compressor cascade	
	$v_{ref} = v_2$ for turbine cascade	

x	dimensionless (with chord) chordwise coordinate	-
x_α	dimensionless (with chord) chordwise position of torsion axis	-
y	dimensionless (with chord) normal-to-chord coordinate	-
y_α	dimensionless (with chord) normal-to-chord position of torsion axis	-
z	dimensionless (with chord) spanwise coordinate	-

Greek Alphabet

$\ddot{\alpha}(t)$	pitching vibration, positive nose-up (Eq. 2)	rad
α	pitching amplitude	rad
β	flow angle, from axial direction, positive in direction of rotation (Fig. 4.1-1)	deg
γ	chordal stagger angle, from axial direction, (Fig. 4.1-1)	deg
δ	bending vibration direction = $\tan^{-1}(h_y/h_x)$	deg
$\Delta\tilde{c}_p(x,t)$	unsteady perturbation pressure difference coefficient (Eq. 8): -	-

$$\Delta\tilde{c}_p(x,t) = \Delta\tilde{c}_p(x) e^{i\{\omega t + \Phi_{\Delta p}(x)\}} = \tilde{c}_p^{ls}(x,t) - \tilde{c}_p^{us}(x,t)$$

$\Delta\tilde{c}_p(x)$	real amplitude of unsteady blade surface perturbation pressure difference coefficient (Eq. 8)	-
$\theta_\alpha^{(m)}$	phase lead of pitching motion towards heaving motion of blade (m)	deg
ν	kinematic viscosity	m/s
Ξ	aeroelastic damping coefficient, positive for stable motion	-
σ	interblade phase angle between blade "m-1" and blade "m". $\sigma^m=0$ for constant interblade phase angle σ^m is positive when blade "m" precedes blade "m-1" For idealized conditions (constant interblade phase angle between adjacent blades, σ , and identical blade vibration amplitude for all blades) the motion of the (m)th blade, for flexion, is given by:	deg

$$\tilde{h}^m(x,y,t) = h^0(x,y) e^{i\{\omega t + m\sigma\}} \hat{e}_h$$

τ	dimensionless (with chord) blade pitch (= gap-to-chord ratio) -	
Φ_f	phase lead of perturbation force coefficient	deg
	towards motion	
Φ_l	phase lead of perturbation lift coefficient towards motion	deg
Φ_m	phase lead of perturbation moment coefficient towards motion	deg
$\Phi_p(x)$	phase lead of perturbation pressure coefficient towards motion	deg
$\Phi_{\Delta p}(x)$	phase lead of perturbation pressure difference coefficient towards motion	deg
Ψ	phase angle in Fourier series	deg
ω	circular frequency = $2\pi f$	rad/s

Subscripts:

A	$A = h$ for bending α for pitching	
aero	aeroelastic damping	
c	stagnation value in the absolute frame of reference	
exp	experimental result (used only in ambiguous contexts)	
G	center of gravity	
global	global (= time-dependent + time-averaged) (see Eq. 7)	
I	imaginary part	
is	"isentropic" values, defined with total head pressure in measuring station "1" upstream of the cascade. This value is thus not the true isentropic value as it includes losses in the static pressure.	
k	k-th harmonic in Fourier series	
LE	leading edge	
mech	mechanical (damping)	
n	n-th harmonic in Fourier series	
R	real part	
ref	reference velocity for reduced frequency $v_{ref} = v_1$ for compressor cascade $v_{ref} = v_2$ for turbine cascade	
TE	trailing edge	
theory	theoretical results (used only in ambiguous contexts)	
w	stagnation value in the relative frame of reference	

x	component in x-direction
y	component in y-direction
z	component in z-direction
α	position of pitch axis (see Fig. 4.1-1)
1	measuring station upstream of cascade
2	measuring station downstream of cascade
$-\infty$	values at "infinity" upstream
$+\infty$	values at "infinity" downstream

Superscripts:

(B)	(B) designates lower or upper surface of profile (B) = (ls) for lower surface of profile (us) " upper " "
c	complex value (used only in ambiguous contexts)
(ls)	lower surface of profile
(m)	blade number m = ... -2, -1, 0, 1, 2, ... If the amplitude, interblade phase angle, etc. are constant for the blades under consideration, this superscript will not be used
(us)	upper surface of profile
-	time-averaged (= steady) values. This superscript will be used only in ambiguous contexts
\sim	time-dependent perturbation values. This superscript will be used only in ambiguous contexts

V. Updating of Nomenclature

Upon the request of some participants, the nomenclature from the first report [4] has been slightly modified. The modifications are:

Symbol	Explanation	Dimension
--------	-------------	-----------

Greek Alphabet

β	flow angle, from axial, positive in direction of rotation (Fig. 4.1-1) (in [4], from circumferential)	deg
γ	chordal stagger angle, from axial, positive in direction of rotation (Fig. 4.1-1) ([4], from circumferential)	deg

Subscripts

c	stagnation value in the absolute frame of reference (in [4], "t" was used)
w	stagnation value in the relative frame of reference (in [4], "t" was used).

Superscripts

- time averaged values (was time-dependent in [4])
- \sim time dependent values (was time-averaged in [4])

Stand Config. No.	Insti- tution	Lin.-Ann./ Thickness/ Camber	Compr./ Turbine	Mach/ Stall Config.	Excitation/ Motion/ Mode	Results	Instru- mentation	Parameters varied
1	United Technol. Research Center	• L (Air) • 6% • 10°	• C	• Incomp. • None	• Controlled • Harmonic • Torsion	• $\bar{c}_p + \tilde{c}_p +$ $\Delta \tilde{c}_p + \tilde{c}_m +$ ≡	• 20 transducers • Strain gauges	• i + $\tilde{\alpha}$ + $\sigma + k$
2	University of Tokyo	• L (Water) • 5% • 16°	• C+T	• Incomp. • None+ Partial+ Fully	• Controlled • Harmonic • Torsion	• $\bar{c}_p + \tilde{c}_l +$ \tilde{c}_m	• Strain gauges	• i + σ + $\gamma + k$
3	Tokyo National Aerospace Lab.	• A (Freon) • 12% • 60°	• T	• Sub + Sub-Super • None+ Partial	• Controlled • Harmonic • Torsion	• $\bar{c}_p + \tilde{c}_p +$ \tilde{c}_m	• 10 transducers • Strain gauges	• $M_2 +$ $\sigma + k$
4	Ecole Polytech. Fédérale Lausanne	• A (Air) • 17% • 45°	• T	• Sub + Sub-Super • None+ Partial	• Controlled • Harmonic • Bending + Torsion	• $\bar{c}_p + \tilde{c}_l +$ ≡	• 12 transducers • Strain gauges	• $\beta_1 + M_2 +$ σ
5	ONERA	• L (Air)/ • 3%/ • 0°	• C	• Subsonic • None + Partial + Fully	• Controlled • Harmonic • Torsion	• $\bar{c}_p + \tilde{c}_p +$ $\Delta \tilde{c}_p + \tilde{c}_m +$ ≡	• 26 transducers • Strain gauges	• i + $M_1 +$ $x_\alpha + k$
6	Ecole Polytech. Fédérale Lausanne	• A (Air) • 5% • 14°	• T	• Sub + Sub-Super • None + Partial	• Controlled • Harmonic • Bending + Torsion	• $\bar{c}_p + \tilde{c}_l +$ ≡	• 10 transducers • Strain gauges	• $\beta_1 + M_2 +$ σ
7	NASA Lewis Research Center	• L (Air) • 3% • -1.3°	• C	• Supersonic+ Super-Sub • None+ Partial	• Controlled • Harmonic • Torsion	• $\bar{c}_p + \tilde{c}_p +$ $\Delta \tilde{c}_p + \tilde{c}_m$	• 12 transducers • Strain gauges	• $M_2 + \sigma$
8	-	• 2-D • 0% • 0°	• -	• Incomp. + Sub. + Super. + Super.→Sub • None	• Controlled • Harmonic • Torsion	• $\tilde{c}_p + \Delta \tilde{c}_p +$ $\tilde{c}_m +$ ≡	• -	• -
9	-	• 2-D • varied • varied	• C	• Incomp. + Sub. + Super. + Super.→Sub • None	• Controlled • Harmonic • Torsion	• $\tilde{c}_p + \Delta \tilde{c}_p +$ $\tilde{c}_m +$ ≡	• -	• -

Table 5.0-1. Brief Summary of nine standard configurations

6. Introduction to the Prediction Models

Several prediction models were applied to the standard configurations. In the beginning of the project, 19 methods were offered as a basis for comparison. Finally, 15 methodologies have been employed up till now.

Table 6.1 identifies the separate models in relationship with the predictions performed on the different standard configurations.

Method N°	Name/Affiliation	Standard Configu- rations Computed
1	D. S. Whitehead/ Cambridge University, Cambridge, UK	1, 2, 5, 8
2	D. S. Whitehead/ Cambridge University, Cambridge, UK	5, 8, 9
3	J. M. Verdon/ United Technologies Research Center, East Hartford, USA	1, 5, 8, 9
4	M. Atassi/ University of Notre Dame, USA	1
5	P. Salaün/ Office National d'Etudes et de la Recherche Aérospatiale, Paris, France	1, 7, 8
6	S. Zhou/ Beijing Institute of Aeronautics and Astronautics, China	1, 2, 5
7	S. G. Newton, R. D. Cedar/ Rolls Royce Ltd, Derby, UK	1, 4, 7, 8

Table 6.1 Continued on next page

8	V. Carstens/ DFVLR-AVA, Göttingen, Germany	1
9	F. Molls/ NASA Lewis Research Center, Cleveland, USA	8
10	S. Kaji/ University of Tokyo, Japan	4, 6
11	O. O. Bendiksen/ Princeton University, USA	8
12	T. Araki/ Toshiba Corporation, Japan	-
13	K. Vogeler/ Technische Hochschule Aachen, Germany	-
14	J. M. R. Graham/ Imperial College, London, UK	1
15	S. Stecco/ University of Florence, Italy	6 (Presently, steady state)
16	D. Nixon/ Nielsen Engineering and Research, Inc., California, USA	-
17	P. Niskode/ General Electric, Cincinnati, USA	-
18	H. Joubert/ SNECMA, Moisy Cramayel, France	7
19	M. Namba/ Kushug University, Japan	6, 8

Table 6.1: Aeroelastic Prediction Models

Method 1: LINSUB (Courtesy of D. S. Whitehead)

The program calculates the unsteady two-dimensional linearized subsonic flow in cascades in travelling wave formulation, using the theory published in [50]. The blades are assumed to be flat plates operating at zero incidence. Both the pressure jump and lift and moment coefficients are computed for different options:

- Translational vibration of the blades normal to their chord.
- Torsional vibration of the blades about the origin at the leading edge.
- Sinusoidal wakes shed from some obstructions upstream, which move relative to the cascade in question.
- Incoming acoustic waves, coming from downstream.
- Incoming acoustic waves, coming from upstream.

Furthermore, the condition of acoustic resonance is calculated.

Method 2: FINSUP (Courtesy of D. S. Whitehead)

As an example of a numerical field method, a computer program called FINSUP will be briefly described. The program has three sections: mesh generation, analysis of steady flow, and analysis of unsteady flow. The mesh generation and analysis of steady flow have been described by Whitehead and Newton (1985) [43]. The analysis of unsteady flow has been described by Whitehead (1982) [44].

A typical mesh is composed of triangular finite elements covering a strip, one blade spacing high, with the blade in the middle. The fluid is assumed to be a perfect gas with no viscosity or thermal conductivity, and the flow is assumed to be adiabatic, reversible and irrotational, so the equations are those for a velocity potential. The potential is continuous, except for a jump across the wake. In order to calculate in regions of supersonic flow it is necessary to use "upwind" densities; that means that instead of taking the density at the element under consideration, the density is taken from the neighbouring element in the most nearly upwind direction. This device stabilizes the computation in supersonic flow, but is unnecessary in subsonic flow. Weak shock waves are well simulated, but are "potential" since there is no entropy increase across the shock, and they are smeared over a few elements. The flow is matched to a linearized solution at the inlet and outlet faces of the computational domain, and is arranged to repeat between corresponding points on the top and bottom faces. The conditions specified to

the program are effectively the inlet circumferential velocity and the jump in potential between the bottom left and the bottom right corners of the domain. This choice of input conditions uniquely specifies the location of a shock in a cascade of flat plates at zero incidence, which no specification of flow conditions at either inlet or outlet can achieve. The non-linear equations are then solved by the Newton-Raphson technique. Convergence is usually achieved in three or four iterations, although up to about twelve may be necessary in difficult cases with supersonic inlet velocities. The nodes are numbered in such a way as to minimize the bandwidth of the dividing matrix at each iteration, so the method is fast. Good agreement with other methods of calculating steady transonic cascade flow in cascades has been demonstrated. The program then goes on to the third stage in which small unsteady perturbations of the steady flow due to vibration of the blades is analysed. Solid body motion of the blades is assumed, either in bending or torsion. The unsteady calculation is therefore similar to one more iteration of the steady calculation, except that the potential perturbation is complex, and the boundary conditions are different. Again the flow at the inlet and exit faces is matched to a linearized solution, which includes propagating or decaying acoustic waves and in the downstream flow the effect of the unsteady wake shed from the trailing edge. The repeat condition between corresponding points on the top and bottom surfaces is arranged to give the required phase difference between neighbouring blades. It is again necessary to use upwind densities in regions of supersonic flow in order to stabilize the calculation. A difficulty arises due to the term

$$(\vec{r} \cdot \Delta \vec{v}) \cdot \vec{n} \quad (\text{M2.1})$$

for the boundary condition at the blade surface. A modified perturbation potential is defined by

$$\theta'' = \theta + \vec{r} \cdot \nabla \Phi \quad (\text{M2.2})$$

where r is given by

$$\vec{r} = \vec{r} + \vec{\alpha} \times \vec{R} \quad (\text{M2.3})$$

and this equation is now extended over the whole domain of calculation, and not just at the blade surface. This device gets rid of the awkward term in the boundary condition at the blade surface, and also eliminates a similar

awkward term in the calculation of the pressure perturbation at the surface. The unsteady pressure perturbations at the surface are then integrated to give the axial and circumferential blade forces and the moment.

Method 3: Linearized Unsteady Aerodynamic Analydes (Courtesy of J. M. Verdon)

The isentropic and irrotational flow of a perfect gas through a two-dimensional cascade of vibrating airfoils is considered. The blades are undergoing identical harmonic motions at frequency ω , but with a constant phase angle ϕ between the motions of adjacent blades. It is assumed that the flow remains attached to the blade surfaces and that the blade motion is the only source of unsteady excitation.

The flow through the cascade is thus governed by the field equations, written in form of the time-dependent velocity potential [5]. In addition to the field equations, the flow must be tangential to the moving blade surfaces and acoustic waves must either attenuate or propagate away from or parallel to the blade row in the far field. Finally, we also require that the mass and tangential momentum be conserved across shocks and that pressure and the normal component of the fluid velocity be continuous across the vortex-sheet unsteady wakes which emanate from the blade trailing edges and extend downstream.

In order to limit the computing resources required to solve the equation system, a small-unsteady-disturbance assumption is involved. Thus, the blades are assumed to undergo small-amplitude unsteady motions around an otherwise steady flow. The resulting first-order or linearized unsteady flow equation is solved subject to both boundary conditions at the mean positions of the blade, shock and wake surfaces and requirements on the behavior of the unsteady disturbances far upstream and downstream from the blade row.

Moreover, because of the cascade geometry and the assumed form of the blade motion, the steady and linearized unsteady flows must exhibit blade-to-blade periodicity. Thus, the numerical resolution of the steady and the linearized unsteady flow equations can be restricted to a single extended blade-passage region of the cascade.

Method 4: Aerodynamic Theory for Two-Dimensional Unsteady Cascades of Oscillating Airfoils in Incompressible Flows (Courtesy of H. Atassi)

A complete first order theory is developed for the analysis of oscillating airfoils in cascade in a uniform upstream flow. The flow is assumed to be incompressible and irrotational. The geometry of the airfoil is arbitrary. The angle of attack of the mean flow and the stagger and solidity of the cascade can assume any prescribed set of values. The airfoils have a small harmonic oscillation about their mean position with a constant interblade phase angle. Both translational and rotational oscillations are considered.

The boundary-value problem for the unsteady component of the velocity is formulated in terms of sectionally analytic functions which must satisfy the impermeability condition along the airfoils surfaces, the Kutta condition at the trailing edges of the airfoils, and the jump condition along the airfoils wakes. The expression for the velocity jump in the wakes is derived to a multiplicative constant from the condition of pressure continuity across the wakes. The velocity field is split into two components: one satisfying the oscillating motion along the airfoils surfaces and the other accounts for a normalized jump conditions along the wakes. This leads to two singular integral equations in the complex plane. The two equations are coupled by Kelvin's theorem of conservation of the circulation around the airfoils and their wakes. The integral equations are solved by a collocation technique.

The results obtained from this theory show that the airfoil geometry and loading and the cascade stagger and solidity strongly affect the aerodynamic forces and moments acting upon oscillating cascades. As a result stability and flutter boundaries are significantly modified for highly loaded cascades.

Method 5: (Courtesy of P. Salaün)

The two-dimensional cascade is an infinite array of thin blades.

The fluid is an inviscid perfect gas and the flow is assumed to be irrotational and isentropic.

The blades are performing harmonic motions of so small amplitude that the theory can be linearized about the undisturbed, uniform flow.

The supersonic theory is restricted to the case of subsonic leading edge locus.

The pressure difference between the two sides of the blades are taken into account when they are replaced by sheets of pressure dipoles in both subsonic and supersonic flow.

Then, the perturbation velocity potential is expressed and the boundary conditions on the blades give an integral equation where the unknown is the pressure difference on the reference blade, and the right hand side the angle of attack.

This integral equation is solved numerically.

Method 6: Zhou Sheng

A finite difference method is used to solve the unsteady velocity potential equation. The velocity potential is split into one steady and one unsteady part, and the unsteady small perturbation is solved with a relaxation procedure.

Method 7: Extended FINSUP (Courtesy of R. D. Cedar)

The flutter calculation used at Rolls Royce is an extension of the finite element method developed by D. S. Whitehead (Method 2). Since the programs introduction to Rolls Royce in 1981 it has been continually developed and evaluated [43]. The finite element mesh generator has been fully automated to the extent that it now contains "rules" about how good a mesh is. Using these "rules" the mesh construction parameters are automatically changed until a satisfactory mesh is obtained.

The steady flow calculation has been extended from being purely two-dimensional to include the quasi-three-dimensional effects of blade rotation and variations of streamtube height and streamline radius [51]. This has allowed the program to be included in the quasi-three-dimensional design system used at Rolls Royce [52]. Improvements to the upwinding scheme has been made that produce sharp shocks. A coupled boundary layer calculation (using both direct and semi-inverse coupling) has been developped [53] as well as a design or inverse calculation [54]. This allows transonic blades to be designed, including the removal of shocks, to give a controlled diffusions.

The unsteady flow calculation has been extended to include the quasi-three-dimensional effects. It has been found that it is essential to include the

effect of variation in streamtube height if test data is to be predicted correctly.

Method 8: Theoretical Flutter Investigation on a Cascade in Incompressible Flow (Courtesy of V. Carstens)

1. Calculation of unsteady aerodynamic coefficients

The calculation of the unsteady aerodynamic coefficients due to harmonic bending and torsion of the cascade's blades is based on an integral equation technique. The main idea of this technique is to replace each blade's surface and its wake by a distribution of vorticity. The kinematic boundary condition and the law of vorticity transport allow the formulation of the flow problem as an integral equation, the solution of which yields the correct value of the unknown unsteady blade vorticity.

Two important items in the formulation of the problem should be mentioned:

- 1) The prescribed harmonic motion of the entire cascade unit is a fundamental mode, in which all blades perform oscillations with the same amplitude but with a constant phase lag from blade to blade (interblade phase angle).
- 2) The influence of the steady flow on the unsteady quantities is obtained by a special linearizing procedure.

The unsteady pressure distribution and the aerodynamic lift and moment coefficients are calculated as a function of the blade vorticity by means of Bernoulli's equation.

2. Flutter analysis

The flutter analysis is done on the basis of a two-degree-of freedom model, which allows for bending perpendicular to the chord and torsion around a given elastic axis. The rearrangement of the two linearized equations of motion for a blade section in nondimensional matrix form yields the formulation of the flutter problem as a nonlinear eigenvalue problem. Stability boundaries are found by determining the real eigenvalues of the matrix equation in an iterative procedure if a set of elastomechanical and aerodynamic parameters is prescribed. The result of each flutter calculation is a stability curve in a reduced frequency - interblade phase angle diagram,

the maximum of which yields the absolute stability boundary and hence the nondimensional flutter speed for the given configuration.

Method 9: (Courtesy of F. Molls)

The model allows for two shock waves to occur in a tip blade passage in which the inlet Mach number is supersonic. A weak oblique shock from the leading edge lies off the pressure surface of the upper blade and its angle is great enough that the shock intersects the lower blade. Off the suction surface of the lower blade there is a normal wave at the trailing edge which intersects the upper blade. The oblique shock angle corresponds to the pressure ratio but not to the metal angle at the leading. The model blade, however, has a wedge angle in agreement with the pressure ratio and inlet Mach number. Where the oblique shock strikes the adjacent blade, the flow turns from the inlet direction through the wedge angle to become parallel to the pressure surface; thus, as observed in actual flow, there is no reflection.

There are two options in the model. Either the pressure and suction surfaces continue uniformly to a blunt trailing edge, or the trailing surfaces are tapered to a specified thickness at the trailing edge. In the former case the differential equations for the unsteady component of the flow have constant coefficients and may be solved analytically. In the latter option, the mean flow in one portion of the blade passage is a slowly varying flow and numerical integration of the disturbance equations is required. A more detailed description with a diagram and references to experimental examples of the modelled flow is given in [37].

Method 10: Semi-Actuator Disk Method (Courtesy of S. Kaji)

The semi-actuator disk model converts an actual blade row to a continuous cascade by inserting many fictitious blades in between and parallel to the original blades. Aerodynamic loading and inter-blade phase change are all shared by inserted blades. Thus the change of physical quantity in the cascade direction is given by crossing each blade stepwise, and we can treat the flow inside a blade channel one-dimensionally.

The first part of the analyses is to solve the linearized governing equations of mass, momentum and energy for the upstream, inside and downstream field

of the cascade separately. We have a pressure wave in the upstream field, two pressure waves going back and forth (and an entropy wave if the total pressure loss is present) inside the cascade and also we have a pressure wave, (an entropy wave) and a vorticity wave due to blade oscillation in the downstream field. The unknown amplitude of each wave is related to the known amplitude of blade oscillation through boundary conditions at the leading edge plane and the trailing edge plane of the cascade.

At the leading edge plane we use

- mass flow continuation,
- relative total enthalpy continuation, and
- the condition of total pressure loss change in accordance with flow incidence.

At the trailing edge plane we can assume a smooth continuation of all physical quantities, i.e., two components of velocity, pressure and density.

The aerodynamic forces acting on blades can be evaluated by use of the momentum principle applied to the control volume taken for a blade channel.

The merits and demerits of the method are:

- Aerodynamic loading
- Total-pressure-loss
- Arbitrary direction of oscillation
- No large inter-blade phase angles

Method 11:

Method 12:

Method 13:

The code is based on the nonlinear transonic small perturbation equation. The disturbances are assumed to be small. Hence the principle of superposition is applied and the problem is split into a steady and an unsteady part. A method of characteristics was developed for both the steady and the unsteady solutions to handle the supersonic flow past a finite cascade of oscillating parabolic - not necessarily symmetric - blades.

Considerable progress was achieved with the extended treatment of the unsteady shocks including a shock equation for the unsteady perturbation

potential. Furthermore the application of the method of characteristics to unsteady sliplines, shock intersections and the crossing of a shock with a slipline was developed.

The results are steady and unsteady pressure distributions, the integrated lift- and moment-coefficients and the shock geometry in the cascade. At the moment the code is for research purposes only. It is planned to rewrite it for industrial application.

Method 14: Discrete Vortex (Cloud-in-Cell) Method for Unsteady Cascade Flows (Courtesy of J. M. R. Graham and J. Basuki)

This method represents shed vortex wakes in two-dimensional incompressible flow by large numbers of discrete point vortices which are convected by the local velocity field. In the cloud-in-cell method the vorticity associated with the moving point vortices is transferred to a fixed Eulerian mesh [32]. The streamfunction and hence velocity distribution is calculated from the vorticity on this mesh using a standard fast Poisson solver.

The present version of this method used to calculate unsteady flow through a cascade represents the individual aerofoils in the cascade by a boundary integral method [33] which uses piecewise constant vorticity panels. The appropriate streamfunction boundary condition is satisfied on the surface of each aerofoil by summing the contributions of the surface vorticity panels (including implied periodicity) and the mesh streamfunction. The boundary condition on the mesh also assumes periodicity along the cascade with the interblade phase angle limited to a small integral number of aerofoils within the mesh flow field. The computation follows the evolution of an unsteady flow by forward time marching, tracking the positions of the vortices.

The program has been used to compute cases with superimposed unsteady flow, upstream wakes, and blade vibration. In the latter case when the interblade phase angle is non-zero, exact application of the boundary integral method requires the influence functions to be recalculated at each time-step to account for changes in the relative blade to blade displacement. This has not been done in the present program for reasons of computational cost. The present boundary condition includes the relative motion but is evaluated on the mean surface of each blade and is therefore limited to small displacement amplitudes compared to the blade spacing.

The program evaluates time histories of surface pressures and forces induced on the aerofoils by the unsteady flows. Since the method involves time

marching from an impulsive start fairly long computations are required to reach a final state free of initial transients.

Method 15: (Courtesy of S. Stecco)

The inviscid planar compressible flow is governed by the continuity, Crocco's and energy equation:

$$\nabla(\rho C) = 0 \quad (M15.1)$$

$$Cx(\nabla x C) + \nabla H - T \nabla S = 0 \quad (M15.2)$$

$$dS/dT = 0 \quad (M15.3)$$

In the case of practical interest it can be assumed that the total enthalpy is constant, and that the flow is homoentropic; this leads to the statement of "irrotational flow".

The assumption of homoentropic flow is not correct in transonic flow where the shock waves can introduce entropy gradients, but such gradients can be neglected, in first approximation, if the shocks are weak as it usually happens in the passage of blades cascades.

In order to get a pseudo-unsteady formulation, after Viviand, it is possible to write Crocco's equation in the streamwise direction:

$$\partial \theta / \partial t = -\{\partial v / \partial x - \partial u / \partial y\} \quad (M15.4)$$

and the continuity equation:

$$\partial Z(\rho) / \partial t = -\{\partial[\rho u] / \partial x + \partial[\rho v] / \partial y\} \quad (M15.5)$$

where Z is a suitable function of density as it will be seen later. The closure equation comes from the conditions:

$$\nabla S = \nabla H = 0 \quad (M15.6)$$

After Viviand the function Z has been chosen in order to achieve good stability all over the working Mach number range:

$$Z(\rho) = -k\rho * M^* \quad (M15.7)$$

where k is an integer number and *refer to critical conditions.

In order to increase the convergence rate of equations (M15.4) and (M15.5) two functions and have now been introduced to multiply the RHS and new stability analysis has been performed.

The choice of these functions is not straight forward because of the presence of high non linear instability; any way a final expression have been found which leads to good results.

The equations (M15.4) and (M15.5) can be written as:

$$\frac{\partial f}{\partial t} + \frac{\partial F}{\partial x} + \frac{\partial G}{\partial y} = 0 \quad (M15.8)$$

where now:

$$\begin{aligned} f &= \begin{vmatrix} Z(\varrho)/\xi \\ \theta/\eta \end{vmatrix} \\ F &= \begin{vmatrix} \varrho u \\ v \end{vmatrix} \\ G &= \begin{vmatrix} \varrho v \\ -u \end{vmatrix} \\ \xi &= M^2 dZ(\varrho)/d\varrho \\ \eta &= |1-M^2| \end{aligned} \quad (M15.9)$$

The numerical solution of these equations will be carried out by an explicit scheme, then the stability condition on the time step has been derived from the CFL criterion that states that the physical dependence domain must be included in the numerical one.

The boundary conditions are:

- upstream the total thermodynamic conditions and the flow angle (if the axial flow is supersonic, also the only Mach number) are fixed.
- downstream the Mach number is fixed, i.e. the pressure ratio across the cascade (if the axial flow is supersonic not any condition is fixed).
- the solid wall require the tangent condition of velocity that substitutes the 2nd equation and impose conditions on the flux terms of first equation.
- the ideal periodic boundaries require the velocity vector to be equal in correspondent point at one pitch distance. When choosing such lines the

normal velocity component must be subsonic. Their treatment results easy in the numerical scheme.

Finally the trailing edge condition is the really delicate one.

In fact there it has to be simulated the base region, from where the shock waves system starts in turbine cascades.

We consider a truncated trailing edge and the velocity vector free on the two points on each side of the trailing edge.

The choice of the truncation must be done carefully owing to its significant influence on the results. It represents roughly the separation points at the trailing edge.

Results are obtained with a coarse grid of 10x57 and a fine mesh of 19x57 points, and by using a finer convergence limit.

Now we test the convergence on the inlet-outlet mass flow difference after the local time variations of the unknowns are within a fixed limit.

Execution time on Honeywell DPS 8:

M _{2is}	CPU time	n. of iteration
1.2	348 s	120
.98	383 s	130
.95	514 s	170

Method 16: Computer Code "Cascade" (Courtesy of D. Nixon)

The code will compute the unsteady transonic flow through a nonstaggered cascade. Thin airfoil boundary conditions are used and the code is an extension of the XTRAN2L code for isolated airfoils. The algorithm is the Rizzetta-Chin algorithm for arbitrary frequencies. The code is used for research purposes and is not a production code.

Method 17:

Method 18: (Courtesy of H. Joubert)

A model has been developed at SNECMA for calculating the unsteady aerodynamic flow through vibrating cascades in view of studying supersonic flutter in axial flow compressors.

The calculation deals with an ideal fluid, in unsteady transonic flow, including shocks, through a quasi three-dimensional cascade.

The explicit Mac Cormack scheme was used to numerically solve the unsteady Euler's equations on a blade to blade surface. An 80×15 grid points mesh was used which was displaced to follow the blade motion. For further details, see ref. [47].

This model has been applied to the seventh standard configuration of the workshop on aeroelasticity in turbomachine-cascades. Two cases were studied, the first one corresponding to an exit Mach number of 1.25 and the second one to an exit Mach a number of 0.99. The unsteady aerodynamic damping coefficients for both cases are represented (see section 7.7) and the magnitude and phase lead of blade surface pressure coefficient for two interblade angles are plotted.

Method 19: Method of Calculating Unsteady Aerodynamic Forces on Two-Dimensional Cascades. (Courtesy of M. Namba.)

The basic assumptions of the method are that the flow should be inviscid and isentropic. The gas should be perfect and the blade oscillations small.

The blades are represented by pressure dipoles of fluctuating strength

$$\Delta p(x_0)e^{i\omega t} + im\alpha \quad (m = 0, \pm 1, \dots) \quad (\text{M19.1})$$

and the problem is reduced to an integral equation for $\Delta p(x_0)$:

$$\int_0^C \Delta p(x_0)K(x-x_0)dx_0 = i\omega\alpha(x) + U\alpha'(x) \quad (\text{M19.2})$$

The Kernel function $K(x-x_0)$ is resolved into:

- a singular part $K(S)(x-x_0)$ in a closed form
- a regular part $K(R)(x-x_0)$ in an infinite series form of uniform convergence (A sufficient convergence with truncation at the 30th term is confirmed.)

The dipole distribution function $\Delta p(x_0)$ is then expanded into a mode function series.

The flow can be either sub- or supersonic:

- Subsonic Cascade:

$$\Delta p(x_0) = \sum_{k=0}^{K-1} P_k Y_k(\psi) \quad (M19.3)$$

where

- $x_0 = 0.5c(1-\cos\psi)$
- $Y_0(\psi) = \cot(0.5\psi)$
- $Y_k(\psi) = \sin(k\psi) \quad (k \geq 1) \quad (\text{Glauert series})$
- Supersonic Cascade:

$$\Delta p(x_0) = g(x_0 + xr) : x_0 - \leq x_0 \leq x_0 + \\ g(x_0) + \sum r \quad : \text{otherwise} \quad (M19.4)$$

where

- r =reflection number (this technique corresponds to the Nagashima & Whitehead' technique)

$$g(x_0) = \sum_{k=0}^{K-1} P_k Y_k(\psi), \text{ with } x_0 = 0.5c(1-\cos\psi) \quad (M19.5)$$

$Y_k(\psi) = \cos k\psi \quad (\text{equivalent to shifted Chebyshev polynomials})$

The integral equation is converted into algebraic equations for P_k ($k = 0, 1, 2, \dots, K-1$).

$$\sum_{k=0}^{K-1} P_k Y_k(x_j) = i\omega\alpha(x_j) + U\alpha'(x_j), \quad j = 1, 2, \dots, K \quad (M19.6)$$

where

$$YK_k(x) = \int_0^c Y_k(\psi) K(S)(x-x_0) dx_0 + \int_0^c Y_k(\psi) K(R)(x-x_0) dx_0 \quad (M19.7)$$

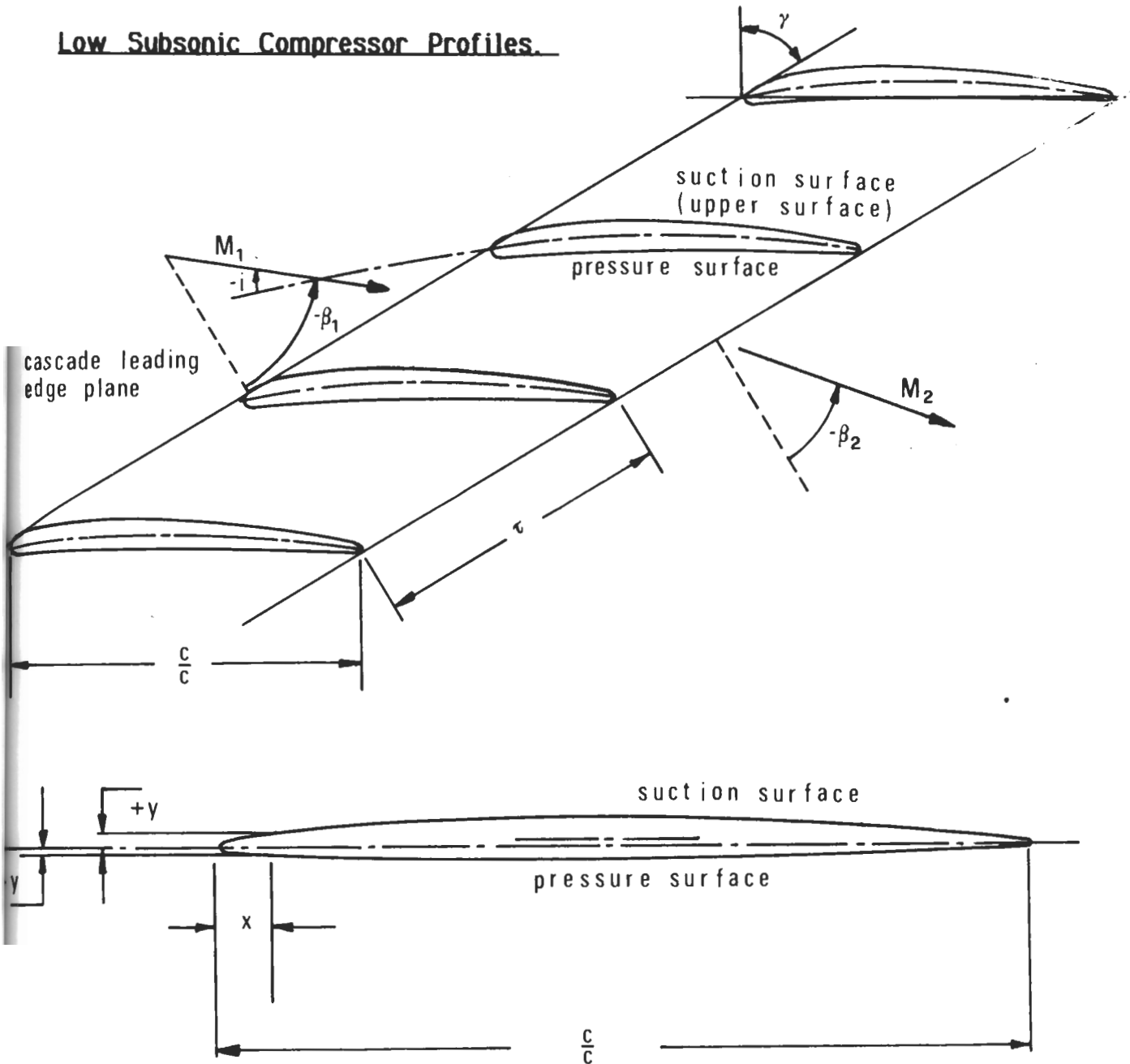
with the first term calculated analytically and the second numerically integrated with about 240 integration points from $x_0 = 0$ to c). In the present cases, calculations were conducted with six control points ($K=6$).

AEROELASTICITY IN TURBOMACHINE-CASCADES

FIRST STANDARD CONFIGURATION

Definition

Low Subsonic Compressor Profiles.



Maximum thickness at x

= 0.5

Vibration in pitch around (x_α, y_α)

= $(0.5, 0.0115)$

d = (thickness/chord)

= 0.06

α = $0.5^\circ, 2.0^\circ$ ($= 0.0087, 0.0349$ rad)

c = 0.1524 m

i = variable ($2^\circ, 6^\circ$)

τ = 0.75

camber = 10°

k = variable

γ = 55°

span = 0.254 m

Working fluid: Air

Fig. 7.1-1. First standard configuration: Cascade geometry

c = 15.24 cm (6 in.)			
SUCTION SURFACE		PRESSURE SURFACE	
X	Y	X	Y
0.0008	0.0020	0.0012	-0.0019
0.0046	0.0053	0.0054	-0.0042
0.0070	0.0064	0.0080	-0.0050
0.0120	0.0083	0.0130	-0.0061
0.0244	0.0116	0.0256	-0.0077
0.0494	0.0164	0.0507	-0.0098
0.0743	0.0204	0.0757	-0.0115
0.0993	0.0237	0.1007	-0.0129
0.1494	0.0290	0.1506	-0.0150
0.1994	0.0331	0.2006	-0.0165
0.2495	0.0364	0.2505	-0.0177
0.2996	0.0387	0.3004	-0.0185
0.3998	0.0411	0.4002	-0.0188
0.5000	0.0406	0.5000	-0.0176
0.6002	0.0370	0.5998	-0.0146
0.7003	0.0306	0.6997	-0.0104
0.8003	0.0223	0.7997	-0.0069
0.8503	0.0176	0.8497	-0.0053
0.9003	0.0127	0.8997	-0.0040
0.9502	0.0078	0.9497	-0.0032
0.9975	0.0030	0.9973	-0.0025

RADIUS CENTER COORDINATES

L.E. RADIUS/c = 0.0024	X = 0.0024, Y = 0.0002
T.E. RADIUS/c = 0.0028	X = 0.9972, Y = 0.0003

Table 7.1-1. First standard configuration: Dimensionless airfoil coordinates.

AERODELASTICITY IN TURBOMACHINE-CASCADES

FIRST STANDARD CONFIGURATION

Aeroelastic Test Cases

Aeroelastic Test Case No	Time averaged				Time Dependent Parameters				
	M ₁ (-)	i (°)	p ₁ /p _{w1} (-)	p ₂ /p _{w1} (-)	β ₂ (°)	k (-)	α (°)	σ (°)	f (Hz)
1	0.18	2	0.9774	0.9818	62.0	0.122	0.5	- 45°	15.5
2	"	"	"	"	"	"	"	+ 45°	"
3	0.17	6	0.9790	0.9852	62.5	"	"	- 45°	"
4	"	"	"	"	"	"	2.0	+ 45°	"
5	"	"	"	"	"	"	"	- 45°	"
6	"	"	"	"	"	"	"	-180°	"
7	"	"	"	"	"	"	"	-135°	"
8	"	"	"	"	"	"	"	- 90°	"
9	"	"	"	"	"	"	"	0°	"
10	"	"	"	"	"	"	"	+ 90°	"
11	"	"	"	"	"	"	"	+135°	"
12	"	"	"	"	"	0.072	"	- 90°	9.2
13	"	"	"	"	"	0.151	"	- 90°	19.2
14	"	"	"	"	"	0.301	"	- 90°	38.4
15	"	"	"	"	"	0.603	"	- 90°	76.8

Table 7.1-2 First standard configuration.

Experimental values for 15 recommended test cases

$c = 15.24 \text{ cm (6 in.)}$

SUCTION SURFACE		PRESSURE SURFACE	
X	Y	X	Y
0.0008	0.0020	0.0012	-0.0019
0.0046	0.0053	0.0054	-0.0042
0.0070	0.0064	0.0080	-0.0050
0.0120	0.0083	0.0130	-0.0061
0.0244	0.0116	0.0256	-0.0077
0.0494	0.0164	0.0507	-0.0098
0.0743	0.0204	0.0757	-0.0115
0.0993	0.0237	0.1007	-0.0129
0.1494	0.0290	0.1506	-0.0150
0.1994	0.0331	0.2006	-0.0165
0.2495	0.0364	0.2505	-0.0177
0.2996	0.0387	0.3004	-0.0185
0.3998	0.0411	0.4002	-0.0188
0.5000	0.0406	0.5000	-0.0176
0.6002	0.0370	0.5998	-0.0146
0.7003	0.0306	0.6997	-0.0104
0.8003	0.0223	0.7997	-0.0069
0.8503	0.0176	0.8497	-0.0053
0.9003	0.0127	0.8997	-0.0040
0.9502	0.0078	0.9497	-0.0032
0.9975	0.0030	0.9973	-0.0025

RADIUS CENTER COORDINATES

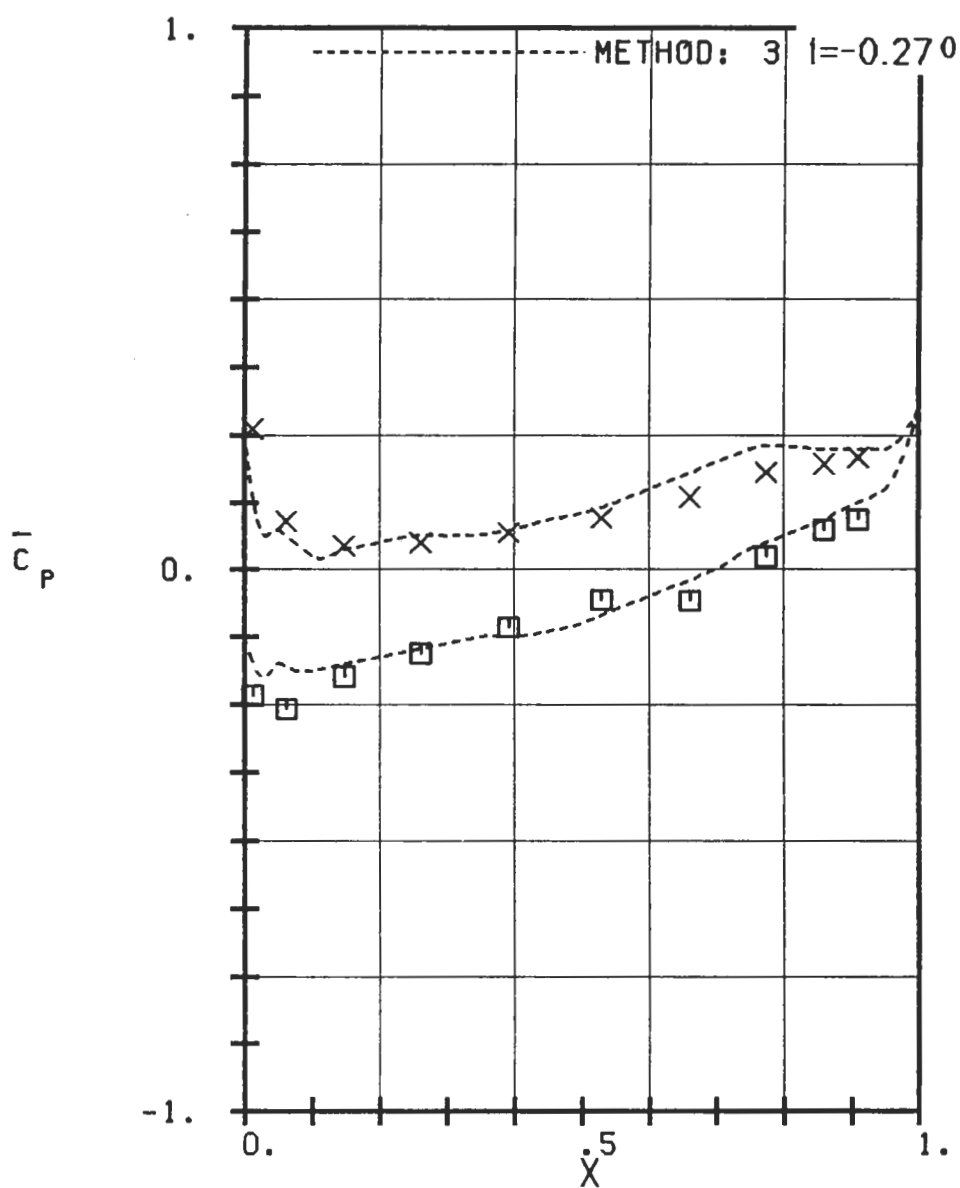
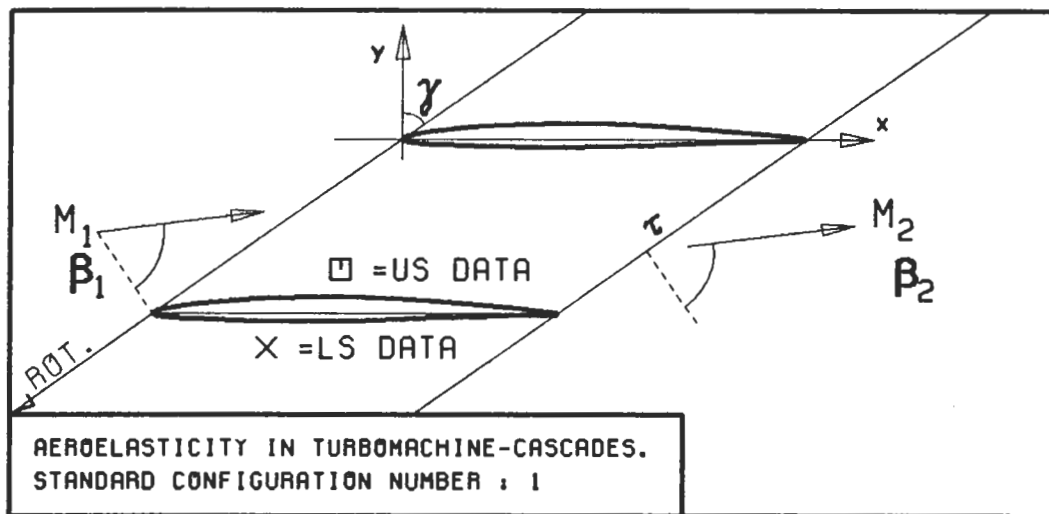
L.E. RADIUS/c = 0.0024	X = 0.0024, Y = 0.0002
T.E. RADIUS/c = 0.0028	X = 0.9972, Y = 0.0003

Table 7.1-1. First standard configuration: Dimensionless airfoil coordinates.

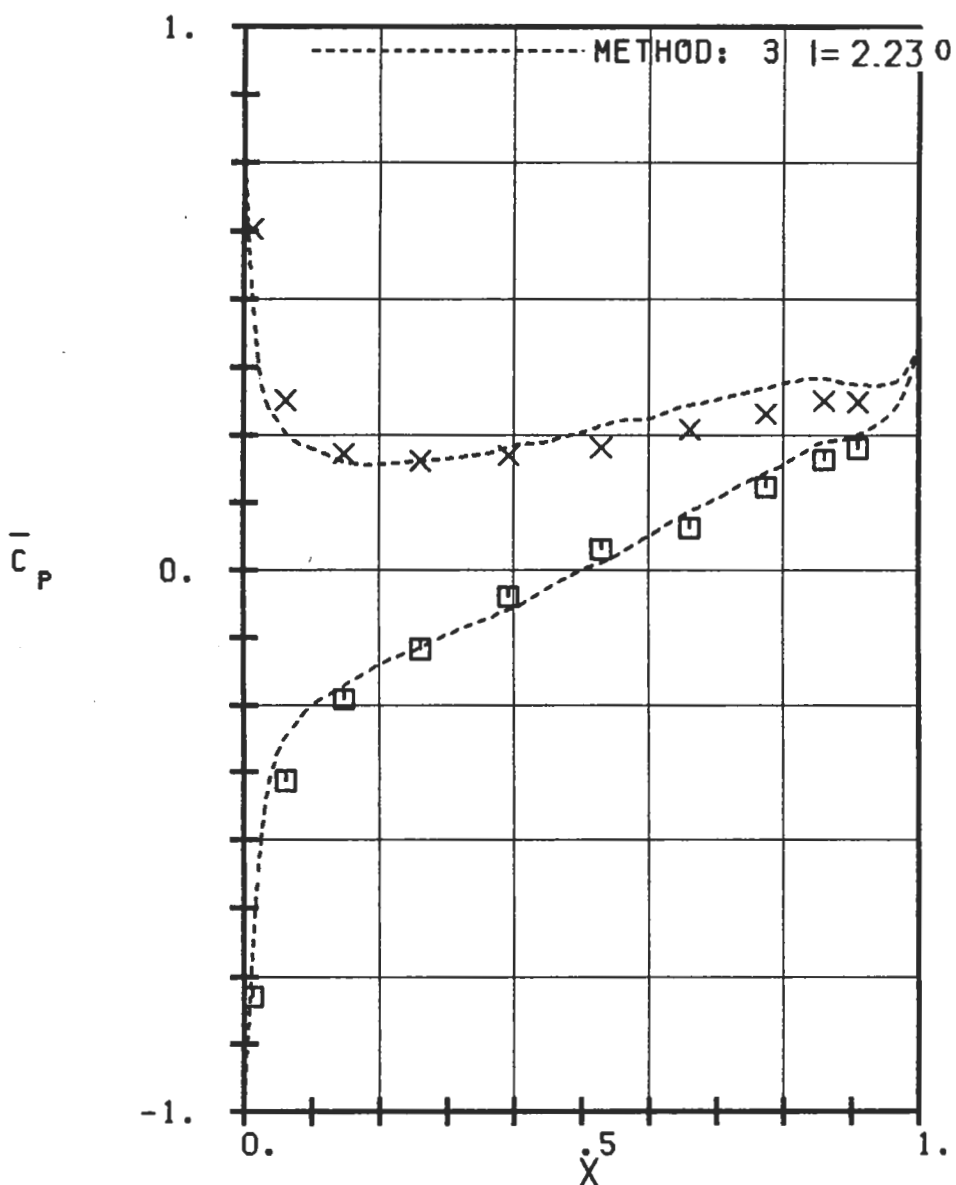
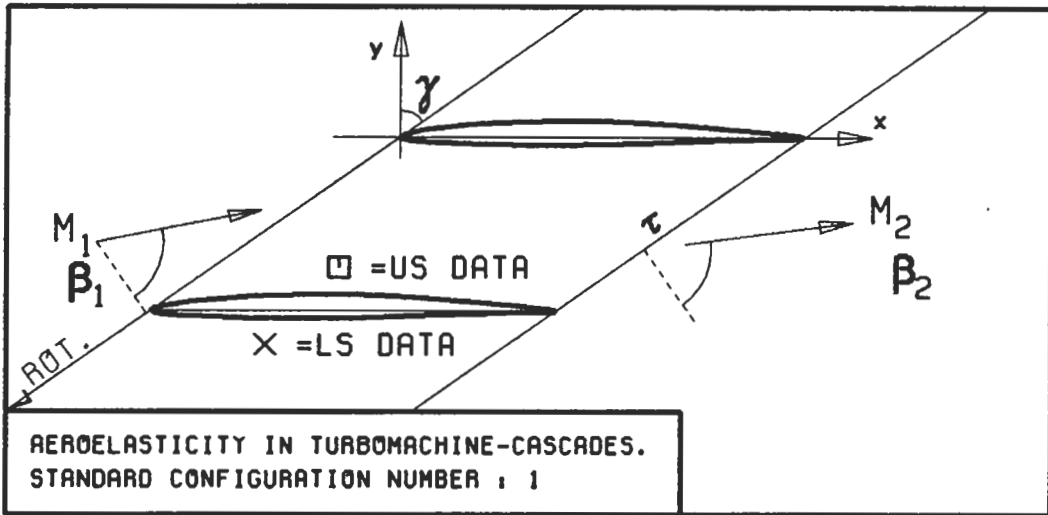
AEROELASTICITY IN TURBOMACHINE-CASCADES

FIRST STANDARD CONFIGURATION

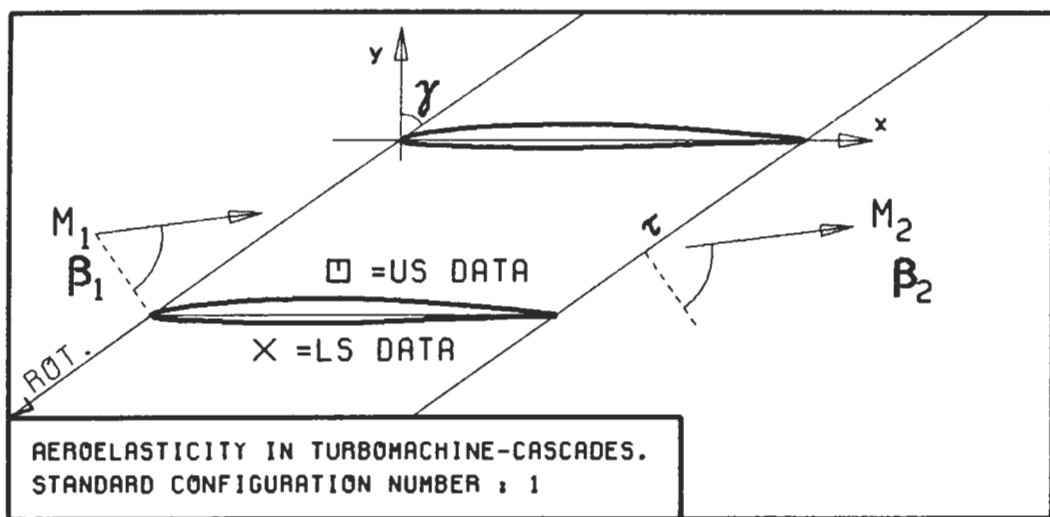
Experimental and Theoretical Results



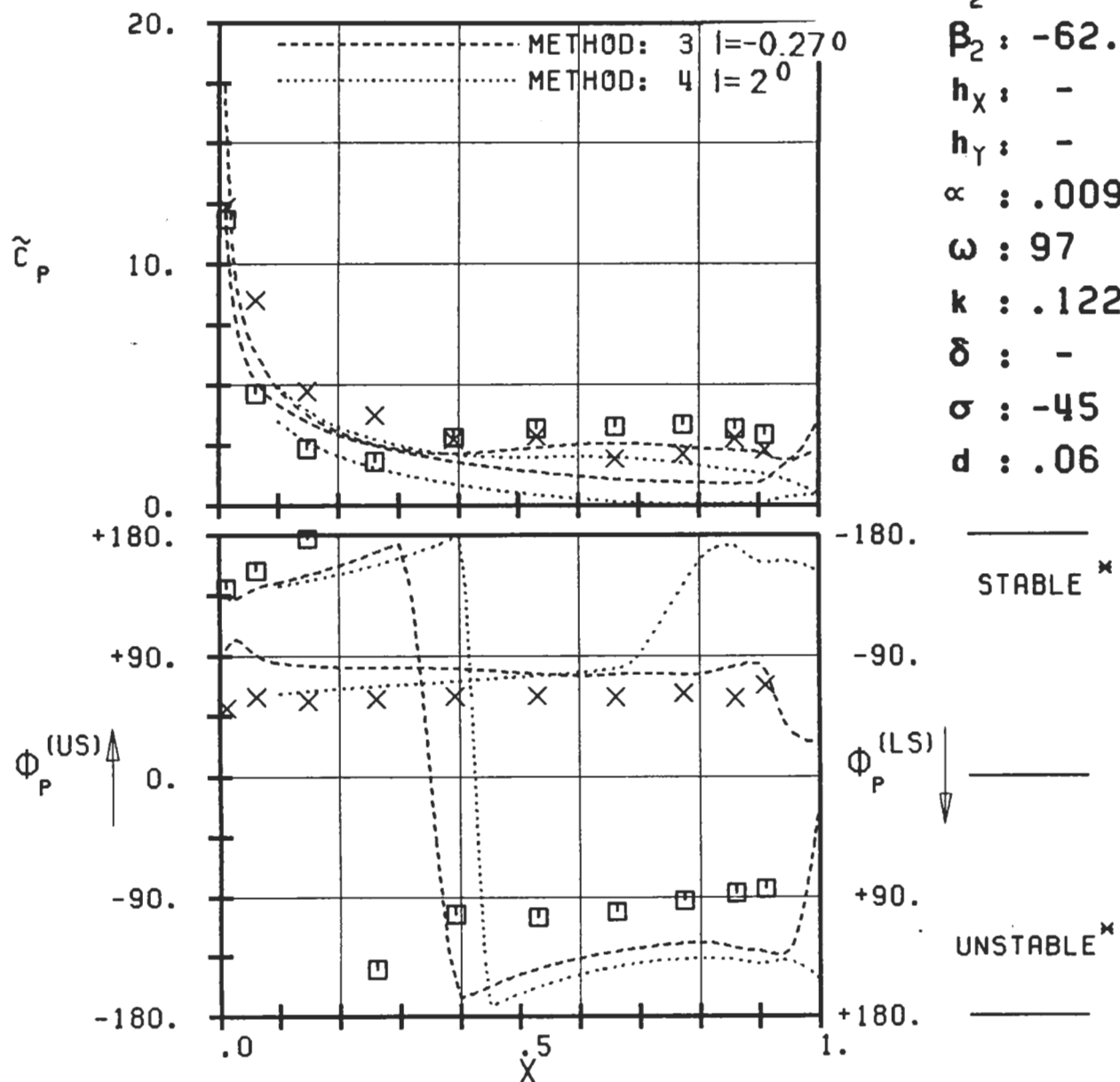
PLOT 7.1-1.1: FIRST STANDARD CONFIGURATION, CASES 1-2.
 TIME AVERAGED BLADE SURFACE PRESSURE
 COEFFICIENT FOR INCIDENCE 2. DEGREES.



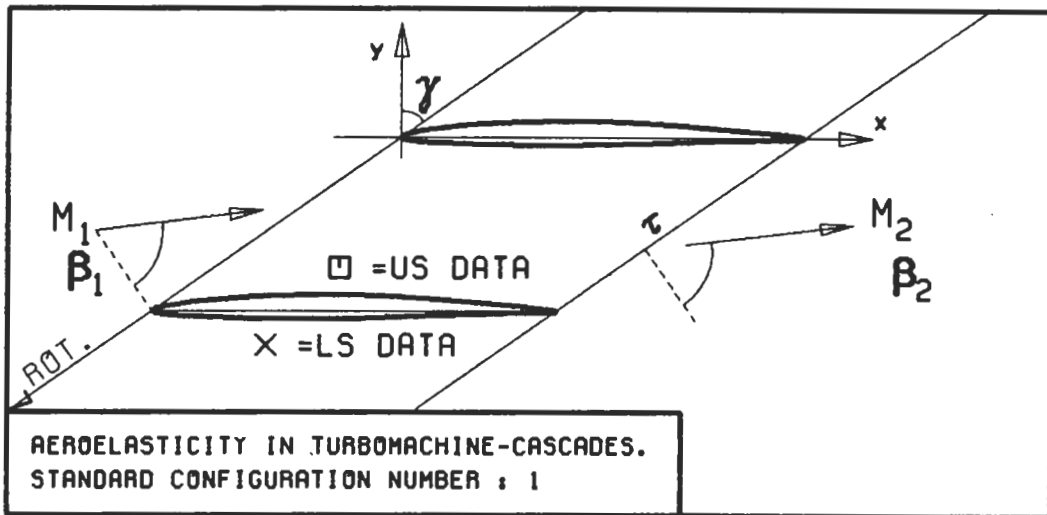
PLOT 7.1-1.2: FIRST STANDARD CONFIGURATION, CASES 3-15.
TIME AVERAGED BLADE SURFACE PRESSURE
COEFFICIENT FOR INCIDENCE 6. DEGREES.



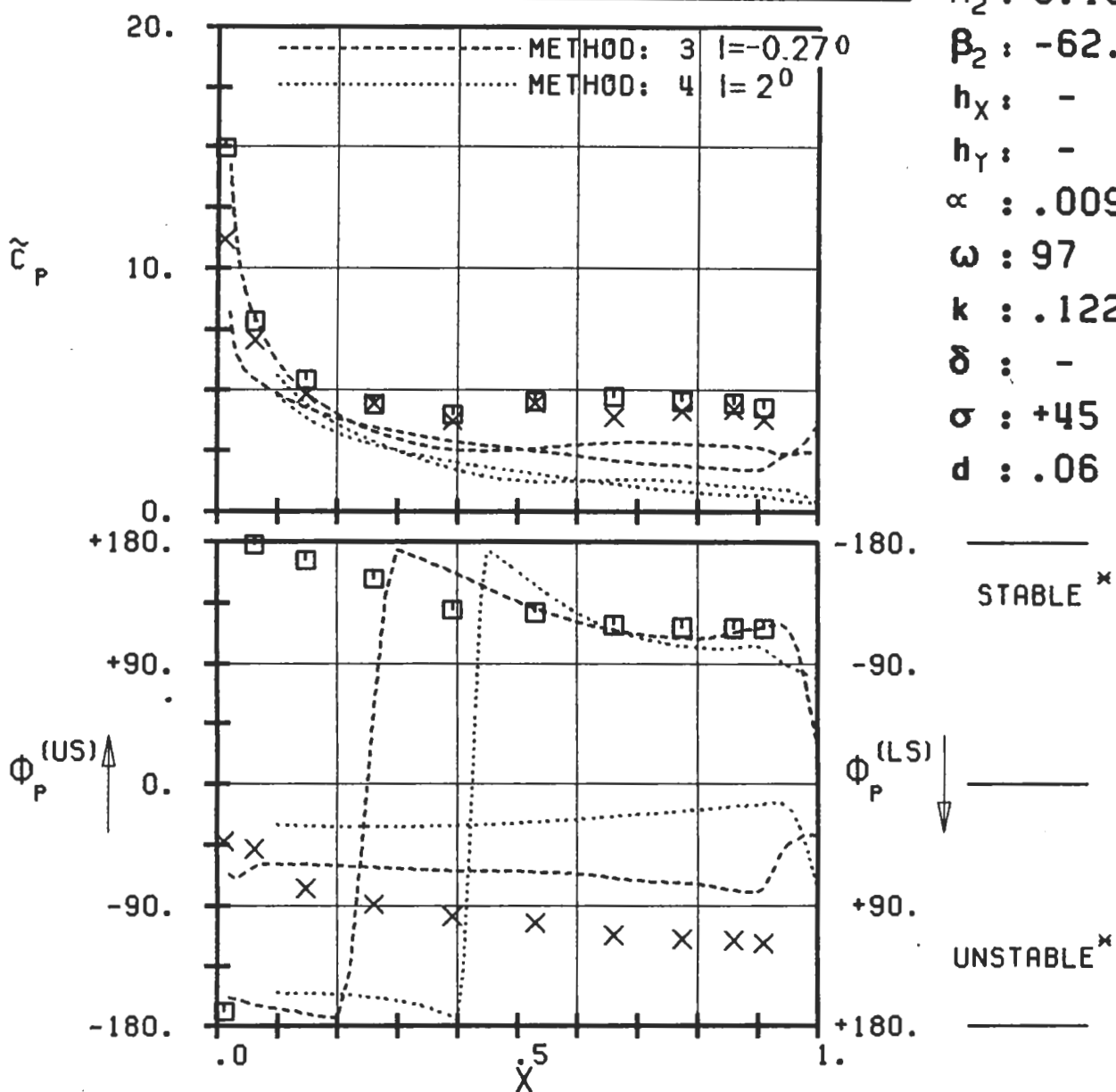
$c : .152M$
 $\tau : .75$
 $\gamma : 55.$
 $x_\alpha : .5$
 $y_\alpha : .0115$
 $M_1 : .18$
 $\beta_1 : -62.$
 $i : 2.$
 $M_2 : 0.16$
 $\beta_2 : -62.$
 $h_X : -$
 $h_Y : -$
 $\alpha : .009$
 $\omega : 97$
 $k : .122$
 $\delta : -$
 $\sigma : -45$
 $d : .06$



PLOT 7.1-2.1: FIRST STANDARD CONFIGURATION, CASE 1.
MAGNITUDE AND PHASE LEAD OF UNSTEADY BLADE
SURFACE PRESSURE COEFFICIENT.
(x: IN PITCH MODE, NOTATION VALID UPSTREAM OF PITCH AXIS)

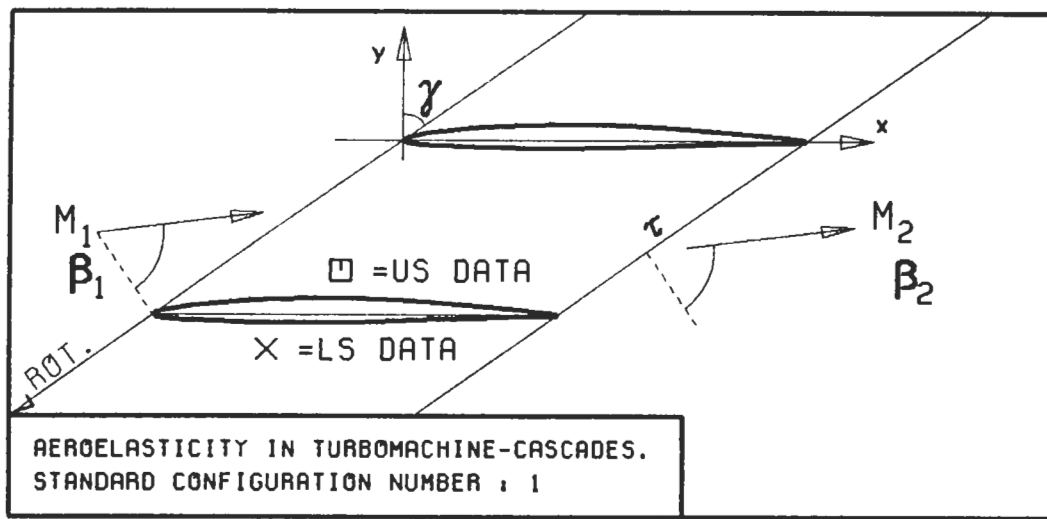


$c : .152M$
 $\tau : .75$
 $\gamma : 55.$
 $x_\alpha : .5$
 $y_\alpha : .0115$
 $M_1 : .18$
 $\beta_1 : -62.$
 $i : 2.$
 $M_2 : 0.16$
 $\beta_2 : -62.$
 $h_x : -$
 $h_y : -$
 $\alpha : .009$
 $\omega : 97$
 $k : .122$
 $\delta : -$
 $\sigma : +45$
 $d : .06$

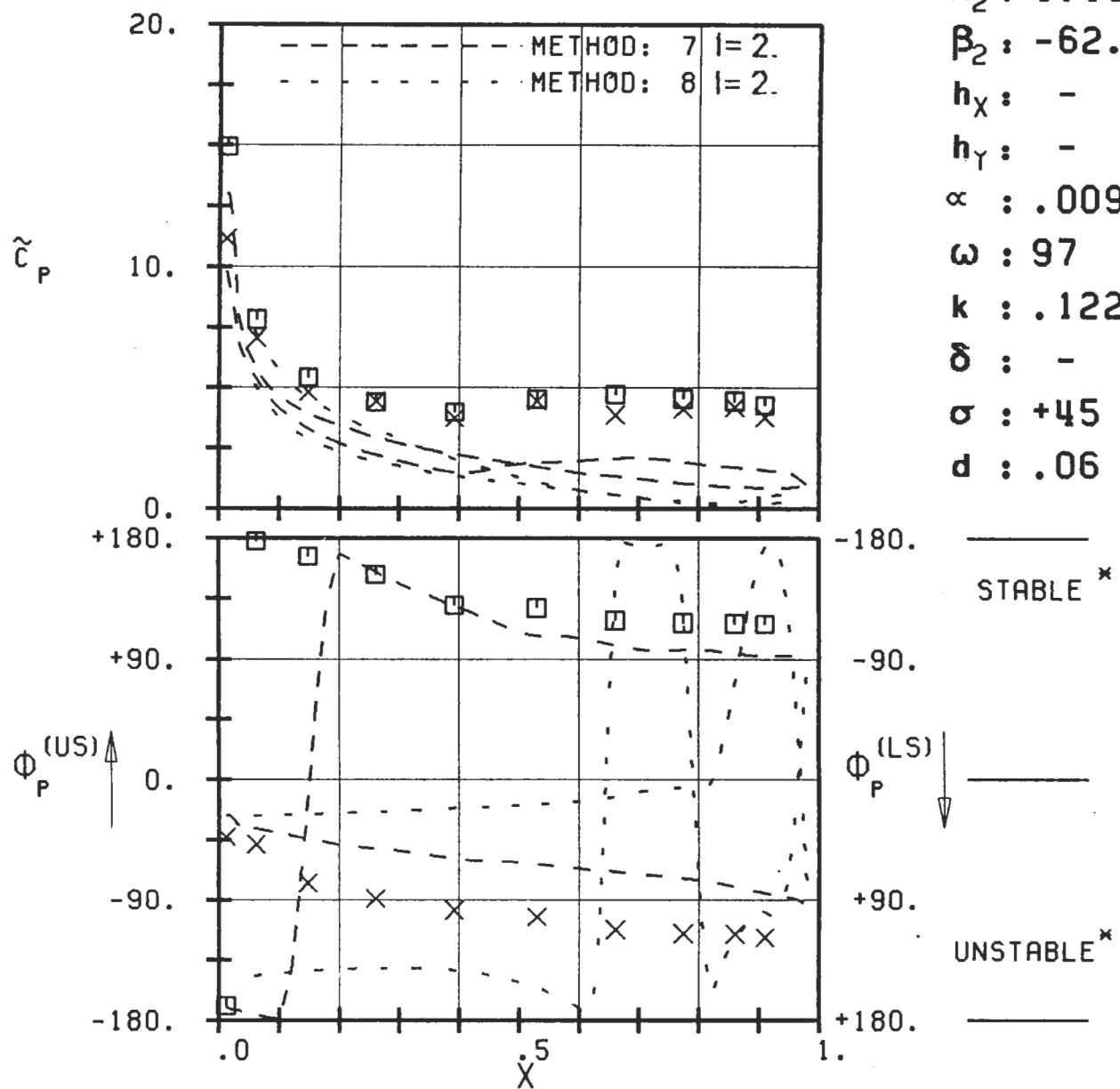


PLOT 7.1-2.2A: FIRST STANDARD CONFIGURATION, CASE 2.
MAGNITUDE AND PHASE LEAD OF UNSTEADY BLADE
SURFACE PRESSURE COEFFICIENT.

(*: IN PITCH MODE, NOTATION VALID UPSTREAM OF PITCH AXIS)

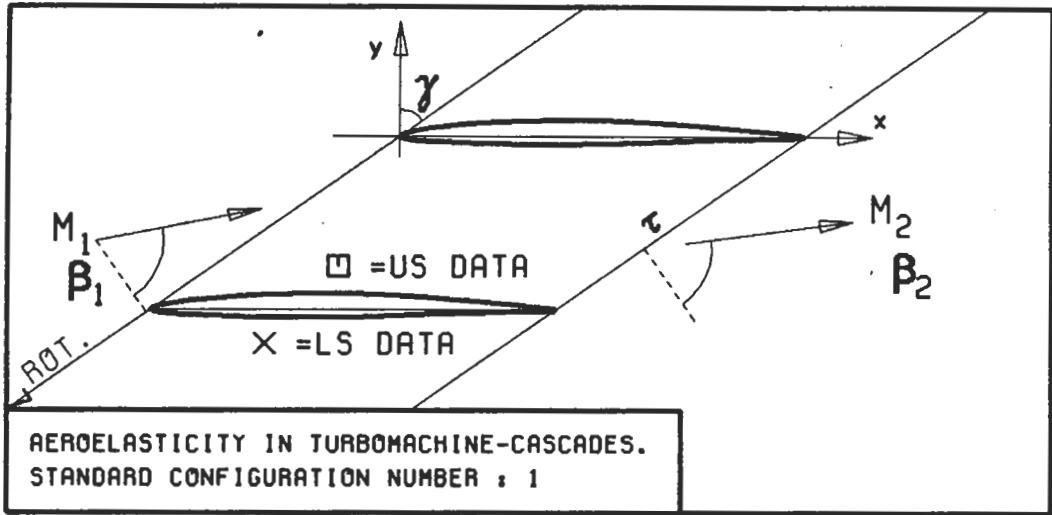


$c : .152M$
 $\tau : .75$
 $\gamma : 55.$
 $x_\alpha : .5$
 $y_\alpha : .0115$
 $M_1 : .18$
 $\beta_1 : -62.$
 $i : 2.$
 $M_2 : 0.16$
 $\beta_2 : -62.$
 $h_X : -$
 $h_Y : -$
 $\alpha : .009$
 $\omega : 97$
 $k : .122$
 $\delta : -$
 $\sigma : +45$
 $d : .06$

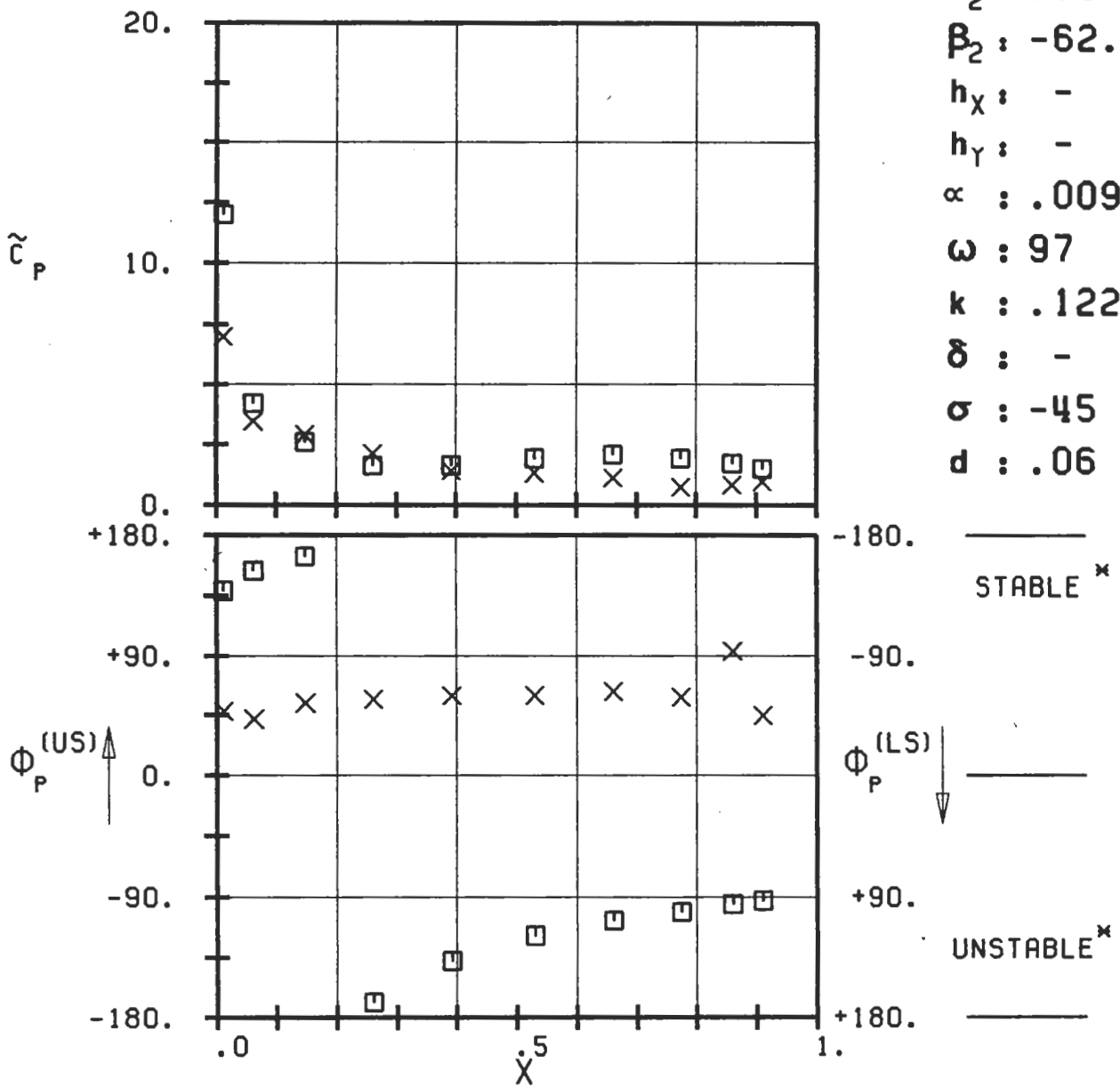


PLOT 7.1-2.2B: FIRST STANDARD CONFIGURATION, CASE 2.
MAGNITUDE AND PHASE LEAD OF UNSTEADY BLADE
SURFACE PRESSURE COEFFICIENT.

(*: IN PITCH MODE, NOTATION VALID UPSTREAM OF PITCH AXIS)

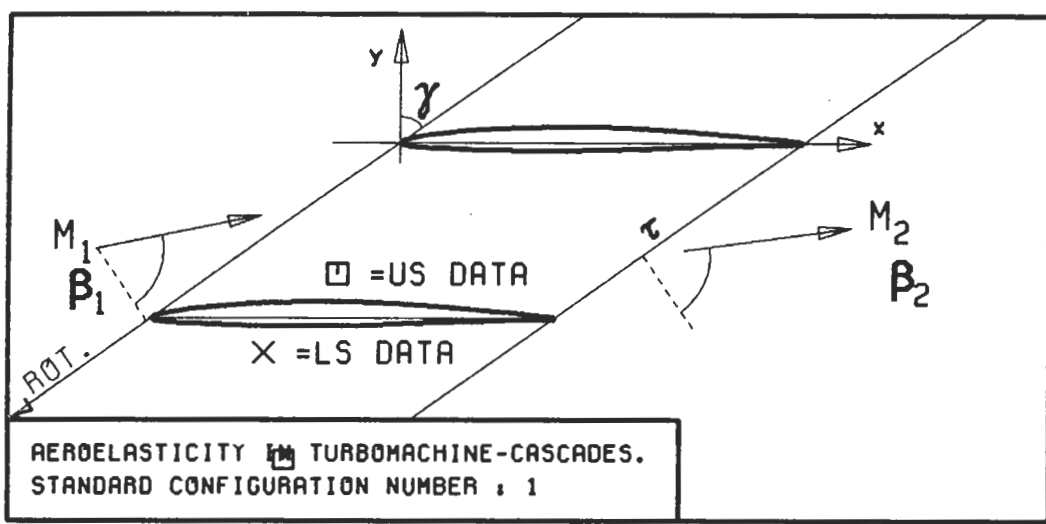


$c : .152M$
 $\tau : .75$
 $\gamma : 55.$
 $x_\alpha : .5$
 $y_\alpha : .0115$
 $M_1 : .17$
 $\beta_1 : -66.$
 $i : 6.$
 $M_2 : 0.15$
 $\beta_2 : -62.5$
 $h_x : -$
 $h_y : -$
 $\alpha : .009$
 $\omega : 97$
 $k : .122$
 $\delta : -$
 $\sigma : -45$
 $d : .06$

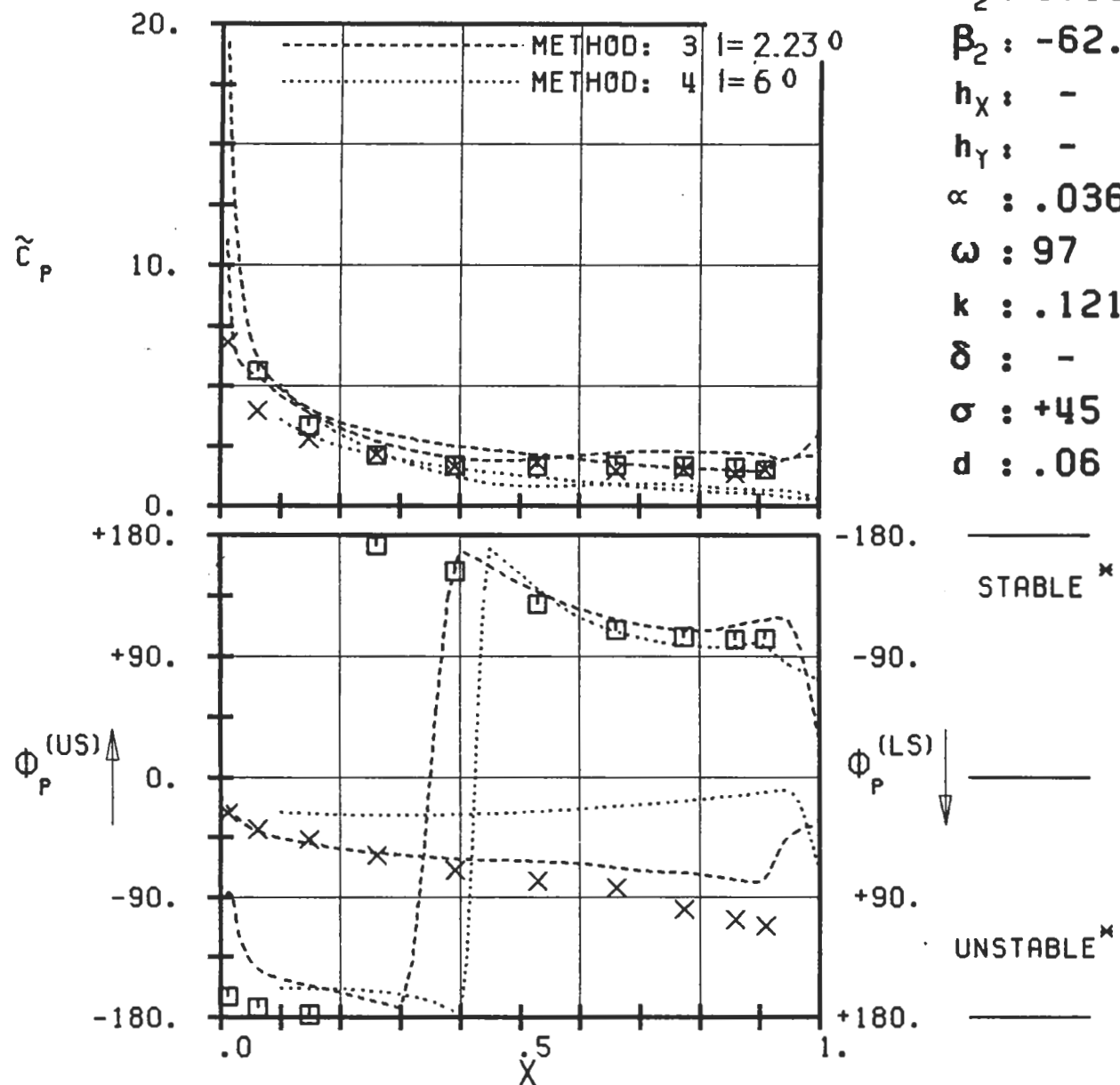


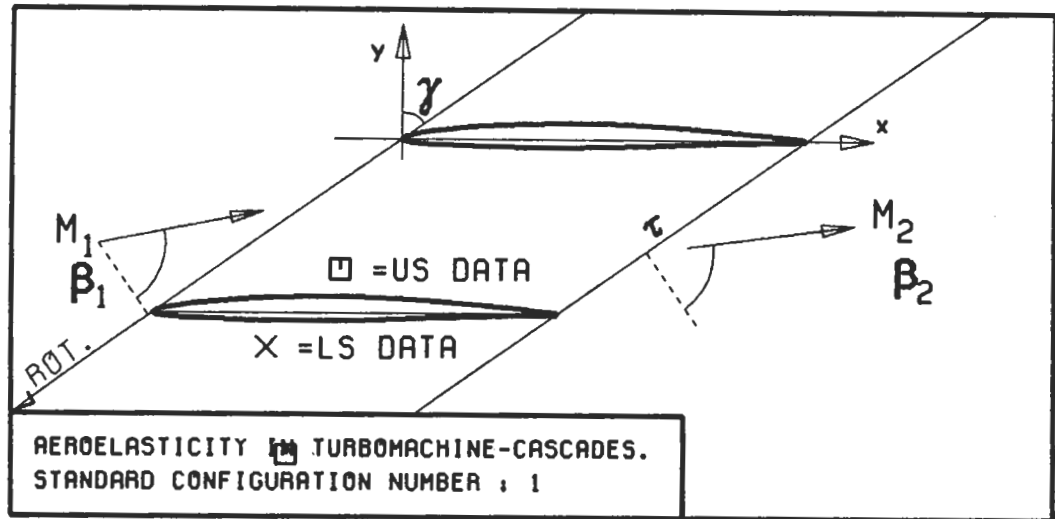
PLOT 7.1-2.3: FIRST STANDARD CONFIGURATION, CASE 3.
MAGNITUDE AND PHASE LEAD OF UNSTEADY BLADE
SURFACE PRESSURE COEFFICIENT.

(x: IN PITCH MODE, NOTATION VALID UPSTREAM OF PITCH AXIS)

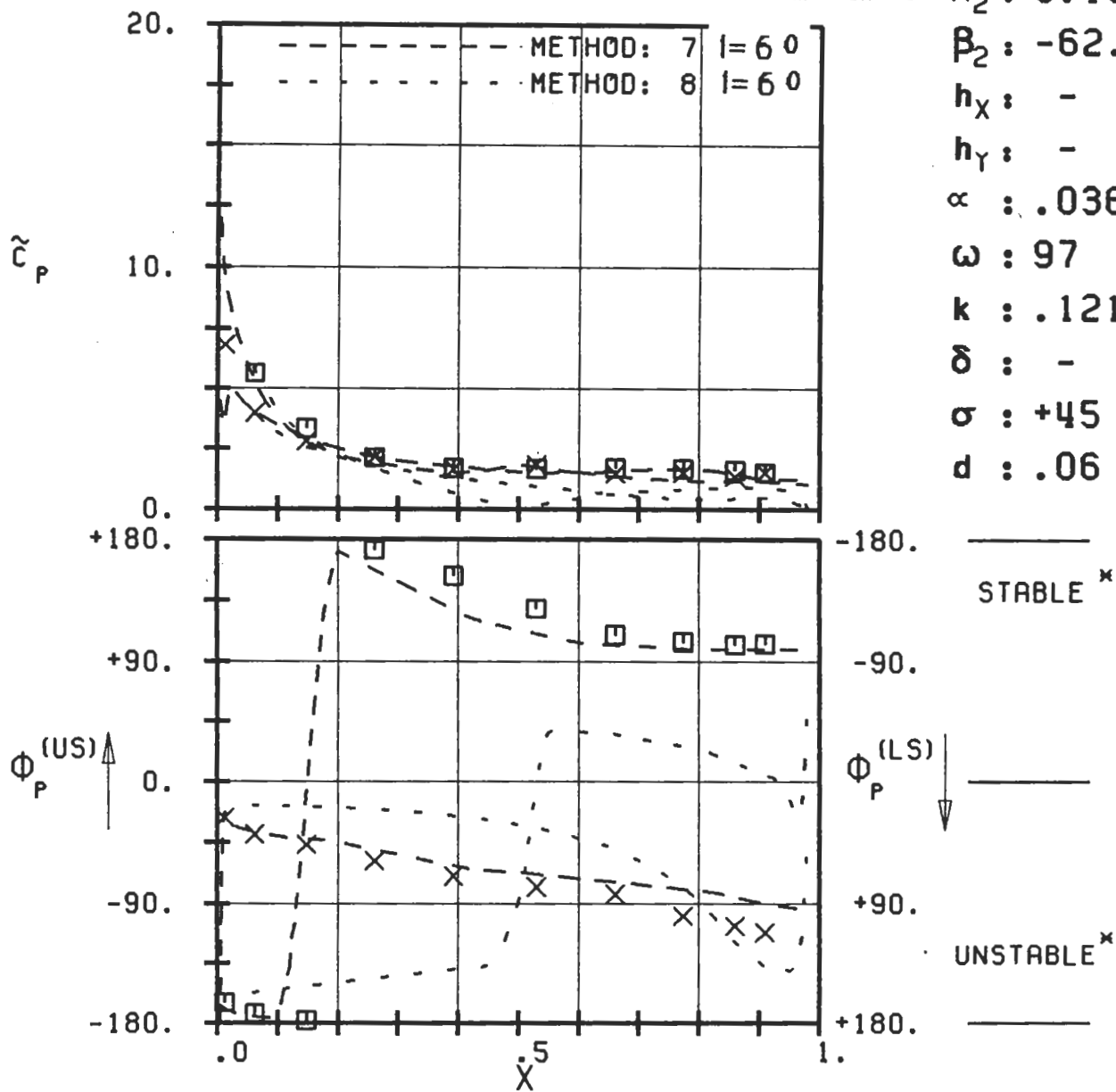


$c : .152M$
 $\tau : .75$
 $\gamma : 55.$
 $x_\infty : .5$
 $y_\infty : .0115$
 $M_1 : .17$
 $\beta_1 : -66.$
 $i : 6.$
 $M_2 : 0.15$
 $\beta_2 : -62.5$
 $h_x : -$
 $h_y : -$
 $\alpha : .036$
 $\omega : 97$
 $k : .121$
 $\delta : -$
 $\sigma : +45$
 $d : .06$



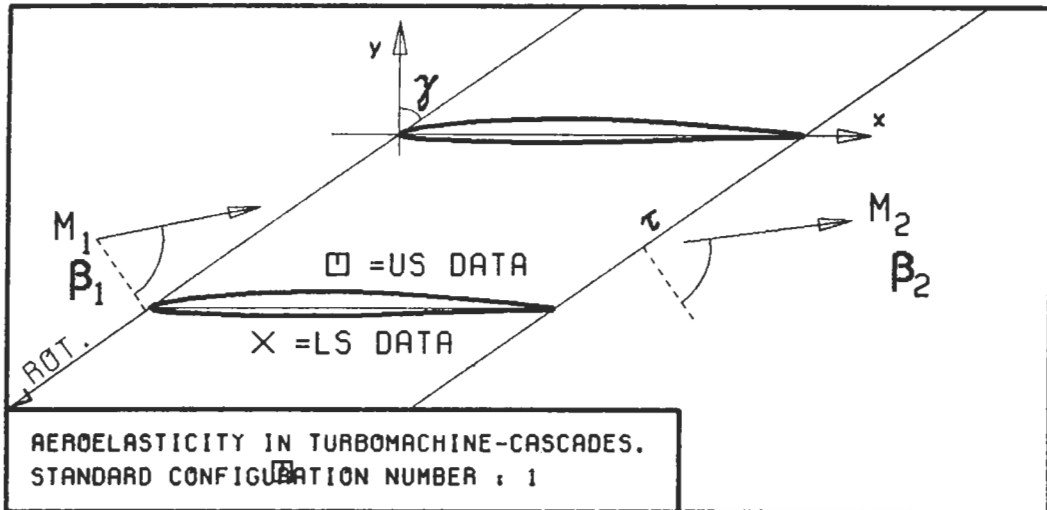


$c : .152M$
 $\tau : .75$
 $\gamma : 55.$
 $x_\alpha : .5$
 $y_\alpha : .0115$
 $M_1 : .17$
 $B_1 : -66.$
 $i : 6.$
 $M_2 : 0.15$
 $B_2 : -62.5$
 $h_X : -$
 $h_Y : -$
 $\alpha : .036$
 $\omega : 97$
 $k : .121$
 $\delta : -$
 $\sigma : +45$
 $d : .06$

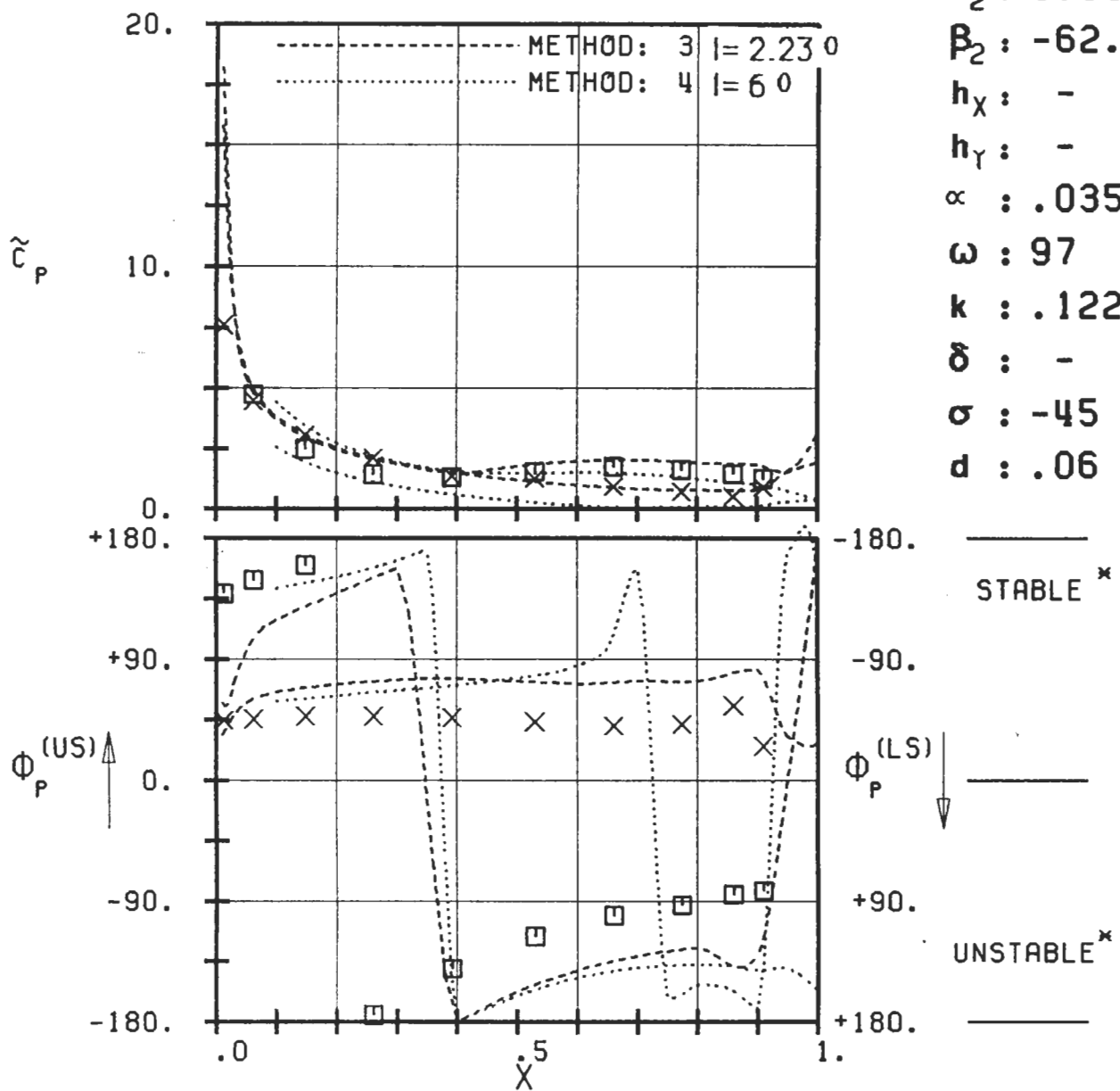


PLOT 7.1-2.4B: FIRST STANDARD CONFIGURATION, CASE 4.
MAGNITUDE AND PHASE LEAD OF UNSTEADY BLADE
SURFACE PRESSURE COEFFICIENT.

(x: IN PITCH MODE, NOTATION VALID UPSTREAM OF PITCH AXIS)

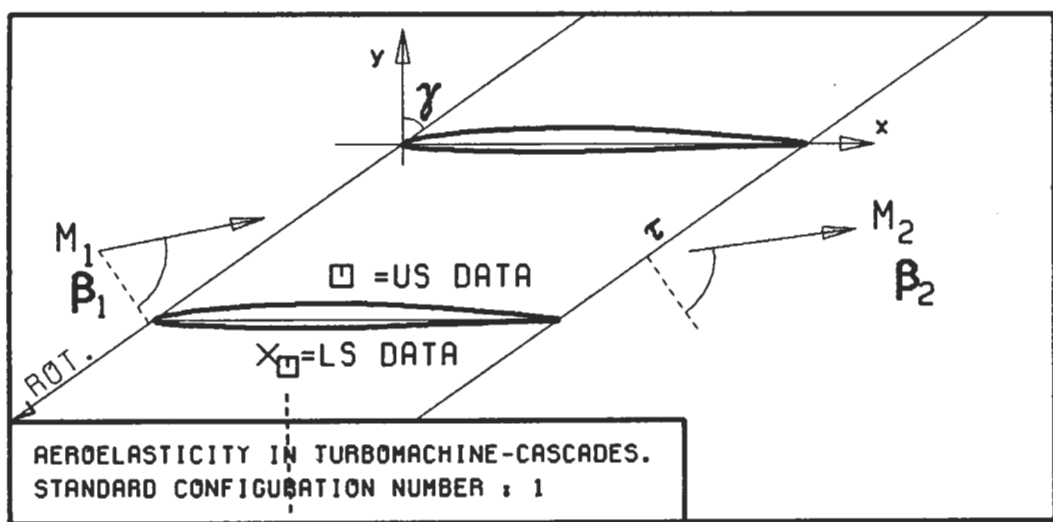


$c : .152M$
 $\tau : .75$
 $\gamma : 55.$
 $x_\infty : .5$
 $y_\infty : .0115$
 $M_1 : .17$
 $B_1 : -66.$
 $i : 6.$
 $M_2 : 0.15$
 $B_2 : -62.5$
 $h_X : -$
 $h_Y : -$
 $\alpha : .035$
 $\omega : 97$
 $k : .122$
 $\delta : -$
 $\sigma : -45$
 $d : .06$

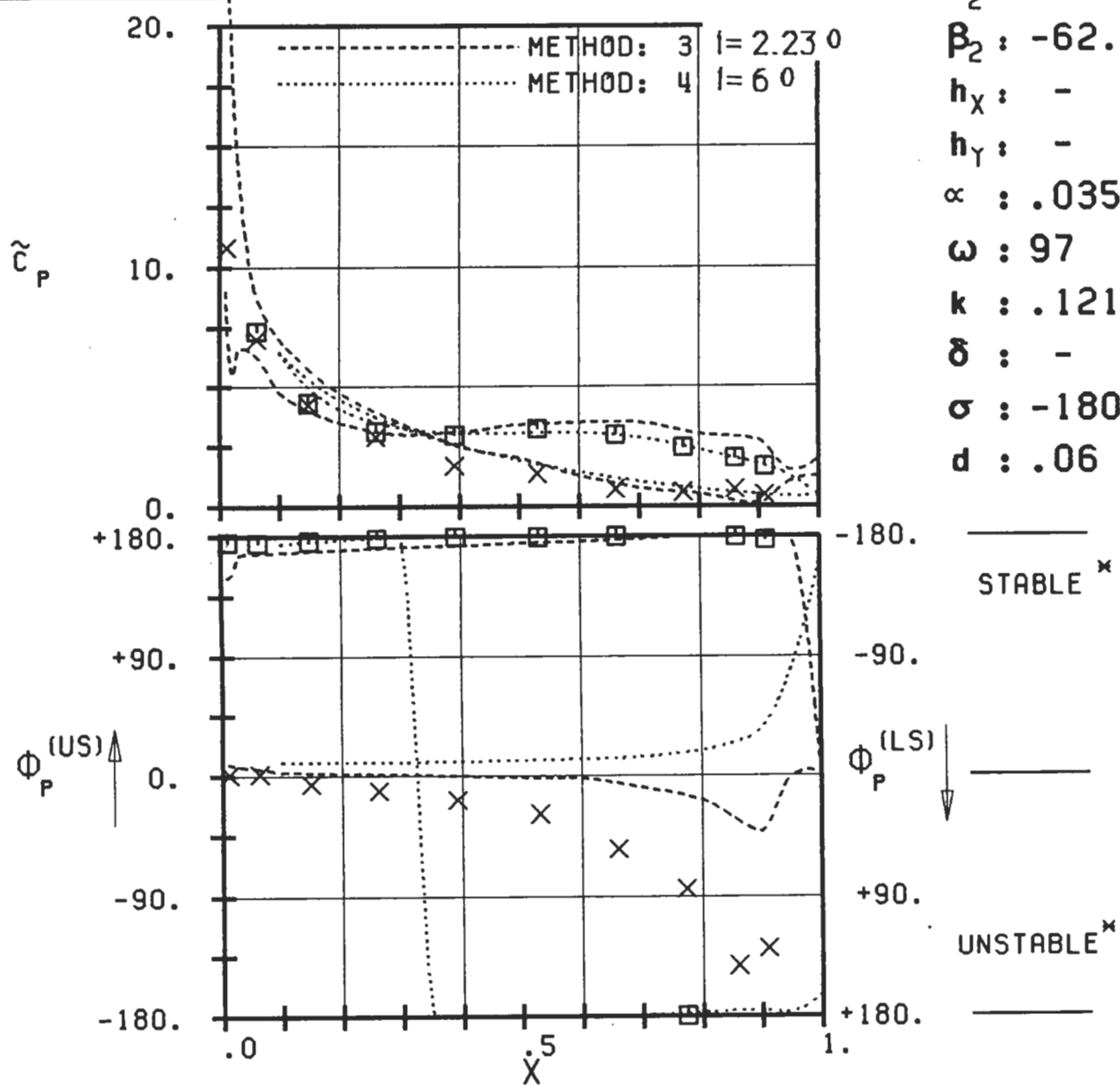


PLOT 7.1-2.5: FIRST STANDARD CONFIGURATION, CASE 5.
MAGNITUDE AND PHASE LEAD OF UNSTEADY BLADE
SURFACE PRESSURE COEFFICIENT.

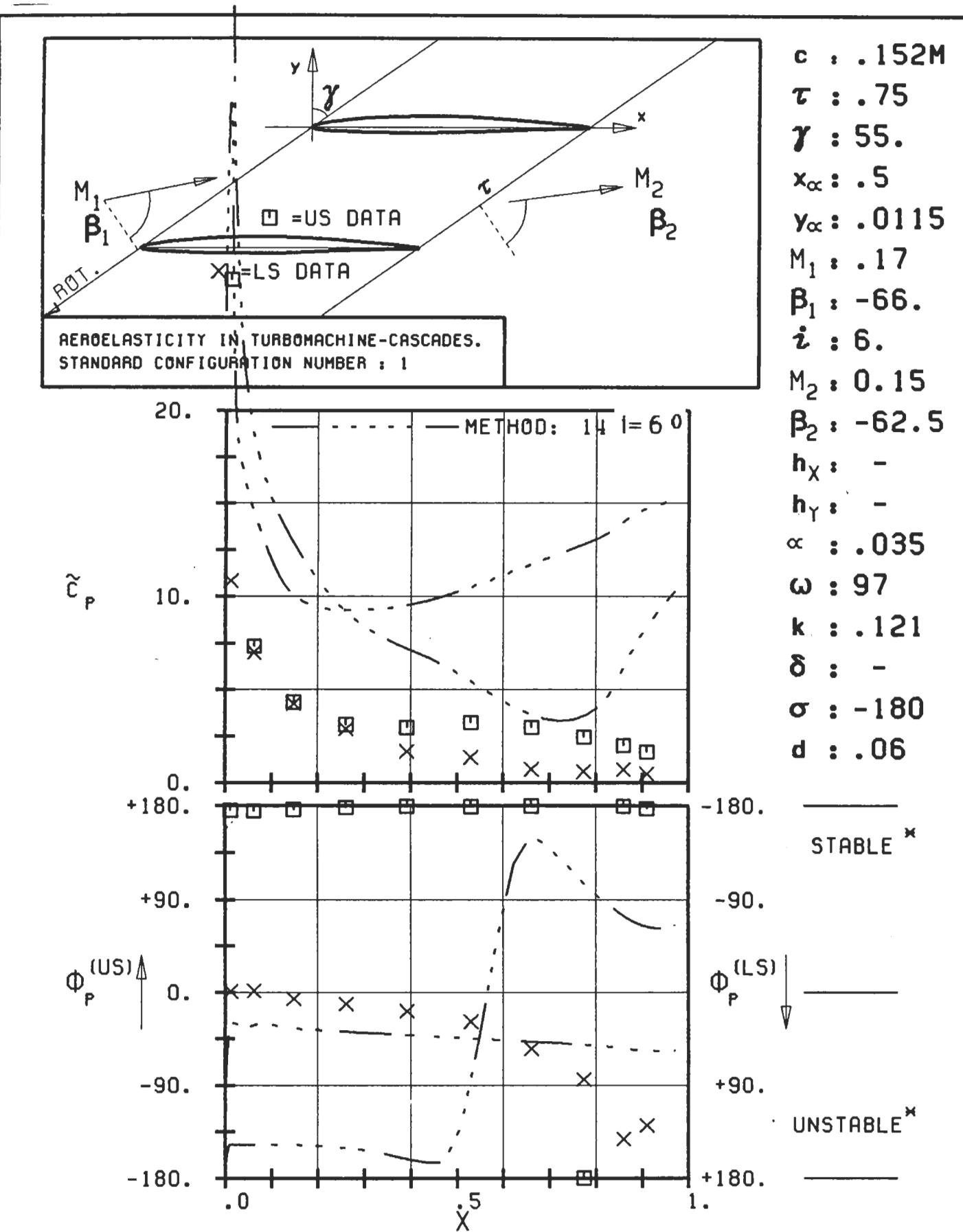
(\times : IN PITCH MODE, NOTATION VALID UPSTREAM OF PITCH AXIS)



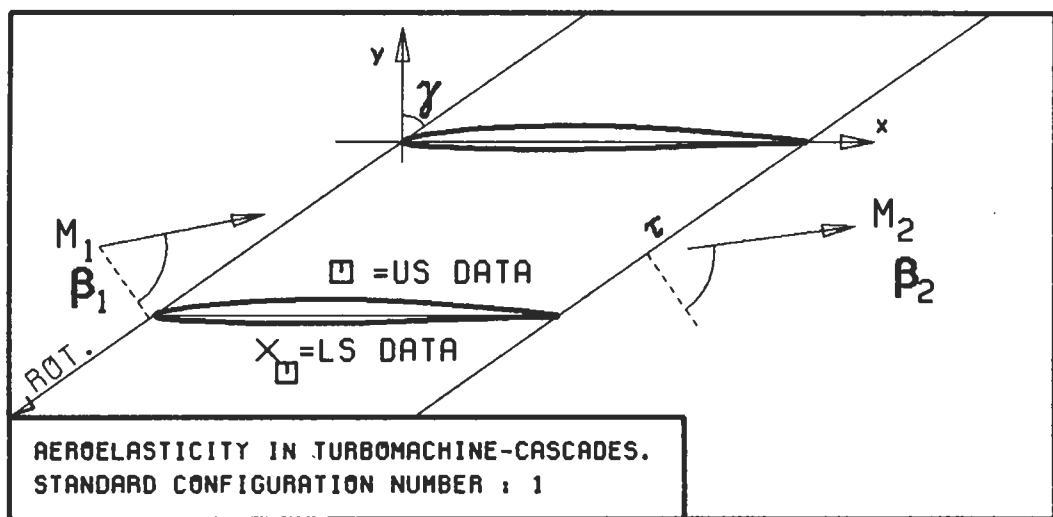
$c : .152M$
 $\tau : .75$
 $\gamma : 55.$
 $x_\infty : .5$
 $y_\infty : .0115$
 $M_1 : .17$
 $\beta_1 : -66.$
 $i : 6.$
 $M_2 : 0.15$
 $\beta_2 : -62.5$
 $h_X : -$
 $h_Y : -$
 $\alpha : .035$
 $\omega : 97$
 $k : .121$
 $\delta : -$
 $\sigma : -180$
 $d : .06$



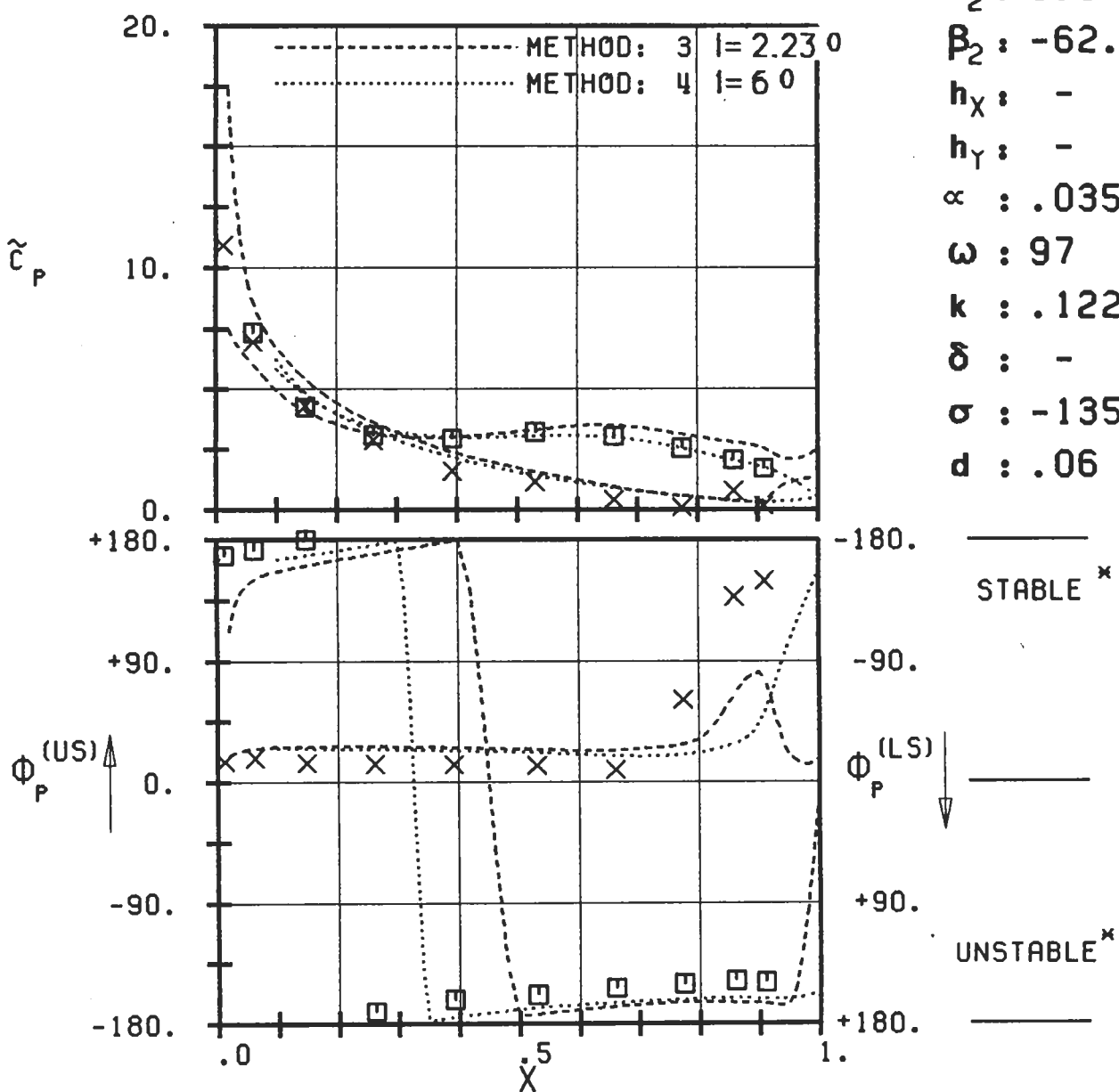
PLOT 7.1-2.6A: FIRST STANDARD CONFIGURATION, CASE 6.
 MAGNITUDE AND PHASE LEAD OF UNSTEADY BLADE
 SURFACE PRESSURE COEFFICIENT.
 (x: IN PITCH MODE, NOTATION VALID UPSTREAM OF PITCH AXIS)



PLOT 7.1-2.6B: FIRST STANDARD CONFIGURATION, CASE 6.
 MAGNITUDE AND PHASE LEAD OF UNSTEADY BLADE
 SURFACE PRESSURE COEFFICIENT.
 (*: IN PITCH MODE, NOTATION VALID UPSTREAM OF PITCH AXIS)

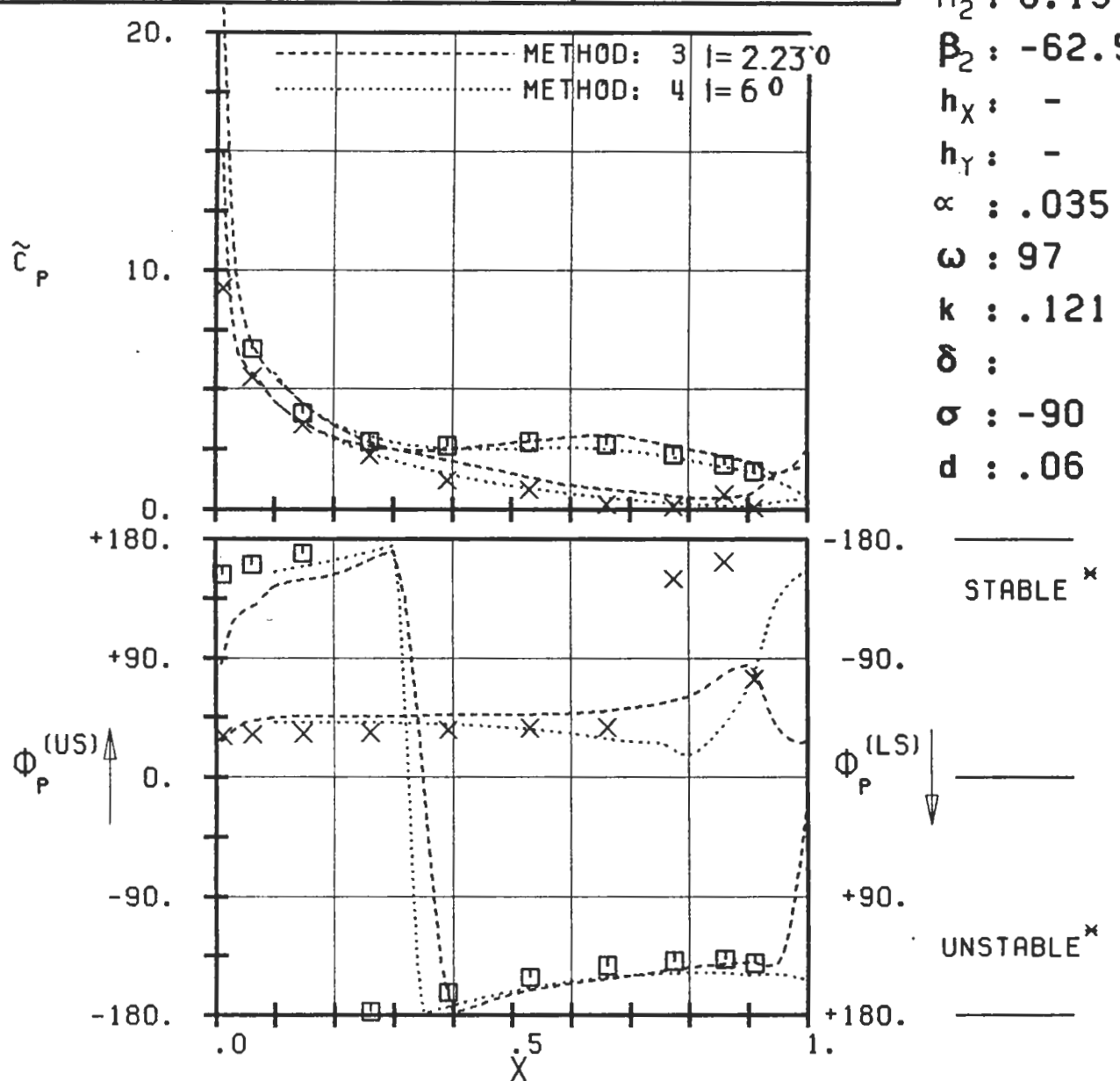
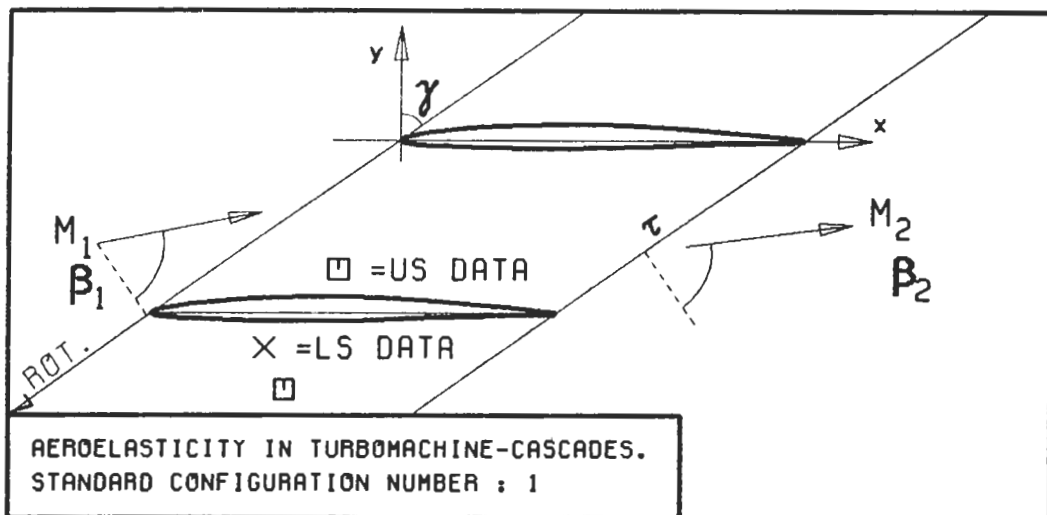


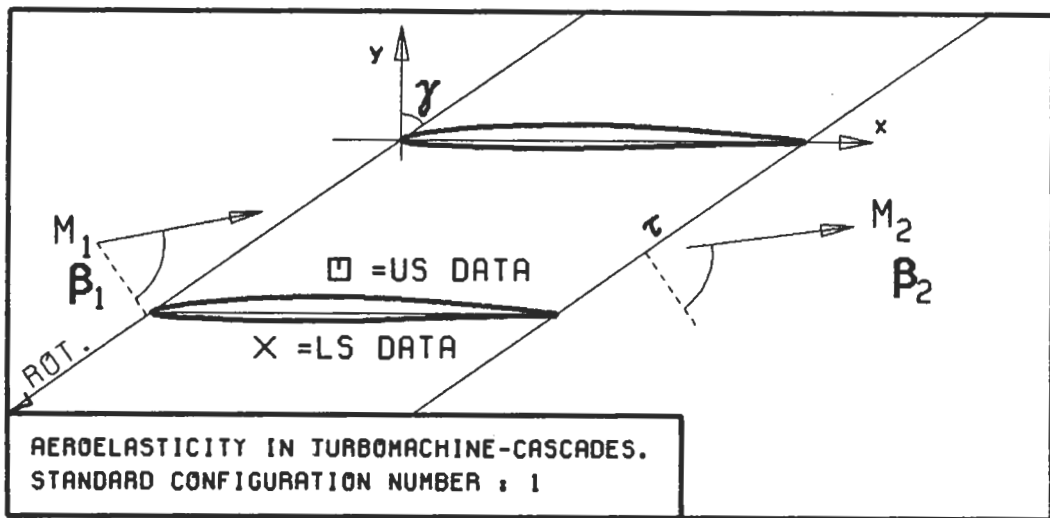
$c : .152M$
 $\tau : .75$
 $\gamma : 55.$
 $x_\alpha : .5$
 $y_\alpha : .0115$
 $M_1 : .17$
 $\beta_1 : -66.$
 $i : 6.$
 $M_2 : 0.15$
 $\beta_2 : -62.5$
 $h_X : -$
 $h_Y : -$
 $\alpha : .035$
 $\omega : 97$
 $k : .122$
 $\delta : -$
 $\sigma : -135$
 $d : .06$



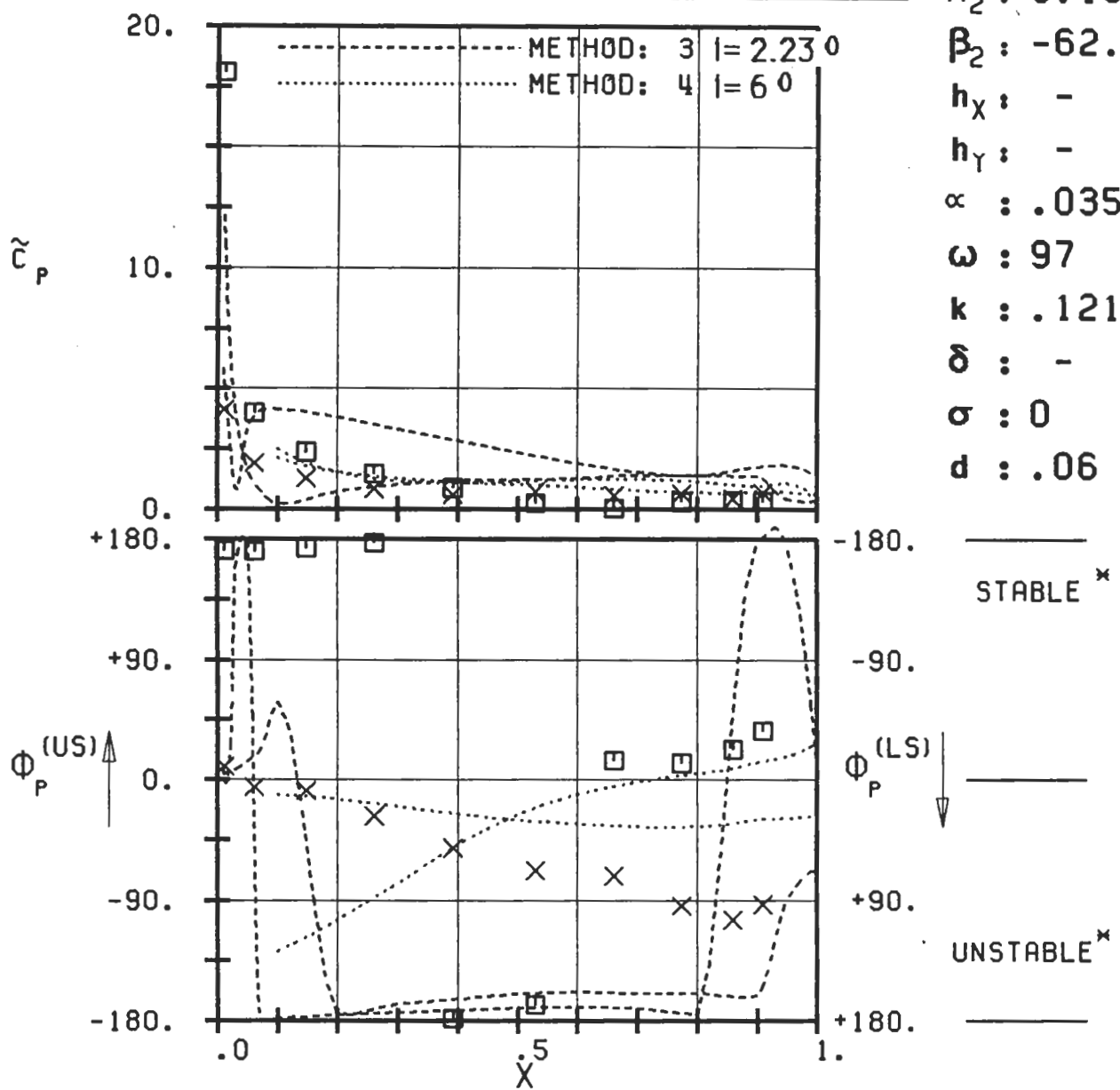
PLOT 7.1-2.7: FIRST STANDARD CONFIGURATION, CASE 7.
MAGNITUDE AND PHASE LEAD OF UNSTEADY BLADE
SURFACE PRESSURE COEFFICIENT.

(x: IN PITCH MODE, NOTATION VALID UPSTREAM OF PITCH AXIS)



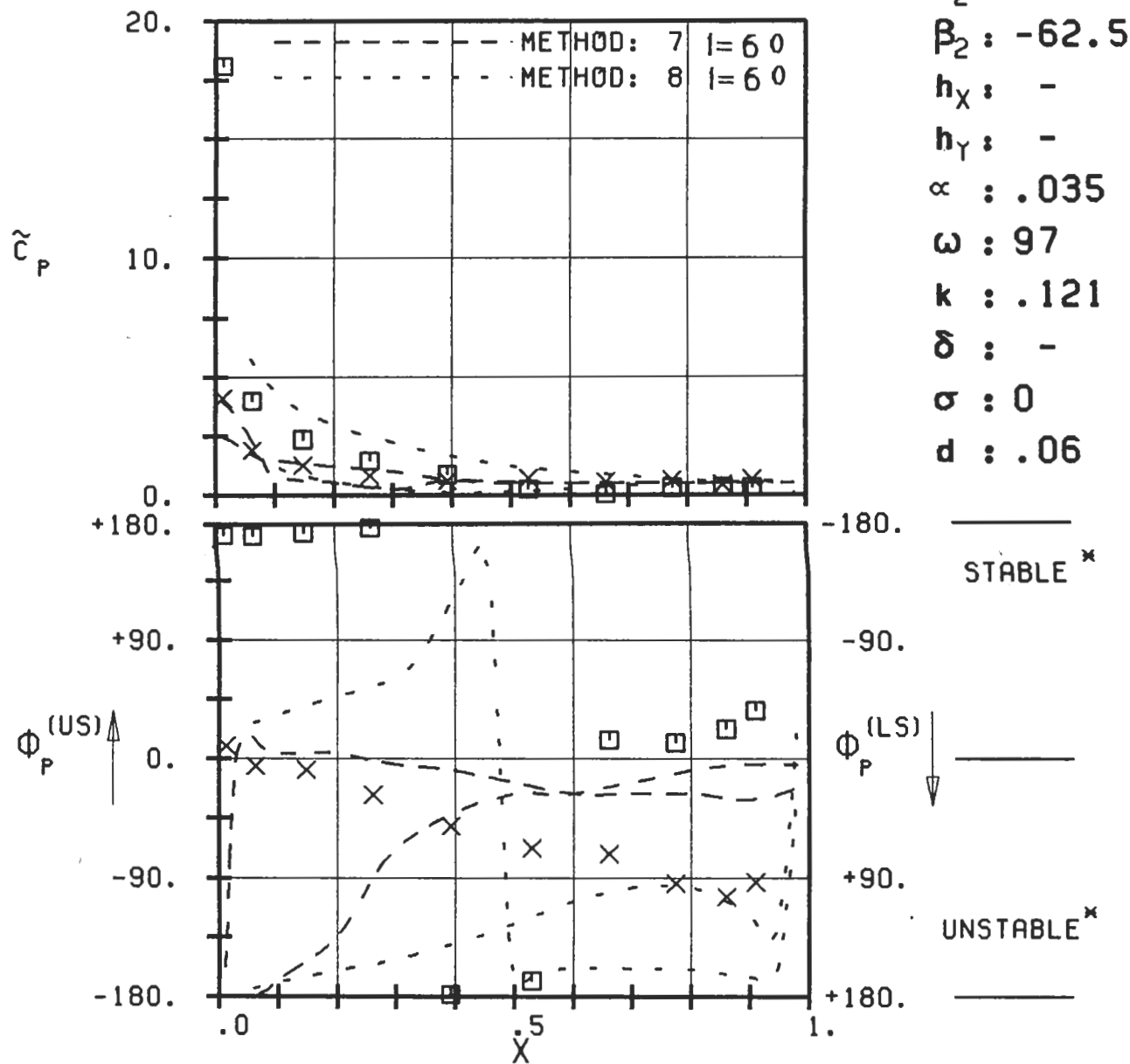
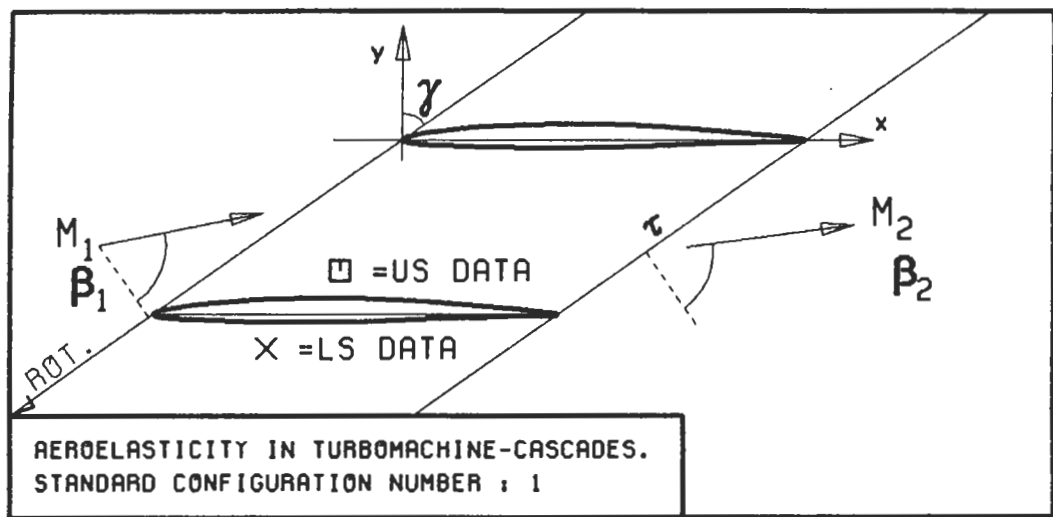


$c : .152M$
 $\tau : .75$
 $\gamma : 55.$
 $x_\infty : .5$
 $y_\infty : .0115$
 $M_1 : .17$
 $B_1 : -66.$
 $i : 6.$
 $M_2 : 0.15$
 $B_2 : -62.5$
 $h_X : -$
 $h_Y : -$
 $\alpha : .035$
 $\omega : 97$
 $k : .121$
 $\delta : -$
 $\sigma : 0$
 $d : .06$



PLOT 7.1-2.9A: FIRST STANDARD CONFIGURATION, CASE 9.
MAGNITUDE AND PHASE LEAD OF UNSTEADY BLADE
SURFACE PRESSURE COEFFICIENT.

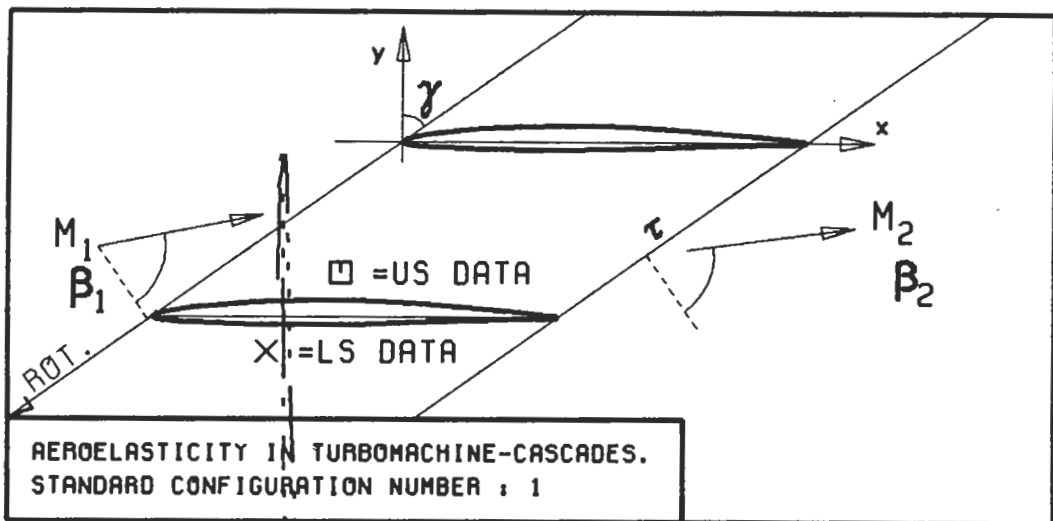
(\times : IN PITCH MODE, NOTATION VALID UPSTREAM OF PITCH AXIS)



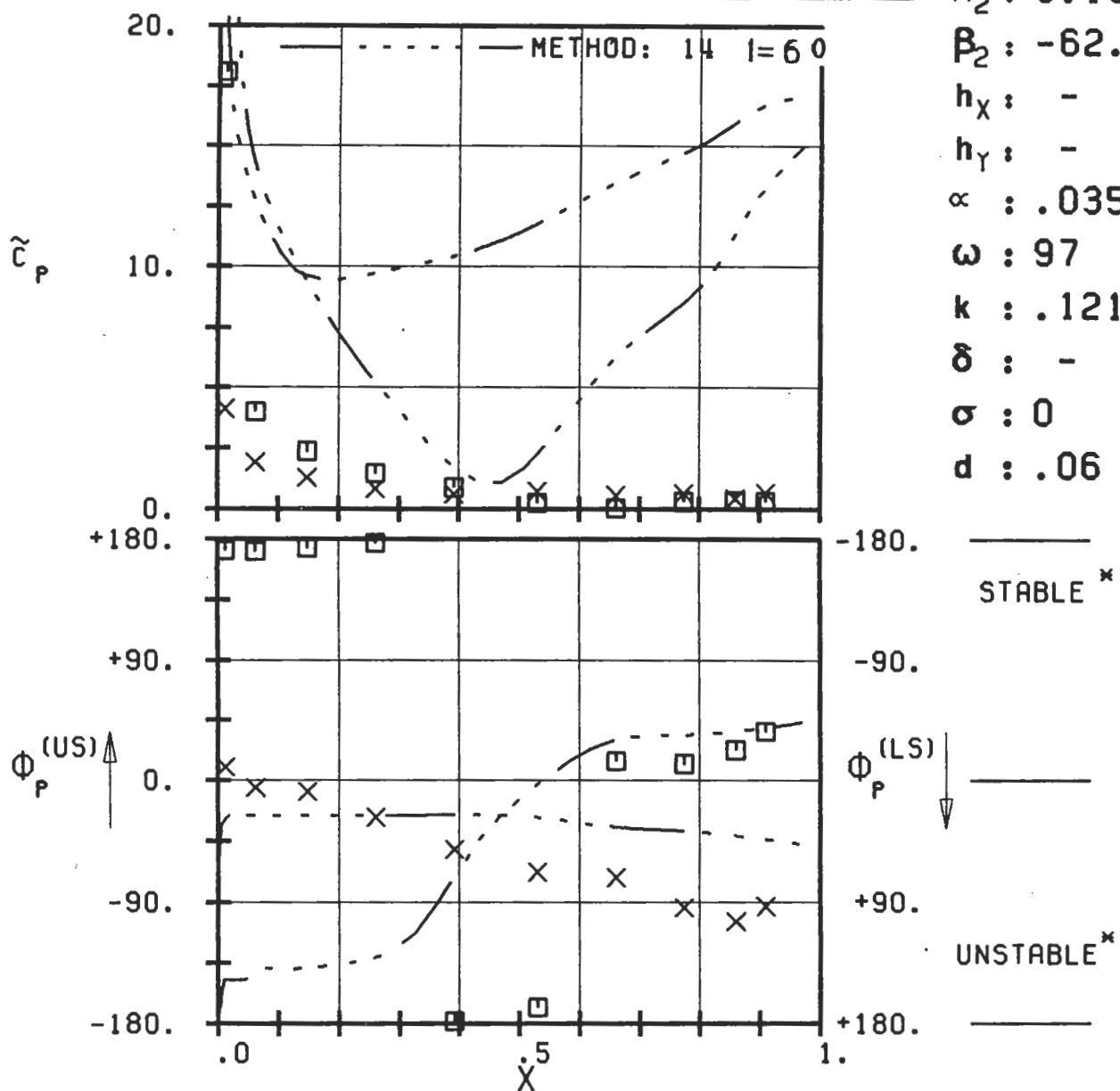
PLOT 7.1-2.9B: FIRST STANDARD CONFIGURATION, CASE 9.
MAGNITUDE AND PHASE LEAD OF UNSTEADY BLADE
SURFACE PRESSURE COEFFICIENT.

(x: IN PITCH MODE, NOTATION VALID UPSTREAM OF PITCH AXIS)

c : .152M
 τ : .75
 γ : 55.
 x_∞ : .5
 y_∞ : .0115
 M_1 : .17
 β_1 : -66.
i : 6.
 M_2 : 0.15
 β_2 : -62.5
 h_X : -
 h_Y : -
 α : .035
 ω : 97
 k : .121
 δ : -
 σ : 0
 d : .06

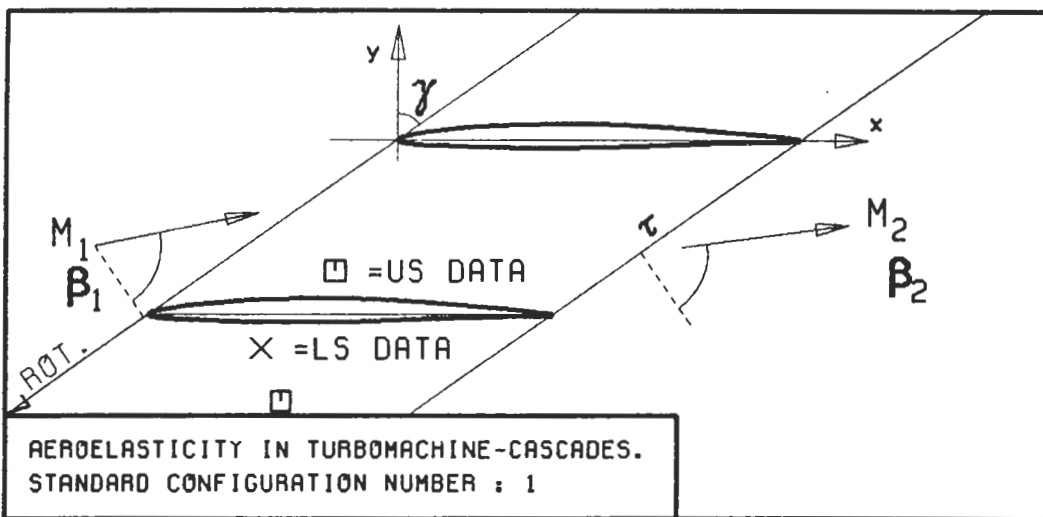


$c : .152M$
 $\tau : .75$
 $\gamma : 55.$
 $x_\alpha : .5$
 $y_\alpha : .0115$
 $M_1 : .17$
 $B_1 : -66.$
 $i : 6.$
 $M_2 : 0.15$
 $B_2 : -62.5$
 $h_x : -$
 $h_y : -$
 $\alpha : .035$
 $\omega : 97$
 $k : .121$
 $\delta : -$
 $\sigma : 0$
 $d : .06$

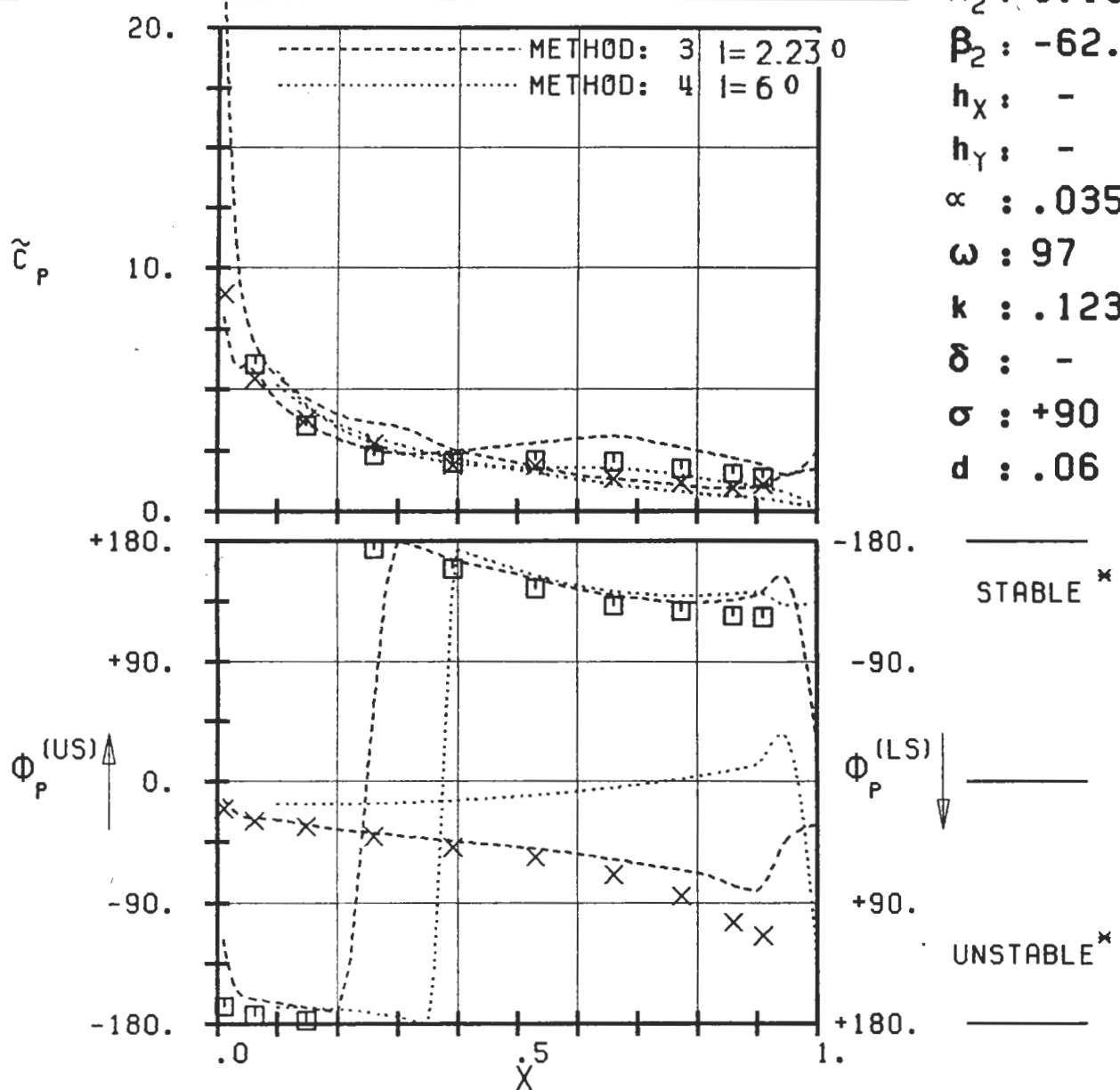


PLOT 7.1-2.9C: FIRST STANDARD CONFIGURATION, CASE 9.
MAGNITUDE AND PHASE LEAD OF UNSTEADY BLADE
SURFACE PRESSURE COEFFICIENT.

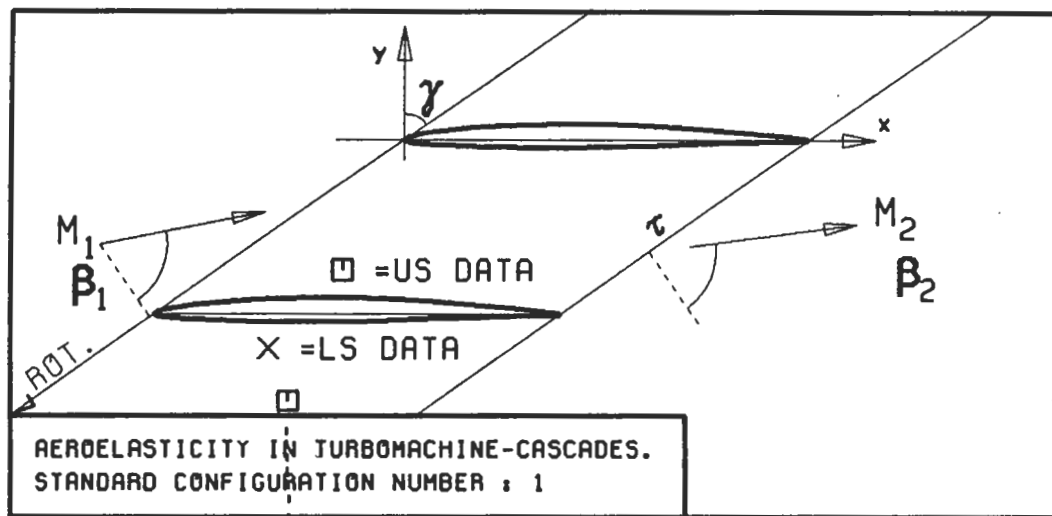
(x: IN PITCH MODE, NOTATION VALID UPSTREAM OF PITCH AXIS)



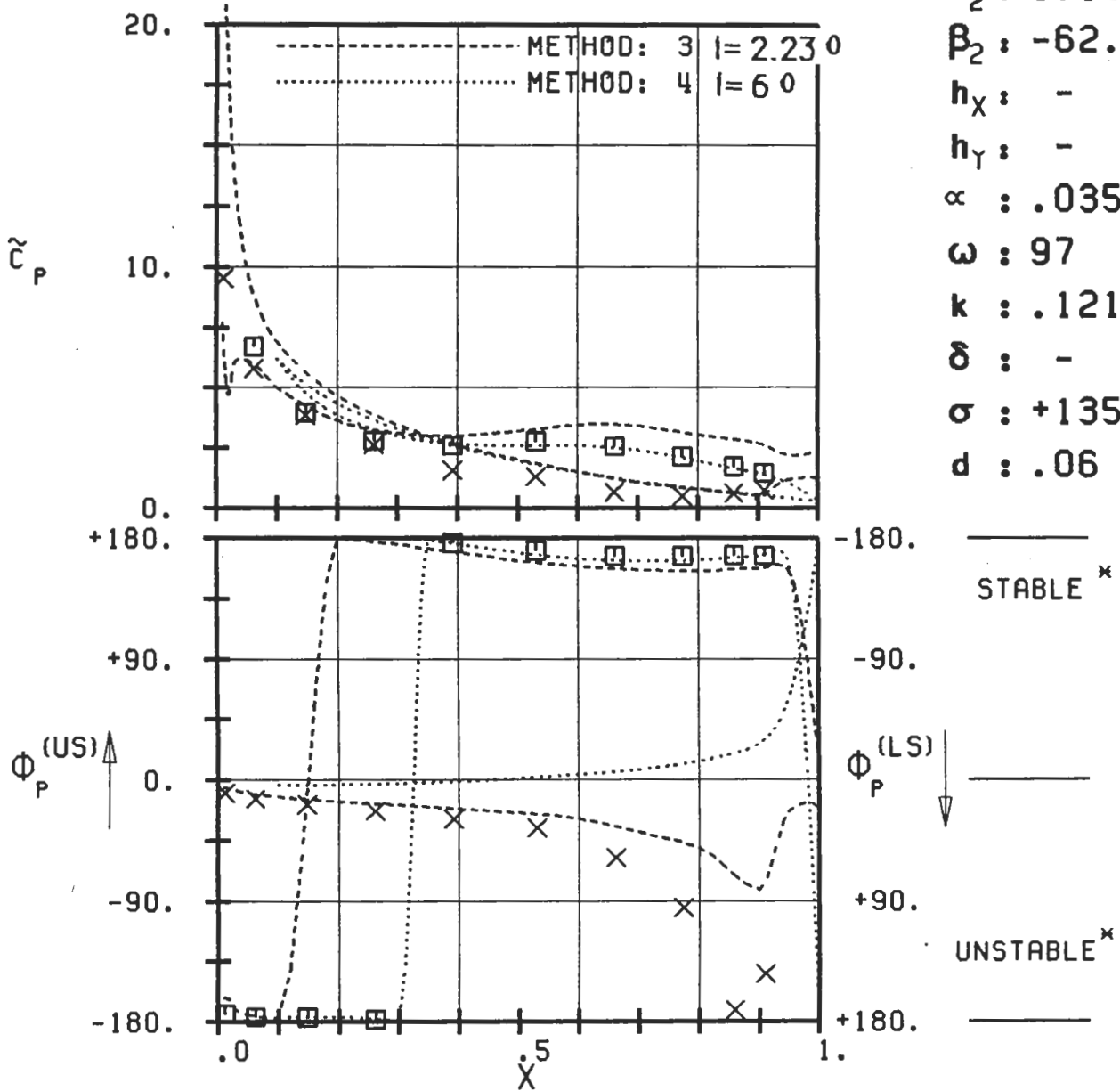
$c : .152M$
 $\tau : .75$
 $\gamma : 55.$
 $x_\infty : .5$
 $y_\infty : .0115$
 $M_1 : .17$
 $\beta_1 : -66.$
 $i : 6.$
 $M_2 : 0.15$
 $\beta_2 : -62.5$
 $h_x : -$
 $h_y : -$
 $\alpha : .035$
 $\omega : 97$
 $k : .123$
 $\delta : -$
 $\sigma : +90$
 $d : .06$



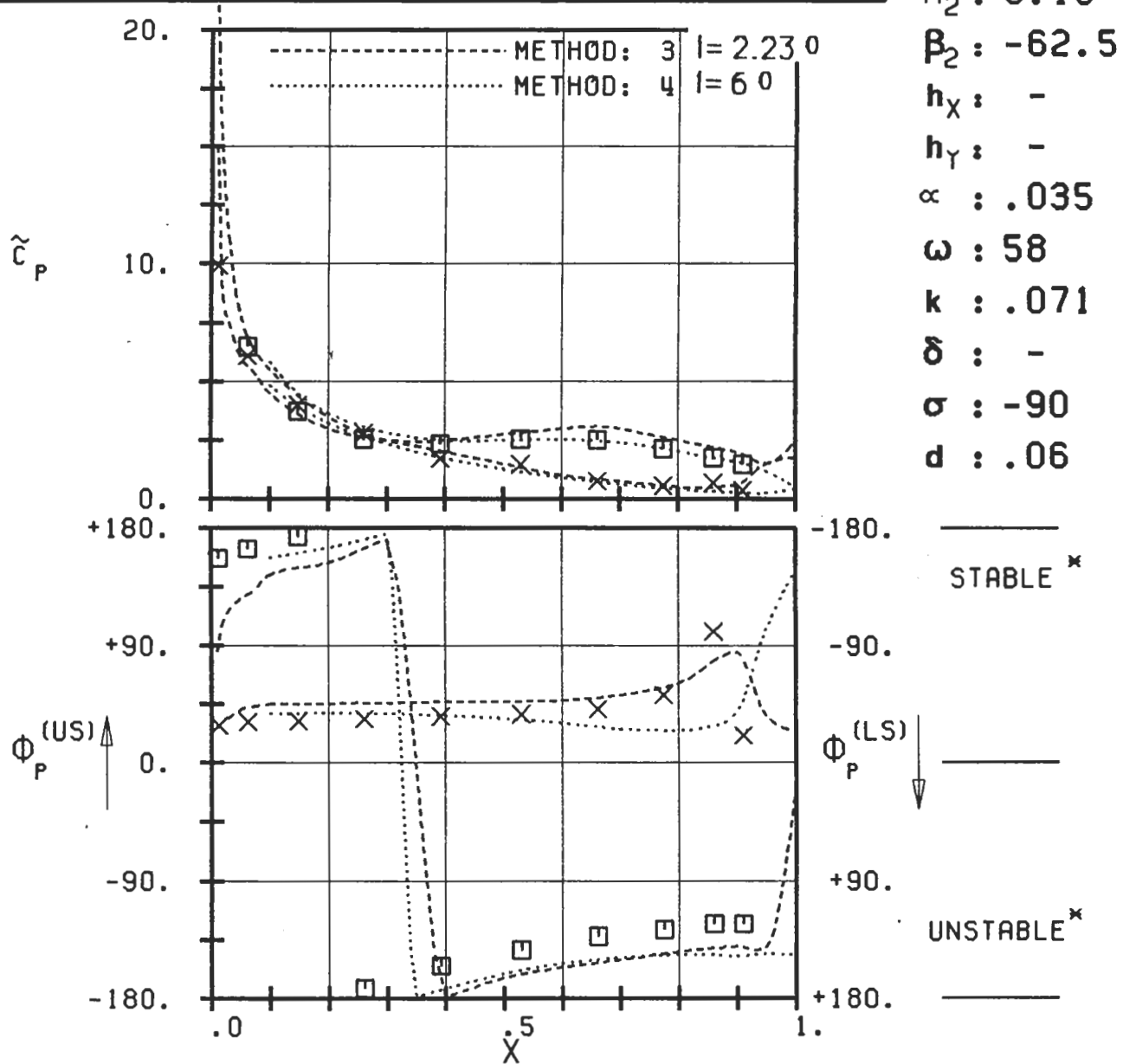
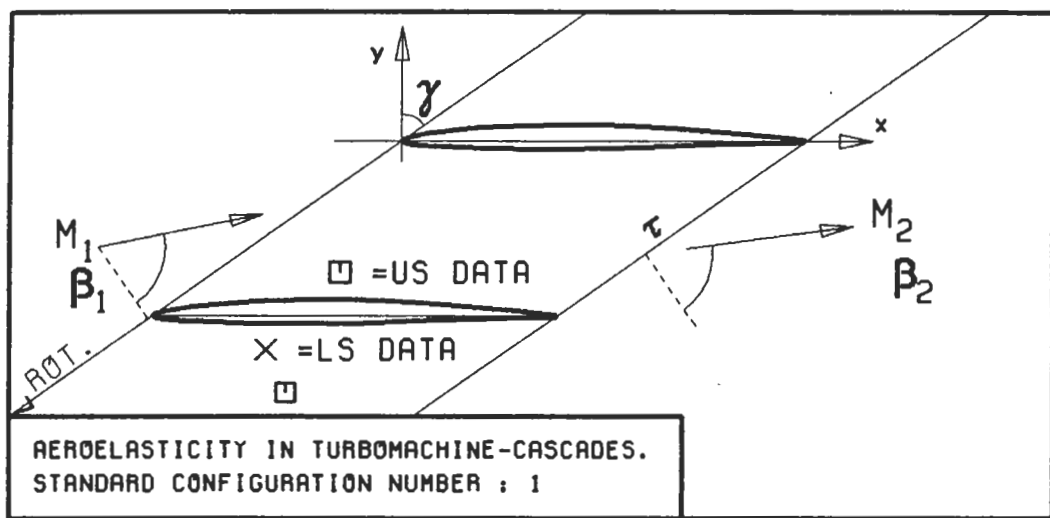
PLOT 7.1-2.10: FIRST STANDARD CONFIGURATION, CASE 10.
 MAGNITUDE AND PHASE LEAD OF UNSTEADY BLADE
 SURFACE PRESSURE COEFFICIENT.
 (*: IN PITCH MODE, NOTATION VALID UPSTREAM OF PITCH AXIS)



$c : .152M$
 $\tau : .75$
 $\gamma : 55.$
 $x_\infty : .5$
 $y_\infty : .0115$
 $M_1 : .17$
 $\beta_1 : -66.$
 $i : 6.$
 $M_2 : 0.15$
 $\beta_2 : -62.5$
 $h_x : -$
 $h_y : -$
 $\alpha : .035$
 $\omega : 97$
 $k : .121$
 $\delta : -$
 $\sigma : +135$
 $d : .06$

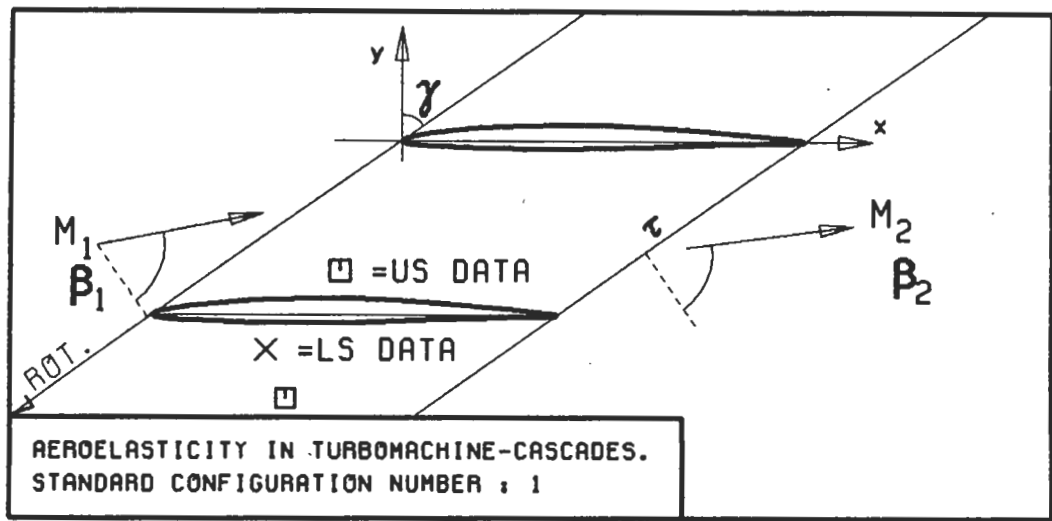


PLOT 7.1-2.11: FIRST STANDARD CONFIGURATION, CASE 11.
MAGNITUDE AND PHASE LEAD OF UNSTEADY BLADE
SURFACE PRESSURE COEFFICIENT.
(\times : IN PITCH MODE, NOTATION VALID UPSTREAM OF PITCH AXIS)

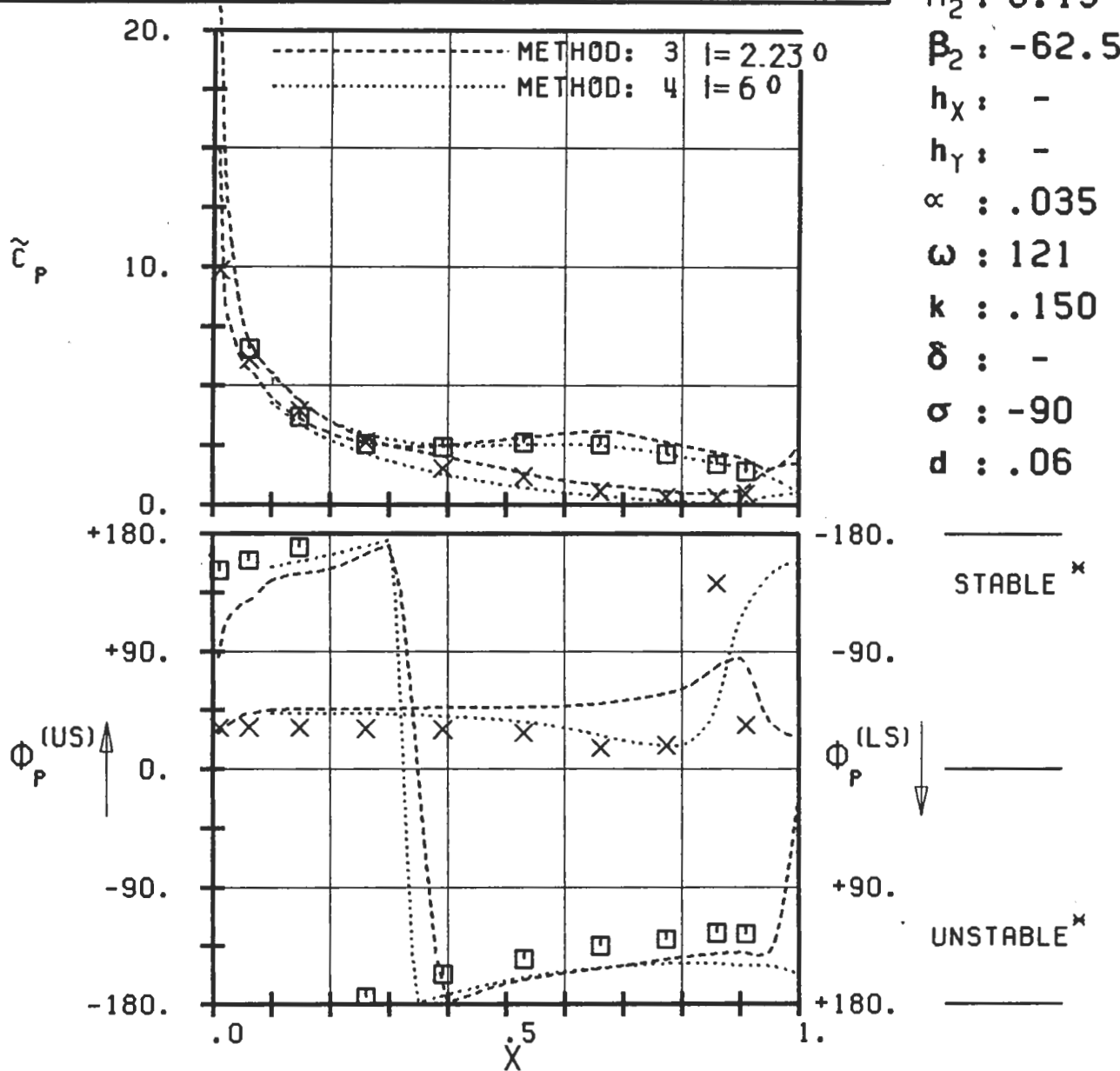


PLOT 7.1-2.12: FIRST STANDARD CONFIGURATION, CASE 12.
MAGNITUDE AND PHASE LEAD OF UNSTEADY BLADE
SURFACE PRESSURE COEFFICIENT.
(\times : IN PITCH MODE, NOTATION VALID UPSTREAM OF PITCH AXIS)

$c : .152M$
 $\tau : .75$
 $\gamma : 55.$
 $x_\alpha : .5$
 $y_\alpha : .0115$
 $M_1 : .17$
 $\beta_1 : -66.$
 $i : 6.$
 $M_2 : 0.15$
 $\beta_2 : -62.5$
 $h_X : -$
 $h_Y : -$
 $\alpha : .035$
 $\omega : 58$
 $k : .071$
 $\delta : -$
 $\sigma : -90$
 $d : .06$

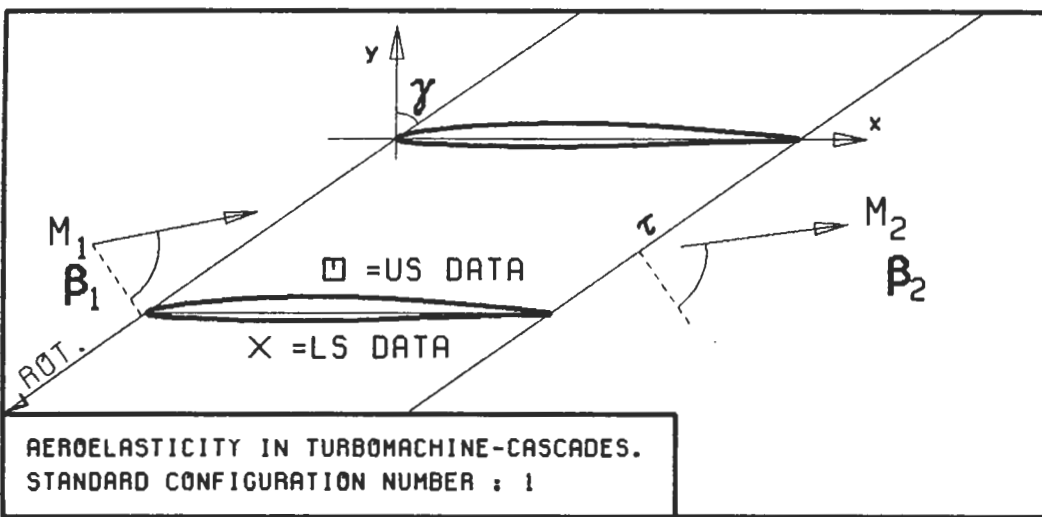


$c : .152M$
 $\tau : .75$
 $\gamma : 55.$
 $x_\alpha : .5$
 $y_\alpha : .0115$
 $M_1 : .17$
 $\beta_1 : -66.$
 $i : 6.$
 $M_2 : 0.15$
 $\beta_2 : -62.5$
 $h_X : -$
 $h_Y : -$
 $\alpha : .035$
 $\omega : 121$
 $k : .150$
 $\delta : -$
 $\sigma : -90$
 $d : .06$

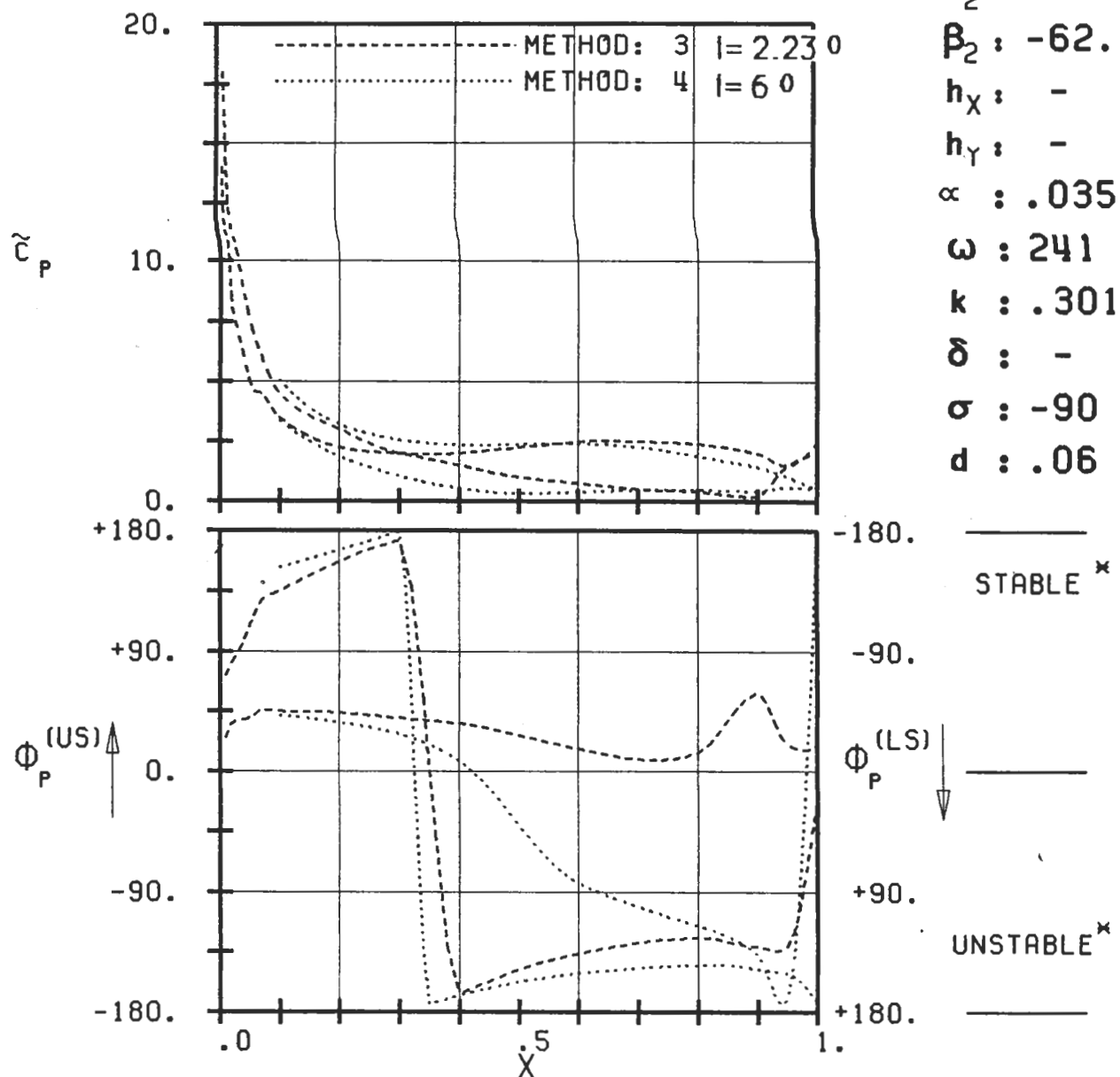


PLOT 7.1-2.13: FIRST STANDARD CONFIGURATION, CASE 13.
MAGNITUDE AND PHASE LEAD OF UNSTEADY BLADE SURFACE PRESSURE COEFFICIENT.

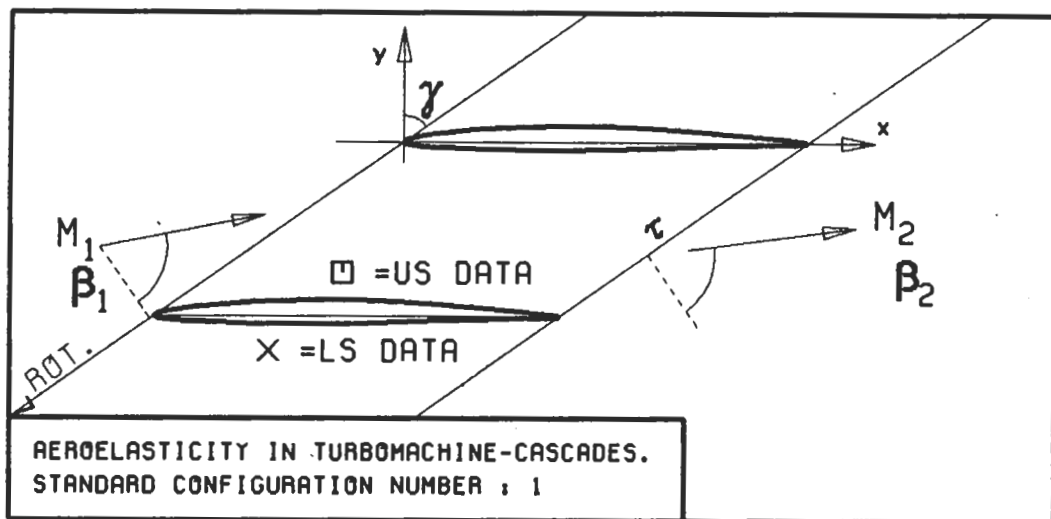
(\times : IN PITCH MODE, NOTATION VALID UPSTREAM OF PITCH AXIS)



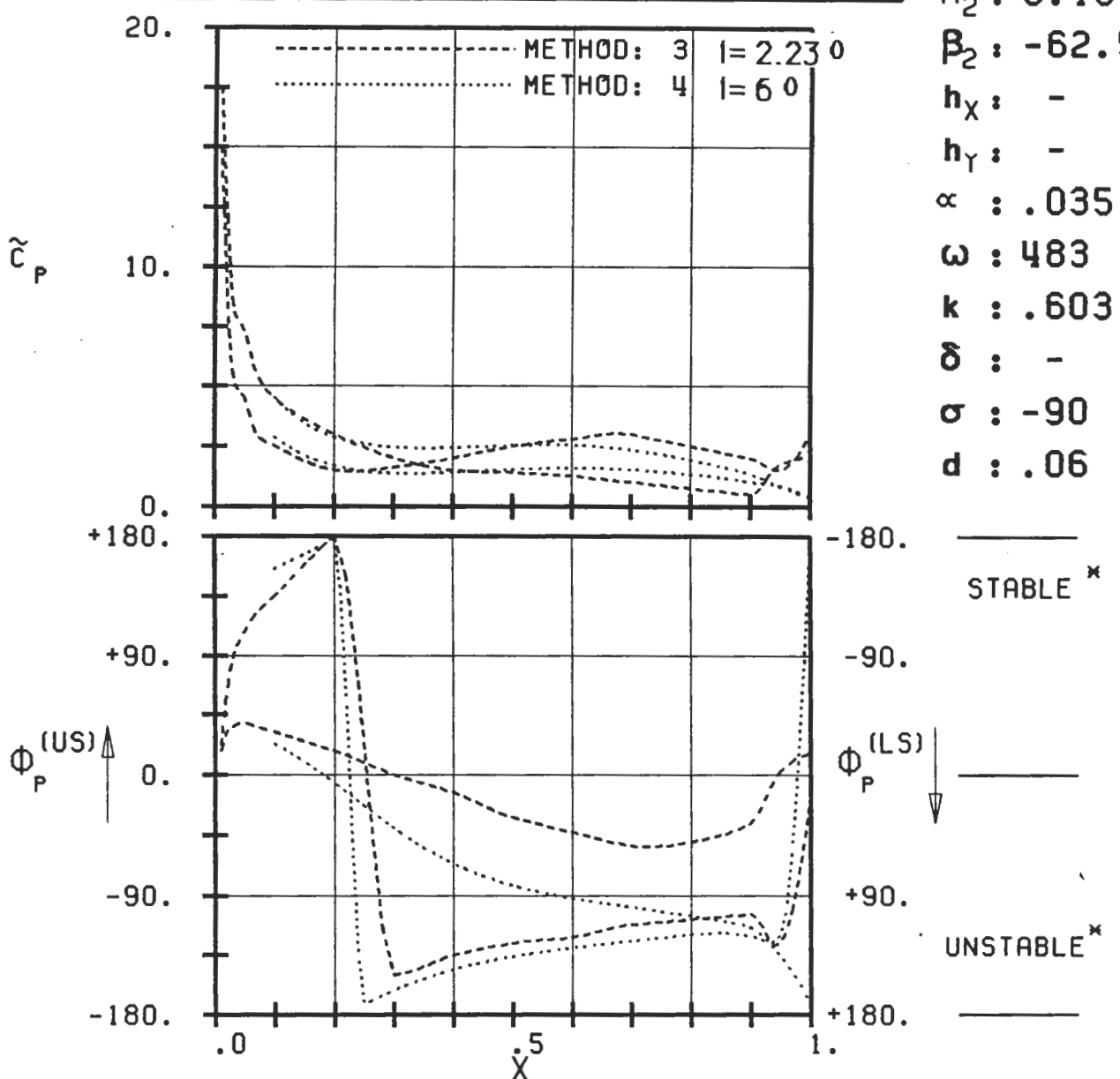
$c \dots .152M$
 $\tau \dots .75$
 $\gamma \dots 55.$
 $x_\alpha \dots .5$
 $y_\alpha \dots .0115$
 $M_1 \dots .17$
 $\beta_1 \dots -66.$
 $i \dots 6.$
 $M_2 \dots 0.15$
 $\beta_2 \dots -62.5$
 $h_x \dots -$
 $h_y \dots -$
 $\alpha \dots .035$
 $\omega \dots 241$
 $k \dots .301$
 $\delta \dots -$
 $\sigma \dots -90$
 $d \dots .06$



PLOT 7.1-2.14: FIRST STANDARD CONFIGURATION, CASE 14.
 MAGNITUDE AND PHASE LEAD OF UNSTEADY BLADE
 SURFACE PRESSURE COEFFICIENT.
 (*: IN PITCH MODE, NOTATION VALID UPSTREAM OF PITCH AXIS)

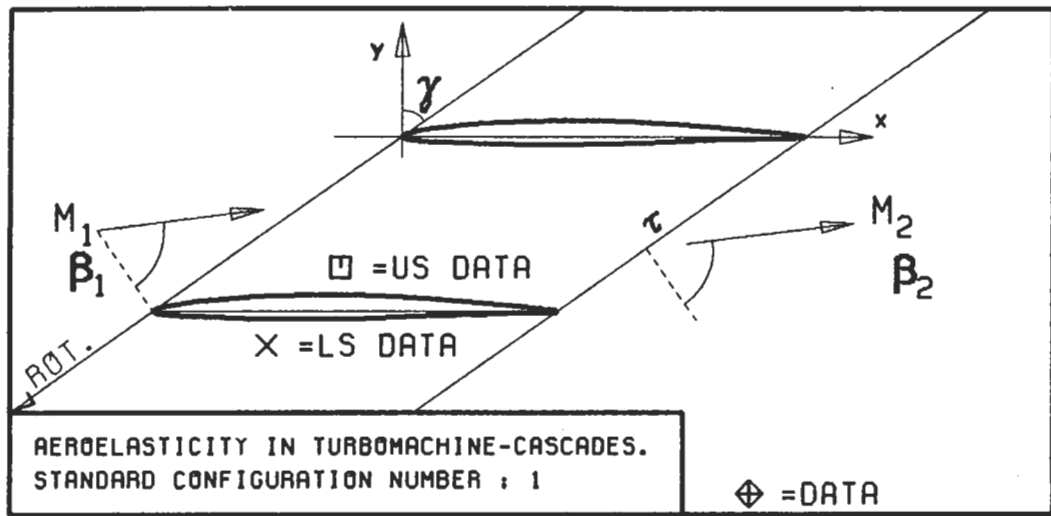


$c : .152M$
 $\tau : .75$
 $\gamma : 55.$
 $x_\infty : .5$
 $y_\infty : .0115$
 $M_1 : .17$
 $\beta_1 : -66.$
 $i : 6.$
 $M_2 : 0.15$
 $\beta_2 : -62.5$
 $h_x : -$
 $h_y : -$
 $\alpha : .035$
 $\omega : 483$
 $k : .603$
 $\delta : -$
 $\sigma : -90$
 $d : .06$

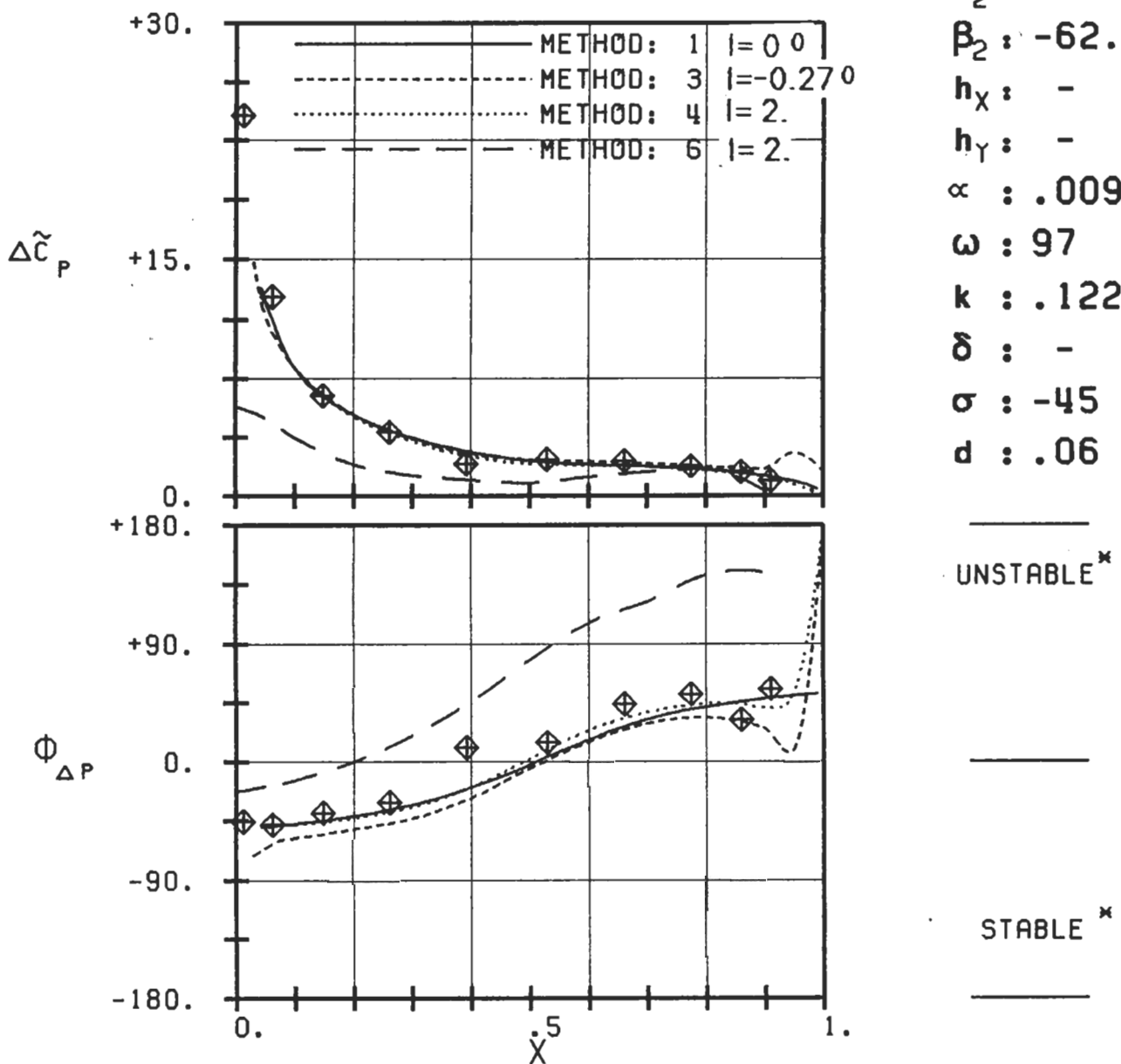


PLOT 7.1-2.15: FIRST STANDARD CONFIGURATION, CASE 15.
MAGNITUDE AND PHASE LEAD OF UNSTEADY BLADE SURFACE PRESSURE COEFFICIENT.

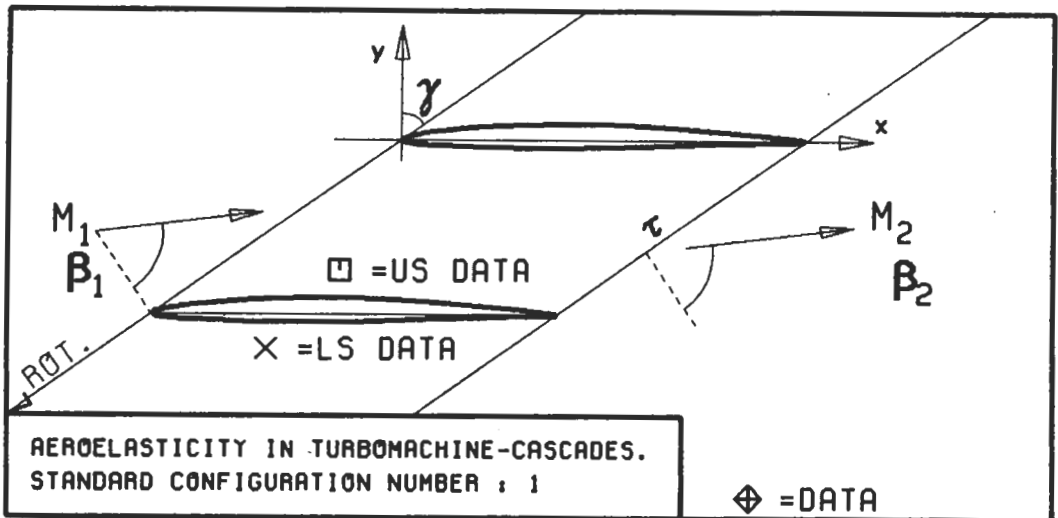
(*: IN PITCH MODE, NOTATION VALID UPSTREAM OF PITCH AXIS)



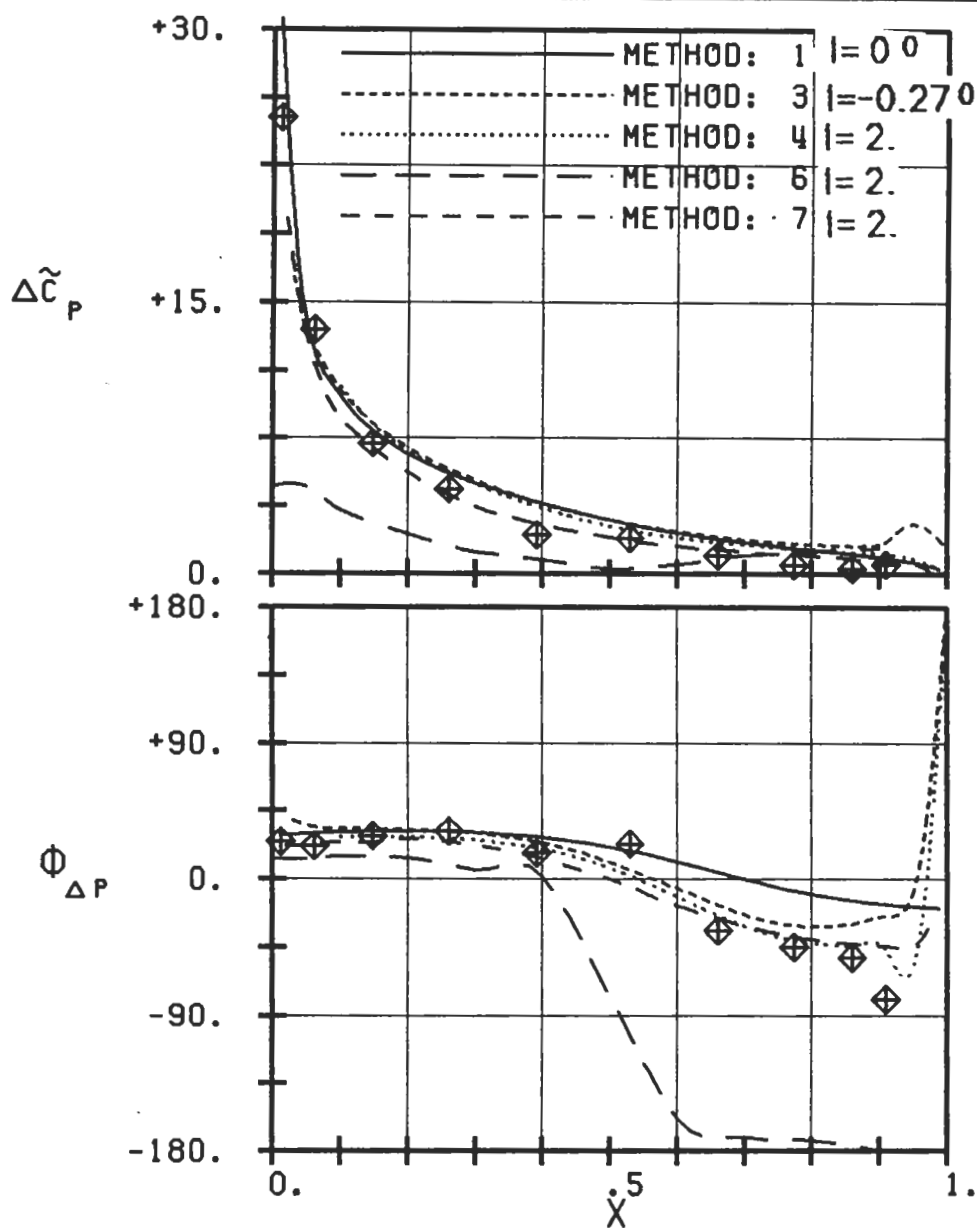
$c : .152M$
 $\tau : .75$
 $\gamma : 55.$
 $x_\alpha : .5$
 $y_\alpha : .0115$
 $M_1 : .18$
 $\beta_1 : -62.$
 $i : 2.$
 $M_2 : 0.16$
 $\beta_2 : -62.$
 $h_x : -$
 $h_y : -$
 $\alpha : .009$
 $\omega : 97$
 $k : .122$
 $\delta : -$
 $\sigma : -45$
 $d : .06$



PLOT 7.1-3.1: FIRST STANDARD CONFIGURATION, CASE 1.
MAGNITUDE AND PHASE LEAD OF UNSTEADY
SURFACE PRESSURE DIFFERENCE COEFFICIENT.
(*: IN PITCH MODE, NOTATION VALID UPSTREAM OF PITCH AXIS)

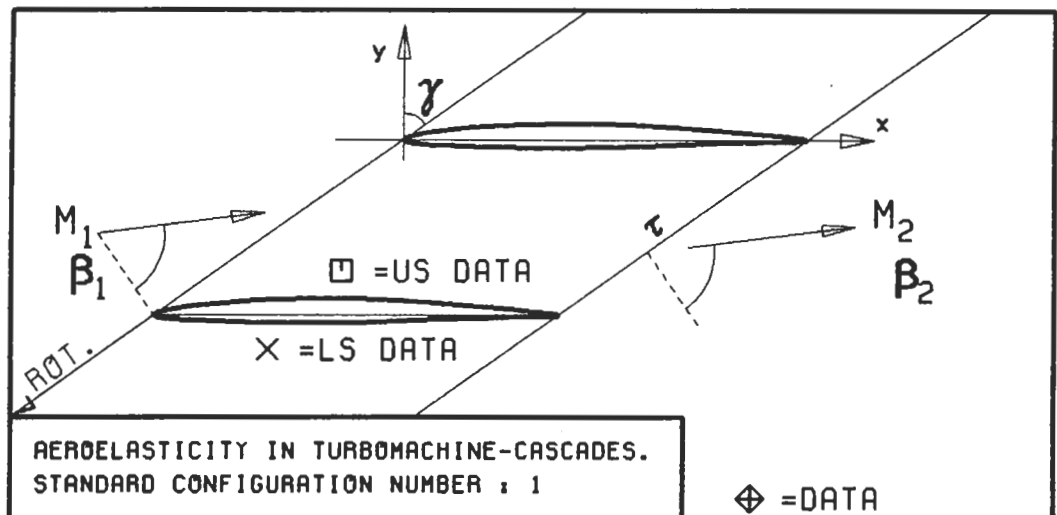


$c : .152M$
 $\tau : .75$
 $\gamma : 55.$
 $x_\alpha : .5$
 $y_\alpha : .0115$
 $M_1 : .18$
 $\beta_1 : -62.$
 $i : 2.$
 $M_2 : 0.16$
 $\beta_2 : -62.$
 $h_X : -$
 $h_Y : -$
 $\alpha : .009$
 $\omega : 97$
 $k : .122$
 $\delta : -$
 $\sigma : +45$
 $d : .06$

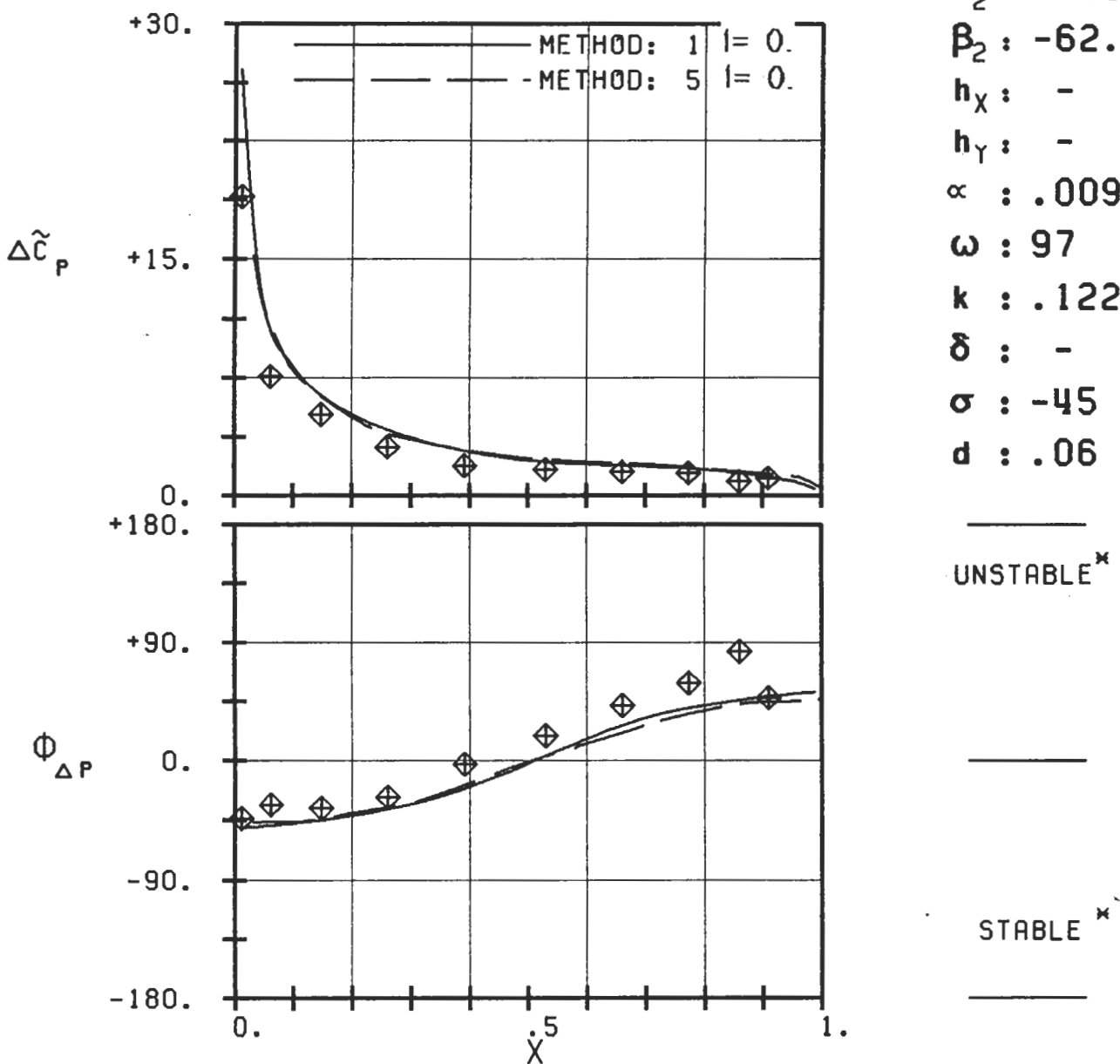


PLOT 7.1-3.2: FIRST STANDARD CONFIGURATION, CASE 2.
MAGNITUDE AND PHASE LEAD OF UNSTEADY
SURFACE PRESSURE DIFFERENCE COEFFICIENT

(x: IN PITCH MODE, NOTATION VALID UPSTREAM OF PITCH AXIS)

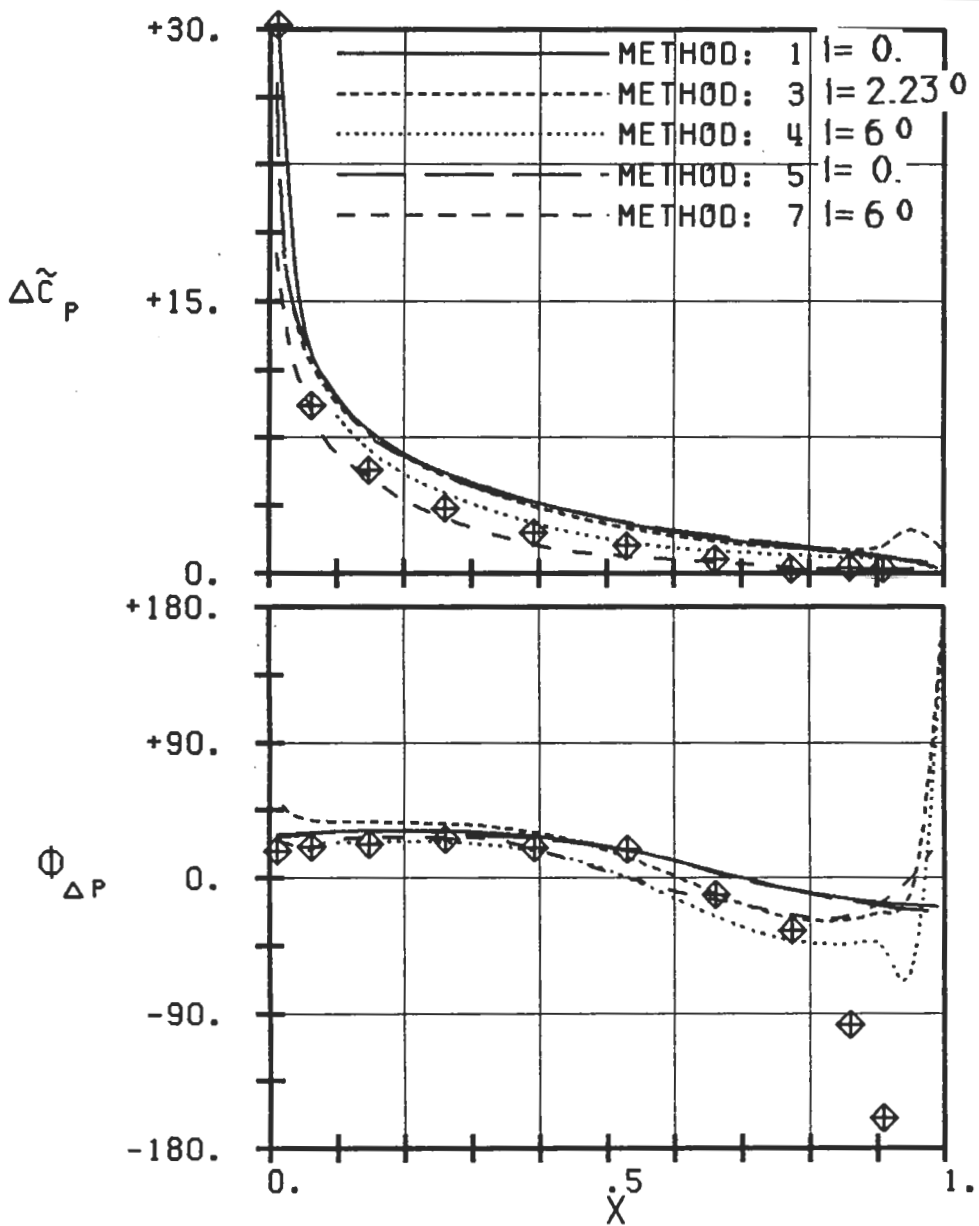
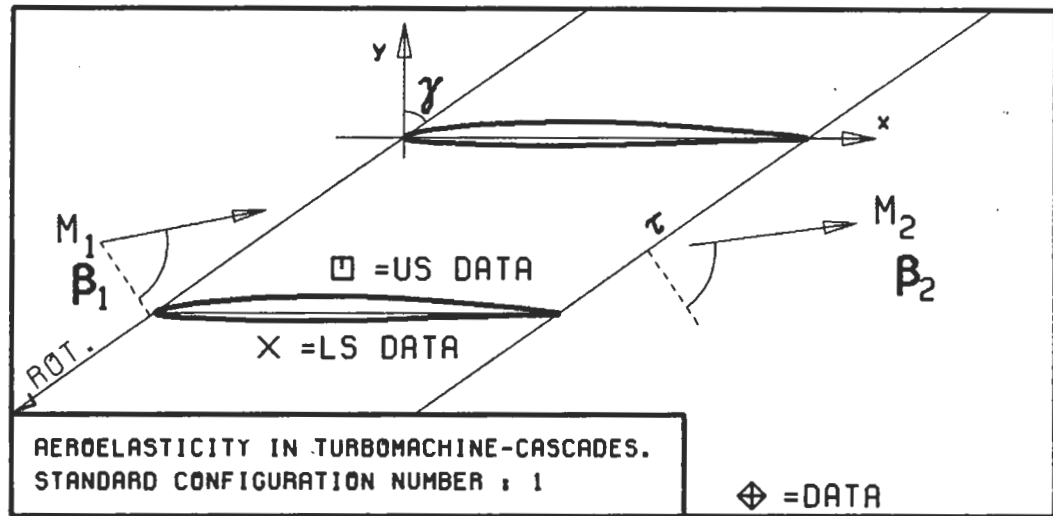


$c : .152M$
 $\tau : .75$
 $\gamma : 55.$
 $x_{\infty} : .5$
 $y_{\infty} : .0115$
 $M_1 : .18$
 $B_1 : -62.$
 $i : 2.$
 $M_2 : 0.16$
 $B_2 : -62.$
 $h_X : -$
 $h_Y : -$
 $\alpha : .009$
 $\omega : 97$
 $k : .122$
 $\delta : -$
 $\sigma : -45$
 $d : .06$



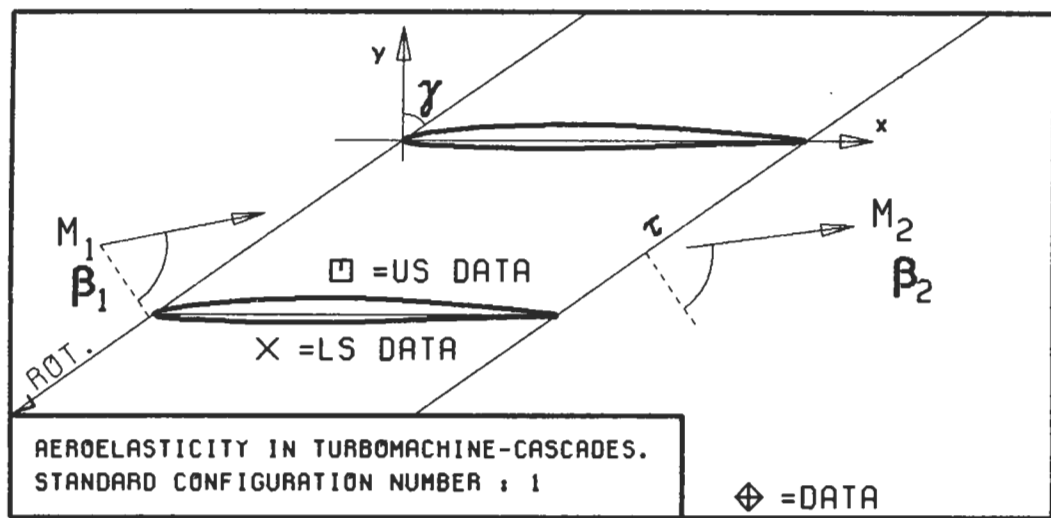
PLOT 7.1-3.3: FIRST STANDARD CONFIGURATION, CASE 3.
MAGNITUDE AND PHASE LEAD OF UNSTEADY
SURFACE PRESSURE DIFFERENCE COEFFICIENT.

(X: IN PITCH MODE, NOTATION VALID UPSTREAM OF PITCH AXIS)

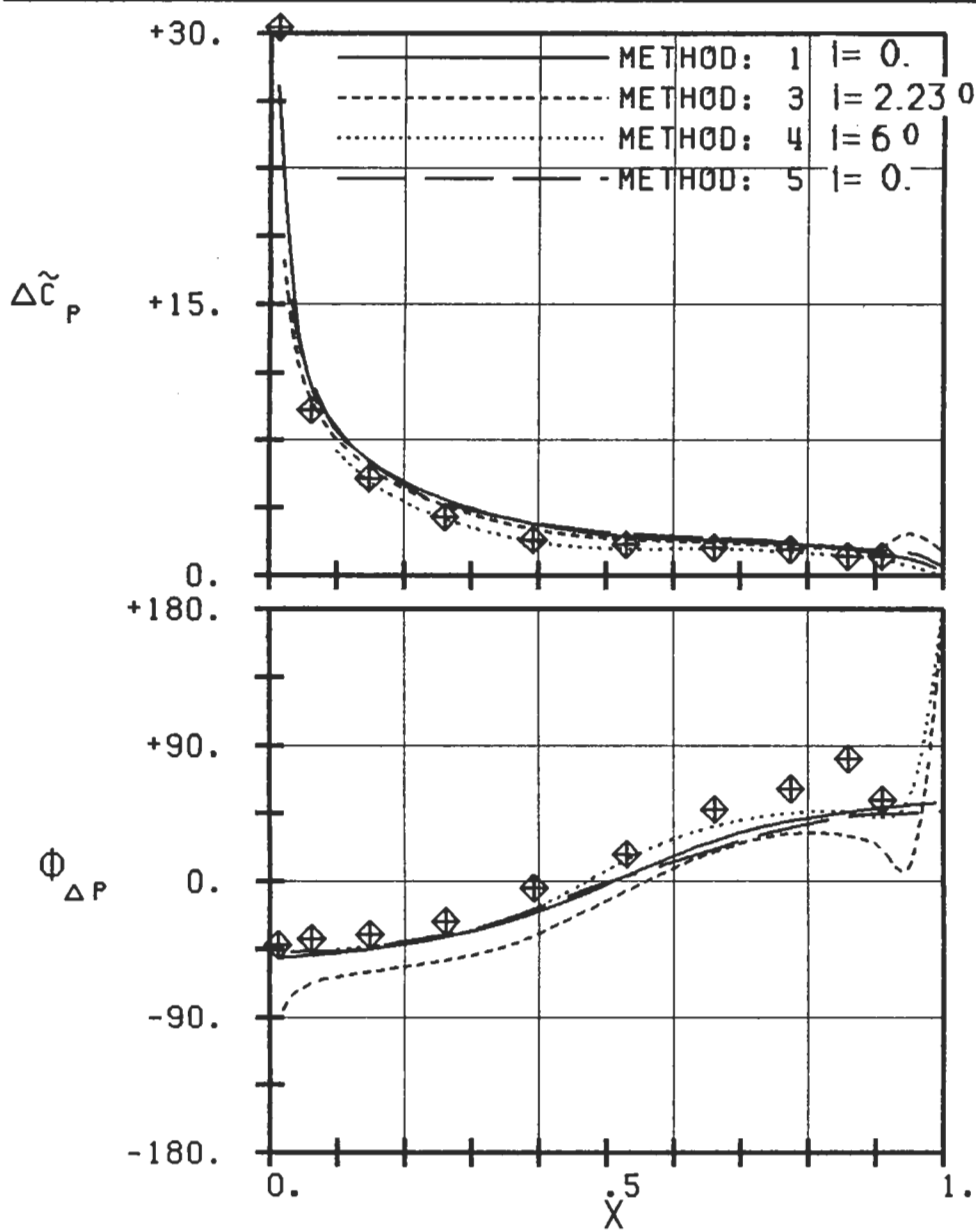


PLOT 7.1-3.4: FIRST STANDARD CONFIGURATION, CASE 4.
 MAGNITUDE AND PHASE LEAD OF UNSTEADY
 SURFACE PRESSURE DIFFERENCE COEFFICIENT.

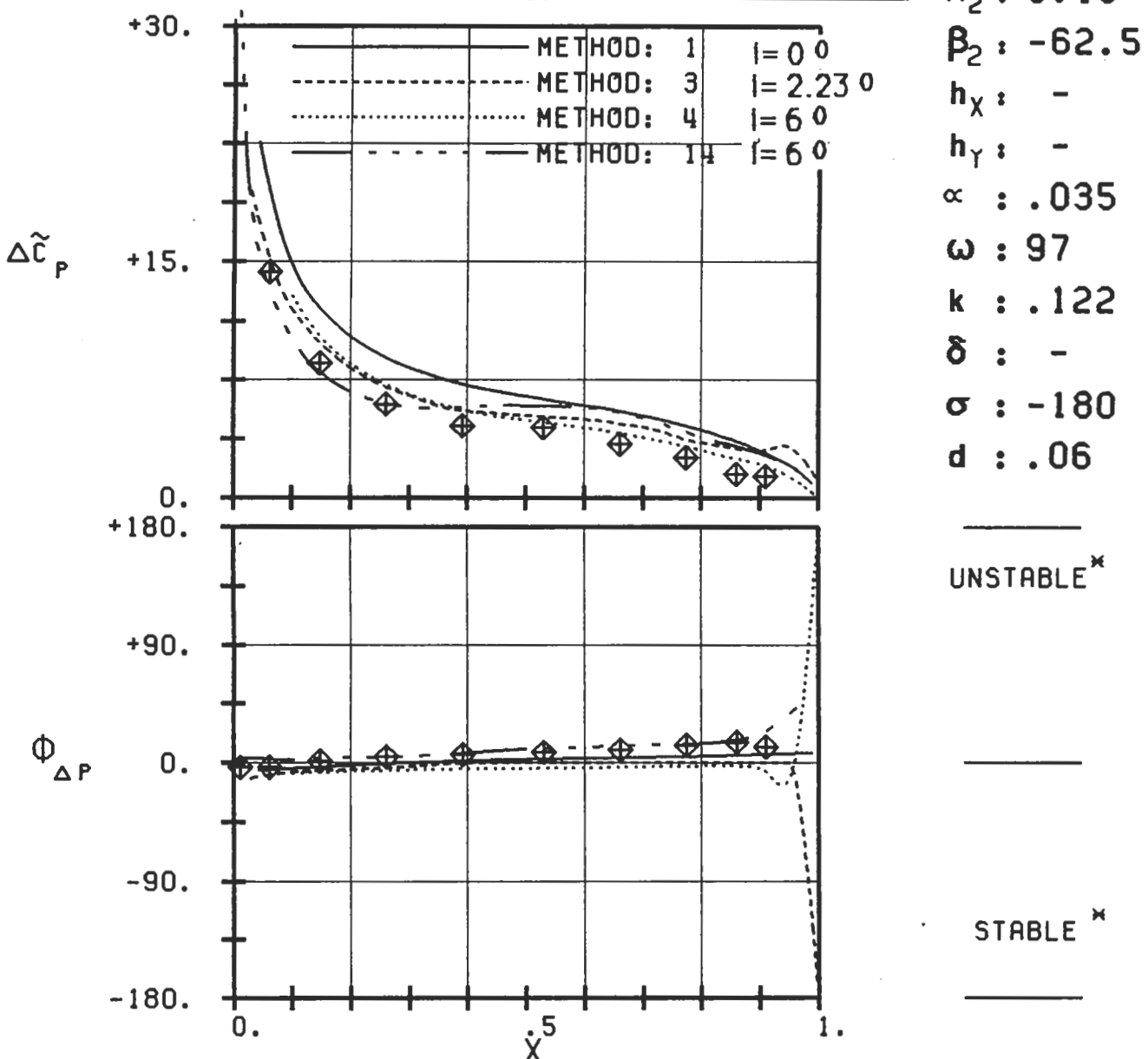
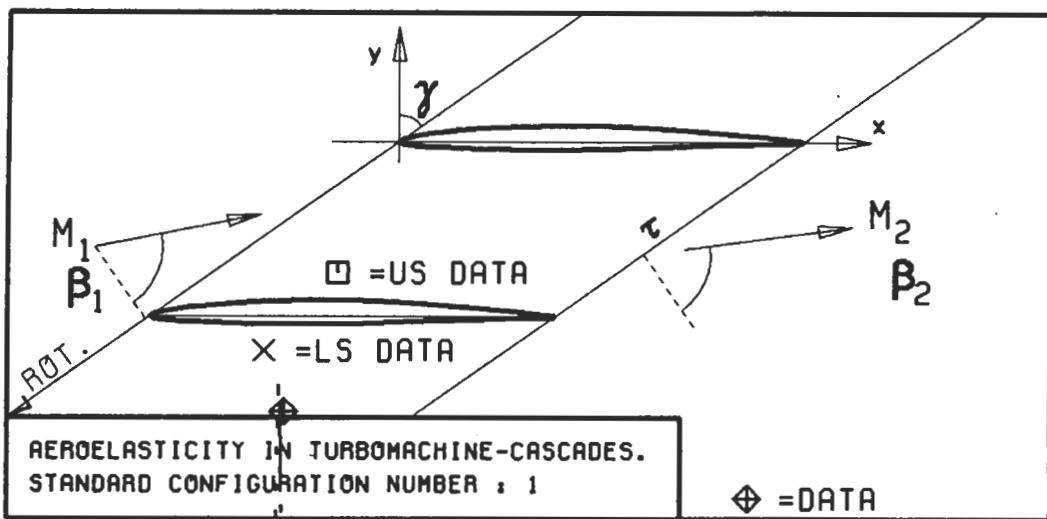
(\times : IN PITCH MODE, NOTATION VALID UPSTREAM OF PITCH AXIS)



$c : .152M$
 $\tau : .75$
 $\gamma : 55.$
 $x_\infty : .5$
 $y_\infty : .0115$
 $M_1 : .18$
 $\beta_1 : -66.$
 $i : 6.$
 $M_2 : 0.15$
 $\beta_2 : -62.5$
 $h_X : -$
 $h_Y : -$
 $\alpha : .035$
 $\omega : 97$
 $k : .122$
 $\delta : -$
 $\sigma : -45$
 $d : .06$



PLOT 7.1-3.5: FIRST STANDARD CONFIGURATION, CASE 5.
MAGNITUDE AND PHASE LEAD OF UNSTEADY
SURFACE PRESSURE DIFFERENCE COEFFICIENT.
(\times : IN PITCH MODE, NOTATION VALID UPSTREAM OF PITCH AXIS)

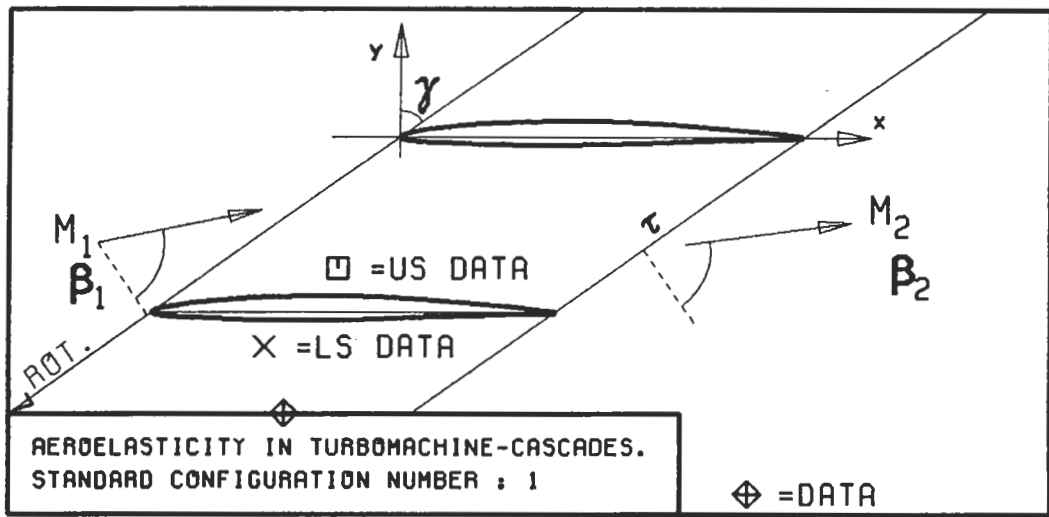


PLOT 7.1-3.6: FIRST STANDARD CONFIGURATION, CASE 6.

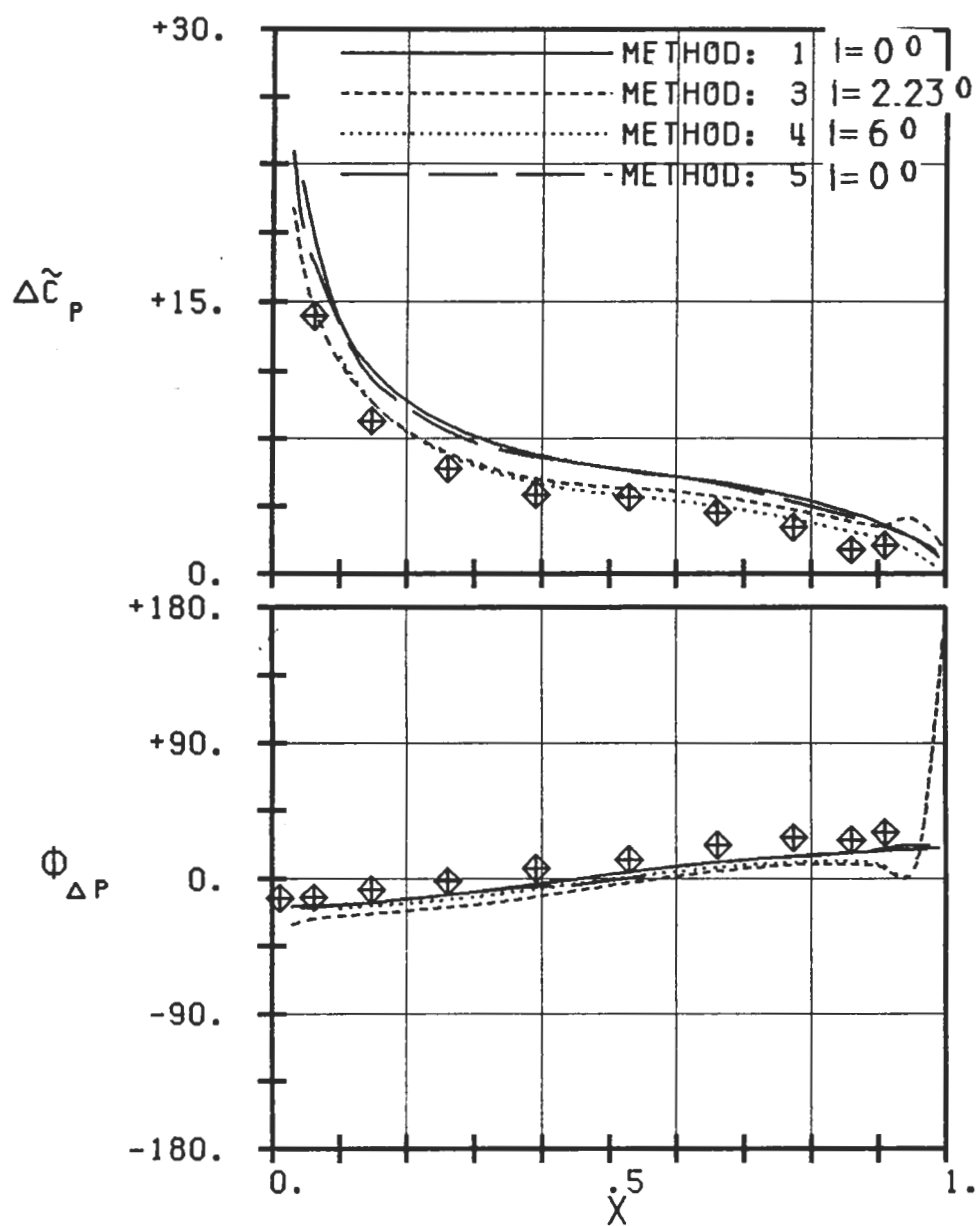
MAGNITUDE AND PHASE LEAD OF UNSTEADY
SURFACE PRESSURE DIFFERENCE COEFFICIENT.

(\times : IN PITCH MODE, NOTATION VALID UPSTREAM OF PITCH AXIS)

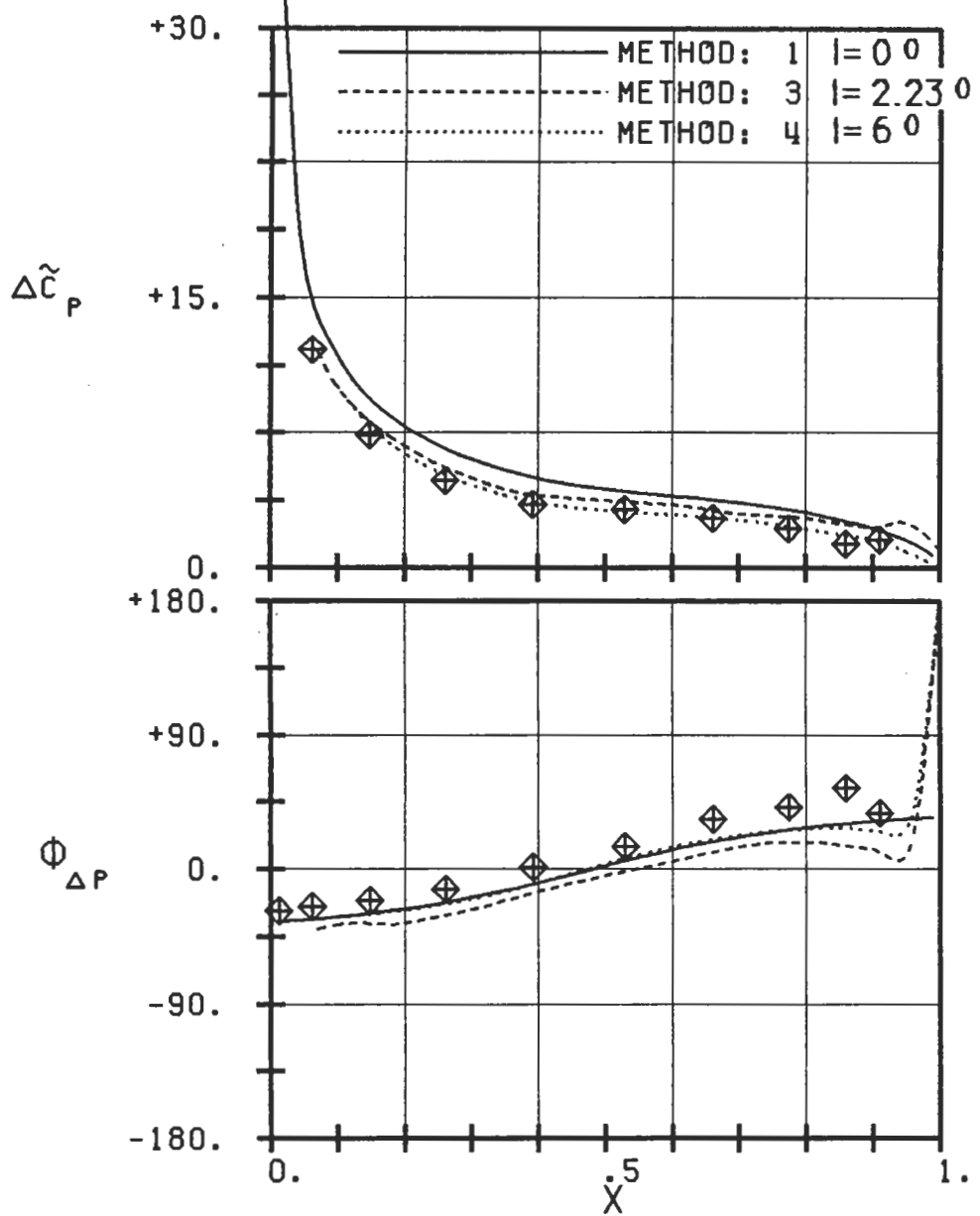
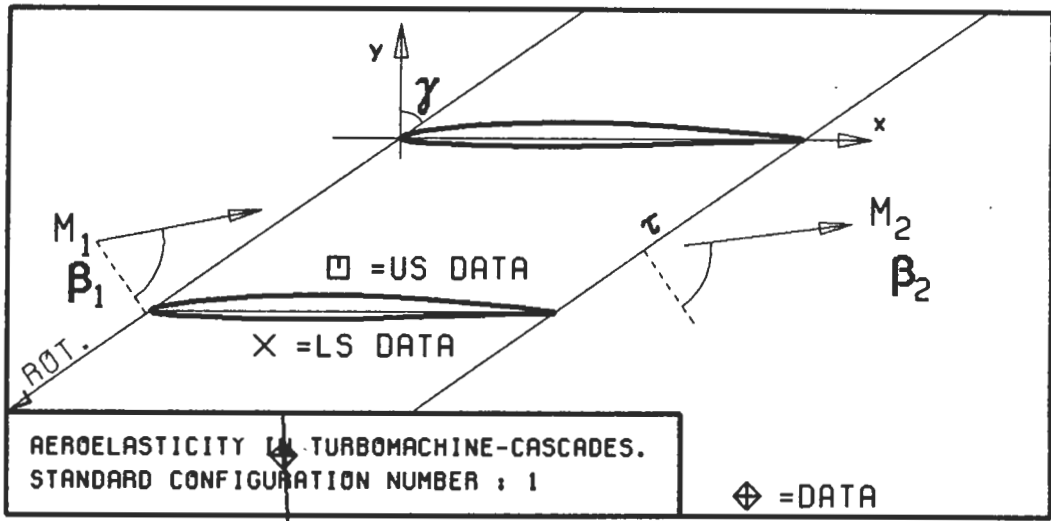
c : .152M
 τ : .75
 γ : 55.
 x_α : .5
 y_α : .0115
 M_1 : .18
 B_1 : -66.
i : 6.
 M_2 : 0.15
 B_2 : -62.5
 h_X : -
 h_Y : -
 α : .035
 ω : 97
k : .122
 δ : -
 σ : -180
d : .06



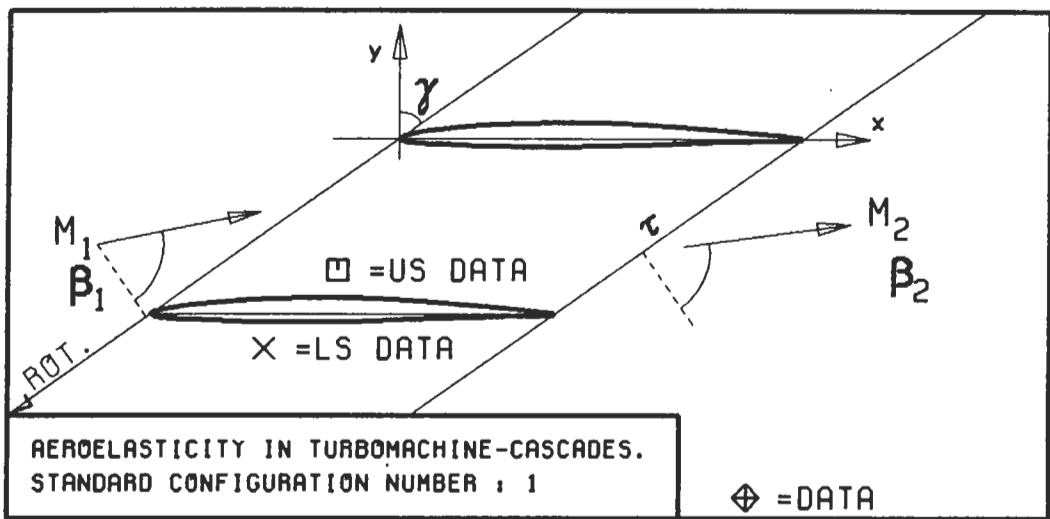
$c : .152M$
 $\tau : .75$
 $\gamma : 55.$
 $x_\infty : .5$
 $y_\infty : .0115$
 $M_1 : .18$
 $\beta_1 : -66.$
 $i : 6.$
 $M_2 : 0.15$
 $\beta_2 : -62.5$
 $h_X : -$
 $h_Y : -$
 $\alpha : .035$
 $\omega : 97$
 $k : .122$
 $\delta : -$
 $\sigma : -135$
 $d : .06$



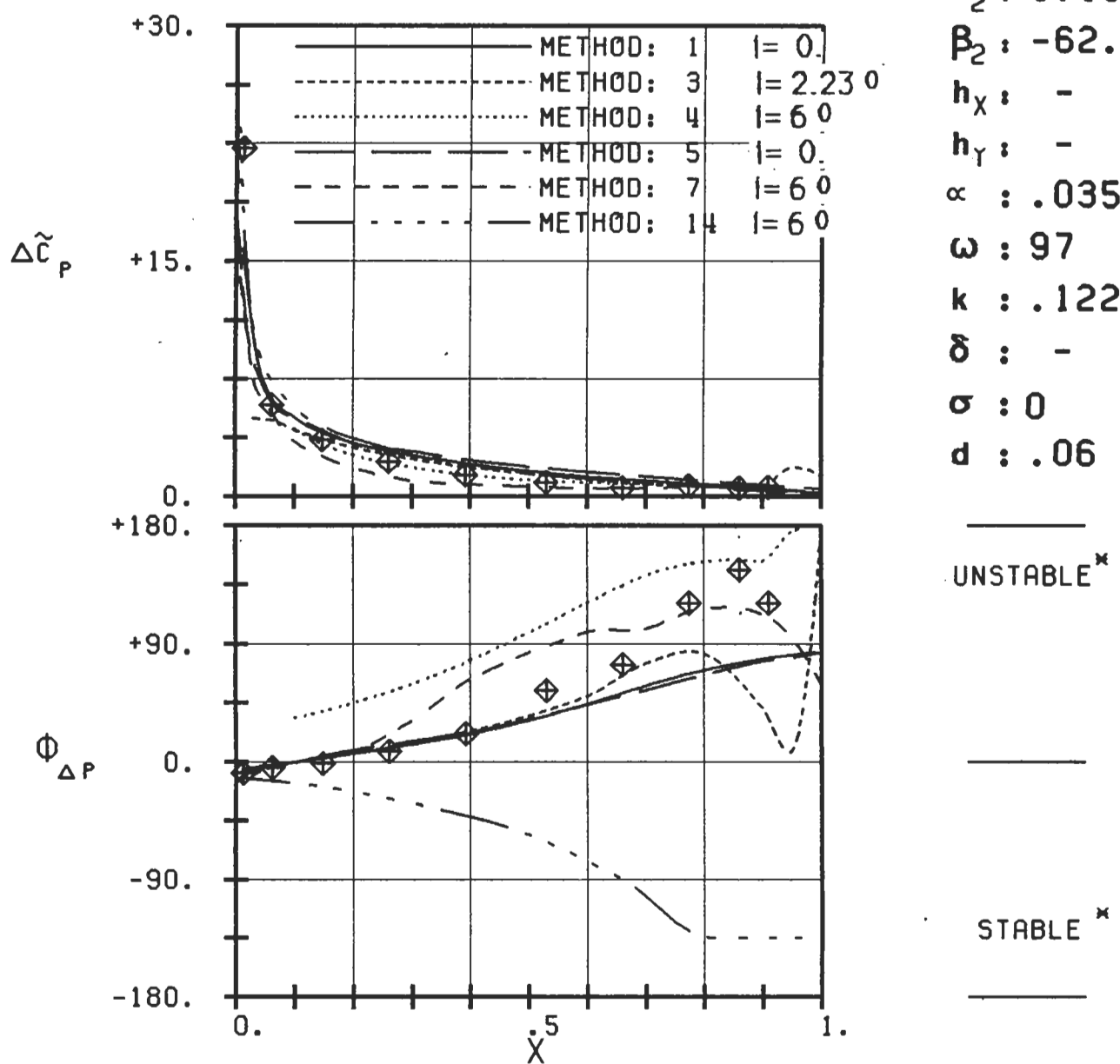
PLOT 7.1-3.7: FIRST STANDARD CONFIGURATION, CASE 7.
 MAGNITUDE AND PHASE LEAD OF UNSTEADY
 SURFACE PRESSURE DIFFERENCE COEFFICIENT.
 (\times : IN PITCH MODE, NOTATION VALID UPSTREAM OF PITCH AXIS)



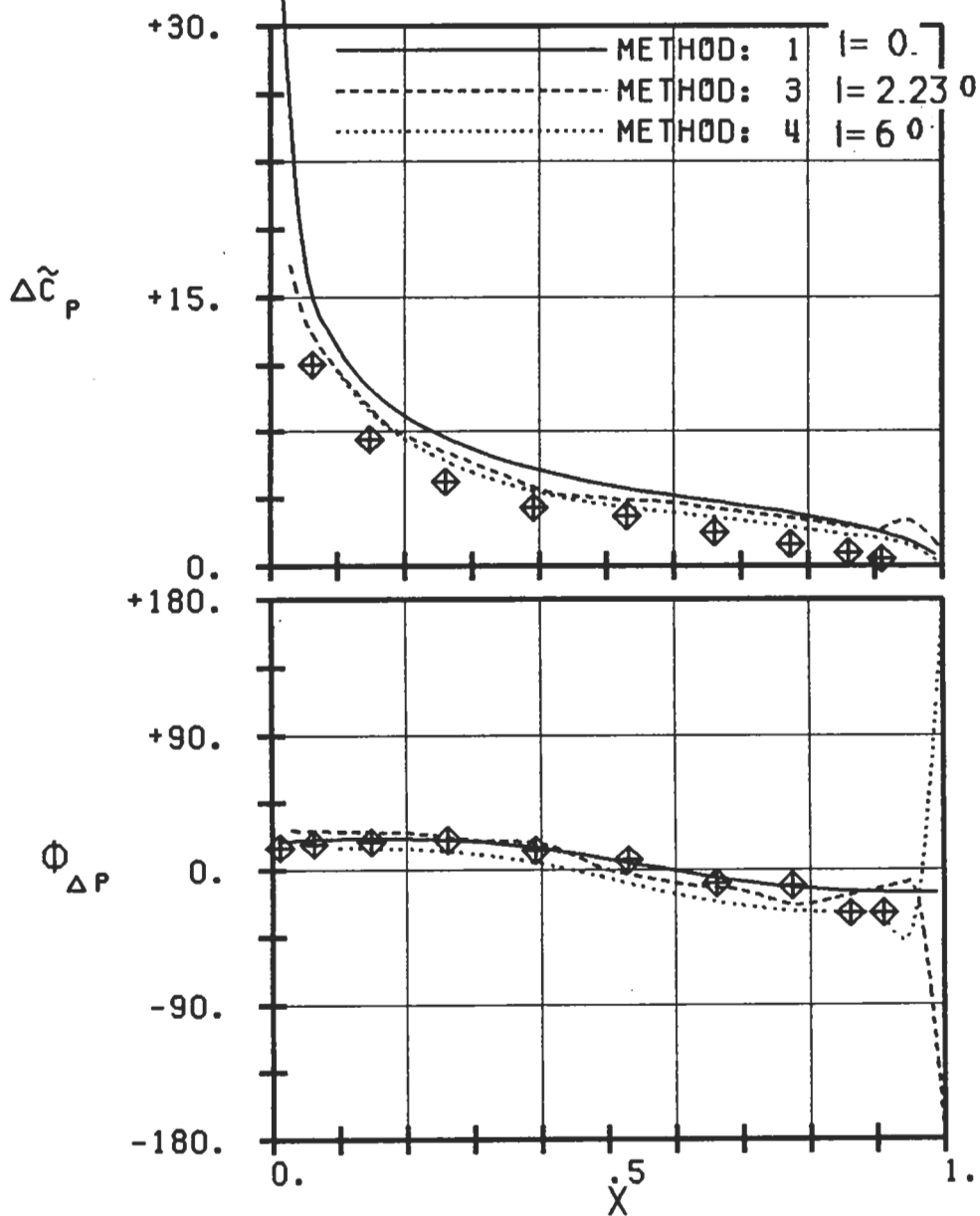
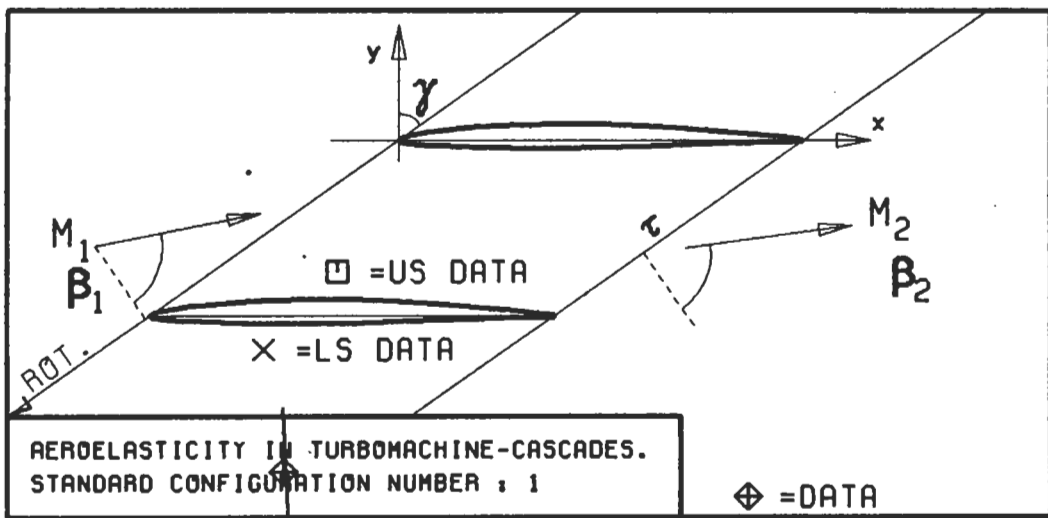
PLOT 7.1-3.8: FIRST STANDARD CONFIGURATION, CASE 8.
 MAGNITUDE AND PHASE LEAD OF UNSTEADY
 SURFACE PRESSURE DIFFERENCE COEFFICIENT.
 (\times : IN PITCH MODE, NOTATION VALID UPSTREAM OF PITCH AXIS)



$c : .152M$
 $\tau : .75$
 $\gamma : 55.$
 $x_\infty : .5$
 $y_\infty : .0115$
 $M_1 : .18$
 $B_1 : -66.$
 $i : 6.$
 $M_2 : 0.15$
 $B_2 : -62.5$
 $h_X : -$
 $h_Y : -$
 $\alpha : .035$
 $\omega : 97$
 $k : .122$
 $\delta : -$
 $\sigma : 0$
 $d : .06$

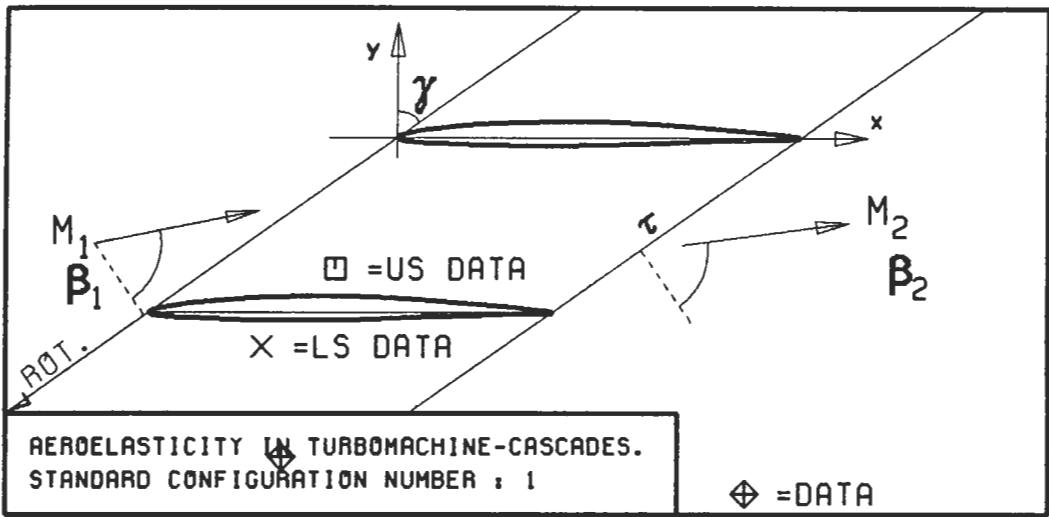


PLOT 7.1-3.9: FIRST STANDARD CONFIGURATION, CASE 9.
MAGNITUDE AND PHASE LEAD OF UNSTEADY
SURFACE PRESSURE DIFFERENCE COEFFICIENT.
(\times : IN PITCH MODE, NOTATION VALID UPSTREAM OF PITCH AXIS)

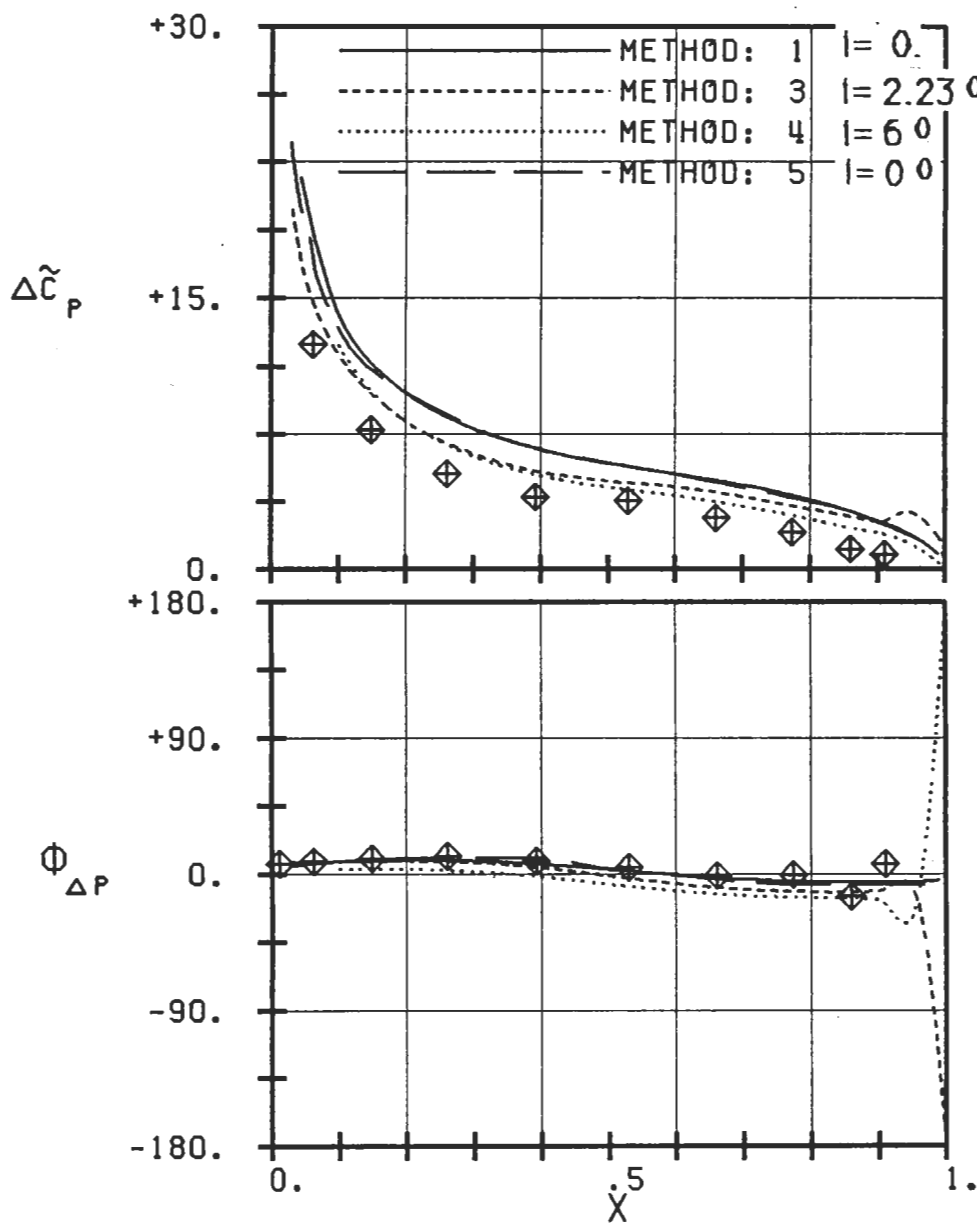


PLOT 7.1-3.10: FIRST STANDARD CONFIGURATION, CASE 10.
MAGNITUDE AND PHASE LEAD OF UNSTEADY
SURFACE PRESSURE DIFFERENCE COEFFICIENT.
(\times : IN PITCH MODE, NOTATION VALID UPSTREAM OF PITCH AXIS)

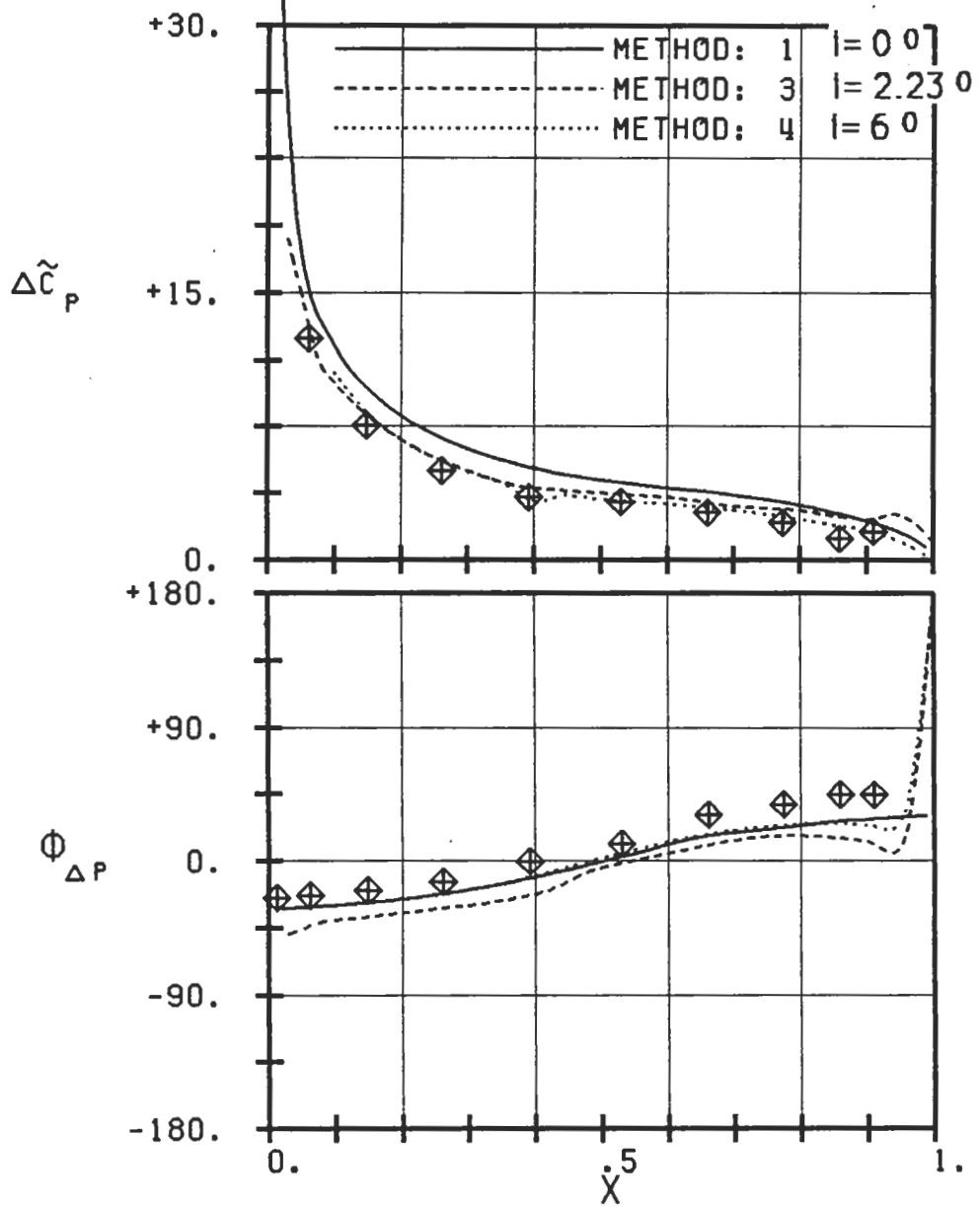
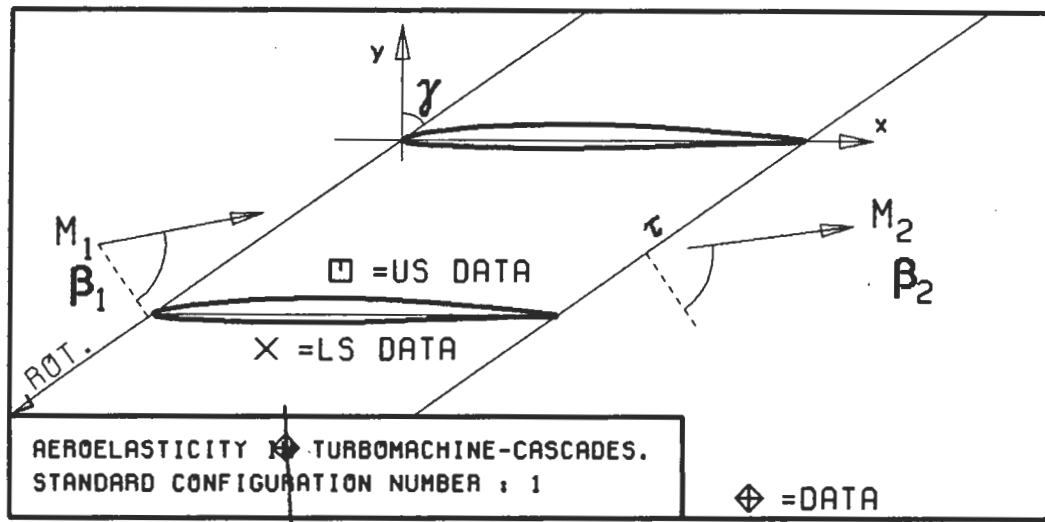
c : .152M
 τ : .75
 γ : 55.
 x_∞ : .5
 y_∞ : .0115
 M_1 : .18
 β_1 : -66.
i : 6.
 M_2 : 0.15
 β_2 : -62.5
 h_X : -
 h_Y : -
 α : .035
 ω : 97
 k : .122
 δ : -
 σ : +90
 d : .06



$c : .152M$
 $\tau : .75$
 $\gamma : 55.$
 $x_\infty : .5$
 $y_\infty : .0115$
 $M_1 : .18$
 $\beta_1 : -66.$
 $i : 6.$
 $M_2 : 0.15$
 $\beta_2 : -62.5$
 $h_X : -$
 $h_Y : -$
 $\alpha : .035$
 $\omega : 97$
 $k : .122$
 $\delta : -$
 $\sigma : +135$
 $d : .06$

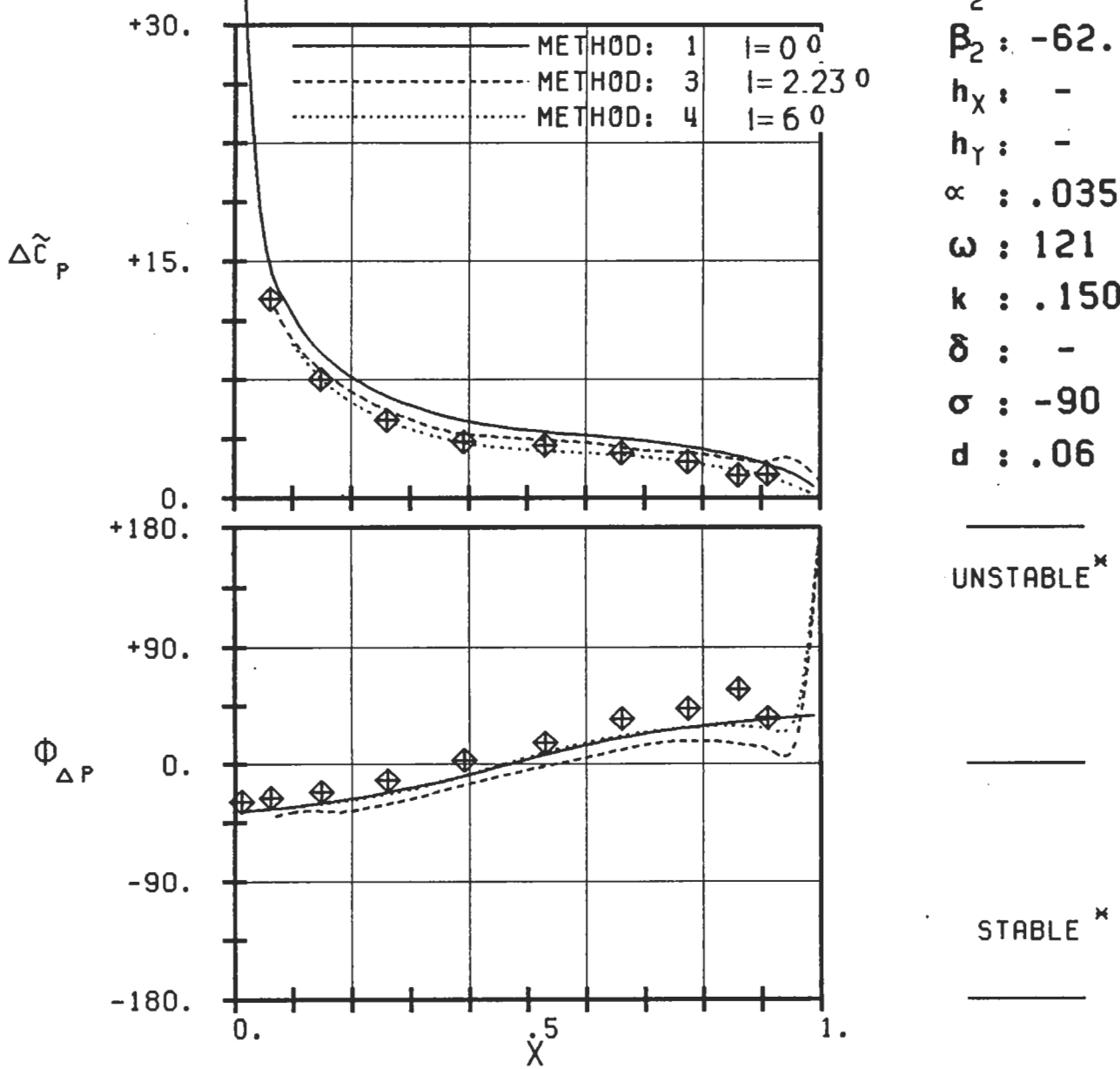
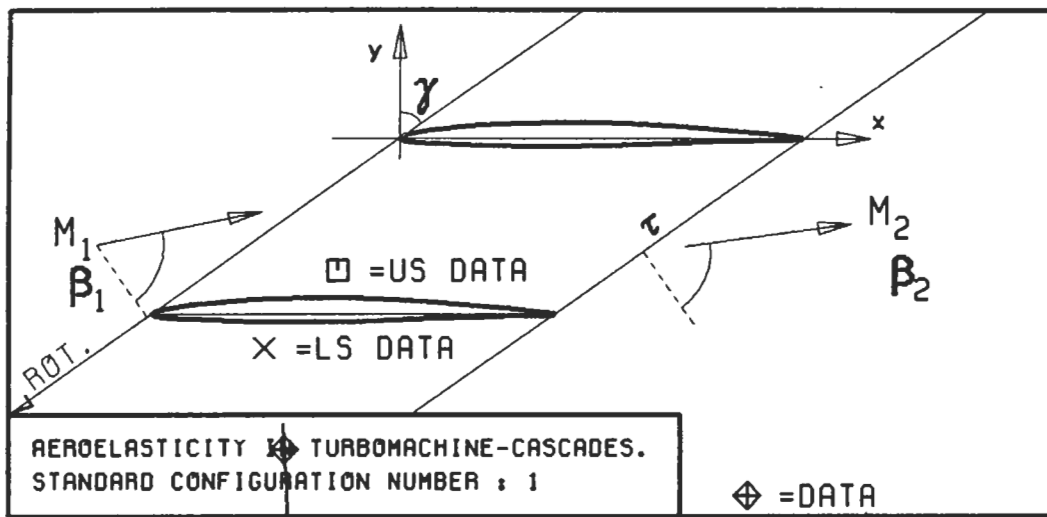


PLOT 7.1-3.11: FIRST STANDARD CONFIGURATION, CASE 11.
MAGNITUDE AND PHASE LEAD OF UNSTEADY
SURFACE PRESSURE DIFFERENCE COEFFICIENT.
(x : IN PITCH MODE, NOTATION VALID UPSTREAM OF PITCH AXIS)

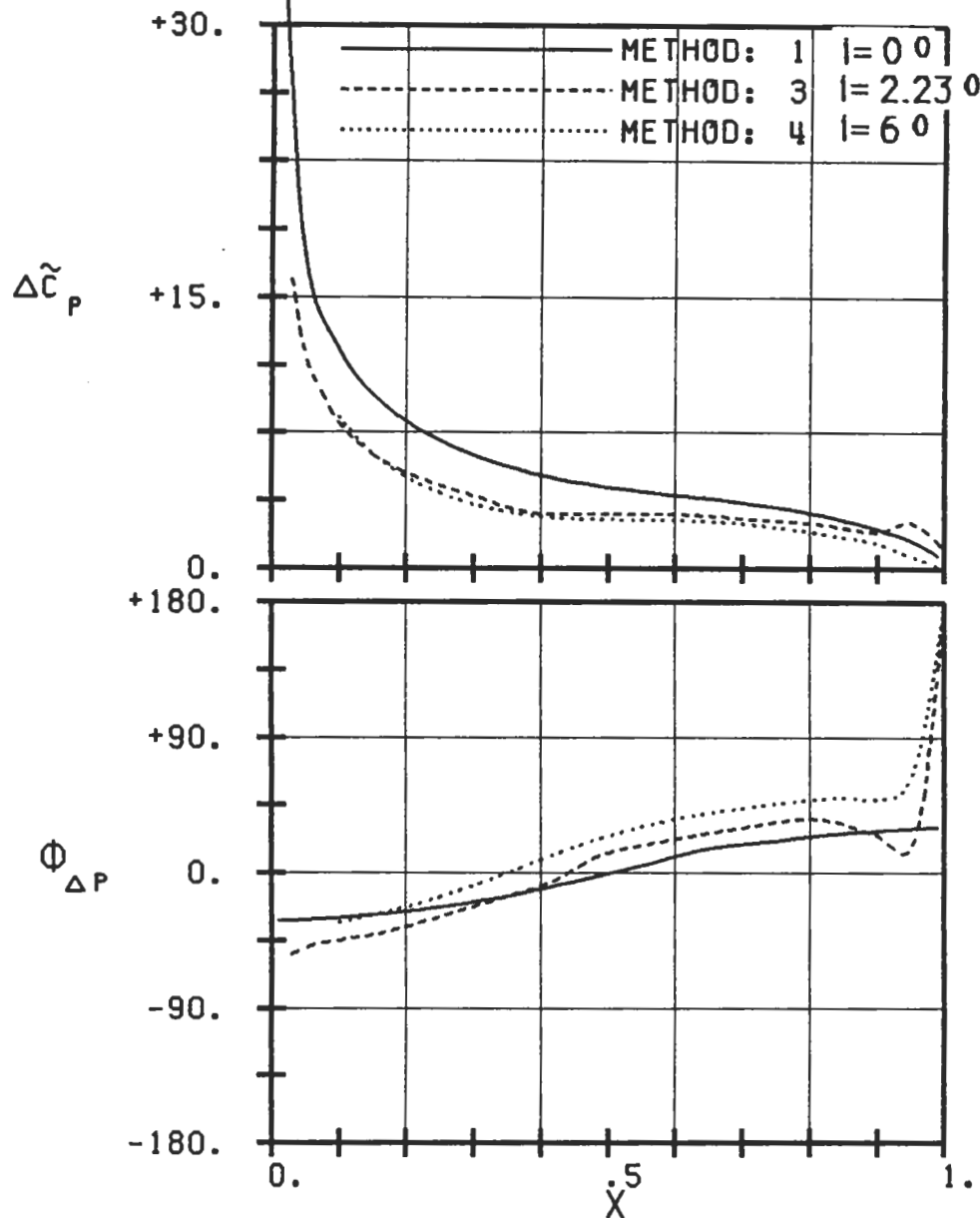
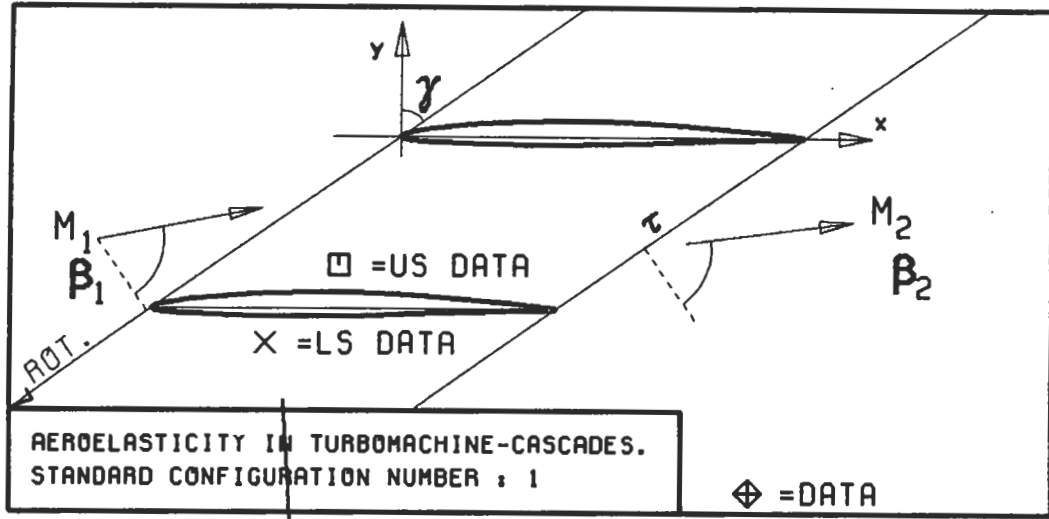


PLT 7.1-3.12: FIRST STANDARD CONFIGURATION, CASE 12.
MAGNITUDE AND PHASE LEAD OF UNSTEADY
SURFACE PRESSURE DIFFERENCE COEFFICIENT.
(\times : IN PITCH MODE, NOTATION VALID UPSTREAM OF PITCH AXIS)

$c : .152M$
 $\tau : .75$
 $\gamma : 55.$
 $x_\alpha : .5$
 $y_\alpha : .0115$
 $M_1 : .18$
 $\beta_1 : -66.$
 $i : 6.$
 $M_2 : 0.15$
 $\beta_2 : -62.5$
 $h_x : -$
 $h_y : -$
 $\alpha : .035$
 $\omega : 58$
 $k : .071$
 $\delta : -$
 $\sigma : -90$
 $d : .06$



PLOT 7.1-3.13: FIRST STANDARD CONFIGURATION, CASE 13.
MAGNITUDE AND PHASE LEAD OF UNSTEADY
SURFACE PRESSURE DIFFERENCE COEFFICIENT.
(X: IN PITCH MODE, NOTATION VALID UPSTREAM OF PITCH AXIS)



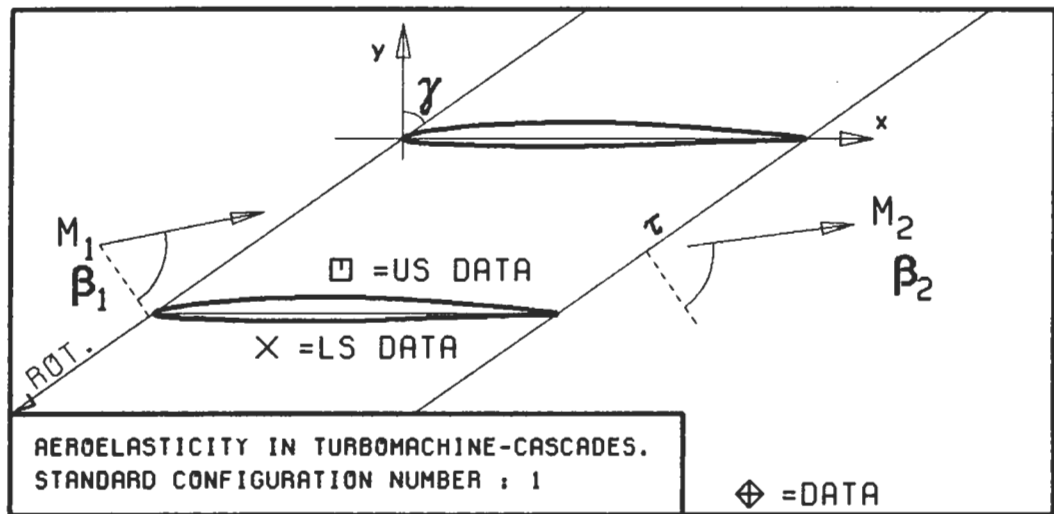
PLOT 7.1-3.14: FIRST STANDARD CONFIGURATION, CASE 14.
 MAGNITUDE AND PHASE LEAD OF UNSTEADY
 SURFACE PRESSURE DIFFERENCE COEFFICIENT.

(\times : IN PITCH MODE, NOTATION VALID UPSTREAM OF PITCH AXIS)

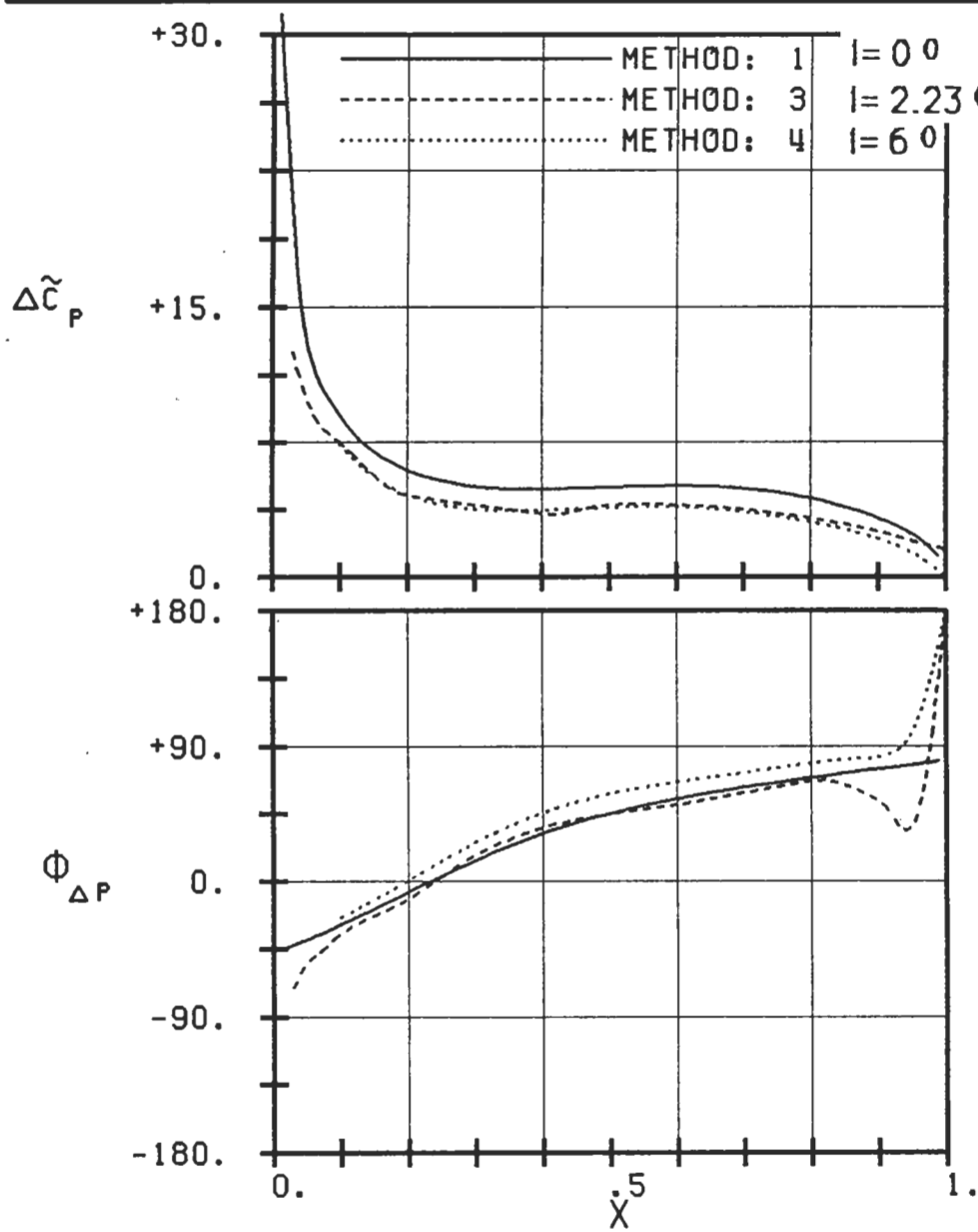
$c : .152M$
 $\tau : .75$
 $\gamma : 55.$
 $x_\infty : .5$
 $y_\infty : .0115$
 $M_1 : .18$
 $\beta_1 : -66.$
 $i : 6.$
 $M_2 : 0.15$
 $\beta_2 : -62.5$
 $h_X : -$
 $h_Y : -$
 $\alpha : .035$
 $\omega : 241$
 $k : .301$
 $\delta : -$
 $\sigma : -90$
 $d : .06$

UNSTABLE \times

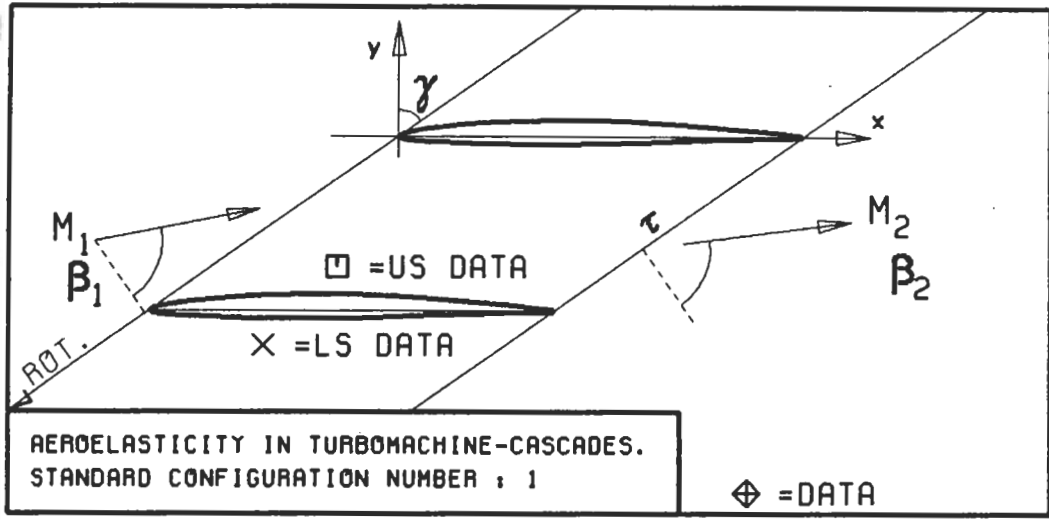
STABLE \times



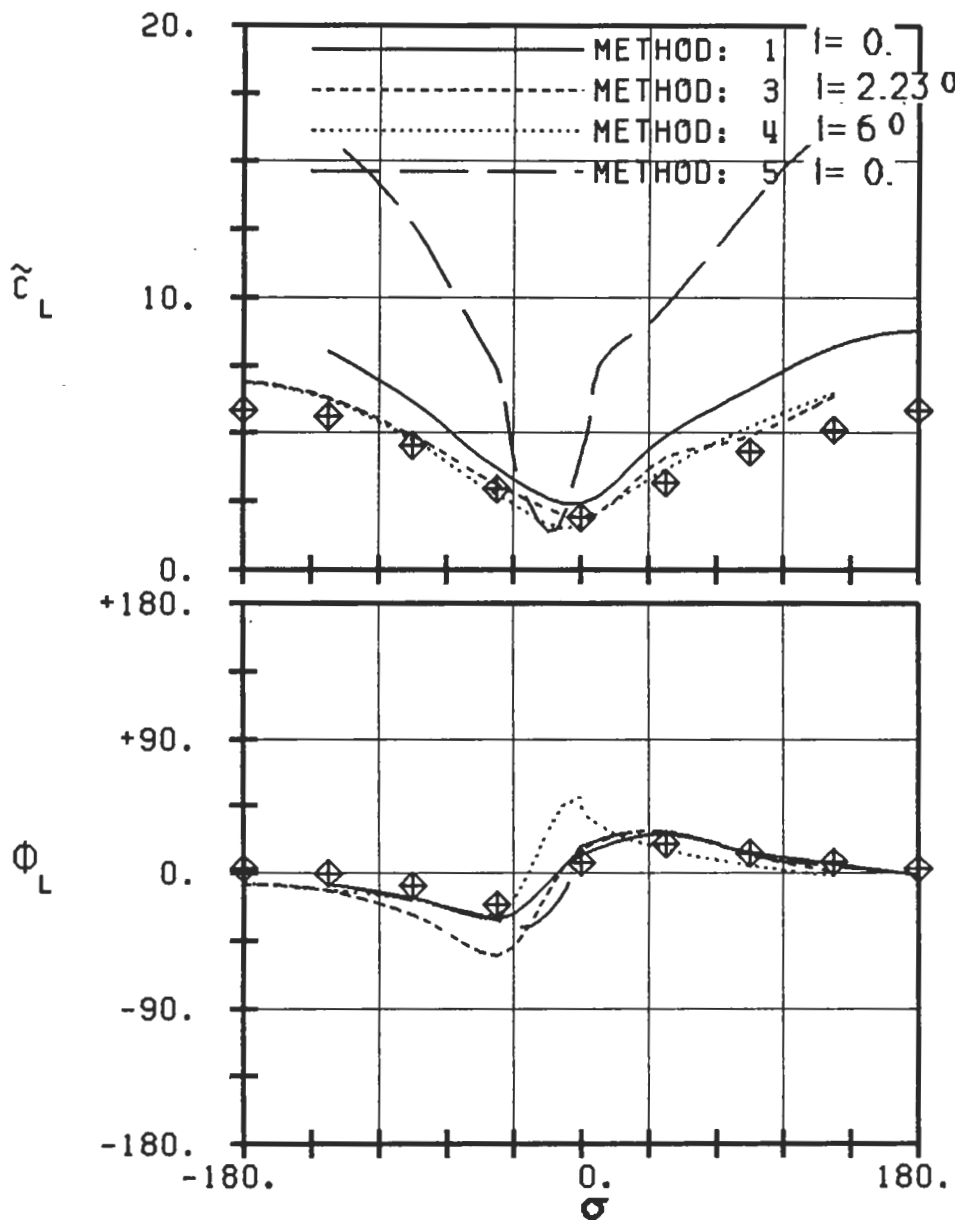
$c : .152M$
 $\tau : .75$
 $\gamma : 55.$
 $x_\infty : .5$
 $y_\infty : .0115$
 $M_1 : .18$
 $\beta_1 : -66.$
 $i : 6.$
 $M_2 : 0.15$
 $\beta_2 : -62.5$
 $h_x : -$
 $h_y : -$
 $\alpha : .035$
 $\omega : 483$
 $k : .603$
 $\delta : -$
 $\sigma : -90$
 $d : .06$



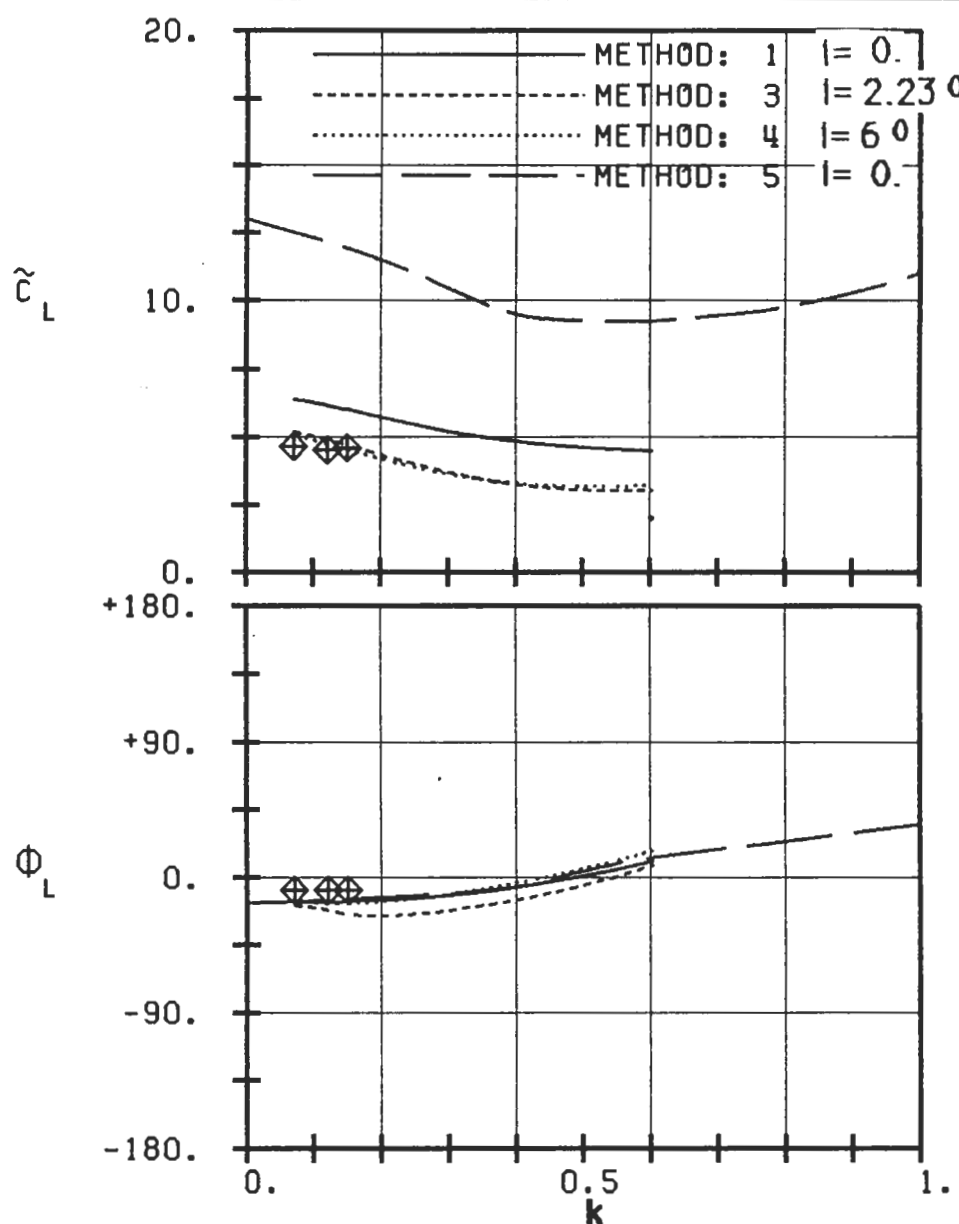
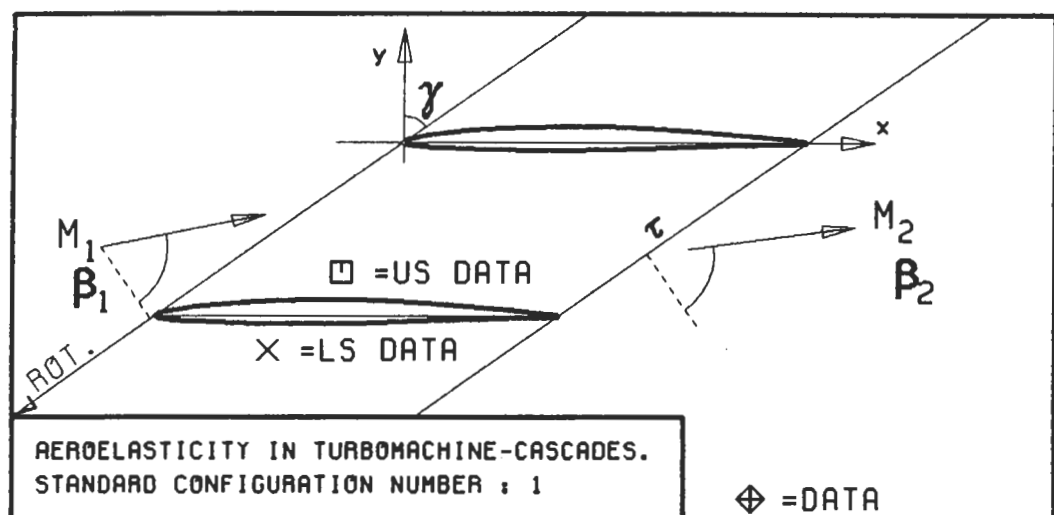
PLOT 7.1-3.15: FIRST STANDARD CONFIGURATION, CASE 15.
MAGNITUDE AND PHASE LEAD OF UNSTEADY
SURFACE PRESSURE DIFFERENCE COEFFICIENT.
(\times : IN PITCH MODE, NOTATION VALID UPSTREAM OF PITCH AXIS)



$c : .152M$
 $\tau : .75$
 $\gamma : 55.$
 $x_\infty : .5$
 $y_\infty : .0115$
 $M_1 : .18$
 $\beta_1 : -66.$
 $i : 6.$
 $M_2 : 0.15$
 $\beta_2 : -62.5$
 $h_x : -$
 $h_y : -$
 $\alpha : .035$
 $\omega : 97$
 $k : .122$
 $\delta : -$
 $\sigma : -$
 $d : .06$

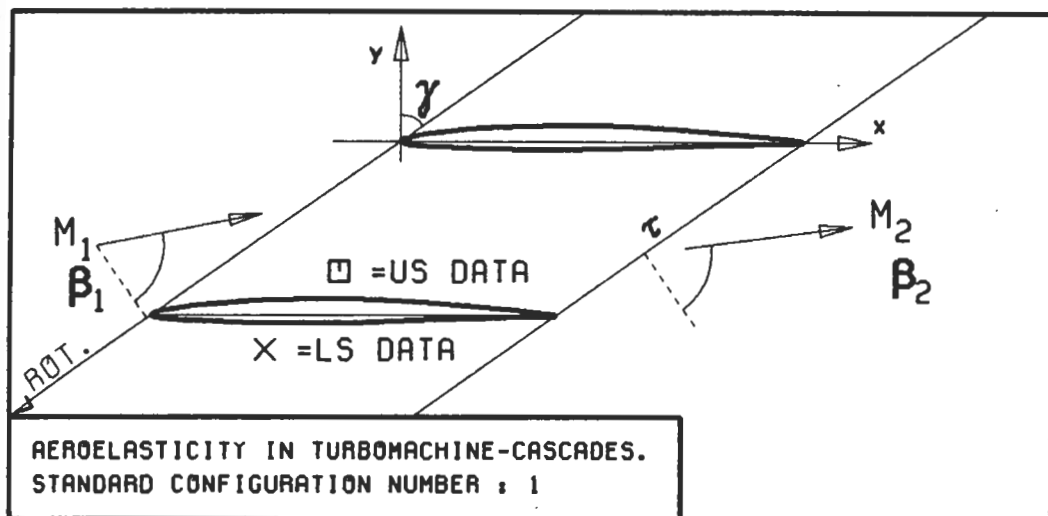


PLOT 7.1-4.1: FIRST STANDARD CONFIGURATION, CASES 4-11.
AERODYNAMIC LIFT COEFFICIENT AND PHASE LEAD
IN DEPENDANCE OF INTERBLADE PHASE ANGLE.

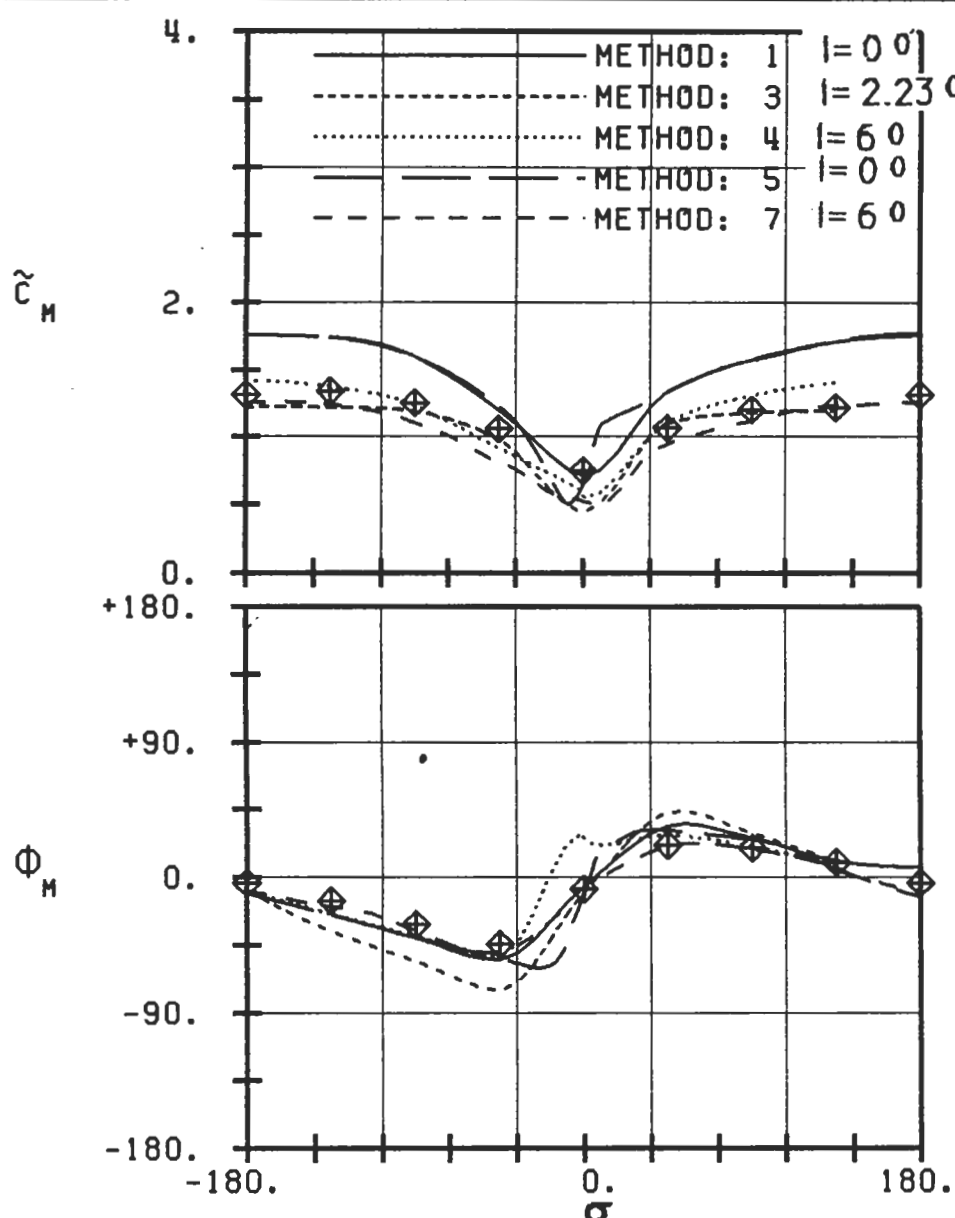


PLOT 7.1-4.2: FIRST STANDARD CONFIGURATION, CASES 8,12-15.
AERODYNAMIC LIFT COEFFICIENT AND PHASE LEAD
IN DEPENDANCE OF REDUCED FREQUENCY.

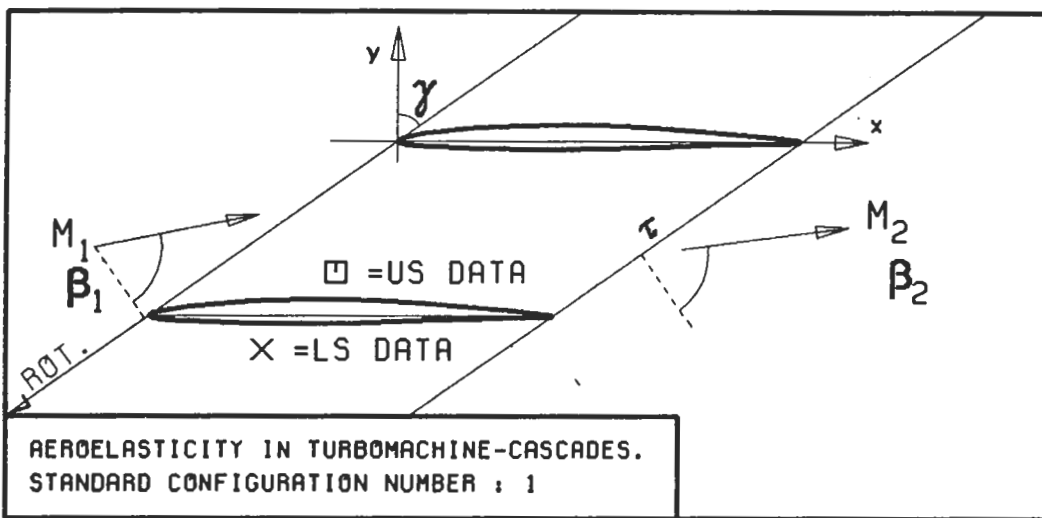
$c : .152M$
 $\tau : .75$
 $\gamma : 55.$
 $x_\infty : .5$
 $y_\infty : .0115$
 $M_1 : .18$
 $\beta_1 : -66.$
 $i : 6.$
 $M_2 : 0.15$
 $\beta_2 : -62.5$
 $h_x : -$
 $h_y : -$
 $\alpha : .035$
 $\omega : -$
 $k : -$
 $\delta : -$
 $\sigma : -90$
 $d : .06$



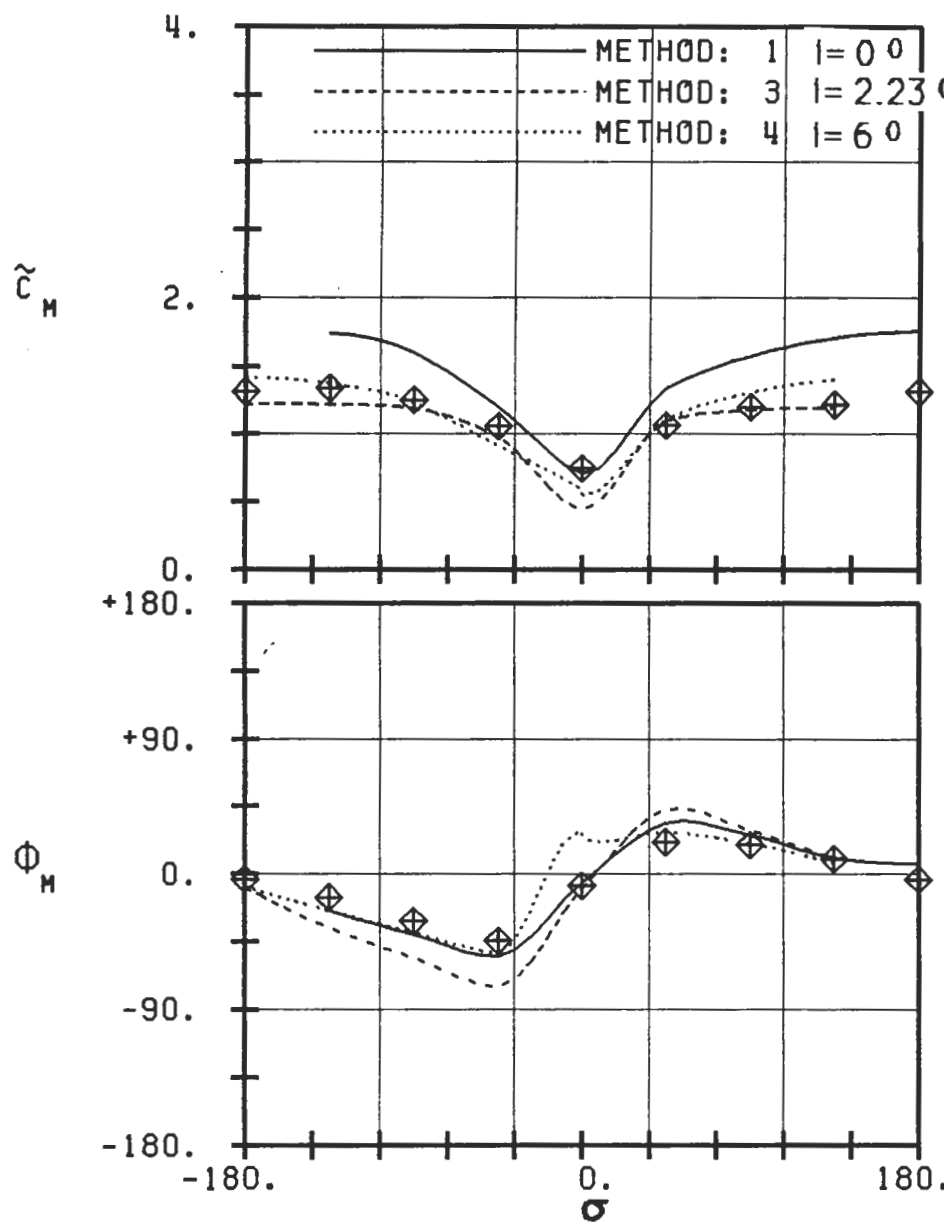
$c : .152M$
 $\tau : .75$
 $\gamma : 55.$
 $x_\infty : .5$
 $y_\infty : .0115$
 $M_1 : .18$
 $\beta_1 : -66.$
 $i : 6.$
 $M_2 : 0.15$
 $\beta_2 : -62.5$
 $h_x : -$
 $h_y : -$
 $\alpha : .035$
 $\omega : 97$
 $k : .122$
 $\delta : -$
 $\sigma : -$
 $d : .06$



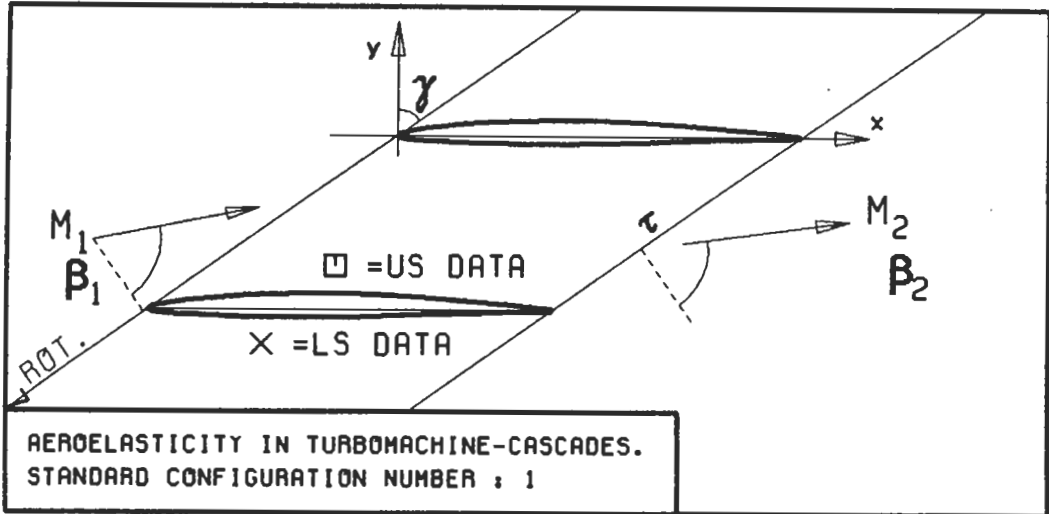
PLOT 7.1-5.1: FIRST STANDARD CONFIGURATION, CASES 4-11.
AERODYNAMIC MOMENT COEFFICIENT AND PHASE LEAD
IN DEPENDANCE OF INTERBLADE PHASE ANGLE.



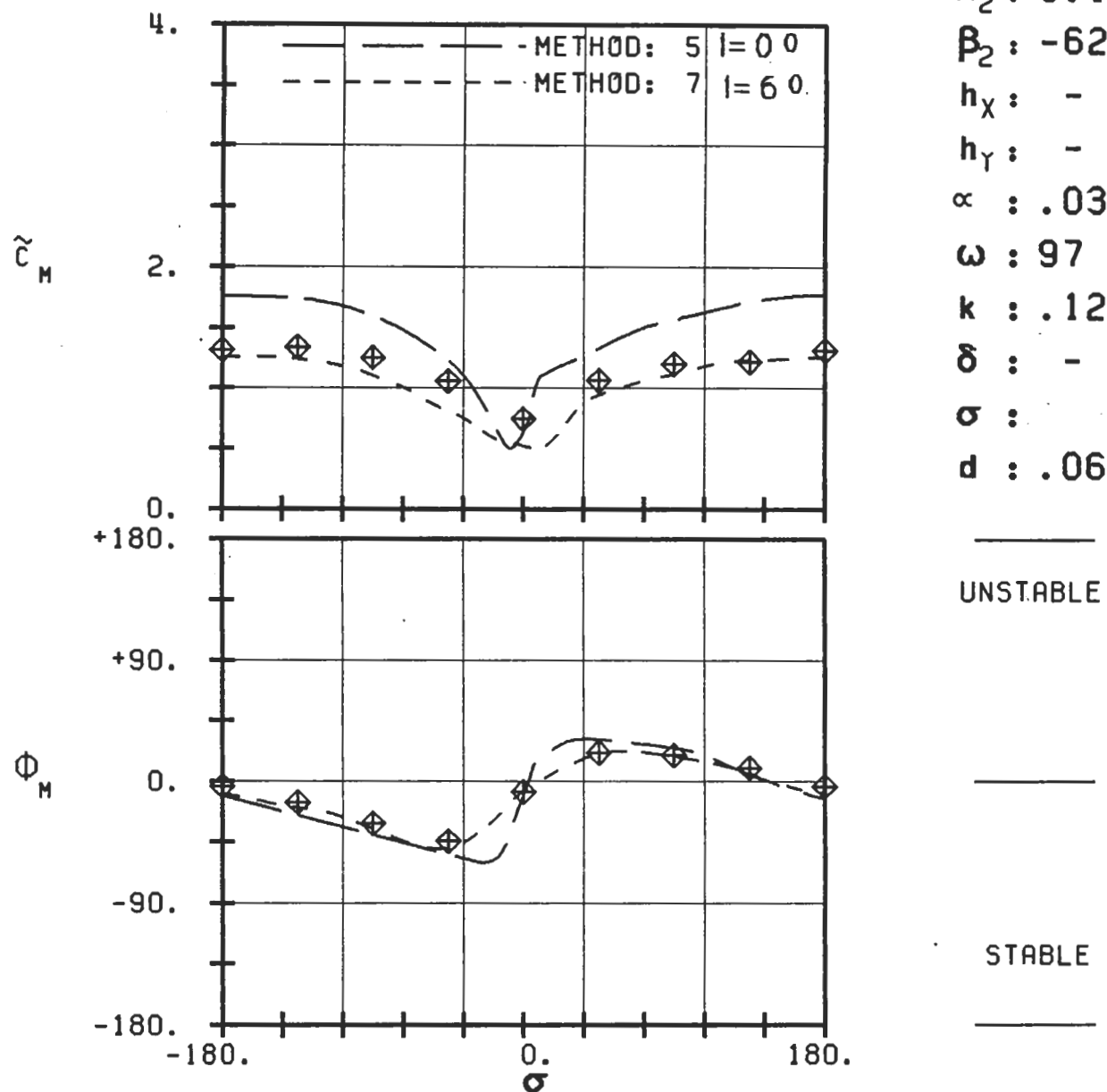
$c : .152M$
 $\tau : .75$
 $\gamma : 55.$
 $x_\infty : .5$
 $y_\infty : .0115$
 $M_1 : .18$
 $\beta_1 : -66.$
 $i : 6.$
 $M_2 : 0.15$
 $\beta_2 : -62.5$
 $h_x : -$
 $h_y : -$
 $\alpha : .035$
 $\omega : 97$
 $k : .122$
 $\delta : -$
 $\sigma : -$
 $d : .06$



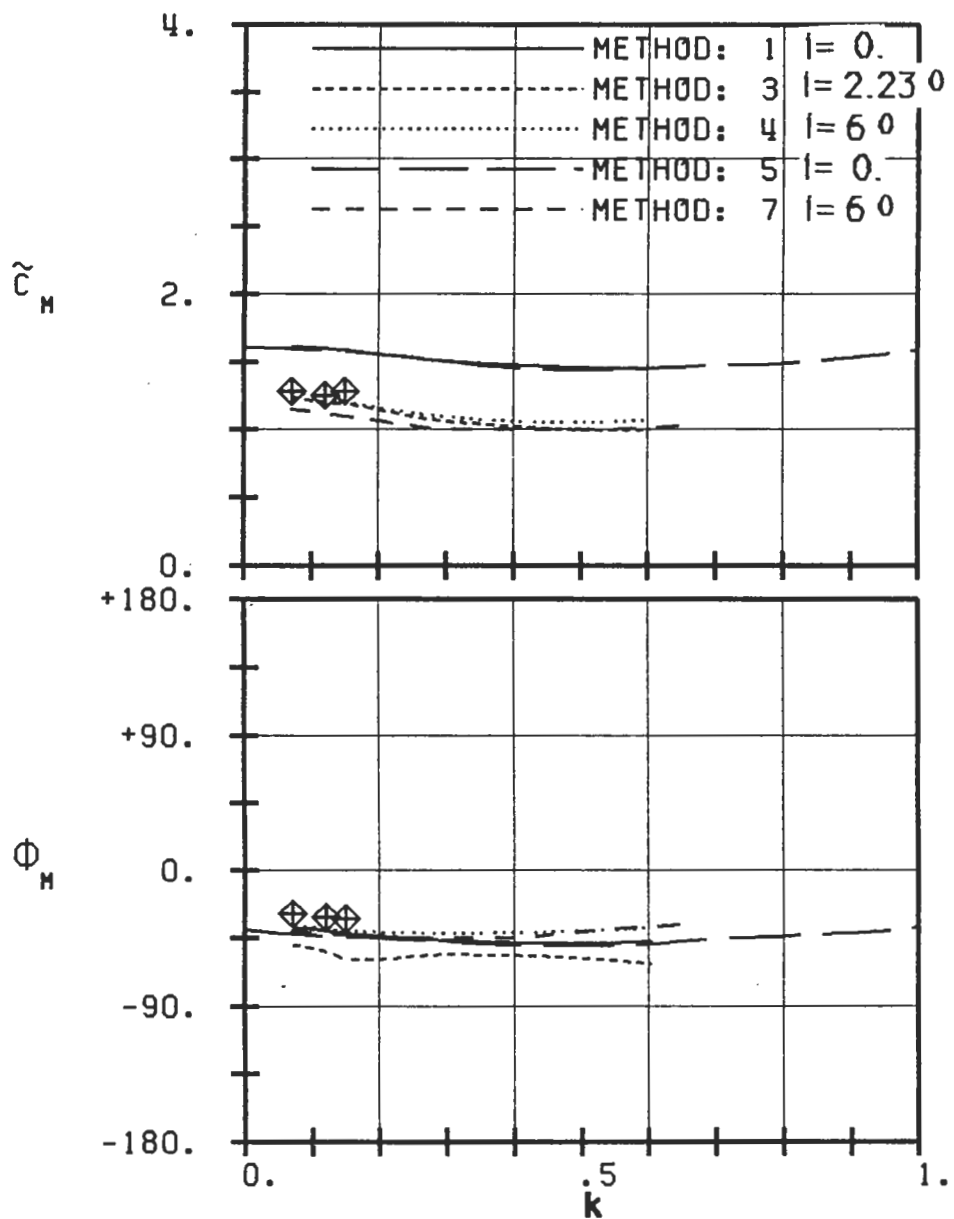
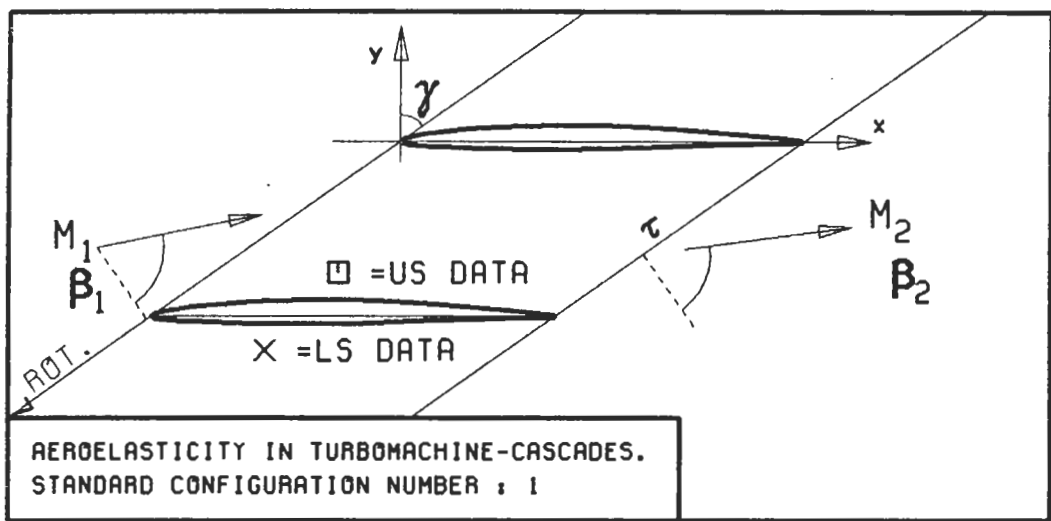
PLOT 7.1-5.1A: FIRST STANDARD CONFIGURATION, CASES 4-11.
AERODYNAMIC MOMENT COEFFICIENT AND PHASE LEAD
IN DEPENDANCE OF INTERBLADE PHASE ANGLE.



c : .152M
 τ : .75
 γ : 55.
 x_∞ : .5
 y_∞ : .0115
 M_1 : .18
 β_1 : -66.
 i : 6.
 M_2 : 0.15
 β_2 : -62.5
 h_X : -
 h_Y : -
 α : .035
 ω : 97
 k : .122
 δ : -
 σ :
 d : .06

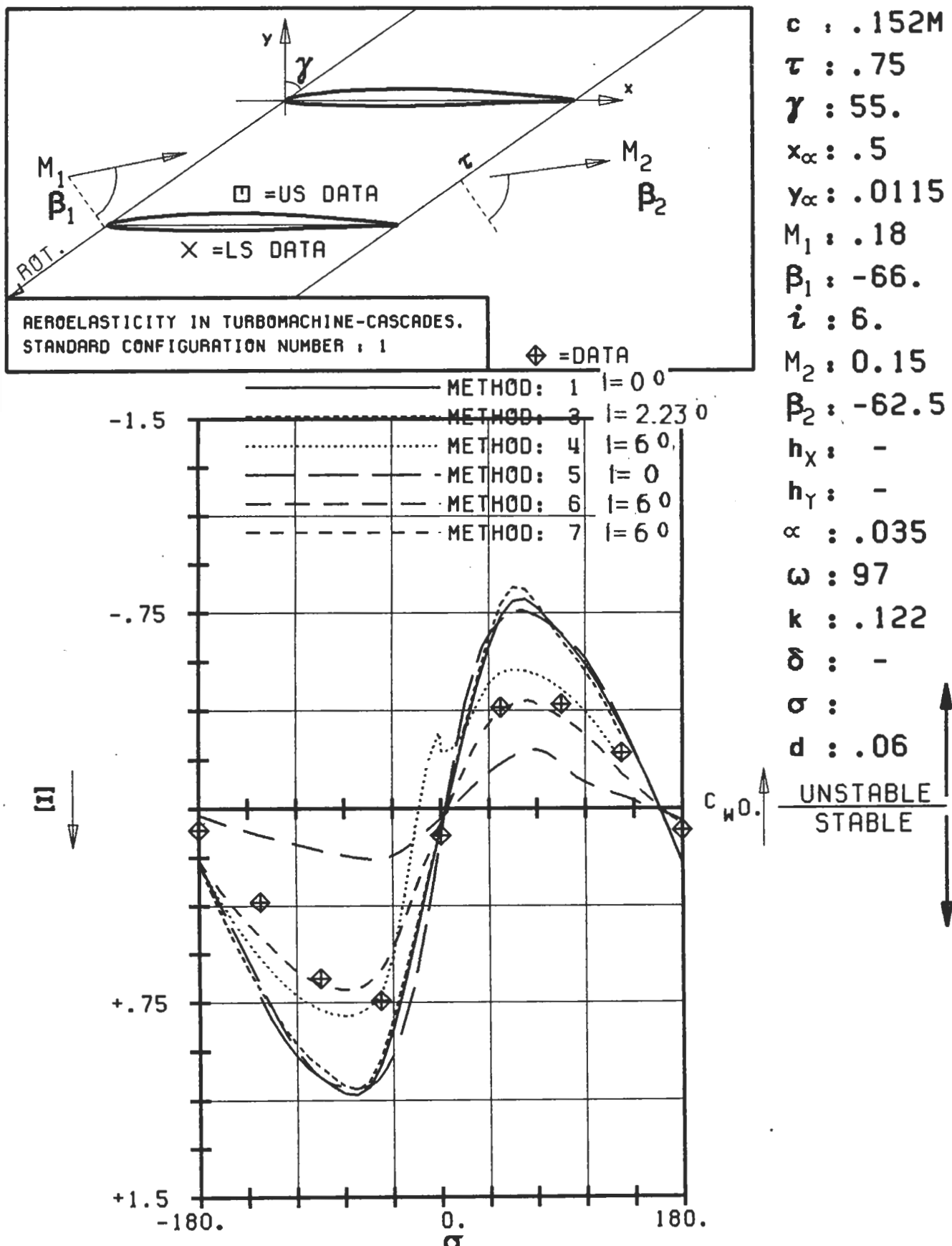


PLOT 7.1-5.1B: FIRST STANDARD CONFIGURATION, CASES 4-11.
AERODYNAMIC MOMENT COEFFICIENT AND PHASE LEAD
IN DEPENDANCE OF INTERBLADE PHASE ANGLE.

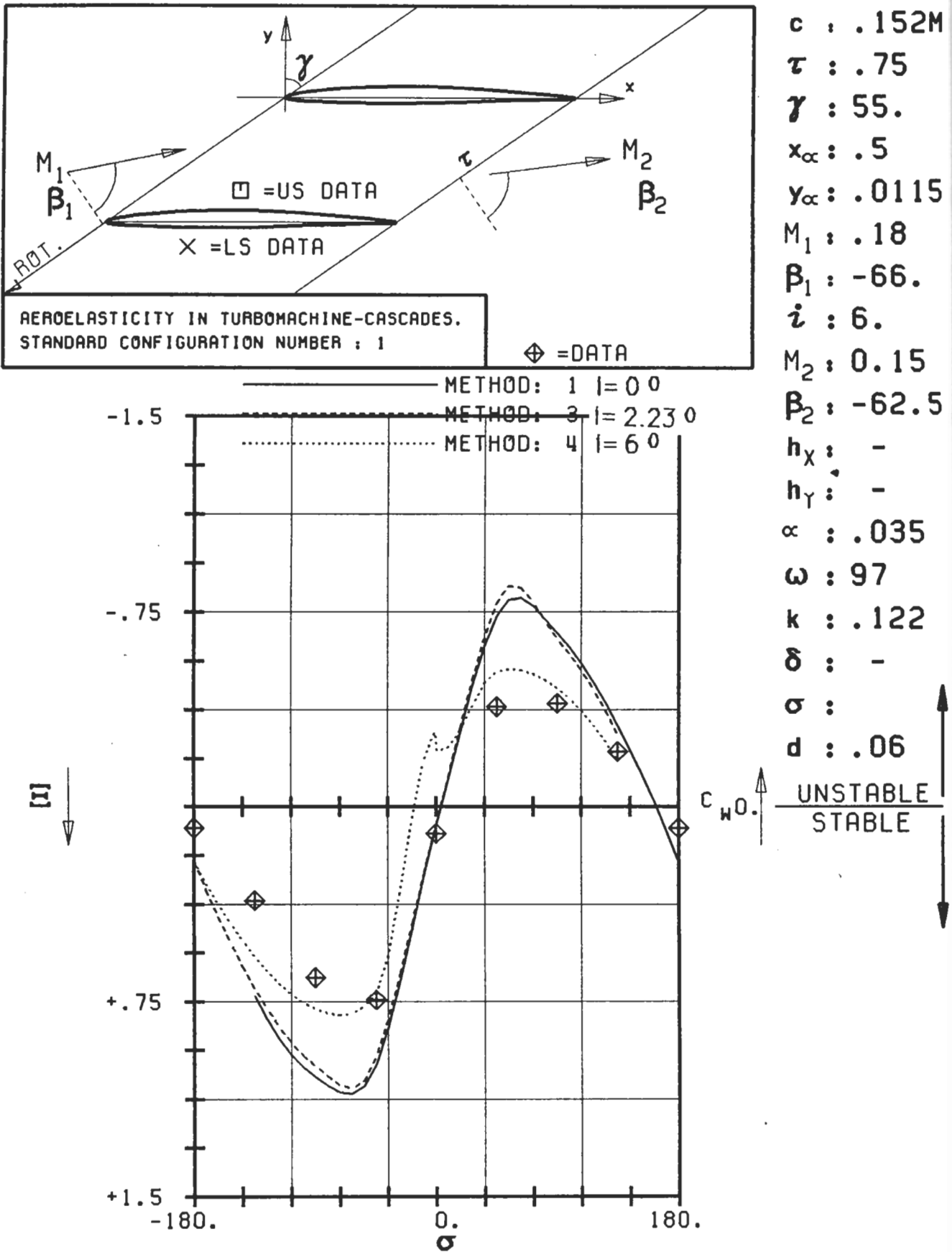


PLOT 7.1-5.2: FIRST STANDARD CONFIGURATION, CASES 8,12-15.
AERODYNAMIC MOMENT COEFFICIENT AND PHASE LEAD
IN DEPENDANCE OF REDUCED FREQUENCY.

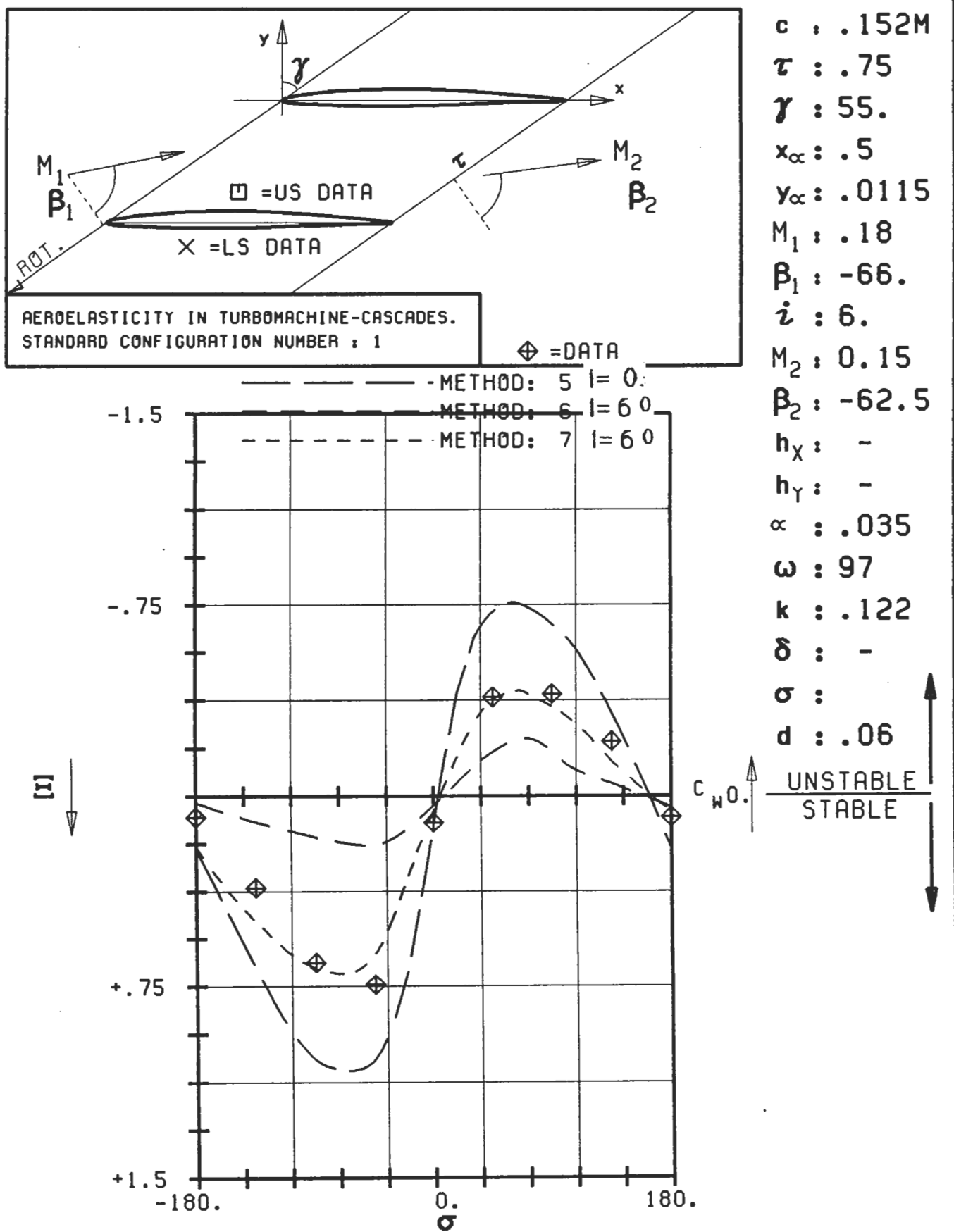
$c : .152M$
 $\tau : .75$
 $\gamma : 55.$
 $x_\infty : .5$
 $y_\infty : .0115$
 $M_1 : .18$
 $\beta_1 : -66.$
 $i : 6.$
 $M_2 : 0.15$
 $\beta_2 : -62.5$
 $h_x : -$
 $h_y : -$
 $\alpha : .035$
 $\omega :$
 $k :$
 $\delta : -$
 $\sigma : -90$
 $d : .06$



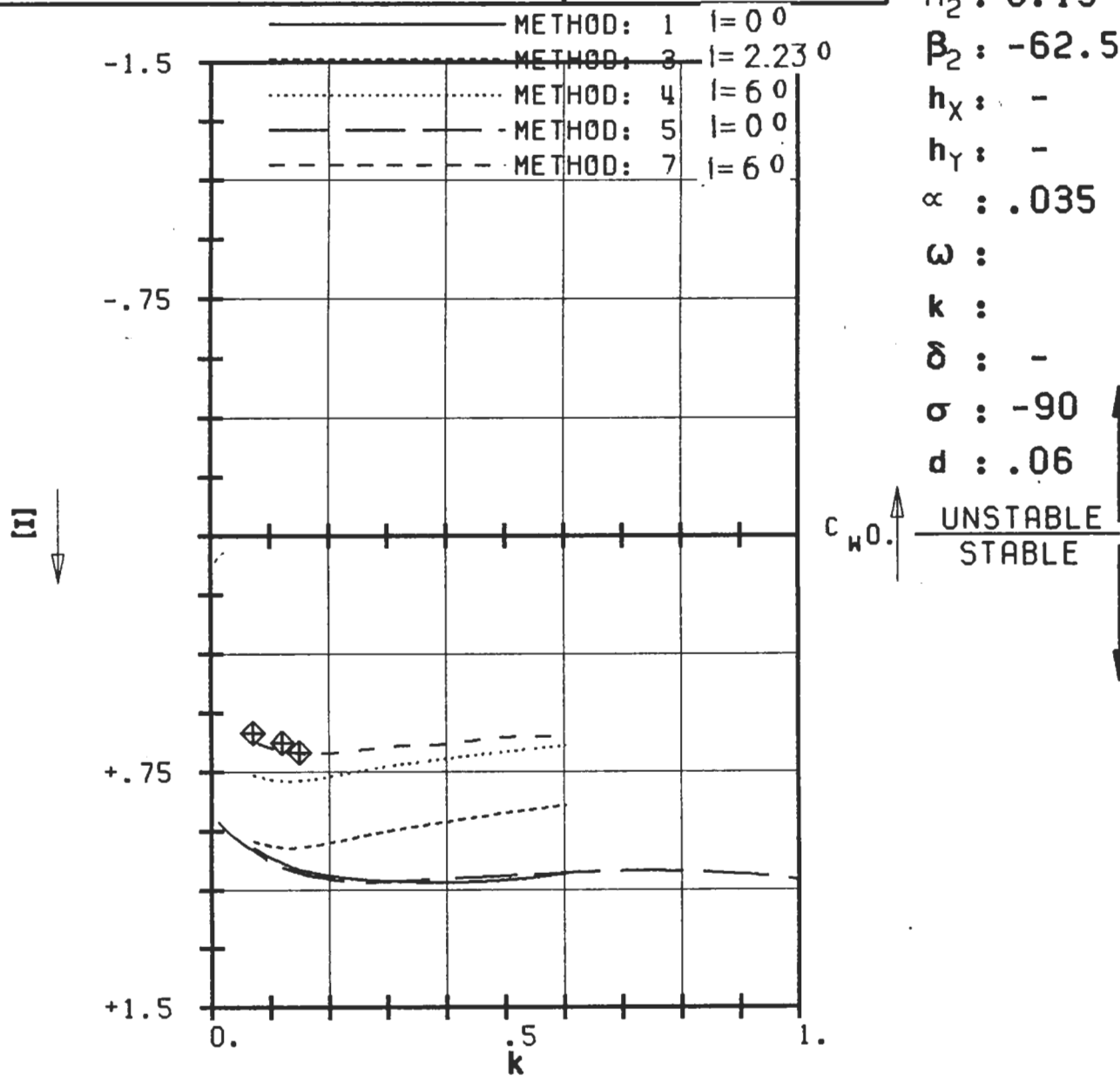
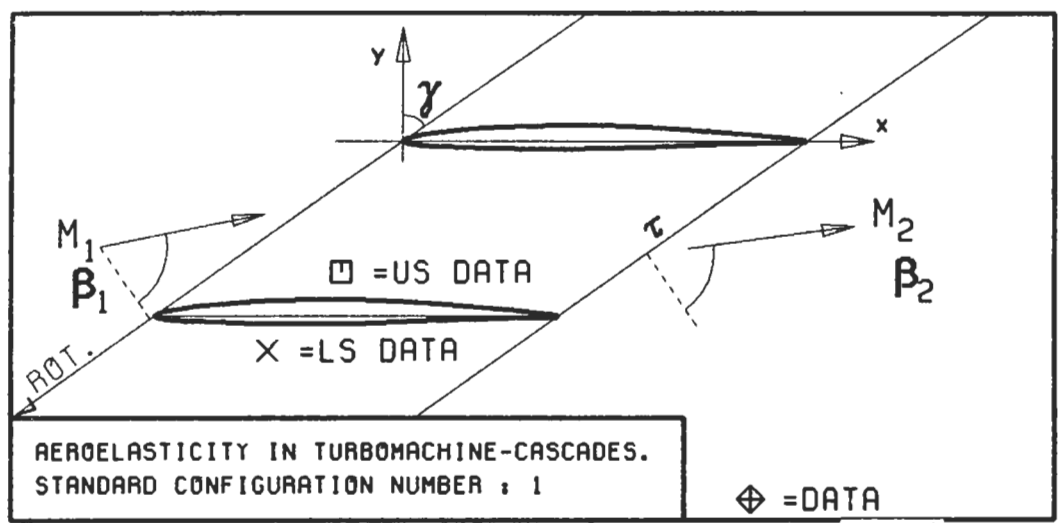
PLOT 7.1-6.1: FIRST STANDARD CONFIGURATION, CASES 4-11.
 AERODYNAMIC WORK AND DAMPING COEFFICIENTS
 IN DEPENDANCE OF INTERBLADE PHASE ANGLE



PLOT 7.1-6.1A: FIRST STANDARD CONFIGURATION, CASES 4-11.
 AERODYNAMIC WORK AND DAMPING COEFFICIENTS
 IN DEPENDANCE OF INTERBLADE PHASE ANGLE



PLOT 7.1-6.1B: FIRST STANDARD CONFIGURATION, CASES 4-11.
 AERODYNAMIC WORK AND DAMPING COEFFICIENTS
 IN DEPENDANCE OF INTERBLADE PHASE ANGLE



PLOT 7.1-6.2: FIRST STANDARD CONFIGURATION, CASES 8,12-15.
 AERODYNAMIC WORK AND DAMPING COEFFICIENTS
 IN DEPENDANCE OF REDUCED FREQUENCY.

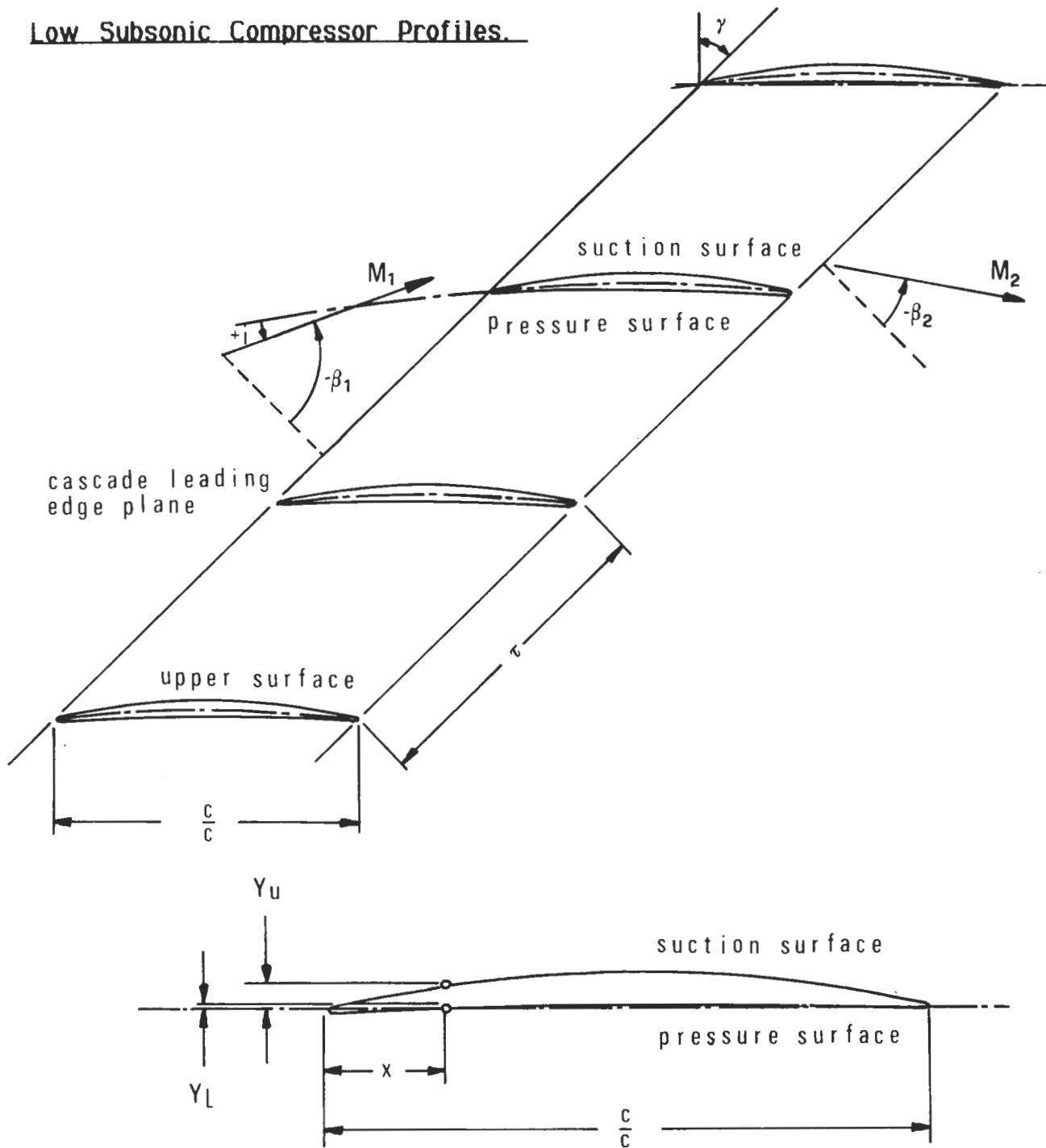
$c : .152M$
 $\tau : .75$
 $\gamma : 55.$
 $x_\infty : .5$
 $y_\infty : .0115$
 $M_1 : .18$
 $\beta_1 : -66.$
 $i : 6.$
 $M_2 : 0.15$
 $\beta_2 : -62.5$
 $h_X : -$
 $h_Y : -$
 $\alpha : .035$
 $\omega :$
 $k :$
 $\delta : -$
 $\sigma : -90$
 $d : .06$

AEROELASTICITY IN TURBOMACHINE-CASCADES

SECOND STANDARD CONFIGURATION

Definition

Low Subsonic Compressor Profiles.



Maximum thickness at x
 Vibration in pitch around (x_a, y_a)
 d = (thickness/chord)
 α = 3.4° ($=0.06$ rad)
 c = 0.050 m
 τ = 1.00
 k = 0.4
 span = 0.100 m
 Working fluid: Air

$= 0.5$
 $= (0.5, 0.0362)$
 $= 0.0524$
 $\beta_1 = -30^\circ$
 $\text{camber} = 16.8^\circ$
 $\gamma = 30^\circ$
 $\sigma = \text{variable}$

Fig. 7.2-1. Second standard configuration: Cascade geometry

Double Circular Arc Blade		
$c=0.050 \text{ m (1.968 in.)}$		
	Suction surface (upper surface)	Pressure surface (lower surface)
x (%)	y (%)	y (%)
0	0	0
5	1.644	-0.404
10	2.637	-0.127
15	3.509	0.115
20	4.262	0.326
25	4.897	0.505
30	5.416	0.650
35	5.818	0.764
40	6.105	0.845
45	6.272	0.893
50	6.334	0.910
55	6.272	0.893
60	6.105	0.845
65	5.818	0.764
70	5.416	0.650
75	4.897	0.505
80	4.262	0.326
85	3.509	0.115
90	2.637	-0.127
95	1.644	-0.404
100	0	0

L.E. and T.E. RADIUS	RADIUS CENTER COORDINATES
L.E. RADIUS/ $c = 0.666 \text{ (%)}$	$x = 0.666 \text{ (%), } y = 0 \text{ (%)}$
T.E. RADIUS/ $c = 0.666 \text{ (%)}$	$x = 0.993 \text{ (%), } y = 0 \text{ (%)}$

Table 7.2-1. Second standard configuration: Dimensionless airfoil coordinates.

AEROELASTICITY IN TURBOMACHINE-CASCADES

SECOND STANDARD CONFIGURATION

Aeroelastic Test Cases

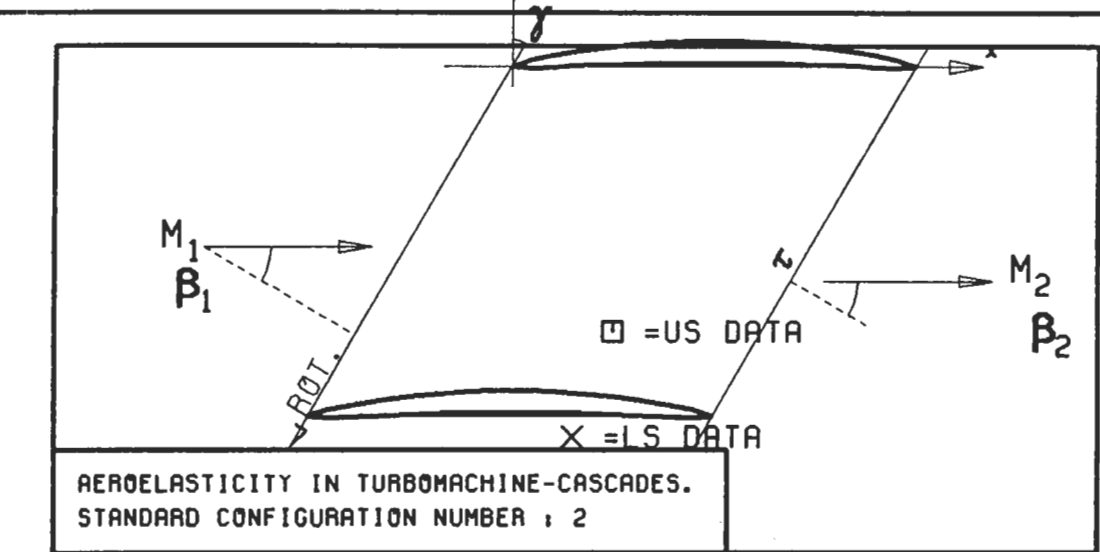
Aeroelastic Test Case No	Time-Averaged Parameters			Time-Dependent Parameters			
	V_1 (m/s)	γ (°)	β_1 (°)	f (Hz)	k (-)	α (rad)	σ (°)
1	2.4	30.0	- 30	6.1	0.4	0.059	- 135
2	"	"	"	"	"	"	- 90
3	"	"	"	"	"	"	- 45
4	"	"	"	"	"	"	0
5	"	"	"	"	"	"	+ 45
6	"	"	"	"	"	"	+ 90
7	"	"	"	"	"	"	+ 135
8	"	"	"	"	"	"	+ 180

Table 7.2-2 Second standard configuration.
8 recommended aerelastic test cases

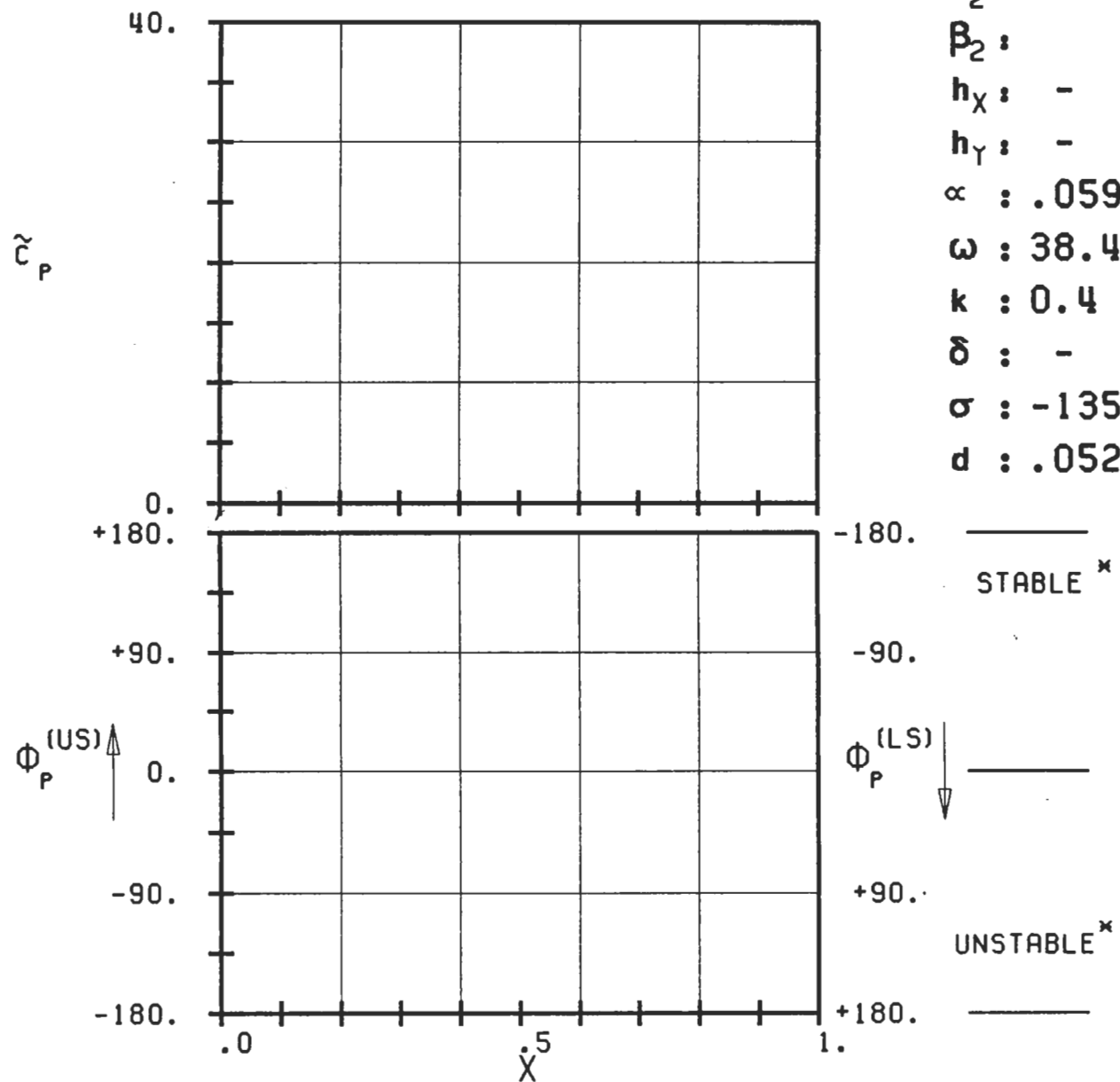
AEROELASTICITY IN TURBOMACHINE-CASCADES

SECOND STANDARD CONFIGURATION

Experimental and Theoretical Results

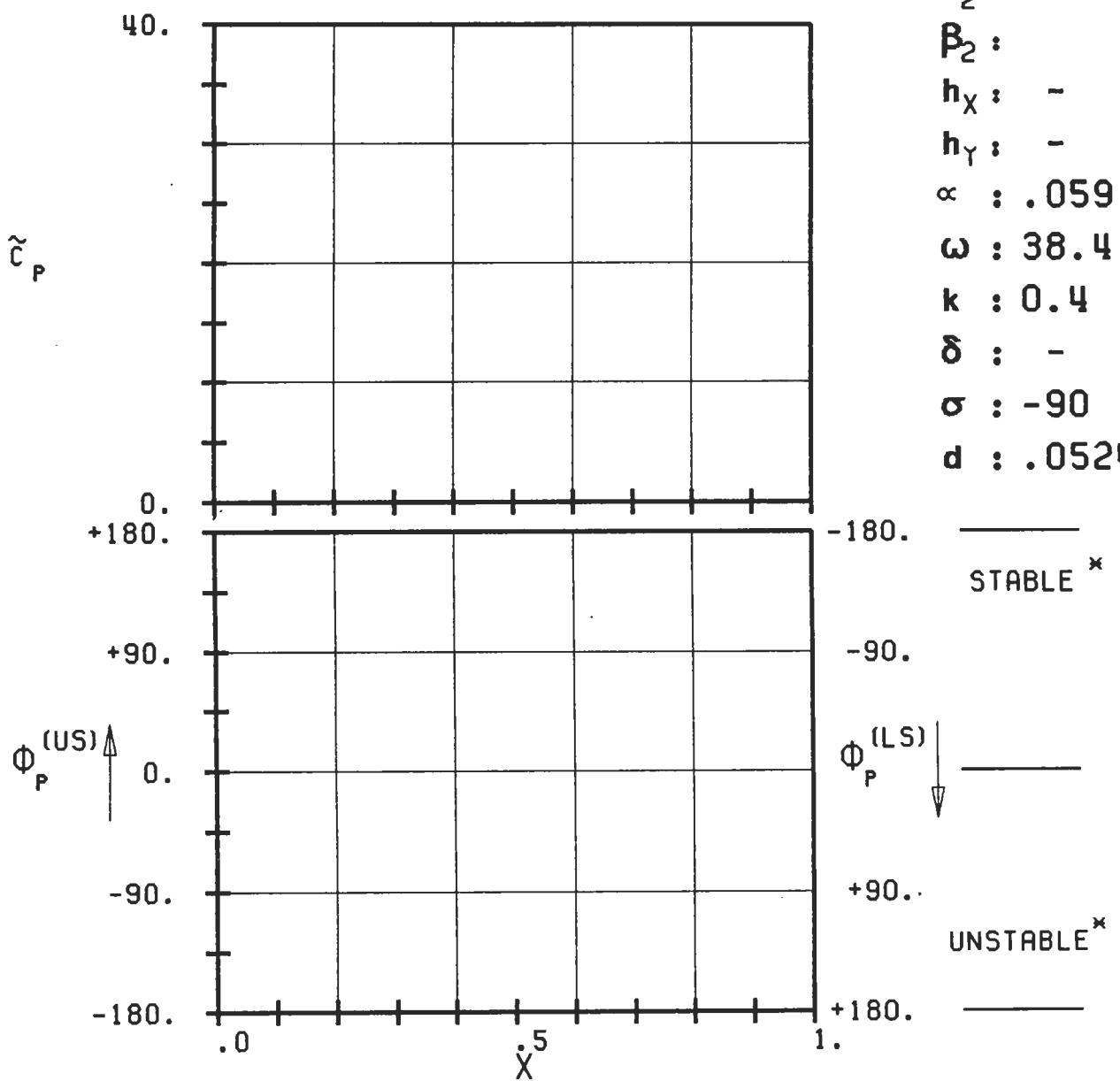
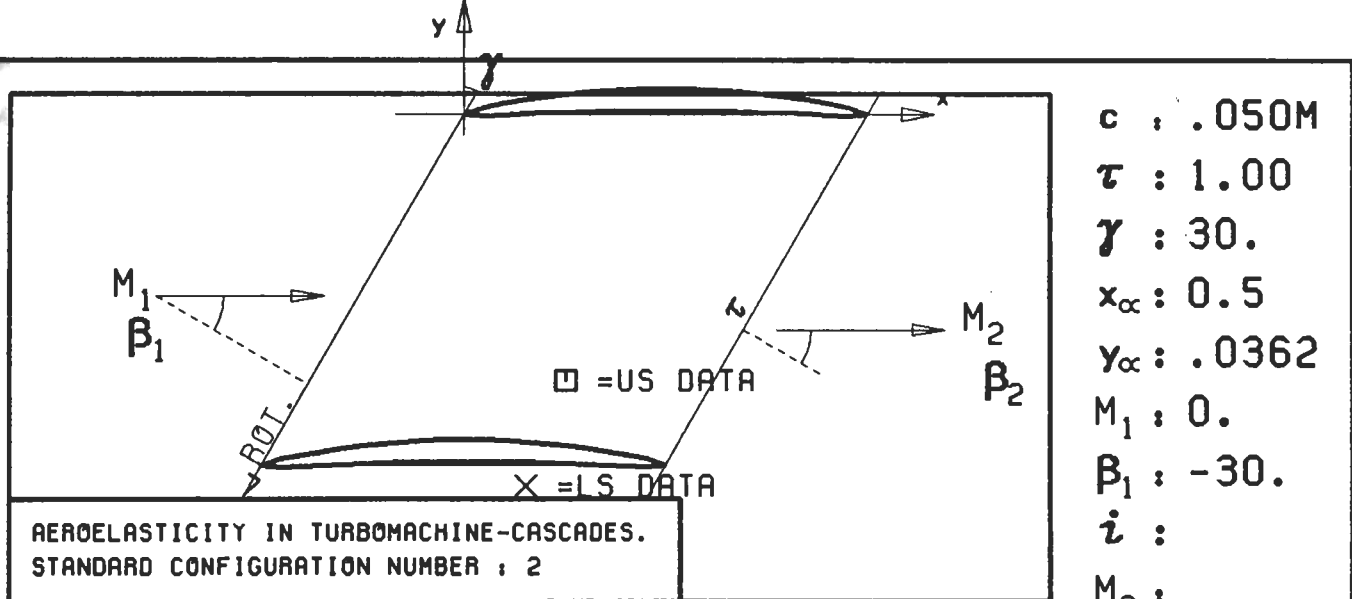


$c : .050M$
 $\tau : 1.00$
 $\gamma : 30.$
 $x_\alpha : 0.5$
 $y_\alpha : .0362$
 $M_1 : 0.$
 $\beta_1 : -30.$
 $i :$
 $M_2 :$
 $\beta_2 :$
 $h_X : -$
 $h_Y : -$
 $\alpha : .059$
 $\omega : 38.4$
 $k : 0.4$
 $\delta : -$
 $\sigma : -135$
 $d : .0524$



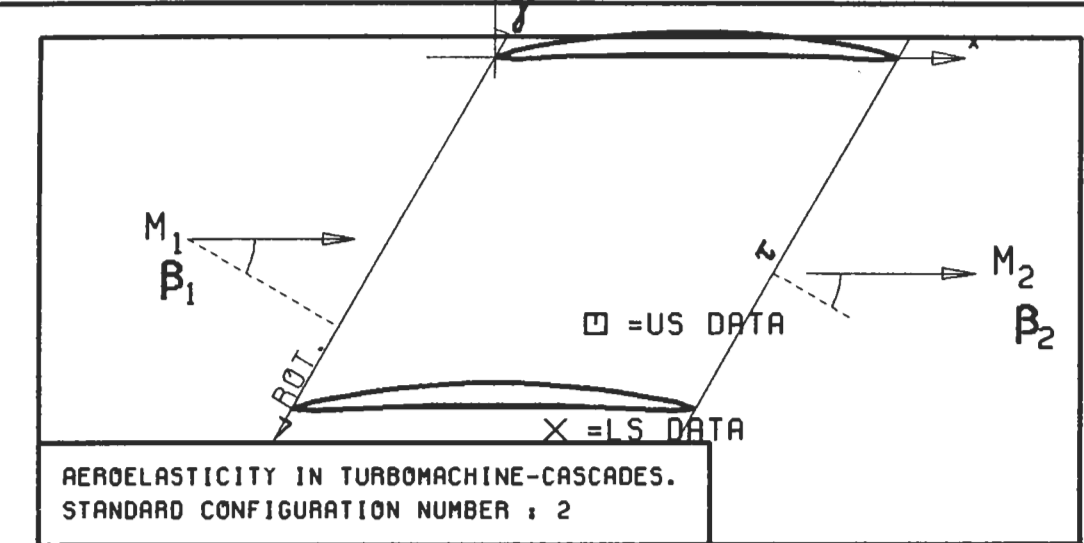
PLOT 7.2-2.1: SECOND STANDARD CONFIGURATION, CASE 1.
MAGNITUDE AND PHASE LEAD OF UNSTEADY BLADE
SURFACE PRESSURE COEFFICIENT.

(x: IN PITCH MODE, NOTATION VALID UPSTREAM OF PITCH AXIS)

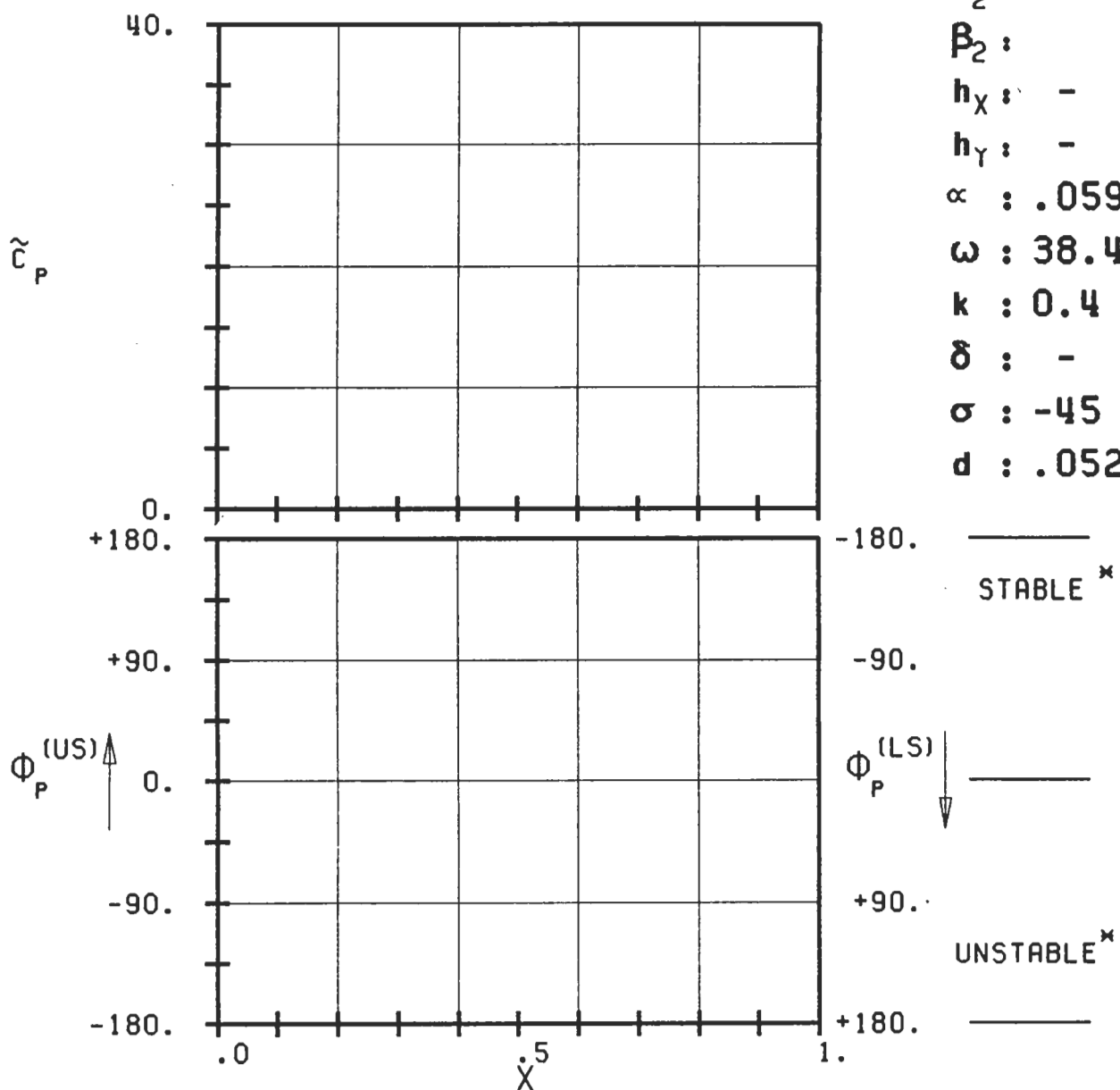


PLOT 7.2-2.2: SECOND STANDARD CONFIGURATION, CASE 2.
 MAGNITUDE AND PHASE LEAD OF UNSTEADY BLADE
 SURFACE PRESSURE COEFFICIENT.

(*: IN PITCH MODE, NOTATION VALID UPSTREAM OF PITCH AXIS)

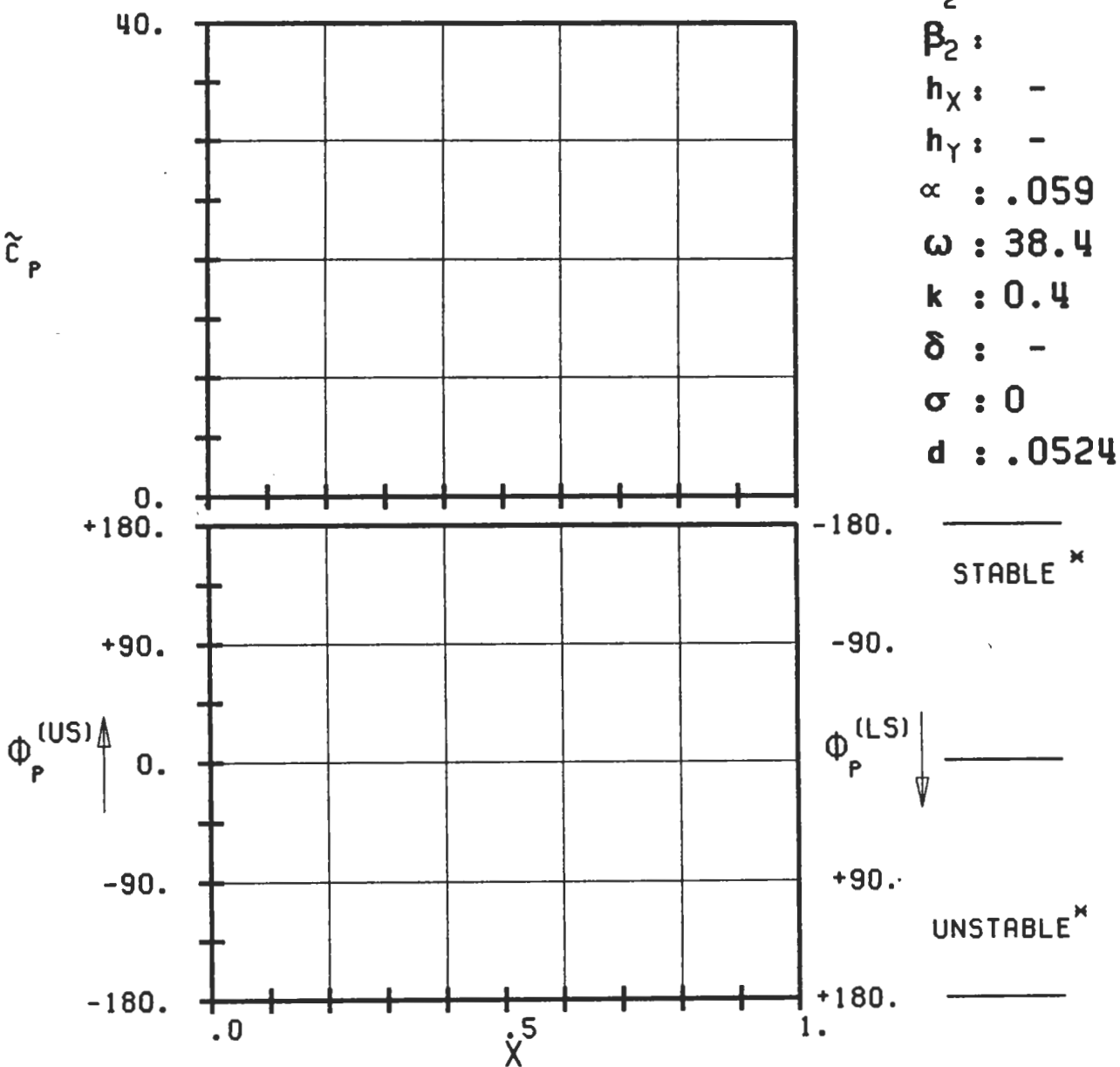
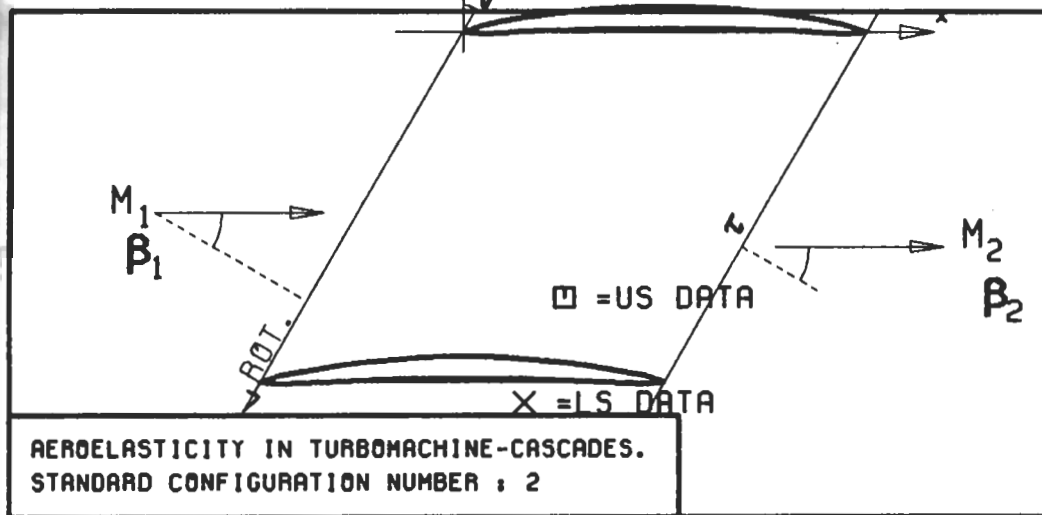


c : .050M
 τ : 1.00
 γ : 30.
 x_∞ : 0.5
 y_∞ : .0362
 M_1 : 0.
 β_1 : -30.
 i :
 M_2 :
 β_2 :
 h_X : -
 h_Y : -
 α : .059
 ω : 38.4
 k : 0.4
 δ : -
 σ : -45
 d : .0524



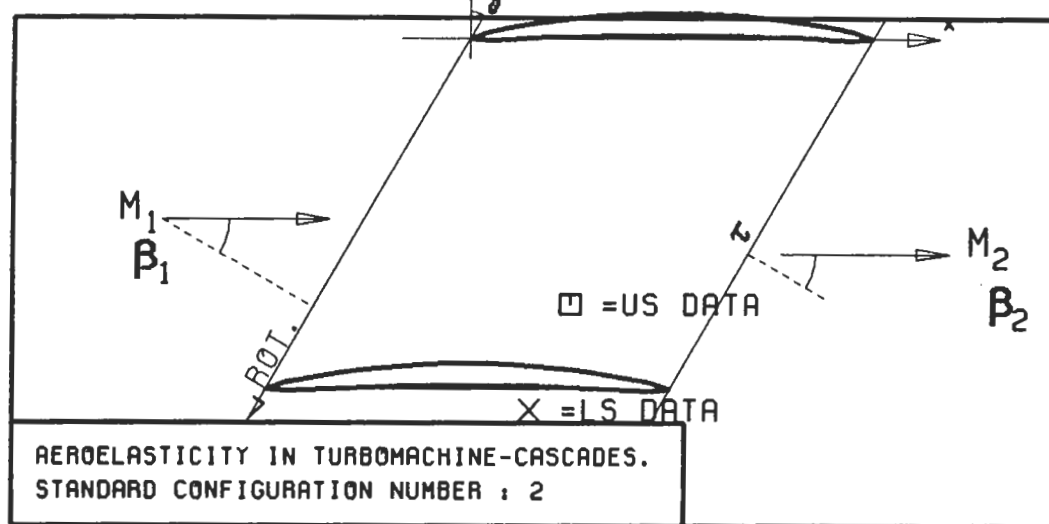
PLOT 7.2-2.3: SECOND STANDARD CONFIGURATION, CASE 3.
MAGNITUDE AND PHASE LEAD OF UNSTEADY BLADE SURFACE PRESSURE COEFFICIENT.

(\times : IN PITCH MODE, NOTATION VALID UPSTREAM OF PITCH AXIS)

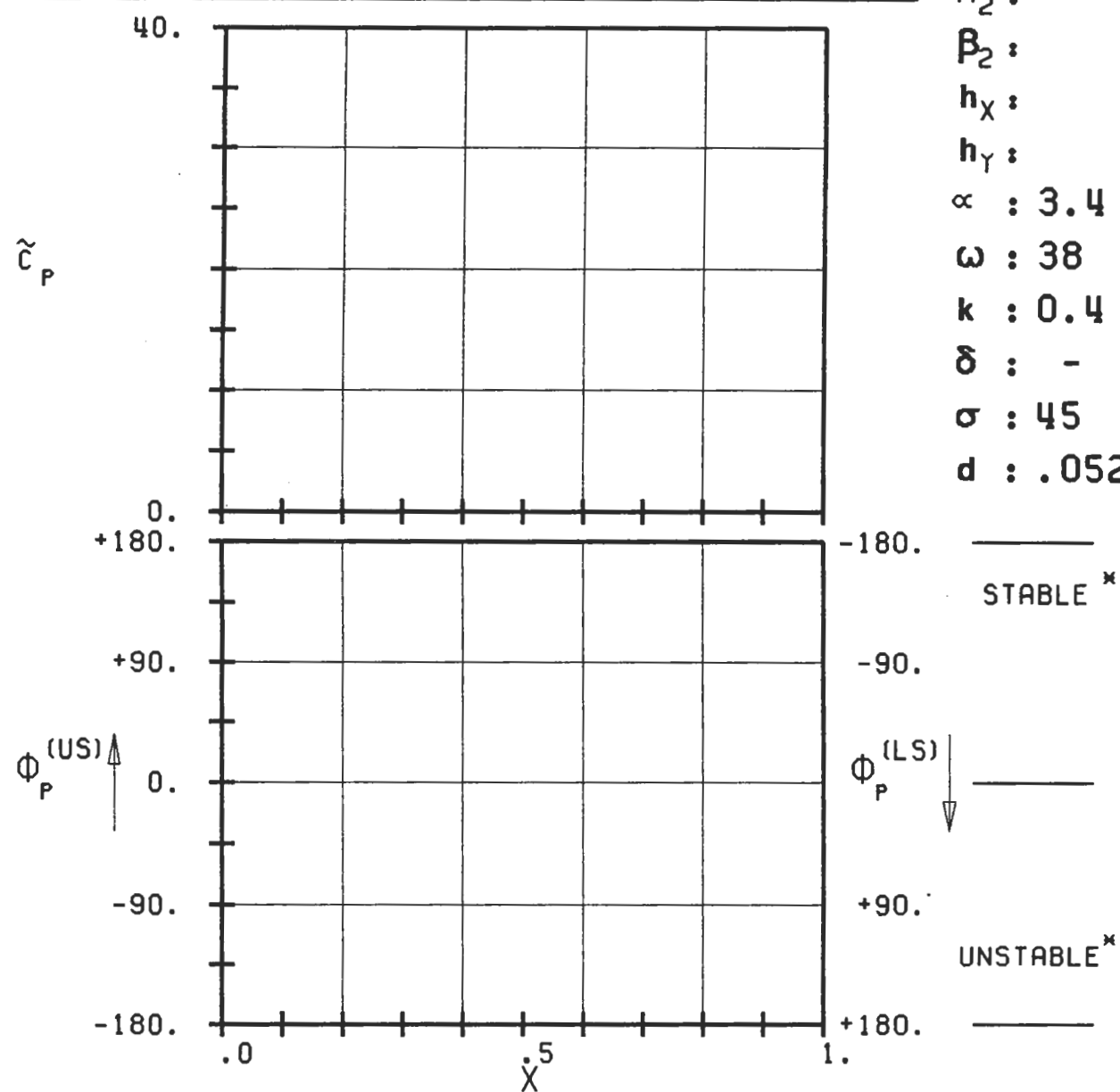


PLOT 7.2-2.4: SECOND STANDARD CONFIGURATION, CASE 4.
MAGNITUDE AND PHASE LEAD OF UNSTEADY BLADE
SURFACE PRESSURE COEFFICIENT.

(*: IN PITCH MODE, NOTATION VALID UPSTREAM OF PITCH AXIS)

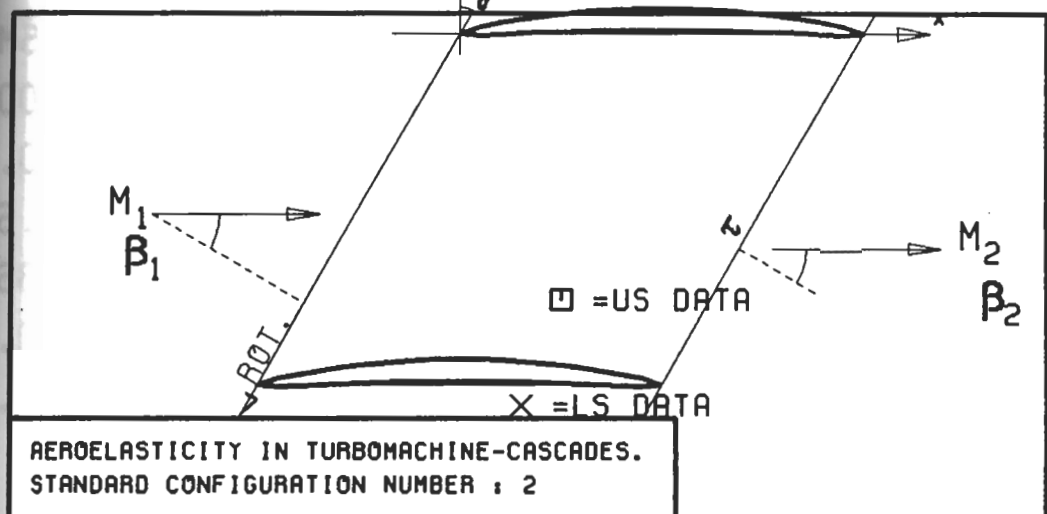


c : .050M
 τ : 1.00
 γ : 30.
 x_∞ : 0.5
 y_∞ : .0362
 M_1 : -
 B_1 : -30.
 i :
 M_2 :
 B_2 :
 h_X :
 h_Y :
 α : 3.4
 ω : 38
 k : 0.4
 δ : -
 σ : 45
 d : .0524

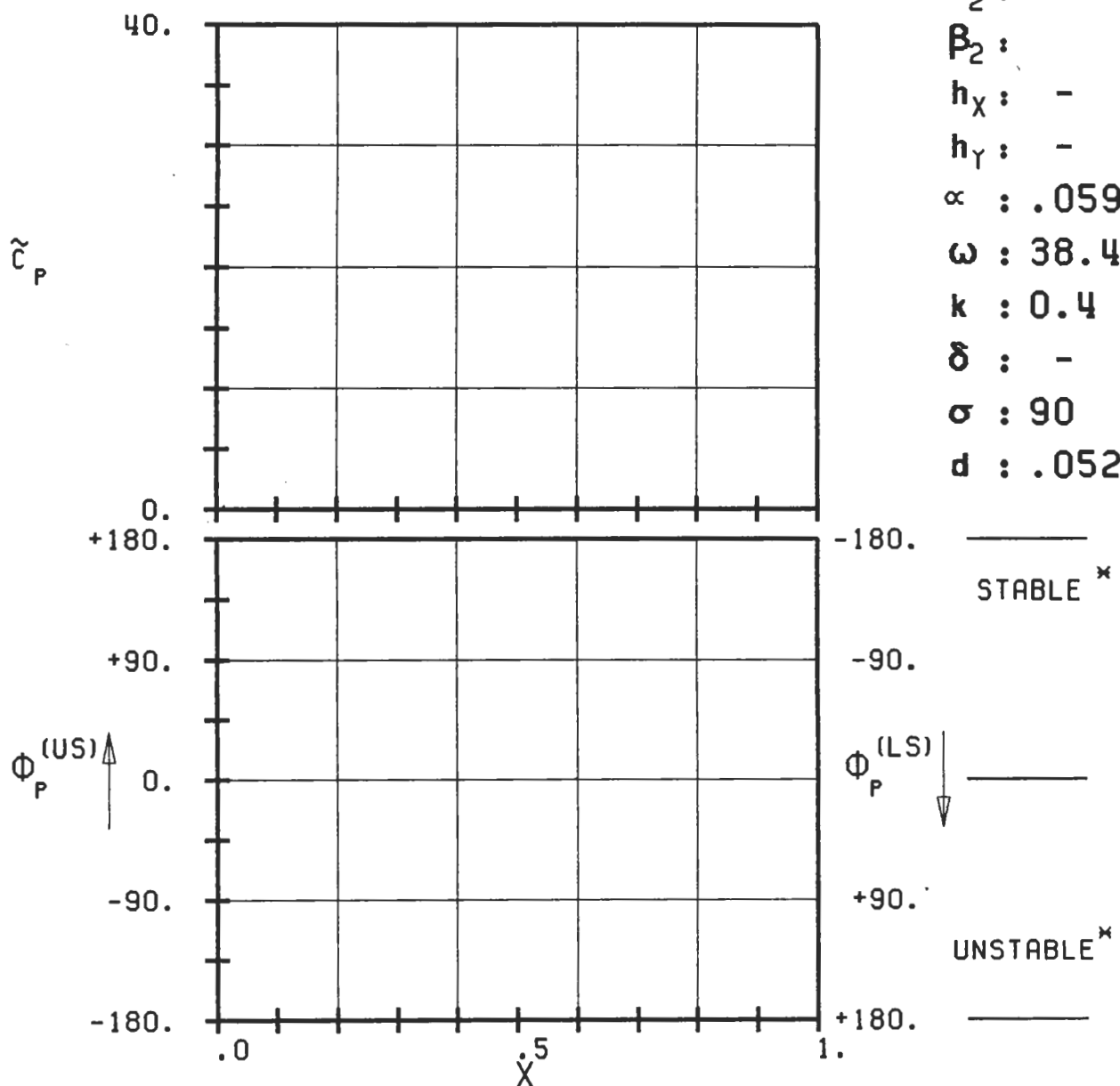


PLOT 7.2-2.5: SECOND STANDARD CONFIGURATION, CASE 5.
MAGNITUDE AND PHASE LEAD OF UNSTEADY BLADE SURFACE PRESSURE COEFFICIENT.

(*: IN PITCH MODE, NOTATION VALID UPSTREAM OF PITCH AXIS)



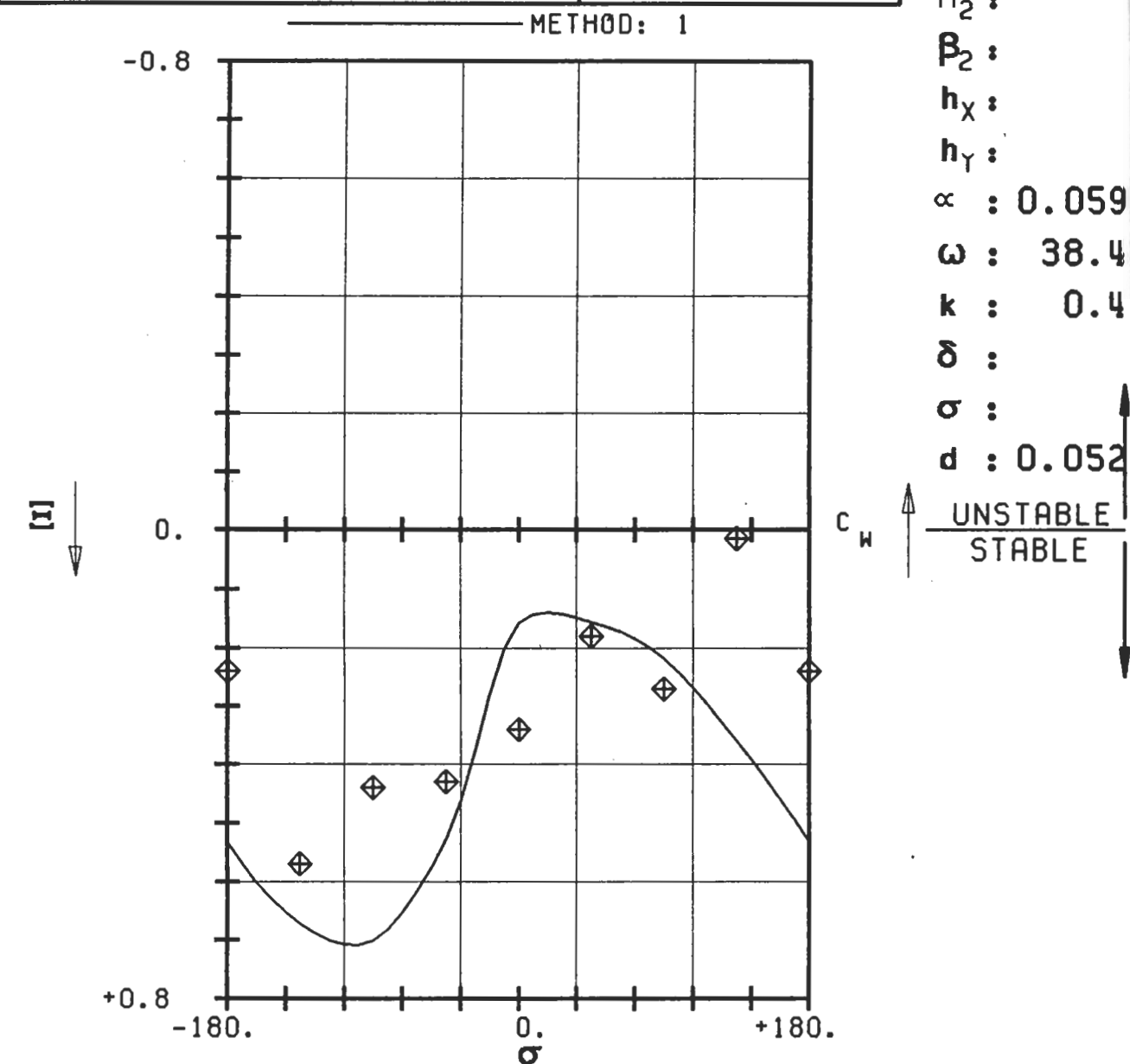
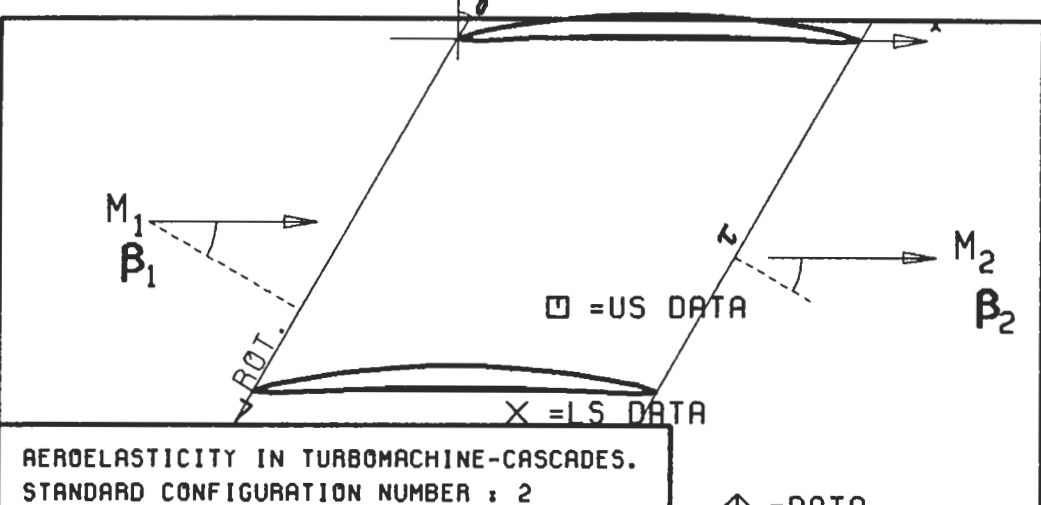
c : .050M
 τ : 1.00
 γ : 30.
 x_α : 0.5
 y_α : .0362
 M_1 : 0.
 β_1 : -30.
 i :
 M_2 :
 β_2 :
 h_X : -
 h_Y : -
 α : .059
 ω : 38.4
 k : 0.4
 δ : -
 σ : 90
 d : .0524



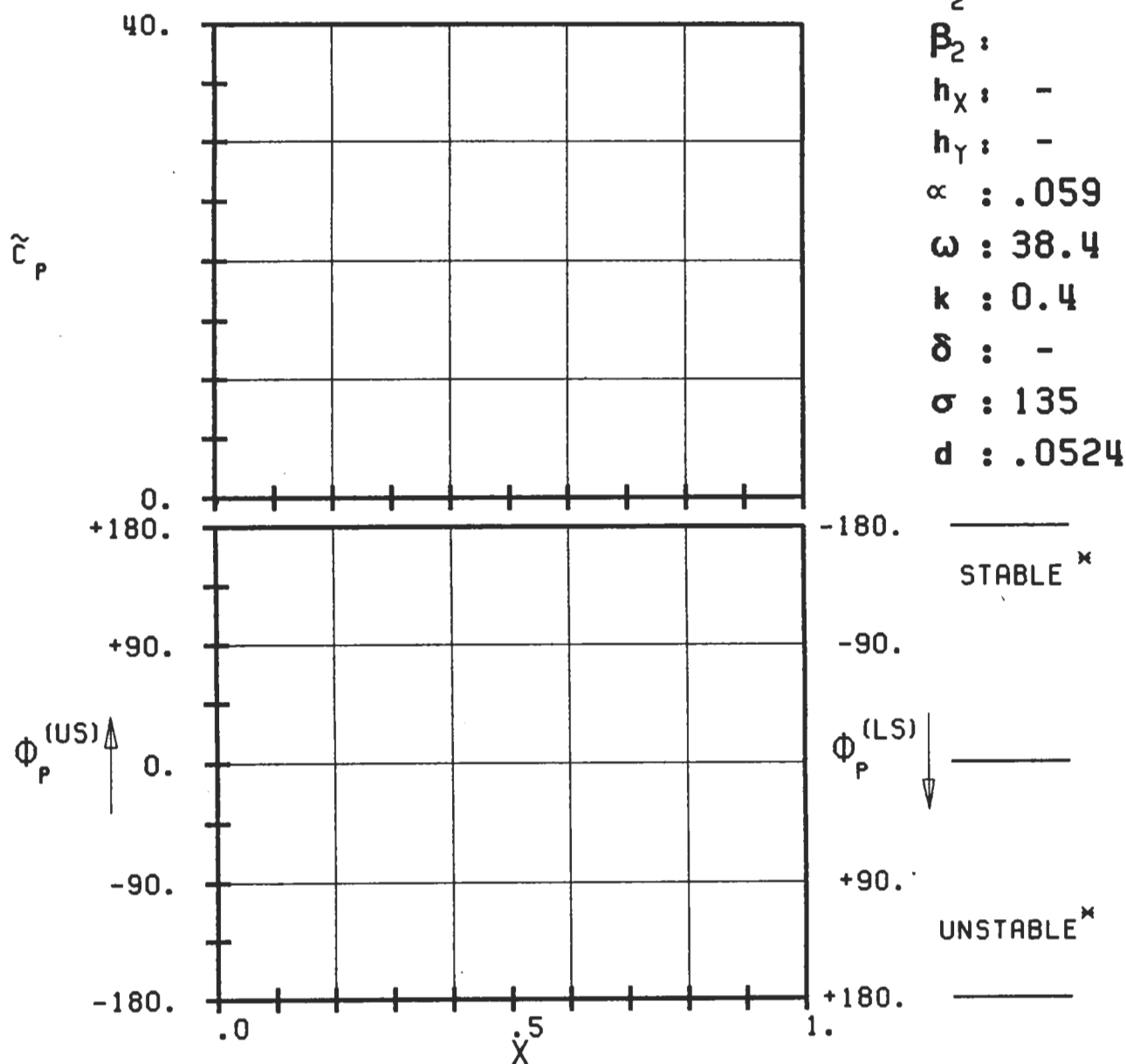
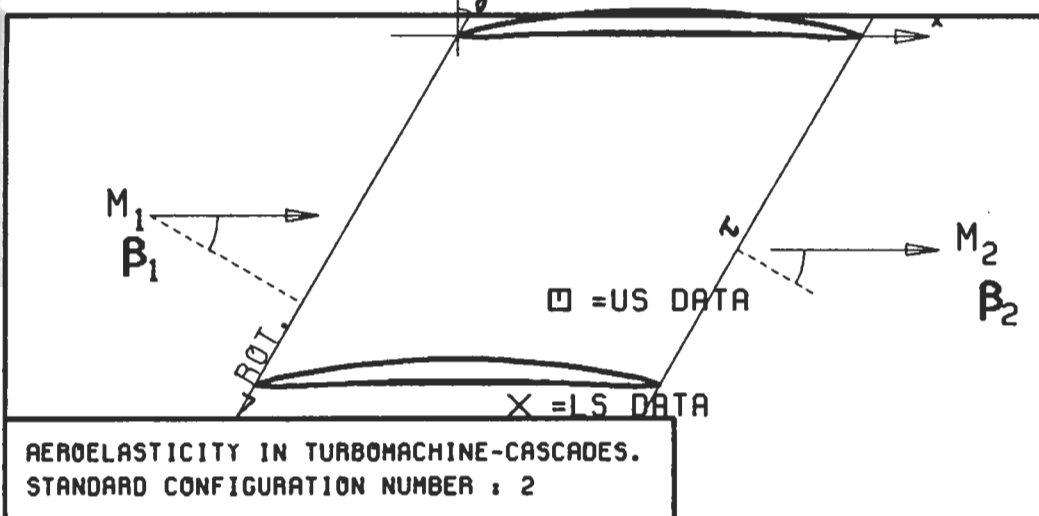
PLOT 7.2-2.6: SECOND STANDARD CONFIGURATION, CASE 6.
MAGNITUDE AND PHASE LEAD OF UNSTEADY BLADE
SURFACE PRESSURE COEFFICIENT.

(x: IN PITCH MODE, NOTATION VALID UPSTREAM OF PITCH AXIS)

Fig. 7.2-2d

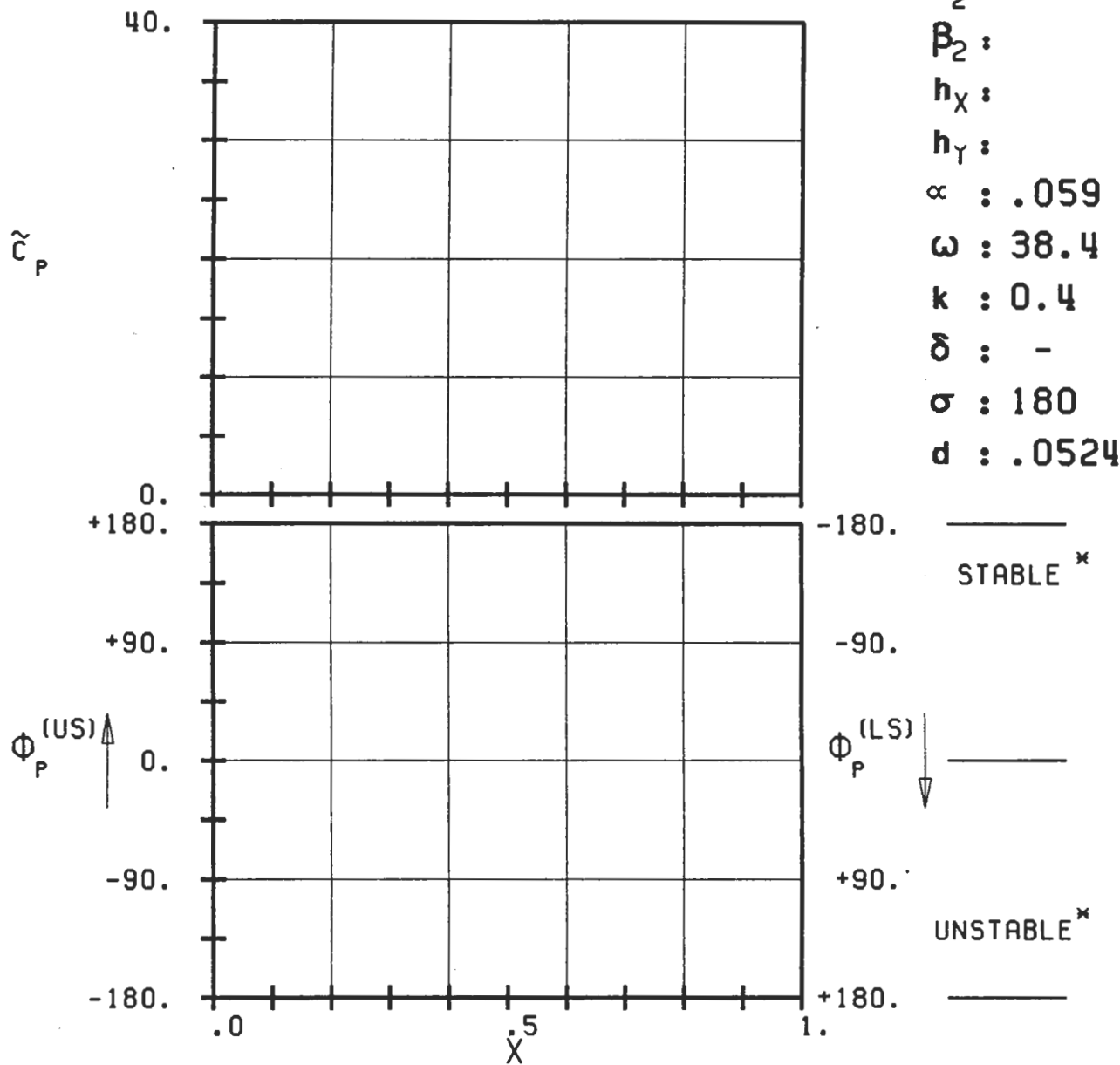
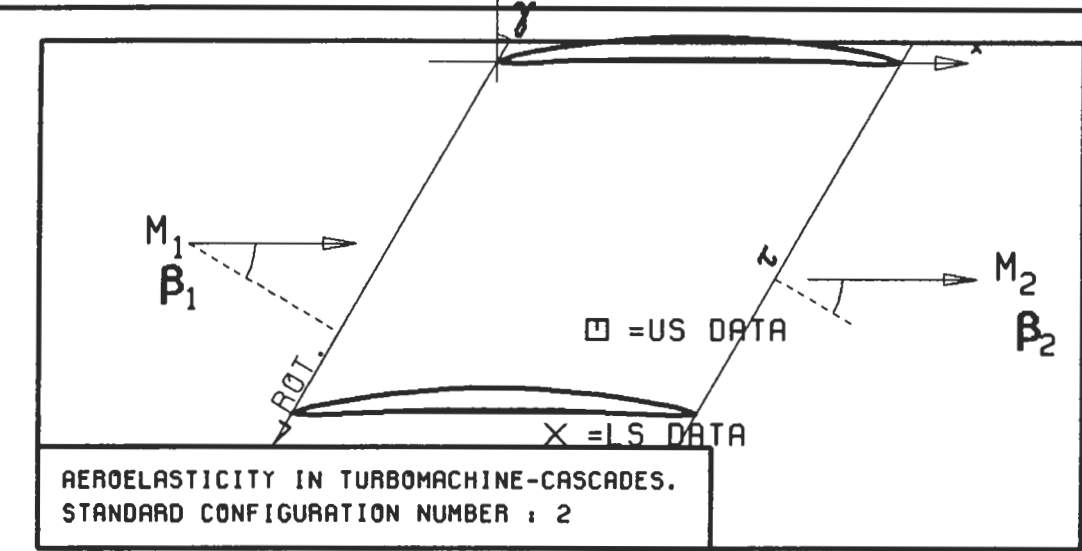


PLOT 7.2-6.1: SECOND STANDARD CONFIGURATION CASES 1-8.
AERODYNAMIC WORK AND DAMPING COEFFICIENTS
IN DEPENDENCE OF INTERBLADE PHASE ANGLE.



PLT 7.2-2.7: SECOND STANDARD CONFIGURATION, CASE 7.
MAGNITUDE AND PHASE LEAD OF UNSTEADY BLADE
SURFACE PRESSURE COEFFICIENT.

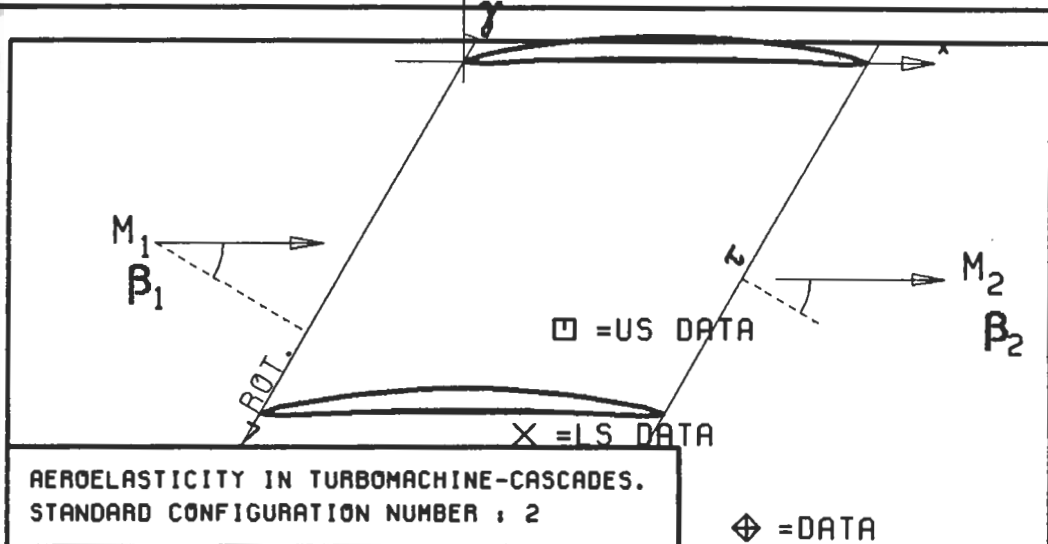
(x: IN PITCH MODE, NOTATION VALID UPSTREAM OF PITCH AXIS)



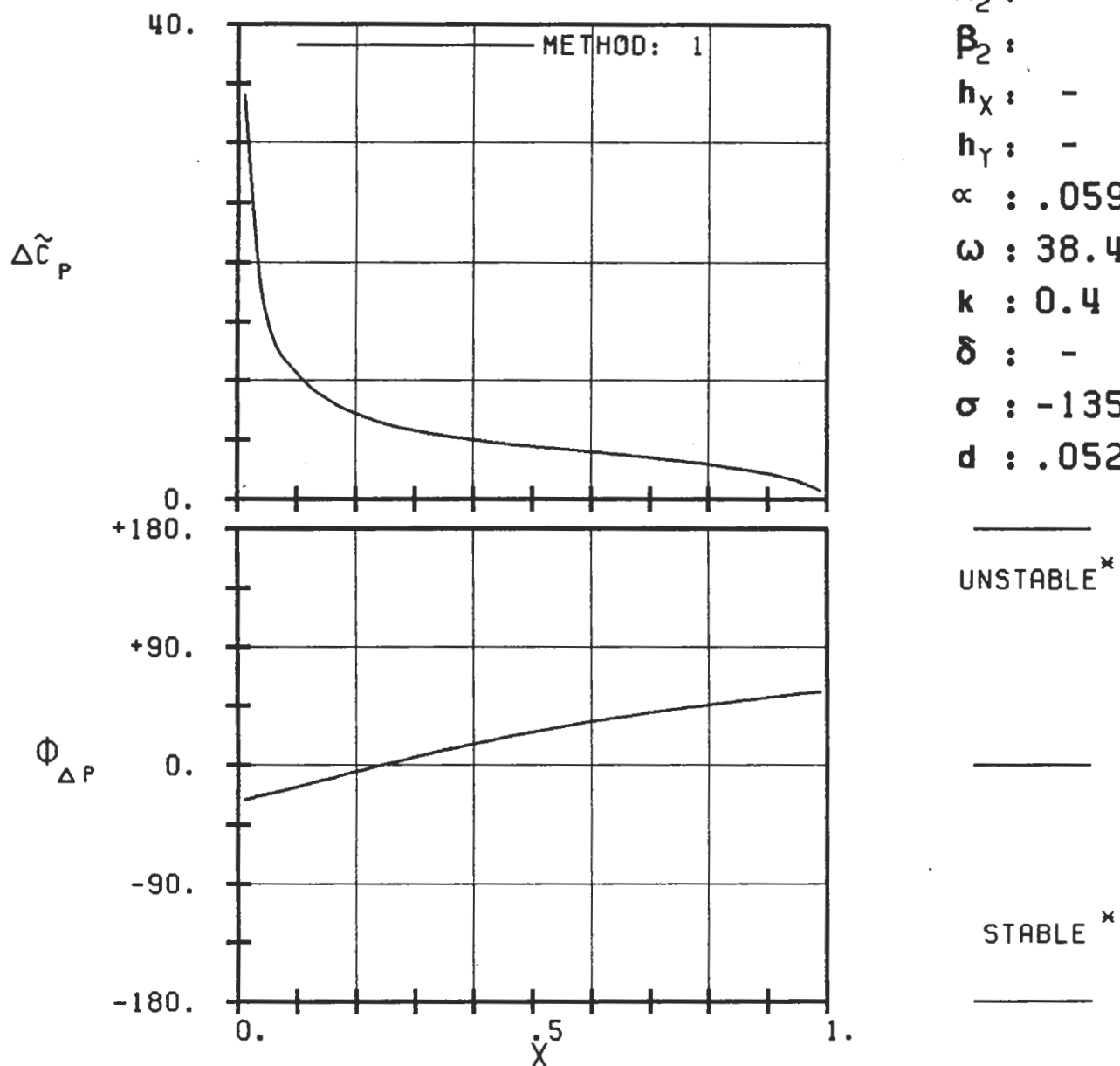
PLOT 7.2-2.8: SECOND STANDARD CONFIGURATION, CASE 8.
MAGNITUDE AND PHASE LEAD OF UNSTEADY BLADE
SURFACE PRESSURE COEFFICIENT.

(x : IN PITCH MODE, NOTATION VALID UPSTREAM OF PITCH AXIS)

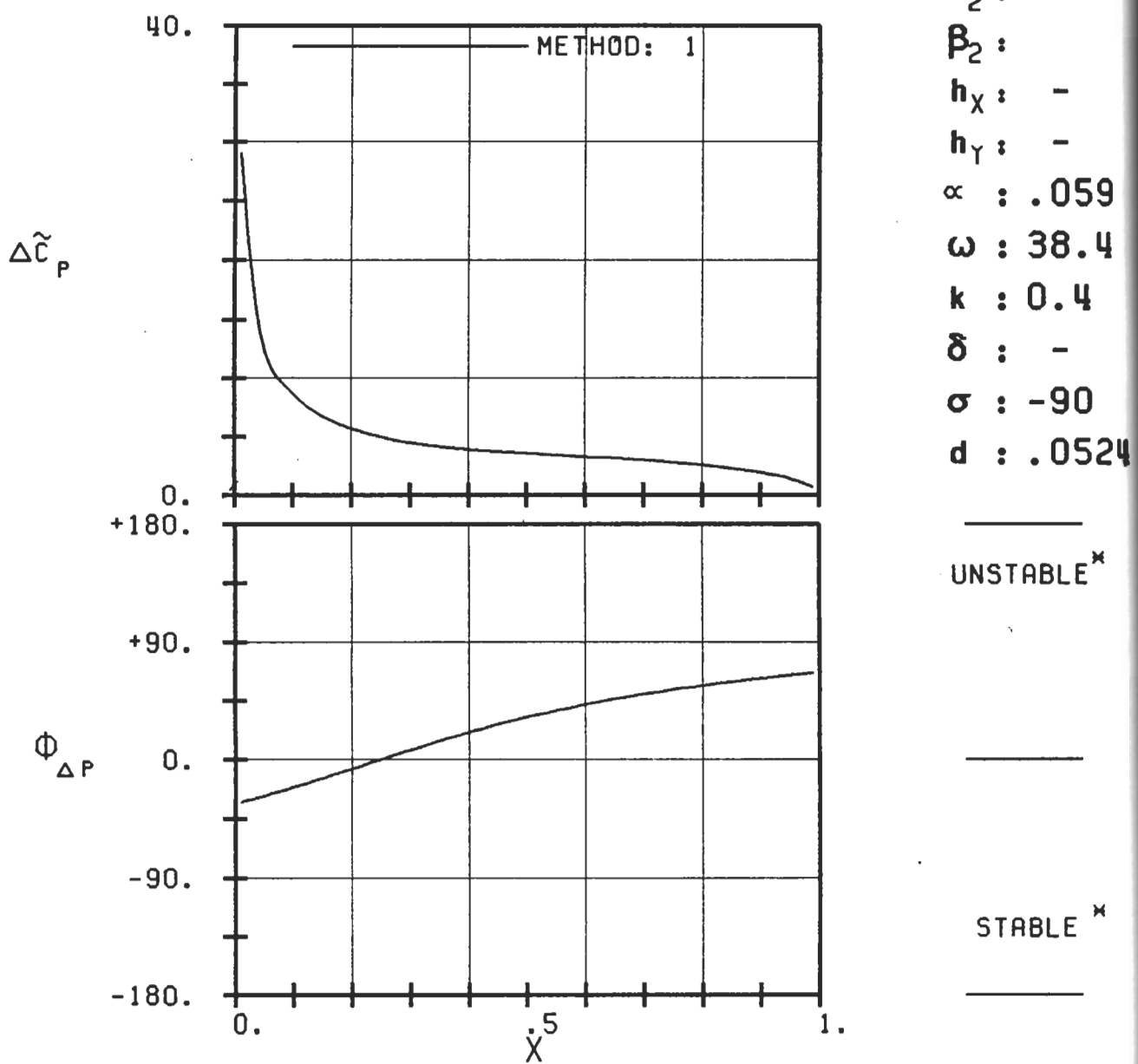
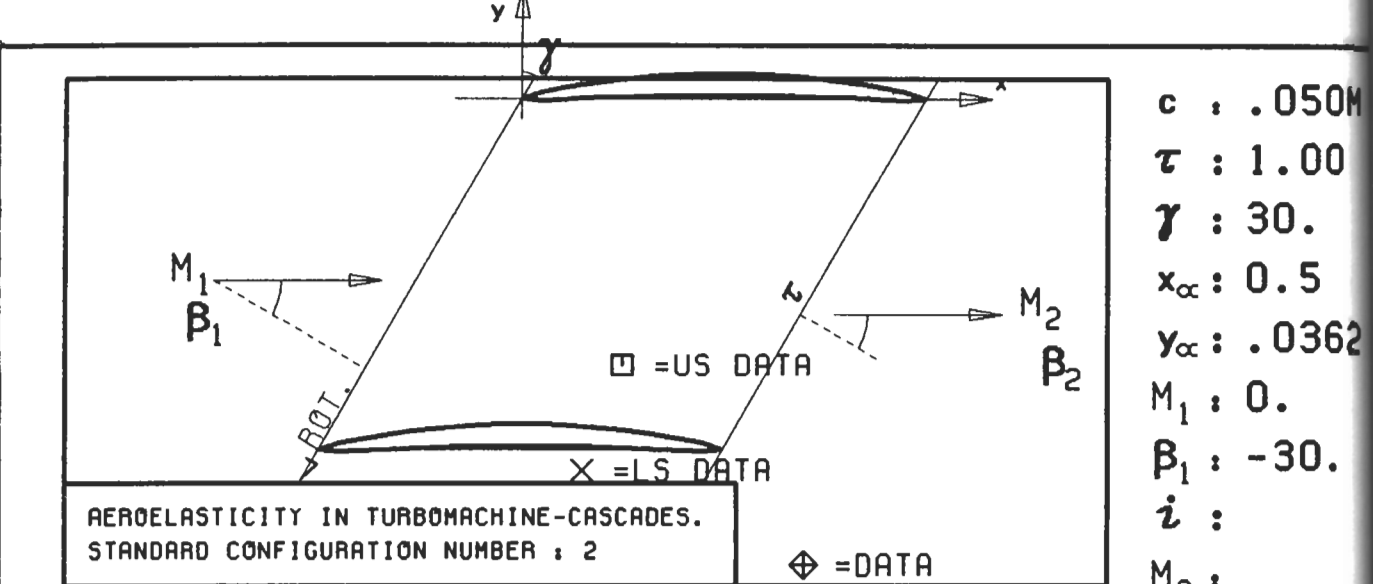
Fig 7.2-2a



$c : .050M$
 $\tau : 1.00$
 $\gamma : 30.$
 $x_\alpha : 0.5$
 $y_\alpha : .0362$
 $M_1 : -$
 $\beta_1 : -30.$
 $i :$
 $M_2 :$
 $\beta_2 :$
 $h_X : -$
 $h_Y : -$
 $\alpha : .059$
 $\omega : 38.4$
 $k : 0.4$
 $\delta : -$
 $\sigma : -135$
 $d : .0524$

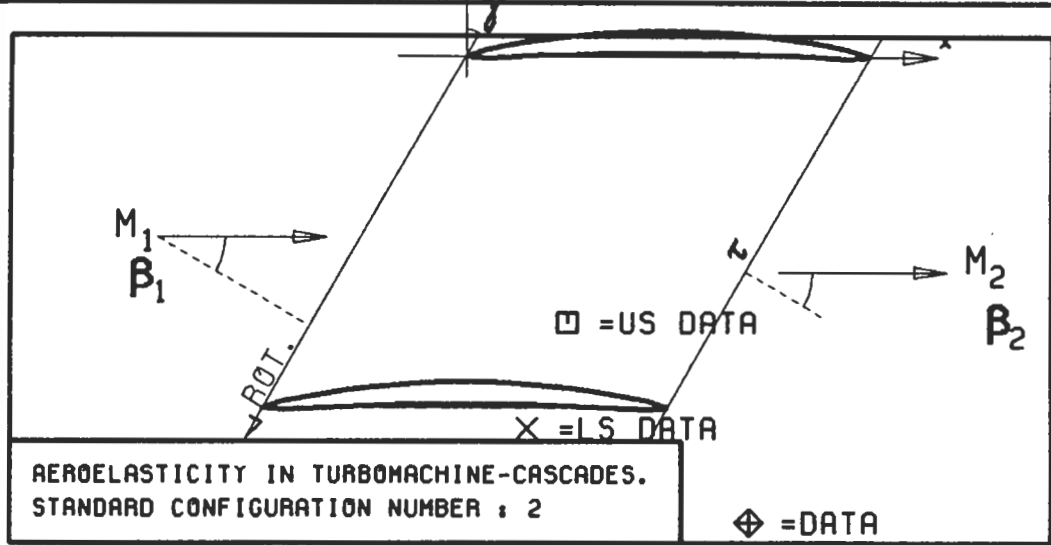


PLOT 7.2-3.1: SECOND STANDARD CONFIGURATION, CASE 1.
 MAGNITUDE AND PHASE LEAD OF UNSTEADY BLADE
 SURFACE PRESSURE DIFFERENCE COEFFICIENT.
 (\times : IN PITCH MODE, NOTATION VALID UPSTREAM OF PITCH AXIS)

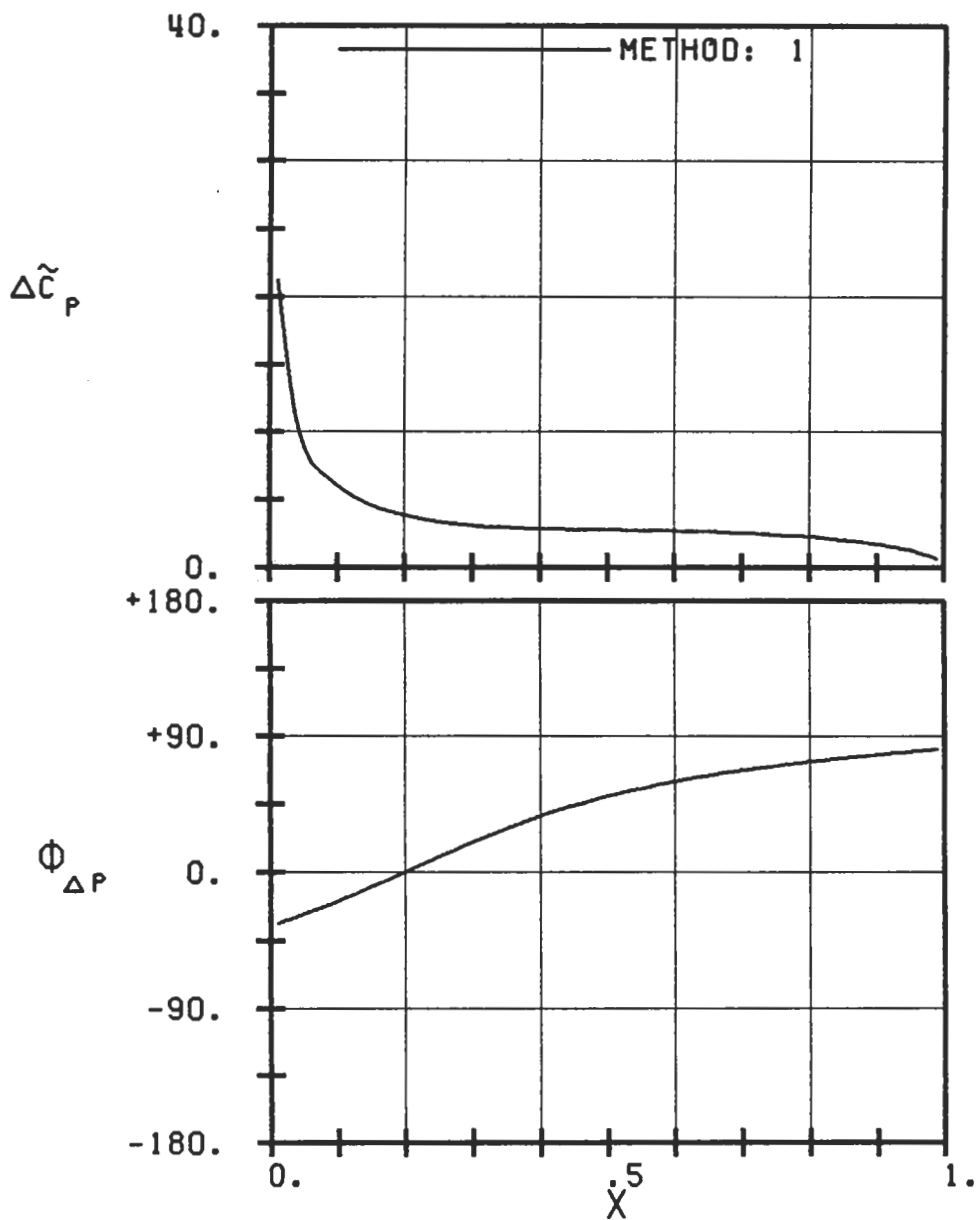


PLOT 7.2-3.2: SECOND STANDARD CONFIGURATION, CASE 2.
 MAGNITUDE AND PHASE LEAD OF UNSTEADY BLADE
 SURFACE PRESSURE DIFFERENCE COEFFICIENT.

(*: IN PITCH MODE, NOTATION VALID UPSTREAM OF PITCH AXIS)



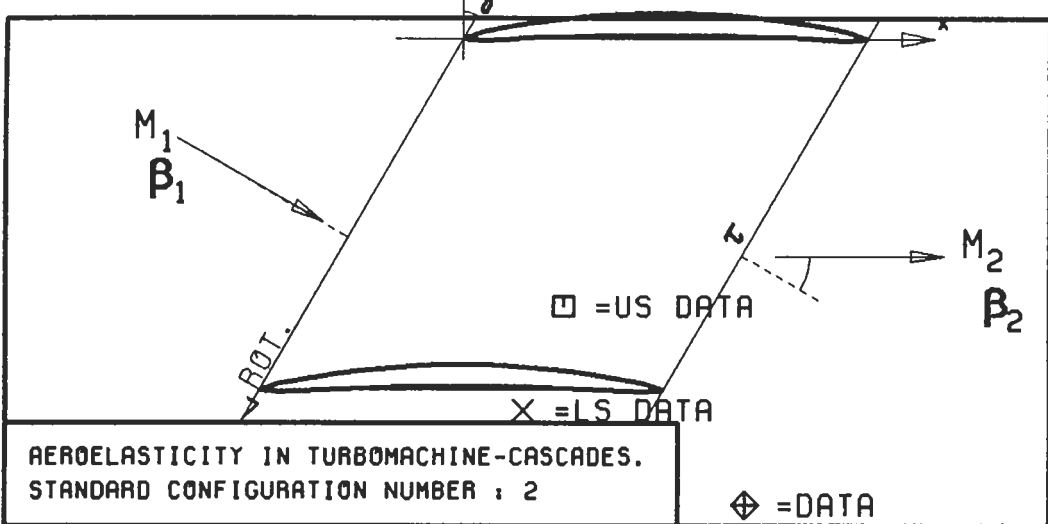
c : .050M
 τ : 1.00
 γ : 30.
 x_α : 0.5
 y_α : .0362
 M_1 : 0.
 β_1 : -30.
 i :
 M_2 :
 β_2 :
 h_X : -
 h_Y : -
 α : .059
 ω : 38.4
 k : 0.4
 δ : -
 σ : -45
 d : .0524



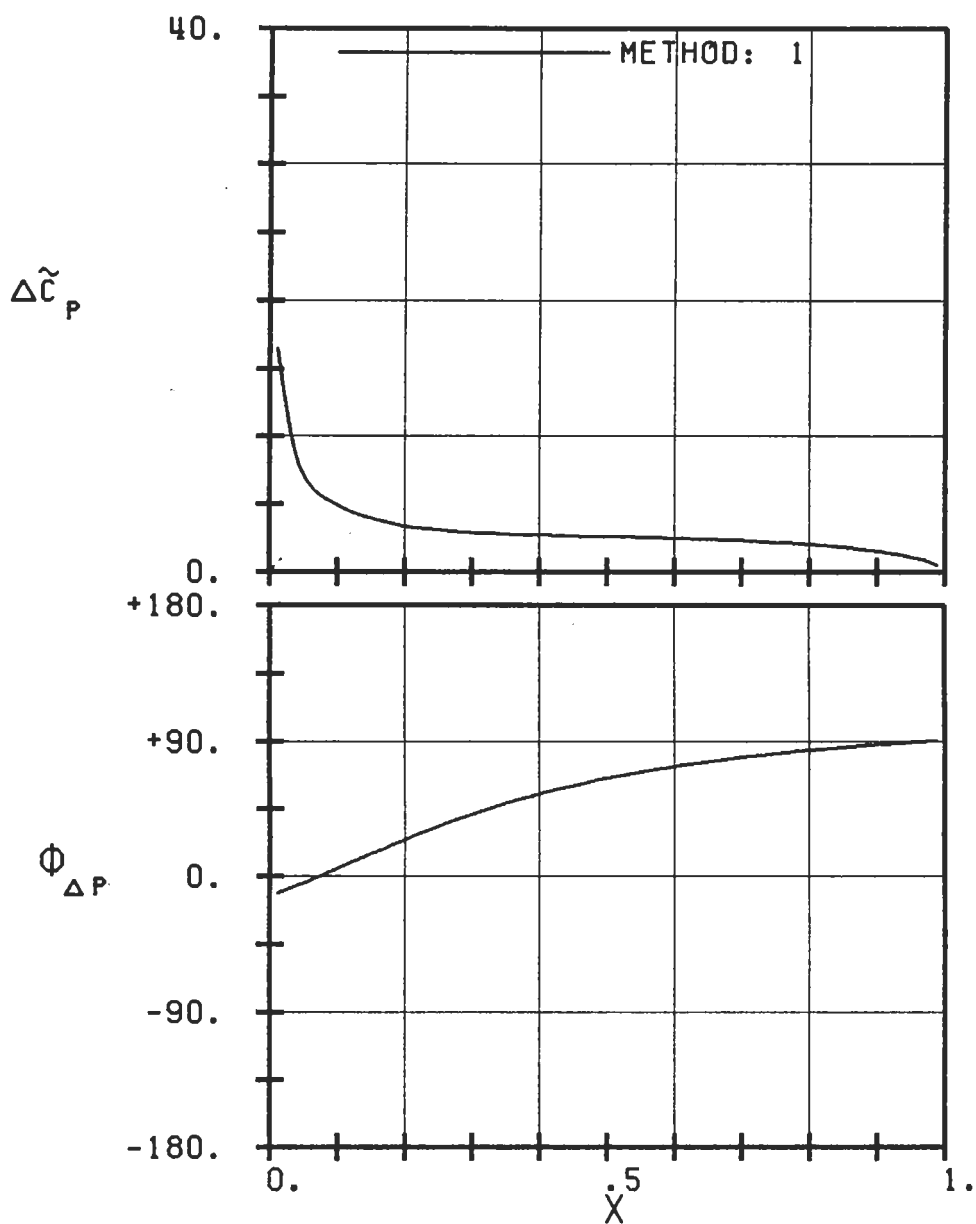
PLOT 7.2-3.3: SECOND STANDARD CONFIGURATION, CASE 3.
MAGNITUDE AND PHASE LEAD OF UNSTEADY BLADE SURFACE PRESSURE DIFFERENCE COEFFICIENT.

(\times : IN PITCH MODE, NOTATION VALID UPSTREAM OF PITCH AXIS)

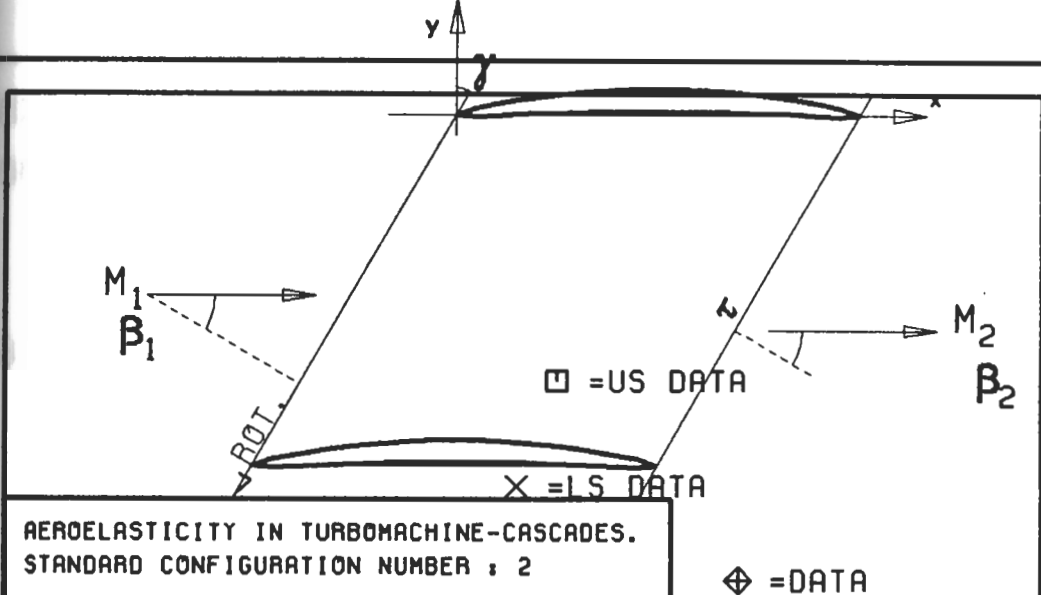
Fig 7.2-2b



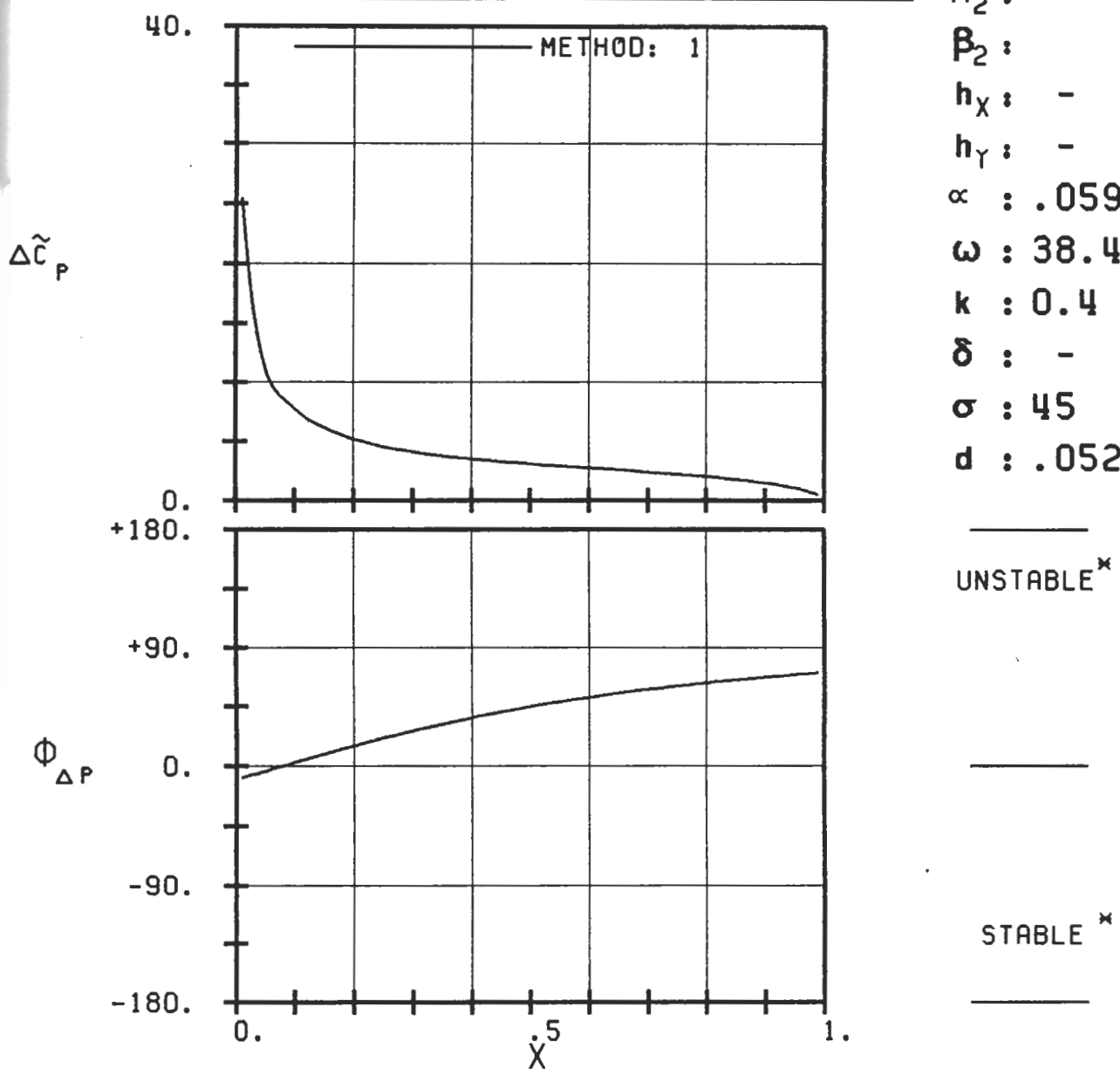
$c : .050M$
 $\tau : 1.00$
 $\gamma : 30.$
 $x_\alpha : 0.5$
 $y_\alpha : .0362$
 $M_1 : 0.$
 $\beta_1 : -30$
 $i :$
 $M_2 :$
 $\beta_2 :$
 $h_x : -$
 $h_y : -$
 $\alpha : .059$
 $\omega : 38.4$
 $k : 0.4$
 $\delta : -$
 $\sigma : 0$
 $d : .0524$



PLOT 7.2-3.4: SECOND STANDARD CONFIGURATION, CASE 4.
MAGNITUDE AND PHASE LEAD OF UNSTEADY BLADE
SURFACE PRESSURE DIFFERENCE COEFFICIENT.
(\times : IN PITCH MODE, NOTATION VALID UPSTREAM OF PITCH AXIS)

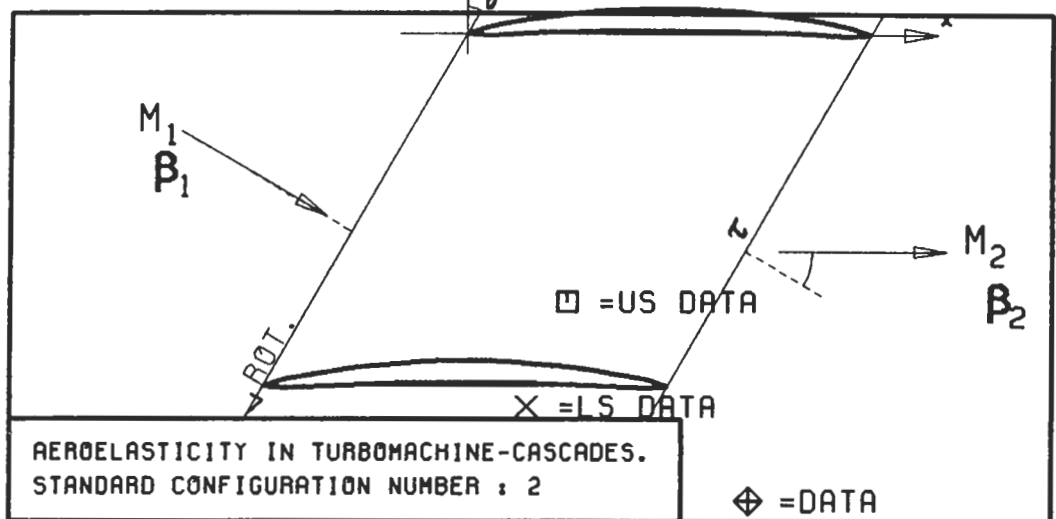


c : .050M
 τ : 1.00
 γ : 30.
 x_α : 0.5
 y_α : .0362
 M_1 : 0.
 B_1 : -30.
 i :
 M_2 :
 B_2 :
 h_X : -
 h_Y : -
 α : .059
 ω : 38.4
 k : 0.4
 δ : -
 σ : 45
 d : .0524

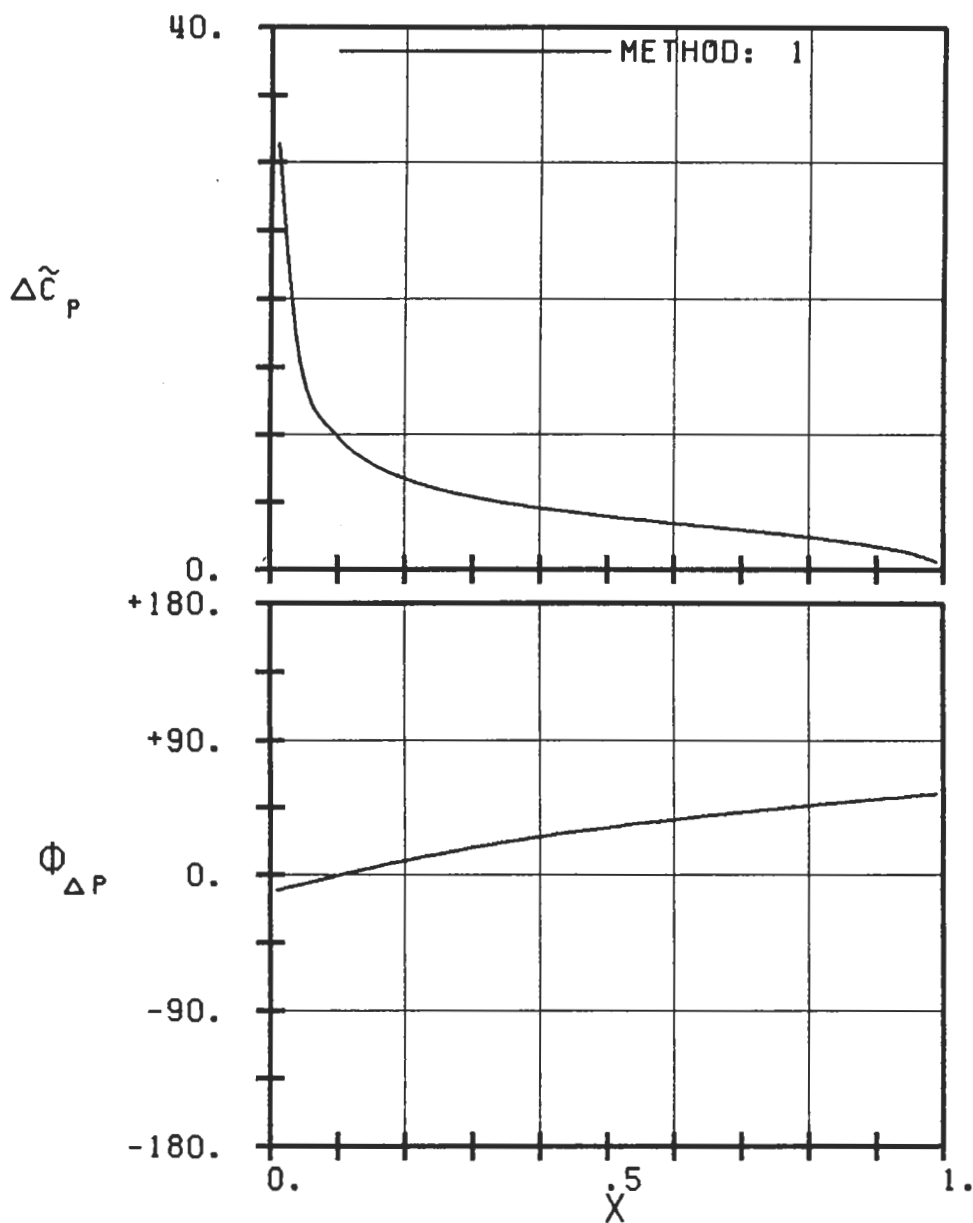


PLOT 7.2-3.5: SECOND STANDARD CONFIGURATION, CASE 5.
MAGNITUDE AND PHASE LEAD OF UNSTEADY BLADE
SURFACE PRESSURE DIFFERENCE COEFFICIENT.

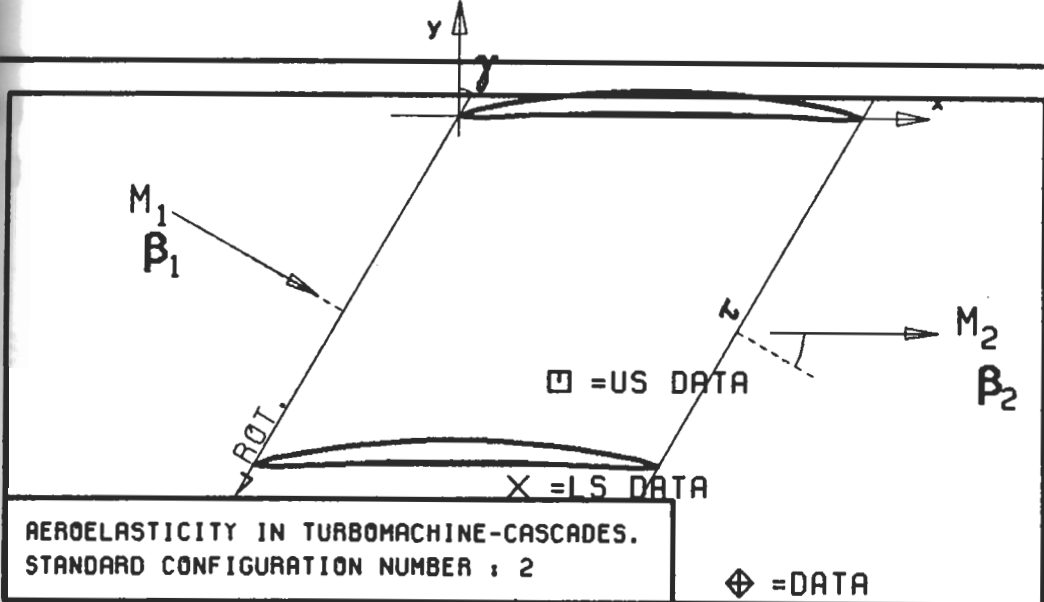
(X: IN PITCH MODE, NOTATION VALID UPSTREAM OF PITCH AXIS)



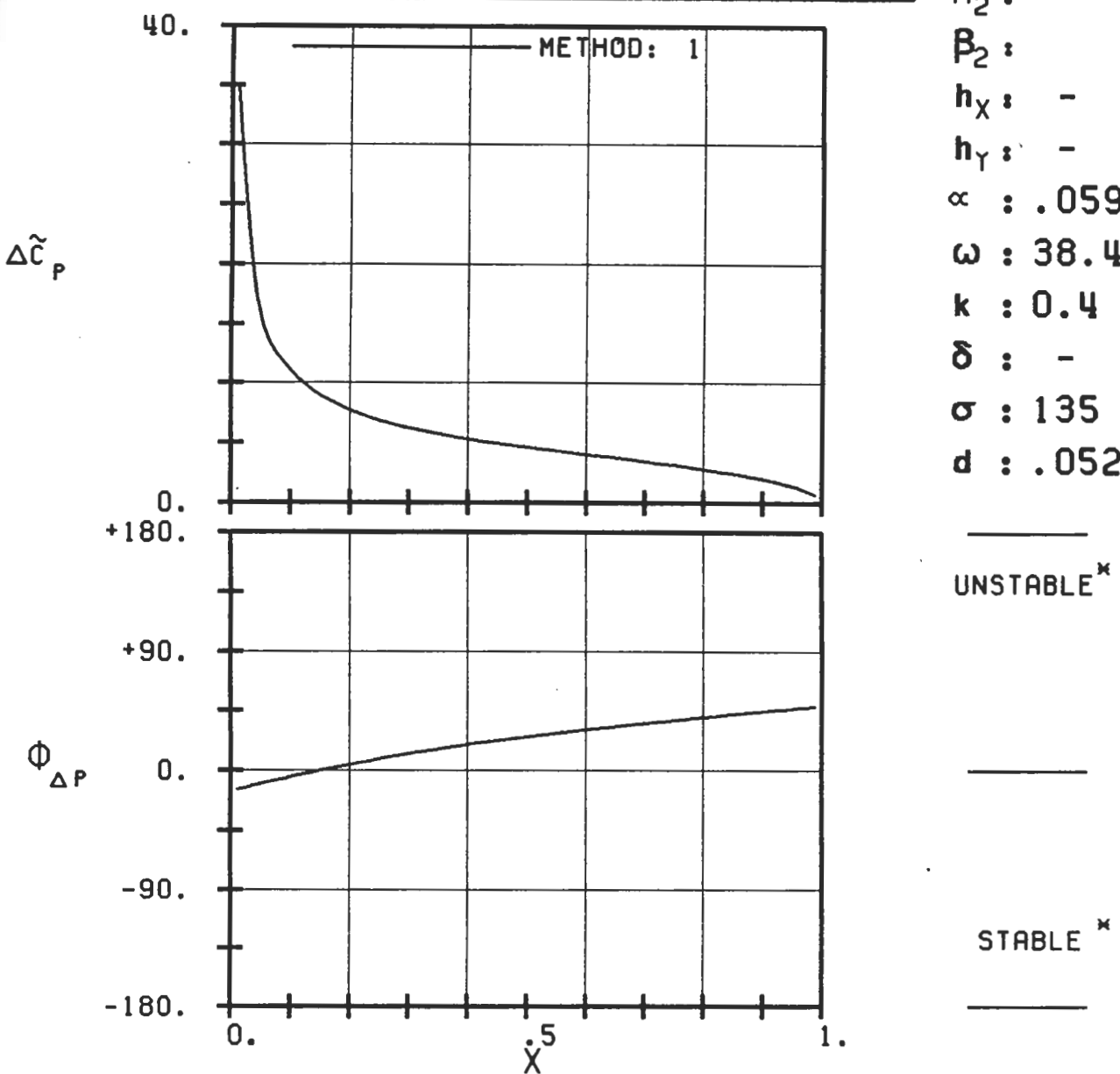
$c : .050M$
 $\tau : 1.00$
 $\gamma : 30.$
 $x_\alpha : 0.5$
 $y_\alpha : .0362$
 $M_1 : 0.$
 $\beta_1 : -30$
 $i :$
 $M_2 :$
 $\beta_2 :$
 $h_X : -$
 $h_Y : -$
 $\alpha : .059$
 $\omega : 38.4$
 $k : 0.4$
 $\delta : -$
 $\sigma : 90$
 $d : .0524$



PLOT 7.2-3.6: SECOND STANDARD CONFIGURATION, CASE 6.
MAGNITUDE AND PHASE LEAD OF UNSTEADY BLADE
SURFACE PRESSURE DIFFERENCE COEFFICIENT.
(x: IN PITCH MODE, NOTATION VALID UPSTREAM OF PITCH AXIS)



c : .050M
 τ : 1.00
 γ : 30.
 x_∞ : 0.5
 y_∞ : .0362
 M_1 : 0.
 β_1 : -30
 i :
 M_2 :
 β_2 :
 h_X : -
 h_Y : -
 α : .059
 ω : 38.4
 k : 0.4
 δ : -
 σ : 135
 d : .0524



PLOT 7.2-3.7: SECOND STANDARD CONFIGURATION, CASE 7.
 MAGNITUDE AND PHASE LEAD OF UNSTEADY BLADE
 SURFACE PRESSURE DIFFERENCE COEFFICIENT.
 (\times : IN PITCH MODE, NOTATION VALID UPSTREAM OF PITCH AXIS)

M_1

β_1

ROT

ω

M_2

β_2

□ = US DATA

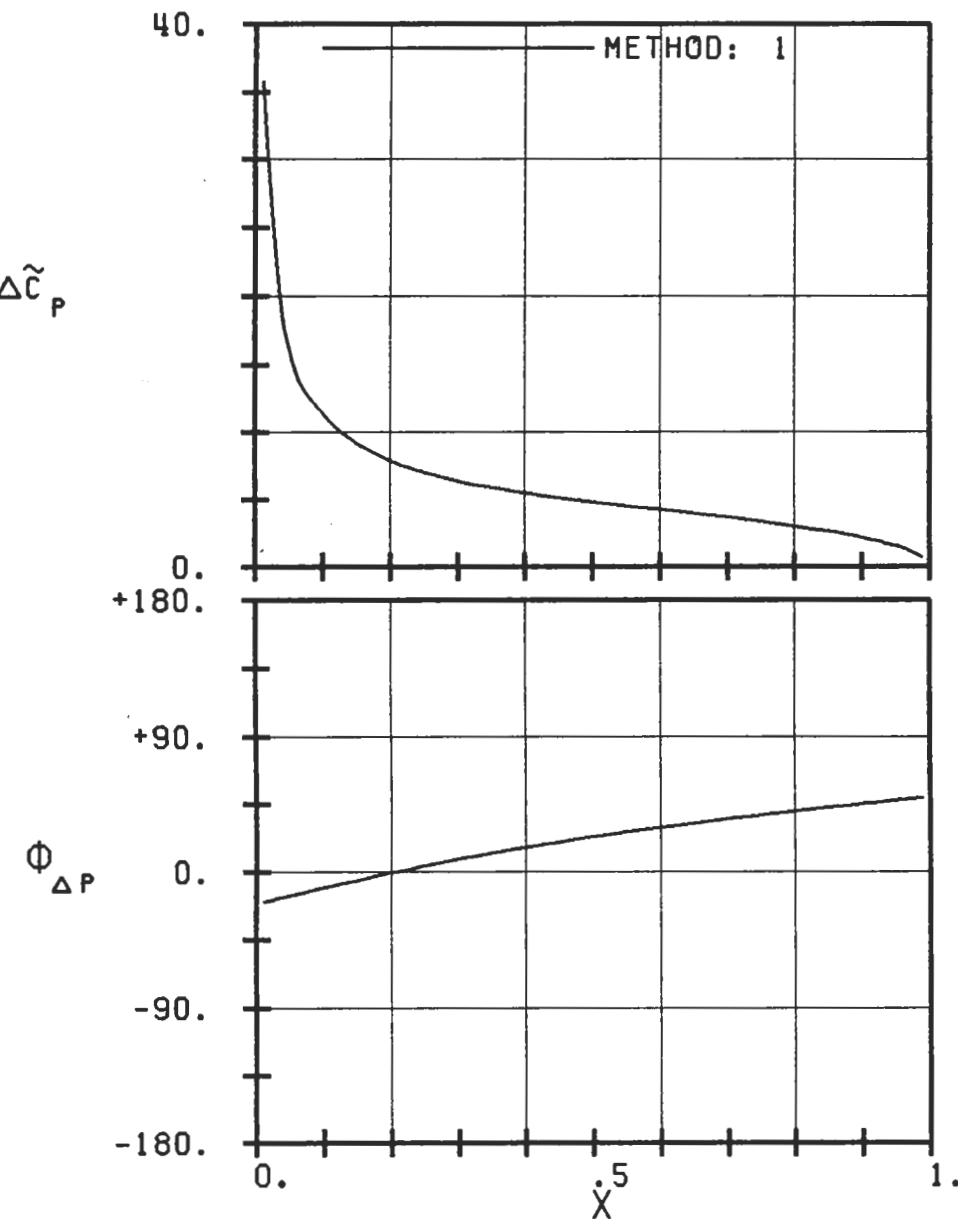
X = LS DATA

◇ = DATA

AEROELASTICITY IN TURBOMACHINE-CASCADES.
STANDARD CONFIGURATION NUMBER : 2

c : .050M
 τ : 1.00
 γ : 30.
 x_∞ : 0.5
 y_∞ : .0362
 M_1 : 0.
 β_1 : -30.
 i :
 M_2 :
 β_2 :
 h_X : -
 h_Y : -
 α : .059
 ω : 38.4
 k : 0.4
 δ : -
 σ : 180
 d : .0524

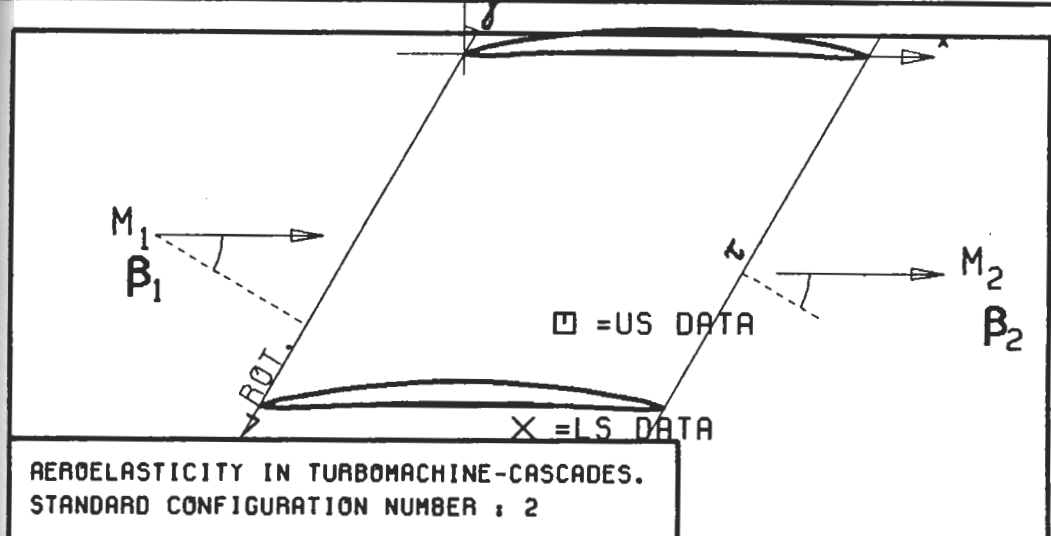
UNSTABLE *



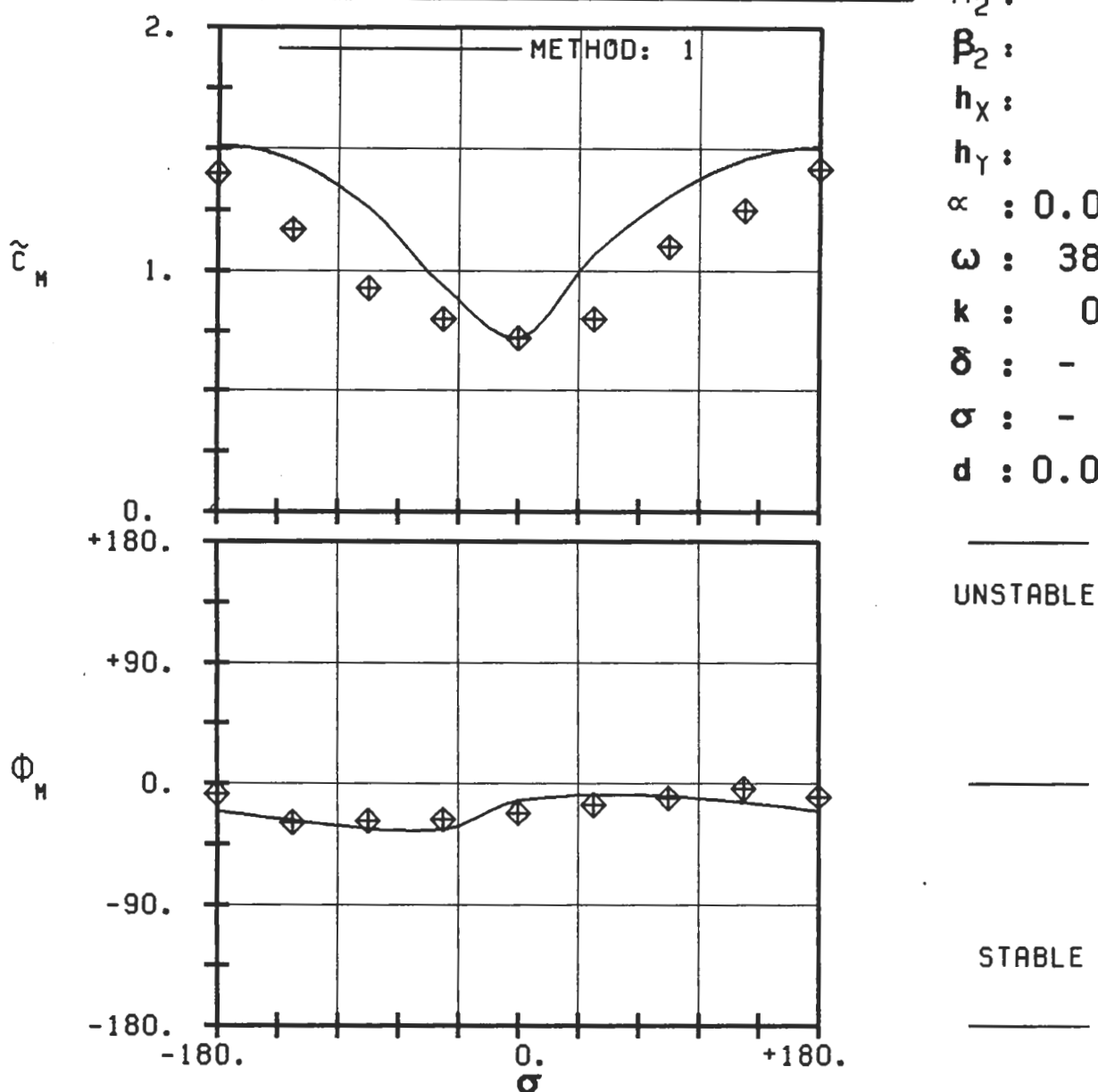
STABLE *

PLOT 7.2-3.8: SECOND STANDARD CONFIGURATION, CASE 8.
MAGNITUDE AND PHASE LEAD OF UNSTEADY BLADE
SURFACE PRESSURE DIFFERENCE COEFFICIENT.
(*: IN PITCH MODE, NOTATION VALID UPSTREAM OF PITCH AXIS)

Fig. 7.2-2c



c : 0.05M
 τ : 1.00
 γ : 30.
 x_∞ : 0.5
 y_∞ : 0.036
 M_1 : 0.
 β_1 : -30.
 i :
 M_2 :
 β_2 :
 h_X :
 h_Y :
 α : 0.059
 ω : 38.4
 k : 0.4
 δ : -
 σ : -
 d : 0.052



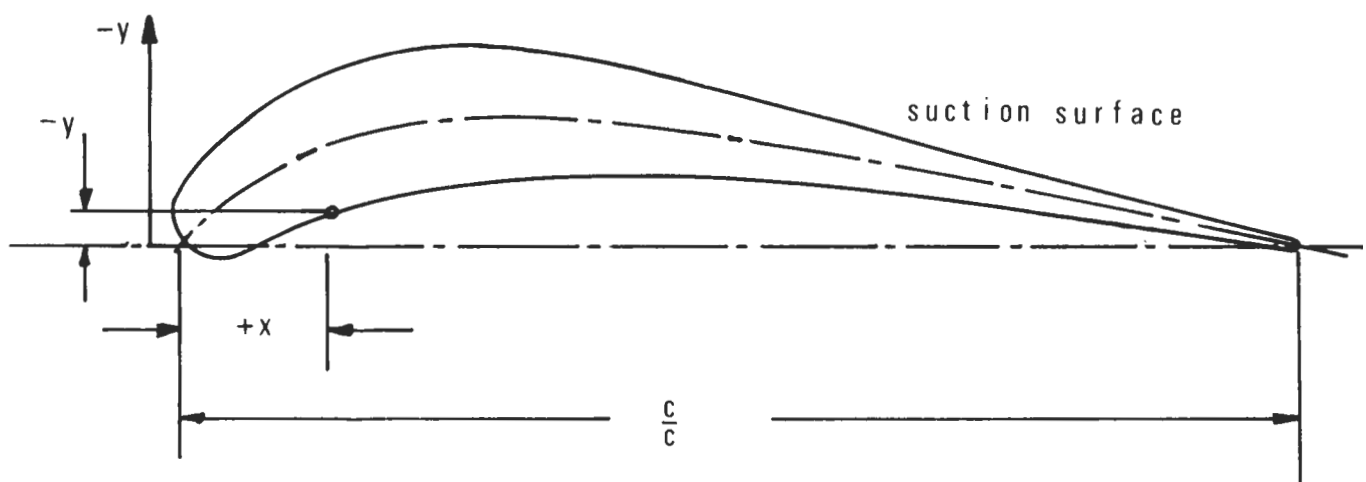
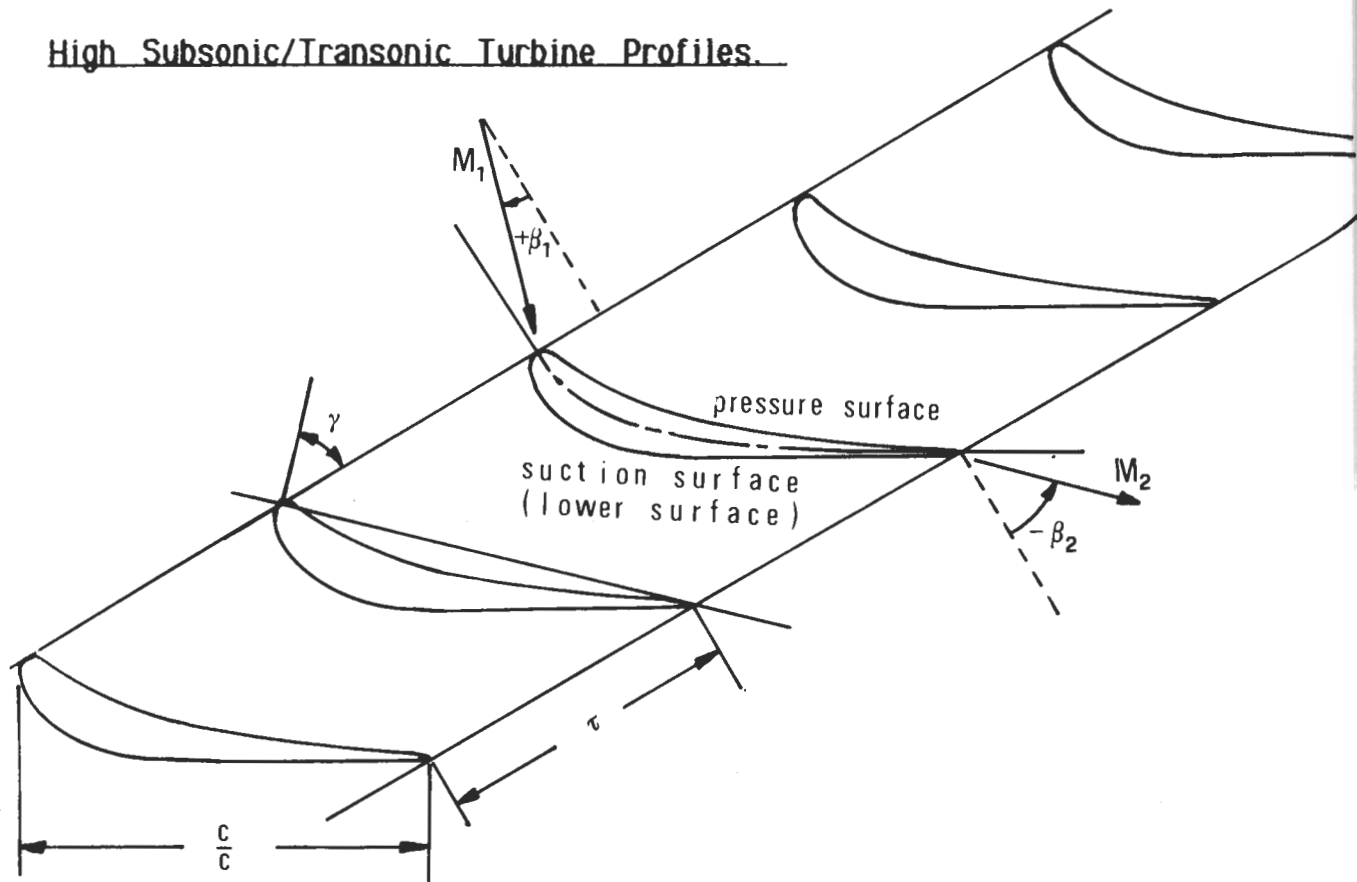
PLOT 7.2-5.1: SECOND STANDARD CONFIGURATION. CASES 1-8.
AERODYNAMIC MOMENT COEFFICIENT AND PHASE LEAD
IN DEPENDENCE OF INTERBLADE PHASE ANGLE.

AEROELASTICITY IN TURBOMACHINE-CASCADES

THIRD STANDARD CONFIGURATION

Definition

High Subsonic/Transonic Turbine Profiles.



Vibration in pitch around (x_α, y_α)

$$= (0.195, -0.1097)$$

d = (thickness/chord)

$$= 0.124$$

α = 0.0172 rad (nominal)

k = variable

C = 0.072 m

span = 0.025 m

T = 0.763 (hub)

camber = 60.83°

0.804 (midspan)

γ = 45.7°

0.873 (tip)

hub/tip = 0.844

M_2 = variable

σ = 67.5° (nominal)

Working fluid: Freon-11 (CFCI_3) with specific heat ratio = 1.137

Fig. 7.3-1. Third standard configuration: Cascade geometry

C = 0.072 m			
SUCTION SURFACE (Lower surface)		PRESSURE SURFACE (Upper surface)	
X	Y _s	X	Y _p
0.0	0.0	0.0	0.0
-0.073	-0.0096	0.0247	+0.0108
-0.0115	-0.0290	0.0439	+0.0066
-0.0051	-0.0487	0.0718	-0.0073
0.0102	-0.0698	0.0932	-0.0144
0.0296	-0.0918	0.1213	-0.0265
0.0462	-0.1080	0.1478	-0.0356
0.0668	-0.1240	0.1742	-0.0434
0.0887	-0.1384	0.2014	-0.0502
0.1117	-0.1508	0.2289	-0.0538
0.1358	-0.1610	0.2563	-0.0601
0.1606	-0.1693	0.2840	-0.0637
0.1864	-0.1749	0.3119	-0.0660
0.2122	-0.1781	0.3395	-0.0674
0.2354	-0.1797	0.3676	-0.0676
0.2584	-0.1800	0.3891	-0.0669
0.2814	-0.1793	0.4113	-0.0662
0.3046	-0.1772	0.4329	-0.0657
0.3274	-0.1745	0.4547	-0.0646
0.3432	-0.1719	0.4765	-0.0639
0.3591	-0.1692	0.4982	-0.0623
0.3748	-0.1657	0.5201	-0.0613
0.3904	-0.1621	0.5419	-0.0596
0.4058	-0.1580	0.5633	-0.0579
0.4806	-0.1396	0.5850	-0.0562
0.5552	-0.1208	0.6069	-0.0540
0.6291	-0.1018	0.6285	-0.0519
0.7038	-0.0829	0.6502	-0.0497
0.7780	-0.0640	0.6721	-0.0470
0.8525	-0.0452	0.6939	-0.0446
0.9270	-0.0264	0.7152	-0.0419
1.0	-0.0075	0.7368	-0.0388
		0.7583	-0.0359
		0.7986	-0.0295
		0.8387	-0.0237
		0.8792	-0.0176
		0.9195	-0.0118
		0.9597	-0.0060
		1.0	0.0

Table 7.3-1. Third standard configuration: Dimensionless airfoil coordinates (spanwise identical).

AEROELASTICITY IN TURBOMACHINE-CASCADES

THIRD STANDARD CONFIGURATION

Aeroelastic Test Cases

Aeroelastic Test Case No	Time - Averaged Parameters					
	M ₁	β ₁	P _{w2} /P _{w1}	P ₁ /P ₂	M ₂	β ₂
1 - 3	0.303	- 1.2	0.984	0.778	0.682	- 58.3
4 - 6	0.334	- 1.1	0.946	0.432	1.242	- 56.1
7 - 9	0.319	- 1.2	0.864	0.345	1.390	- 55.5

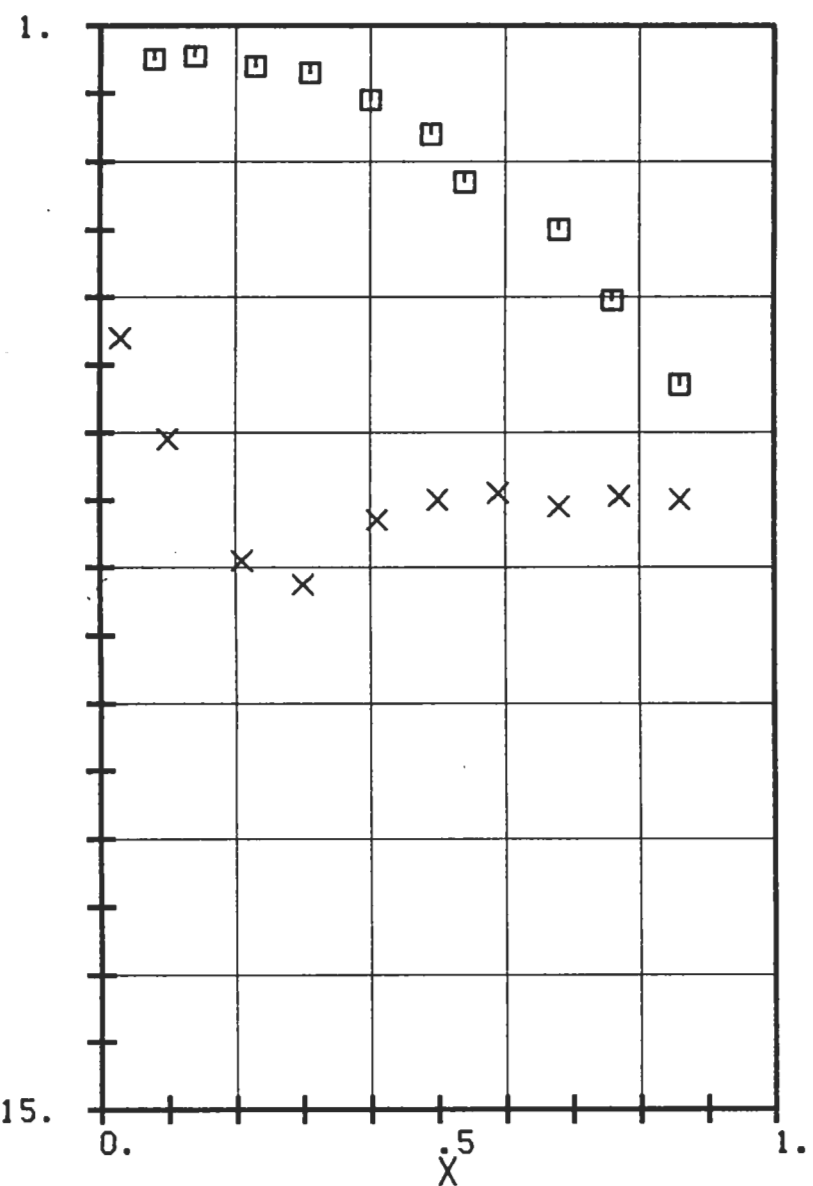
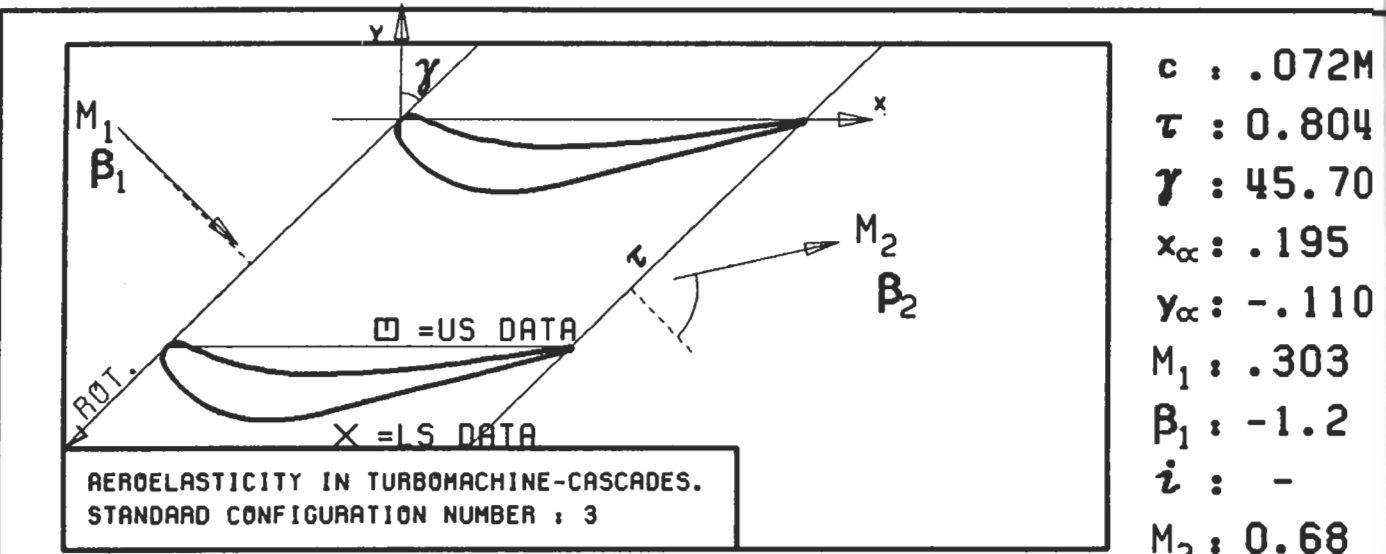
Aeroelastic Test Case No	Time-Dependent Parameters											
	Amplitude (Nominal = 0.01745rad)					Frequency (Hz)f	Reduced Frequency K	Interblade phase angle measured (Nominal = 67.5°)				
	$\frac{(-2)}{\alpha}$	$\frac{(-1)}{\alpha}$	$\frac{(0)}{\alpha}$ (rad)	$\frac{(+1)}{\alpha}$	$\frac{(+2)}{\alpha}$			$\delta^{(-2)}$	$\delta^{(-1)}$	$\delta^{(0)}$	$\delta^{(+1)}$	$\delta^{(+2)}$
1	0.965	0.952	0.0172	0.996	1.028	25	0.057	65.5	73.6	66.6	67.9	70.2
2	1.008	0.973	0.0172	1.026	1.032	100	0.229	76.4	67.4	67.6	64.6	70.5
3	1.087	1.024	0.0171	0.966	1.075	200	0.457	71.2	66.7	71.8	68.5	70.3
4	0.965	0.952	0.0172	0.996	1.028	25	0.031	65.5	73.6	66.6	67.9	70.2
5	1.008	0.973	0.0172	1.026	1.032	100	0.126	76.4	67.4	67.6	64.6	70.5
6	1.087	1.024	0.0171	0.966	1.075	200	0.251	71.2	68.7	71.8	68.5	70.3
7	0.965	0.952	0.0172	0.996	1.028	25	0.028	65.5	73.6	66.6	67.9	70.2
8	1.008	0.973	0.0172	1.026	1.032	100	0.112	76.4	67.4	67.6	64.6	70.5
9	1.087	1.024	0.0171	0.966	1.075	200	0.223	71.2	68.7	71.8	68.5	70.3

Table 7.3-2. Third standard configuration: 9 recommended aeroelastic test cases (Fluid used is Freon-11; all values are at midspan)

AEROELASTICITY IN TURBOMACHINE-CASCADES

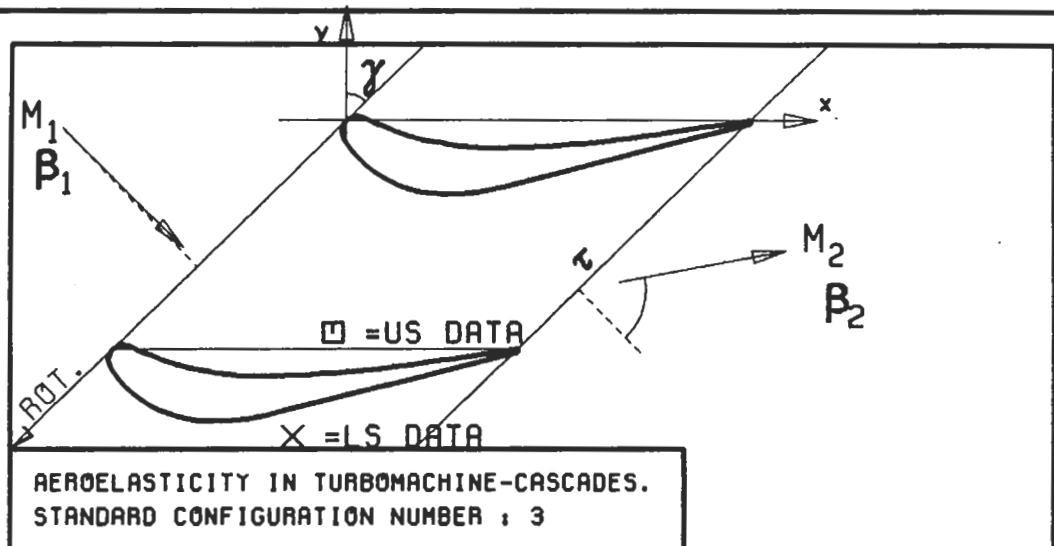
THIRD STANDARD CONFIGURATION

Experimental and Theoretical Results

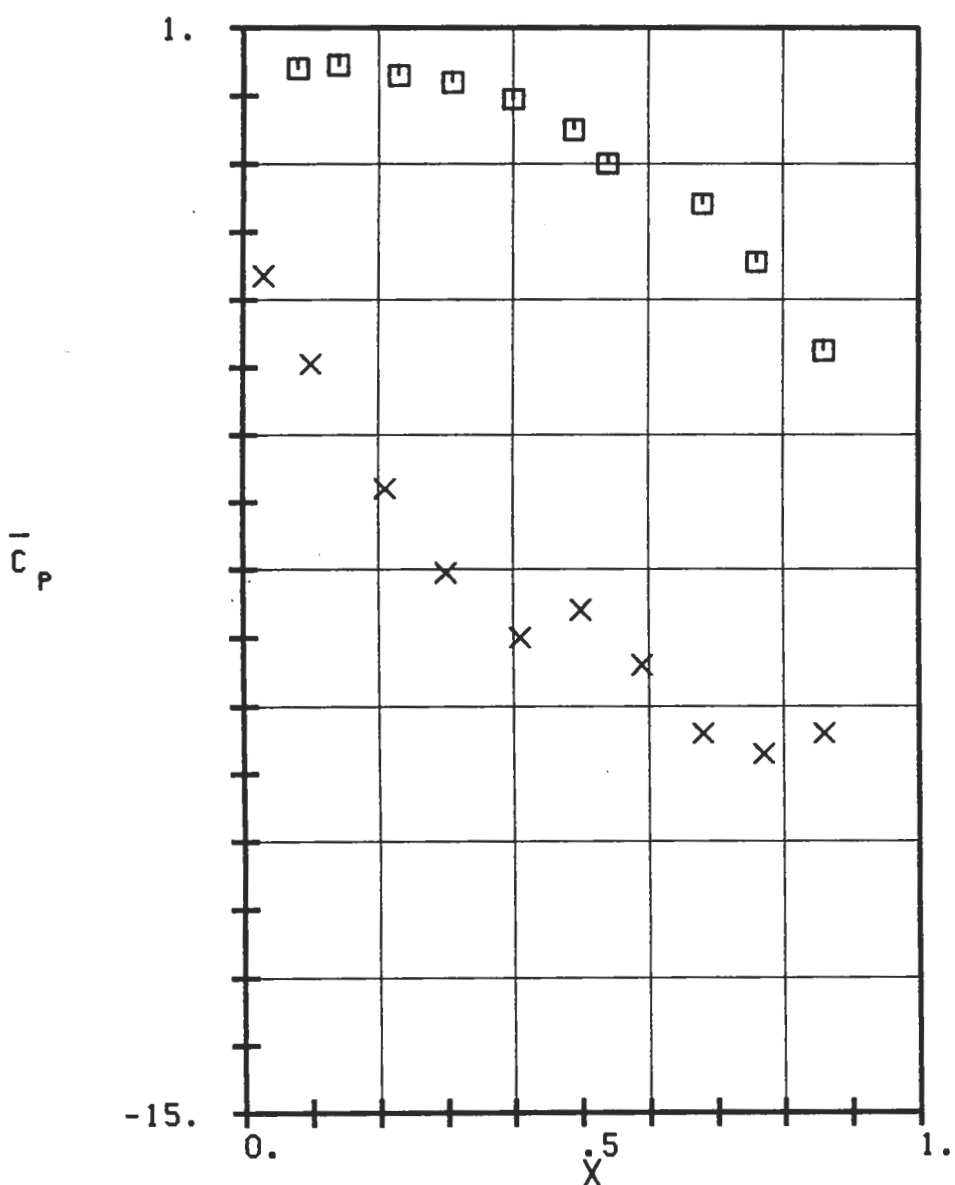


PLOT 7.3-1.1: THIRD STANDARD CONFIGURATION , CASES 1-3:
 TIME AVERAGED BLADE SURFACE PRESSURE
 COEFFICIENT.

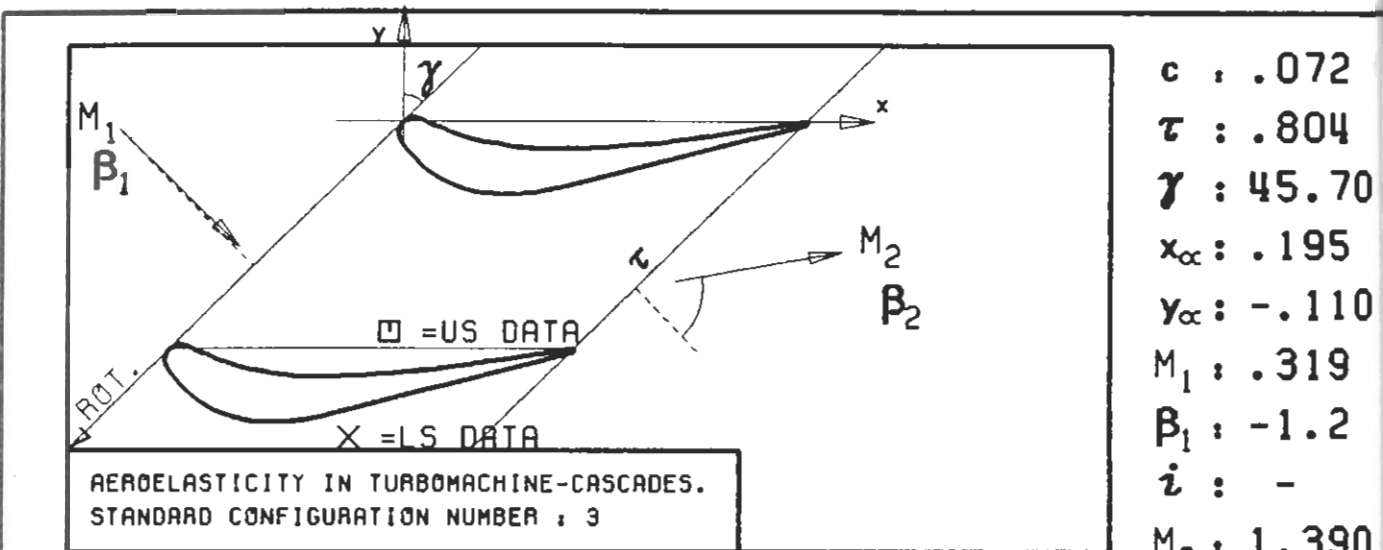
$c : .072M$
 $\tau : 0.804$
 $\gamma : 45.70$
 $x_\alpha : .195$
 $y_\alpha : -.110$
 $M_1 : .303$
 $\beta_1 : -1.2$
 $i : -$
 $M_2 : 0.68$
 $\beta_2 : -58.3$
 $h_X : -$
 $h_Y : -$
 $\alpha : -$
 $\omega : -$
 $k : -$
 $\delta : -$
 $\sigma : -$
 $d : .124$



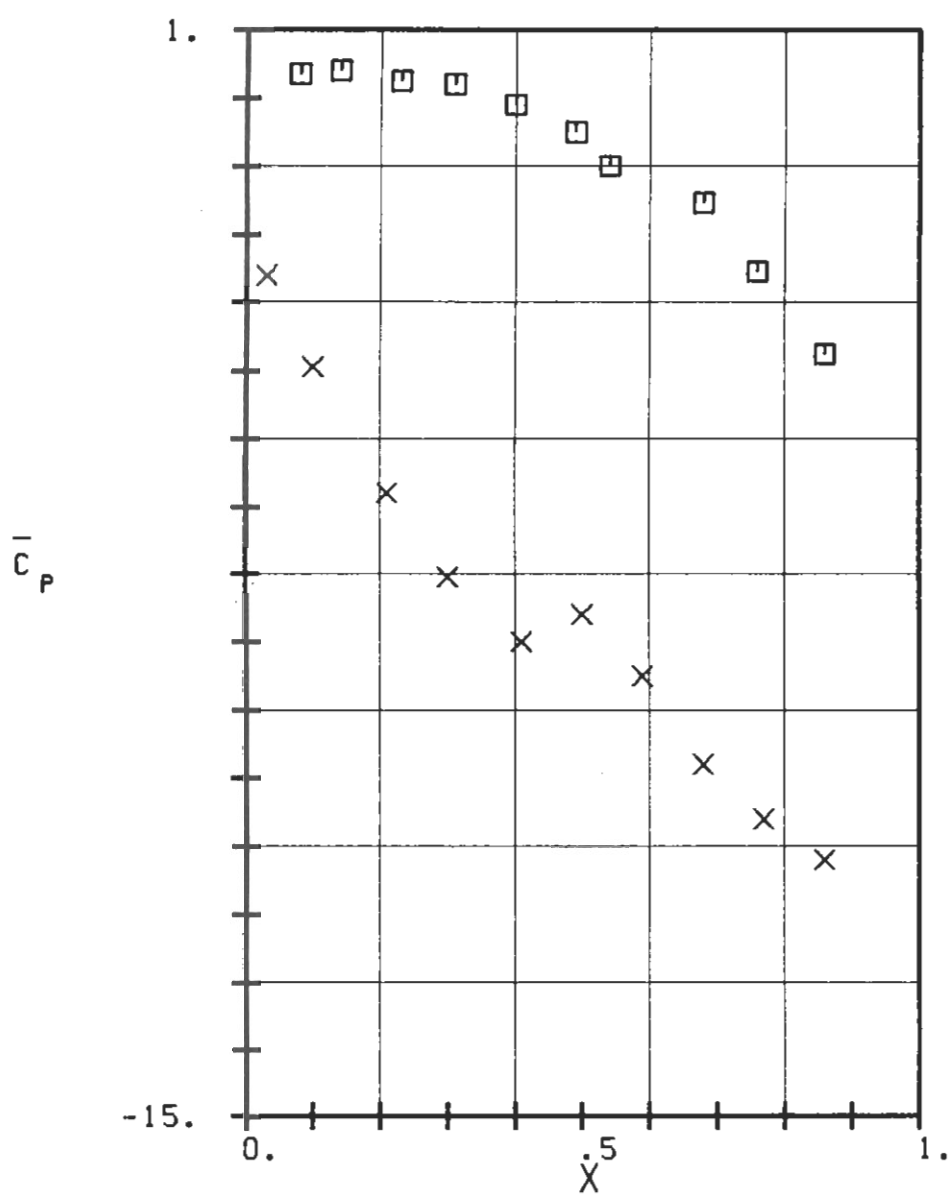
$c : .072$
 $\tau : .804$
 $\gamma : 45.70$
 $x_\alpha : .195$
 $y_\alpha : -.110$
 $M_1 : .334$
 $B_1 : -1.1$
 $i : -$
 $M_2 : 1.242$
 $B_2 : -56.1$
 $h_X : -$
 $h_Y : -$
 $\alpha : -$
 $\omega : -$
 $k : -$
 $\delta : -$
 $\sigma : -$
 $d : .124$



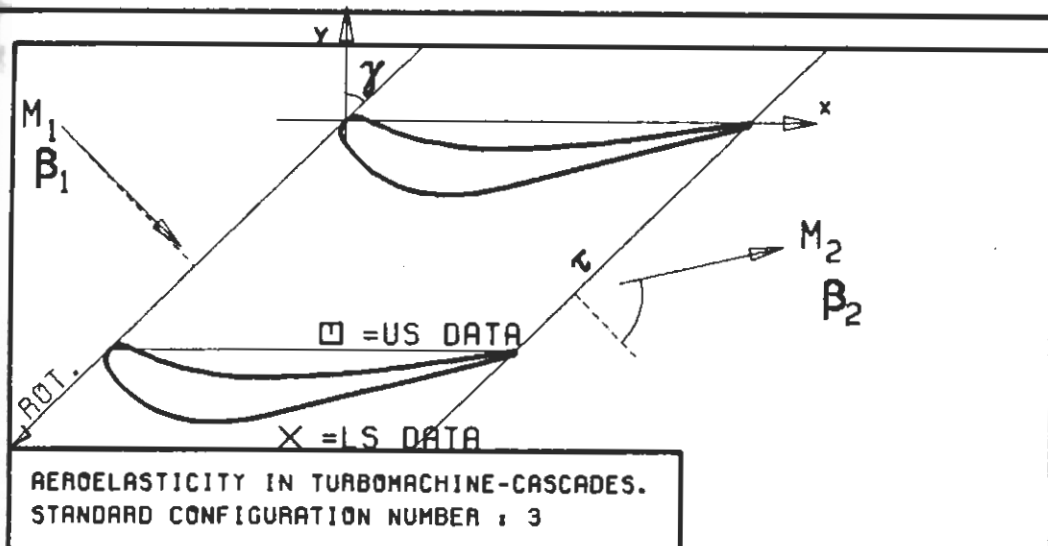
PLOT 7.3-1.2: THIRD STANDARD CONFIGURATION , CASES 4-6:
TIME AVERAGED BLADE SURFACE PRESSURE
COEFFICIENT.



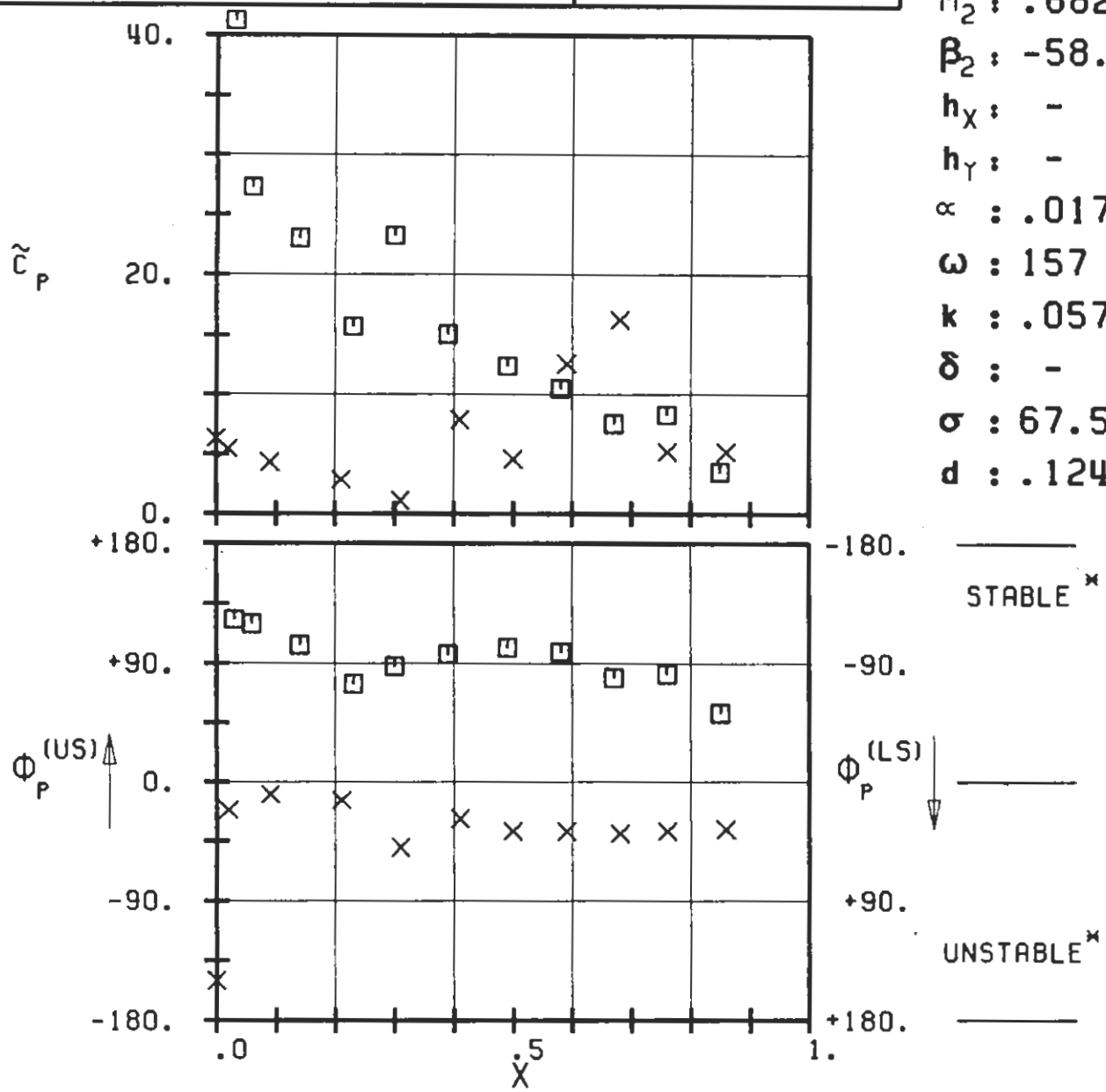
c : .072
 τ : .804
 γ : 45.70
 x_{∞} : .195
 y_{∞} : -.110
 M_1 : .319
 β_1 : -1.2
 i : -
 M_2 : 1.390
 β_2 : -55.5
 h_x : -
 h_y : -
 α : -
 ω : -
 k : -
 δ : -
 σ : -
 d : .124



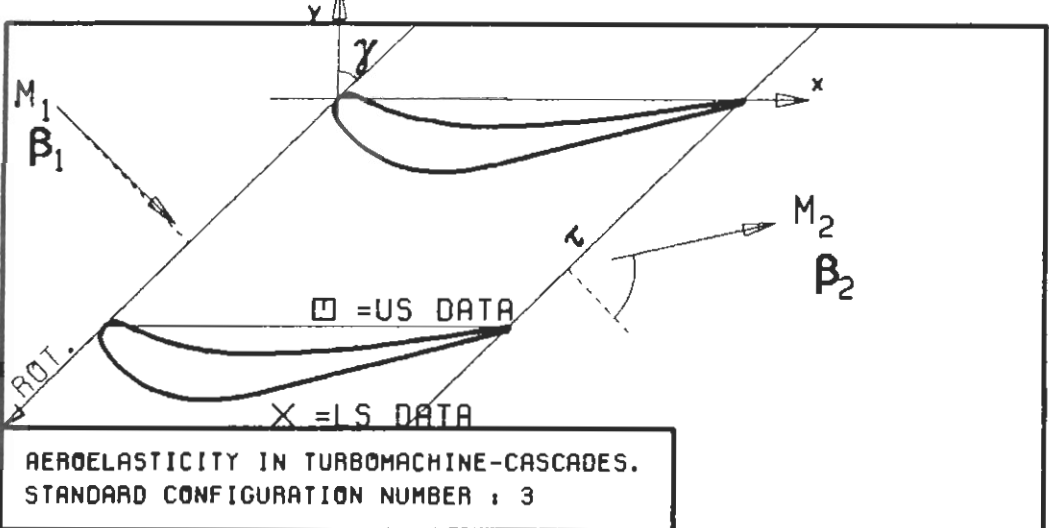
PLOT 7.3-1.3: THIRD STANDARD CONFIGURATION , CASES 7-9:
 TIME AVERAGED BLADE SURFACE PRESSURE
 COEFFICIENT.



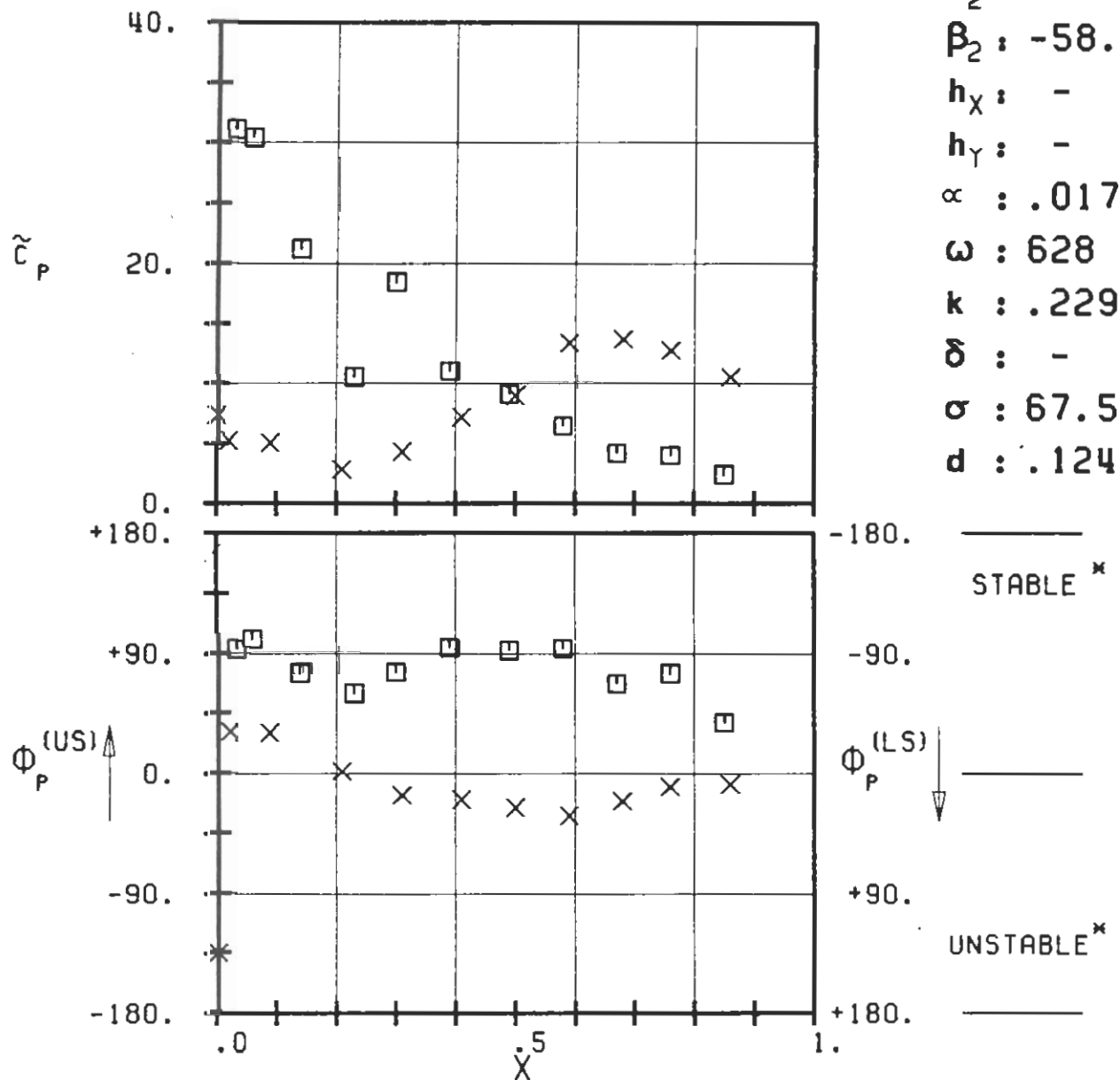
c : .072M
 τ : .804
 γ : 45.7
 x_α : .195
 y_α : -.110
 M_1 : .303
 β_1 : -1.2
 i :
 M_2 : .682
 β_2 : -58.3
 h_x : -
 h_y : -
 α : .0172
 ω : 157
 k : .057
 δ : -
 σ : 67.5
 d : .124



PLOT 7.3-2.1: THIRD STANDARD CONFIGURATION , CASE 1.
MAGNITUDE AND PHASE LEAD OF UNSTEADY BLADE
SURFACE PRESSURE COEFFICIENT.
(X: IN PITCH MODE, NOTATION VALID UPSTREAM OF PITCH AXIS)

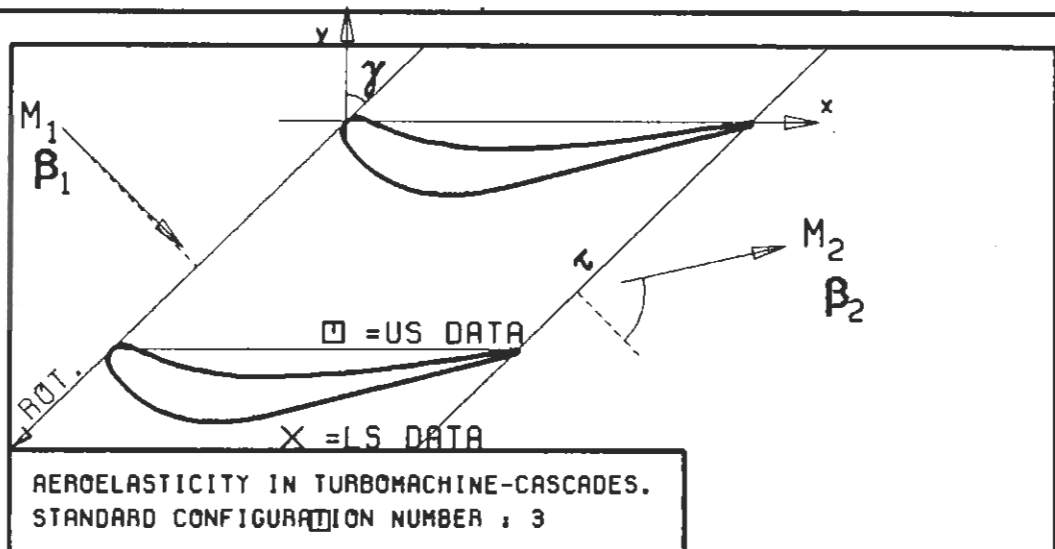


$c : .072M$
 $\tau : .804$
 $\gamma : 45.7$
 $x_\infty : .195$
 $y_\infty : -.110$
 $M_1 : .303$
 $\beta_1 : -1.2$
 $i :$
 $M_2 : .682$
 $\beta_2 : -58.3$
 $h_X : -$
 $h_Y : -$
 $\alpha : .0172$
 $\omega : 628$
 $k : .229$
 $\delta : -$
 $\sigma : 67.5$
 $d : .124$

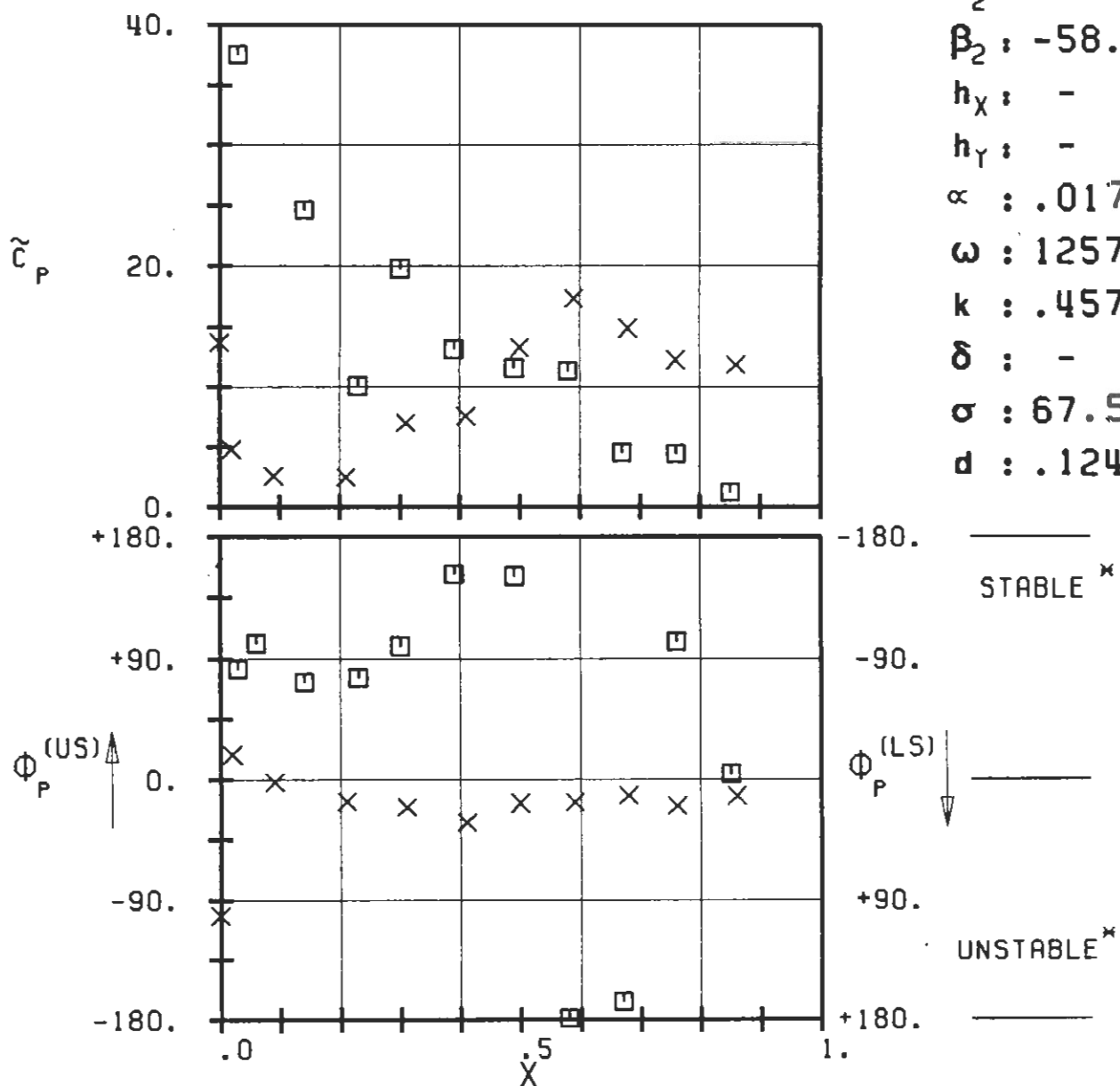


PLOT 7.3-2.2: THIRD STANDARD CONFIGURATION , CASE 2.
MAGNITUDE AND PHASE LEAD OF UNSTEADY BLADE
SURFACE PRESSURE COEFFICIENT.

(*: IN PITCH MODE, NOTATION VALID UPSTREAM OF PITCH AXIS)

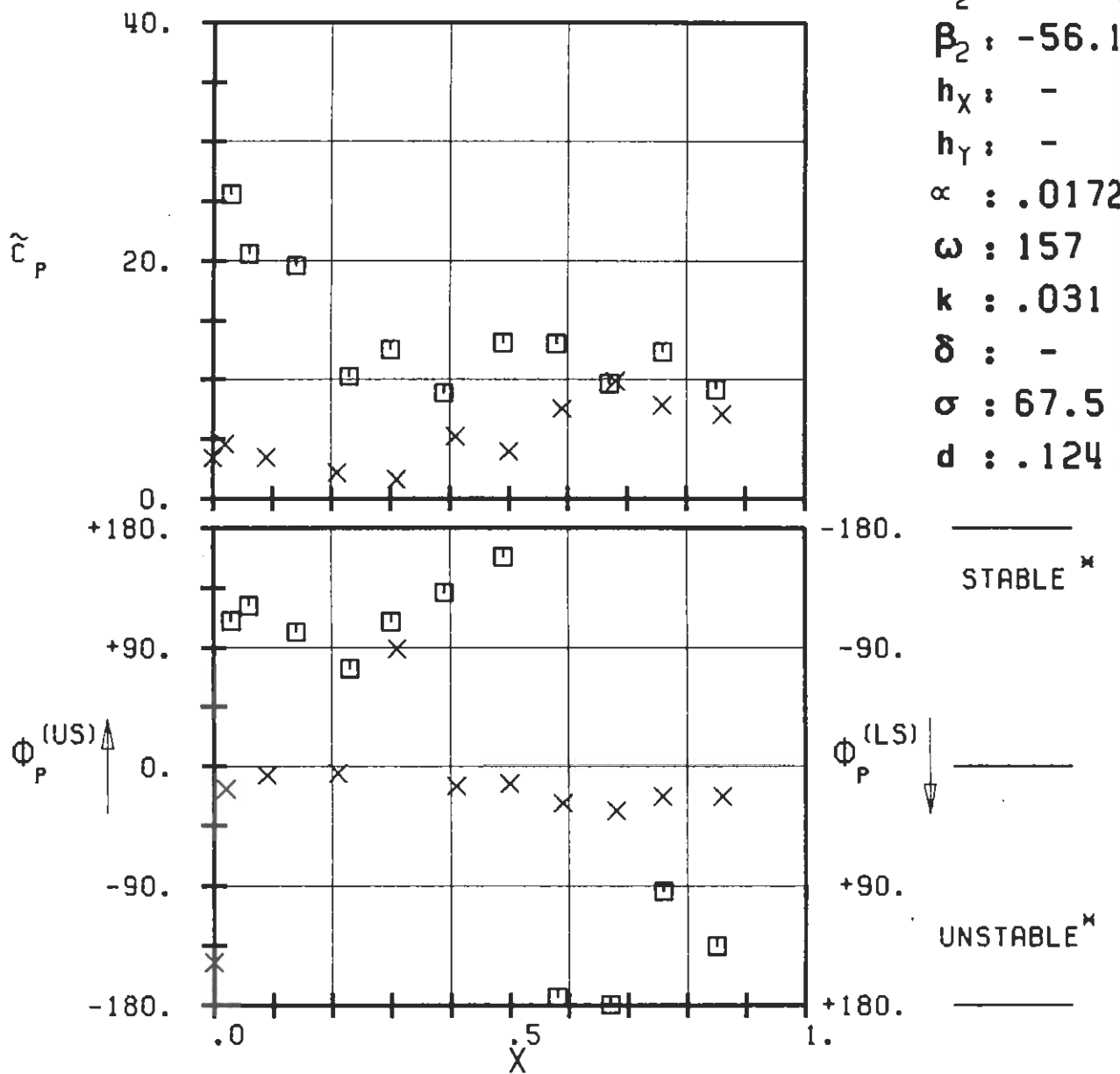
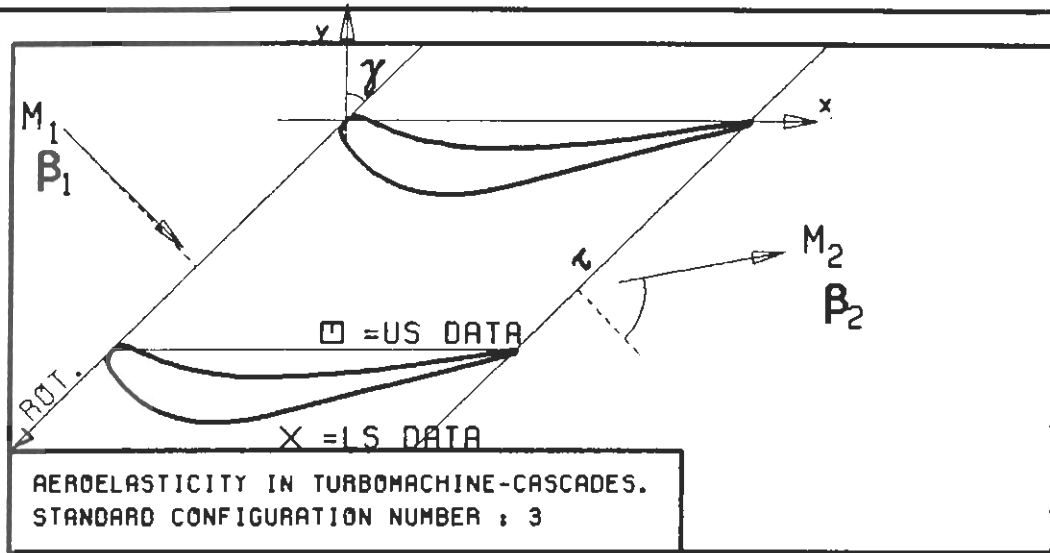


$c : .072M$
 $\tau : .804$
 $\gamma : 45.7$
 $x_\alpha : .195$
 $y_\alpha : -.110$
 $M_1 : .303$
 $\beta_1 : -1.2$
 $i :$
 $M_2 : .682$
 $\beta_2 : -58.3$
 $h_X : -$
 $h_Y : -$
 $\alpha : .0172$
 $\omega : 1257$
 $k : .457$
 $\delta : -$
 $\sigma : 67.5$
 $d : .124$



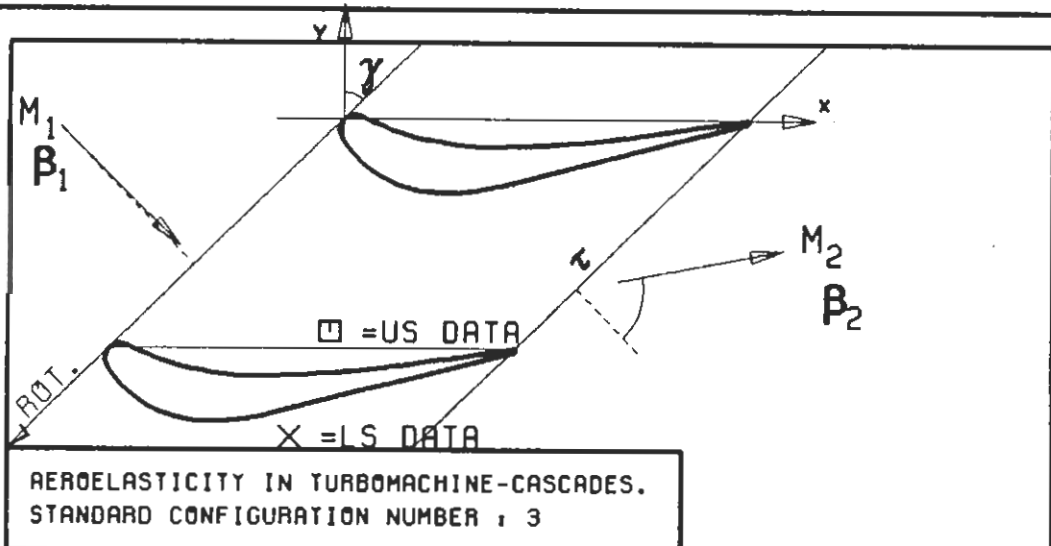
PLOT 7.3-2.3: THIRD STANDARD CONFIGURATION , CASE 3.
MAGNITUDE AND PHASE LEAD OF UNSTEADY BLADE
SURFACE PRESSURE COEFFICIENT.

(*: IN PITCH MODE, NOTATION VALID UPSTREAM OF PITCH AXIS)

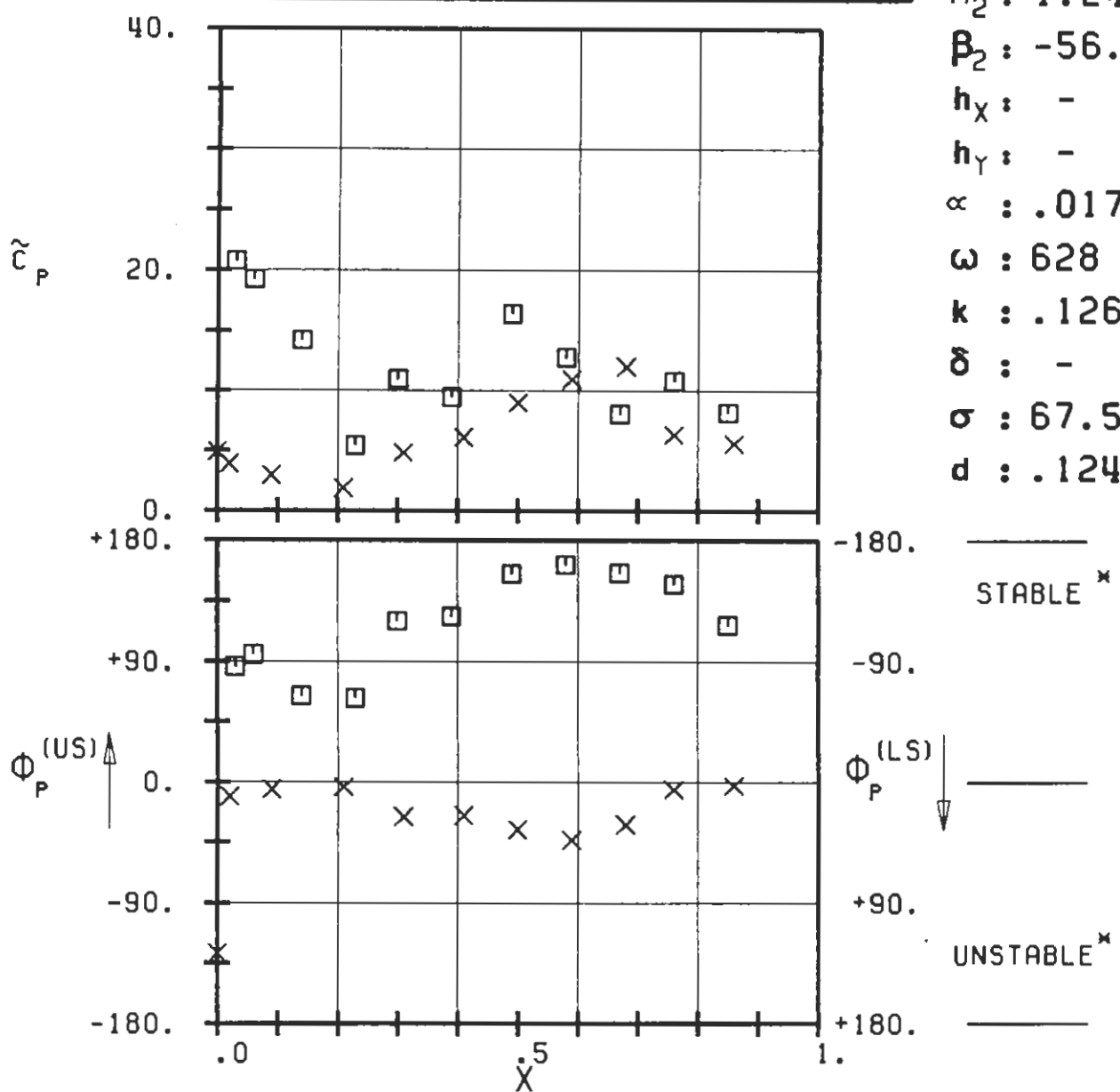


PLOT 7.3-2.4: THIRD STANDARD CONFIGURATION . CRSE 4.
MAGNITUDE AND PHASE LEAD OF UNSTEADY BLADE
SURFACE PRESSURE COEFFICIENT.

(*: IN PITCH MODE, NOTATION VALID UPSTREAM OF PITCH AXIS)

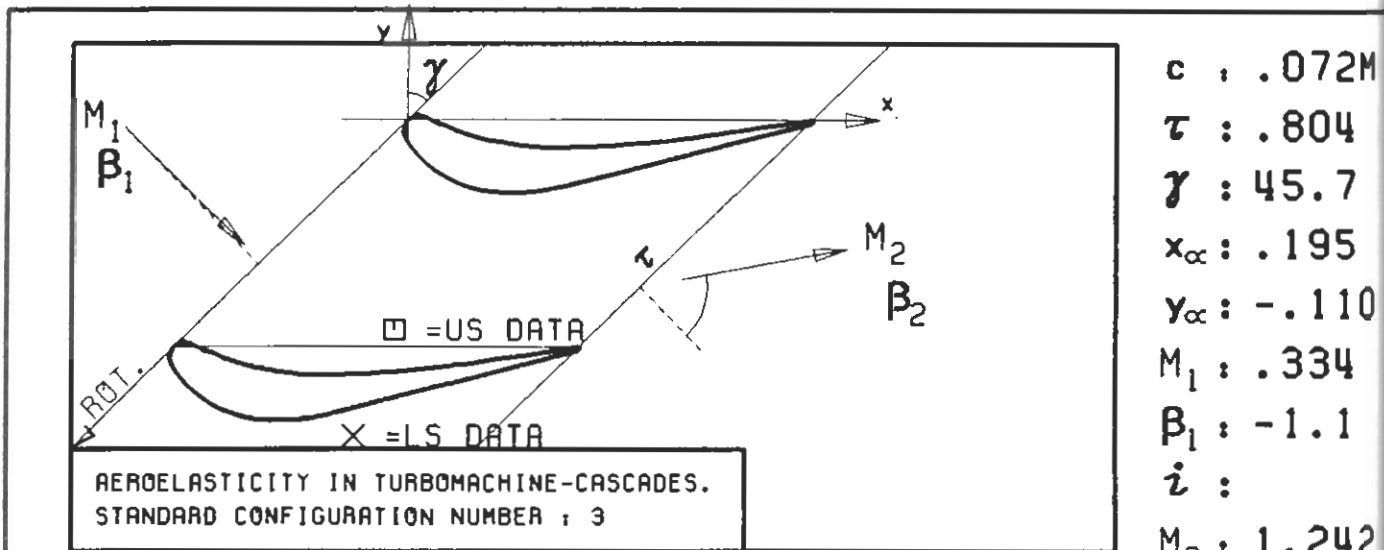


$c = .072M$
 $\tau = .804$
 $\gamma = 45.7$
 $x_\alpha = .195$
 $y_\alpha = -.110$
 $M_1 = .334$
 $\beta_1 = -1.1$
 $i =$
 $M_2 = 1.242$
 $\beta_2 = -56.1$
 $h_X = -$
 $h_Y = -$
 $\alpha = .0172$
 $\omega = 628$
 $k = .126$
 $\delta = -$
 $\sigma = 67.5$
 $d = .124$

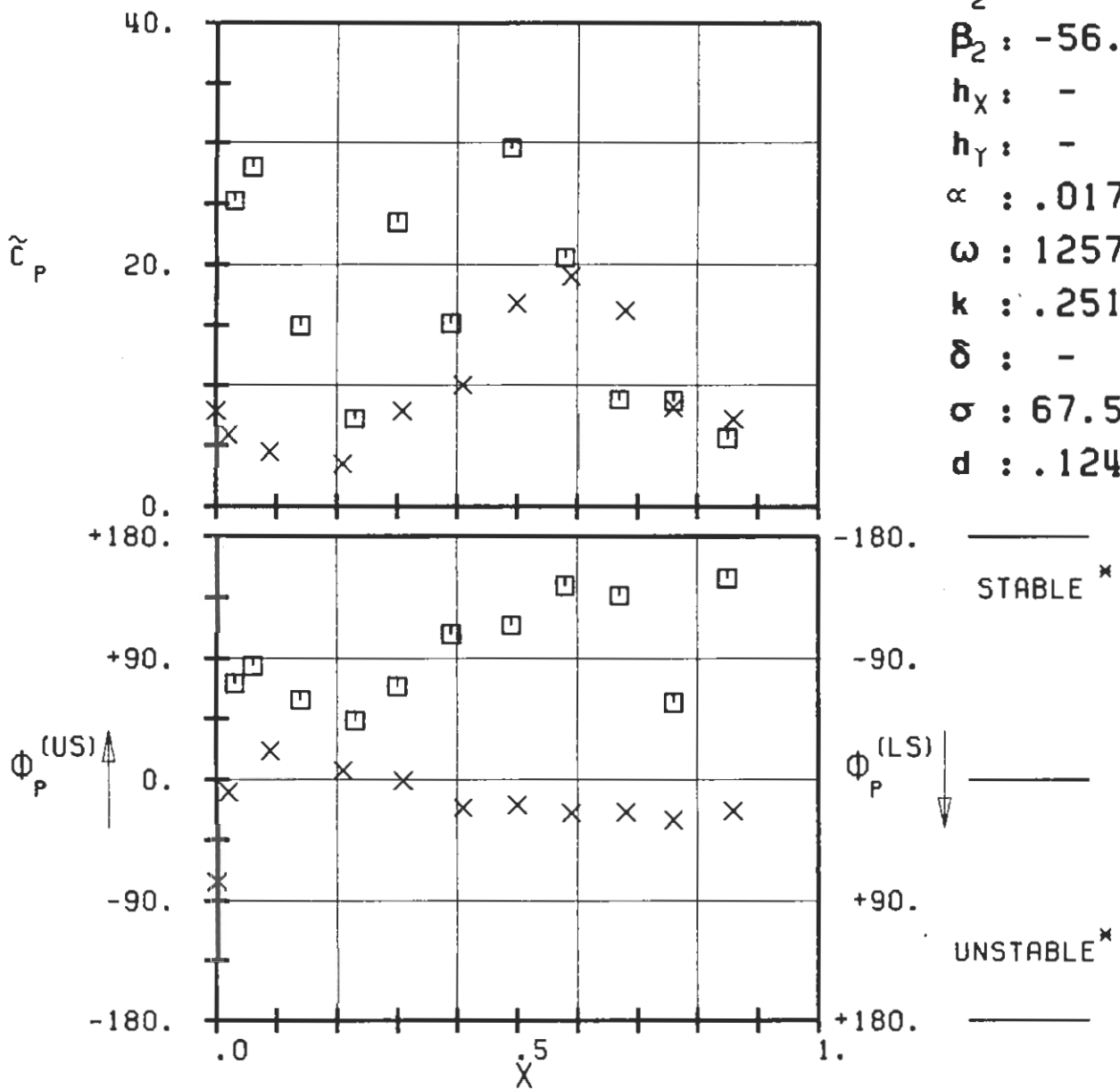


PLOT 7.3-2.5: THIRD STANDARD CONFIGURATION , CASE 5.
 MAGNITUDE AND PHASE LEAD OF UNSTEADY BLADE
 SURFACE PRESSURE COEFFICIENT.

(x: IN PITCH MODE, NOTATION VALIO UPSTREAM OF PITCH AXIS)

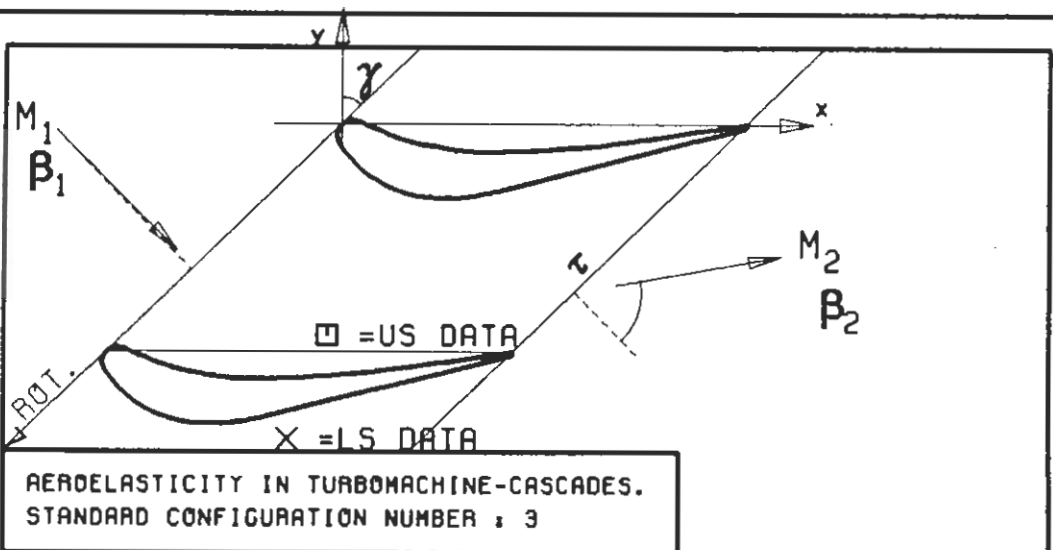


$c : .072M$
 $\tau : .804$
 $\gamma : 45.7$
 $x_\infty : .195$
 $y_\infty : -.110$
 $M_1 : .334$
 $B_1 : -1.1$
 $i :$
 $M_2 : 1.242$
 $B_2 : -56.1$
 $h_x : -$
 $h_y : -$
 $\alpha : .0172$
 $\omega : 1257$
 $k : .251$
 $\delta : -$
 $\sigma : 67.5$
 $d : .124$

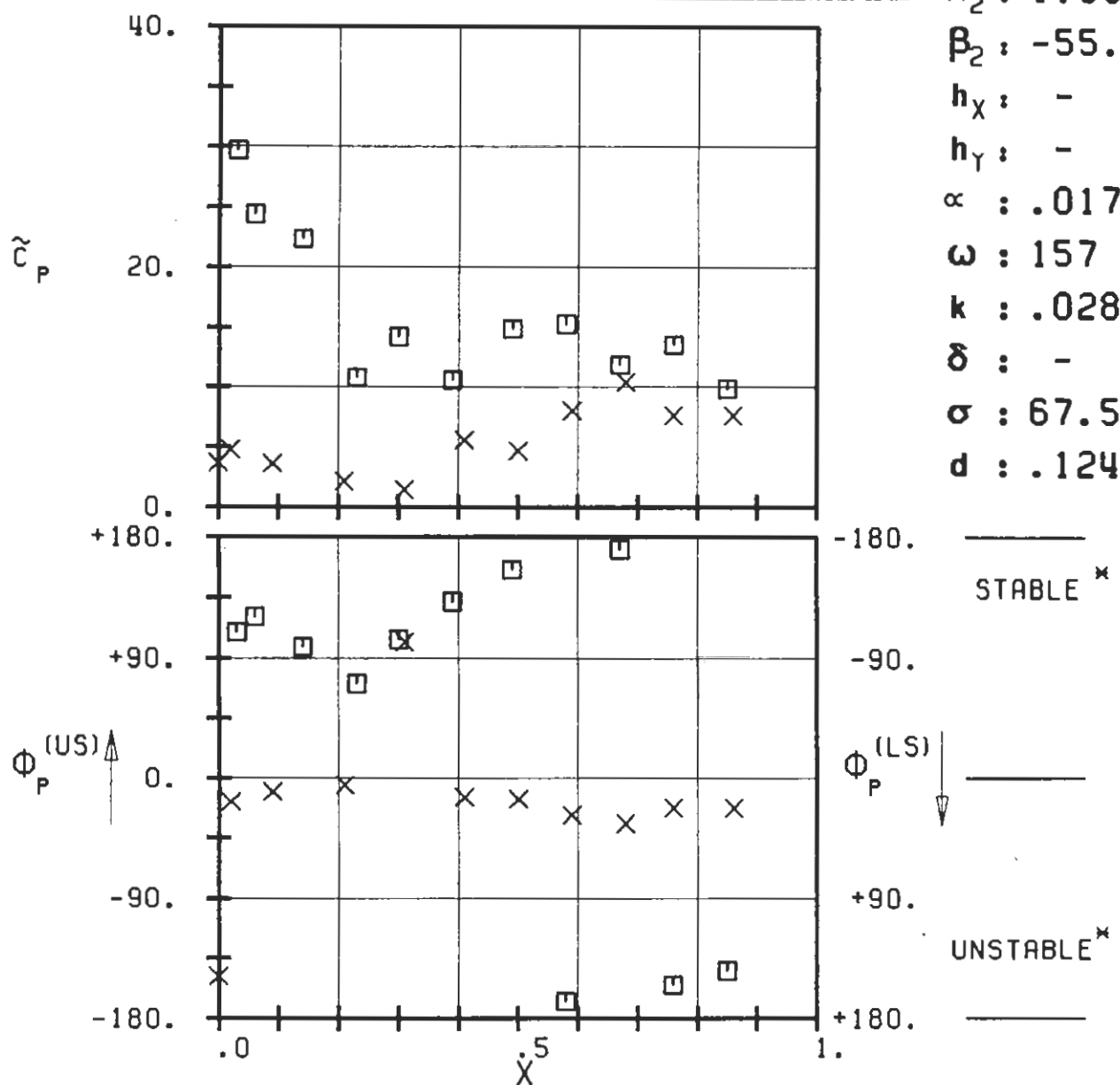


PLOT 7.3-2.6: THIRD STANDARD CONFIGURATION , CASE 6.
MAGNITUDE AND PHASE LEAD OF UNSTEADY BLADE
SURFACE PRESSURE COEFFICIENT.

(*: IN PITCH MODE, NOTATION VALID UPSTREAM OF PITCH AXIS)

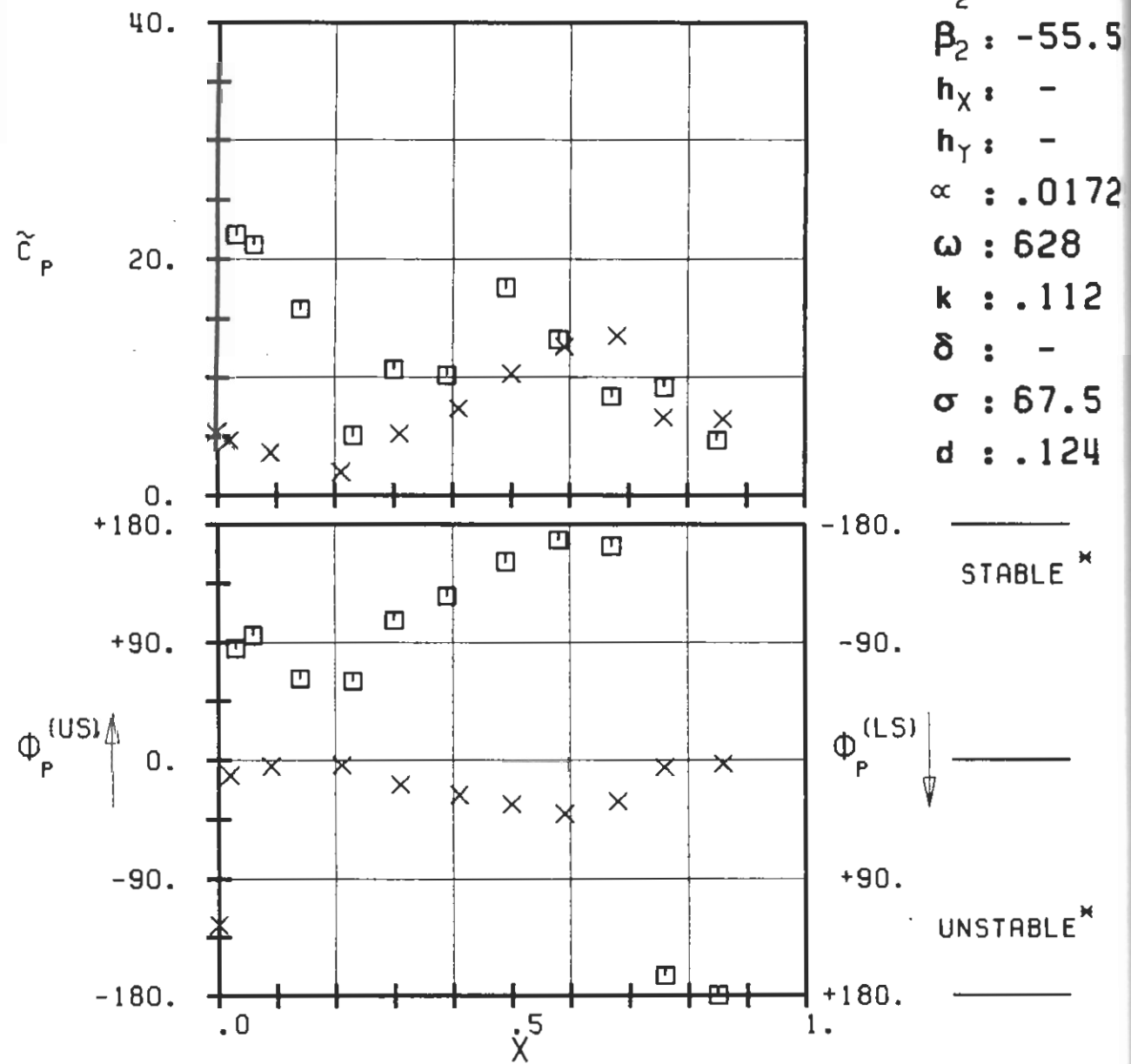
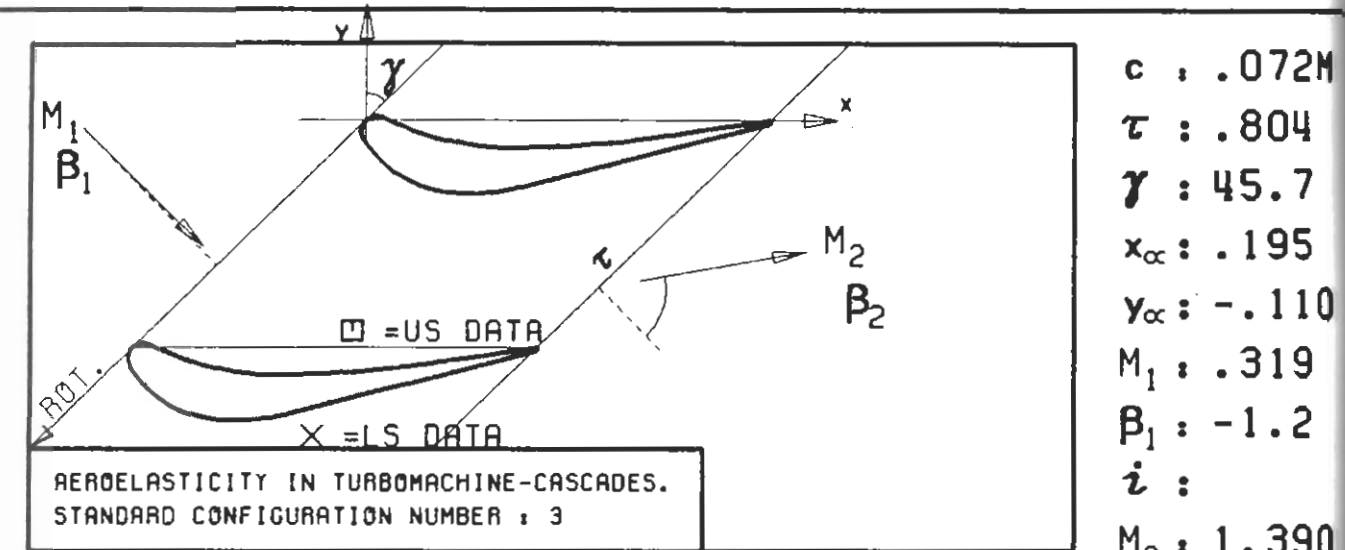


$c : .072M$
 $\tau : .804$
 $\gamma : 45.7$
 $x_\alpha : .195$
 $y_\alpha : -.110$
 $M_1 : .319$
 $\beta_1 : -1.2$
 $i :$
 $M_2 : 1.390$
 $\beta_2 : -55.5$
 $h_X : -$
 $h_Y : -$
 $\alpha : .0172$
 $\omega : 157$
 $k : .028$
 $\delta : -$
 $\sigma : 67.5$
 $d : .124$



PLOT 7.3-2.7: THIRD STANDARD CONFIGURATION , CASE 7.
 MAGNITUDE AND PHASE LEAD OF UNSTEADY BLADE SURFACE PRESSURE COEFFICIENT.

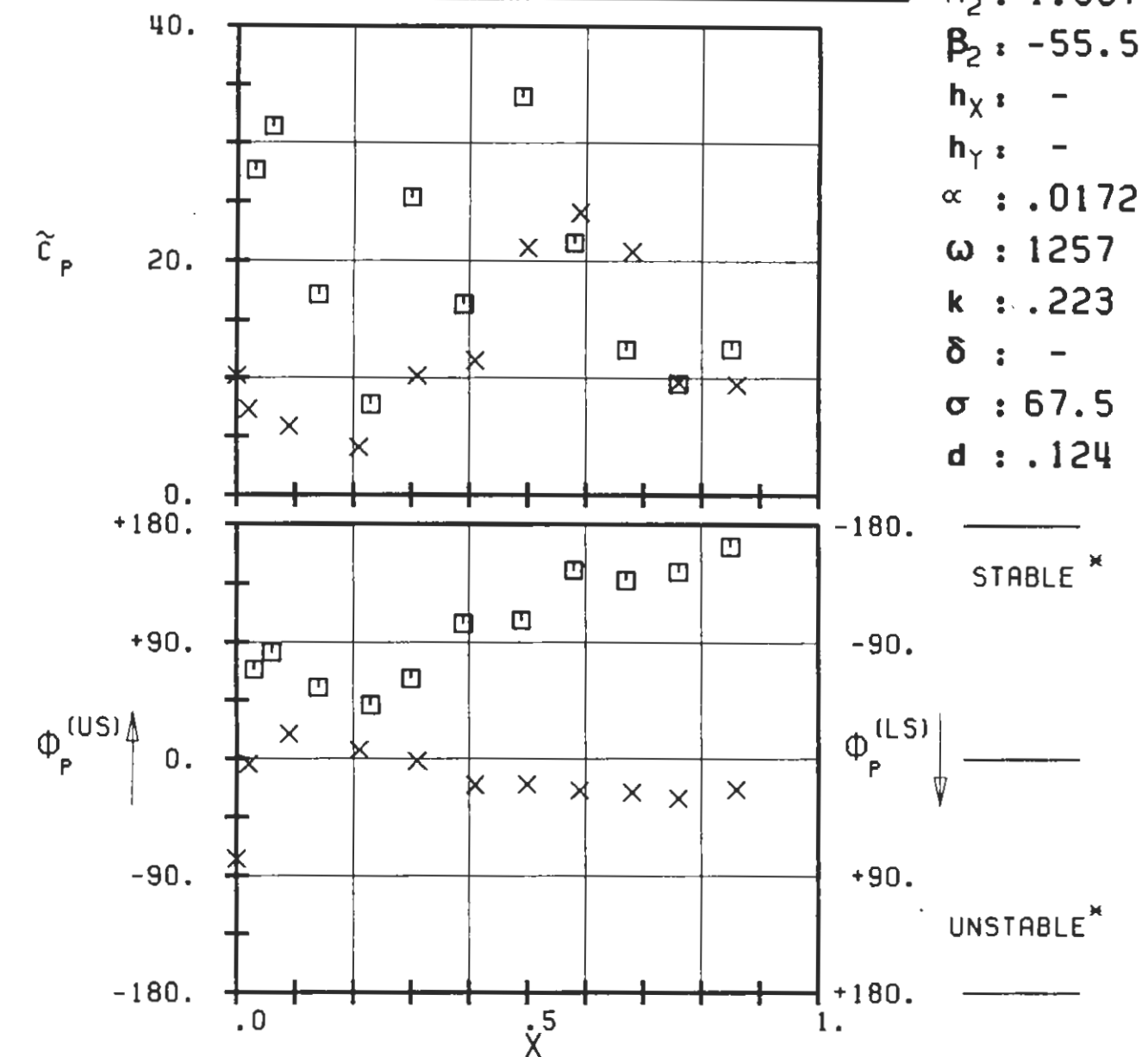
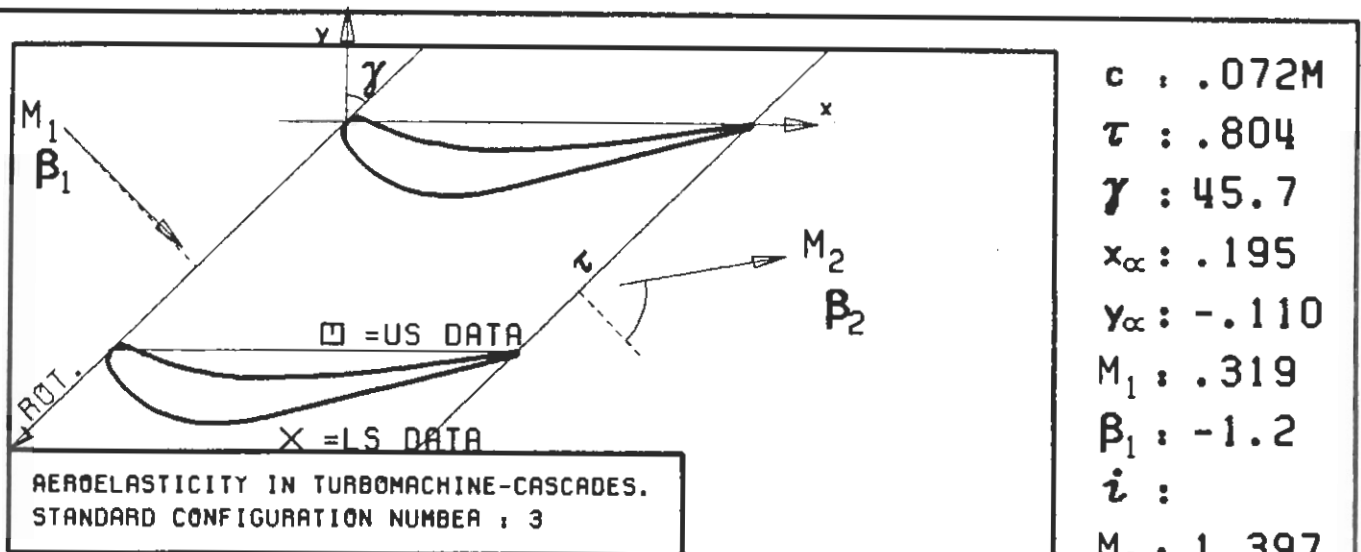
(\times : IN PITCH MODE, NOTATION VALID UPSTREAM OF PITCH AXIS)



PLOT 7.3-2.8: THIRD STANDARD CONFIGURATION , CASE 8.
MAGNITUDE AND PHASE LEAD OF UNSTEADY BLADE SURFACE PRESSURE COEFFICIENT.

(\times : IN PITCH MODE, NOTATION VALID UPSTREAM OF PITCH AXIS)

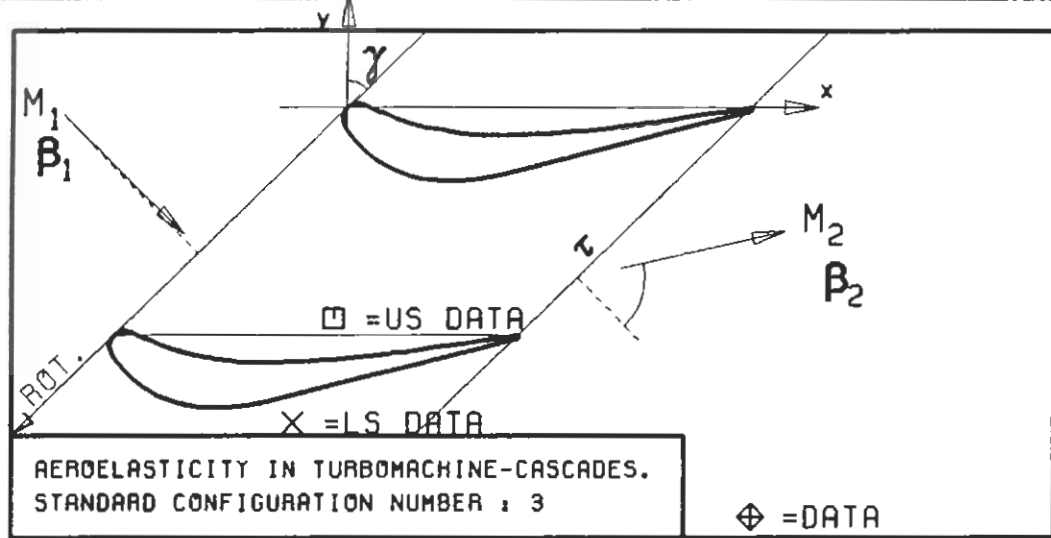
$c : .072M$
 $\tau : .804$
 $\gamma : 45.7$
 $x_{\infty} : .195$
 $y_{\infty} : -.110$
 $M_1 : .319$
 $\beta_1 : -1.2$
 $i :$
 $M_2 : 1.390$
 $\beta_2 : -55.5$
 $h_X : -$
 $h_Y : -$
 $\alpha : .0172$
 $\omega : 628$
 $k : .112$
 $\delta : -$
 $\sigma : 67.5$
 $d : .124$



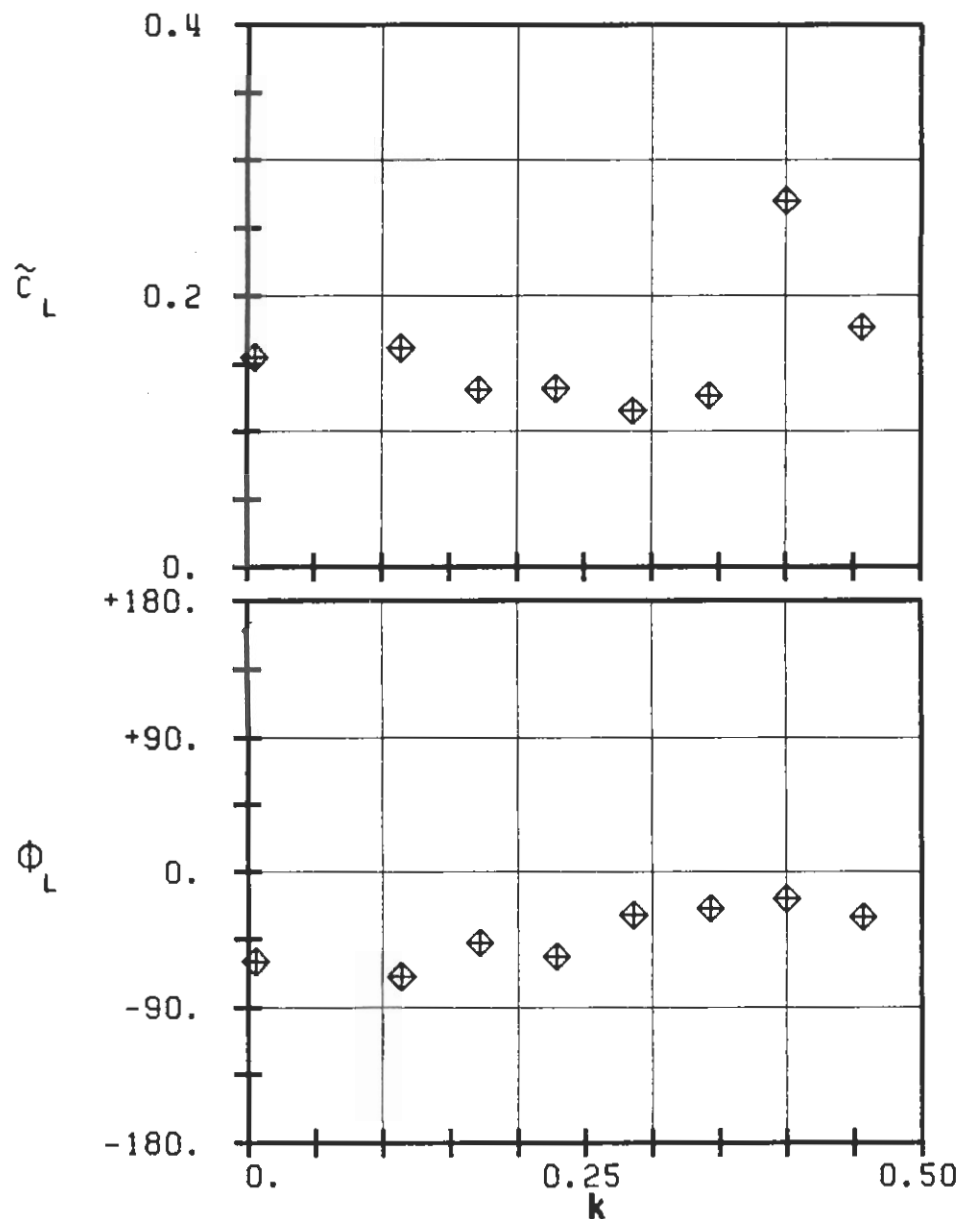
PLOT 7.3-2.9: THIRD STANDARD CONFIGURATION , CASE 9.
MAGNITUDE AND PHASE LEAD OF UNSTEADY BLADE
SURFACE PRESSURE COEFFICIENT.

(\times : IN PITCH MODE, NOTATION VALID UPSTREAM OF PITCH AXIS)

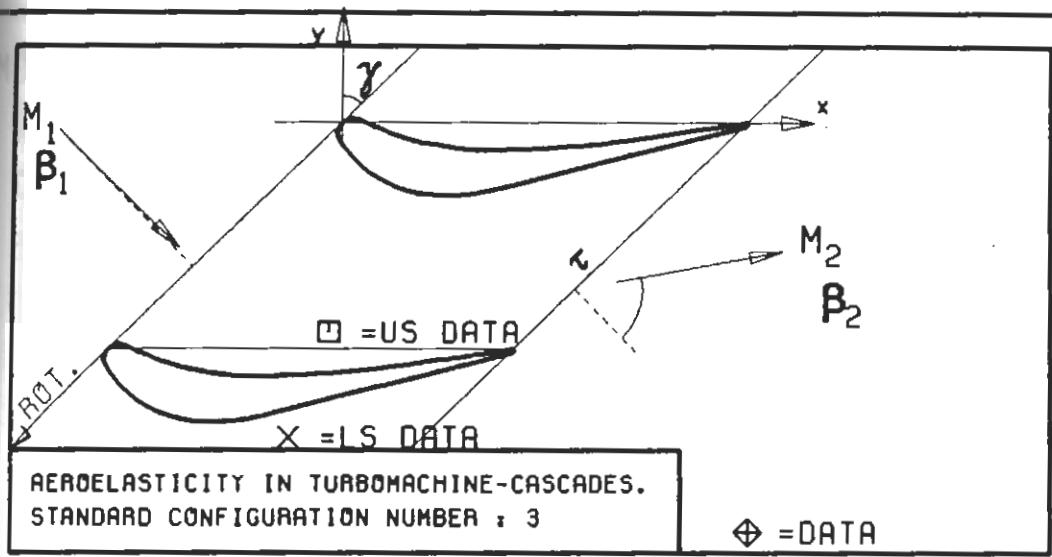
$c : .072M$
 $\tau : .804$
 $\gamma : 45.7$
 $x_\alpha : .195$
 $y_\alpha : -.110$
 $M_1 : .319$
 $\beta_1 : -1.2$
 $i :$
 $M_2 : 1.397$
 $\beta_2 : -55.5$
 $h_X : -$
 $h_Y : -$
 $\alpha : .0172$
 $\omega : 1257$
 $k : .223$
 $\delta : -$
 $\sigma : 67.5$
 $d : .124$



c : .072M
 τ : .804
 γ : 45.7
 x_∞ : .195
 y_∞ : -.110
 M_1 : .303
 β_1 : -1.2
 i : -
 M_2 : 0.682
 β_2 : -58.3
 h_x : -
 h_y : -
 α : .017
 ω :
 k :
 δ : -
 σ : 67.5
 d : .124



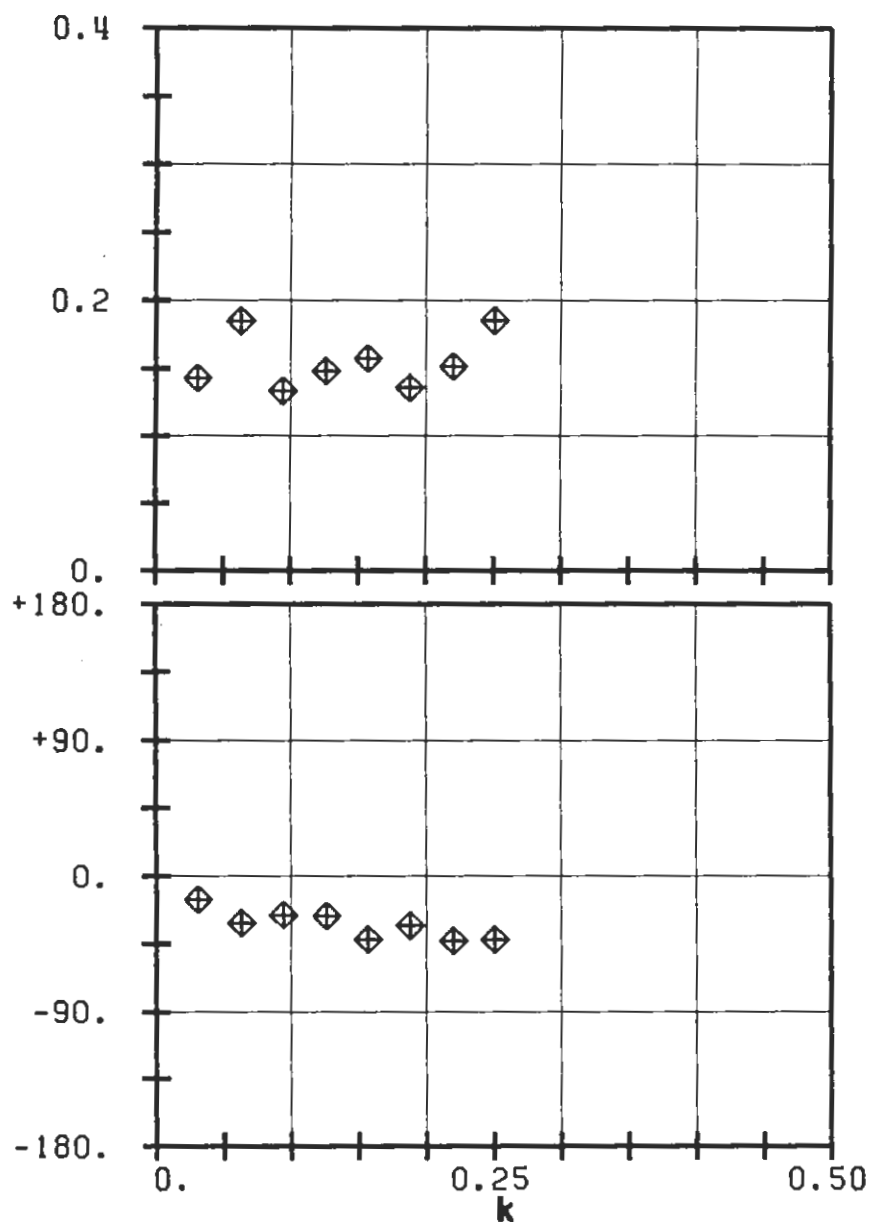
PLOT 7.3-4.1: THIRD STANDARD CONFIGURATION.
AERODYNAMIC LIFT COEFFICIENT AND PHASE LEAD
IN DEPENDENCE OF REDUCED FREQUENCY.



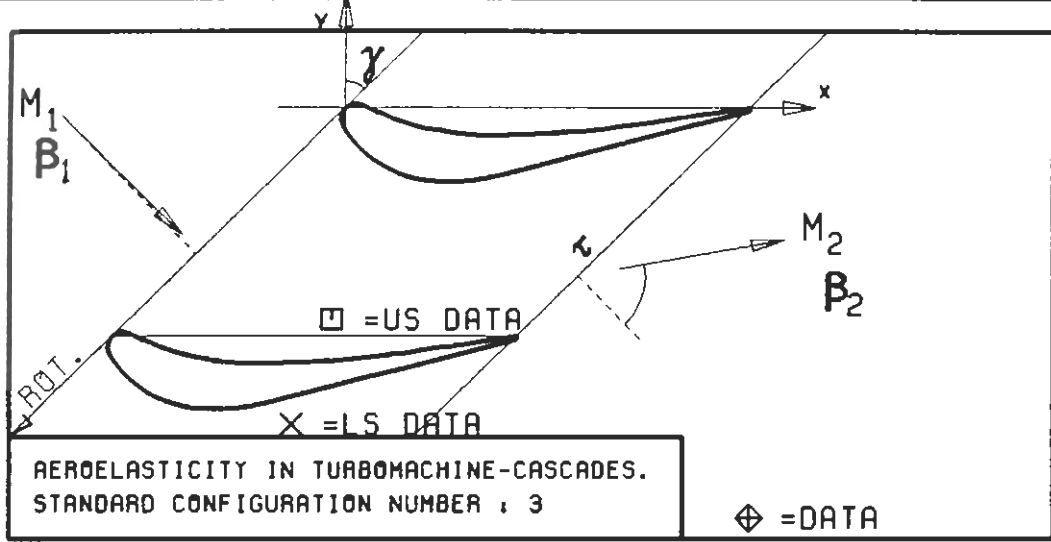
$c : .072M$
 $\tau : .804$
 $\gamma : 45.7$
 $x_\infty : .195$
 $y_\infty : -.110$
 $M_1 : .334$
 $\beta_1 : -1.1$
 $i : -$
 $M_2 : 1.242$
 $\beta_2 : -56.1$
 $h_x : -$
 $h_y : -$
 $\alpha : .017$
 $\omega :$
 $k :$
 $\delta : -$
 $\sigma : 67.5$
 $d : .124$

UNSTABLE

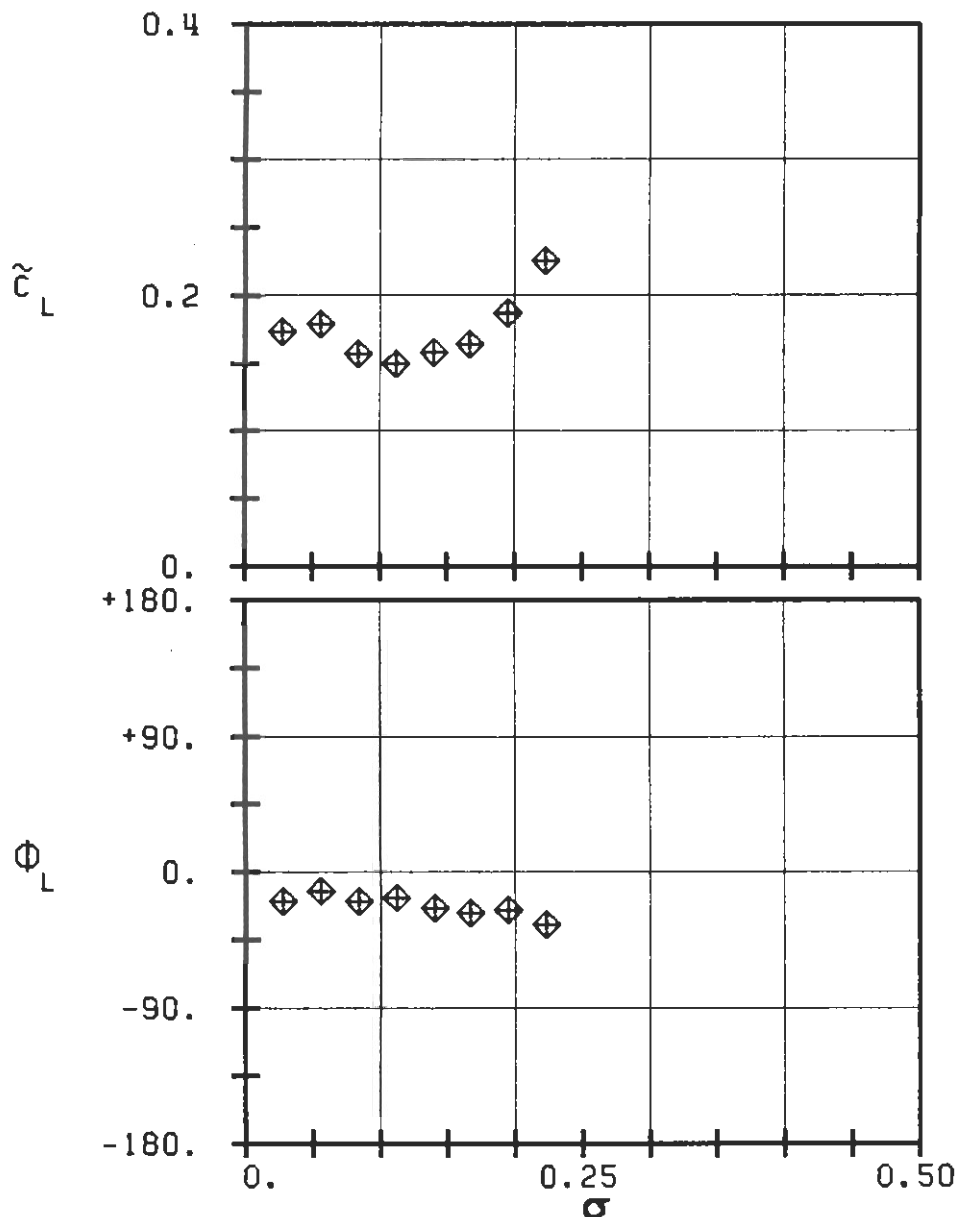
STABLE



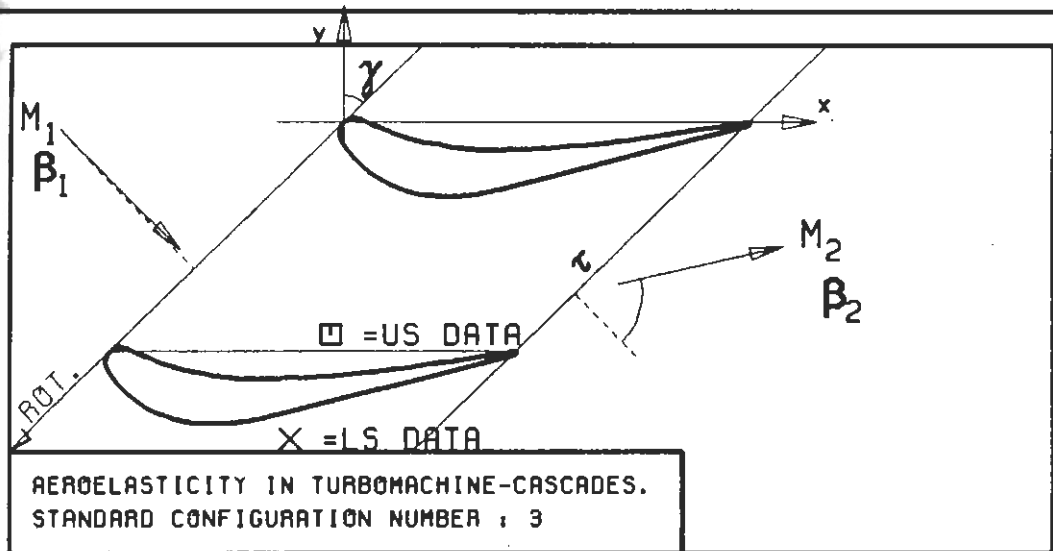
PLOT 7.3-4.2: THIRD STANDARD CONFIGURATION.
AERODYNAMIC LIFT COEFFICIENT AND PHASE LEAD
IN DEPENDENCE OF REDUCED FREQUENCY.



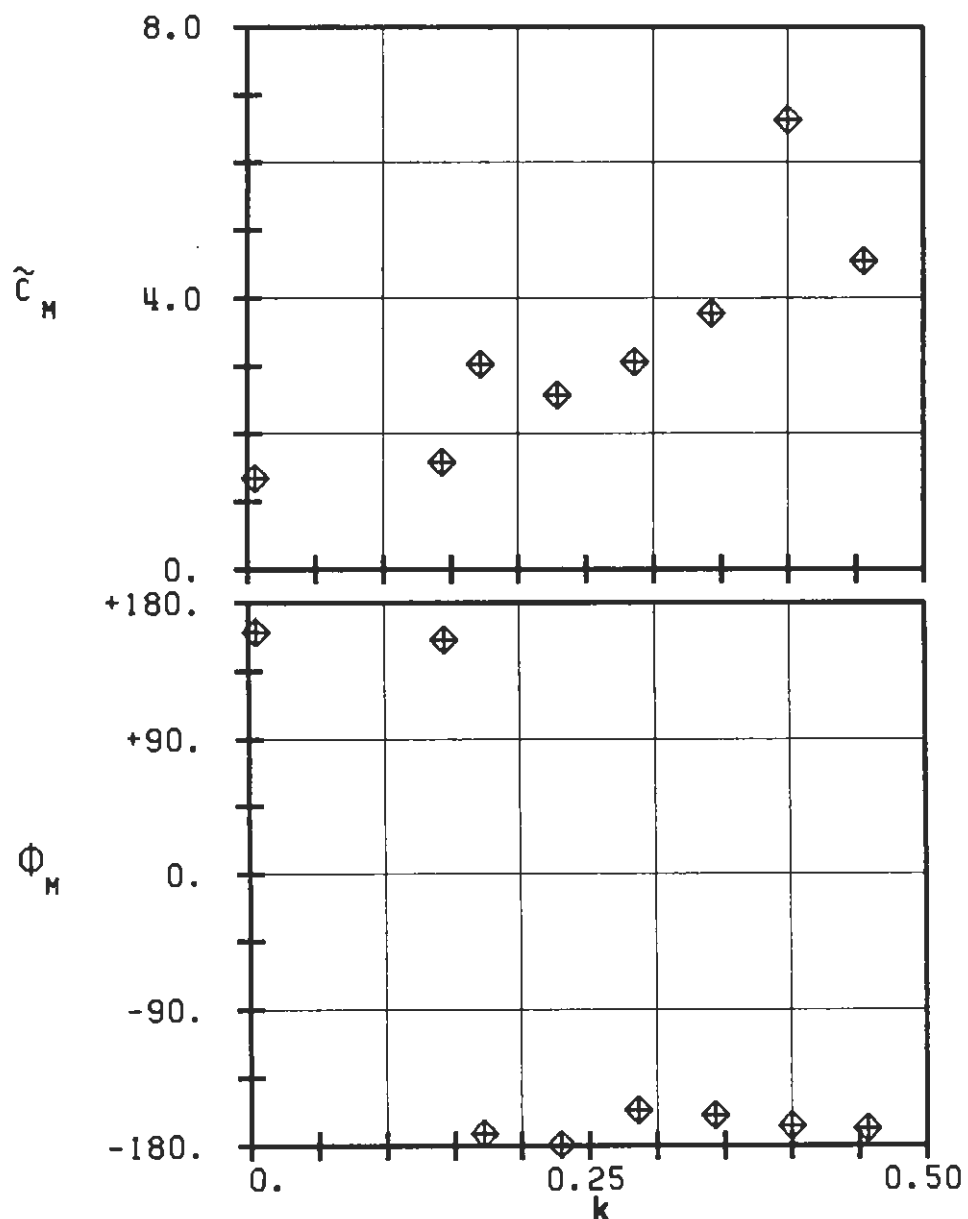
c : .072M
 τ : .804
 γ : 45.7
 x_α : .195
 y_α : .110
 M_1 : .303
 β_1 : -1.2
 i : -
 M_2 : 1.397
 β_2 : -55.5
 h_x : -
 h_y : -
 α : .017
 ω :
 k :
 δ : -
 σ : 67.5
 d : .124



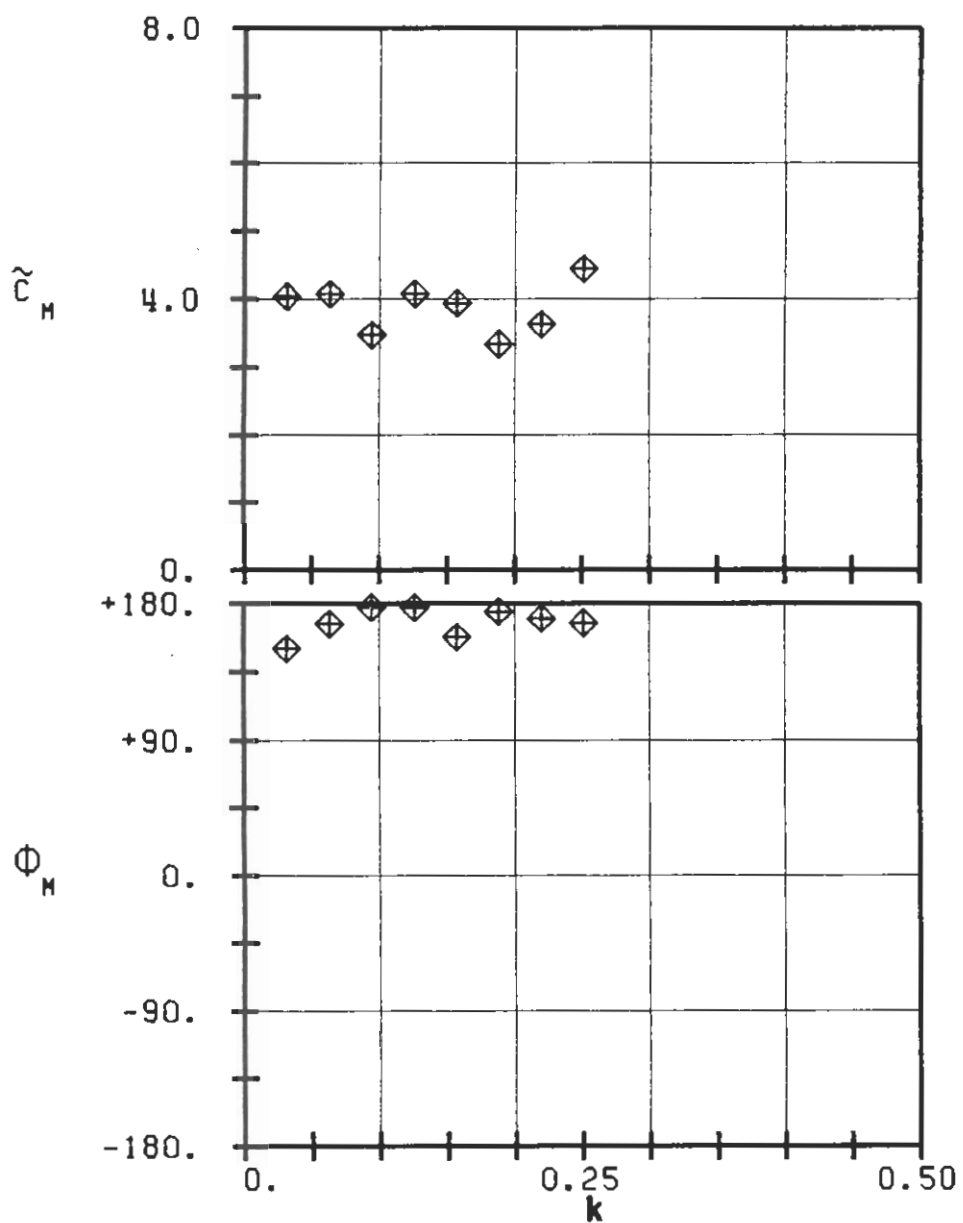
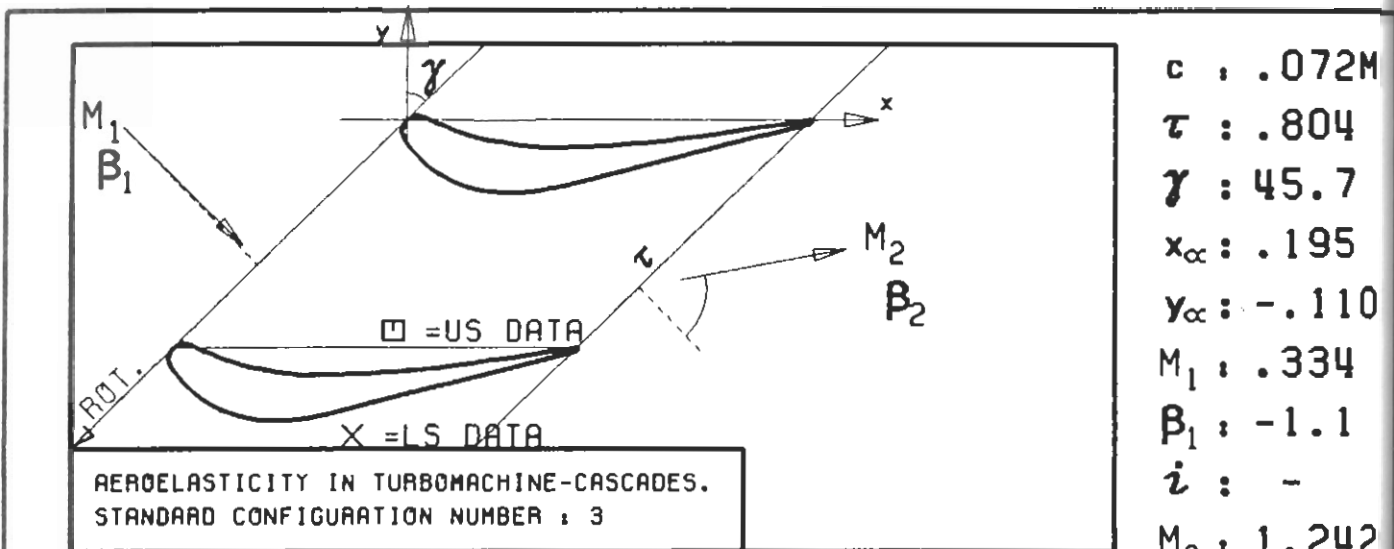
PLOT 7.3-4.3: THIRD STANDARD CONFIGURATION.
AERODYNAMIC LIFT COEFFICIENT AND PHASE LEAD
IN DEPENDENCE OF REDUCED FREQUENCY.



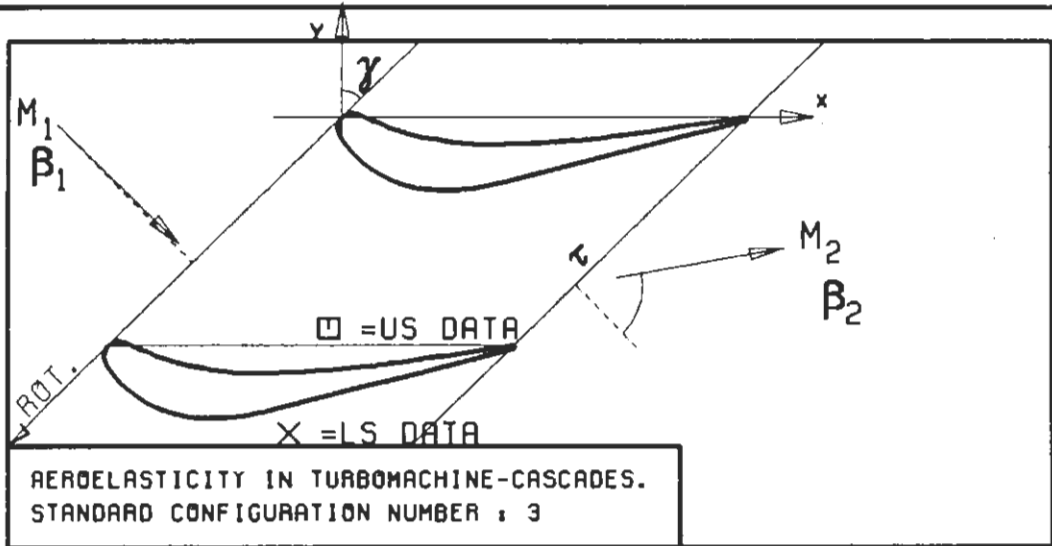
c	: .072M
τ	: .804
γ	: 45.7
x_α	: .195
y_α	: -.110
M_1	: .303
B_1	: -1.2
i	: -
M_2	: 0.682
B_2	: -58.3
h_x	: -
h_y	: -
α	: .017
ω	:
k	:
δ	: -
σ	: 67.5
d	: .124



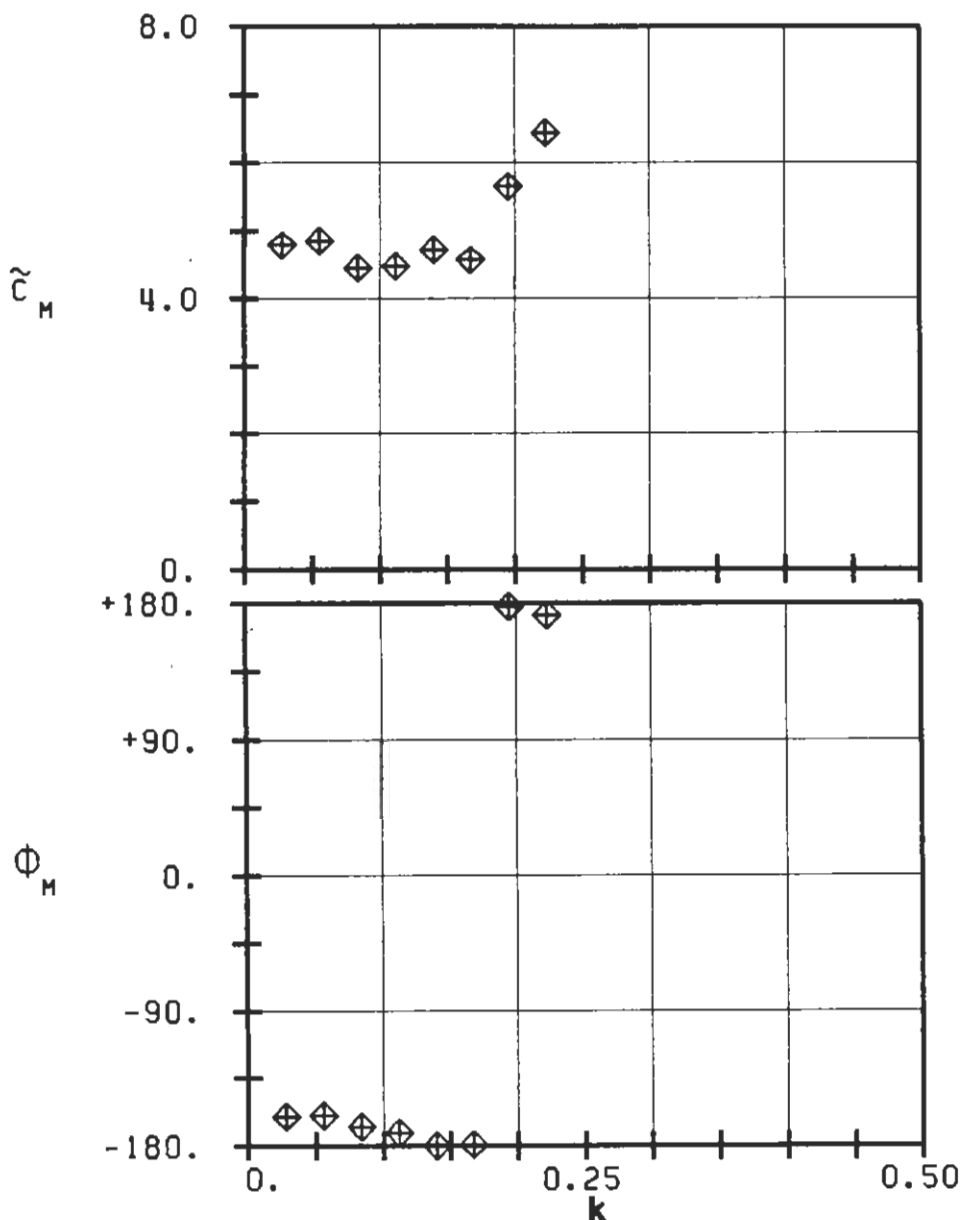
PLOT 7.3-5.1: THIRD STANDARD CONFIGURATION.
AERODYNAMIC MOMENT COEFFICIENT AND PHASE LEAD
IN DEPENDENCE OF REDUCED FREQUENCY.



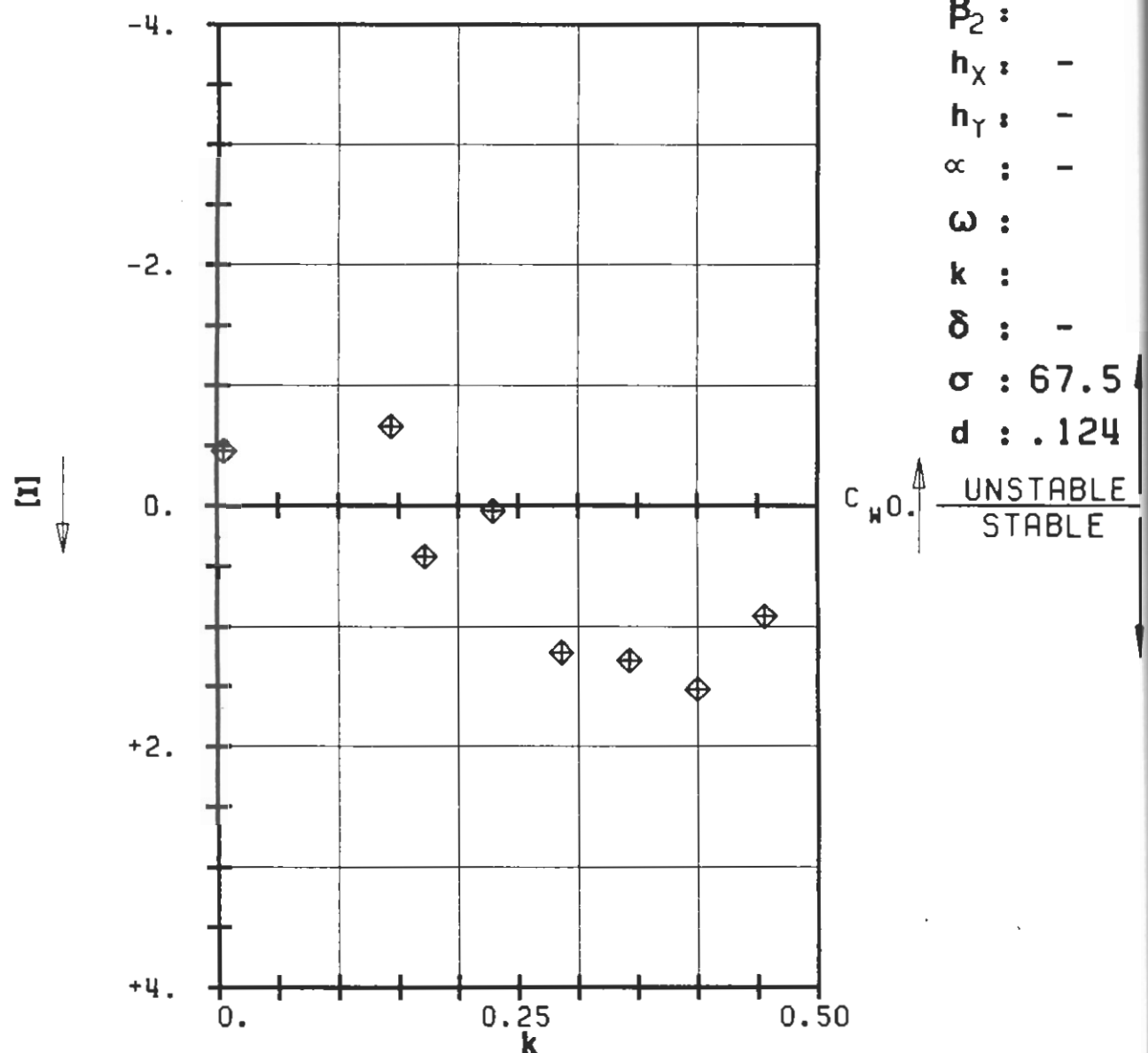
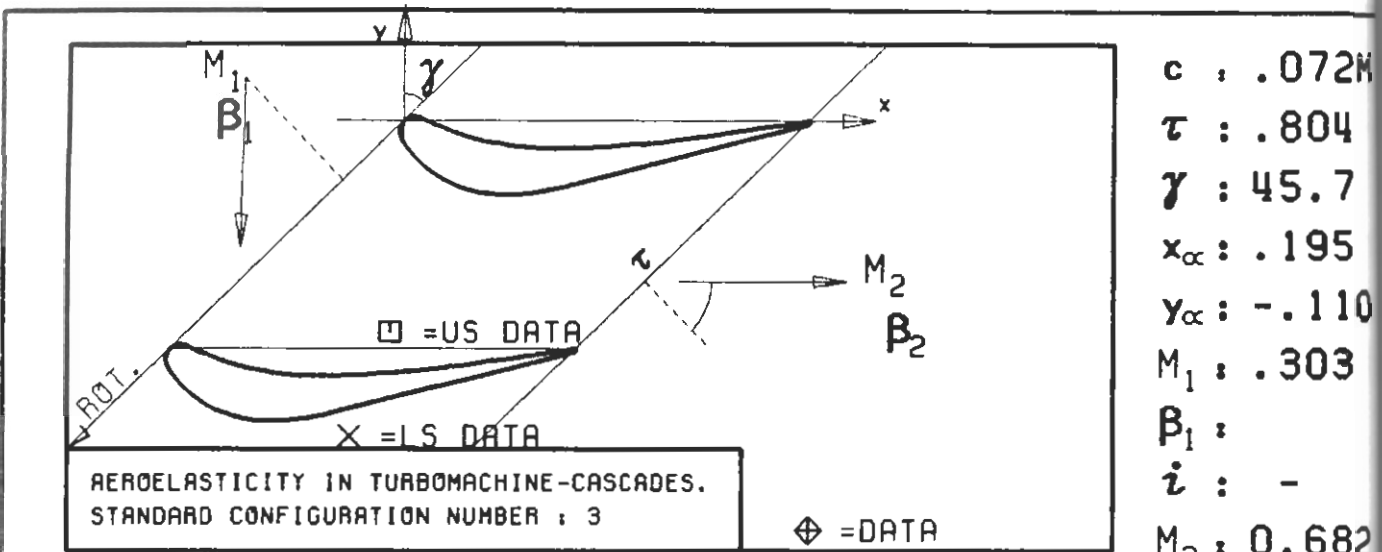
PLOT 7.3-5.2: THIRD STANDARD CONFIGURATION.
AERODYNAMIC MOMENT COEFFICIENT AND PHASE LEAD
IN DEPENDENCE OF REDUCED FREQUENCY.



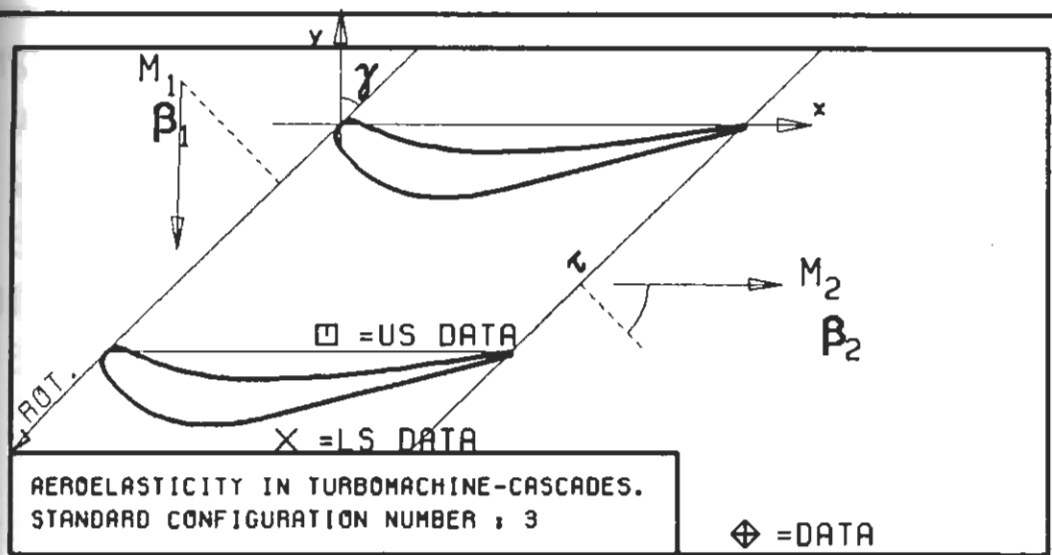
$c : .072M$
 $\tau : .804$
 $\gamma : 45.7$
 $x_\alpha : .195$
 $y_\alpha : -.110$
 $M_1 : .303$
 $\beta_1 : -1.2$
 $i : -$
 $M_2 : 1.397$
 $\beta_2 : -55.5$
 $h_x : -$
 $h_y : -$
 $\alpha : .017$
 $\omega : -$
 $k : -$
 $\delta : -$
 $\sigma : 67.5$
 $d : .124$



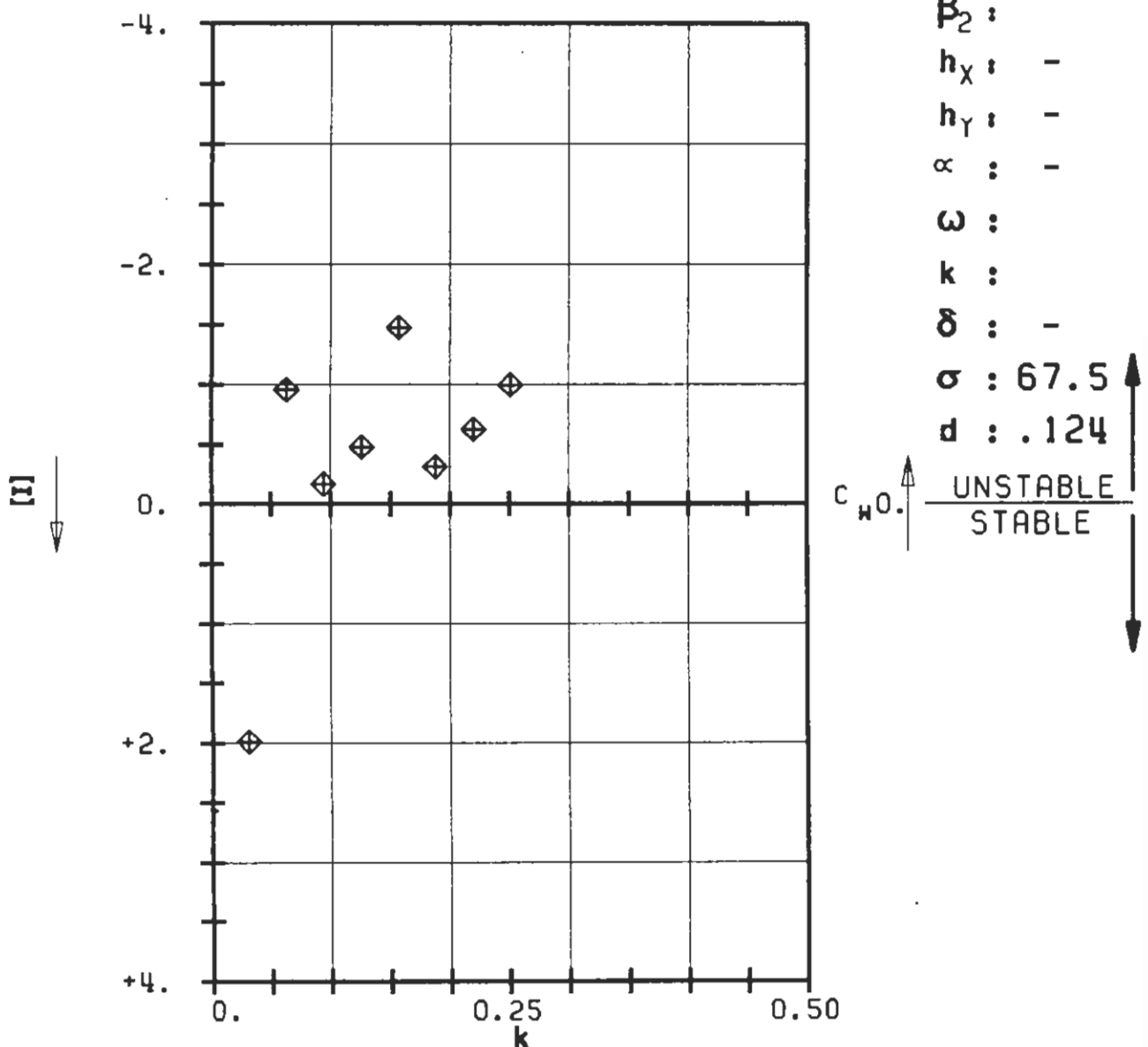
PLOT 7.3-5.3: THIRD STANDARD CONFIGURATION.
AERODYNAMIC MOMENT COEFFICIENT AND PHASE LEAD
IN DEPENDENCE OF REDUCED FREQUENCY.



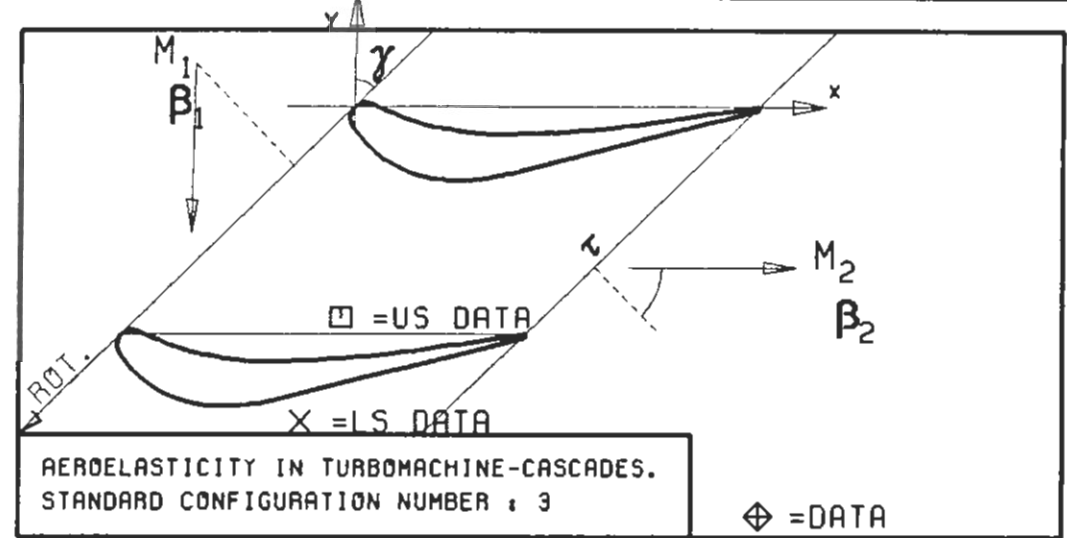
PLOT 7.3-6.1: THIRD STANDARD CONFIGURATION.
AERODYNAMIC WORK AND DAMPING COEFFICIENTS
IN DEPENDENCE OF REDUCED FREQUENCY.



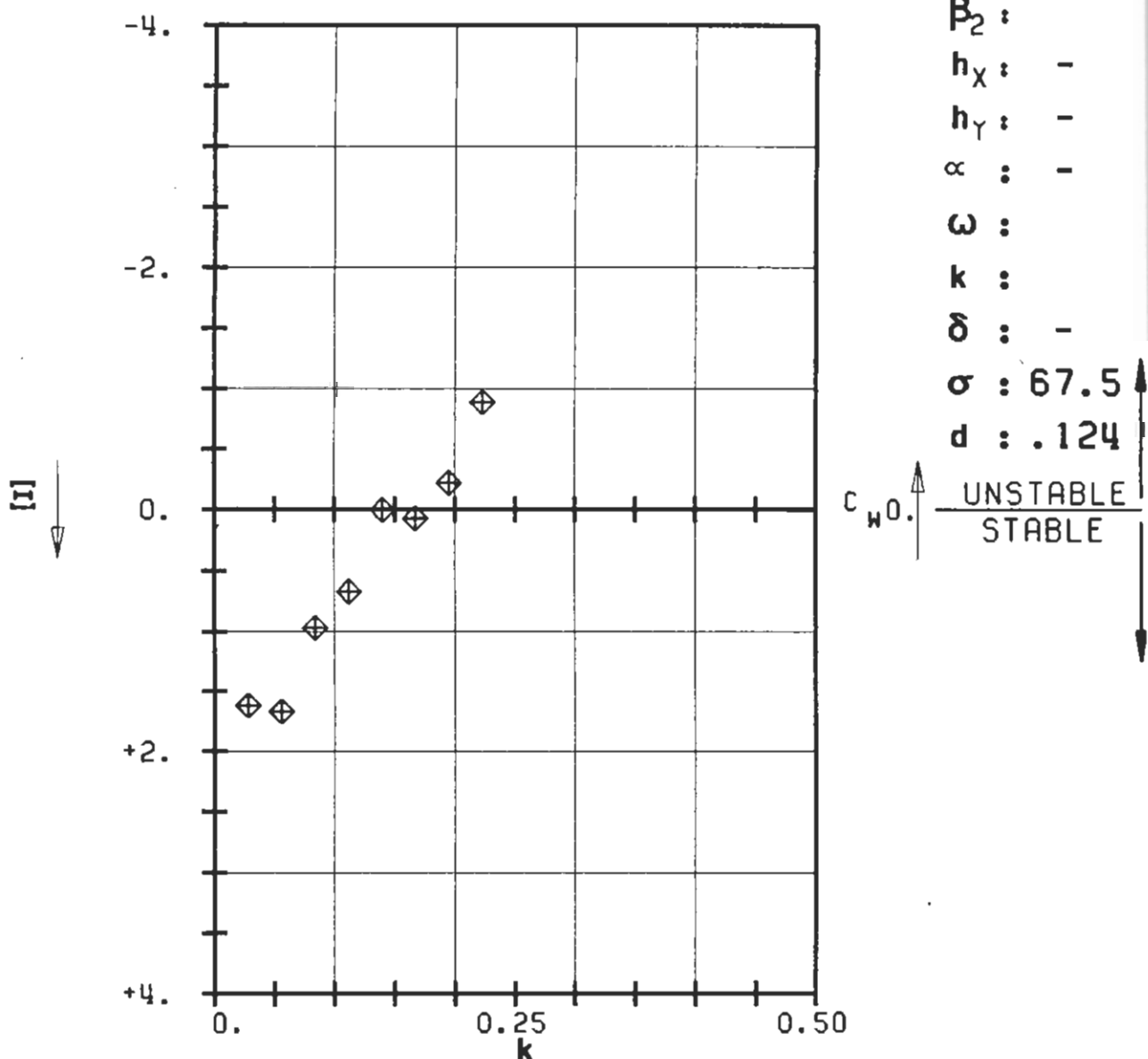
$c : .072M$
 $\tau : .804$
 $\gamma : 45.7$
 $x_\alpha : .195$
 $y_\alpha : -.110$
 $M_1 : .334$
 $\beta_1 :$
 $i : -$
 $M_2 : 1.242$
 $\beta_2 :$
 $h_x : -$
 $h_y : -$
 $\alpha : -$
 $\omega : -$
 $k : -$
 $\delta : -$
 $\sigma : 67.5$
 $d : .124$



PLOT 7.3-6.2: THIRD STANDARD CONFIGURATION.
AERODYNAMIC WORK AND DAMPING COEFFICIENTS
IN DEPENDENCE OF REDUCED FREQUENCY.



c : .072M
 τ : .804
 γ : 45.7
 x_α : .195
 y_α : -.110
 M_1 : .303
 β_1 :
 i : -
 M_2 : 1.397



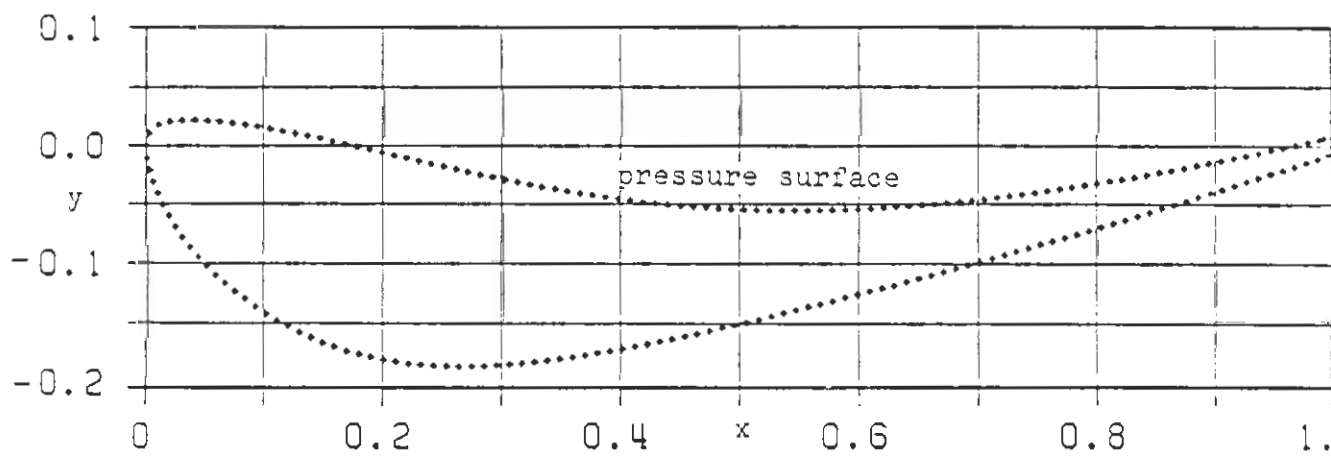
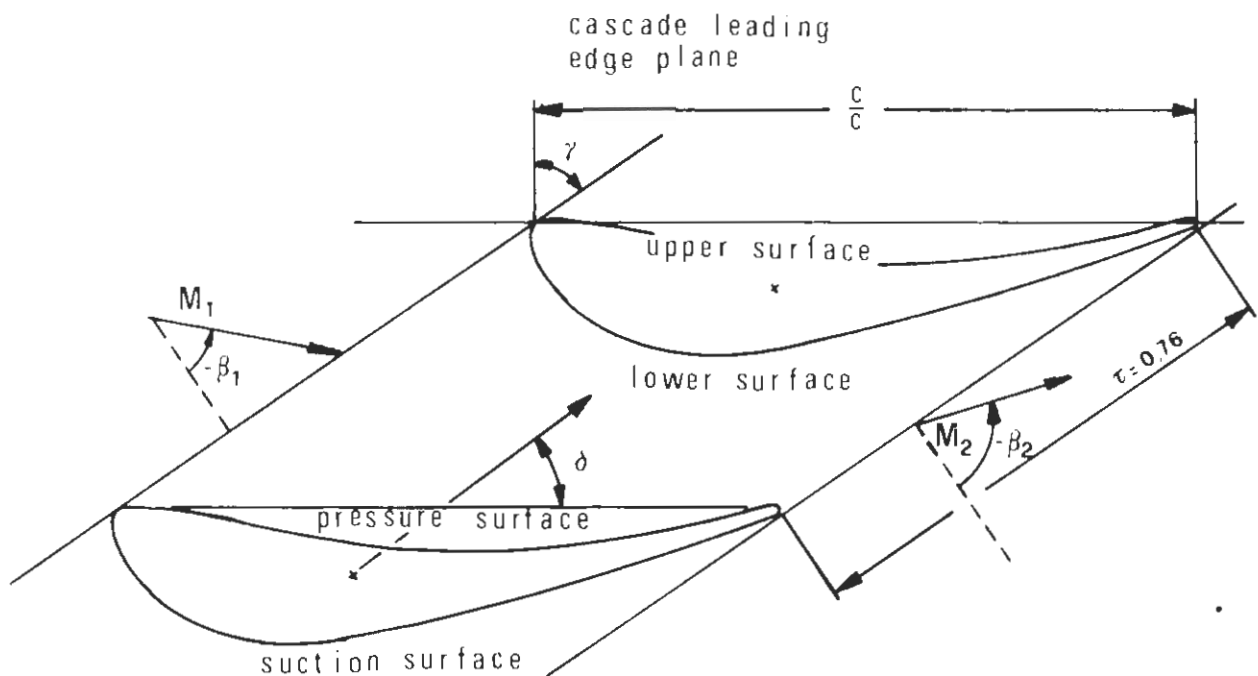
PLOT 7.3-6.3: THIRD STANDARD CONFIGURATION.
AERODYNAMIC WORK AND DAMPING COEFFICIENTS
IN DEPENDENCE OF REDUCED FREQUENCY.

AEROELASTICITY IN TURBOMACHINE-CASCADES

FOURTH STANDARD CONFIGURATION

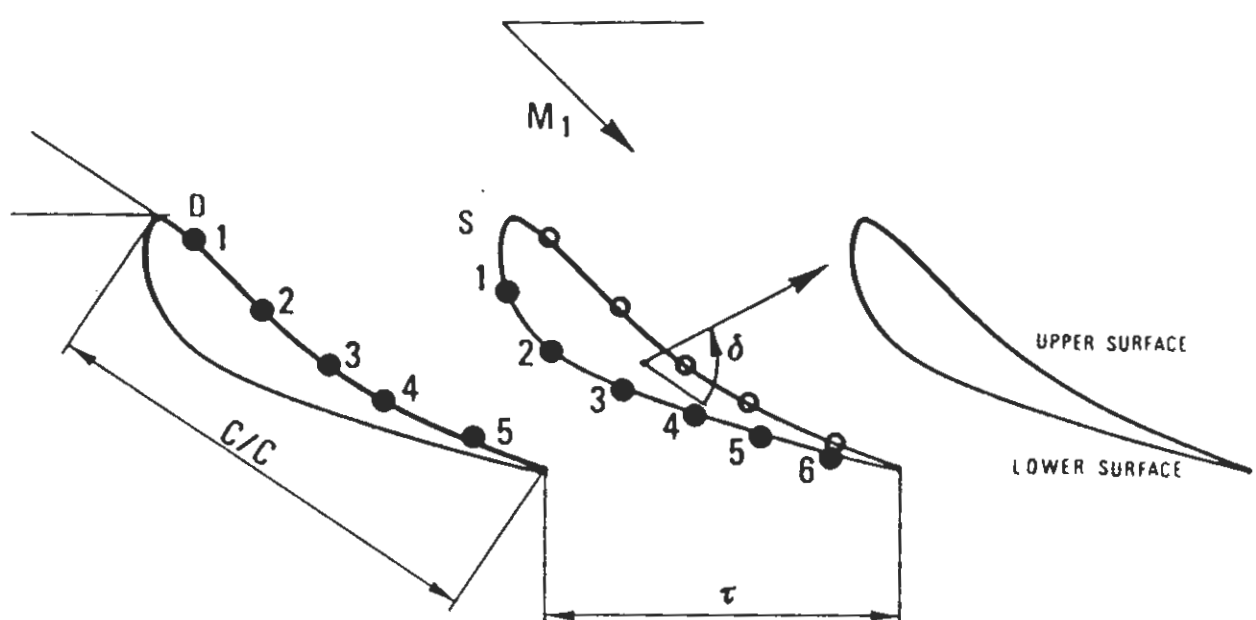
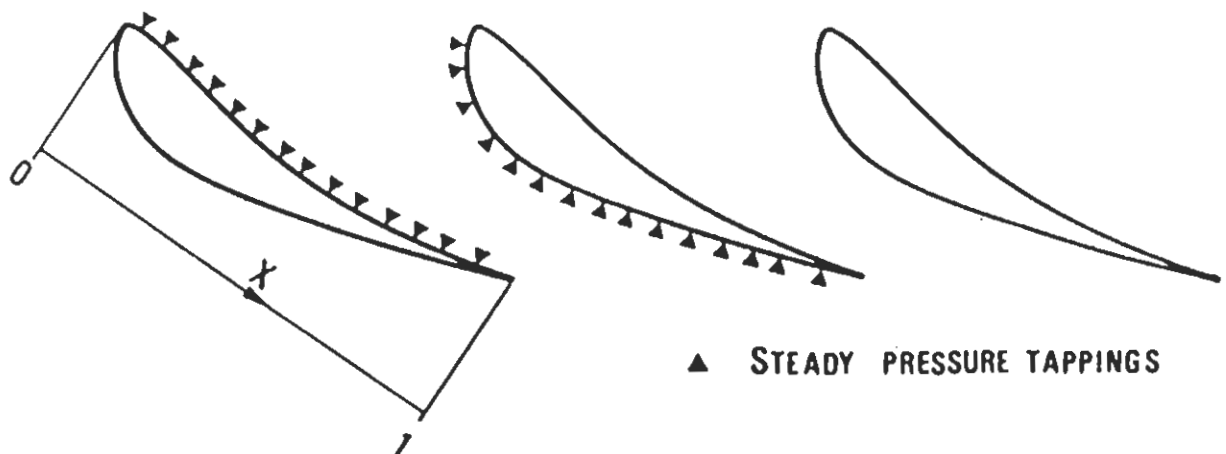
Definition

High Subsonic/Transonic Turbine Profiles.



Vibration in first bending mode	δ	= 60.4°
d = (thickness/chord)		= 0.17
γ = 56.6°	k	= variable
C = 0.0744 m	span	= 0.040 m
τ = 0.67 (hub) 0.76 (midspan) 0.84 (tip)	camber	= $45.^\circ$
M_{2is} = variable	hub/tip	= 0.8
Nominal values: $M_1=0.31$; $\beta_1=-44.1^\circ$; $M_2=0.90$; $\beta_2=-72.4^\circ$	f	= 150 Hz
Working fluid: Air	σ	= variable

Fig. 7.4-1a. Fourth standard configuration: Cascade geometry



● UNSTEADY PRESSURE TRANSDUCERS

Fig. 7.4-1b. Fourth standard configuration: Location of pressure measurements on blade surfaces.

C = .0744 M

UPPER SURFACE				LOWER SURFACE			
X	Y	X	Y	X	Y	X	Y
0.000	0.000	.514	-.055	0.000	0.000	.443	-.163
.003	.010	.524	-.055	.001	-.011	.453	-.160
.010	.018	.535	-.055	.003	-.021	.464	-.158
.020	.021	.546	-.055	.006	-.031	.474	-.156
.031	.022	.556	-.055	.010	-.041	.485	-.154
.042	.022	.567	-.055	.014	-.051	.495	-.151
.052	.021	.578	-.055	.020	-.060	.505	-.149
.063	.020	.588	-.055	.025	-.069	.516	-.146
.074	.019	.599	-.054	.031	-.078	.526	-.144
.084	.018	.610	-.054	.038	-.087	.536	-.141
.095	.016	.620	-.053	.044	-.095	.547	-.139
.105	.014	.631	-.052	.052	-.102	.557	-.136
.116	.012	.642	-.052	.059	-.110	.568	-.134
.126	.010	.652	-.051	.067	-.117	.578	-.131
.136	.008	.663	-.050	.076	-.124	.588	-.129
.147	.006	.673	-.049	.084	-.130	.598	-.126
.157	.004	.684	-.048	.093	-.136	.609	-.123
.168	.001	.695	-.047	.102	-.142	.619	-.121
.178	-.001	.705	-.046	.111	-.147	.629	-.118
.188	-.003	.716	-.044	.120	-.153	.640	-.115
.199	-.006	.726	-.043	.130	-.157	.650	-.113
.209	-.008	.737	-.042	.139	-.162	.660	-.110
.220	-.011	.747	-.040	.149	-.166	.671	-.107
.230	-.013	.758	-.039	.159	-.170	.681	-.104
.240	-.015	.768	-.037	.169	-.173	.691	-.101
.251	-.018	.779	-.036	.179	-.176	.701	-.099
.261	-.020	.790	-.034	.190	-.179	.712	-.096
.271	-.022	.800	-.032	.200	-.181	.722	-.093
.282	-.025	.811	-.030	.211	-.182	.732	-.090
.292	-.027	.821	-.029	.221	-.184	.742	-.087
.303	-.029	.832	-.027	.232	-.185	.753	-.084
.313	-.031	.842	-.025	.243	-.185	.763	-.081
.324	-.033	.852	-.023	.253	-.186	.773	-.078
.334	-.035	.863	-.021	.264	-.186	.783	-.075
.345	-.037	.873	-.019	.274	-.186	.794	-.072
.355	-.039	.884	-.017	.285	-.186	.804	-.069
.365	-.041	.894	-.015	.296	-.185	.814	-.066
.376	-.043	.905	-.013	.306	-.184	.824	-.063
.387	-.044	.915	-.010	.317	-.183	.834	-.060
.397	-.046	.926	-.008	.328	-.182	.844	-.057
.408	-.047	.936	-.006	.338	-.181	.855	-.054
.418	-.048	.946	-.004	.349	-.179	.865	-.050
.429	-.049	.957	-.001	.359	-.178	.875	-.047
.439	-.051	.967	.001	.370	-.176	.885	-.044
.450	-.051	.978	.003	.380	-.175	.895	-.041
.461	-.052	.988	.006	.391	-.173	.905	-.037
.471	-.053			.401	-.171	.926	-.031
.482	-.054			.412	-.169	.936	-.028
.493	-.054			.422	-.167	.946	-.024
.503	-.055			.433	-.165	.956	-.021
						.966	-.017
						.976	-.014
						.986	-.011
						.996	-.007

Table 7.4-1. Fourth standard configuration: Dimensionless airfoil coordinates (spanwise identical).

AEROELASTICITY IN TURBOMACHINE-CASCADES

FOURTH STANDARD CONFIGURATION

Aeroelastic Test Cases

Aeroelastic Test Case	Time-Averaged Parameters				Time-Dependent Parameters			
	M ₁ (-)	β ₁ (°)	M _{2is} (-)	β ₂ (°)	σ (°)	k (-)	h ⁰ (-)	δ (°)
1	0.19	- 45	0.58	- 71	- 90	0.168	0.0038	60.4
2	0.26	"	0.76	"	"	0.128	"	"
3	0.28	"	0.90	"	"	0.107	"	"
4	0.29	"	1.02	"	"	0.095	0.0033	"
5	"	"	1.19	"	"	0.082	0.0038	"
6	0.28	"	0.90	"	+ 180	0.107	0.0033	"
7	"	"	"	"	+ 90	"	"	"
8	"	"	"	"	0	"	"	"

Table 7.4-2. Fourth Standard Configuration.
8 Recommended Aeroelastic Test Cases.

AEROELASTICITY IN TURBOMACHINE-CASCADES

FOURTH STANDARD CONFIGURATION

Experimental and Theoretical Results

4TH STANDARD CONFIGURATION : Unsteady Test Data

Aeroelastic case Nr. : 1

TEST: 553D-1 Date : 8-AUG-84

Inlet and outlet flow conditions :

$P_{c1} = 2318 \text{ mb}$	$P_{s1} = 2259 \text{ mb}$	$P_{s2} = 1843 \text{ mb}$
$\beta_{c1} = 45 \text{ deg}$	$M_{1is} = 0.19$	$M_{2is} = 0.58$

Unsteady test parameters :

Blade frequency :	$f = 150.0 \text{ Hz}$	$k = 0.1722$
Phase control setpoint :	$\sigma = -90 \text{ deg}$	
Total record time :	$T_{rec} = 11.72 \text{ sec}$	
Number of periods detected :	$N_{Per} = 1748$	
Total number of samples :	$N_{Samp} = 25600$	
Number of sample sets :	$N_{Set} = 10$	

Error limits estimated for 95% confidence level, based on variance
of mean values of sample sets

Blade vibration data :

Blade	Amplitude (mm)	$h*1000 (-)$	$\phi (\text{deg})$	$\sigma (\text{deg})$	signal ratio
B 4	0.242 ± 0.004	3.25 ± 0.05	180. ± 0.9		0.992
B 5	0.275 ± 0.004	3.69 ± 0.06	90. ± 0.9	-89.4	0.996
B 6	0.255 ± 0.003	3.43 ± 0.04	0. ± 0.6	-90.4	0.995
B 7	0.244 ± 0.006	3.28 ± 0.08	-90. ± 1.4	-89.9	0.995

Unsteady pressure data :

(Phase angles referenced to transducer blade motions)

Transducer	x	P (mb)	$P/P_{c1}/h (-)$	cP (-)	$\phi (\text{deg})$	signal ratio
US B5:D1	0.101	0.44	0.050	1.97 ± 1.10	51. ± 29.	0.523
US B5:D2	0.302	1.07	0.125	4.92 ± 0.70	106. ± 8.	0.490
US B5:D3	0.501	1.62	0.189	7.43 ± 1.05	126. ± 8.	0.567
US B5:D4	0.638	2.18	0.254	9.98 ± 1.05	146. ± 6.	0.704
US B5:D5	0.840	3.27	0.382	15.01 ± 1.08	170. ± 4.	0.848
LS B6:S1	0.101	5.04	0.633	24.88 ± 1.81	173. ± 4.	0.776
LS B6:S2	0.236	5.38	0.676	26.57 ± 2.01	160. ± 4.	0.819
LS B6:S3	0.437	1.99	0.250	9.81 ± 1.59	152. ± 9.	0.520
LS B6:S4	0.571	1.25	0.157	6.18 ± 1.37	137. ± 13.	0.399
LS B6:S5	0.706	0.91	0.114	4.48 ± 1.30	132. ± 16.	0.310
LS B6:S6	0.840	0.96	0.120	4.73 ± 1.28	126. ± 15.	0.306

Unsteady force coefficients :

Side	$ch (-)$	$\phi(ch) (\text{deg})$	ch_{re}	ch_{im}
US B5:CH	5.94	-35.	4.87	-3.41
LS B6:CH	12.44	161.	-11.78	3.98
Combined	6.94 ± 0.73	175. ± 6.	-6.91	0.57

Aerodynamic damping coefficient : $\chi_{si} = -0.571 ± 0.518$

4TH STANDARD CONFIGURATION : Unsteady Test Data

Aeroelastic case Nr. : 2

TEST: 553C-1 Date : 8-AUG-84

Inlet and outlet flow conditions :

$P_{c1} = 2131 \text{ mb}$	$P_{s1} = 2034 \text{ mb}$	$P_{s2} = 1449 \text{ mb}$
$\beta_{a1} = 45 \text{ deg}$	$M_{1is} = 0.26$	$M_{2is} = 0.76$

Unsteady test parameters :

Blade frequency :	$f = 150.0 \text{ Hz}$	$k = 0.1338$
Phase control setpoint :	$\sigma = -90 \text{ deg}$	
Total record time :	$T_{rec} = 11.72 \text{ sec}$	
Number of periods detected :	$N_{Per} = 1746$	
Total number of samples :	$N_{Samp} = 25600$	
Number of sample sets :	$N_{Set} = 10$	

Error limits estimated for 95% confidence level, based on variance
of mean values of sample sets

Blade vibration data :

Blade	Amplitude (mm)	$h*1000 (-)$	$\phi (\text{deg})$	$\sigma (\text{deg})$	signal ratio
B 4	0.240 ± 0.006	3.23 ± 0.09	180. ± 1.6		0.980
B 5	0.272 ± 0.010	3.65 ± 0.14	91. ± 2.2	-88.9	0.985
B 6	0.254 ± 0.004	3.41 ± 0.06	-0. ± 1.0	-90.9	0.985
B 7	0.242 ± 0.012	3.25 ± 0.16	-89. ± 2.9	-89.5	0.983

Unsteady pressure data :

(Phase angles referenced to transducer blade motions)

Transducer	x	p (mb)	$p/p_{c1}/h (-)$	$c_p (-)$	$\phi (\text{deg})$	signal ratio
US B5:D1	0.101	0.37	0.045	0.99 ± 0.83	41. ± 40.	0.483
US B5:D2	0.302	0.93	0.118	2.60 ± 0.63	101. ± 14.	0.453
US B5:D3	0.501	1.58	0.203	4.45 ± 0.80	121. ± 10.	0.557
US B5:D4	0.638	2.26	0.290	6.37 ± 0.92	148. ± 8.	0.721
US B5:D5	0.840	3.92	0.504	11.07 ± 1.29	175. ± 7.	0.889
LS B6:S1	0.101	5.66	0.779	17.11 ± 1.57	171. ± 5.	0.832
LS B6:S2	0.236	6.70	0.921	20.24 ± 1.81	158. ± 5.	0.873
LS B6:S3	0.437	2.55	0.348	7.64 ± 2.56	148. ± 19.	0.501
LS B6:S4	0.571	1.93	0.262	5.75 ± 2.40	133. ± 23.	0.436
LS B6:S5	0.706	1.39	0.186	4.10 ± 2.37	128. ± 30.	0.322
LS B6:S6	0.840	1.40	0.186	4.09 ± 2.36	127. ± 30.	0.324

Unsteady force coefficients :

Side	$ch (-)$	$\phi(ch) (\text{deg})$	ch_{re}	ch_{im}
US B5:CH	3.80	-29.	3.32	-1.85
LS B6:CH	9.30	158.	-8.60	3.55
Combined	5.55 ± 0.84	162. ± 9.	-5.28	1.70

Aerodynamic damping coefficient : $x_{si} = -1.705 ± 0.593$

4TH STANDARD CONFIGURATION : Unsteady Test Data

Aeroelastic case Nr. : 3

TEST: 552B-1 Date : 8-AUG-84

Inlet and outlet flow conditions :

$P_{c1} = 2058 \text{ mb}$	$P_{s1} = 1949 \text{ mb}$	$P_{s2} = 1212 \text{ mb}$
$\beta_{c1} = 45 \text{ deg}$	$M_{1is} = 0.28$	$M_{2is} = 0.90$

Unsteady test parameters :

Blade frequency :	$f = 150.0 \text{ Hz}$	$k = 0.1153$
Phase control setpoint :	$\sigma = -90 \text{ deg}$	
Total record time :	$T_{rec} = 11.72 \text{ sec}$	
Number of periods detected :	$N_{Per} = 1745$	
Total number of samples :	$N_{Samp} = 25600$	
Number of sample sets :	$N_{Set} = 10$	

Error limits estimated for 95% confidence level, based on variance
of mean values of sample sets

Blade vibration data :

Blade	Amplitude (mm)	$h*1000 (-)$	$\phi (\text{deg})$	$\sigma (\text{deg})$	signal ratio
B 4	0.213 ± 0.117	2.86 ± 0.12	180. ± 2.3		0.967
B 5	0.227 ± 0.006	3.05 ± 0.08	90. ± 1.4	-89.6	0.984
B 6	0.226 ± 0.006	3.04 ± 0.08	0. ± 1.5	-90.0	0.975
B 7	0.229 ± 0.017	3.07 ± 0.23	-90. ± 4.3	-90.1	0.974

Unsteady pressure data :

(Phase angles referenced to transducer blade motions)

Transducer	x	P (mb)	$P/P_{c1}/h (-)$	$C_P (-)$	$\phi (\text{deg})$	signal ratio
US B5:D1	0.101	0.67	0.100	1.89 ± 1.84	37. ± 44.	0.392
US B5:D2	0.302	0.83	0.130	2.46 ± 0.87	97. ± 20.	0.320
US B5:D3	0.501	1.34	0.212	4.00 ± 1.03	97. ± 14.	0.429
US B5:D4	0.638	1.95	0.309	5.83 ± 1.01	146. ± 10.	0.585
US B5:D5	0.840	3.58	0.568	10.73 ± 1.13	176. ± 6.	0.819
LS B6:S1	0.101	5.26	0.840	15.86 ± 1.69	170. ± 6.	0.746
LS B6:S2	0.236	5.44	0.869	16.41 ± 0.93	157. ± 3.	0.880
LS B6:S3	0.437	2.54	0.404	7.63 ± 2.50	139. ± 18.	0.483
LS B6:S4	0.571	2.64	0.418	7.89 ± 3.09	130. ± 21.	0.462
LS B6:S5	0.706	2.48	0.390	7.36 ± 4.22	154. ± 30.	0.327
LS B6:S6	0.840	1.90	0.298	5.63 ± 3.21	149. ± 30.	0.340

Unsteady force coefficients :

Side	$ch (-)$	$\phi(ch) (\text{deg})$	ch_{re}	ch_{im}
US B5:CH	3.31	-34.	2.73	-1.87
LS B6:CH	9.28	157.	-8.54	3.63
Combined	6.08 ± 1.02	163. ± 10.	-5.81	1.76

Aerodynamic damping coefficient : $\chi_{si} = -1.762 ± 0.720$

4TH STANDARD CONFIGURATION : Unsteady Test Data

Aeroelastic case Nr. : 4

TEST: 552A-1 Date : 8-AUG-84

Inlet and outlet flow conditions :

$P_{c1} = 2020 \text{ mb}$	$P_{s1} = 1907 \text{ mb}$	$P_{s2} = 1043 \text{ mb}$
$\beta_{a1} = 45 \text{ deg}$	$M_{1is} = 0.29$	$M_{2is} = 1.02$

Unsteady test parameters :

Blade frequency :	$f = 150.0 \text{ Hz}$	$k = 0.1041$
Phase control setpoint :	$\sigma = -90 \text{ deg}$	
Total record time :	$T_{rec} = 11.72 \text{ sec}$	
Number of periods detected :	$N_{Per} = 1745$	
Total number of samples :	$N_{Samp} = 25600$	
Number of sample sets :	$N_{Set} = 10$	

Error limits estimated for 95% confidence level, based on variance
of mean values of sample sets

Blade vibration data :

Blade	Amplitude (mm)	$h*1000 (-)$	$\phi (\text{deg})$	$\sigma (\text{deg})$	signal ratio
B 4	0.217 ± 0.008	2.91 ± 0.12	179. ± 2.3		0.984
B 5	0.231 ± 0.007	3.10 ± 0.09	90. ± 1.7	-89.0	0.995
B 6	0.231 ± 0.004	3.11 ± 0.06	0. ± 1.1	-90.3	0.989
B 7	0.232 ± 0.017	3.12 ± 0.23	-91. ± 4.2	-90.6	0.986

Unsteady pressure data :

(Phase angles referenced to transducer blade motions)

Transducer	x	p (mb)	$p/p_{c1}/h (-)$	$c_p (-)$	$\phi (\text{deg})$	signal ratio
US B5:D1	0.101	0.34	0.051	0.91 ± 0.85	53. ± 43.	0.375
US B5:D2	0.302	0.85	0.135	2.42 ± 0.56	104. ± 13.	0.318
US B5:D3	0.501	1.37	0.219	3.91 ± 0.75	107. ± 11.	0.428
US B5:D4	0.638	2.07	0.329	5.89 ± 0.71	146. ± 7.	0.582
US B5:D5	0.840	4.03	0.642	11.48 ± 0.78	176. ± 4.	0.851
LS B6:S1	0.101	5.16	0.822	14.69 ± 1.41	174. ± 5.	0.741
LS B6:S2	0.236	4.21	0.670	11.98 ± 0.75	160. ± 4.	0.906
LS B6:S3	0.437	2.42	0.384	6.87 ± 1.02	-180. ± 8.	0.660
LS B6:S4	0.571	1.08	0.172	3.07 ± 0.57	68. ± 11.	0.495
LS B6:S5	0.706	1.62	0.257	4.59 ± 0.63	98. ± 8.	0.645
LS B6:S6	0.840	2.38	0.379	6.77 ± 0.80	107. ± 7.	0.626

Unsteady force coefficients :

Side	$ch (-)$	$\phi(ch) (\text{deg})$	ch_{re}	ch_{im}
US B5:CH	3.66	-29.	3.20	-1.77
LS B6:CH	6.80	156.	-6.22	2.73
Combined	3.17 ± 0.49	162. ± 9.	-3.02	0.96

Aerodynamic damping coefficient : $\xi = -0.964 ± 0.349$

4TH STANDARD CONFIGURATION : Unsteady Test Data

Aeroelastic case Nr. : 5

TEST: 553B-1 Date : 8-AUG-84

Inlet and outlet flow conditions :

$p_{c1} = 2196 \text{ mb}$	$p_{s1} = 2071 \text{ mb}$	$p_{s2} = 914 \text{ mb}$
$\beta_{c1} = 45 \text{ deg}$	$M_{1is} = 0.29$	$M_{2is} = 1.19$

Unsteady test parameters :

Blade frequency :	$f = 150.0 \text{ Hz}$	$k = 0.0917$
Phase control setpoint :	$\sigma = -90 \text{ deg}$	
Total record time :	$T_{rec} = 11.72 \text{ sec}$	
Number of periods detected :	$N_{Per} = 1746$	
Total number of samples :	$N_{Samp} = 25600$	
Number of sample sets :	$N_{Set} = 10$	

Error limits estimated for 95% confidence level, based on variance
of mean values of sample sets

Blade vibration data :

Blade	Amplitude (mm)	$h \times 1000 (-)$	$\phi (\text{deg})$	$\sigma (\text{deg})$	signal ratio
B 4	0.242 ± 0.011	3.25 ± 0.14	180. ± 2.4		0.987
B 5	0.273 ± 0.009	3.67 ± 0.12	91. ± 1.9	-88.9	0.990
B 6	0.254 ± 0.005	3.41 ± 0.07	0. ± 1.2	-91.0	0.988
B 7	0.242 ± 0.011	3.25 ± 0.14	-89. ± 2.5	-89.0	0.988

Unsteady pressure data :

(Phase angles referenced to transducer blade motions)

Transducer	x	P (mb)	$P/P_{c1}/h (-)$	$c_P (-)$	$\phi (\text{deg})$	signal ratio
US B5:D1	0.101	0.39	0.046	0.81 ± 0.69	41. ± 41.	0.445
US B5:D2	0.302	0.95	0.118	2.07 ± 0.37	96. ± 10.	0.428
US B5:D3	0.501	1.63	0.202	3.55 ± 0.49	116. ± 8.	0.525
US B5:D4	0.638	2.10	0.260	4.56 ± 0.47	143. ± 6.	0.670
US B5:D5	0.840	4.05	0.502	8.81 ± 0.52	176. ± 3.	0.872
LS B6:S1	0.101	8.47	1.131	19.87 ± 1.47	166. ± 4.	0.853
LS B6:S2	0.236	10.02	1.338	23.51 ± 1.01	146. ± 2.	0.972
LS B6:S3	0.437	5.15	0.687	12.07 ± 1.28	-117. ± 6.	0.859
LS B6:S4	0.571	9.94	1.328	23.33 ± 1.36	-110. ± 3.	0.951
LS B6:S5	0.706	2.78	0.371	6.51 ± 1.54	146. ± 13.	0.531
LS B6:S6	0.840	4.46	0.595	10.46 ± 1.26	-162. ± 7.	0.829

Unsteady force coefficients :

Side	$ch (-)$	$\phi(ch) (\text{deg})$	ch_{re}	ch_{im}
US B5:CH	2.88	-31.	2.47	-1.47
LS B6:CH	11.03	-177.	-11.01	-0.64
Combined	8.80 ± 0.54	-166. ± 4.	-8.54	-2.12

Aerodynamic damping coefficient : $x_{si} = 2.115 ± 0.381$

4TH STANDARD CONFIGURATION : Unsteady Test Data

Aeroelastic case Nr. : 6

TEST: 552B-2 Date : 8-AUG-84

Inlet and outlet flow conditions :

$P_{c1} = 2058 \text{ mb}$	$P_{s1} = 1949 \text{ mb}$	$P_{s2} = 1212 \text{ mb}$
$\beta_{c1} = 45 \text{ deg}$	$M_{1is} = 0.28$	$M_{2is} = 0.90$

Unsteady test parameters :

Blade frequency :	$f = 150.0 \text{ Hz}$	$k = 0.1153$
Phase control setpoint :	$\sigma = 180 \text{ deg}$	
Total record time :	$T_{rec} = 11.72 \text{ sec}$	
Number of periods detected :	$N_{Per} = 1743$	
Total number of samples :	$N_{Samp} = 25600$	
Number of sample sets :	$N_{Set} = 10$	

Error limits estimated for 95% confidence level, based on variance
of mean values of sample sets

Blade vibration data :

Blade	Amplitude (mm)	$h@1000 \text{ (-)}$	$\phi \text{ (deg)}$	$\sigma \text{ (deg)}$	signal ratio
B 4	0.214 ± 0.184	2.87 ± 0.18	0. ± 3.7		0.973
B 5	0.227 ± 0.008	3.06 ± 0.10	-179. ± 1.9	-179.6	0.982
B 6	0.225 ± 0.007	3.02 ± 0.10	0. ± 1.8	179.5	0.971
B 7	0.232 ± 0.022	3.11 ± 0.30	180. ± 5.5	179.9	0.974

Unsteady pressure data :

(Phase angles referenced to transducer blade motions)

Transducer	x	p (mb)	$P/P_{c1}/h \text{ (-)}$	$c_p \text{ (-)}$	$\phi \text{ (deg)}$	signal ratio
US B5:D1	0.101	0.77	0.117	2.20 ± 1.94	29. ± 41.	0.437
US B5:D2	0.302	0.71	0.113	2.13 ± 0.66	42. ± 17.	0.281
US B5:D3	0.501	1.18	0.187	3.52 ± 0.67	52. ± 11.	0.390
US B5:D4	0.638	1.11	0.175	3.31 ± 0.90	105. ± 15.	0.381
US B5:D5	0.840	4.12	0.656	12.38 ± 0.96	150. ± 4.	0.867
LS B6:S1	0.101	6.52	1.048	19.79 ± 1.64	-160. ± 5.	0.823
LS B6:S2	0.236	6.29	1.011	19.09 ± 1.20	-175. ± 4.	0.916
LS B6:S3	0.437	2.60	0.416	7.85 ± 2.15	164. ± 15.	0.501
LS B6:S4	0.571	3.01	0.482	9.10 ± 2.53	154. ± 16.	0.526
LS B6:S5	0.706	2.93	0.466	8.79 ± 3.25	155. ± 20.	0.384
LS B6:S6	0.840	2.50	0.400	7.56 ± 2.27	145. ± 17.	0.441

Unsteady force coefficients :

Side	$ch \text{ (-)}$	$\phi(ch) \text{ (deg)}$	ch_{re}	ch_{im}
US B5:CH	2.91	-62.	1.35	-2.58
LS B6:CH	10.71	-179.	-10.71	-0.14
Combined	9.75 ± 0.87	-164. ± 5.	-9.36	-2.72

Aerodynamic damping coefficient : $x_{si} = 2.719 ± 0.612$

4TH STANDARD CONFIGURATION : Unsteady Test Data

Aeroelastic case Nr. : 7

TEST: 552B-3 Date : 8-AUG-84

Inlet and outlet flow conditions :

$p_{c1} = 2058 \text{ mb}$	$p_{s1} = 1949 \text{ mb}$	$p_{s2} = 1212 \text{ mb}$
$\beta_{a1} = 45 \text{ deg}$	$M_{1is} = 0.28$	$M_{2is} = 0.90$

Unsteady test parameters :

Blade frequency :	$f = 150.0 \text{ Hz}$	$k = 0.1153$
Phase control setpoint :	$\sigma = 90 \text{ deg}$	
Total record time :	$T_{rec} = 11.72 \text{ sec}$	
Number of Periods detected :	$N_{Per} = 1746$	
Total number of samples :	$N_{Samp} = 25600$	
Number of sample sets :	$N_{Set} = 10$	

Error limits estimated for 95% confidence level, based on variance
of mean values of sample sets

Blade vibration data :

Blade	Amplitude (mm)	$h*1000 (-)$	$\phi (\text{deg})$	$\sigma (\text{deg})$	signal ratio
B 4	0.211 ± 0.191	2.84 ± 0.19	-180. ± 3.8		0.970
B 5	0.228 ± 0.007	3.06 ± 0.10	-90. ± 1.9	90.1	0.983
B 6	0.225 ± 0.006	3.02 ± 0.09	0. ± 1.6	89.9	0.975
B 7	0.227 ± 0.014	3.05 ± 0.19	90. ± 3.5	90.2	0.968

Unsteady pressure data :

(Phase angles referenced to transducer blade motions)

Transducer	x	$p (\text{mb})$	$p/p_{c1}/h (-)$	$\phi_p (-)$	$\phi (\text{deg})$	signal ratio
US B5:D1	0.101	0.47	0.062	1.18 ± 1.84	13. ± 57.	0.289
US B5:D2	0.302	0.32	0.050	0.95 ± 0.49	-30. ± 27.	0.135
US B5:D3	0.501	0.86	0.136	2.57 ± 0.68	-8. ± 15.	0.299
US B5:D4	0.638	0.25	0.037	0.69 ± 0.59	103. ± 40.	0.092
US B5:D5	0.840	2.39	0.379	7.16 ± 0.77	124. ± 6.	0.682
LS B6:S1	0.101	4.67	0.750	14.17 ± 1.63	-128. ± 7.	0.707
LS B6:S2	0.236	4.67	0.750	14.17 ± 1.20	-148. ± 5.	0.840
LS B6:S3	0.437	3.03	0.484	9.14 ± 2.18	-150. ± 13.	0.557
LS B6:S4	0.571	2.62	0.416	7.86 ± 2.52	-159. ± 18.	0.464
LS B6:S5	0.706	1.91	0.298	5.64 ± 3.54	162. ± 32.	0.257
LS B6:S6	0.840	1.56	0.243	4.60 ± 2.42	158. ± 28.	0.290

Unsteady force coefficients :

Side	$ch (-)$	$\phi(ch) (\text{deg})$	ch_{re}	ch_{im}
US B5:CH	1.22	-85.	0.10	-1.21
LS B6:CH	7.95	-149.	-6.79	-4.13
Combined	8.56 ± 0.86	-141. ± 6.	-6.69	-5.35

Aerodynamic damping coefficient : $x_{si} = 5.347 ± 0.609$

4TH STANDARD CONFIGURATION : Unsteady Test Data

Aeroelastic case Nr. : 8

TEST: 552B-4 Date : 8-AUG-84

Inlet and outlet flow conditions :

P_{c1} = 2058 mb	P_{s1} = 1949 mb	P_{s2} = 1212 mb
β_{a1} = 45 deg	M_{1is} = 0.28	M_{2is} = 0.90

Unsteady test parameters :

Blade frequency :	f = 150.0 Hz	k = 0.1153
Phase control setpoint :	σ = 0 deg	
Total record time :	T_{rec} = 11.72 sec	
Number of periods detected :	N_{Per} = 1742	
Total number of samples :	N_{Samp} = 25600	
Number of sample sets :	N_{Set} = 10	

Error limits estimated for 95% confidence level, based on variance of mean values of sample sets

Blade vibration data :

Blade	Amplitude (mm)	$h \times 1000$ (-)	ϕ (deg)	σ (deg)	signal ratio
B 4	0.210 ± 0.222	2.82 ± 0.22	0. ± 4.5		0.961
B 5	0.227 ± 0.007	3.06 ± 0.09	-0. ± 1.6	-0.4	0.980
B 6	0.226 ± 0.005	3.04 ± 0.06	-0. ± 1.2	0.2	0.974
B 7	0.226 ± 0.020	3.03 ± 0.27	0. ± 5.0	0.2	0.962

Unsteady pressure data :

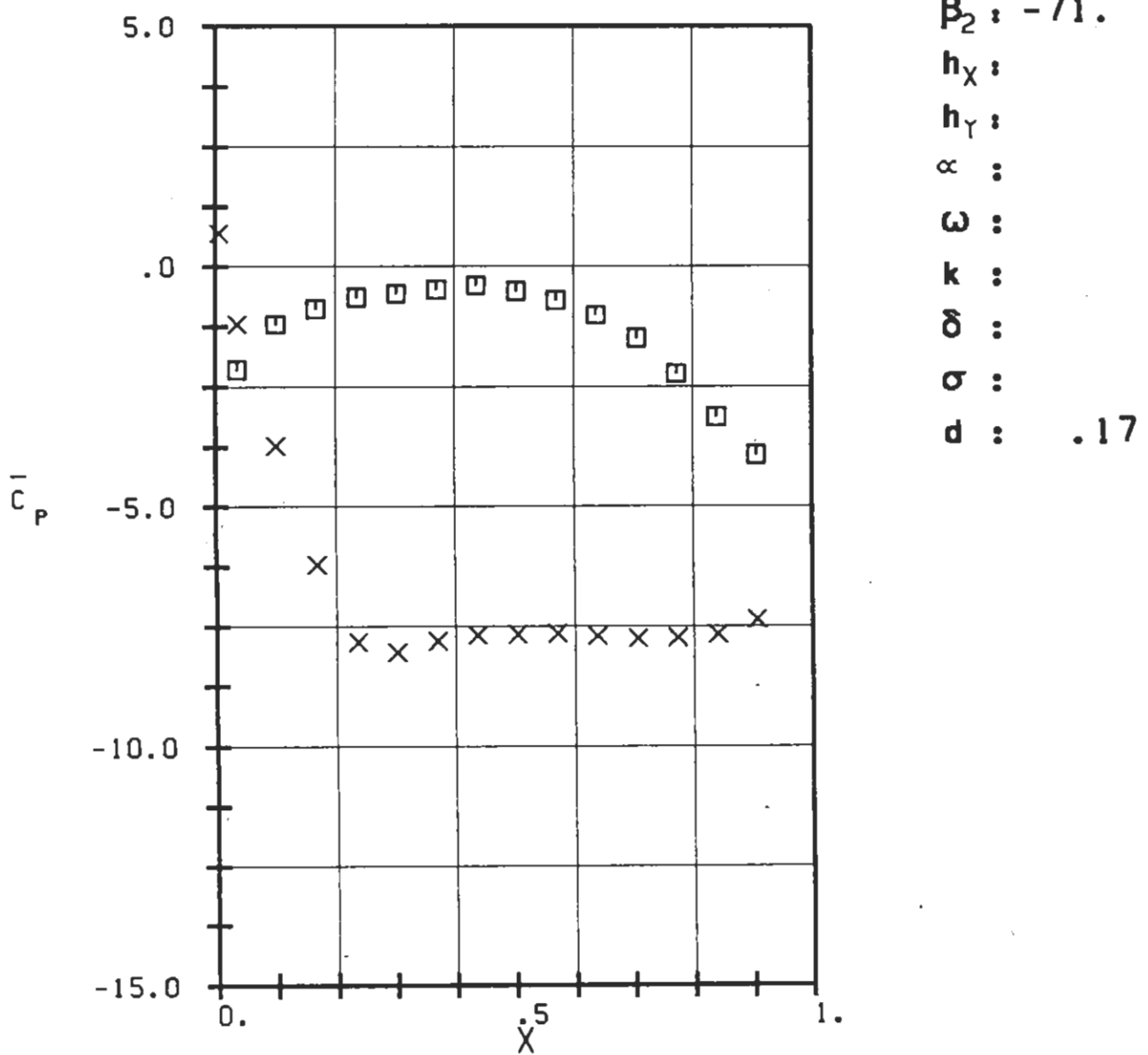
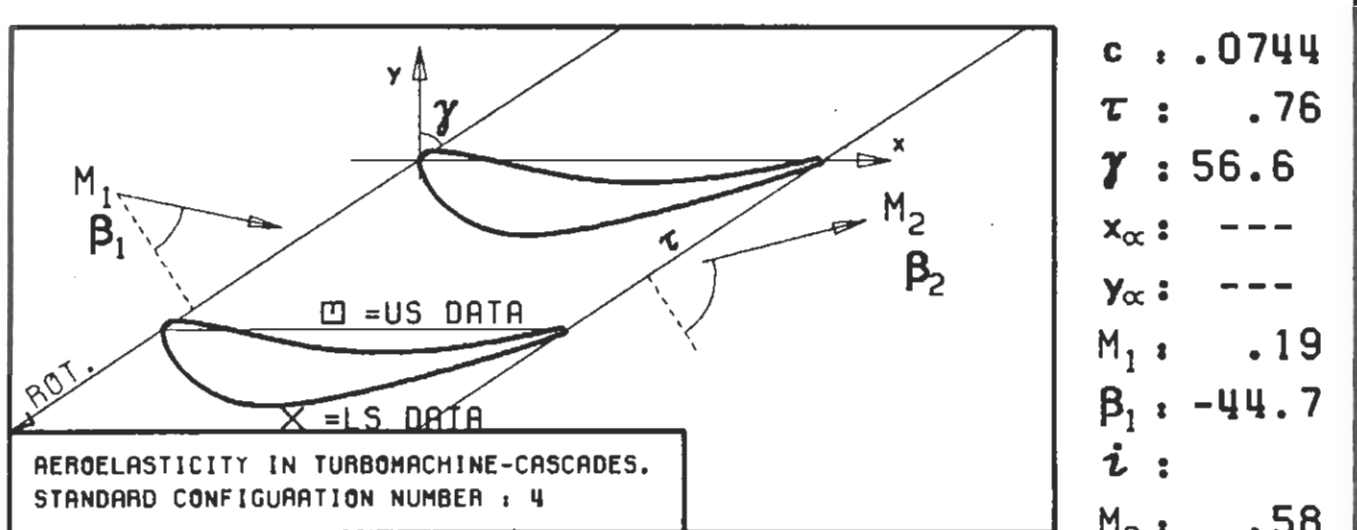
(Phase angles referenced to transducer blade motions)

Transducer	x	p (mb)	$p/p_{c1}/h$ (-)	c_p (-)	ϕ (deg)	signal ratio
US B5:D1	0.101	0.42	0.052	0.99 ± 1.95	116. ± 63.	0.267
US B5:D2	0.302	0.87	0.137	2.58 ± 0.66	160. ± 14.	0.346
US B5:D3	0.501	0.56	0.087	1.64 ± 0.72	163. ± 24.	0.198
US B5:D4	0.638	1.40	0.221	4.18 ± 0.74	179. ± 10.	0.470
US B5:D5	0.840	1.63	0.258	4.86 ± 0.97	178. ± 11.	0.532
LS B6:S1	0.101	1.54	0.244	4.62 ± 1.11	-174. ± 14.	0.301
LS B6:S2	0.236	1.81	0.289	5.46 ± 1.10	169. ± 11.	0.488
LS B6:S3	0.437	0.90	0.128	2.41 ± 2.93	-23. ± 51.	0.194
LS B6:S4	0.571	0.76	0.094	1.78 ± 3.29	5. ± 62.	0.152
LS B6:S5	0.706	1.31	0.199	3.75 ± 4.43	126. ± 50.	0.182
LS B6:S6	0.840	0.65	0.059	1.12 ± 3.66	108. ± 73.	0.126

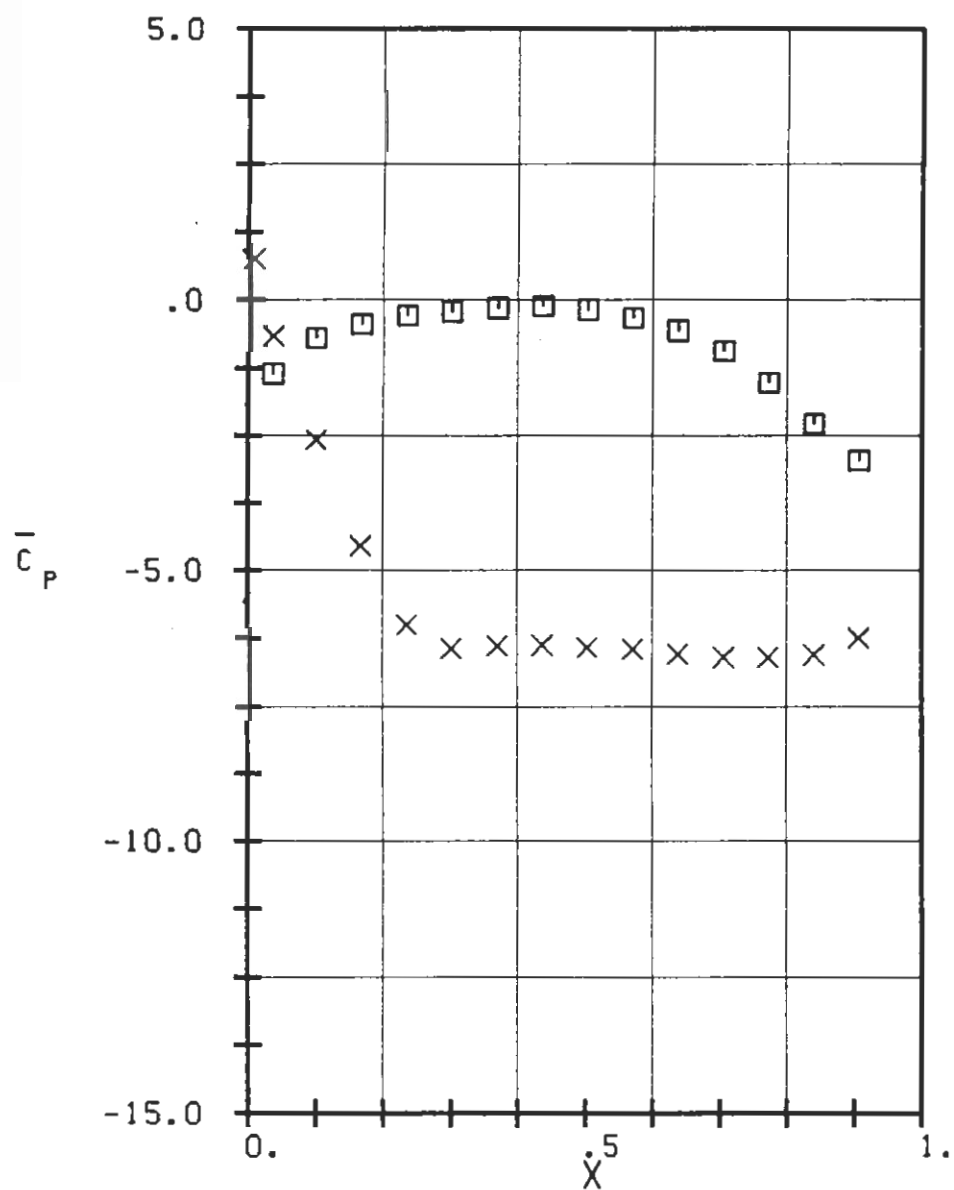
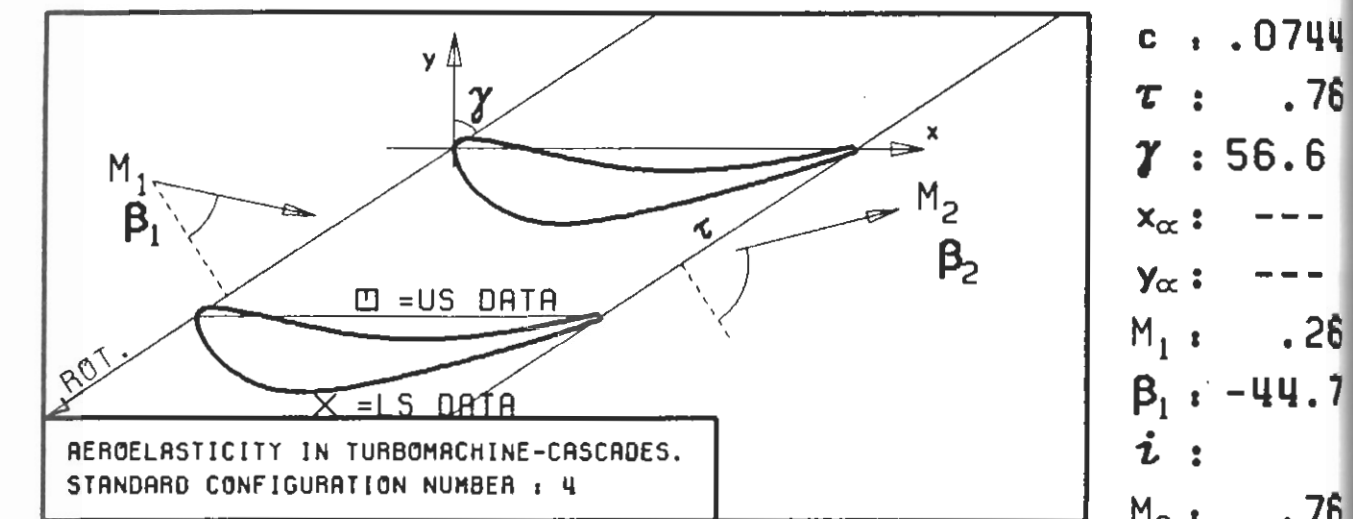
Unsteady force coefficients :

Side	ch (-)	$\phi(ch)$ (deg)	ch_{re}	ch_{im}
US B5:CH	2.40	-11.	2.36	-0.45
LS B6:CH	1.72	166.	-1.67	0.41
Combined	0.69 ± 1.03	-3. ± 56.	0.69	-0.04

Aerodynamic damping coefficient : $\xi = 0.040 ± 0.730$

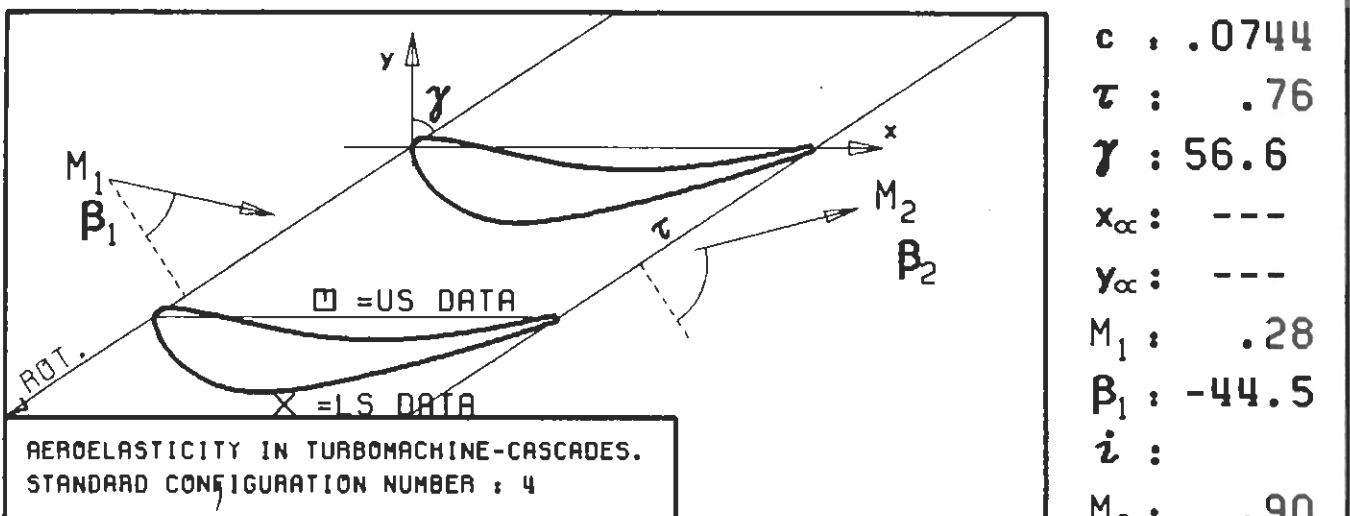


PLOT 7.4-1.1: FOURTH STANDARD CONFIGURATION CASE : 1
 TIME AVERAGED BLADE SURFACE PRESSURE DISTRIBUTION

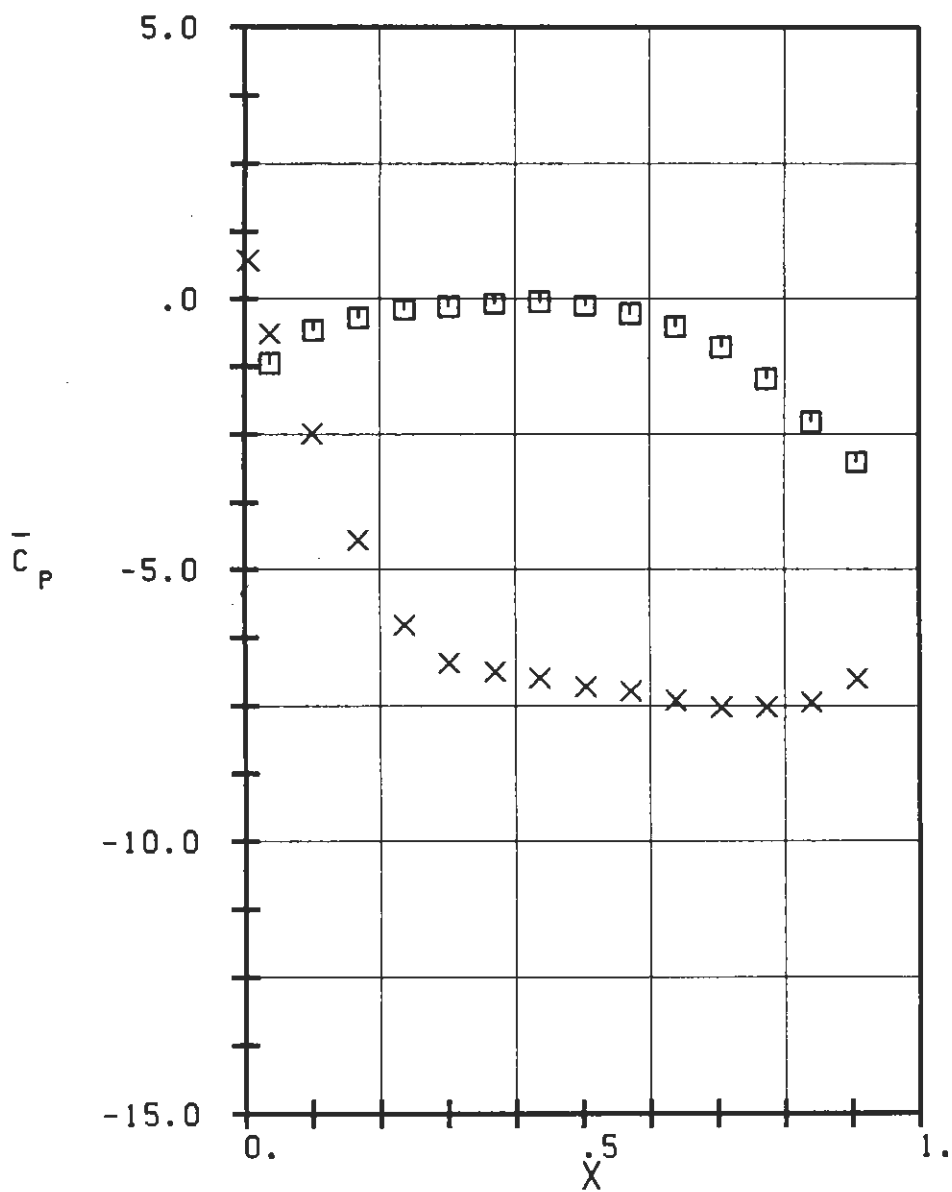


PLOT 7.4-1.2: FOURTH STANDARD CONFIGURATION CASE : 2
TIME AVERAGED BLADE SURFACE PRESSURE DISTRIBUTION

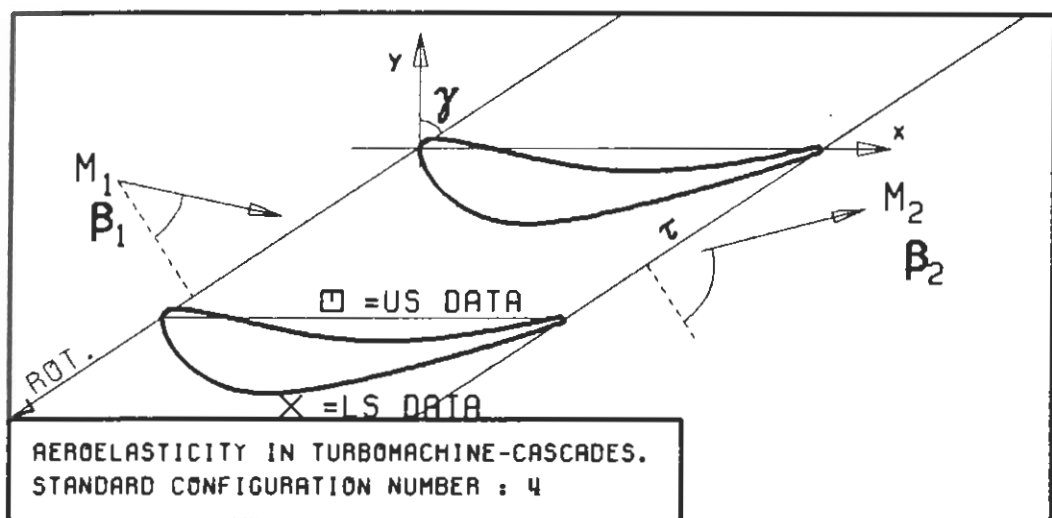
553C-1



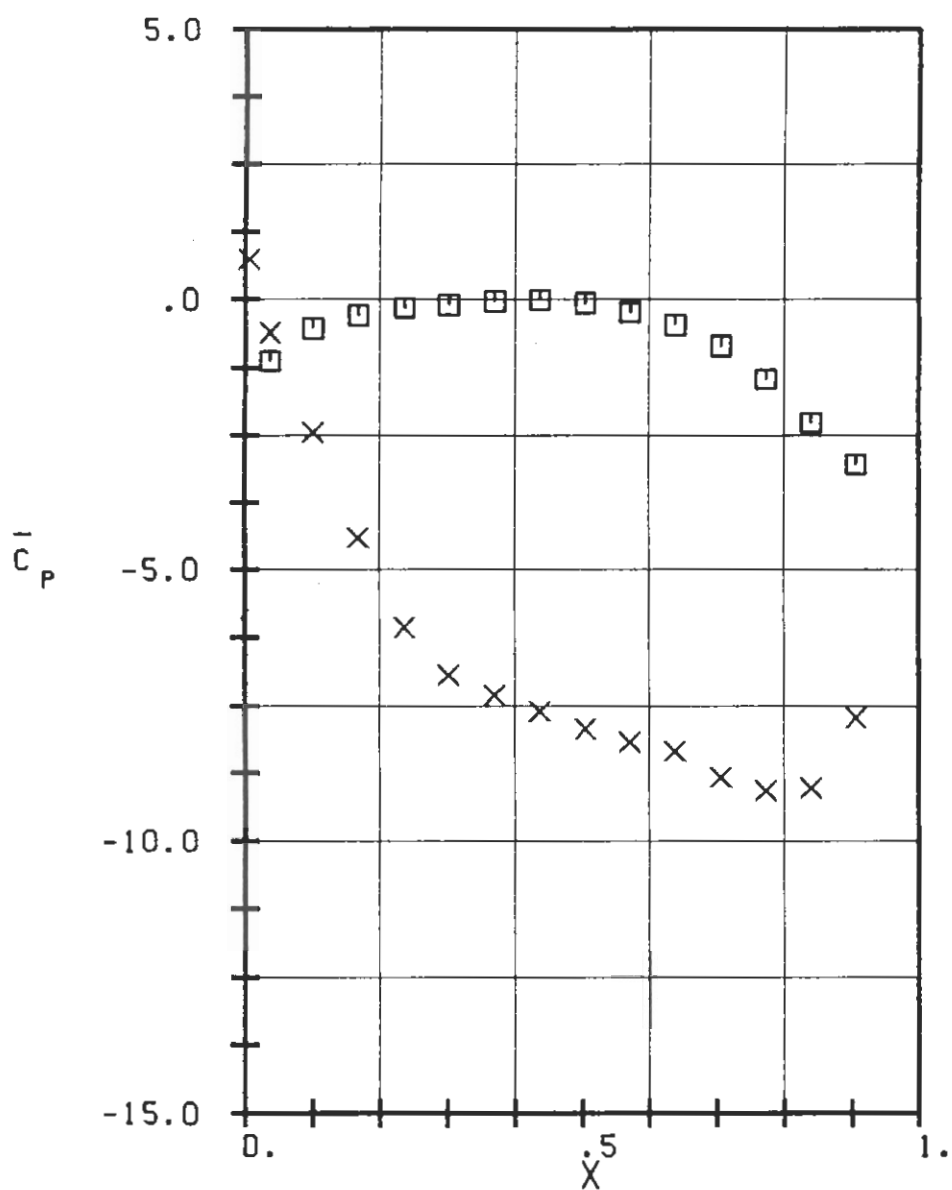
$c = .0744$
 $\tau = .76$
 $\gamma = 56.6$
 $x_\infty = \text{---}$
 $y_\infty = \text{---}$
 $M_1 = .28$
 $\beta_1 = -44.5$
 $i =$
 $M_2 = .90$
 $\beta_2 = -71.$
 $h_X =$
 $h_Y =$
 $\alpha =$
 $\omega =$
 $k =$
 $\delta =$
 $\sigma = -91.$
 $d = .17$



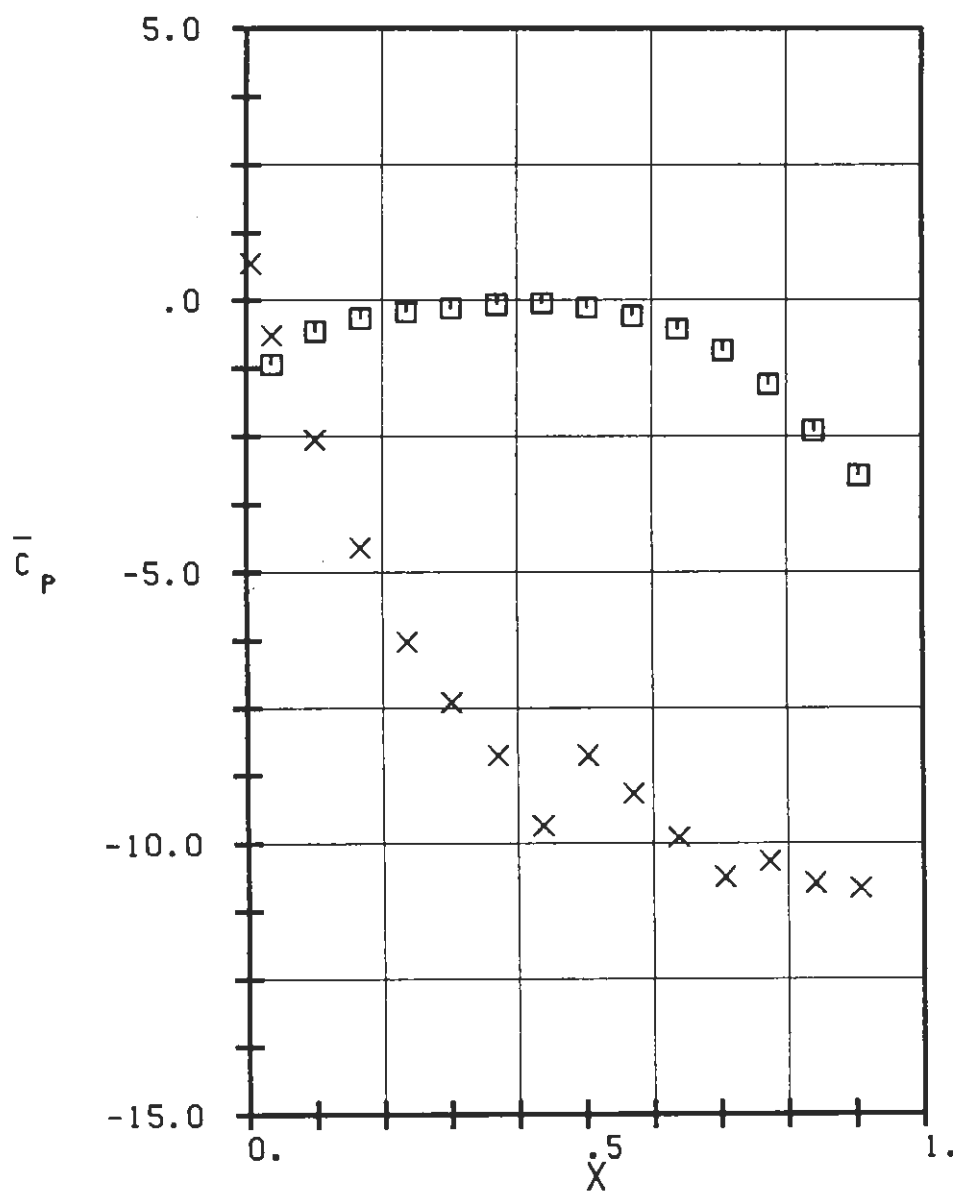
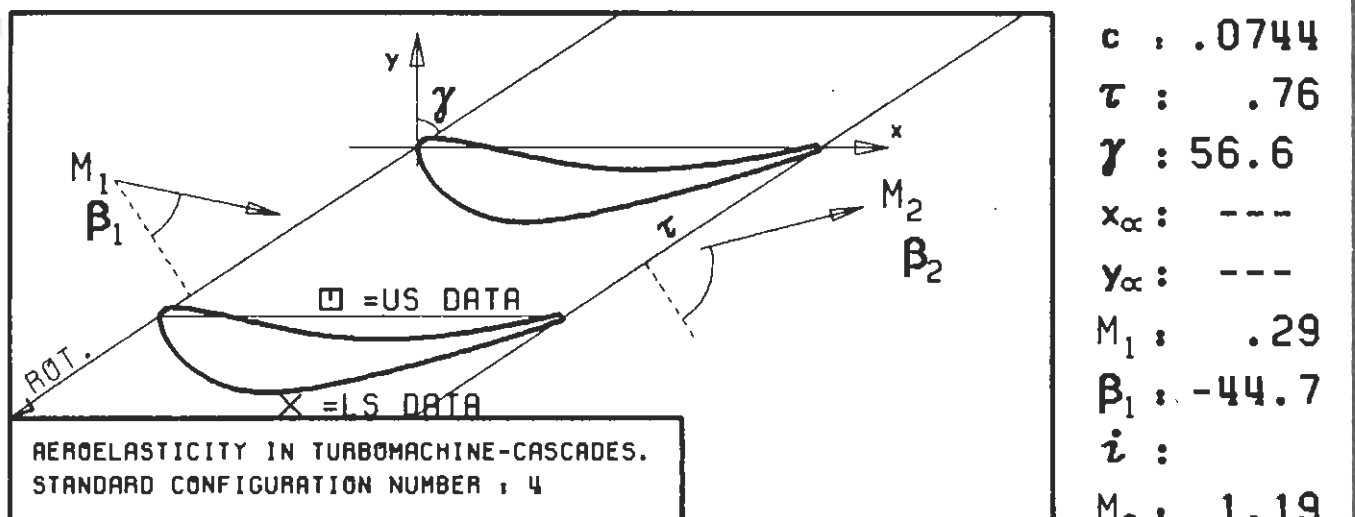
PLOT 7.4-1.3: FOURTH STANDARD CONFIGURATION CASES: 3+6-8
TIME AVERAGED BLADE SURFACE PRESSURE DISTRIBUTION



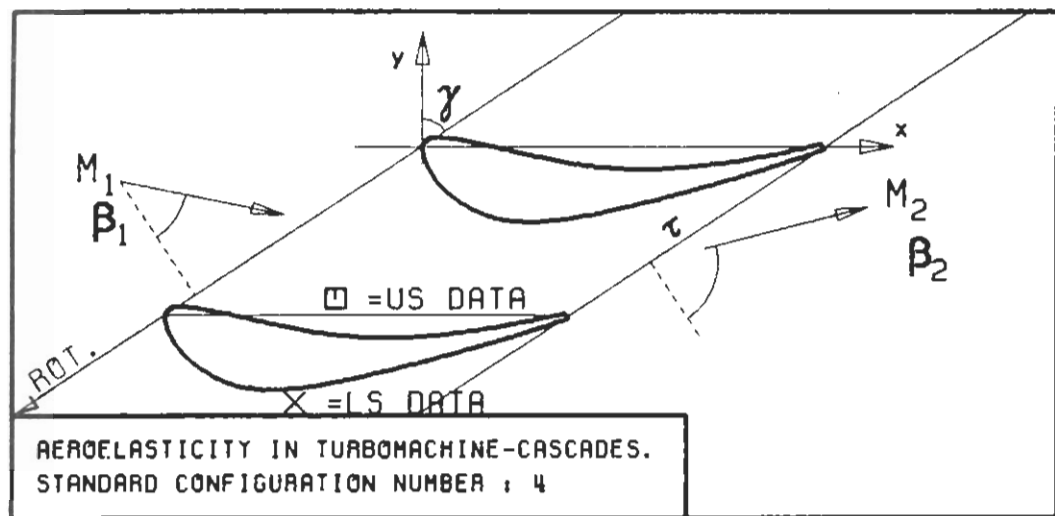
c :	.0744
τ :	.76
γ :	56.6
x_∞ :	---
y_∞ :	---
M_1 :	.29
β_1 :	-44.5
i :	
M_2 :	1.02
β_2 :	-71.
h_X :	
h_Y :	
α :	
ω :	
k :	
δ :	
σ :	
d :	.17



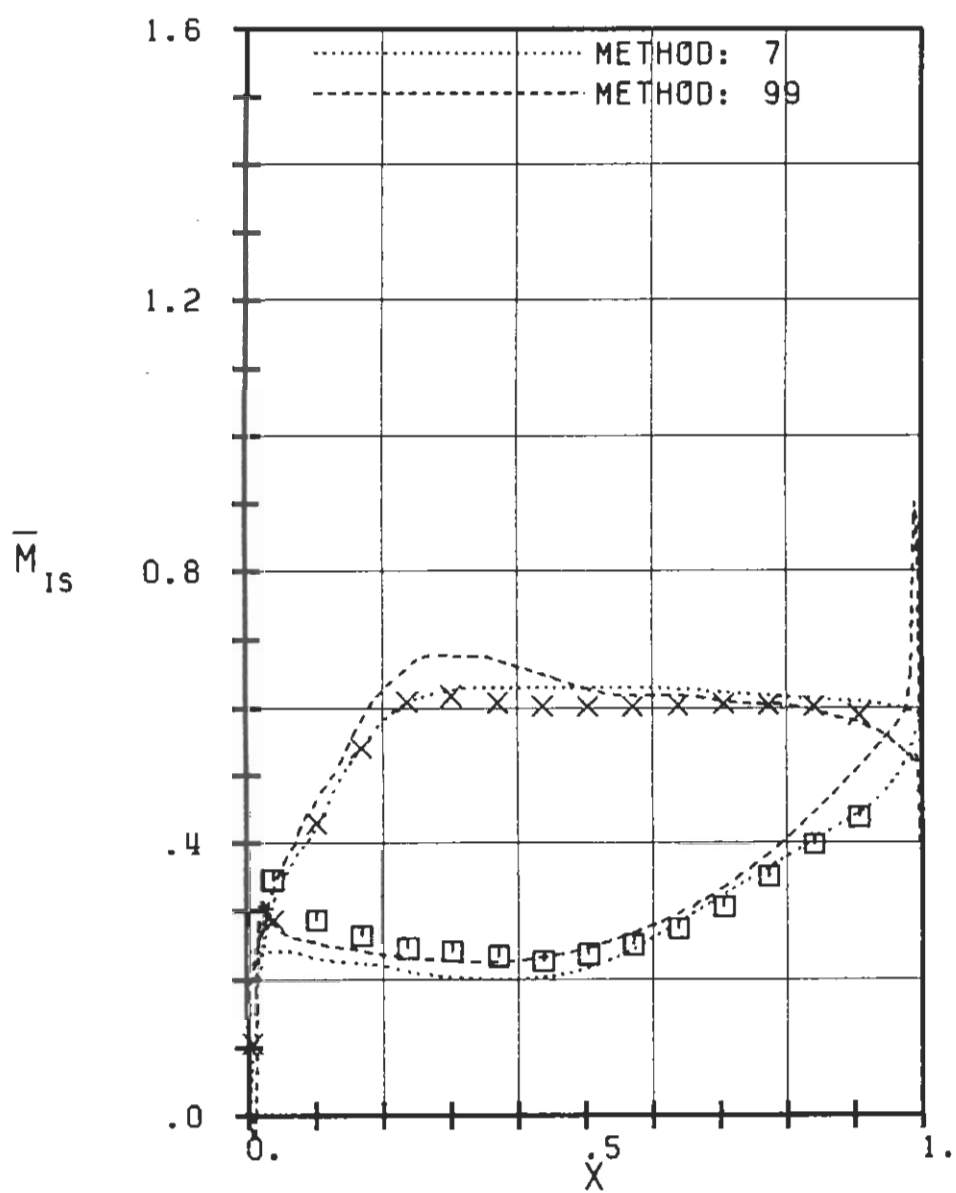
PLOT 7.4-1.4: FOURTH STANDARD CONFIGURATION CASE : 4
TIME AVERAGED BLADE SURFACE PRESSURE DISTRIBUTION



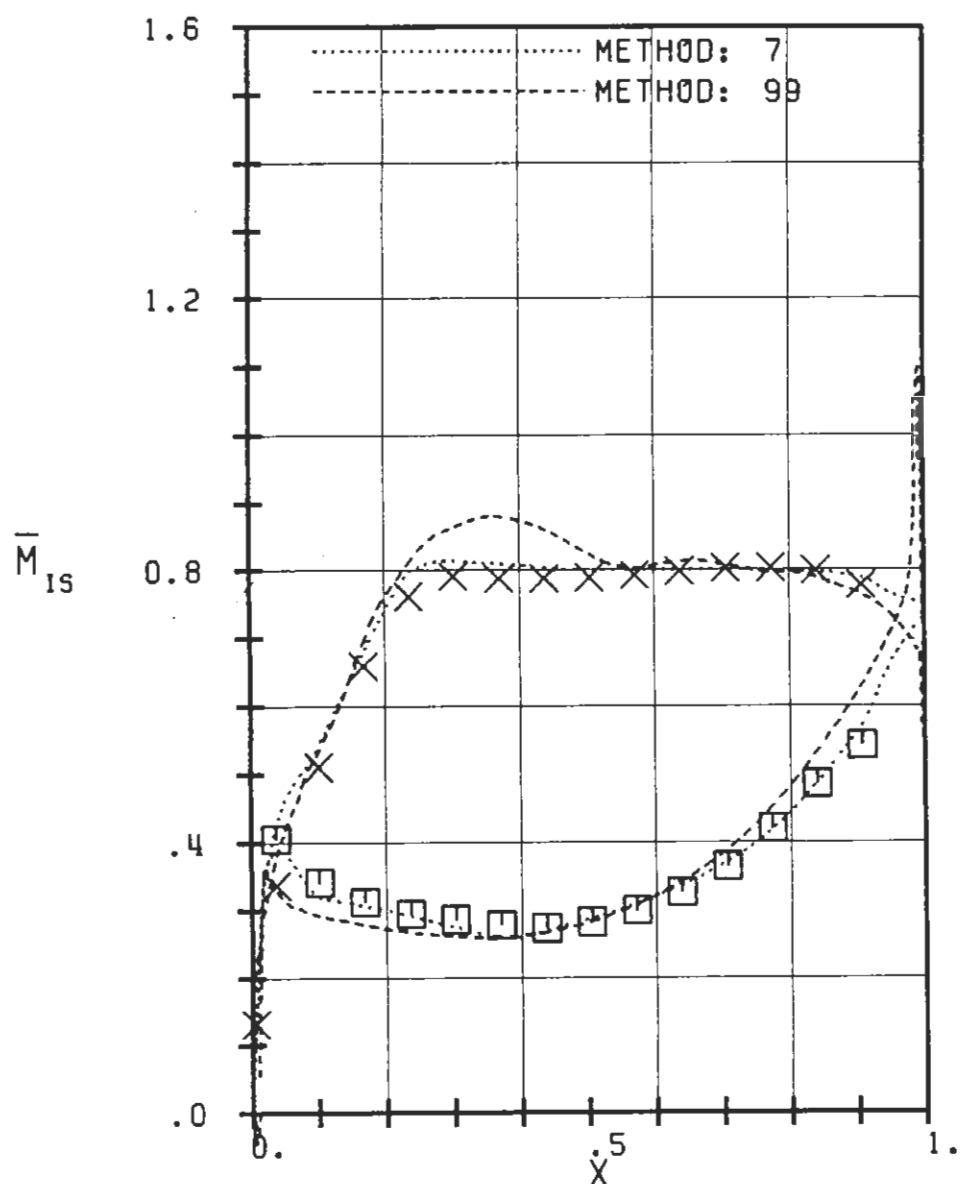
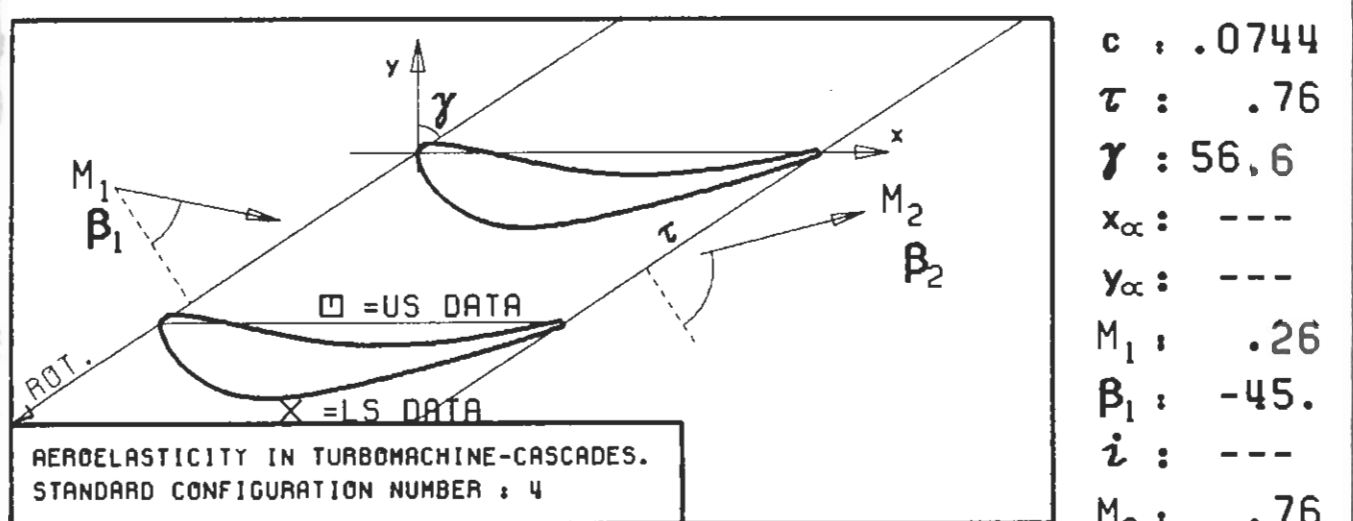
PLOT 7.4-1.5: FOURTH STANDARD CONFIGURATION CASE : 5
TIME AVERAGED BLADE SURFACE PRESSURE DISTRIBUTION



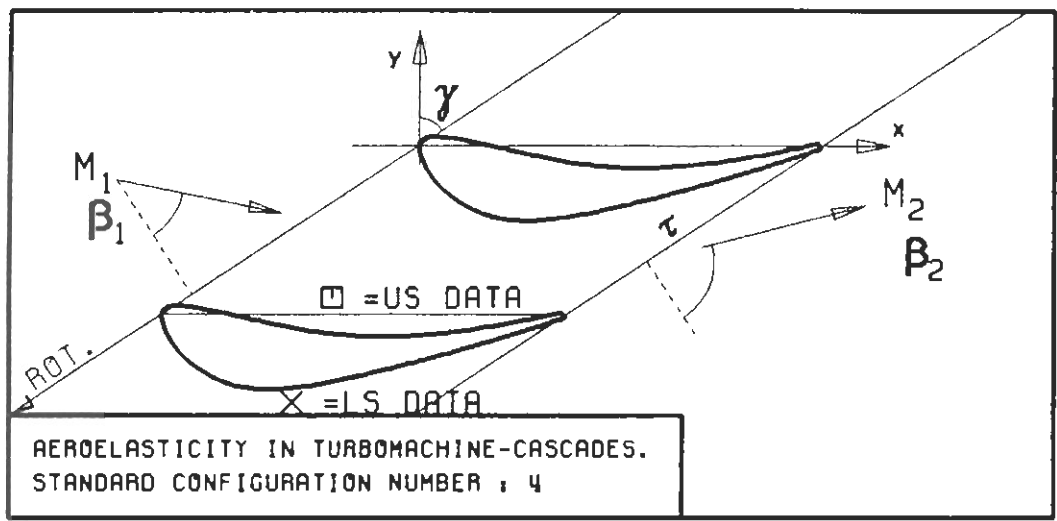
c	: .0744
τ	: .76
γ	: 56.6
x_{∞}	: ---
y_{∞}	: ---
M_1	: .19
β_1	: -45.
i	: ---
M_2	: .58
β_2	: -71.
h_x	:
h_y	:
α	: ---
ω	:
k	:
δ	: 60.4
σ	:
d	: .17



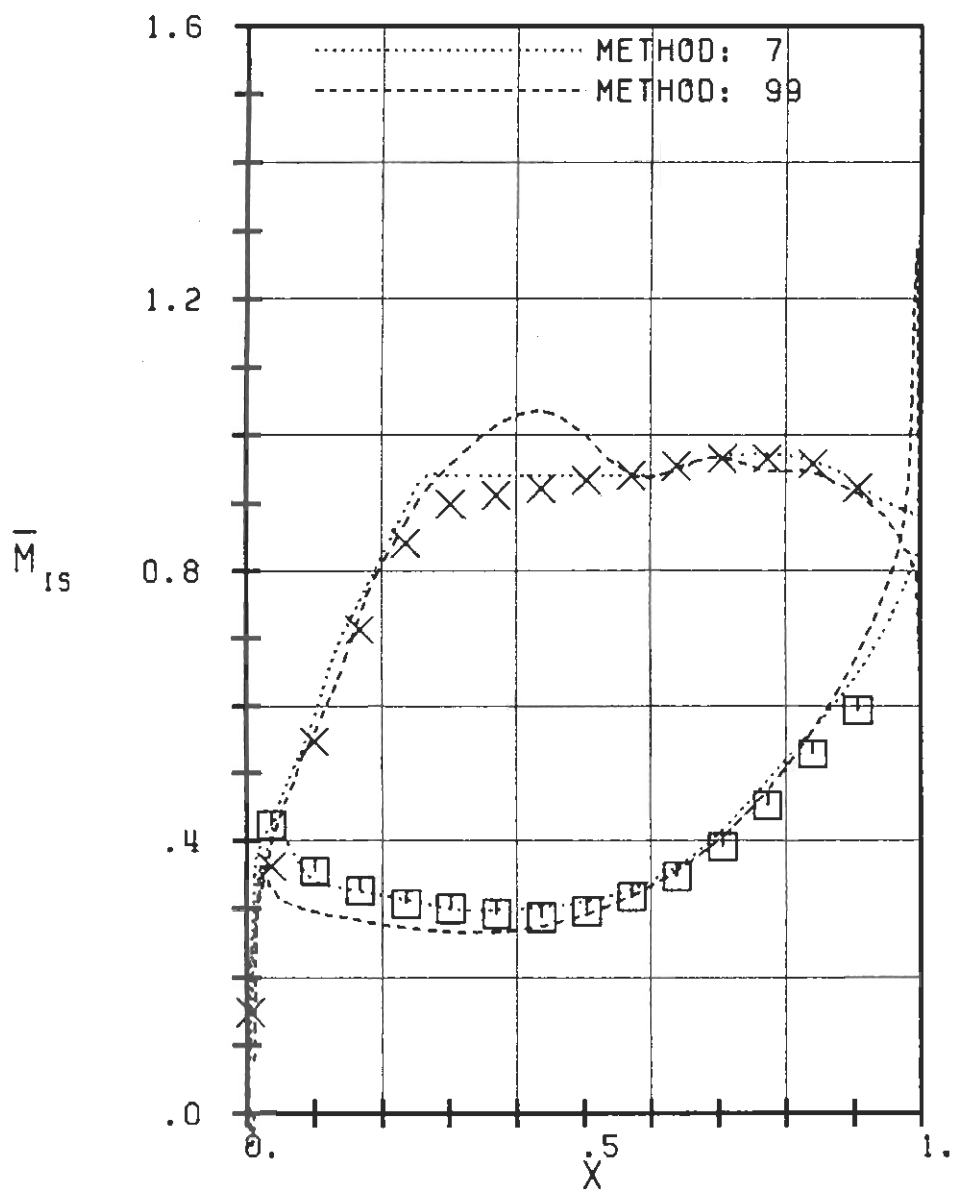
PLOT 7.4-1.6: FOURTH STANDARD CONFIGURATION CASE : 1
 EPFL-LTT MD ISENTROPIC MACH NUMBER DISTRIBUTION
 553D-1 ON THE BLADE



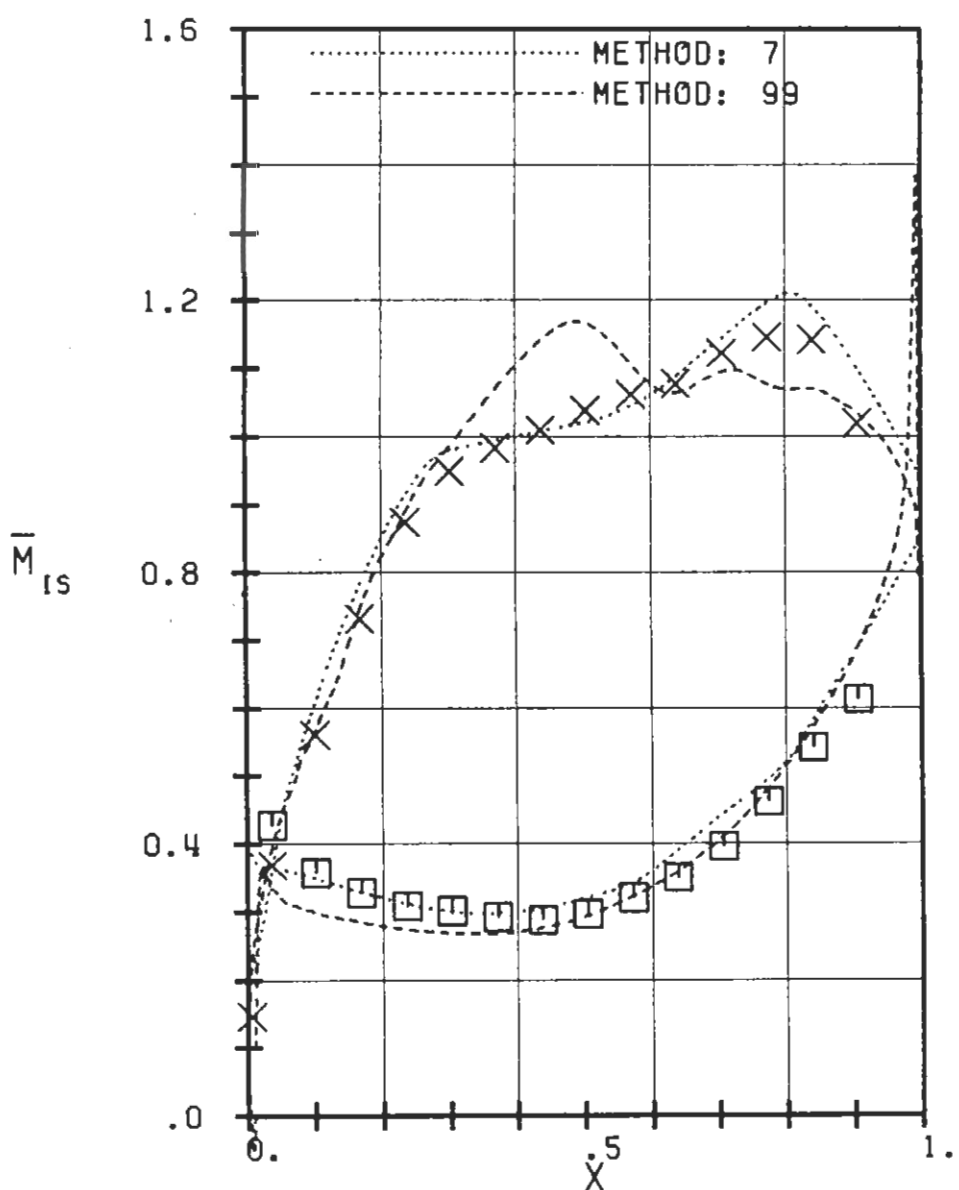
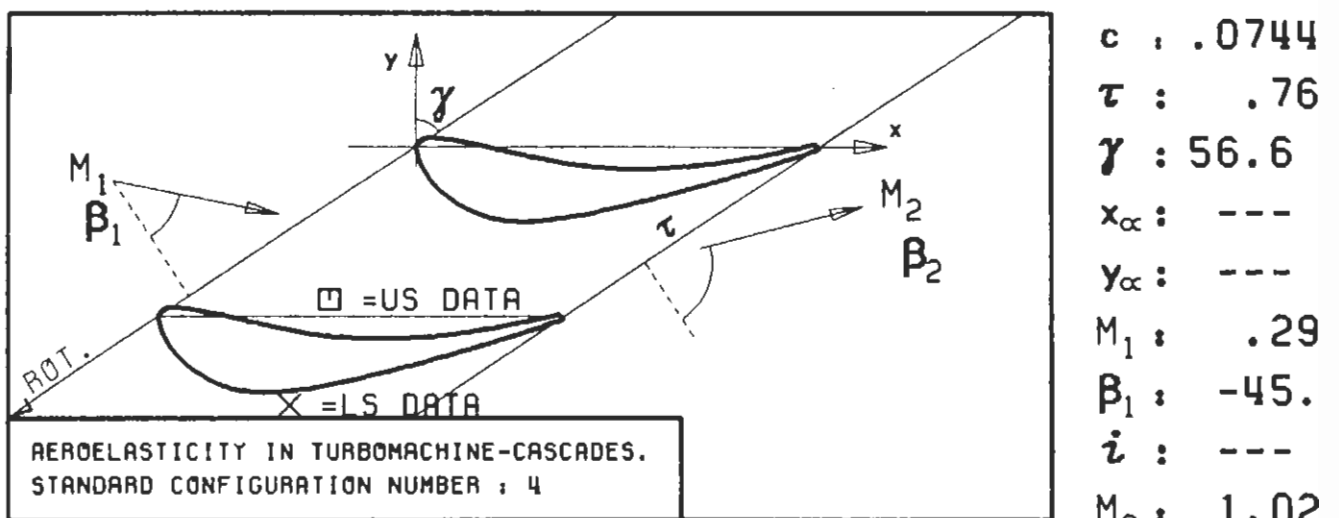
PLOT 7.4-1.7: FOURTH STANDARD CONFIGURATION CASE : 2
 EPFL-LTT MD ISENTROPIC MACH NUMBER DISTRIBUTION
 553C-1 ON THE BLADE



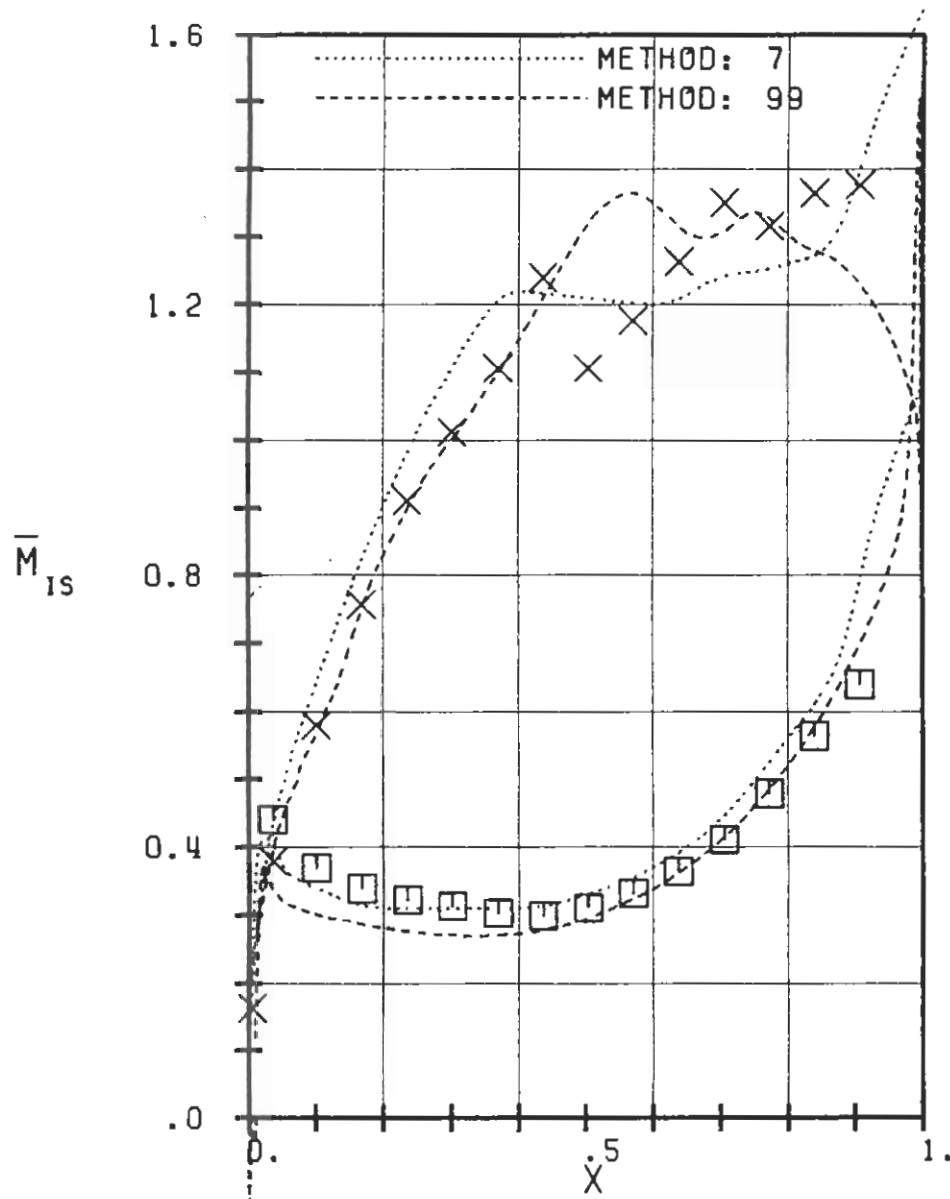
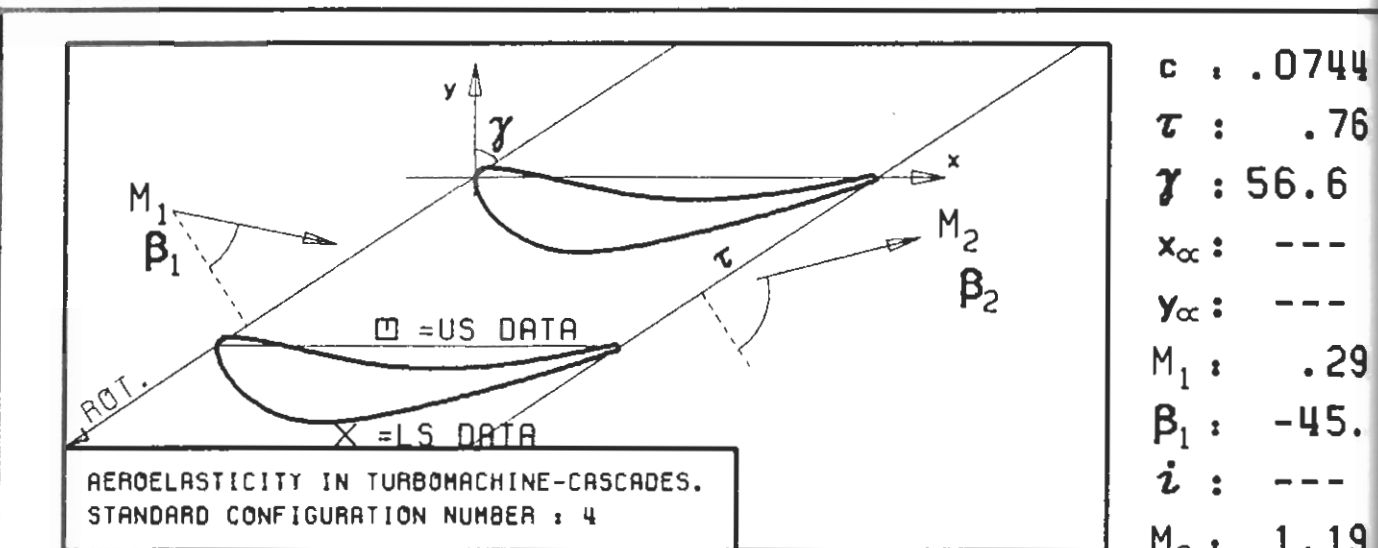
c	: .0744
τ	: .76
γ	: 56.6
x_∞	: ---
y_∞	: ---
M_1	: .28
β_1	: -45.
i	: ---
M_2	: .90
β_2	: -71.
h_X	: ---
h_Y	: ---
α	: ---
ω	: ---
k	: ---
δ	: 60.4
σ	: ---
d	: .17



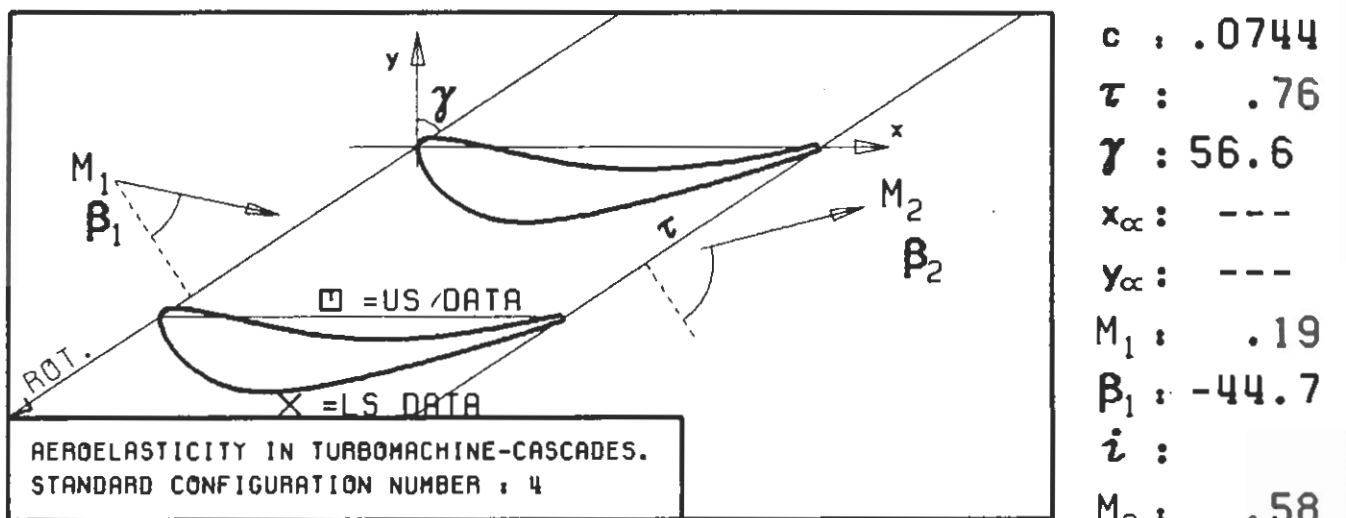
PLOT 7.4-1.8: FOURTH STANDARD CONFIGURATION CASES: 3+6-8
EPFL-LTT MD ISENTROPIC MACH NUMBER DISTRIBUTION
552B-1 ON THE BLADE



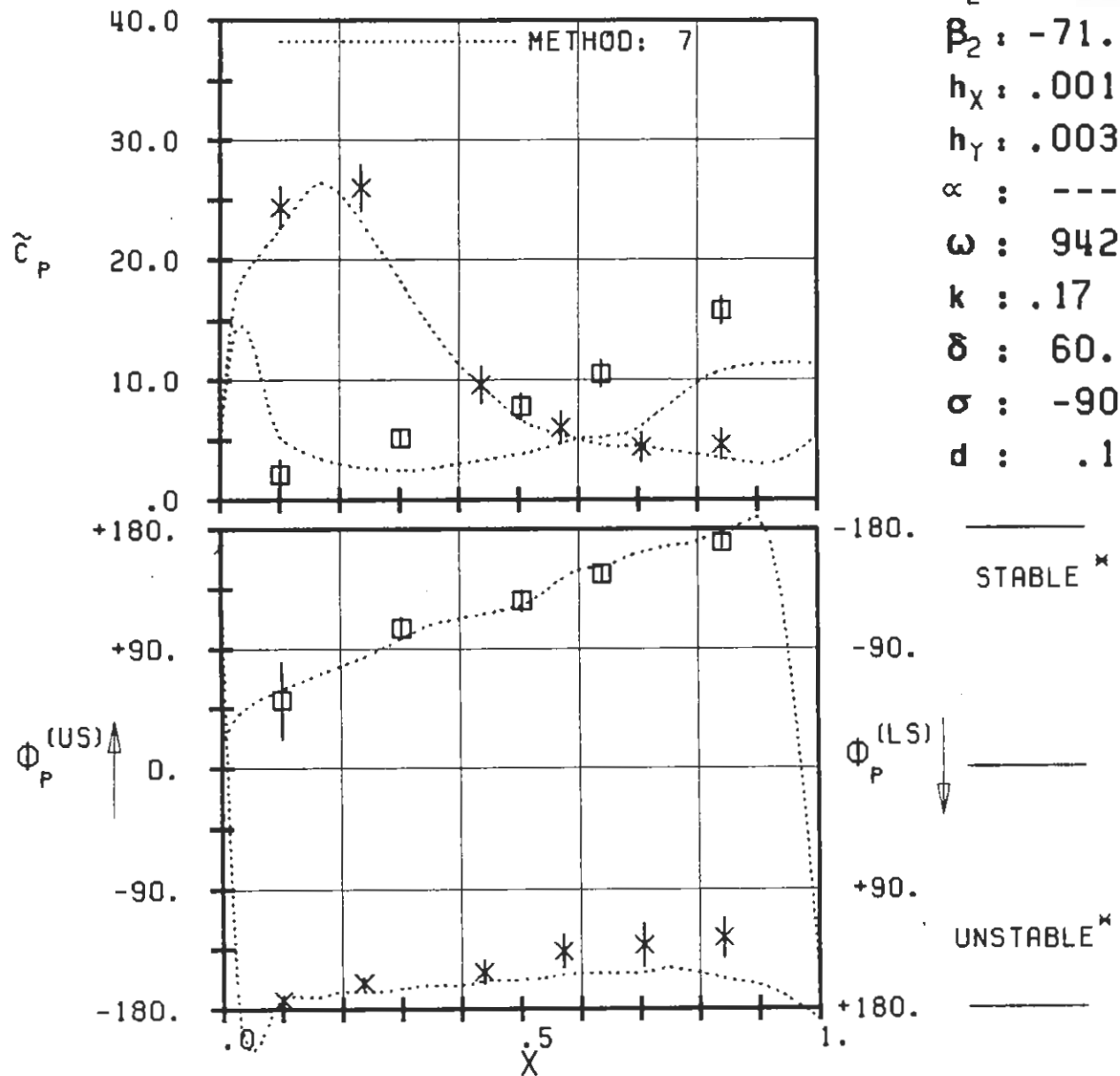
PLOT 7.4-1.9: FOURTH STANDARD CONFIGURATION CASE : 4
 EPFL-LTT MD ISENTROPIC MACH NUMBER DISTRIBUTION
 552A-1 ON THE BLADE



PLOT 7.4-1.10: FOURTH STANDARD CONFIGURATION CASE : 5
 EPFL-LTT MD ISENTROPIC MACH NUMBER DISTRIBUTION
 553B-1 ON THE BLADE

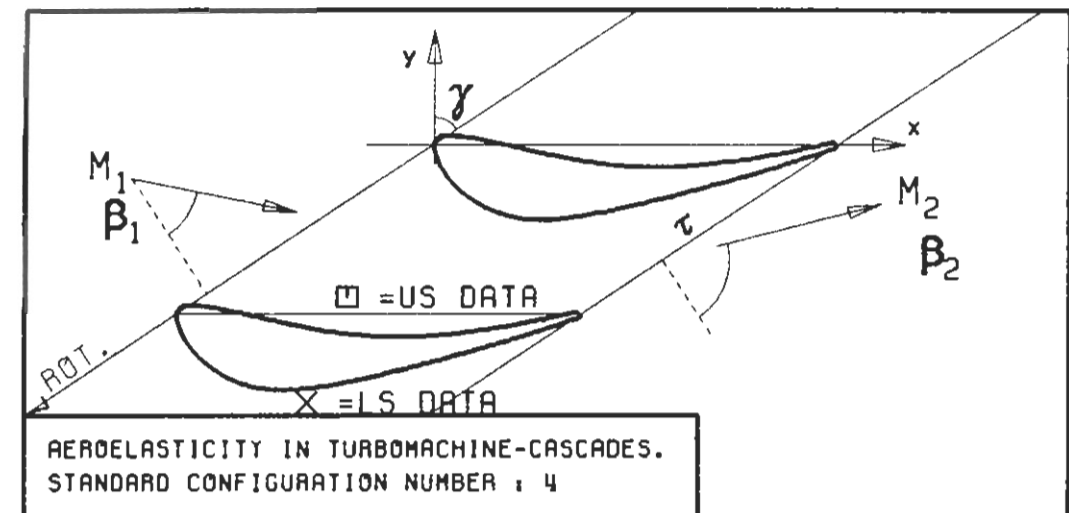


$c : .0744$
 $\tau : .76$
 $\gamma : 56.6$
 $x_\infty : ---$
 $y_\infty : ---$
 $M_1 : .19$
 $\beta_1 : -44.7$
 $i :$
 $M_2 : .58$
 $\beta_2 : -71.$
 $h_x : .0019$
 $h_y : .0033$
 $\alpha : ---$
 $\omega : 942.$
 $k : .17$
 $\delta : 60.4$
 $\sigma : -90.$
 $d : .17$

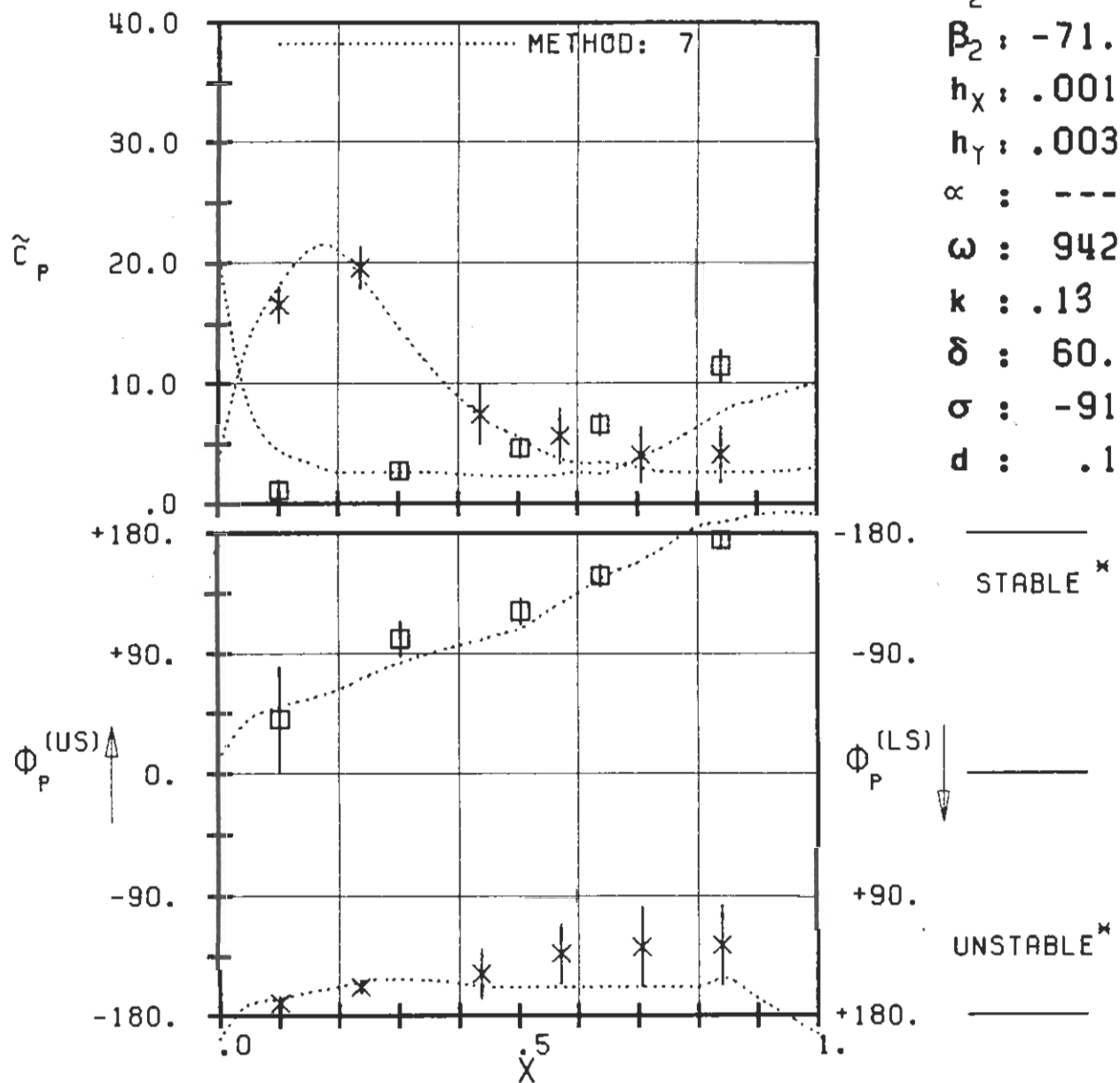


PLOT 7.4-2.1: FOURTH STANDARD CONFIGURATION CASE : 1
 MAGNITUDE AND PHASE LEAD OF UNSTEADY BLADE SURFACE PRESSURE COEFFICIENT.
 553D-1

(*: IN PITCH MODE, NOTATION VALID UPSTREAM OF PITCH AXIS)

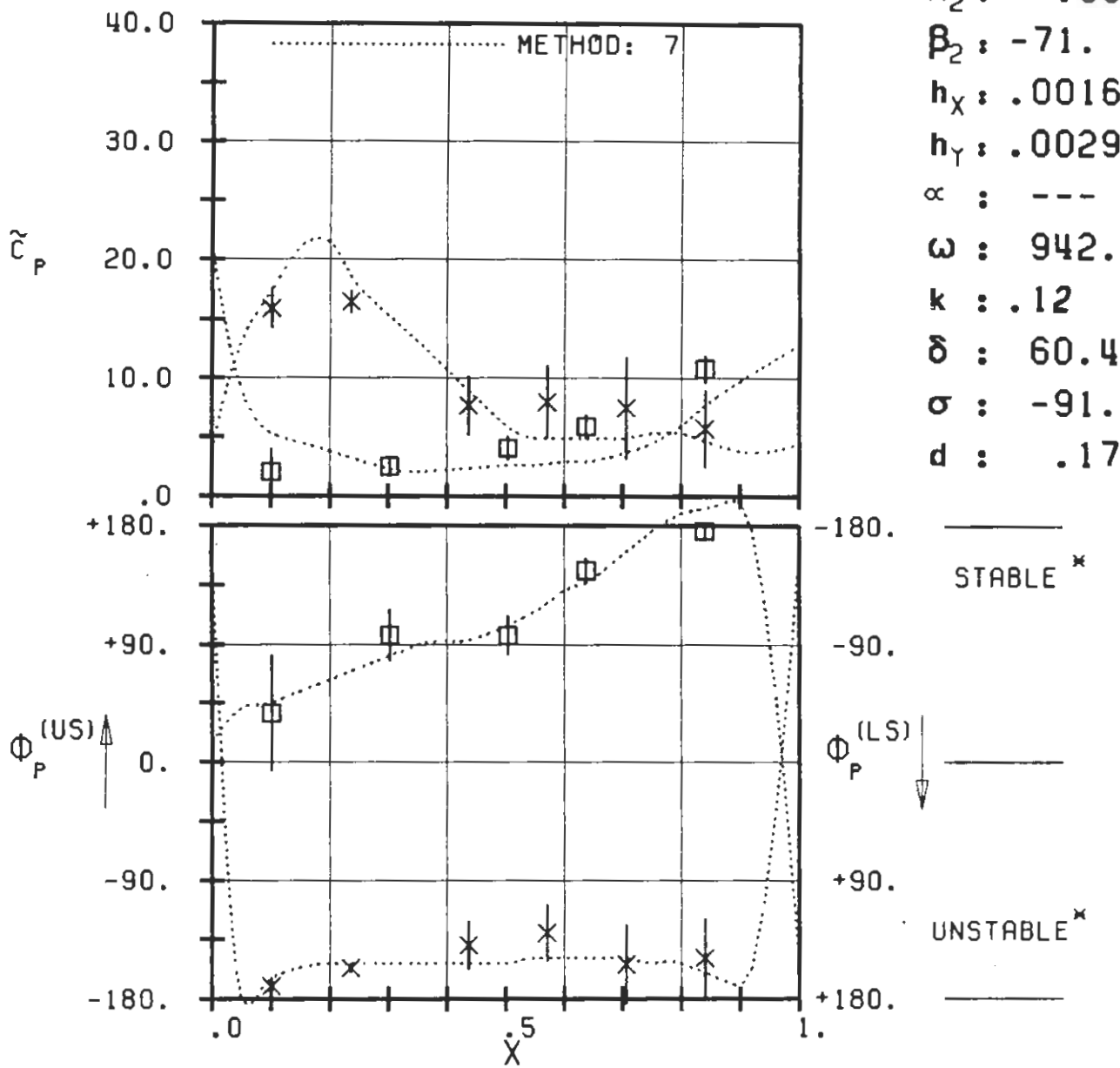
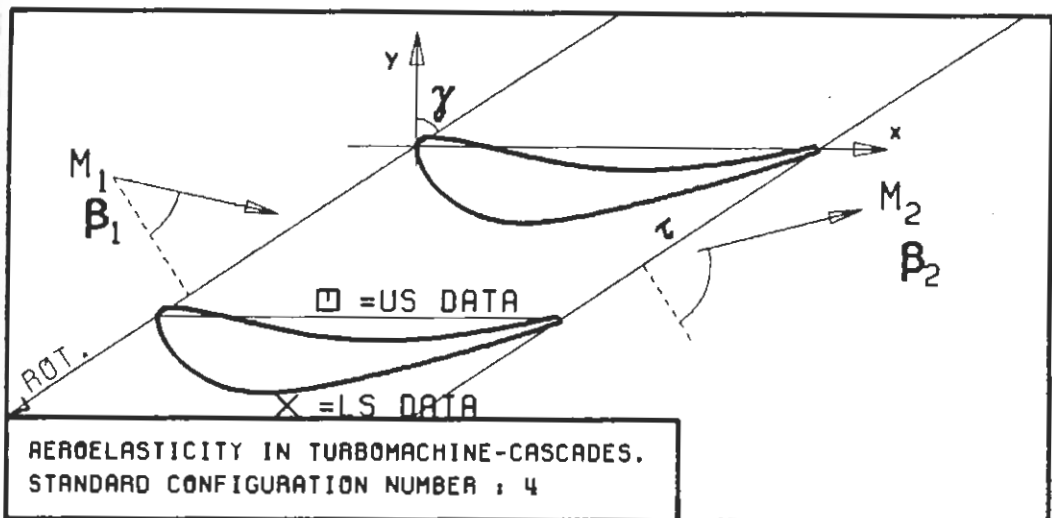


$c : .0744$
 $\tau : .76$
 $\gamma : 56.6$
 $x_\infty : ---$
 $y_\infty : ---$
 $M_1 : .26$
 $\beta_1 : -45.$
 $i :$
 $M_2 : .76$
 $\beta_2 : -71.$
 $h_x : .0019$
 $h_y : .0033$
 $\alpha : ---$
 $\omega : 942.$
 $k : .13$
 $\delta : 60.4$
 $\sigma : -91.$
 $d : .17$

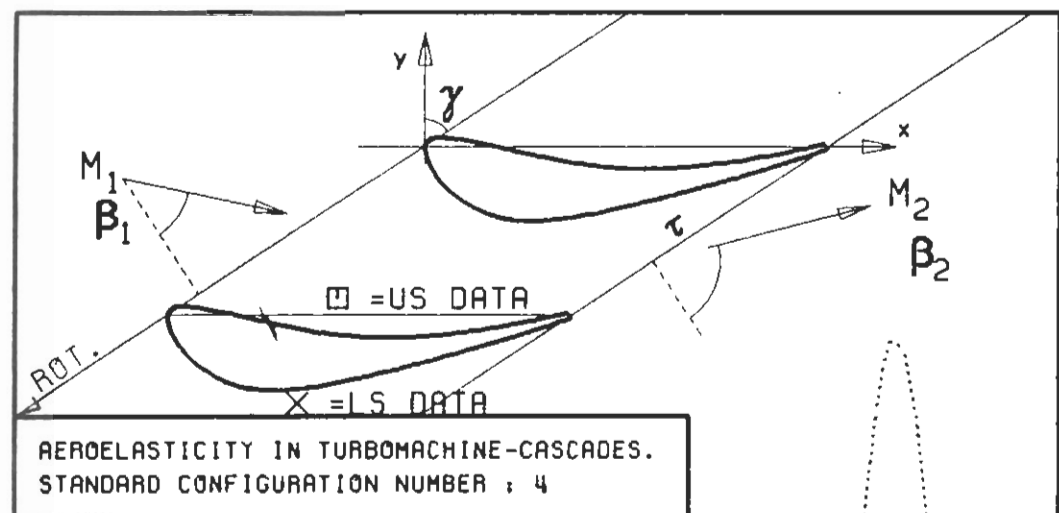


PLOT 7.4-2.2: FOURTH STANDARD CONFIGURATION CASE : 2
MAGNITUDE AND PHASE LEAD OF UNSTEADY BLADE
SURFACE PRESSURE COEFFICIENT.

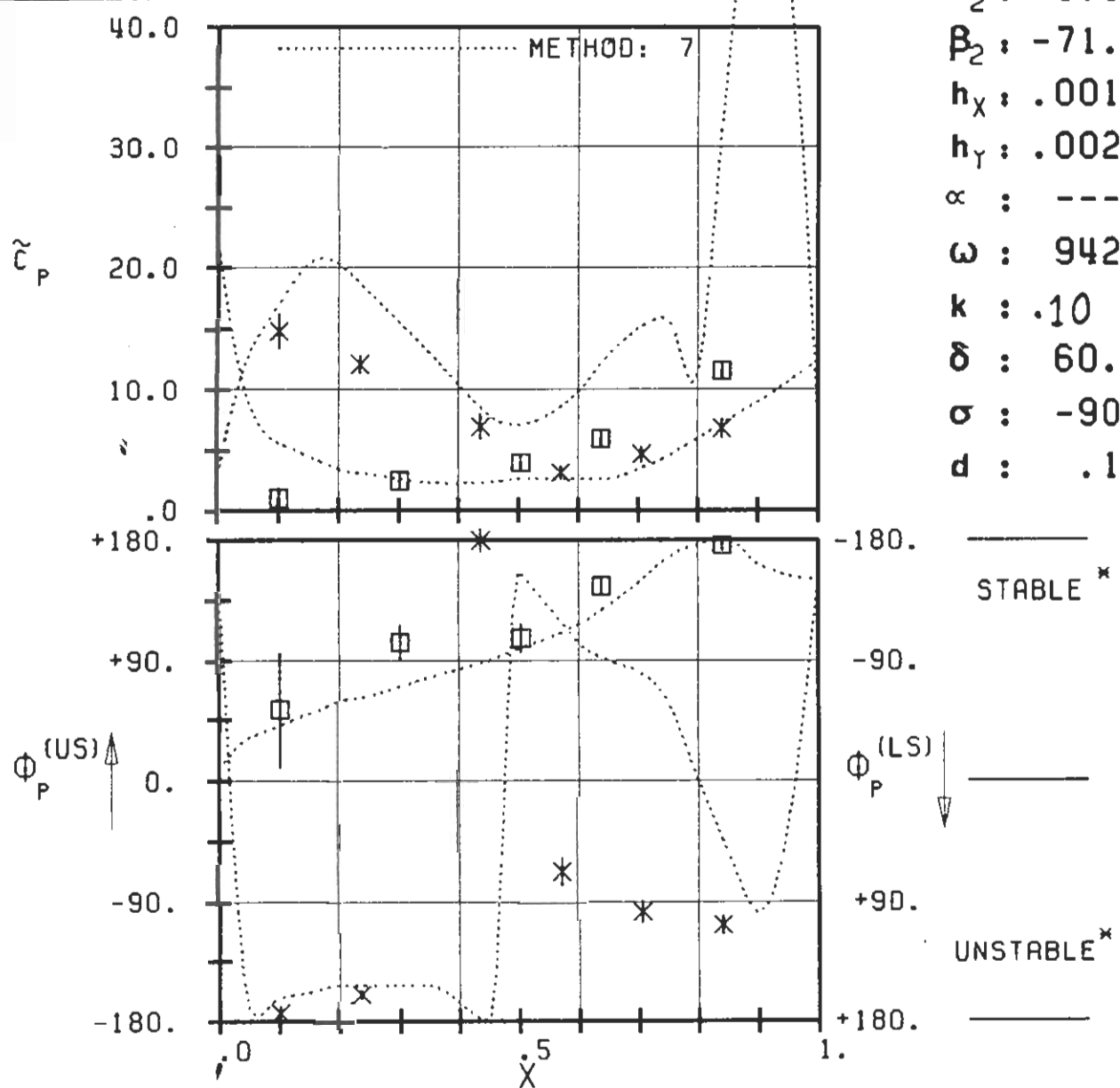
(x: IN PITCH MODE, NOTATION VALID UPSTREAM OF PITCH AXIS)



PLOT 7.4-2.3: FOURTH STANDARD CONFIGURATION CASE : 3
MAGNITUDE AND PHASE LEAD OF UNSTEADY BLADE SURFACE PRESSURE COEFFICIENT.

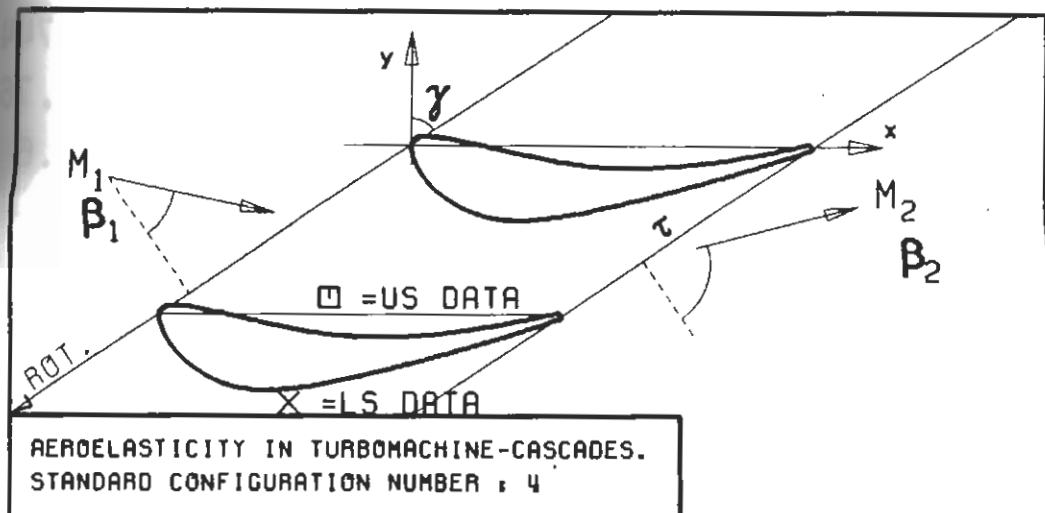


$c : .0744$
 $\tau : .76$
 $\gamma : 56.6$
 $x_{\infty} : \text{---}$
 $y_{\infty} : \text{---}$
 $M_1 : .29$
 $\beta_1 : -44.5$
 $i :$
 $M_2 : 1.02$
 $\beta_2 : -71.$
 $h_x : .0016$
 $h_y : .0029$
 $\alpha : \text{---}$
 $\omega : 942.$
 $k : .10$
 $\delta : 60.4$
 $\sigma : -90.$
 $d : .17$

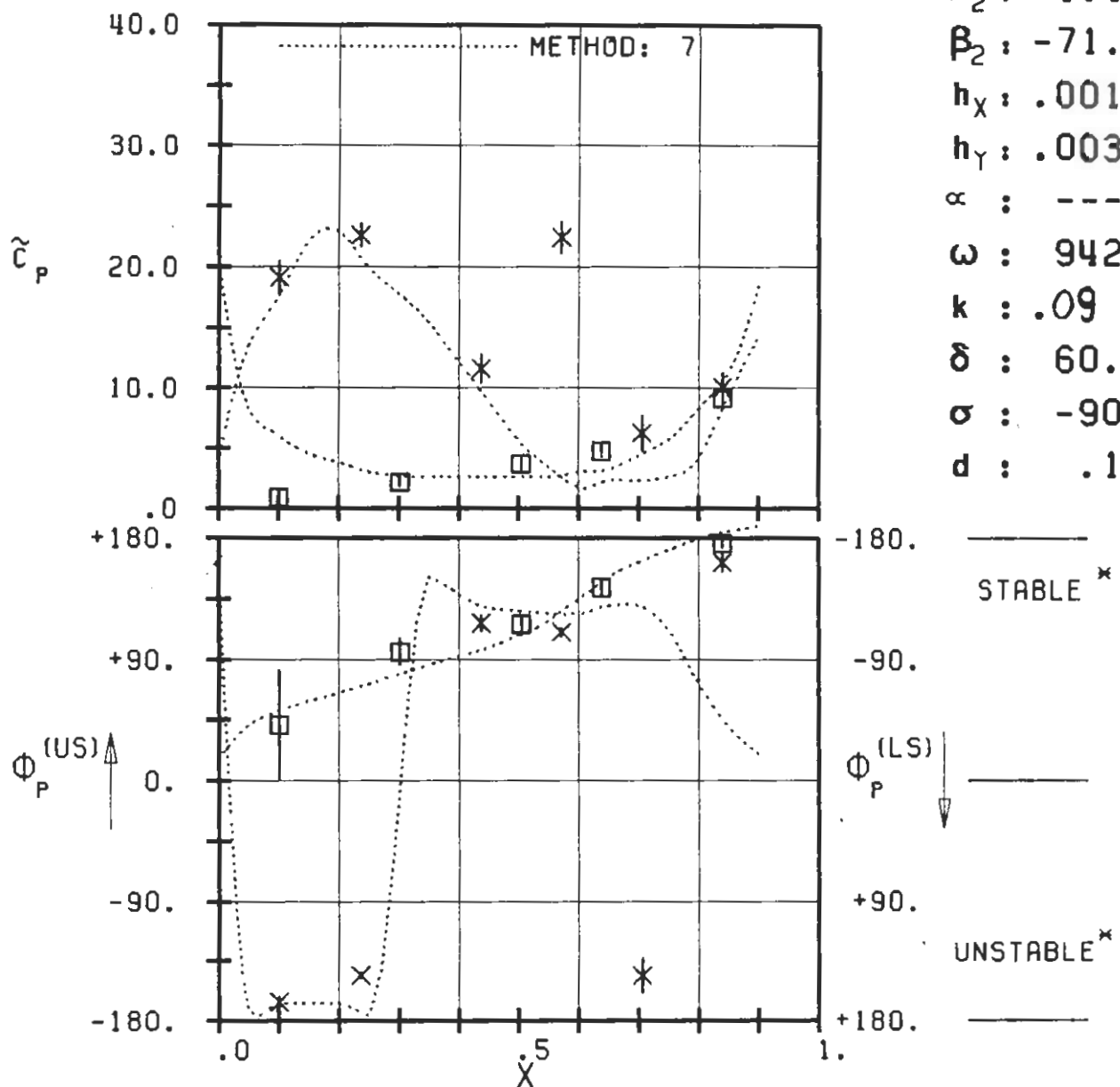


PLOT 7.4-2.4: FOURTH STANDARD CONFIGURATION CASE : 4
MAGNITUDE AND PHASE LEAD OF UNSTEADY BLADE SURFACE PRESSURE COEFFICIENT.
552A-1

(*: IN PITCH MODE, NOTATION VALID UPSTREAM OF PITCH AXIS)

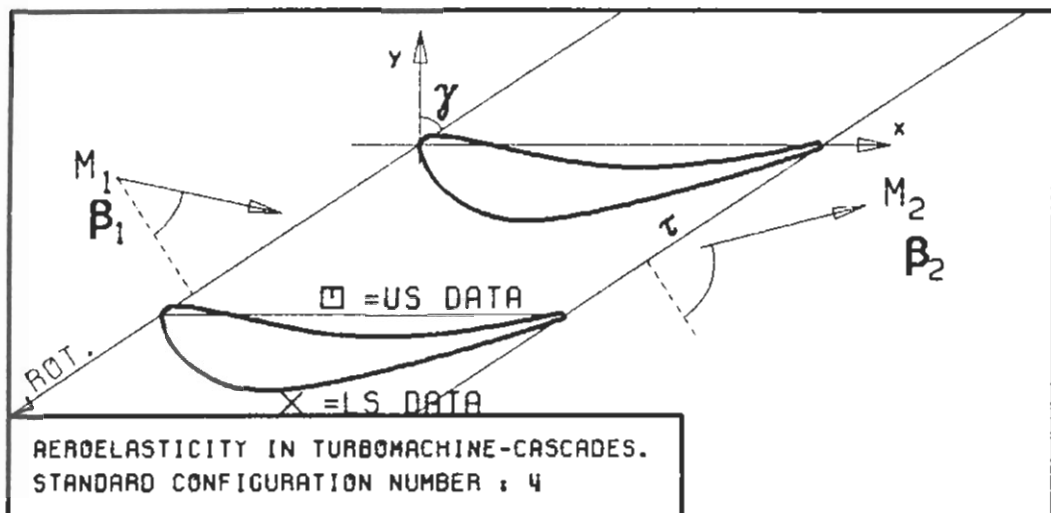


$c : .0744$
 $\tau : .76$
 $\gamma : 56.6$
 $x_\infty : ---$
 $y_\infty : ---$
 $M_1 : .29$
 $\beta_1 : -44.7$
 $i :$
 $M_2 : 1.19$
 $\beta_2 : -71.$
 $h_x : .0019$
 $h_y : .0033$
 $\alpha : ---$
 $\omega : 942.$
 $k : .09$
 $\delta : 60.4$
 $\sigma : -90.$
 $d : .17$

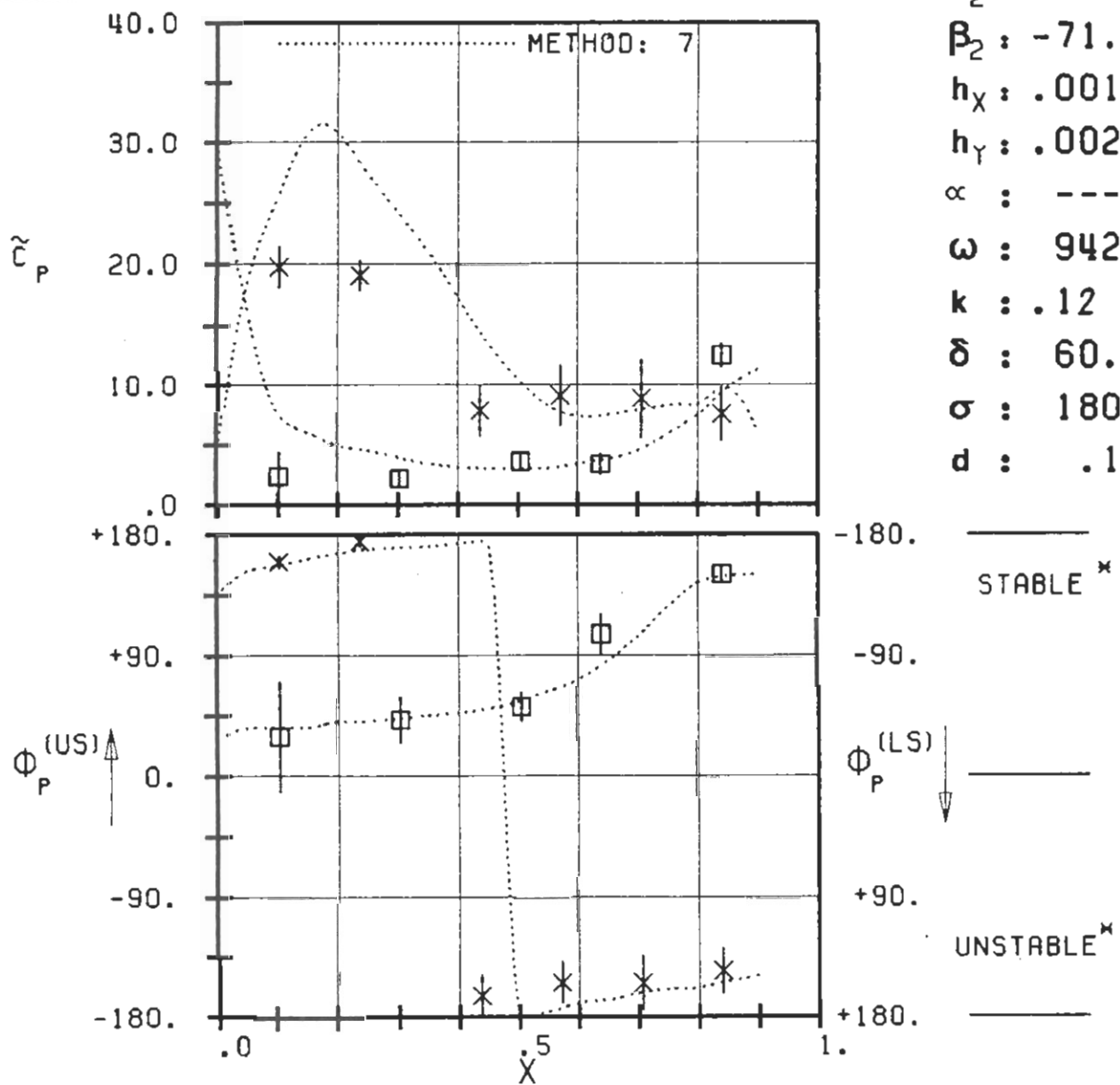


PLOT 7.4-2.5: FOURTH STANDARD CONFIGURATION CASE : 5
MAGNITUDE AND PHASE LEAD OF UNSTEADY BLADE SURFACE PRESSURE COEFFICIENT.
553B-1

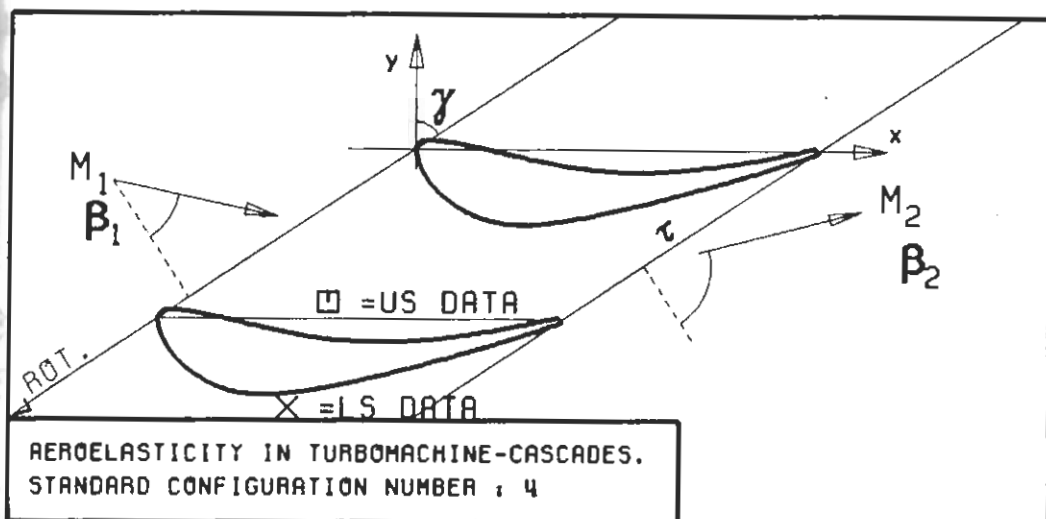
(\times : IN PITCH MODE, NOTATION VALID UPSTREAM OF PITCH AXIS)



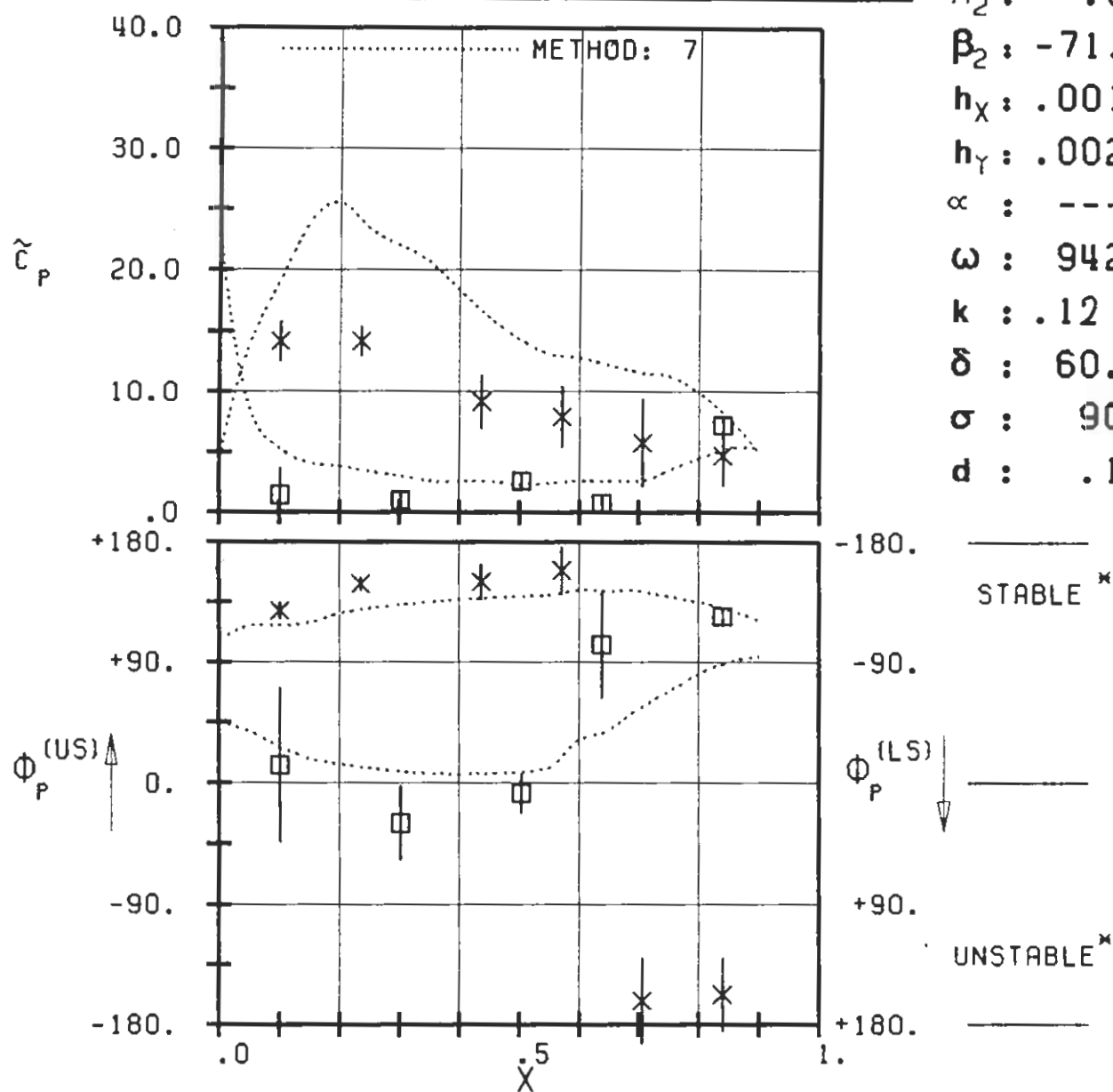
$c : .0744$
 $\tau : .76$
 $\gamma : 56.6$
 $x_\infty : \text{---}$
 $y_\infty : \text{---}$
 $M_1 : .28$
 $\beta_1 : -44.5$
 $i :$
 $M_2 : .90$
 $\beta_2 : -71.$
 $h_X : .0016$
 $h_Y : .0029$
 $\alpha : \text{---}$
 $\omega : 942.$
 $k : .12$
 $\delta : 60.4$
 $\sigma : 180.$
 $d : .17$



PLOT 7.4-2.6: FOURTH STANDARD CONFIGURATION CASE : 6
MAGNITUDE AND PHASE LEAD OF UNSTEADY BLADE SURFACE PRESSURE COEFFICIENT.

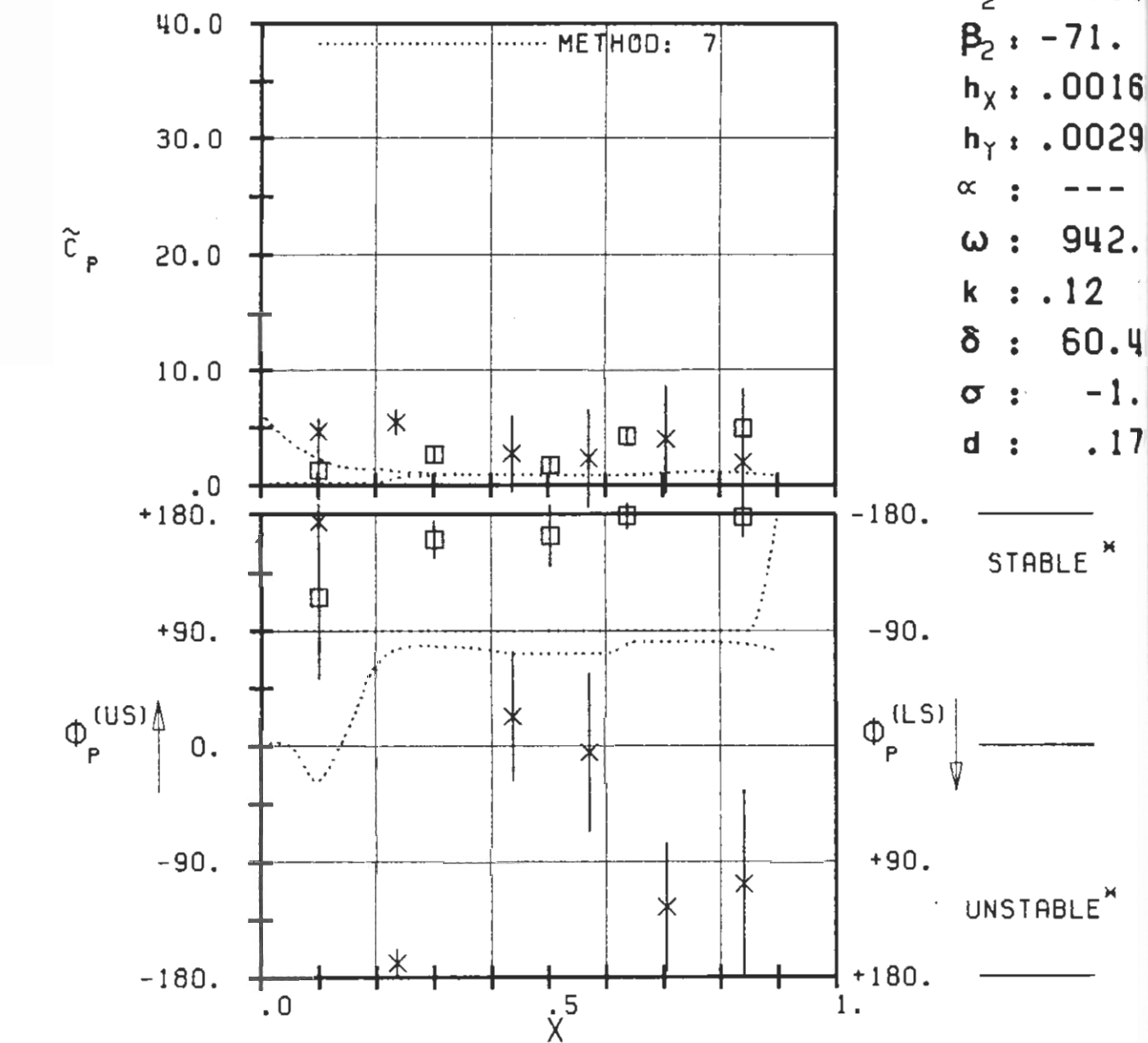
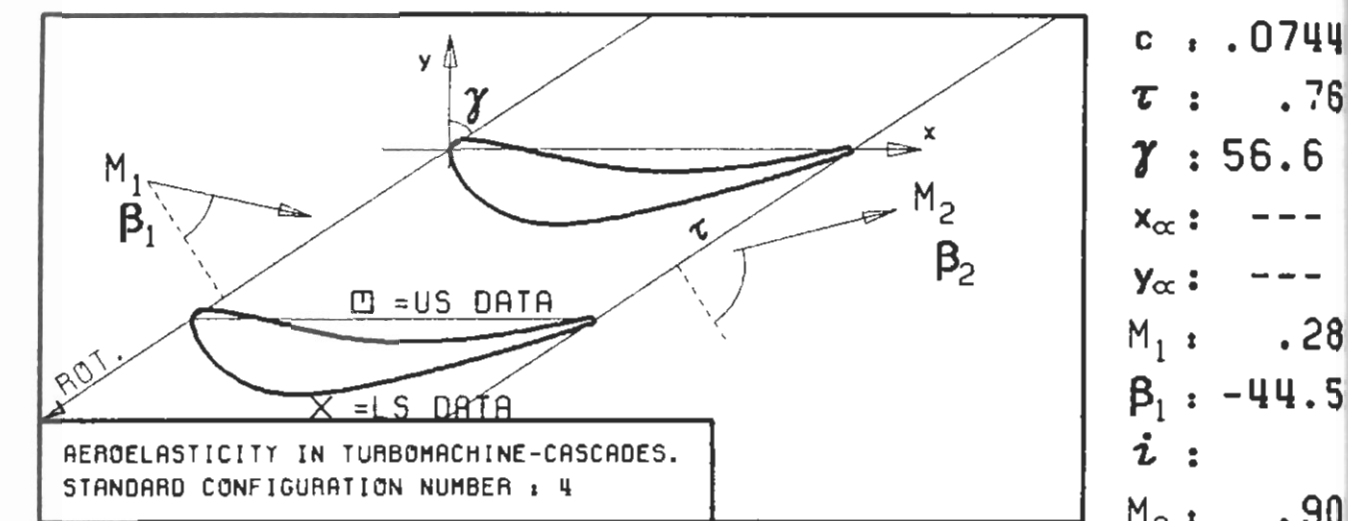


$c : .0744$
 $\tau : .76$
 $\gamma : 56.6$
 $x_\infty : ---$
 $y_\infty : ---$
 $M_1 : .28$
 $\beta_1 : -44.5$
 $i :$
 $M_2 : .90$
 $\beta_2 : -71.$
 $h_x : .0016$
 $h_y : .0029$
 $\infty : ---$
 $\omega : 942.$
 $k : .12$
 $\delta : 60.4$
 $\sigma : 90.$
 $d : .17$



PLOT 7.4-2.7: FOURTH STANDARD CONFIGURATION CASE : 7
MAGNITUDE AND PHASE LEAD OF UNSTEADY BLADE SURFACE PRESSURE COEFFICIENT.
552B-3

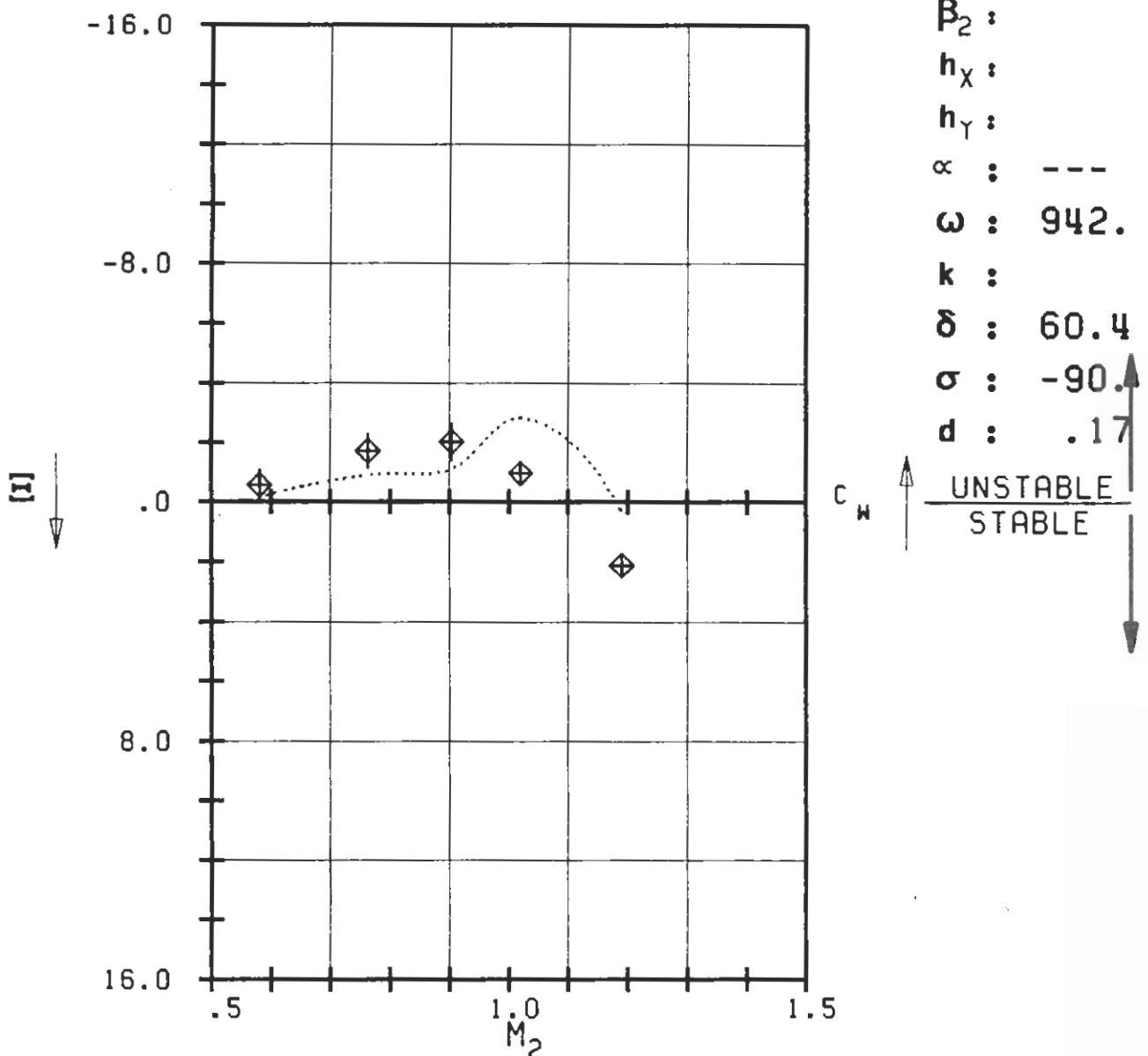
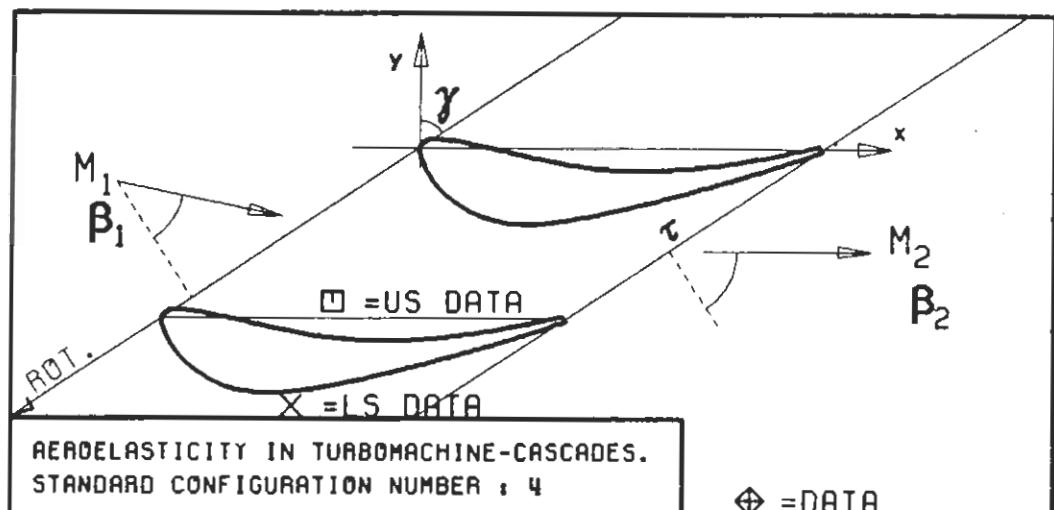
(*: IN PITCH MODE, NOTATION VALID UPSTREAM OF PITCH AXIS)



PLOT 7.4-2.8: FOURTH STANDARD CONFIGURATION CASE : 8
MAGNITUDE AND PHASE LEAD OF UNSTEADY BLADE SURFACE PRESSURE COEFFICIENT.
552B-4

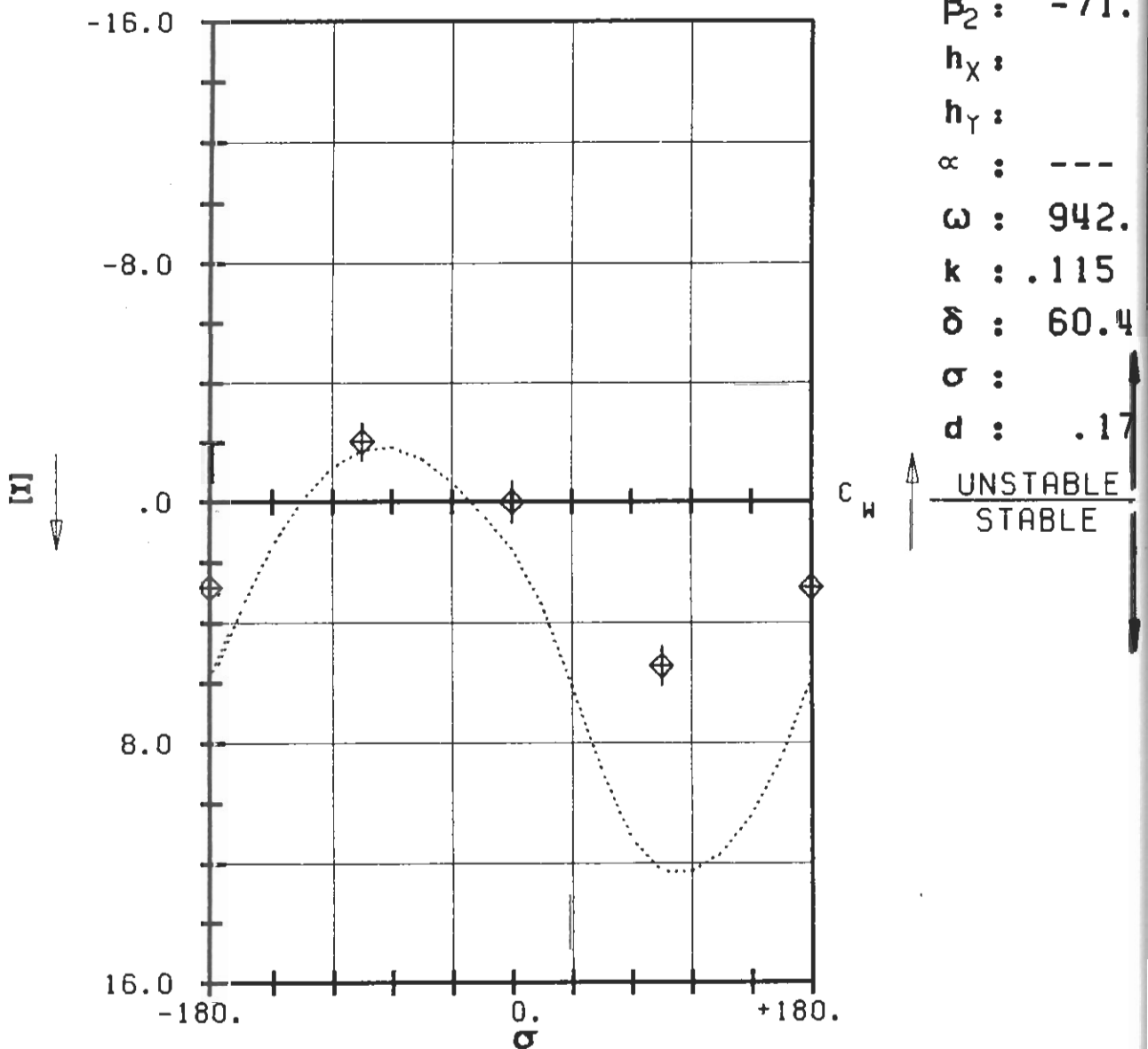
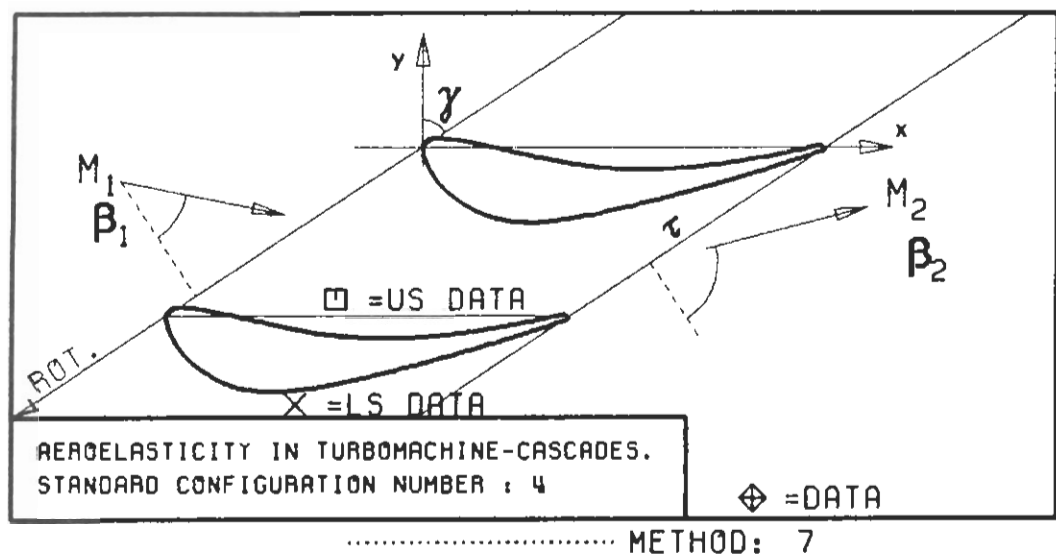
(X: IN PITCH MODE, NOTATION VALID UPSTREAM OF PITCH AXIS)

$c : .0744$
 $\tau : .76$
 $\gamma : 56.6$
 $x_\infty : ---$
 $y_\infty : ---$
 $M_1 : .28$
 $\beta_1 : -44.5$
 $i : ---$
 $M_2 : .90$
 $\beta_2 : -71.$
 $h_x : .0016$
 $h_y : .0029$
 $\alpha : ---$
 $\omega : 942.$
 $k : .12$
 $\delta : 60.4$
 $\sigma : -1.$
 $d : .17$



PLOT 7.4-6.1: FOURTH STANDARD CONFIGURATION CASES: 1-5
EPFL-LTT MD AERODYNAMIC WORK AND DAMPING COEFFICIENTS
553D-1 IN DEPENDANCE OF OUTLET ISENTROPIC MACH NUMBER

c	: .0744
τ	: .76
γ	: 56.6
x_α	: ---
y_α	: ---
M_1	: .19
β_1	: -45.
i	: ---
M_2	:
β_2	:
h_X	:
h_Y	:
α	: ---
ω	: 942.
k	:
δ	: 60.4
σ	: -90.4
d	: .17



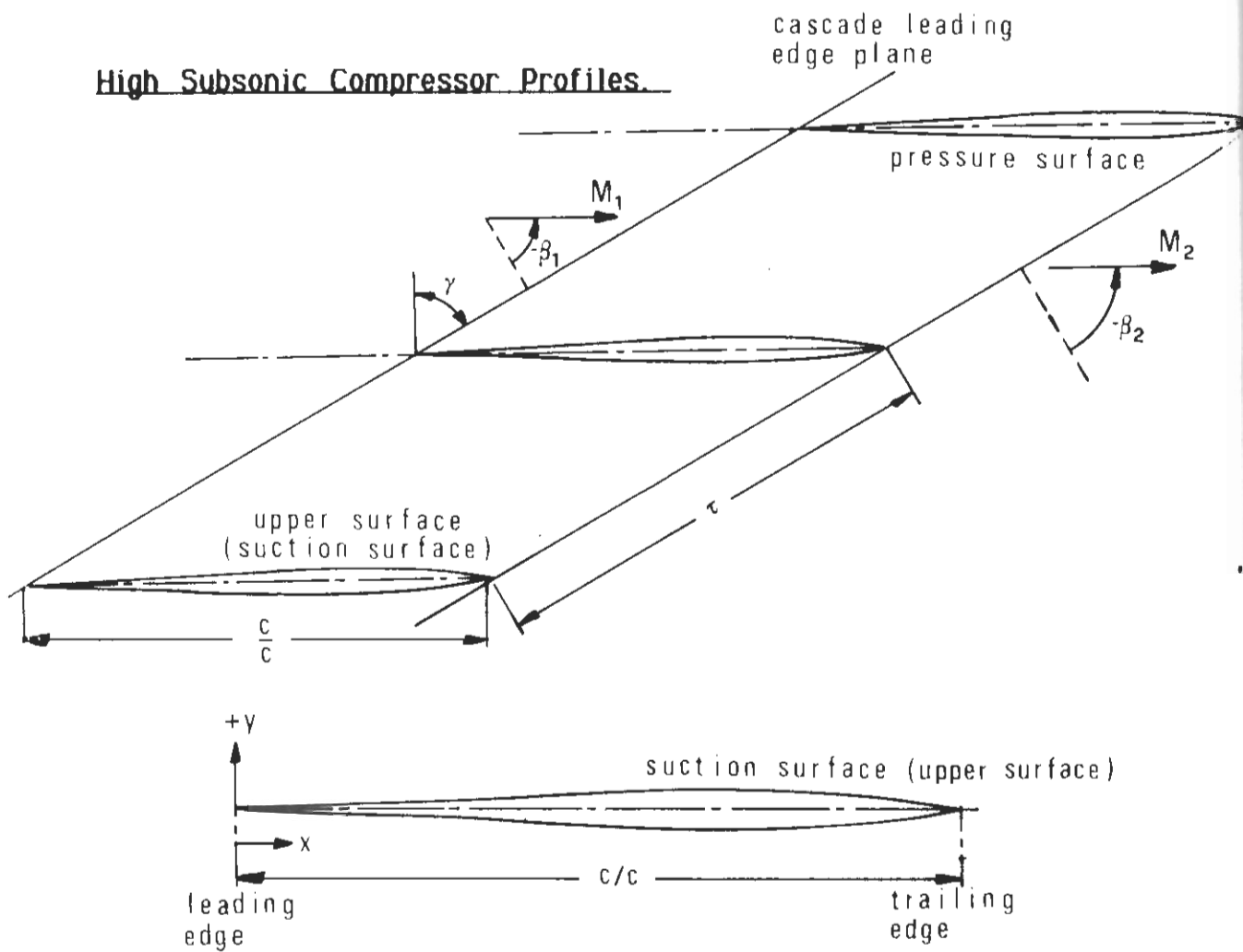
PLOT 7.4-6.2: FOURTH STANDARD CONFIGURATION CASES: 3,6-8
 EPFL-LTT MD AERODYNAMIC WORK AND DAMPING COEFFICIENTS
 552B-2 IN DEPENDANCE OF INTERBLADE PHASE ANGLE

AEROELASTICITY IN TURBOMACHINE-CASCADES

FIFTH STANDARD CONFIGURATION

Definition

High Subsonic Compressor Profiles.



Maximum thickness at x	= 0.67
Vibration in pitch around (x_α, y_α)	= (0.5, 0.)
d = (thickness/chord)	= 0.027
α = 0.00524 rad	f = variable (75-550 Hz)
c = 0.090 m	i = variable (2°-15°)
τ = 0.95	camber = 0°
k = variable	γ = 59.3°
span = 0.120 m	σ : Only one blade vibrated
M_1 = variable (0.5-1.0)	
Working fluid: Air	

Fig. 7.5-1. Fifth standard configuration: Cascade geometry

$c = 0.090 \text{ m}$				
x	Upper surface (Suction surface)		Lower surface (Pressure surface)	
	y	y	y	
0.	0.	0.	0.	
0.0124	0.0016	-0.0016		
0.0250	0.0018	-0.0018		
0.0500	0.0026	-0.0026		
0.0750	0.0033	-0.0033		
0.1000	0.0041	-0.0041		
0.1500	0.0053	-0.0053		
0.2000	0.0062	-0.0062		
0.2500	0.0079	-0.0079		
0.3000	0.0101	-0.0101		
0.3500	0.0103	-0.0103		
0.4000	0.0111	-0.0111		
0.4500	0.0119	-0.0119		
0.5000	0.0124	-0.0124		
0.5500	0.0128	-0.0128		
0.6000	0.0133	-0.0133		
0.6500	0.0135	-0.0135		
0.7000	0.0135	-0.0135		
0.7500	0.0128	-0.0128		
0.8000	0.0116	-0.0116		
0.8500	0.0098	-0.0098		
0.9000	0.0076	-0.0076		
0.9500	0.0048	-0.0048		
1.0000	0.	0.		

$\frac{\text{LE radius}}{c} = \frac{\text{TE radius}}{c} = 0.002$

Table 7.5-1 Fifth standard configuration : Dimensionless Airfoil Coordinates

AEROELASTICITY IN TURBOMACHINE-CASCADES

FIFTH STANDARD CONFIGURATION

Aeroelastic Test Cases

Aeroelastic Test Case No.	Time Averaged				Time Dependent Parameters				Flow
	M ₁	i	p ₂ /p _{w1}	α	σ	f	k		
(-)	(°)	(-)	(rad)	(°)	(Hz)	(-)			
1	0.5	2	0.84	0.00524	180	200	0.37		Attached
2	"	4	0.86	"	"	"	"		"
3	"	6	0.87	"	"	"	"		Part. sep.
4	"	4	0.86	"	"	75	0.14		Attached
5	"	"	"	"	"	125	0.22		"
6	"	"	"	"	"	300	0.54		"
7	"	"	"	"	"	550	1.02		"
8	"	6	0.87	"	"	75	0.14		Part. sep.
9	"	"	"	"	"	125	0.22		"
10	"	"	"	"	"	300	0.56		"
11	"	"	"	"	"	550	1.02		"

Pitch axis at $(x_\alpha, y_\alpha) = (0.5, 0.)$ for all the above aeroelastic test cases

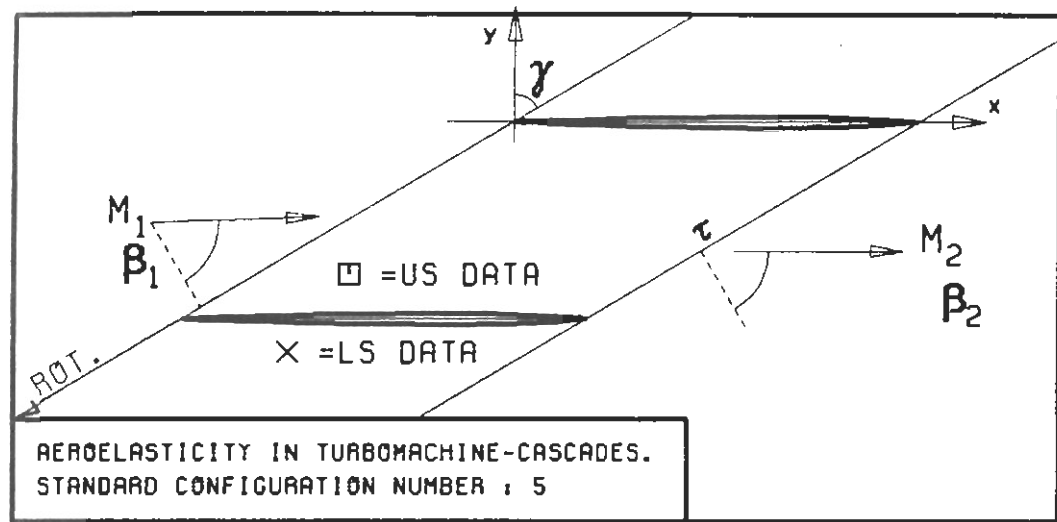
Table 7.5-2. Fifth standard configuration.

11 recommended aeroelastic test cases (restricted set from /4/)

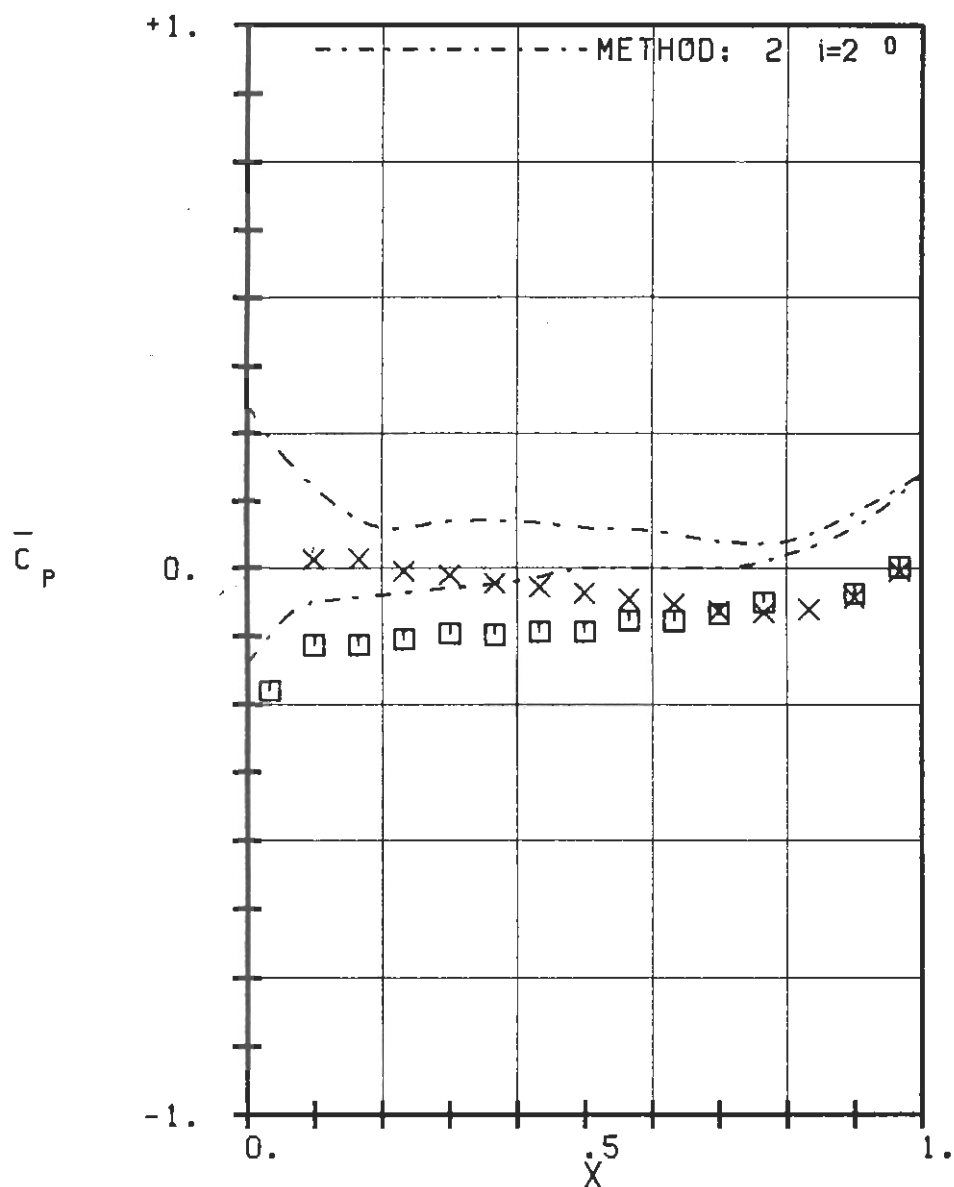
AEROELASTICITY IN TURBOMACHINE-CASCADES

FIFTH STANDARD CONFIGURATION

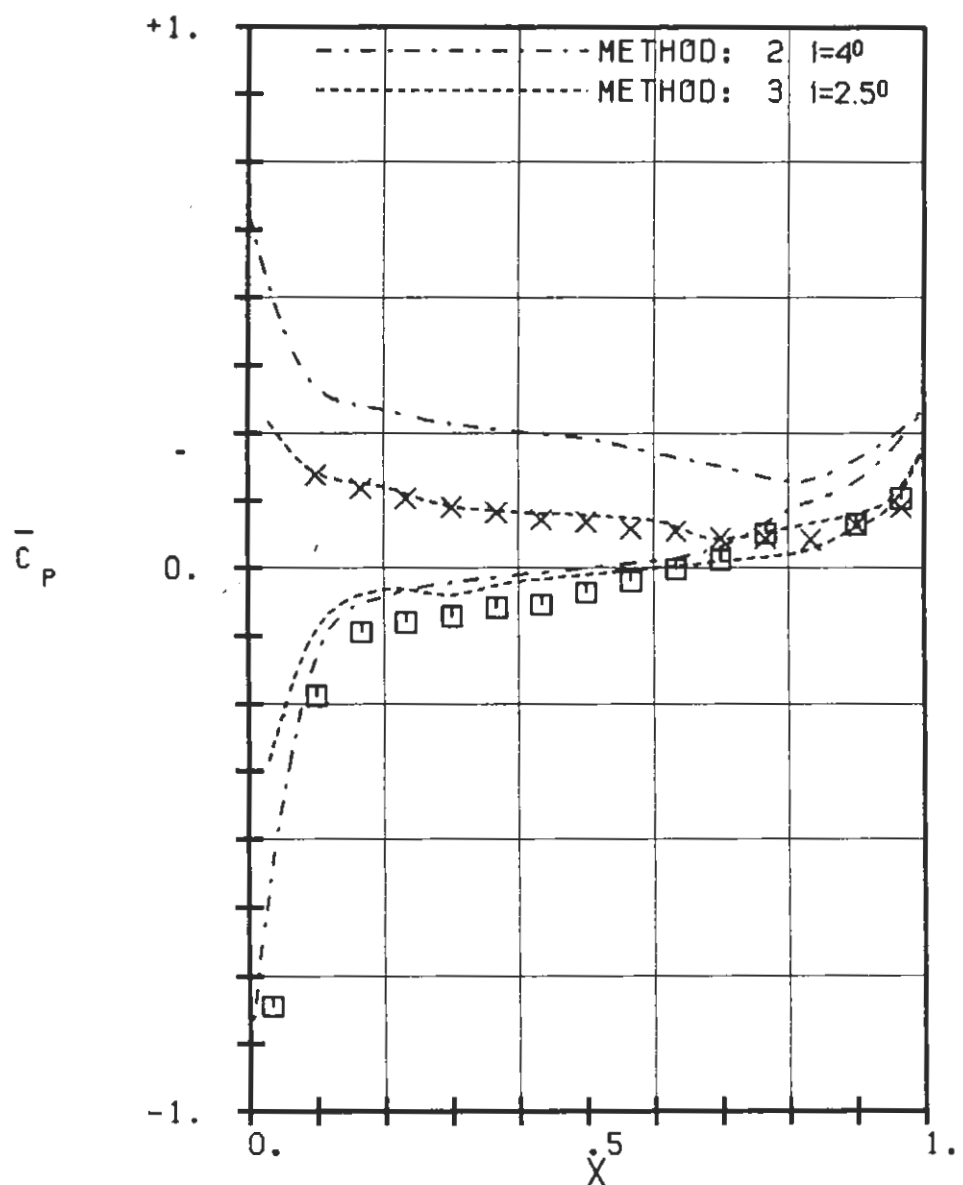
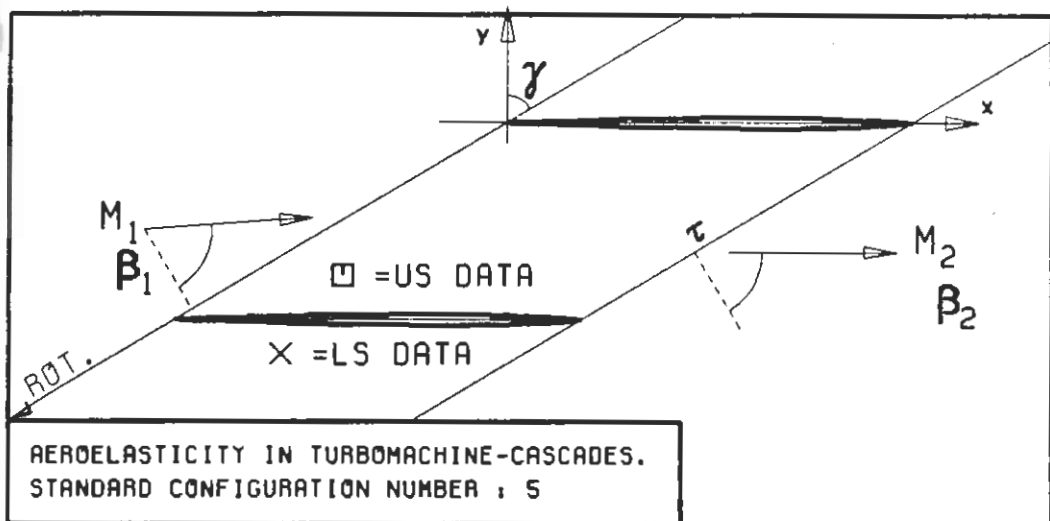
Experimental and Theoretical Results



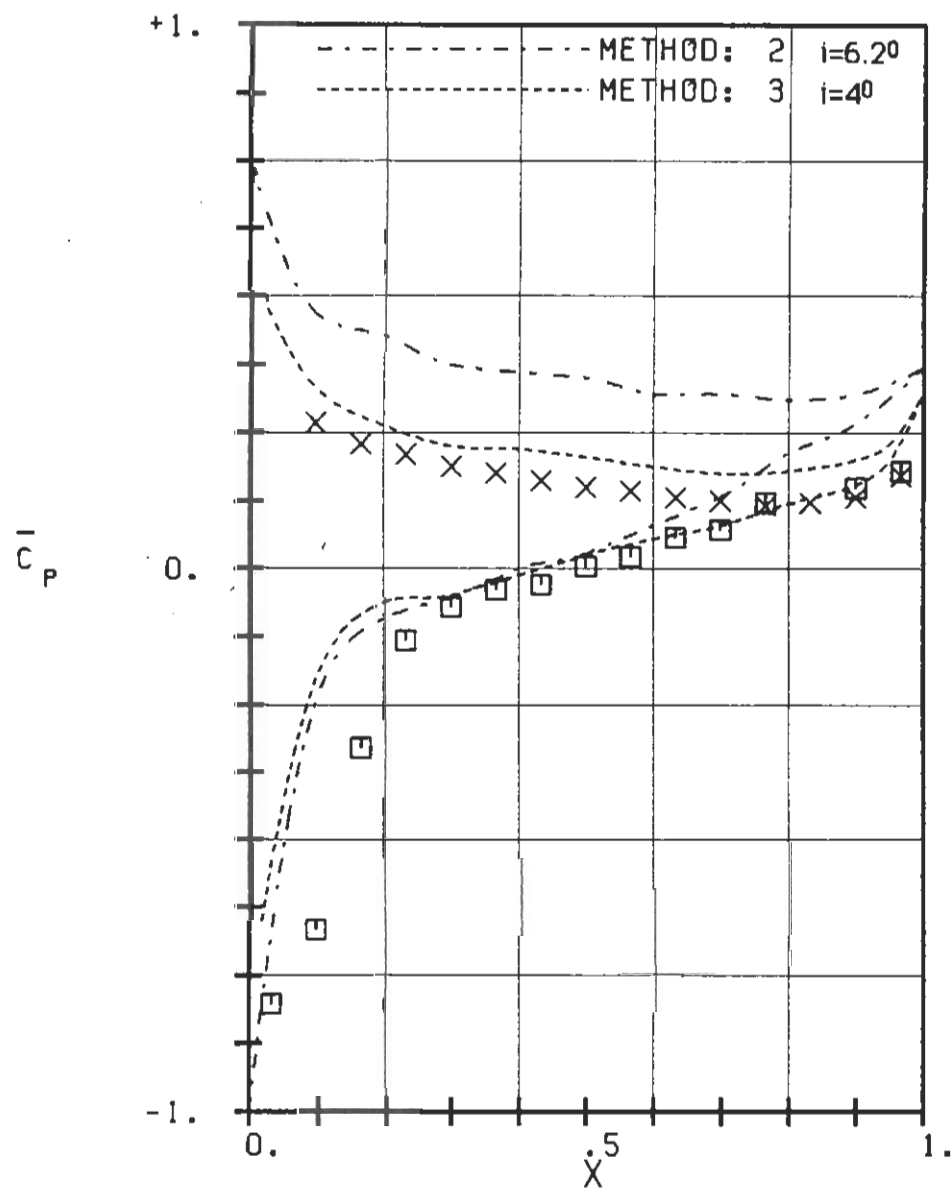
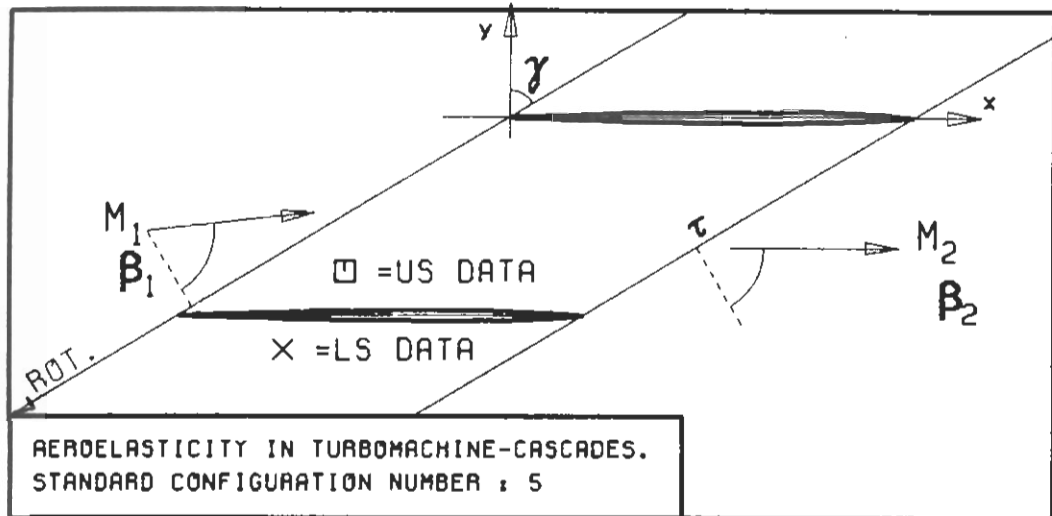
c : .090M
 τ : .95
 γ : 59.3
 x_∞ : -
 y_∞ : -
 M_1 : .5
 β_1 : -61.3
 i : 2.
 M_2 : -
 β_2 :
 h_X : -
 h_Y : -
 ∞ : -
 ω : -
 k : -
 δ : -
 σ : -
 d : .027



PLOT 7.5-1.1: FIFTH STANDARD CONFIGURATION, CASE 1.
 TIME AVERAGED BLADE SURFACE PRESSURE
 DISTRIBUTION FOR $M_1=0.5$ AND $INCIDENCE=2$ DEG.

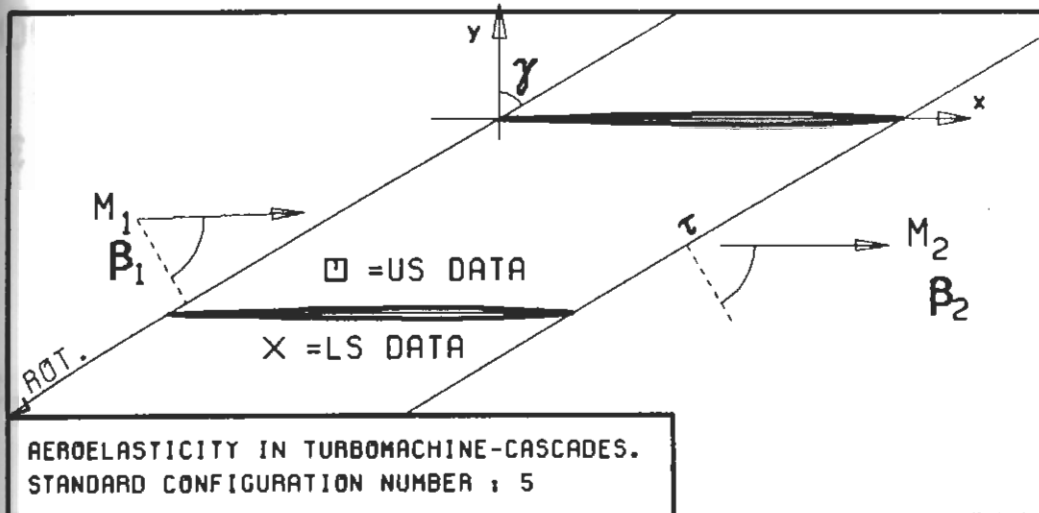


PLOT 7.5-1.2: FIFTH STANDARD CONFIGURATION, CASES 2.4-7.
TIME AVERAGED BLADE SURFACE PRESSURE
DISTRIBUTION FOR $M_1=0.5$ AND $INCIDENCE=4$ DEG.

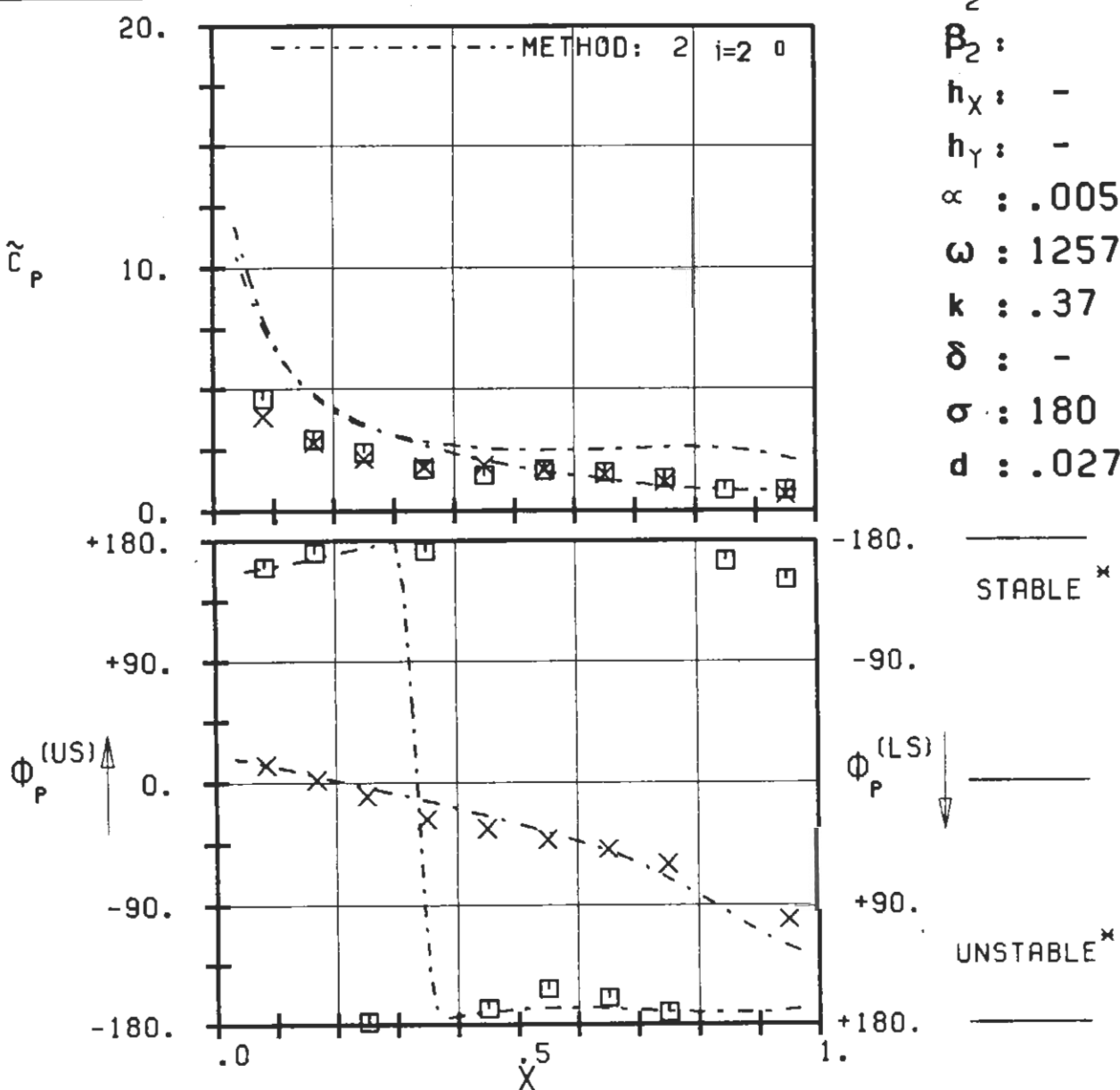


PLOT 7.5-1.3: FIFTH STANDARD CONFIGURATION, CASES 3,8-11.
 TIME AVERAGED BLADE SURFACE PRESSURE
 DISTRIBUTION FOR $M_1=0.5$ AND INCIDENCE=6 DEG.

$c : .090M$
 $\tau : .95$
 $\gamma : 59.3$
 $x_\infty : -$
 $y_\infty : -$
 $M_1 : .5$
 $\beta_1 : -65.3$
 $i : 6.$
 $M_2 : -$
 $\beta_2 : -$
 $h_X : -$
 $h_Y : -$
 $\alpha : -$
 $\omega : -$
 $k : -$
 $\delta : -$
 $\sigma : -$
 $d : .027$

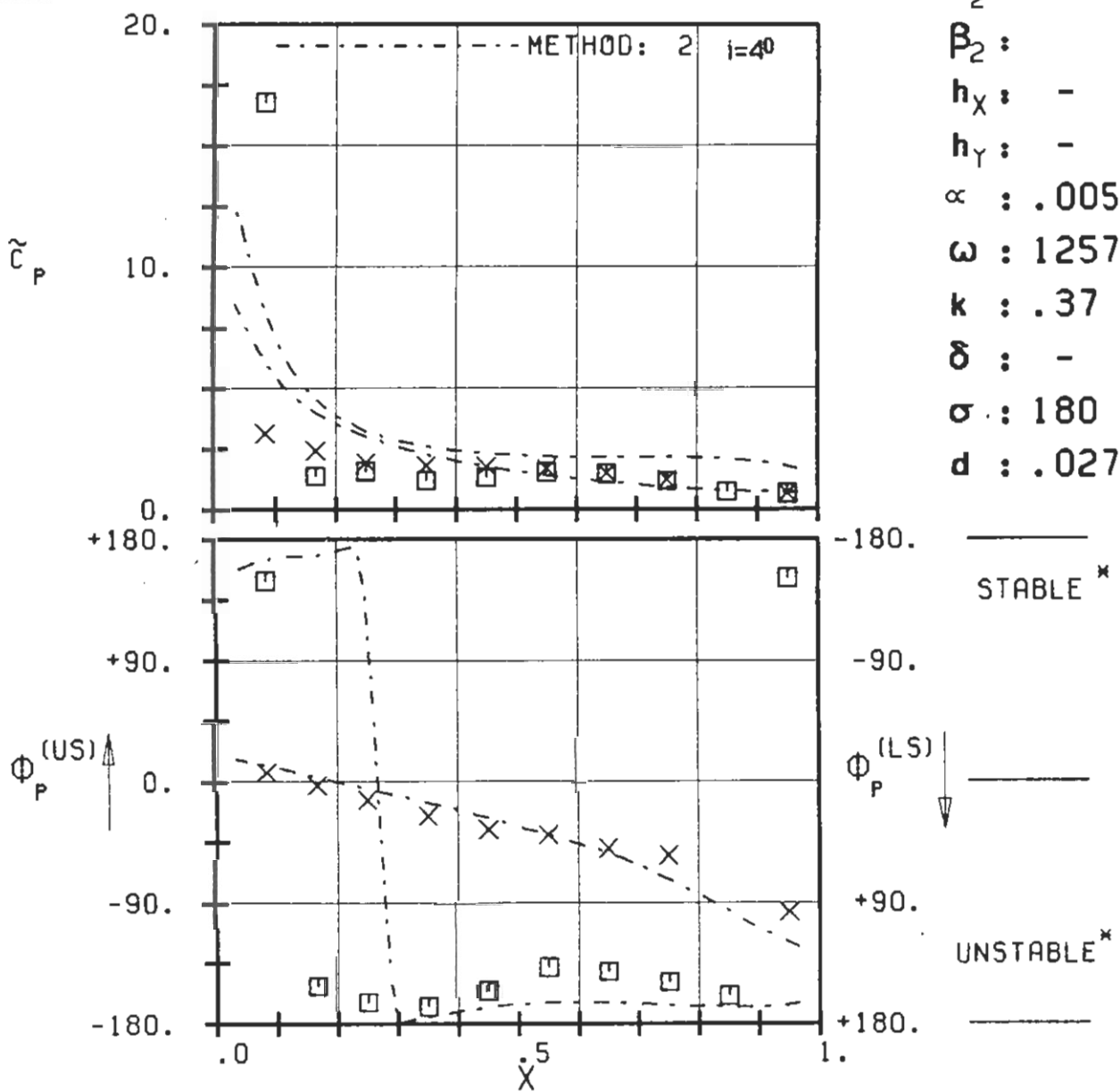
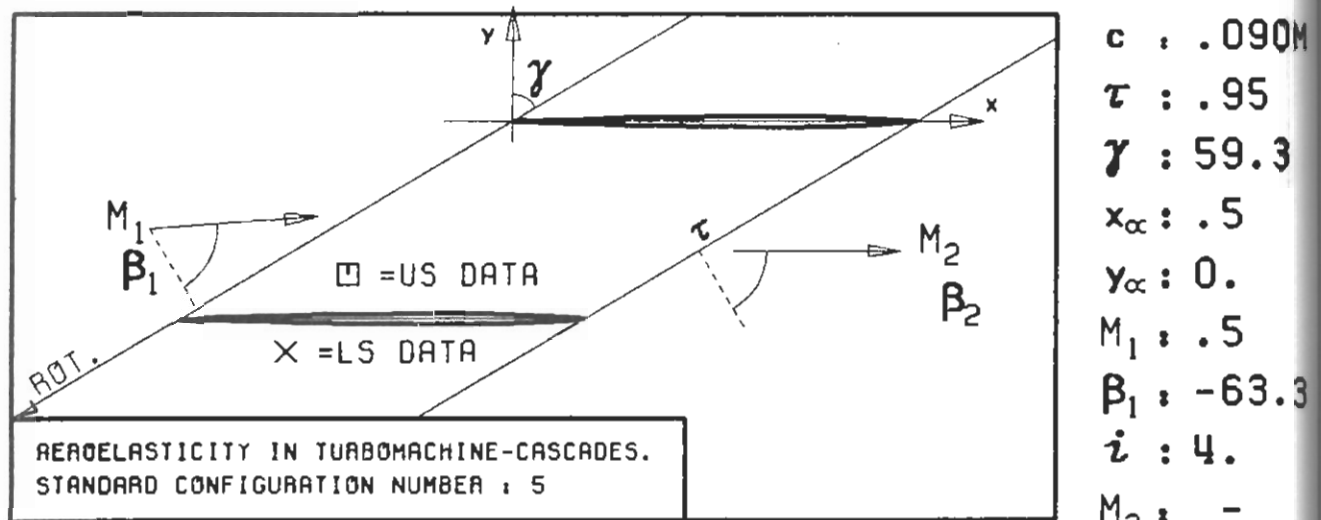


c : .090M
 τ : .95
 γ : 59.3
 x_∞ : .5
 y_∞ : 0.
 M_1 : .5
 β_1 : -61.3
 i : 2.
 M_2 : -
 β_2 :
 h_x : -
 h_y : -
 α : .0052
 ω : 1257
 k : .37
 δ : -
 σ : 180
 d : .027



PLOT 7.5-2.1: FIFTH STANDARD CONFIGURATION, CASE 1.
MAGNITUDE AND PHASE LEAD OF BLADE SURFACE
PRESSURE COEFFICIENT.

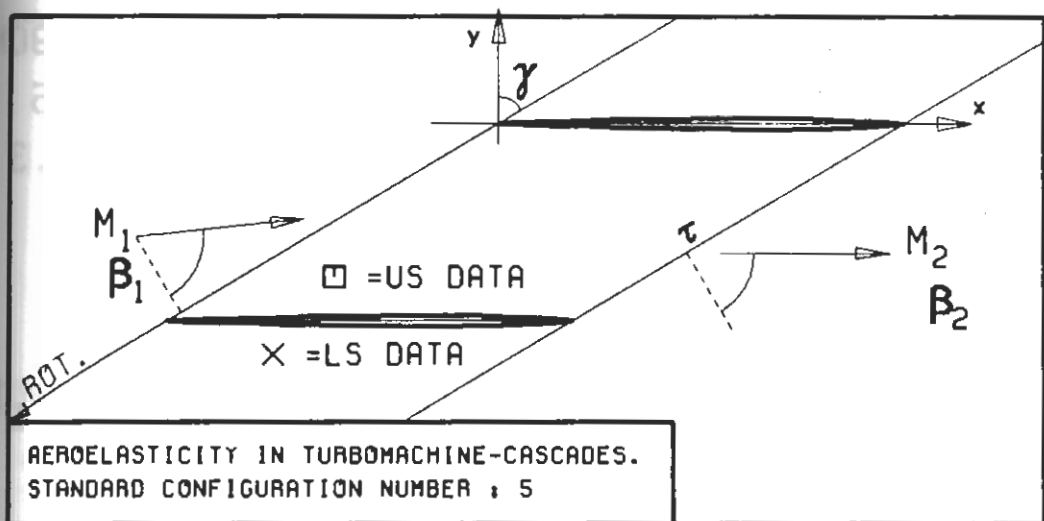
(x: IN PITCH MODE, NOTATION VALID UPSTREAM OF PITCH AXIS)



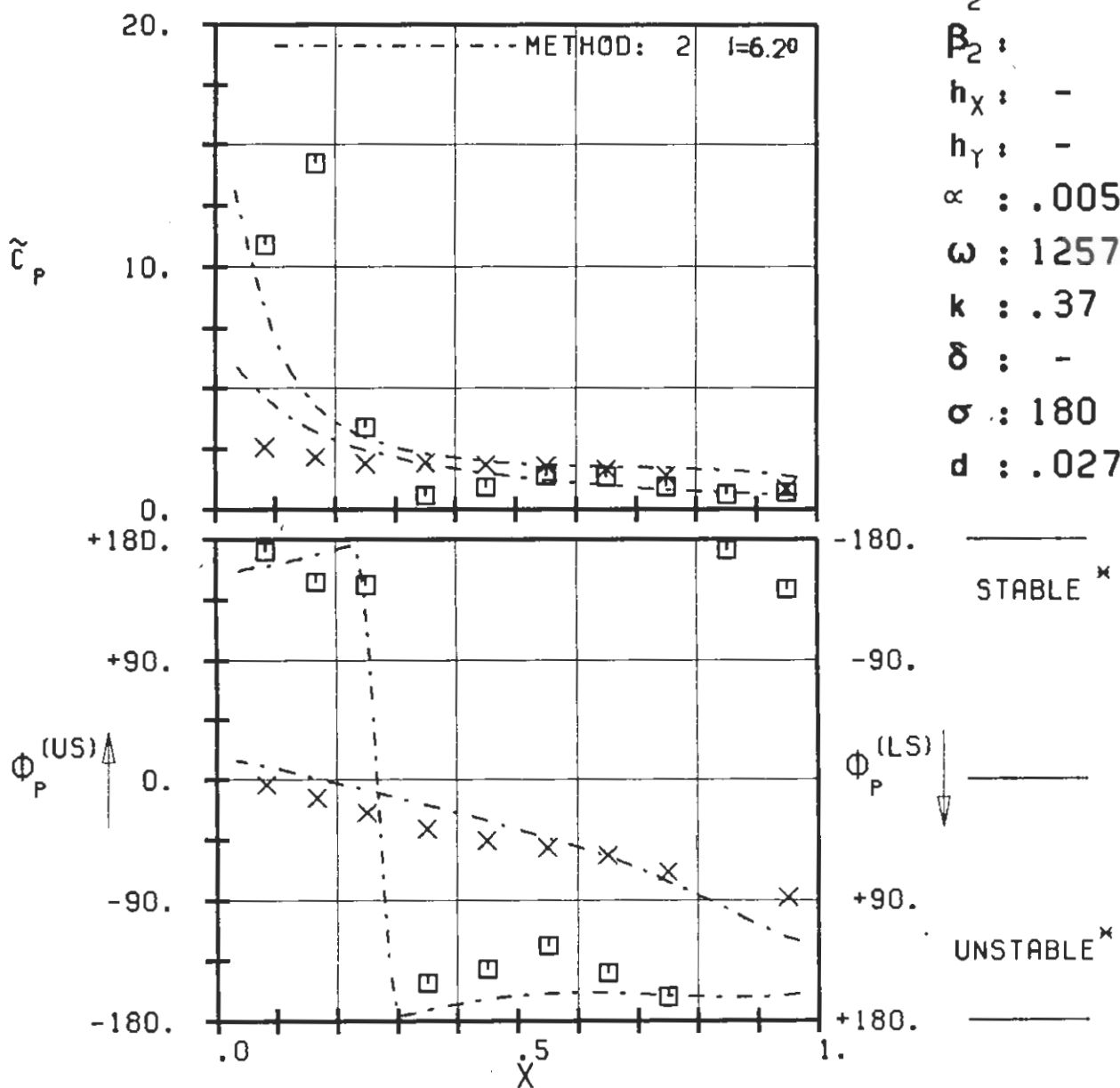
PLOT 7.5-2.2: FIFTH STANDARD CONFIGURATION, CASE 2.
 MAGNITUDE AND PHASE LEAD OF BLADE SURFACE
 PRESSURE COEFFICIENT.

(*: IN PITCH MODE, NOTATION VALID UPSTREAM OF PITCH AXIS)

$c : .090M$
 $\tau : .95$
 $\gamma : 59.3$
 $x_\infty : .5$
 $y_\infty : 0.$
 $M_1 : .5$
 $\beta_1 : -63.3$
 $i : 4.$
 $M_2 : -$
 $\beta_2 : -$
 $h_x : -$
 $h_y : -$
 $\alpha : .0052$
 $\omega : 1257$
 $k : .37$
 $\delta : -$
 $\sigma : 180$
 $d : .027$

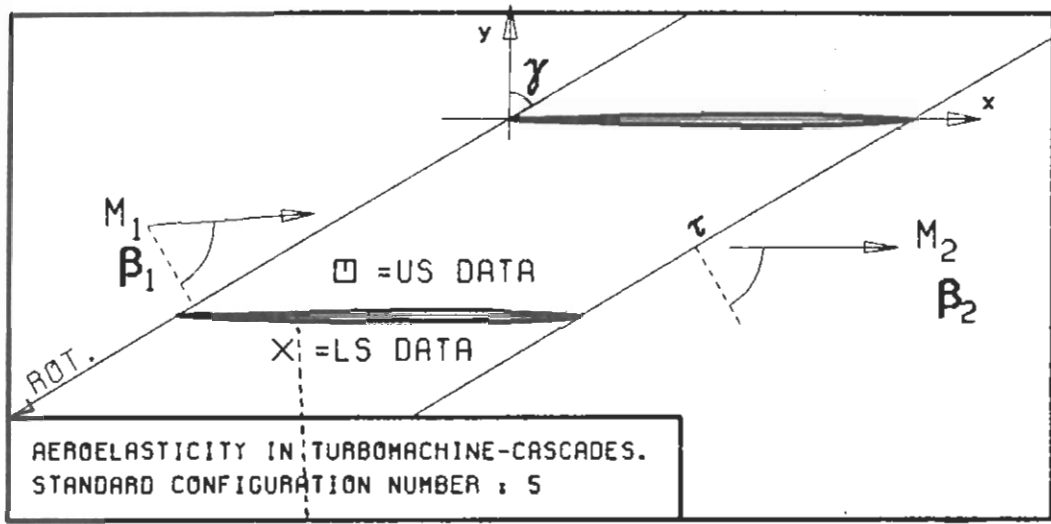


$c : .090M$
 $\tau : .95$
 $\gamma : 59.3$
 $x_\alpha : .5$
 $y_\alpha : 0.$
 $M_1 : .5$
 $B_1 : -65.3$
 $i : 6.$
 $M_2 : -$
 $B_2 : -$
 $h_X : -$
 $h_Y : -$
 $\alpha : .0052$
 $\omega : 1257$
 $k : .37$
 $\delta : -$
 $\sigma : 180$
 $d : .027$

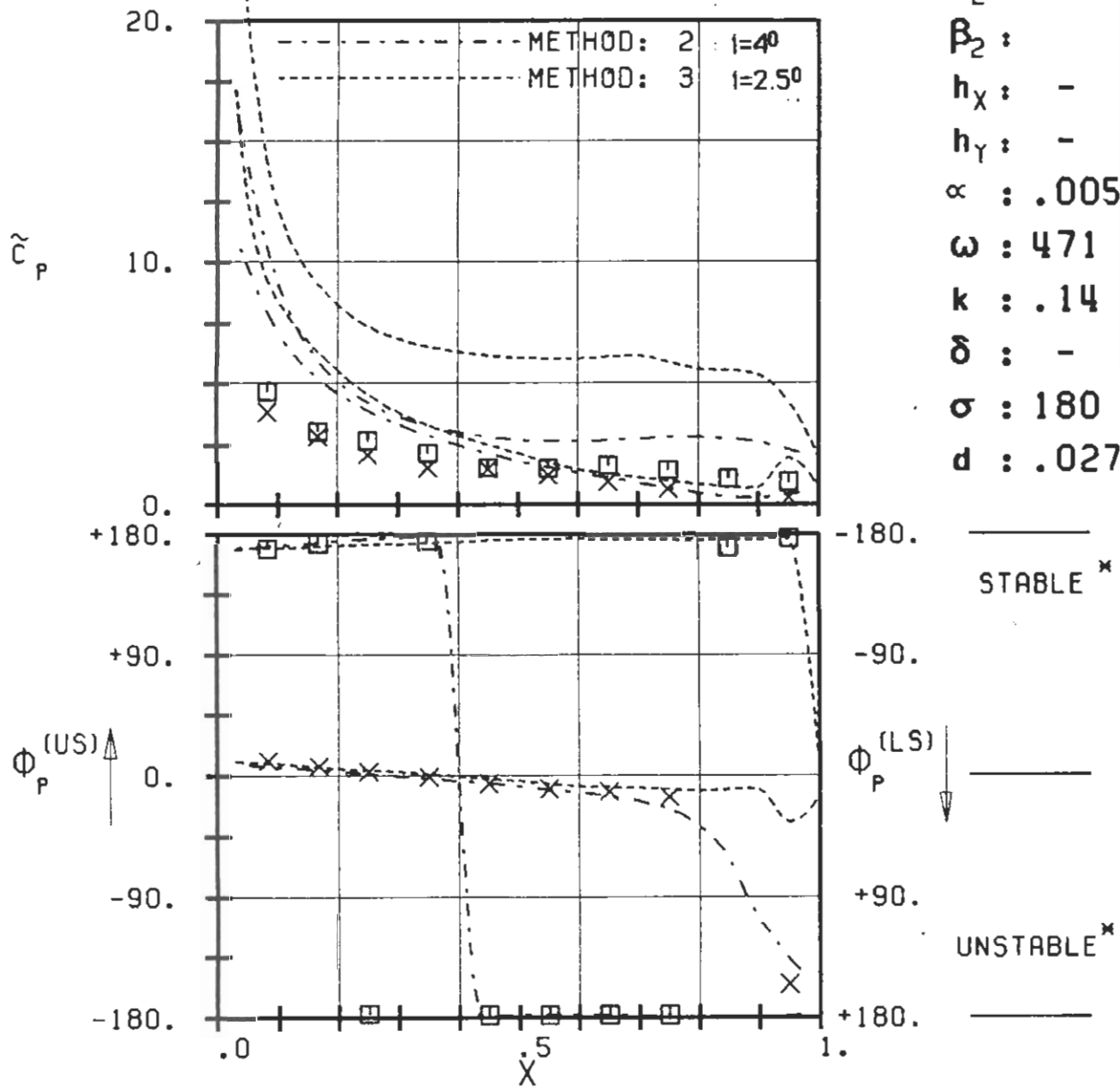


PLOT 7.5-2.3: FIFTH STANDARD CONFIGURATION, CASE 3.
MAGNITUDE AND PHASE LEAD OF BLADE SURFACE
PRESSURE COEFFICIENT.

(\times : IN PITCH MODE, NOTATION VALID UPSTREAM OF PITCH AXIS)

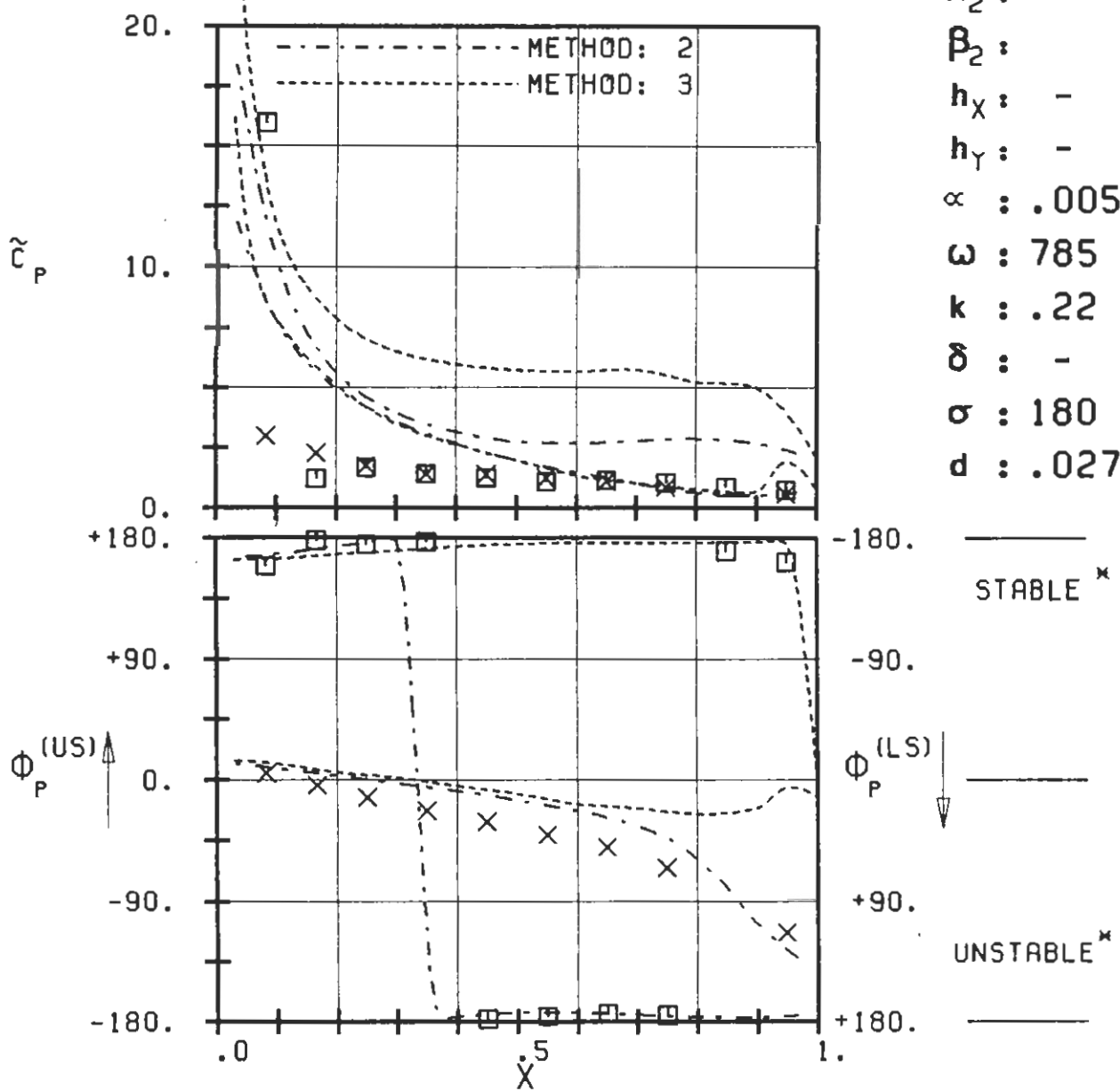
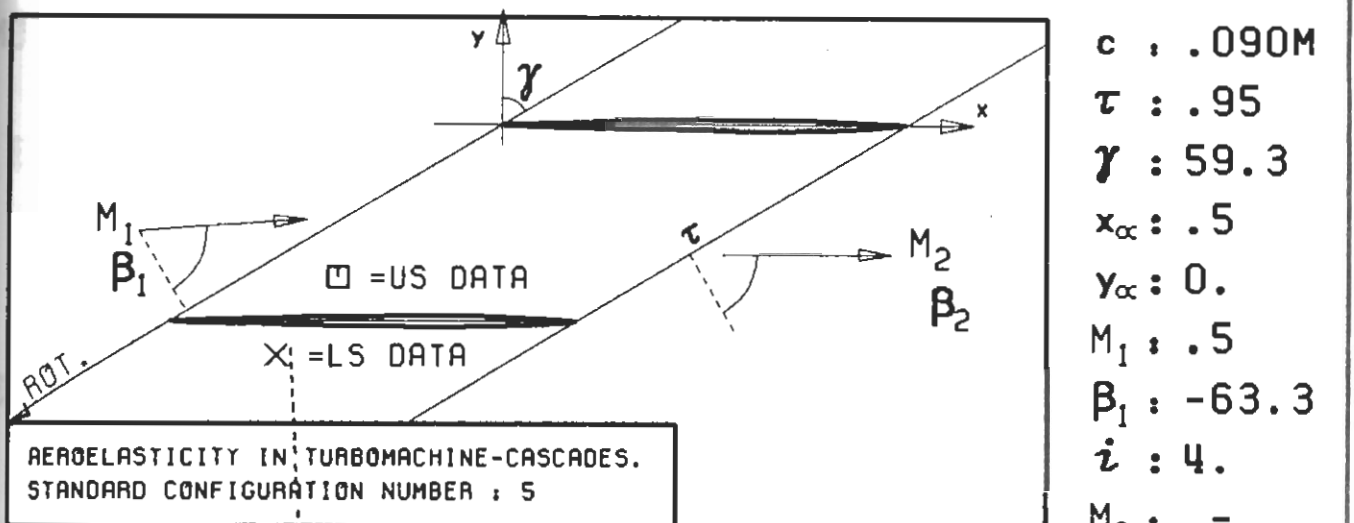


c : .090M
 τ : .95
 γ : 59.3
 x_α : .5
 y_α : 0.
 M_1 : .5
 β_1 : -63.3
 i : 4.
 M_2 : -
 β_2 :
 h_X : -
 h_Y : -
 α : .0052
 ω : 471
 k : .14
 δ : -
 σ : 180
 d : .027



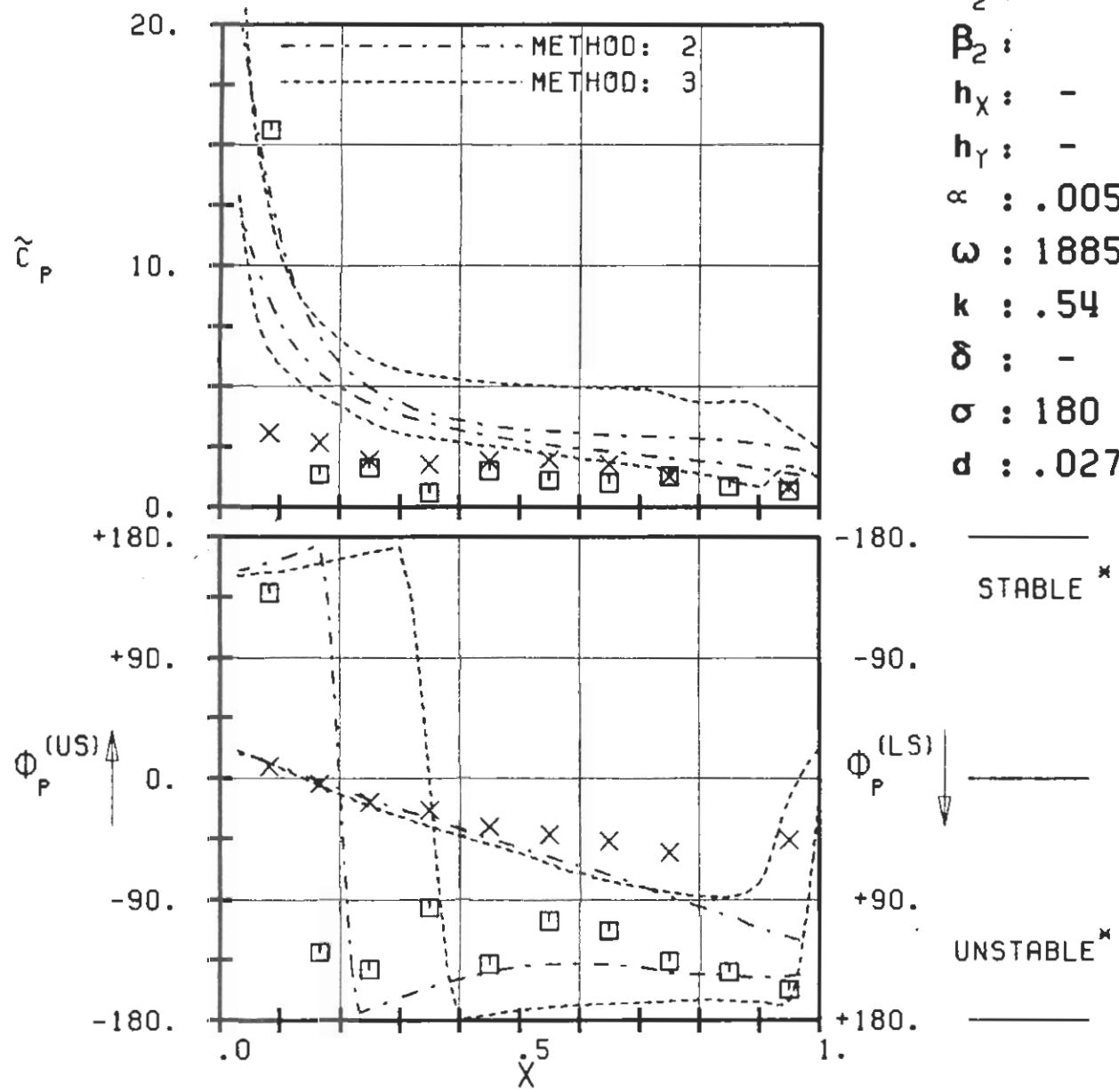
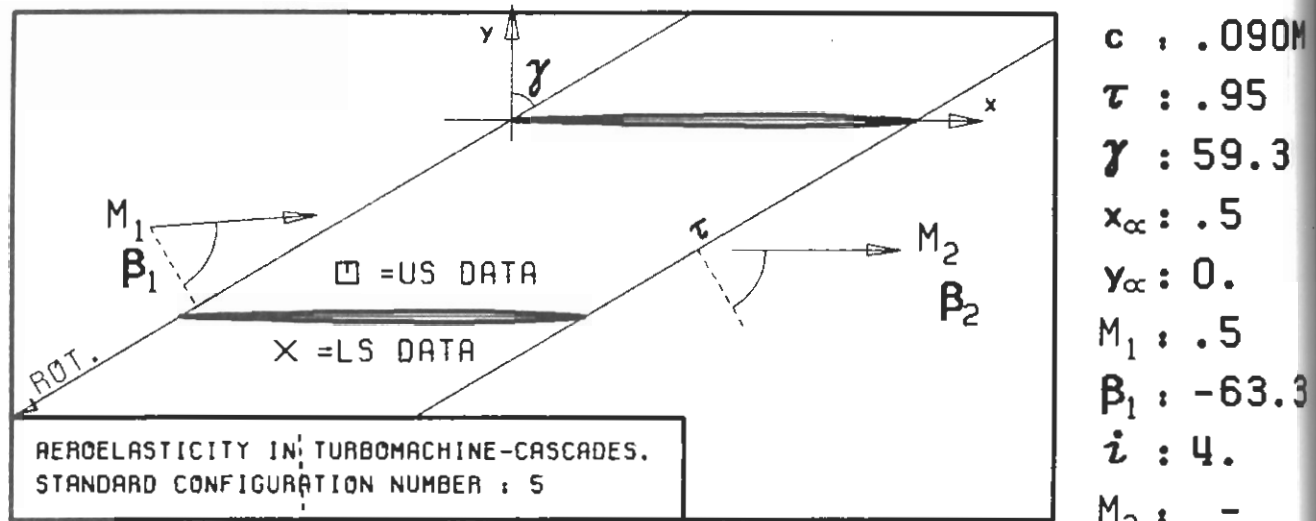
PLOT 7.5-2.4: FIFTH STANDARD CONFIGURATION, CASE 4.
MAGNITUDE AND PHASE LEAD OF BLADE SURFACE
PRESSURE COEFFICIENT.

(x: IN PITCH MODE, NOTATION VALID UPSTREAM OF PITCH AXIS)



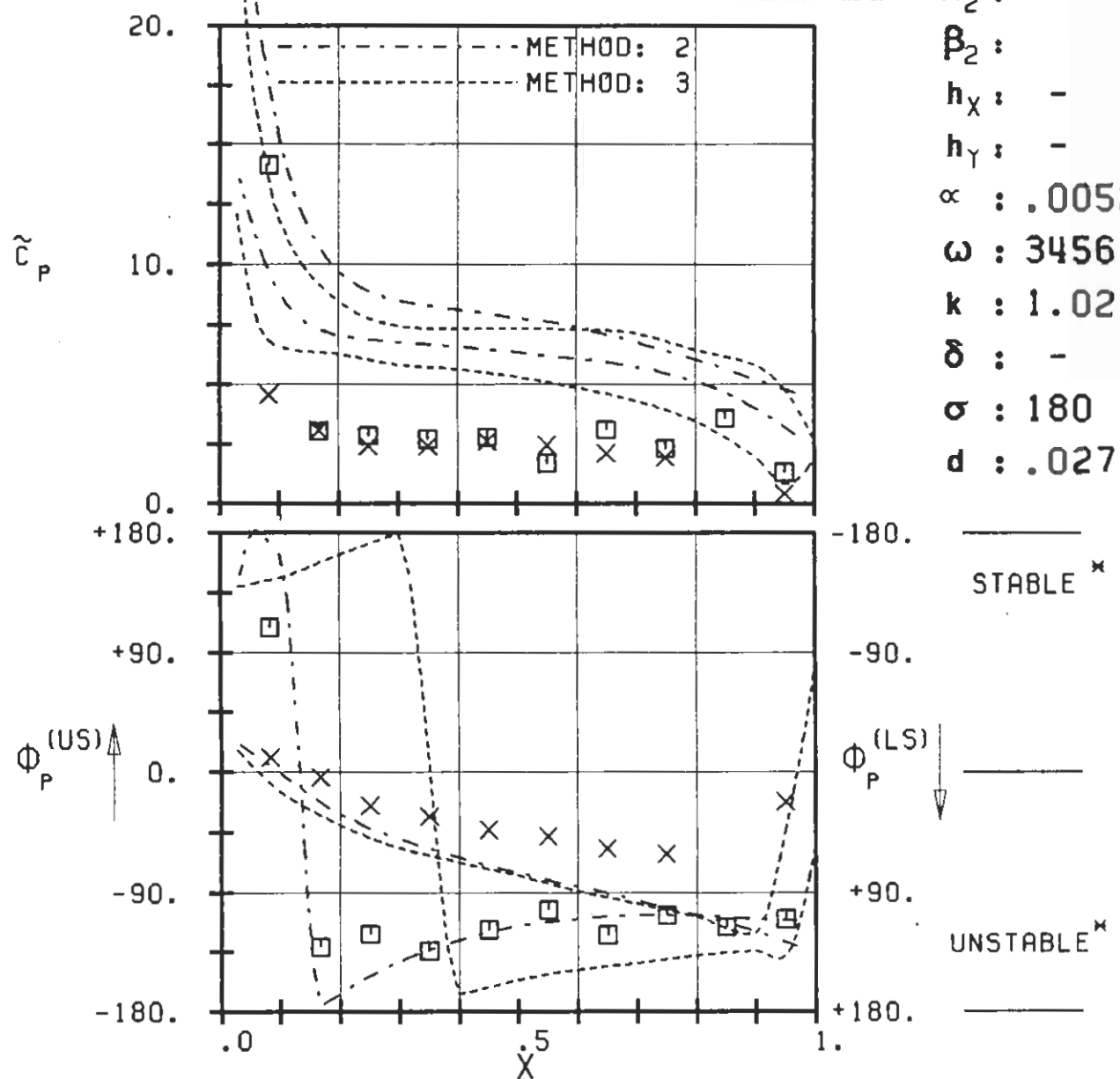
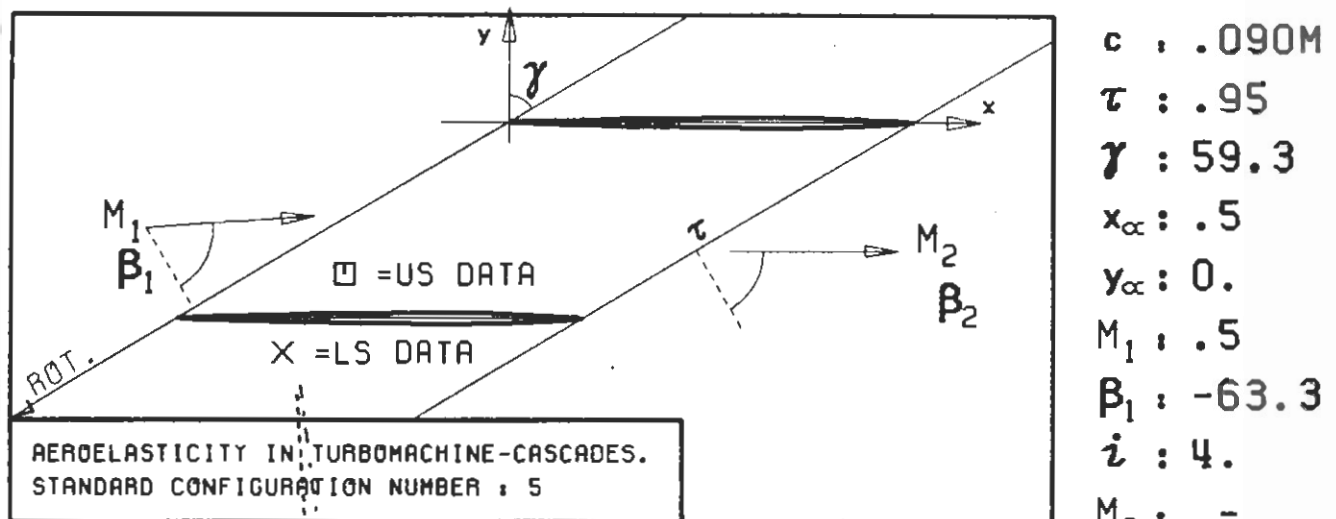
PLOT 7.5-2.5: FIFTH STANDARD CONFIGURATION, CASE 5.
MAGNITUDE AND PHASE LEAD OF BLADE SURFACE
PRESSURE COEFFICIENT.

(x: IN PITCH MODE, NOTATION VALID UPSTREAM OF PITCH AXIS)



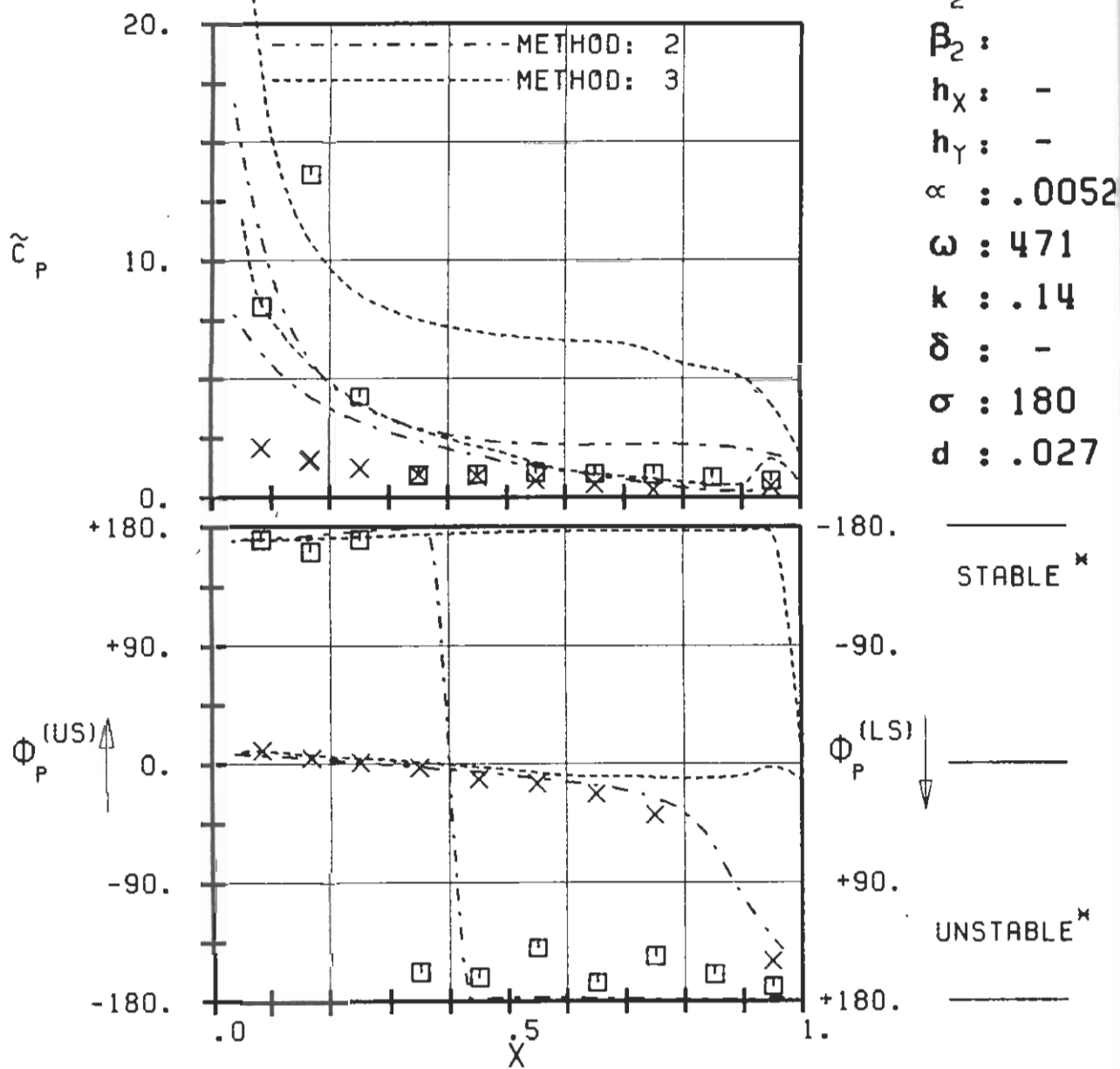
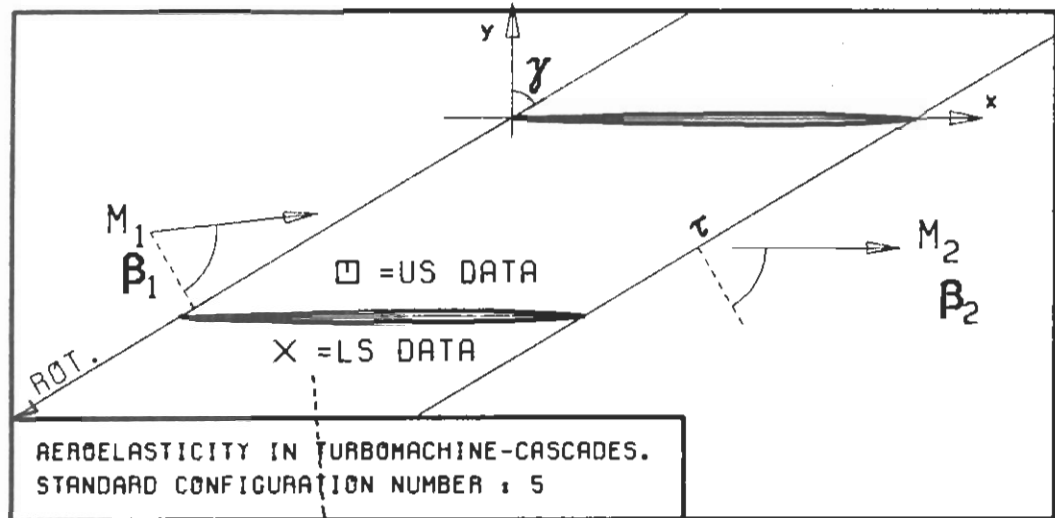
PLOT 7.5-2.6: FIFTH STANDARD CONFIGURATION, CASE 6.
MAGNITUDE AND PHASE LEAD OF BLADE SURFACE
PRESSURE COEFFICIENT.

(*: IN PITCH MODE, NOTATION VALID UPSTREAM OF PITCH AXIS)



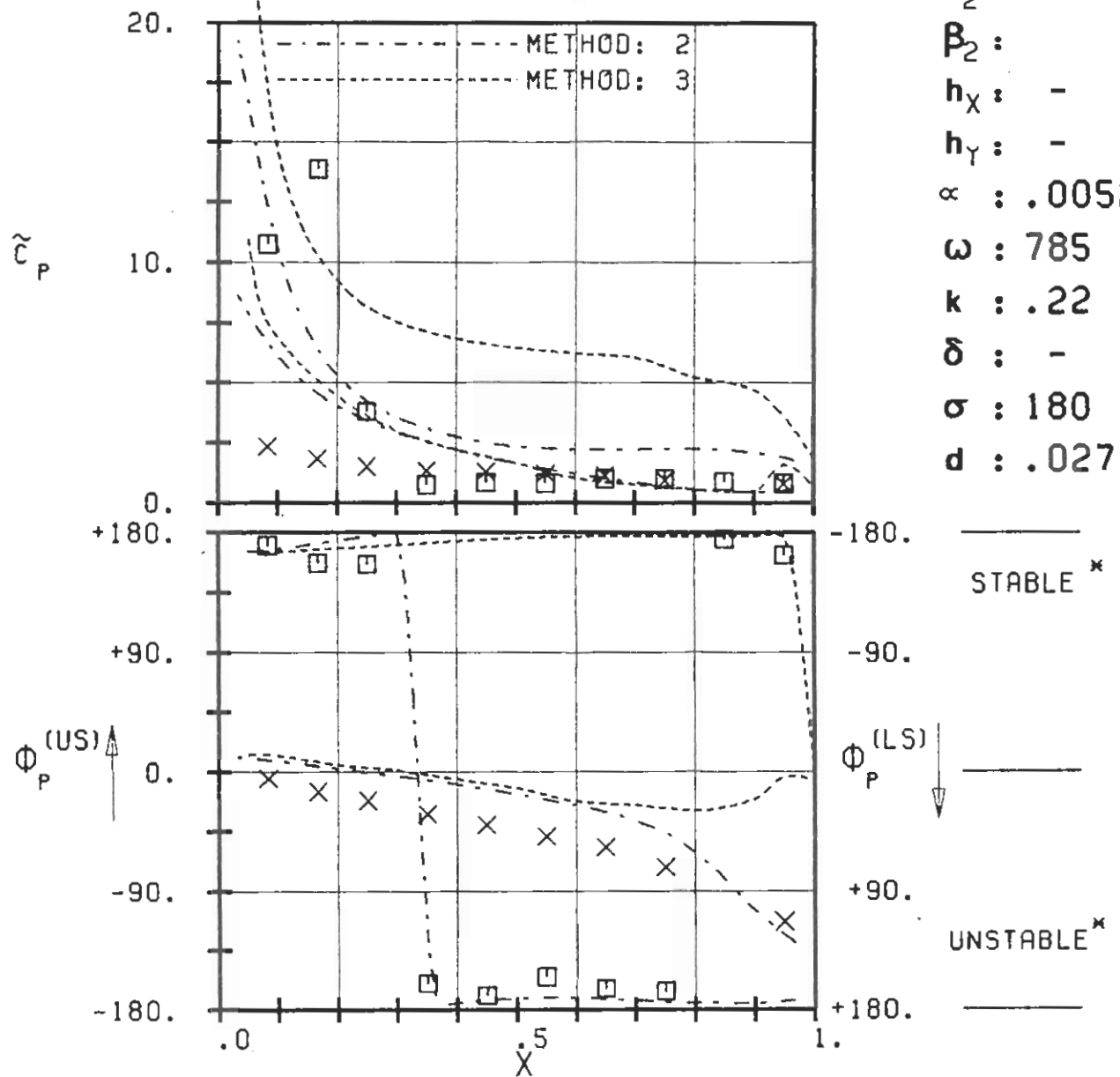
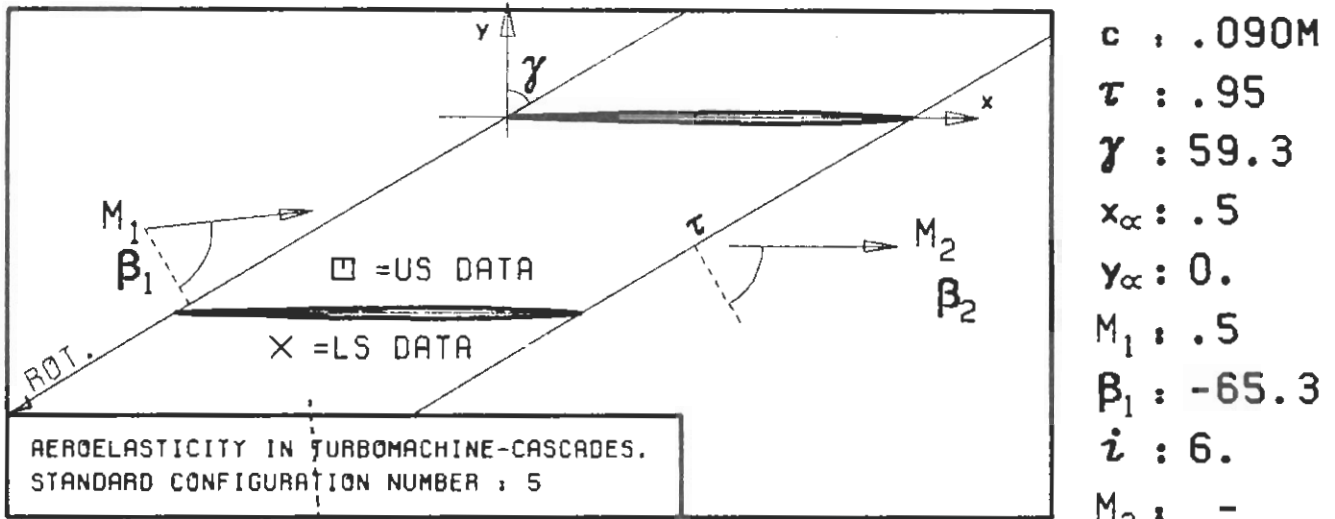
PLOT 7.5-2.7: FIFTH STANDARD CONFIGURATION, CASE 7.
 MAGNITUDE AND PHASE LEAD OF BLADE SURFACE
 PRESSURE COEFFICIENT.

(\times : IN PITCH MODE, NOTATION VALID UPSTREAM OF PITCH AXIS)



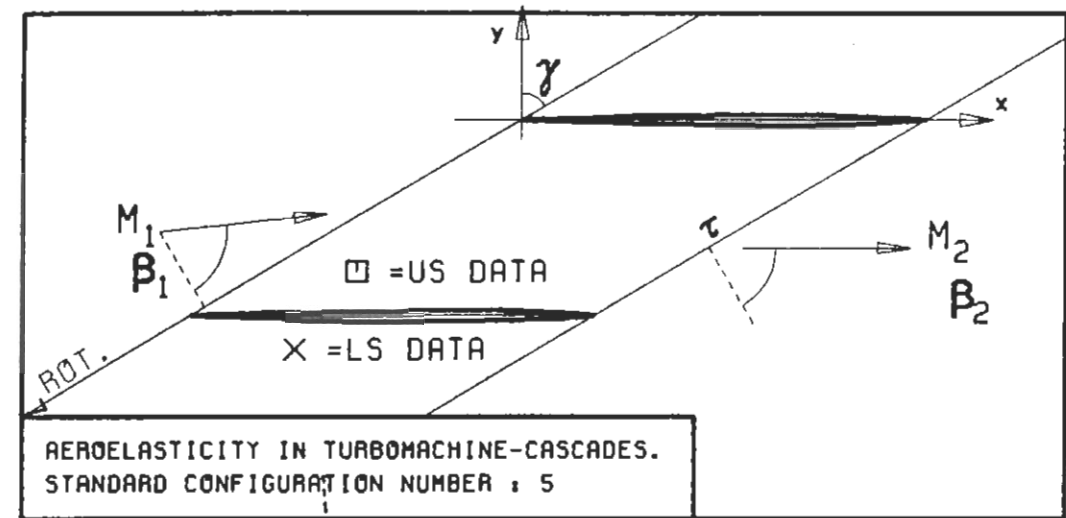
PLOT 7.5-2.8: FIFTH STANDARD CONFIGURATION, CASE 8.
MAGNITUDE AND PHASE LEAD OF BLADE SURFACE
PRESSURE COEFFICIENT.

(\times : IN PITCH MODE, NOTATION VALID UPSTREAM OF PITCH AXIS)

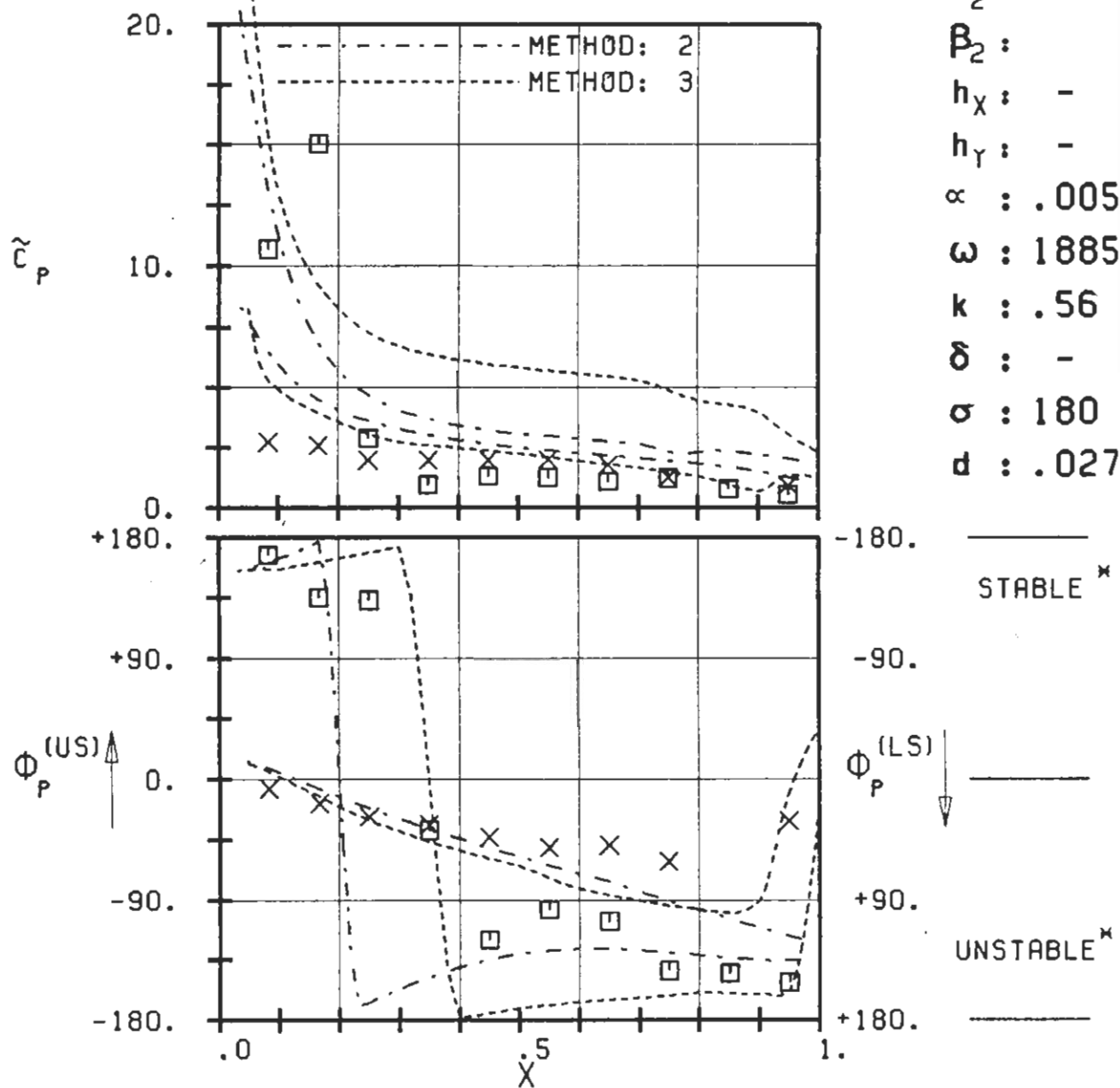


PLOT 7.5-2.9: FIFTH STANDARD CONFIGURATION, CASE 9.
MAGNITUDE AND PHASE LEAD OF BLADE SURFACE
PRESSURE COEFFICIENT.

(x: IN PITCH MODE, NOTATION VALID UPSTREAM OF PITCH AXIS)

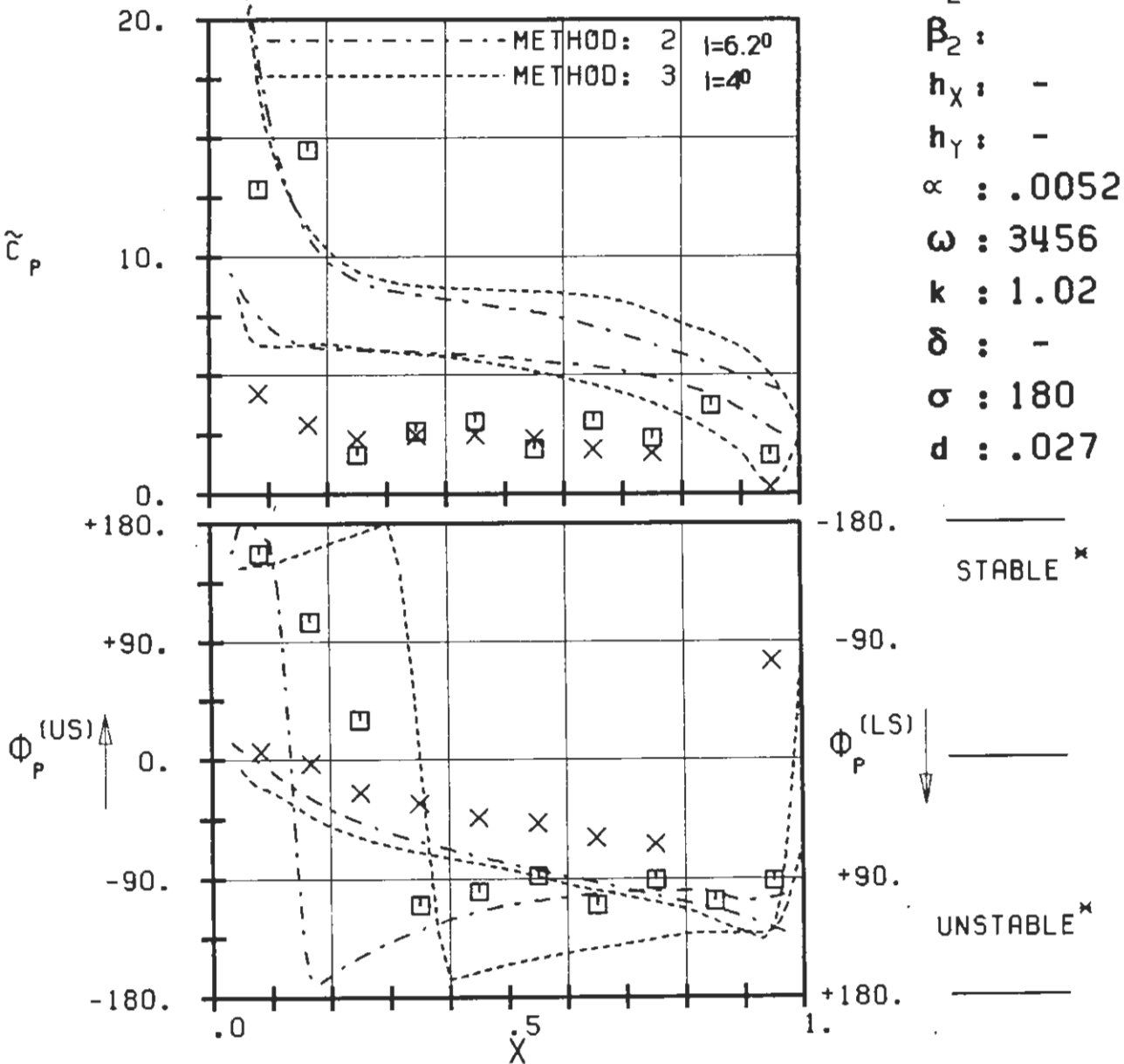
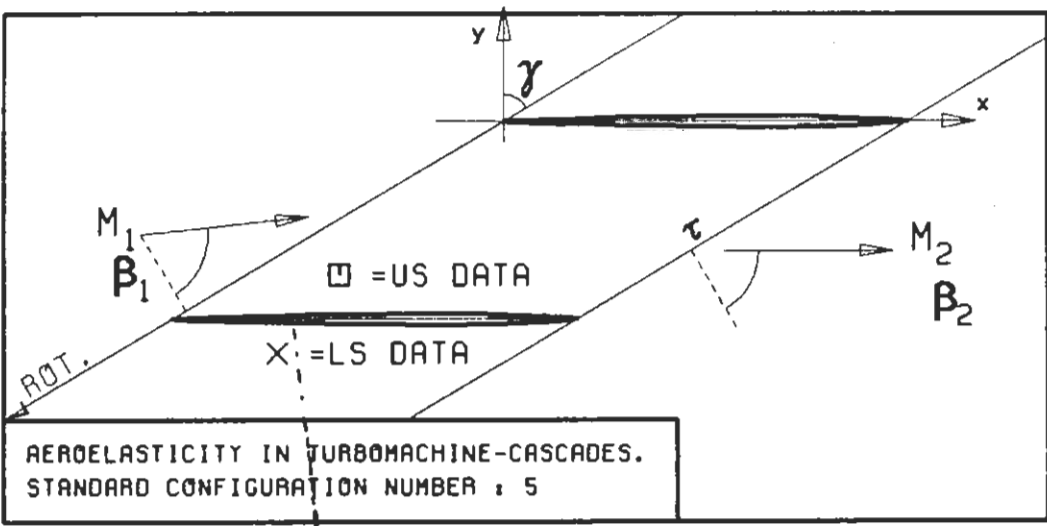


c : .090M
 τ : .95
 γ : 59.3
 x_∞ : .5
 y_∞ : 0.
 M_1 : .5
 B_1 : -65.3
 i : 6.
 M_2 : -
 B_2 :
 h_x : -
 h_y : -
 α : .0052
 ω : 1885
 k : .56
 δ : -
 σ : 180
 d : .027



PLOT 7.5-2.10: FIFTH STANDARD CONFIGURATION, CASE 10.
MAGNITUDE AND PHASE LEAD OF BLADE SURFACE
PRESSURE COEFFICIENT.

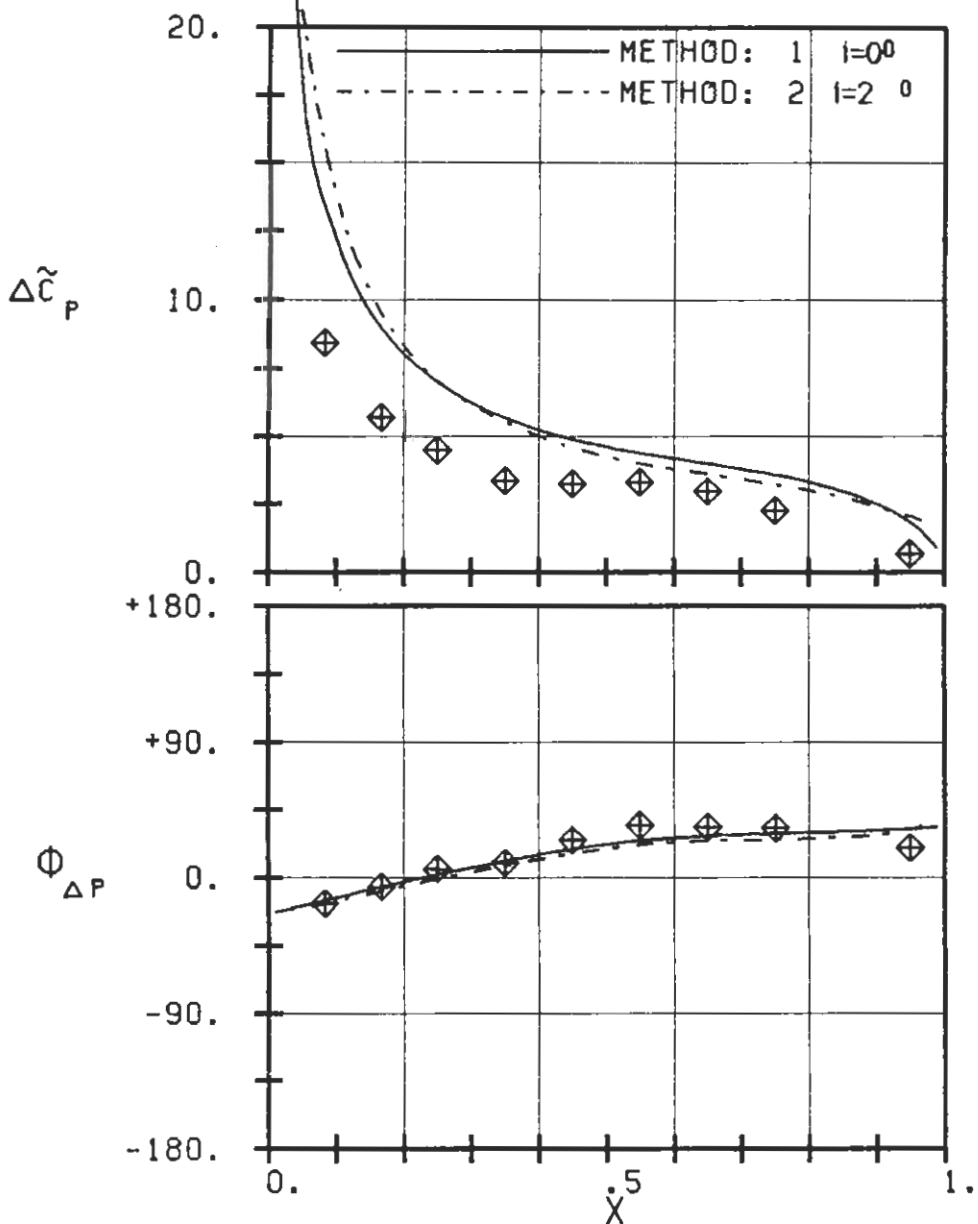
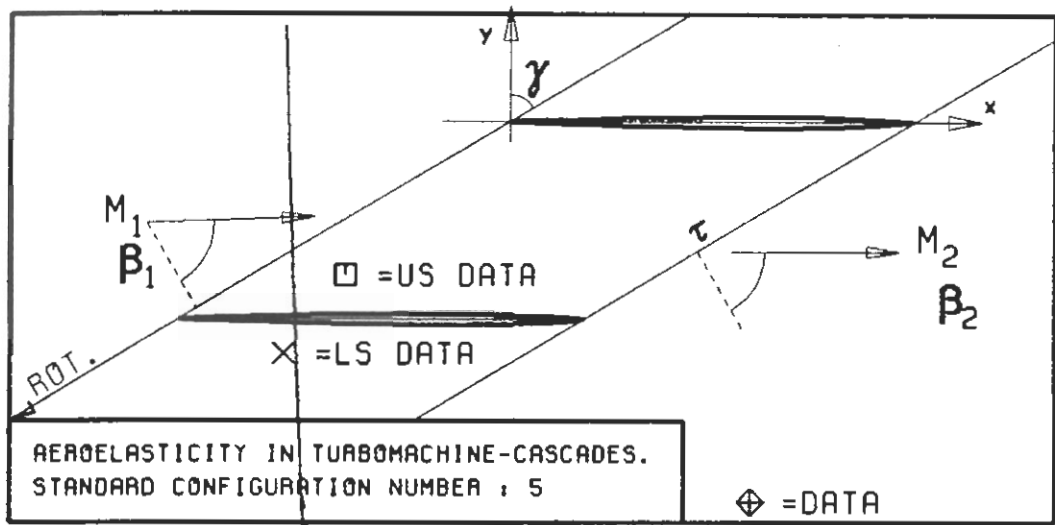
(x: IN PITCH MODE, NOTATION VALID UPSTREAM OF PITCH AXIS)



PLOT 7.5-2.11: FIFTH STANDARD CONFIGURATION, CASE 11.
MAGNITUDE AND PHASE LEAD OF BLADE SURFACE
PRESSURE COEFFICIENT.

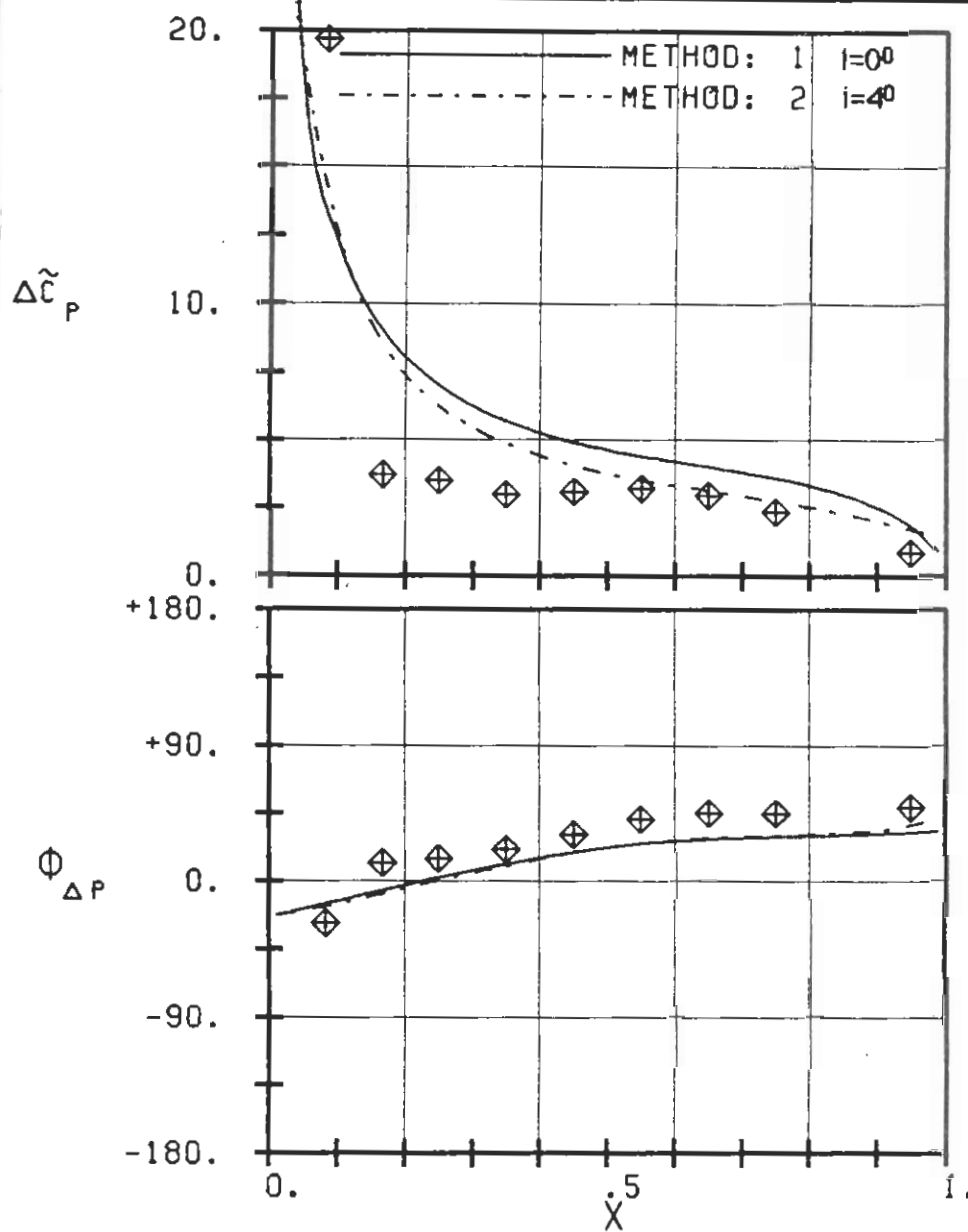
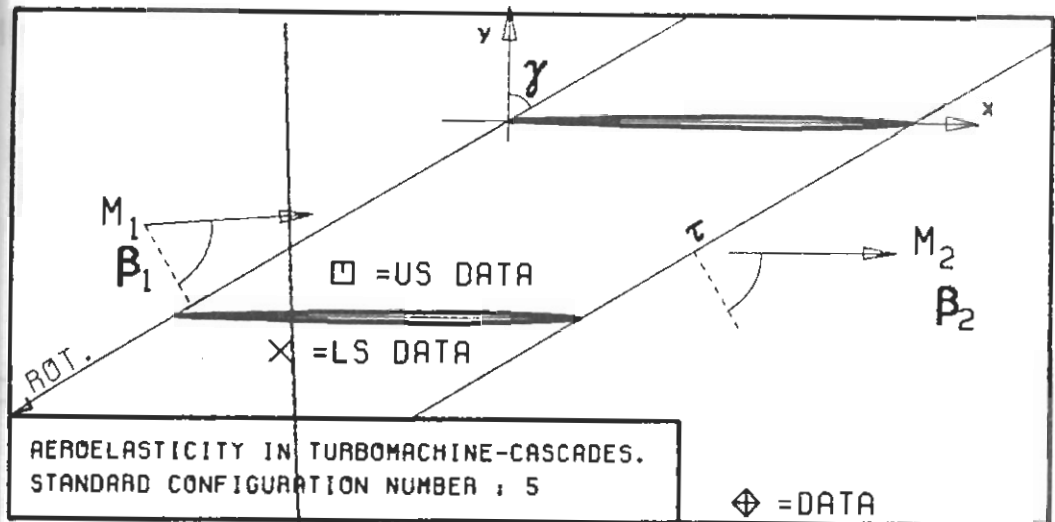
(x: IN PITCH MODE, NOTATION VALID UPSTREAM OF PITCH AXIS)

c : .090M
 τ : .95
 γ : 59.3
 x_α : .5
 y_α : 0.
 M_1 : .5
 β_1 : -65.3
i : 6.
 M_2 : -
 β_2 : -
 h_X : -
 h_Y : -
 α : .0052
 ω : 3456
 k : 1.02
 δ : -
 σ : 180
 d : .027



PLOT 7.5-3.1: FIFTH STANDARD CONFIGURATION, CASE 1.
MAGNITUDE AND PHASE LEAD OF BLADE SURFACE
PRESSURE DIFFERENCE COEFFICIENT.

(\times : IN PITCH MODE, NOTATION VALID UPSTREAM OF PITCH AXIS)



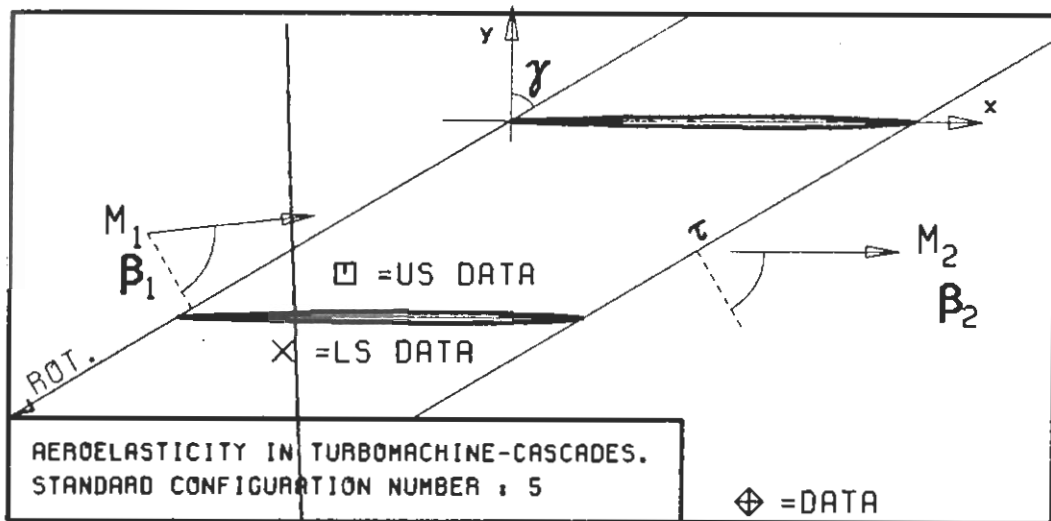
PLOT 7.5-3.2: FIFTH STANDARD CONFIGURATION, CASE 2.
MAGNITUDE AND PHASE LEAD OF BLADE SURFACE
PRESSURE DIFFERENCE COEFFICIENT.

(*: IN PITCH MODE, NOTATION VALID UPSTREAM OF PITCH AXIS)

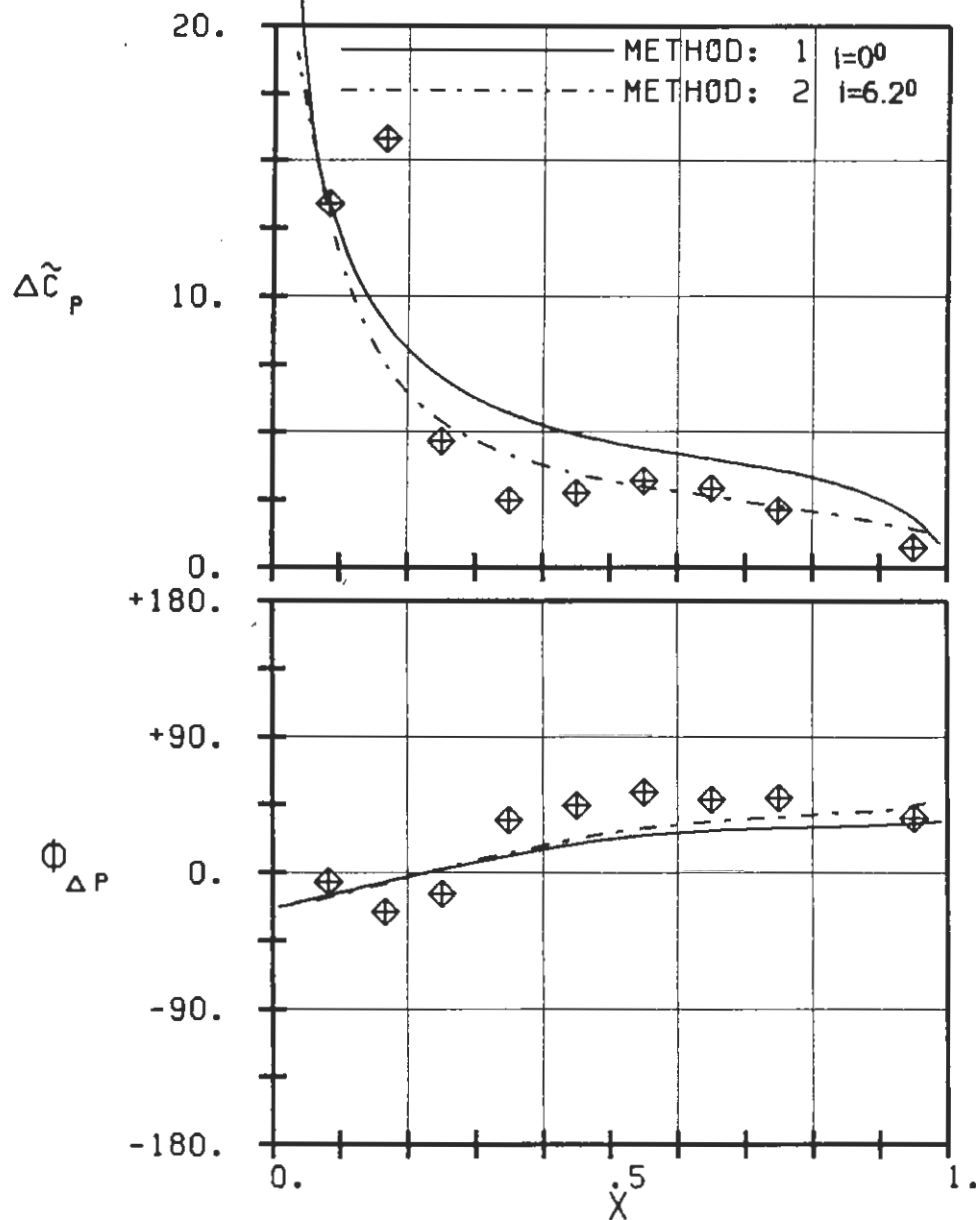
c : .090M
 τ : .95
 γ : 59.3
 x_α : .5
 y_α : 0.
 M_1 : .5
 B_1 : -63.3
 i : 4.
 M_2 : -
 B_2 : -
 h_x : -
 h_y : -
 α : .0052
 ω : 1257
 k : .37
 δ : -
 σ : 180
 d : .027

UNSTABLE*

STABLE *

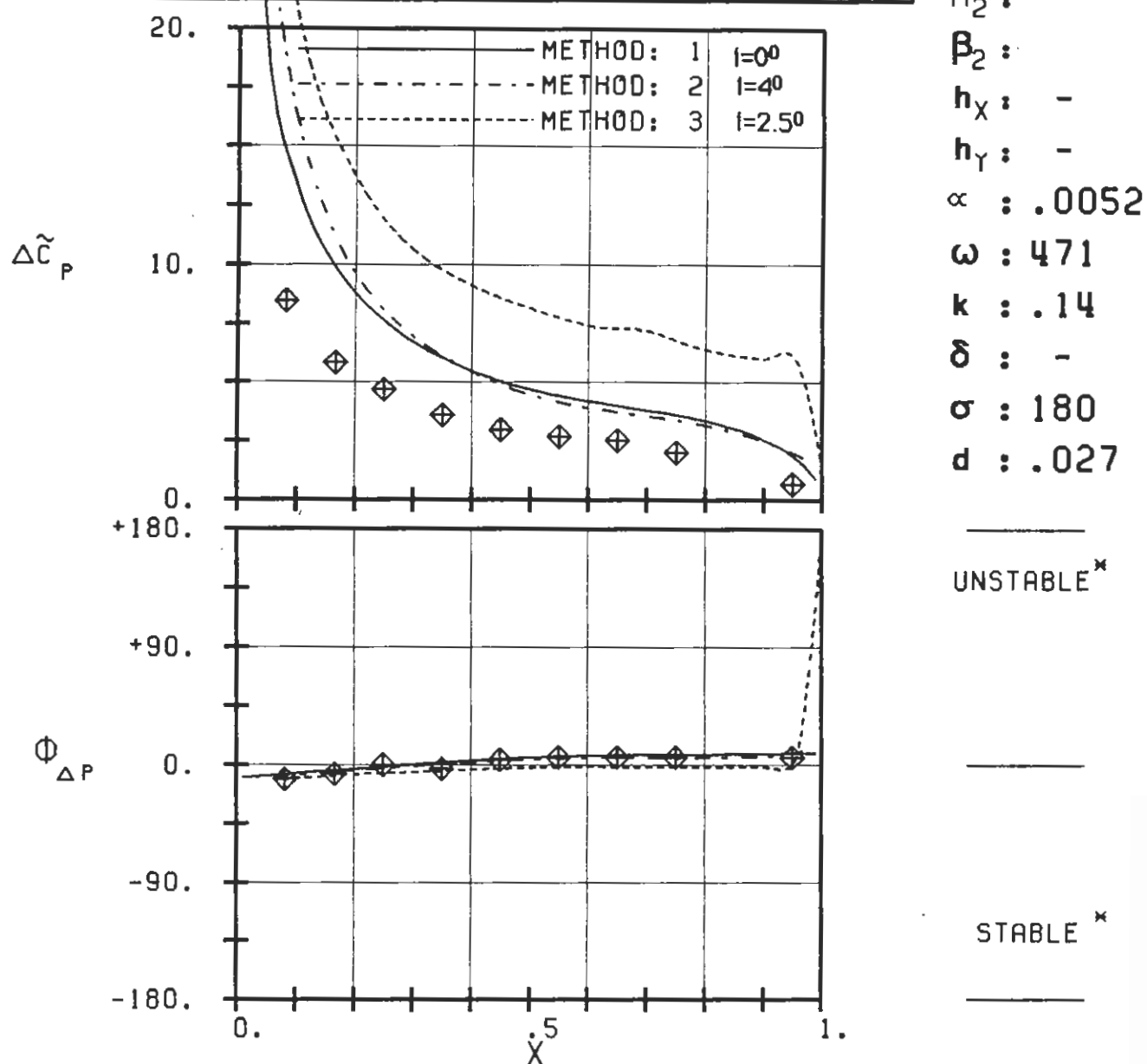
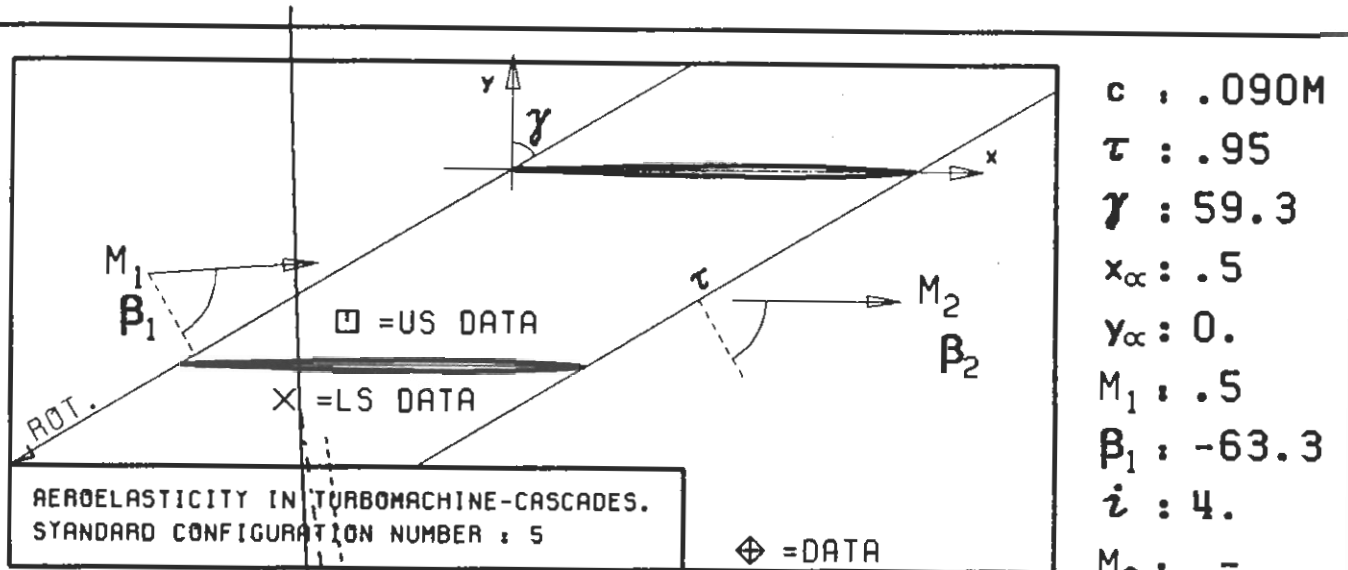


c : .090M
 τ : .95
 γ : 59.3
 x_∞ : .5
 y_∞ : 0.
 M_1 : .5
 β_1 : -65.3
 i : 6.
 M_2 : -
 β_2 : -
 h_x : -
 h_y : -
 α : .0052
 ω : 1257
 k : .37
 δ : -
 σ : 180
 d : .027



PLOT 7.5-3.3: FIFTH STANDARD CONFIGURATION, CASE 3.
MAGNITUDE AND PHASE LEAD OF BLADE SURFACE
PRESSURE DIFFERENCE COEFFICIENT.

(\times : IN PITCH MODE, NOTATION VALID UPSTREAM OF PITCH AXIS)



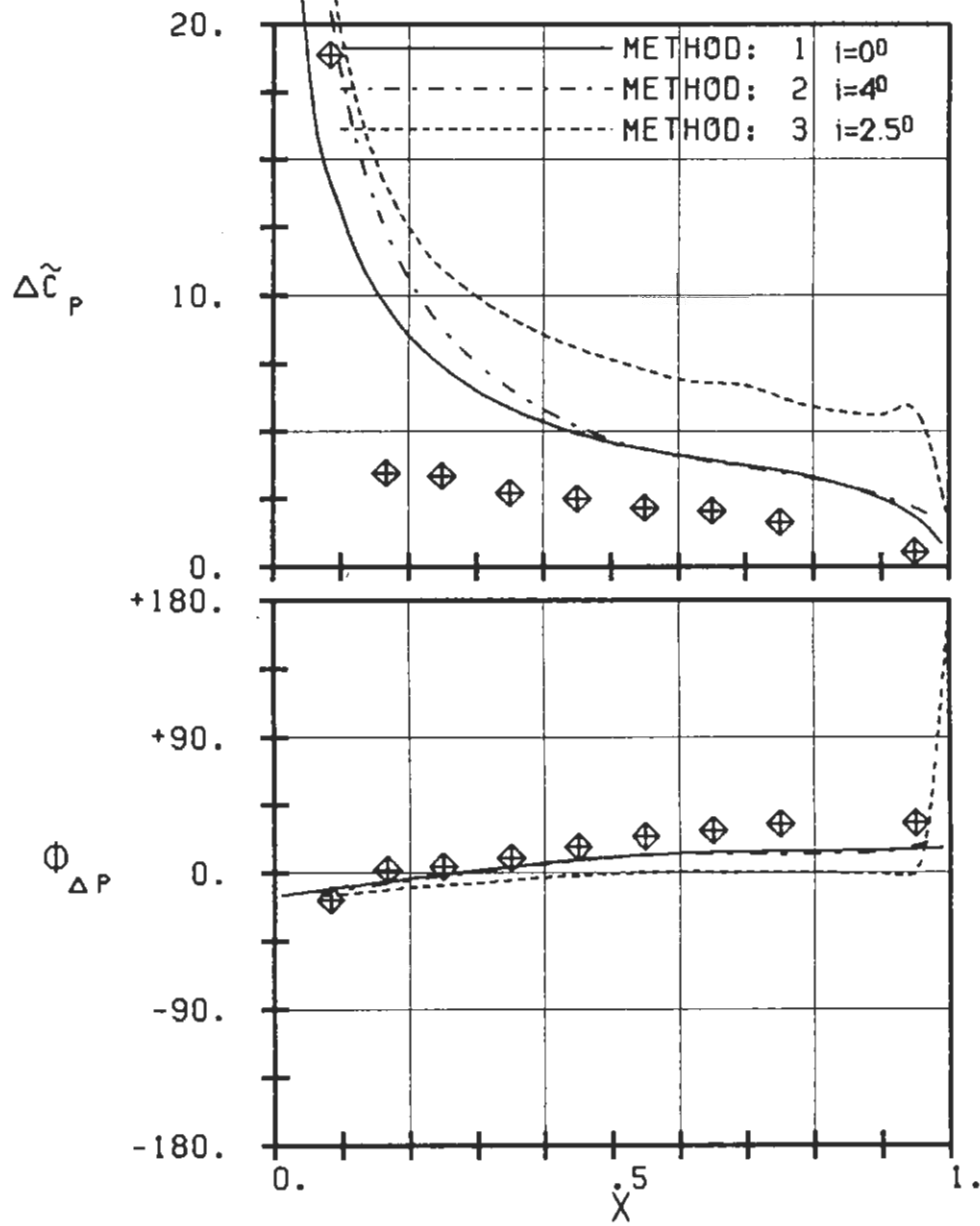
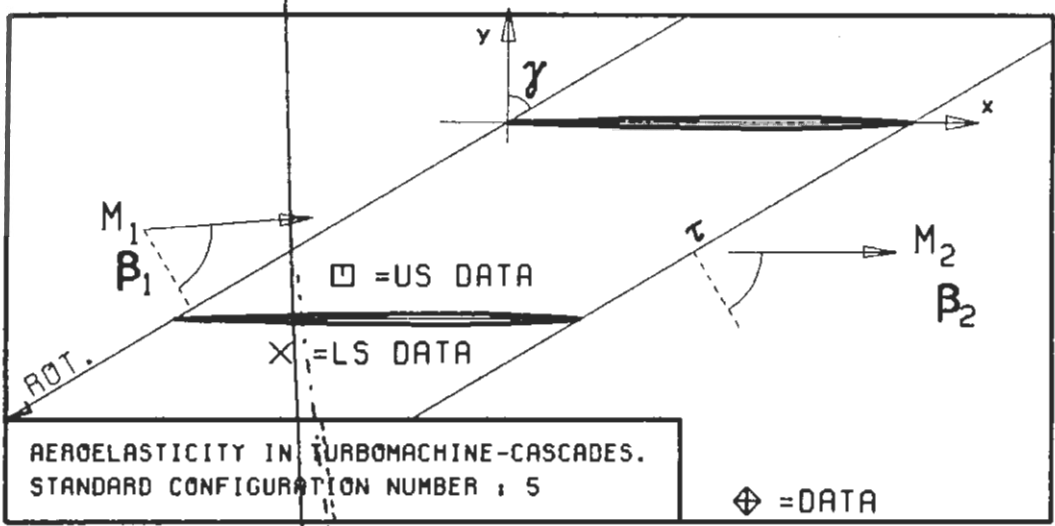
PLOT 7.5-3.4: FIFTH STANDARD CONFIGURATION, CASE 4.
 MAGNITUDE AND PHASE LEAD OF BLADE SURFACE
 PRESSURE DIFFERENCE COEFFICIENT.

(*: IN PITCH MODE, NOTATION VALID UPSTREAM OF PITCH AXIS)

$c : .090M$
 $\tau : .95$
 $\gamma : 59.3$
 $x_\infty : .5$
 $y_\infty : 0.$
 $M_1 : .5$
 $\beta_1 : -63.3$
 $i : 4.$
 $M_2 : -$
 $\beta_2 : -$
 $h_x : -$
 $h_y : -$
 $\alpha : .0052$
 $\omega : 471$
 $k : .14$
 $\delta : -$
 $\sigma : 180$
 $d : .027$

UNSTABLE *

STABLE *



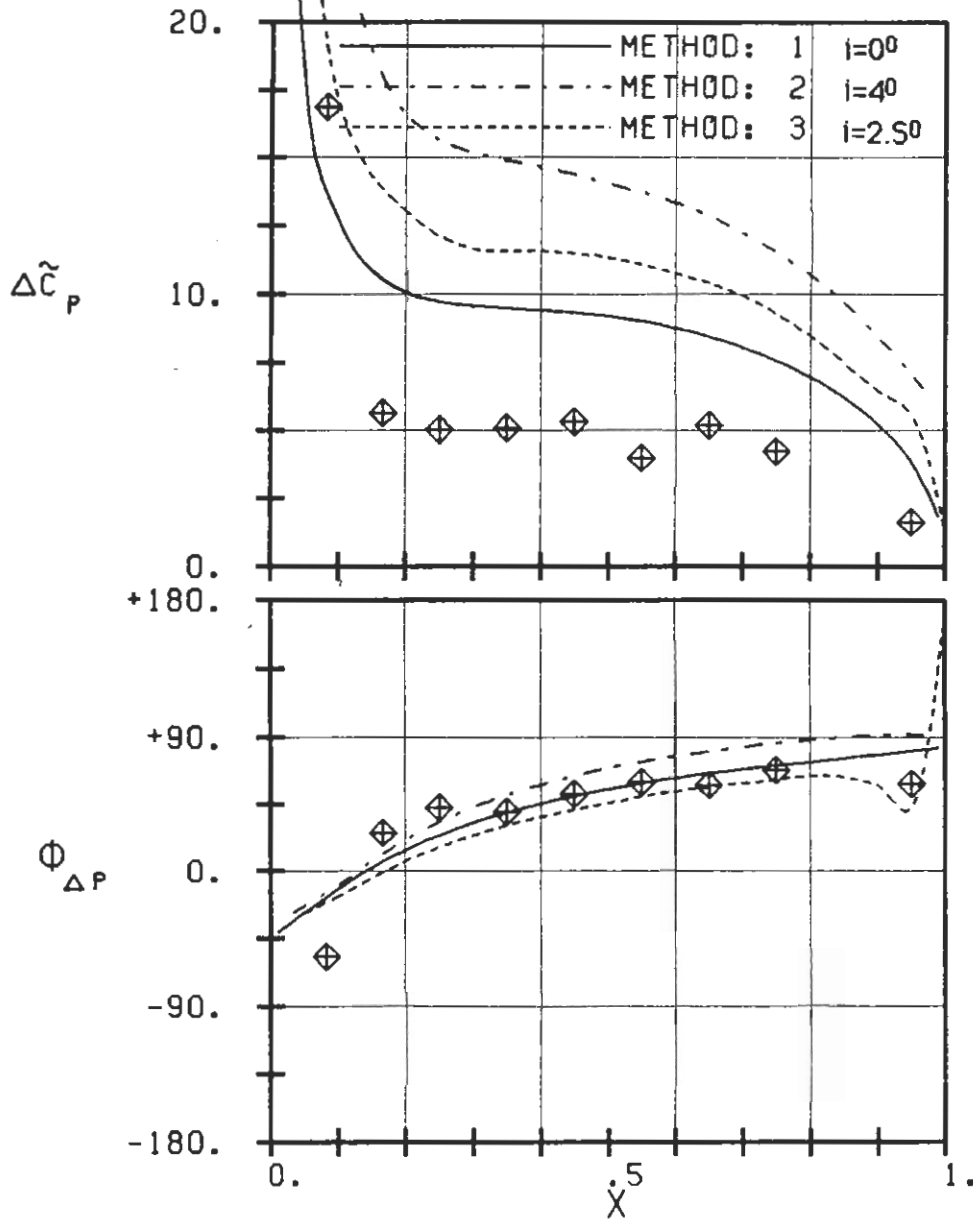
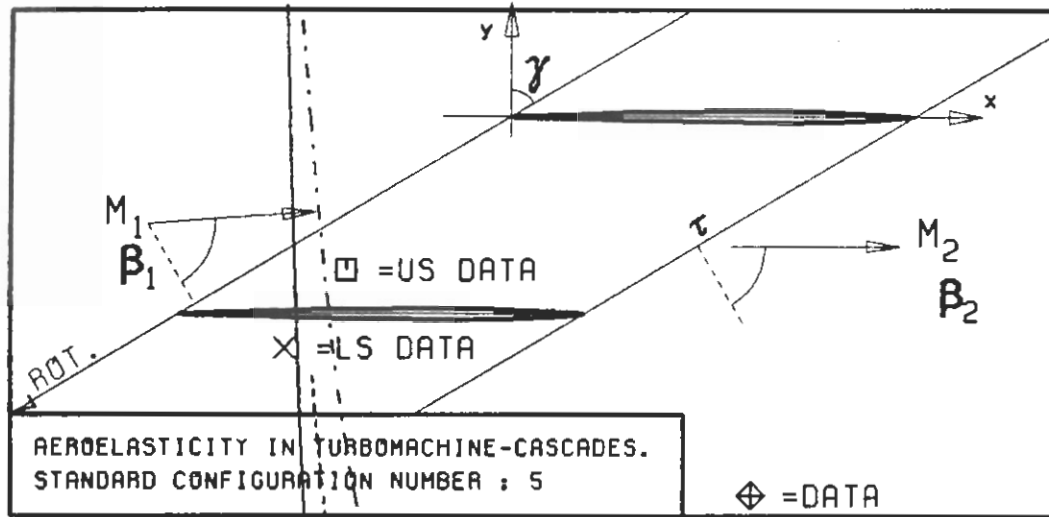
PLOT 7.5-3.5: FIFTH STANDARD CONFIGURATION, CASE 5.
MAGNITUDE AND PHASE LEAD OF BLADE SURFACE
PRESSURE DIFFERENCE COEFFICIENT.

(*: IN PITCH MODE, NOTATION VALID UPSTREAM OF PITCH AXIS)

$c : .090M$
 $\tau : .95$
 $\gamma : 59.3$
 $x_\alpha : .5$
 $y_\alpha : 0.$
 $M_1 : .5$
 $\beta_1 : -63.3$
 $i : 4.$
 $M_2 : -$
 $\beta_2 : -$
 $h_X : -$
 $h_Y : -$
 $\alpha : .0052$
 $\omega : 785$
 $k : .22$
 $\delta : -$
 $\sigma : 180$
 $d : .027$

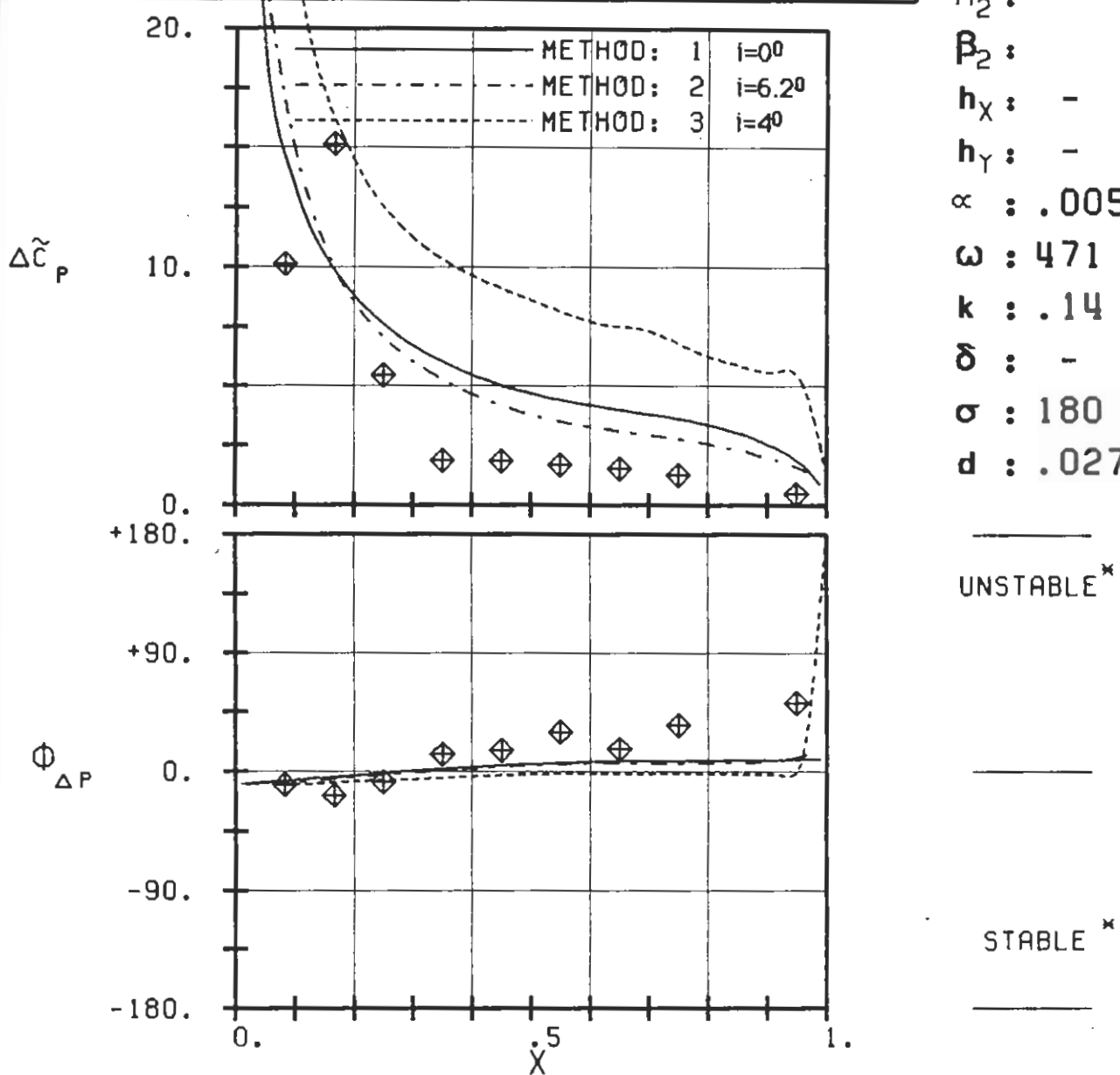
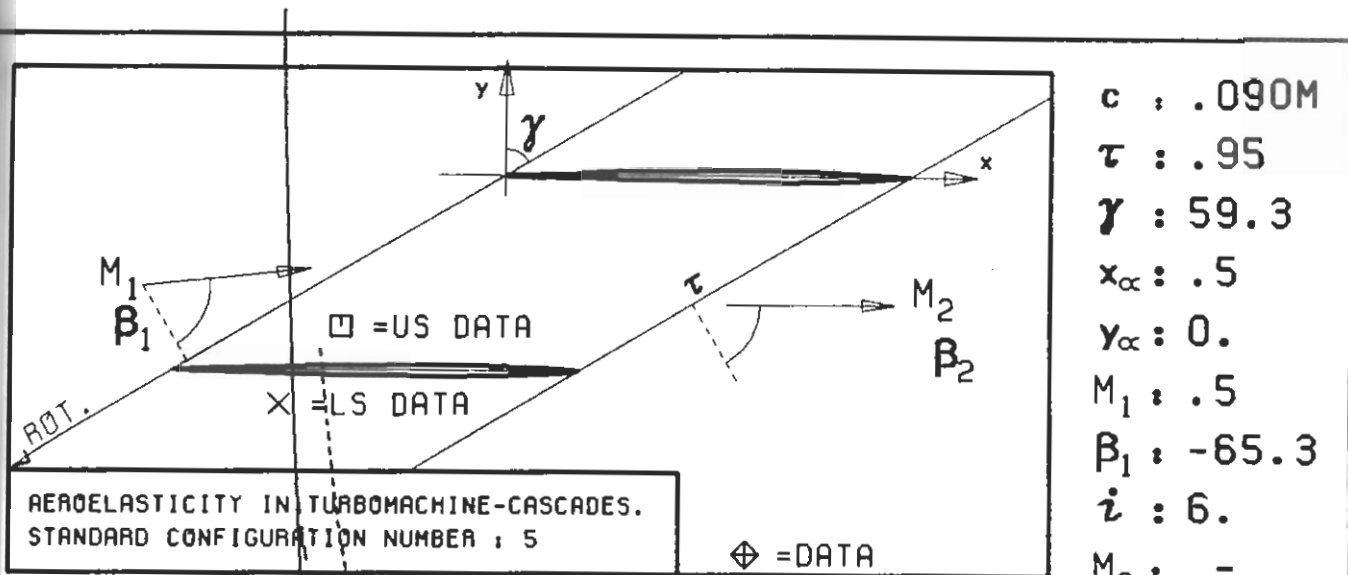
UNSTABLE *

STABLE *



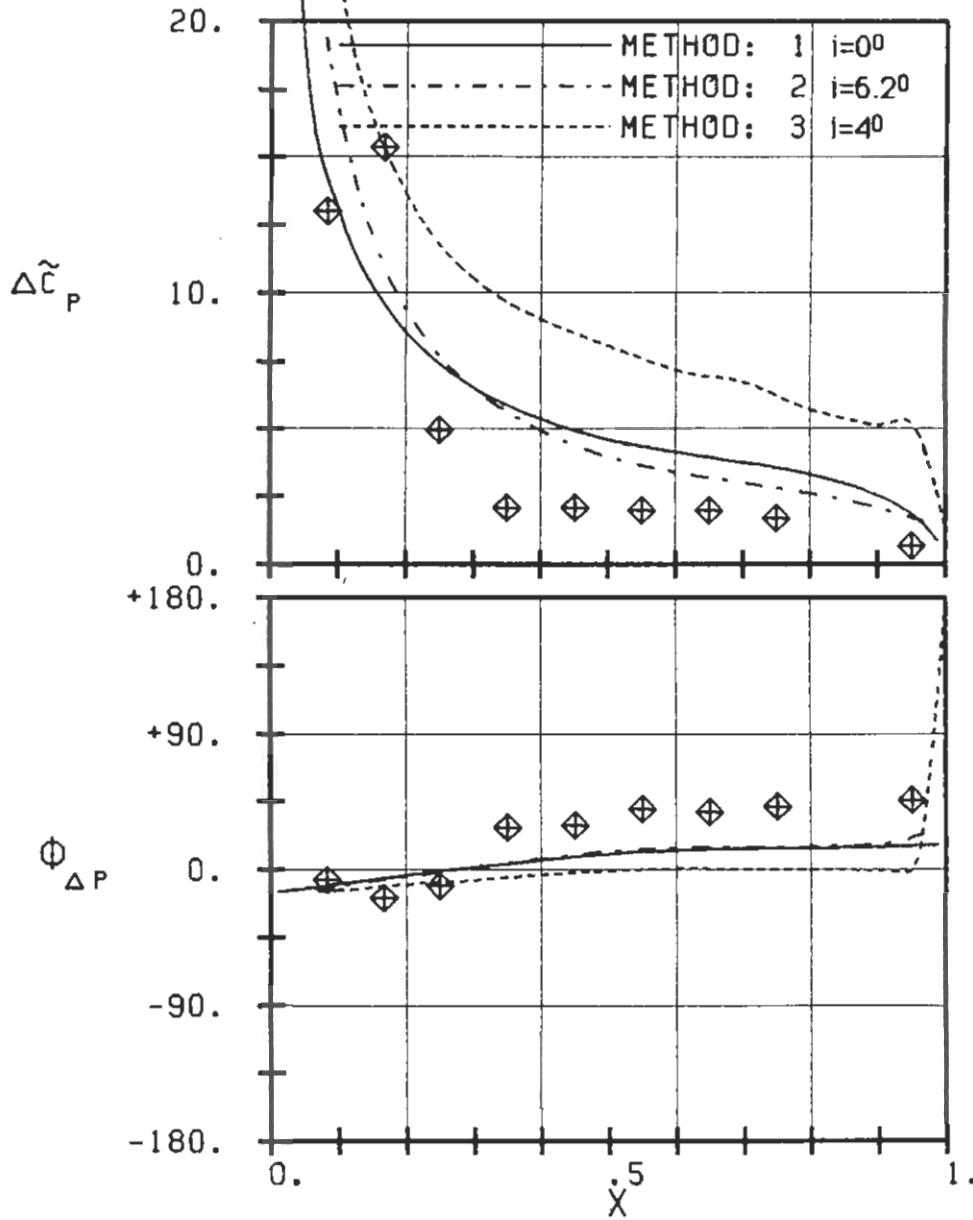
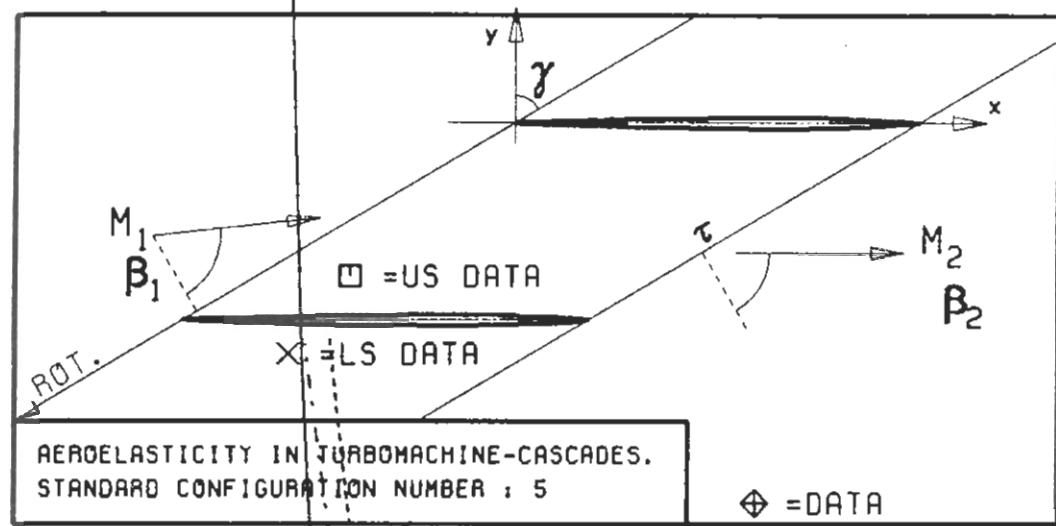
PLOT 7.5-3.7: FIFTH STANDARD CONFIGURATION, CASE 7.
MAGNITUDE AND PHASE LEAD OF BLADE SURFACE
PRESSURE DIFFERENCE COEFFICIENT.

(*: IN PITCH MODE, NOTATION VALID UPSTREAM OF PITCH AXIS)



PLOT 7.5-3.8: FIFTH STANDARD CONFIGURATION, CASE 8.
MAGNITUDE AND PHASE LEAD OF BLADE SURFACE
PRESSURE DIFFERENCE COEFFICIENT.

(*: IN PITCH MODE, NOTATION VALID UPSTREAM OF PITCH AXIS)



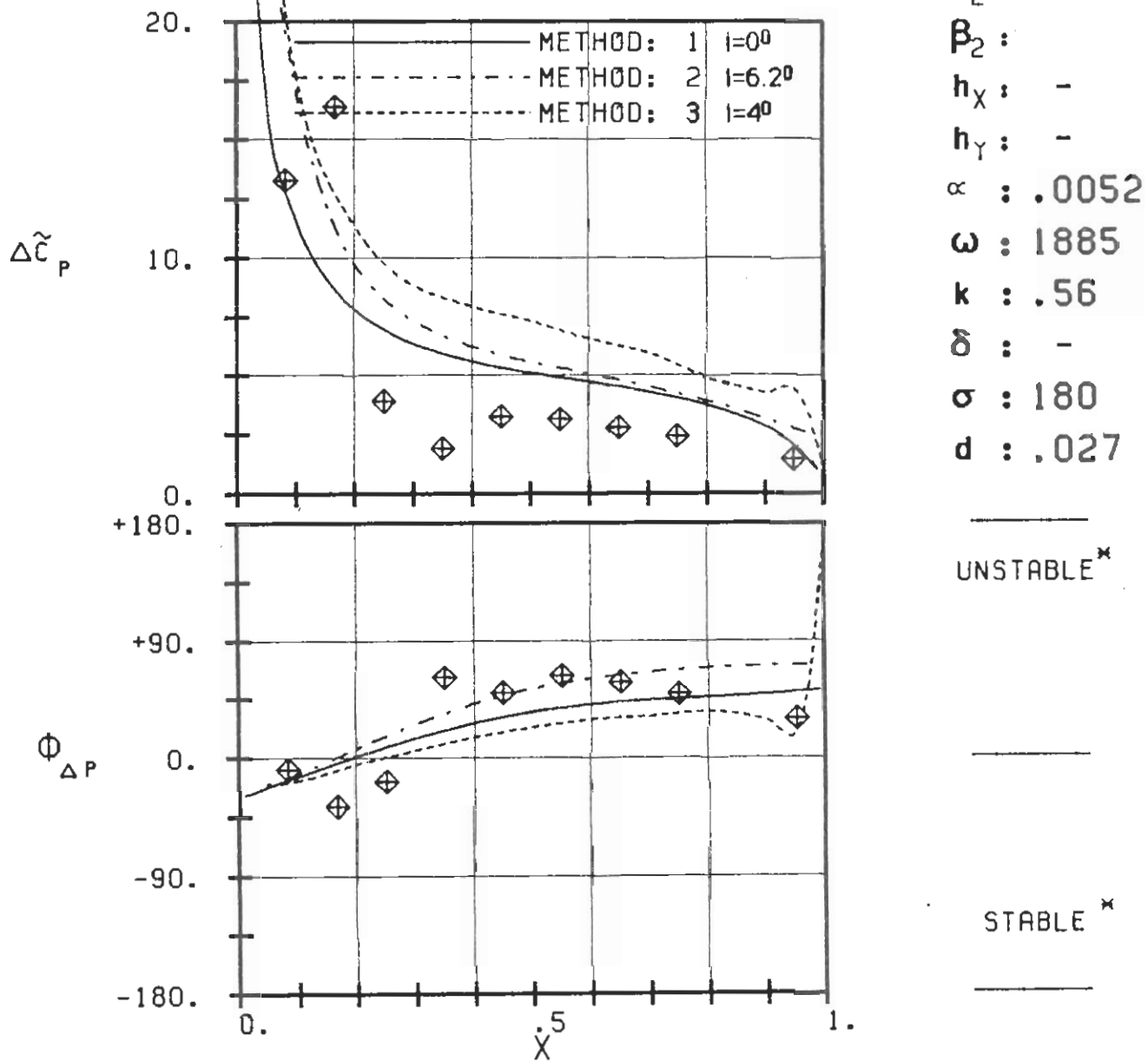
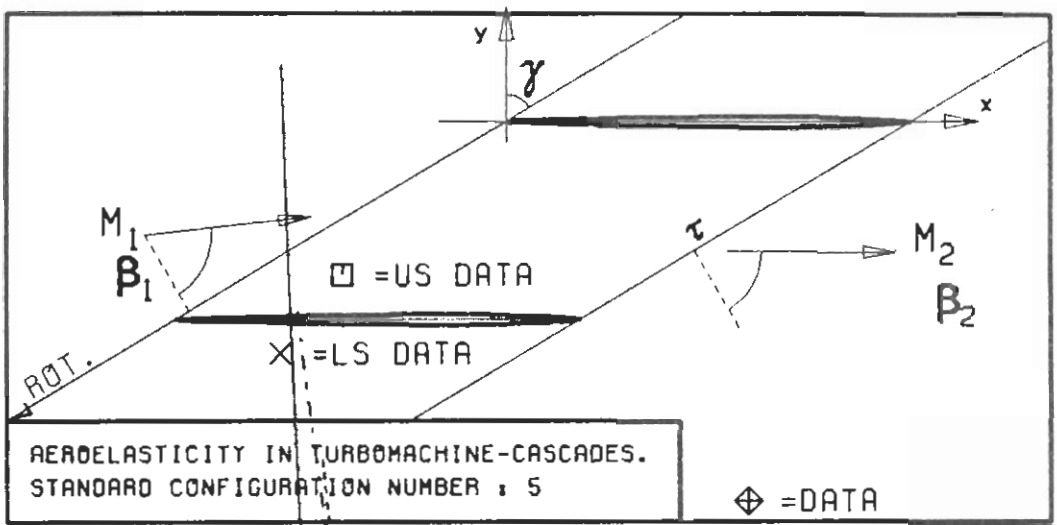
PLOT 7.5-3.9: FIFTH STANDARD CONFIGURATION, CASE 9.
MAGNITUDE AND PHASE LEAD OF BLADE SURFACE
PRESSURE DIFFERENCE COEFFICIENT.

(\times : IN PITCH MODE, NOTATION VALID UPSTREAM OF PITCH AXIS)

c : .090M
 τ : .95
 γ : 59.3
 x_∞ : .5
 y_∞ : 0.
 M_1 : .5
 β_1 : -65.3
 i : 6.
 M_2 : -
 β_2 :
 h_x : -
 h_y : -
 α : .0052
 ω : 785
 k : .22
 δ : -
 σ : 180
 d : .027

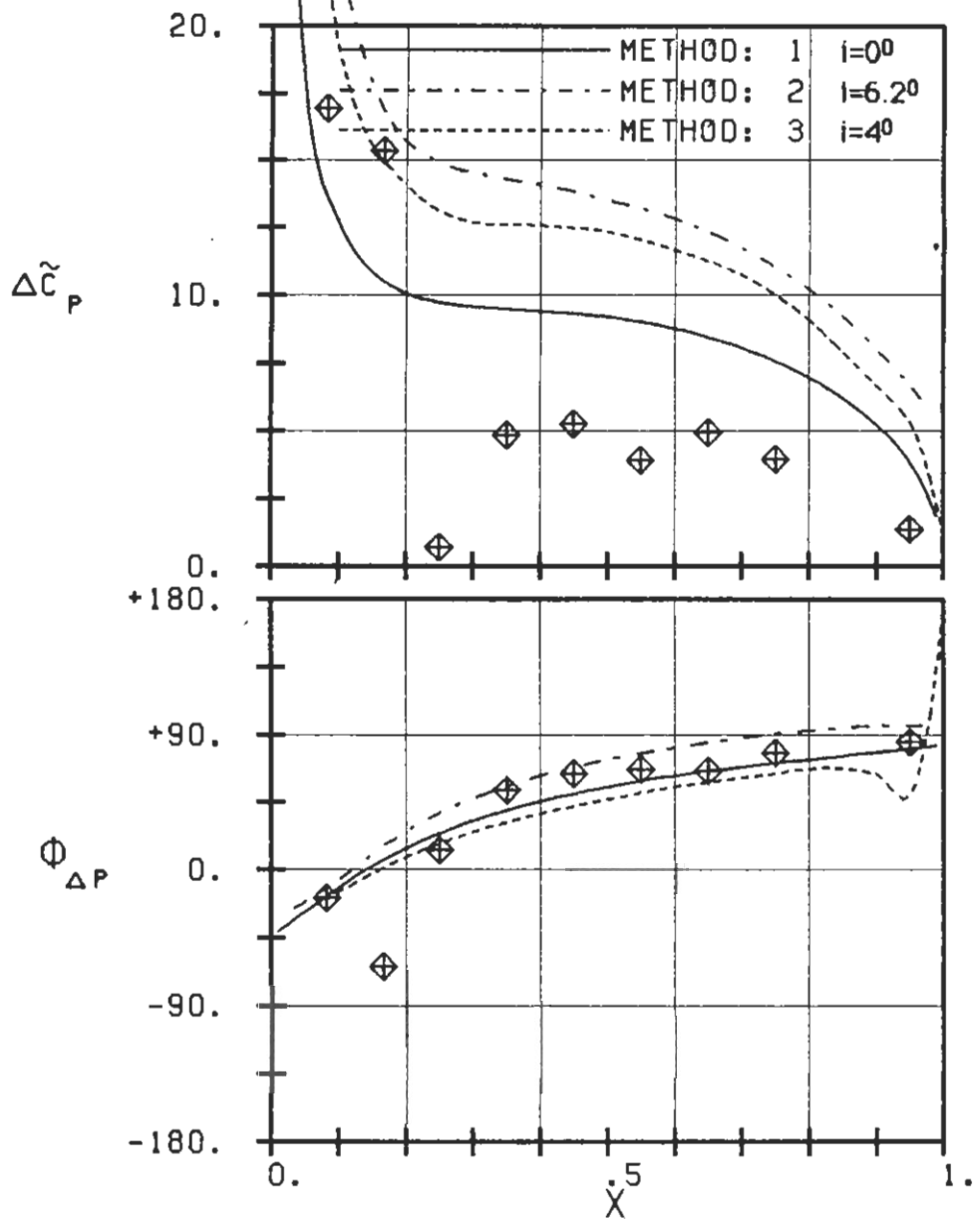
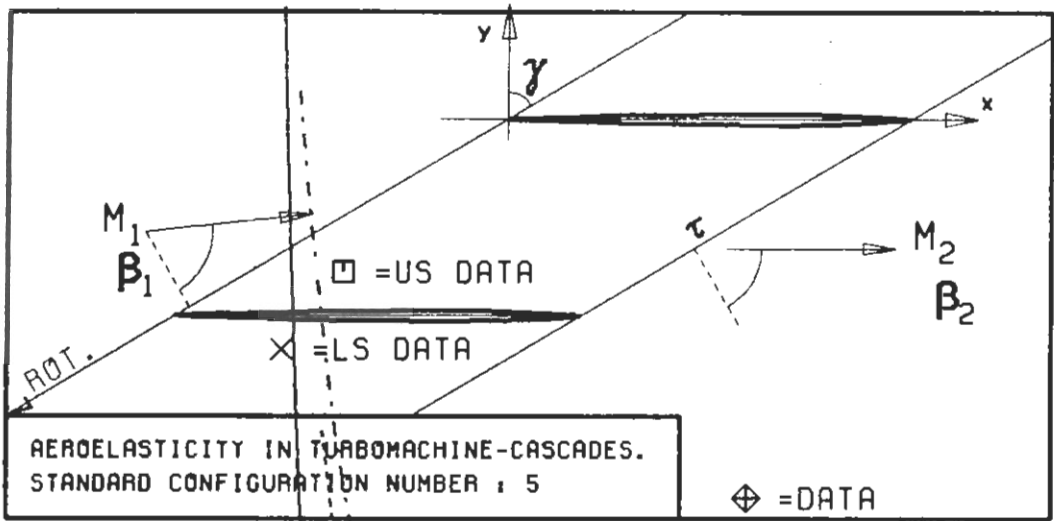
UNSTABLE \times

STABLE \times



PLOT 7.5-3.10: FIFTH STANDARD CONFIGURATION, CASE 10.
MAGNITUDE AND PHASE LEAD OF BLADE SURFACE
PRESSURE DIFFERENCE COEFFICIENT.

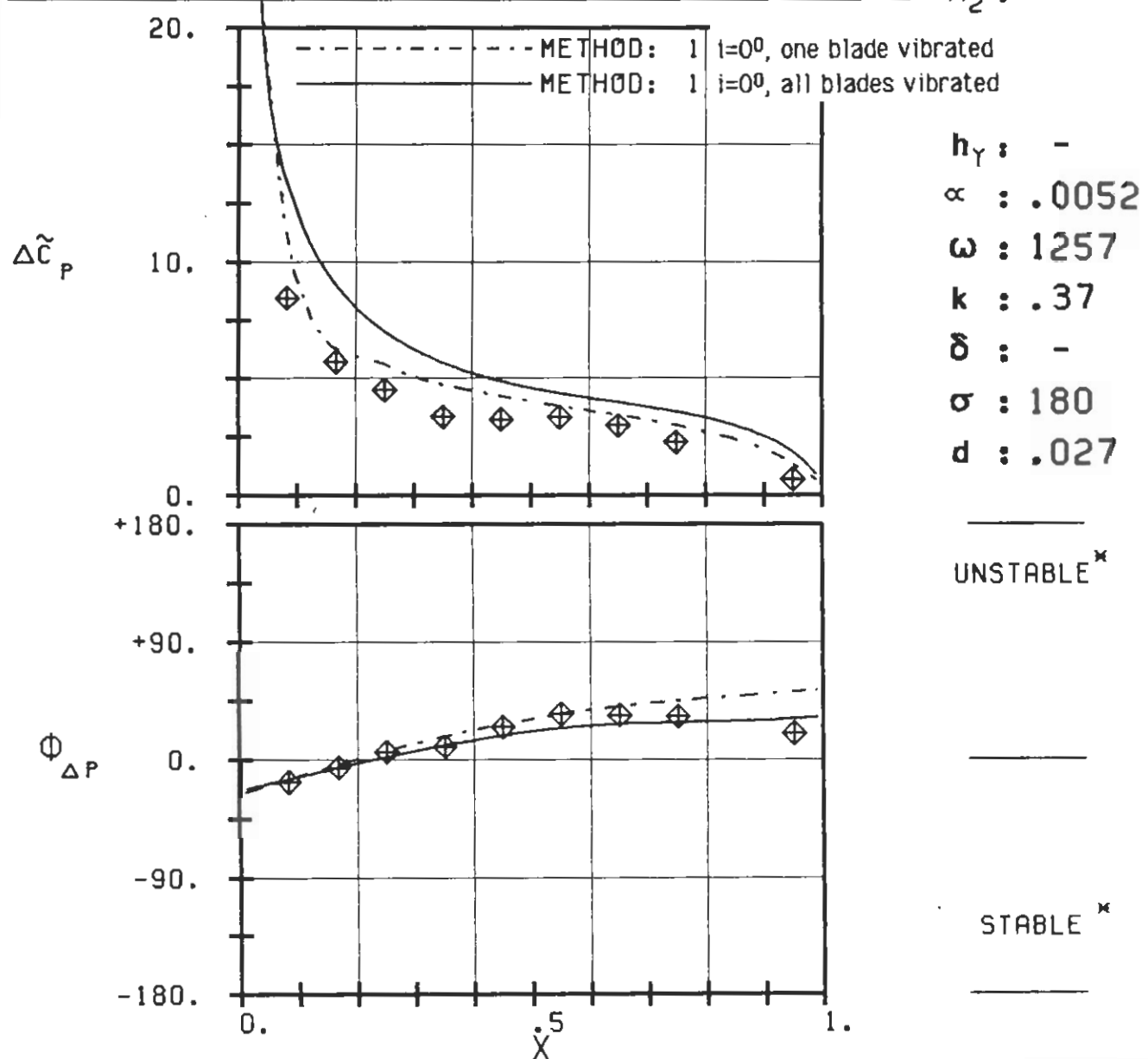
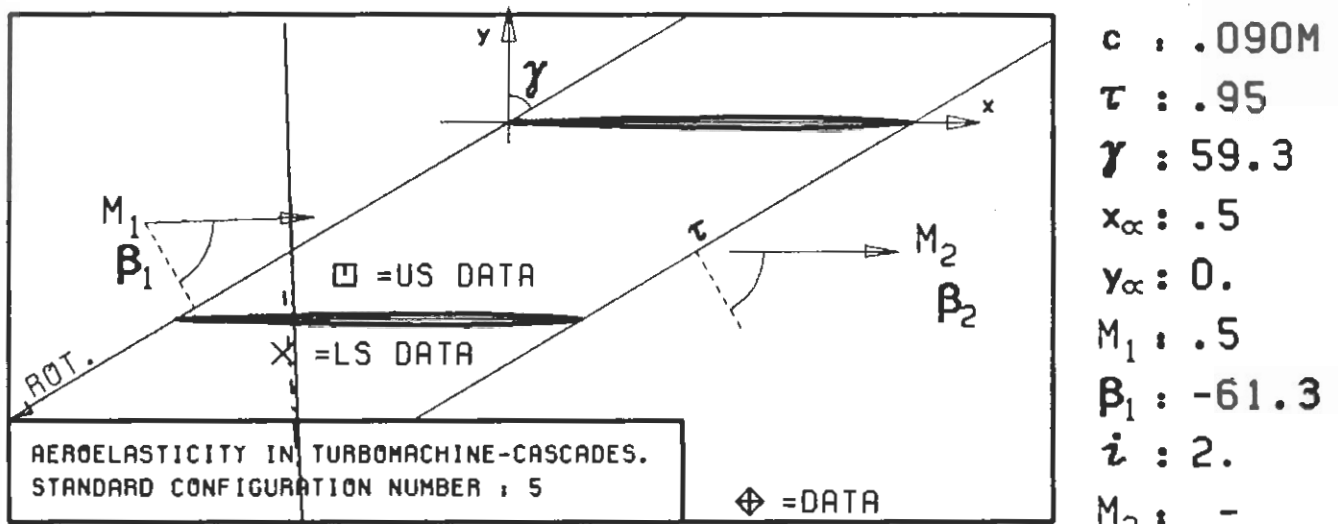
(*: IN PITCH MODE, NOTATION VALID UPSTREAM OF PITCH AXIS)



PLOT 7.5-3.11: FIFTH STANDARD CONFIGURATION, CASE II.
MAGNITUDE AND PHASE LEAD OF BLADE SURFACE
PRESSURE DIFFERENCE COEFFICIENT.

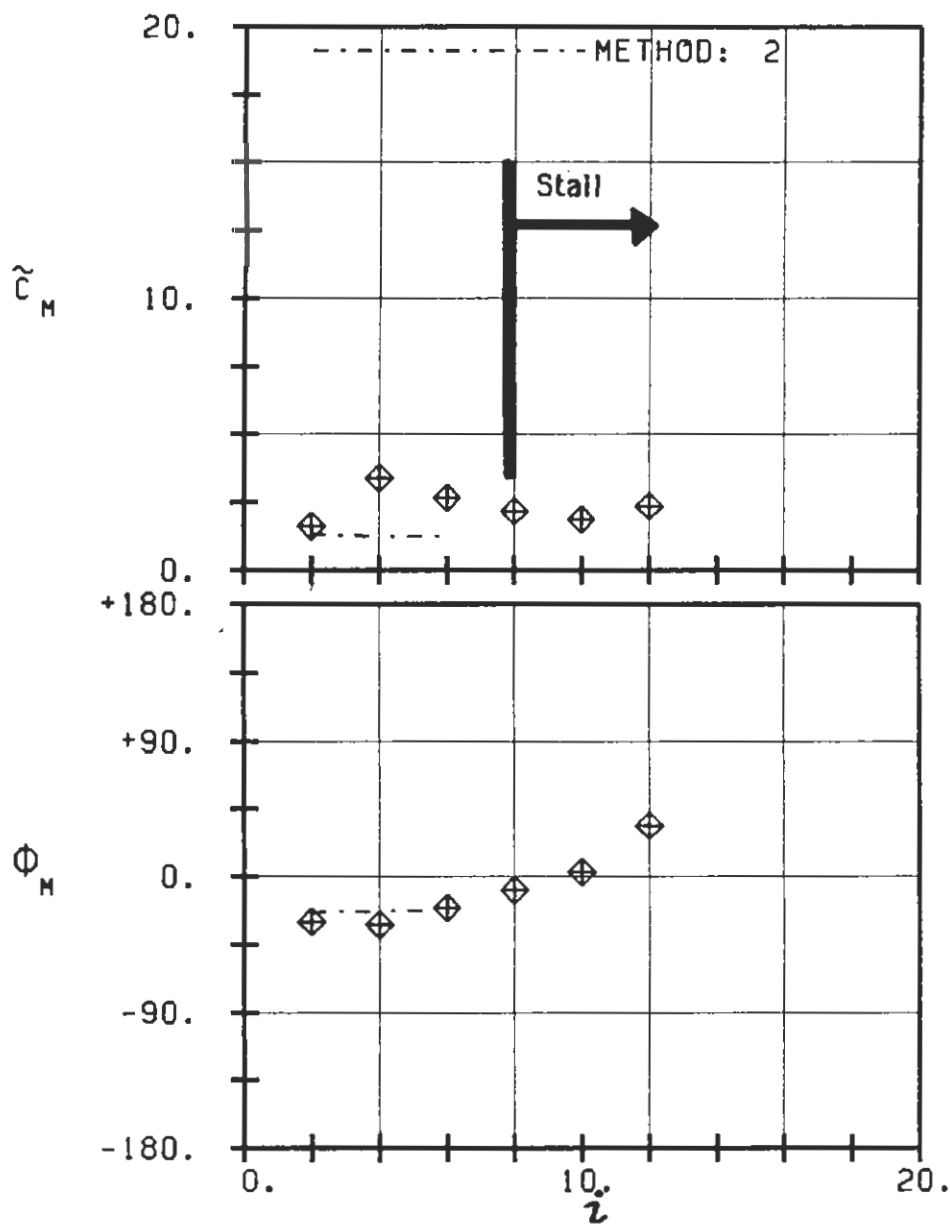
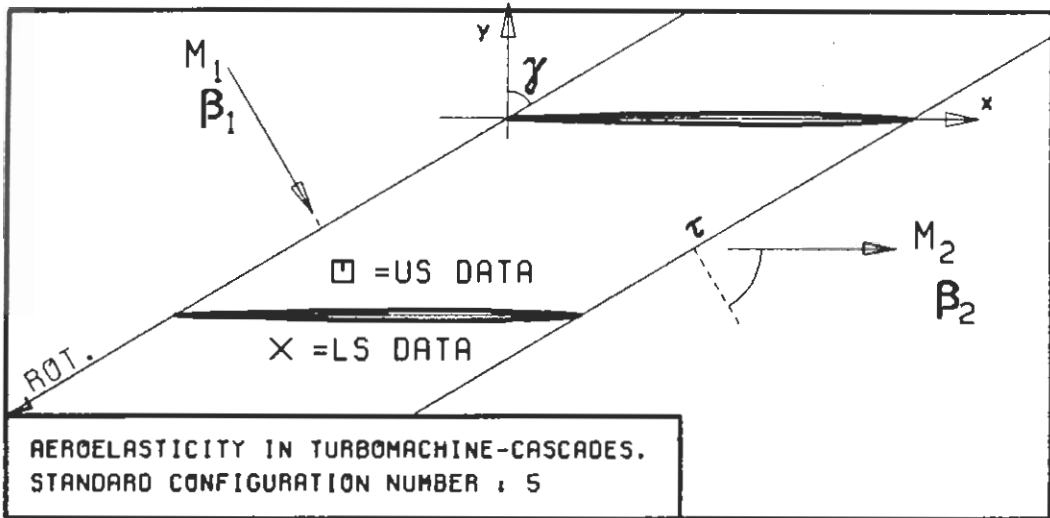
(*: IN PITCH MODE, NOTATION VALID UPSTREAM OF PITCH AXIS)

c : .090M
 τ : .95
 γ : 59.3
 x_∞ : .5
 y_∞ : 0.
 M_1 : .5
 β_1 : -65.3
i : 6.
 M_2 : -
 β_2 : -
 h_X : -
 h_Y : -
 α : .0052
 ω : 3456
 k : 1.02
 δ : -
 σ : 180
 d : .027

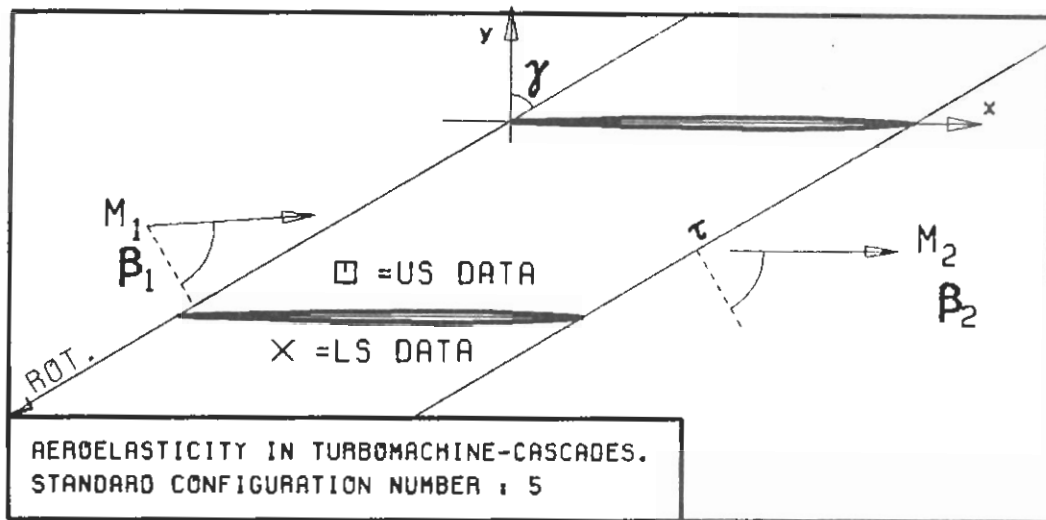


PLOT 7.5-3.12: FIFTH STANDARD CONFIGURATION, CASE 1.
INFLUENCE OF AERODYNAMIC COUPLING ON BLADE
SURFACE PRESSURE DIFFERENCE COEFFICIENT.

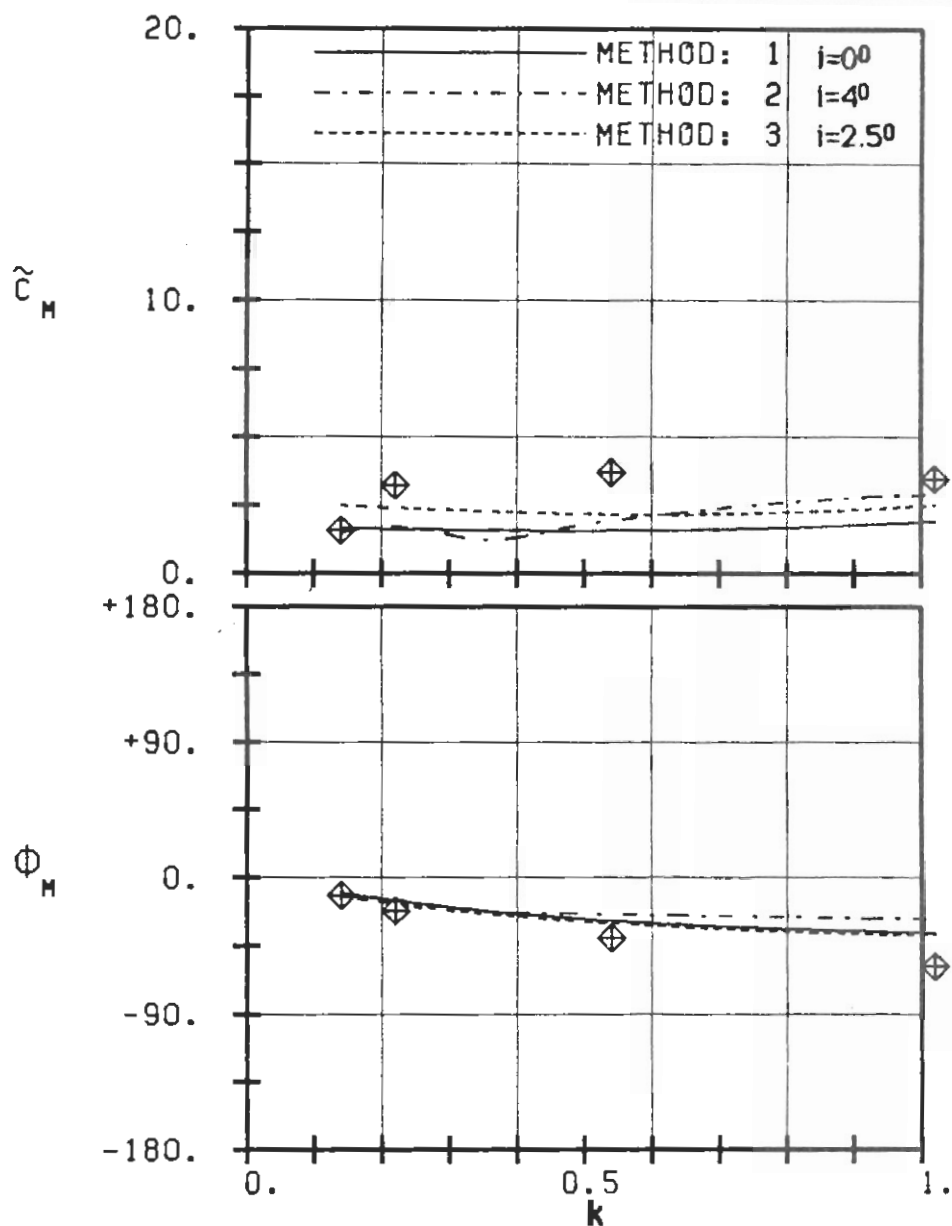
(\times : IN PITCH MODE, NOTATION VALID UPSTREAM OF PITCH AXIS)



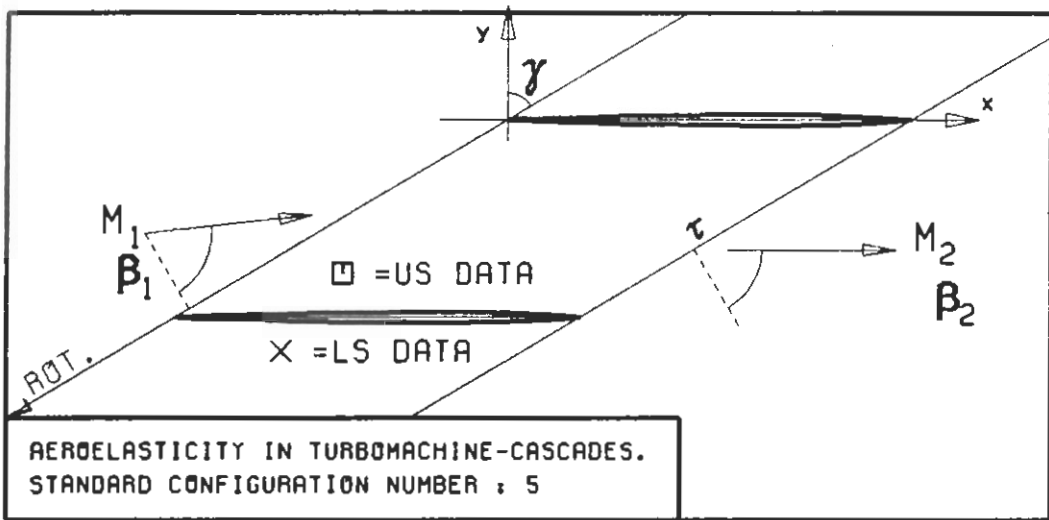
PLOT 7.5-5.1: FIFTH STANDARD CONFIGURATION, CASES 1-3+EXTRA.
AERODYNAMIC MOMENT COEFFICIENT AND PHASE LEAD
IN DEPENDANCE OF INCIDENCE ANGLE.



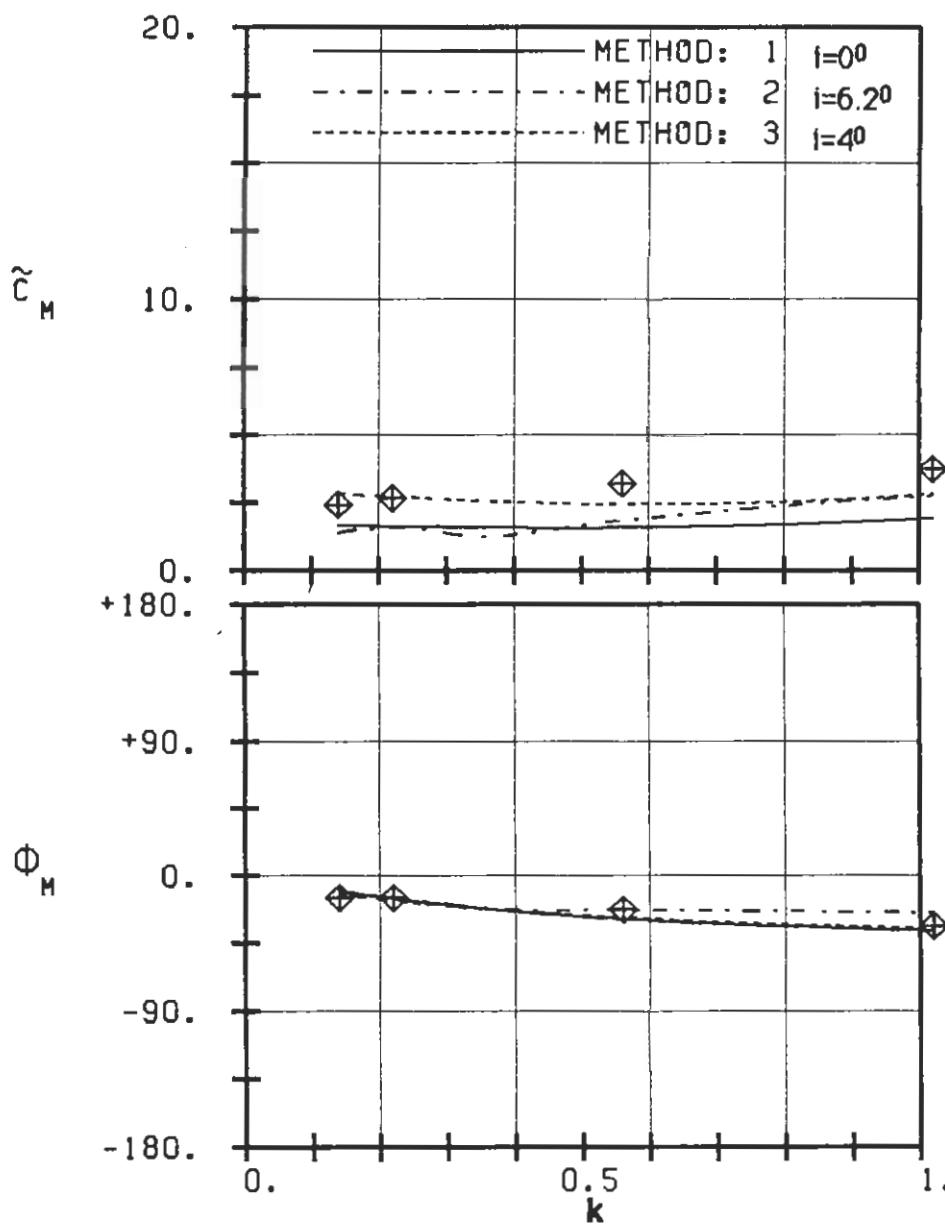
$c : .090M$
 $\tau : .95$
 $\gamma : 59.3$
 $x_\infty : .5$
 $y_\infty : 0.$
 $M_1 : 0.5$
 $\beta_1 : -63.3$
 $i : 4.$
 $M_2 : -$
 $\beta_2 : -$
 $h_x : -$
 $h_y : -$
 $\alpha : .0052$
 $\omega : -$
 $k : -$
 $\delta : -$
 $\sigma : 180$
 $d : .027$



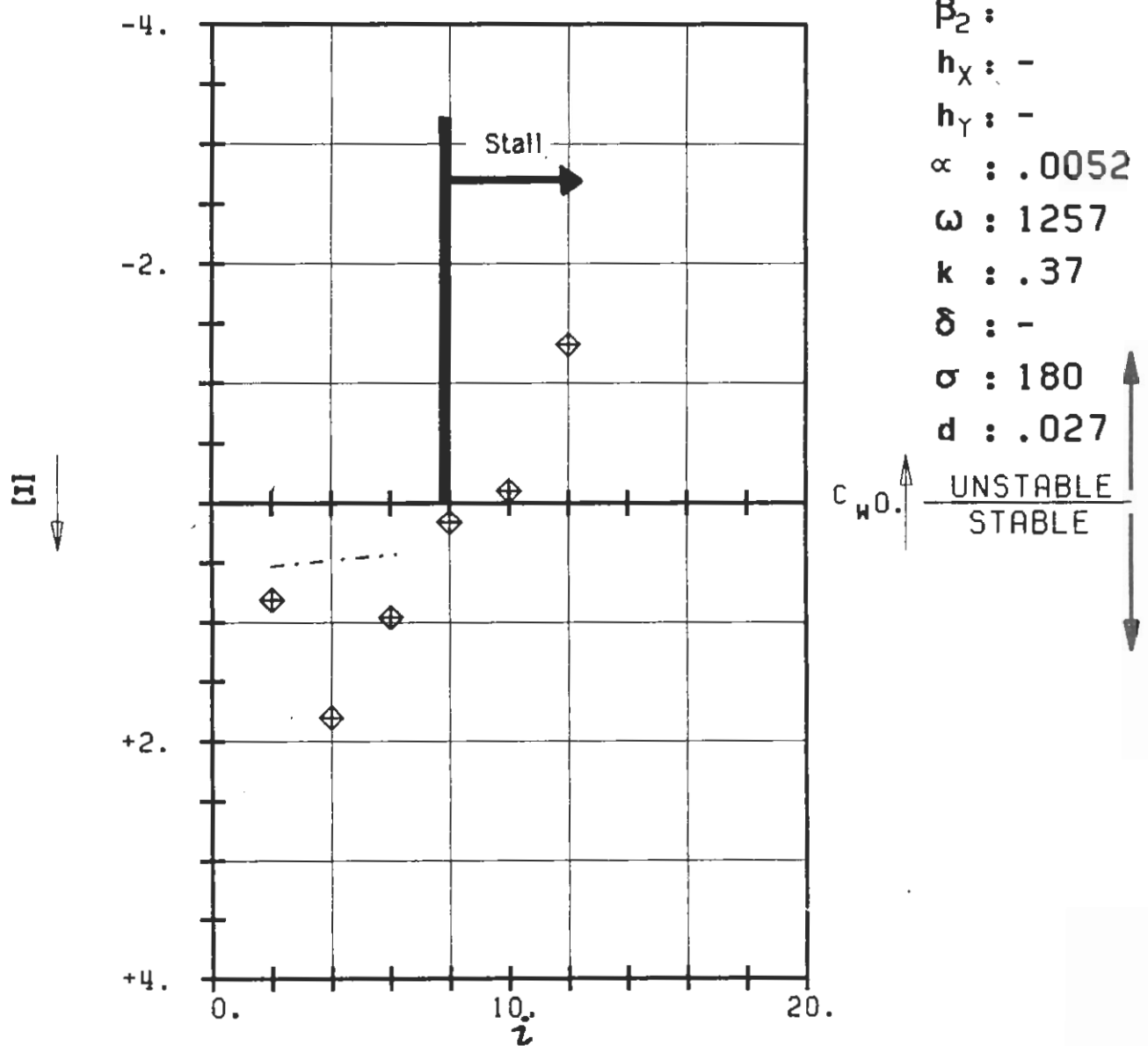
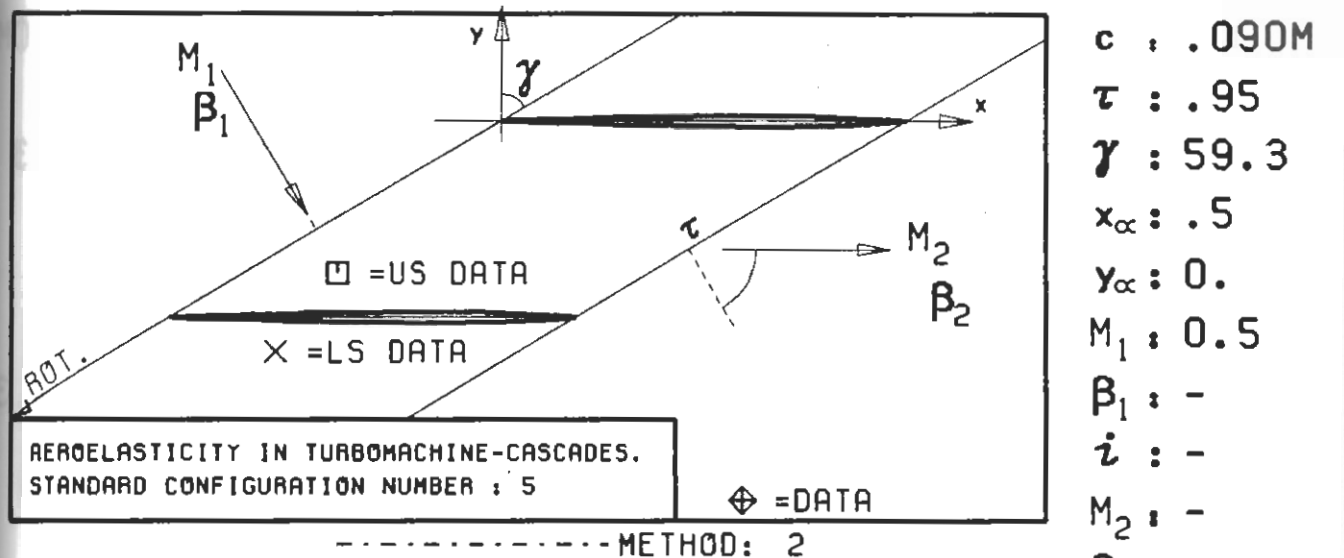
PLOT 7.5-5.2: FIFTH STANDARD CONFIGURATION, CASES 4-7.
AERODYNAMIC MOMENT COEFFICIENT AND PHASE LEAD
IN DEPENDANCE OF REDUCED FREQUENCY.



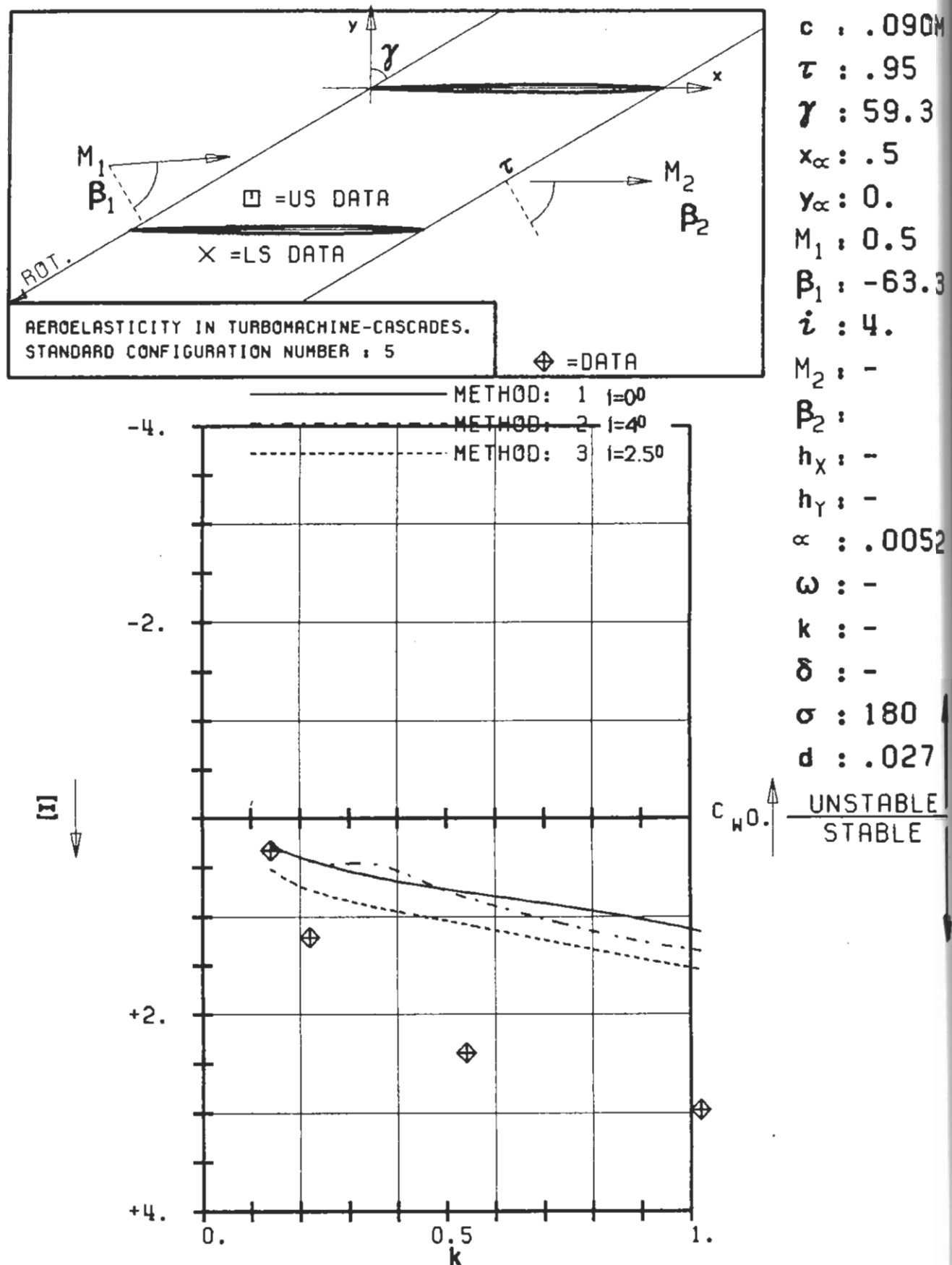
c : .090M
 τ : .95
 γ : 59.3
 x_∞ : .5
 y_∞ : 0.
 M_1 : 0.5
 β_1 : -65.3
 i : 6.
 M_2 : -
 β_2 :
 h_x : -
 h_y : -
 α : .0052
 ω : -
 k : -
 δ : -
 σ : 180
 d : .027



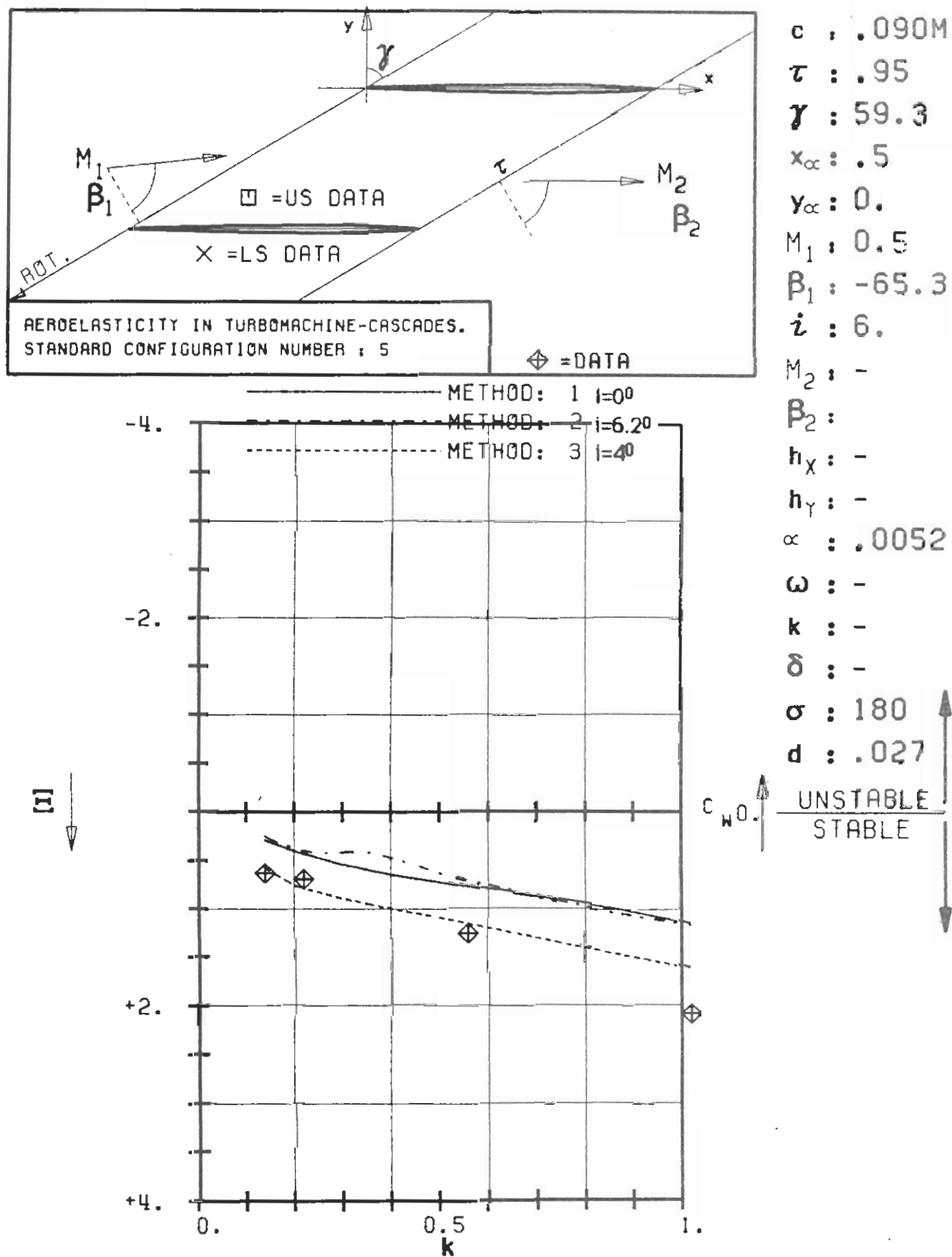
PLOT 7.5-5.3: FIFTH STANDARD CONFIGURATION, CASES 8-11.
AERODYNAMIC MOMENT COEFFICIENT AND PHASE LEAD
IN DEPENDANCE OF REDUCED FREQUENCY .



PLOT 7.5-6.1: FIFTH STANDARD CONFIGURATION, CASES 1-3+EXTRA.
AERODYNAMIC WORK AND DAMPING COEFFICIENTS
IN DEPENDANCE OF INCIDENCE ANGLE.



PLOT 7.5-6.2: FIFTH STANDARD CONFIGURATION, CASES 4-7.
 AERODYNAMIC WORK AND DAMPING COEFFICIENTS
 IN DEPENDANCE OF REDUCED FREQUENCY.

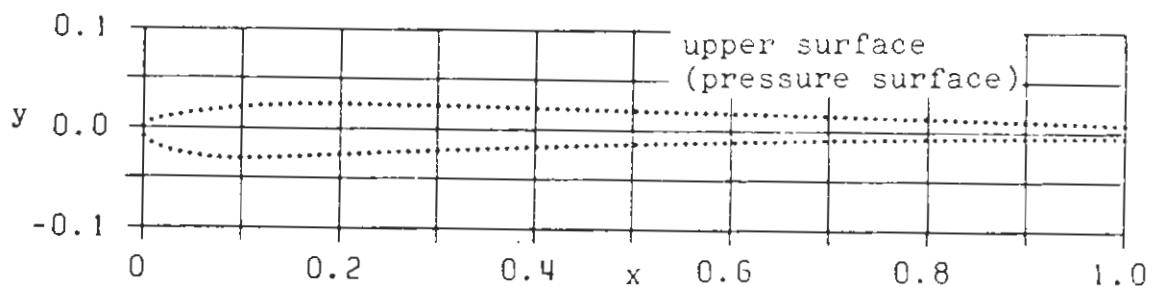
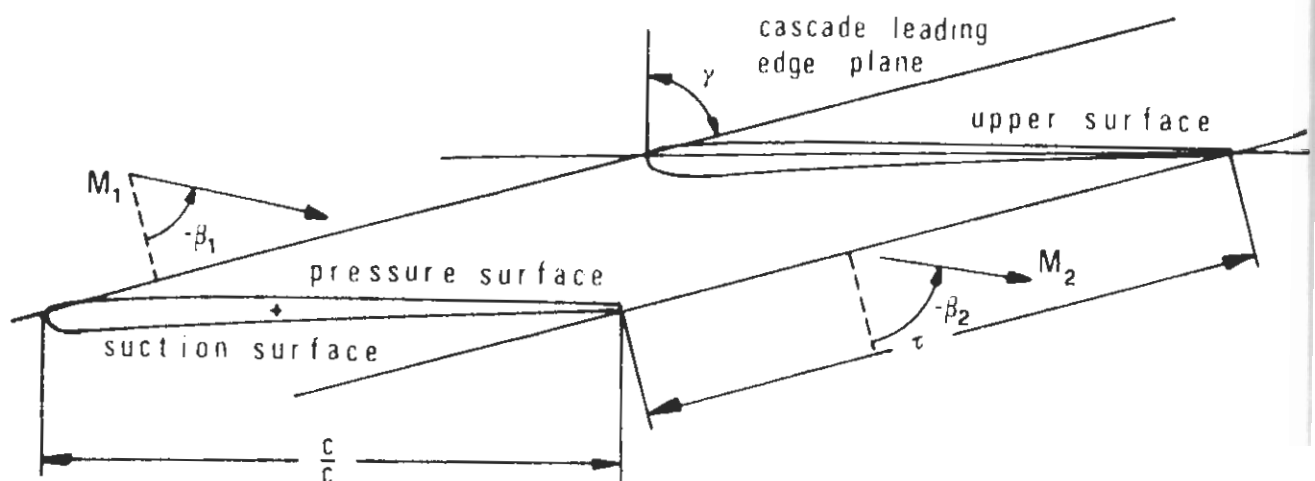


PLOT 7.5-6.3: FIFTH STANDARD CONFIGURATION, CASES 8-11.
 AERODYNAMIC WORK AND DAMPING COEFFICIENTS
 IN DEPENDANCE OF REDUCED FREQUENCY.

AEROELASTICITY IN TURBOMACHINE-CASCADES

SIXTH STANDARD CONFIGURATION

Definition



Transonic Steam Turbine Profiles.

Vibration in first bending mode	δ	= 43.2°
d = (thickness/chord)		= 0.0526
γ = 73.4°	k	= variable
c = 0.0528 m	span	= 0.040 m
τ = 0.952 (hub)	camber	= 14°
1.071 (midspan)	hub/tip	= 0.8
1.190 (tip)	f	= 226 Hz
M_2 = varied	β_1	= varied
σ = varied		

Nominal values: $M_1=0.40$; $\beta_1=-62^\circ$; $M_2=1.34$; $\beta_2=-71^\circ$

Working fluid: Air

Fig. 7.6-1. Sixth standard configuration: Cascade geometry

C = 0.05277 M							
UPPER SURFACE				LOWER SURFACE			
X	Y	X	Y	X	Y	X	Y
0.0000	0.0000	.5033	.0191	0.0000	0.0000	.4930	-.0151
.0078	.0063	.5135	.0189	.0008	-.0097	.5032	-.0148
.0176	.0090	.5236	.0187	.0085	-.0161	.5133	-.0145
.0275	.0109	.5338	.0185	.0178	-.0202	.5234	-.0142
.0375	.0127	.5439	.0183	.0275	-.0232	.5336	-.0138
.0475	.0143	.5540	.0181	.0373	-.0255	.5437	-.0135
.0575	.0157	.5642	.0179	.0473	-.0274	.5538	-.0132
.0676	.0171	.5743	.0177	.0573	-.0288	.5640	-.0130
.0777	.0184	.5845	.0175	.0674	-.0298	.5741	-.0127
.0877	.0195	.5946	.0173	.0775	-.0305	.5843	-.0124
.0978	.0204	.6047	.0171	.0877	-.0309	.5944	-.0121
.1079	.0213	.6149	.0169	.0978	-.0311	.6045	-.0119
.1181	.0221	.6250	.0167	.1080	-.0310	.6147	-.0116
.1282	.0225	.6352	.0165	.1181	-.0307	.6248	-.0113
.1383	.0230	.6453	.0162	.1282	-.0303	.6349	-.0111
.1484	.0235	.6554	.0160	.1384	-.0298	.6451	-.0108
.1586	.0239	.6656	.0158	.1485	-.0294	.6552	-.0106
.1687	.0242	.6757	.0156	.1586	-.0289	.6654	-.0104
.1789	.0243	.6859	.0153	.1688	-.0284	.6755	-.0101
.1890	.0243	.6960	.0151	.1789	-.0278	.6856	-.0099
.1991	.0243	.7061	.0149	.1890	-.0274	.6958	-.0097
.2093	.0242	.7163	.0147	.1991	-.0269	.7059	-.0095
.2194	.0240	.7264	.0144	.2093	-.0264	.7161	-.0093
.2296	.0239	.7366	.0142	.2194	-.0259	.7262	-.0091
.2397	.0237	.7467	.0140	.2295	-.0254	.7363	-.0089
.2498	.0236	.7568	.0137	.2397	-.0250	.7465	-.0087
.2600	.0235	.7670	.0135	.2498	-.0245	.7566	-.0085
.2701	.0235	.7771	.0133	.2599	-.0240	.7668	-.0083
.2803	.0234	.7873	.0130	.2701	-.0236	.7769	-.0082
.2904	.0233	.7974	.0128	.2802	-.0232	.7870	-.0080
.3006	.0232	.8075	.0125	.2903	-.0227	.7972	-.0078
.3107	.0231	.8177	.0123	.3005	-.0223	.8073	-.0077
.3208	.0229	.8278	.0120	.3106	-.0219	.8175	-.0075
.3310	.0227	.8380	.0118	.3207	-.0214	.8276	-.0074
.3411	.0225	.8481	.0115	.3309	-.0210	.8377	-.0072
.3513	.0223	.8582	.0112	.3410	-.0206	.8479	-.0071
.3614	.0220	.8684	.0110	.3511	-.0202	.8580	-.0070
.3715	.0218	.8785	.0107	.3613	-.0198	.8682	-.0068
.3817	.0215	.8886	.0104	.3714	-.0194	.8783	-.0067
.3918	.0213	.8988	.0102	.3815	-.0190	.8884	-.0066
.4019	.0211	.9089	.0099	.3917	-.0186	.8986	-.0065
.4121	.0210	.9191	.0096	.4018	-.0183	.9087	-.0064
.4222	.0208	.9292	.0093	.4119	-.0179	.9189	-.0063
.4324	.0206	.9393	.0090	.4221	-.0175	.9290	-.0062
.4425	.0204	.9495	.0088	.4322	-.0172	.9392	-.0061
.4526	.0202	.9596	.0085	.4423	-.0168	.9493	-.0060
.4628	.0200	.9697	.0082	.4525	-.0164	.9594	-.0060
.4729	.0198	.9799	.0079	.4626	-.0161	.9696	-.0059
.4831	.0195	.9900	.0076	.4727	-.0158	.9797	-.0058
.4932	.0193	1.0002	.0073	.4829	-.0154	1.0000	-.0057

Table 7.6-1. Sixth standard configuration: Dimensionless airfoil coordinates (spanwise identical)

AEROELASTICITY IN TURBOMACHINE-CASCADES

SIXTH STANDARD CONFIGURATION

Aeroelastic Test Cases

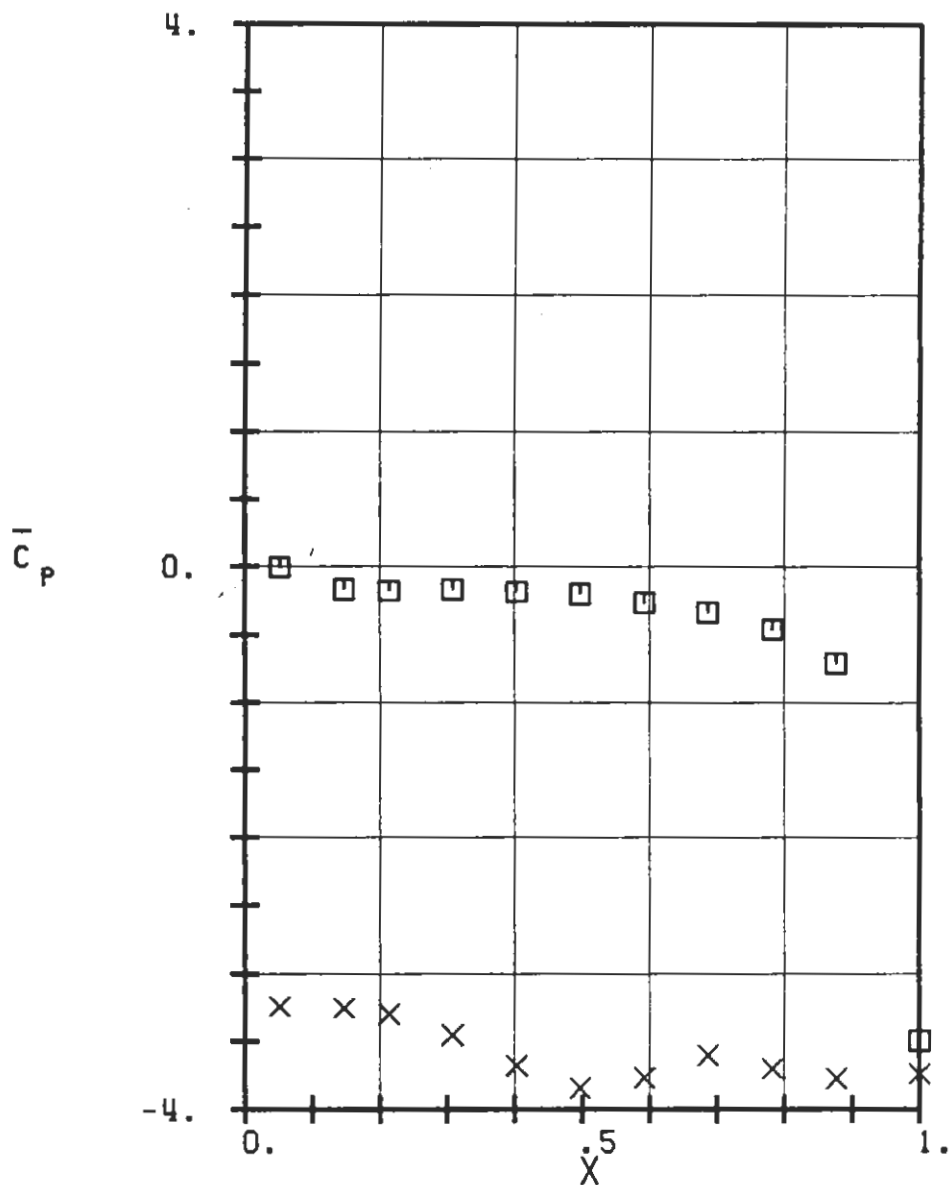
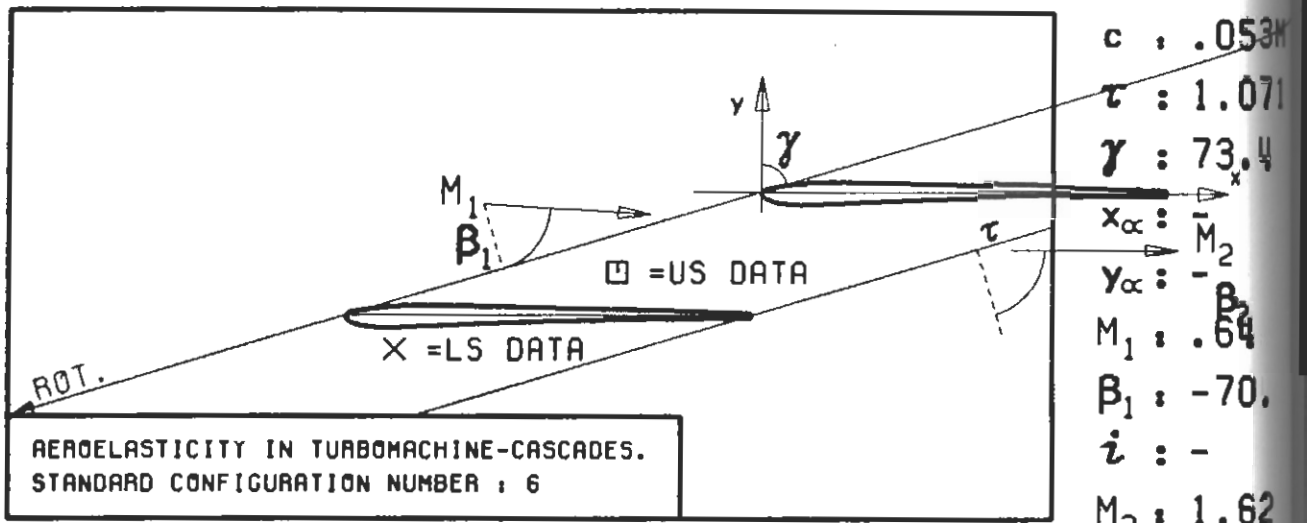
Aeroelastic Test Case No.	Time Averaged				Time Dependent Parameters					
	M_1 (-)	β_1 (°)	p_2/p_1 (-)	M_{2is} (-)	h^0 (-)	f (Hz)	K (-)	σ (°)	δ (°)	
1	0.53	70	0.27	1.63	0.0030	226	0.068	0	+43.2	
2	"	"	"	"	"	"	"	+45	"	
3	"	"	"	"	"	"	"	+90	"	
4	"	"	"	"	"	"	"	+135	"	
5	"	"	"	"	"	"	"	-180	"	
6	"	"	"	"	"	"	"	+135	"	
7	"	"	"	"	"	"	"	-90	"	
8	"	"	"	"	"	"	"	-45	"	
9	0.52	"	0.50	1.20	"	"	0.092	-90	"	
10	"	"	0.54	1.14	"	"	0.097	"	"	
11	"	"	0.62	1.02	"	"	0.108	"	"	
12	"	"	0.65	0.98	"	"	0.113	"	"	

Table 7.6-2. Sixth standard configuration: Recommended aeroelastic test cases.

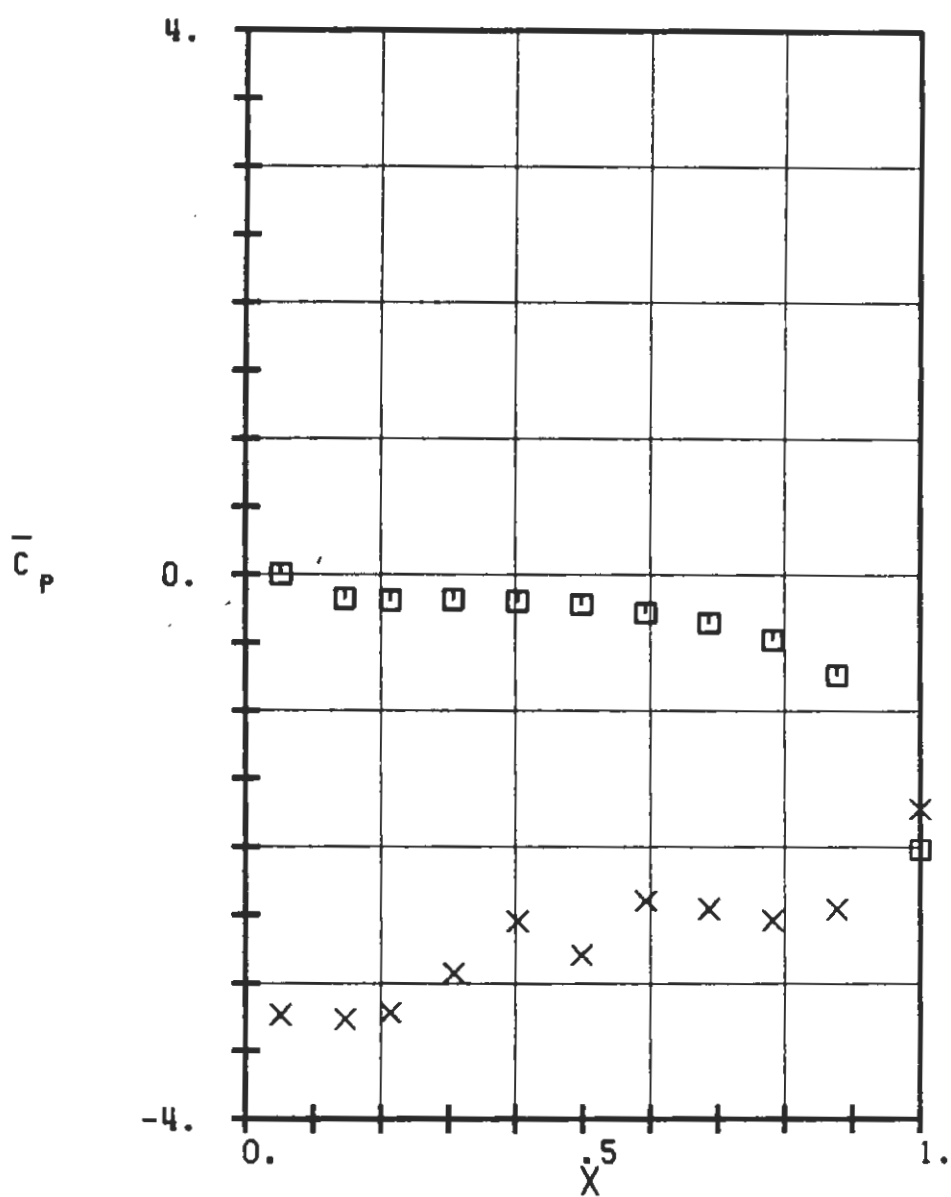
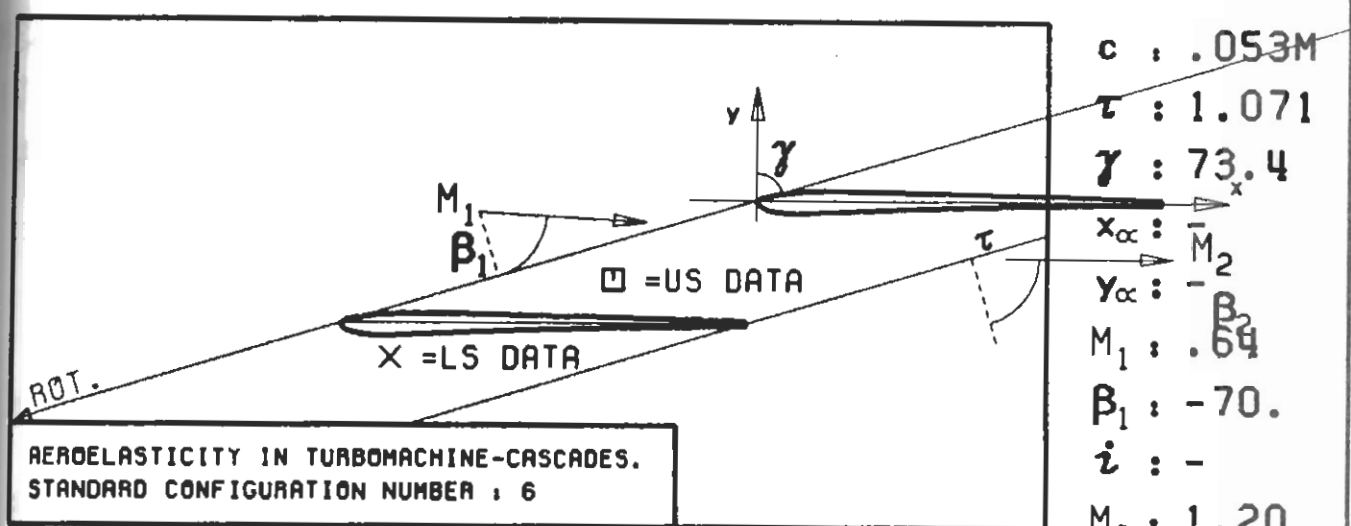
AERODELASTICITY IN TURBOMACHINE-CASCADES

SIXTH STANDARD CONFIGURATION

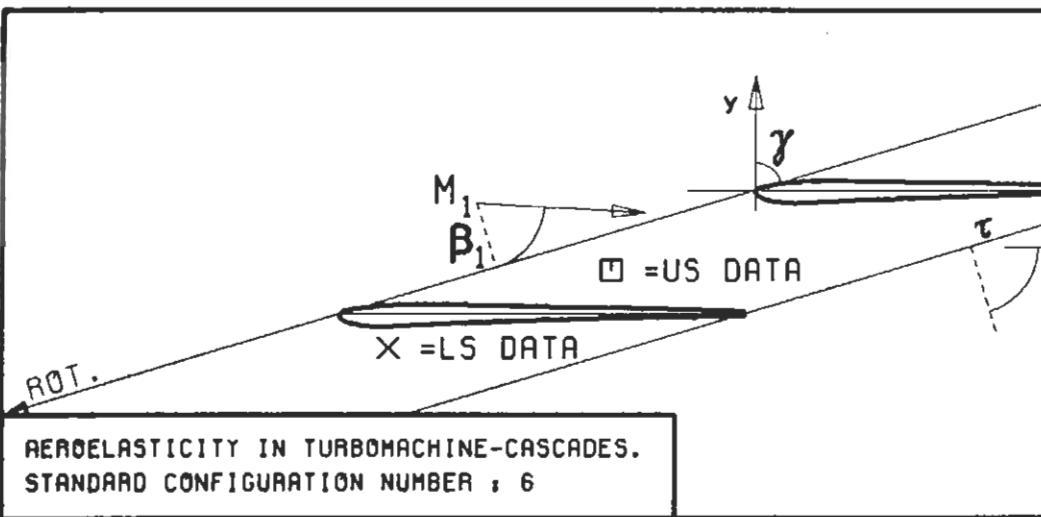
Experimental and Theoretical Results



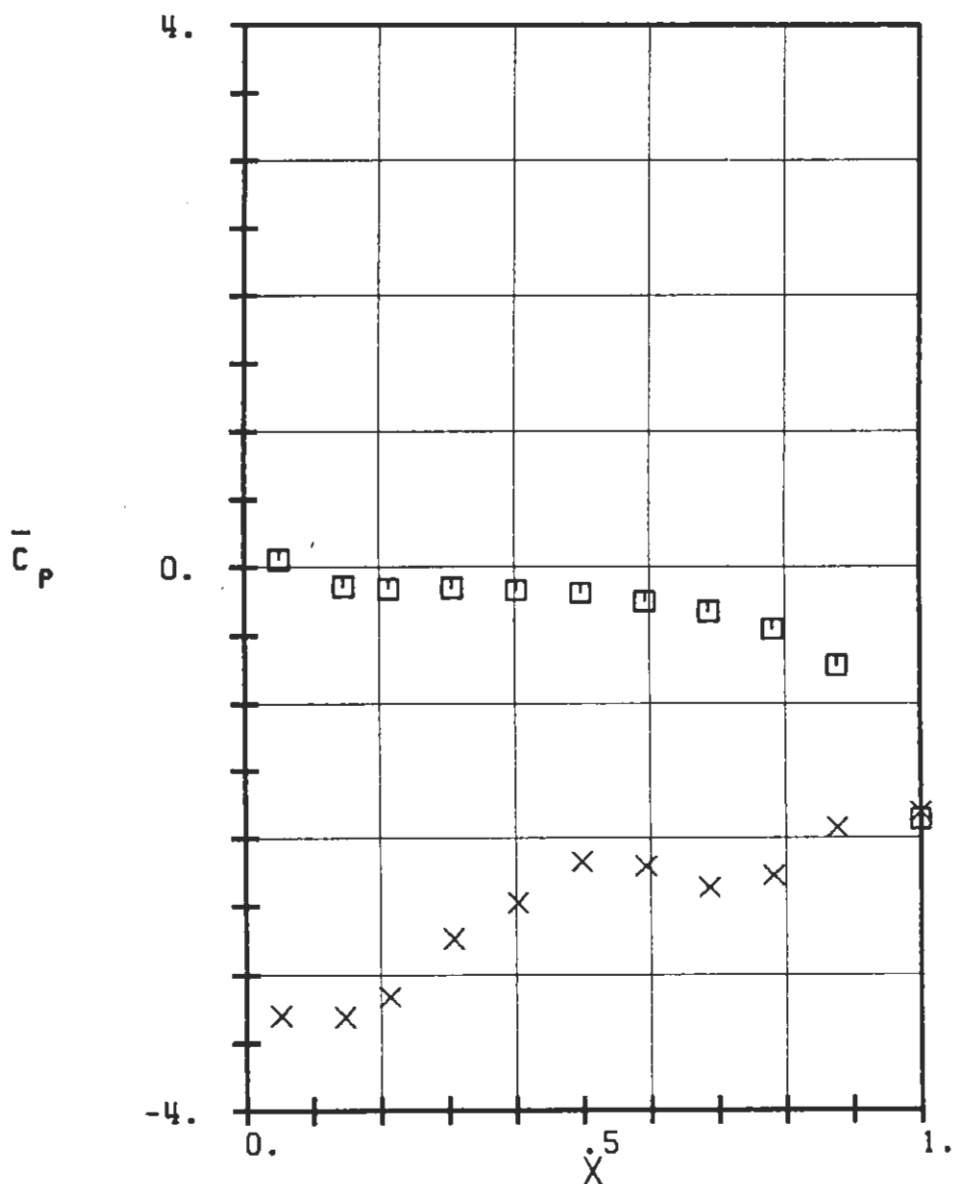
PLT 7.6-1.1: SIXTH STANDARD CONFIGURATION, CASES 1-8.
TIME AVERAGED BLADE SURFACE PRESSURE COEFFICIENT



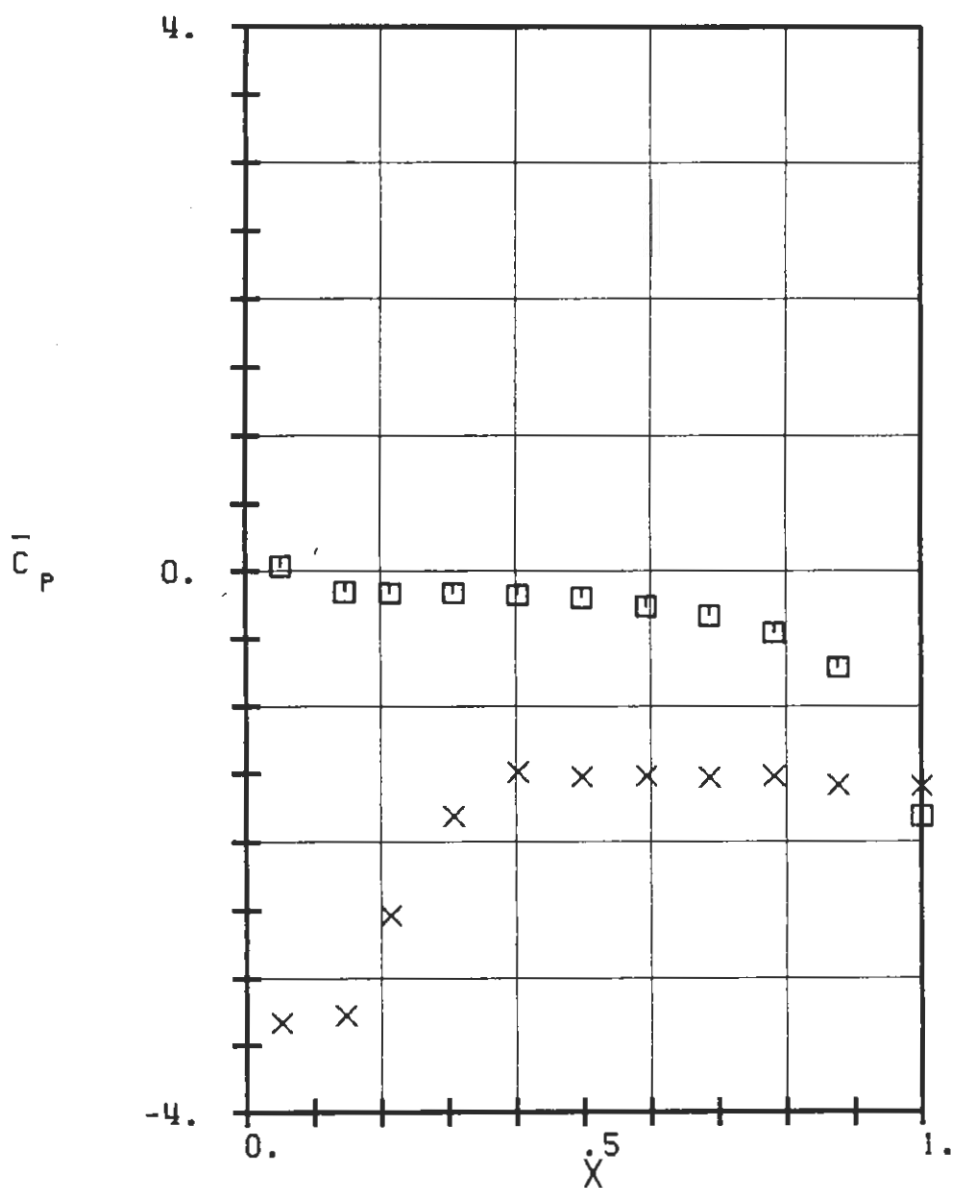
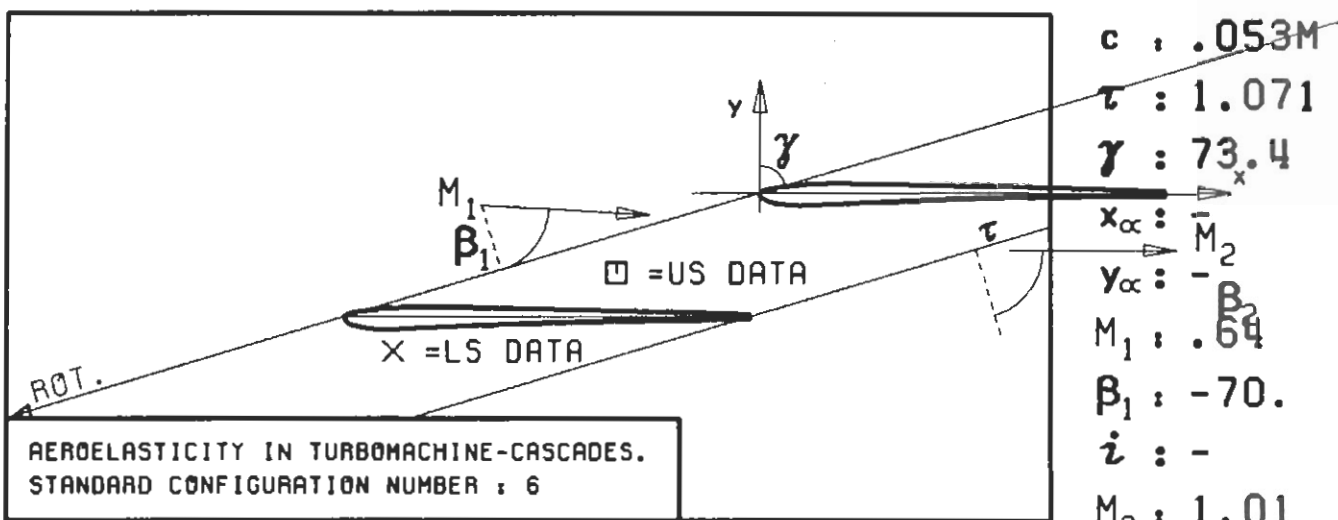
PLOT 7.6-1.2: SIXTH STANDARD CONFIGURATION, CASE 9.
TIME AVERAGED BLADE SURFACE PRESSURE
COEFFICIENT



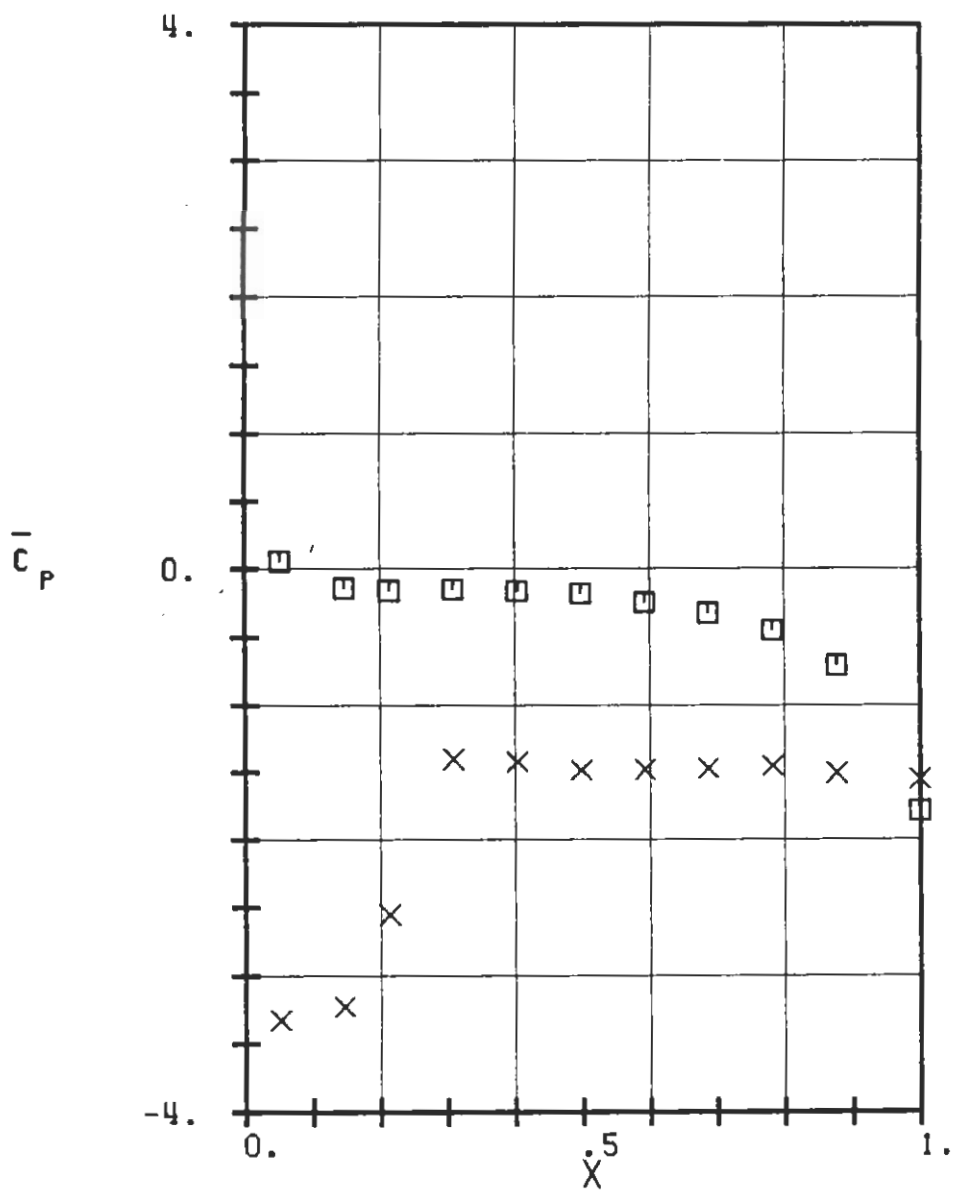
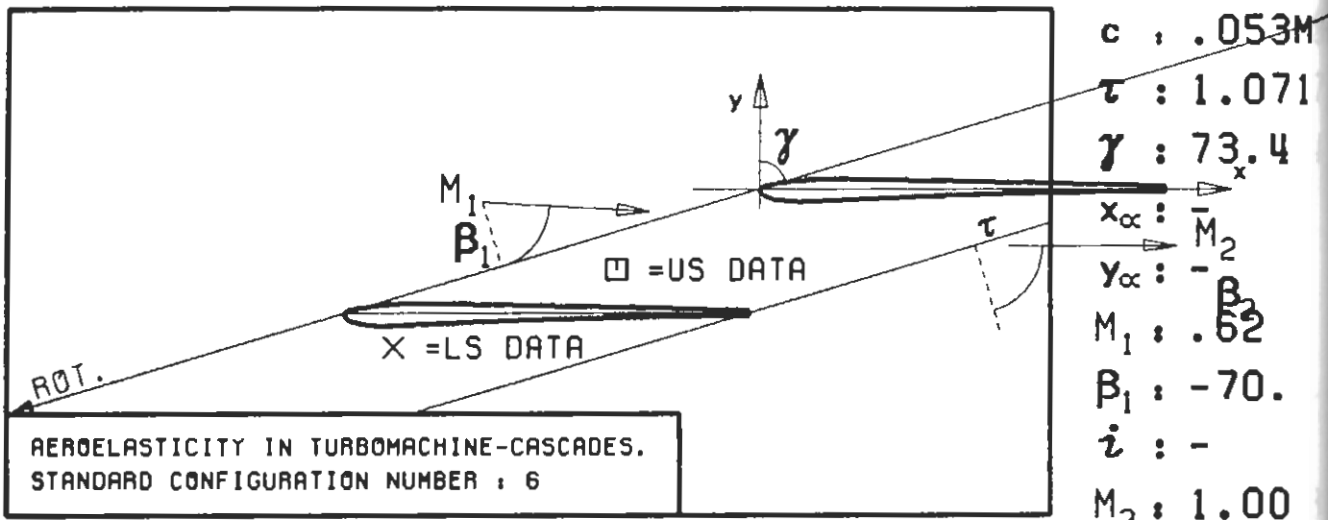
$c : .053M$
 $\tau : 1.071$
 $\gamma : 73.4$
 $x_\alpha : -\bar{M}_2$
 $y_\alpha : -\bar{B}_2$
 $M_1 : .64$
 $\beta_1 : -70.$
 $i : -$
 $M_2 : 1.13$
 $\beta_2 :$
 $h_X : .0040$
 $h_Y : .0038$
 $\alpha : -$
 $\omega : 1420$
 $k : .0916$
 $\delta : 43.2$
 $\sigma : -92.$
 $d : .0526$



PLOT 7.6-1.3: SIXTH STANDARD CONFIGURATION, CASE 10.
 TIME AVERAGED BLADE SURFACE PRESSURE
 COEFFICIENT

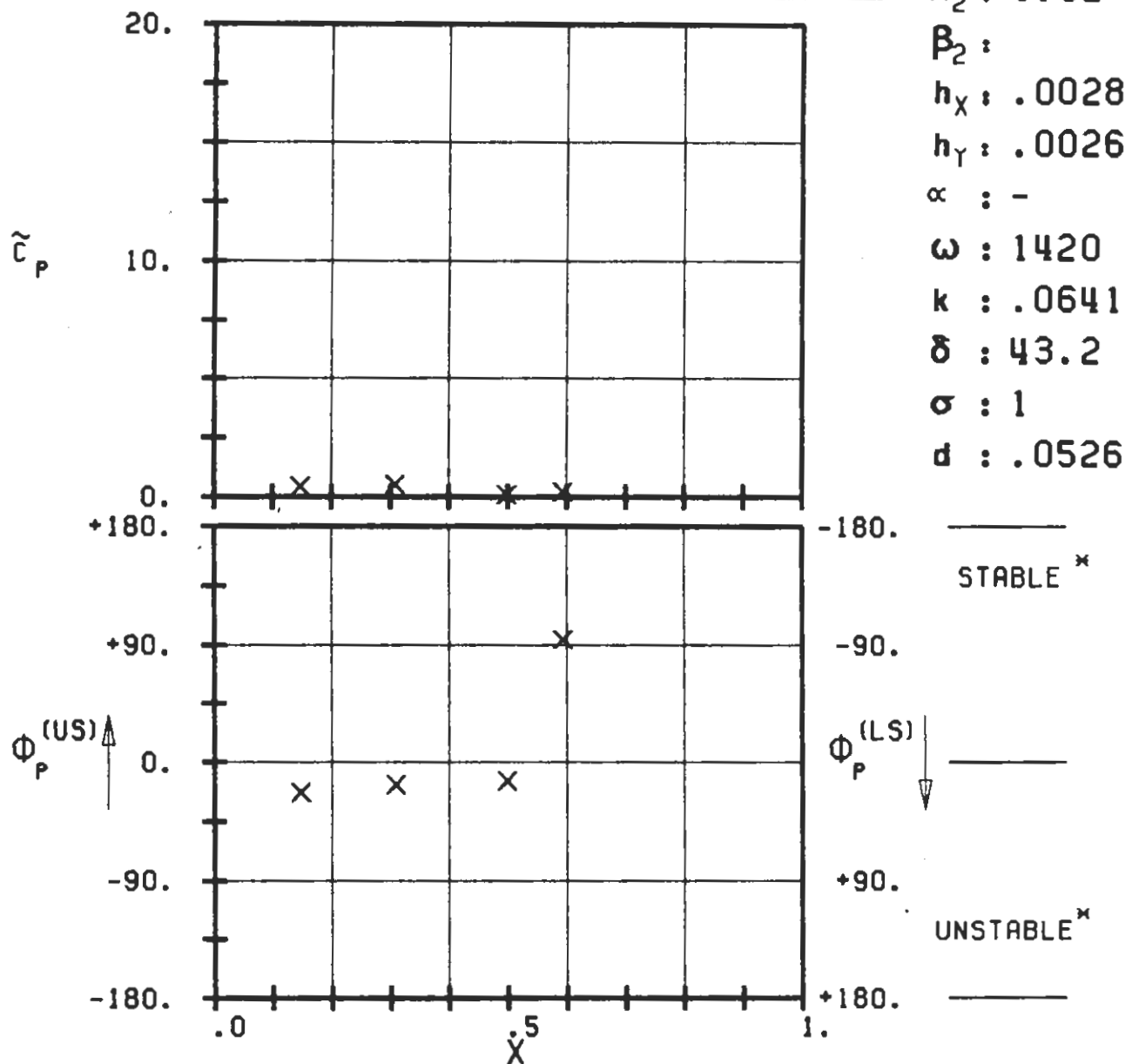
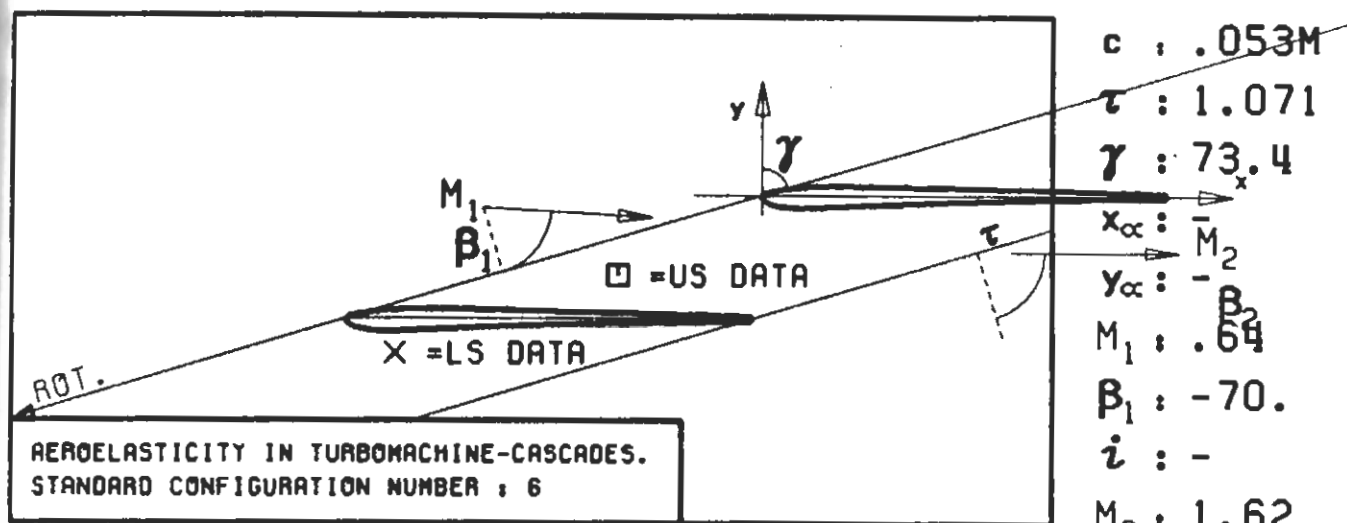


PLOT 7.6-1.4: SIXTH STANDARD CONFIGURATION, CASE 11.
TIME AVERAGED BLADE SURFACE PRESSURE COEFFICIENT



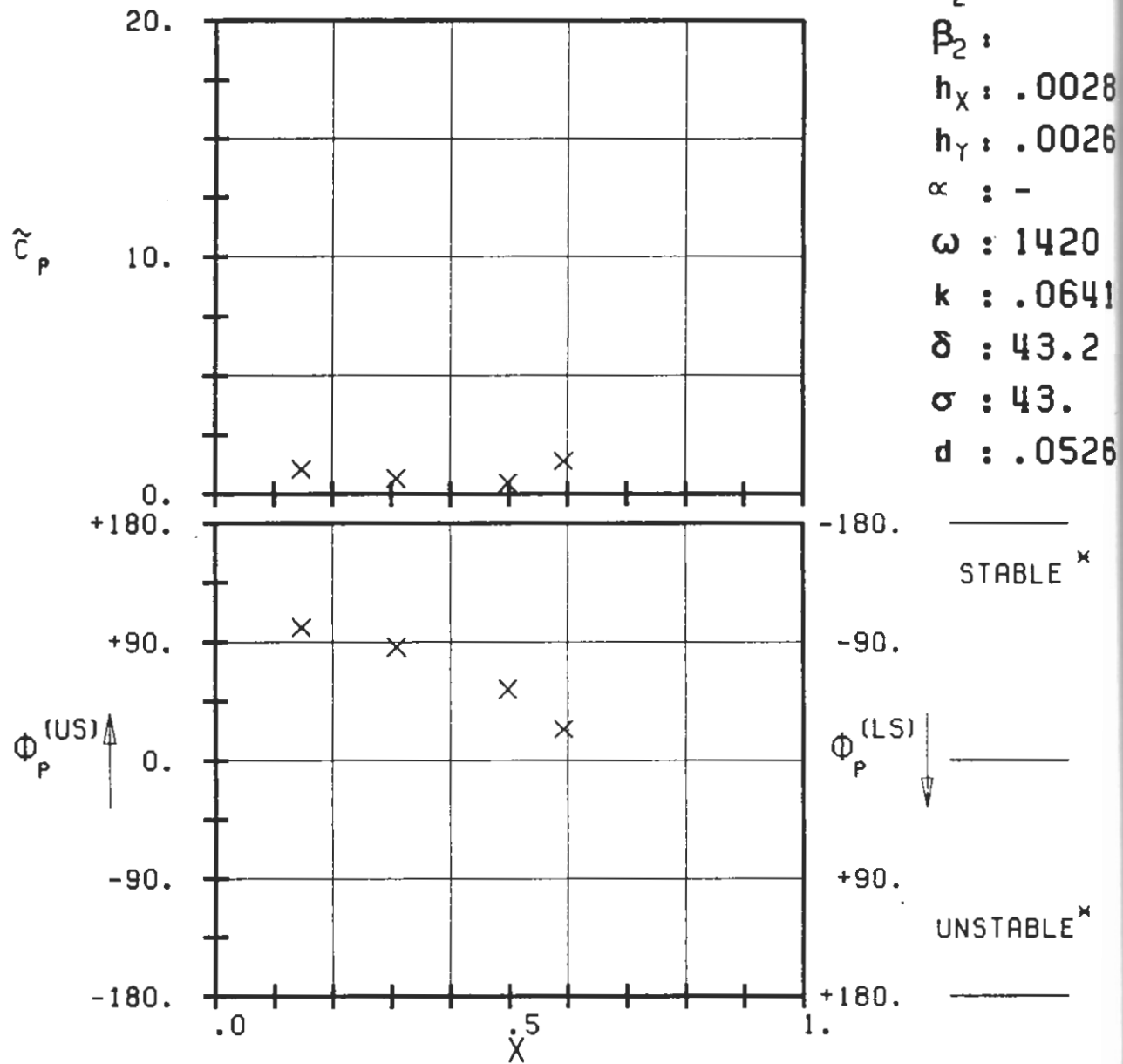
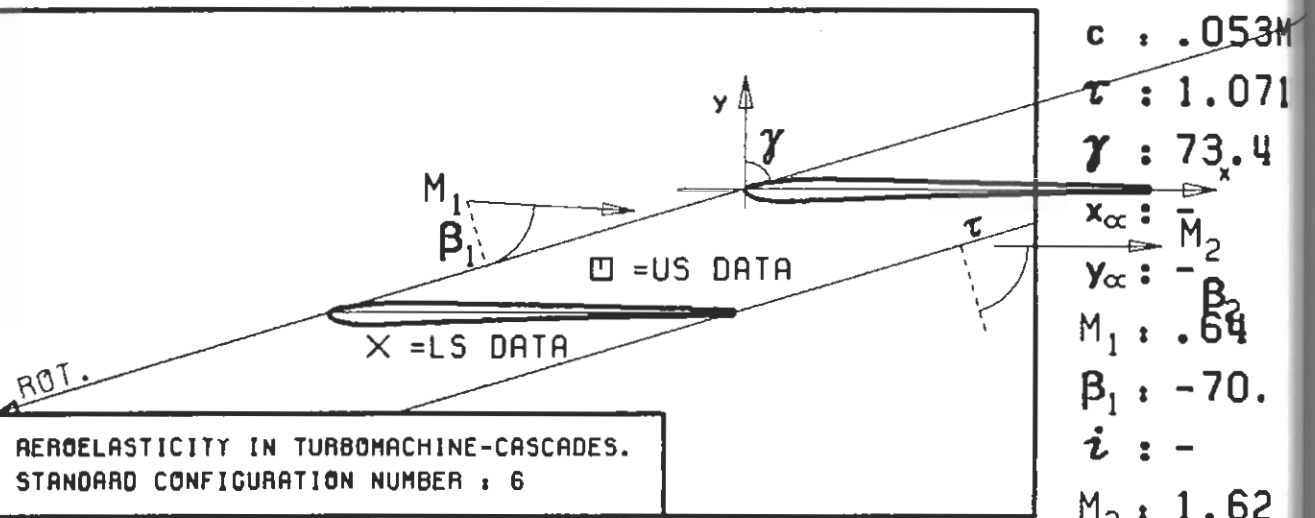
PLOT 7.6-1.5: SIXTH STANDARD CONFIGURATION, CASE 12.
 TIME AVERAGED BLADE SURFACE PRESSURE
 COEFFICIENT

$c : .053M$
 $\tau : 1.071$
 $\gamma : 73.4$
 $x_\alpha : \bar{M}_2$
 $y_\alpha : -B_1$
 $M_1 : .62$
 $B_1 : -70.$
 $i : -$
 $M_2 : 1.00$
 $B_2 :$
 $h_X : .0033$
 $h_Y : .0031$
 $\alpha : -$
 $\omega : 1420$
 $k : .1039$
 $\delta : 43.2$
 $\sigma : -$
 $d : .0526$



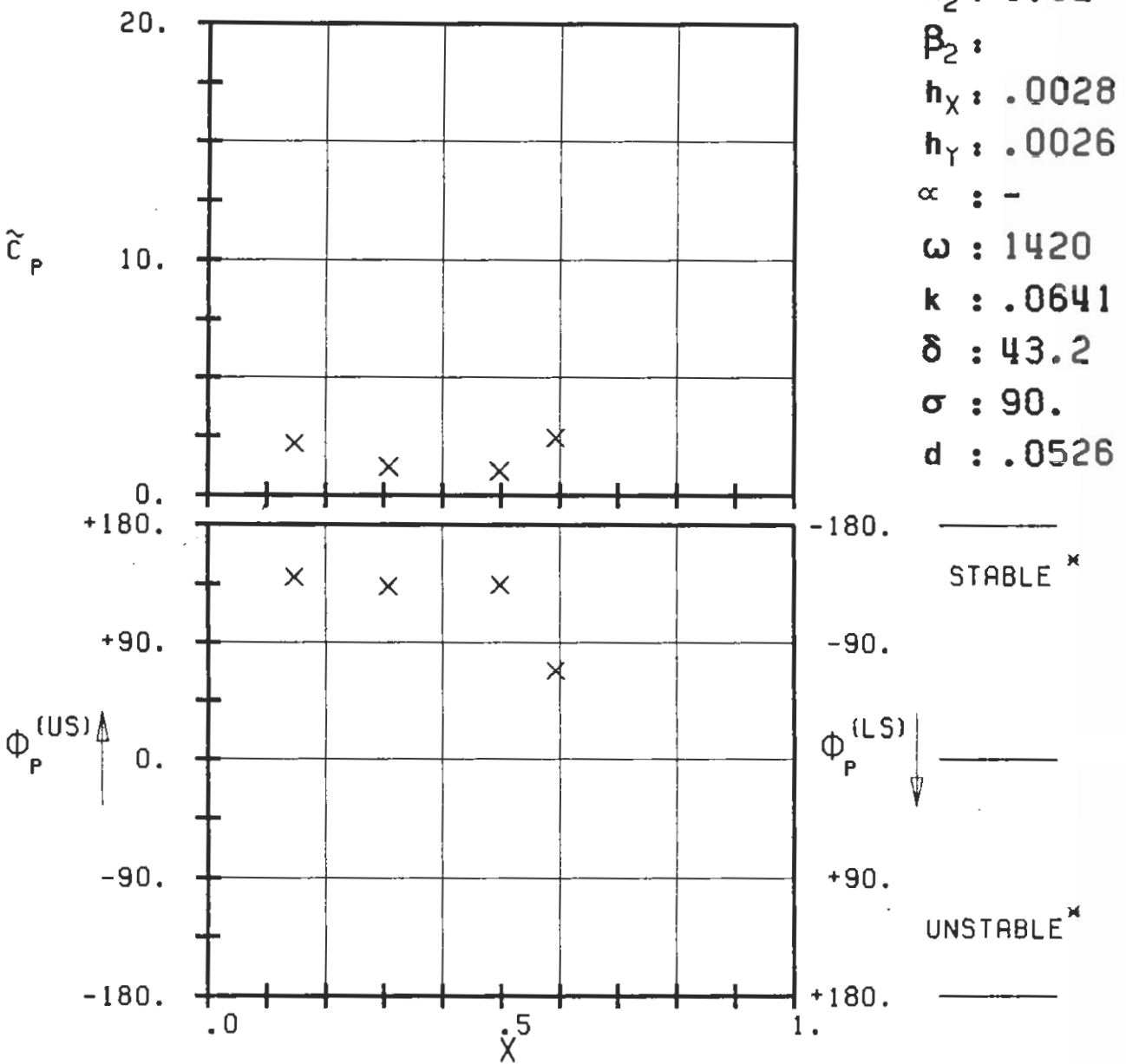
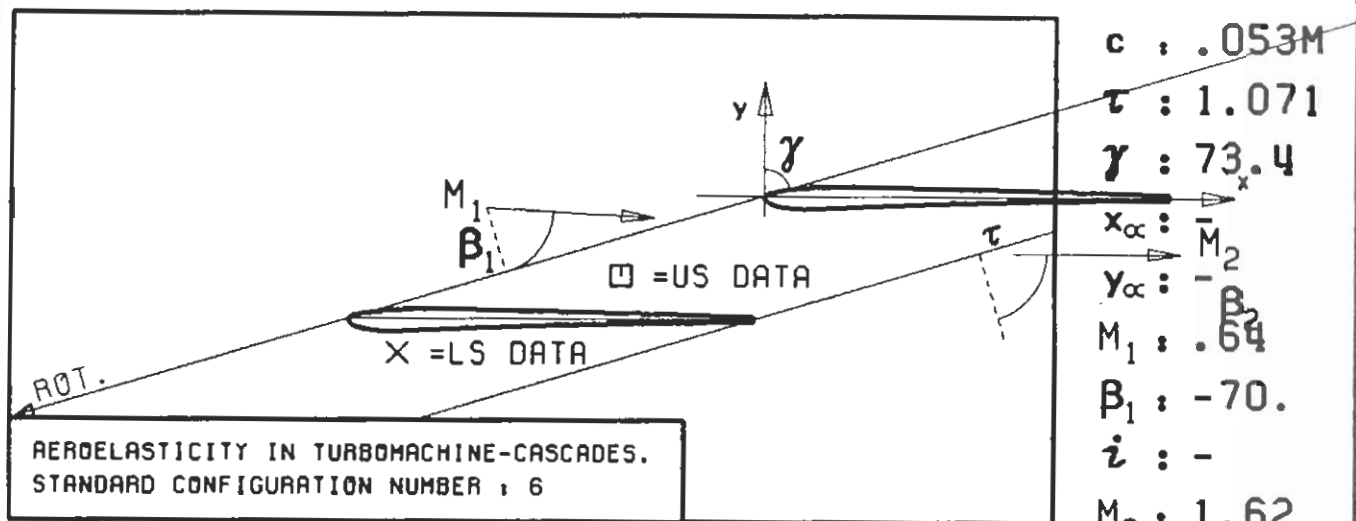
PLOT 7.6-2.1: SIXTH STANDARD CONFIGURATION, CASE 1.
 MAGNITUDE AND PHASE LEAD OF UNSTEADY BLADE
 SURFACE PRESSURE COEFFICIENT.

(x: IN PITCH MODE, NOTATION VALID UPSTREAM OF PITCH AXIS)



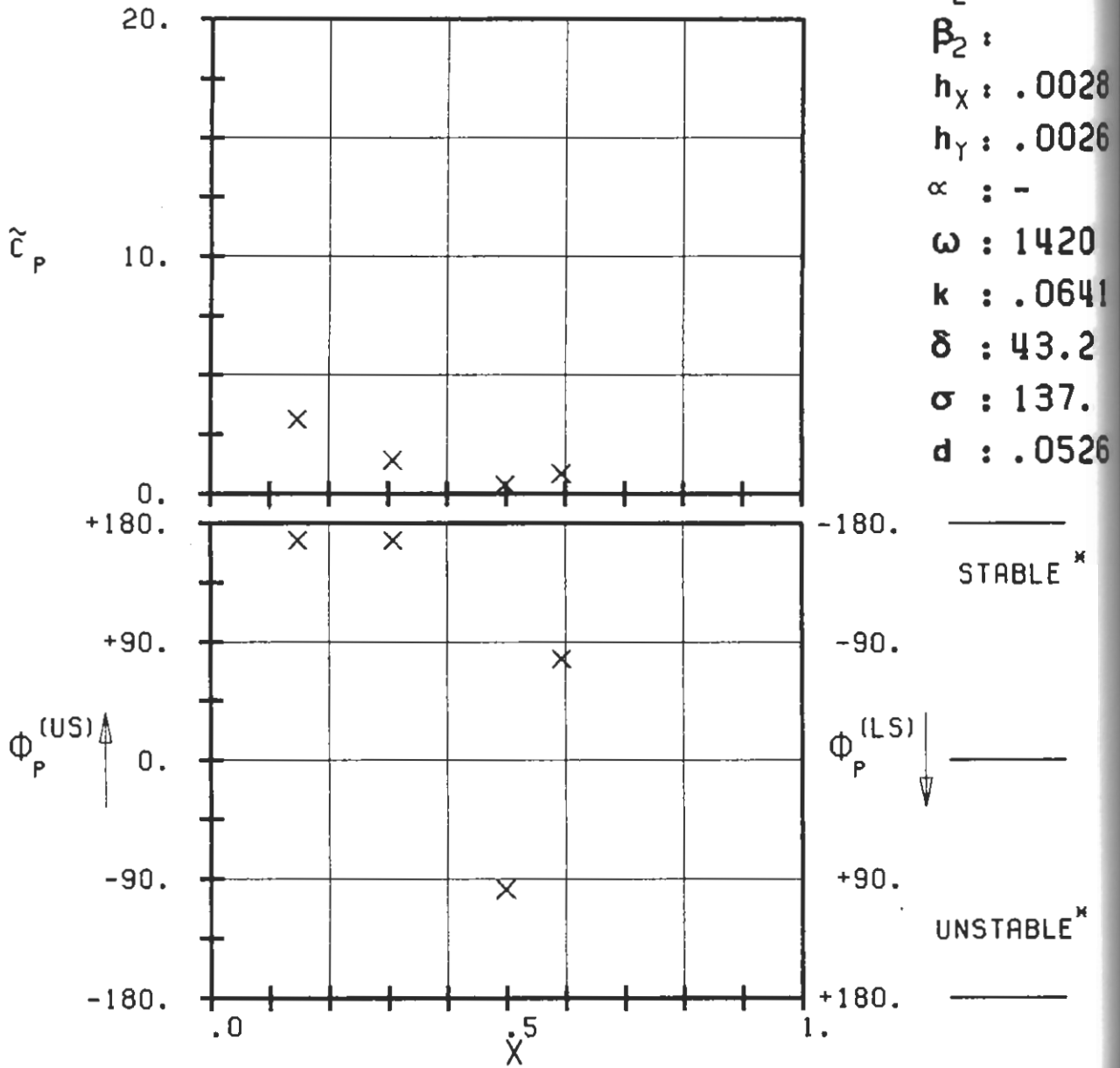
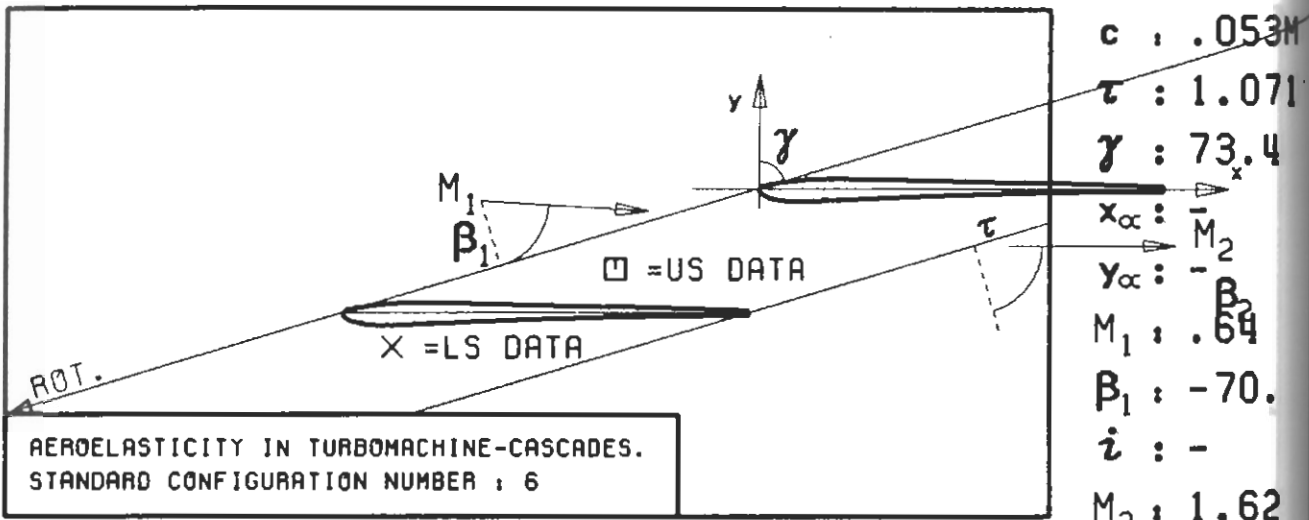
PLOT 7.6-2.2: SIXTH STANDARD CONFIGURATION, CASE 2.
 MAGNITUDE AND PHASE LEAD OF UNSTEADY BLADE
 SURFACE PRESSURE COEFFICIENT.

(X: IN PITCH MODE, NOTATION VALID UPSTREAM OF PITCH AXIS)



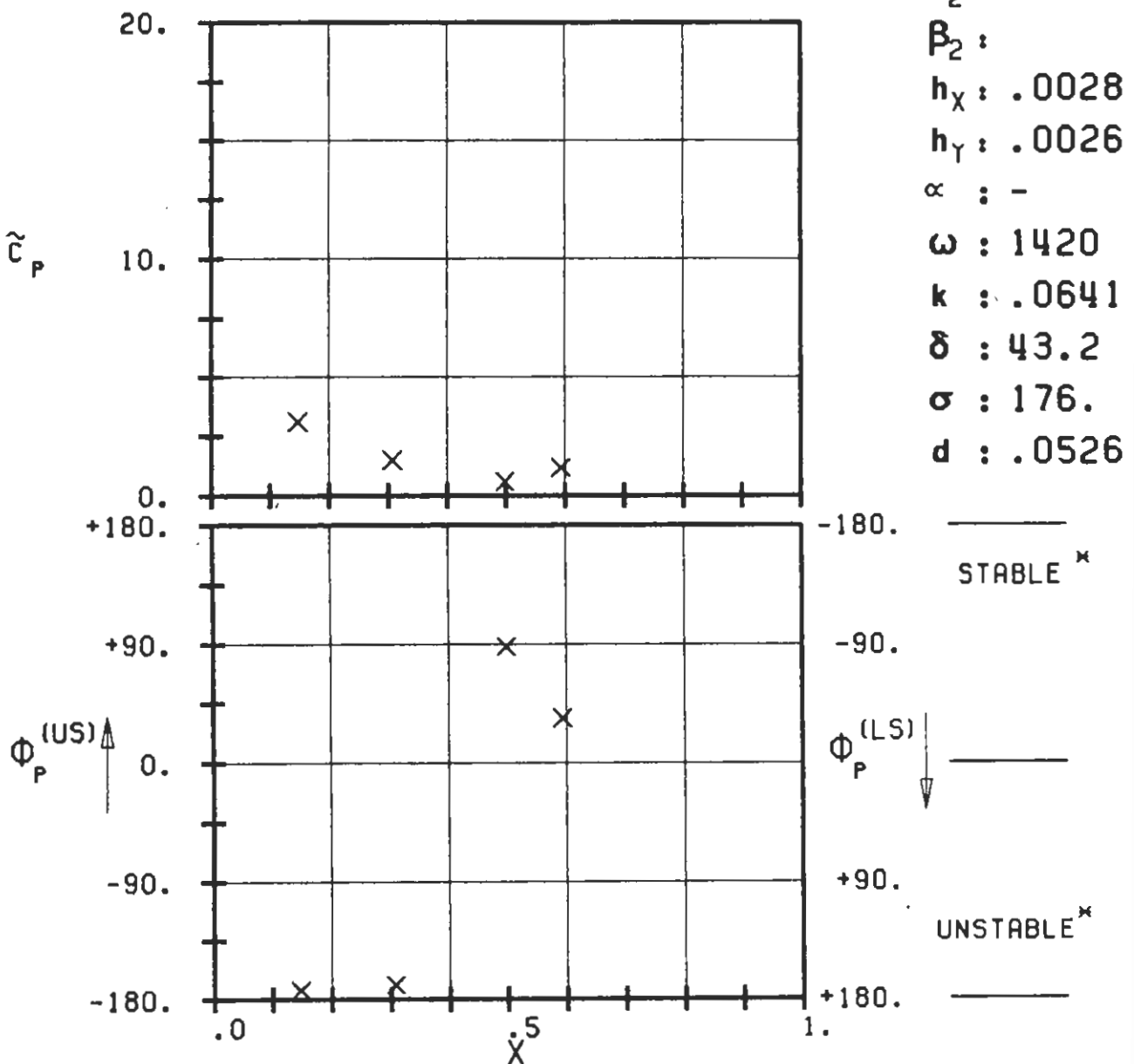
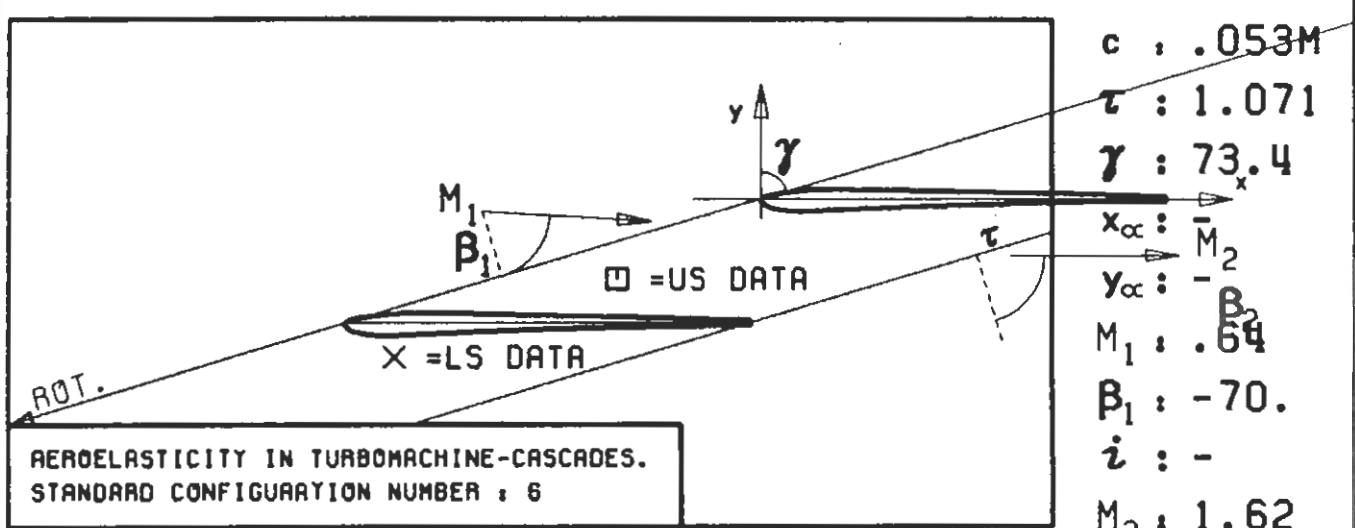
PLOT 7.6-2.3: SIXTH STANDARD CONFIGURATION, CASE 3.
 MAGNITUDE AND PHASE LEAD OF UNSTEADY BLADE
 SURFACE PRESSURE COEFFICIENT.

(\times : IN PITCH MODE, NOTATION VALID UPSTREAM OF PITCH AXIS)



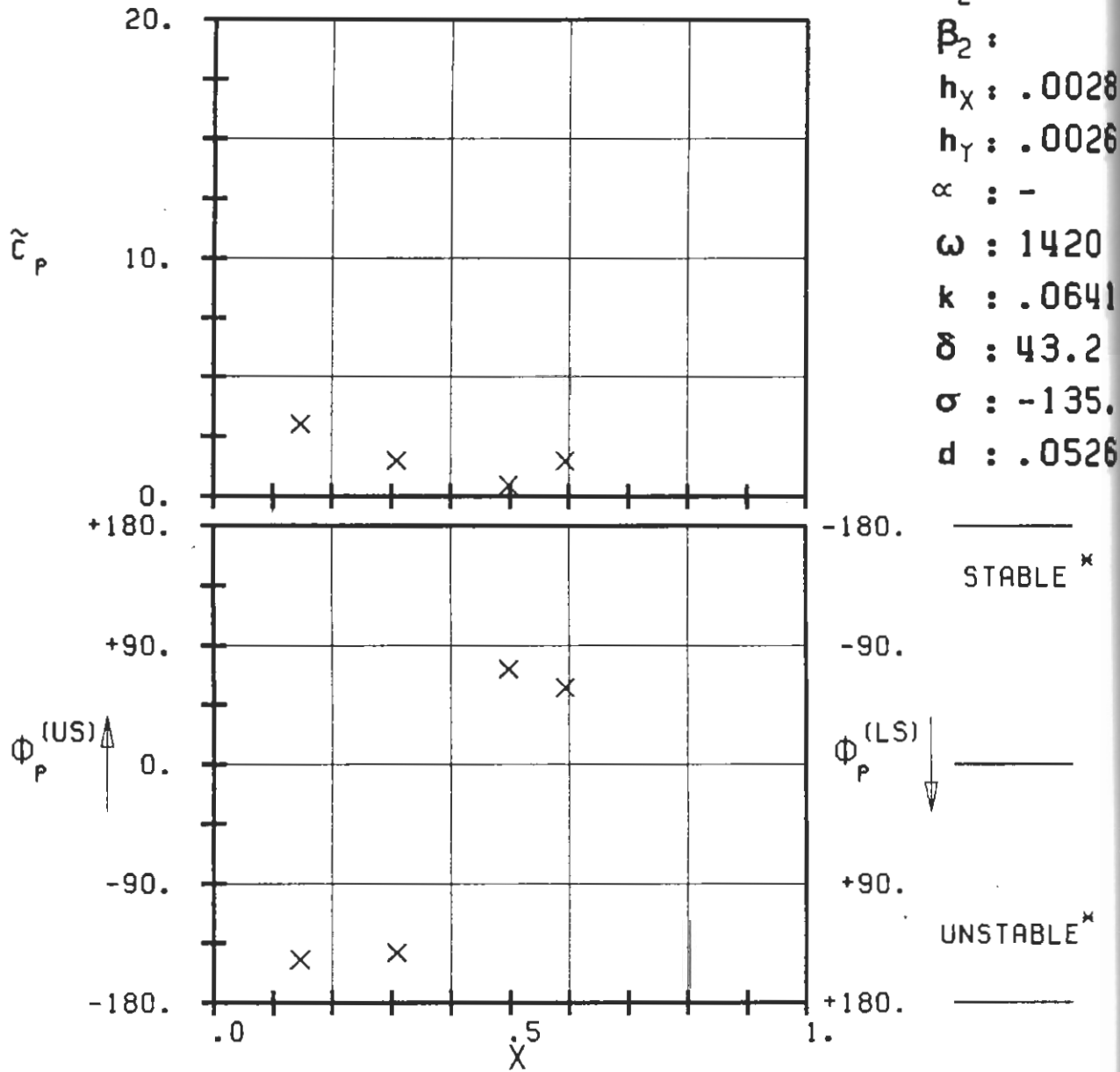
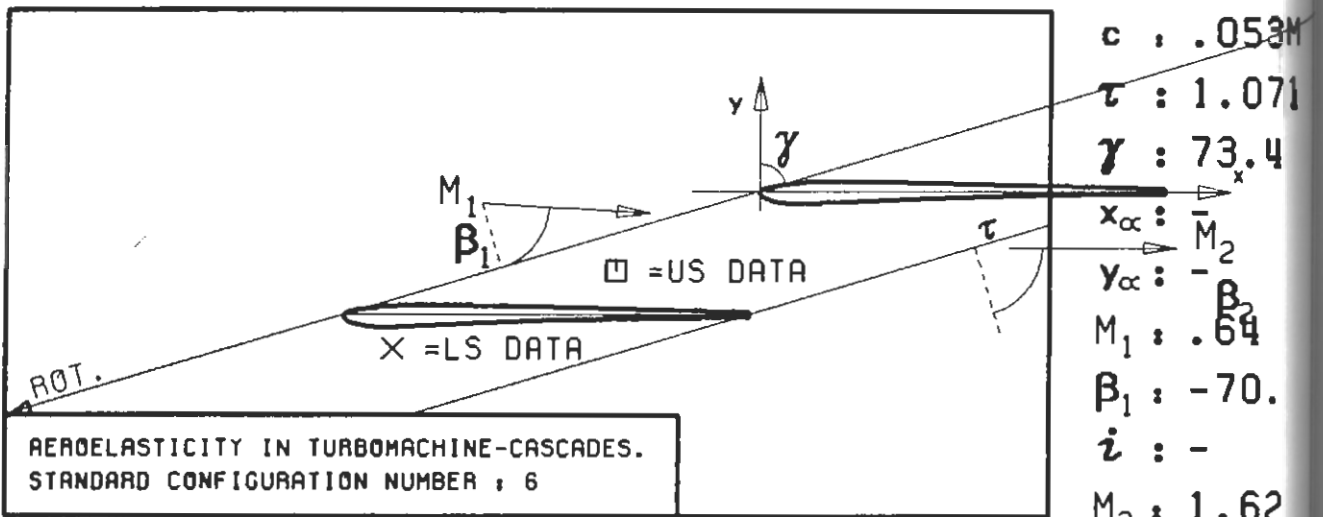
PLOT 7.6-2.4: SIXTH STANDARD CONFIGURATION, CASE 4.
MAGNITUDE AND PHASE LEAD OF UNSTEADY BLADE
SURFACE PRESSURE COEFFICIENT.

(*:IN PITCH MODE,NOTATION VALID UPSTREAM OF PITCH AXIS)



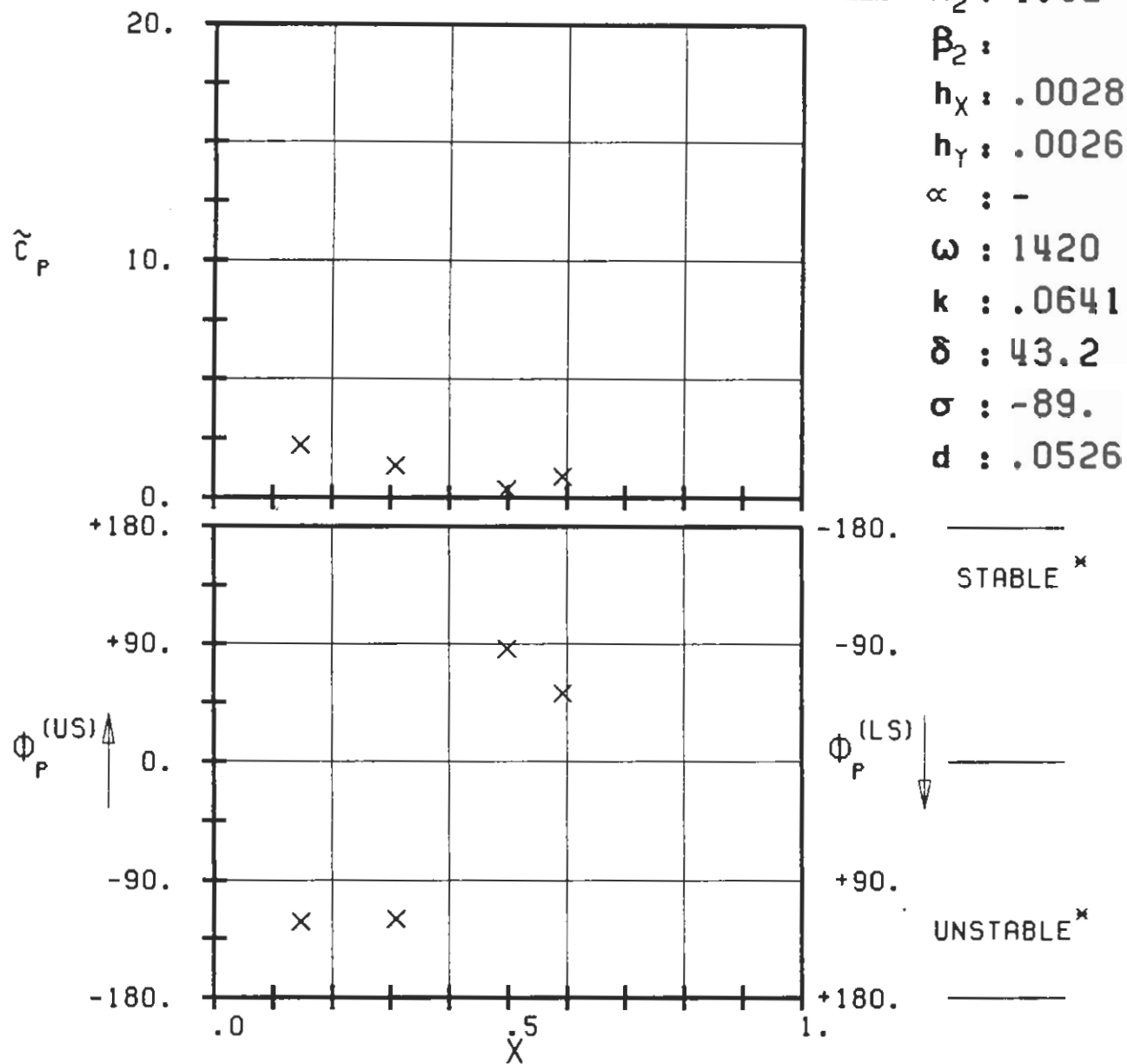
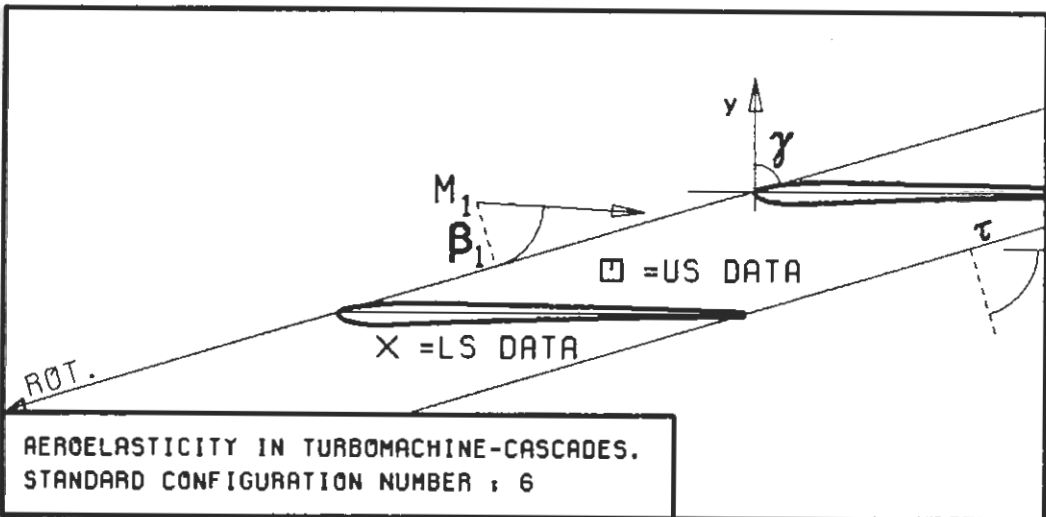
PLOT 7.6-2.5: SIXTH STANDARD CONFIGURATION, CASE 5.
 MAGNITUDE AND PHASE LEAD OF UNSTEADY BLADE
 SURFACE PRESSURE COEFFICIENT.

(x: IN PITCH MODE, NOTATION VALID UPSTREAM OF PITCH AXIS)



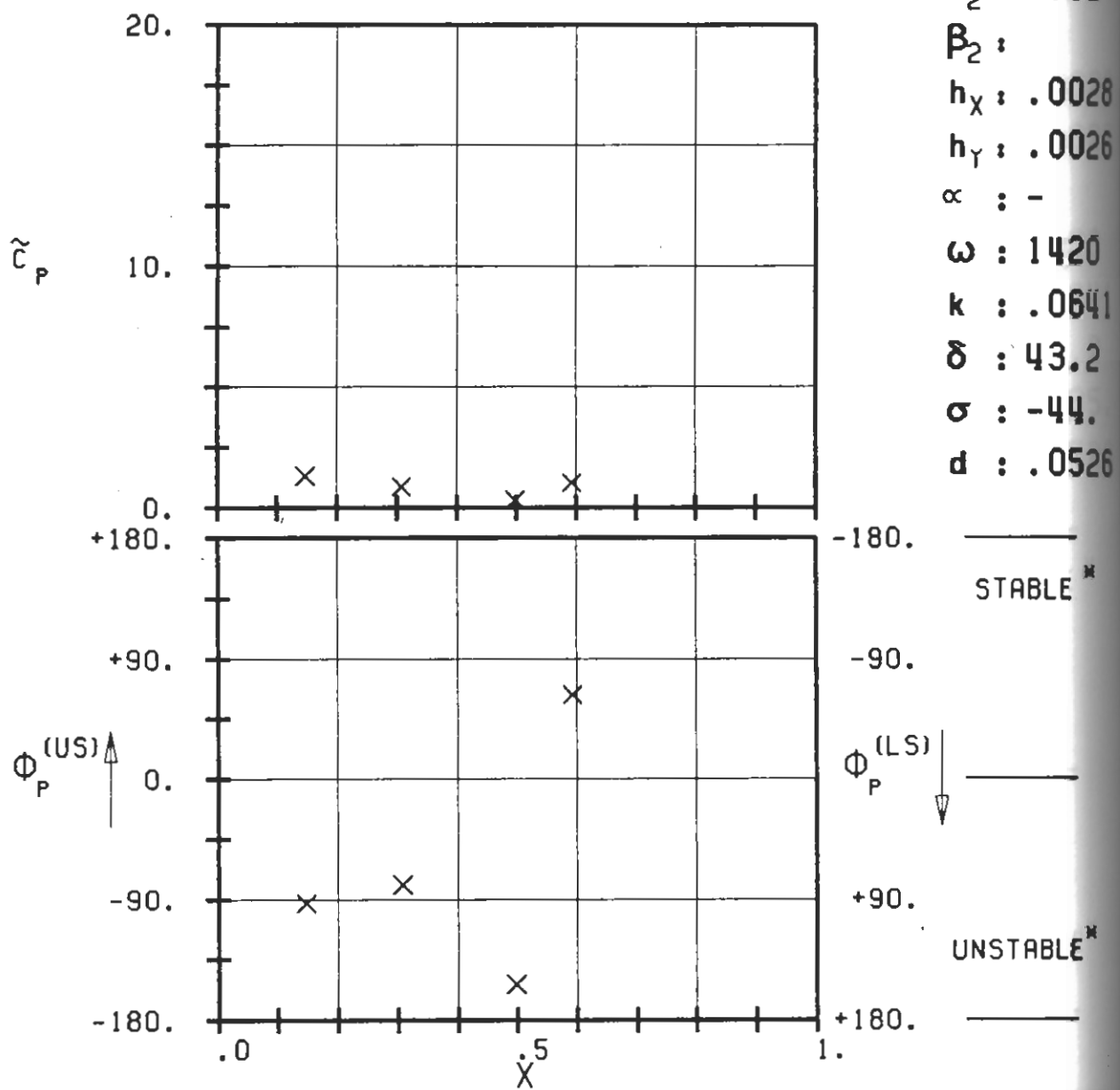
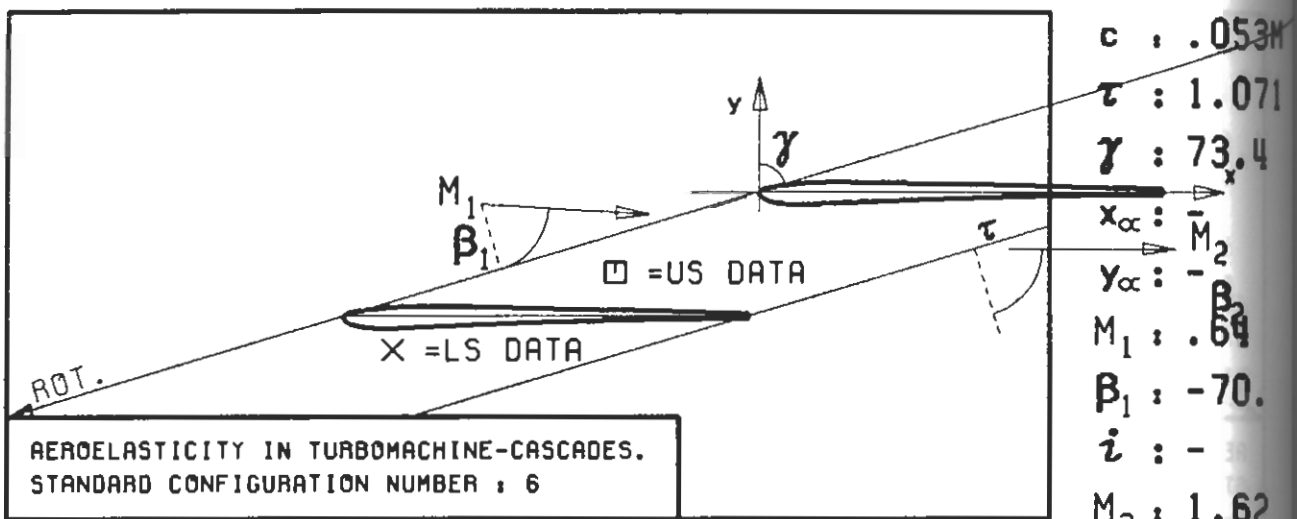
PLT 7.6-2.6: SIXTH STANDARD CONFIGURATION, CASE 6.
MAGNITUDE AND PHASE LEAD OF UNSTEADY BLADE
SURFACE PRESSURE COEFFICIENT.

(X: IN PITCH MODE, NOTATION VALID UPSTREAM OF PITCH AXIS)



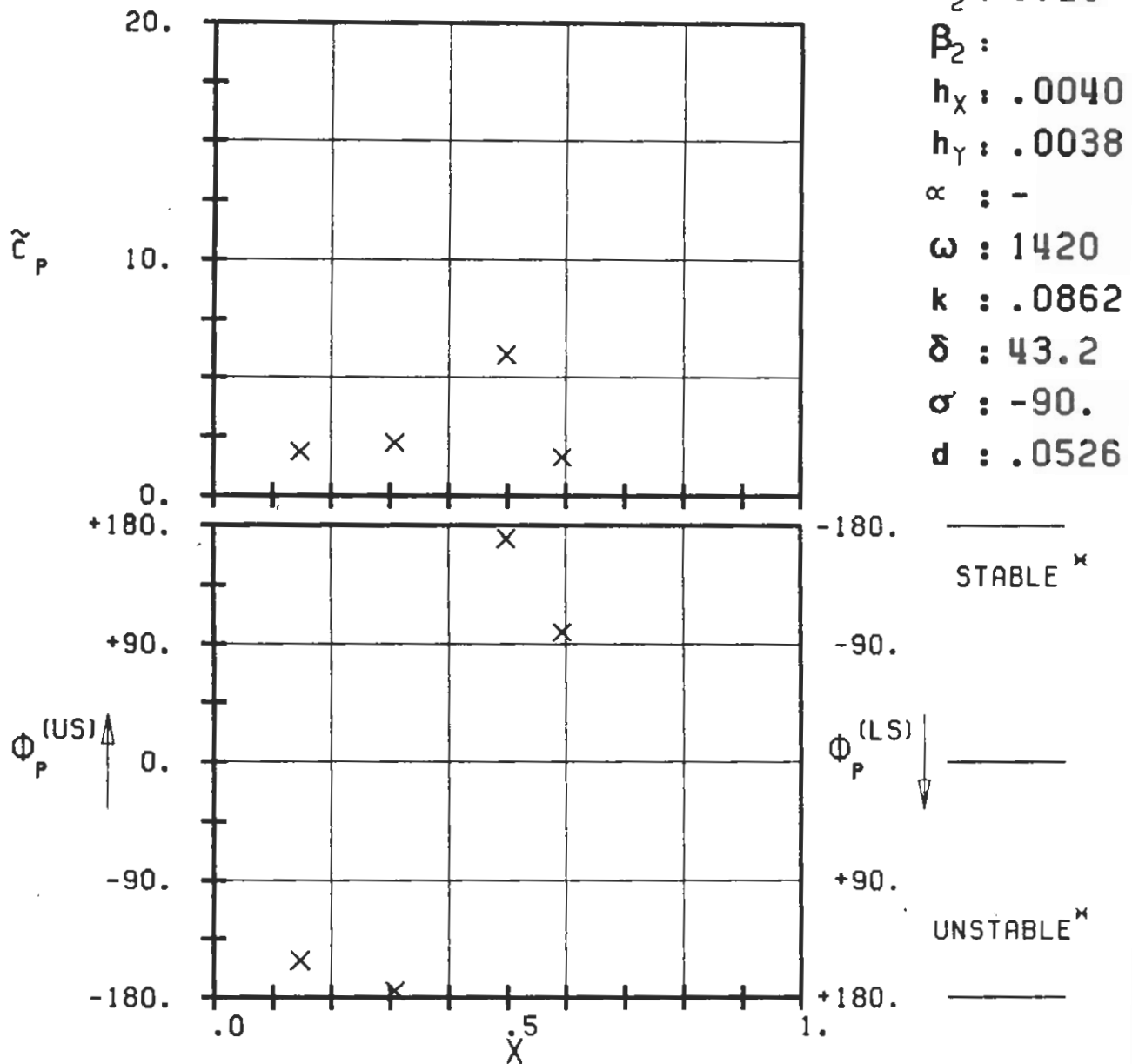
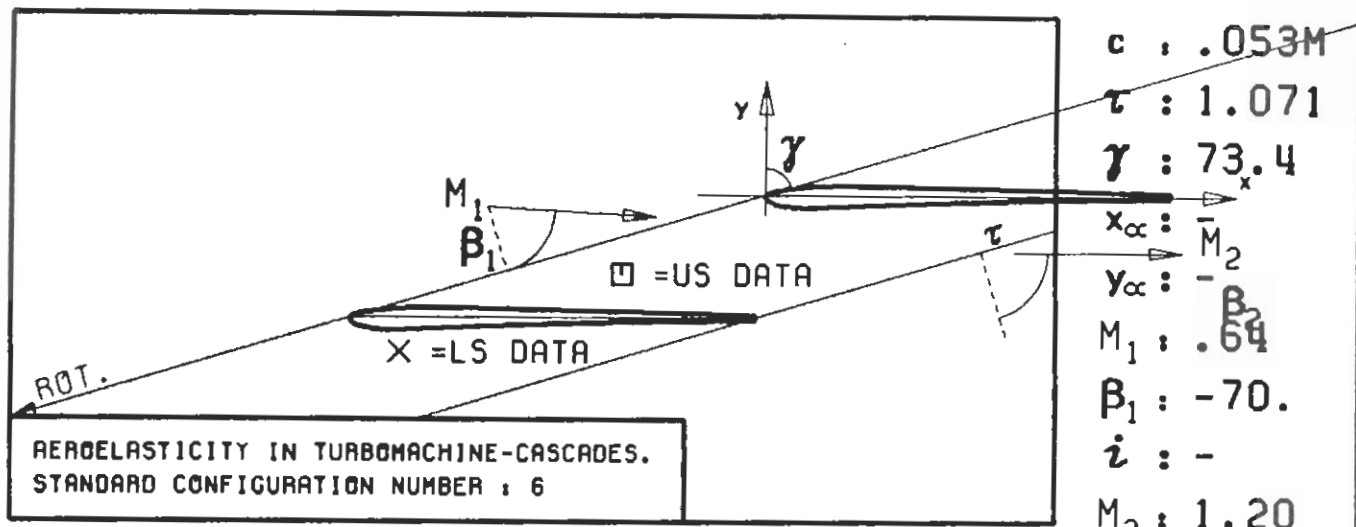
PLOT 7.6-2.7: SIXTH STANDARD CONFIGURATION, CASE 7.
MAGNITUDE AND PHASE LEAD OF UNSTEADY BLADE
SURFACE PRESSURE COEFFICIENT.

(x: IN PITCH MODE, NOTATION VALID UPSTREAM OF PITCH AXIS)



PLOT 7.6-2.8: SIXTH STANDARD CONFIGURATION, CASE 8.
MAGNITUDE AND PHASE LEAD OF UNSTEADY BLADE SURFACE PRESSURE COEFFICIENT.

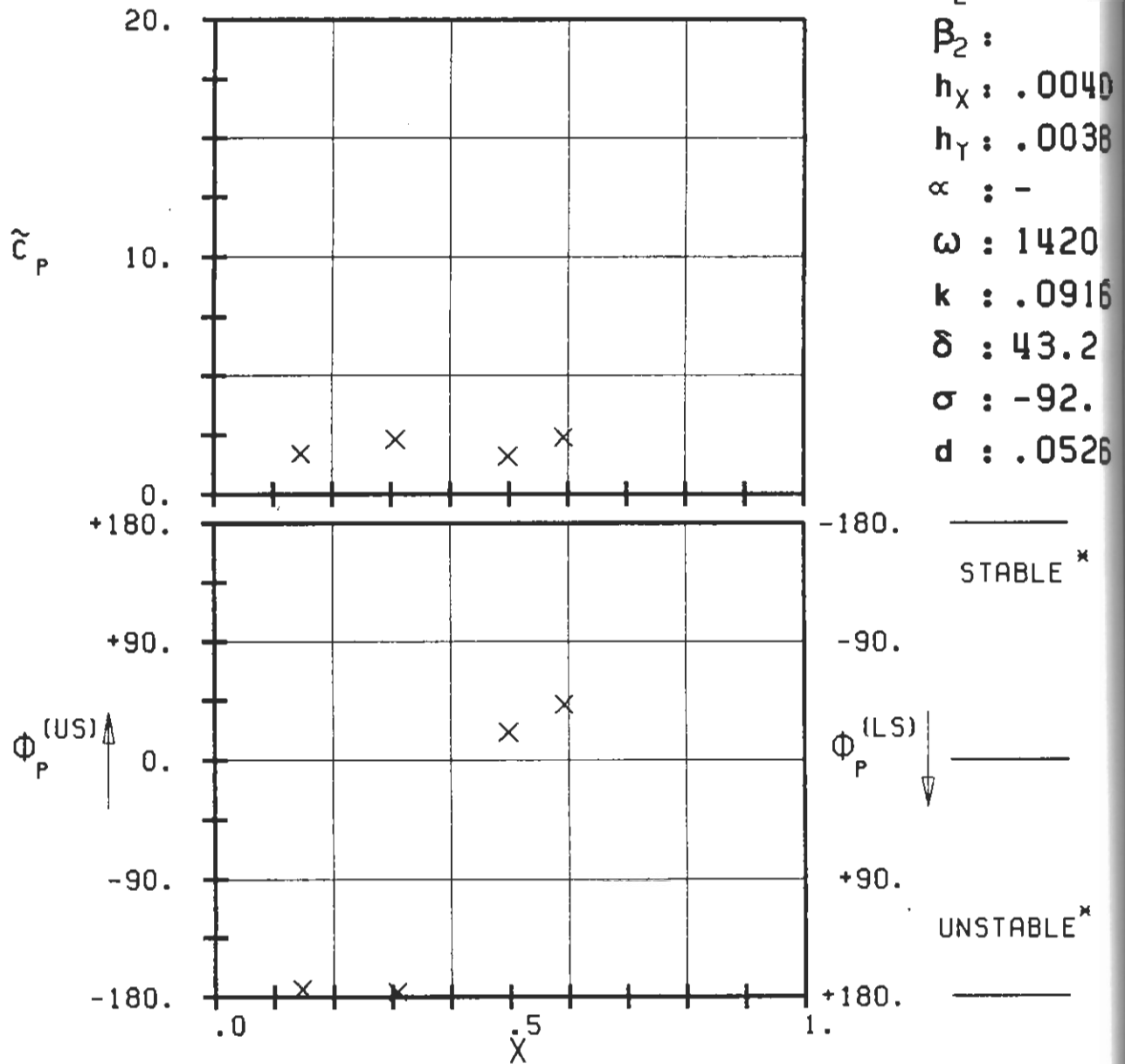
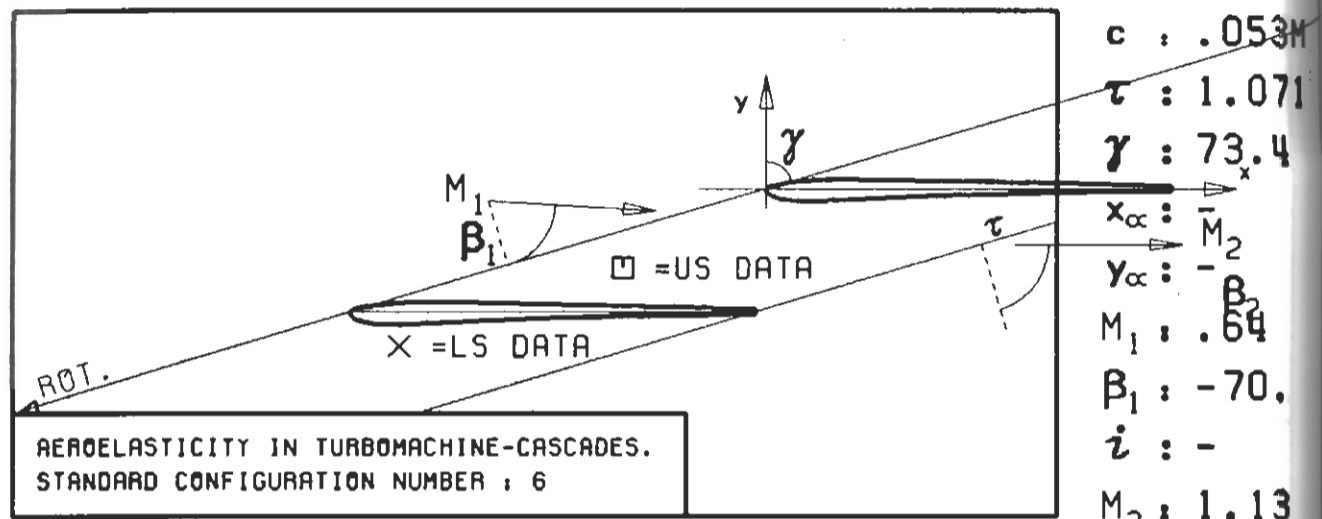
(x: IN PITCH MODE, NOTATION VALID UPSTREAM OF PITCH AXIS)



PLOT 7.6-2.9: SIXTH STANDARD CONFIGURATION, CASE 9.
 MAGNITUDE AND PHASE LEAD OF UNSTEADY BLADE
 SURFACE PRESSURE COEFFICIENT.

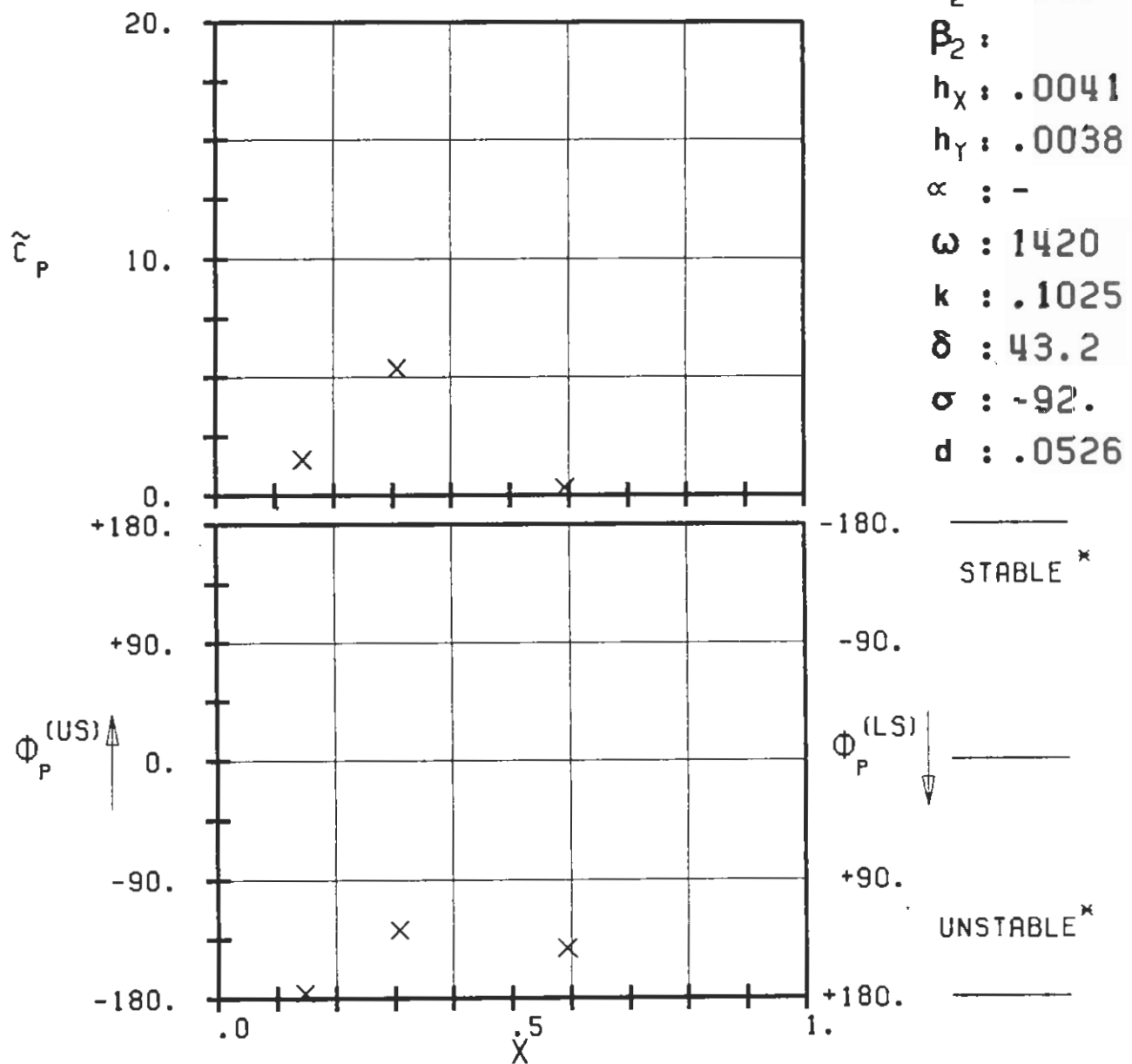
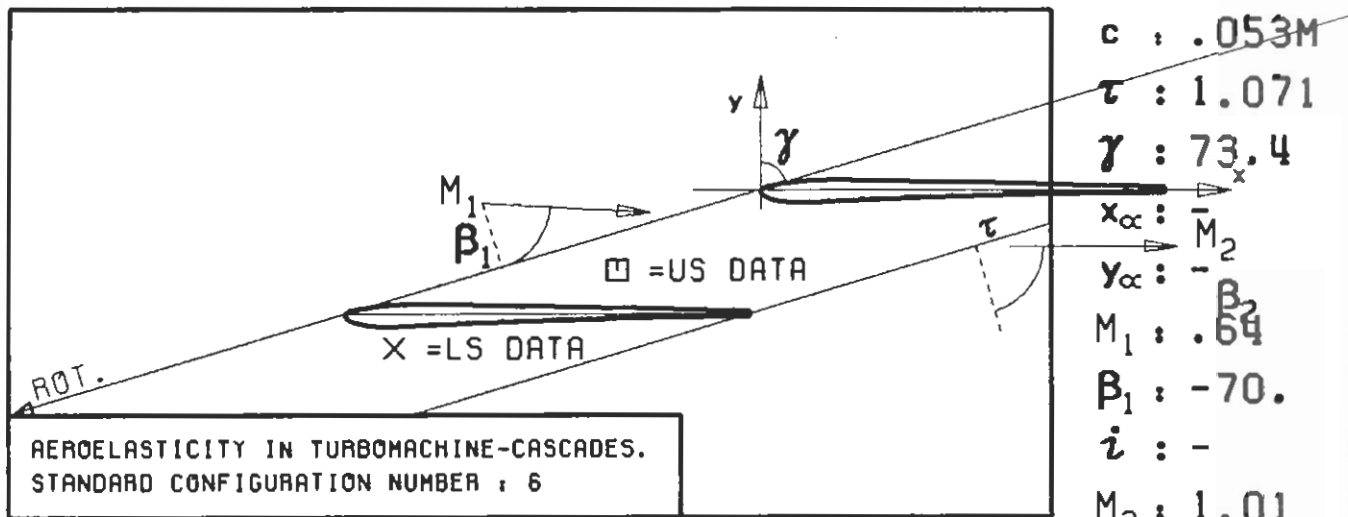
(\times : IN PITCH MODE, NOTATION VALID UPSTREAM OF PITCH AXIS)

$c : .053M$
 $\tau : 1.071$
 $\gamma : 73.4$
 $x_{\infty} : M_2$
 $y_{\infty} : -\beta_2$
 $M_1 : .64$
 $\beta_1 : -70.$
 $i : -$
 $M_2 : 1.20$
 $\beta_2 :$
 $h_X : .0040$
 $h_Y : .0038$
 $\alpha : -$
 $\omega : 1420$
 $k : .0862$
 $\delta : 43.2$
 $\sigma : -90.$
 $d : .0526$



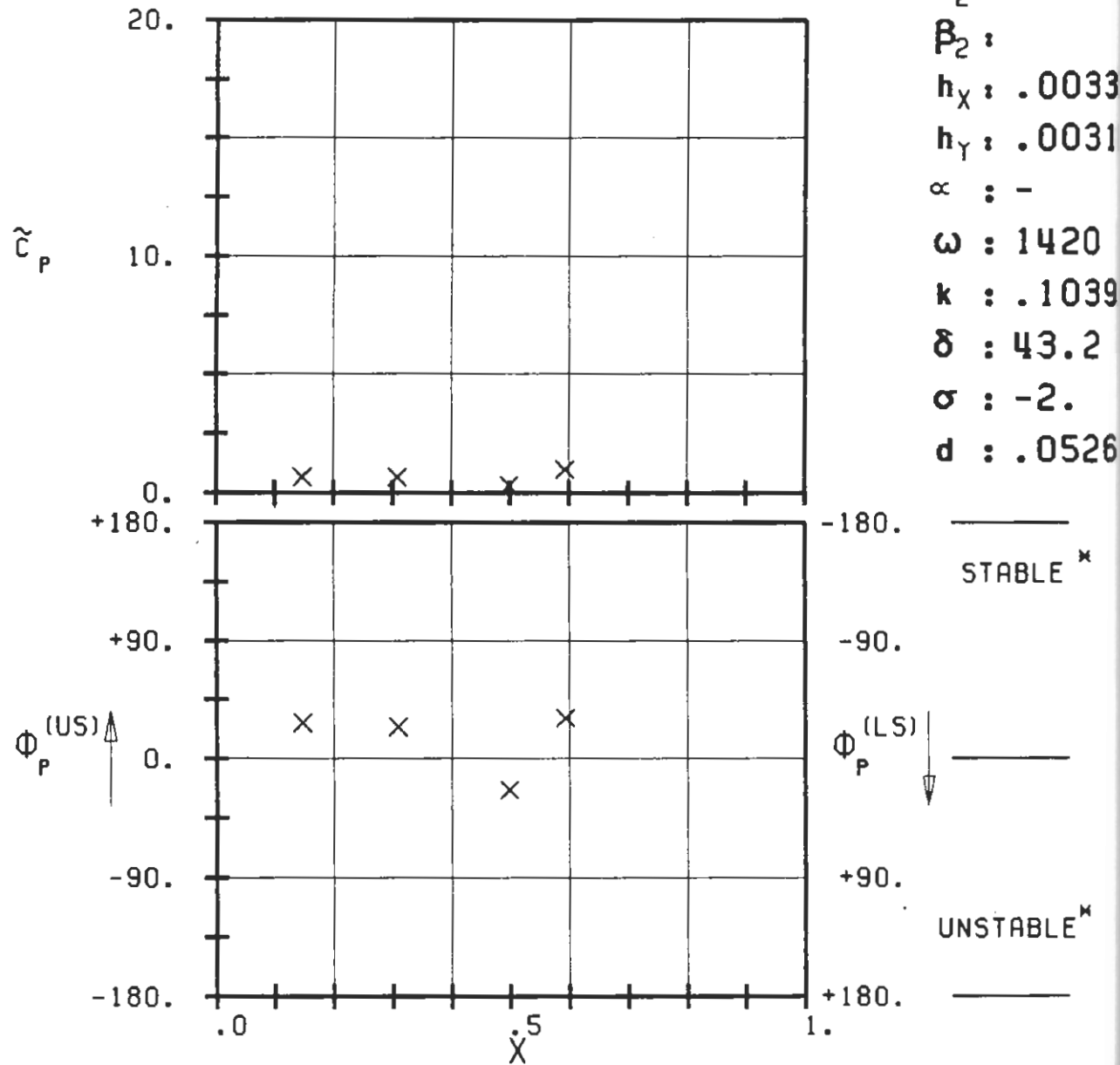
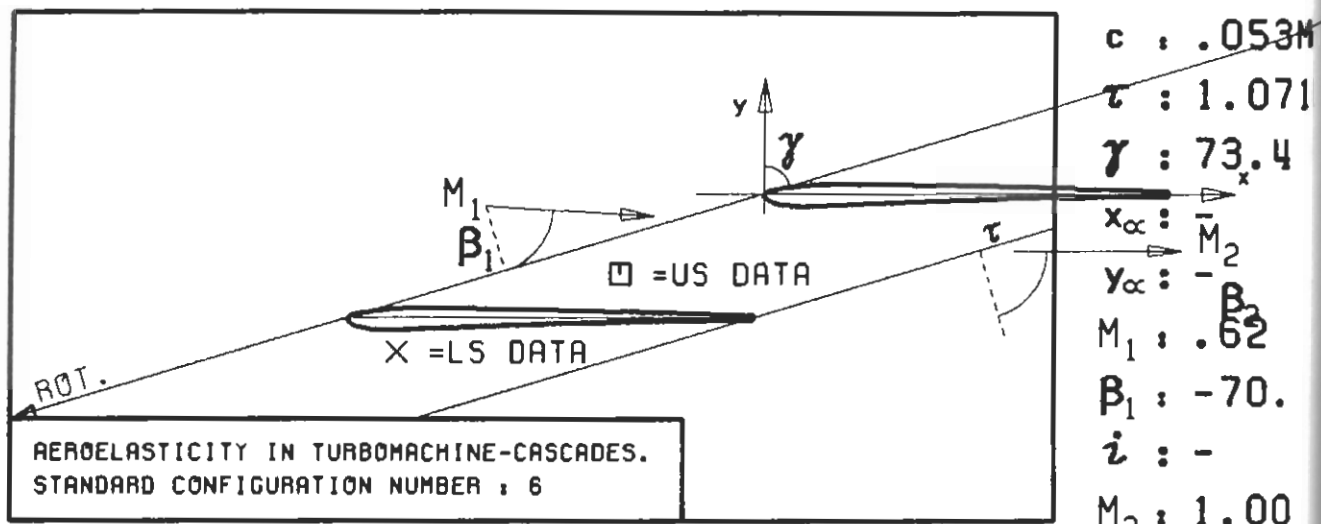
PLOT 7.6-2.10: SIXTH STANDARD CONFIGURATION, CASE 10.
MAGNITUDE AND PHASE LEAD OF UNSTEADY BLADE
SURFACE PRESSURE COEFFICIENT.

(x: IN PITCH MODE, NOTATION VALID UPSTREAM OF PITCH AXIS)



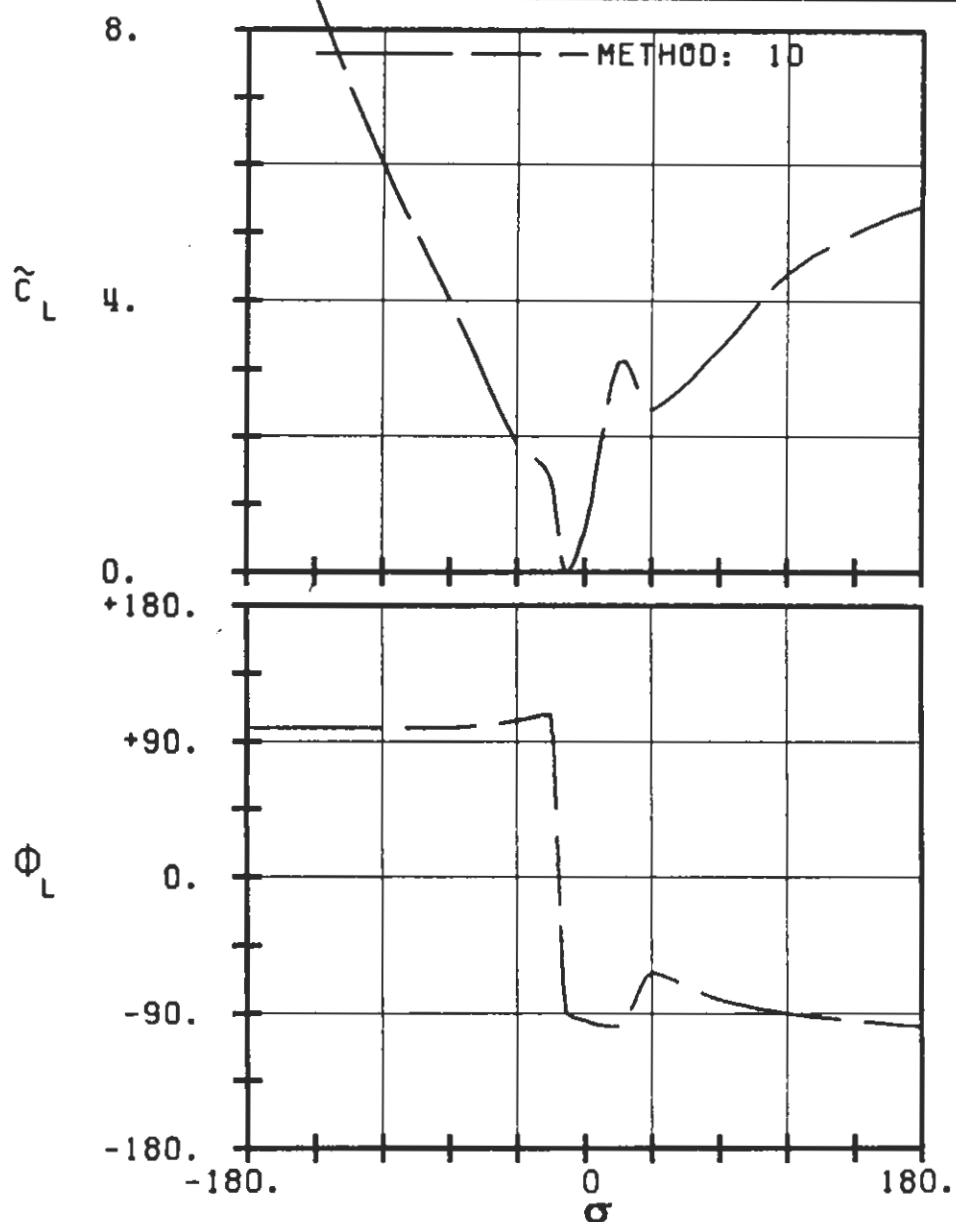
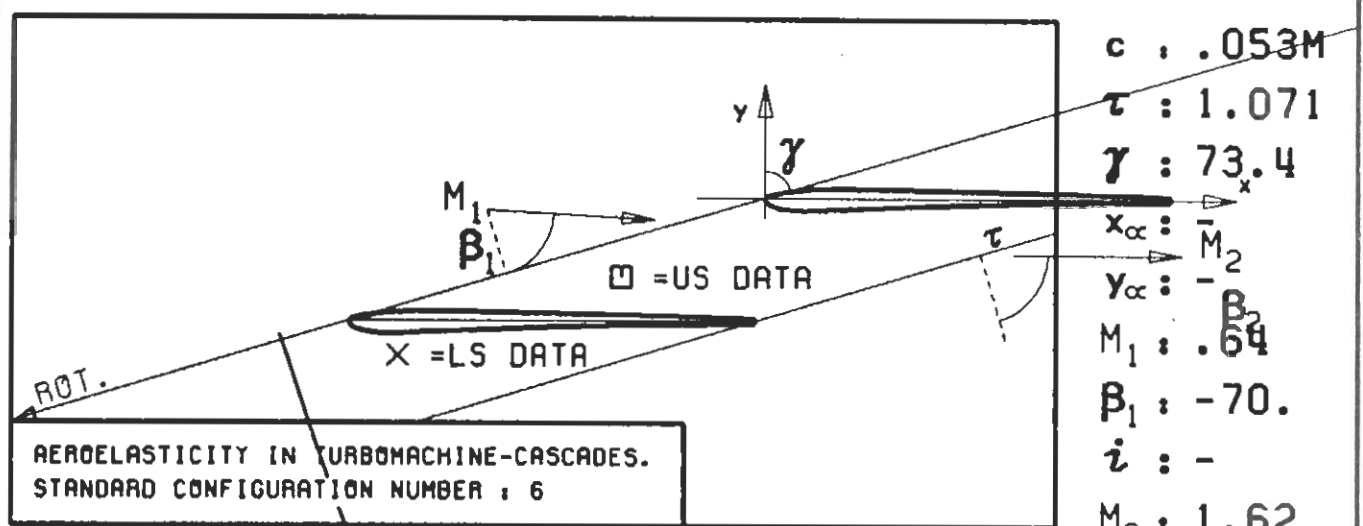
PLOT 7.6-2.11: SIXTH STANDARD CONFIGURATION, CASE 11.
 MAGNITUDE AND PHASE LEAD OF UNSTEADY BLADE
 SURFACE PRESSURE COEFFICIENT.

(*: IN PITCH MODE, NOTATION VALID UPSTREAM OF PITCH AXIS)

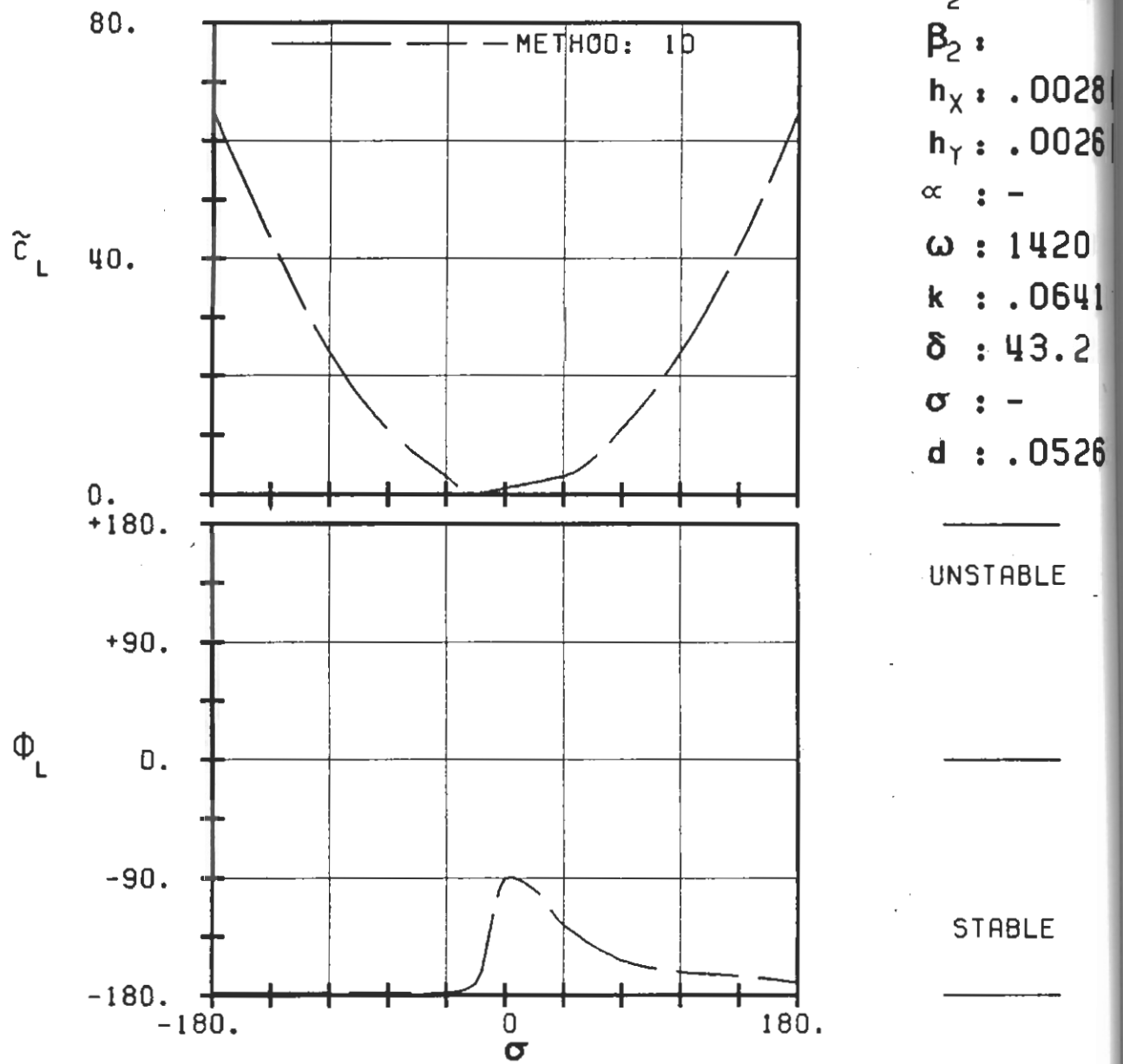
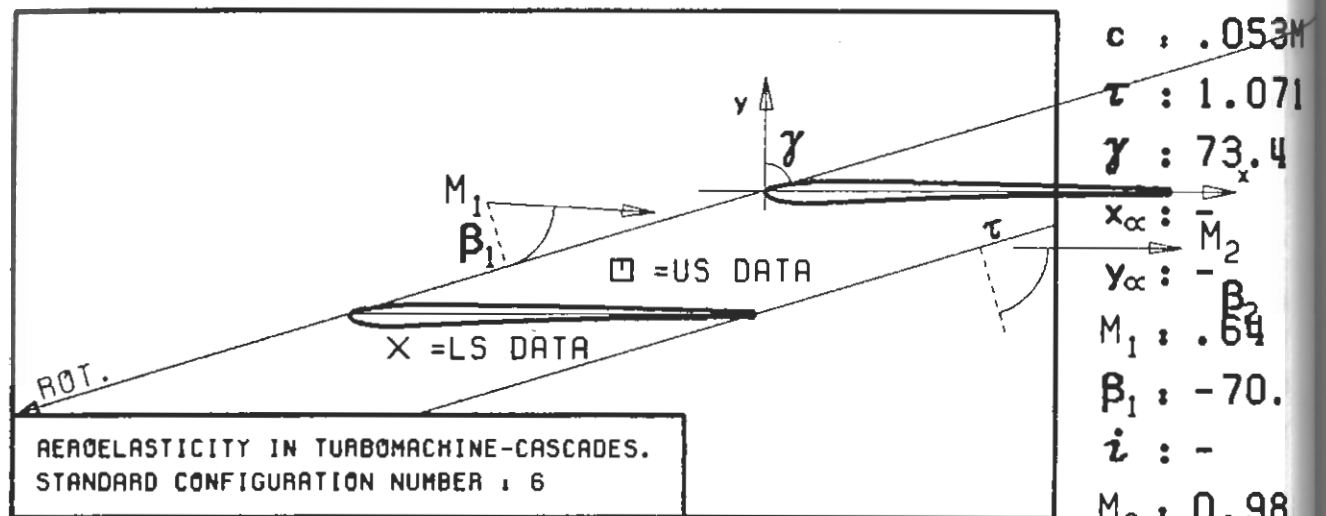


PLOT 7.6-2.12: SIXTH STANDARD CONFIGURATION, CASE 12.
 MAGNITUDE AND PHASE LEAD OF UNSTEADY BLADE
 SURFACE PRESSURE COEFFICIENT.

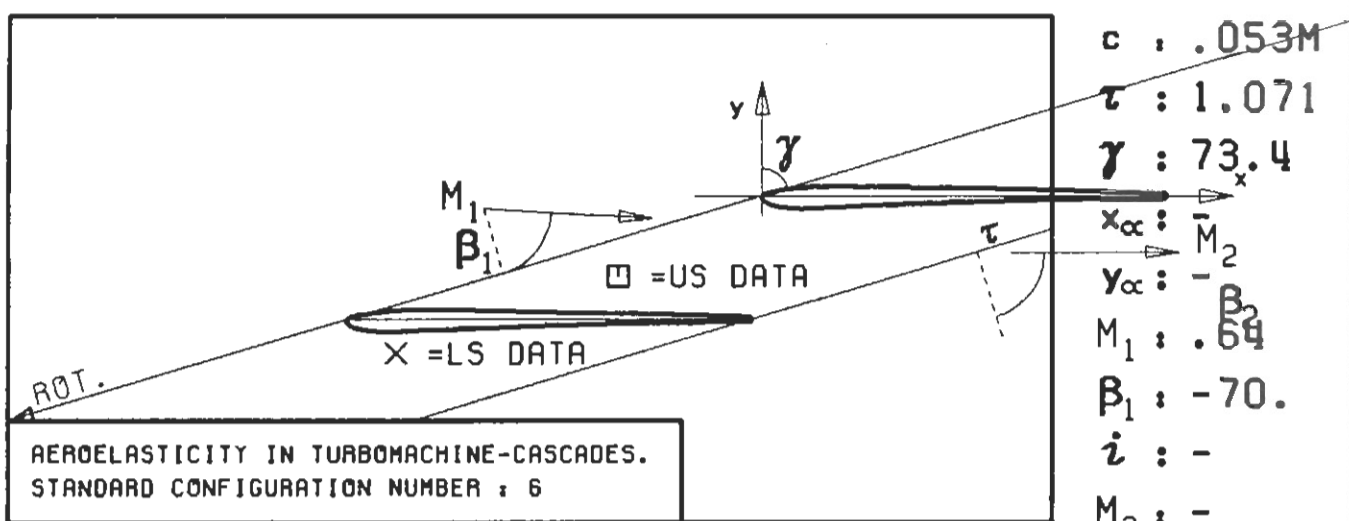
(x: IN PITCH MODE, NOTATION VALID UPSTREAM OF PITCH AXIS)



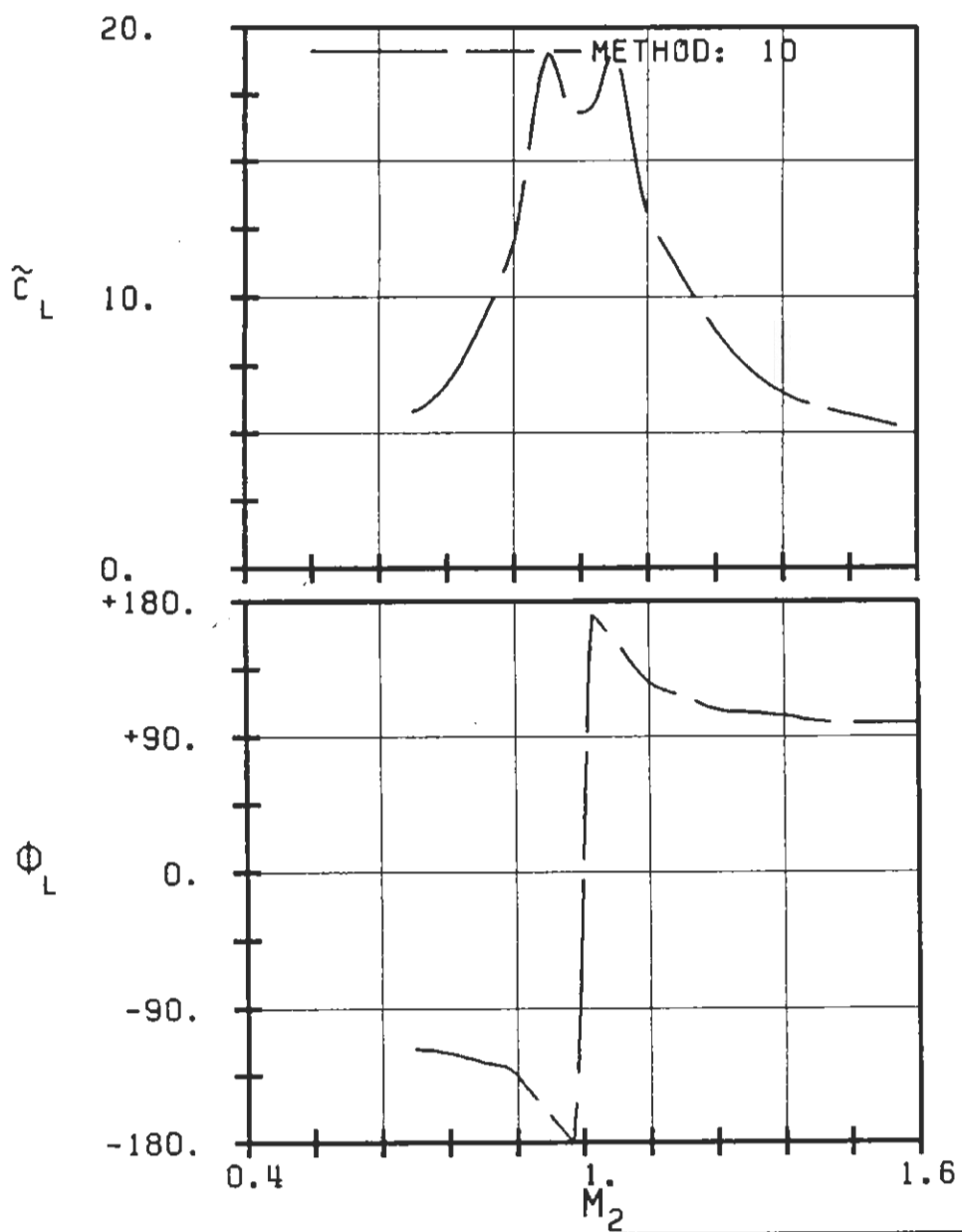
PLOT 7.6-4.1: SIXTH STANDARD CONFIGURATION, CASES 1-8.
 AERODYNAMIC LIFT COEFFICIENT AND PHASE LEAD
 IN DEPENDENCE OF INTERBLADE PHASE ANGLE.



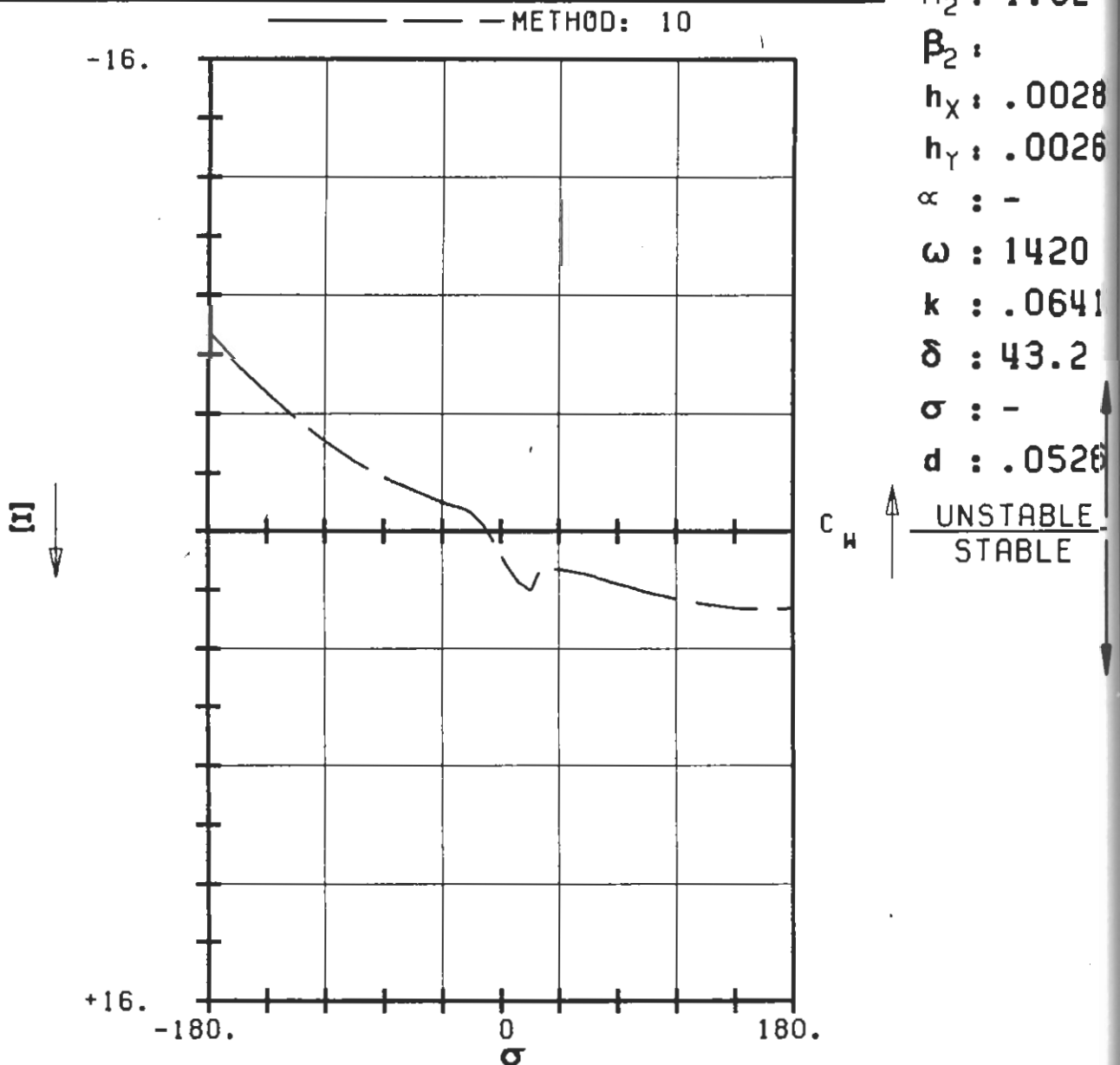
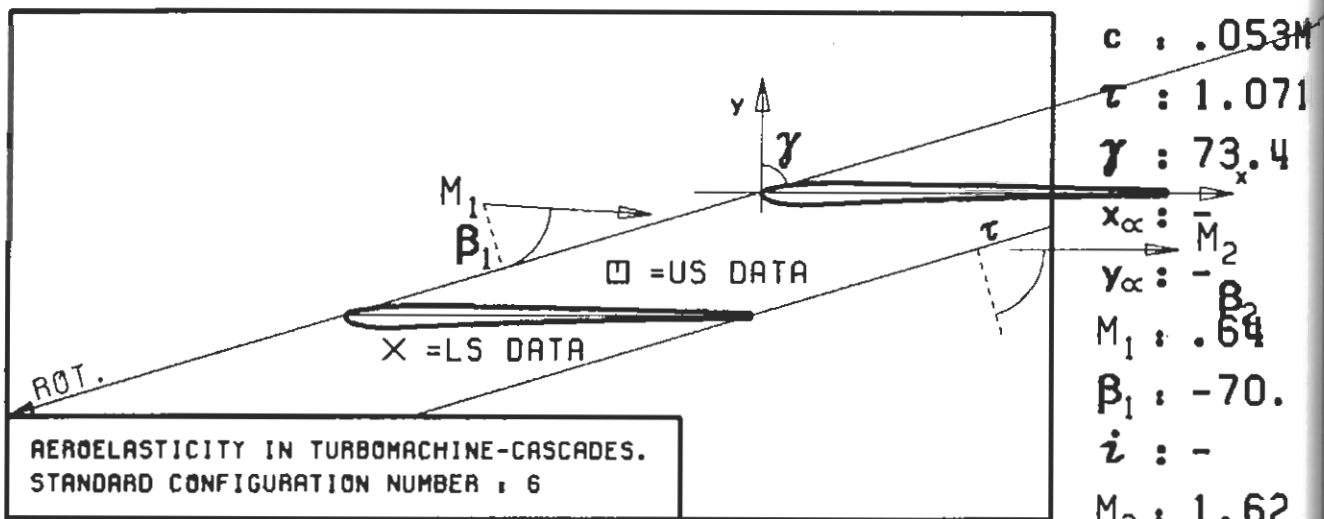
PLOT 7.6-4.2: SIXTH STANDARD CONFIGURATION.
 AERODYNAMIC LIFT COEFFICIENT AND PHASE LEAD
 IN DEPENDANCE OF INTERBLADE PHASE ANGLE.



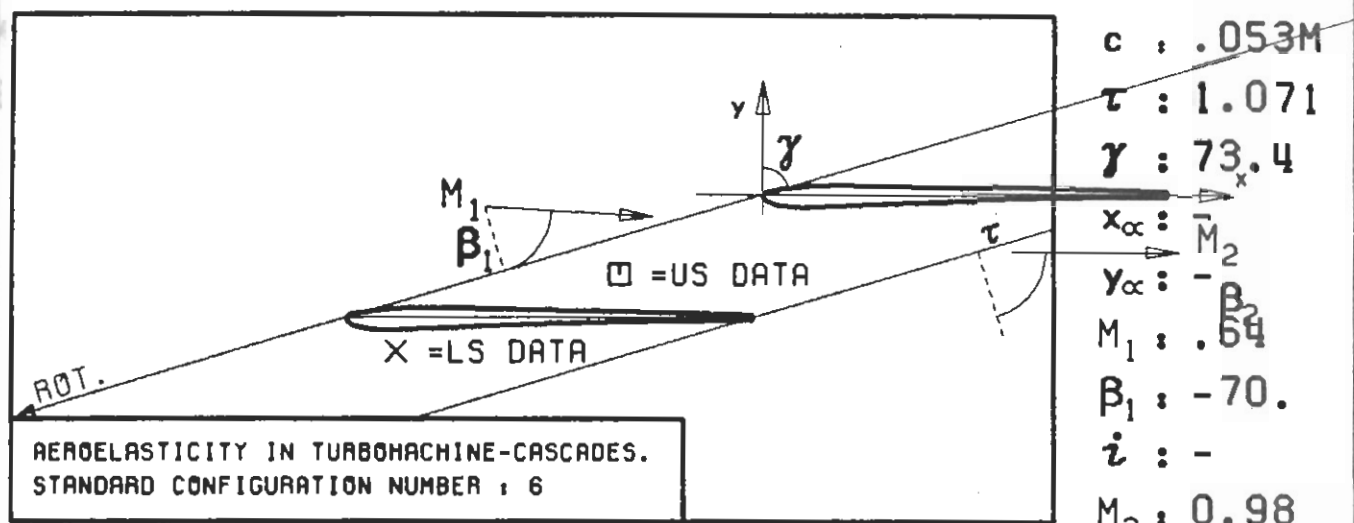
$c : .053M$
 $\tau : 1.071$
 $\gamma : 73.4$
 $x_\alpha : -M_2$
 $y_\alpha : -B_2$
 $M_1 : .64$
 $B_1 : -70.$
 $i : -$
 $M_2 : -$
 $B_2 : -$
 $h_x : -$
 $h_y : -$
 $\alpha : -$
 $\omega : 1420$
 $k : -$
 $\delta : 43.2$
 $\sigma : -90$
 $d : .0526$



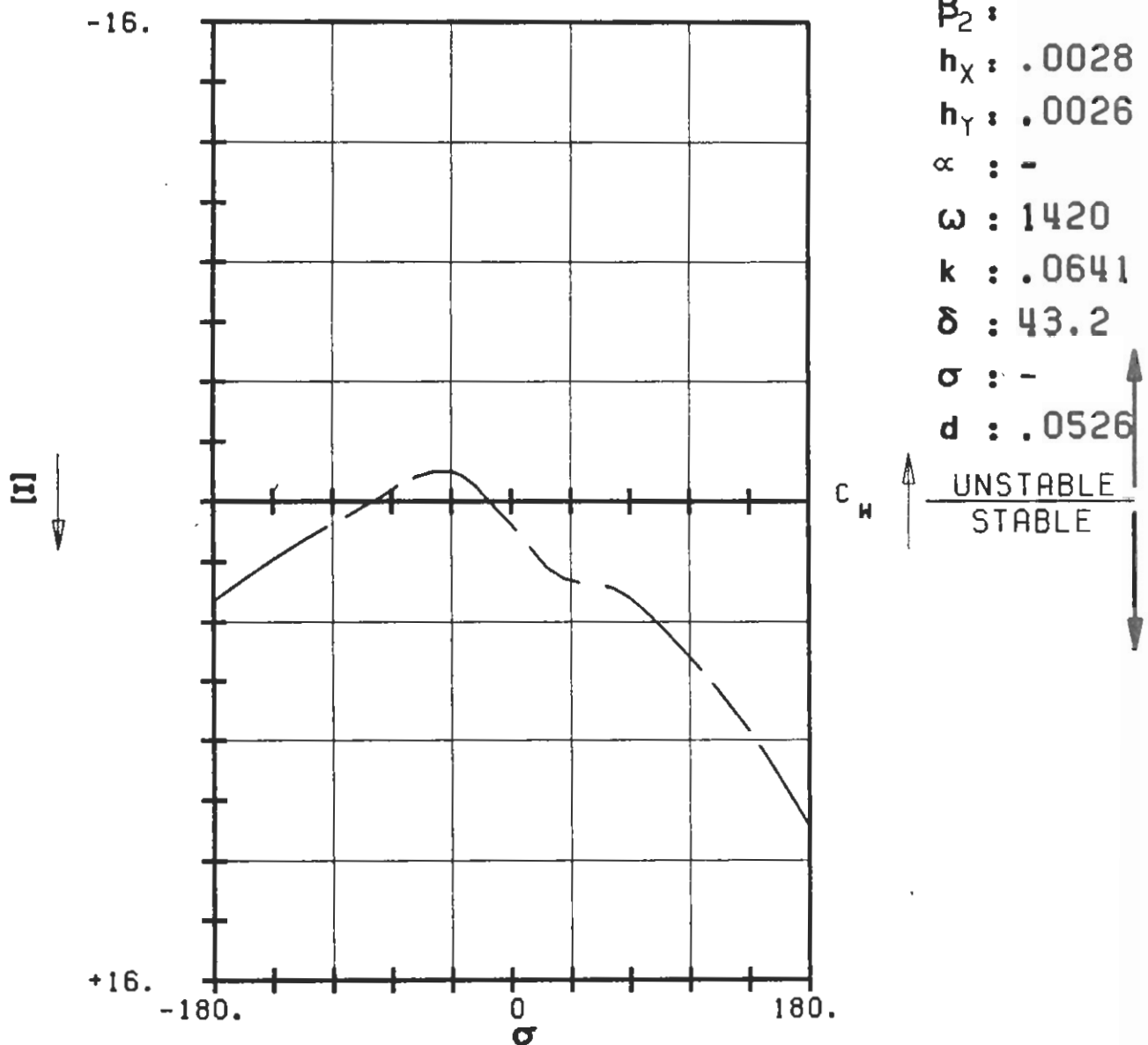
PLOT 7.6-4.3: SIXTH STANDARD CONFIGURATION.
 AERODYNAMIC LIFT COEFFICIENT AND PHASE LEAD
 IN DEPENDENCE OF OUTLET ISENTROPIC VELOCITY



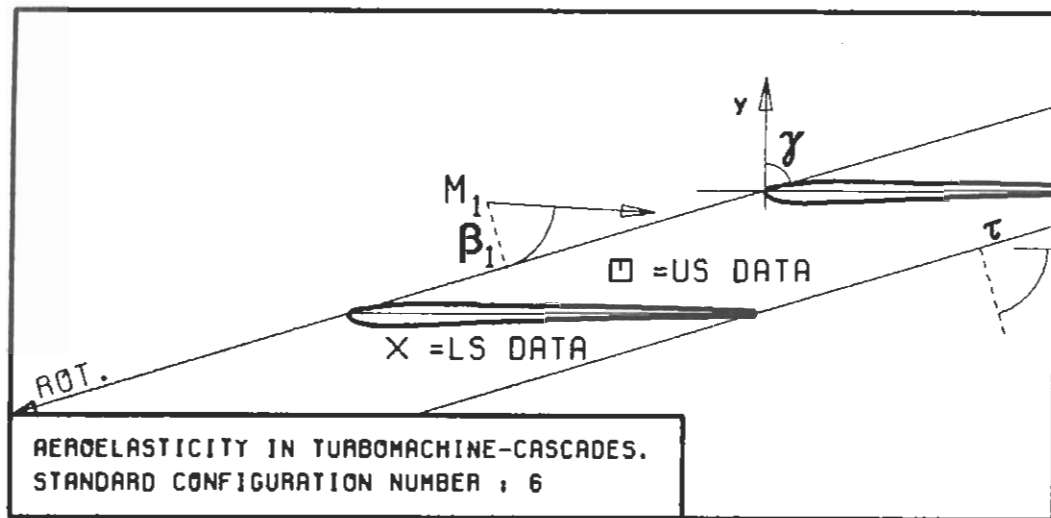
**PLOT 7.6-6.1: SIXTH STANDARD CONFIGURATION, CASES 1-8.
AERODYNAMIC WORK AND DAMPING COEFFICIENTS
IN DEPENDANCE OF INTERBLADE PHASE ANGLE.**



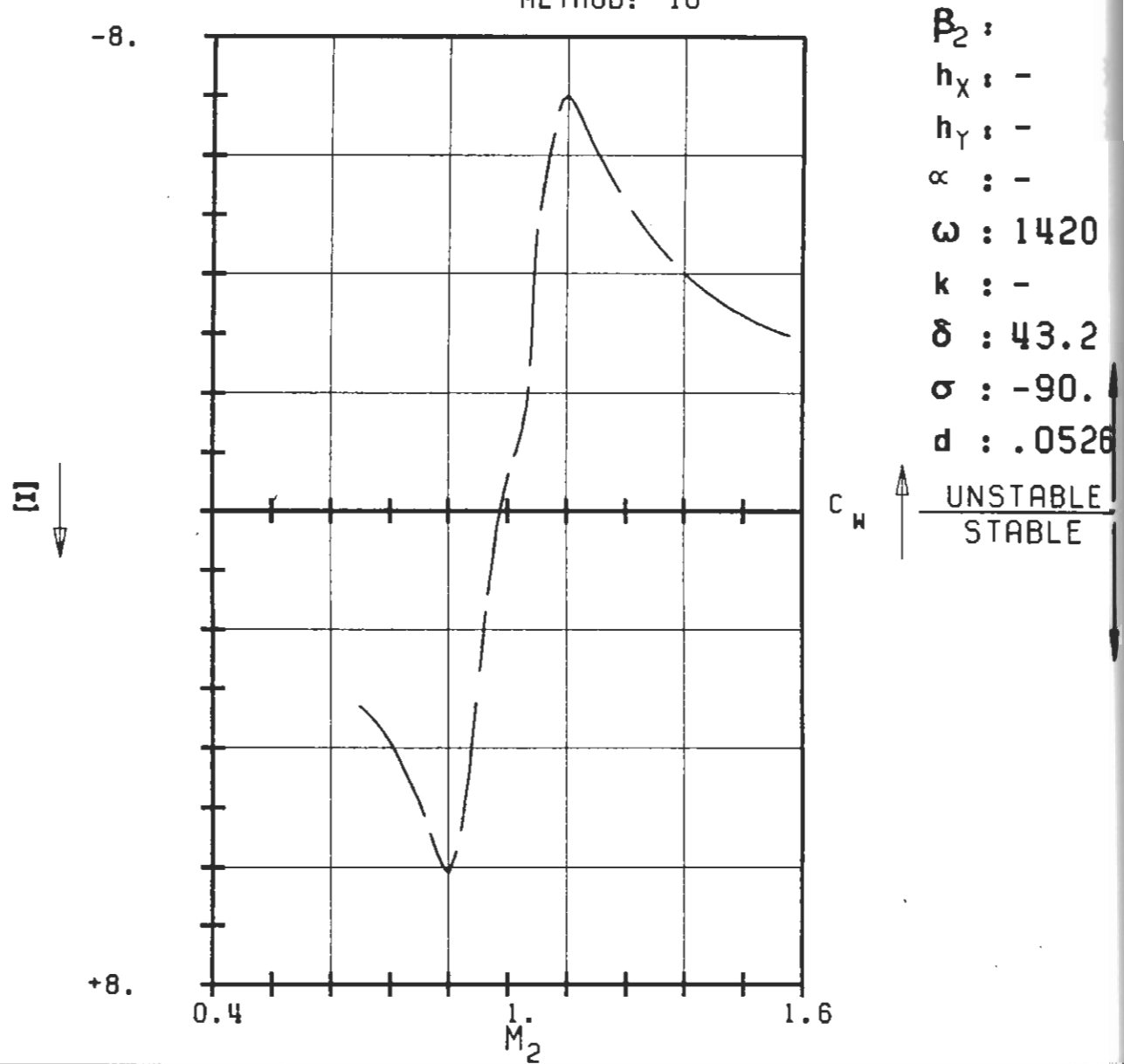
— — — METHOD: 10



PLOT 7.6-6.2: SIXTH STANDARD CONFIGURATION.
 AERODYNAMIC WORK AND DAMPING COEFFICIENTS
 IN DEPENDANCE OF INTERBLADE PHASE ANGLE.



c : .0531
 τ : 1.071
 γ : 73.4
 x_{α} : M_2
 y_{α} : -
 M_1 : .64
 β_1 : -70.
 i : -
 M_2 : -
 β_2 : -
 h_x : -
 h_y : -
 α : -
 ω : 1420
 k : -
 δ : 43.2
 σ : -90.
 d : .0526



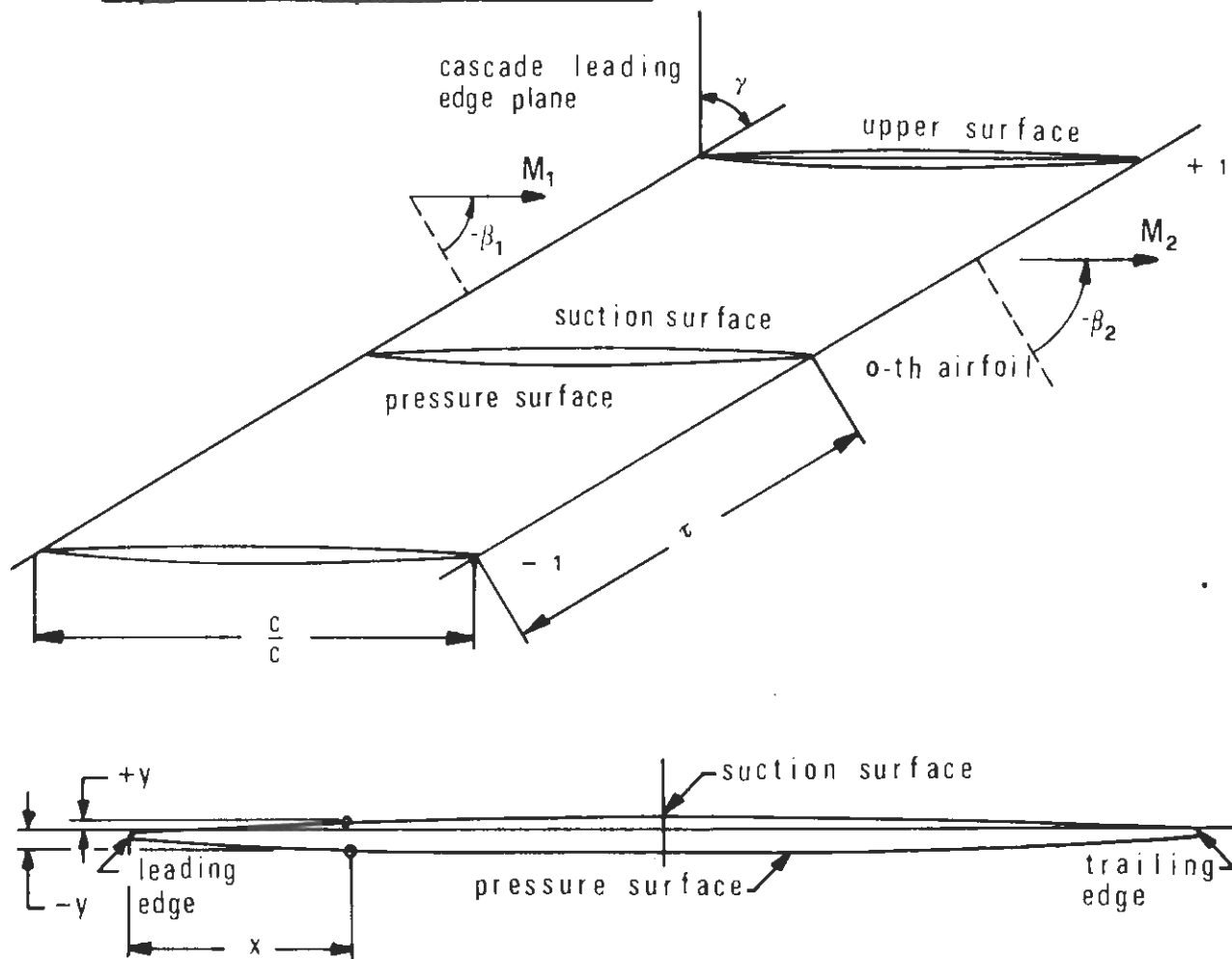
PLOT 7.6-6.3: SIXTH STANDARD CONFIGURATION,
AERODYNAMIC WORK AND DAMPING COEFFICIENTS
IN DEPENDANCE OF OUTLET ISENTROPIC VELOCITY

AEROELASTICITY IN TURBOMACHINE-CASCADES

SEVENTH STANDARD CONFIGURATION

Definition

Supersonic Compressor Profiles.



Vibration in pitch around (x_α, y_α)	= (0.5,0.0)
d = (thickness/chord)	= 0.034
α = 0.06-0.2°	M_2 = variable
c = 0.0762 m	β_1 = 64.0°
τ = 0.855	camber = -1.30°
k = variable	γ = 61.55°
span = 0.0762 m	f = 710-730 Hz
Working fluid: Air	

Fig. 7.7-1. Seventh standard configuration: Cascade geometry

C = 0.0762 m (3.00 in)					
	Upper surface (SUCTION SURFACE)		Lower surface (PRESSURE SURFACE)		
	X	+Y	X	-Y	
	0	-0.0029		0	0.0029
	0.0026	-0.0004		0.0027	0.0056
	0.0078	0.0015		0.0279	0.0066
	0.0655	0.0041		0.0657	0.0079
	0.1032	0.0065		0.1035	0.0092
	0.1410	0.0087		0.1412	0.0103
	0.1788	0.0107		0.1790	0.0113
	0.2165	0.0124		0.2168	0.0123
	0.2543	0.0139		0.2546	0.0131
	0.2921	0.0152		0.2923	0.0138
	0.3299	0.0162		0.3301	0.0144
	0.3551	0.0168		0.3552	0.0148
	0.3929	0.0175		0.3930	0.0152
	0.4307	0.0179		0.4308	0.0155
	0.4685	0.0181		0.4685	0.0158
	0.5063	0.0181		0.5063	0.0159
	0.5441	0.0179		0.5440	0.0159
	0.5820	0.0174		0.5818	0.0158
	0.6198	0.0167		0.6195	0.0156
	0.6576	0.0158		0.6573	0.0153
	0.6828	0.0150		0.6824	0.0151
	0.7205	0.0157		0.7202	0.0146
	0.7583	0.0122		0.7580	0.0140
	0.7961	0.0105		0.7958	0.0153
	0.8338	0.0087		0.8336	0.0124
	0.8716	0.0067		0.8714	0.0112
	0.9093	0.0047		0.9092	0.0098
	0.9471	0.0026		0.9470	0.0082
	0.9848	0.0003		0.9848	0.0063
	0.9974	-0.0005		0.9974	0.0057
	1.0000	-0.0029		1.0000	0.0029

L.E. RADIUS/C = 0.0027
T.E. RADIUS/C = 0.0027

Table 7.7-1. Seventh Standard Configuration: Dimensionless Airfoil Coordinates.

AEROELASTICITY IN TURBOMACHINE-CASCADES

SEVENTH STANDARD CONFIGURATION

Aeroelastic Test Cases

Aeroelastic Test Case No	M ₁ (-)	β_1 ($^{\circ}$)	P _{w2} /P _{w1} (-)	P ₂ /P ₁ (-)	M ₂ (-)	β_2 ($^{\circ}$)
1-6	1.315	- 64.0	0.958	1.04	1.25	- 62.8
7-12	"	"	0.957	1.45	0.99	- 63.6

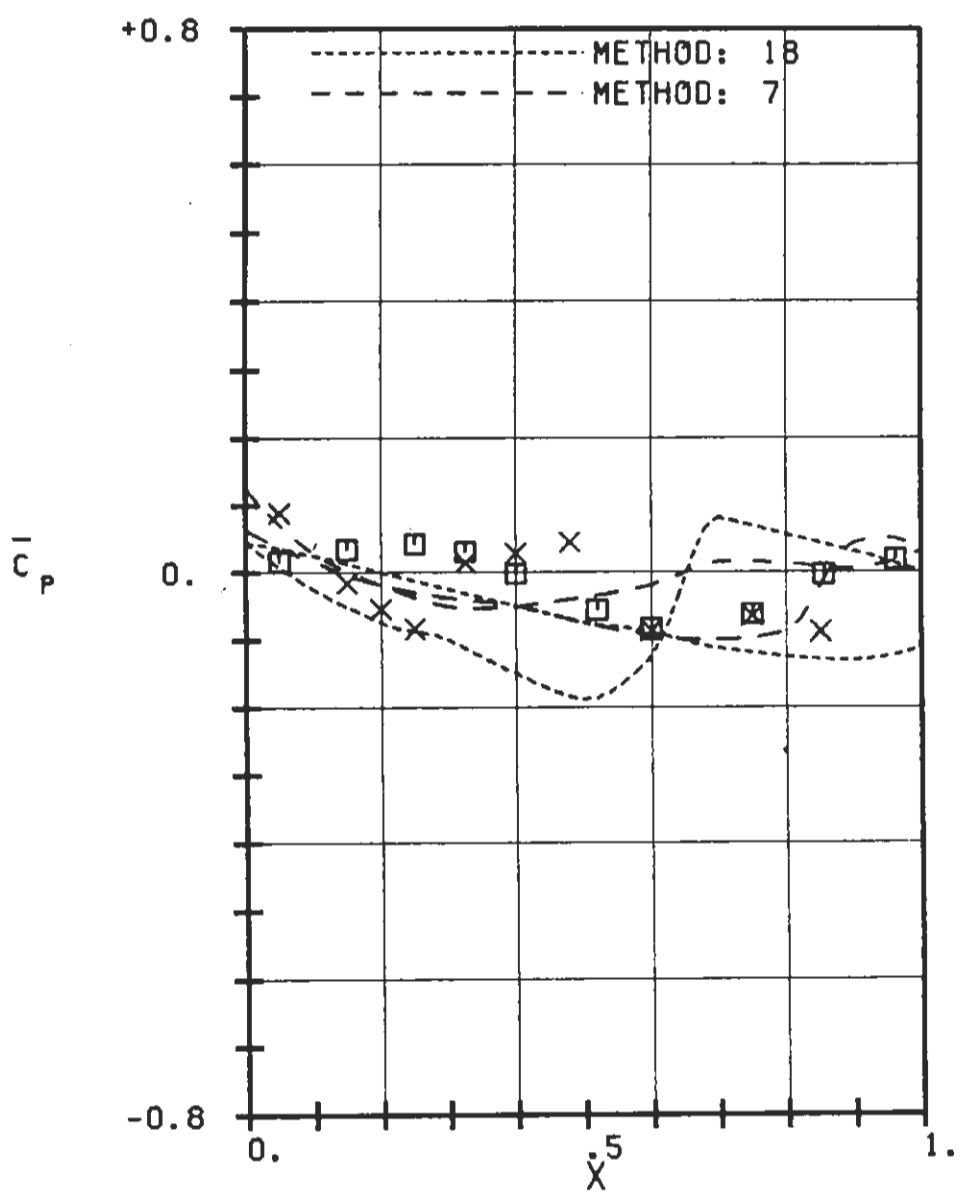
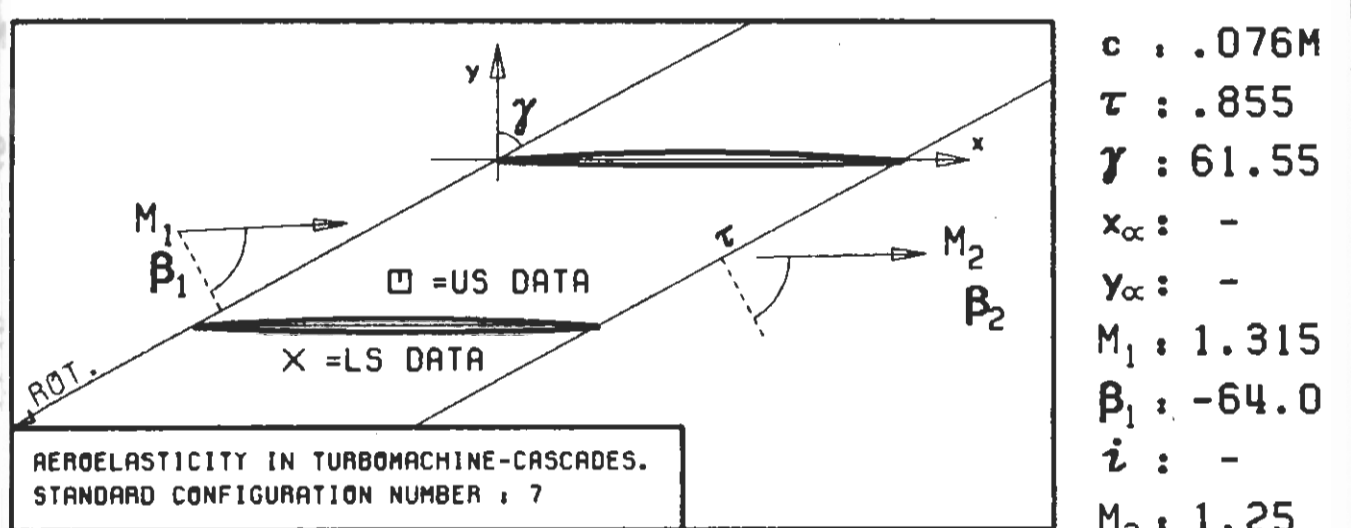
Aeroelastic Test Case No	Time-Dependent Parameters						$\alpha_{nominal}$ (rad)	$\alpha_{nominal}$ (rad)	α^{-2}/α^* ($^{\circ}$)	α^{-1}/α^* ($^{\circ}$)	α^0/α^* ($^{\circ}$)	α^{+1}/α^* ($^{\circ}$)	α^{+2}/α^* ($^{\circ}$)					
	f _{nominal} (Hz)	k (-)	σ^{-1} ($^{\circ}$)	σ^0 ($^{\circ}$)	σ^{+1} ($^{\circ}$)	σ^{+2} ($^{\circ}$)												
1	725	725	0.44	-180	-173	-187	-178	-180	0.00349	0.76	0.52	0.00122	1.27	0.0				
2	"	714	0.43	-90	-91	-65	-81	-80	"	0.87	0.20	"	"	0.67				
3	"	-	0.44	-45	-	-	-	-	"	-	-	-	-	-				
4	"	724	"	0	+	4	+	6	"	0.34	0.61	0.00379	0.75	"				
5	"	745	0.45	+ 45	+	48	+	53	+	54	+ 50	"	0.00206	0.32	"			
6	"	724	0.44	+ 90	+	91	+	91	+	84	+ 90	"	0.56	0.59	0.00187			
7	"	"	"	-180	-172	-168	-163	-170	"	1.21	0.85	0.00131	0.60	"				
8	"	725	"	-45	-	66	-69	-61	-66	"	0.54	0.44	0.00178	0.34	"			
9	"	724	"	0	-	4	+	8	- 5	0	"	0.64	0.96	0.00202	1.11	"		
10	"	"	"	+ 45	+	66	+	59	+	60	+	60	0.36	0.65	0.00386	0.50	"	
11	"	725	"	+ 90	+	92	+	74	+	86	+	85	"	0.66	0.96	0.00227	0.73	"
12	"	"	"	+ 120	+	96	+	115	+	98	+	100	"	0.35	0.40	0.00129	0.25	"

Table 7.7-2 Seventh standard configuration. 12 experimental aeroelastic test cases (defined from /57,58/)

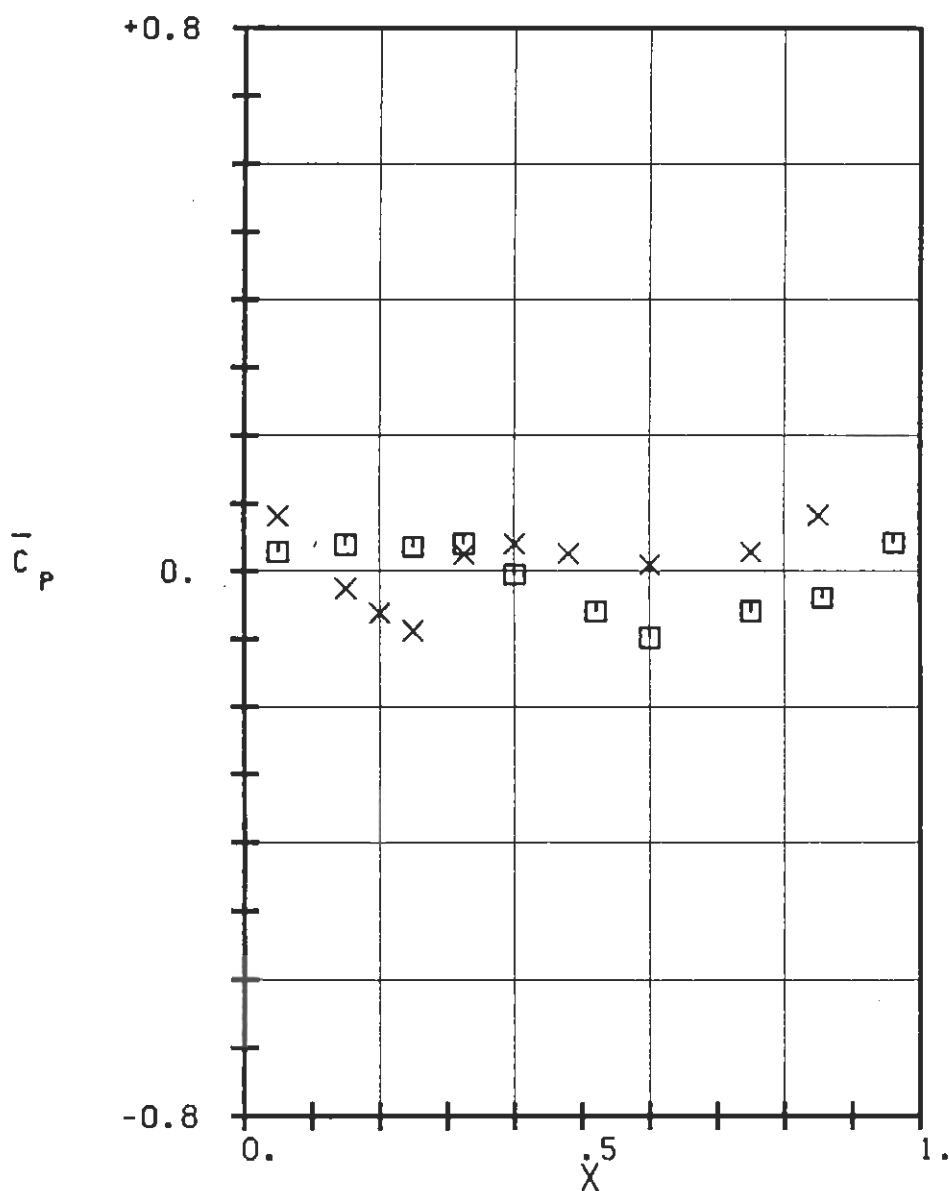
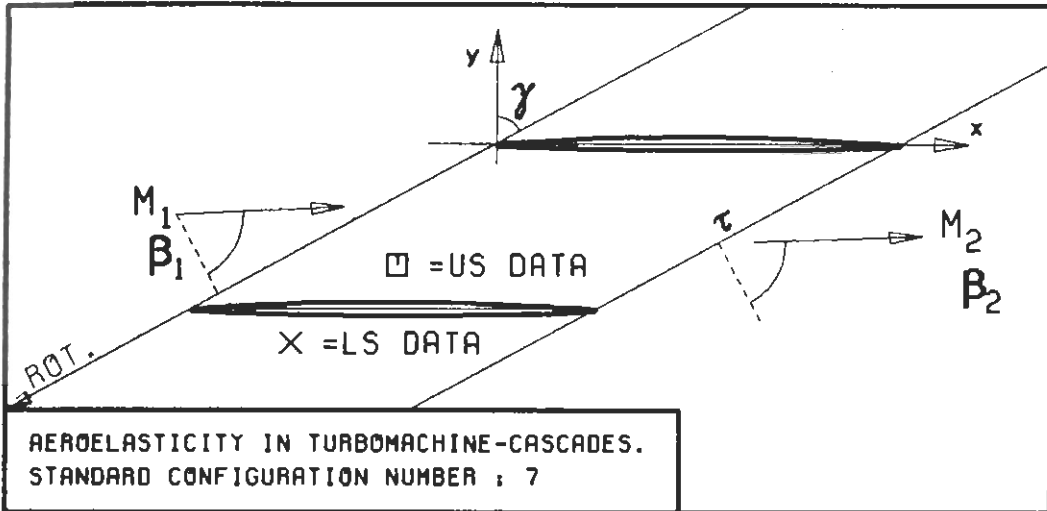
AEROELASTICITY IN TURBOMACHINE-CASCADES

SEVENTH STANDARD CONFIGURATION

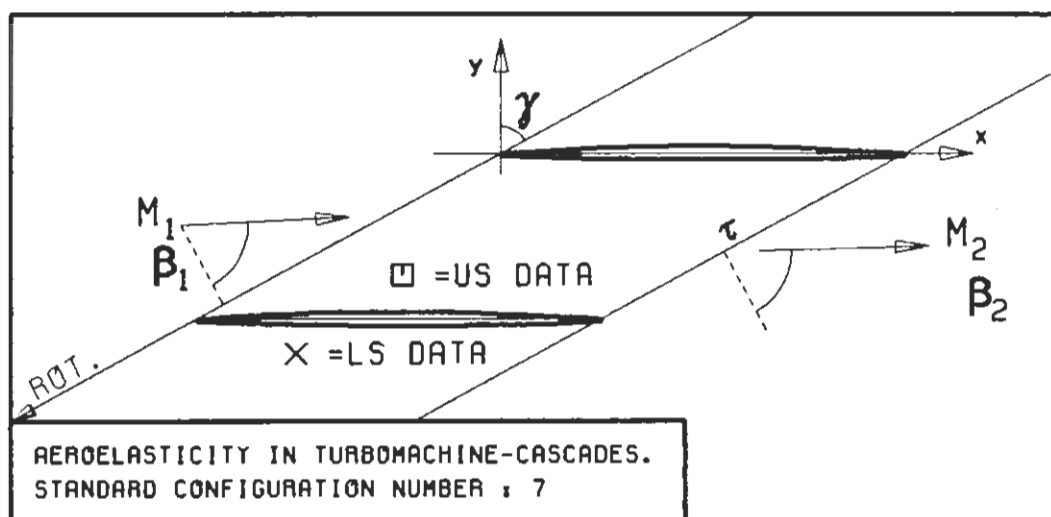
Experimental and Theoretical Results



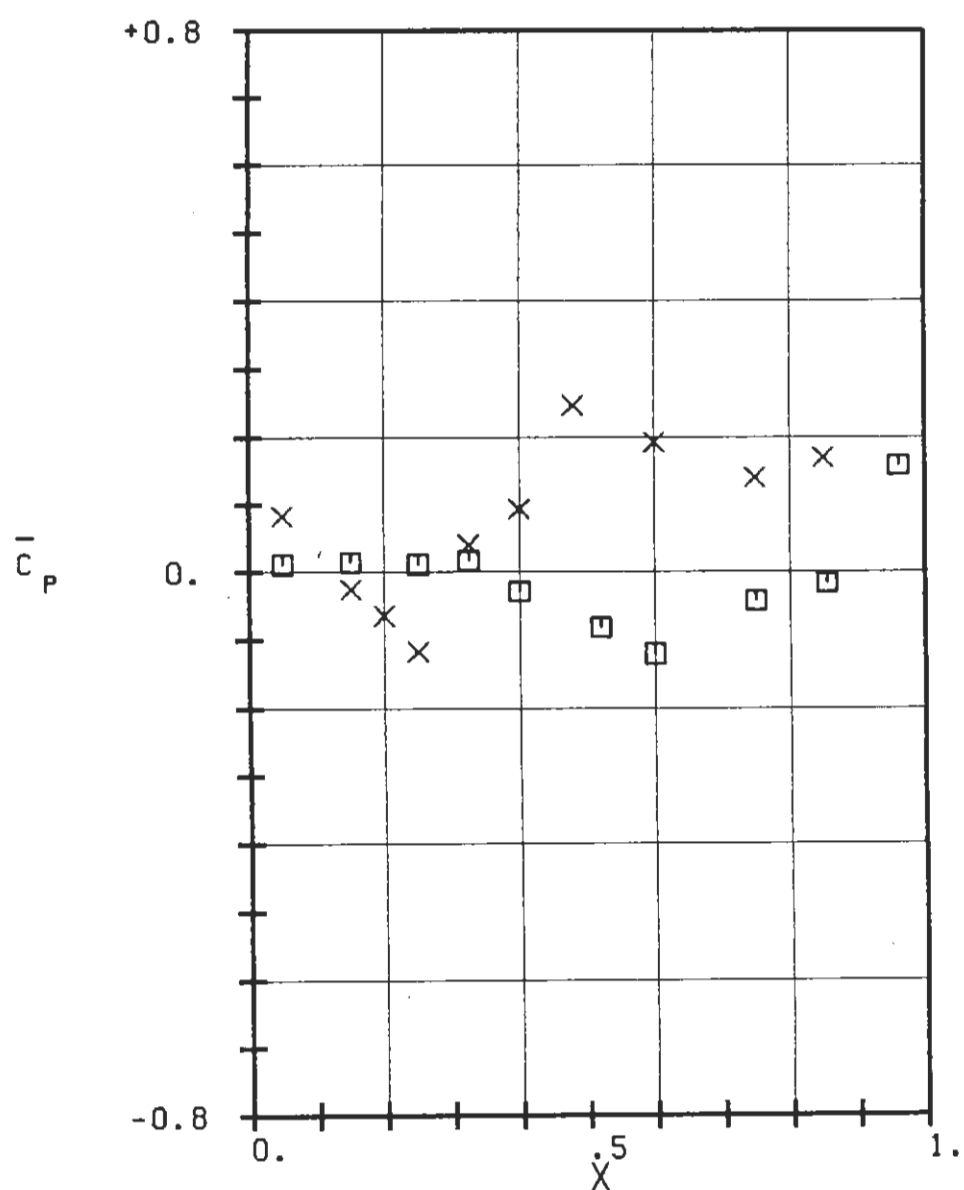
PLOT 7.7-1.1: SEVENTH STANDARD CONFIGURATION, CASES 1-5.
TIME AVERAGED BLADE SURFACE PRESSURE
DISTRIBUTION FOR OUTLET VELOCITY $M_2 = 1.25$.



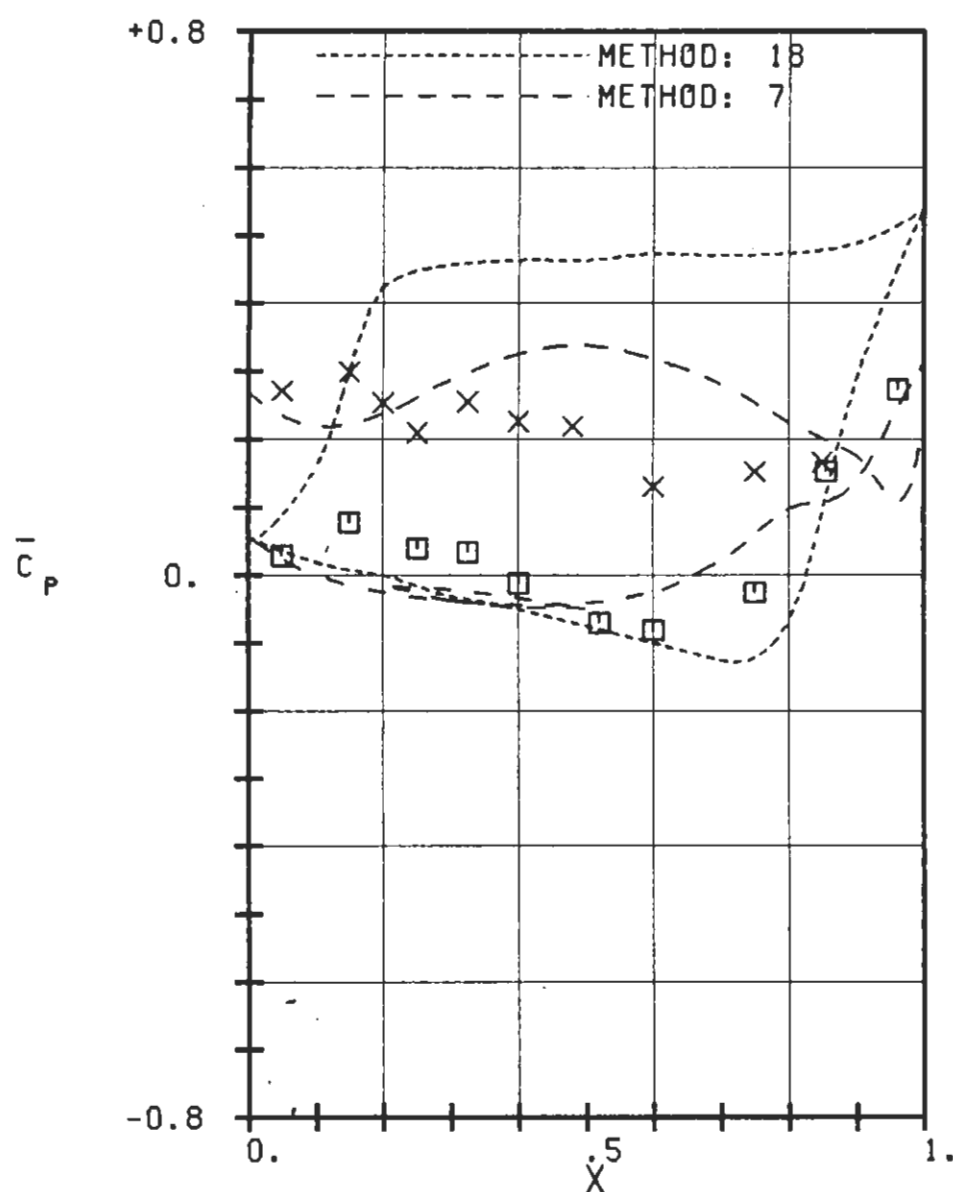
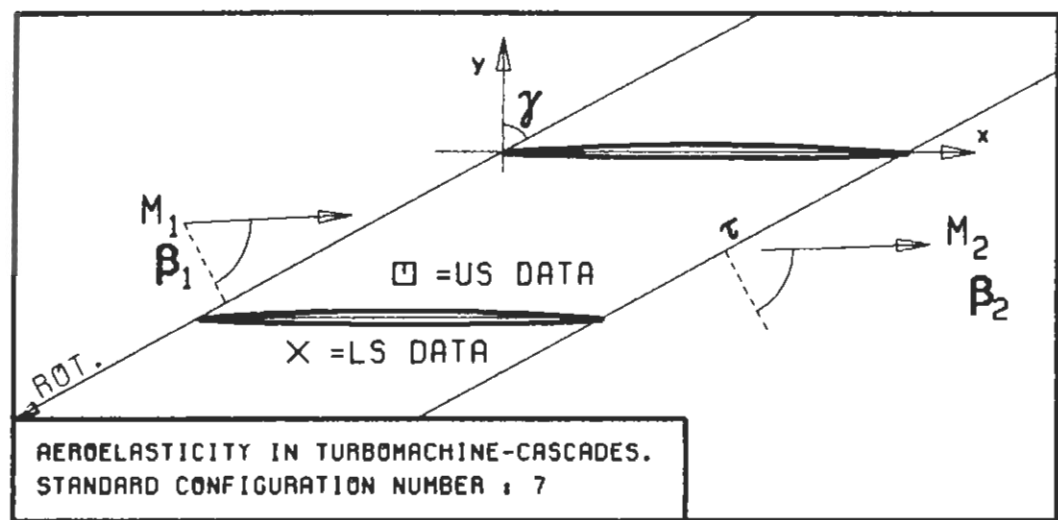
PLOT 7.7-1.2: SEVENTH STANDARD CONFIGURATION, EXTRA CASES.
TIME AVERAGED BLADE SURFACE PRESSURE
DISTRIBUTION FOR OUTLET VELOCITY $M_2 = 1.14$.



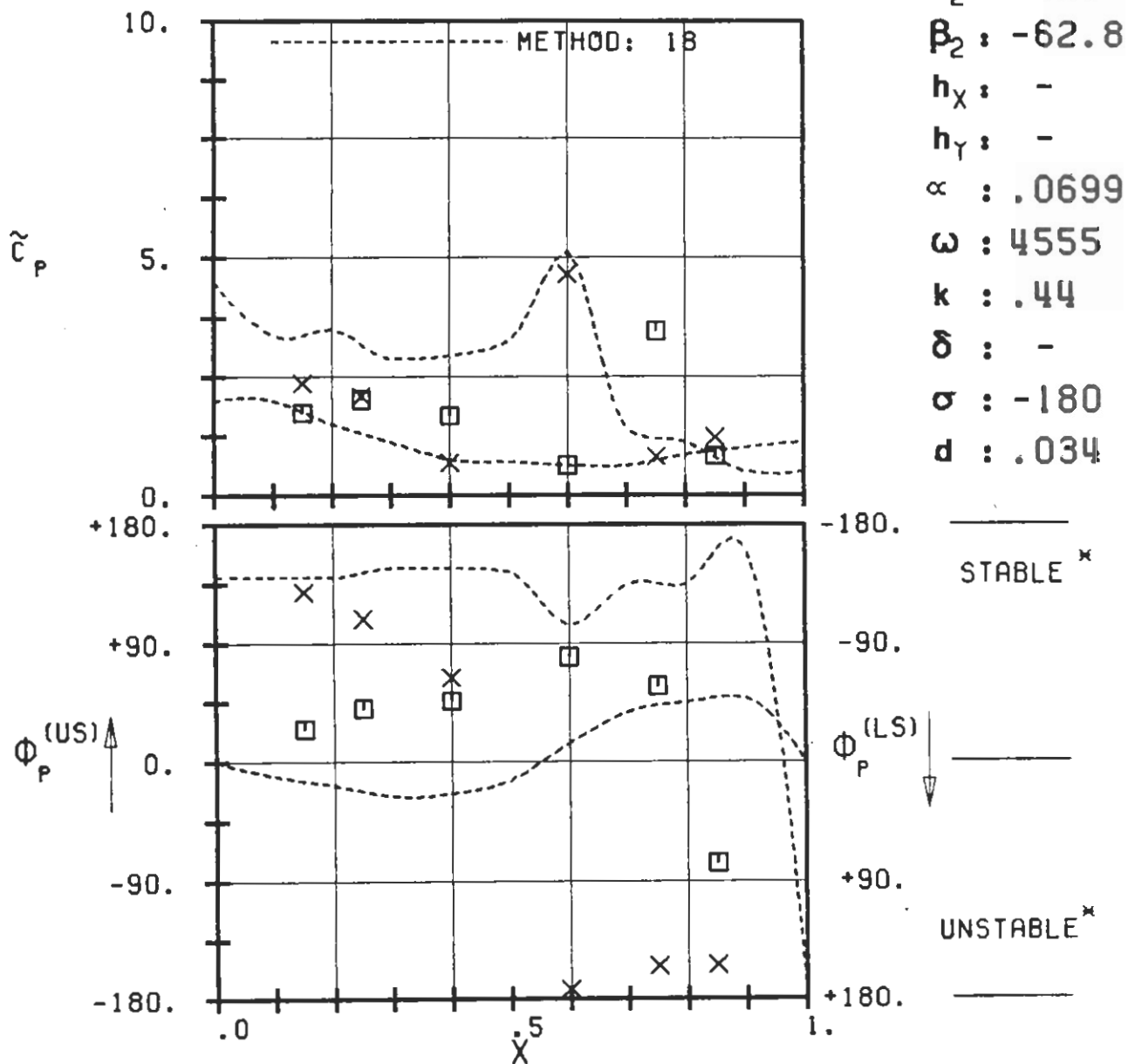
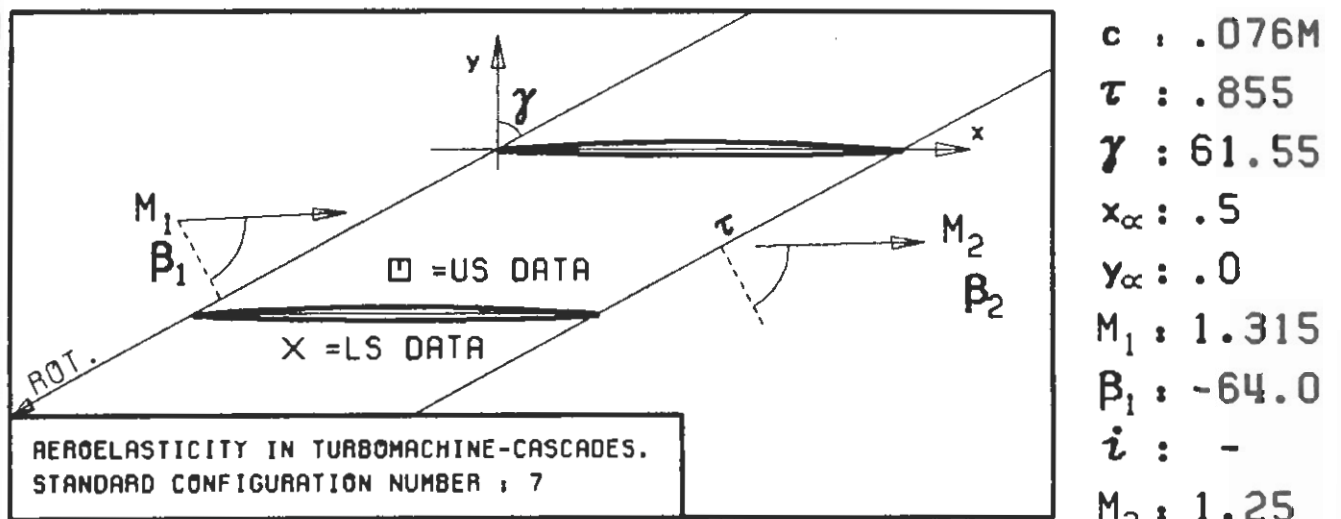
$c : .076M$
 $\tau : .855$
 $\gamma : 61.55$
 $x_\infty : -$
 $y_\infty : -$
 $M_1 : 1.315$
 $\beta_1 : -64.0$
 $i : -$
 $M_2 : 1.05$
 $\beta_2 : -63.3$
 $h_x : -$
 $h_y : -$
 $\alpha : -$
 $\omega : -$
 $k : -$
 $\delta : -$
 $\sigma : -$
 $d : .034$



PLOT 7.7-1.3: SEVENTH STANDARD CONFIGURATION, EXTRA CASES.
TIME AVERAGED BLADE SURFACE PRESSURE
DISTRIBUTION FOR OUTLET VELOCITY $M_2=1.05$.

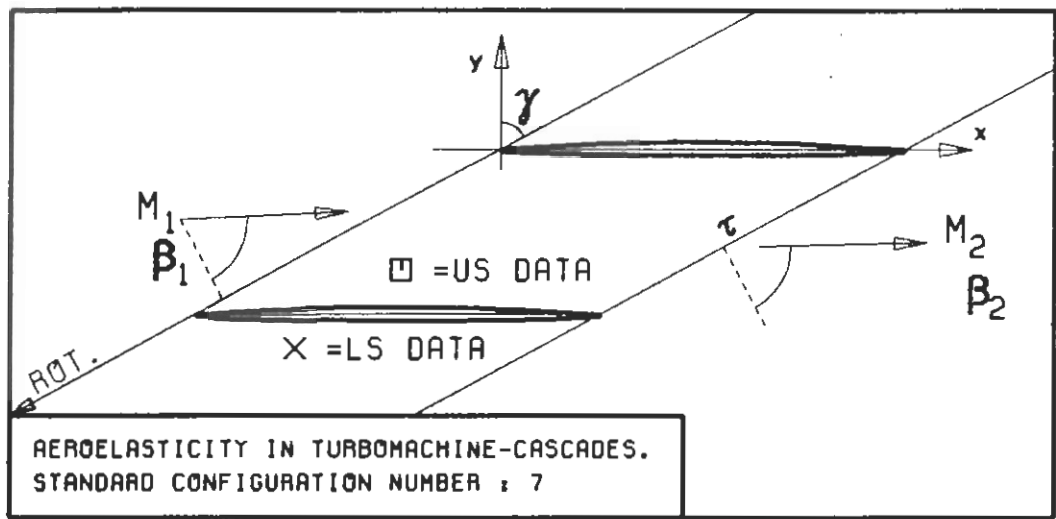


PLOT 7.7-1.4: SEVENTH STANDARD CONFIGURATION, CASES 7-12.
TIME AVERAGED BLADE SURFACE PRESSURE
DISTRIBUTION FOR OUTLET VELOCITY $M_2=0.99$.

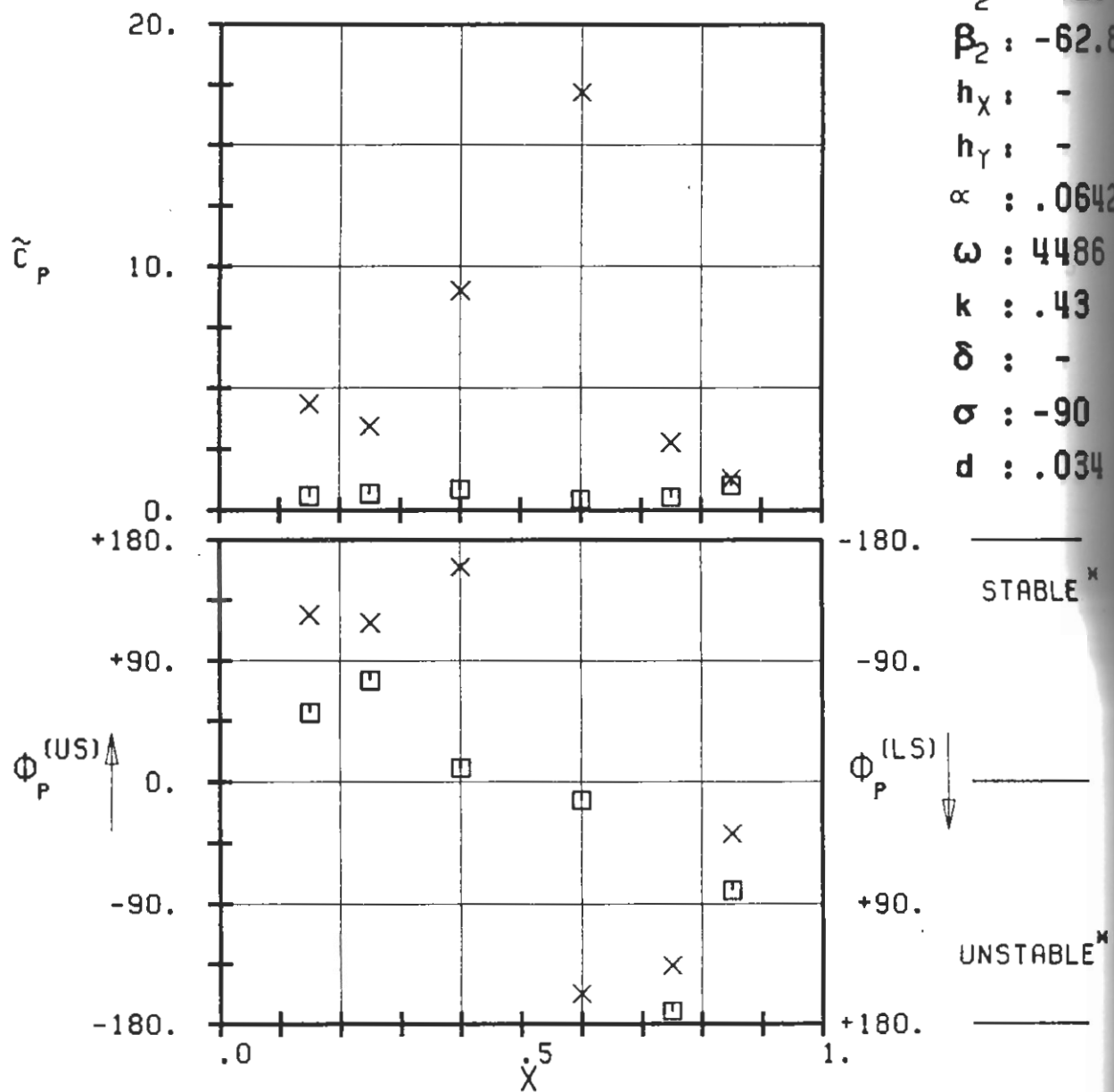


PLOT 7.7-2.1: SEVENTH STANDARD CONFIGURATION, CASE 1.
MAGNITUDE AND PHASE LEAD OF BLADE SURFACE
PRESSURE COEFFICIENT.

(x: IN PITCH MODE, NOTATION VALID UPSTREAM OF PITCH AXIS)

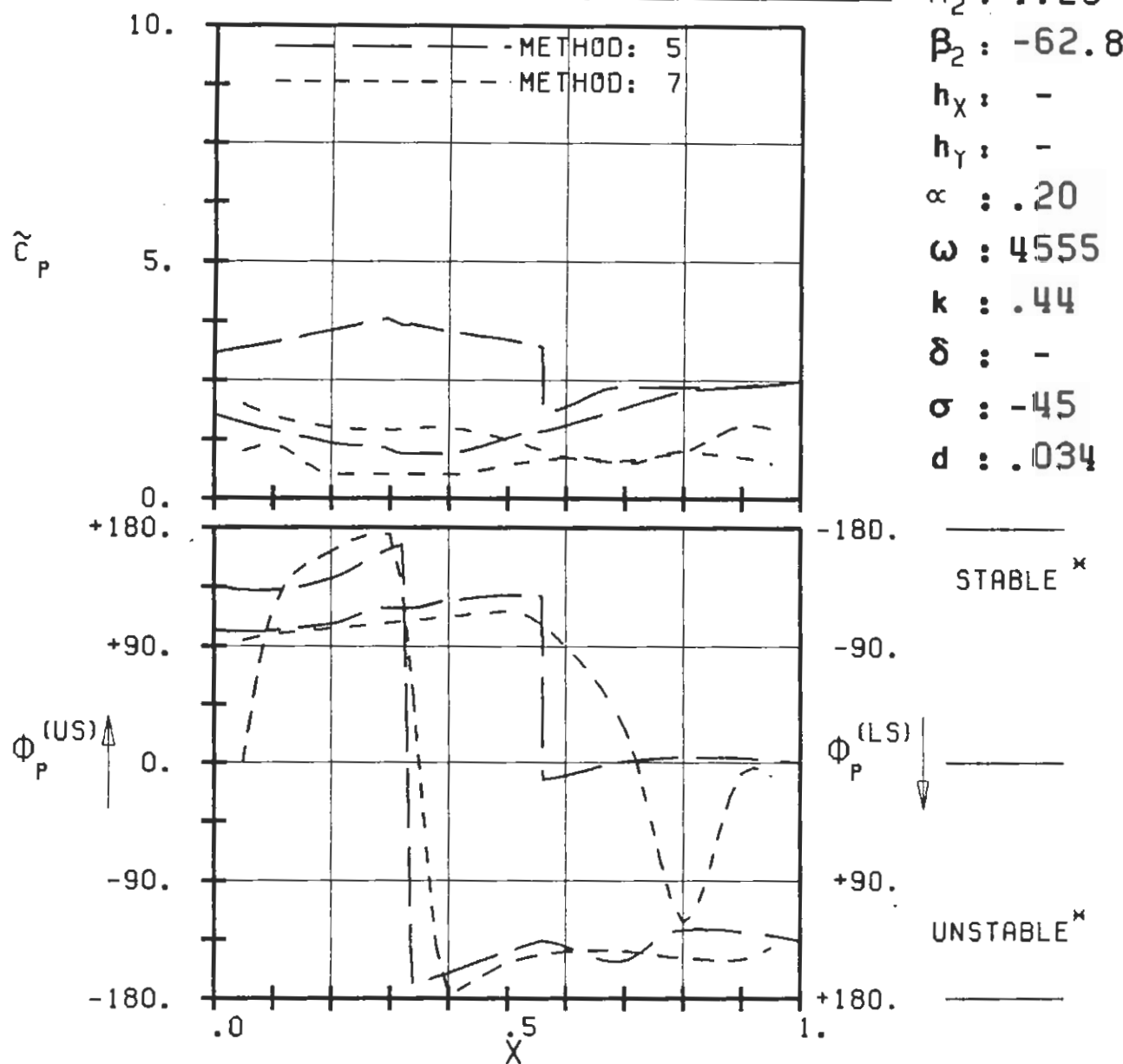
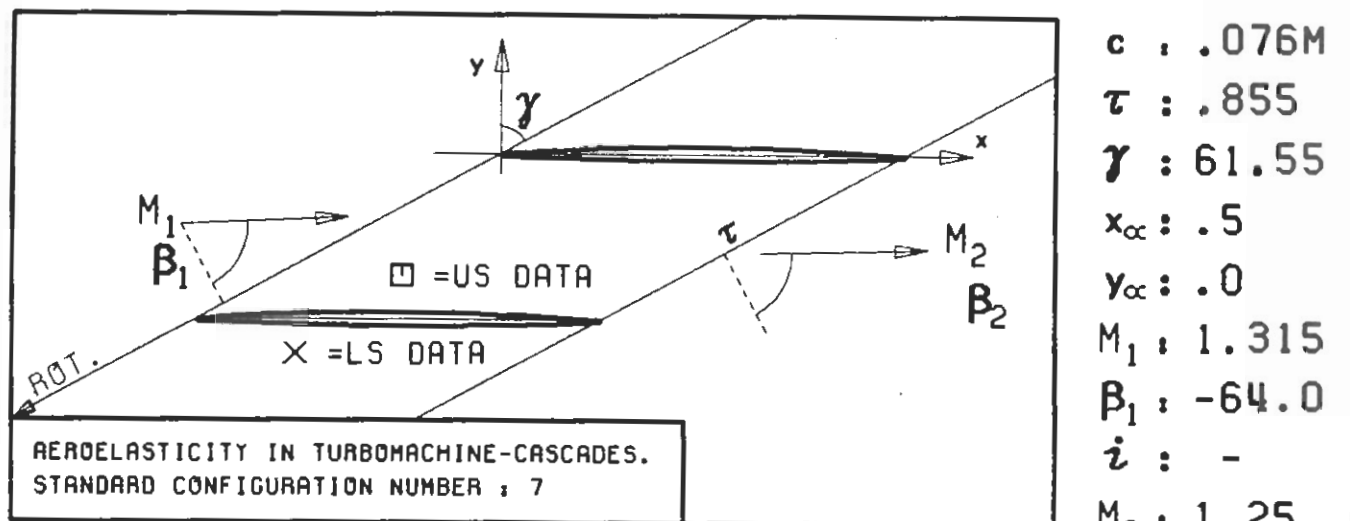


$c : .076M$
 $\tau : .855$
 $\gamma : 61.55$
 $x_\alpha : .5$
 $y_\alpha : .0$
 $M_1 : 1.315$
 $\beta_1 : -64.0$
 $i : -$
 $M_2 : 1.25$
 $\beta_2 : -62.8$
 $h_x : -$
 $h_y : -$
 $\alpha : .0642$
 $\omega : 4486$
 $k : .43$
 $\delta : -$
 $\sigma : -90$
 $d : .034$



PLOT 7.7-2.1: SEVENTH STANDARD CONFIGURATION, CASE 2.
 MAGNITUDE AND PHASE LEAD OF BLADE SURFACE
 PRESSURE COEFFICIENT.

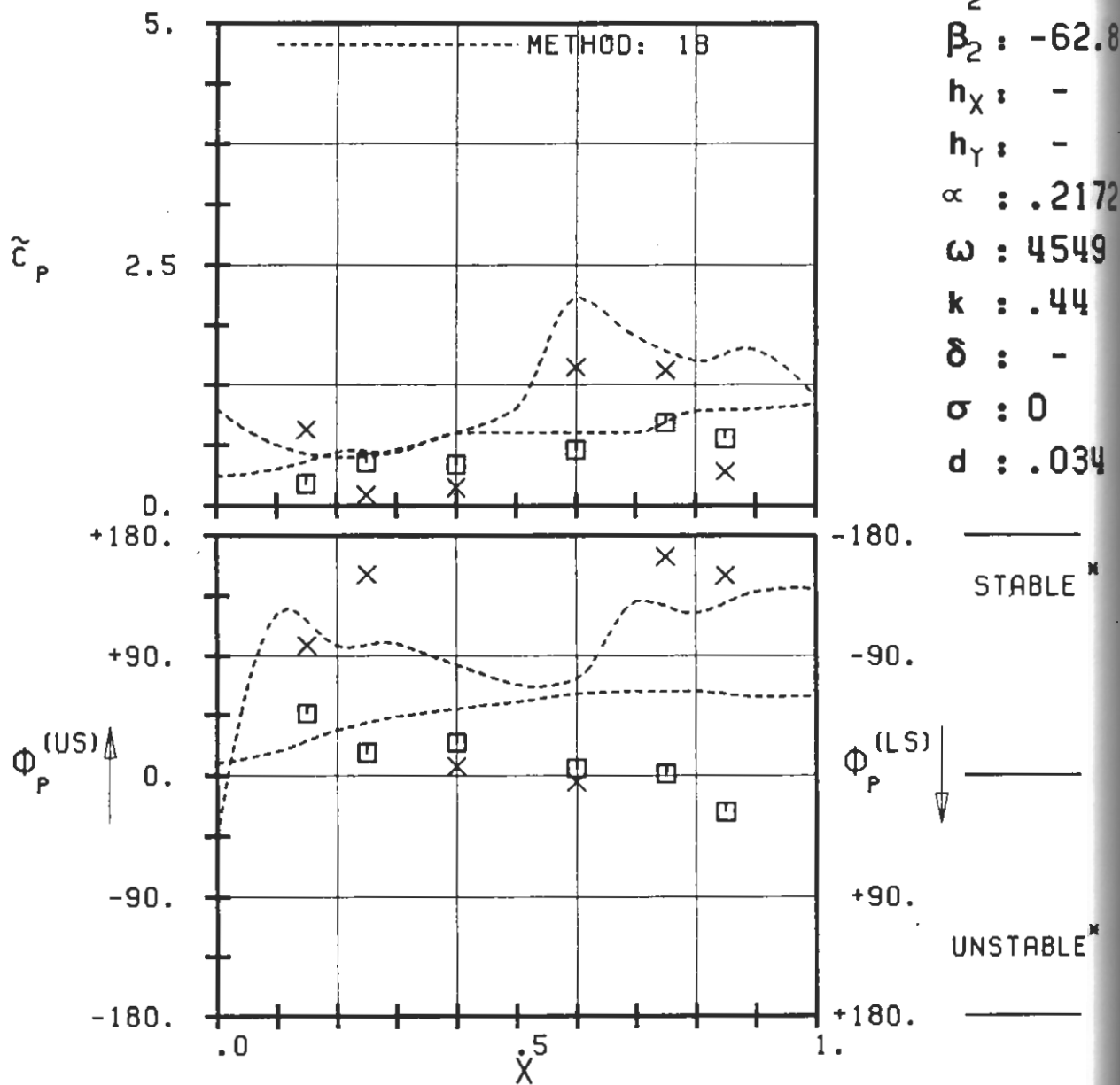
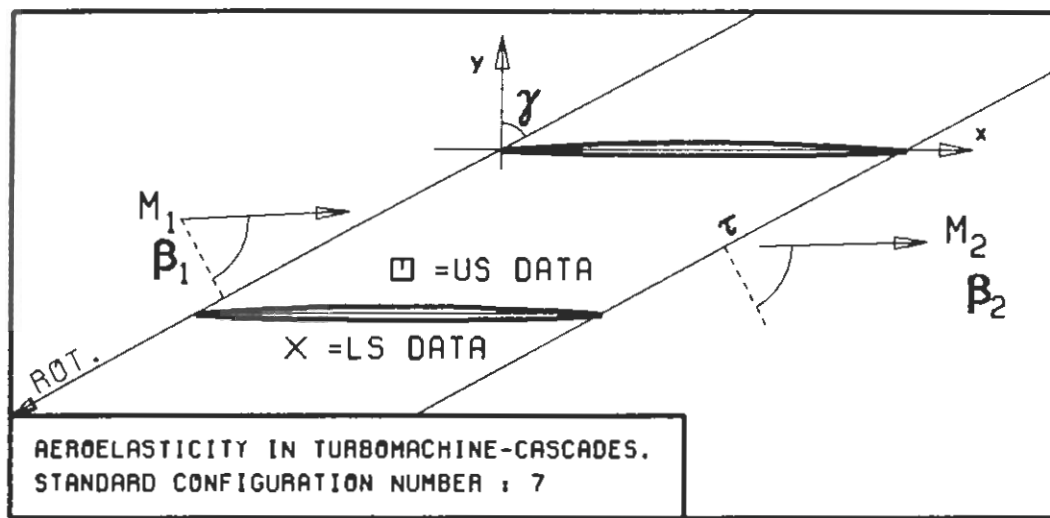
(\times : IN PITCH MODE, NOTATION VALID UPSTREAM OF PITCH AXIS)



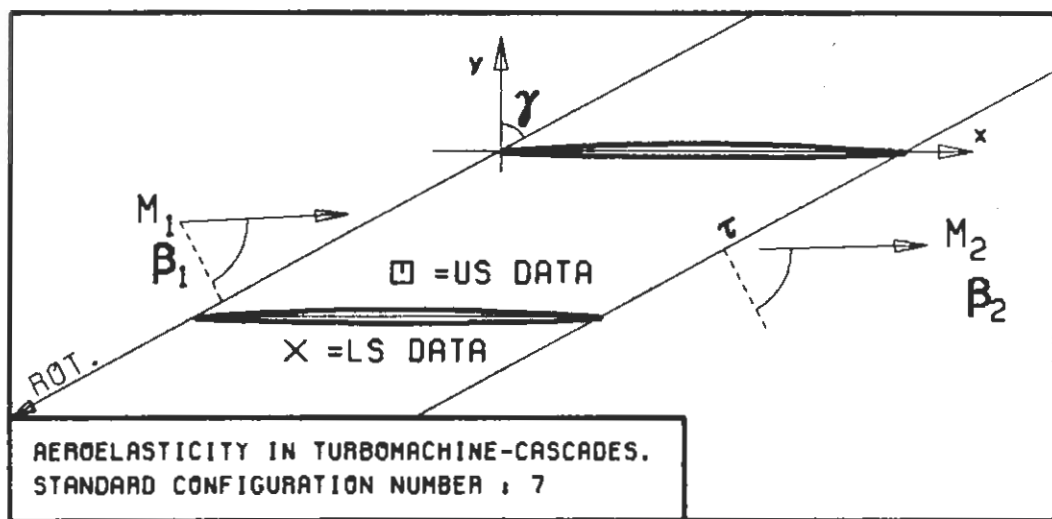
PLOT 7.7-2.3: SEVENTH STANDARD CONFIGURATION, CASE 3.
 MAGNITUDE AND PHASE LEAD OF BLADE SURFACE
 PRESSURE COEFFICIENT.

(x: IN PITCH MODE, NOTATION VALID UPSTREAM OF PITCH AXIS)

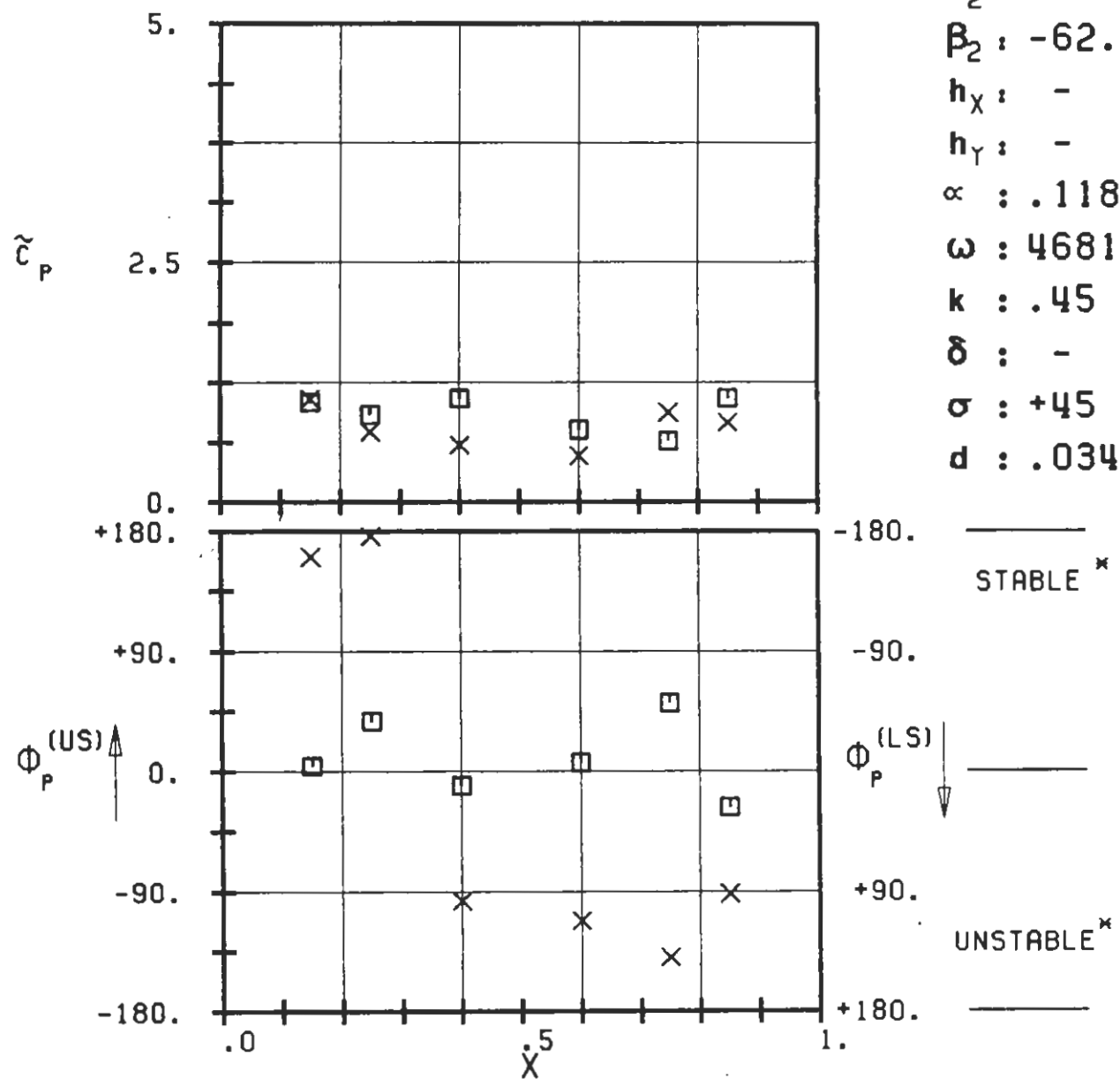
$c : .076M$
 $\tau : .855$
 $\gamma : 61.55$
 $x_\alpha : .5$
 $y_\alpha : .0$
 $M_1 : 1.315$
 $B_1 : -64.0$
 $i : -$
 $M_2 : 1.25$
 $B_2 : -62.8$
 $h_X : -$
 $h_Y : -$
 $\alpha : .20$
 $\omega : 4555$
 $k : .44$
 $\delta : -$
 $\sigma : -45$
 $d : .034$



c : .076M
 τ : .855
 γ : 61.55
 x_α : .5
 y_α : .0
 M_1 : 1.315
 β_1 : -64.0
 i : -
 M_2 : 1.25
 β_2 : -62.8
 h_X : -
 h_Y : -
 α : .2172
 ω : 4549
 k : .44
 δ : -
 σ : 0
 d : .034

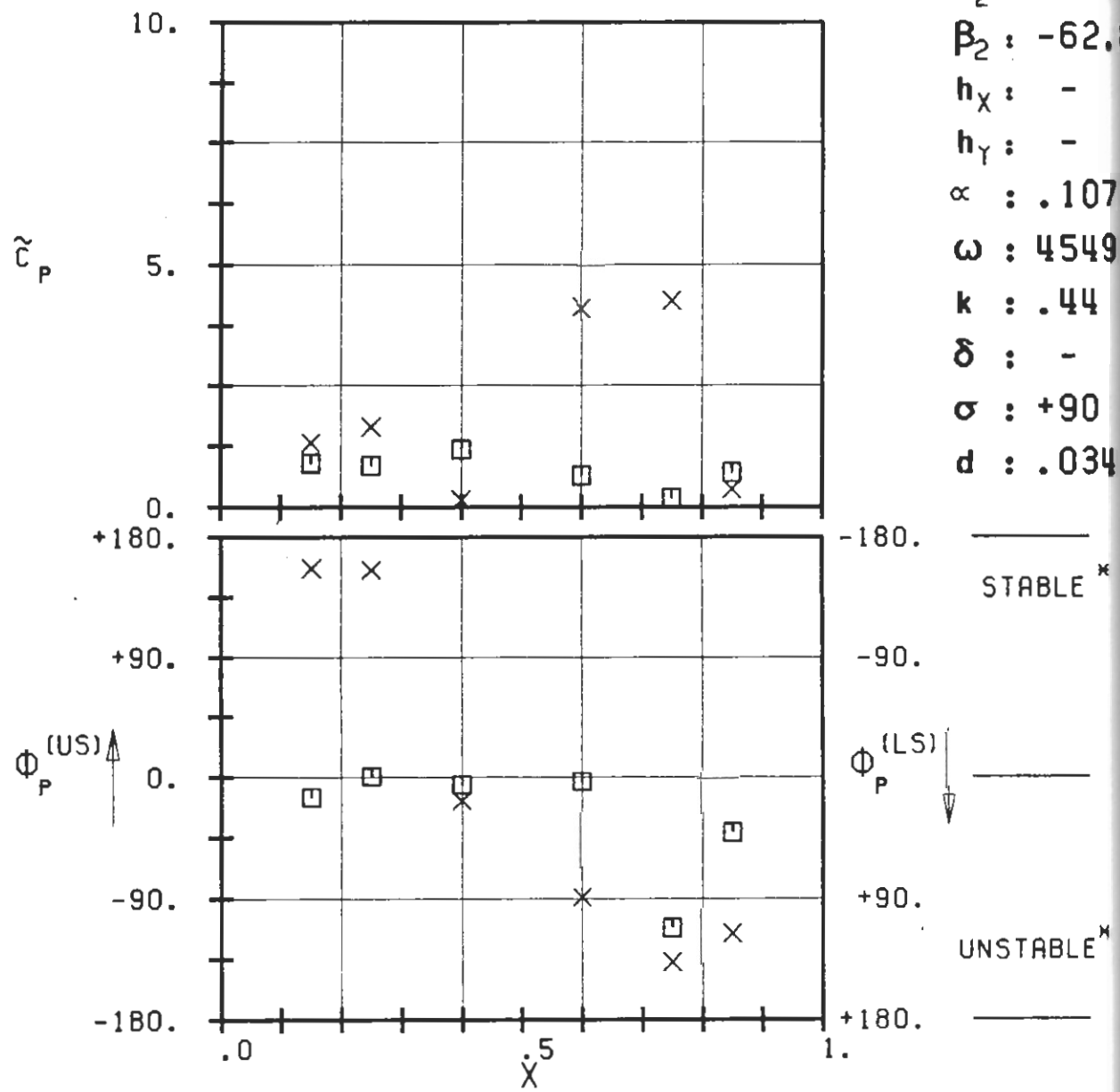
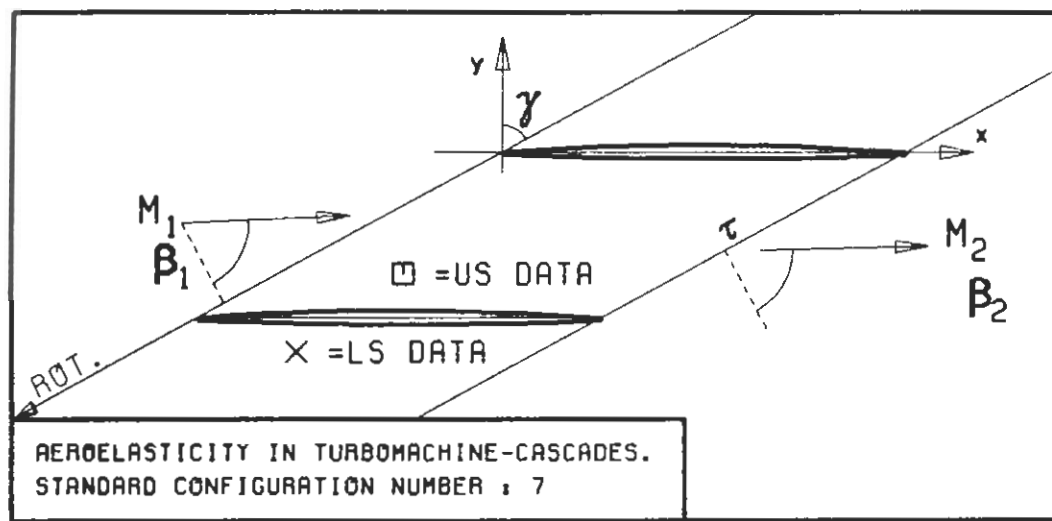


c : .076M
 τ : .855
 γ : 61.55
 x_∞ : .5
 y_∞ : .0
 M_1 : 1.315
 β_1 : -64.0
 i : -
 M_2 : 1.25
 β_2 : -62.8
 h_x : -
 h_y : -
 α : .1180
 ω : 4681
 k : .45
 δ : -
 σ : +45
 d : .034



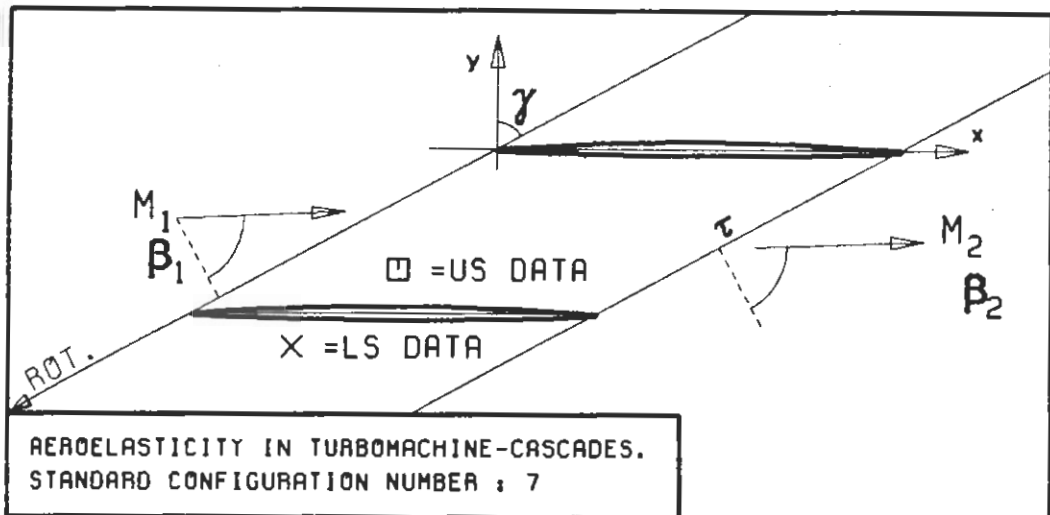
PLOT 7.7-2.5: SEVENTH STANDARD CONFIGURATION, CASE 5.
MAGNITUDE AND PHASE LEAD OF BLADE SURFACE
PRESSURE COEFFICIENT.

(\times : IN PITCH MODE, NOTATION VALID UPSTREAM OF PITCH AXIS)

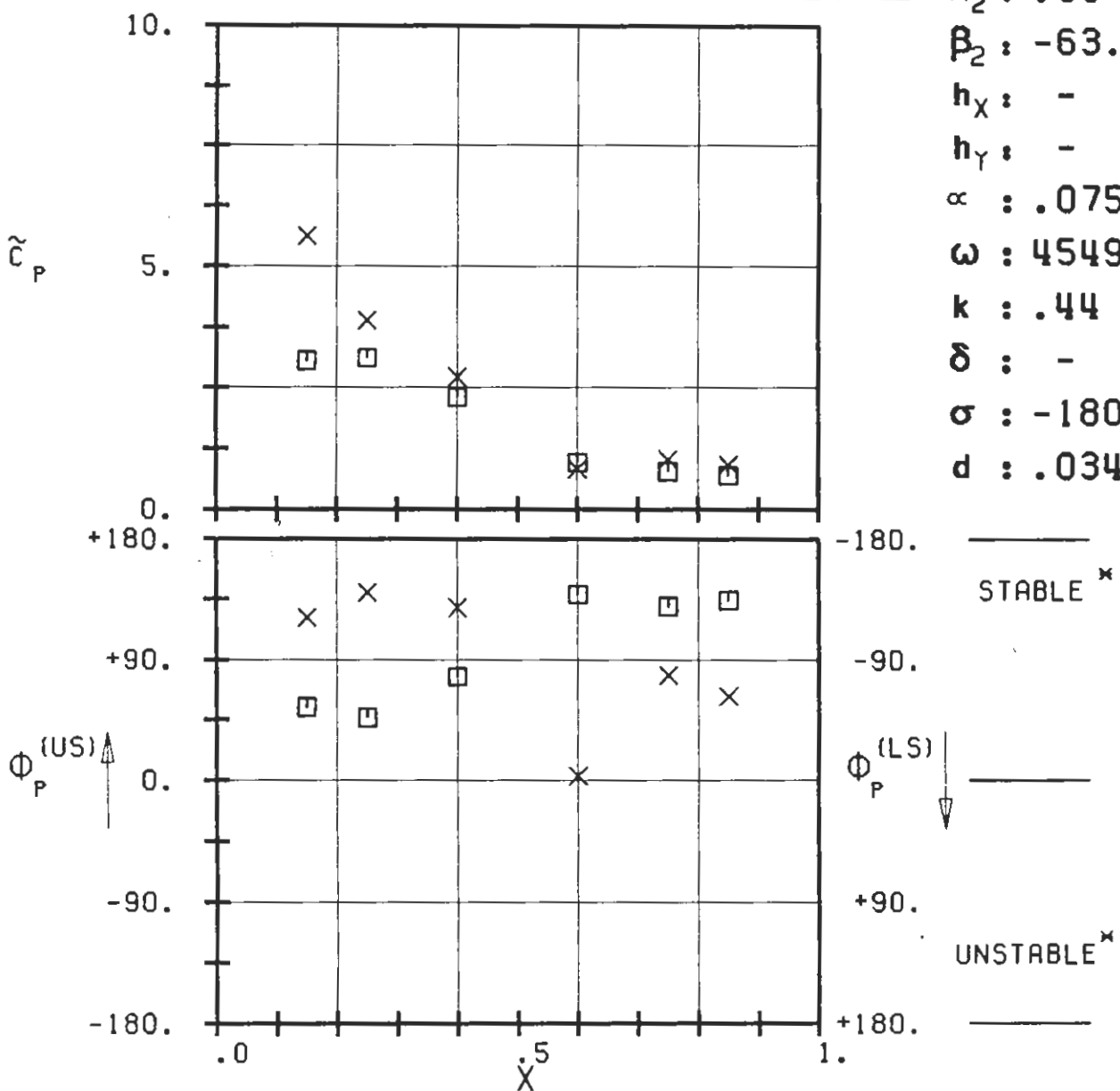


PLOT 7.7-9.6: SEVENTH STANDARD CONFIGURATION, CASE 6.
MAGNITUDE AND PHASE LEAD OF BLADE SURFACE
PRESSURE COEFFICIENT.

(x: IN PITCH MODE, NOTATION VALID UPSTREAM OF PITCH AXIS)

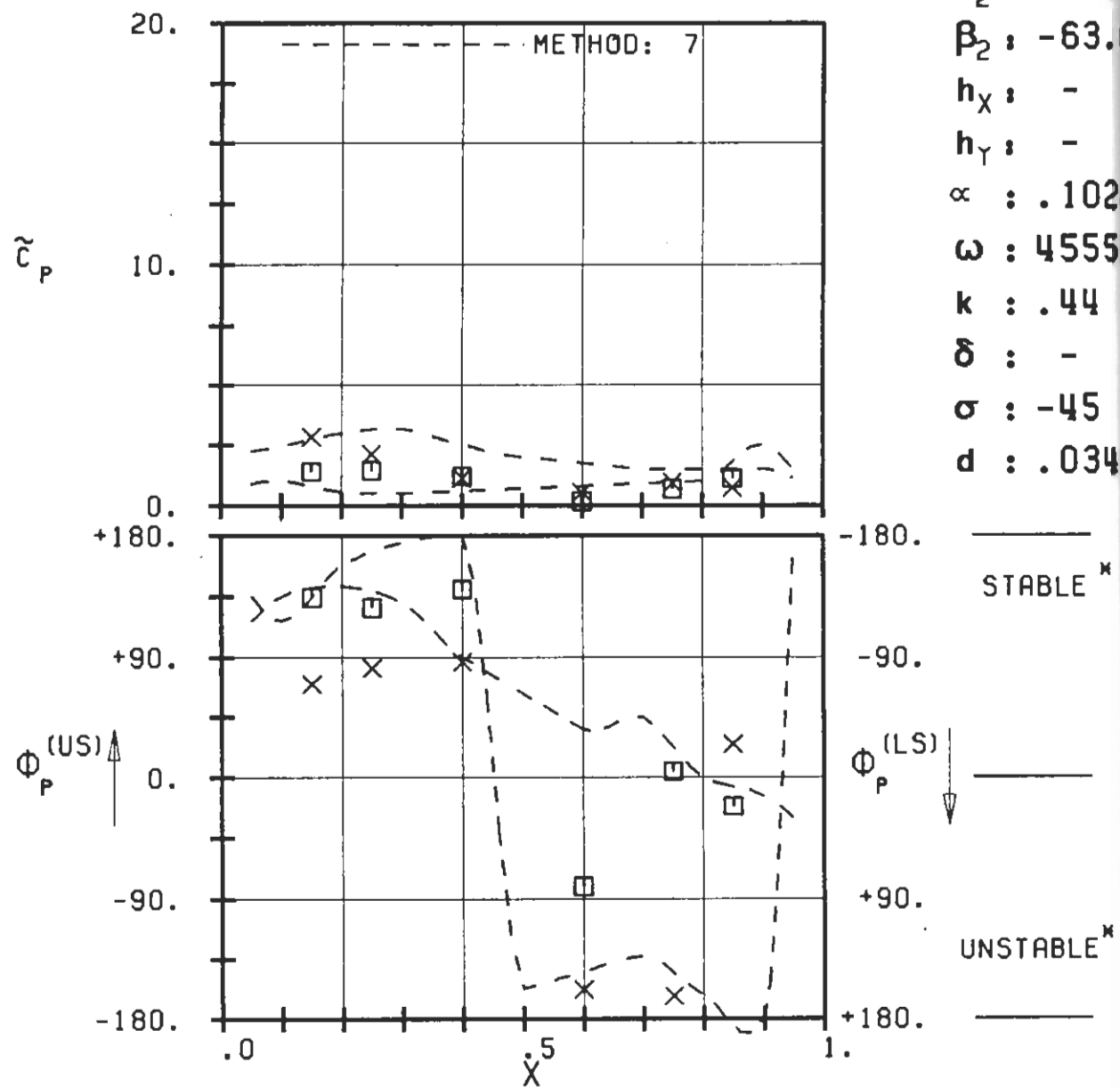
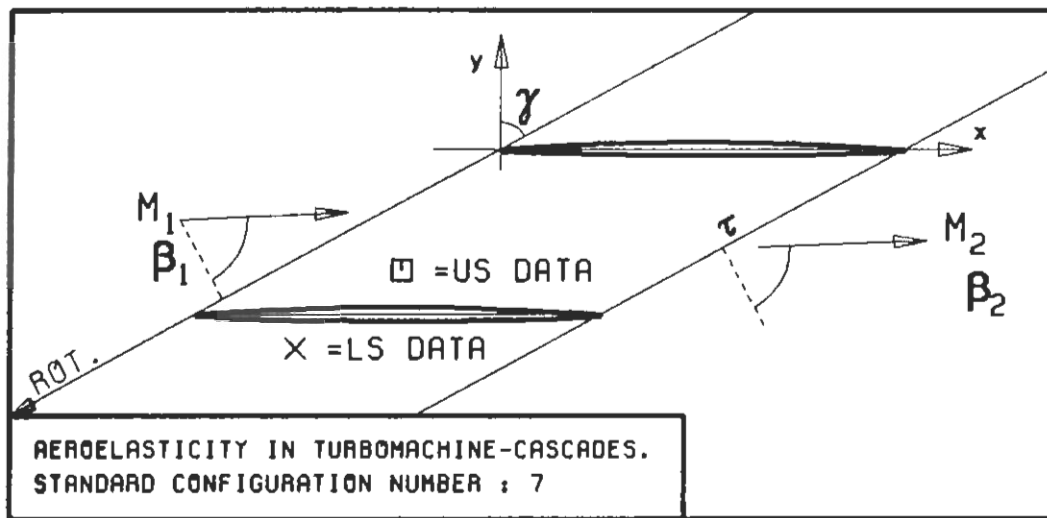


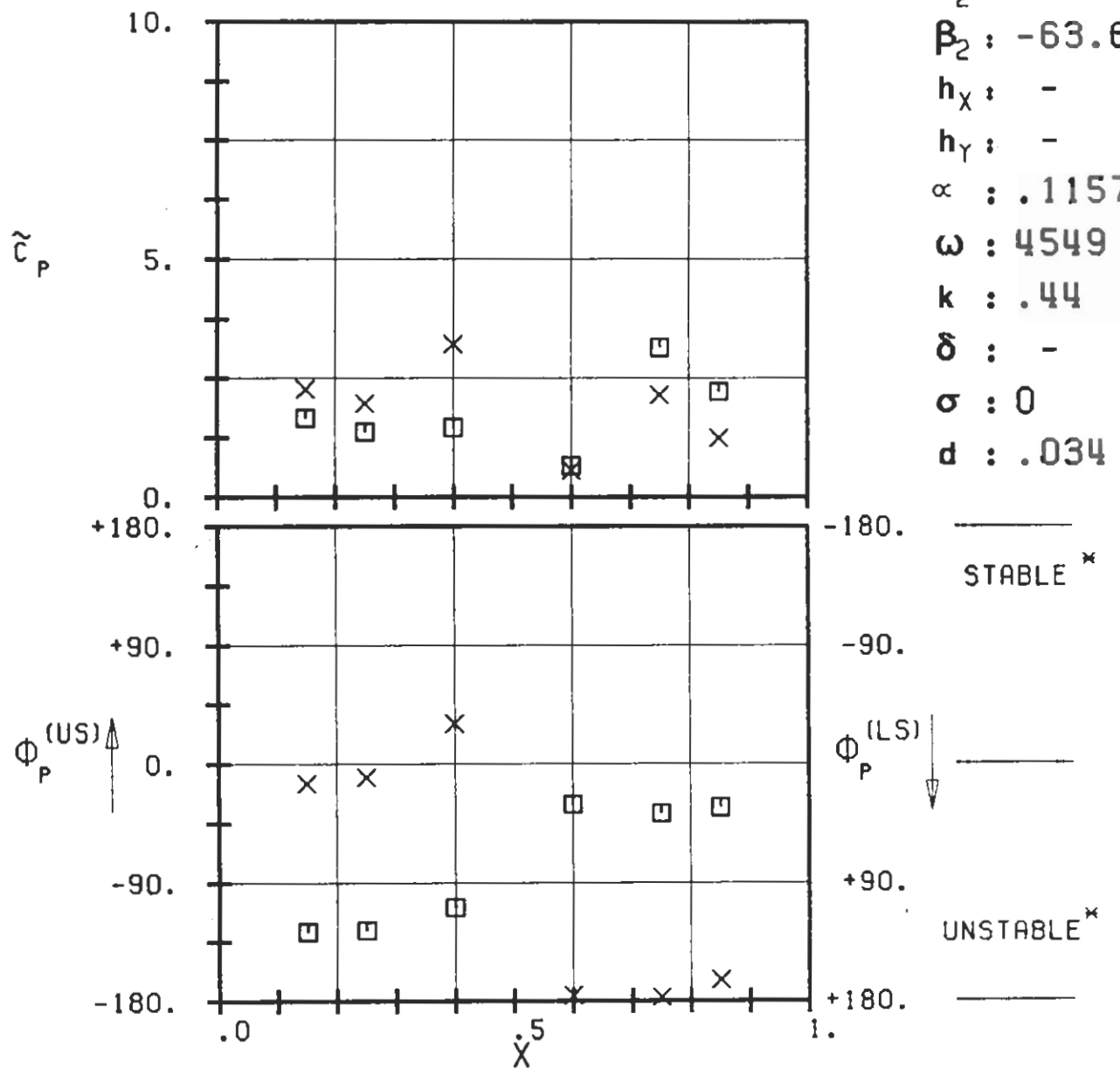
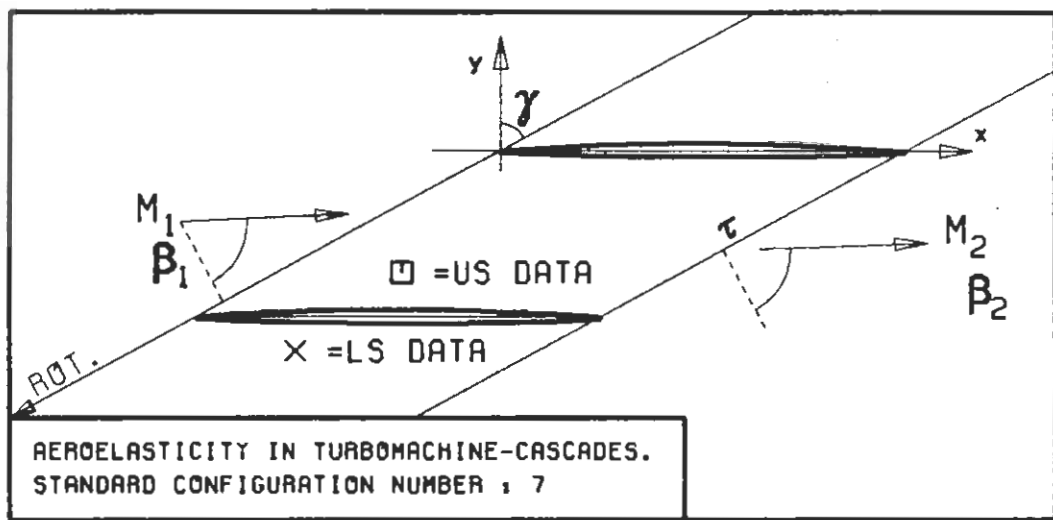
$c : .076M$
 $\tau : .855$
 $\gamma : 61.55$
 $x_{\alpha} : .5$
 $y_{\alpha} : .0$
 $M_1 : 1.315$
 $\beta_1 : -64.0$
 $i : -$
 $M_2 : .99$
 $\beta_2 : -63.6$
 $h_x : -$
 $h_y : -$
 $\alpha : .0751$
 $\omega : 4549$
 $k : .44$
 $\delta : -$
 $\sigma : -180$
 $d : .034$



PLOT 7.7-2.7 : SEVENTH STANDARD CONFIGURATION, CASE 7.
MAGNITUDE AND PHASE LEAD OF BLADE SURFACE
PRESSURE COEFFICIENT.

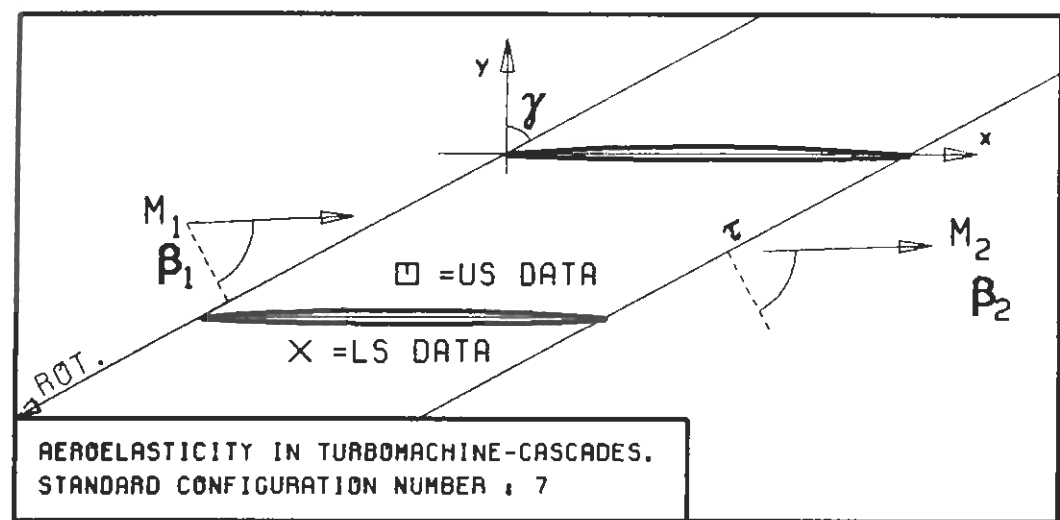
(X: IN PITCH MODE, NOTATION VALID UPSTREAM OF PITCH AXIS)



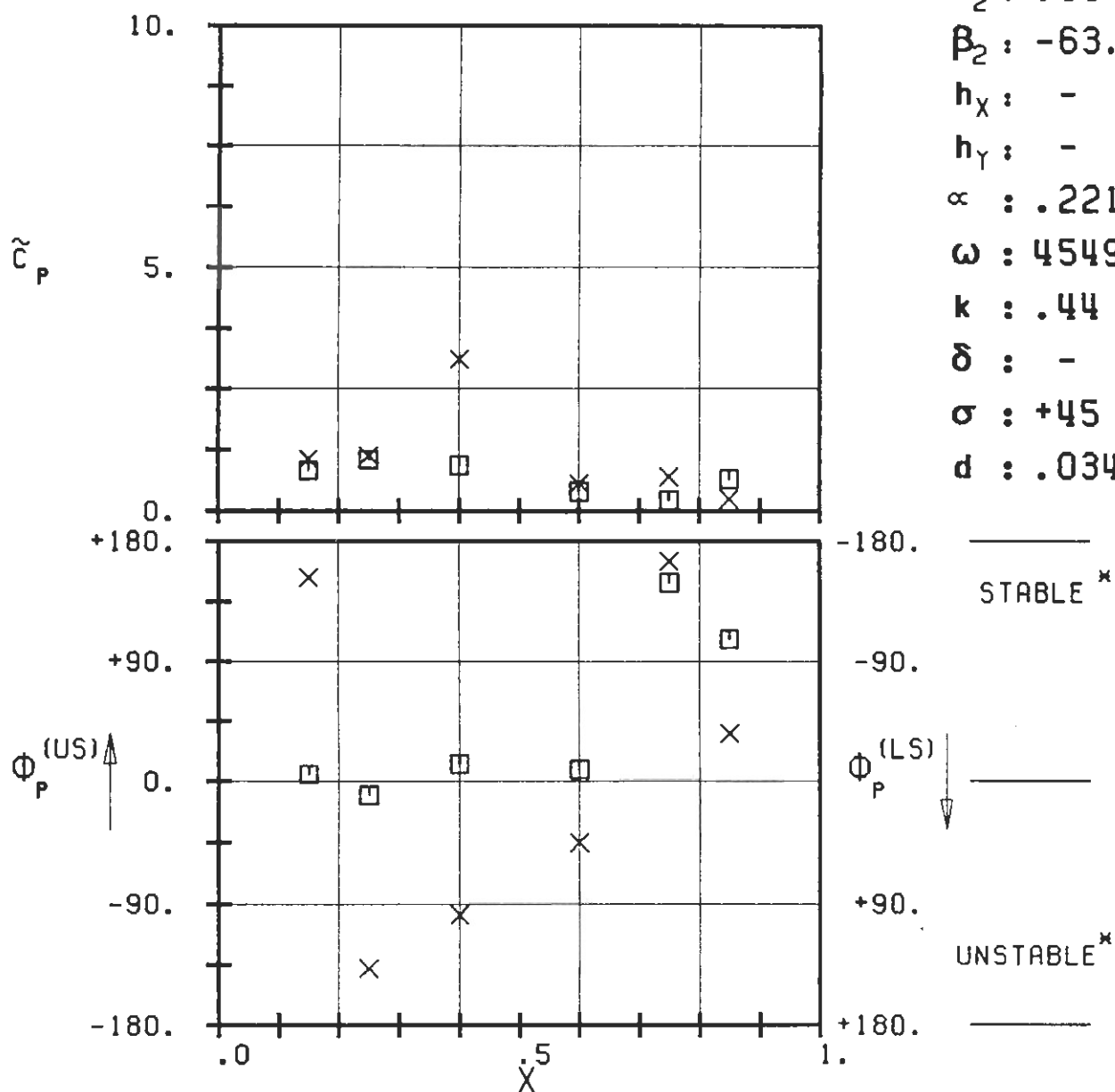


PLOT 7.7-9.9: SEVENTH STANDARD CONFIGURATION, CASE 9.
MAGNITUDE AND PHASE LEAD OF BLADE SURFACE
PRESSURE COEFFICIENT.

(X: IN PITCH MODE, NOTATION VALID UPSTREAM OF PITCH AXIS)

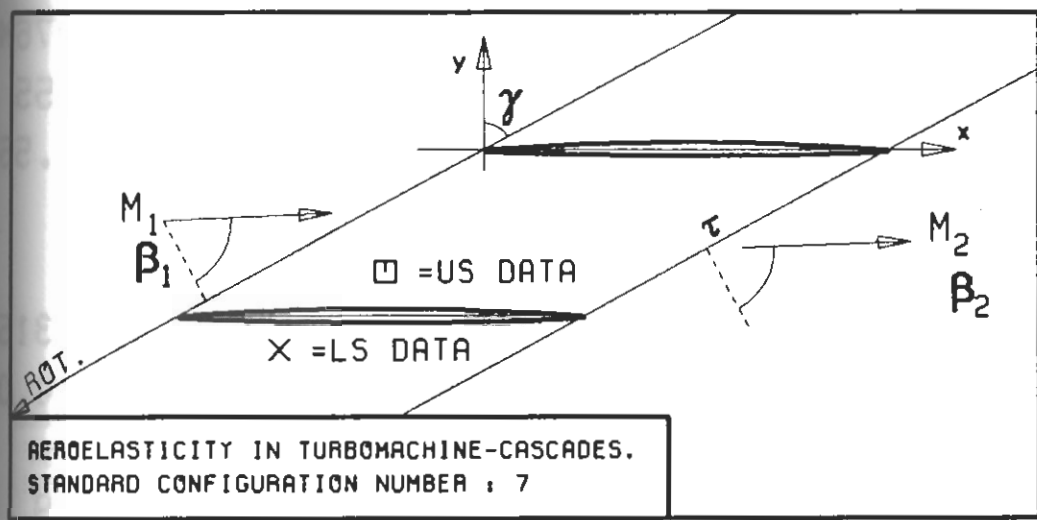


$c : .076M$
 $\tau : .855$
 $\gamma : 61.55$
 $x_\infty : .5$
 $y_\infty : .0$
 $M_1 : 1.315$
 $\beta_1 : -64.0$
 $i : -$
 $M_2 : .99$
 $\beta_2 : -63.6$
 $h_x : -$
 $h_y : -$
 $\alpha : .2212$
 $\omega : 4549$
 $k : .44$
 $\delta : -$
 $\sigma : +45$
 $d : .034$

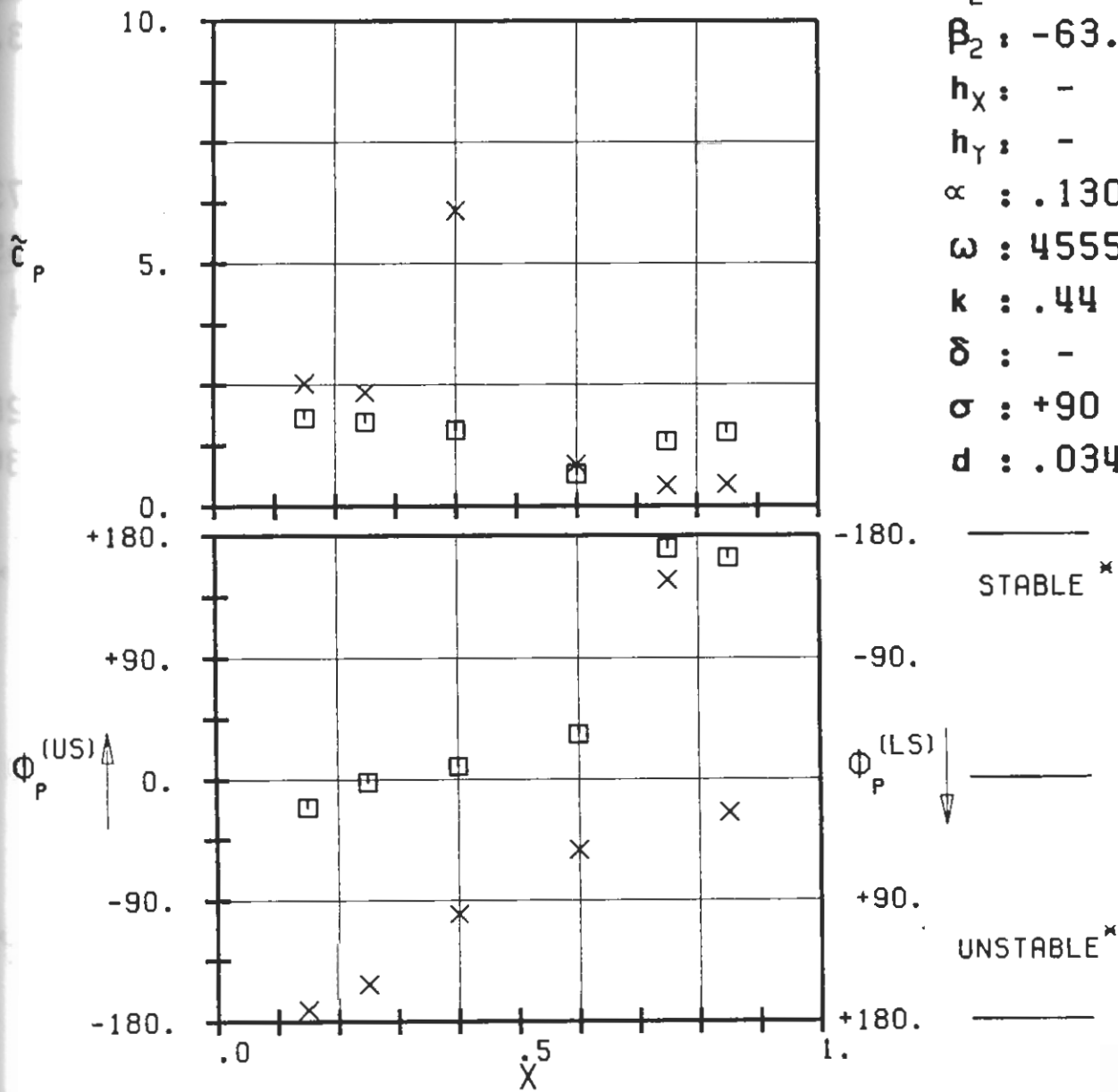


PLOT 7.7-2.10: SEVENTH STANDARD CONFIGURATION, CASE 10.
MAGNITUDE AND PHASE LEAD OF BLADE SURFACE
PRESSURE COEFFICIENT.

(X: IN PITCH MODE, NOTATION VALID UPSTREAM OF PITCH AXIS)

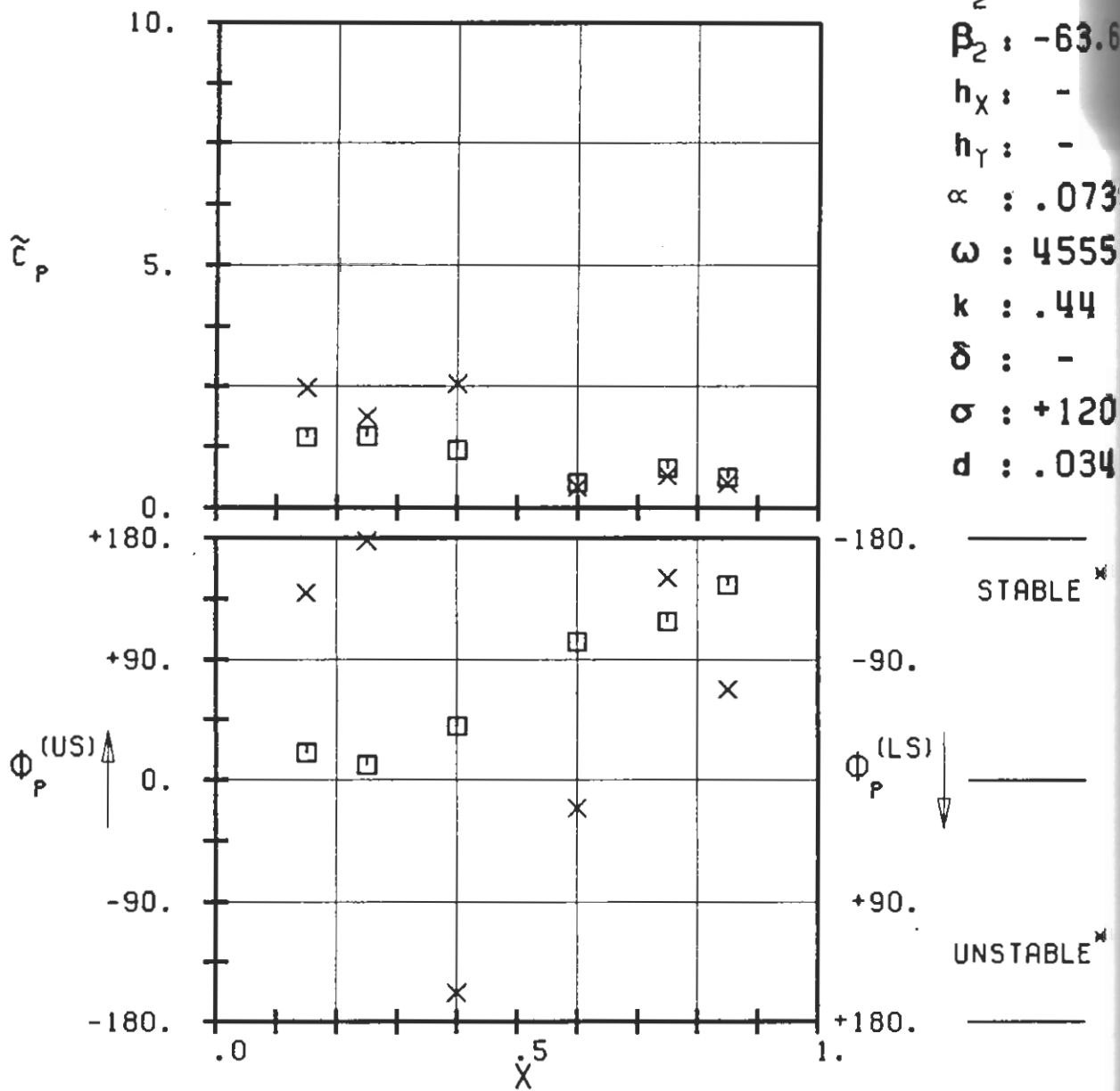
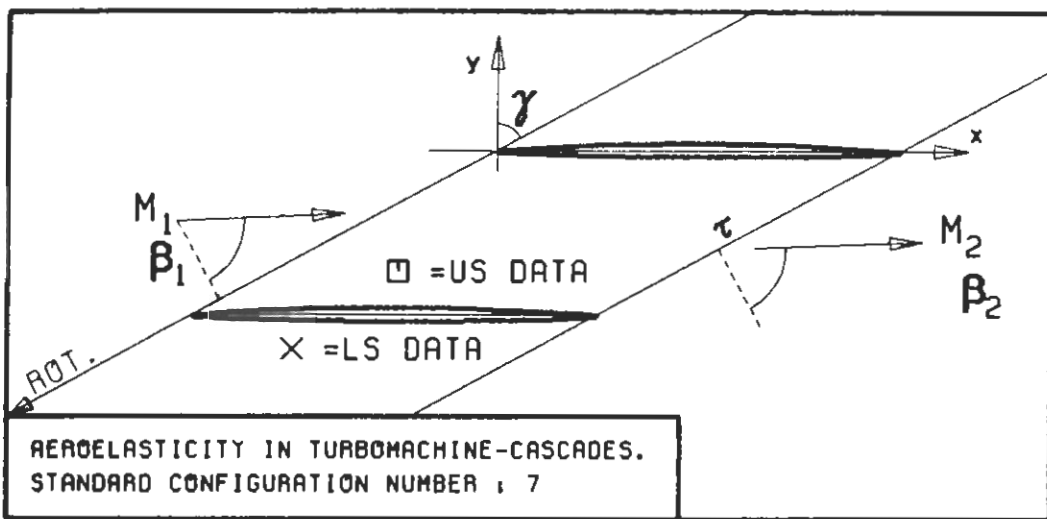


c : .076M
 τ : .855
 γ : 61.55
 x_α : .5
 y_α : .0
 M_1 : 1.315
 β_1 : -64.0
 i : -
 M_2 : .99
 β_2 : -63.6
 h_x : -
 h_y : -
 α : .1301
 ω : 4555
 k : .44
 δ : -
 σ : +90
 d : .034



PLOT 7.7-2.11: SEVENTH STANDARD CONFIGURATION, CASE 11.
MAGNITUDE AND PHASE LEAD OF BLADE SURFACE
PRESSURE COEFFICIENT.

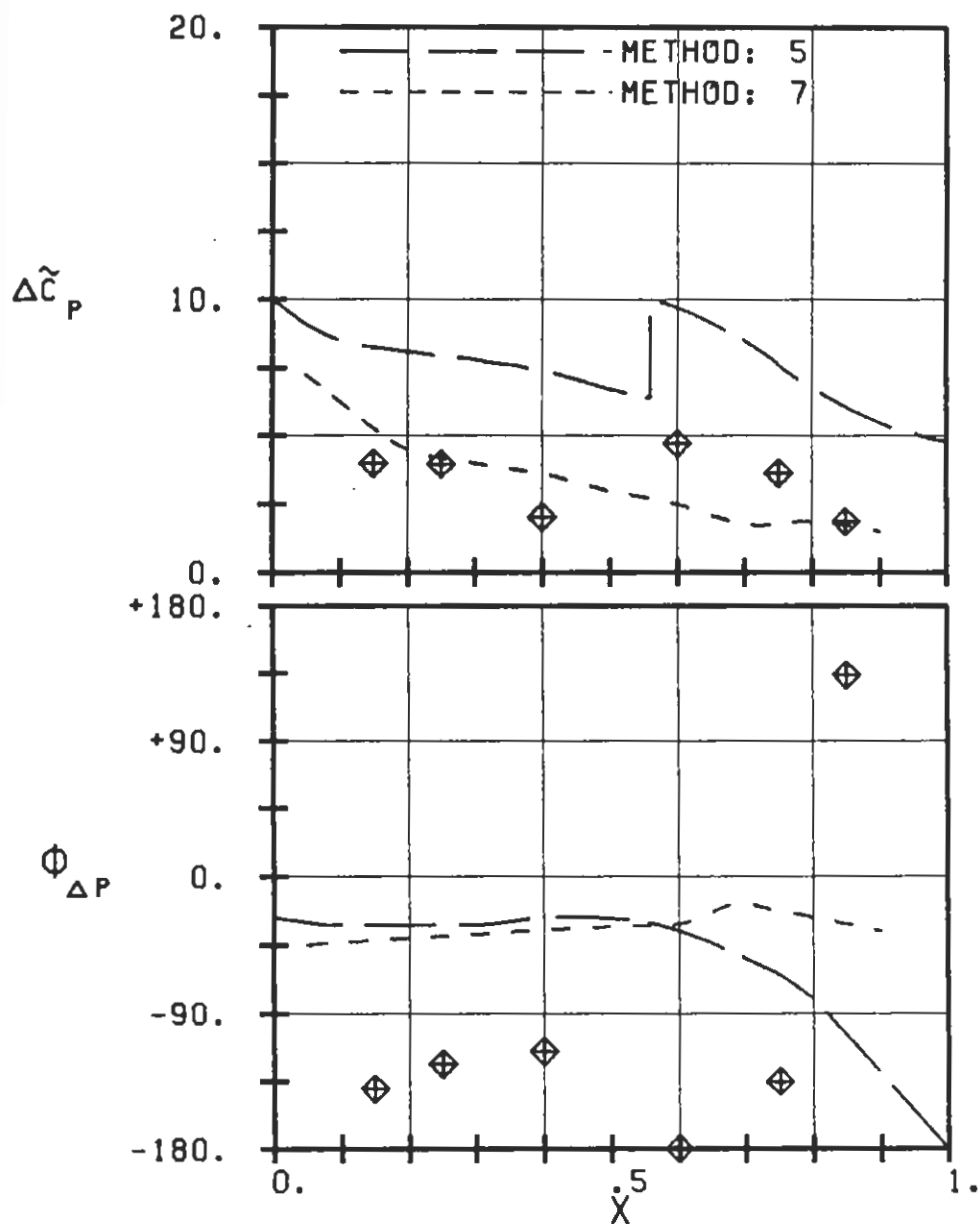
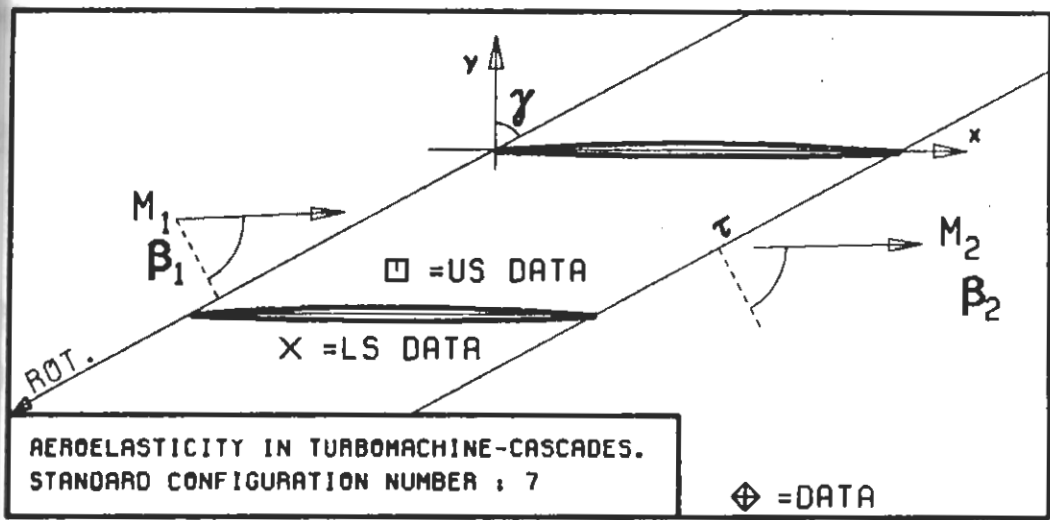
(x: IN PITCH MODE, NOTATION VALID UPSTREAM OF PITCH AXIS)



PLOT 7.7-2.12: SEVENTH STANDARD CONFIGURATION, CASE 12.
MAGNITUDE AND PHASE LEAD OF BLADE SURFACE
PRESSURE COEFFICIENT.

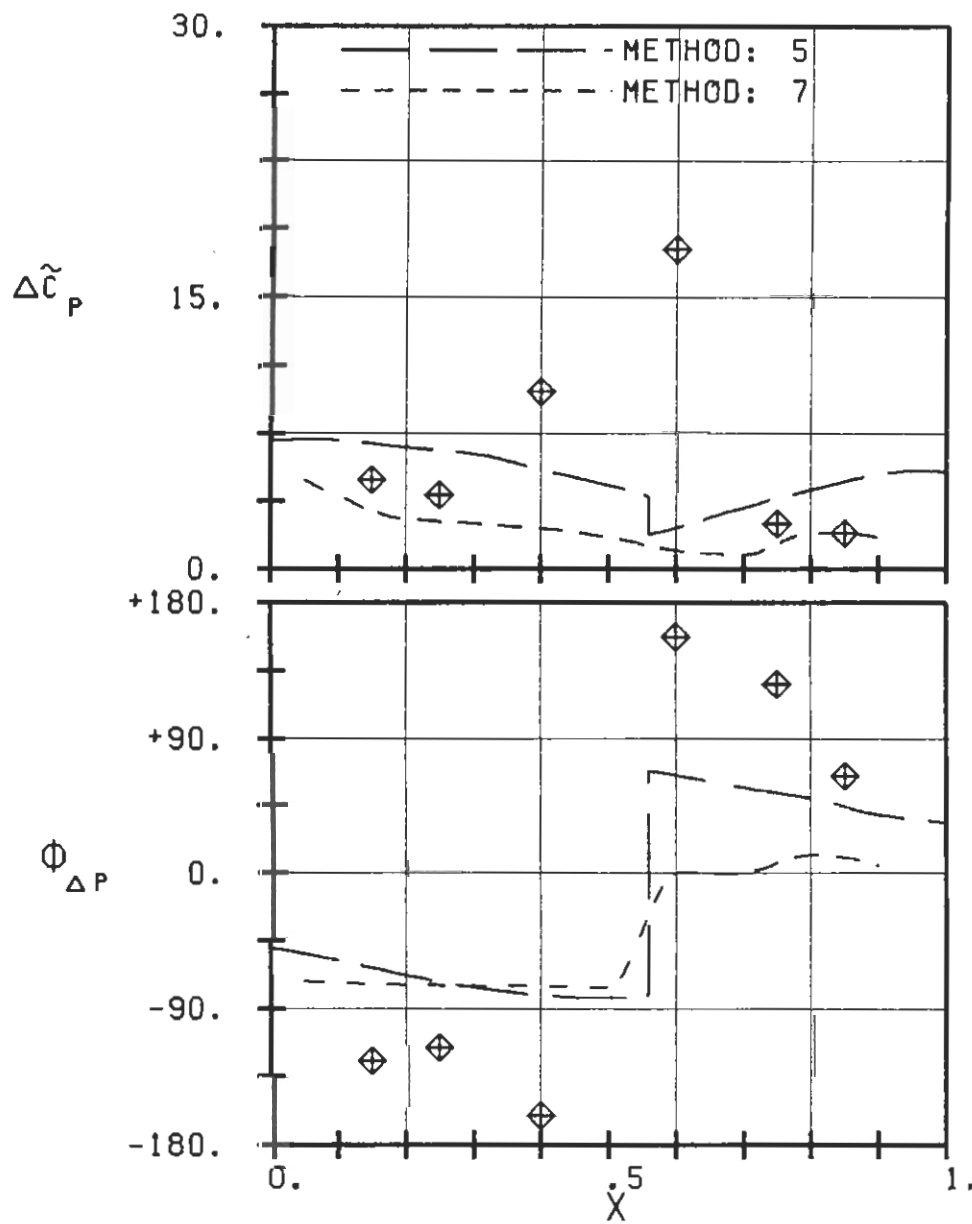
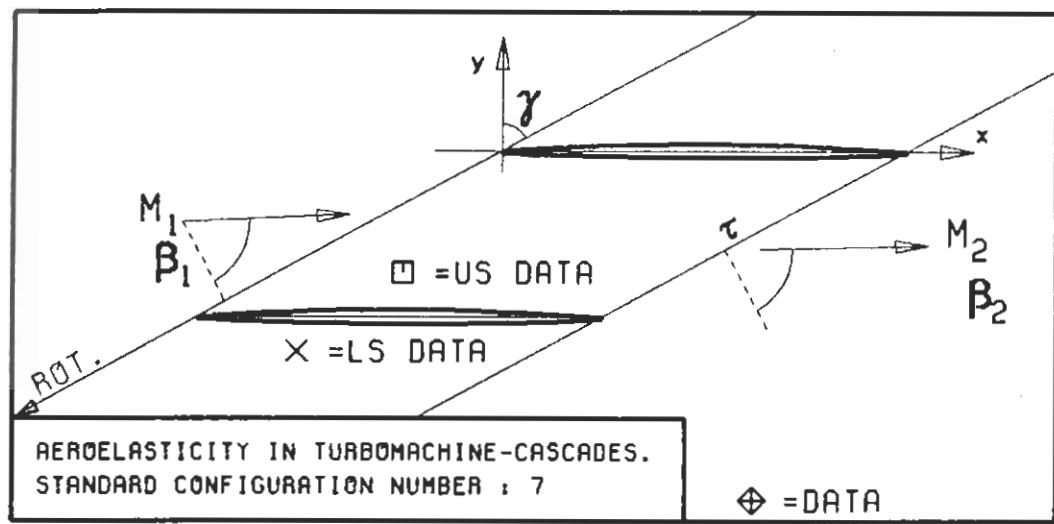
(x: IN PITCH MODE, NOTATION VALID UPSTREAM OF PITCH AXIS)

$c = .076$
 $\tau = .855$
 $\gamma = 61.55$
 $x_\alpha = .5$
 $y_\alpha = .0$
 $M_1 = 1.315$
 $\beta_1 = -64.0$
 $i = -$
 $M_2 = .99$
 $\beta_2 = -63.6$
 $h_x = -$
 $h_y = -$
 $\alpha = .0739$
 $\omega = 4555$
 $k = .44$
 $\delta = -$
 $\sigma = +120$
 $d = .034$



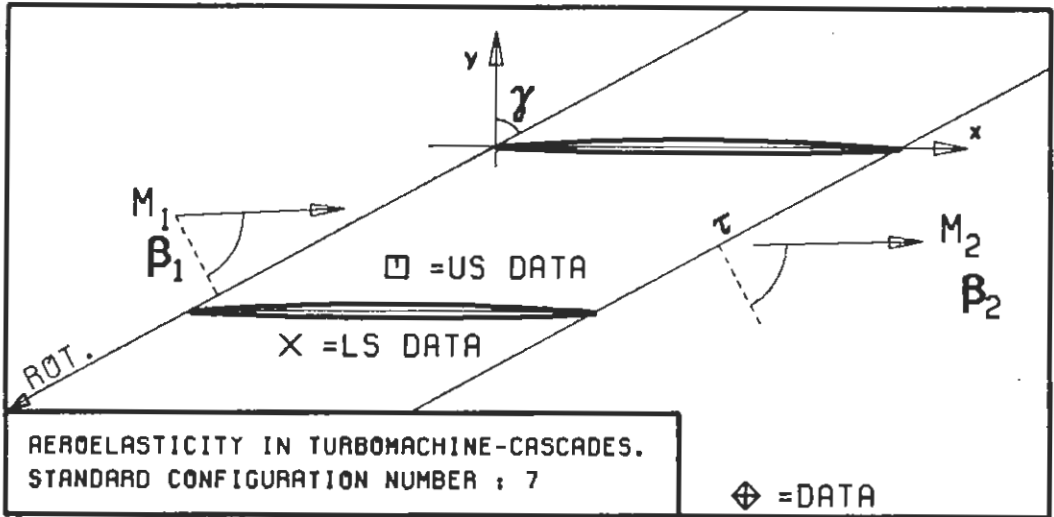
PLOT 7.7-3.1: SEVENTH STANDARD CONFIGURATION, CASE 1.
 MAGNITUDE AND PHASE LEAD OF BLADE SURFACE
 PRESSURE DIFFERENCE COEFFICIENT.

(*: IN PITCH MODE, NOTATION VALID UPSTREAM OF PITCH AXIS)

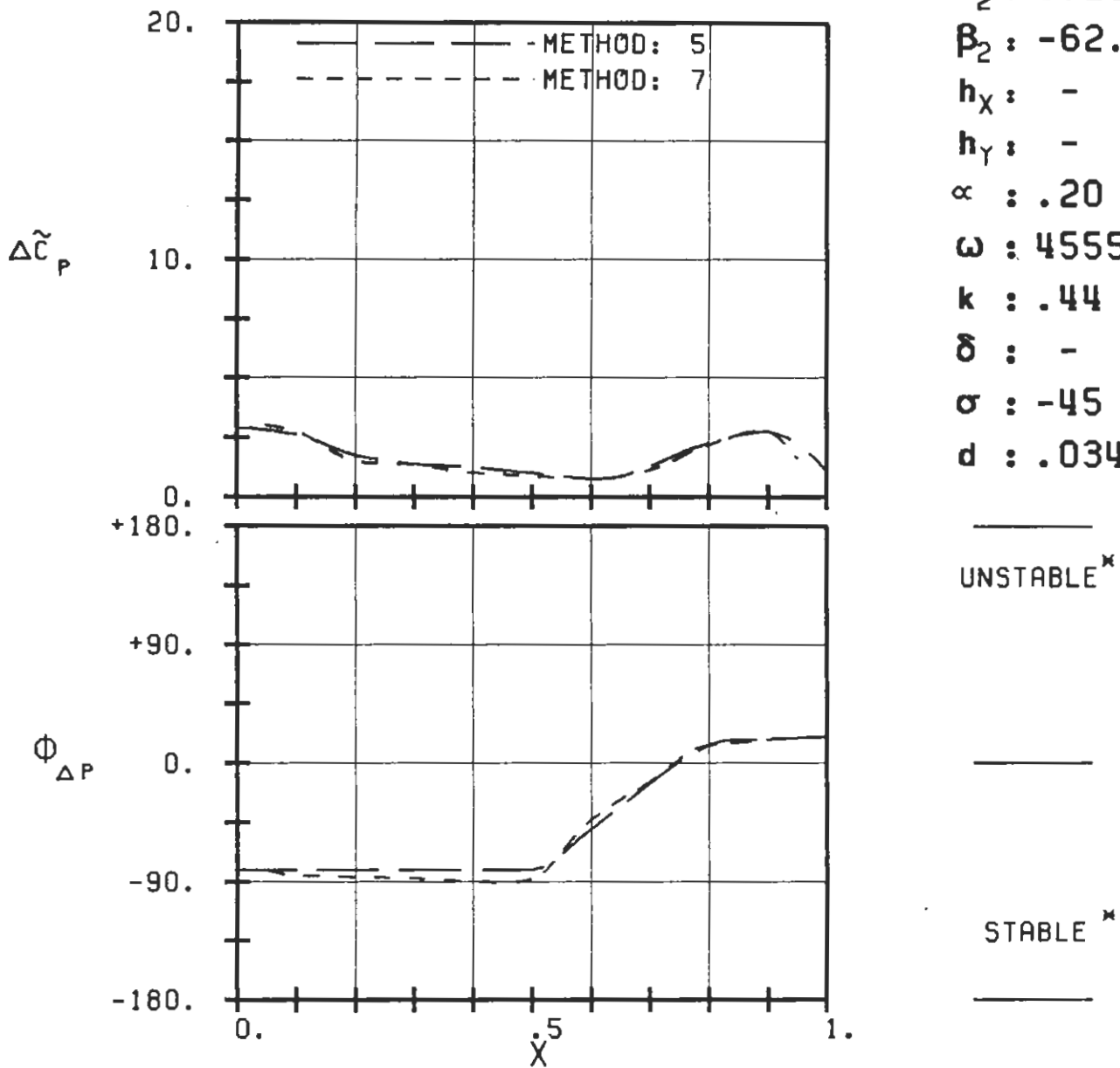


PLOT 7.7-3.2: SEVENTH STANDARD CONFIGURATION, CASE 2.
MAGNITUDE AND PHASE LEAD OF BLADE SURFACE
PRESSURE DIFFERENCE COEFFICIENT.

(*: IN PITCH MODE, NOTATION VALID UPSTREAM OF PITCH AXIS)

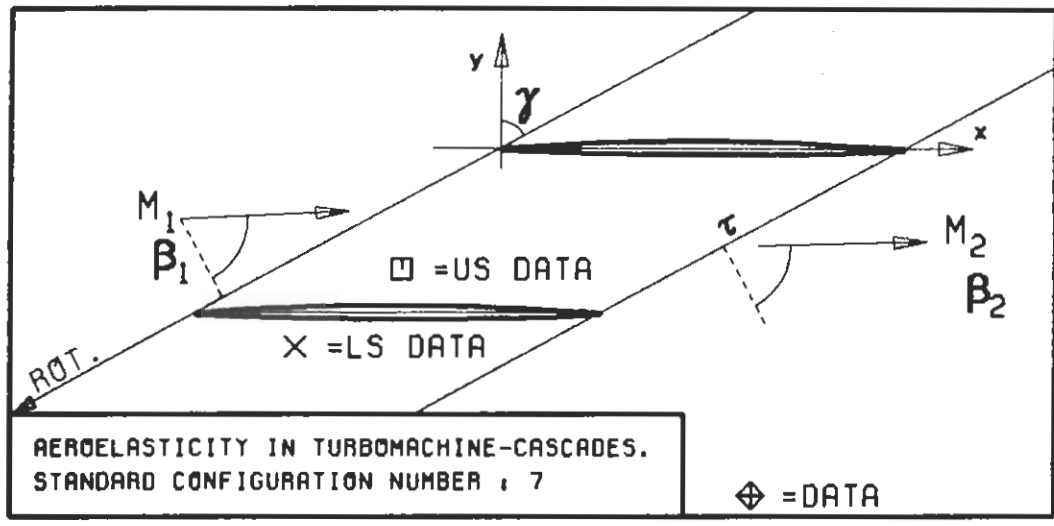


c : .076M
 τ : .855
 γ : 61.55
 x_α : .5
 y_α : .0
 M_1 : 1.315
 B_1 : -64.0
 i : -
 M_2 : 1.25
 B_2 : -62.8
 h_x : -
 h_y : -
 α : .20
 ω : 4555
 k : .44
 δ : -
 σ : -45
 d : .034

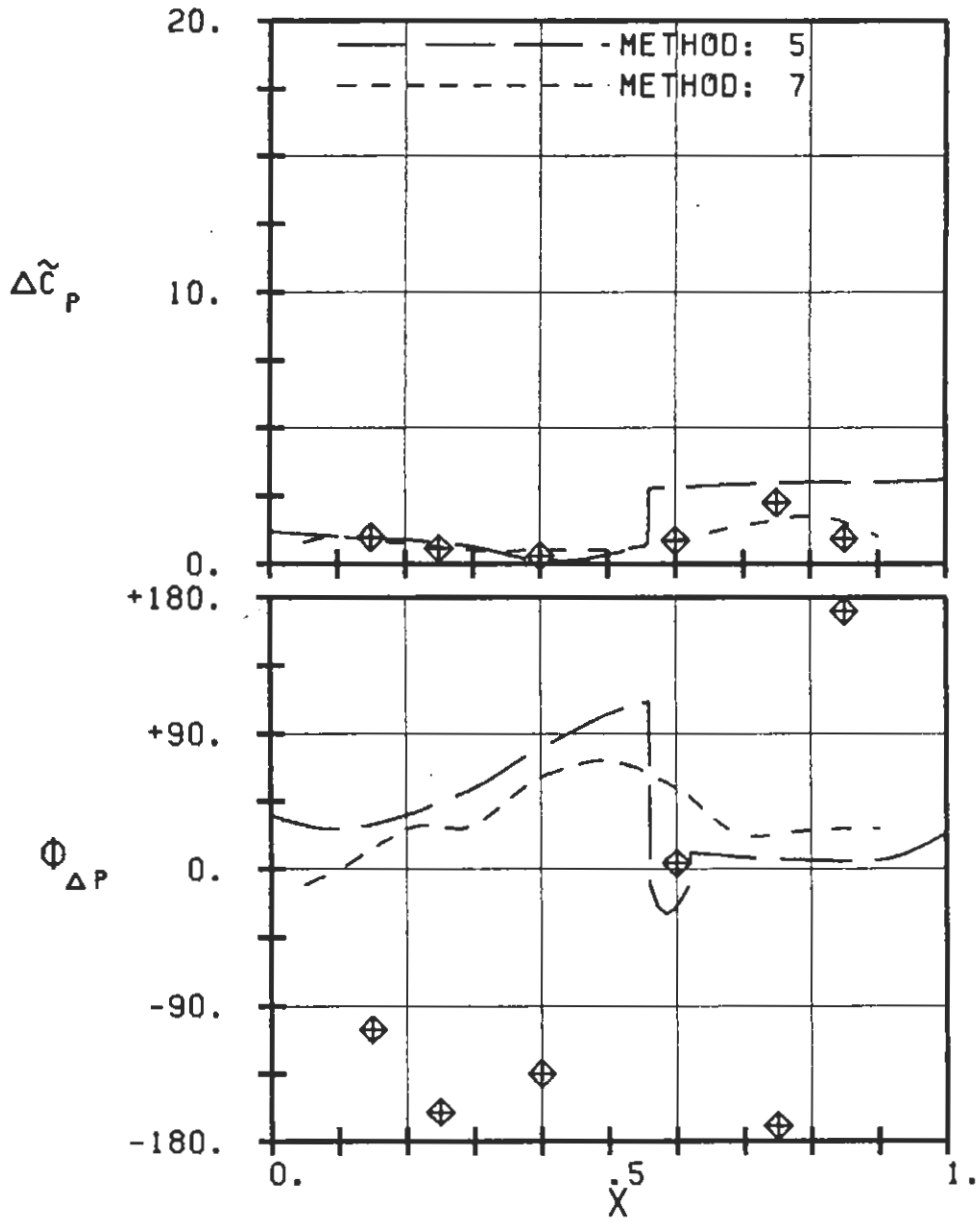


PL0T 7.7-3.3: SEVENTH STANDARD CONFIGURATION, CASE 3.
MAGNITUDE AND PHASE LEAD OF BLADE SURFACE
PRESSURE DIFFERENCE COEFFICIENT.

(*: IN PITCH MODE, NOTATION VALID UPSTREAM OF PITCH AXIS)

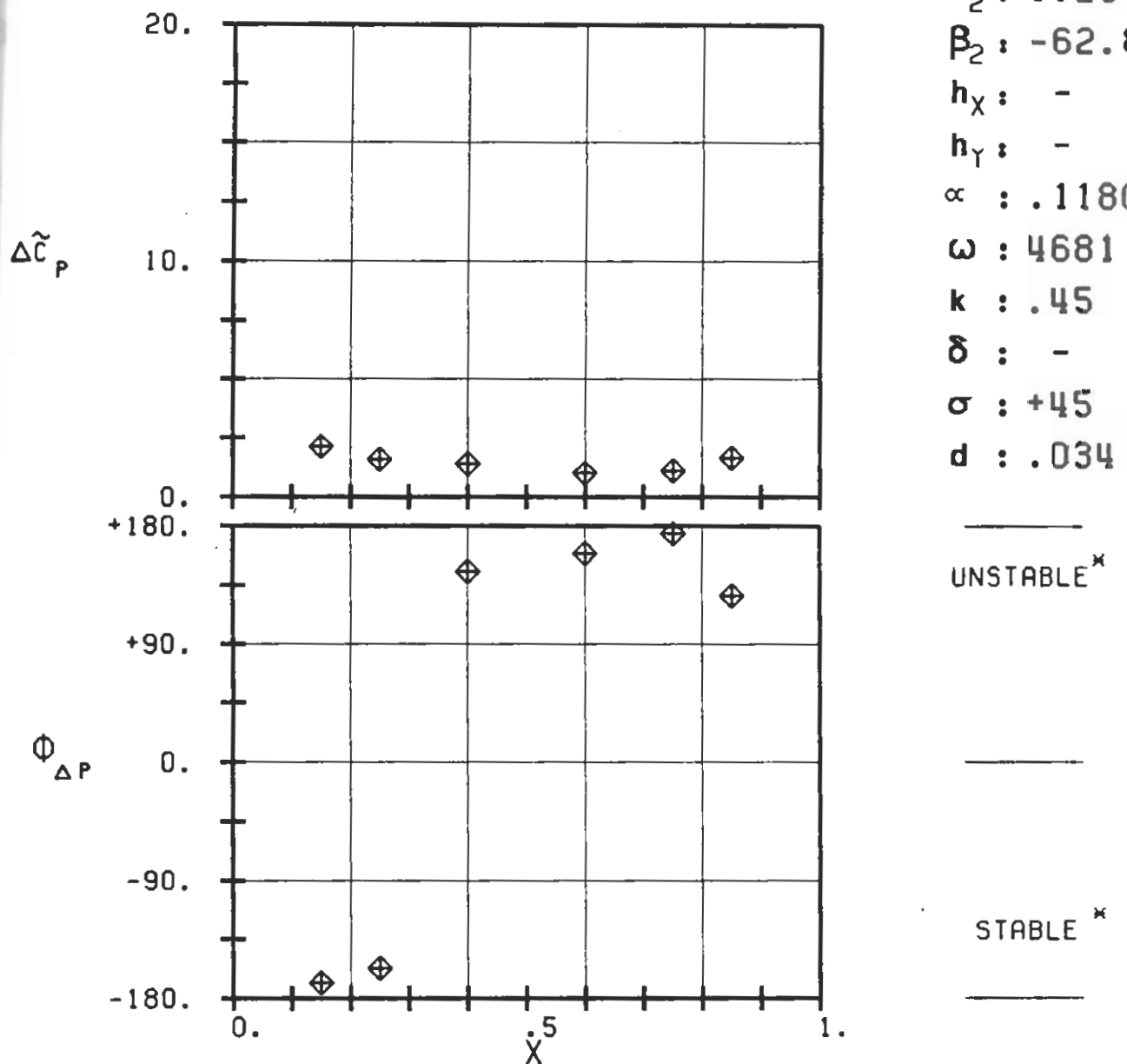
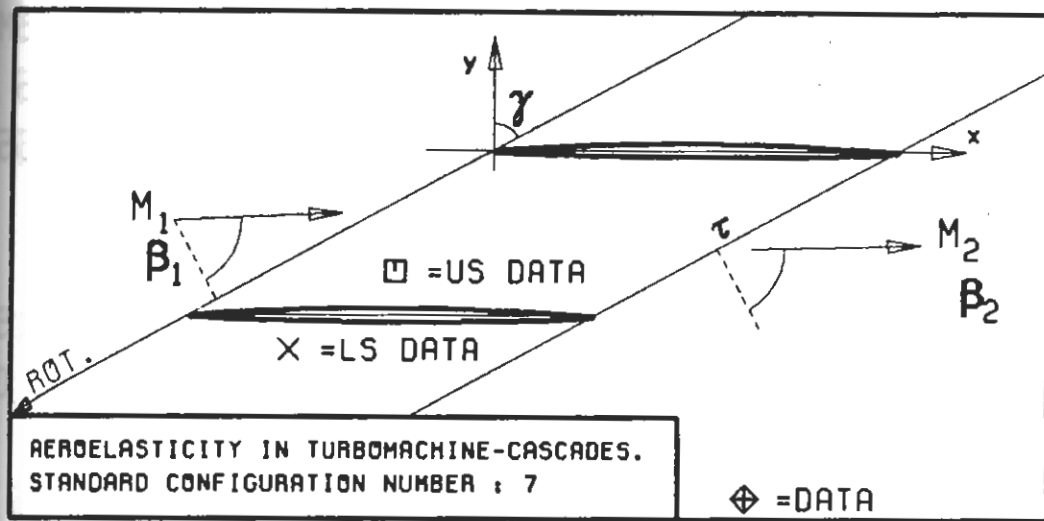


$c : .076M$
 $\tau : .855$
 $\gamma : 61.55$
 $x_\alpha : .5$
 $y_\alpha : .0$
 $M_1 : 1.315$
 $B_1 : -64.0$
 $i : -$
 $M_2 : 1.25$
 $B_2 : -62.8$
 $h_x : -$
 $h_y : -$
 $\alpha : .2172$
 $\omega : 4549$
 $k : .44$
 $\delta : -$
 $\sigma : 0$
 $d : .034$



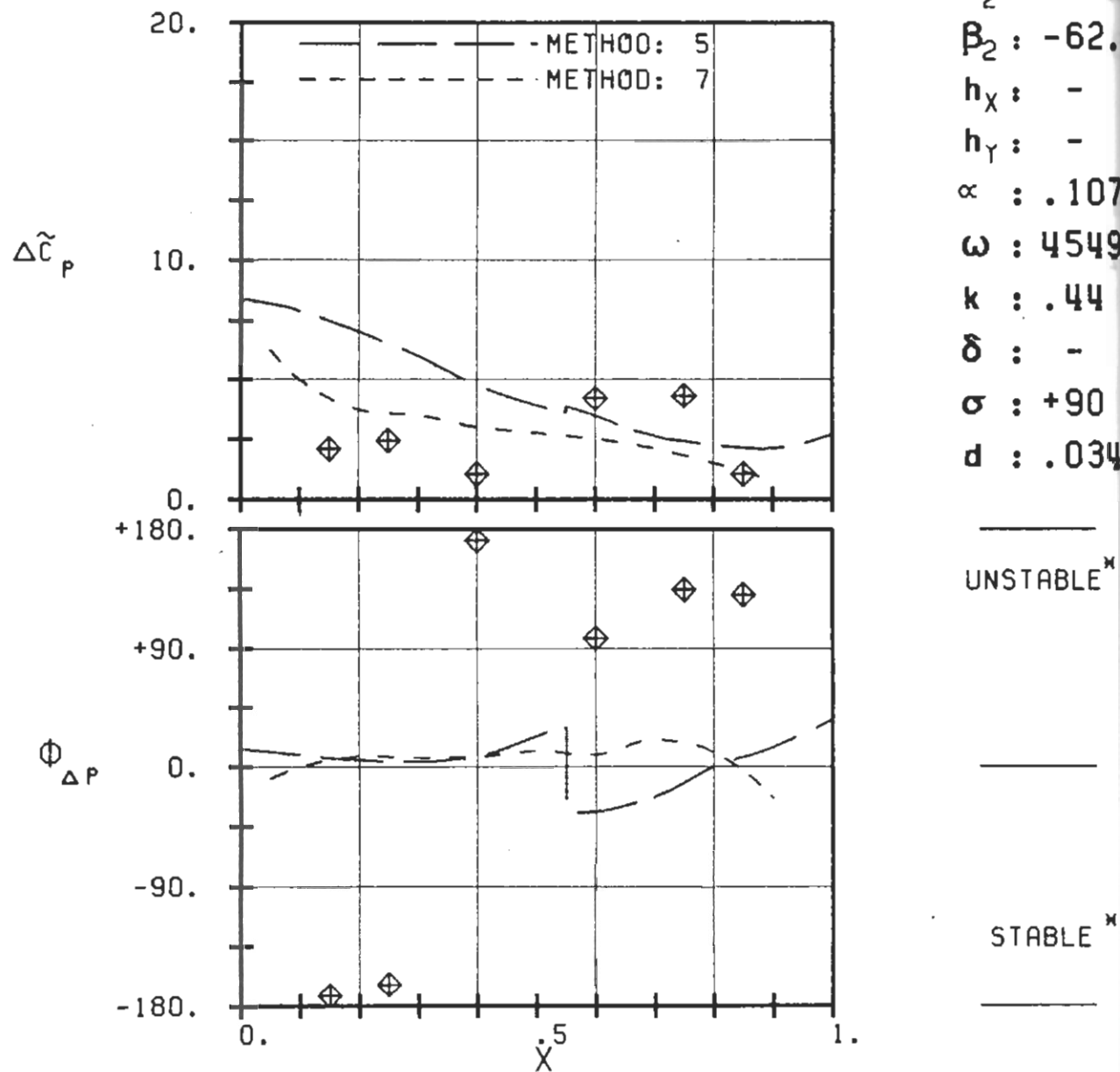
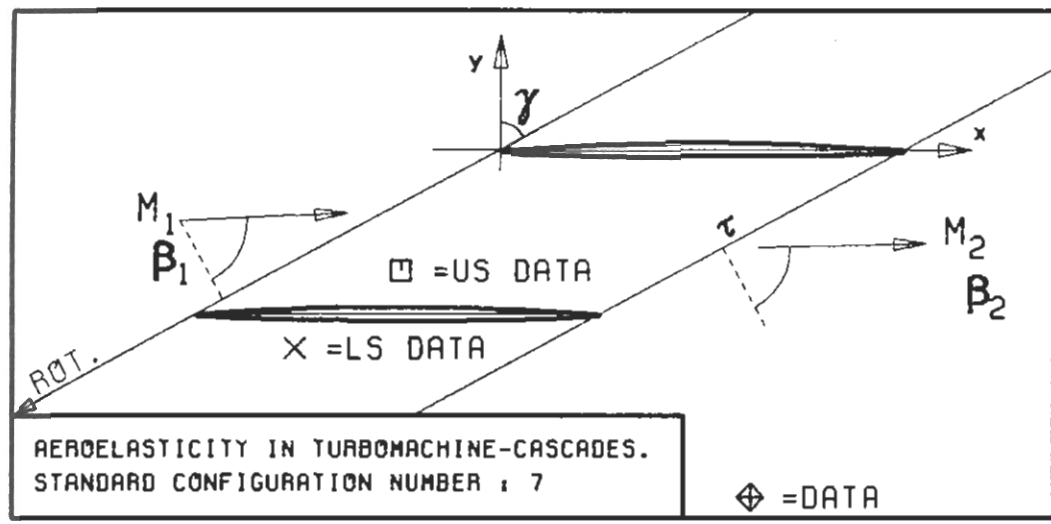
PLOT 7.7-3.4: SEVENTH STANDARD CONFIGURATION, CASE 4.
MAGNITUDE AND PHASE LEAD OF BLADE SURFACE
PRESSURE DIFFERENCE COEFFICIENT.

(*: IN PITCH MODE, NOTATION VALID UPSTREAM OF PITCH AXIS)



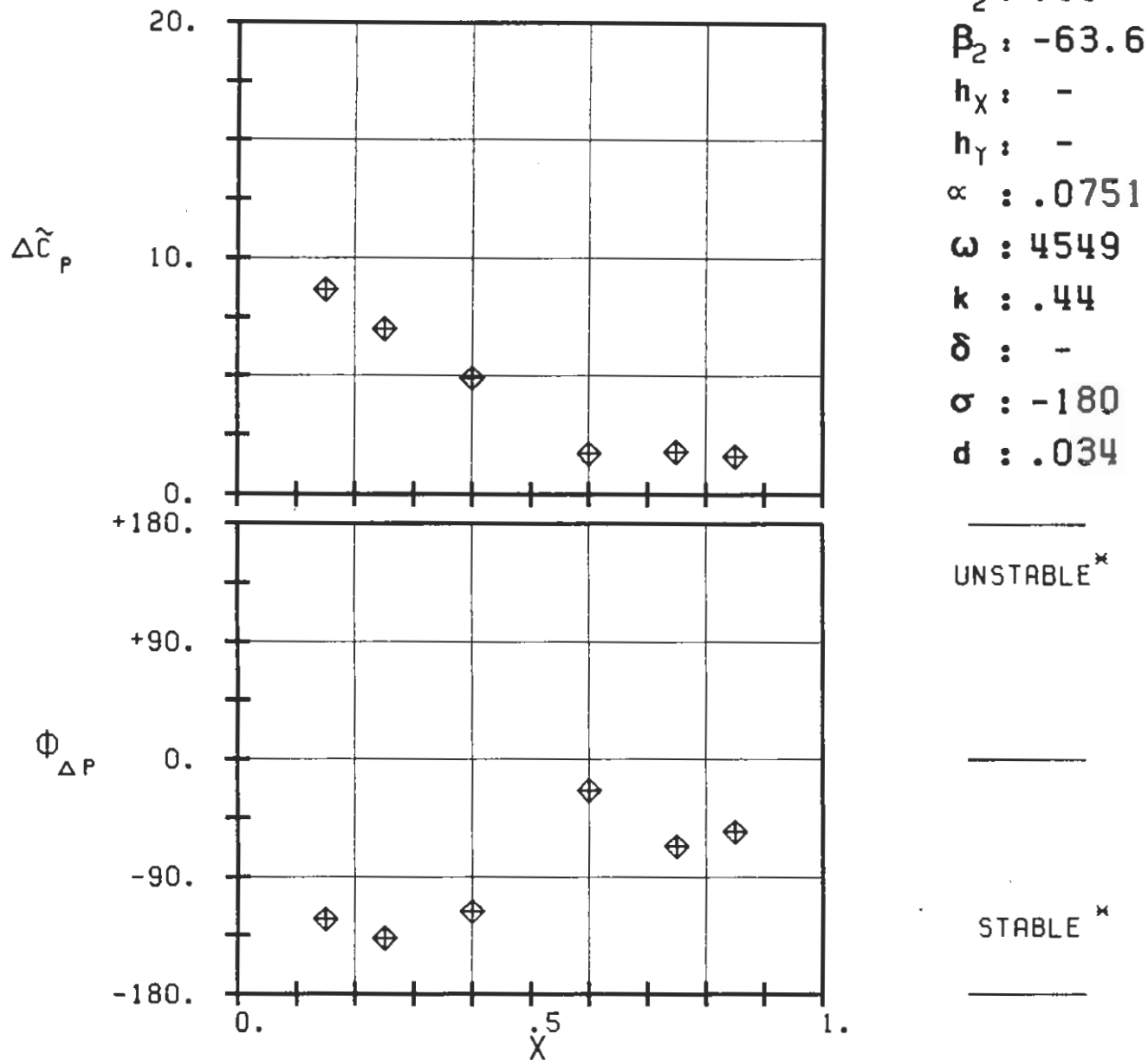
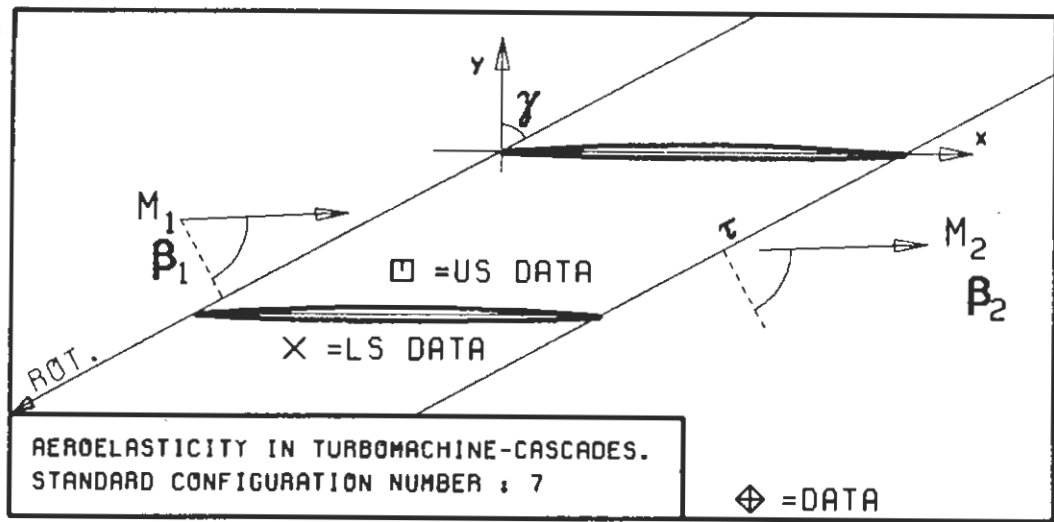
PLOT 7.7-3.5: SEVENTH STANDARD CONFIGURATION, CASE 5.
MAGNITUDE AND PHASE LEAD OF BLADE SURFACE
PRESSURE DIFFERENCE COEFFICIENT.

(*: IN PITCH MODE, NOTATION VALID UPSTREAM OF PITCH AXIS)



PLOT 7.7-3.6: SEVENTH STANDARD CONFIGURATION, CASE 6.
MAGNITUDE AND PHASE LEAD OF BLADE SURFACE
PRESSURE DIFFERENCE COEFFICIENT.

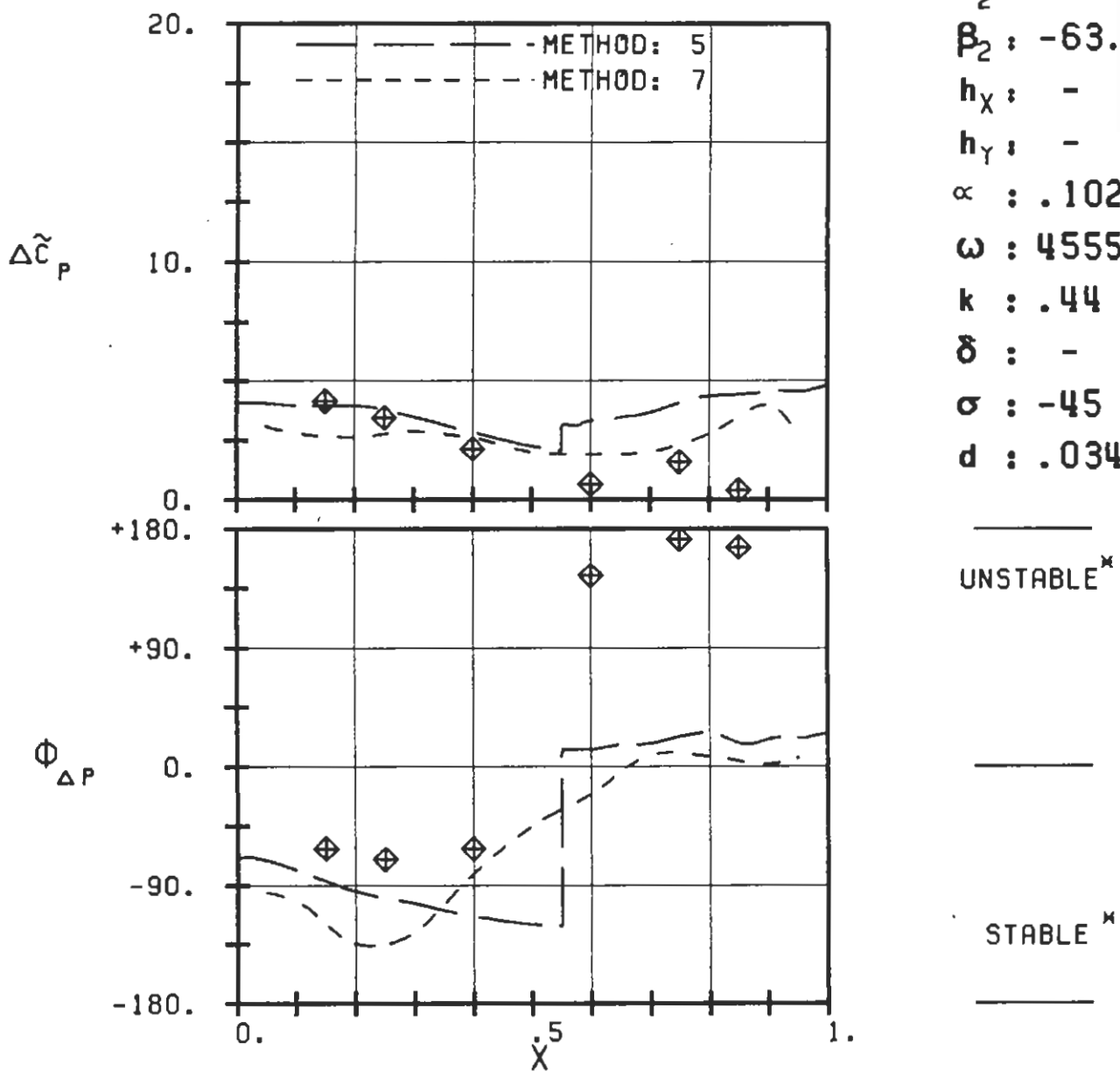
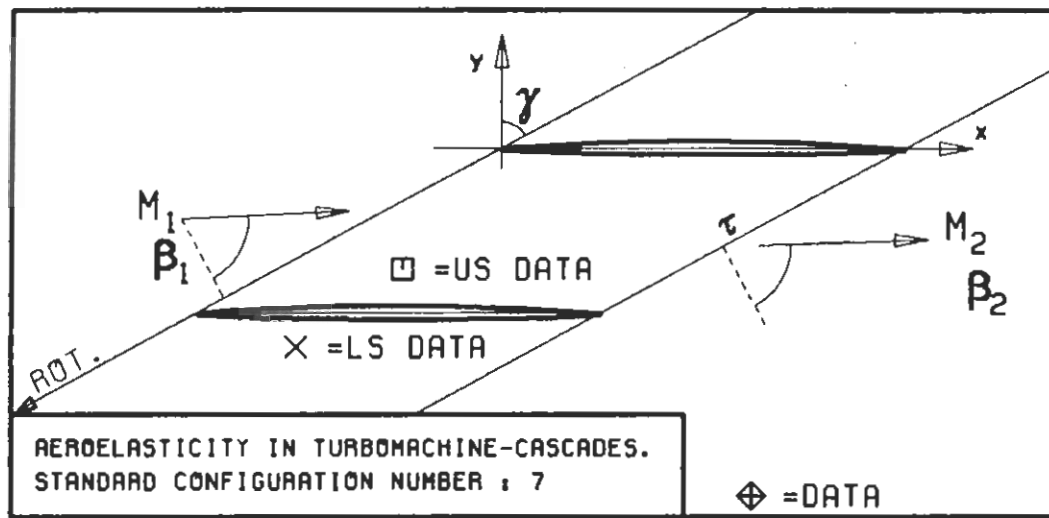
(*: IN PITCH MODE, NOTATION VALID UPSTREAM OF PITCH AXIS)



PLOT 7.7-3.7: SEVENTH STANDARD CONFIGURATION, CASE 7.
 MAGNITUDE AND PHASE LEAD OF BLADE SURFACE
 PRESSURE DIFFERENCE COEFFICIENT.

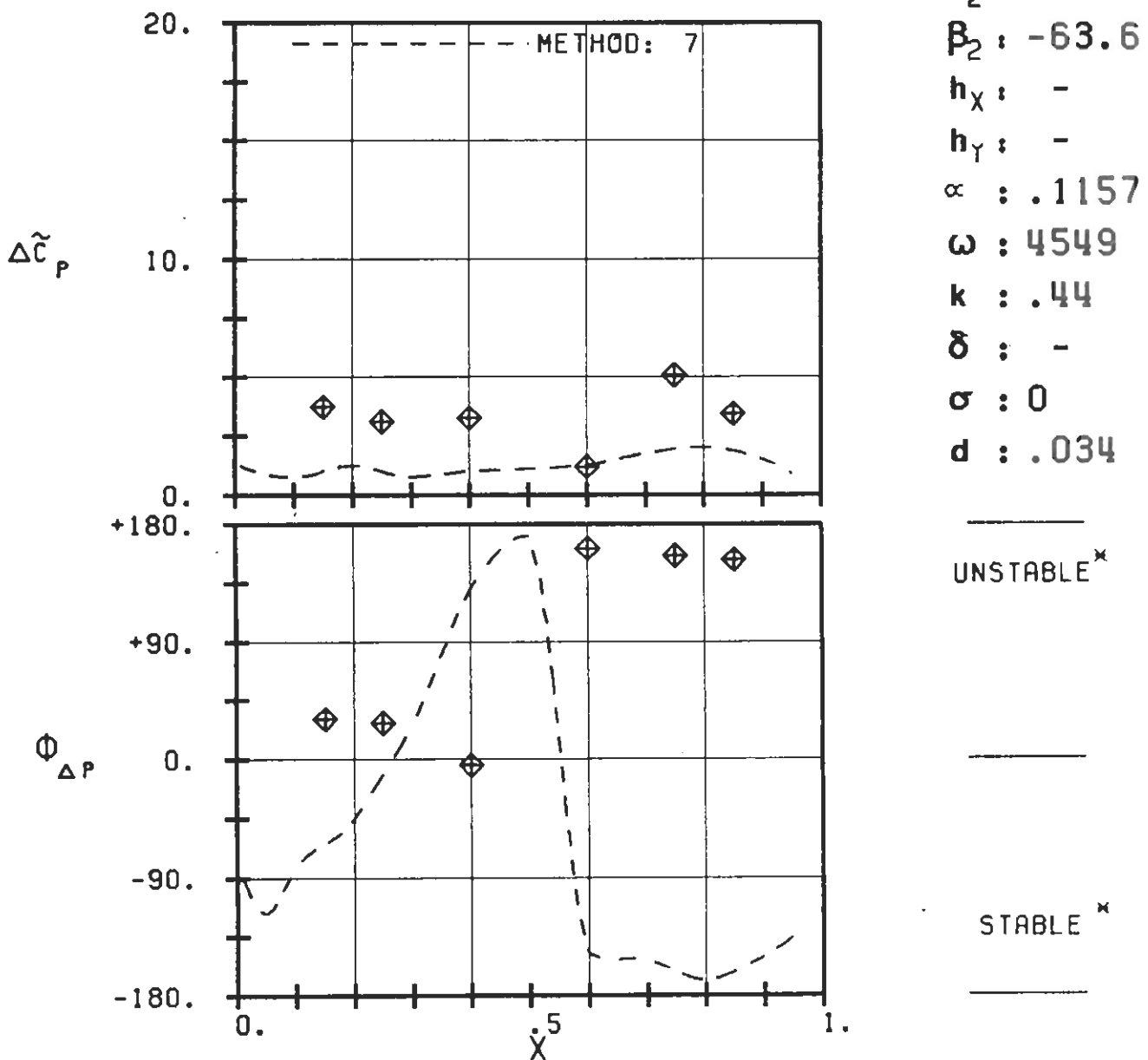
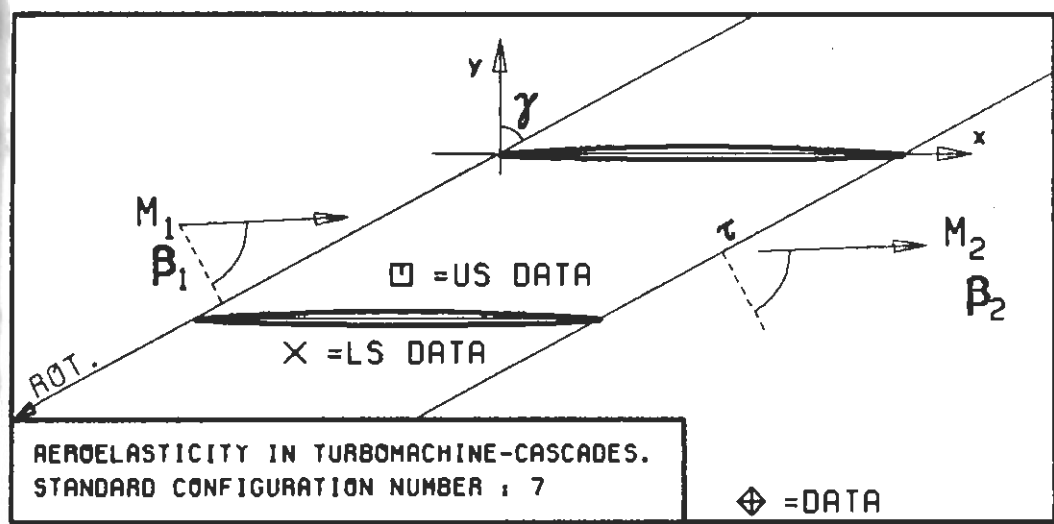
(\times : IN PITCH MODE, NOTATION VALID UPSTREAM OF PITCH AXIS)

$c : .076M$
 $\tau : .855$
 $\gamma : 61.55$
 $x_\alpha : .5$
 $y_\alpha : .0$
 $M_1 : 1.315$
 $\beta_1 : -64.0$
 $i : -$
 $M_2 : .99$
 $\beta_2 : -63.6$
 $h_X : -$
 $h_Y : -$
 $\alpha : .0751$
 $\omega : 4549$
 $k : .44$
 $\delta : -$
 $\sigma : -180$
 $d : .034$



PLOT 7.7-3.8: SEVENTH STANDARD CONFIGURATION, CASE 8.
MAGNITUDE AND PHASE LEAD OF BLADE SURFACE
PRESSURE DIFFERENCE COEFFICIENT.

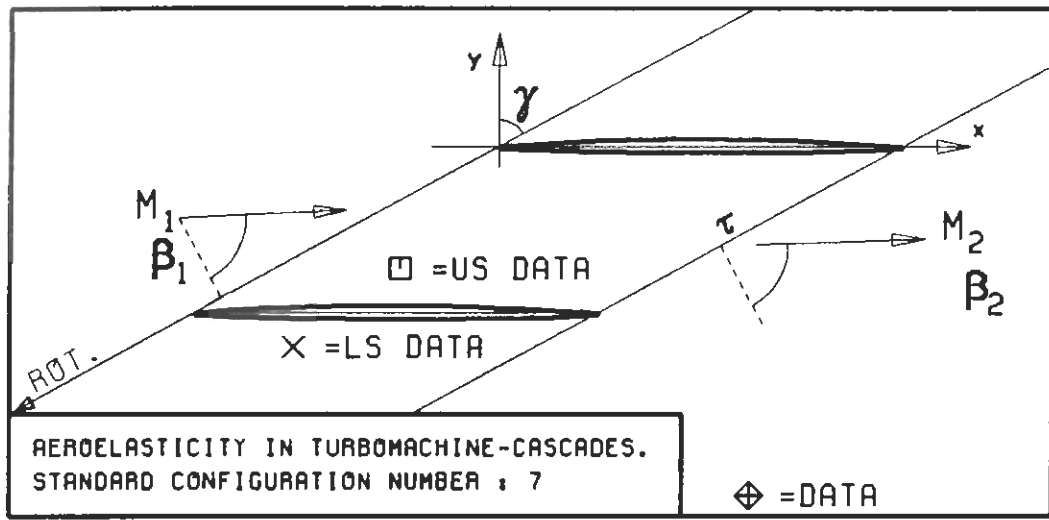
(x: IN PITCH MODE, NOTATION VALID UPSTREAM OF PITCH AXIS)



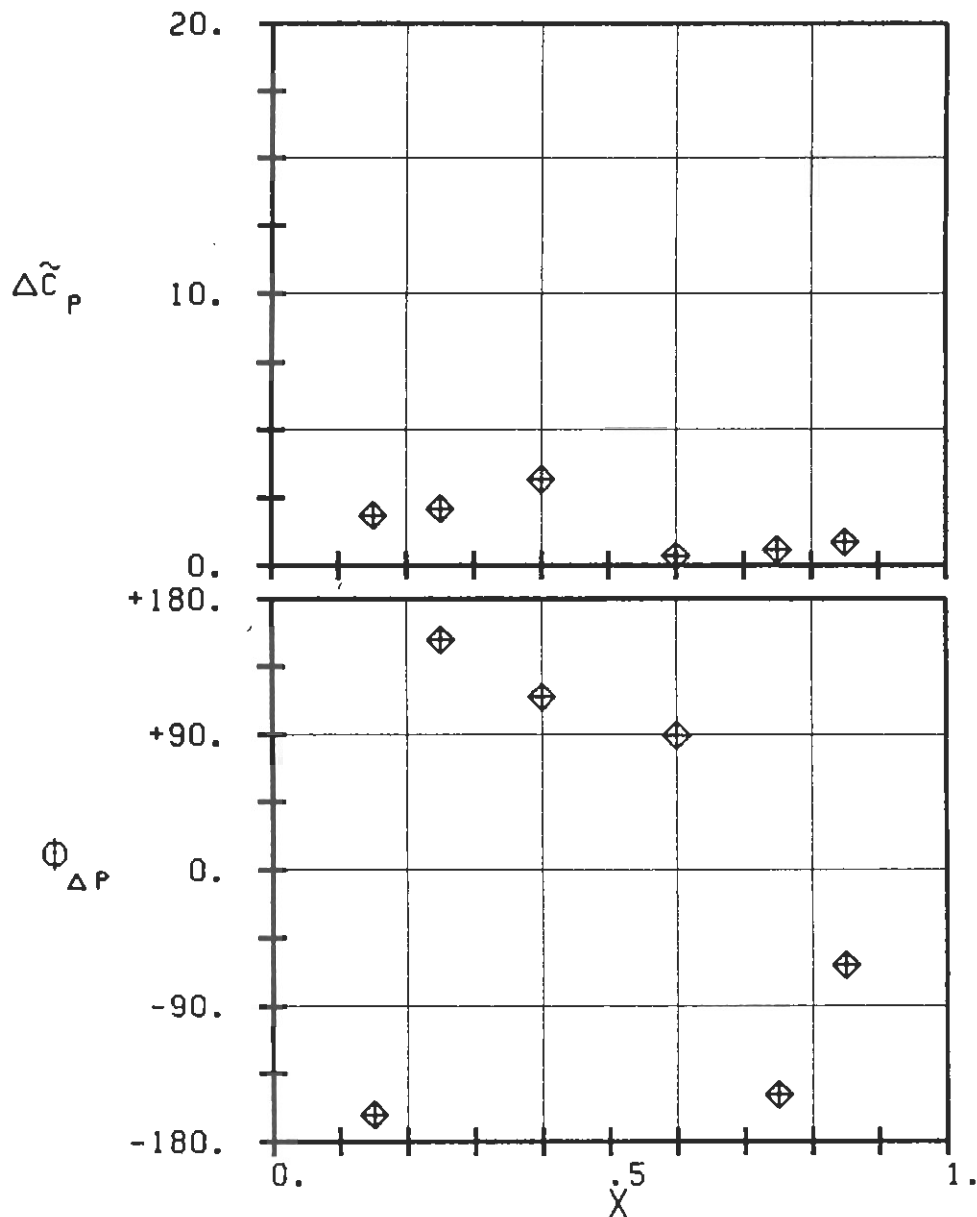
PLOT 7.7-3.9: SEVENTH STANDARD CONFIGURATION, CASE 9.
MAGNITUDE AND PHASE LEAD OF BLADE SURFACE
PRESSURE DIFFERENCE COEFFICIENT.

(x: IN PITCH MODE, NOTATION VALID UPSTREAM OF PITCH AXIS)

c : .076M
 τ : .855
 γ : 61.55
 x_∞ : .5
 y_∞ : .0
 M_1 : 1.315
 B_1 : -64.0
 i : -
 M_2 : .99
 B_2 : -63.6
 h_X : -
 h_Y : -
 α : .1157
 ω : 4549
 k : .44
 δ : -
 σ : 0
 d : .034

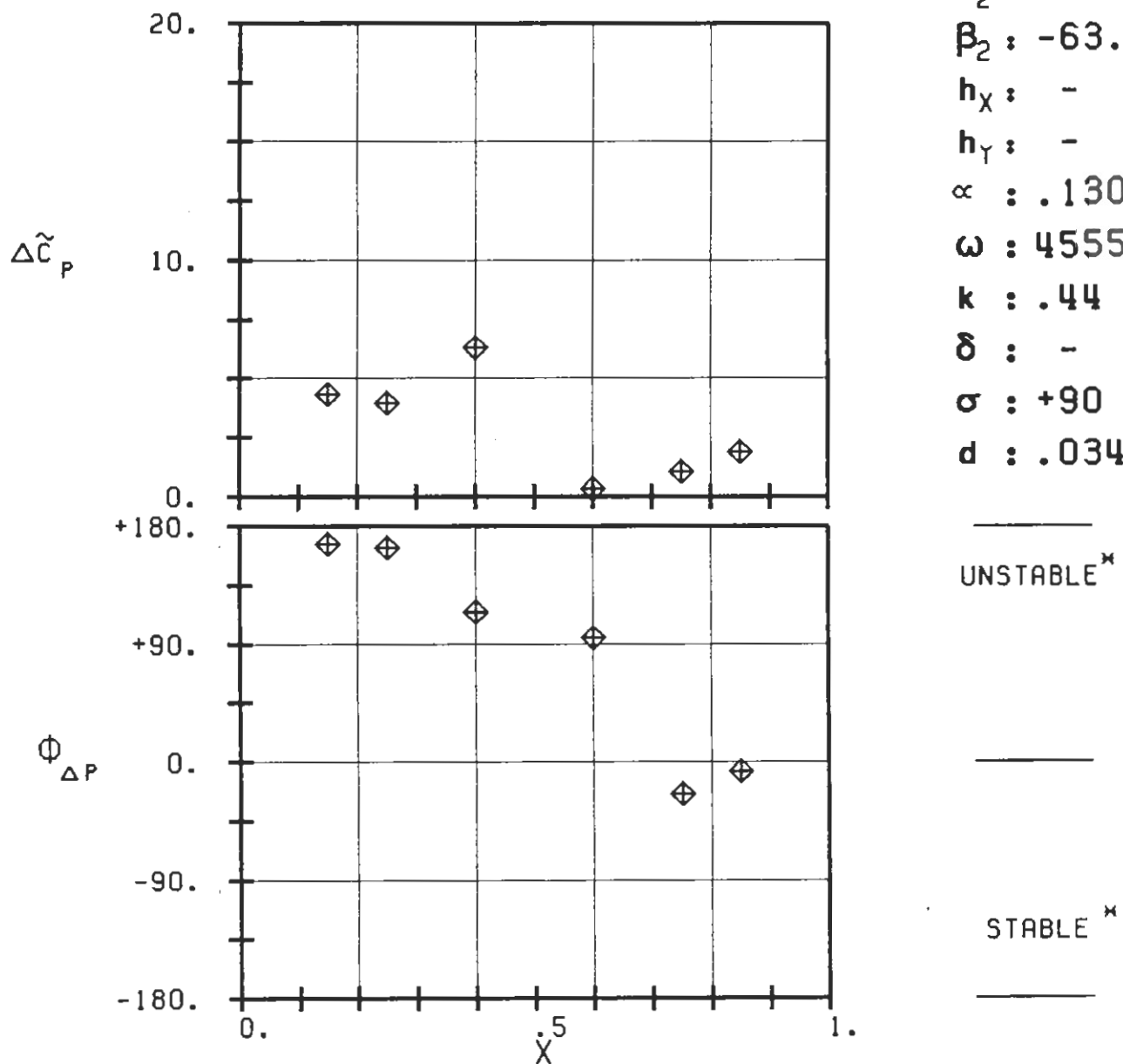
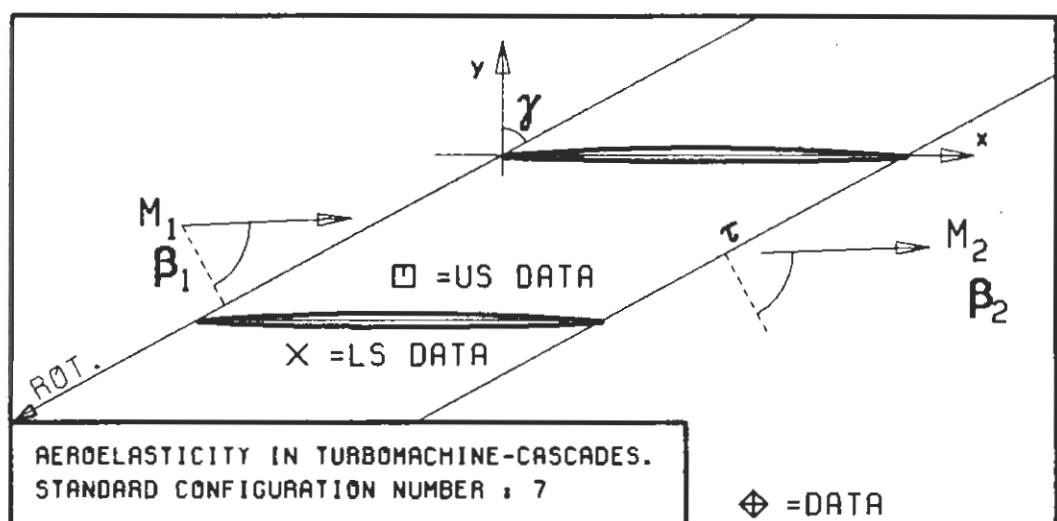


$c : .076M$
 $\tau : .855$
 $\gamma : 61.55$
 $x_\infty : .5$
 $y_\infty : .0$
 $M_1 : 1.315$
 $\beta_1 : -64.0$
 $i : -$
 $M_2 : .99$
 $\beta_2 : -63.6$
 $h_x : -$
 $h_y : -$
 $\alpha : .2212$
 $\omega : 4549$
 $k : .44$
 $\delta : -$
 $\sigma : +45$
 $d : .034$



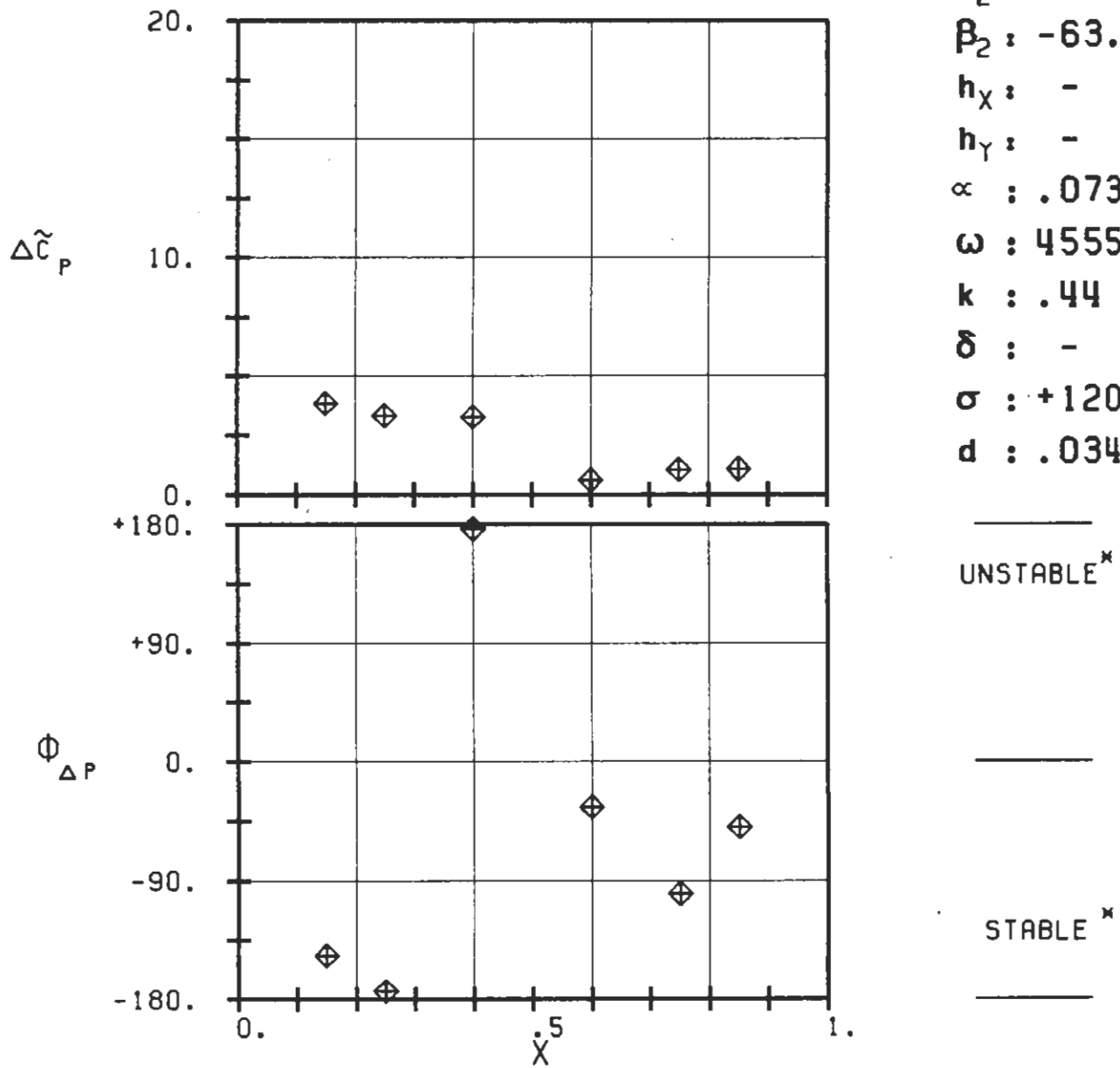
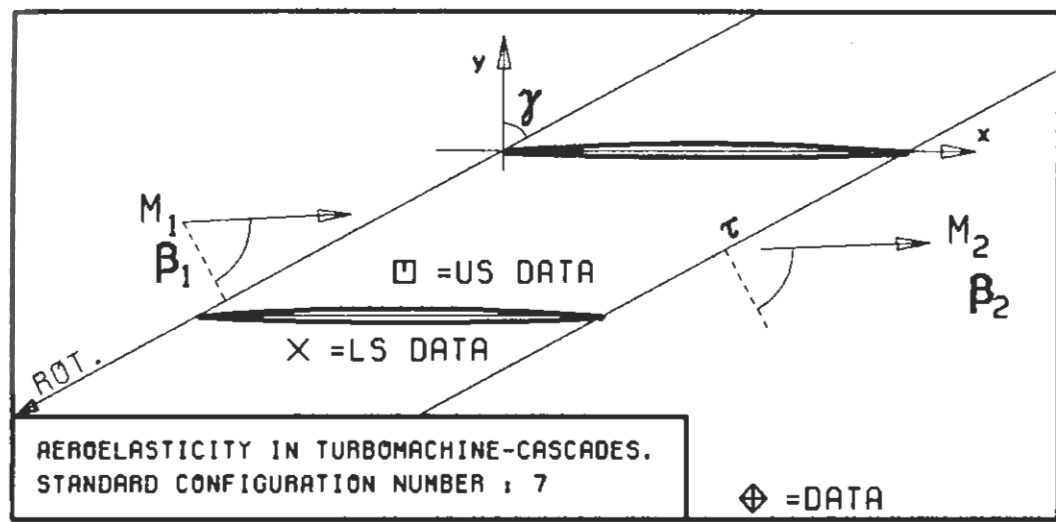
PLOT 7.7-3.10 SEVENTH STANDARD CONFIGURATION, CASE 10.
 MAGNITUDE AND PHASE LEAD OF BLADE SURFACE
 PRESSURE DIFFERENCE COEFFICIENT.

(*: IN PITCH MODE, NOTATION VALID UPSTREAM OF PITCH AXIS)



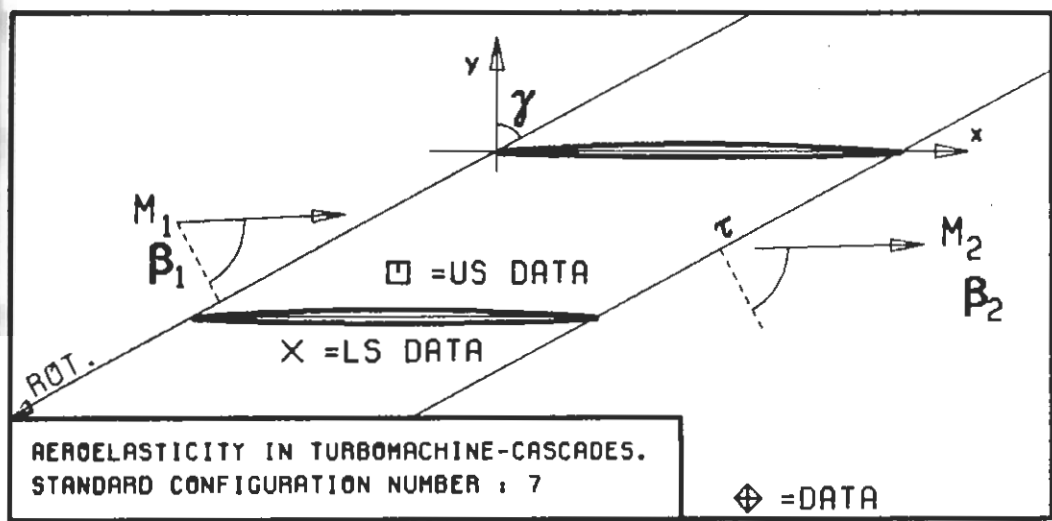
PLOT 7.7-3.11 SEVENTH STANDARD CONFIGURATION, CASE 11.
MAGNITUDE AND PHASE LEAD OF BLADE SURFACE
PRESSURE DIFFERENCE COEFFICIENT.

(\times : IN PITCH MODE, NOTATION VALID UPSTREAM OF PITCH AXIS)

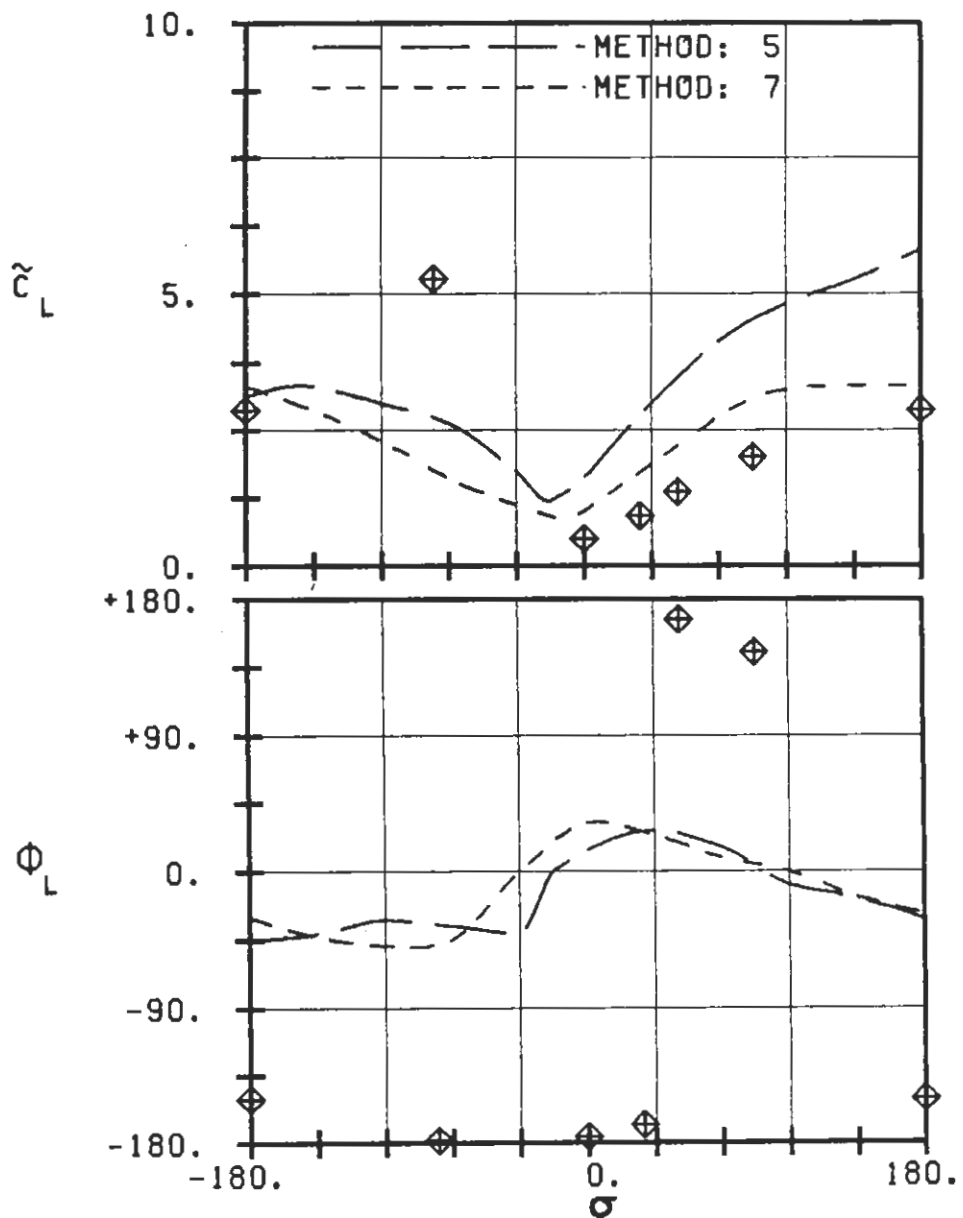


PLOT 7.7-3.12: SEVENTH STANDARD CONFIGURATION, CASE 12.
MAGNITUDE AND PHASE LEAD OF BLADE SURFACE
PRESSURE DIFFERENCE COEFFICIENT.

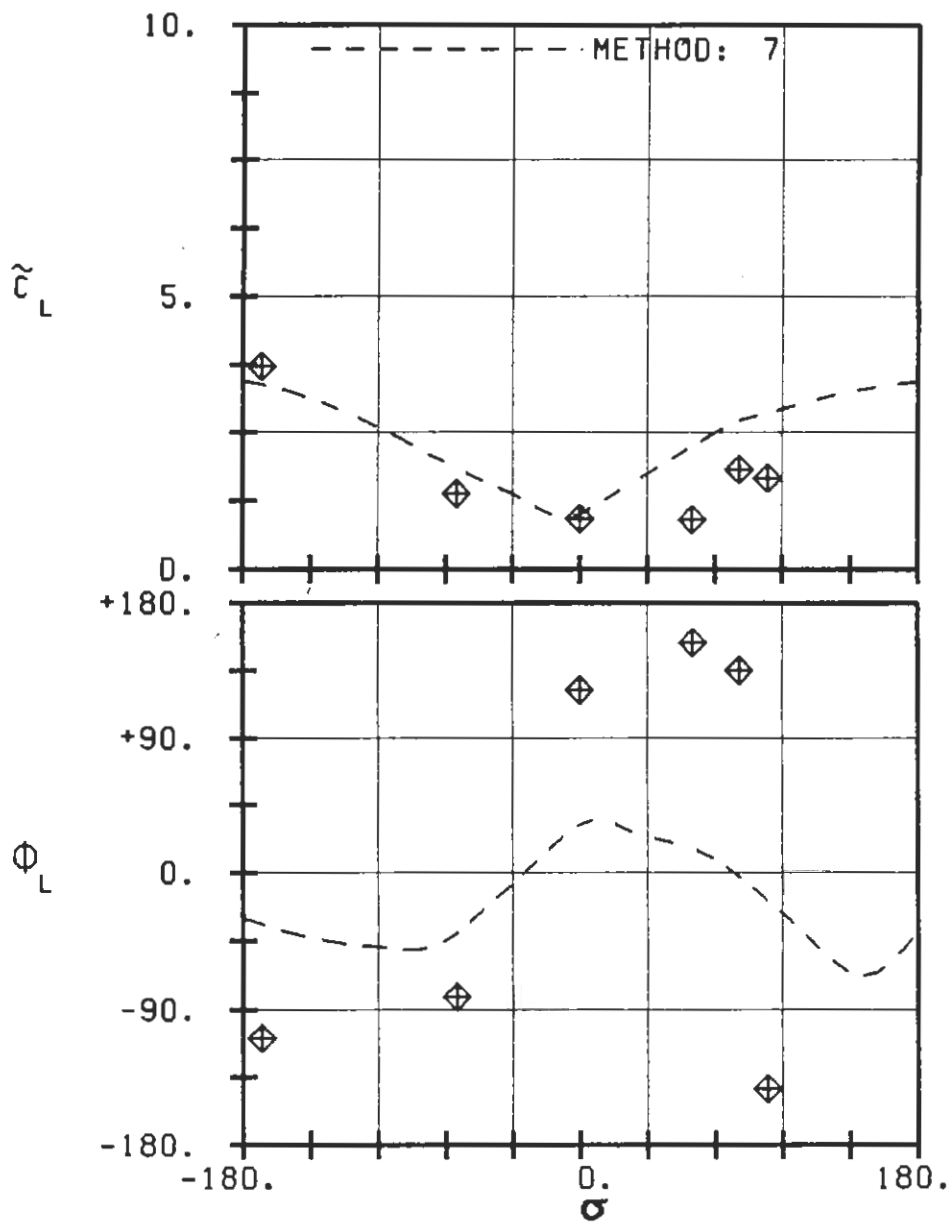
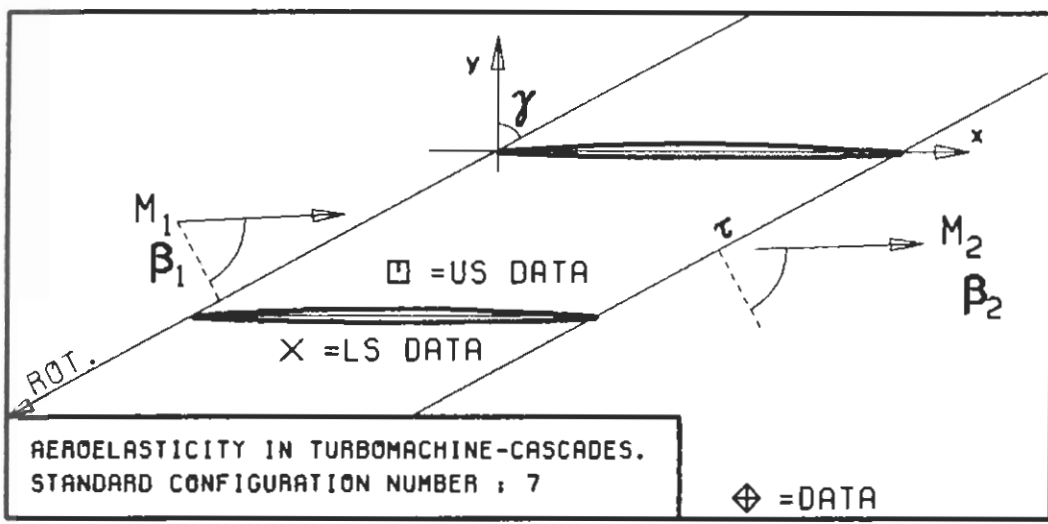
(x: IN PITCH MODE, NOTATION VALID UPSTREAM OF PITCH AXIS)



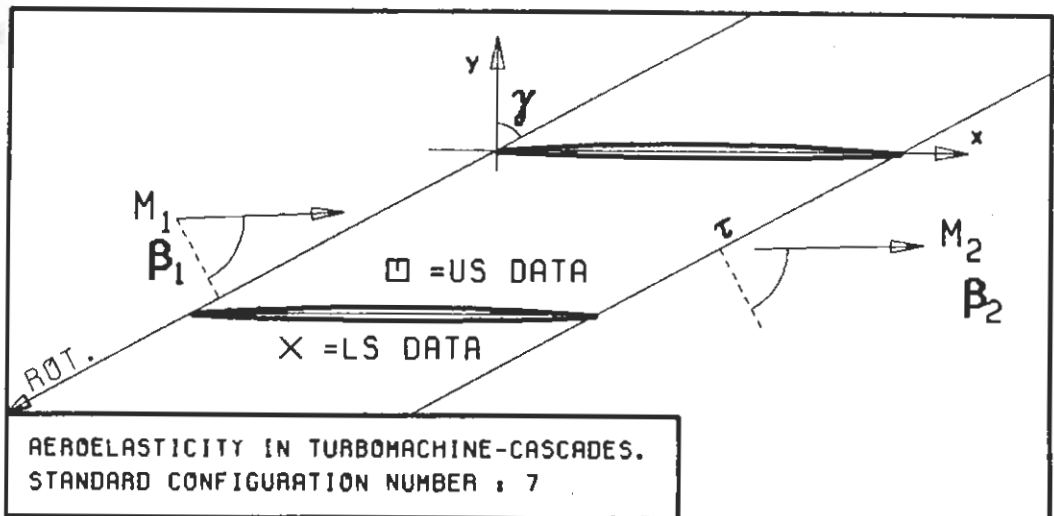
c : .076M
 τ : .855
 γ : 61.55
 x_α : .5
 y_α : 0.
 M_1 : 1.315
 B_1 : -64.0
 i : -
 M_2 : 1.25
 B_2 : -62.8
 h_x : -
 h_y : -
 α : -
 ω : -
 k : .44
 δ : -
 σ : -
 d : .034



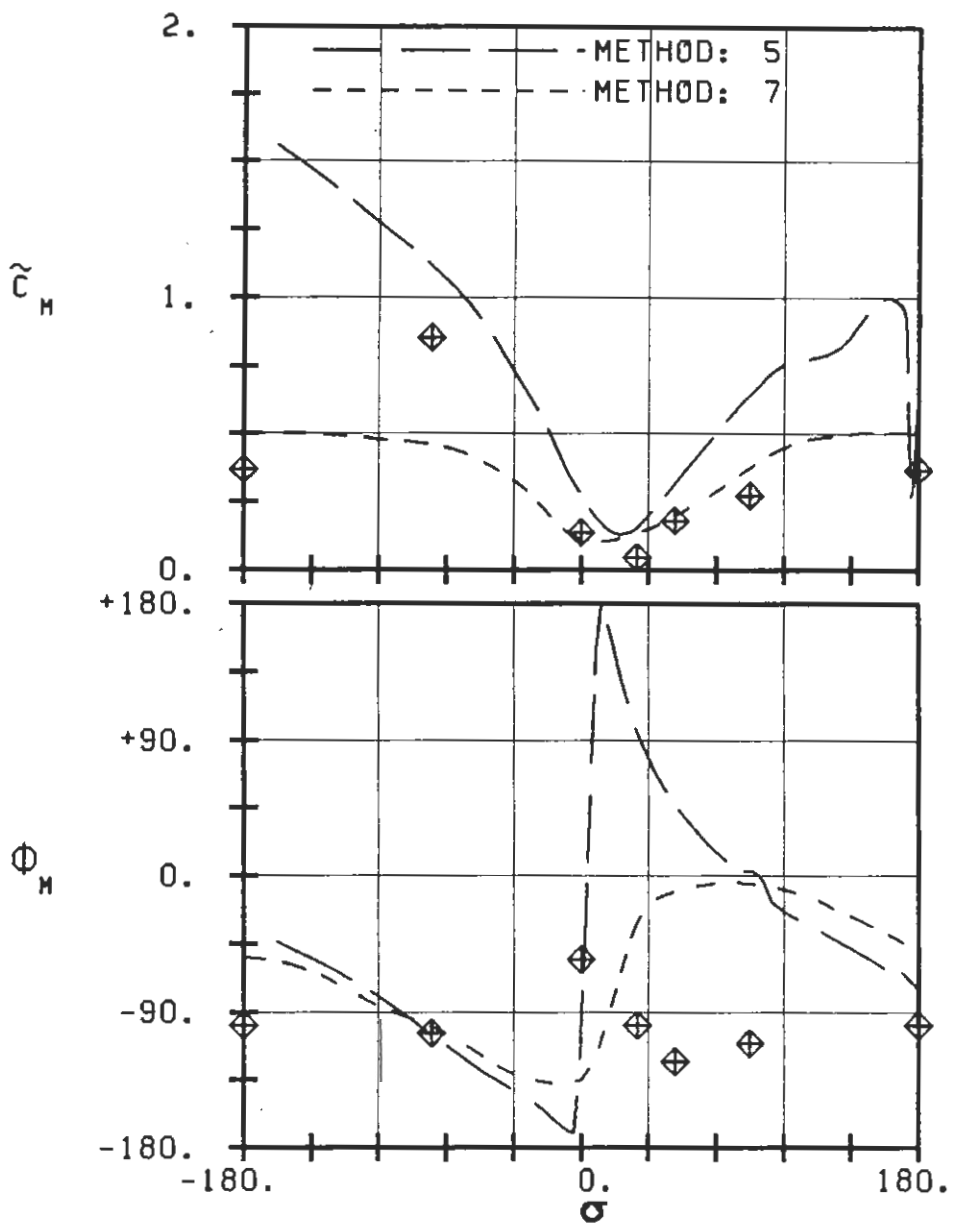
PLOT 7.7-4.1: SEVENTH STANDARD CONFIGURATION, CASES 1-6.
 AERODYNAMIC LIFT COEFFICIENT AND PHASE LEAD
 IN DEPENDANCE OF INTERBLADE PHASE ANGLE.



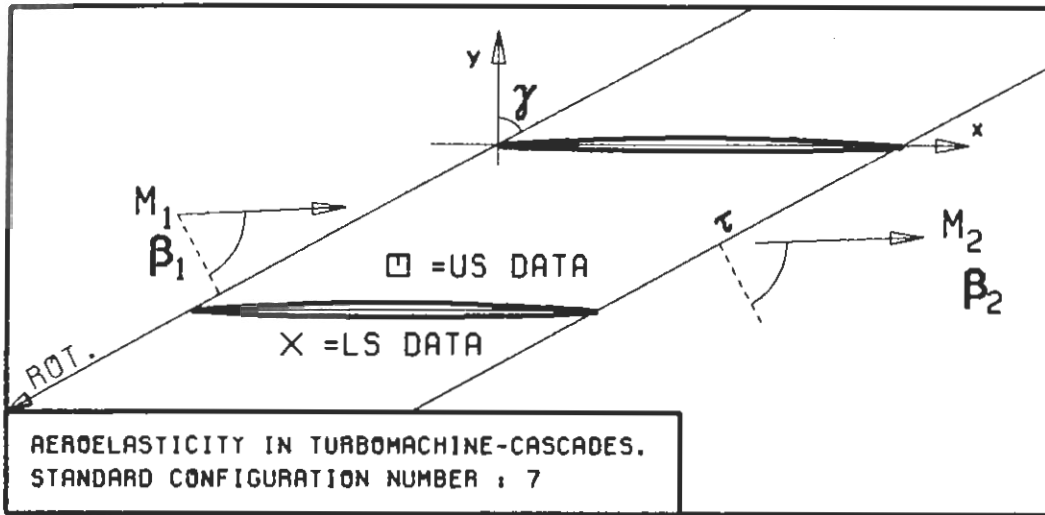
PLOT 7.7-4.2: SEVENTH STANDARD CONFIGURATION, CASES 7-12.
AERODYNAMIC LIFT COEFFICIENT AND PHASE LEAD
IN DEPENDANCE OF INTERBLADE PHASE ANGLE.



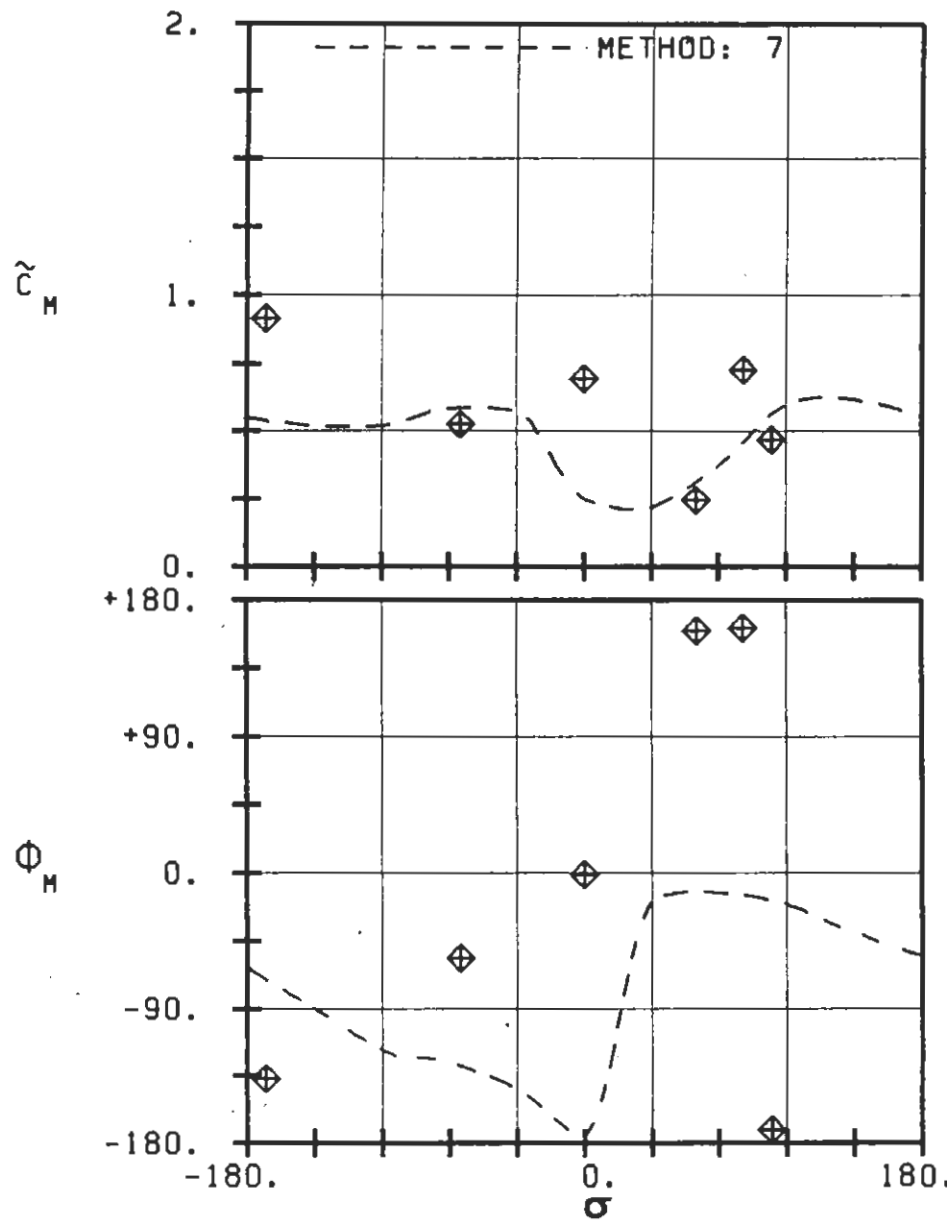
c : .076M
 τ : .855
 γ : 61.55
 x_{α} : .5
 y_{α} : 0.
 M_1 : 1.315
 β_1 : -64.0
 i : -
 M_2 : 1.25
 β_2 : -62.8
 h_x : -
 h_y : -
 α : -
 ω : -
 k : .44
 δ : -
 σ : -
 d : .034



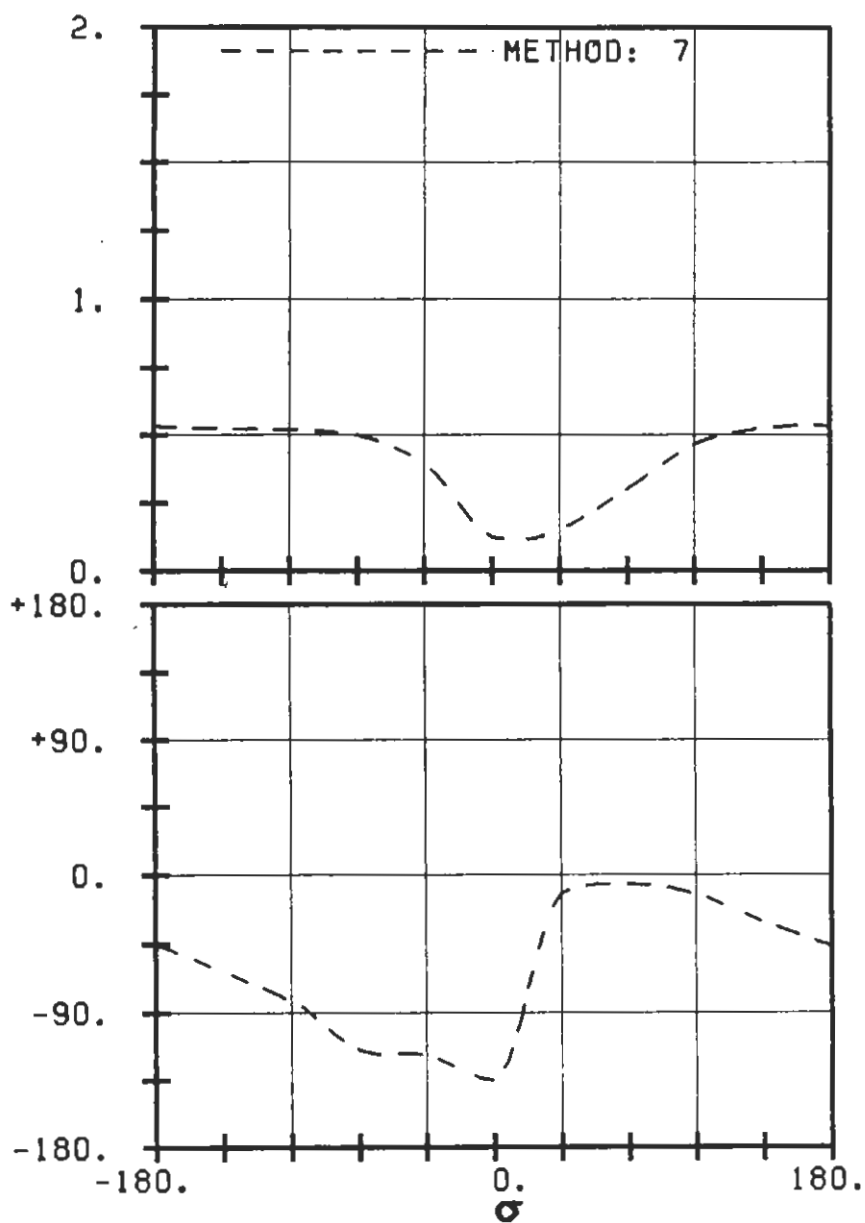
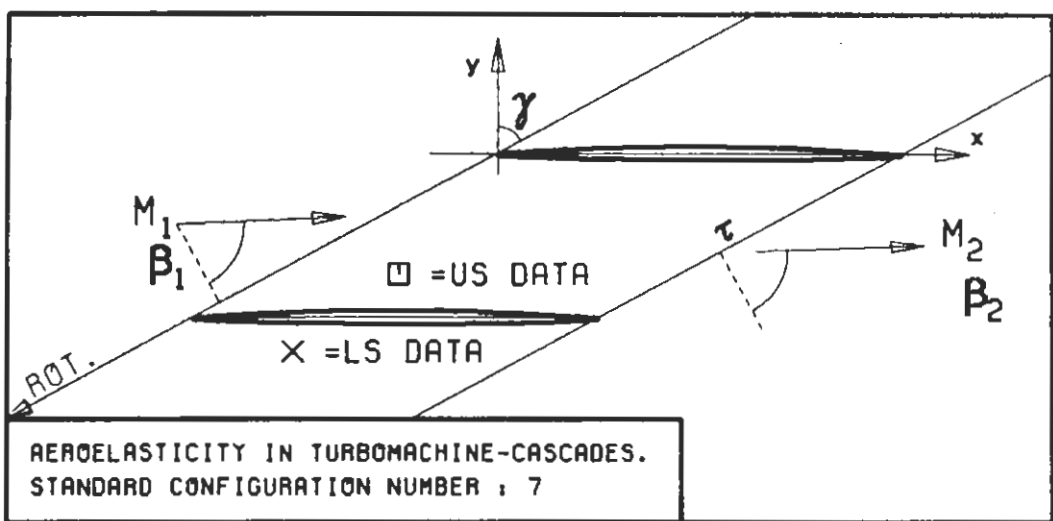
PLOT 7.7-5.1: SEVENTH STANDARD CONFIGURATION, CASES 1-6.
AERODYNAMIC MOMENT COEFFICIENT AND PHASE LEAD
IN DEPENDANCE OF INTERBLADE PHASE ANGLE.



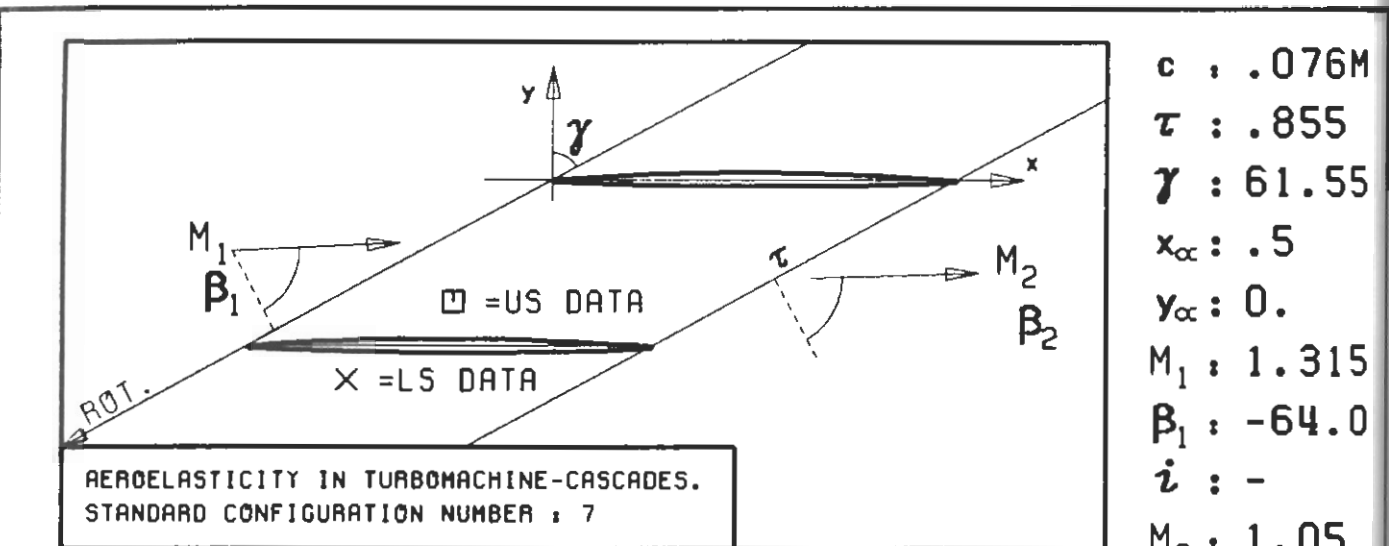
$c : .076M$
 $\tau : .855$
 $\gamma : 61.55$
 $x_\alpha : .5$
 $y_\alpha : 0.$
 $M_1 : 1.315$
 $\beta_1 : -64.0$
 $i : -$
 $M_2 : .99$
 $\beta_2 : -63.6$
 $h_x : -$
 $h_y : -$
 $\alpha : -$
 $\omega : -$
 $k : .44$
 $\delta : -$
 $\sigma : -$
 $d : .034$



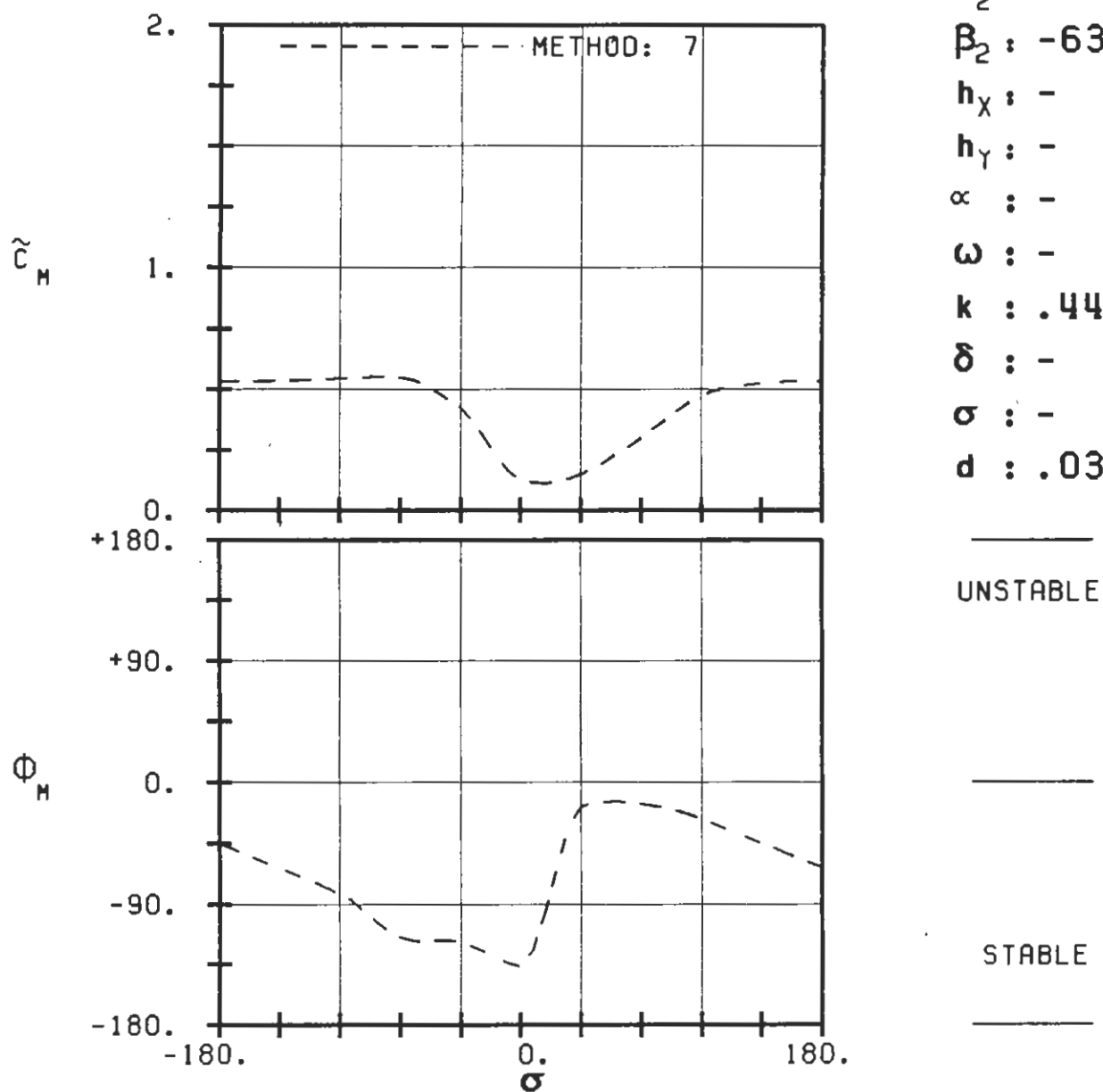
PLOT 7.7-5.2: SEVENTH STANDARD CONFIGURATION, CASES 7-12.
AERODYNAMIC MOMENT COEFFICIENT AND PHASE LEAD
IN DEPENDANCE OF INTERBLADE PHASE ANGLE.



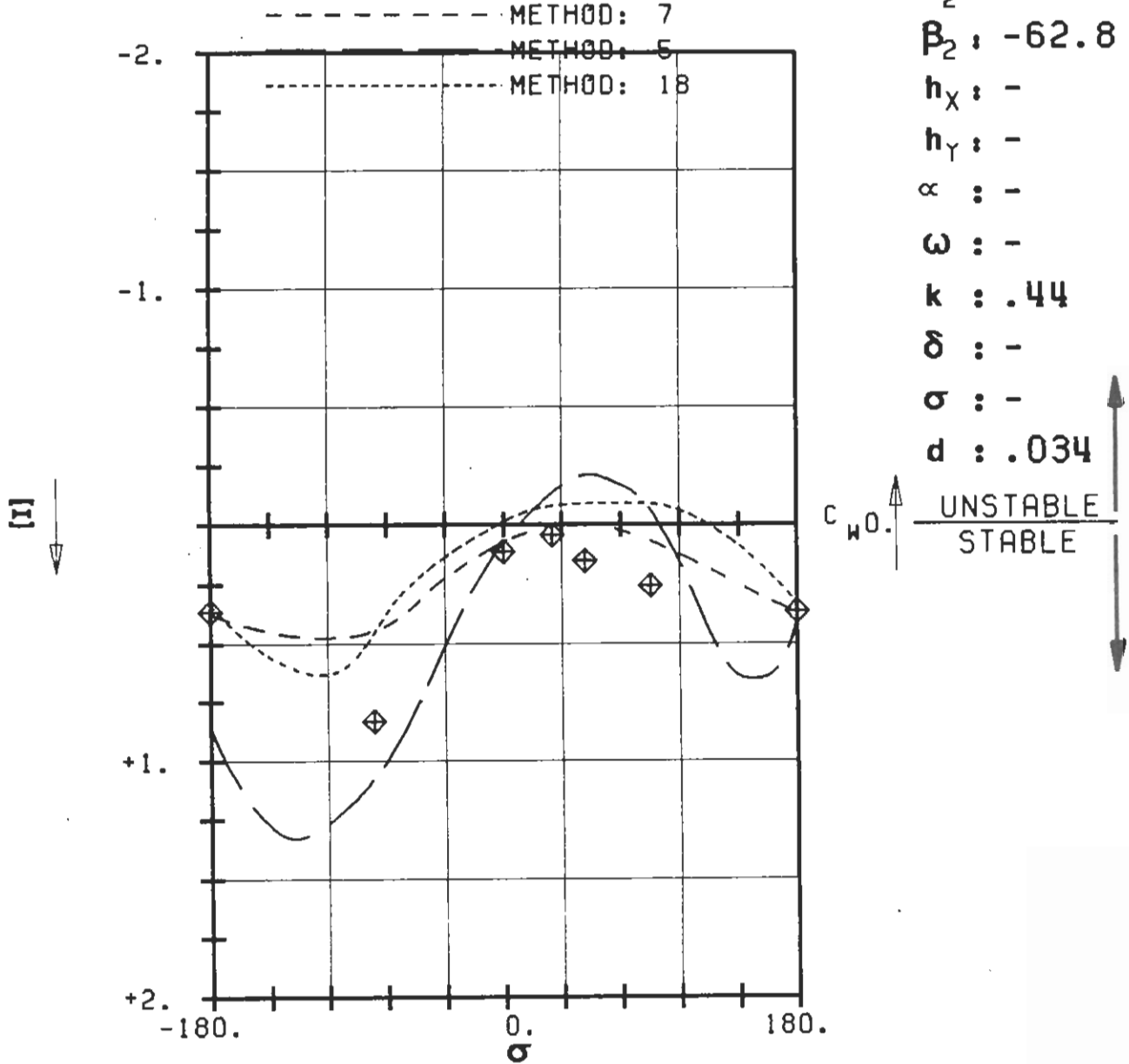
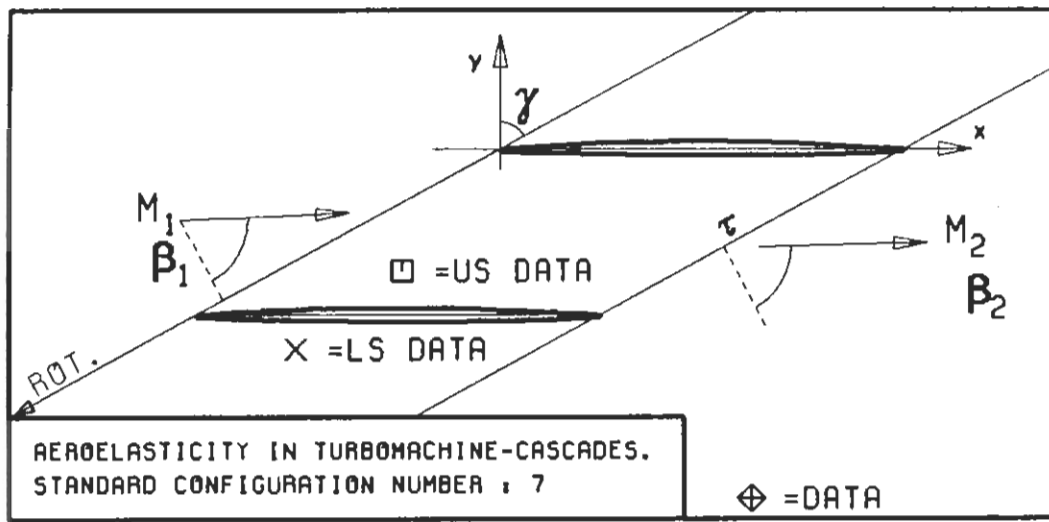
PLOT 7.7-5.3: SEVENTH STANDARD CONFIGURATION. EXTRA CASES.
AERODYNAMIC MOMENT COEFFICIENT AND PHASE LEAD
IN DEPENDANCE OF INTERBLADE PHASE ANGLE.



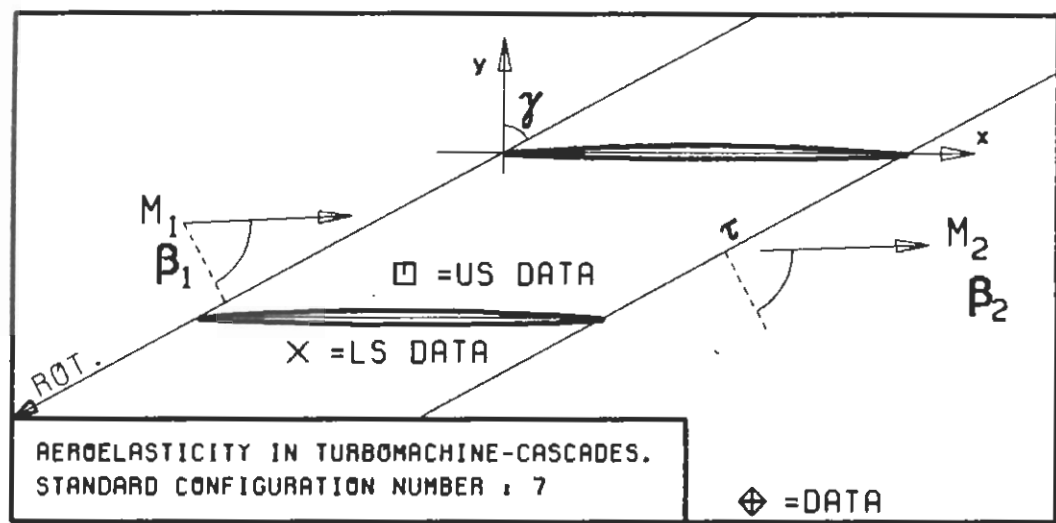
$c : .076M$
 $\tau : .855$
 $\gamma : 61.55$
 $x_{\alpha} : .5$
 $y_{\alpha} : 0.$
 $M_1 : 1.315$
 $\beta_1 : -64.0$
 $i : -$
 $M_2 : 1.05$
 $\beta_2 : -63.3$
 $h_x : -$
 $h_y : -$
 $\alpha : -$
 $\omega : -$
 $k : .44$
 $\delta : -$
 $\sigma : -$
 $d : .034$



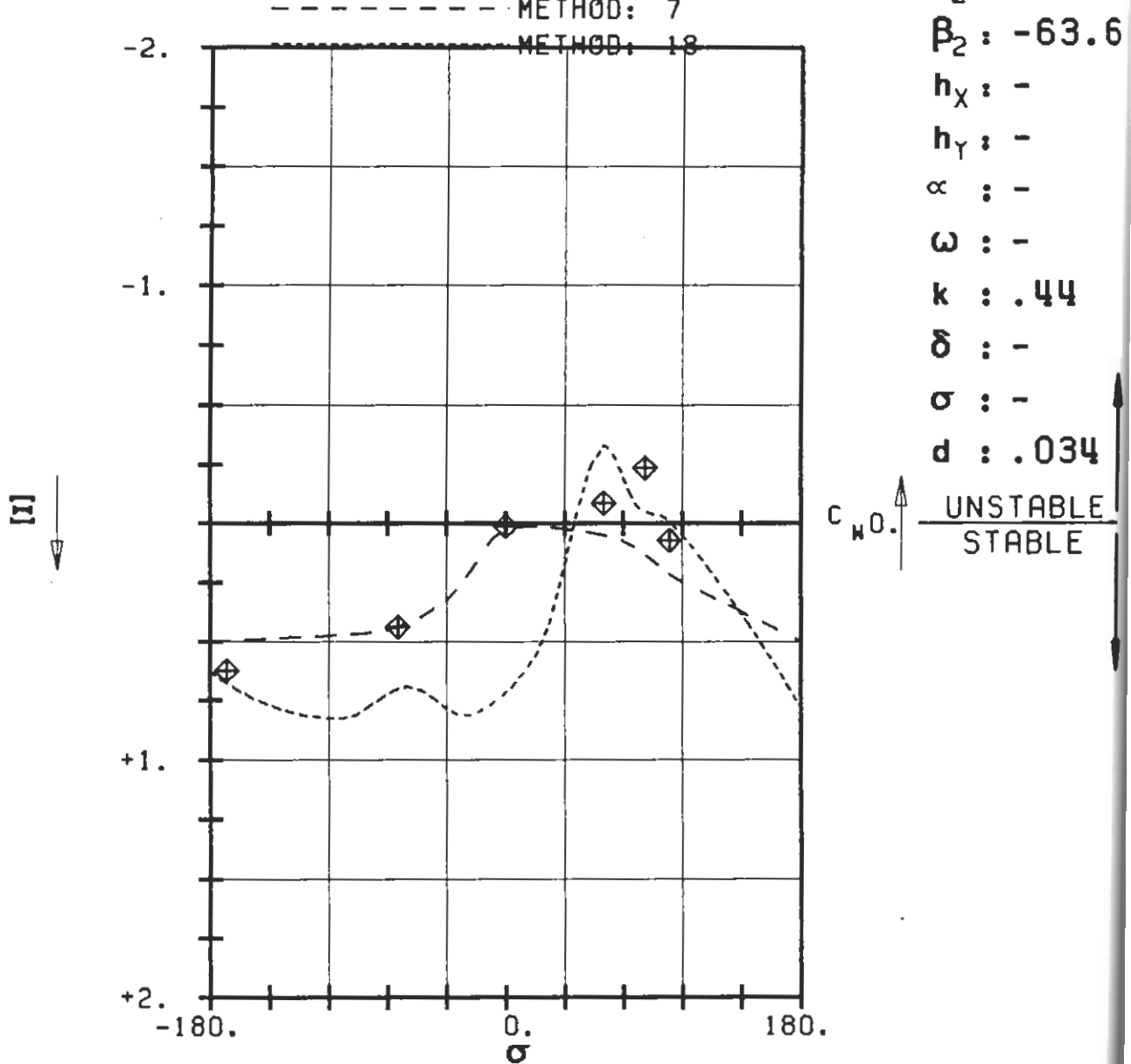
PLOT 7.7-5.4: SEVENTH STANDARD CONFIGURATION. EXTRA CASES.
AERODYNAMIC MOMENT COEFFICIENT AND PHASE LEAD
IN DEPENDANCE OF INTERBLADE PHASE ANGLE.



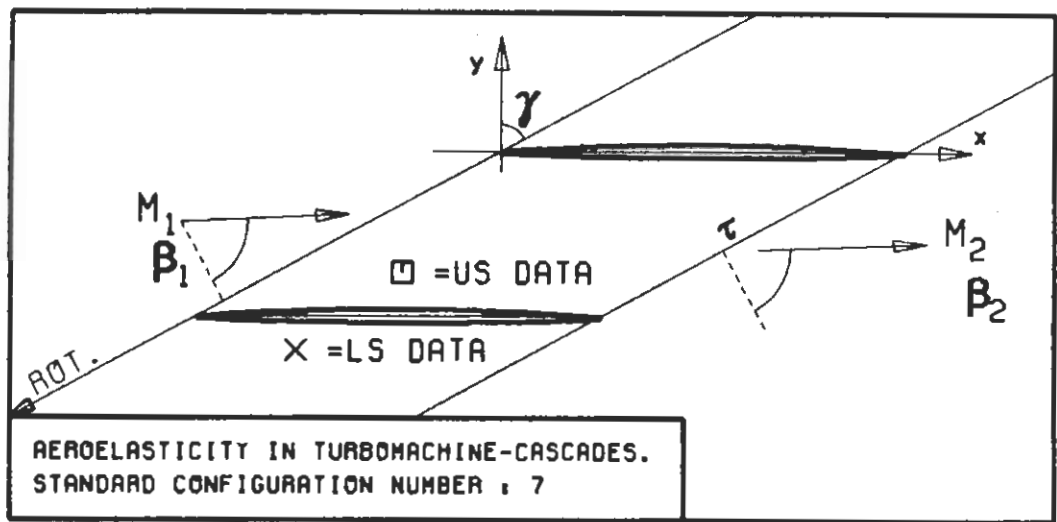
PLOT 7.7-6.1: SEVENTH STANDARD CONFIGURATION, CASES 1-6.
AERODYNAMIC WORK AND DAMPING COEFFICIENTS
IN DEPENDANCE OF INTERBLADE PHASE ANGLE,



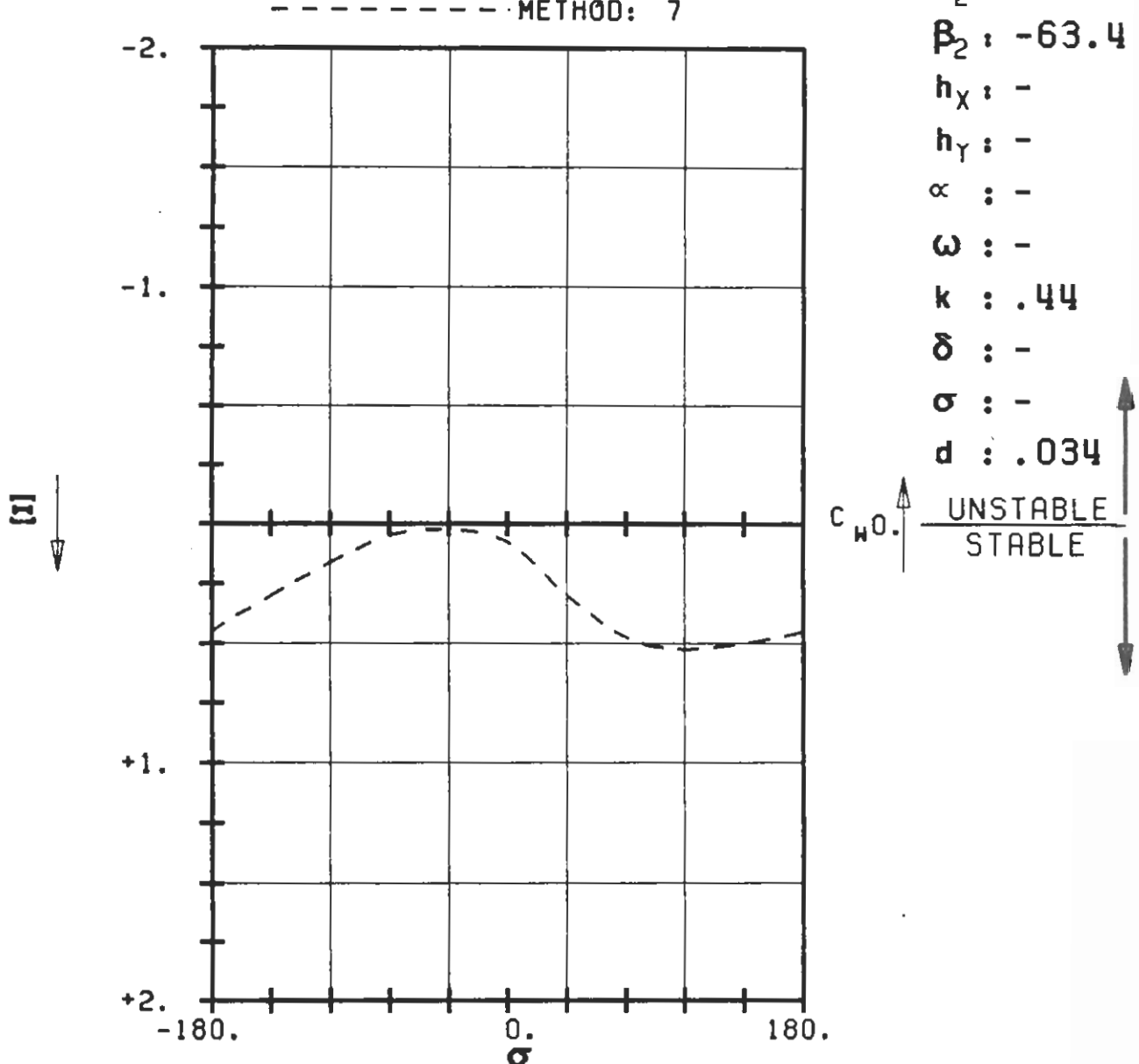
$c : .076M$
 $\tau : .855$
 $\gamma : 61.55$
 $x_\alpha : .5$
 $y_\alpha : 0.$
 $M_1 : 1.315$
 $\beta_1 : -64.0$
 $i : -$
 $M_2 : 0.99$
 $\beta_2 : -63.6$
 $h_X : -$
 $h_Y : -$
 $\alpha : -$
 $\omega : -$
 $k : .44$
 $\delta : -$
 $\sigma : -$
 $d : .034$



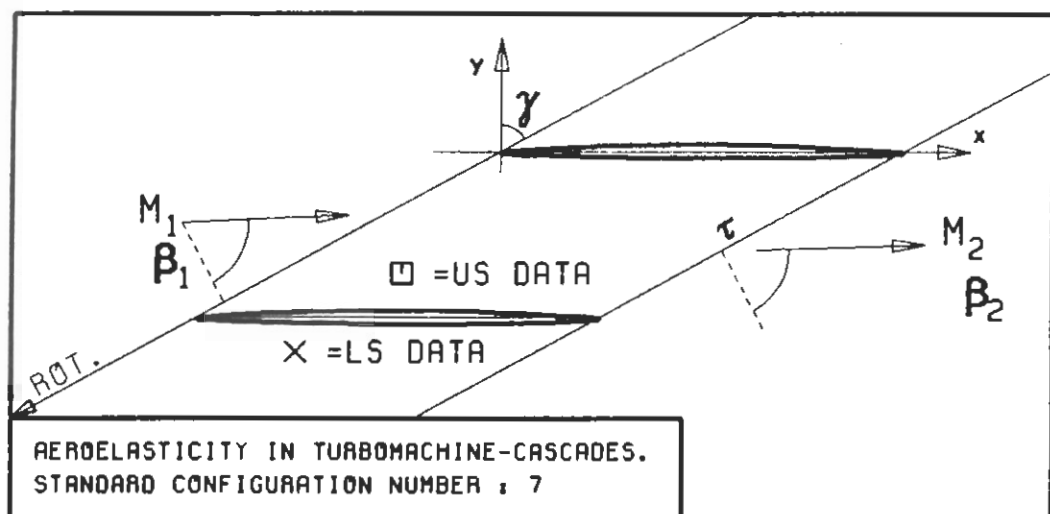
PLOT 7.7-6.2: SEVENTH STANDARD CONFIGURATION, CASES 7-12.
 AERODYNAMIC WORK AND DAMPING COEFFICIENTS
 IN DEPENDANCE OF INTERBLADE PHASE ANGLE,



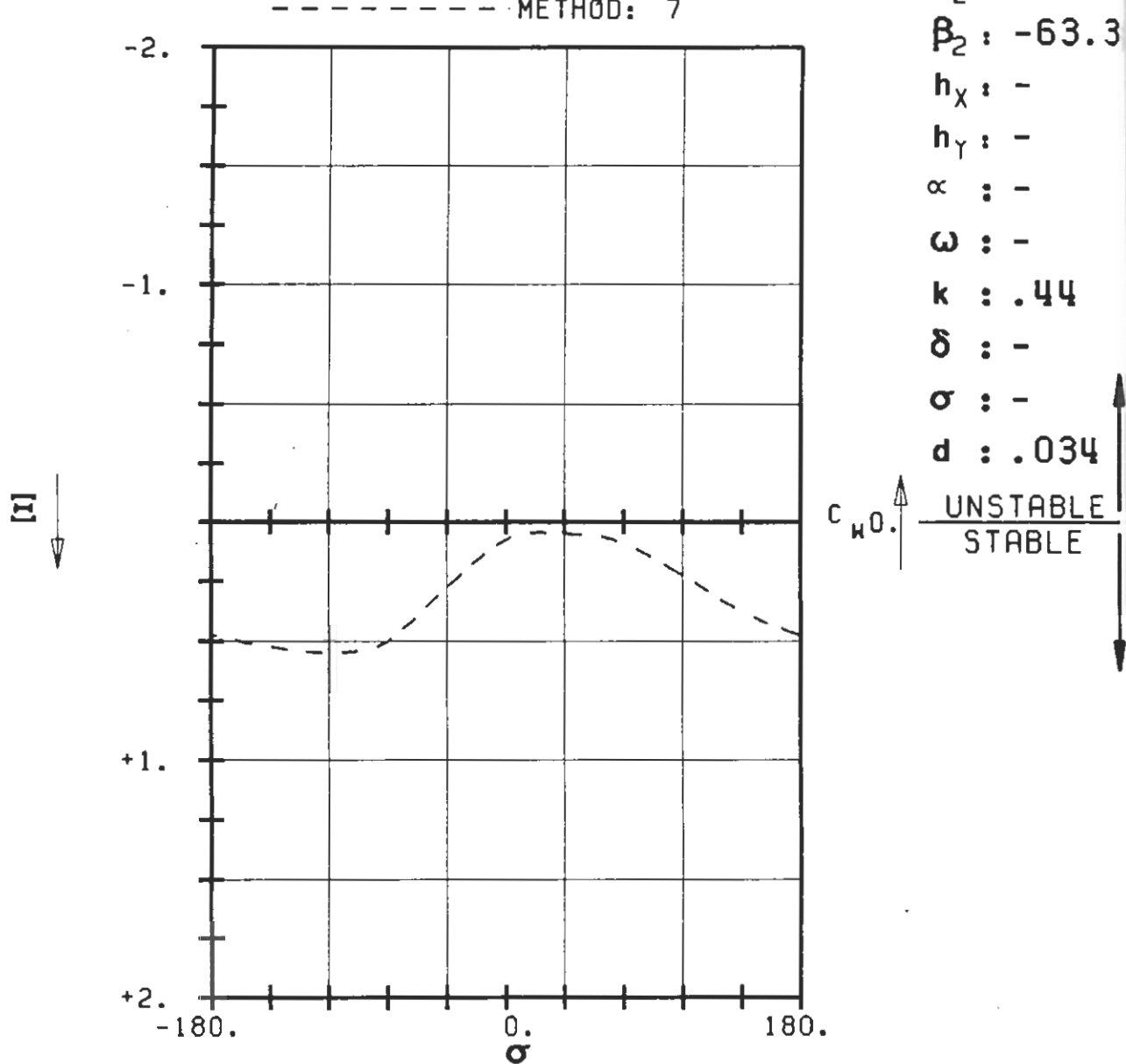
$c : .076M$
 $\tau : .855$
 $\gamma : 61.55$
 $x_\alpha : .5$
 $y_\alpha : 0.$
 $M_1 : 1.315$
 $\beta_1 : -64.0$
 $i : -$
 $M_2 : 1.14$
 $\beta_2 : -63.4$
 $h_x : -$
 $h_y : -$
 $\alpha : -$
 $\omega : -$
 $k : .44$
 $\delta : -$
 $\sigma : -$
 $d : .034$



PLOT 7.7-6.3: SEVENTH STANDARD CONFIGURATION, EXTRA CASES.
 AERODYNAMIC WORK AND DAMPING COEFFICIENTS
 IN DEPENDANCE OF INTERBLADE PHASE ANGLE. $M_2=1$.



$c : .076M$
 $\tau : .855$
 $\gamma : 61.55$
 $x_\alpha : .5$
 $y_\alpha : 0.$
 $M_1 : 1.315$
 $\beta_1 : -64.0$
 $i : -$
 $M_2 : 1.05$
 $\beta_2 : -63.3$
 $h_x : -$
 $h_y : -$
 $\alpha : -$
 $\omega : -$
 $k : .44$
 $\delta : -$
 $\sigma : -$
 $d : .034$



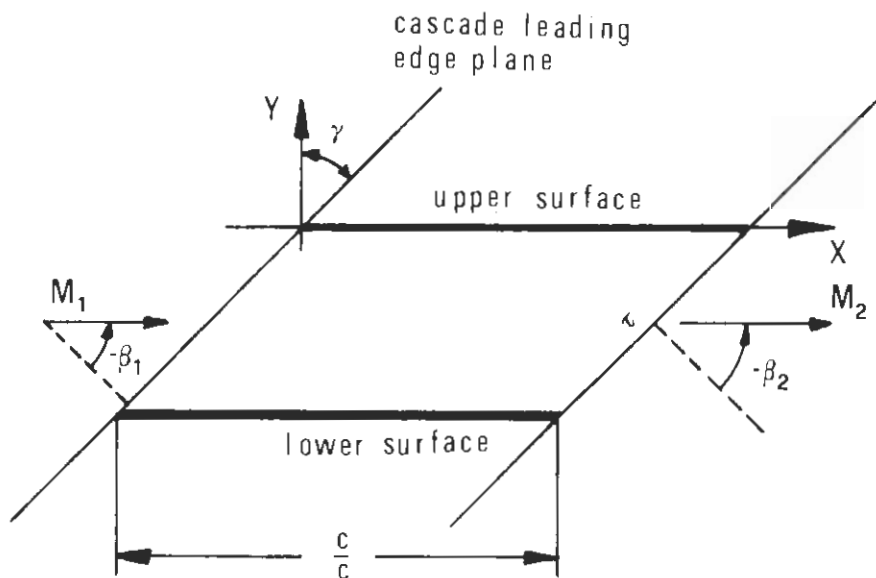
PLOT 7.7-6.4: SEVENTH STANDARD CONFIGURATION, EXTRA CASES.
 AERODYNAMIC WORK AND DAMPING COEFFICIENTS
 IN DEPENDANCE OF INTERBLADE PHASE ANGLE, $M_2=1$.

AEROELASTICITY IN TURBOMACHINE-CASCADES

EIGHTH STANDARD CONFIGURATION

Definition

Flat Plate Profiles.



Vibration in pitch around (x_α, y_α)	= (0.5,0.)
α	= 2.0° ($=0.0349$ rad)
c	= 0.1 m
τ	= variable (0.5-1.0)
k	= 1.0
σ	= 90°
i	= 0°
camber	= 0°
γ	= variable (0° - 60°)
M_1	= variable (0.0-1.5)

Fig. 7.8-1. Eighth standard configuration: Cascade geometry

AEROELASTICITY IN TURBOMACHINE-CASCADES

EIGHTH STANDARD CONFIGURATION

Aeroelastic Test Cases

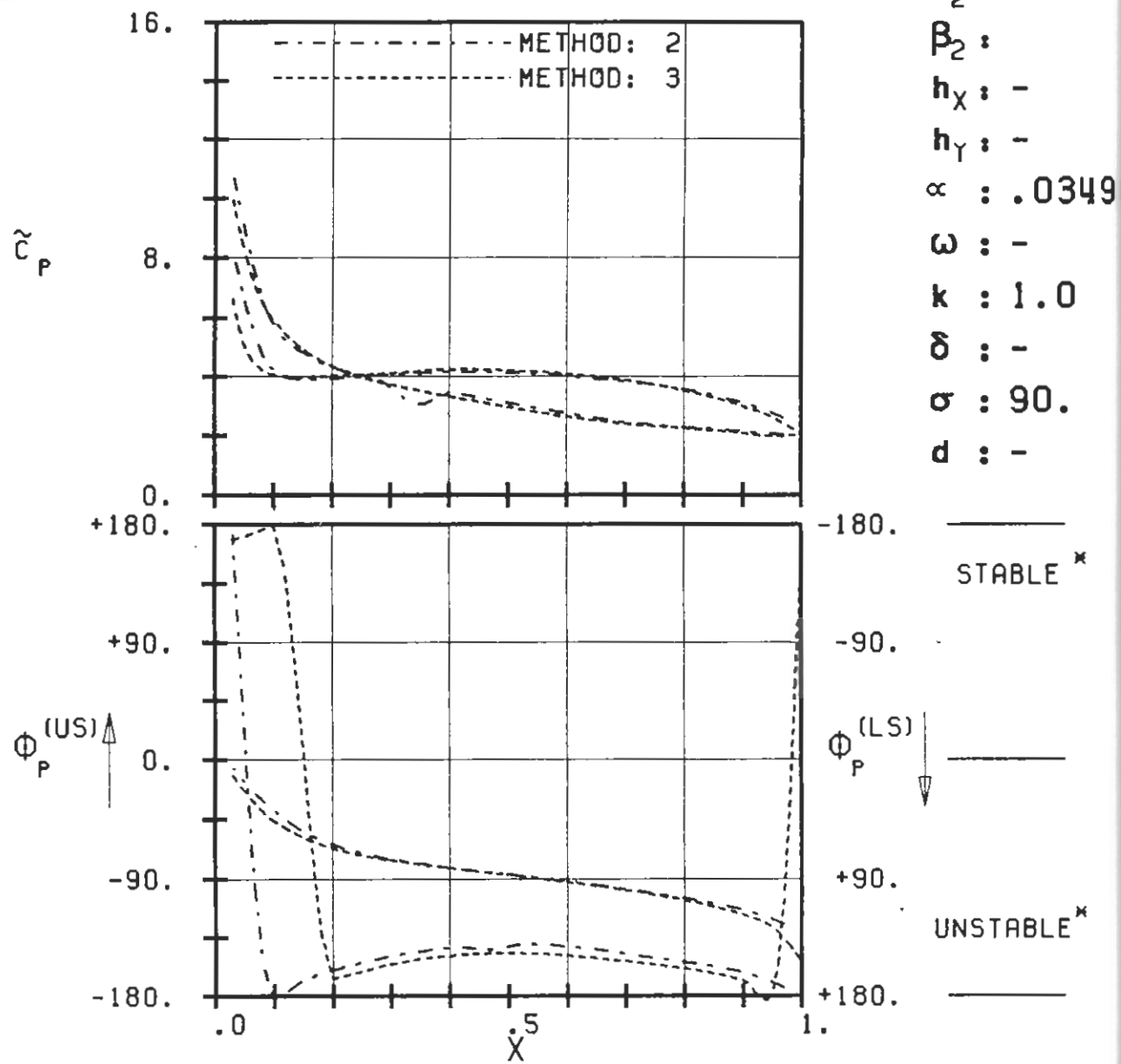
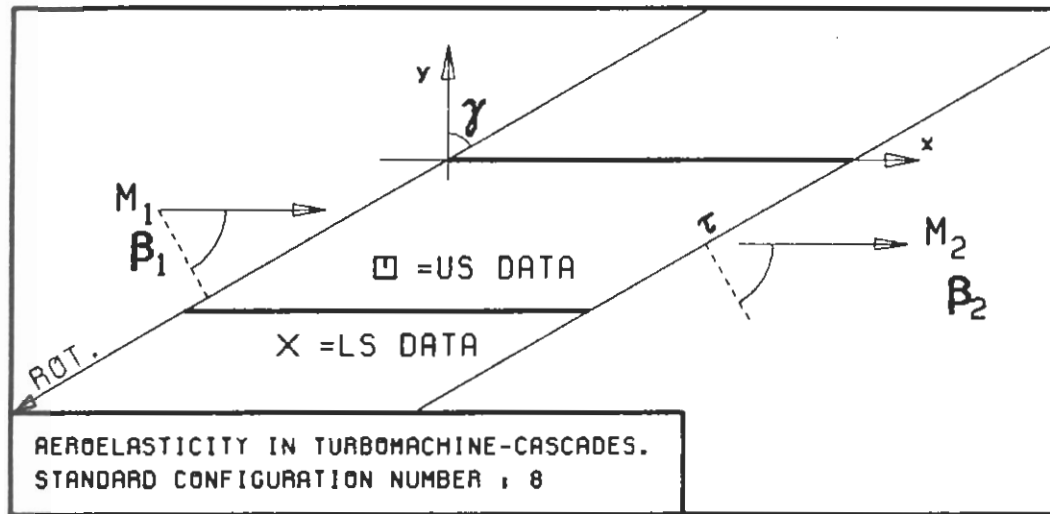
Aeroelastic Test Case No	Time-Averaged Parameters					
	M_1 (-)	γ (°)	β_1 (°)	H_+ (-)	H_- (-)	d (-)
1	0.0	60	- 60	0.01	0.01	0.02
2	"	"	"	0.02	0.02	0.04
3	"	"	"	0.03	0.03	0.06
4	"	"	"	0.05	0.05	0.10
5	0.5	"	"	0.01	0.01	0.02
6	0.7	"	"	0.005	0.005	0.01
7	"	"	"	0.01	0.01	0.02
8	"	"	"	0.0015	0.0015	0.03
9	"	"	"	0.02	0.02	0.04
10	0.8	"	"	0.01	0.01	0.02
11	1.3	"	"	"	"	"
12	1.4	"	"	"	"	"
13	1.5	"	"	"	"	"
14	0.0	45	- 45	"	"	"
15	0.5	"	"	"	"	"
16	0.7	"	"	"	"	"
17	0.8	"	"	"	"	"
18	0.5	"	"	0.05	0.0	0.05
19	0.7	"	"	"	"	"
20	0.8	"	"	"	"	"
21	0.9	"	"	"	"	"

Table 7.9-1 Ninth standard configuration. 21 aeroelastic test cases

AEROELASTICITY IN TURBOMACHINE-CASCADES

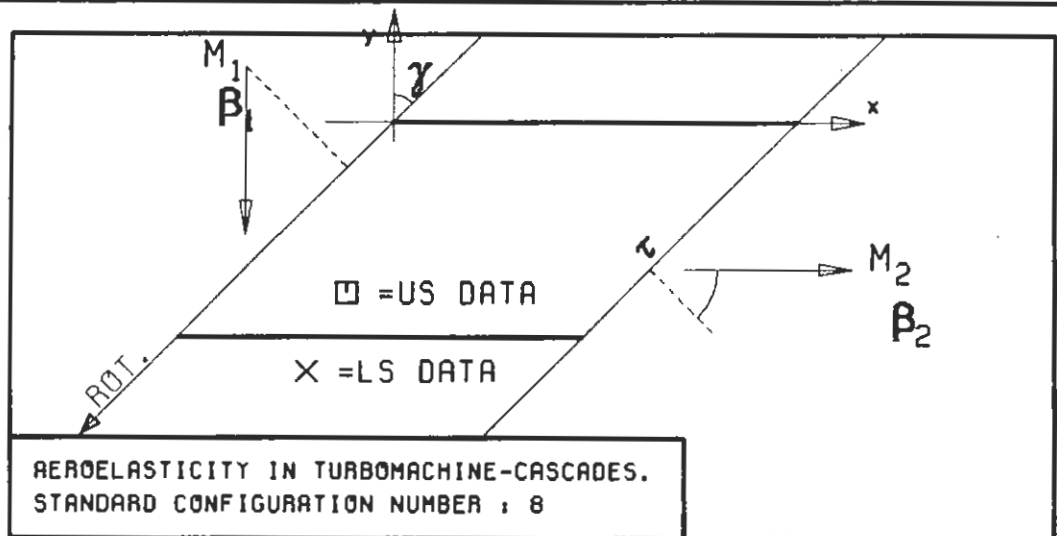
EIGHTH STANDARD CONFIGURATION

Experimental and Theoretical Results

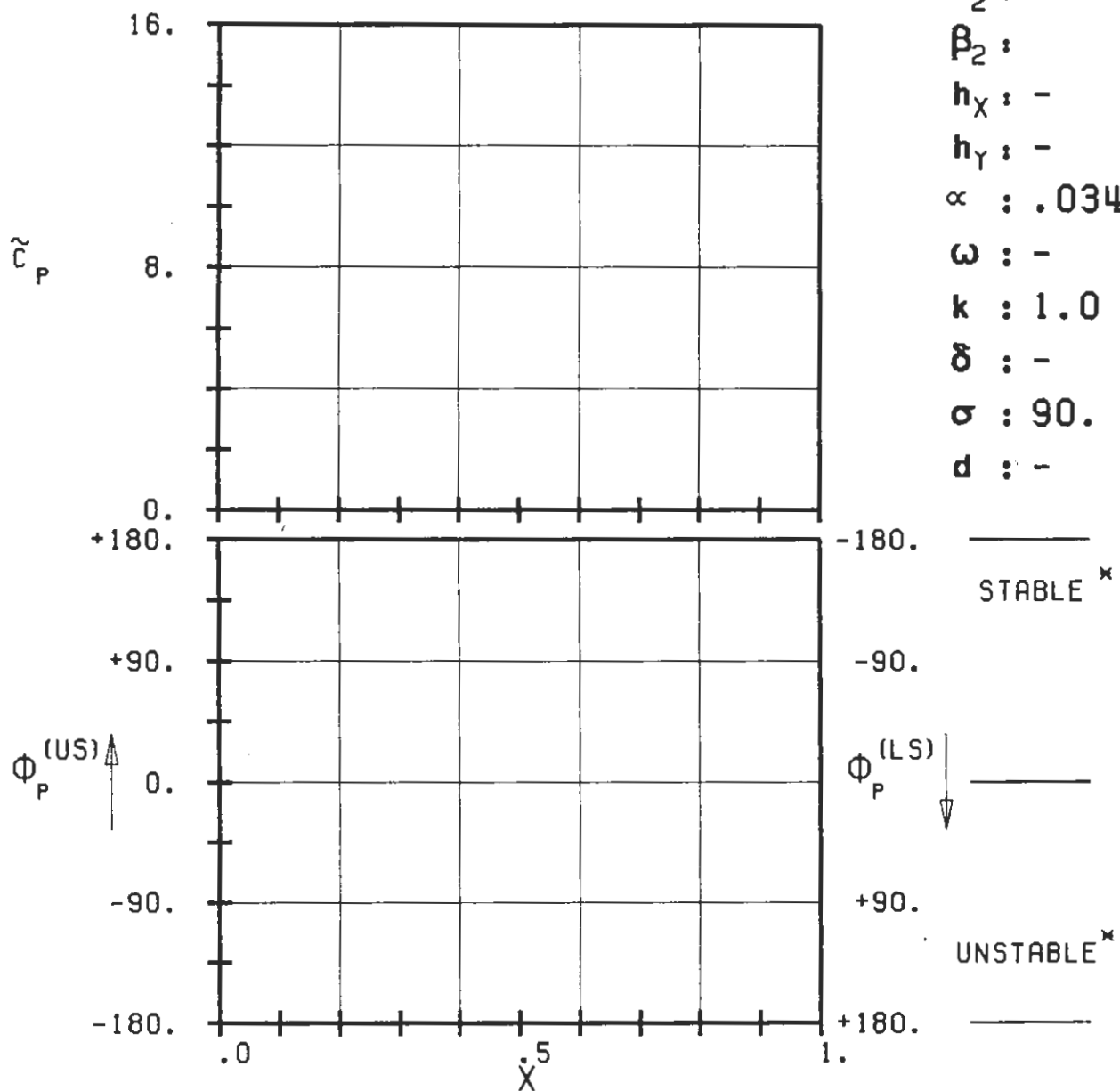


PLOT 7.8-2.1: EIGHTH STANDARD CONFIGURATION, CASE 1.
MAGNITUDE AND PHASE LEAD OF UNSTEADY BLADE SURFACE PRESSURE DISTRIBUTION.

(x: IN PITCH MODE, NOTATION VALID UPSTREAM OF PITCH AXIS)

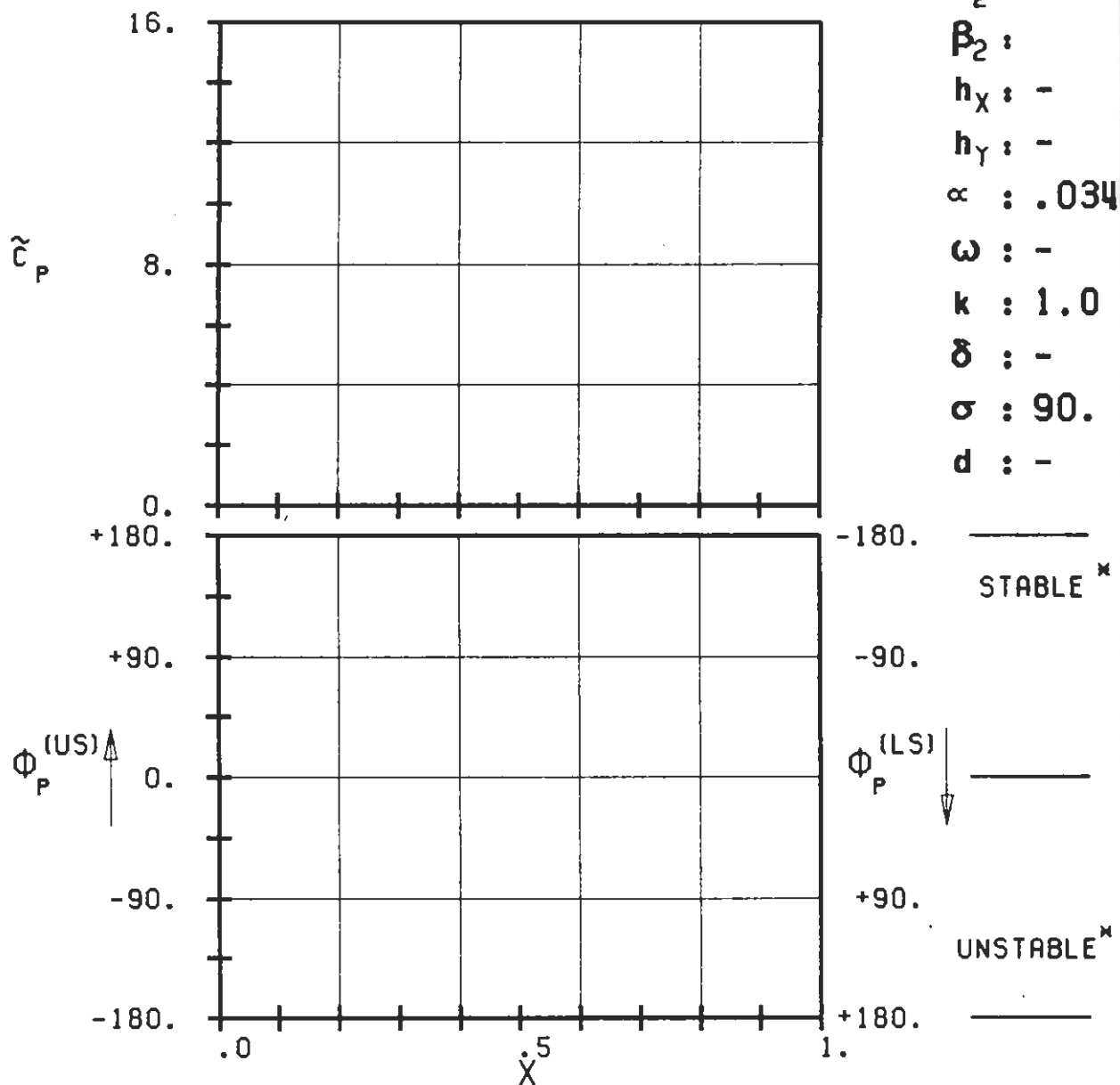
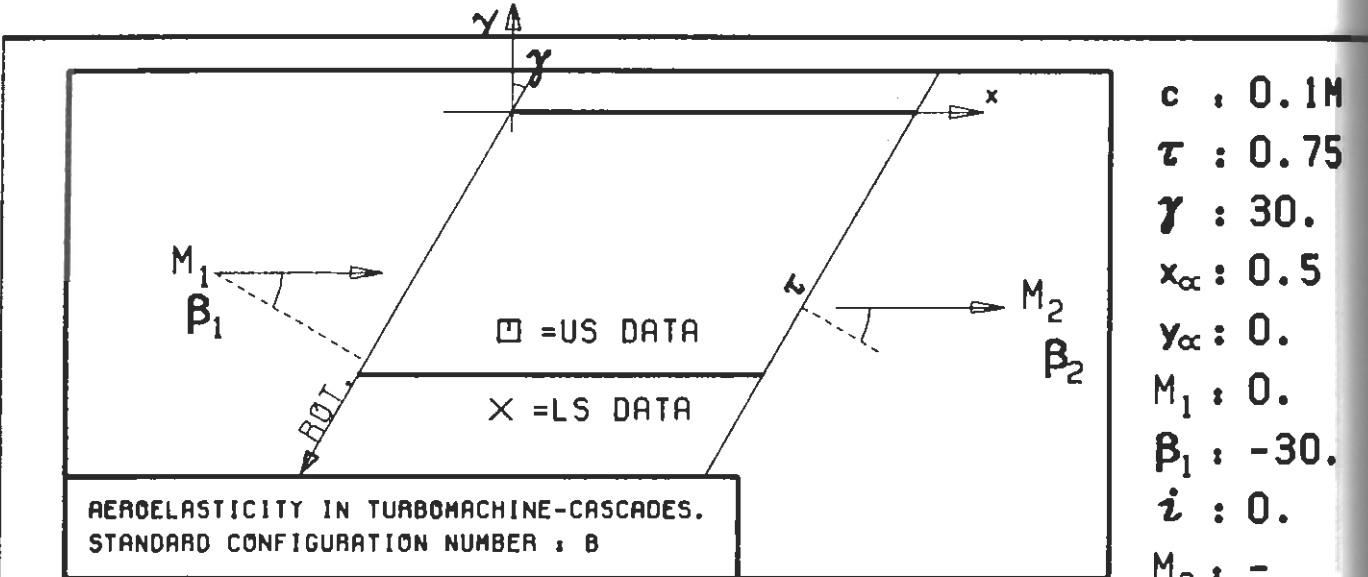


$c : 0.1M$
 $\tau : 0.75$
 $\gamma : 45.$
 $x_\infty : 0.5$
 $y_\infty : 0.$
 $M_1 : 0.$
 $\beta_1 : 45.$
 $i : 0.$
 $M_2 : -$
 $\beta_2 : -$
 $h_x : -$
 $h_y : -$
 $\alpha : .0349$
 $\omega : -$
 $k : 1.0$
 $\delta : -$
 $\sigma : 90.$
 $d : -$



PLOT 7.7-2.2: EIGHTH STANDARD CONFIGURATION, CASE 2.
MAGNITUDE AND PHASE LEAD OF UNSTEADY BLADE
SURFACE PRESSURE DISTRIBUTION.

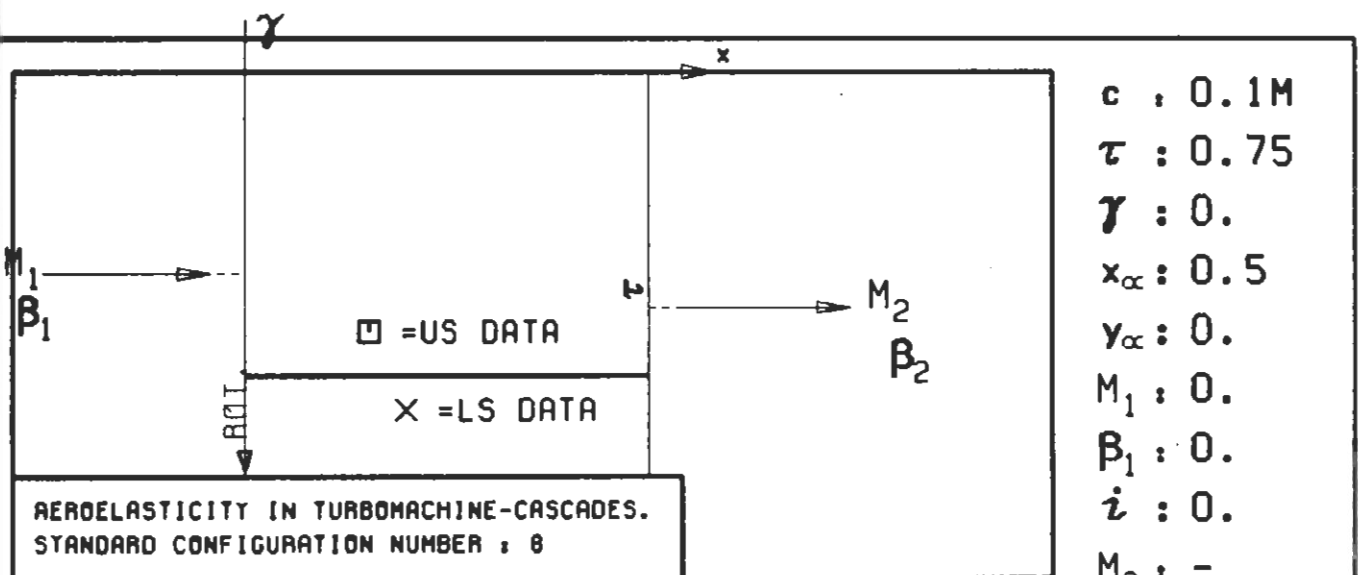
(x : IN PITCH MODE, NOTATION VALID UPSTREAM OF PITCH AXIS)



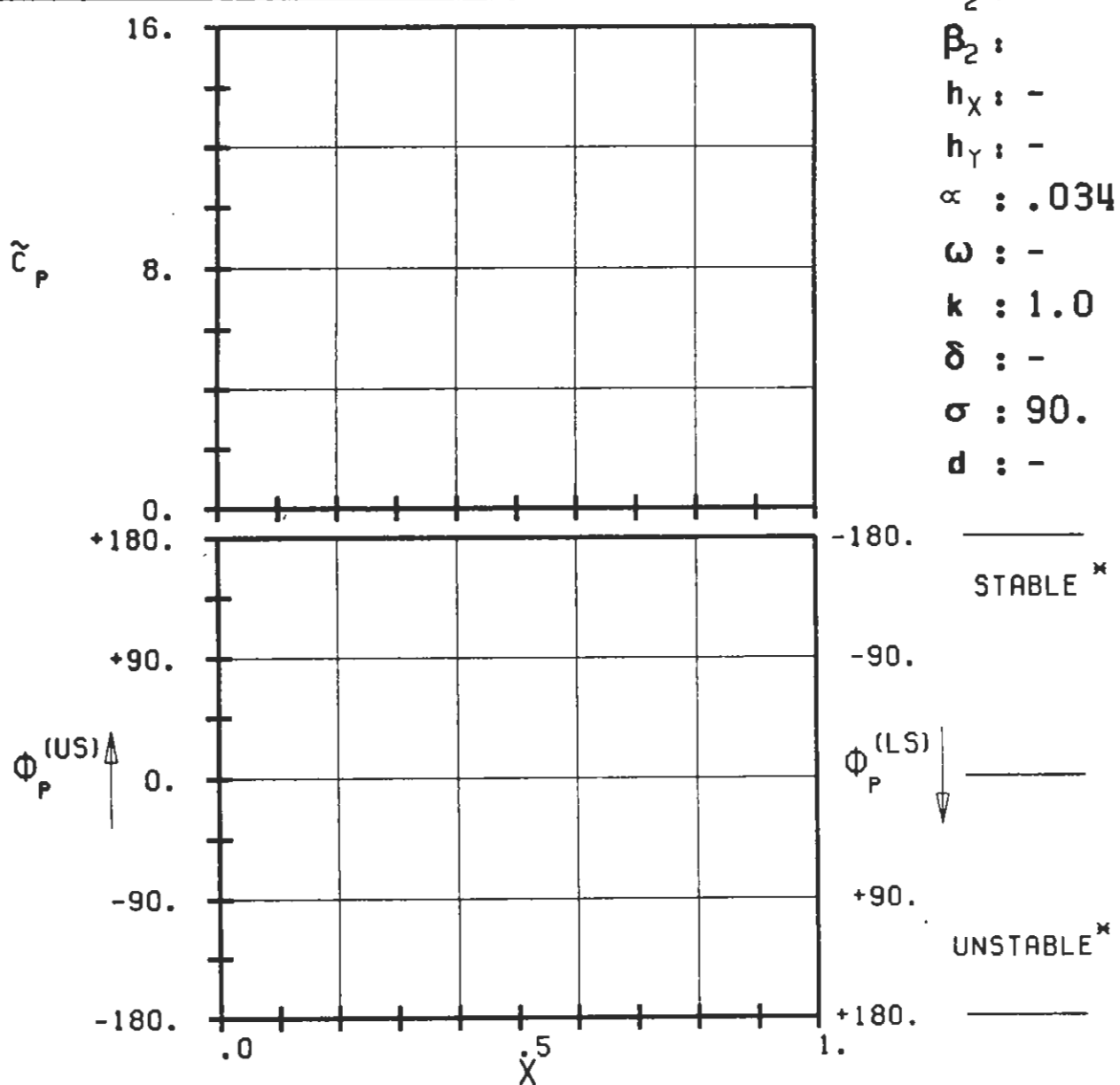
PLOT 7.8-2.3: EIGHTH STANDARD CONFIGURATION, CASE 3.
 MAGNITUDE AND PHASE LEAD OF UNSTEADY BLADE
 SURFACE PRESSURE DISTRIBUTION.

(x : IN PITCH MODE, NOTATION VALID UPSTREAM OF PITCH AXIS)

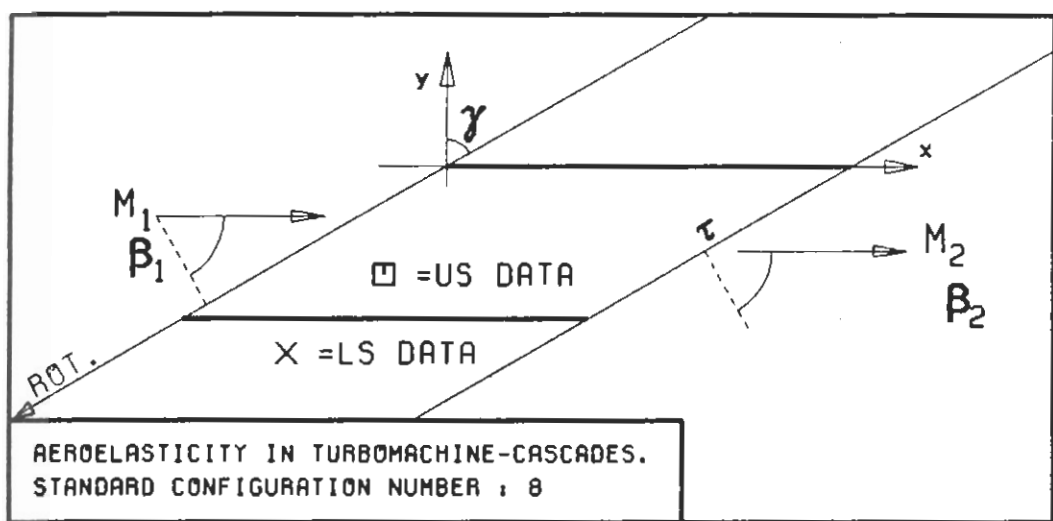
$c : 0.1M$
 $\tau : 0.75$
 $\gamma : 30.$
 $x_{\infty} : 0.5$
 $y_{\infty} : 0.$
 $M_1 : 0.$
 $\beta_1 : -30.$
 $i : 0.$
 $M_2 : -$
 $\beta_2 : -$
 $h_x : -$
 $h_y : -$
 $\alpha : .0349$
 $\omega : -$
 $k : 1.0$
 $\delta : -$
 $\sigma : 90.$
 $d : -$



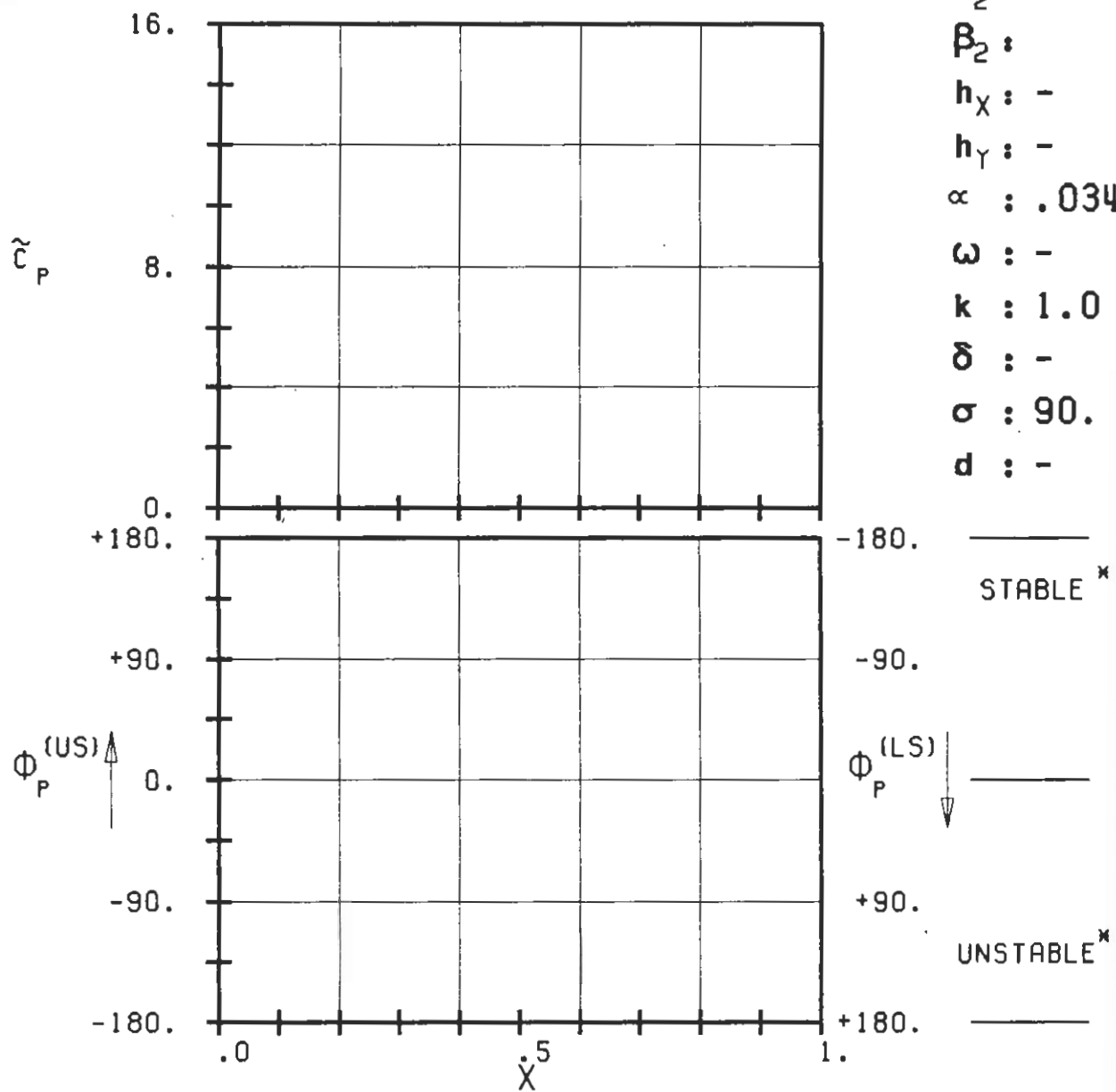
$c : 0.1M$
 $\tau : 0.75$
 $\gamma : 0.$
 $x_\alpha : 0.5$
 $y_\alpha : 0.$
 $M_1 : 0.$
 $B_1 : 0.$
 $i : 0.$
 $M_2 : -$
 $B_2 : -$
 $h_X : -$
 $h_Y : -$
 $\alpha : .0349$
 $\omega : -$
 $k : 1.0$
 $\delta : -$
 $\sigma : 90.$
 $d : -$



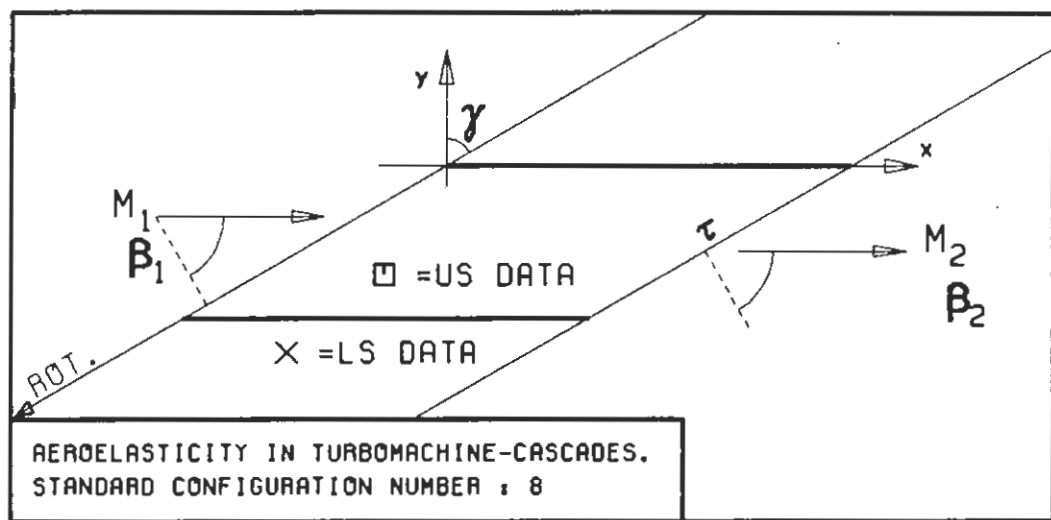
PLOT 7.8-2.4: EIGHTH STANDARD CONFIGURATION, CASE 4.
MAGNITUDE AND PHASE LEAD OF UNSTEADY BLADE SURFACE PRESSURE DISTRIBUTION.
 (x: IN PITCH MODE, NOTATION VALID UPSTREAM OF PITCH AXIS)



$c : 0.1M$
 $\tau : 0.75$
 $\gamma : 60.$
 $x_\alpha : 0.5$
 $y_\alpha : 0.$
 $M_1 : 0.5$
 $B_1 : -60.$
 $i : 0.$
 $M_2 : -$
 $B_2 : -$
 $h_X : -$
 $h_Y : -$
 $\alpha : .0349$
 $\omega : -$
 $k : 1.0$
 $\delta : -$
 $\sigma : 90.$
 $d : -$

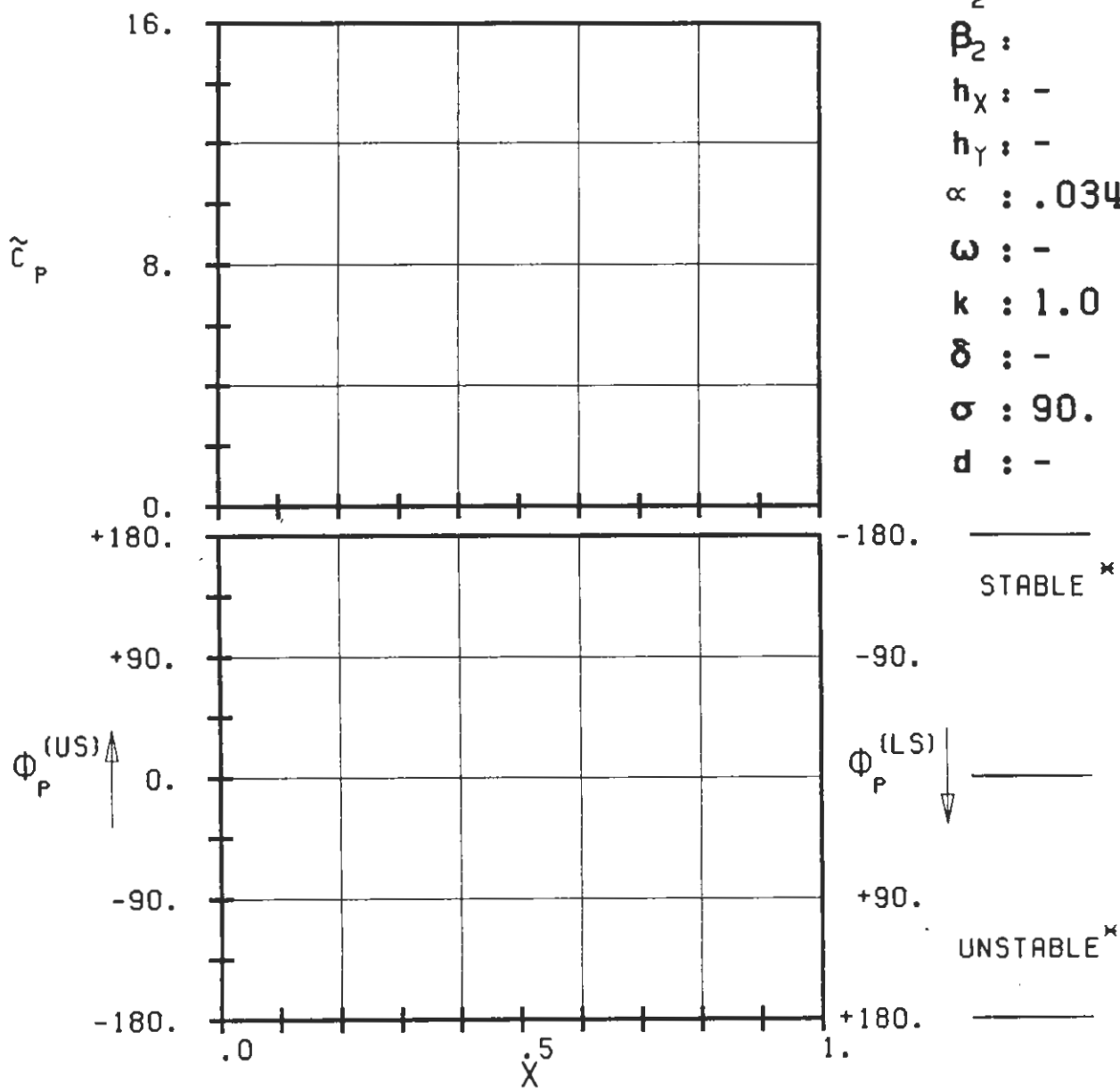


PLOT 7.8-2.5: EIGHTH STANDARD CONFIGURATION, CASE 5.
 MAGNITUDE AND PHASE LEAD OF UNSTEADY BLADE
 SURFACE PRESSURE DISTRIBUTION.
 (x: IN PITCH MODE, NOTATION VALID UPSTREAM OF PITCH AXIS)



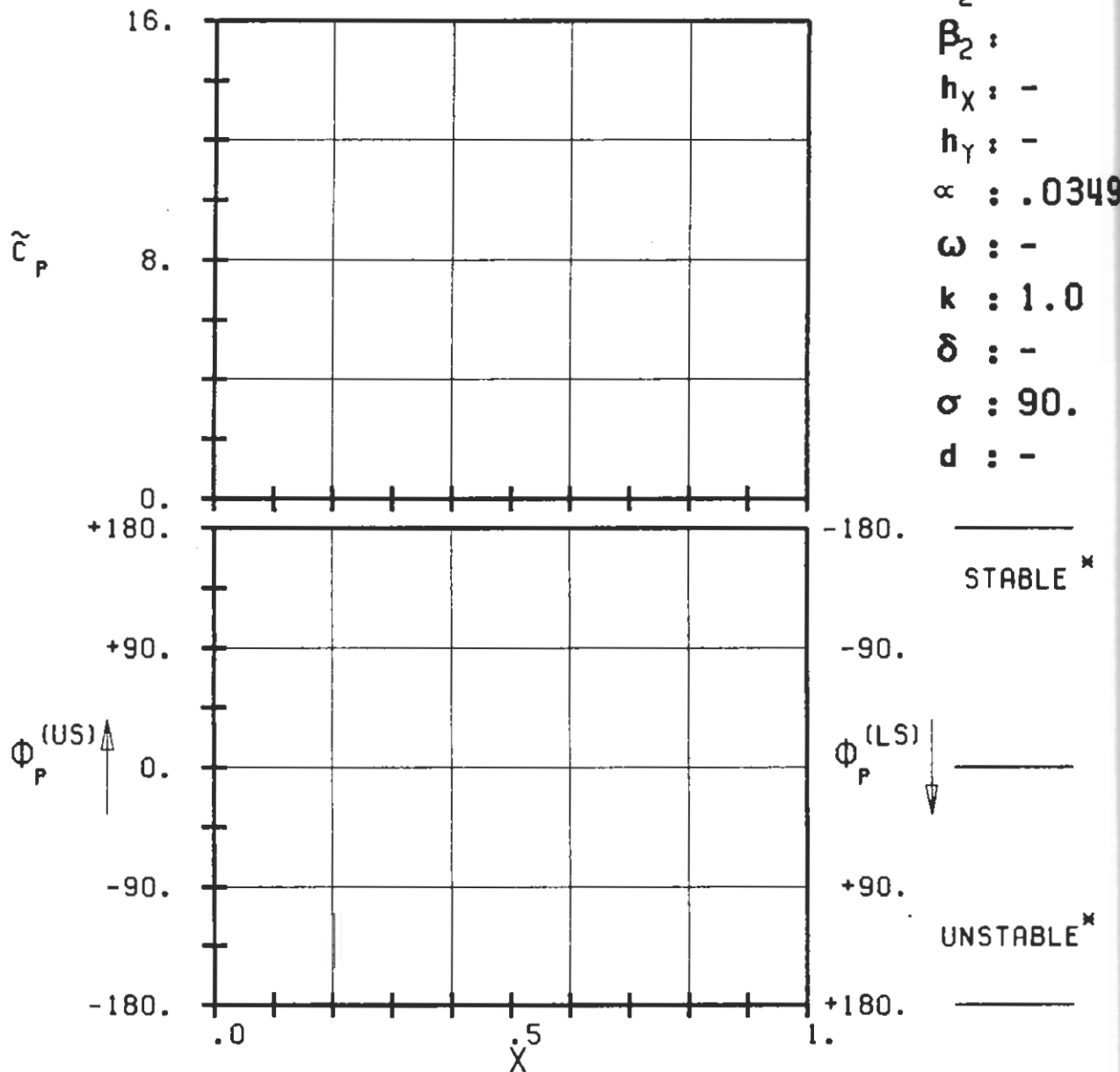
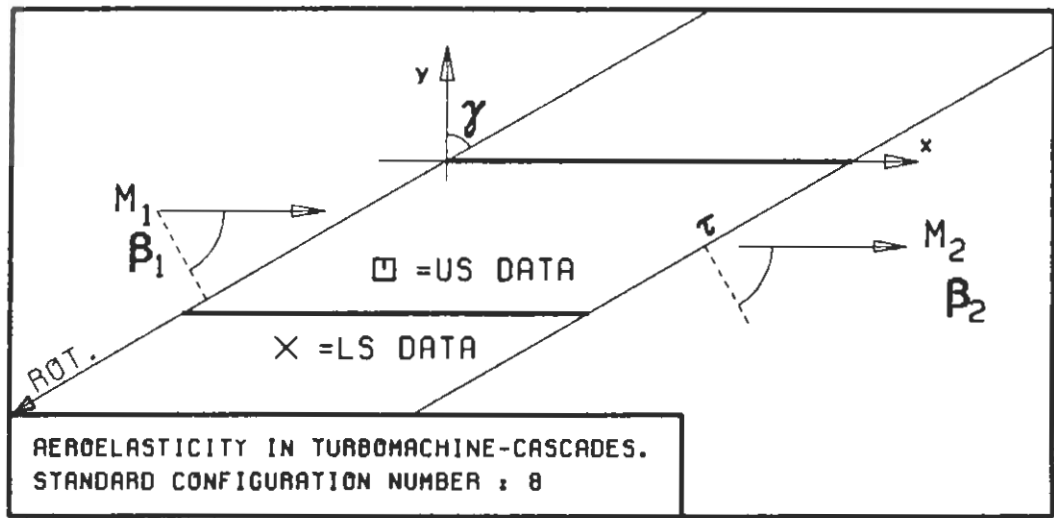
$c : 0.1M$
 $\tau : 0.75$
 $\gamma : 60.$
 $x_\infty : 0.5$
 $y_\infty : 0.$
 $M_1 : 0.6$
 $\beta_1 : -60.$
 $i : 0.$
 $M_2 : -$
 $\beta_2 : -$
 $h_x : -$
 $h_y : -$
 $\alpha : .0349$

$\omega : -$
 $k : 1.0$
 $\delta : -$
 $\sigma : 90.$
 $d : -$

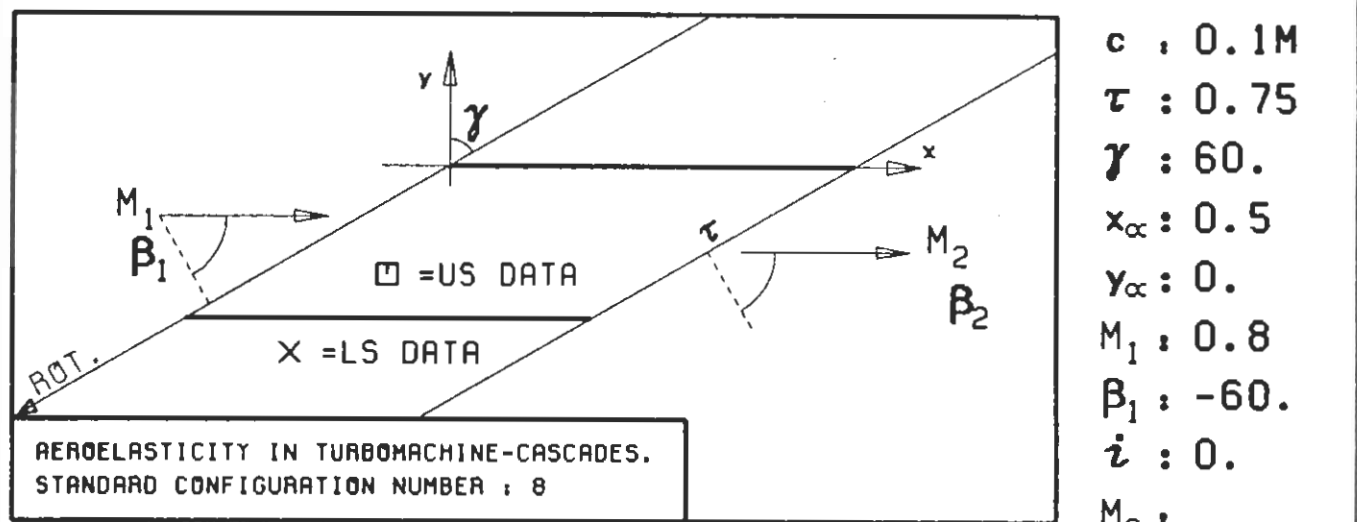


PLOT 7.8-2.6: EIGHTH STANDARD CONFIGURATION, CASE 6.
 MAGNITUDE AND PHASE LEAD OF UNSTEADY BLADE
 SURFACE PRESSURE DISTRIBUTION.

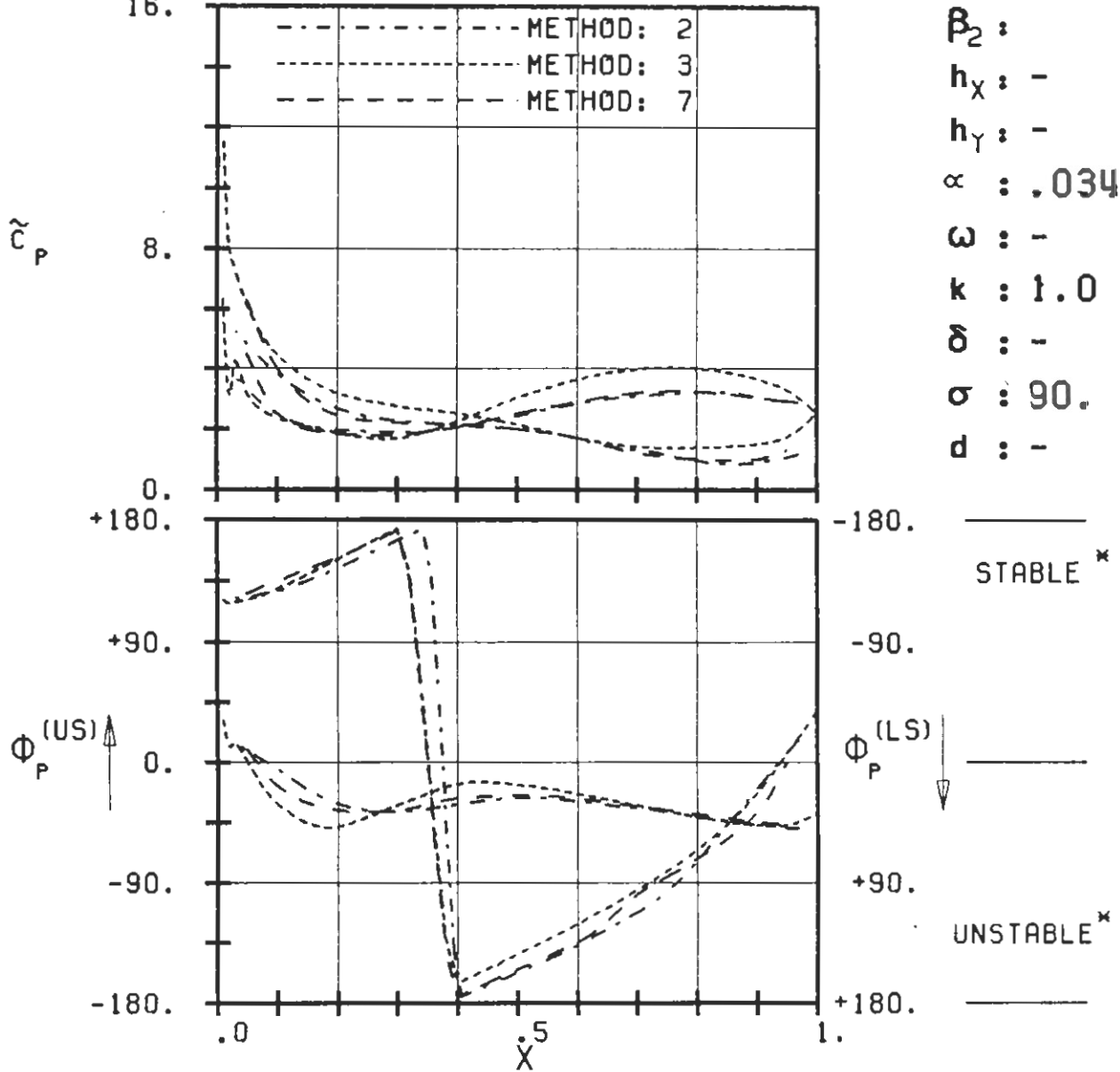
(*: IN PITCH MODE, NOTATION VALID UPSTREAM OF PITCH AXIS)



PLOT 7.8-2.7: EIGHTH STANDARD CONFIGURATION, CASE 7.
 MAGNITUDE AND PHASE LEAD OF UNSTEADY BLADE
 SURFACE PRESSURE DISTRIBUTION.
 (x: IN PITCH MODE, NOTATION VALID UPSTREAM OF PITCH AXIS)

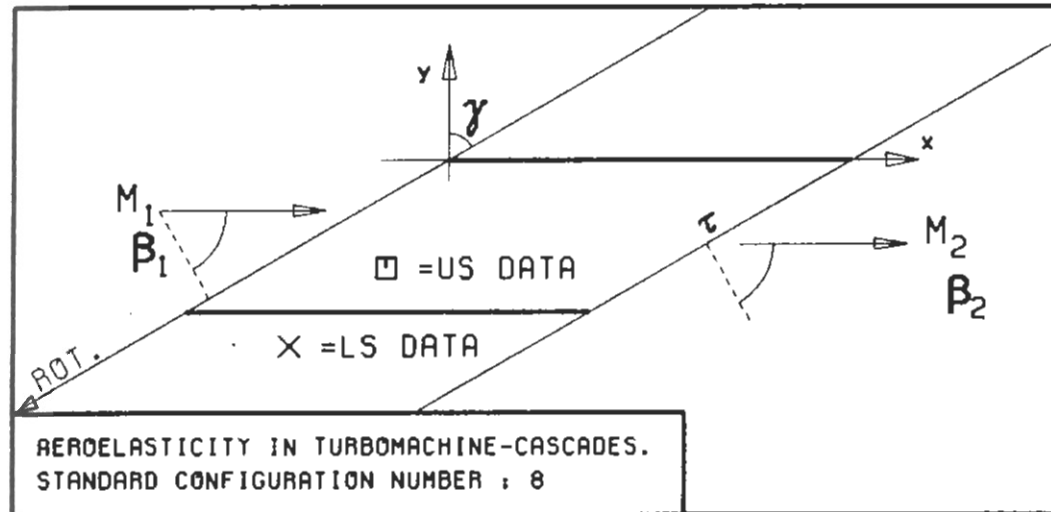


16.



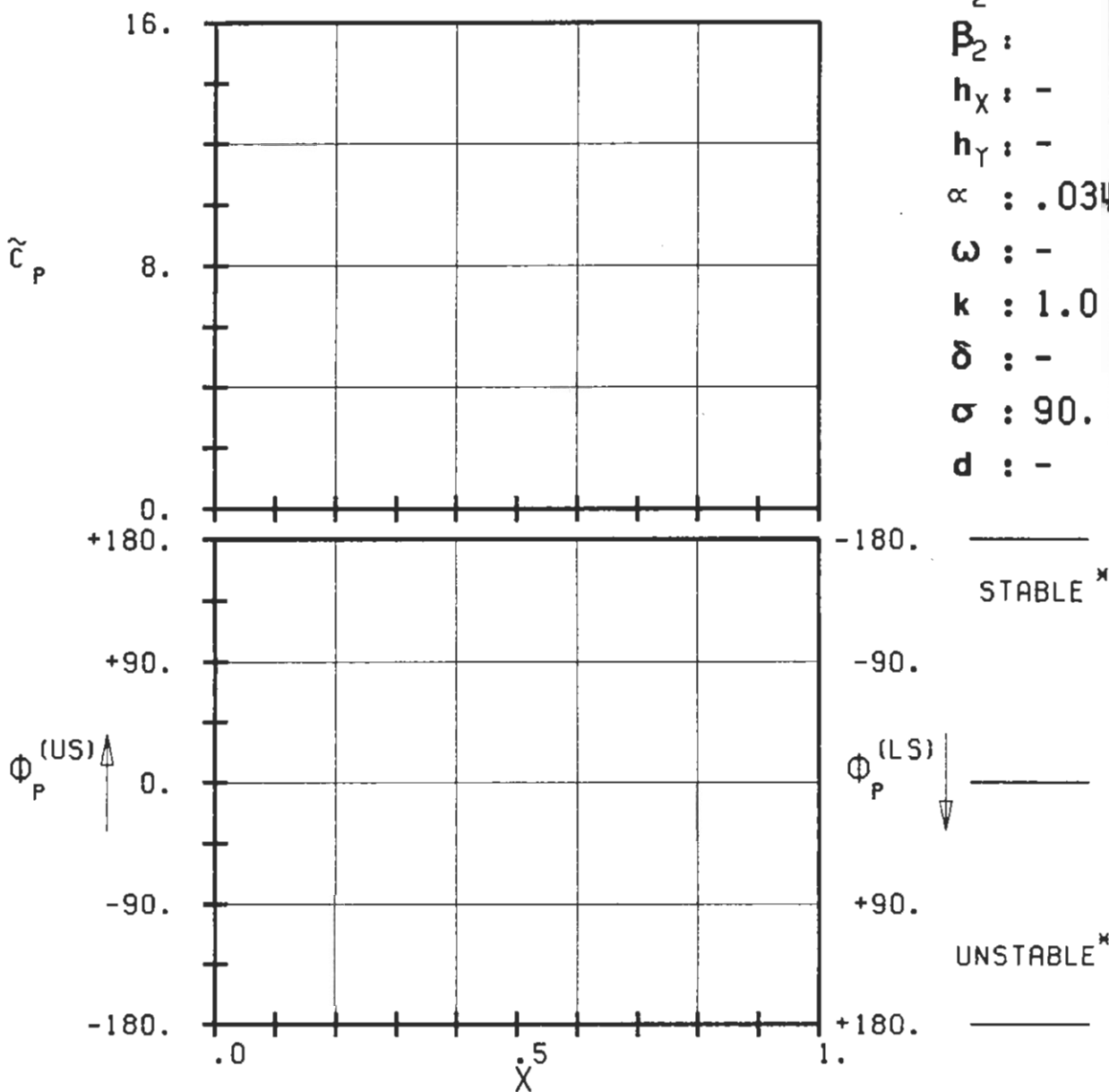
PLOT 7.8-2.8: EIGHTH STANDARD CONFIGURATION, CASE 8.
MAGNITUDE AND PHASE LEAD OF UNSTEADY BLADE
SURFACE PRESSURE DISTRIBUTION.

(x: IN PITCH MODE, NOTATION VALID UPSTREAM OF PITCH AXIS)



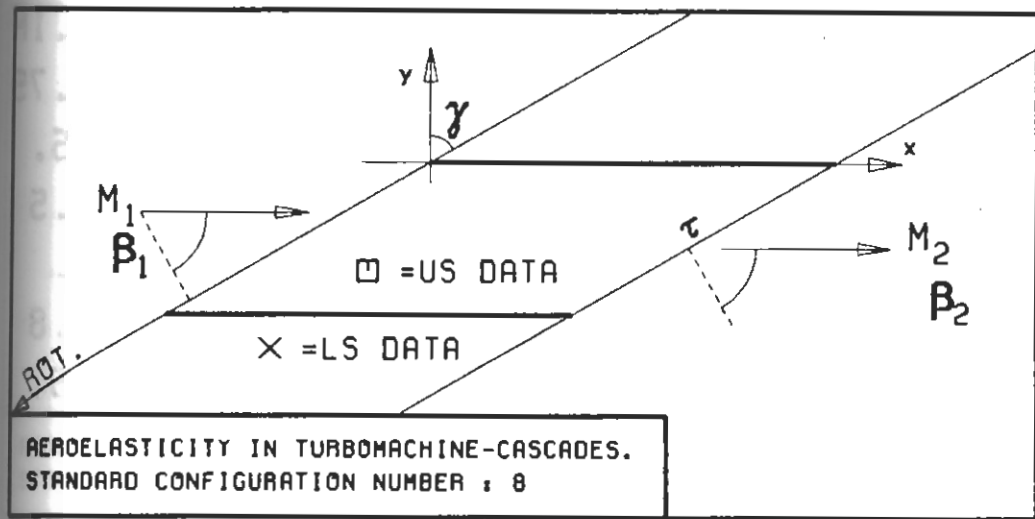
c : 0.1
 τ : 0.75
 γ : 60.
 x_∞ : 0.5
 y_∞ : 0.
 M_1 : 0.9
 β_1 : -60.
 i : 0.
 M_2 : -
 β_2 :
 h_x : -
 h_y : -
 α : .0349

ω : -
 k : 1.0
 δ : -
 σ : 90.
 d : -



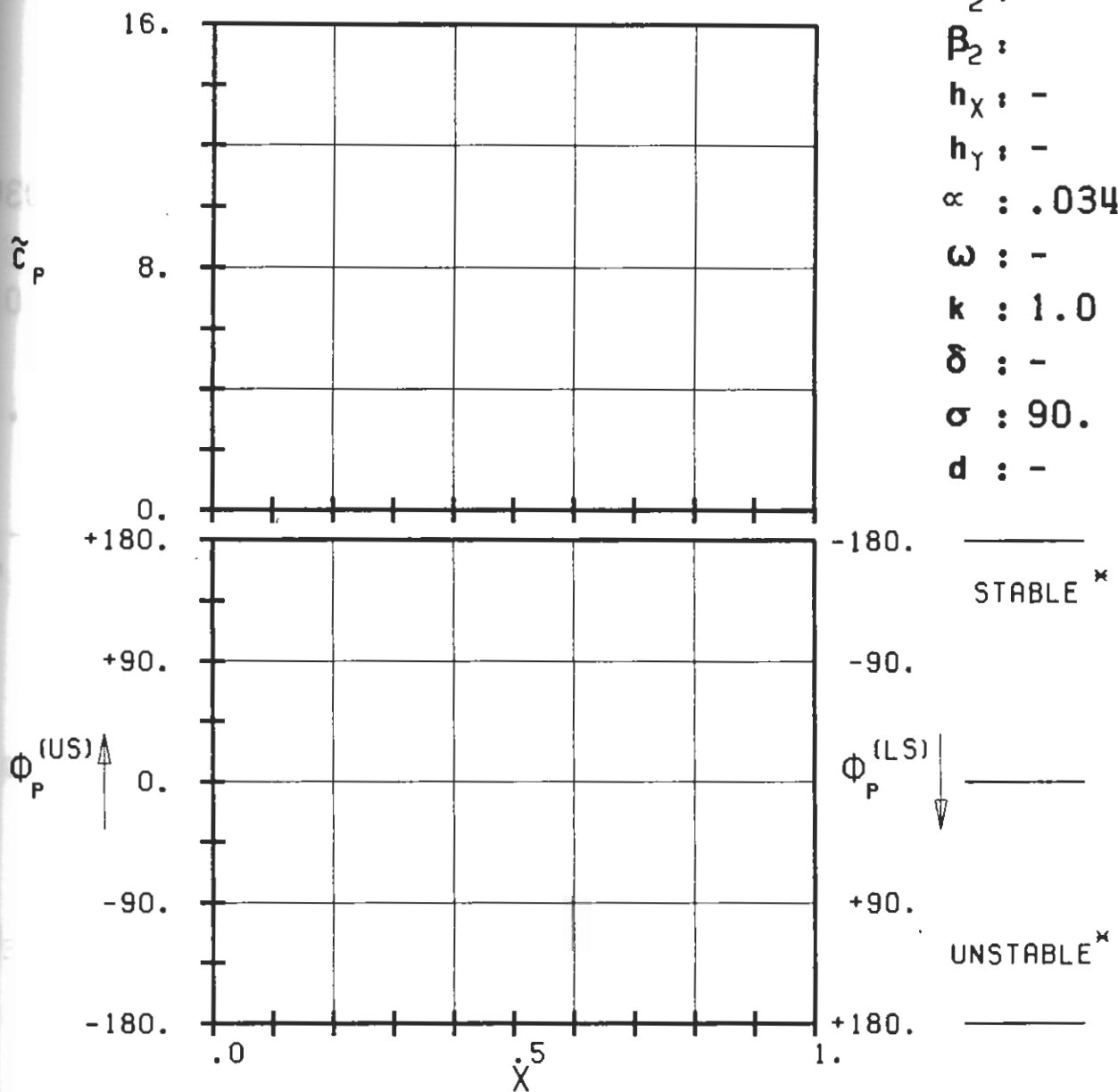
PLOT 7.8-2.9: EIGHTH STANDARD CONFIGURATION, CASE 9.
MAGNITUDE AND PHASE LEAD OF UNSTEADY BLADE SURFACE PRESSURE DISTRIBUTION.

(*: IN PITCH MODE, NOTATION VALID UPSTREAM OF PITCH AXIS)



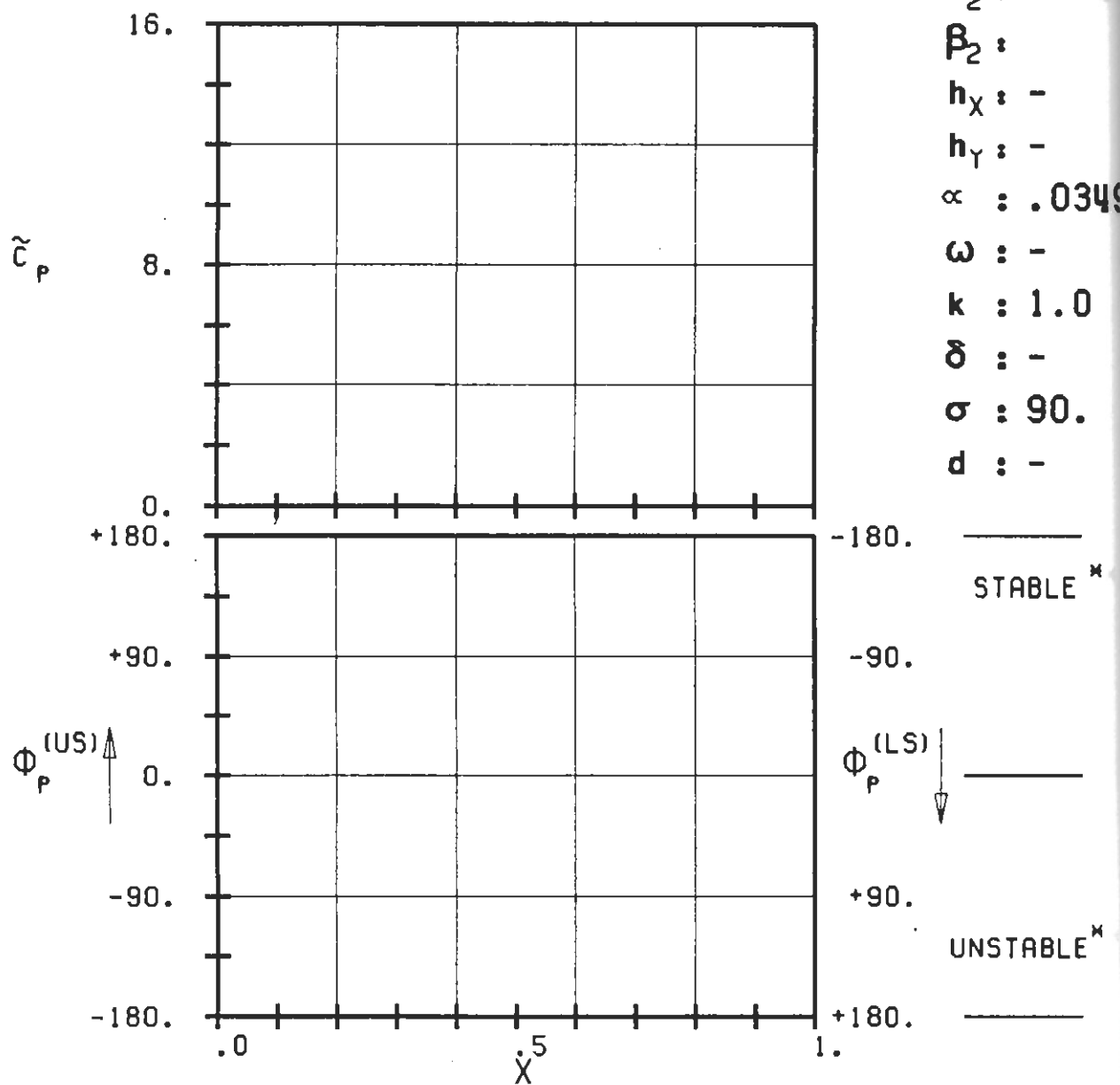
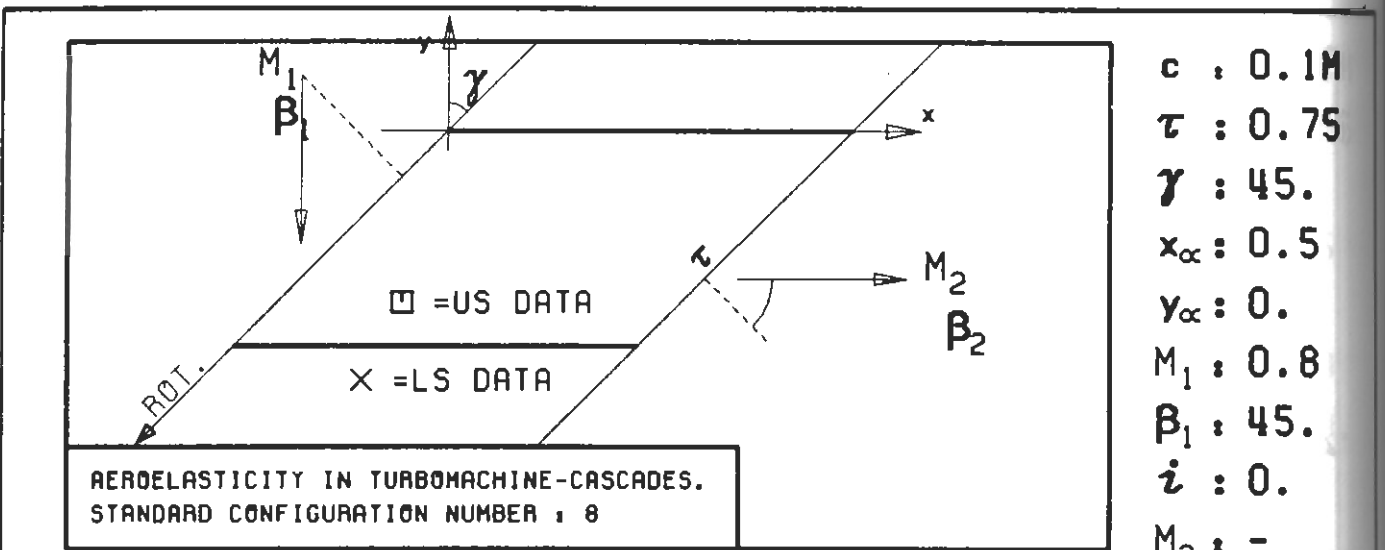
$c : 0.1M$
 $\tau : 0.75$
 $\gamma : 60.$
 $x_\alpha : 0.5$
 $y_\alpha : 0.$
 $M_1 : 0.95$
 $\beta_1 : -60.$
 $i : 0.$
 $M_2 : -$
 $\beta_2 : -$
 $h_x : -$
 $h_y : -$
 $\alpha : .0349$

$\omega : -$
 $k : 1.0$
 $\delta : -$
 $\sigma : 90.$
 $d : -$

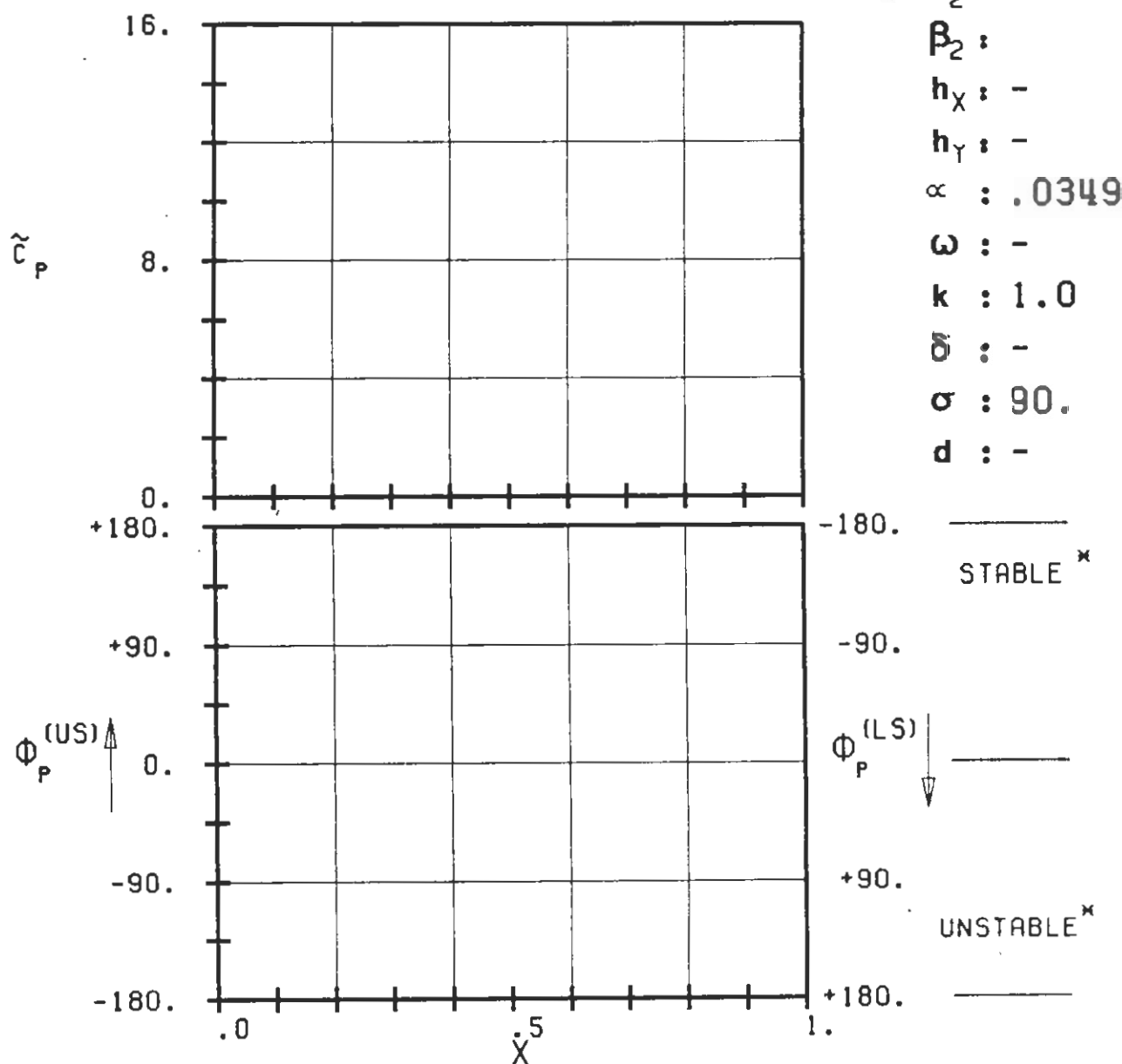
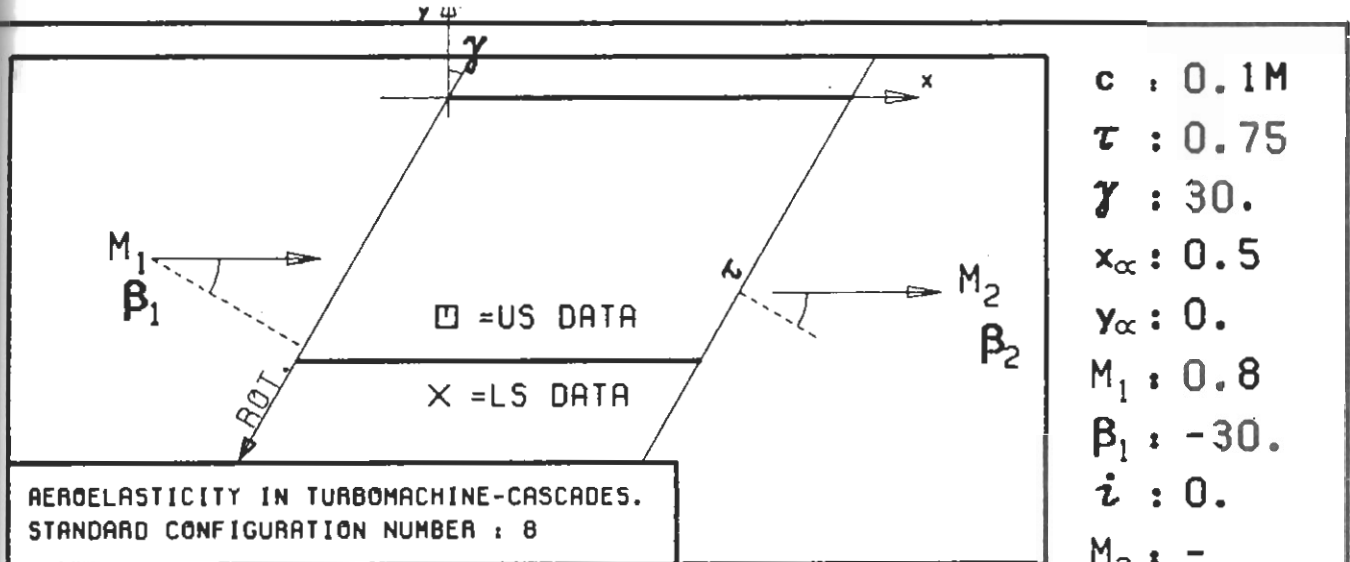


PLOT 7.8-2.10: EIGHTH STANDARD CONFIGURATION, CASE 10.
MAGNITUDE AND PHASE LEAD OF UNSTEADY BLADE
SURFACE PRESSURE DISTRIBUTION.

(x: IN PITCH MODE, NOTATION VALID UPSTREAM OF PITCH AXIS)

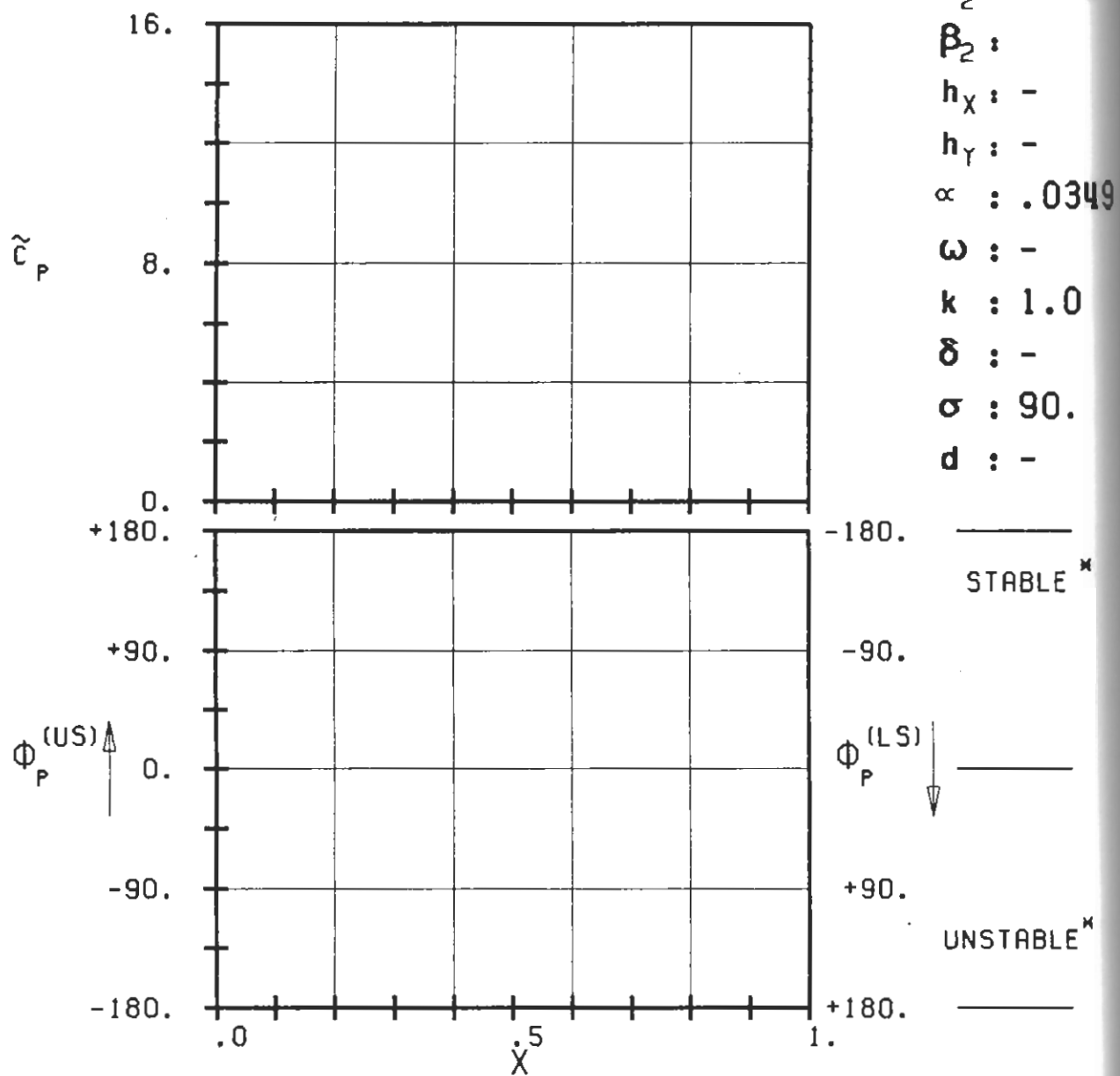
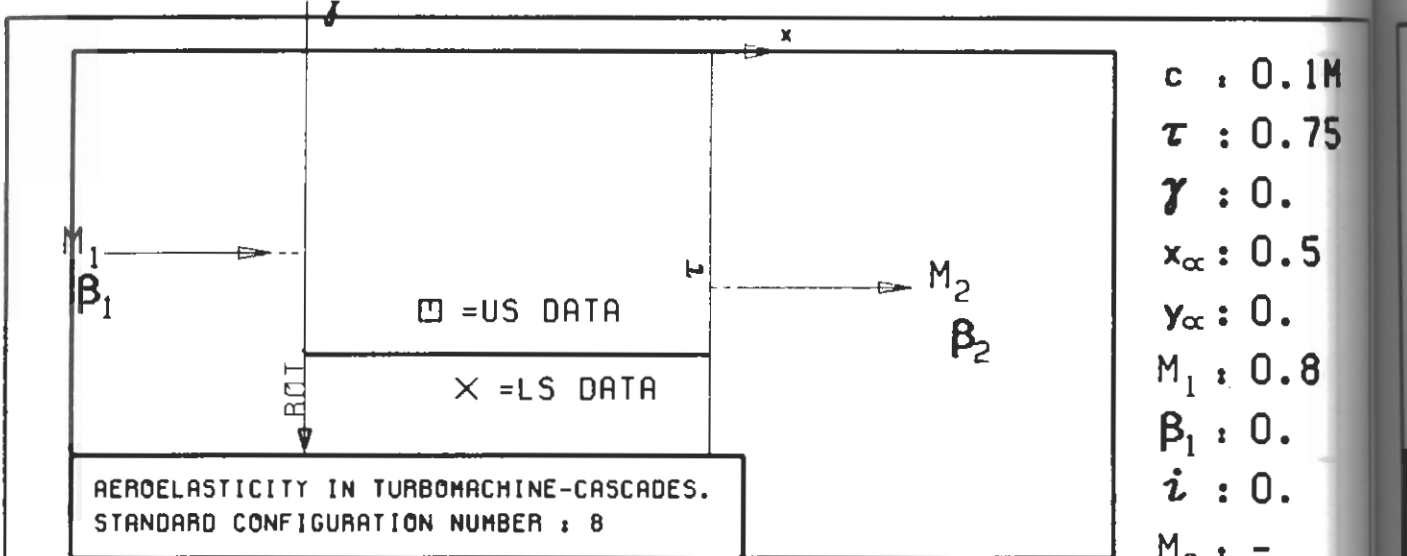


PLOT 7.8-2.11: EIGHTH STANDARD CONFIGURATION, CASE 11.
MAGNITUDE AND PHASE LEAD OF UNSTEADY BLADE SURFACE PRESSURE DISTRIBUTION.
(*: IN PITCH MODE, NOTATION VALID UPSTREAM OF PITCH AXIS)

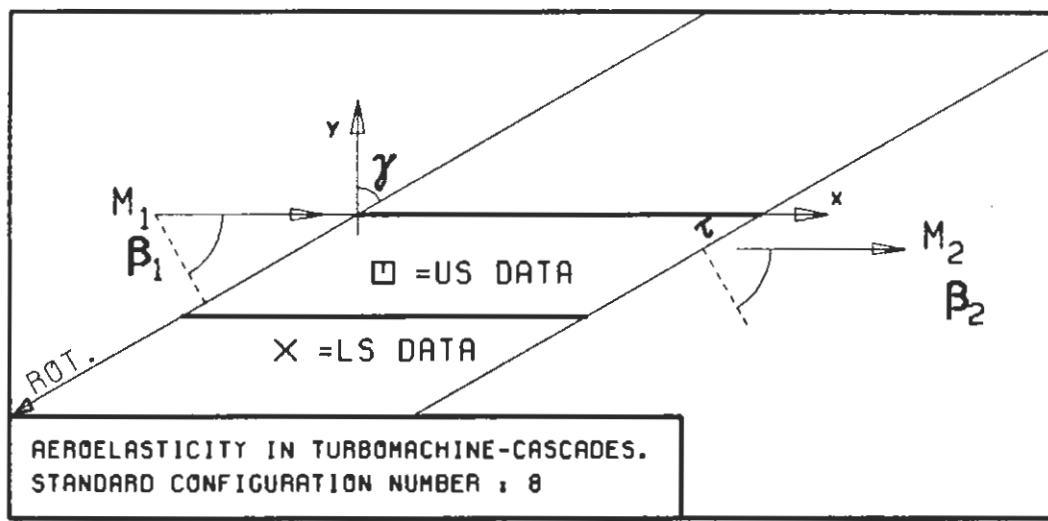


PLOT 7.8-2.12: EIGHTH STANDARD CONFIGURATION, CASE 12.
MAGNITUDE AND PHASE LEAD OF UNSTEADY BLADE
SURFACE PRESSURE DISTRIBUTION.

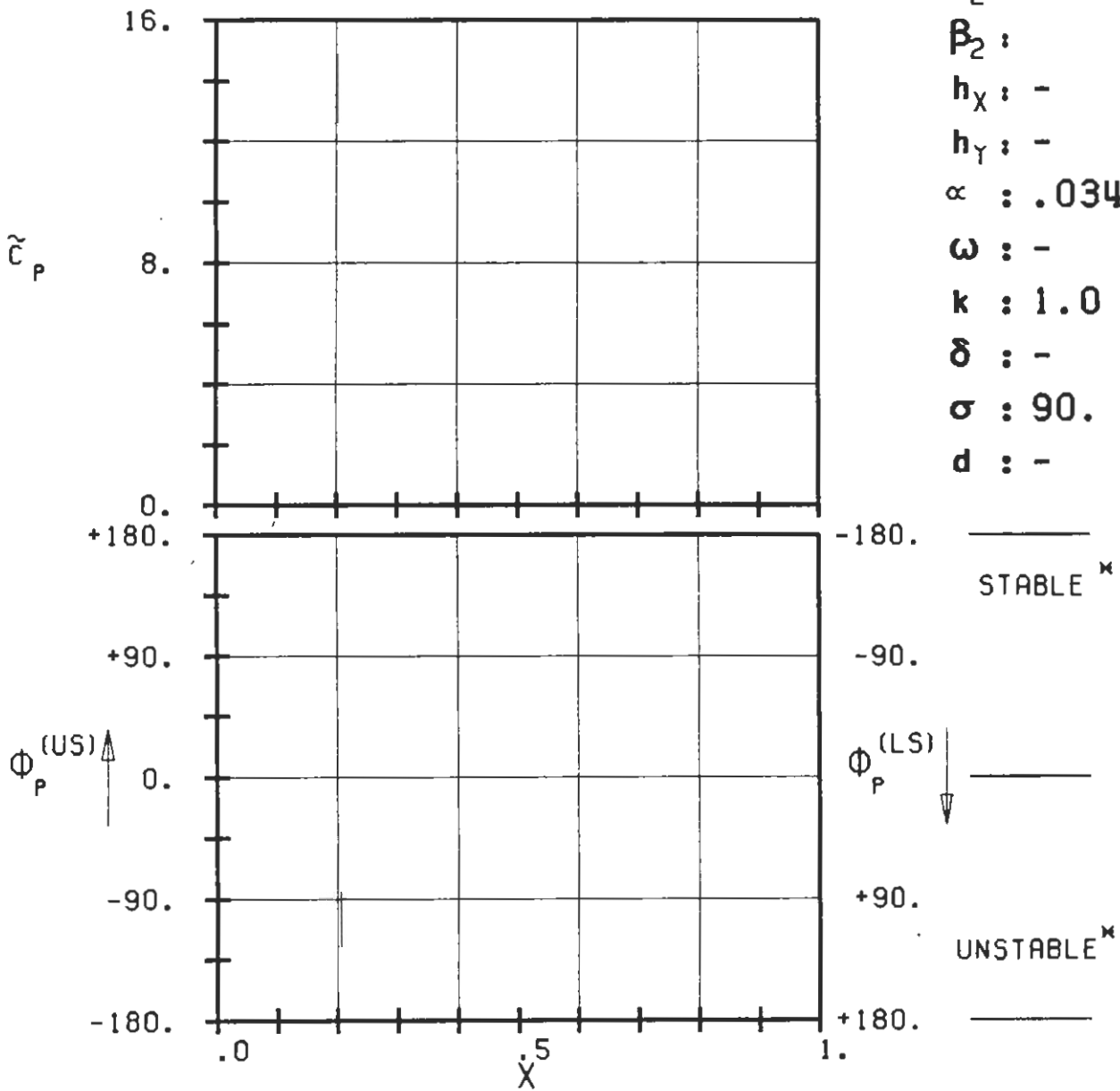
(*: IN PITCH MODE, NOTATION VALID UPSTREAM OF PITCH AXIS)



PLOT 7.8-2.13: EIGHTH STANDARD CONFIGURATION, CASE 13.
 MAGNITUDE AND PHASE LEAD OF UNSTEADY BLADE SURFACE PRESSURE DISTRIBUTION.
 (*: IN PITCH MODE, NOTATION VALID UPSTREAM OF PITCH AXIS)

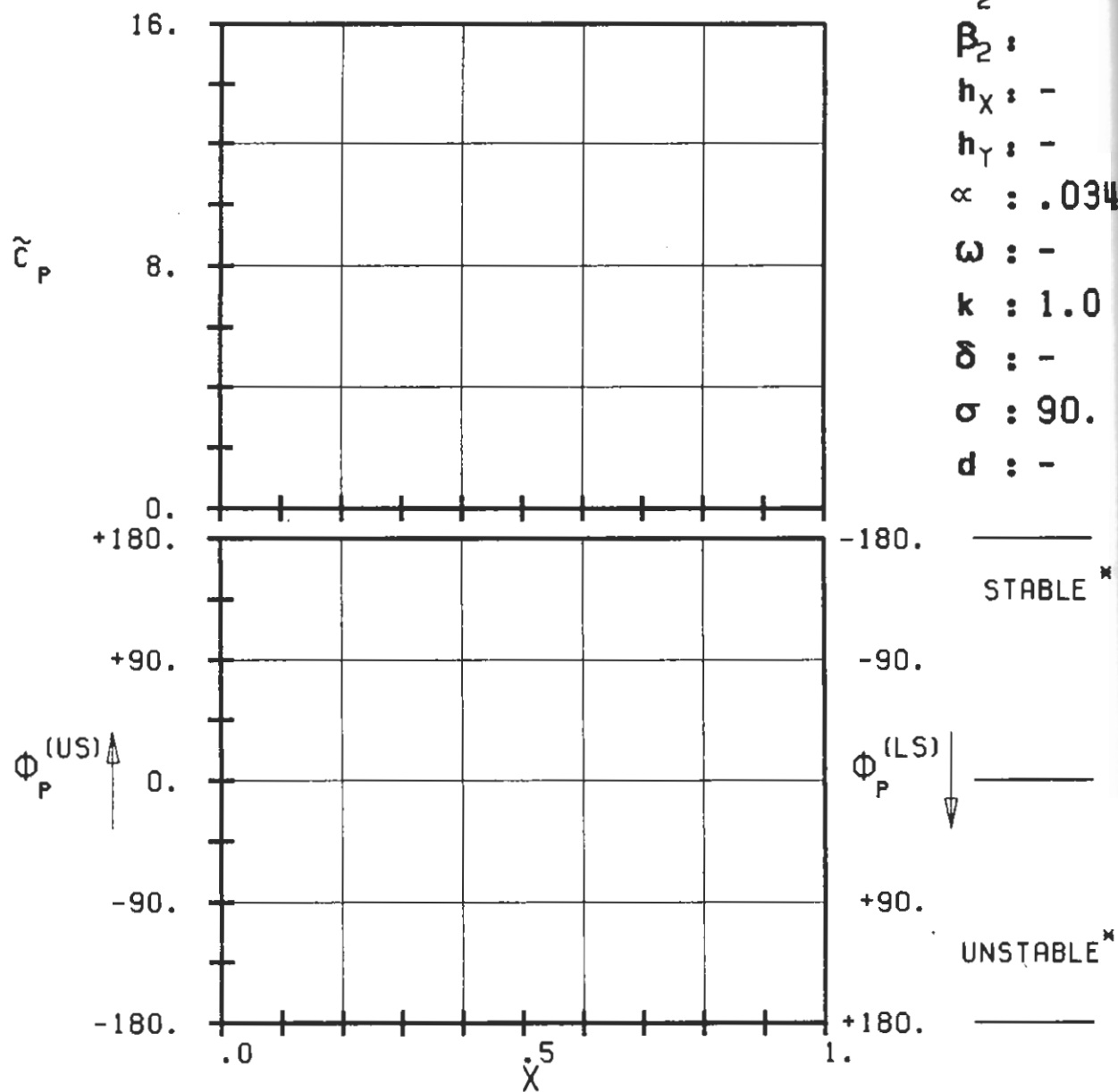
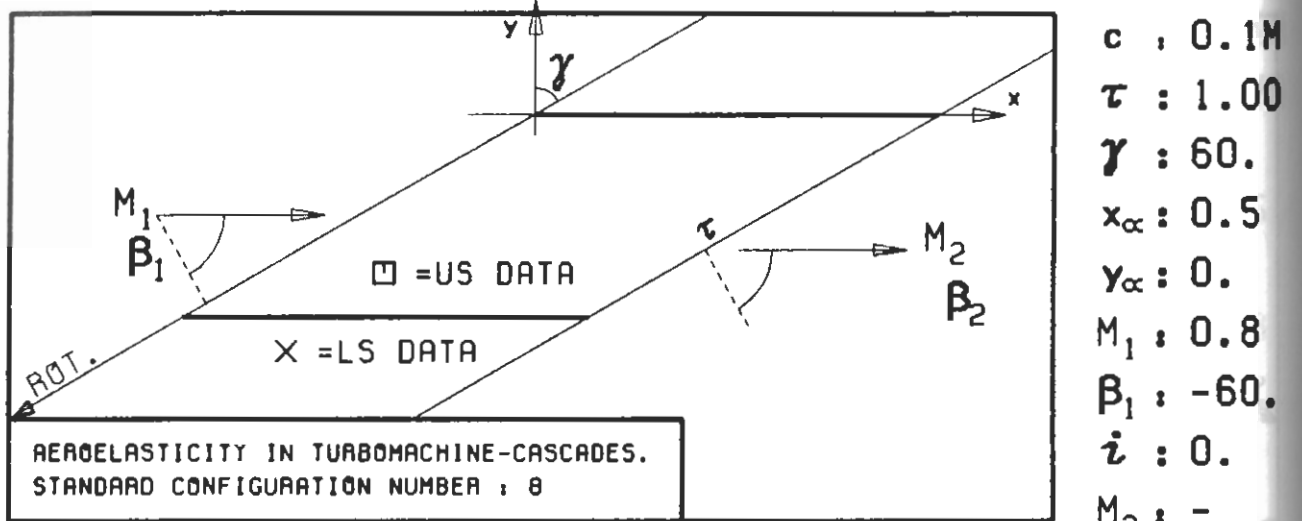


$c : 0.1M$
 $\tau : 0.50$
 $\gamma : 60.$
 $x_\infty : 0.5$
 $y_\infty : 0.$
 $M_1 : 0.8$
 $\beta_1 : -60.$
 $i : 0.$
 $M_2 : -$
 $\beta_2 : -$
 $h_X : -$
 $h_Y : -$
 $\alpha : .0349$
 $\omega : -$
 $k : 1.0$
 $\delta : -$
 $\sigma : 90.$
 $d : -$



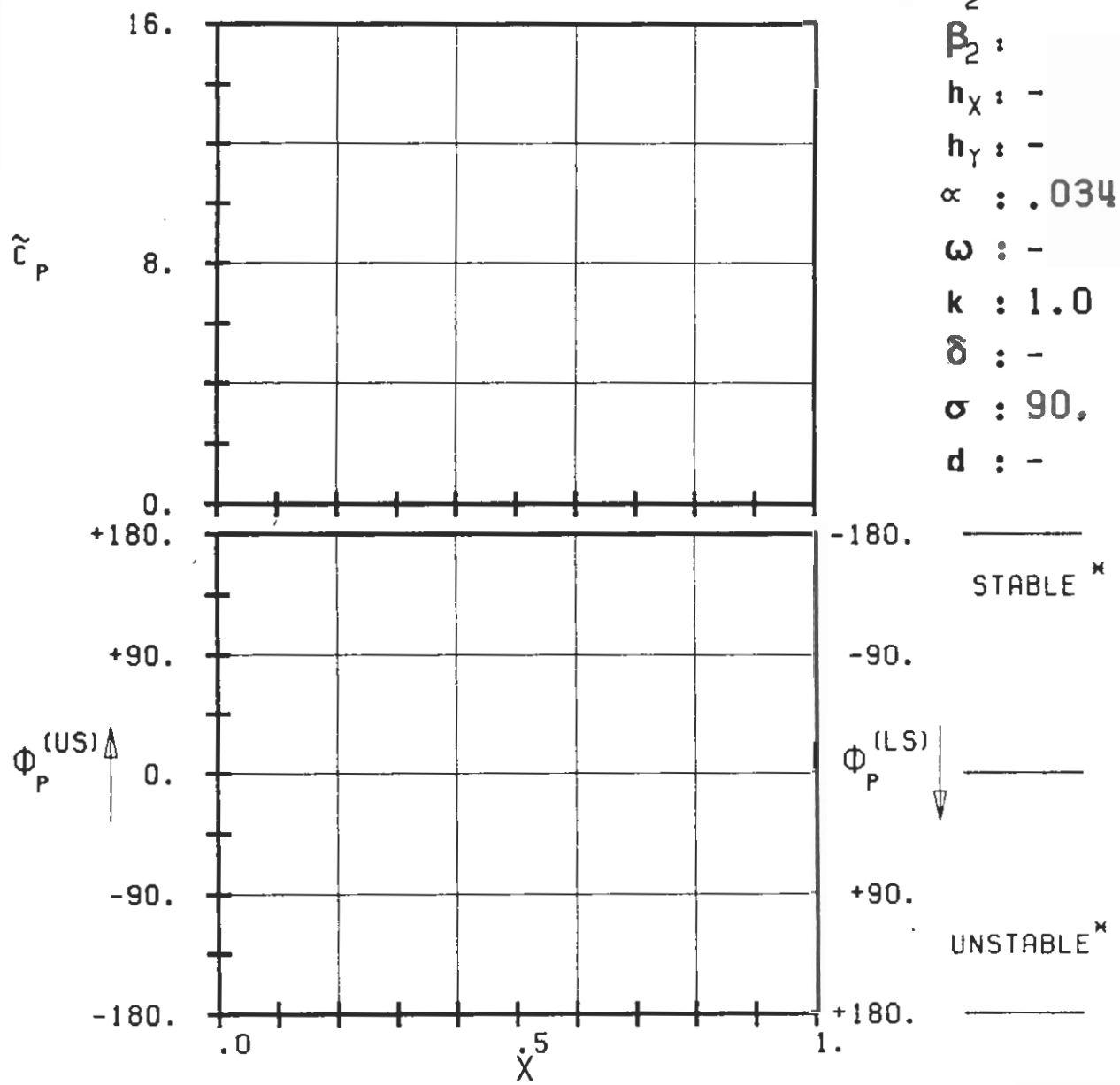
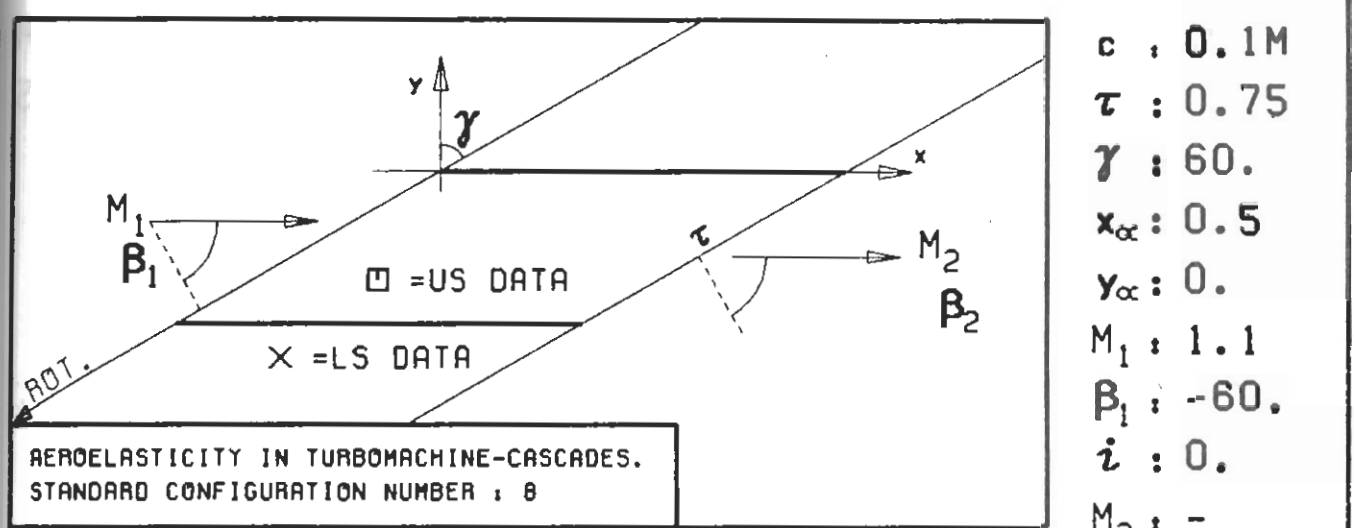
PLOT 7.8-2.14: EIGHTH STANDARD CONFIGURATION, CASE 14.
MAGNITUDE AND PHASE LEAD OF UNSTEADY BLADE
SURFACE PRESSURE DISTRIBUTION.

(*: IN PITCH MODE, NOTATION VALID UPSTREAM OF PITCH AXIS)



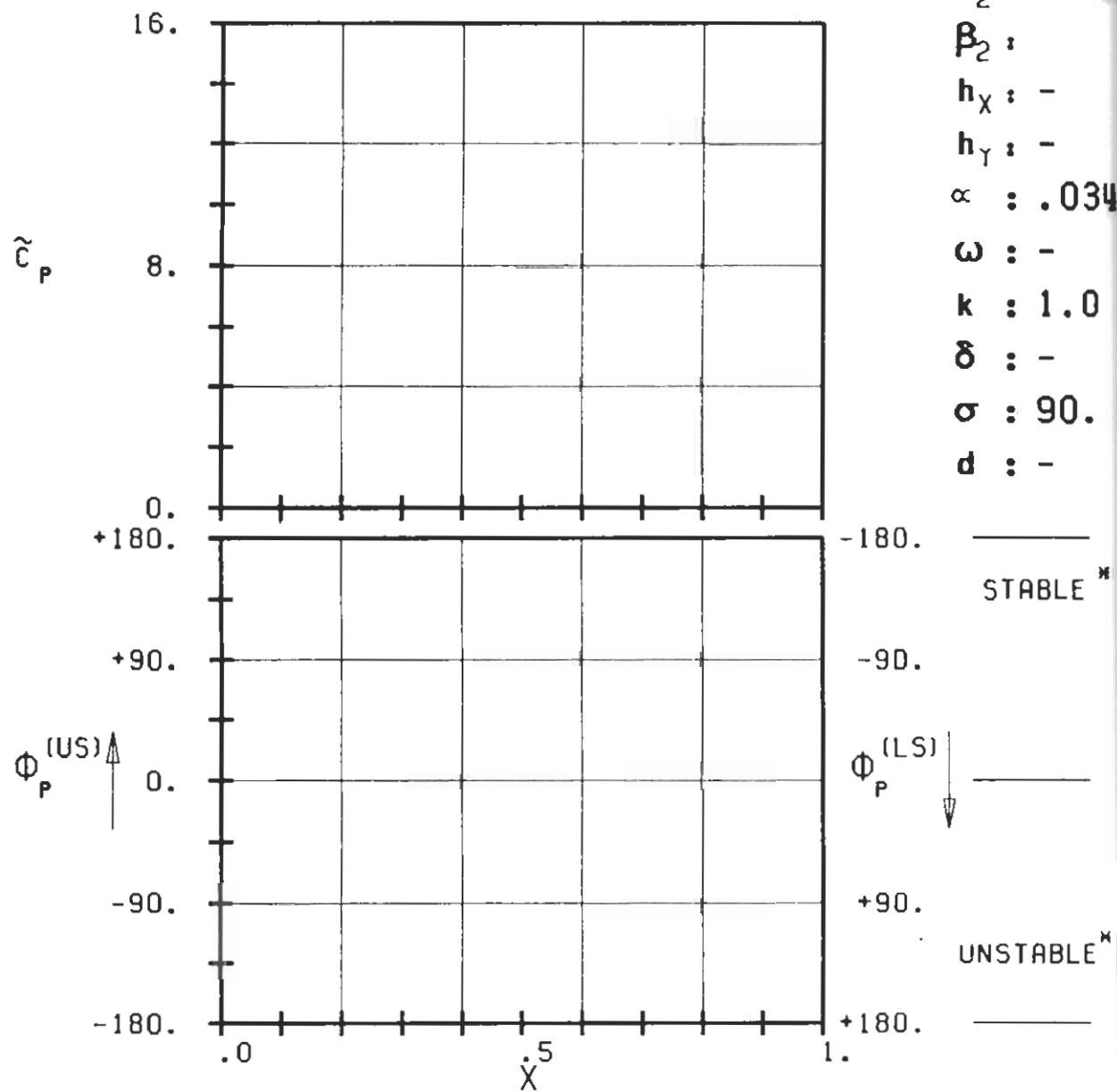
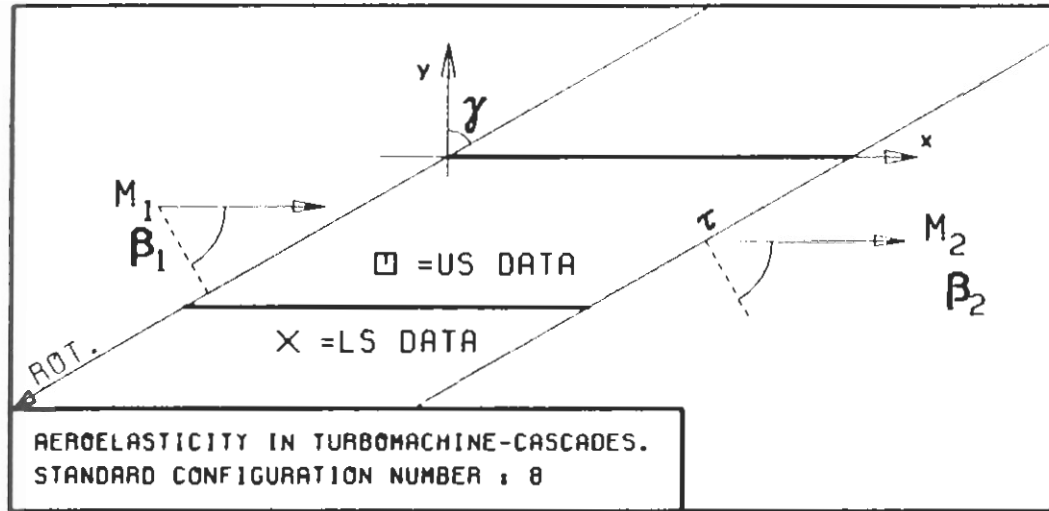
PLOT 7.8-2.15: EIGHTH STANDARD CONFIGURATION, CASE 15.
MAGNITUDE AND PHASE LEAD OF UNSTEADY BLADE
SURFACE PRESSURE DISTRIBUTION.

(*: IN PITCH MODE, NOTATION VALID UPSTREAM OF PITCH AXIS)



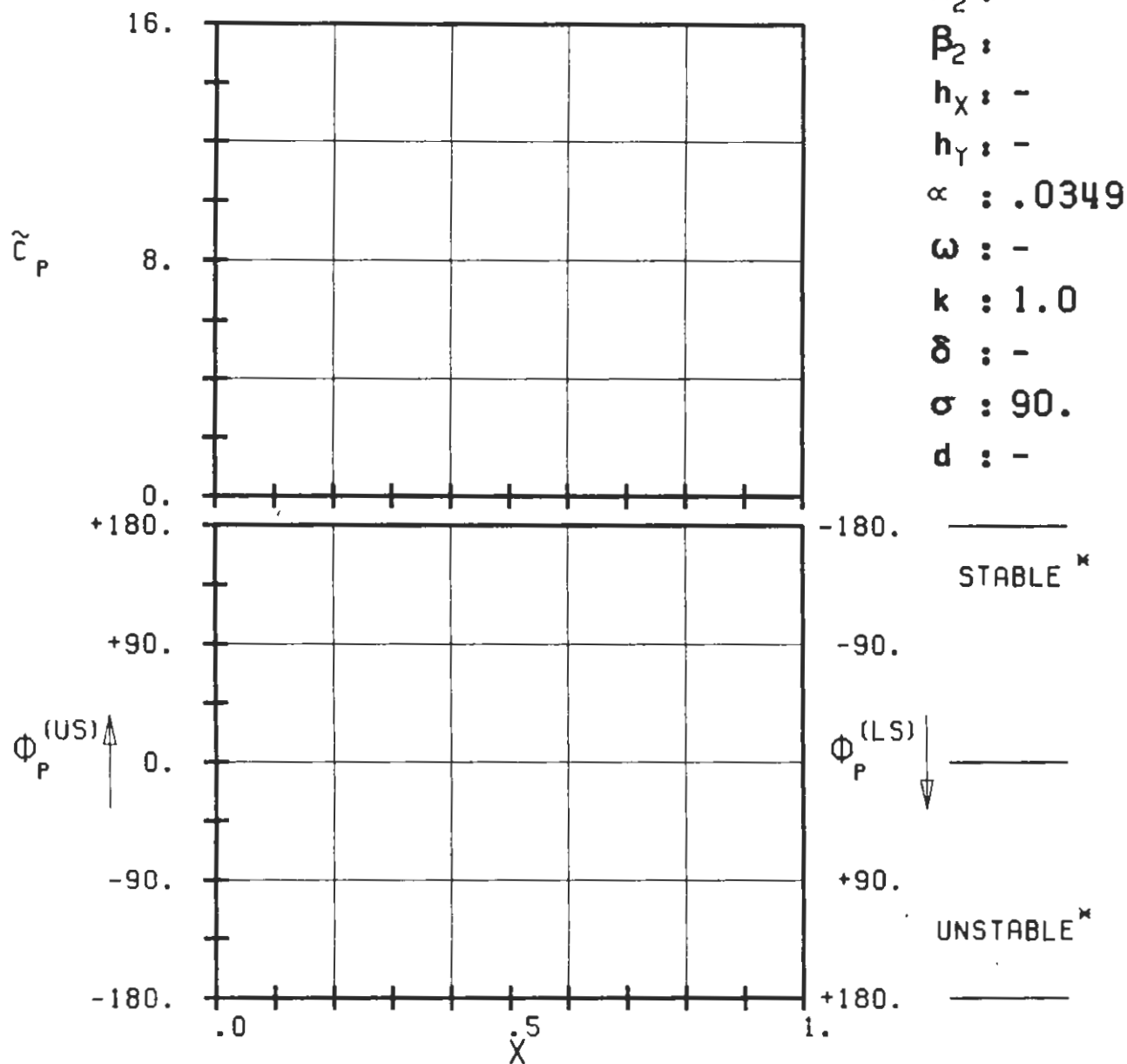
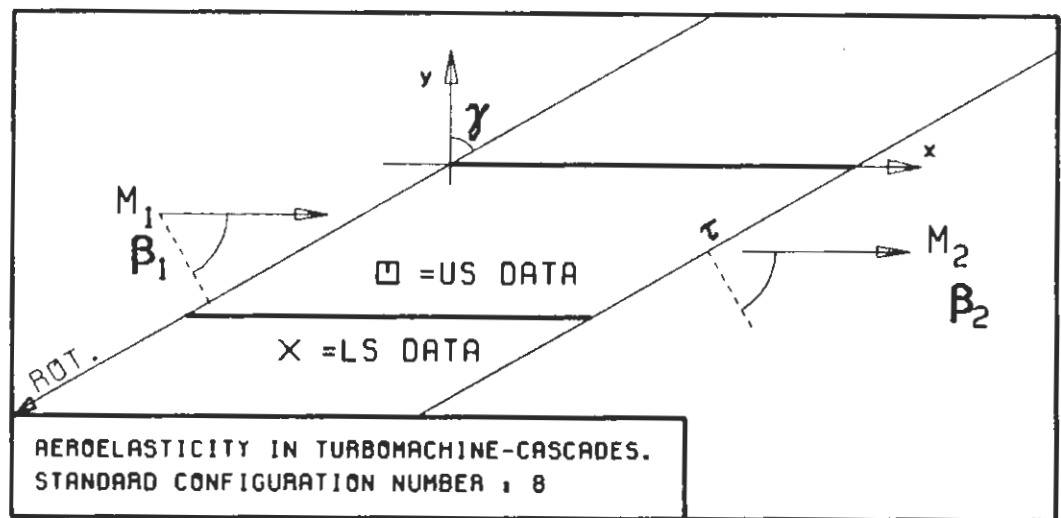
PLOT 7.8-2.16: EIGHTH STANDARD CONFIGURATION, CASE 16.
MAGNITUDE AND PHASE LEAD OF UNSTEADY BLADE SURFACE PRESSURE DISTRIBUTION.

(x: IN PITCH MODE, NOTATION VALID UPSTREAM OF PITCH AXIS)

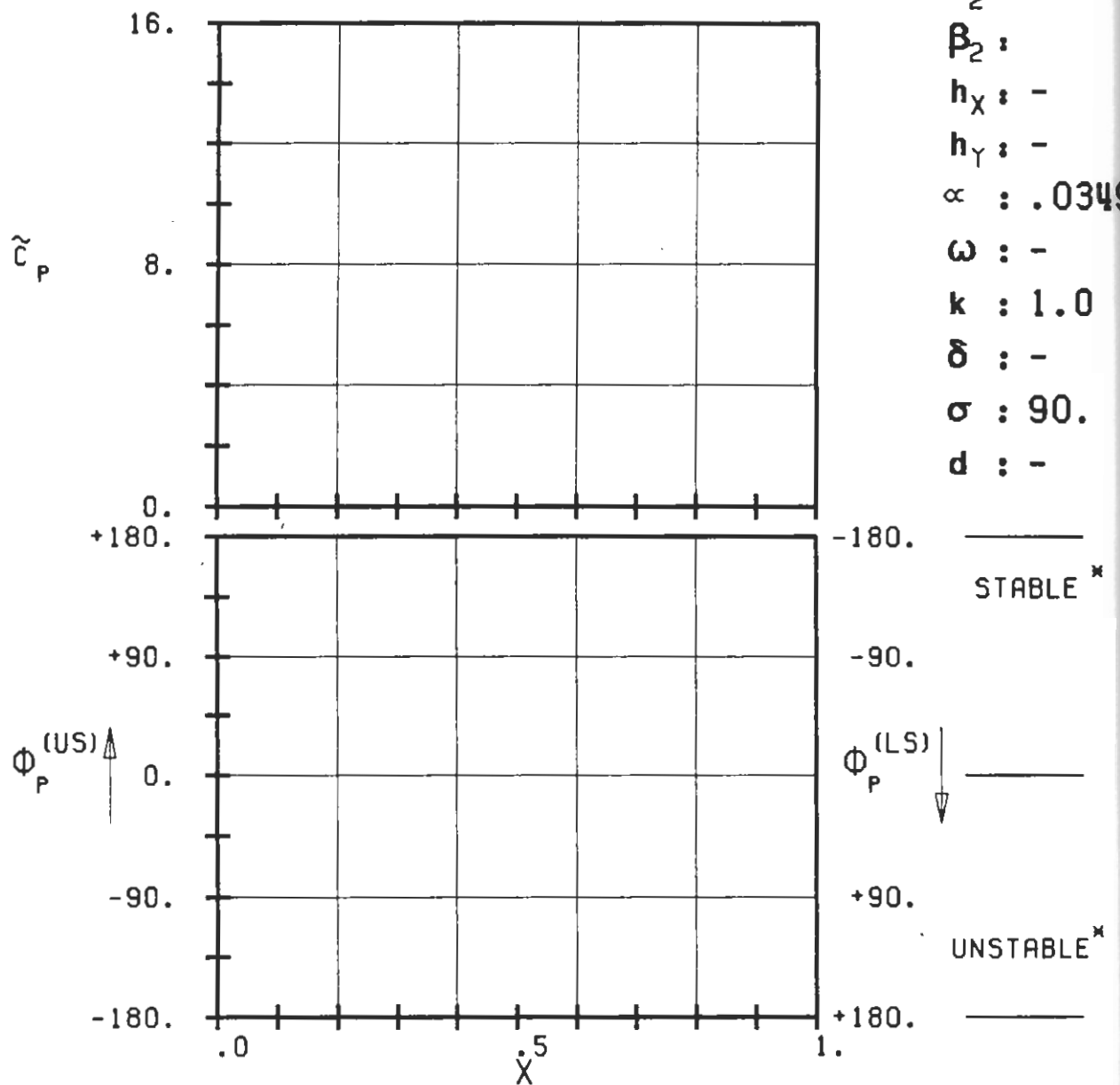
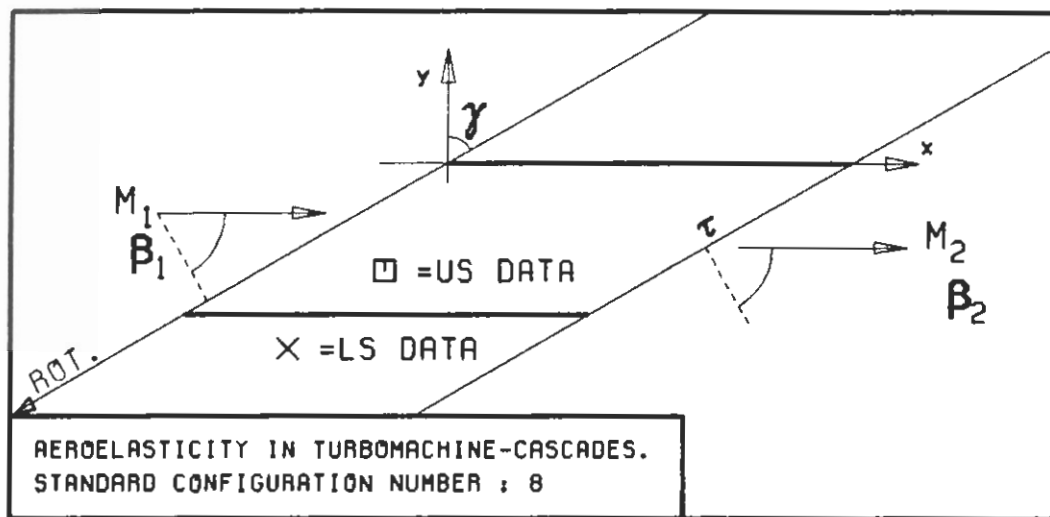


PLOT 7.8-2.17: EIGHTH STANDARD CONFIGURATION, CASE 17.
MAGNITUDE AND PHASE LEAD OF UNSTEADY BLADE SURFACE PRESSURE DISTRIBUTION.

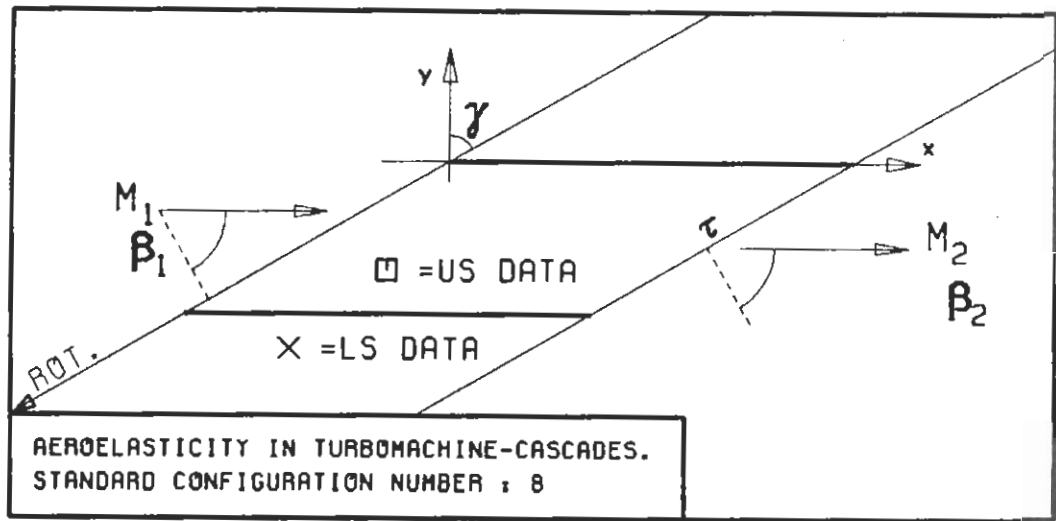
(x: IN PITCH MODE, NOTATION VALID UPSTREAM OF PITCH AXIS)



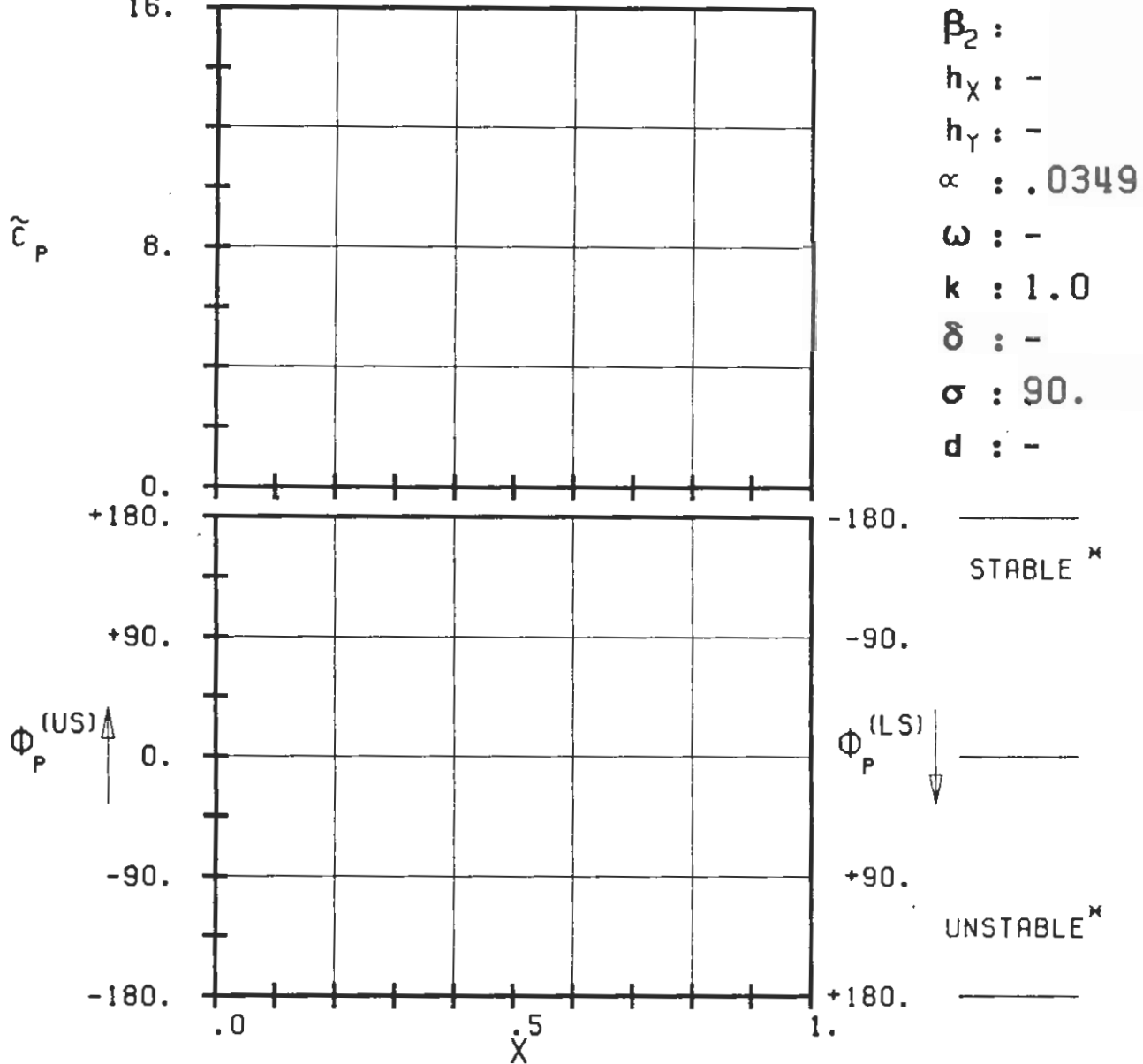
PLOT 7.8-2.18: EIGHTH STANDARD CONFIGURATION, CASE 18.
MAGNITUDE AND PHASE LEAD OF UNSTEADY BLADE
SURFACE PRESSURE DISTRIBUTION.
(*: IN PITCH MODE, NOTATION VALID UPSTREAM OF PITCH AXIS)



PLOT 7.8-2.19: EIGHTH STANDARD CONFIGURATION, CASE 19.
MAGNITUDE AND PHASE LEAD OF UNSTEADY BLADE
SURFACE PRESSURE DISTRIBUTION.
(\times : IN PITCH MODE, NOTATION VALID UPSTREAM OF PITCH AXIS)

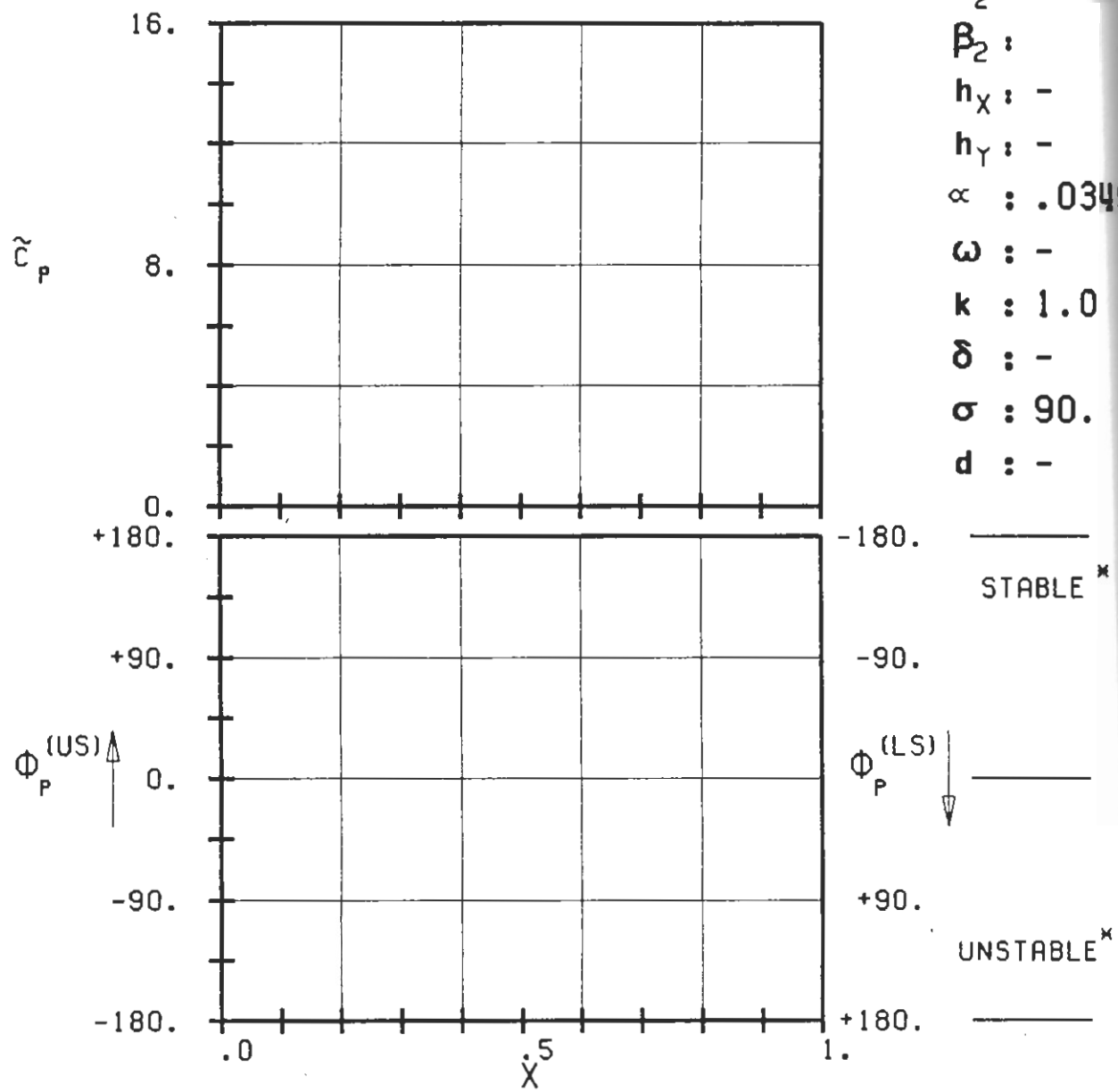
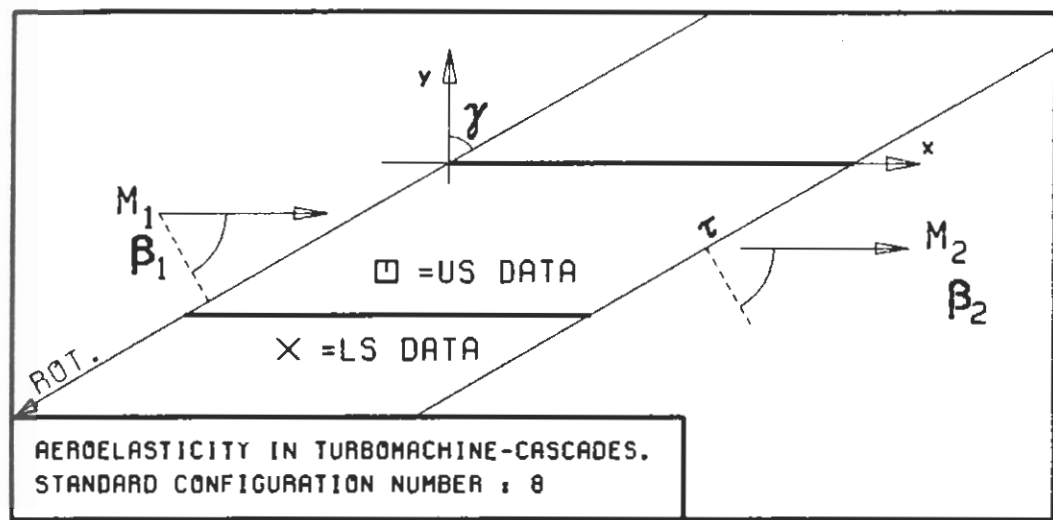


16.



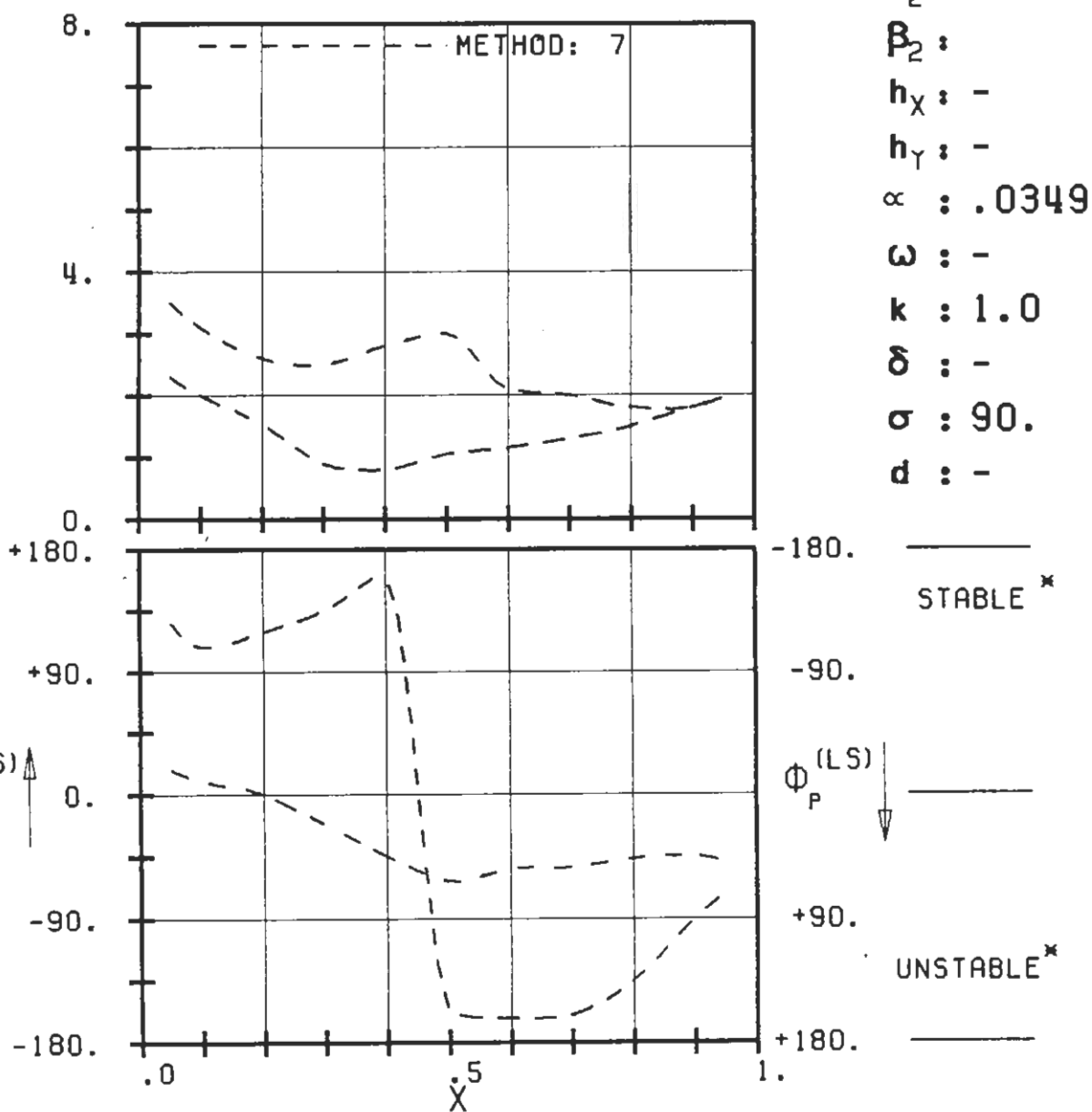
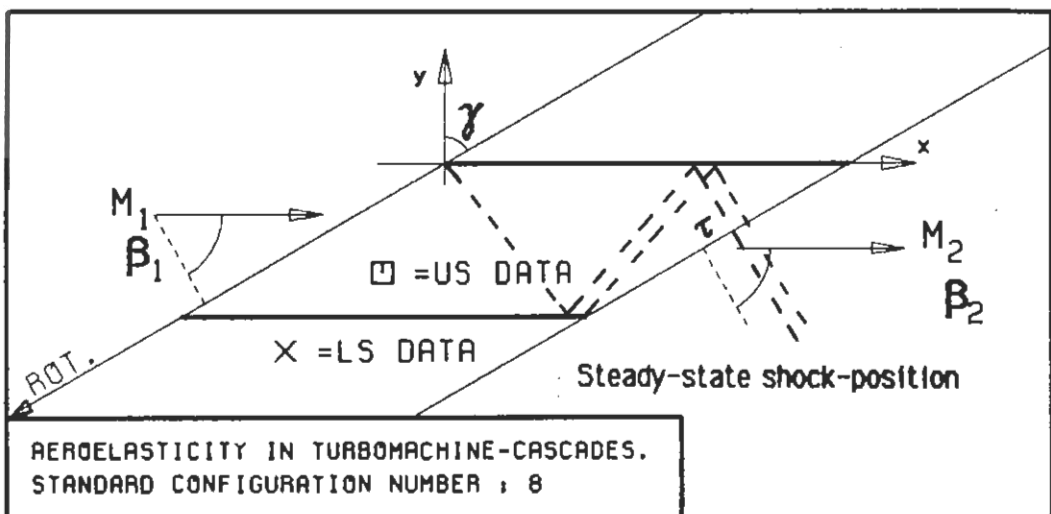
PLOT 7.8-2.20: EIGHTH STANDARD CONFIGURATION, CASE 20.
MAGNITUDE AND PHASE LEAD OF UNSTEADY BLADE SURFACE PRESSURE DISTRIBUTION.

(*: IN PITCH MODE, NOTATION VALID UPSTREAM OF PITCH AXIS)

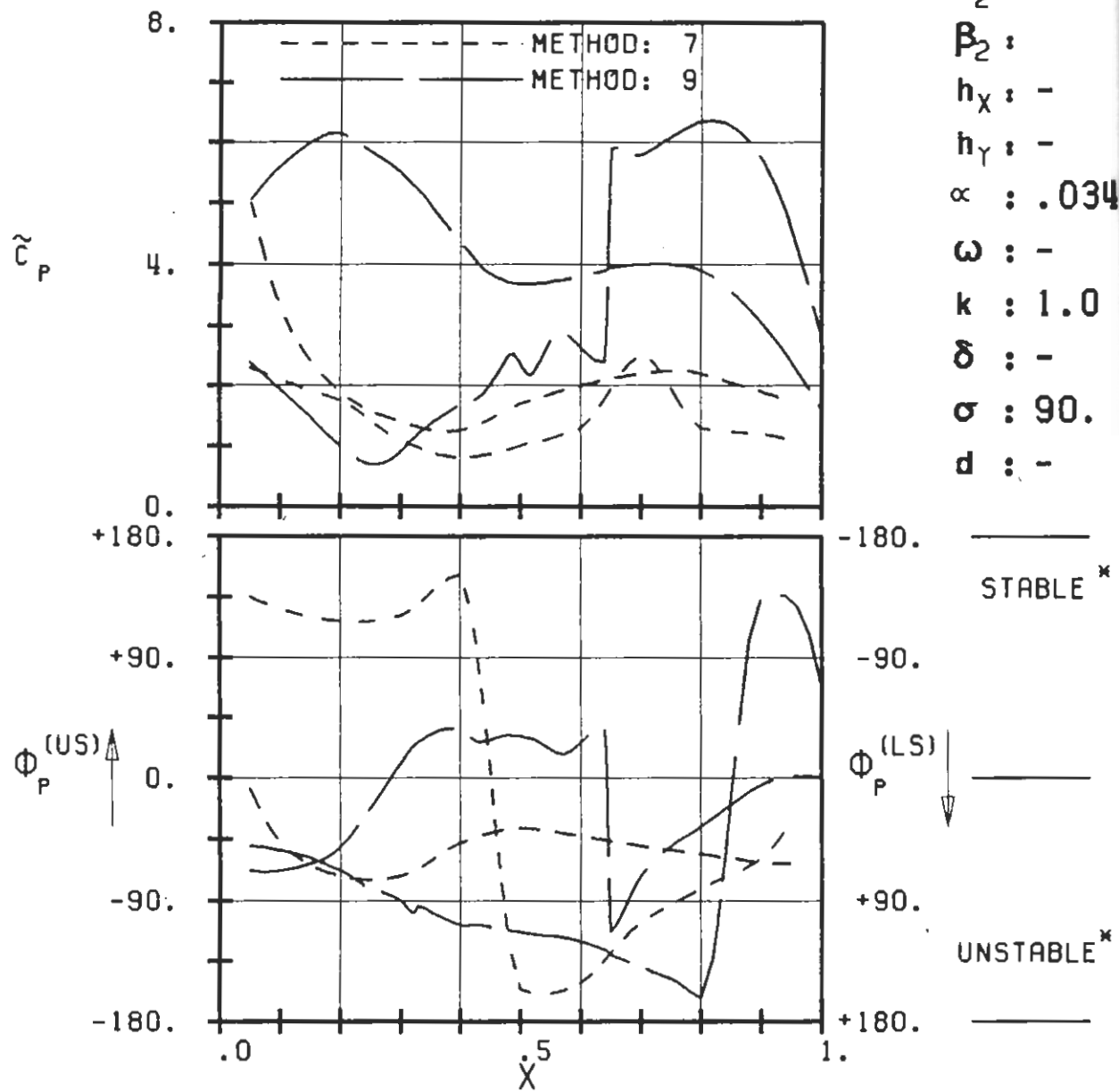
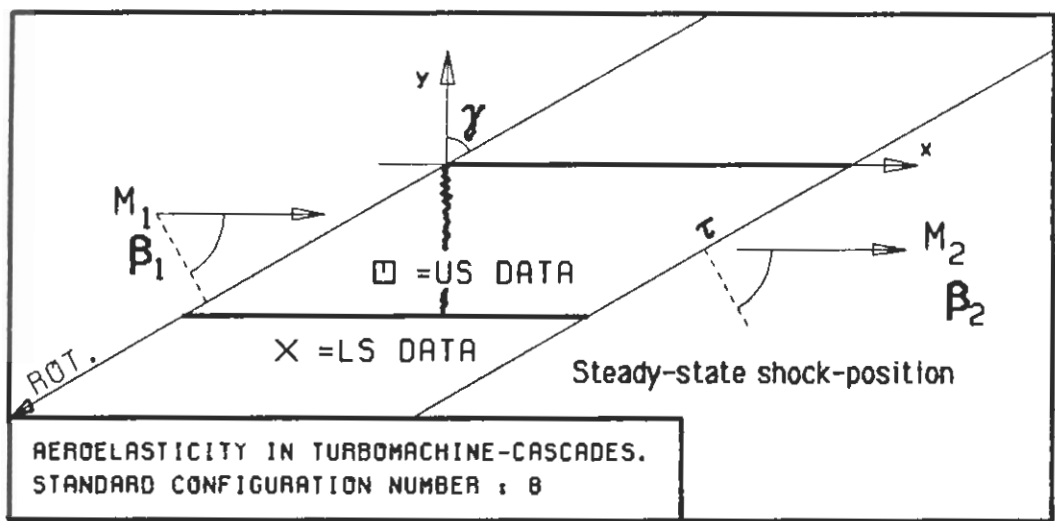


PLOT 7.8-2.21: EIGHTH STANDARD CONFIGURATION, CASE 21.
MAGNITUDE AND PHASE LEAD OF UNSTEADY BLADE SURFACE PRESSURE DISTRIBUTION.

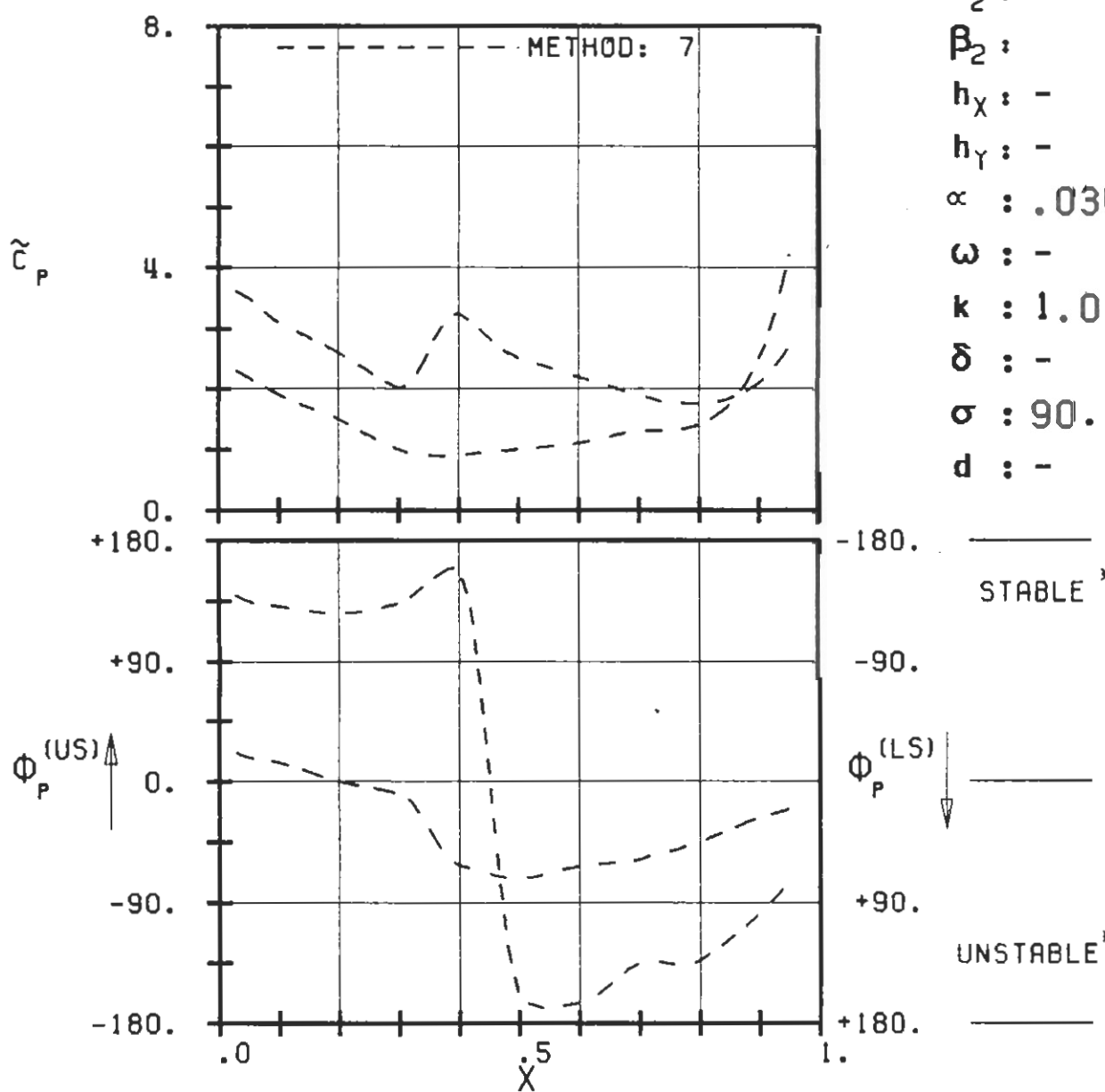
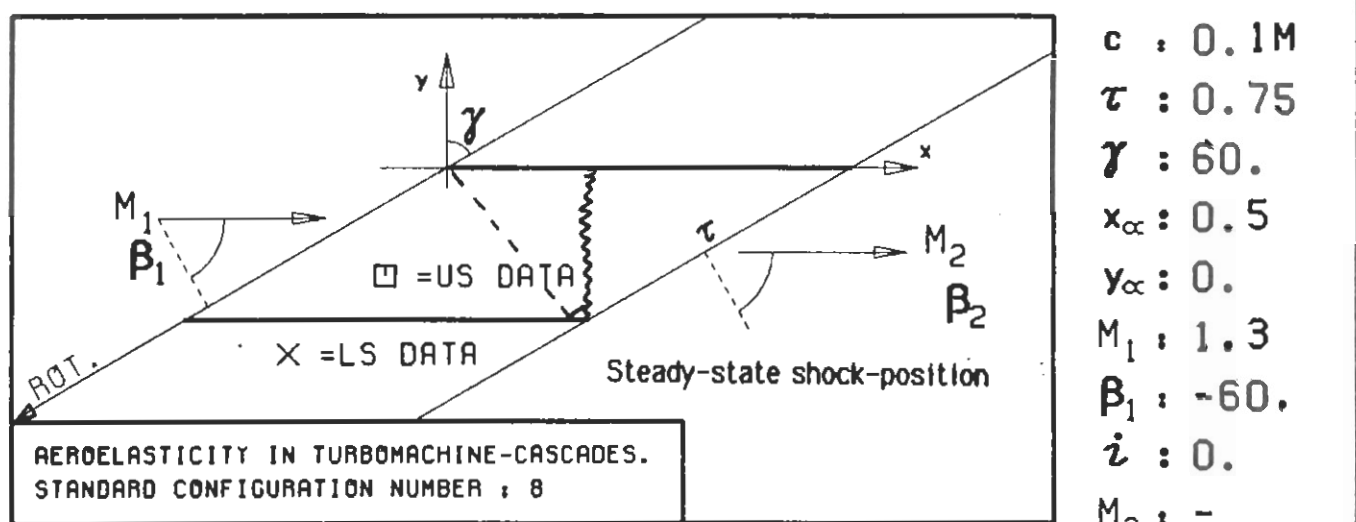
(*: IN PITCH MODE, NOTATION VALID UPSTREAM OF PITCH AXIS)



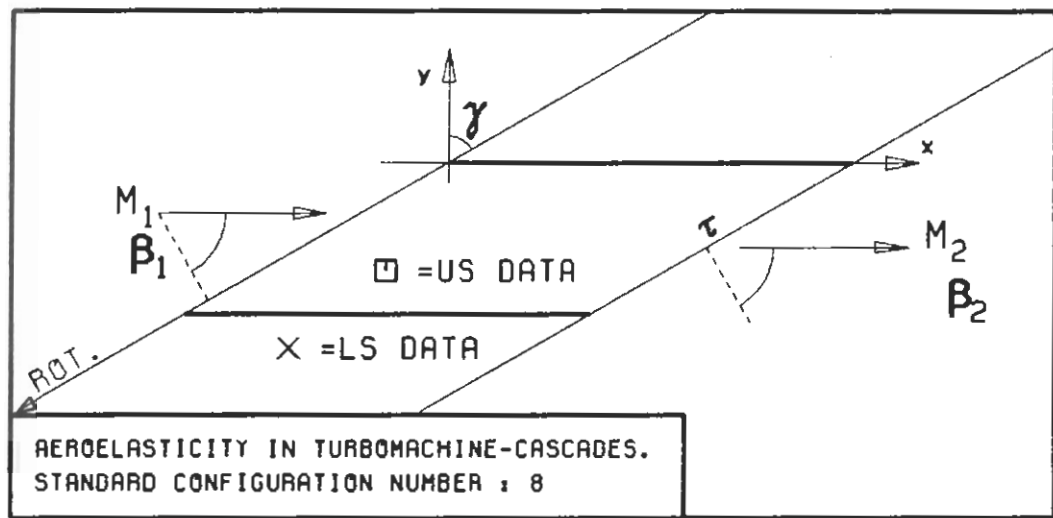
PLOT 7.8-2.22: EIGHTH STANDARD CONFIGURATION, CASE 22.
 MAGNITUDE AND PHASE LEAD OF UNSTEADY BLADE
 SURFACE PRESSURE DISTRIBUTION.
 (*: IN PITCH MODE. NOTATION VALID UPSTREAM OF PITCH AXIS)



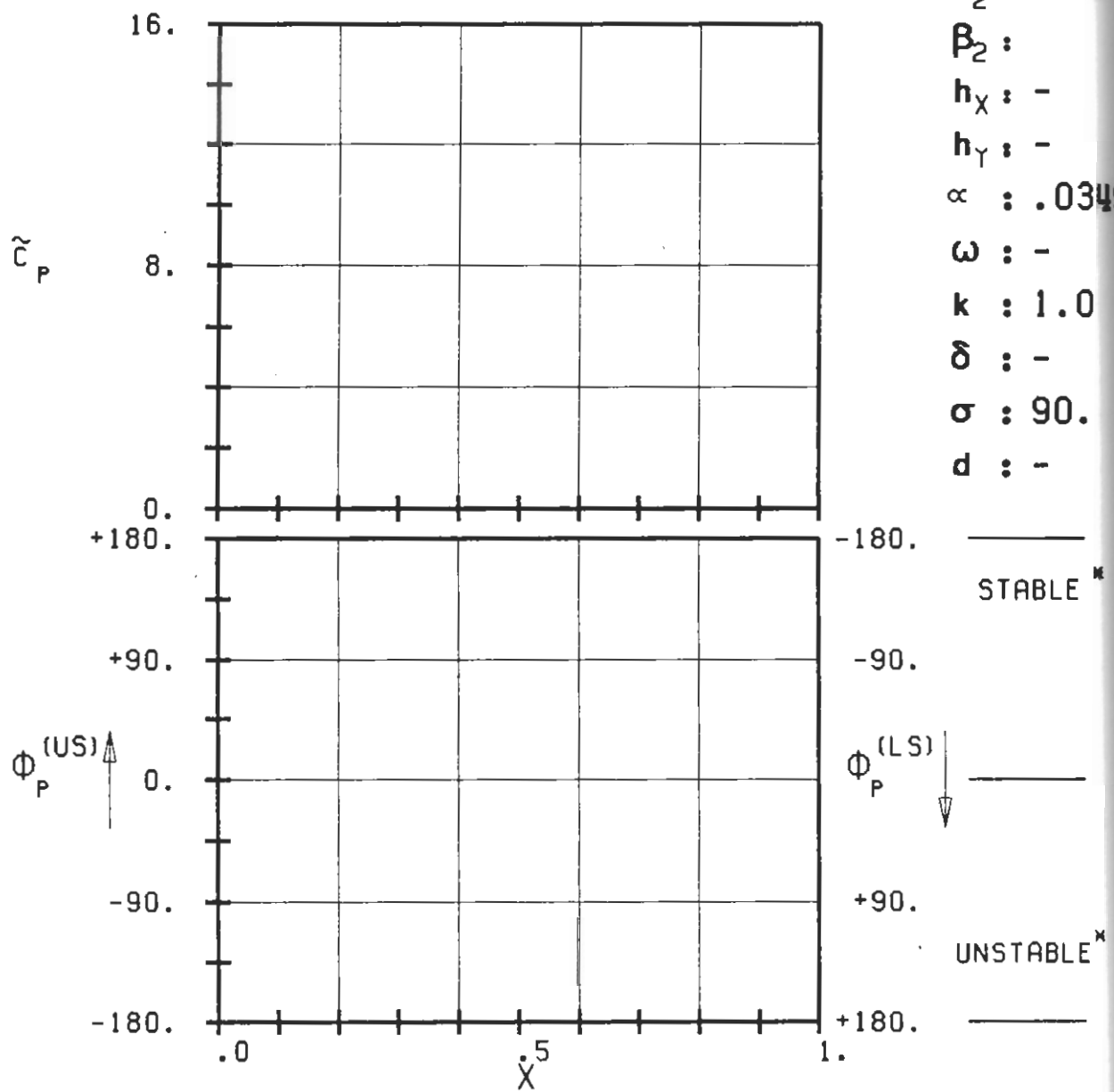
PLOT 7.8-2.23: EIGHTH STANDARD CONFIGURATION, CASE 23.
 MAGNITUDE AND PHASE LEAD OF UNSTEADY BLADE
 SURFACE PRESSURE DISTRIBUTION.
 (*: IN PITCH MODE, NOTATION VALID UPSTREAM OF PITCH AXIS)



PLOT 7.8-2.24: EIGHTH STANDARD CONFIGURATION, CASE 24.
MAGNITUDE AND PHASE LEAD OF UNSTEADY BLADE
SURFACE PRESSURE DISTRIBUTION.
(X: IN PITCH MODE, NOTATION VALID UPSTREAM OF PITCH AXIS)

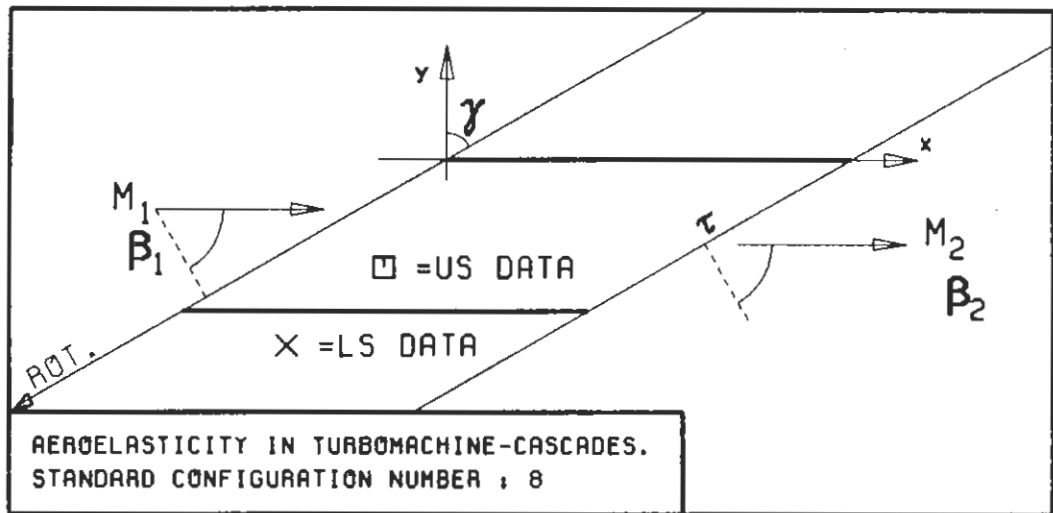


$c : 0.1M$
 $\tau : 0.75$
 $\gamma : 60.$
 $x_\alpha : 0.5$
 $y_\alpha : 0.$
 $M_1 : 1.4$
 $\beta_1 : -60.$
 $i : 0.$
 $M_2 : -$
 $\beta_2 : -$
 $h_x : -$
 $h_y : -$
 $\alpha : .0349$
 $\omega : -$
 $k : 1.0$
 $\delta : -$
 $\sigma : 90.$
 $d : -$



PLOT 7.8-2.25: EIGHTH STANDARD CONFIGURATION, CASE 25
MAGNITUDE AND PHASE LEAD OF UNSTEADY BLADE SURFACE PRESSURE DISTRIBUTION.

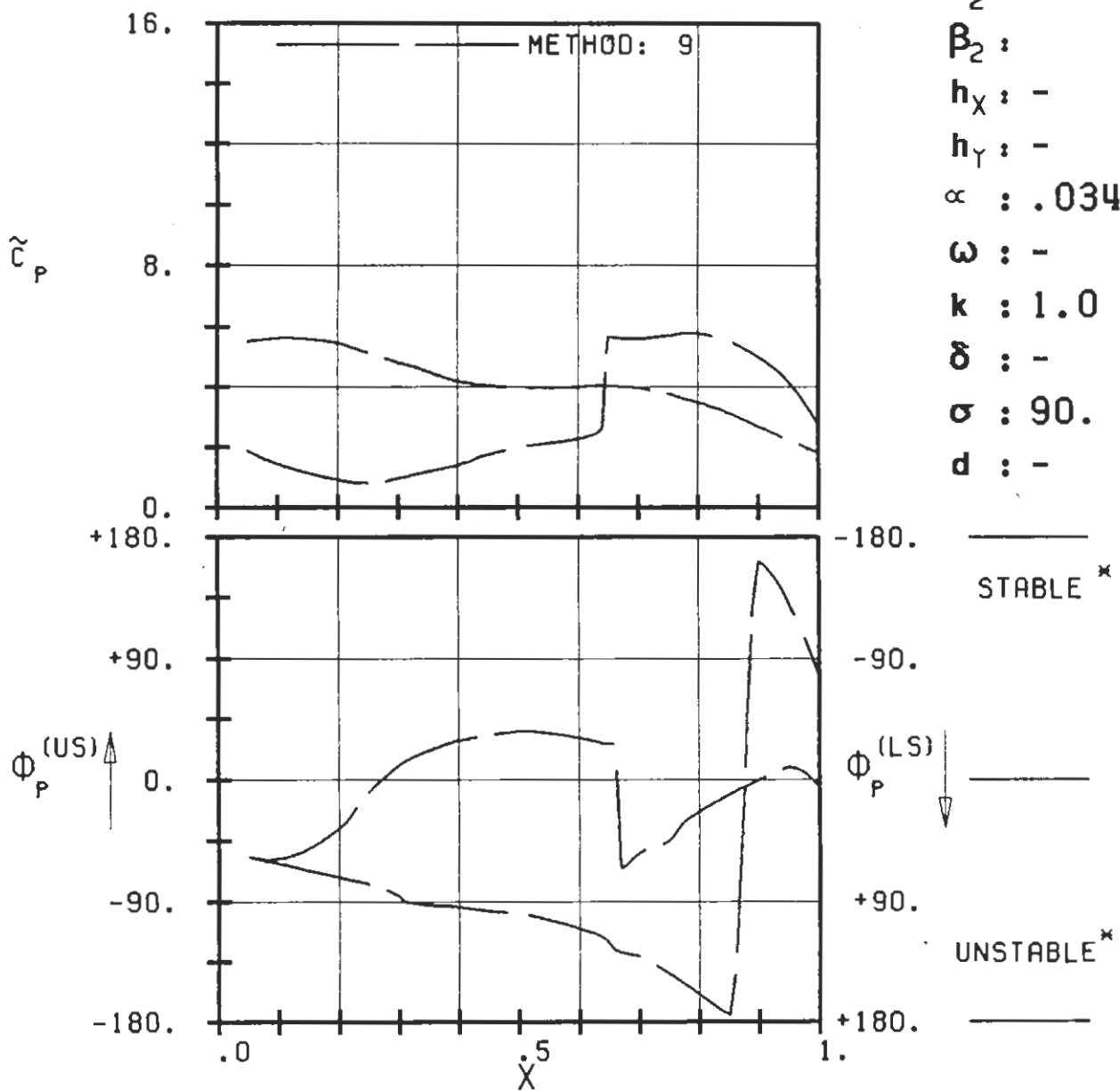
(*: IN PITCH MODE, NOTATION VALID UPSTREAM OF PITCH AXIS)

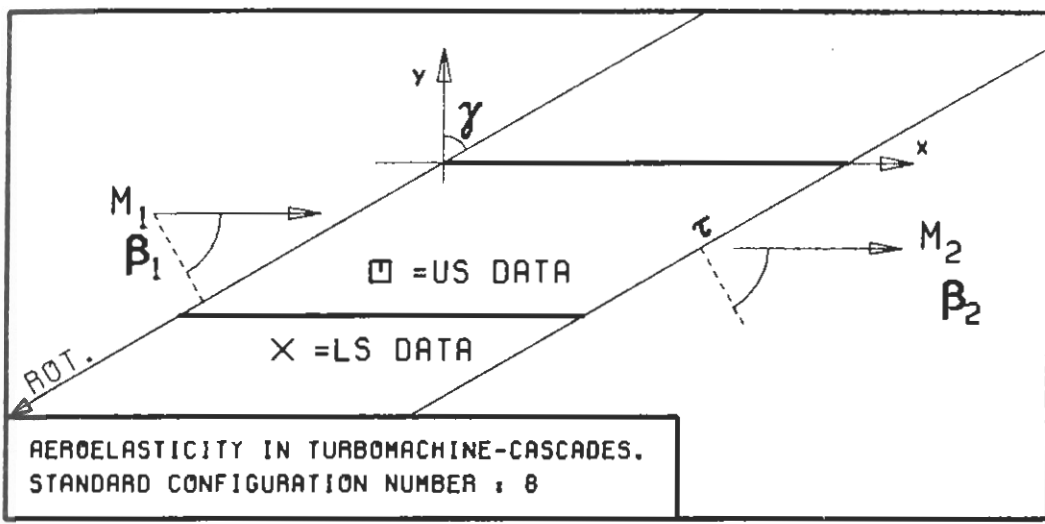


c : 0.1M
 τ : 0.75
 γ : 60.
 x_α : 0.5
 y_α : 0.
 M_1 : 1.4
 β_1 : -60.
 i : 0.
 M_2 : -
 β_2 :
 h_X : -
 h_Y : -
 α : .0349

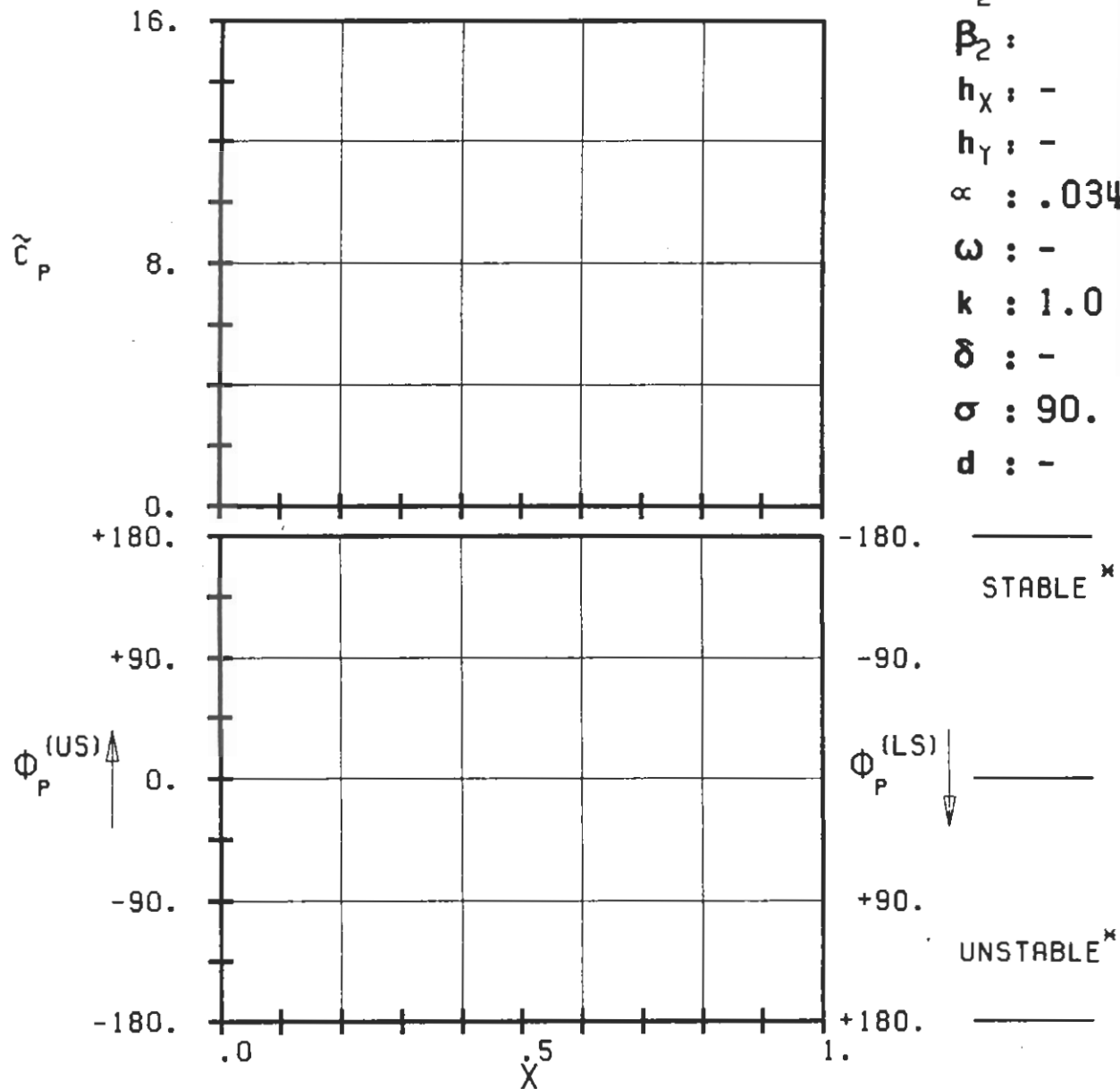
ω : -
 k : 1.0
 δ : -
 σ : 90.
 d : -

STABLE *

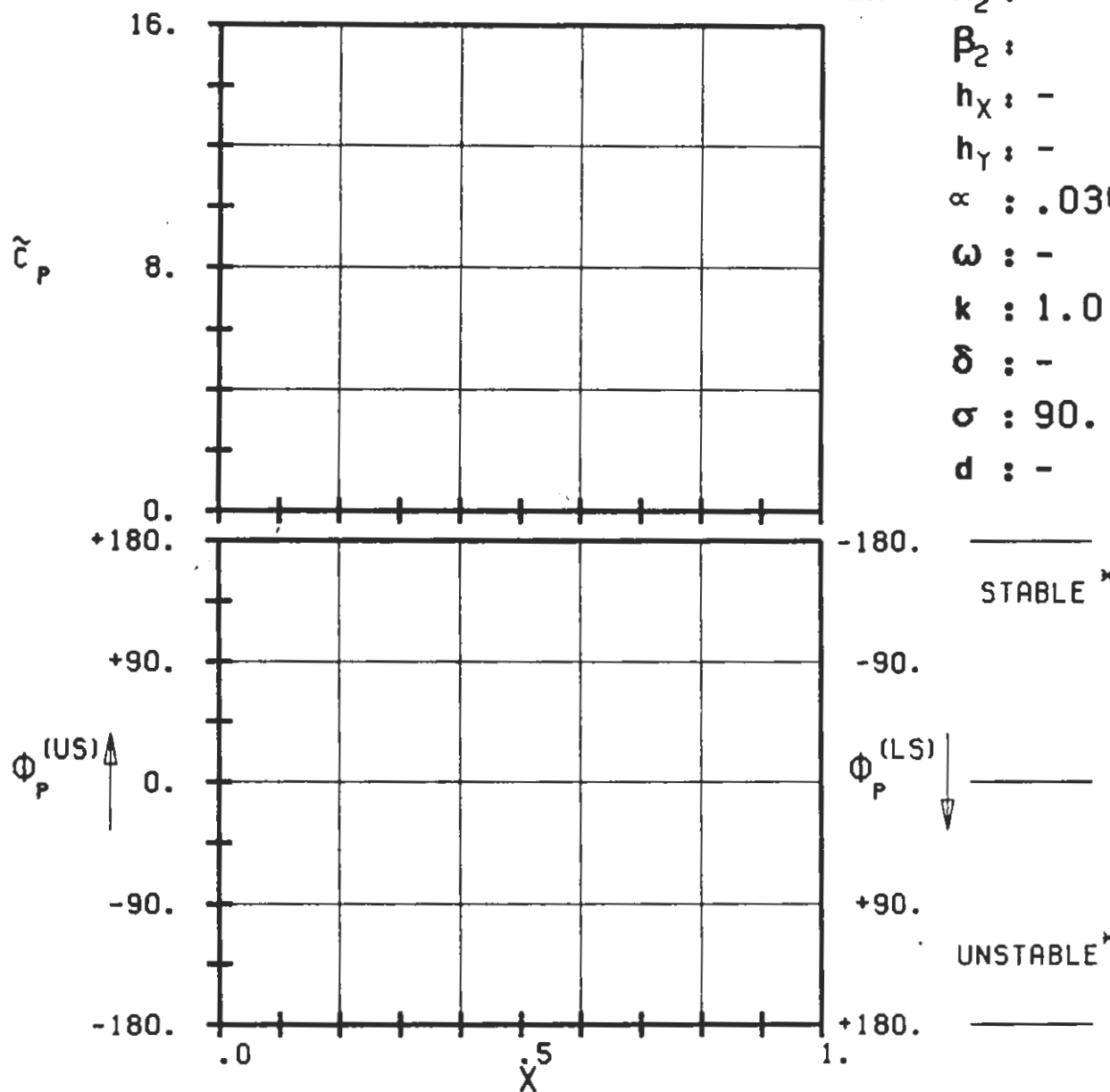
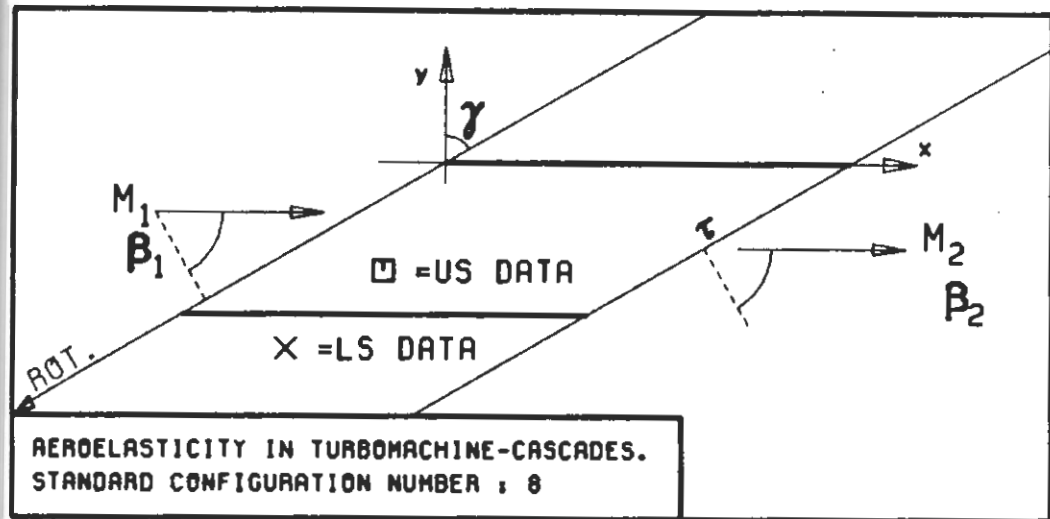




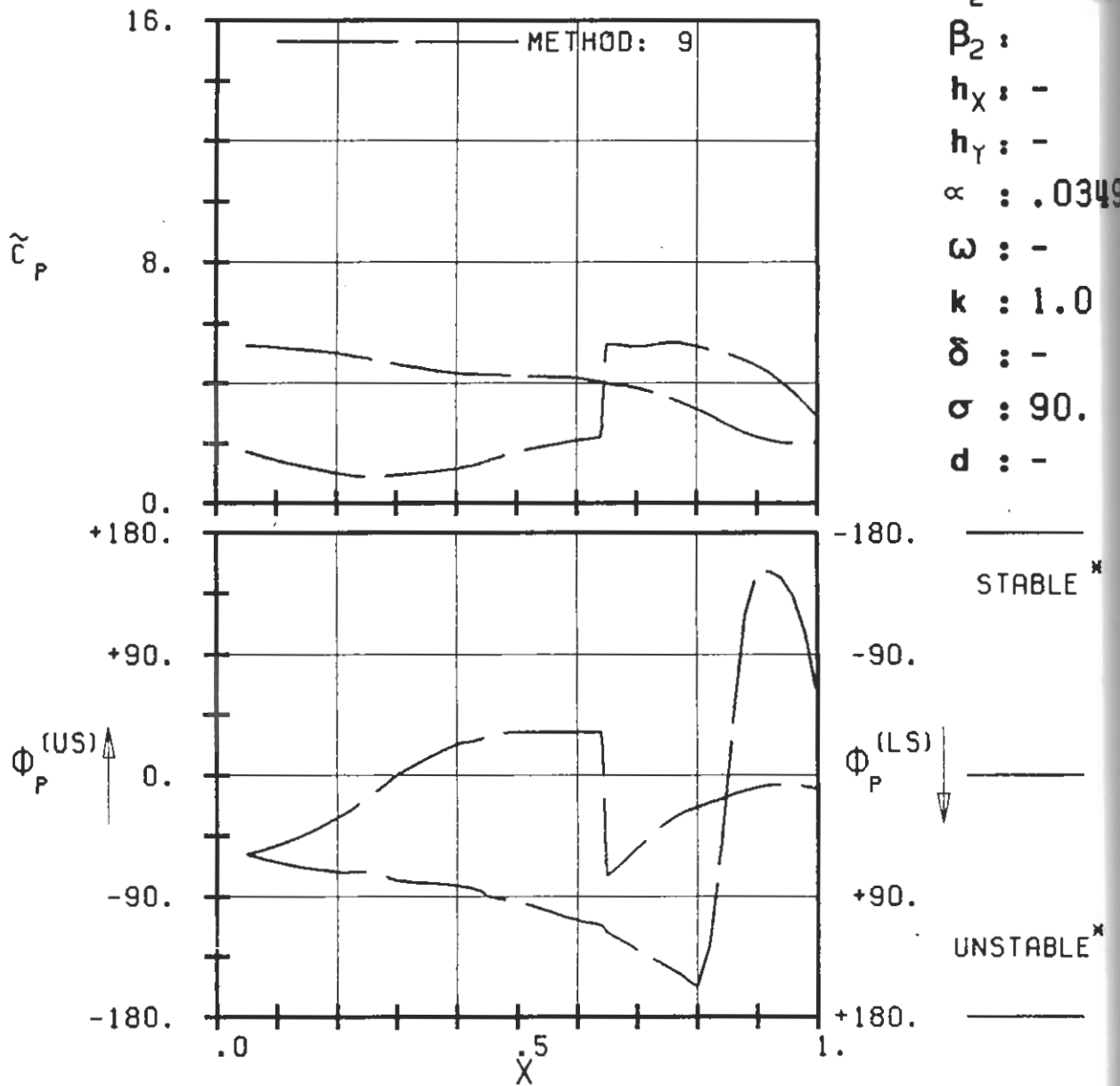
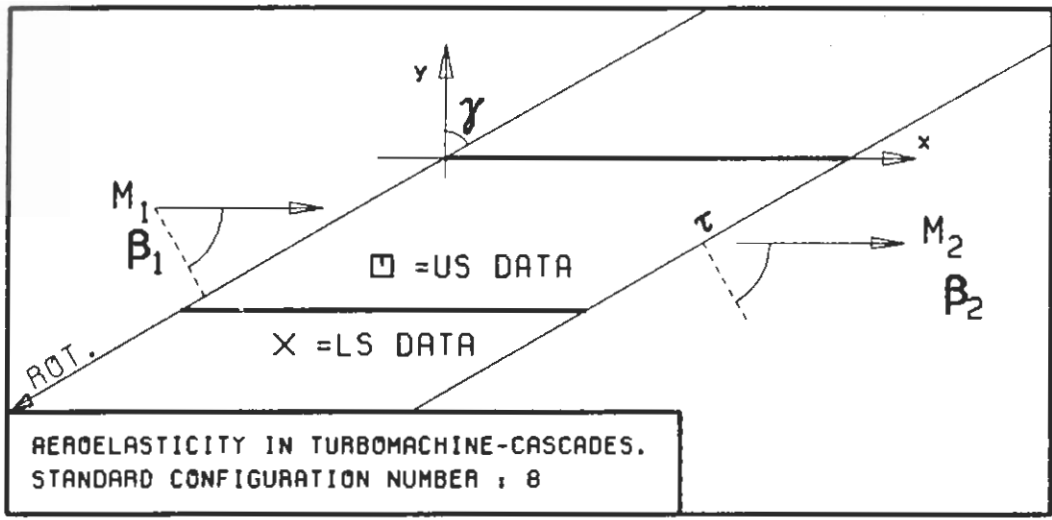
c : 0.1M
 τ : 0.75
 γ : 60.
 x_∞ : 0.5
 y_∞ : 0.
 M_1 : 1.4
 β_1 : -60.
 i : 0.
 M_2 : -
 β_2 :
 h_x : -
 h_y : -
 α : .0349
 ω : -
 k : 1.0
 δ : -
 σ : 90.
 d : -



PLOT 7.8-2.27: EIGHTH STANDARD CONFIGURATION, CASE 27.
 MAGNITUDE AND PHASE LEAD OF UNSTEADY BLADE
 SURFACE PRESSURE DISTRIBUTION.
 (\times : IN PITCH MODE, NOTATION VALID UPSTREAM OF PITCH AXIS)

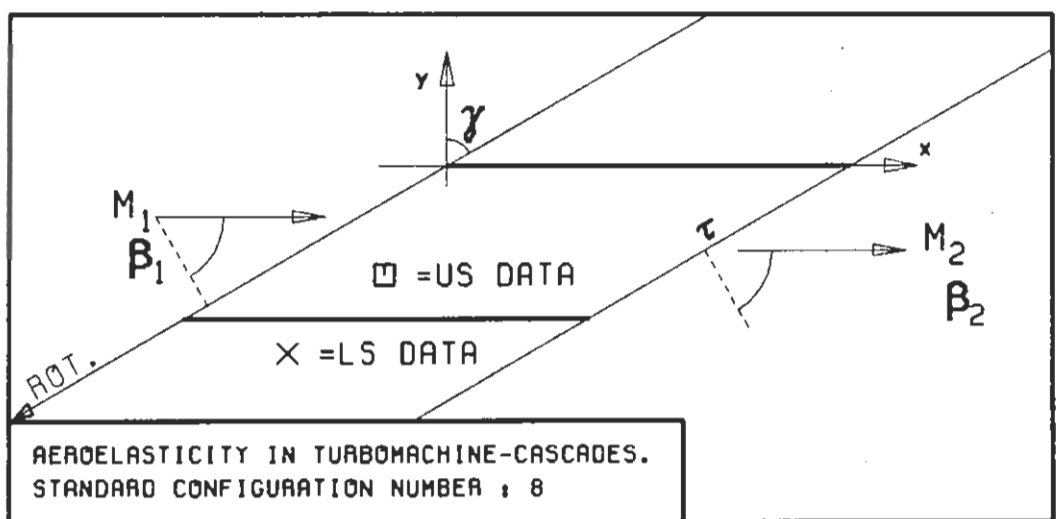


PLOT 7.8-2.28: EIGHTH STANDARD CONFIGURATION, CASE 28.
 MAGNITUDE AND PHASE LEAD OF UNSTEADY BLADE
 SURFACE PRESSURE DISTRIBUTION.
 (\times : IN PITCH MODE, NOTATION VALID UPSTREAM OF PITCH AXIS)

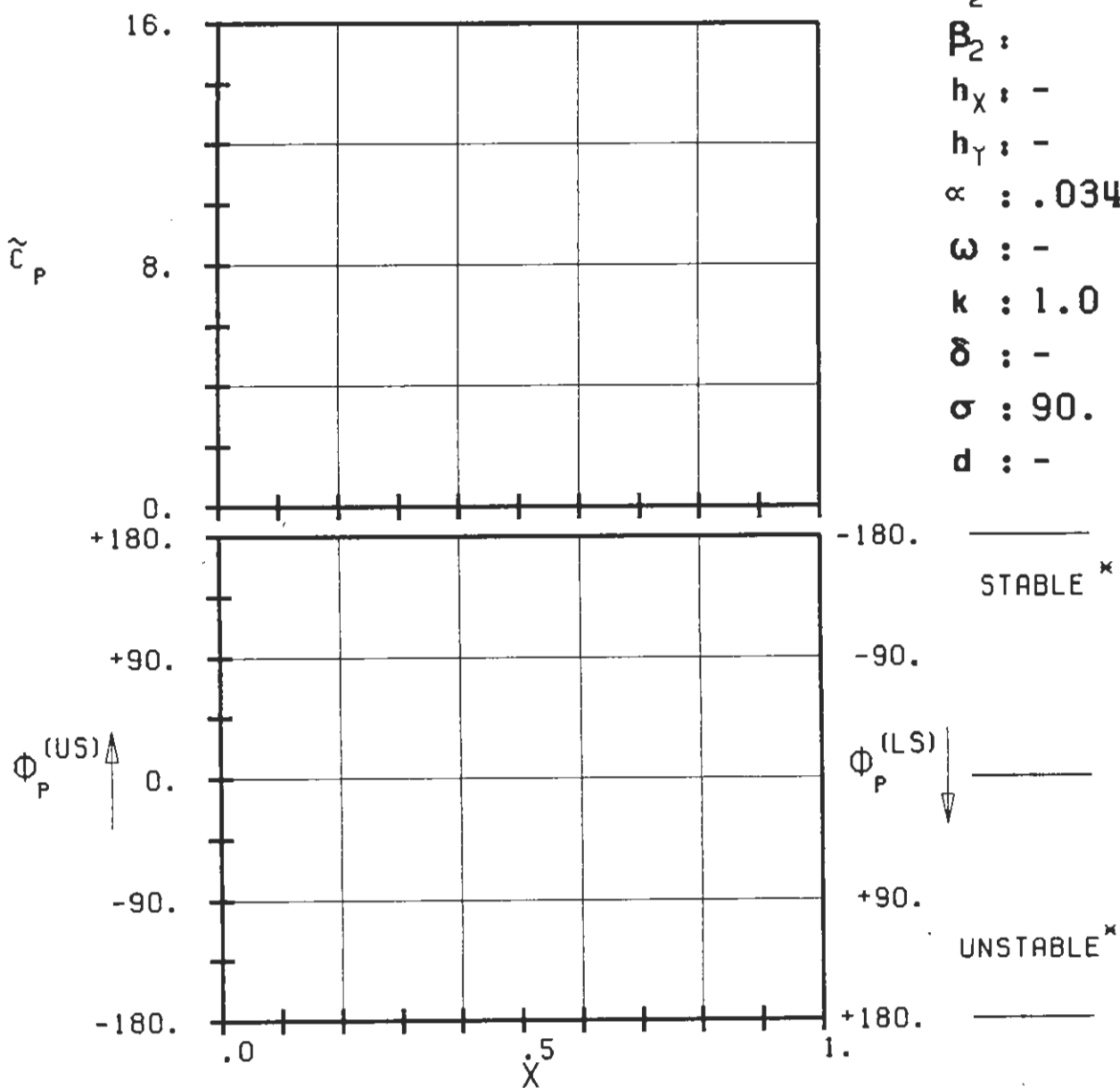


PLOT 7.8-2.29: EIGHTH STANDARD CONFIGURATION, CASE 29.
MAGNITUDE AND PHASE LEAD OF UNSTEADY BLADE
SURFACE PRESSURE DISTRIBUTION.

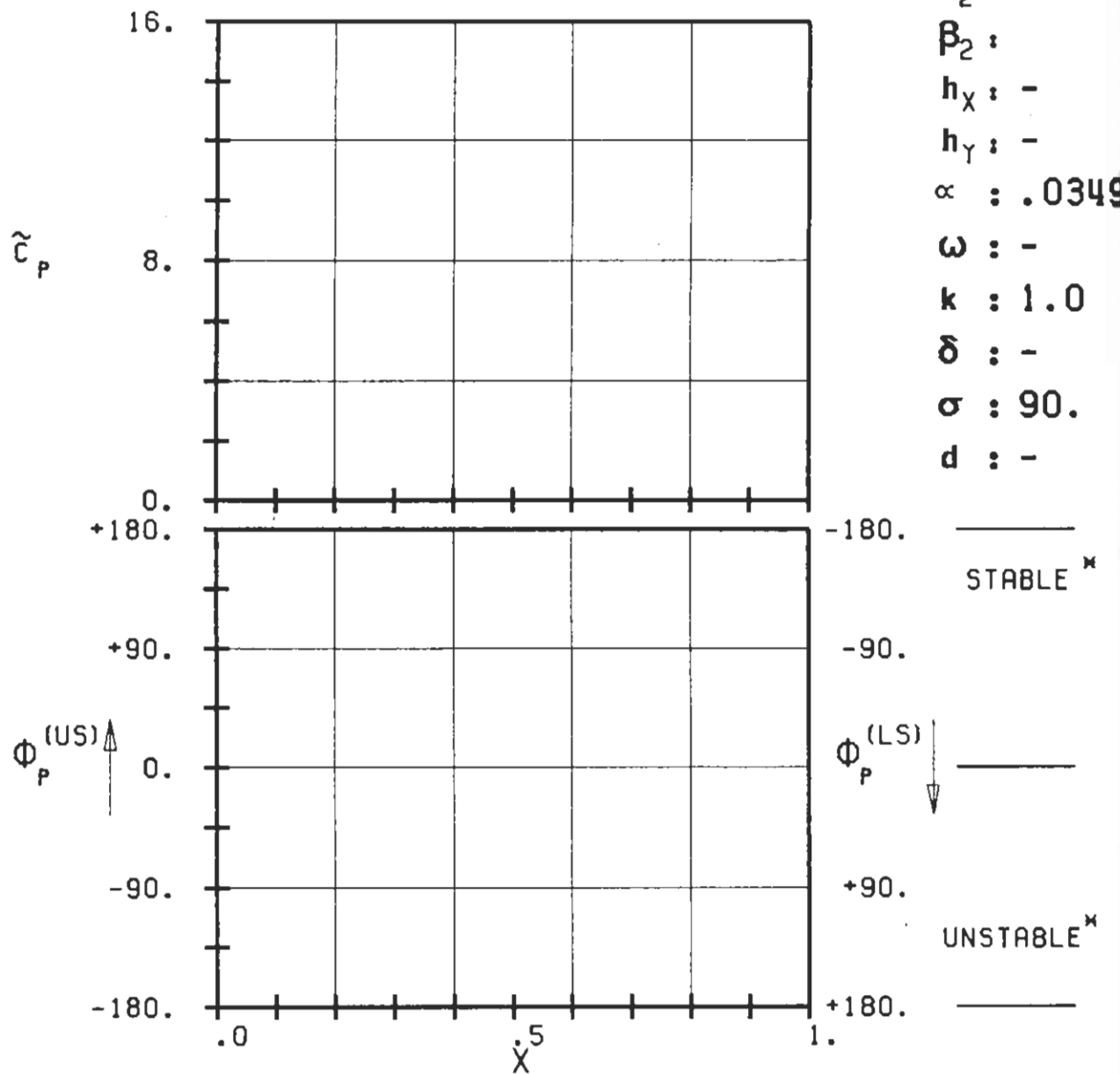
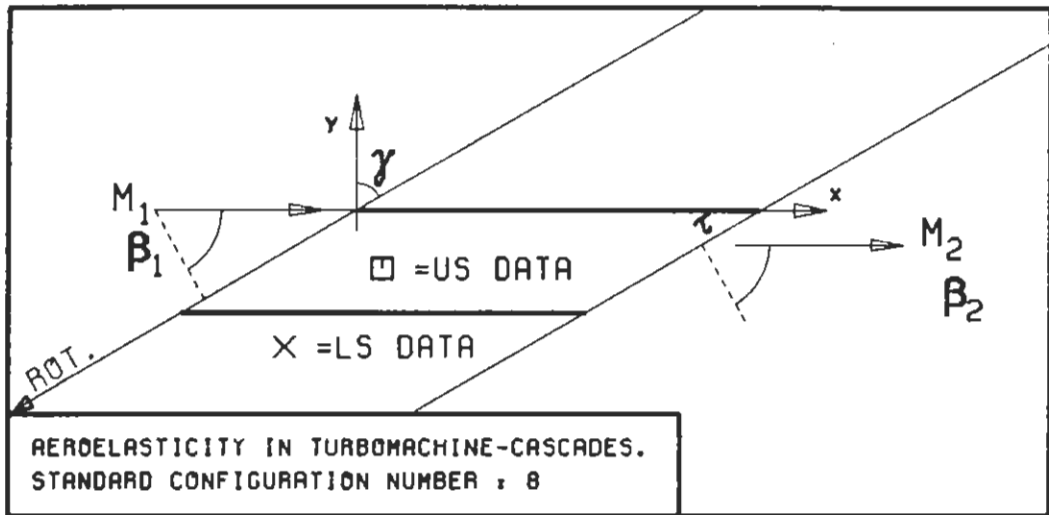
(*: IN PITCH MODE, NOTATION VALID UPSTREAM OF PITCH AXIS)



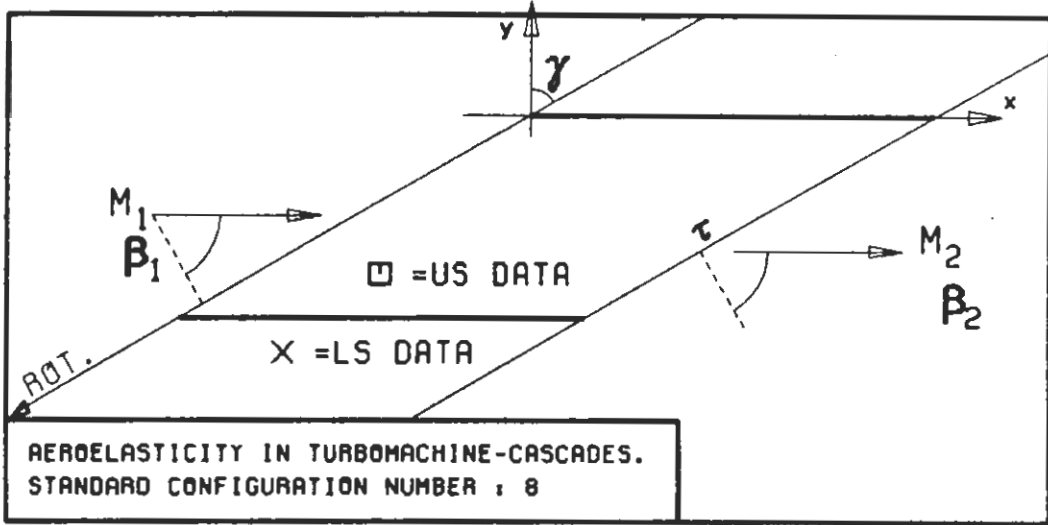
$c : 0.1M$
 $\tau : 0.75$
 $\gamma : 60.$
 $x_\infty : 0.5$
 $y_\infty : 0.$
 $M_1 : 1.5$
 $\beta_1 : -60.$
 $i : 0.$
 $M_2 : -$
 $\beta_2 : -$
 $h_x : -$
 $h_y : -$
 $\alpha : .0349$
 $\omega : -$
 $k : 1.0$
 $\delta : -$
 $\sigma : 90.$
 $d : -$



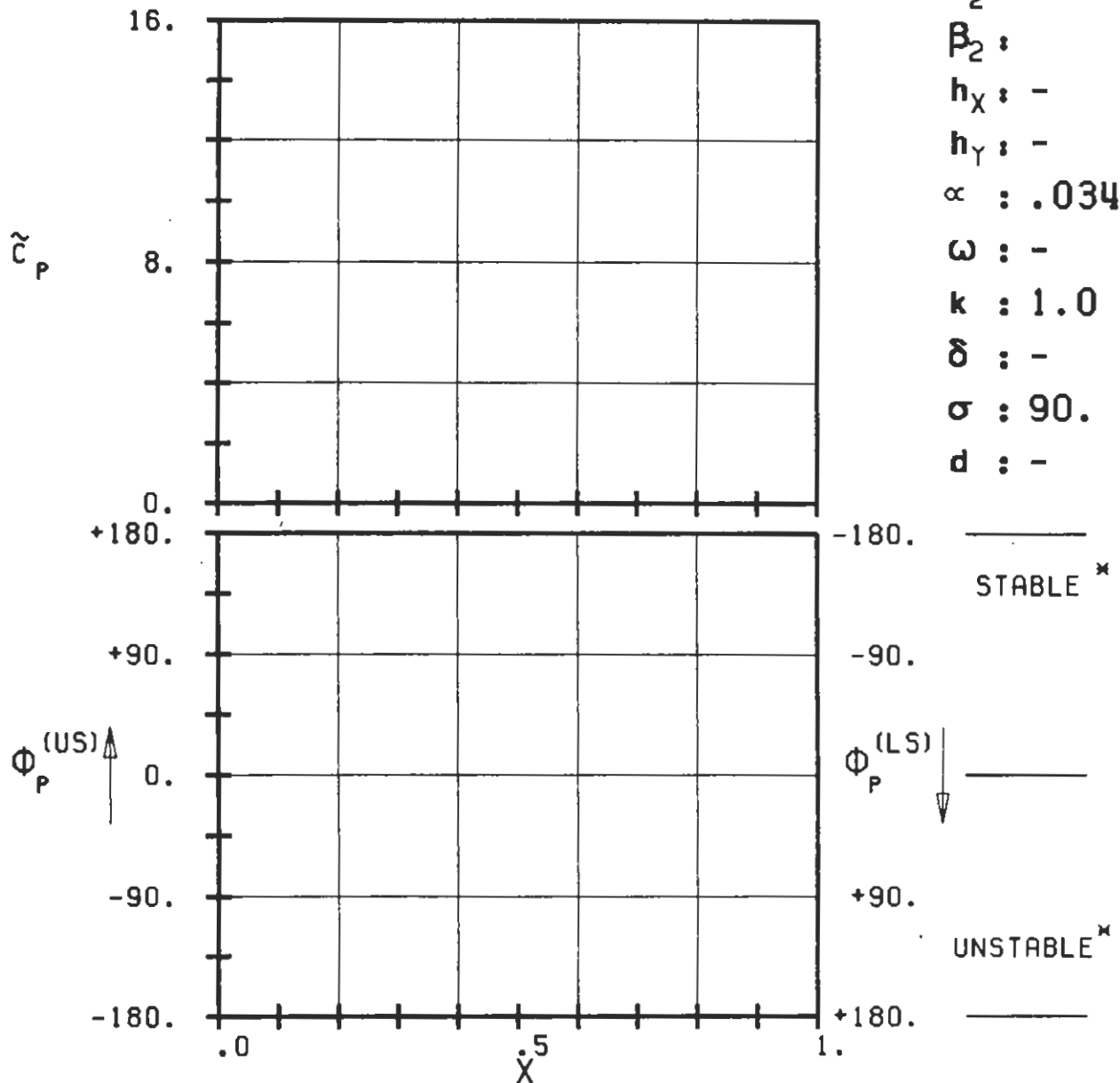
PLOT 7.8-2.30: EIGHTH STANDARD CONFIGURATION, CASE 30.
MAGNITUDE AND PHASE LEAD OF UNSTEADY BLADE
SURFACE PRESSURE DISTRIBUTION.
(*: IN PITCH MODE, NOTATION VALID UPSTREAM OF PITCH AXIS)



PLOT 7.8-2.31: EIGHTH STANDARD CONFIGURATION, CASE 31.
 MAGNITUDE AND PHASE LEAD OF UNSTEADY BLADE
 SURFACE PRESSURE DISTRIBUTION.
 (X: IN PITCH MODE, NOTATION VALID UPSTREAM OF PITCH AXIS)

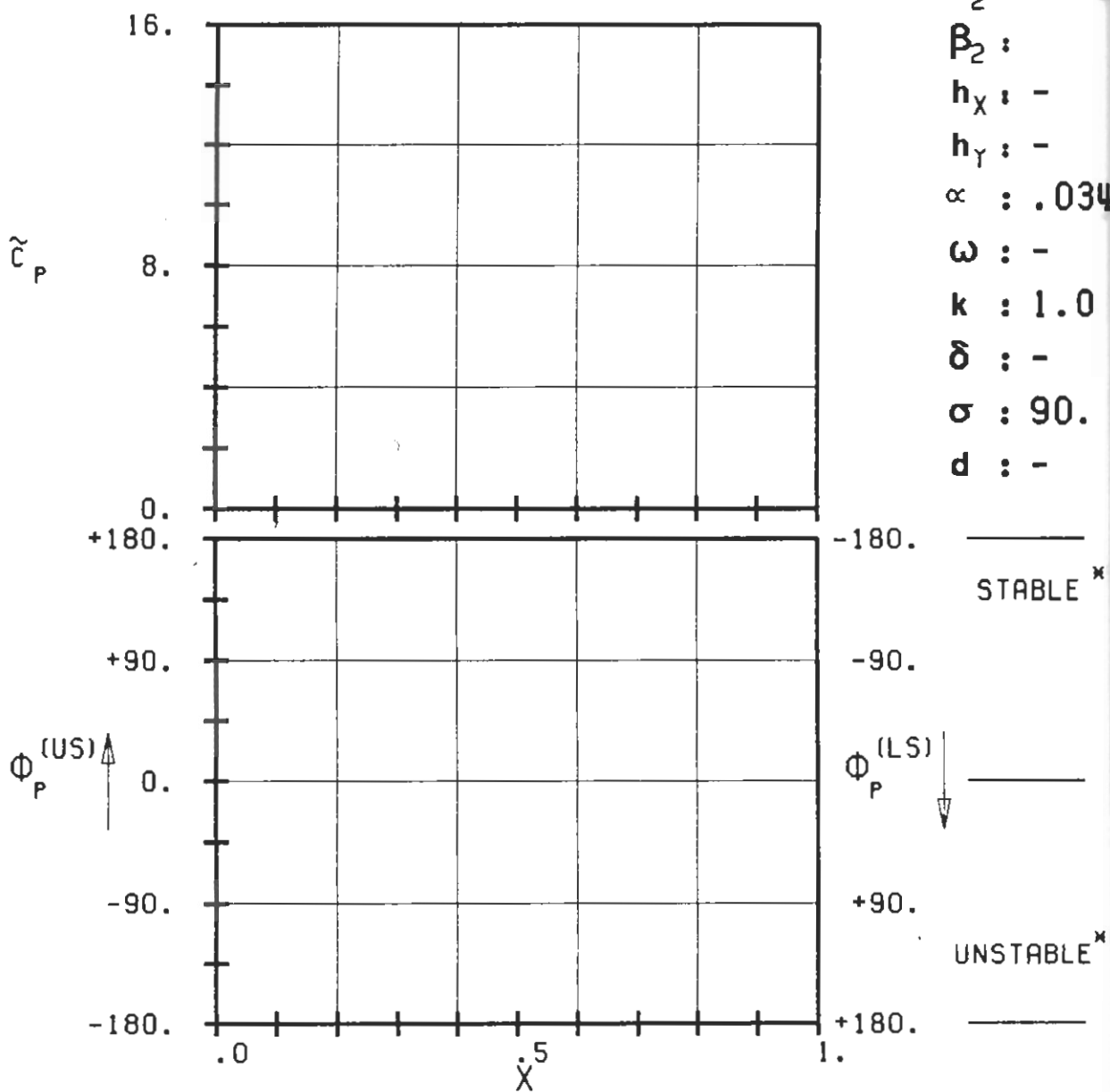
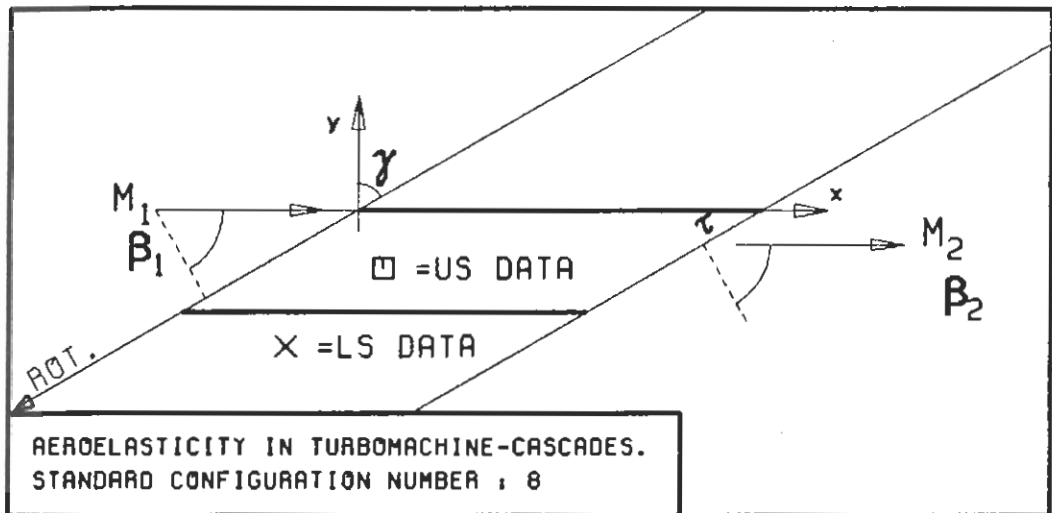


$c : 0.1M$
 $\tau : 1.00$
 $\gamma : 60.$
 $x_\alpha : 0.5$
 $y_\alpha : 0.$
 $M_1 : 1.3$
 $\beta_1 : -60.$
 $i : 0.$
 $M_2 : -$
 $\beta_2 : -$
 $h_X : -$
 $h_Y : -$
 $\alpha : .0349$
 $\omega : -$
 $k : 1.0$
 $\delta : -$
 $\sigma : 90.$
 $d : -$

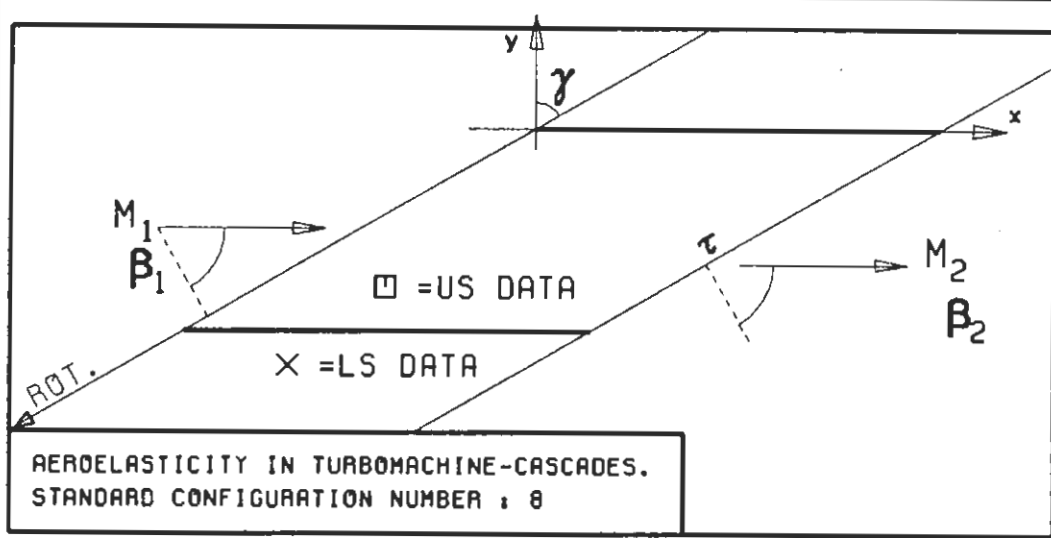


PLOT 7.8-2.32: EIGHTH STANDARD CONFIGURATION, CASE 32.
MAGNITUDE AND PHASE LEAD OF UNSTEADY BLADE
SURFACE PRESSURE DISTRIBUTION.

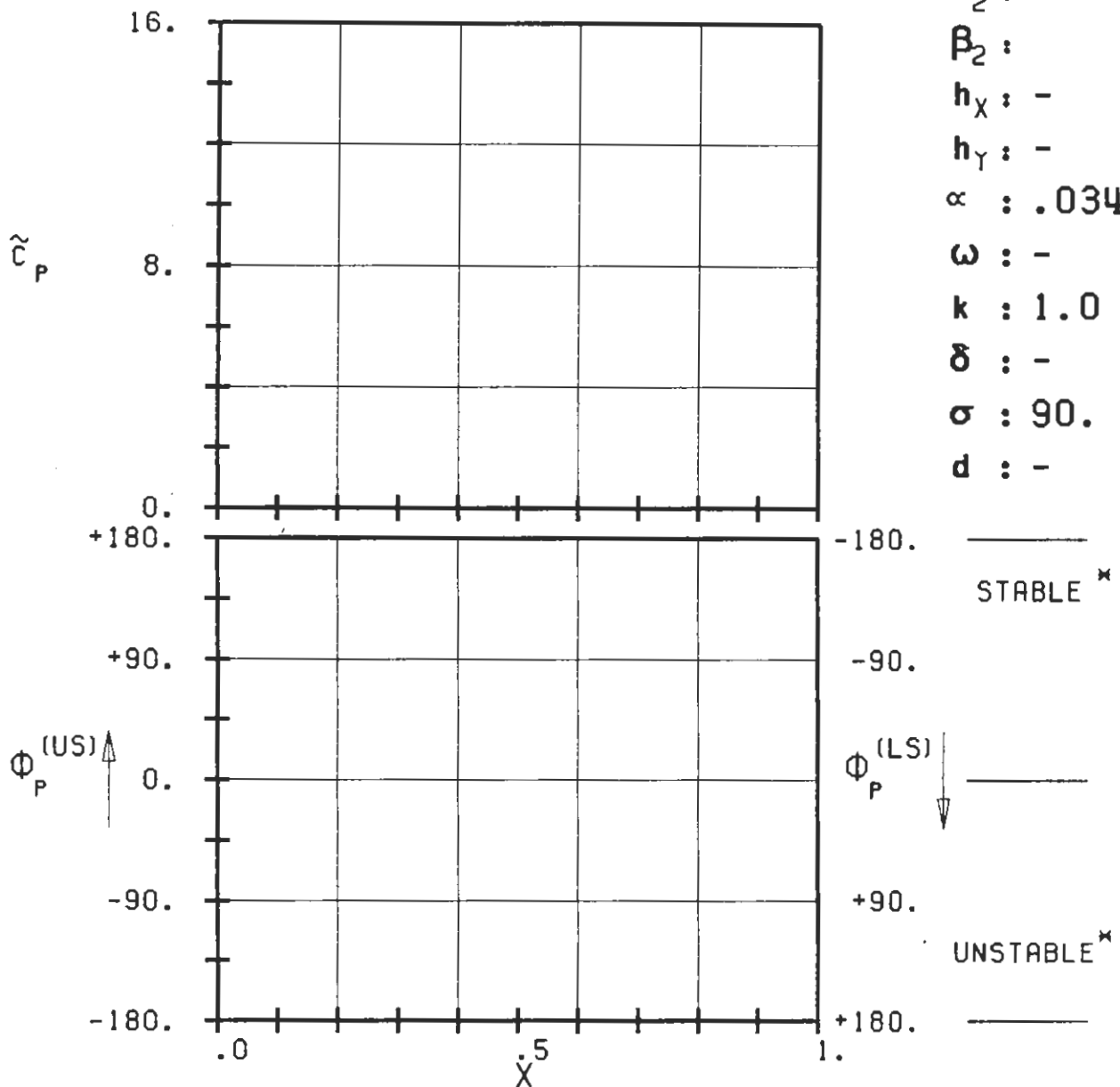
(x: IN PITCH MODE, NOTATION VALID UPSTREAM OF PITCH AXIS)



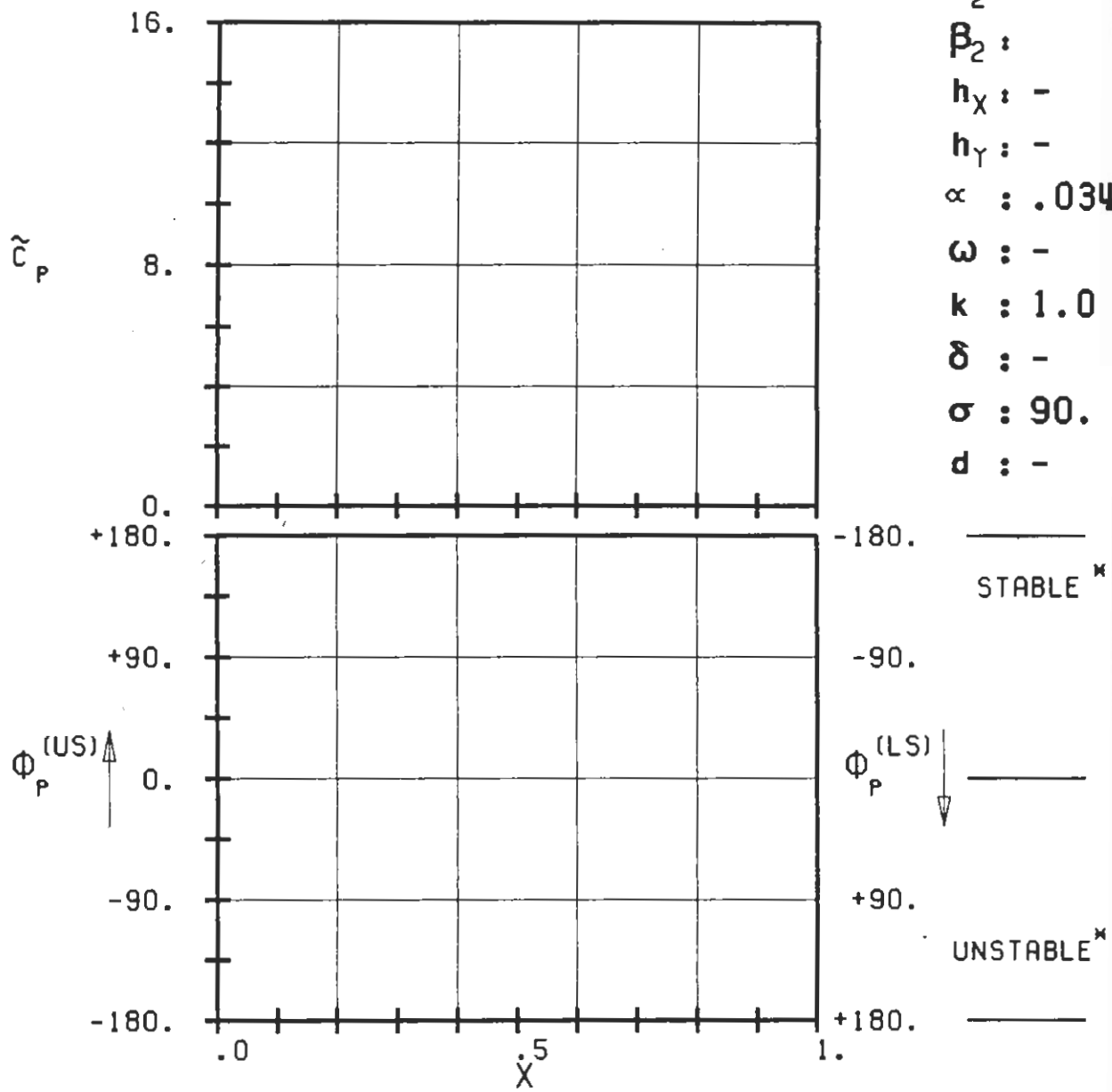
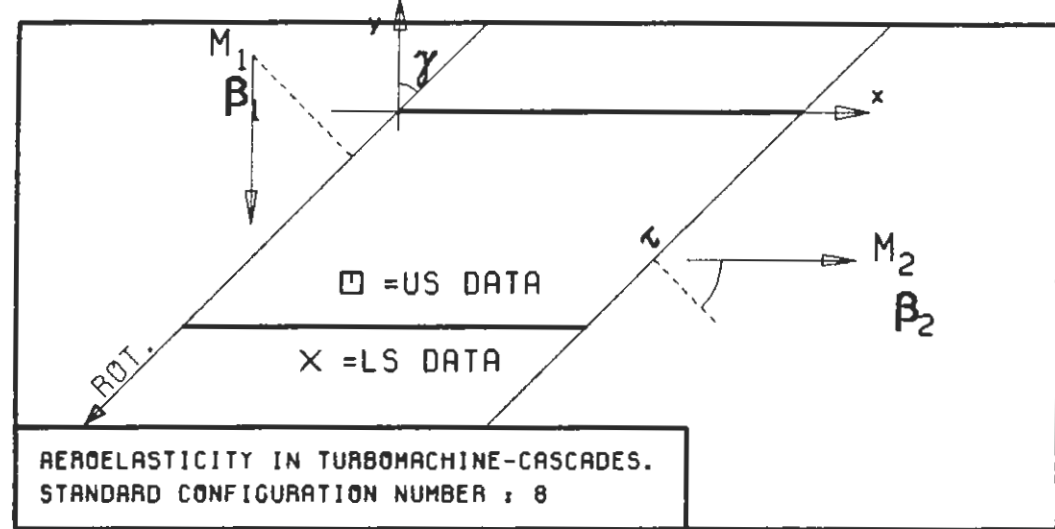
PLOT 7.8-2.33: EIGHTH STANDARD CONFIGURATION, CASE 33.
 MAGNITUDE AND PHASE LEAD OF UNSTEADY BLADE
 SURFACE PRESSURE DISTRIBUTION.
 (*: IN PITCH MODE, NOTATION VALID UPSTREAM OF PITCH AXIS)



c : 0.1M
 τ : 1.00
 γ : 60.
 x_∞ : 0.5
 y_∞ : 0.
 M_1 : 1.3
 β_1 : -60.
 i : 0.
 M_2 : -
 β_2 :
 h_x : -
 h_y : -
 α : .0349
 ω : -
 k : 1.0
 δ : -
 σ : 90.
 d : -

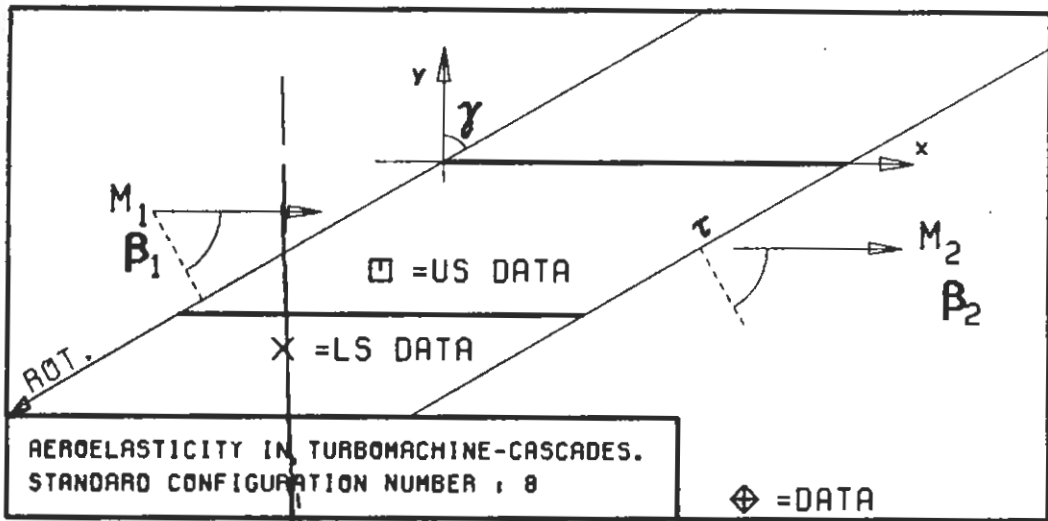


PLOT 7.8-2.34: EIGHTH STANDARD CONFIGURATION, CASE 34.
MAGNITUDE AND PHASE LEAD OF UNSTEADY BLADE SURFACE PRESSURE DISTRIBUTION.
(\times : IN PITCH MODE, NOTATION VALID UPSTREAM OF PITCH AXIS)

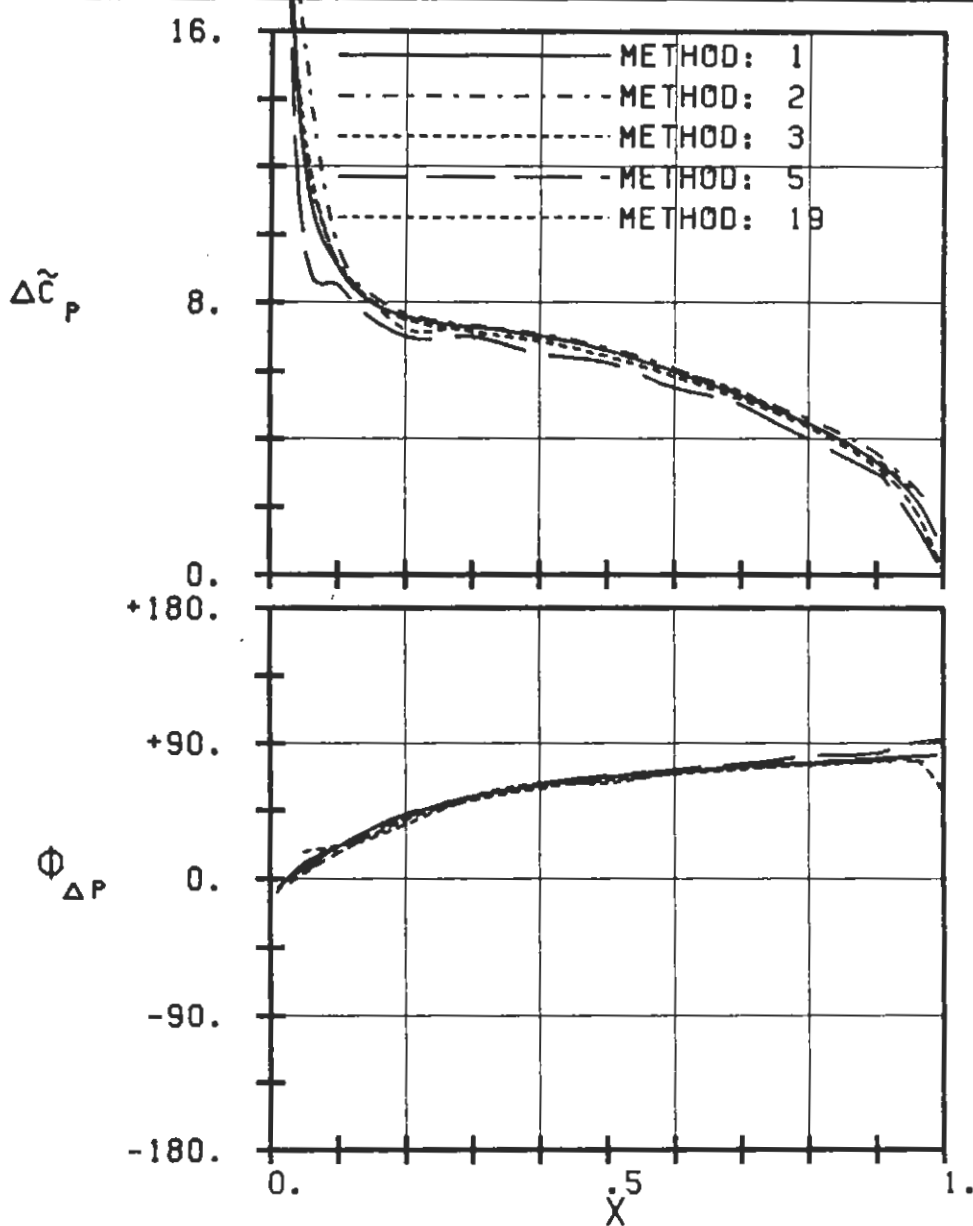


PLOT 7.8-2.35: EIGHTH STANDARD CONFIGURATION, CASE 35.
 MAGNITUDE AND PHASE LEAD OF UNSTEADY BLADE
 SURFACE PRESSURE DISTRIBUTION.

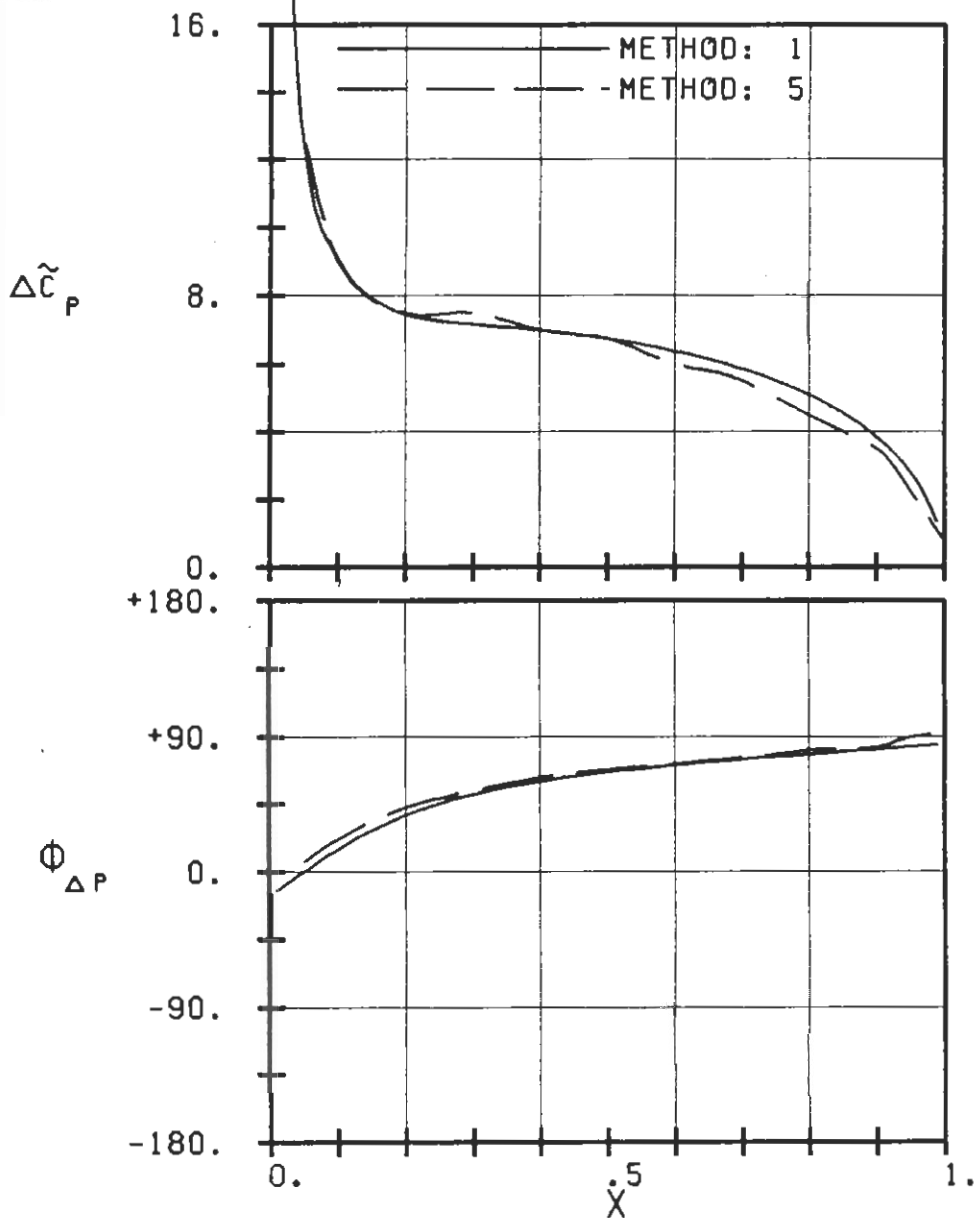
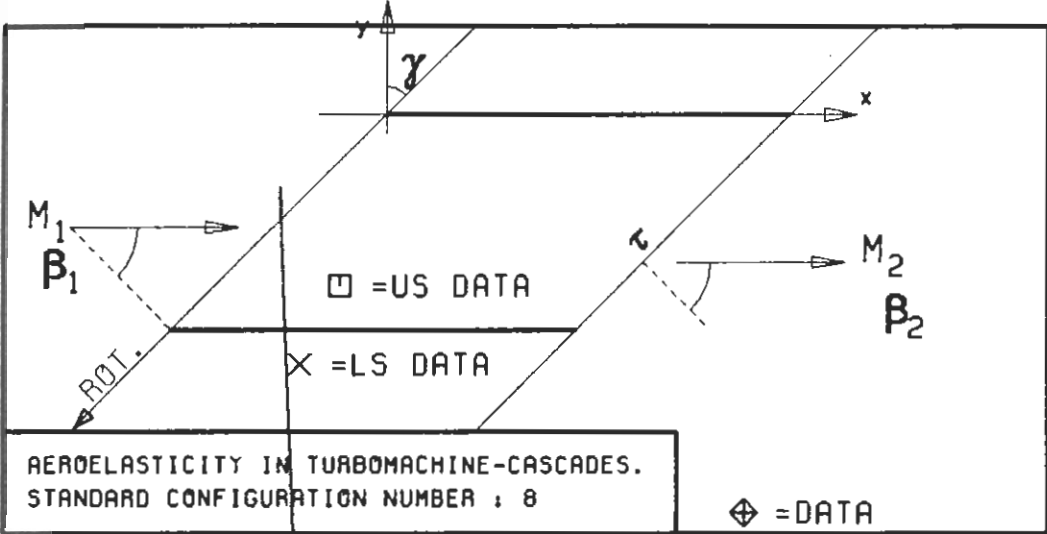
(*: IN PITCH MODE, NOTATION VALID UPSTREAM OF PITCH AXIS)



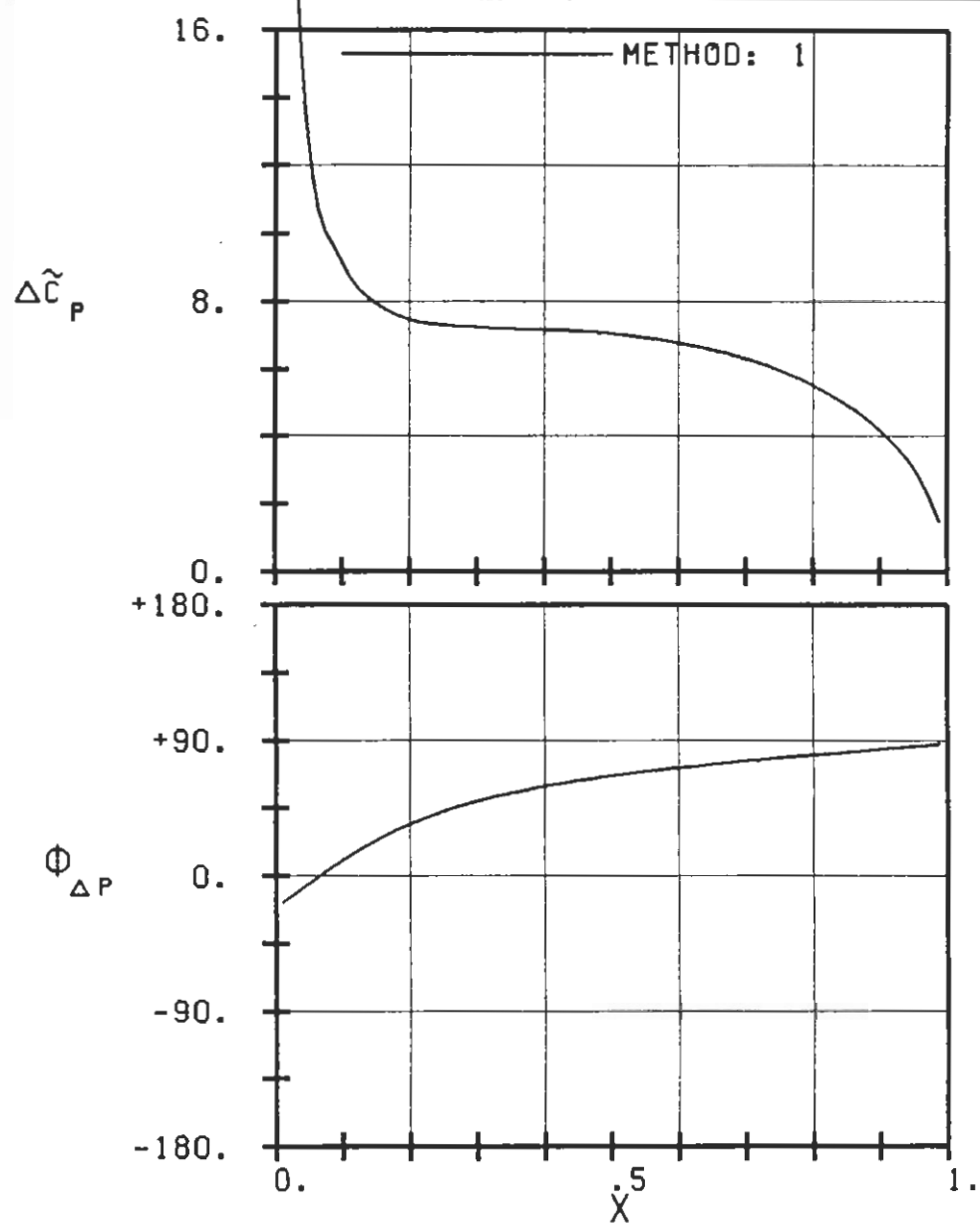
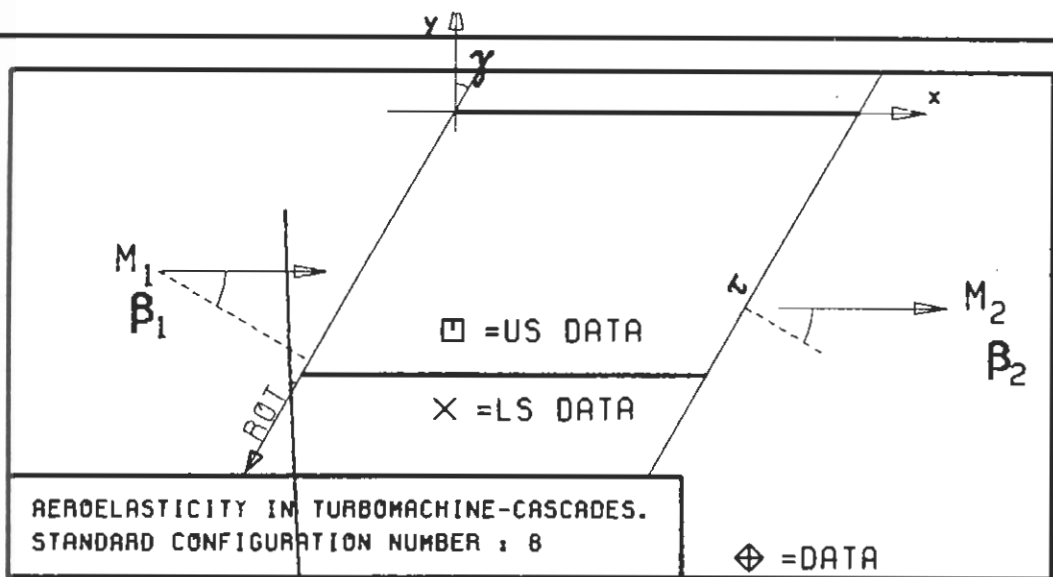
$c : 0.1M$
 $\tau : 0.75$
 $\gamma : 60.$
 $x_\alpha : 0.5$
 $y_\alpha : 0.$
 $M_1 : 0.$
 $\beta_1 : -60.$
 $i : 0.$
 $M_2 : -$
 $\beta_2 : -$
 $h_x : -$
 $h_y : -$
 $\alpha : .0349$



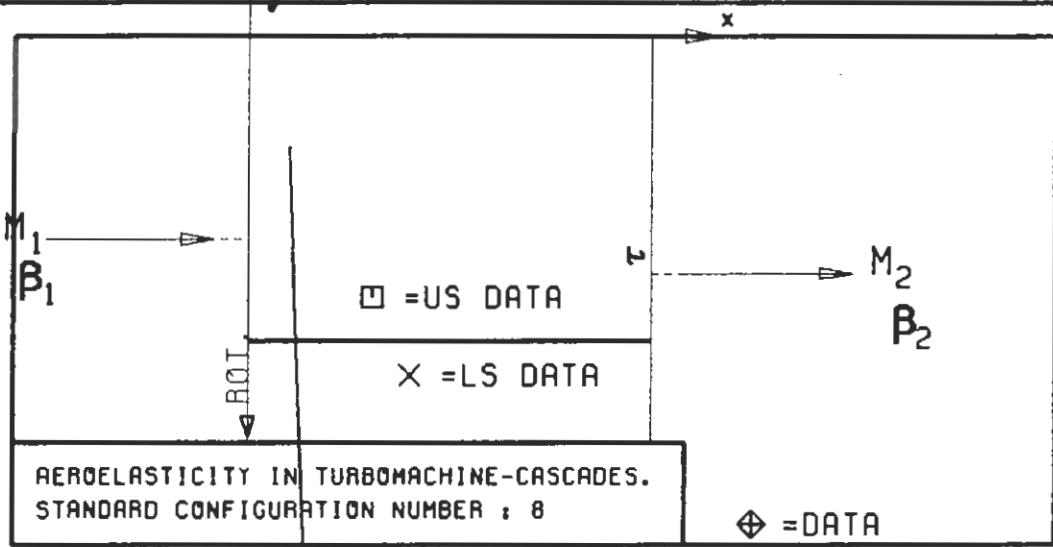
PLOT 7.8-3.1: EIGHTH STANDARD CONFIGURATION, CASE 1.
 MAGNITUDE AND PHASE LEAD OF UNSTEADY BLADE
 SURFACE PRESSURE DIFFERENCE DISTRIBUTION.
 (*: IN PITCH MODE, NOTATION VALID UPSTREAM OF PITCH AXIS)



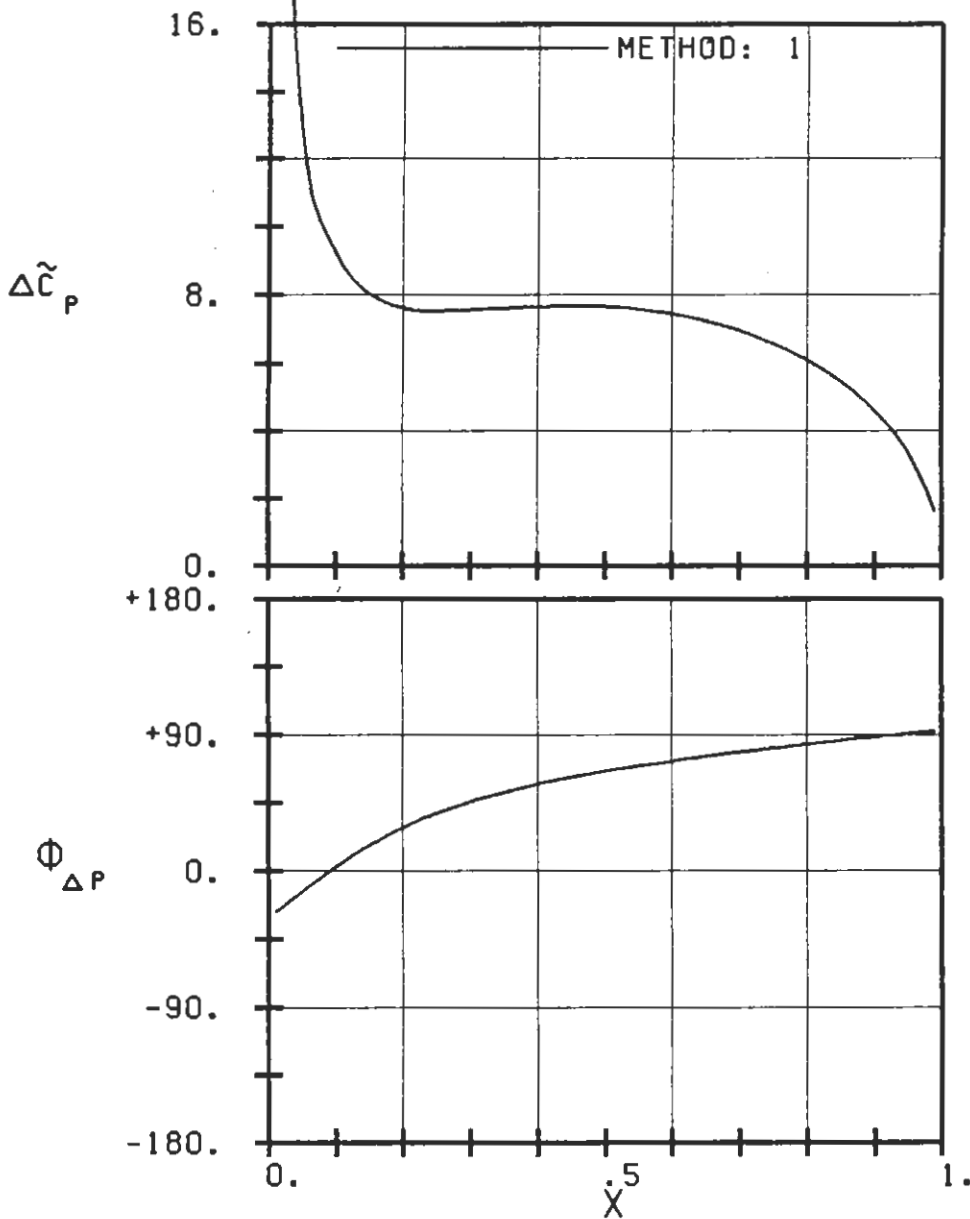
PLOT 7.8-3.2: EIGHTH STANDARD CONFIGURATION, CASE 2.
 MAGNITUDE AND PHASE LEAD OF UNSTEADY BLADE
 SURFACE PRESSURE DIFFERENCE DISTRIBUTION.
 (x: IN PITCH MODE, NOTATION VALID UPSTREAM OF PITCH AXIS)



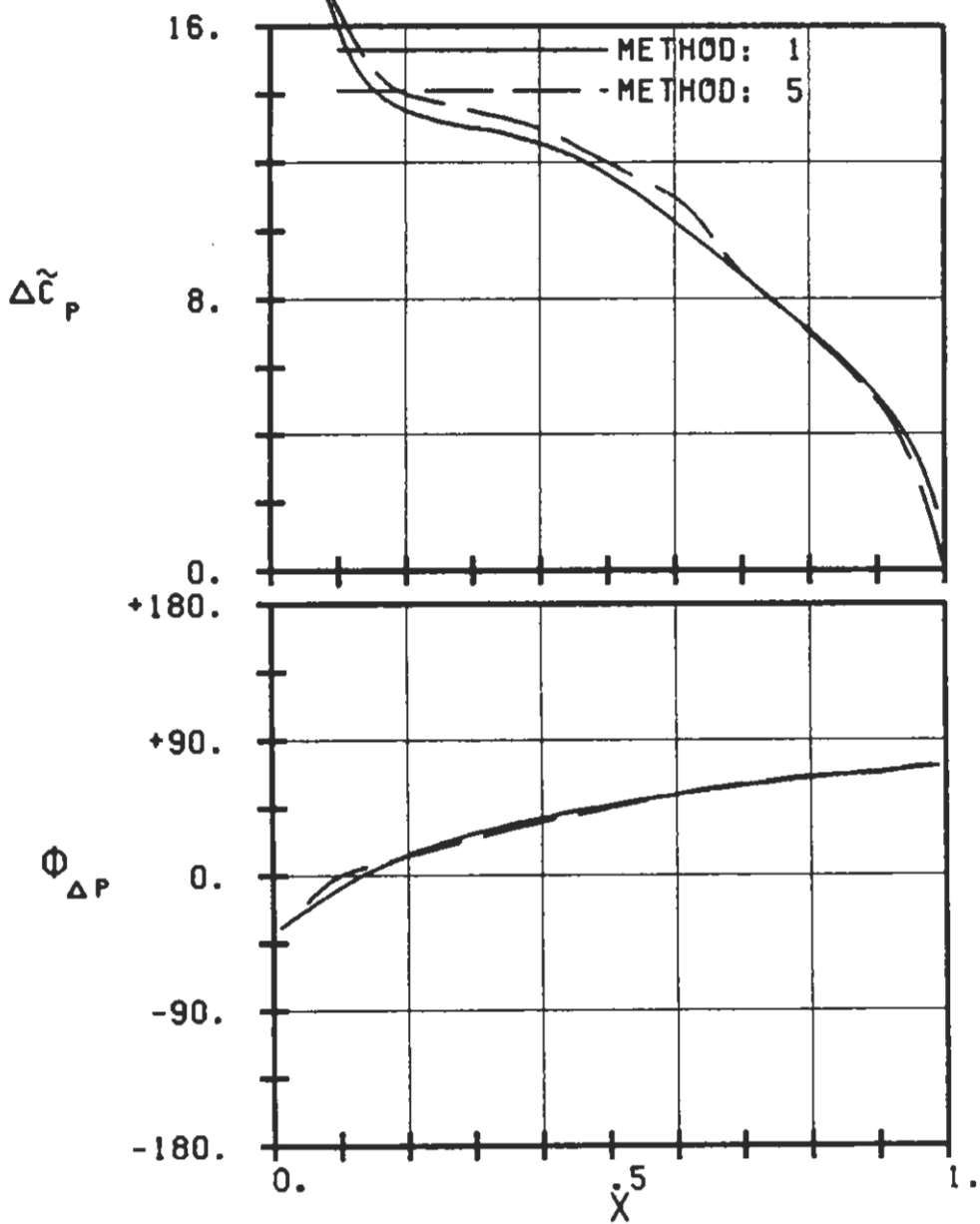
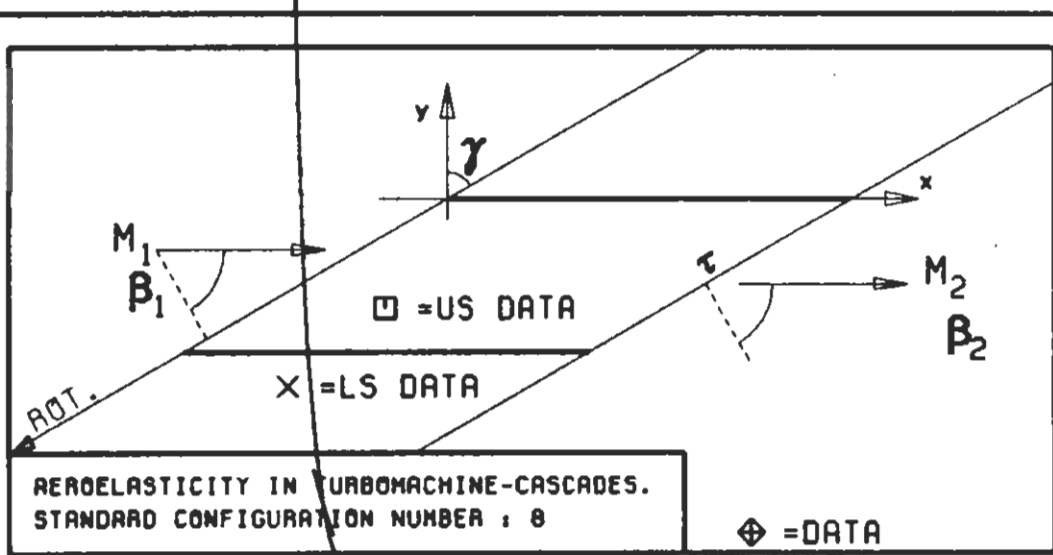
PLOT 7.8-3.3: EIGHTH STANDARD CONFIGURATION, CASE 3.
 MAGNITUDE AND PHASE LEAD OF UNSTEADY BLADE
 SURFACE PRESSURE DIFFERENCE DISTRIBUTION.
 (*: IN PITCH MODE, NOTATION VALID UPSTREAM OF PITCH AXIS)



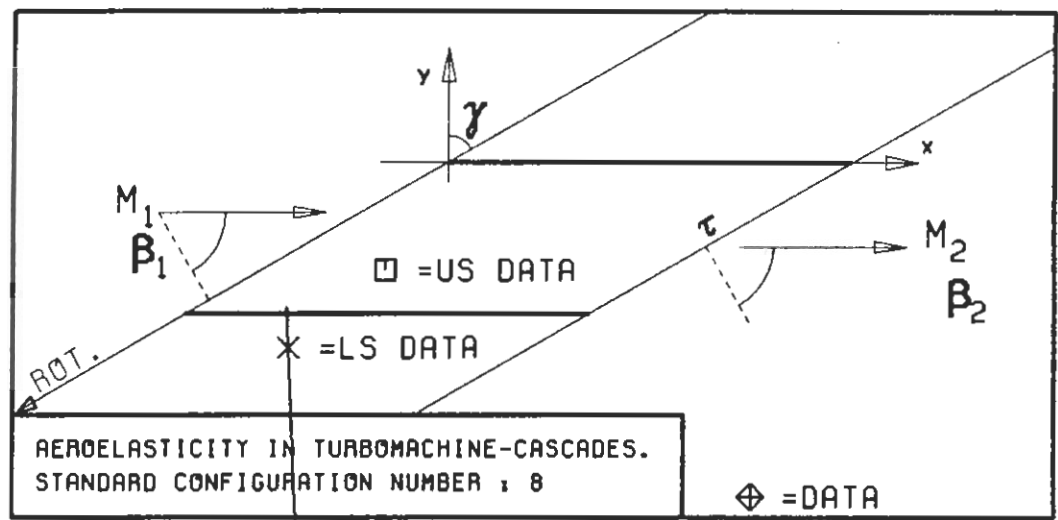
$c : 0.1M$
 $\tau : 0.75$
 $\gamma : 0.0$
 $x_\alpha : 0.5$
 $y_\alpha : 0.$
 $M_1 : 0.$
 $\beta_1 : 0.0$
 $i : 0.$
 $M_2 : -$
 $\beta_2 : -$
 $h_x : -$
 $h_y : -$
 $\alpha : .0349$
 $\omega : -$
 $k : 1.0$
 $\delta : -$
 $\sigma : 90.$
 $d : -$



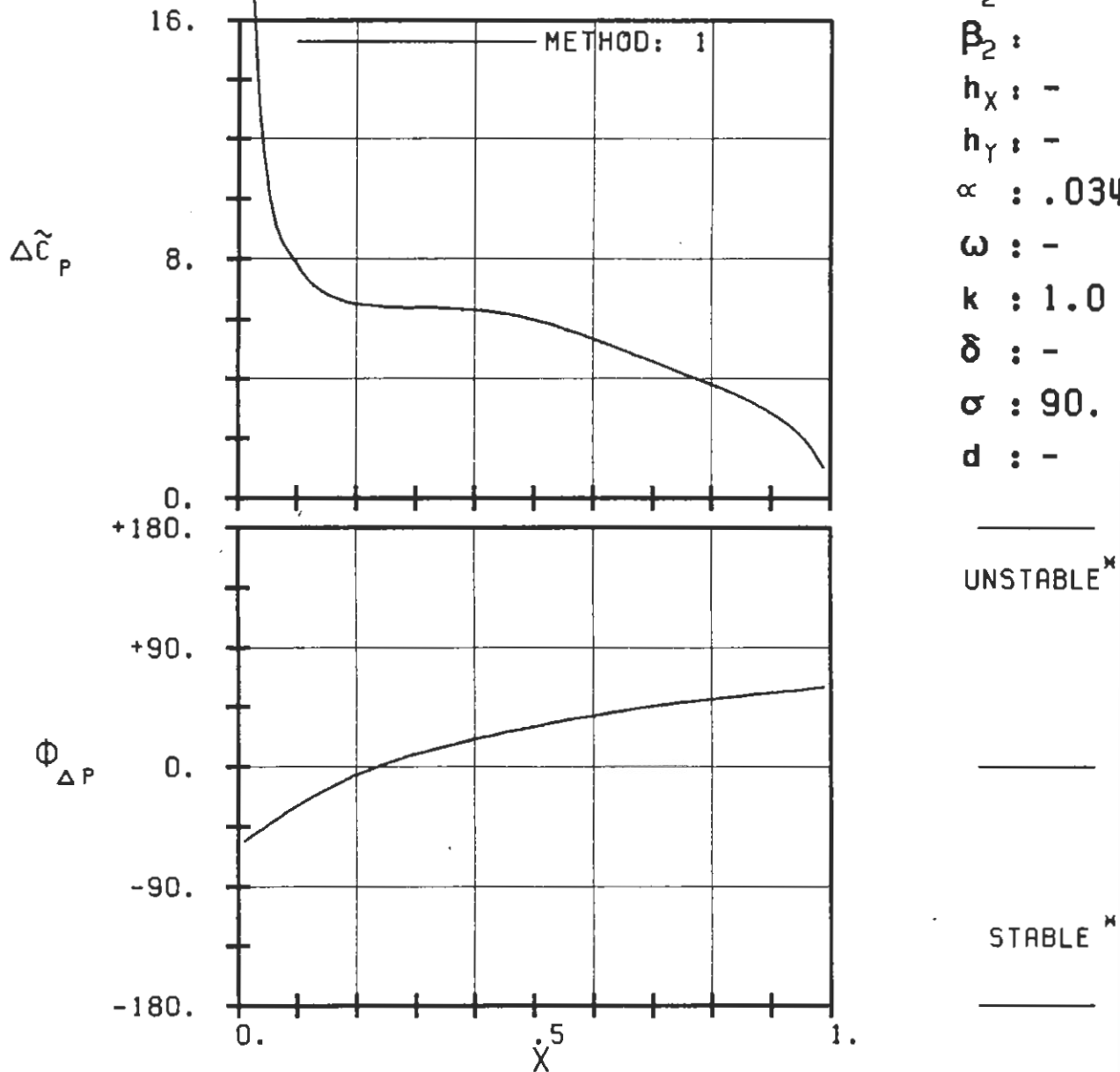
PLOT 7.8-3.4: EIGHTH STANDARD CONFIGURATION, CASE 4.
 MAGNITUDE AND PHASE LEAD OF UNSTEADY BLADE SURFACE PRESSURE DIFFERENCE DISTRIBUTION.
 (*: IN PITCH MODE, NOTATION VAL10 UPSTREAM OF PITCH AXIS)

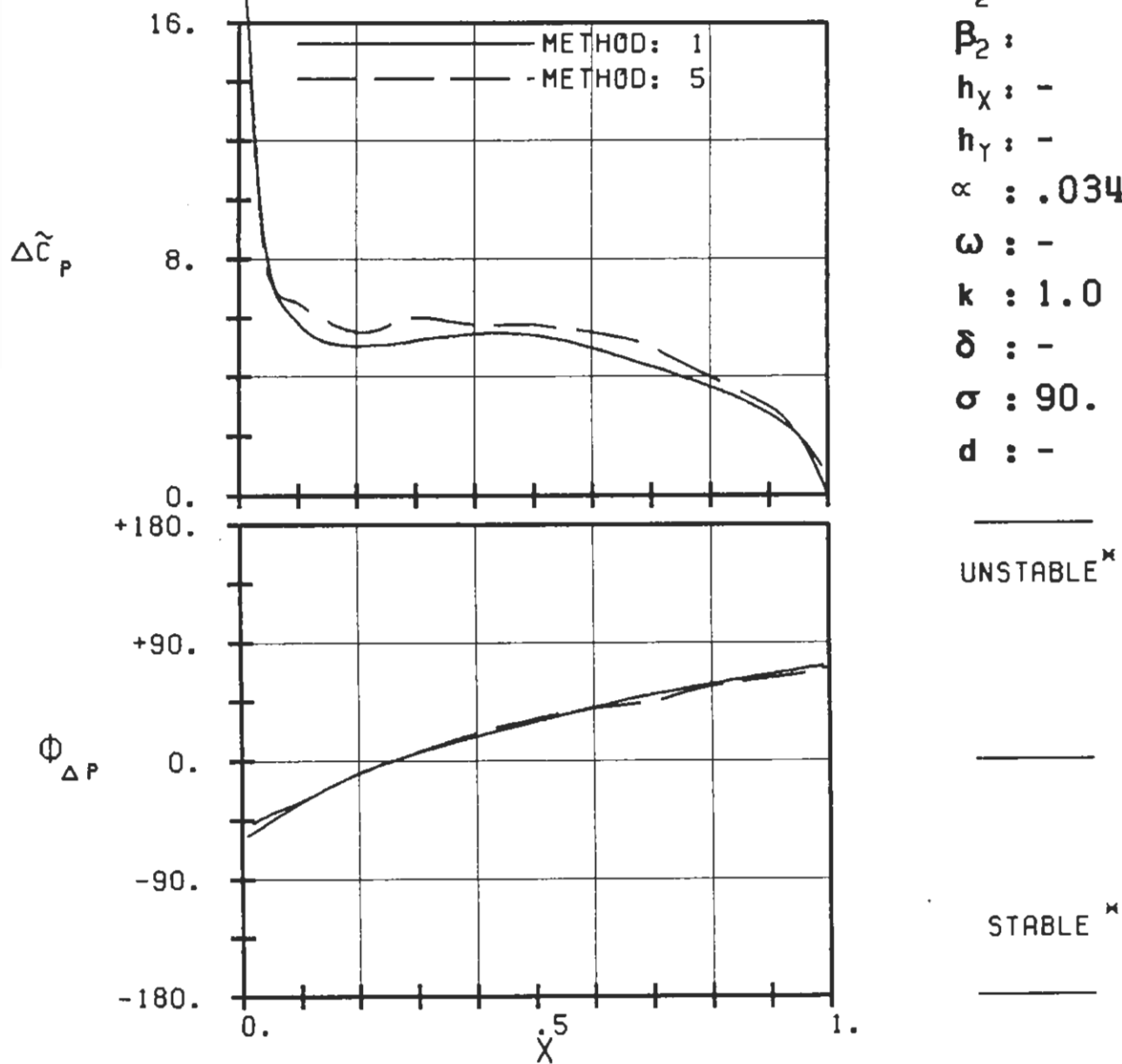
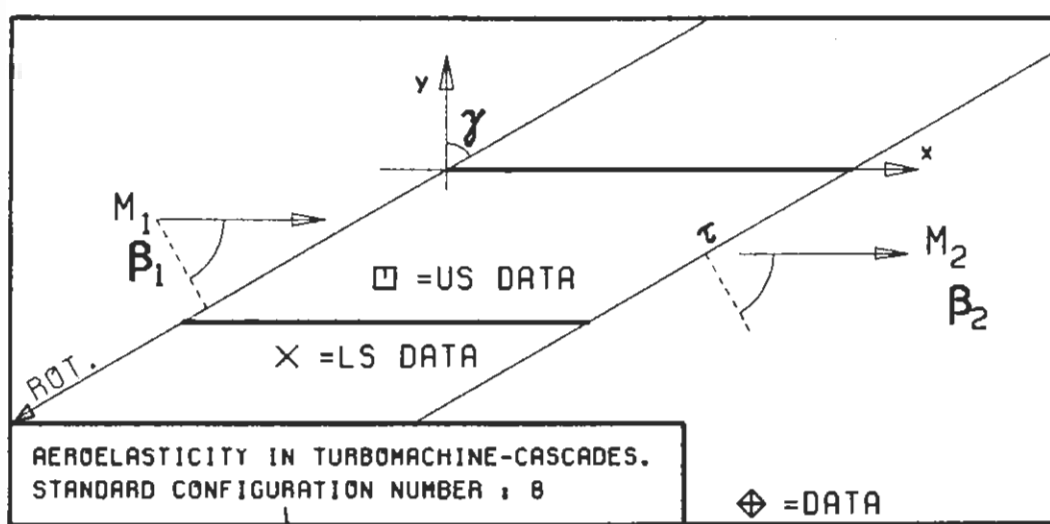


PLOT 7.8-3.5: EIGHTH STANDARD CONFIGURATION, CASE 5.
 MAGNITUDE AND PHASE LEAD OF UNSTEADY BLADE
 SURFACE PRESSURE DIFFERENCE DISTRIBUTION.
 (\times : IN PITCH MODE, NOTATION VALID UPSTREAM OF PITCH AXIS)

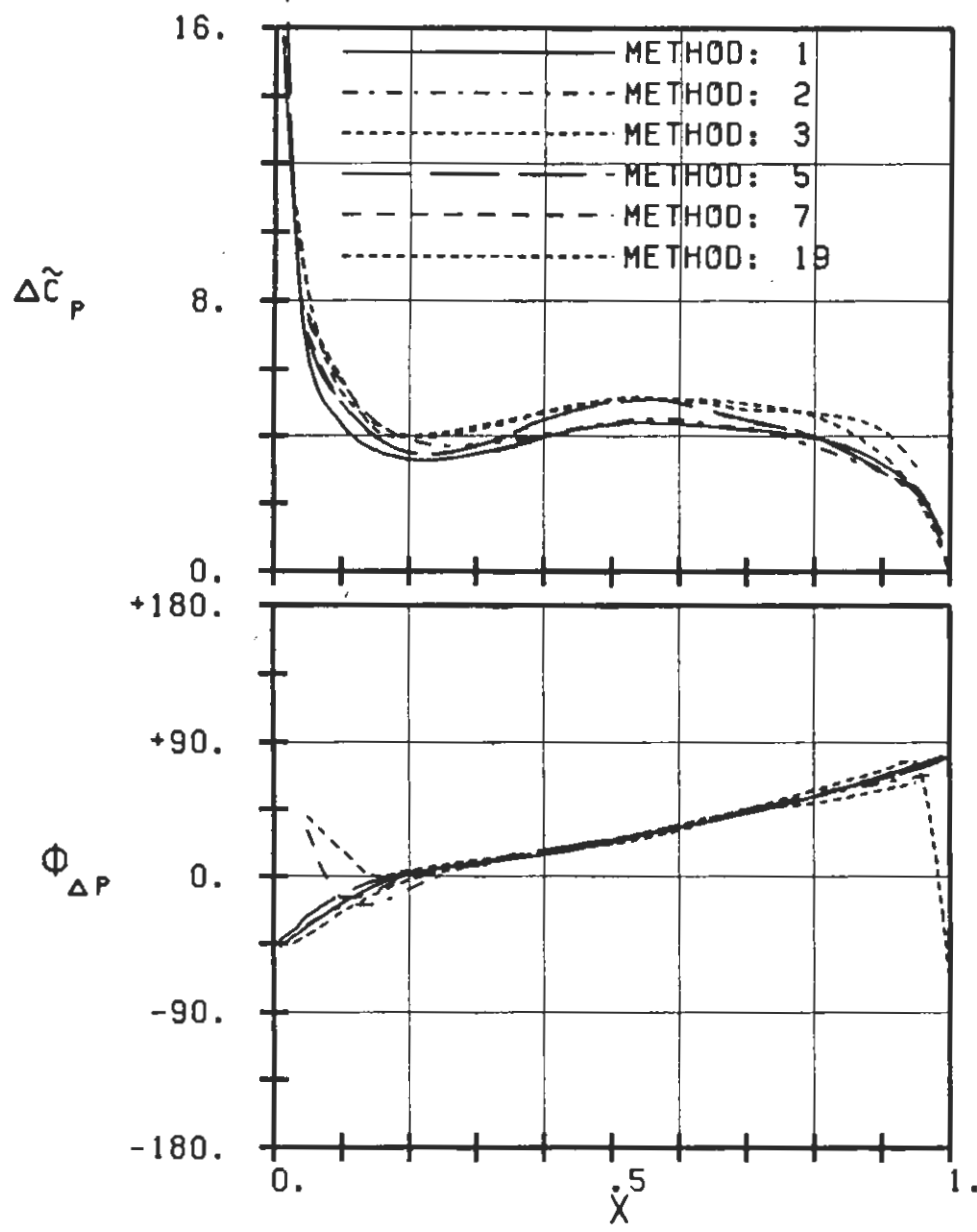
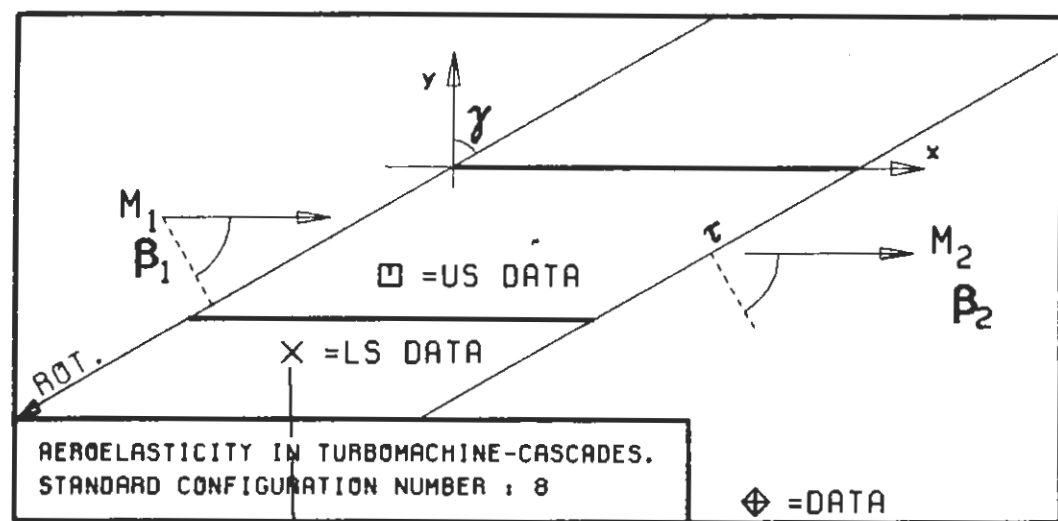


c : 0.1M
 τ : 0.75
 γ : 60.
 x_∞ : 0.5
 y_∞ : 0.
 M_1 : 0.6
 B_1 : -60.
 i : 0.
 M_2 : -
 B_2 : -
 h_X : -
 h_Y : -
 α : .0349
 ω : -
 k : 1.0
 δ : -
 σ : 90.
 d : -





PLOT 7.8-3.7: EIGHTH STANDARD CONFIGURATION, CASE 7.
MAGNITUDE AND PHASE LEAD OF UNSTEADY BLADE SURFACE PRESSURE DIFFERENCE DISTRIBUTION.
(\times : IN PITCH MODE, NOTATION VALID UPSTREAM OF PITCH AXIS)

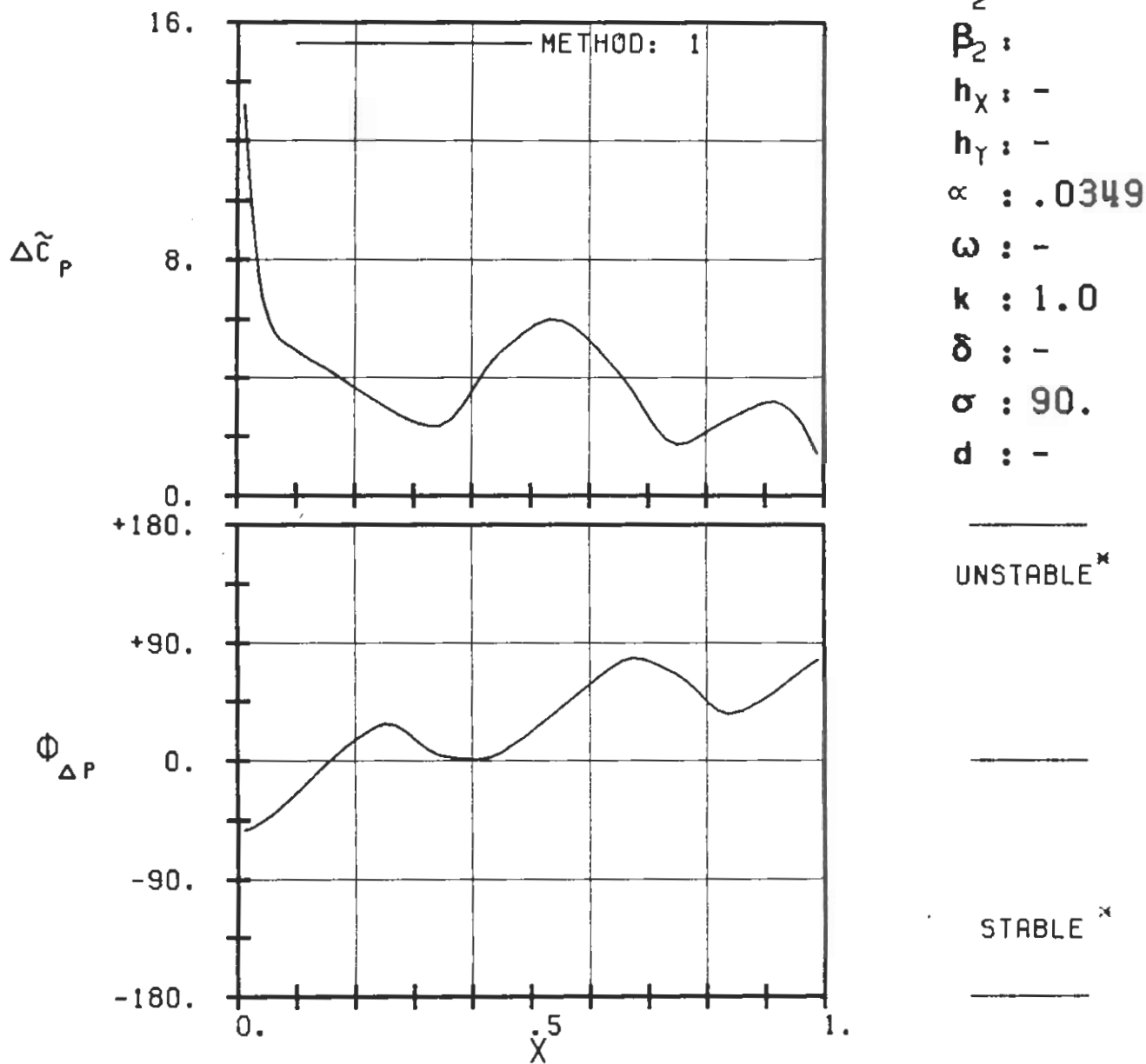
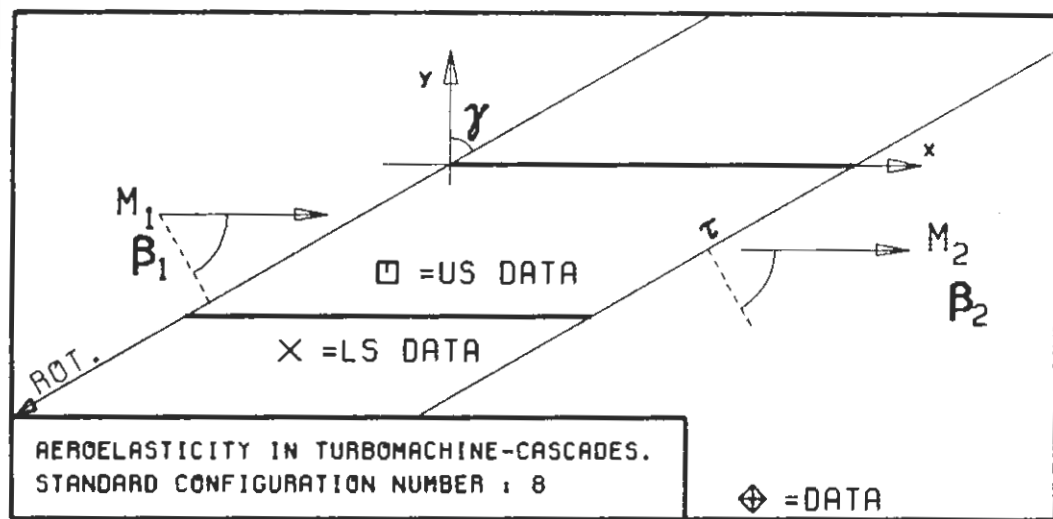


PLOT 7.8-3.8: EIGHTH STANDARD CONFIGURATION, CASE 8.
MAGNITUDE AND PHASE LEAD OF UNSTEADY BLADE
SURFACE PRESSURE DIFFERENCE DISTRIBUTION.
(\times : IN PITCH MODE, NOTATION VALID UPSTREAM OF PITCH AXIS)

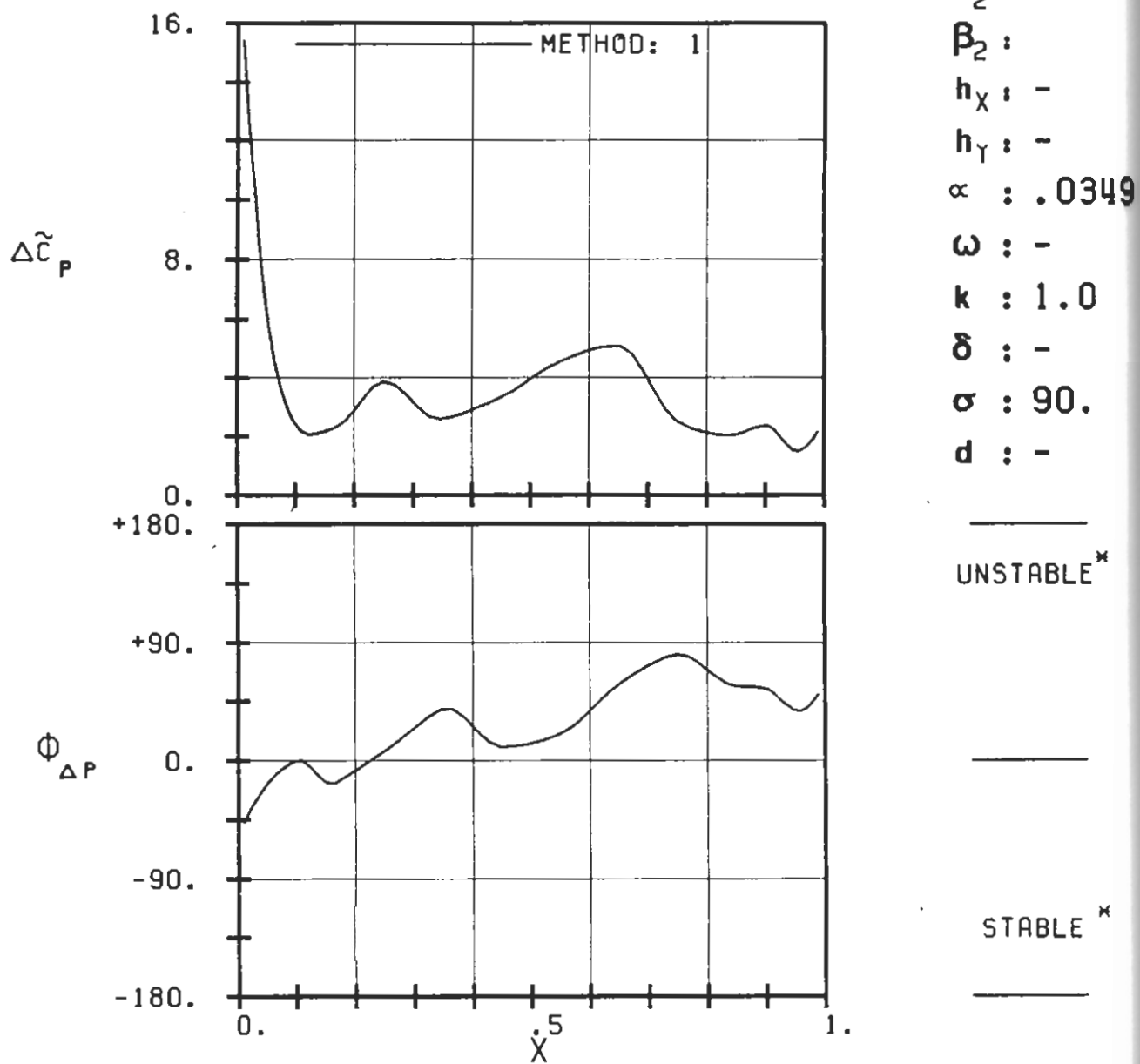
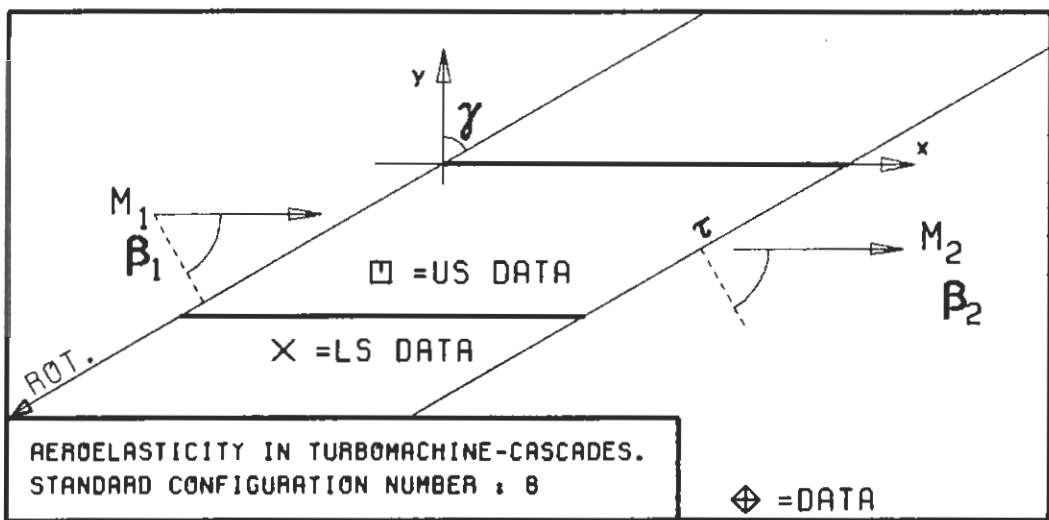
$c = 0.1M$
 $\tau = 0.75$
 $\gamma = 60.$
 $x_\alpha = 0.5$
 $y_\alpha = 0.$
 $M_1 = 0.8$
 $\beta_1 = -60.$
 $i = 0.$
 $M_2 = -$
 $\beta_2 = -$
 $h_X = -$
 $h_Y = -$
 $\alpha = .0349$
 $\omega = -$
 $k = 1.0$
 $\delta = -$
 $\sigma = 90.$
 $d = -$

UNSTABLE*

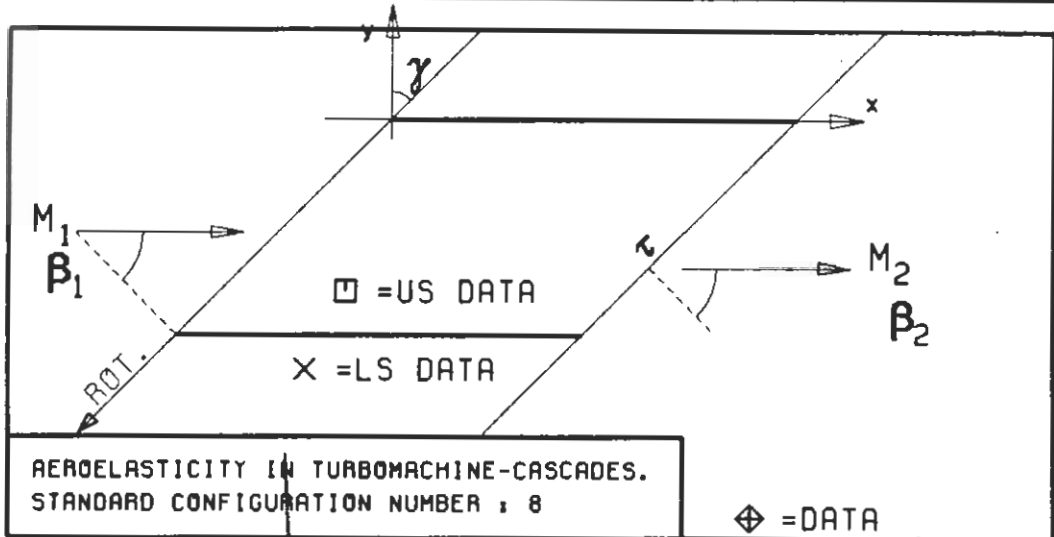
STABLE *



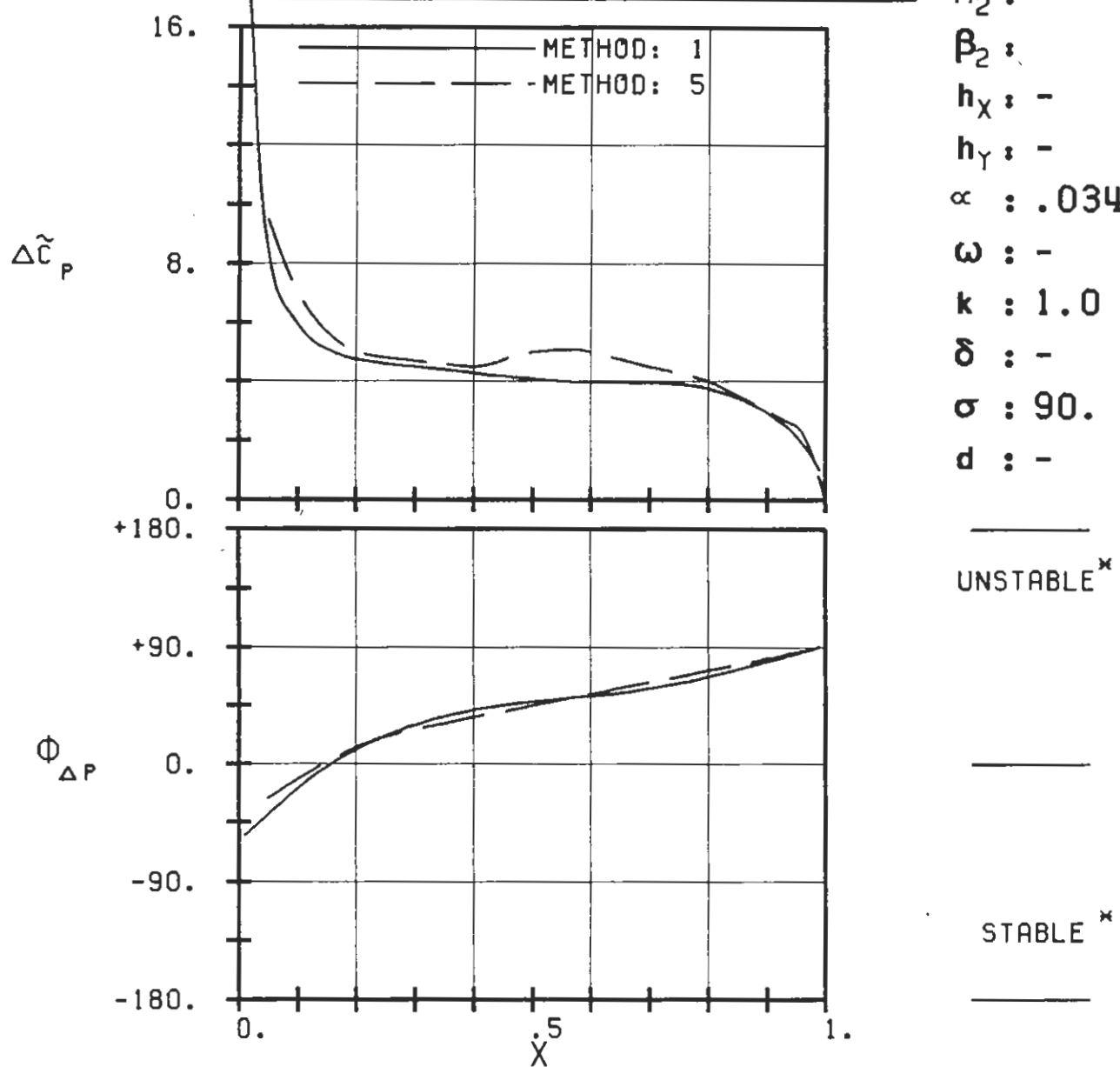
PLOT 7.8-3.9: EIGHTH STANDARD CONFIGURATION, CASE 9.
MAGNITUDE AND PHASE LEAD OF UNSTEADY BLADE
SURFACE PRESSURE DIFFERENCE DISTRIBUTION.
(*: IN PITCH MODE, NOTATION VALID UPSTREAM OF PITCH AXIS)



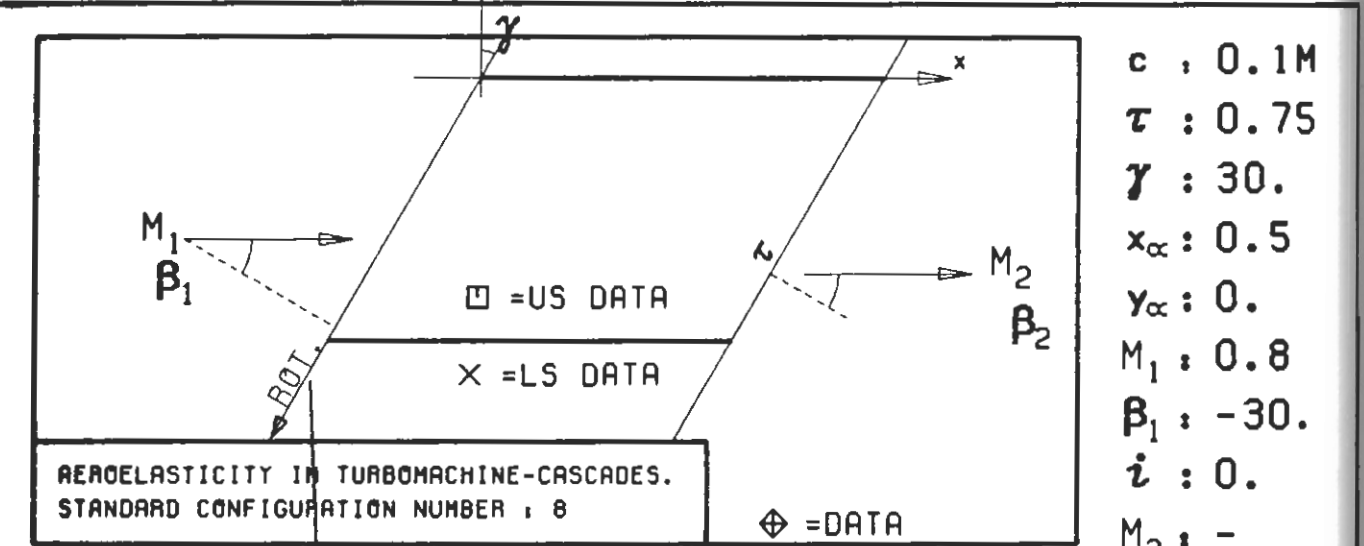
PLOT 7.8-3.10: EIGHTH STANDARD CONFIGURATION, CASE 10.
MAGNITUDE AND PHASE LEAD OF UNSTEADY BLADE
SURFACE PRESSURE DIFFERENCE DISTRIBUTION.
(\times : IN PITCH MODE, NOTATION VALID UPSTREAM OF PITCH AXIS)



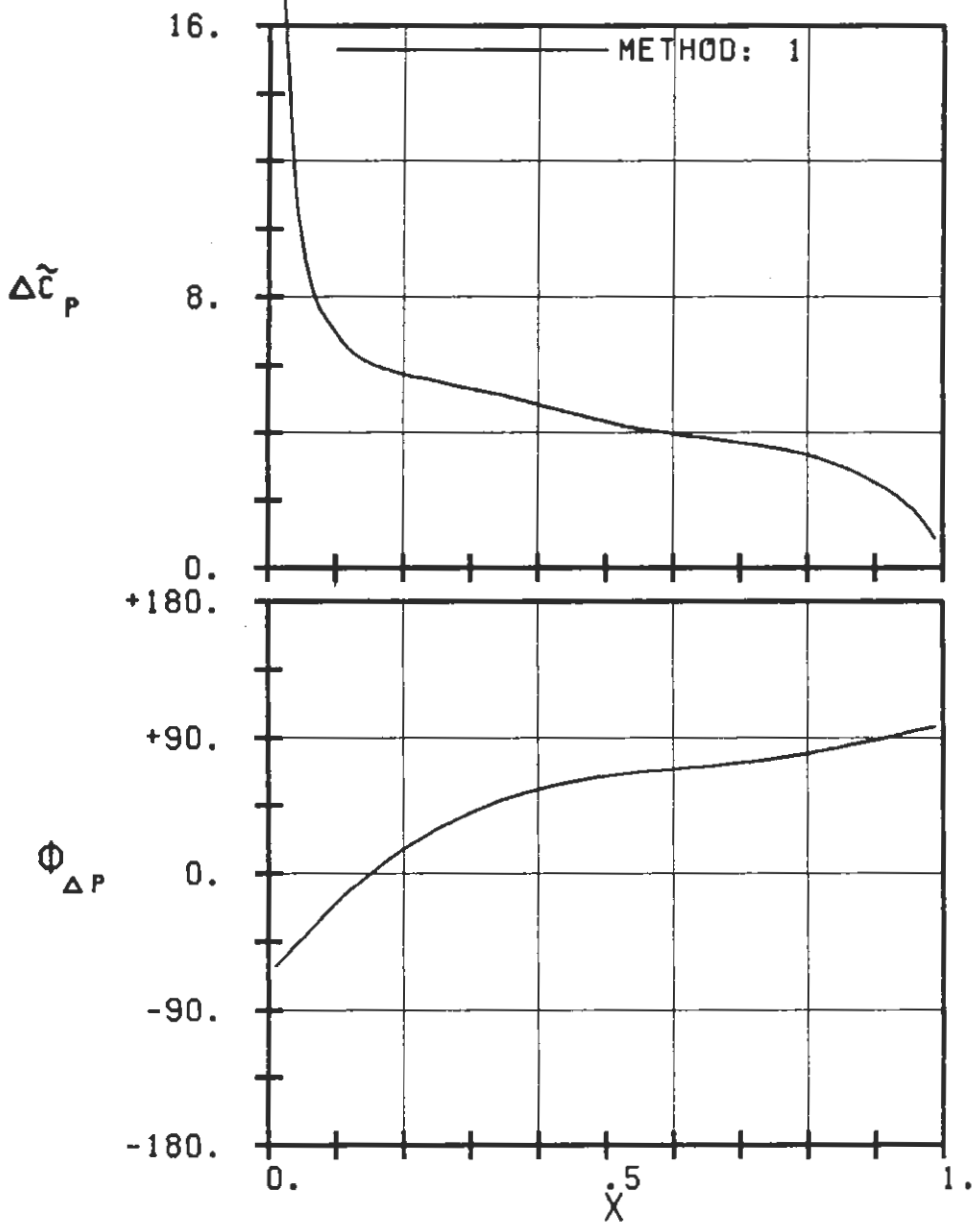
c : 0.1M
 τ : 0.75
 γ : 45.
 x_∞ : 0.5
 y_∞ : 0.
 M_1 : 0.8
 β_1 : -45.
 i : 0.
 M_2 : -
 β_2 : -
 h_X : -
 h_Y : -
 α : .0349
 ω : -
 k : 1.0
 δ : -
 σ : 90.
 d : -



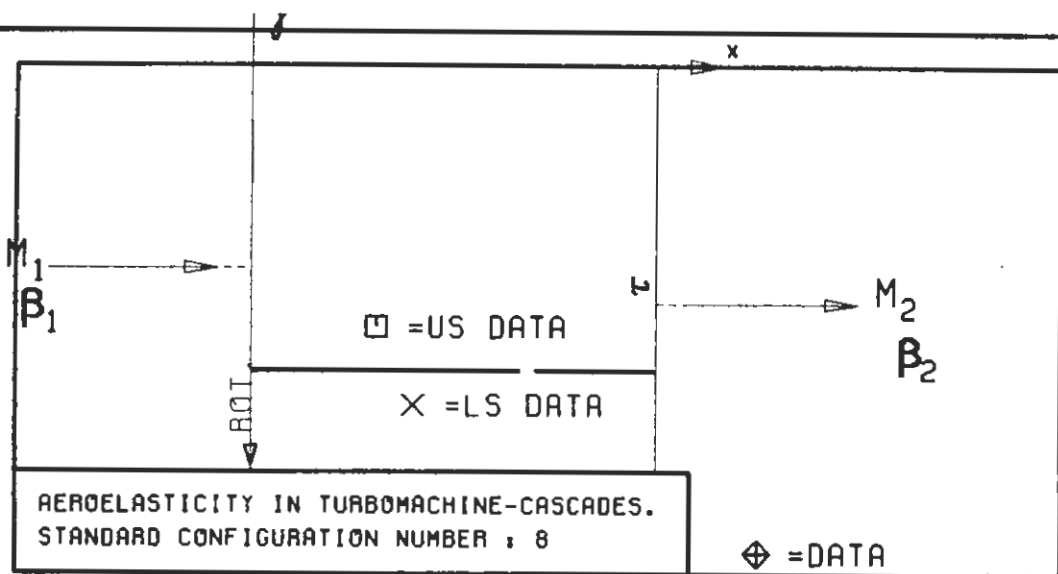
PLOT 7.8-3.11: EIGHTH STANDARD CONFIGURATION, CASE 11.
 MAGNITUDE AND PHASE LEAD OF UNSTEADY BLADE
 SURFACE PRESSURE DIFFERENCE DISTRIBUTION.
 (\times : IN PITCH MODE, NOTATION VALID UPSTREAM OF PITCH AXIS)



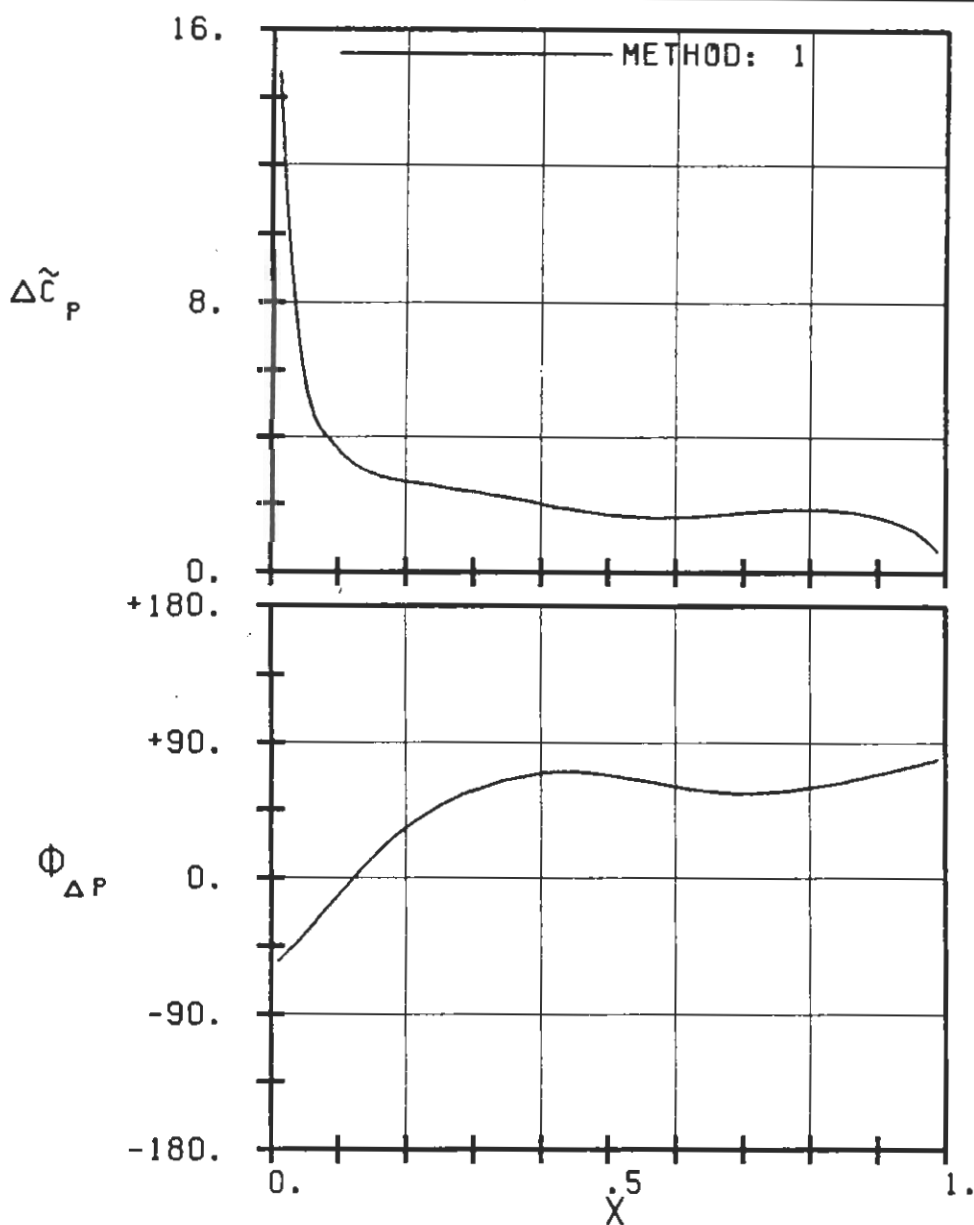
c : 0.1M
 τ : 0.75
 γ : 30.
 x_α : 0.5
 y_α : 0.
 M_1 : 0.8
 β_1 : -30.
 i : 0.
 M_2 : -
 β_2 :
 h_X : -
 h_Y : -
 α : .0349
 ω : -
 k : 1.0
 δ : -
 σ : 90.
 d : -



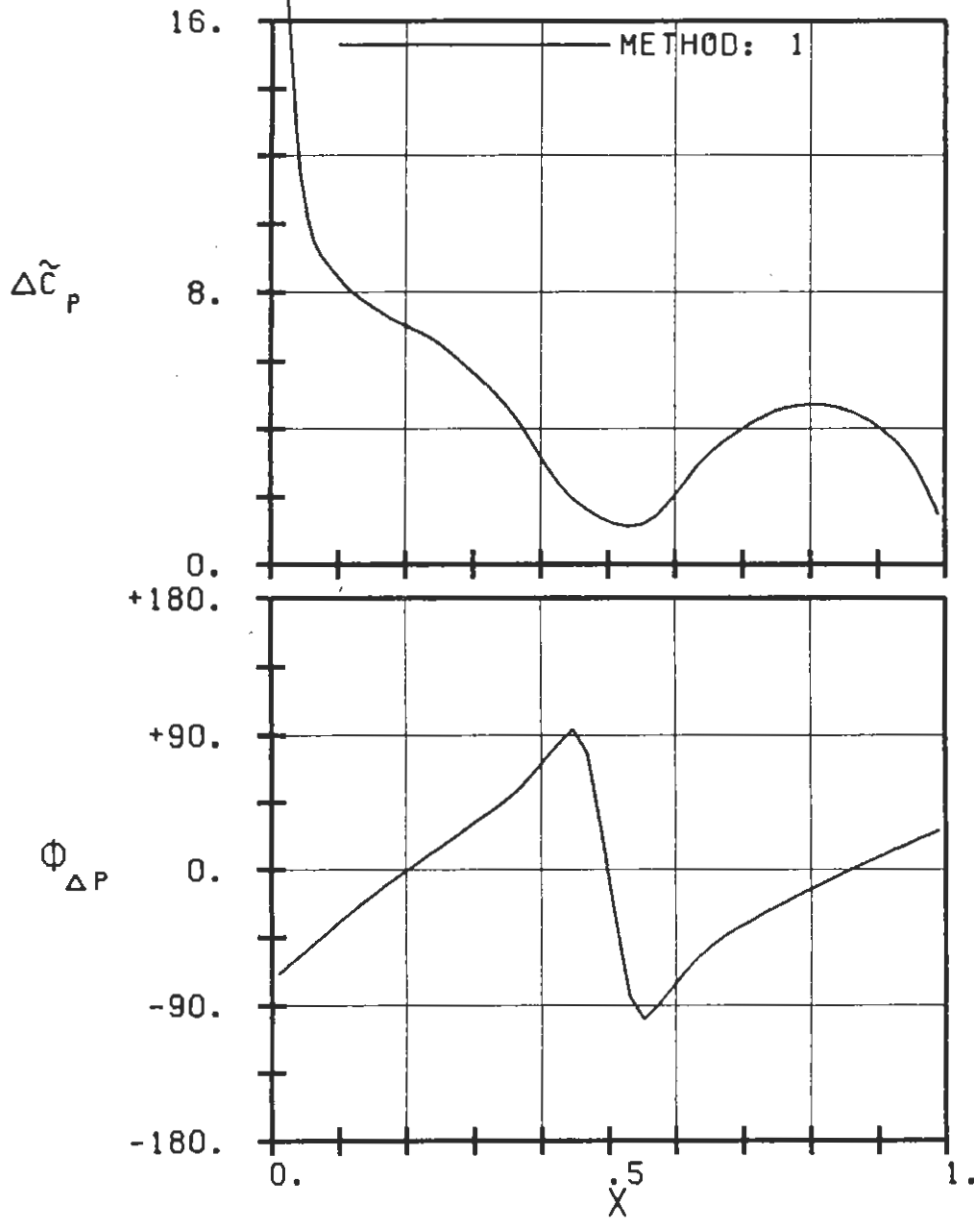
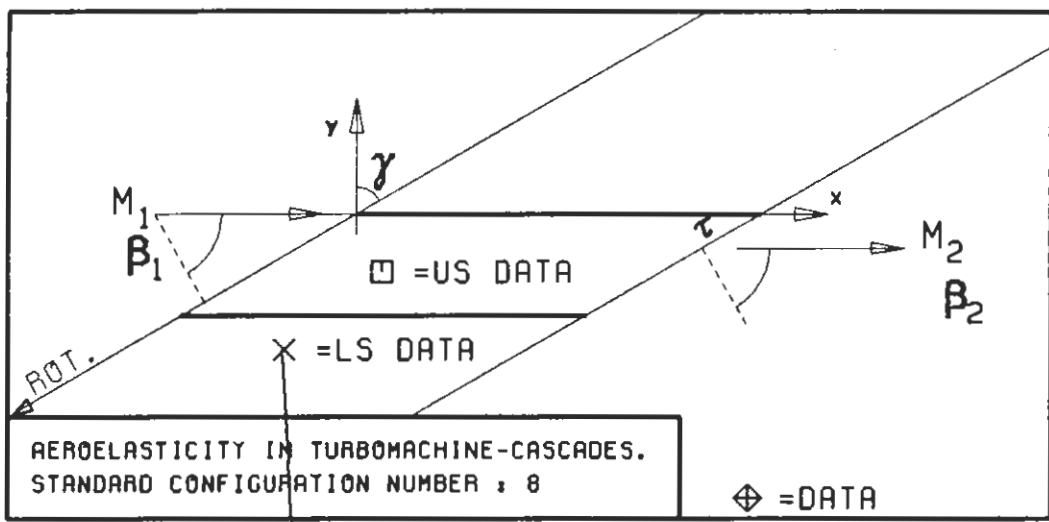
PLOT 7.8-3.12: EIGHTH STANDARD CONFIGURATION, CASE 12.
 MAGNITUDE AND PHASE LEAD OF UNSTEADY BLADE
 SURFACE PRESSURE DIFFERENCE DISTRIBUTION.
 (*: IN PITCH MODE, NOTATION VALID UPSTREAM OF PITCH AXIS)



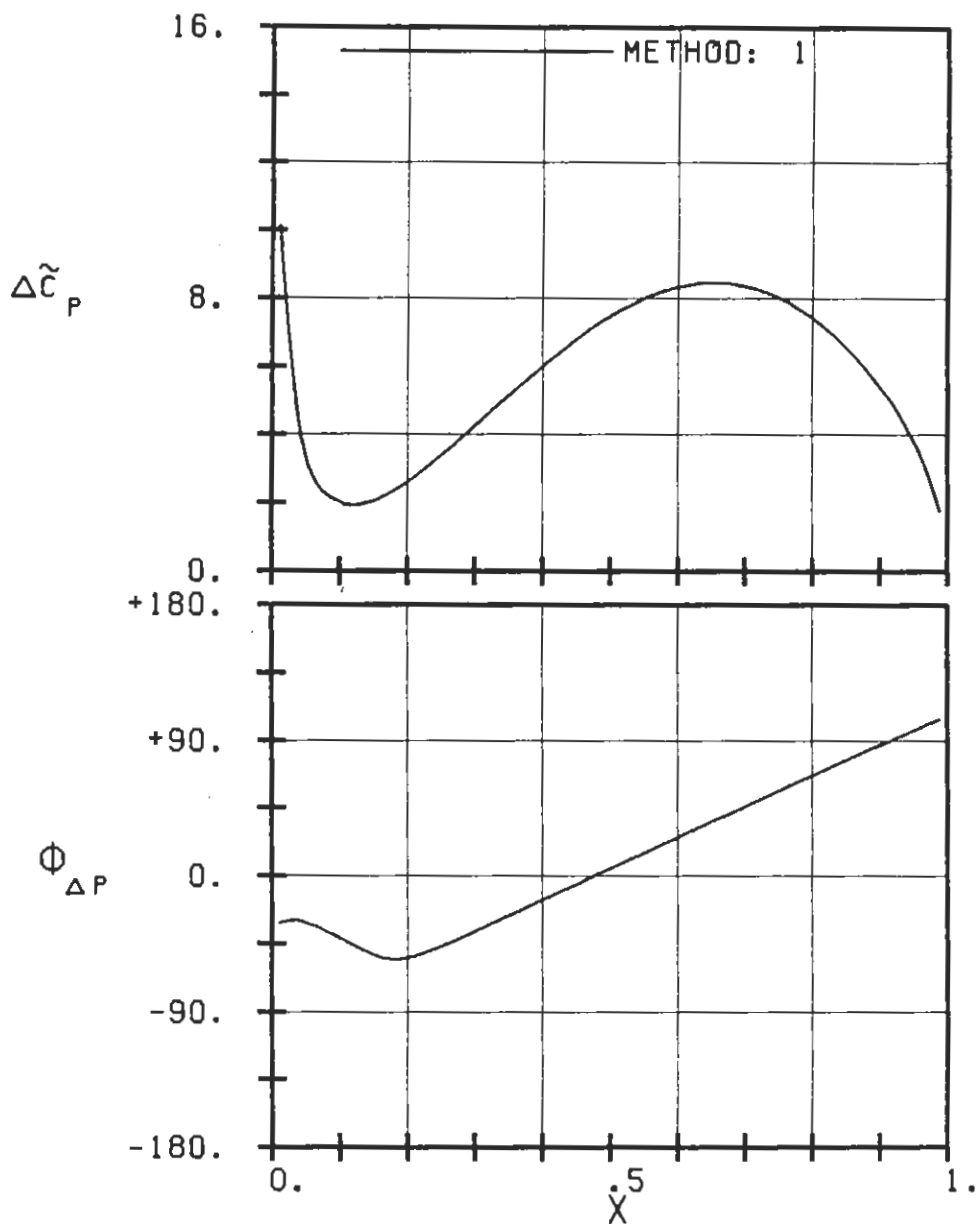
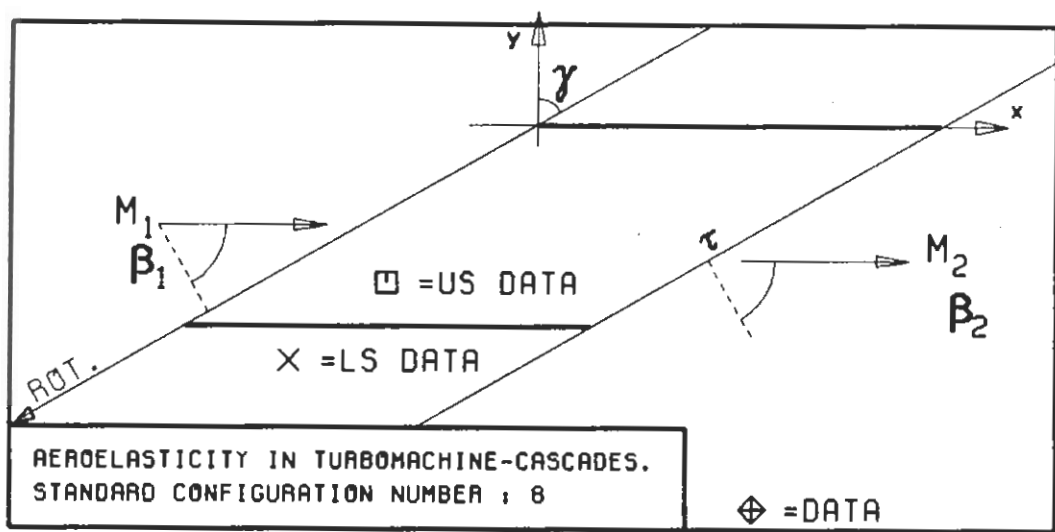
$c : 0.1M$
 $\tau : 0.75$
 $\gamma : 0.0$
 $x_\infty : 0.5$
 $y_\infty : 0.$
 $M_1 : 0.8$
 $\beta_1 : 0.0$
 $i : 0.$
 $M_2 : -$
 $\beta_2 : -$
 $h_x : -$
 $h_y : -$
 $\alpha : .0349$
 $\omega : -$
 $k : 1.0$
 $\delta : -$
 $\sigma : 90.$
 $d : -$



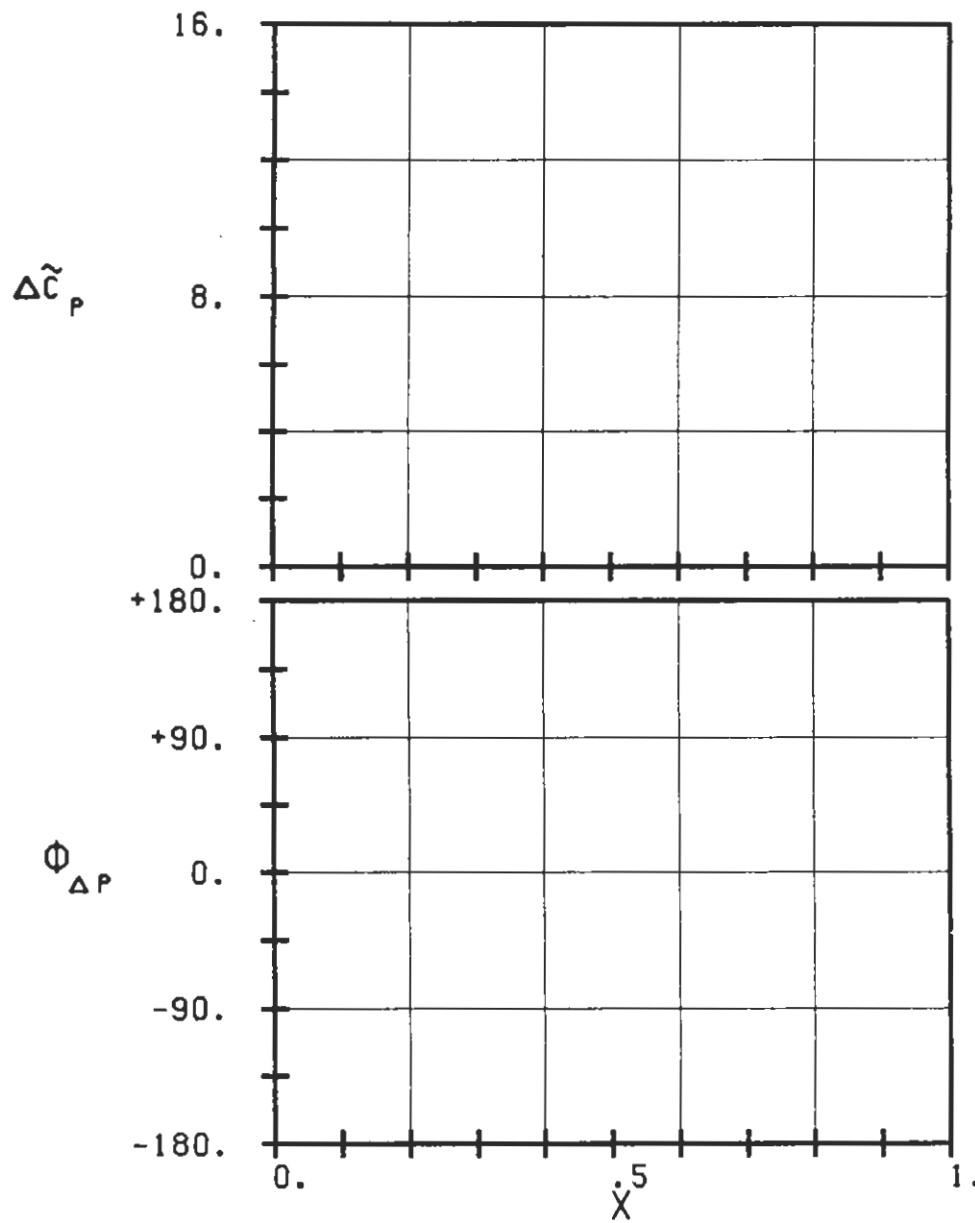
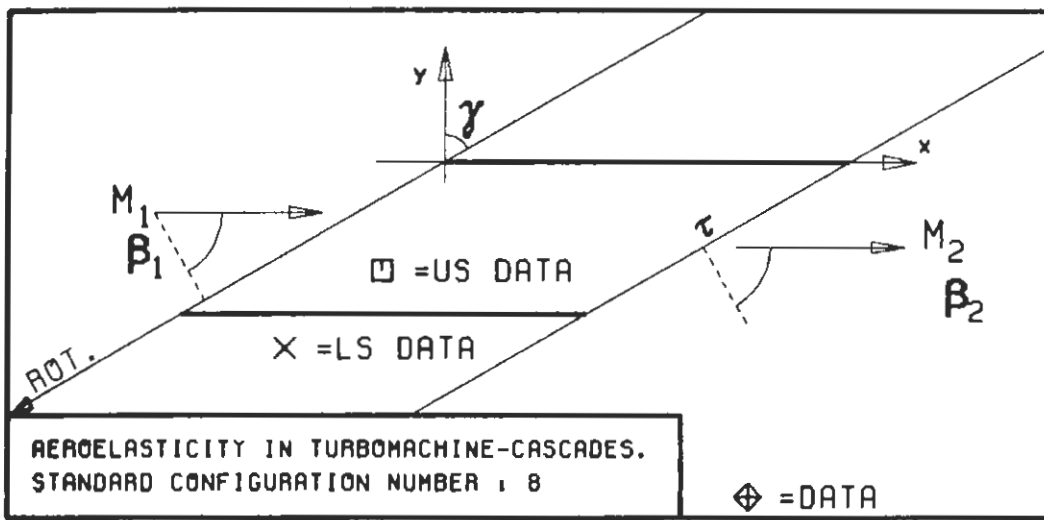
PLOT 7.8-3.13: EIGHTH STANDARD CONFIGURATION, CASE 13.
 MAGNITUDE AND PHASE LEAD OF UNSTEADY BLADE
 SURFACE PRESSURE DIFFERENCE DISTRIBUTION.
 (*: IN PITCH MODE, NOTATION VALID UPSTREAM OF PITCH AXIS)



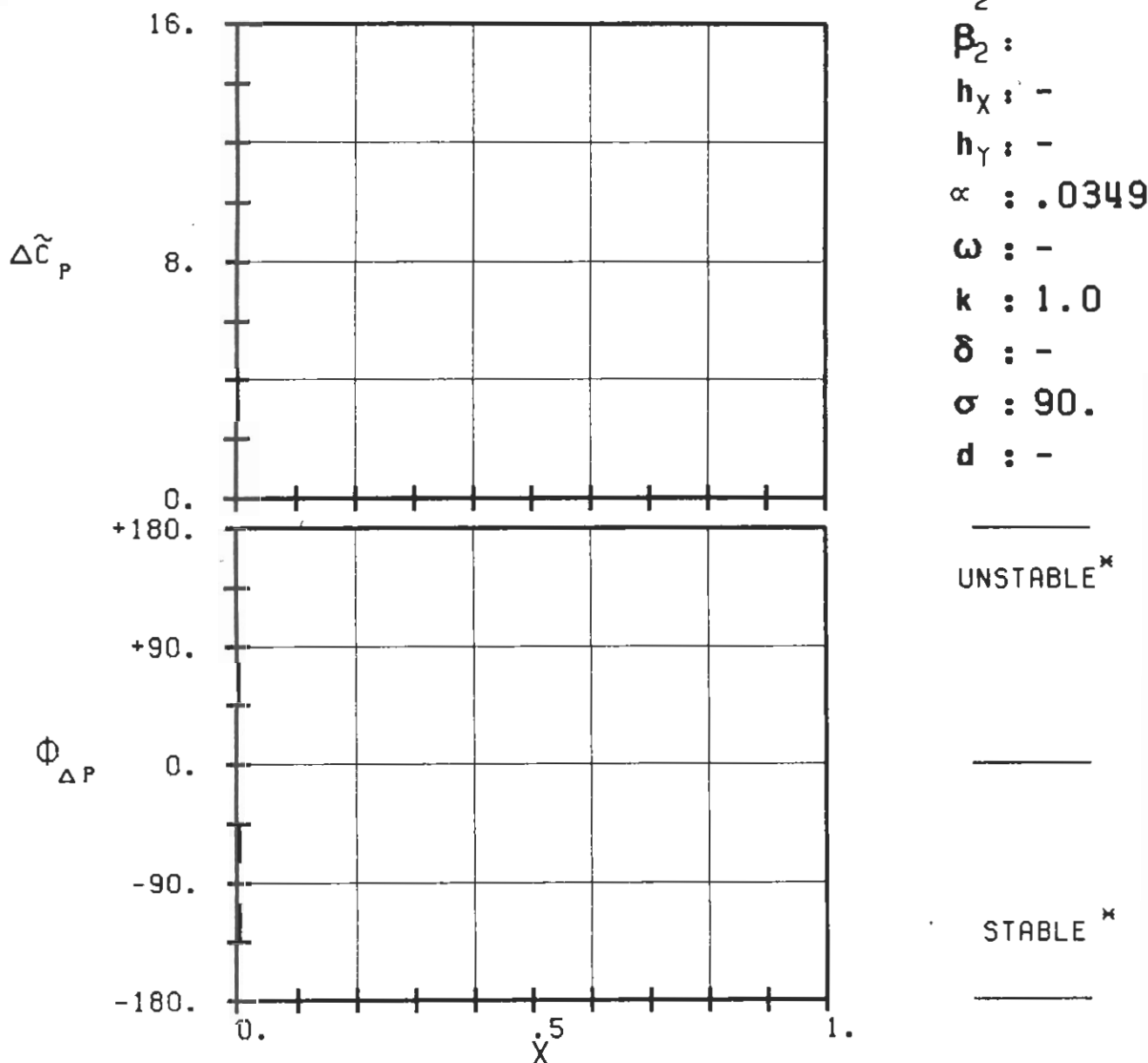
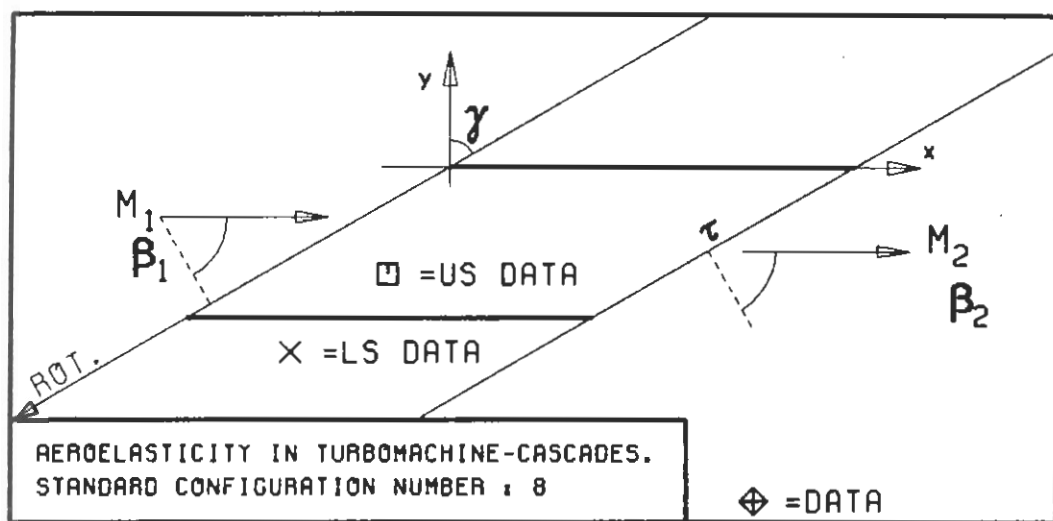
PLOT 7.8-3.14: EIGHTH STANDARD CONFIGURATION, CASE 14.
 MAGNITUDE AND PHASE LEAD OF UNSTEADY BLADE
 SURFACE PRESSURE DIFFERENCE DISTRIBUTION.
 (*: IN PITCH MODE, NOTATION VALID UPSTREAM OF PITCH AXIS)



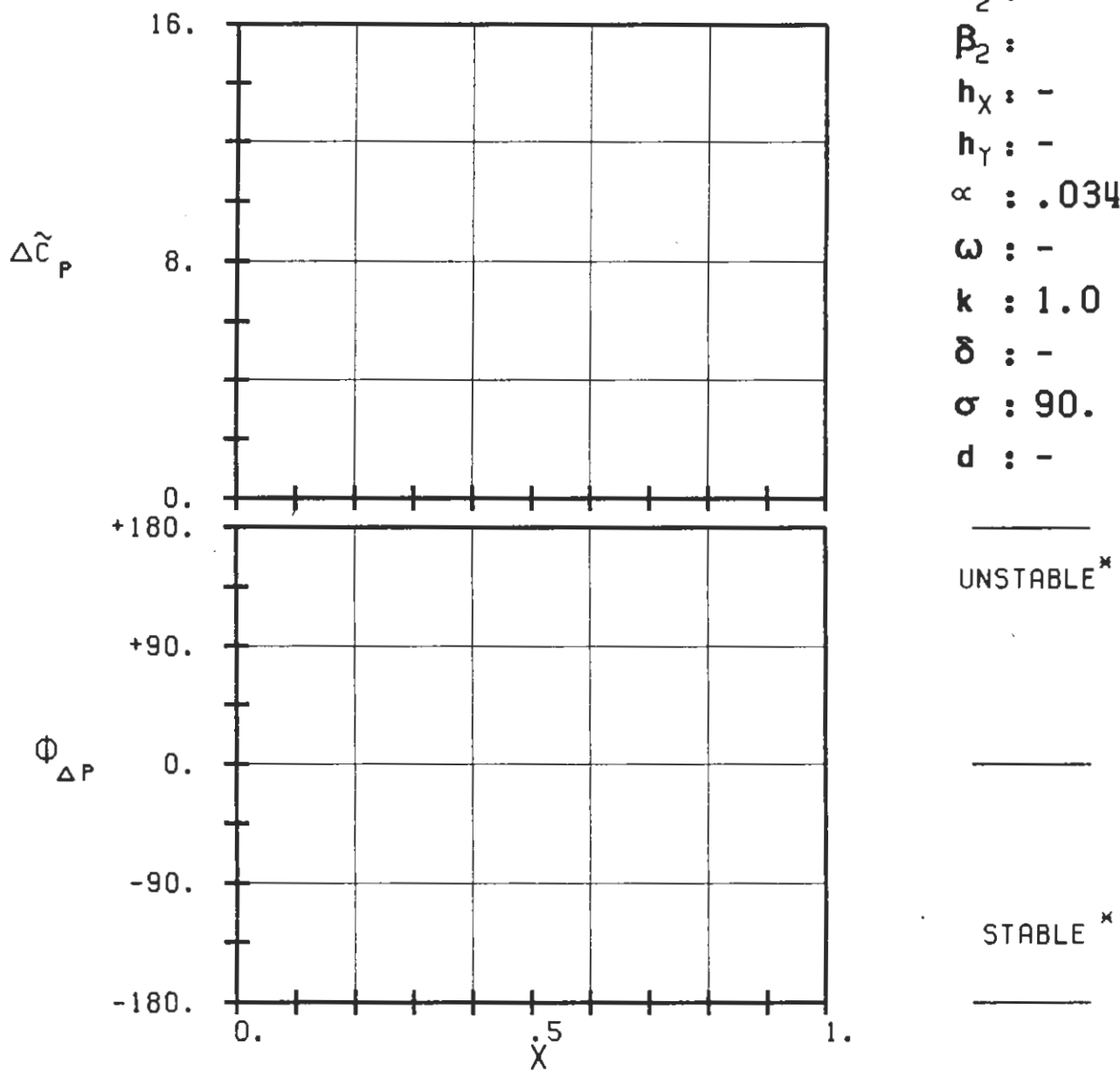
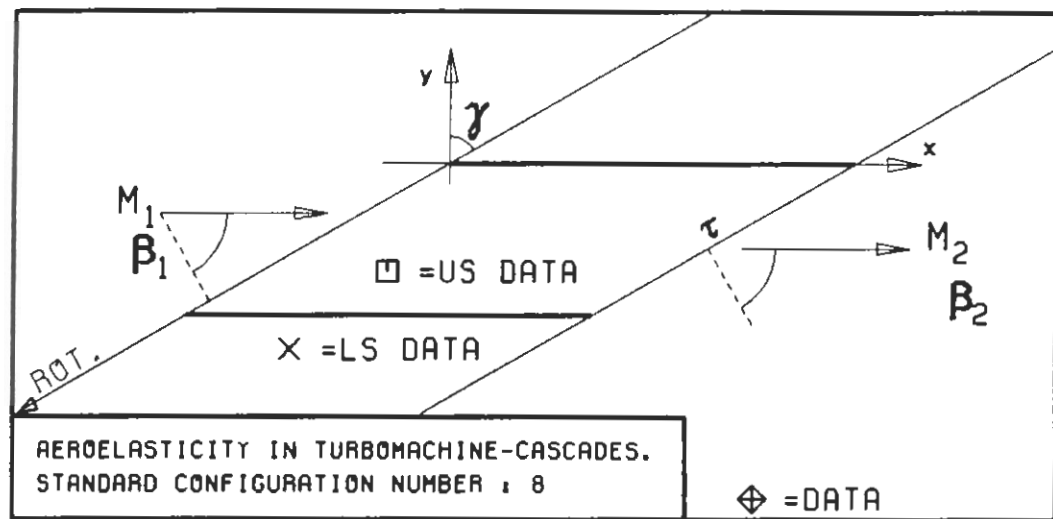
PLOT 7.8-3.15: EIGHTH STANDARD CONFIGURATION, CASE 15.
 MAGNITUDE AND PHASE LEAD OF UNSTEADY BLADE
 SURFACE PRESSURE DIFFERENCE DISTRIBUTION.
 (*: IN PITCH MODE, NOTATION VALID UPSTREAM OF PITCH AXIS)



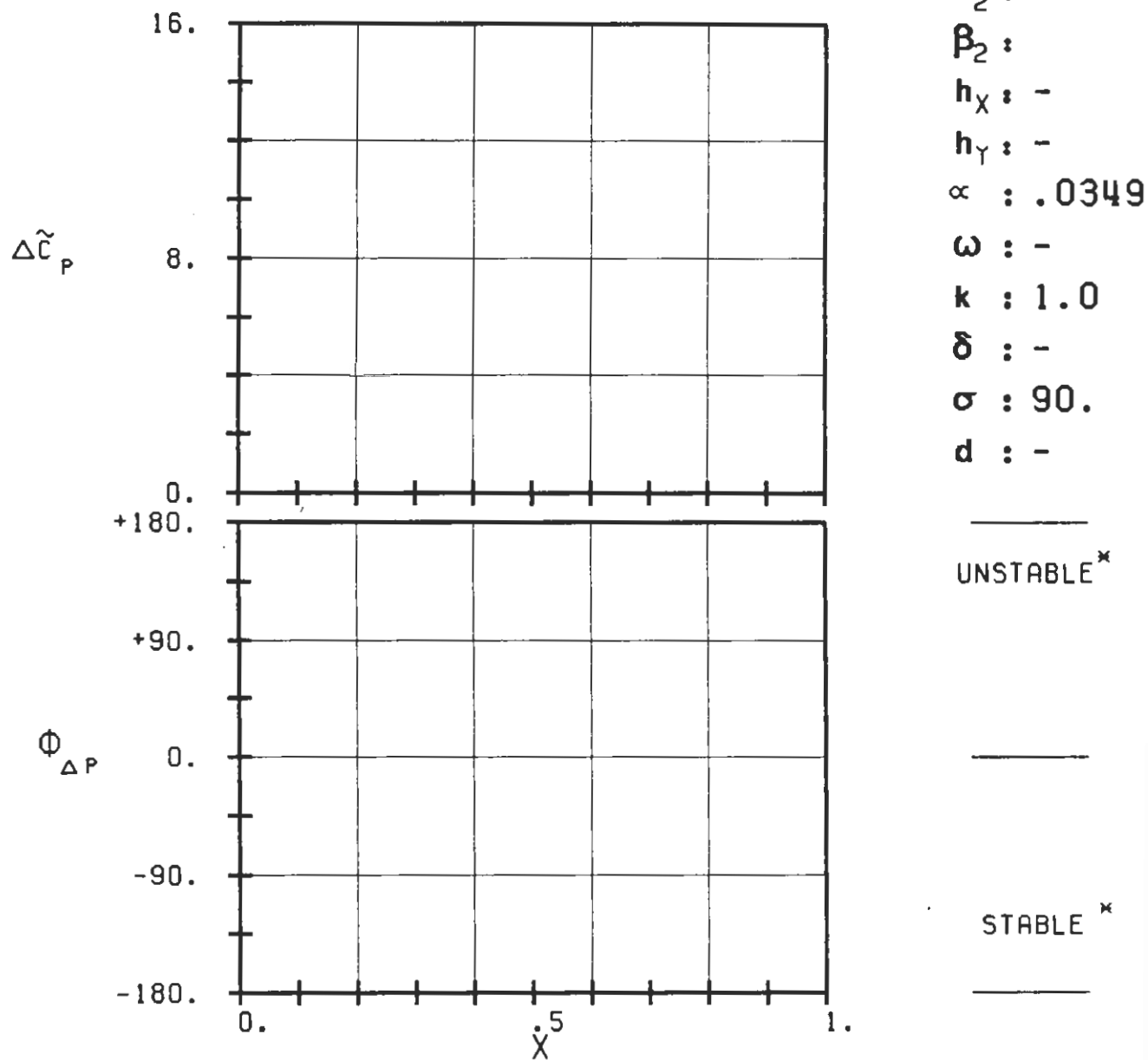
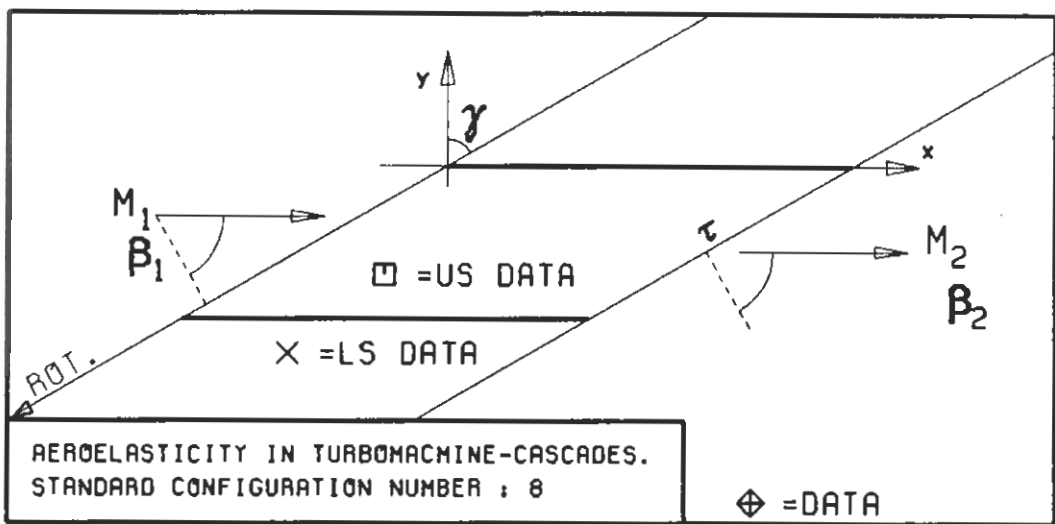
PLOT 7.8-3.16: EIGHTH STANDARD CONFIGURATION, CASE 16.
MAGNITUDE AND PHASE LEAD OF UNSTEADY BLADE
SURFACE PRESSURE DIFFERENCE DISTRIBUTION.
(*: IN PITCH MODE, NOTATION VALID UPSTREAM OF PITCH AXIS)



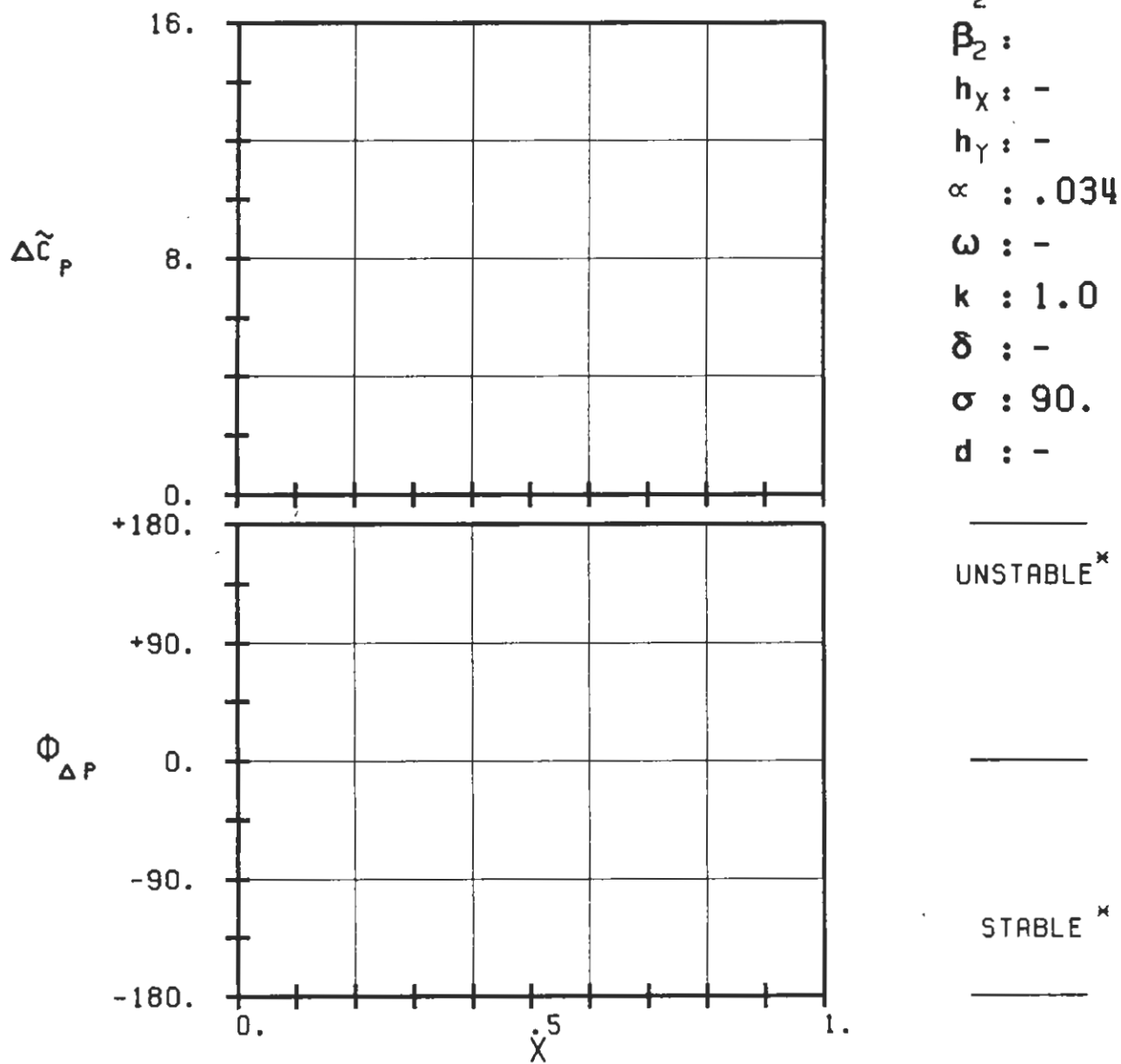
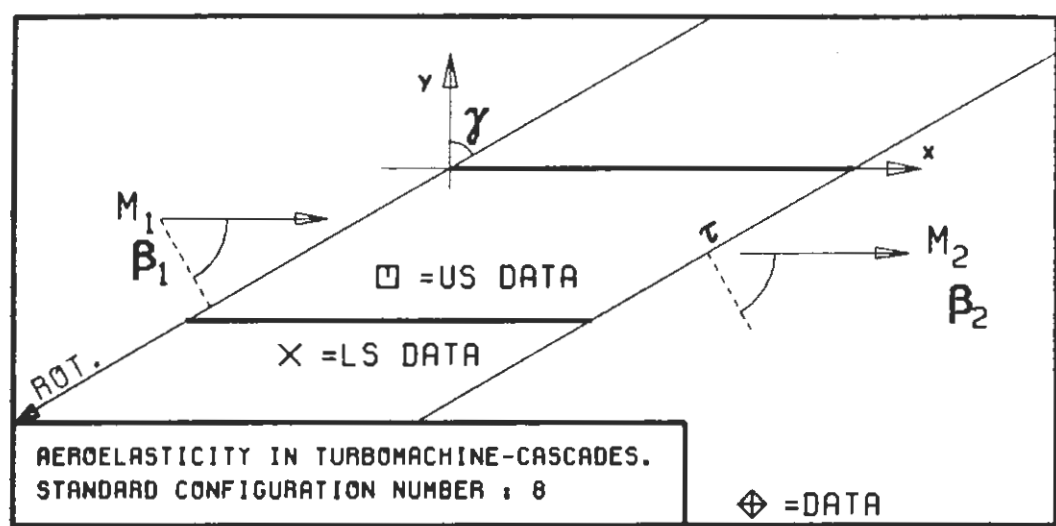
PLOT 7.8-3.17: EIGHTH STANDARD CONFIGURATION, CASE 17.
MAGNITUDE AND PHASE LEAD OF UNSTEADY BLADE
SURFACE PRESSURE DIFFERENCE DISTRIBUTION.
(*: IN PITCH MODE, NOTATION VALID UPSTREAM OF PITCH AXIS)



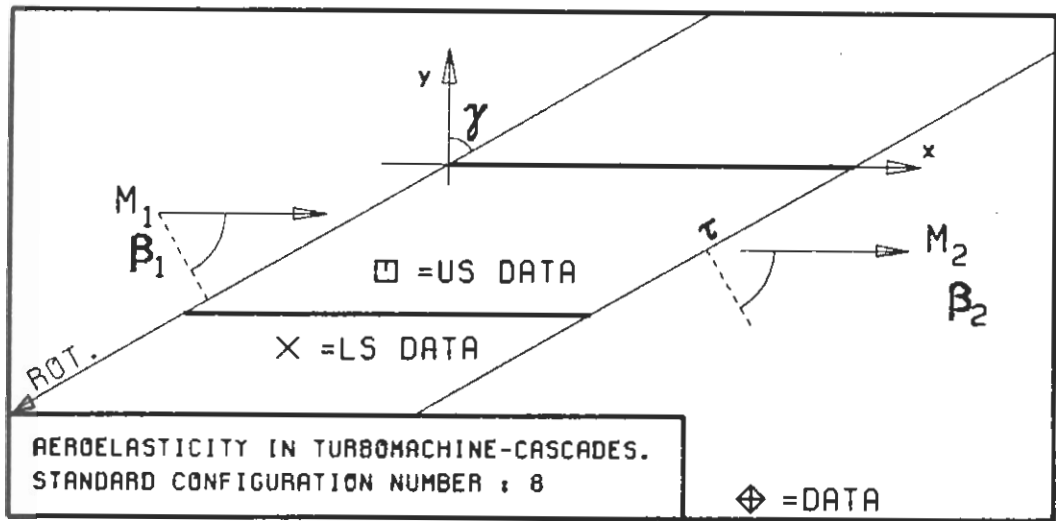
PLOT 7.8-3.18: EIGHTH STANDARD CONFIGURATION, CASE 18.
MAGNITUDE AND PHASE LEAD OF UNSTEADY BLADE
SURFACE PRESSURE DIFFERENCE DISTRIBUTION.
(*: IN PITCH MODE, NOTATION VALID UPSTREAM OF PITCH AXIS)



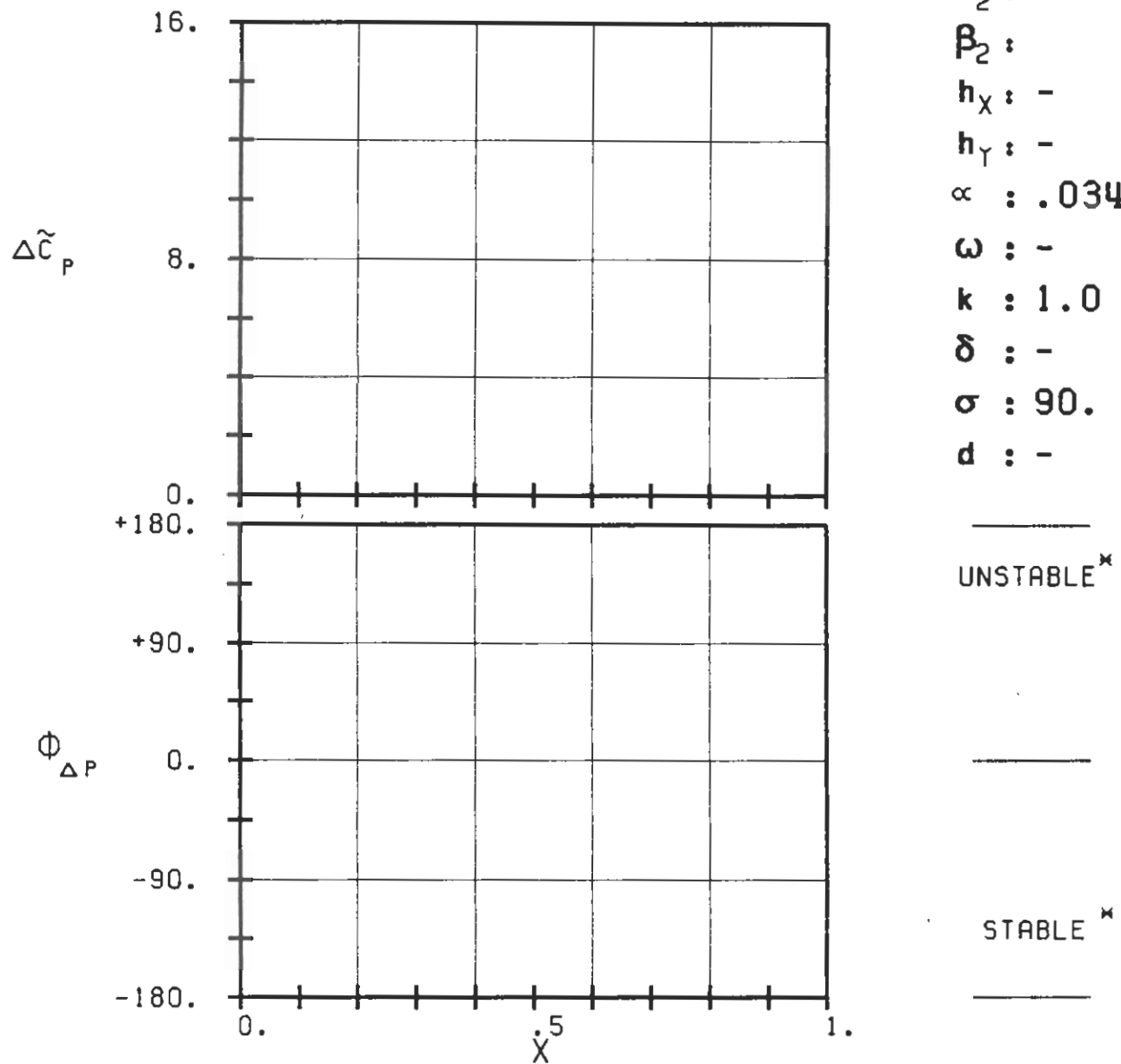
PLOT 7.8-3.19: EIGHTH STANDARD CONFIGURATION, CASE 19.
MAGNITUDE AND PHASE LEAD OF UNSTEADY BLADE
SURFACE PRESSURE DIFFERENCE DISTRIBUTION.
(*: IN PITCH MODE, NOTATION VALID UPSTREAM OF PITCH AXIS)



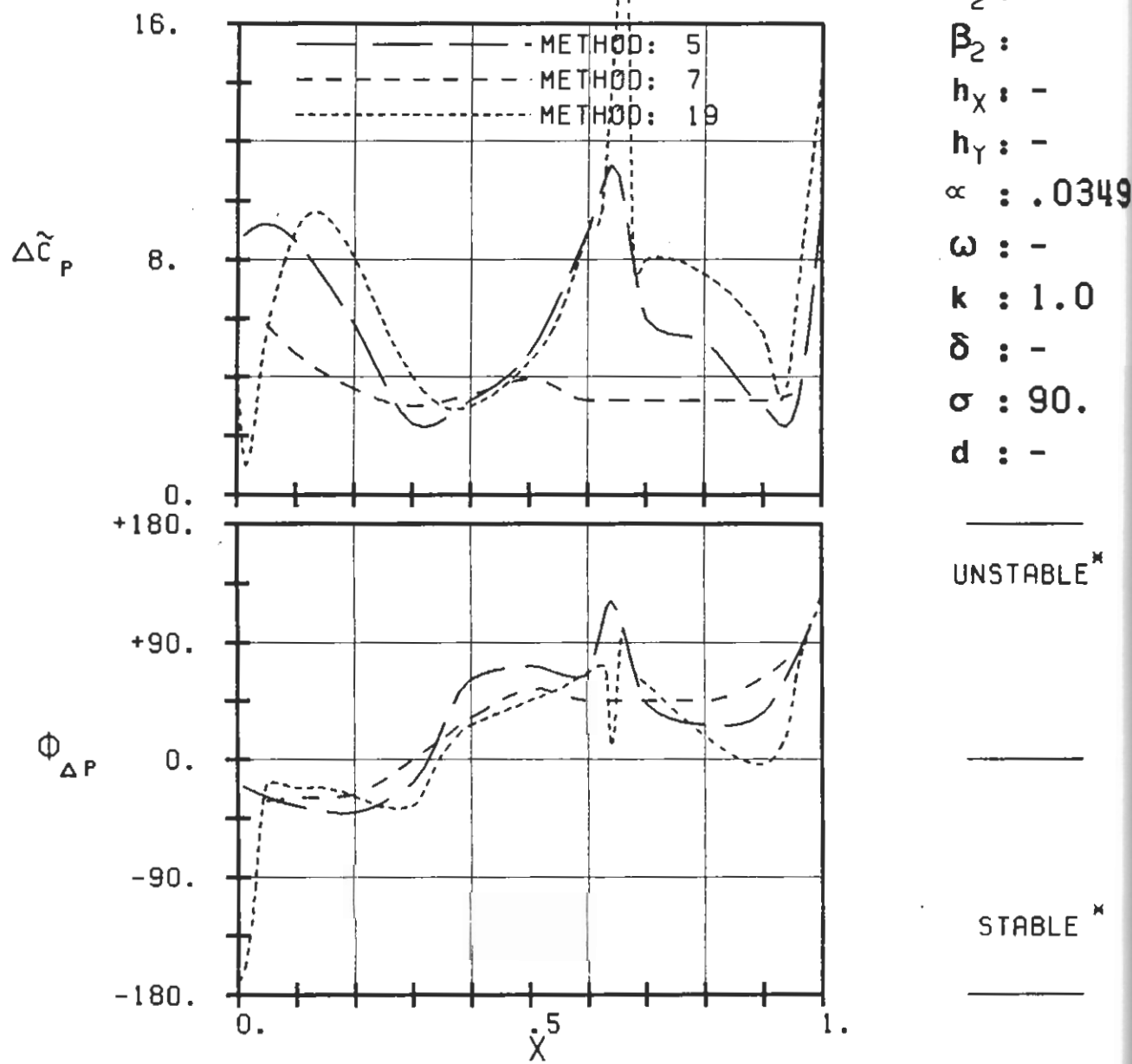
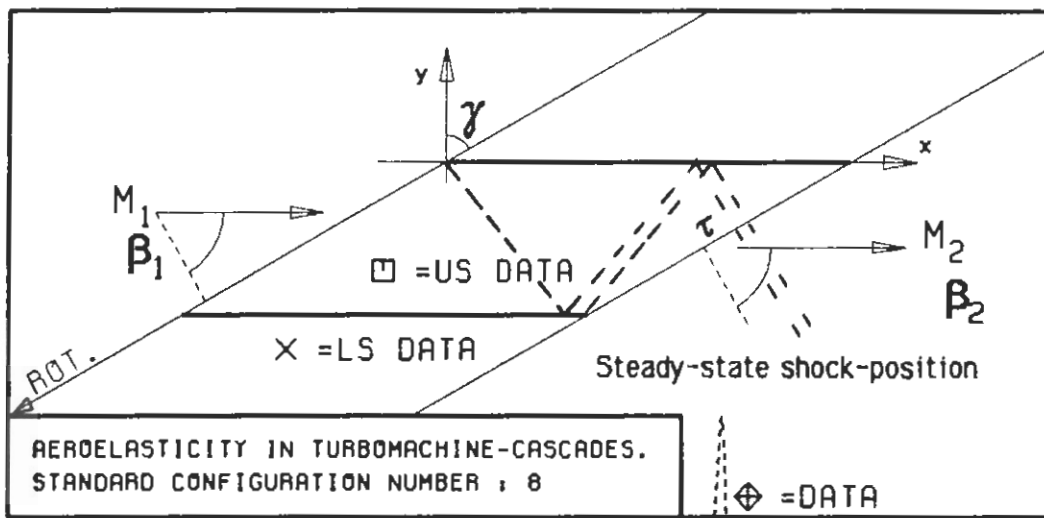
PLOT 7.8-3.20: EIGHTH STANDARD CONFIGURATION, CASE 20.
 MAGNITUDE AND PHASE LEAD OF UNSTEADY BLADE
 SURFACE PRESSURE DIFFERENCE DISTRIBUTION.
 (*: IN PITCH MODE, NOTATION VALID UPSTREAM OF PITCH AXIS)



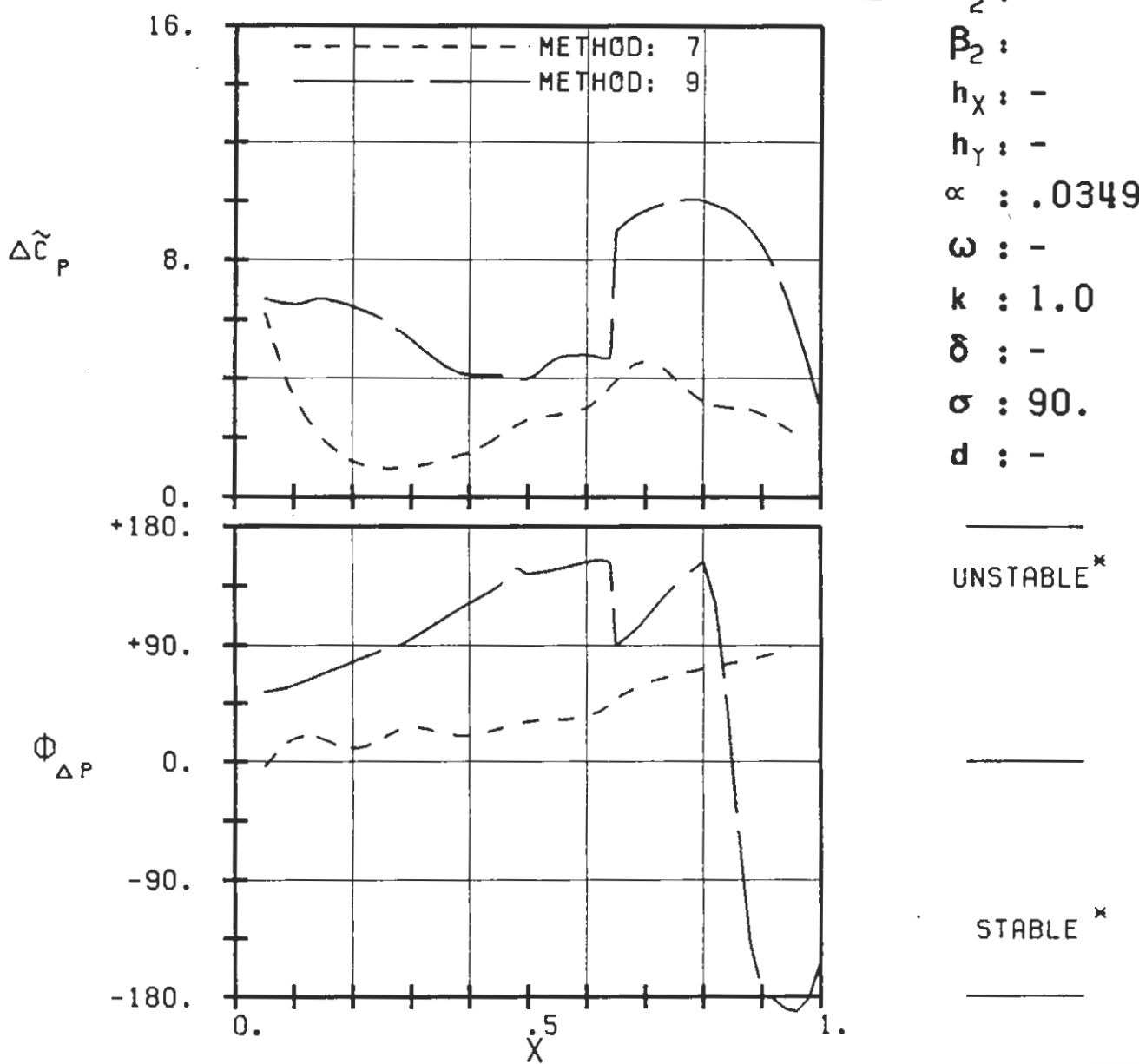
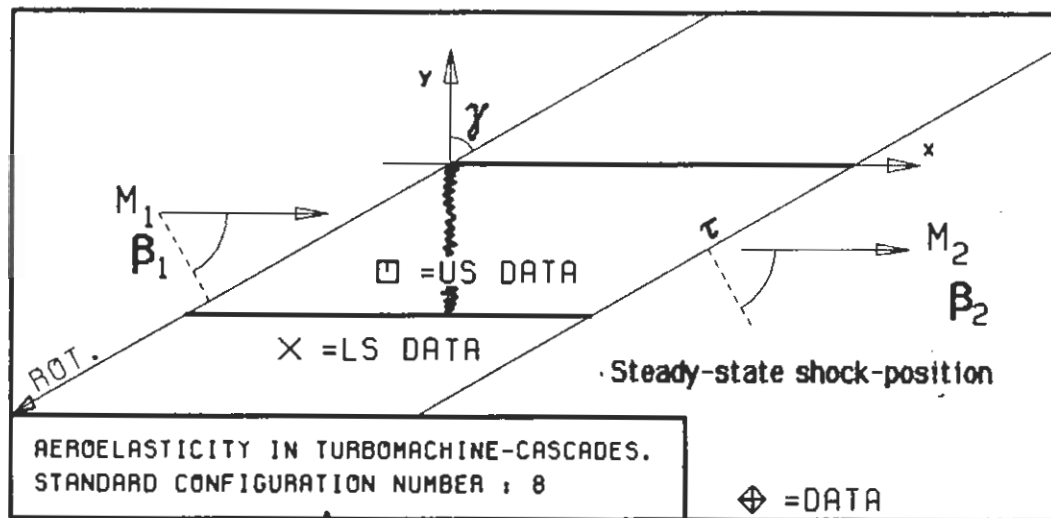
$c : 0.1M$
 $\tau : 0.75$
 $\gamma : 60.$
 $x_\infty : 0.5$
 $y_\infty : 0.$
 $M_1 : 1.2$
 $\beta_1 : -60.$
 $i : 0.$
 $M_2 : -$
 $\beta_2 : -$
 $h_x : -$
 $h_y : -$
 $\alpha : .0349$
 $\omega : -$
 $k : 1.0$
 $\delta : -$
 $\sigma : 90.$
 $d : -$



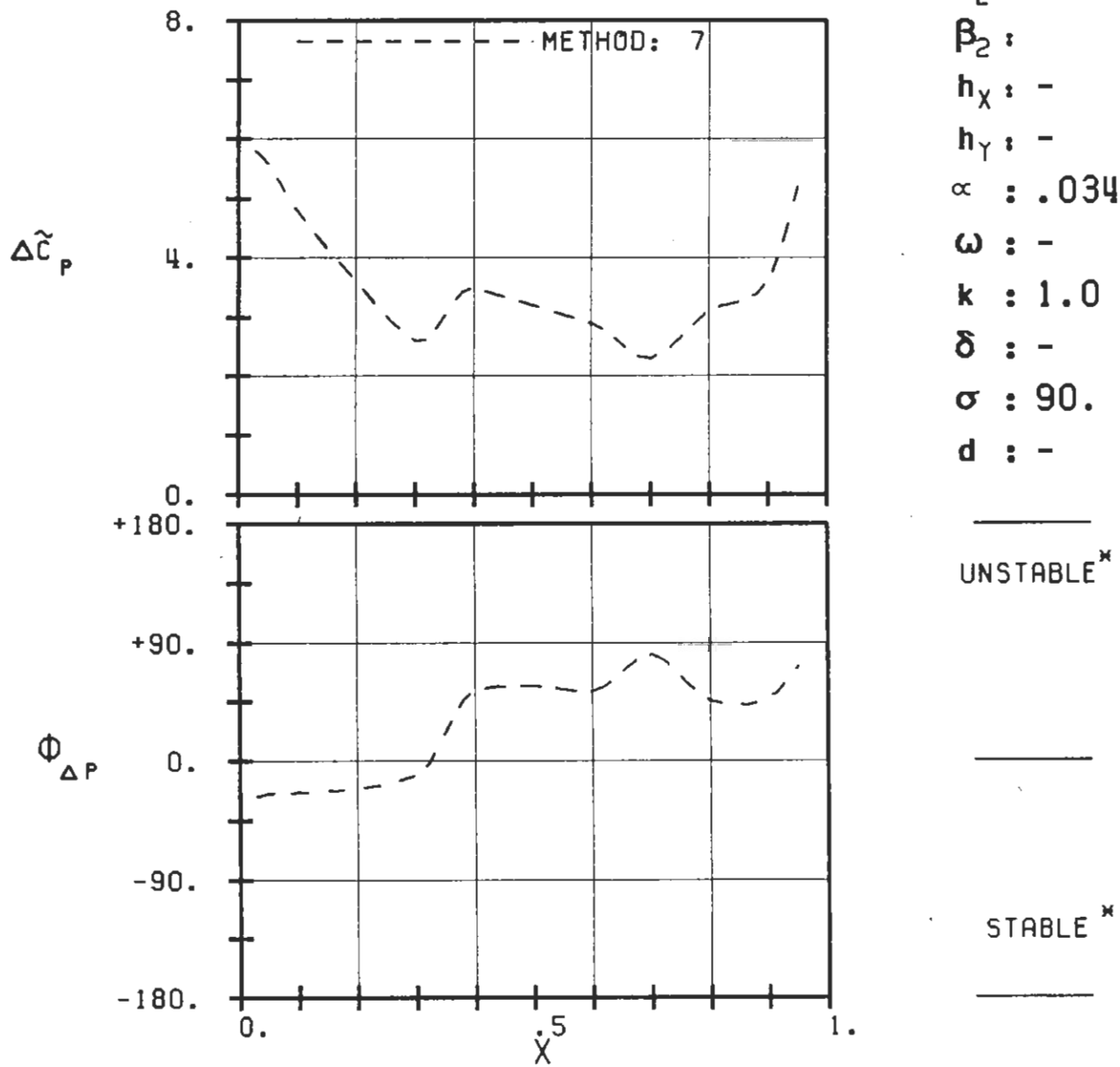
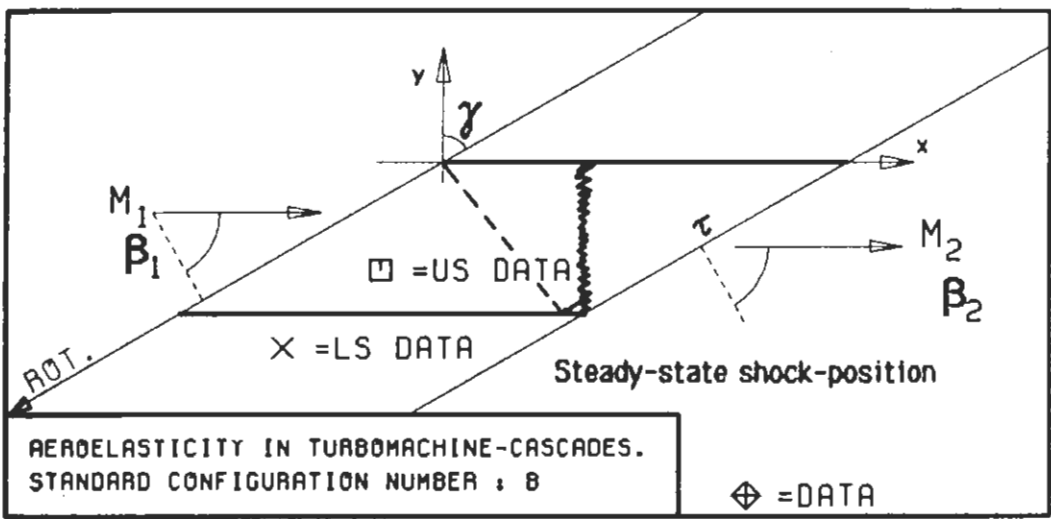
PLOT 7.8-3.21: EIGHTH STANDARD CONFIGURATION, CASE 21.
 MAGNITUDE AND PHASE LEAD OF UNSTEADY BLADE
 SURFACE PRESSURE DIFFERENCE DISTRIBUTION.
 (*: IN PITCH MODE, NOTATION VALID UPSTREAM OF PITCH AXIS)



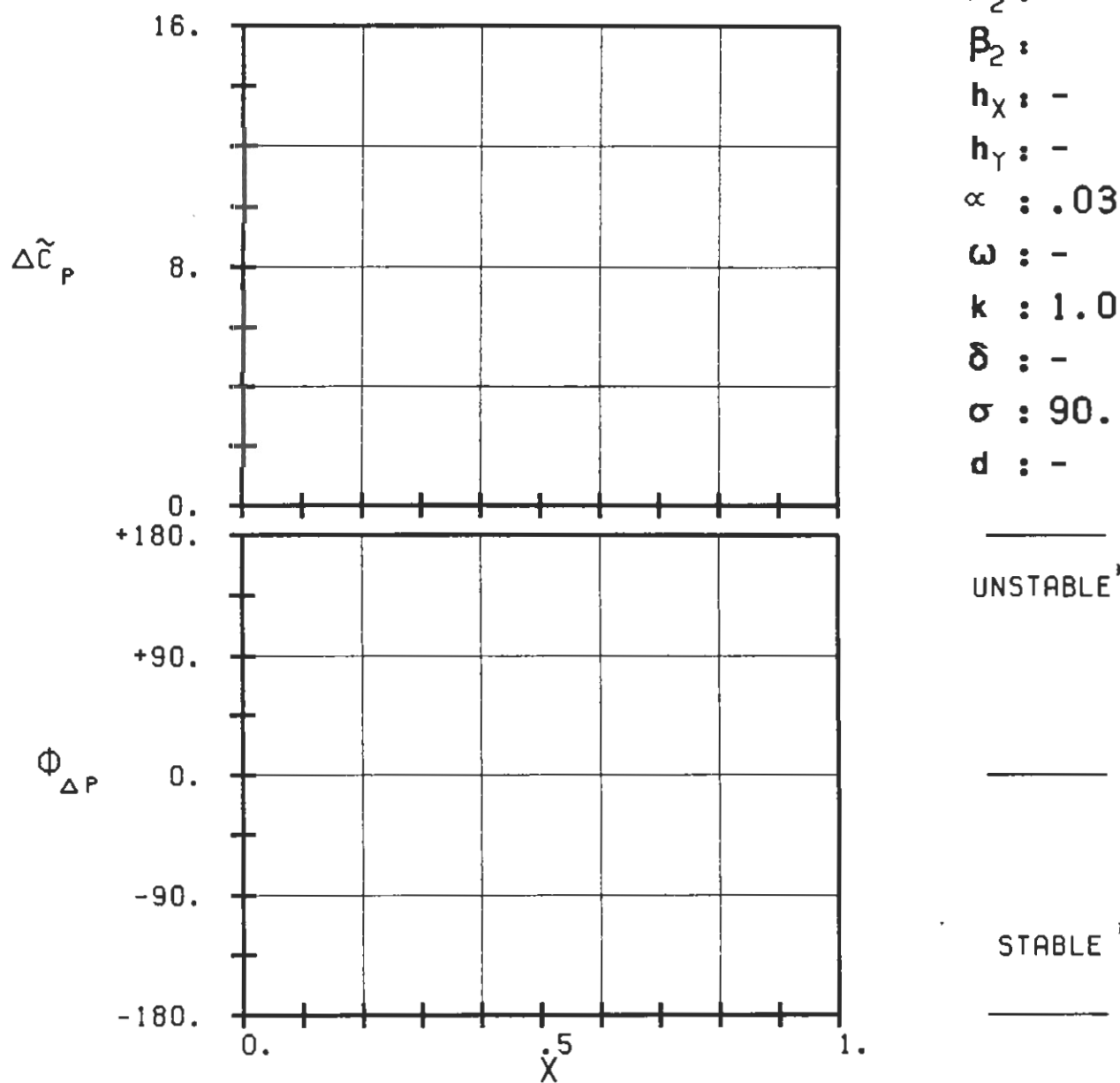
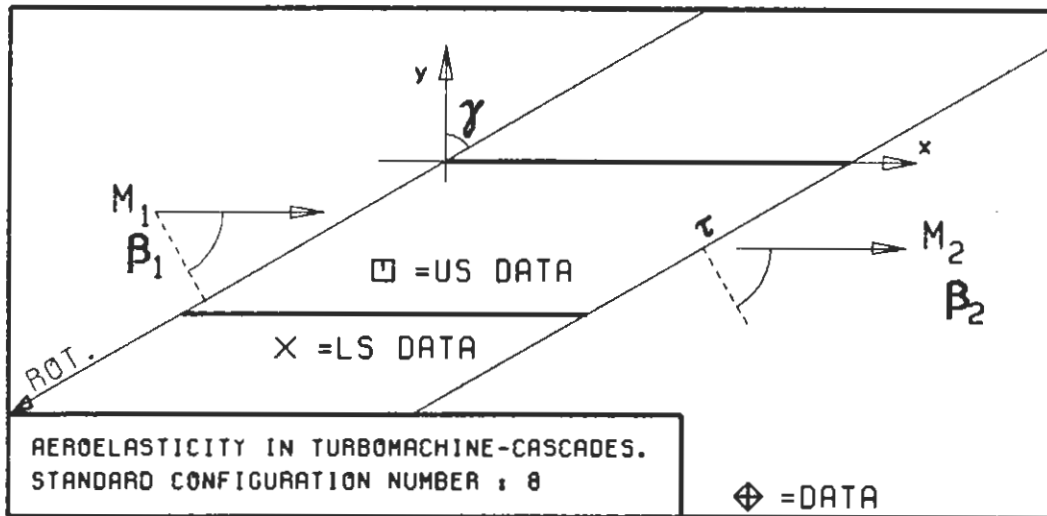
PLOT 7.8-3.22: EIGHTH STANDARD CONFIGURATION, CASE 22.
MAGNITUDE AND PHASE LEAD OF UNSTEADY BLADE
SURFACE PRESSURE DIFFERENCE DISTRIBUTION.
(*: IN PITCH MODE, NOTATION VALID UPSTREAM OF PITCH AXIS)



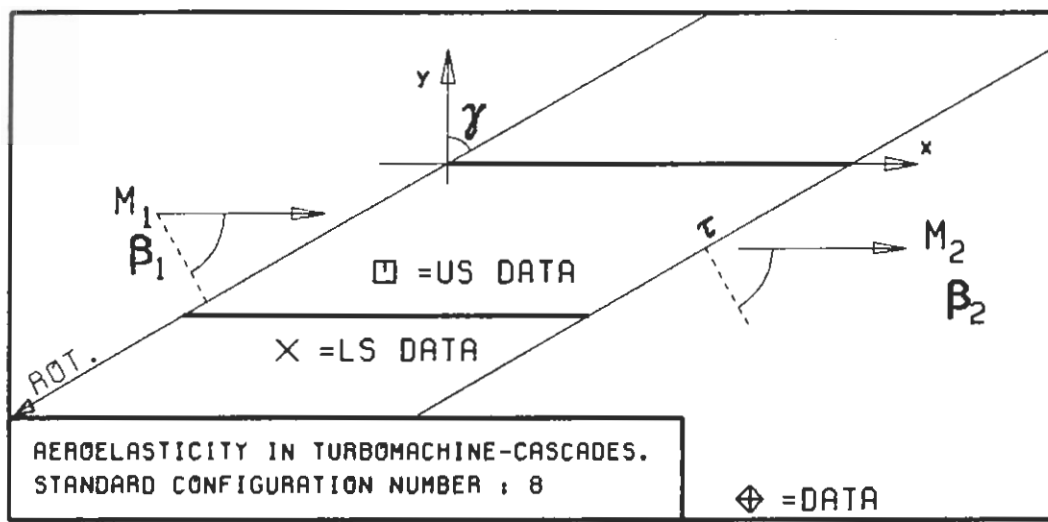
PLOT 7.8-3.23: EIGHTH STANDARD CONFIGURATION, CASE 23.
MAGNITUDE AND PHASE LEAD OF UNSTEADY BLADE SURFACE PRESSURE DIFFERENCE DISTRIBUTION.
(x: IN PITCH MODE, NOTATION VALID UPSTREAM OF PITCH AXIS)



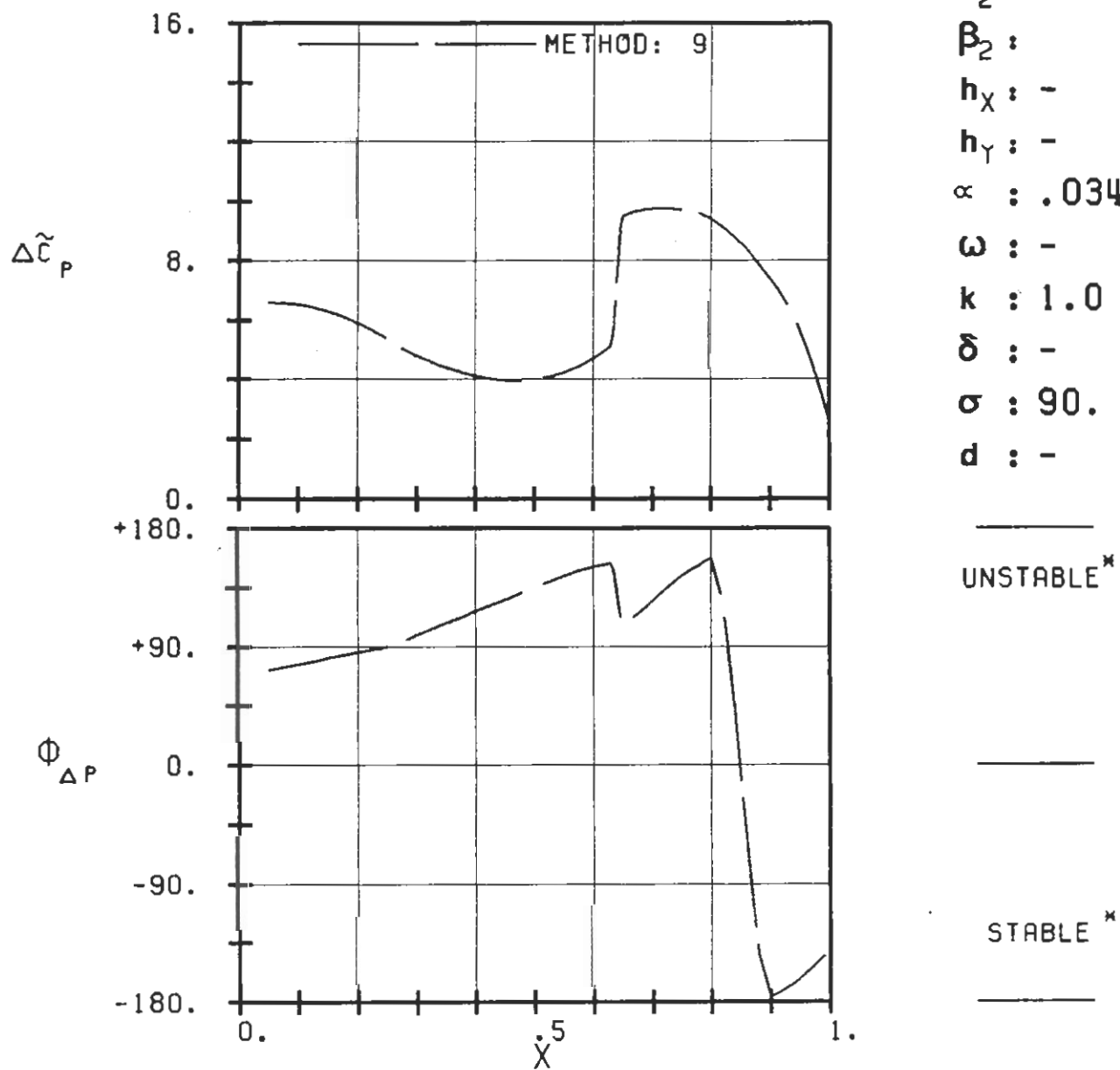
PLOT 7.8-3.24: EIGHTH STANDARD CONFIGURATION, CASE 24.
MAGNITUDE AND PHASE LEAD OF UNSTEADY BLADE
SURFACE PRESSURE DIFFERENCE DISTRIBUTION.
(*: IN PITCH MODE, NOTATION VALID UPSTREAM OF PITCH AXIS)



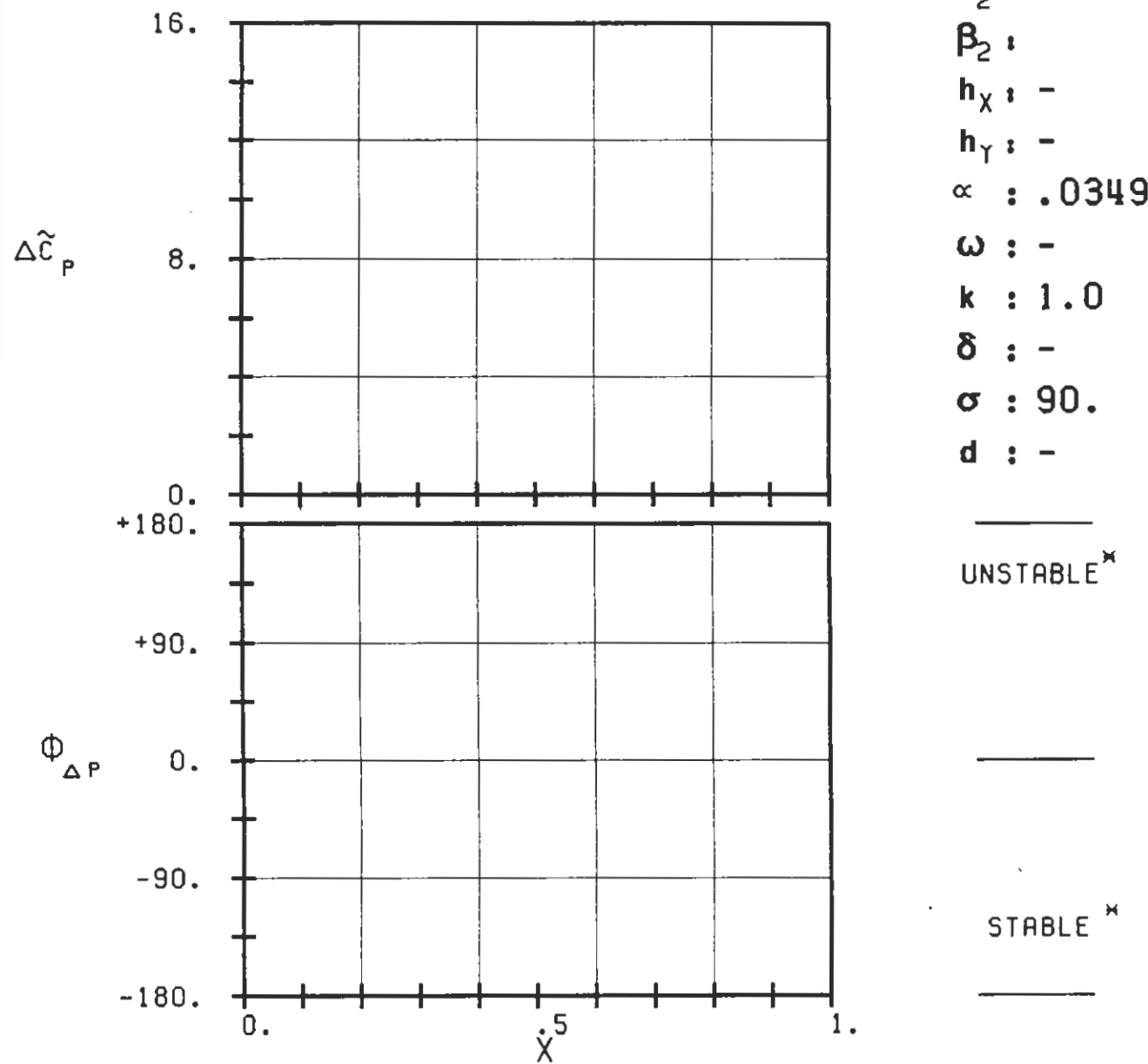
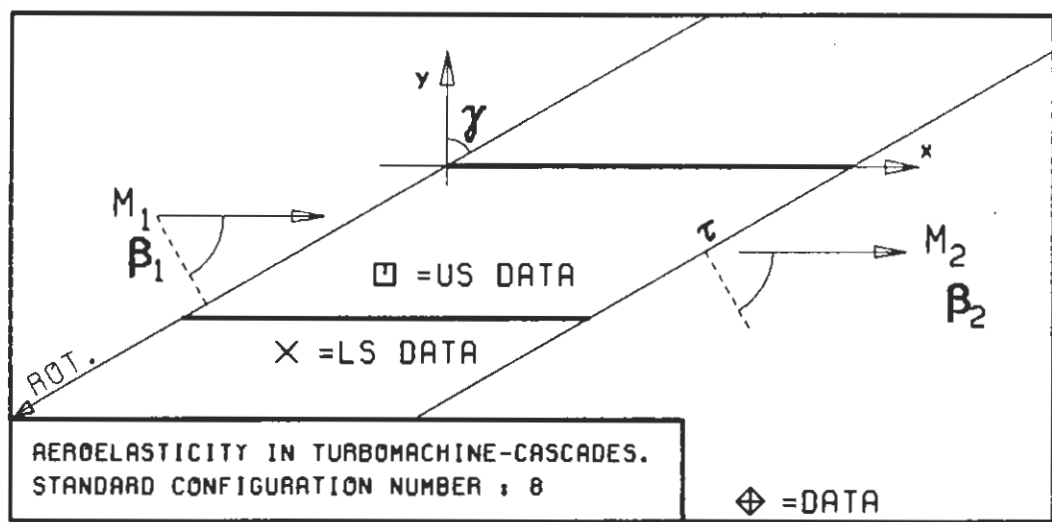
PLOT 7.8-3.25: EIGHTH STANDARD CONFIGURATION, CASE 25
MAGNITUDE AND PHASE LEAD OF UNSTEADY BLADE
SURFACE PRESSURE DIFFERENCE DISTRIBUTION.
(*: IN PITCH MODE, NOTATION VALID UPSTREAM OF PITCH AXIS)



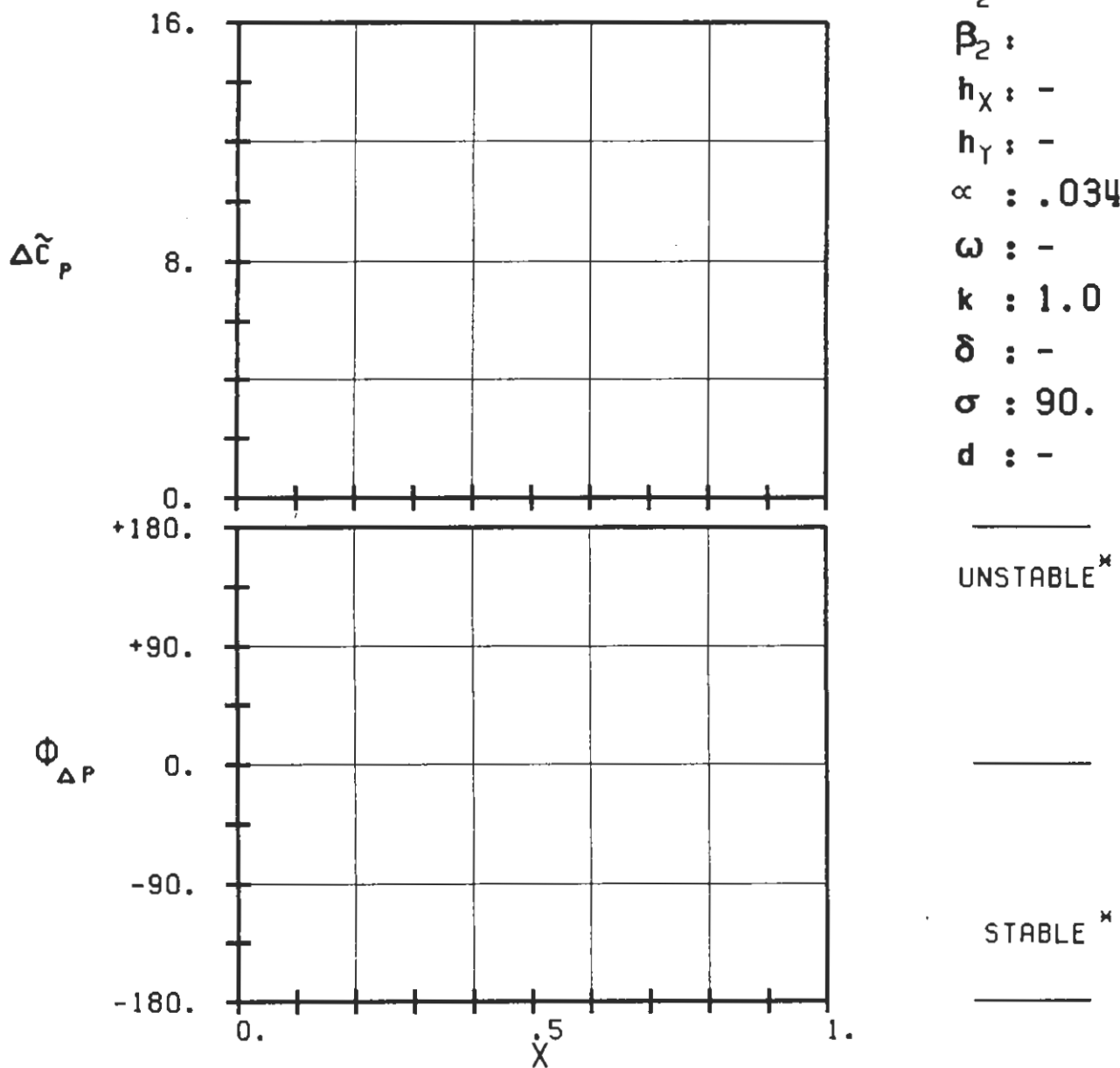
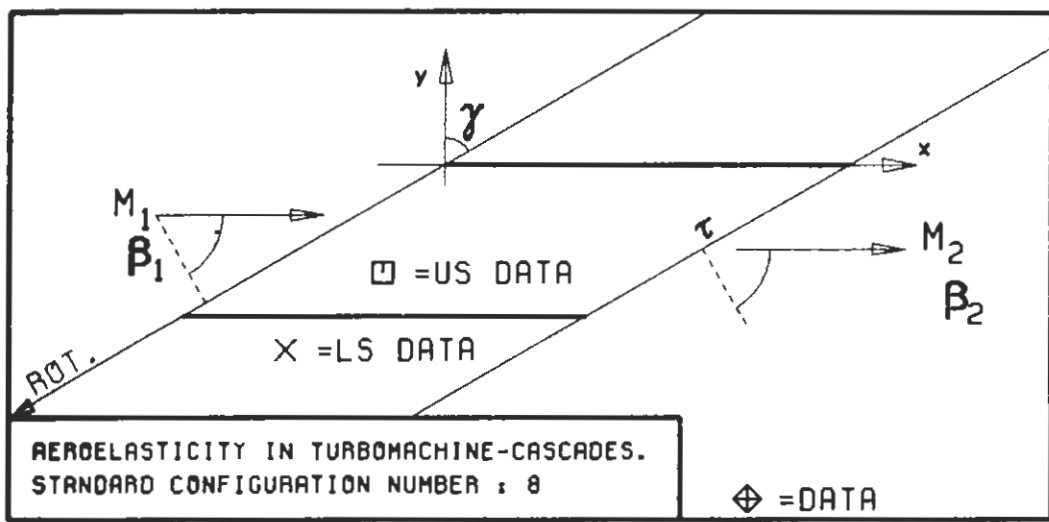
c : 0.1M
 τ : 0.75
 γ : 60.
 x_α : 0.5
 y_α : 0.
 M_1 : 1.4
 β_1 : -60.
 i : 0.
 M_2 : -
 β_2 : -
 h_X : -
 h_Y : -
 α : .0349
 ω : -
 k : 1.0
 δ : -
 σ : 90.
 d : -



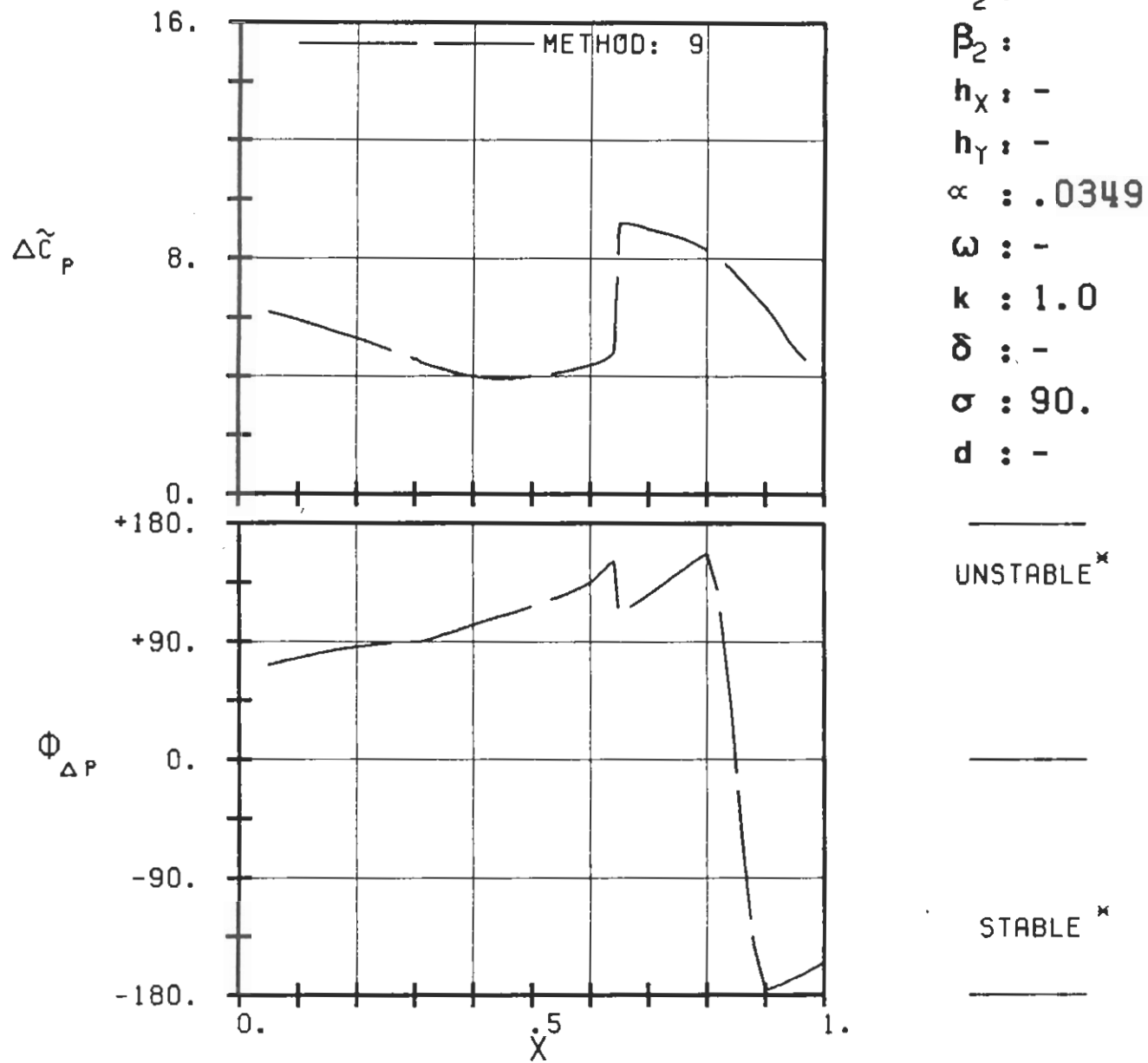
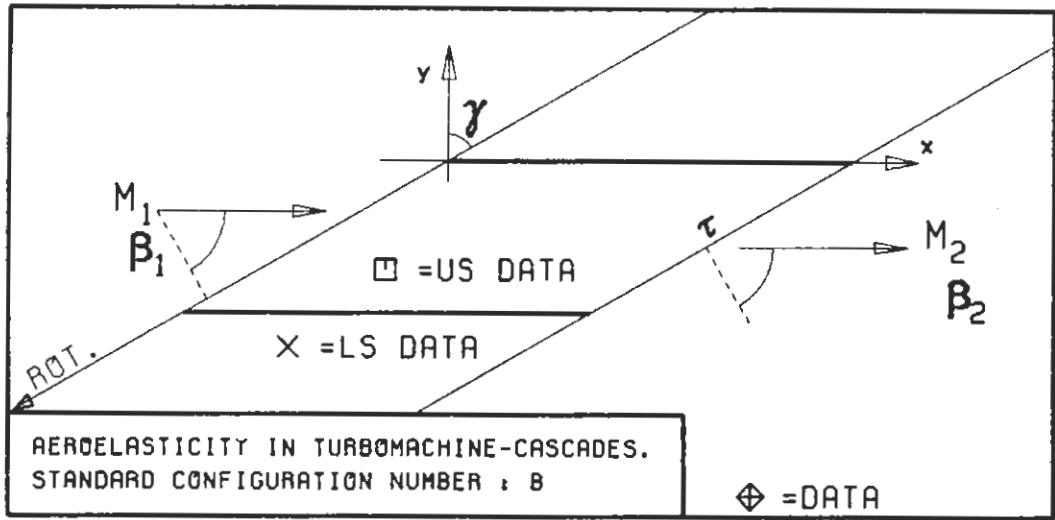
PLOT 7.8-3.26: EIGHTH STANDARD CONFIGURATION, CASE 26.
 MAGNITUDE AND PHASE LEAD OF UNSTEADY BLADE
 SURFACE PRESSURE DIFFERENCE DISTRIBUTION.
 (*: IN PITCH MODE, NOTATION WRT UPSTREAM OF PITCH AXIS)



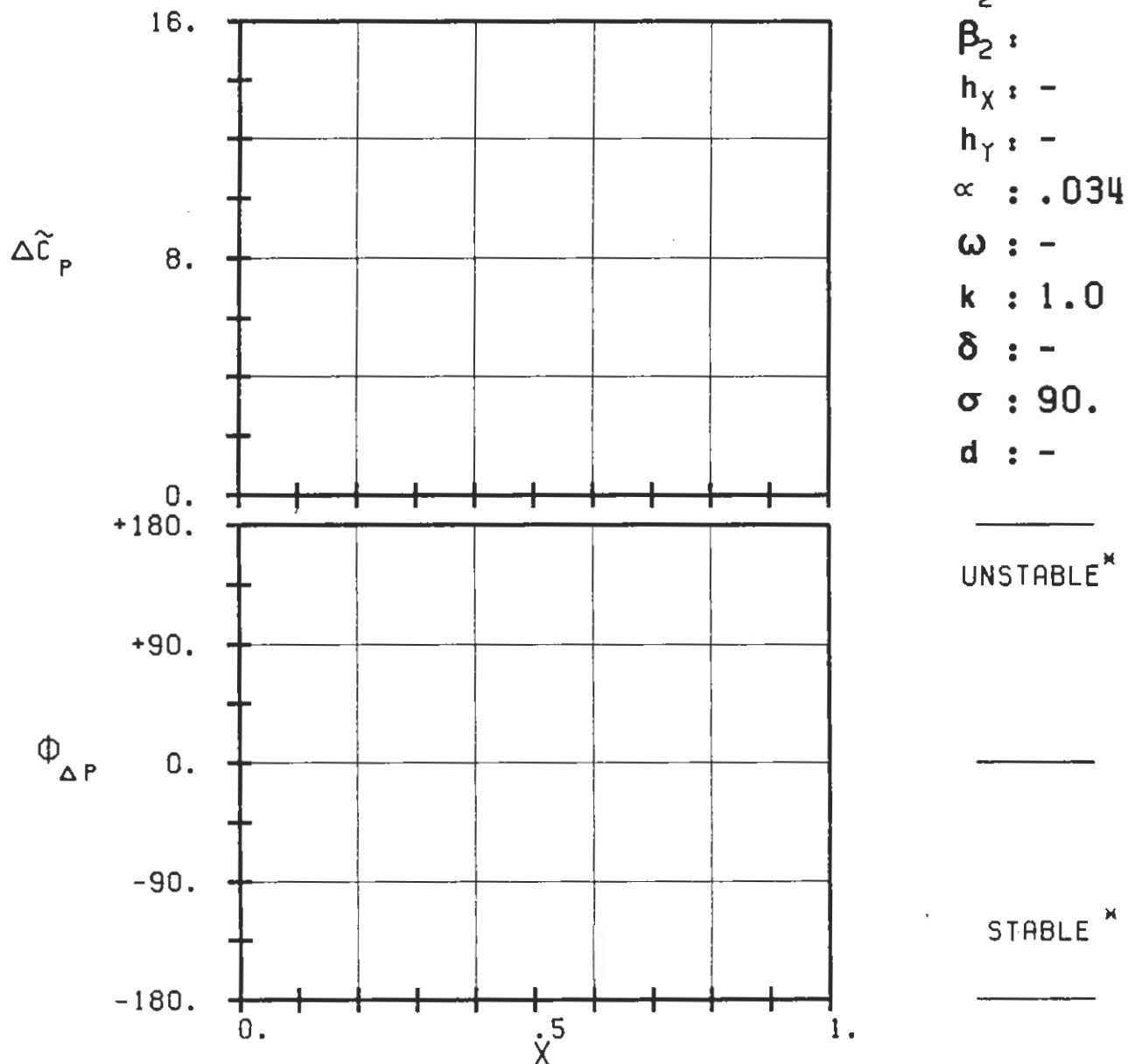
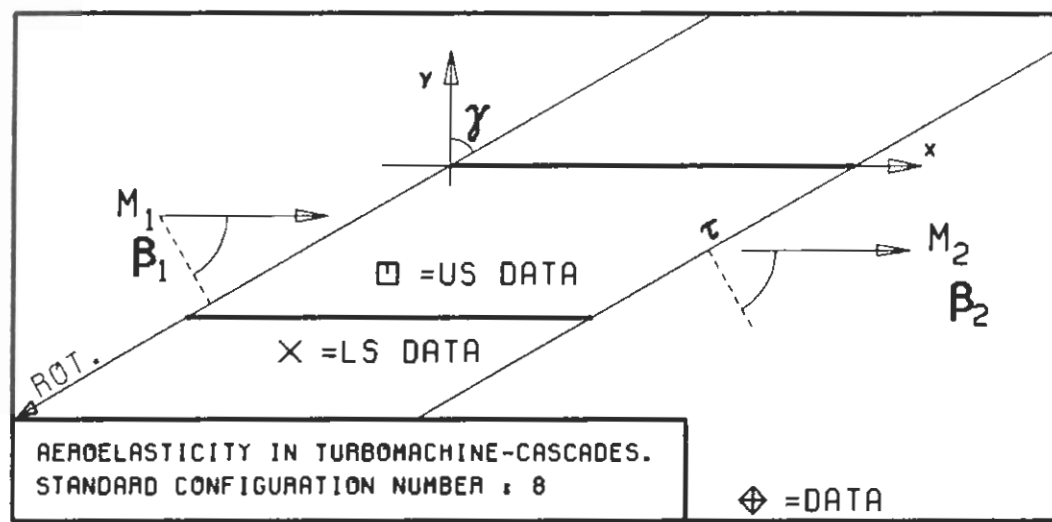
PLOT 7.8-3.27: EIGHTH STANDARD CONFIGURATION, CASE 27.
 MAGNITUDE AND PHASE LEAD OF UNSTEADY BLADE
 SURFACE PRESSURE DIFFERENCE DISTRIBUTION.
 (\times : IN PITCH MODE, NOTATION VALID UPSTREAM OF PITCH AXIS)



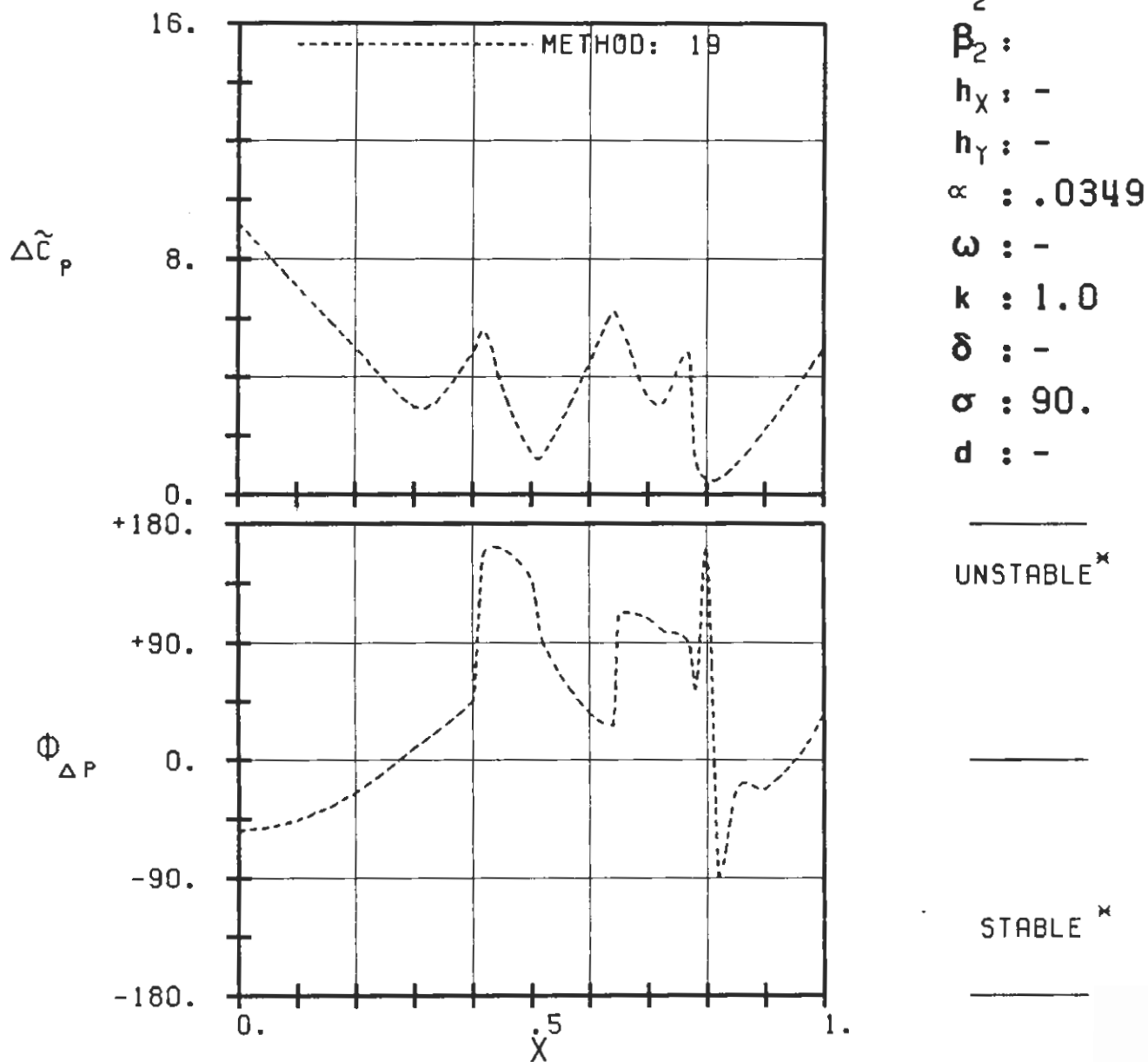
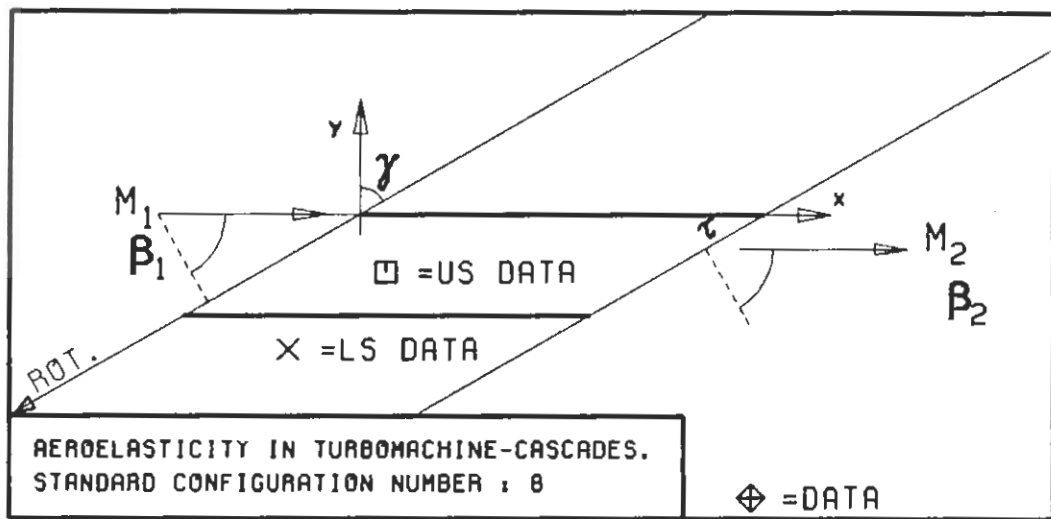
$c : 0.1M$
 $\tau : 0.75$
 $\gamma : 60.$
 $x_\alpha : 0.5$
 $y_\alpha : 0.$
 $M_1 : 1.5$
 $\beta_1 : -60.$
 $i : 0.$
 $M_2 : -$
 $\beta_2 : -$
 $h_X : -$
 $h_Y : -$
 $\alpha : .0349$
 $\omega : -$
 $k : 1.0$
 $\delta : -$
 $\sigma : 90.$
 $d : -$



PLOT 7.8-3.29: EIGHTH STANDARD CONFIGURATION, CASE 29.
 MAGNITUDE AND PHASE LEAD OF UNSTEADY BLADE
 SURFACE PRESSURE DIFFERENCE DISTRIBUTION.
 (*: IN PITCH MODE, NOTATION VALID UPSTREAM OF PITCH AXIS)

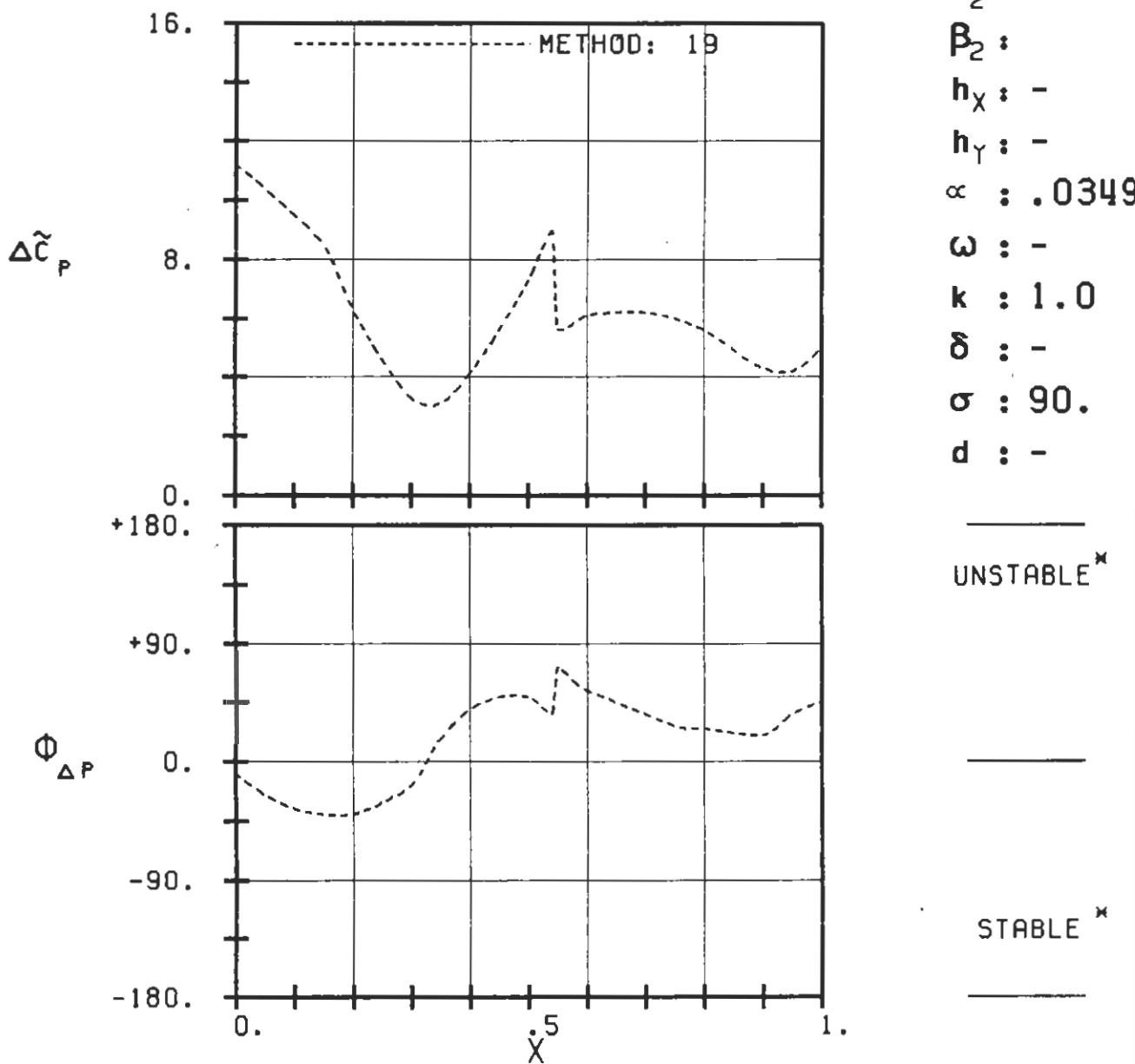
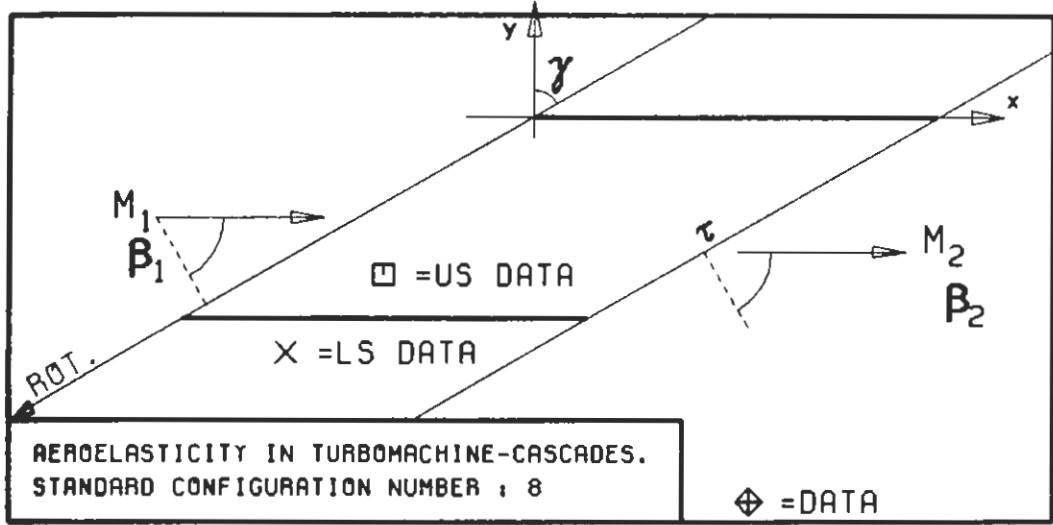


PLOT 7.8-3.30: EIGHTH STANDARD CONFIGURATION, CASE 30.
MAGNITUDE AND PHASE LEAD OF UNSTEADY BLADE
SURFACE PRESSURE DIFFERENCE DISTRIBUTION.
(*: IN PITCH MODE, NOTATION VALID UPSTREAM OF PITCH AXIS)

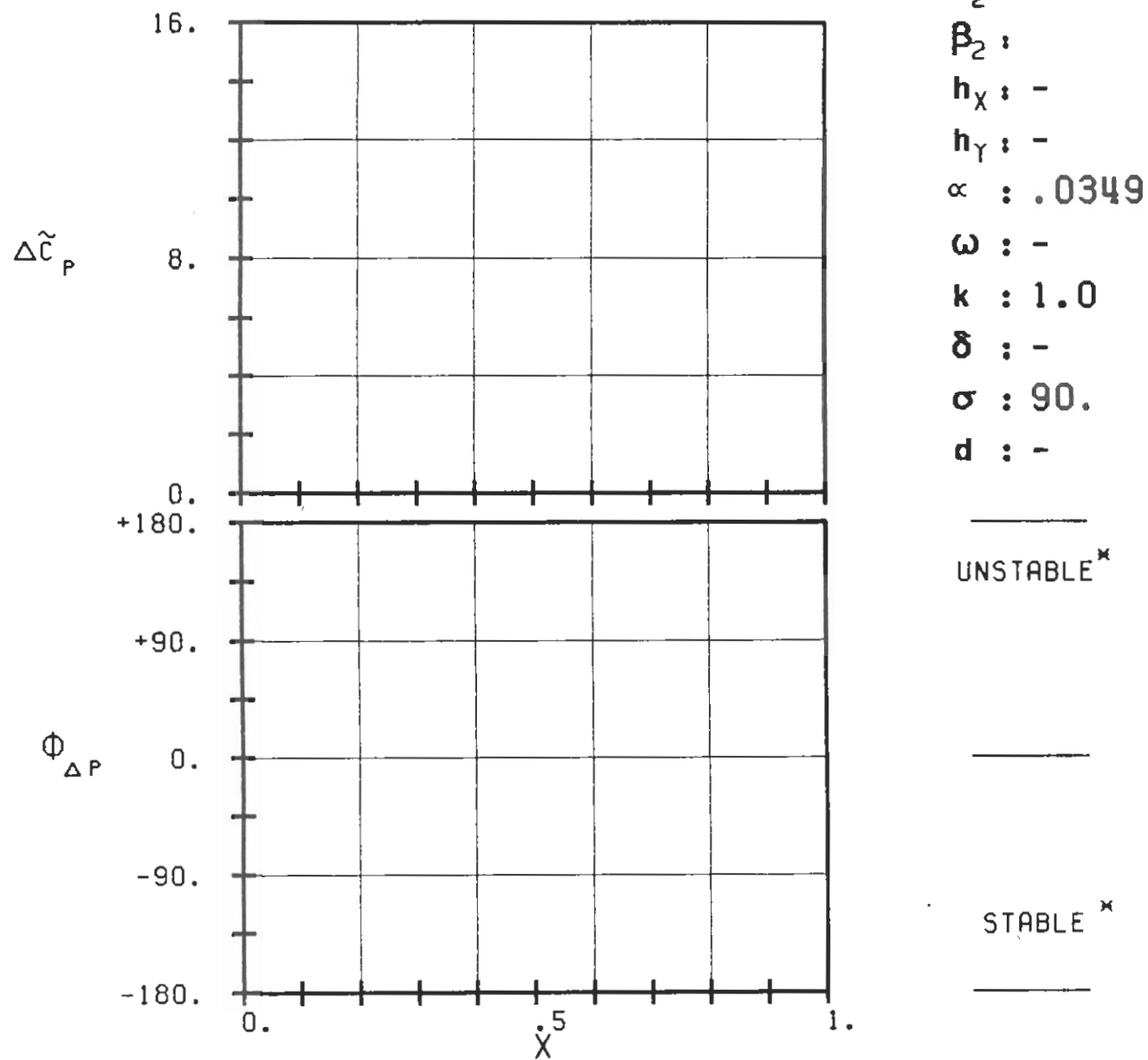
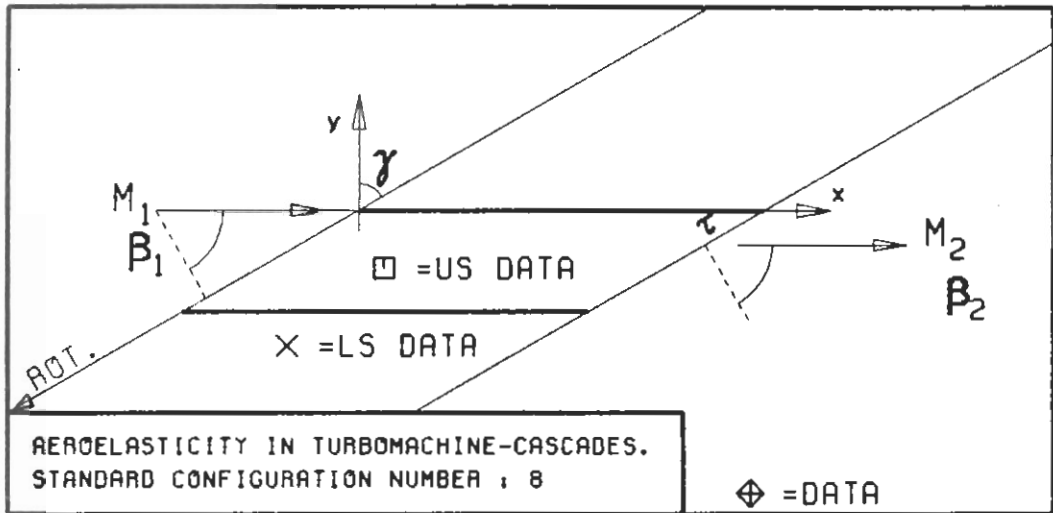


PLOT 7.8-3.31: EIGHTH STANDARD CONFIGURATION, CASE 31.
MAGNITUDE AND PHASE LEAD OF UNSTEADY BLADE
SURFACE PRESSURE DIFFERENCE DISTRIBUTION.

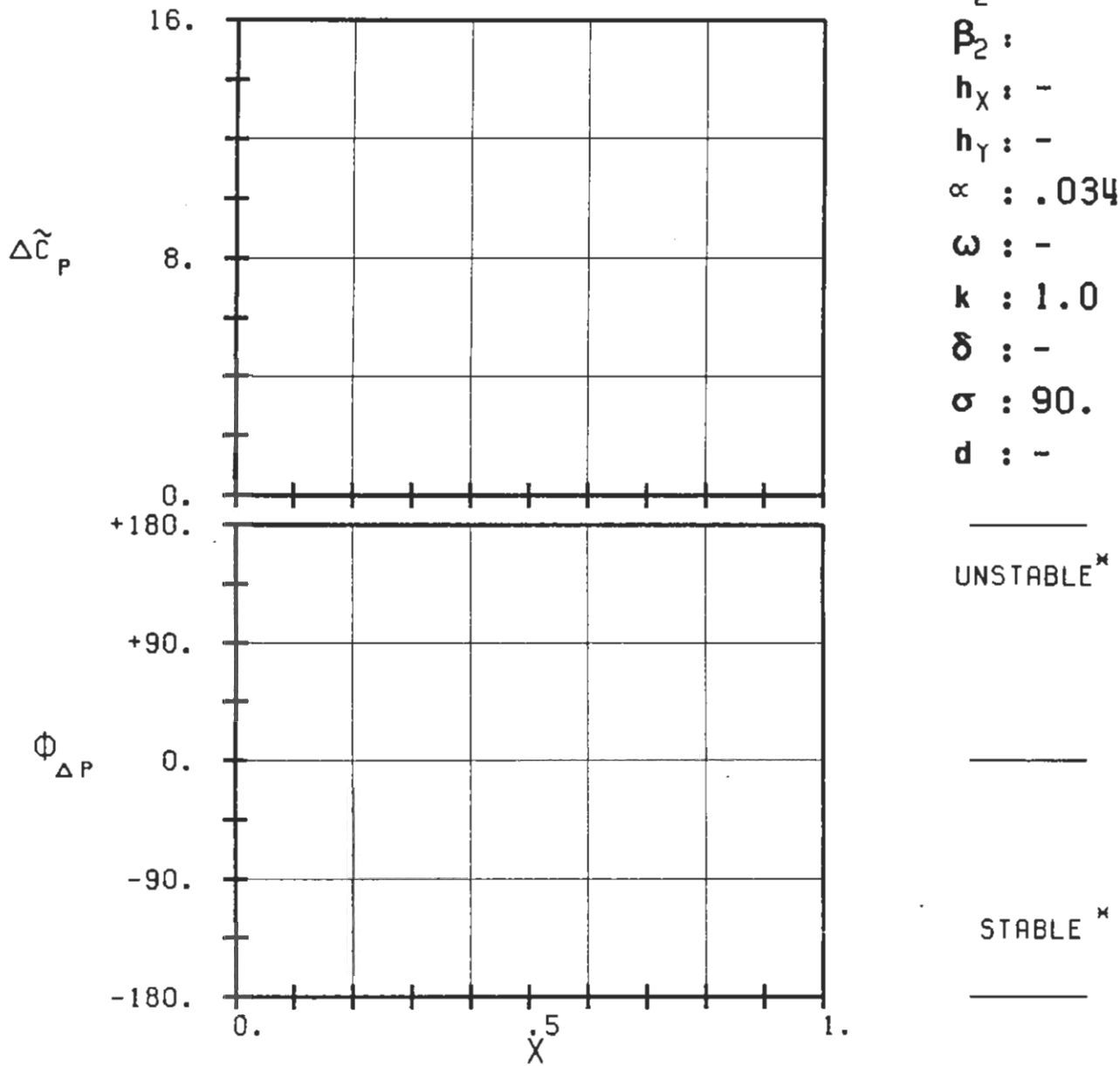
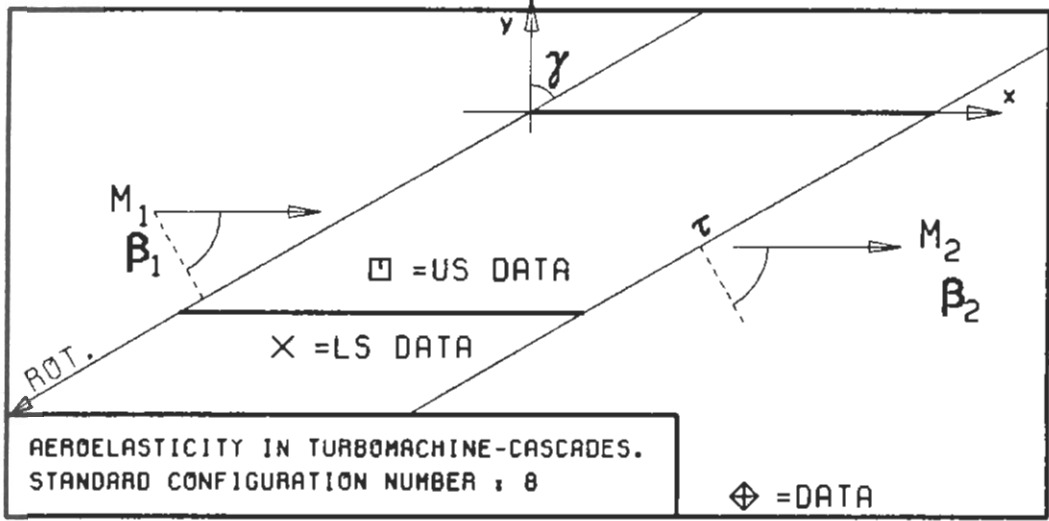
(X: IN PITCH MODE, NOTATION VALID UPSTREAM OF PITCH AXIS)



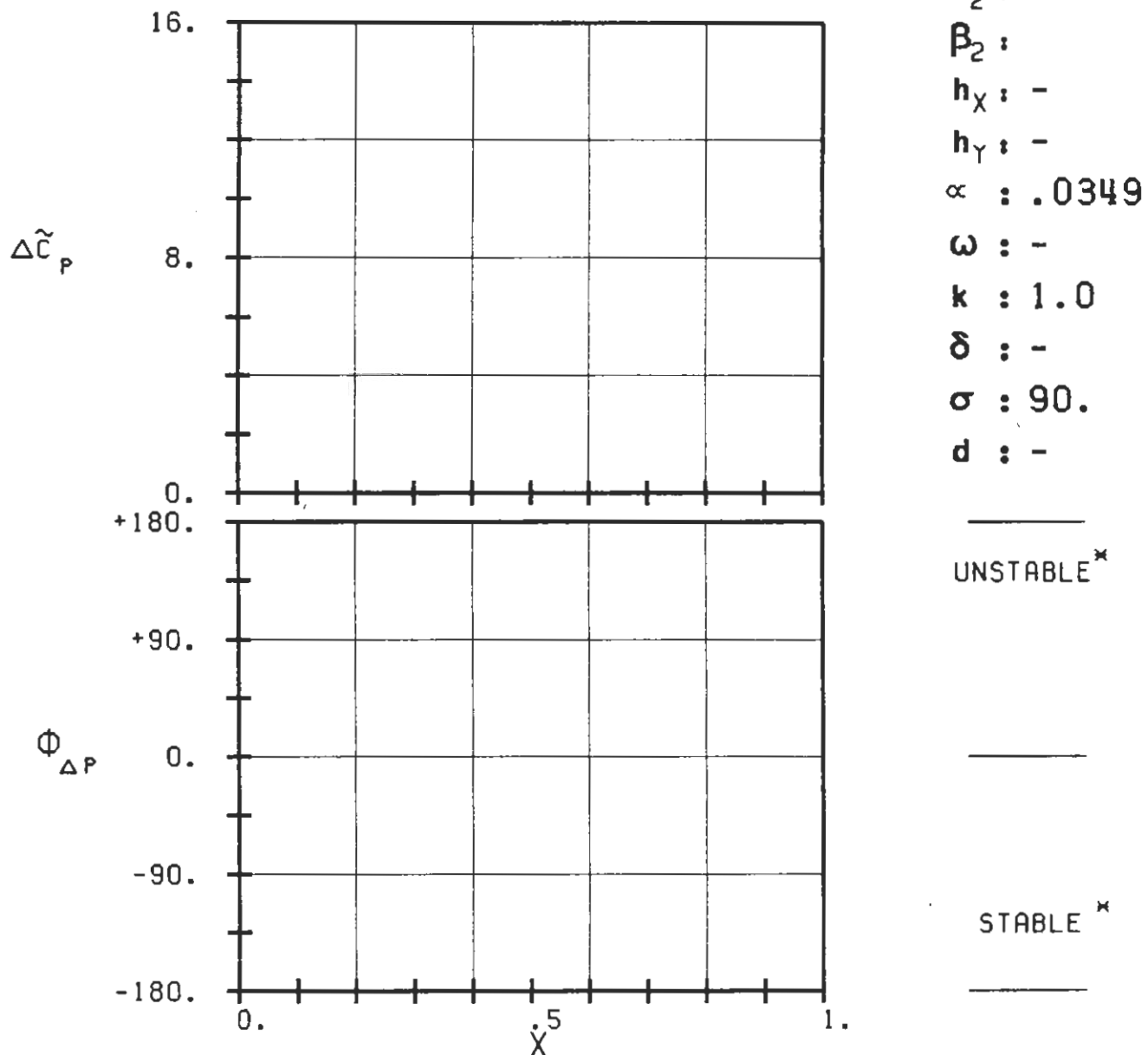
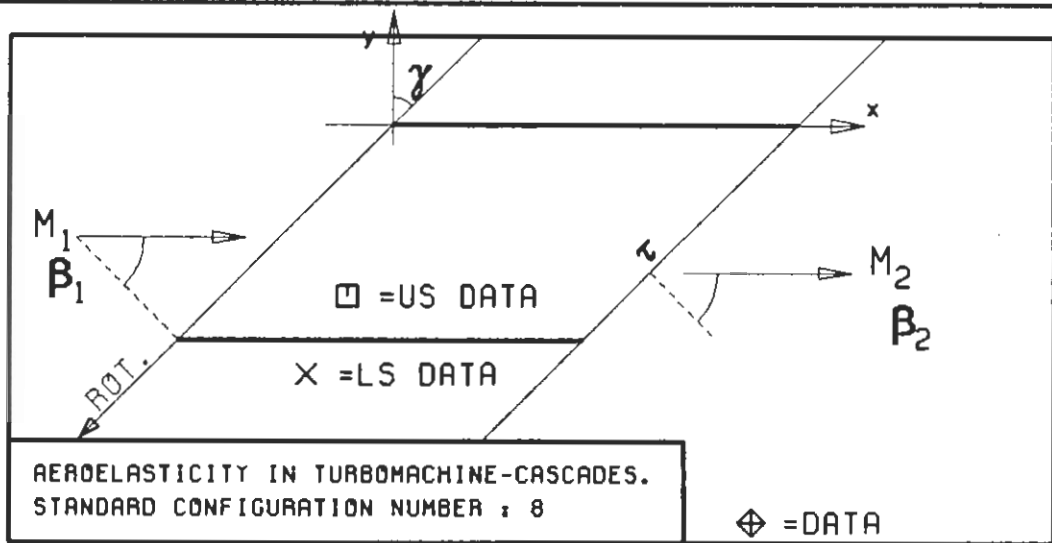
PLOT 7.8-3.32: EIGHTH STANDARD CONFIGURATION, CASE 32.
MAGNITUDE AND PHASE LEAD OF UNSTEADY BLADE
SURFACE PRESSURE DIFFERENCE DISTRIBUTION.
(\times : IN PITCH MODE, NOTATION VALID UPSTREAM OF PITCH AXIS)



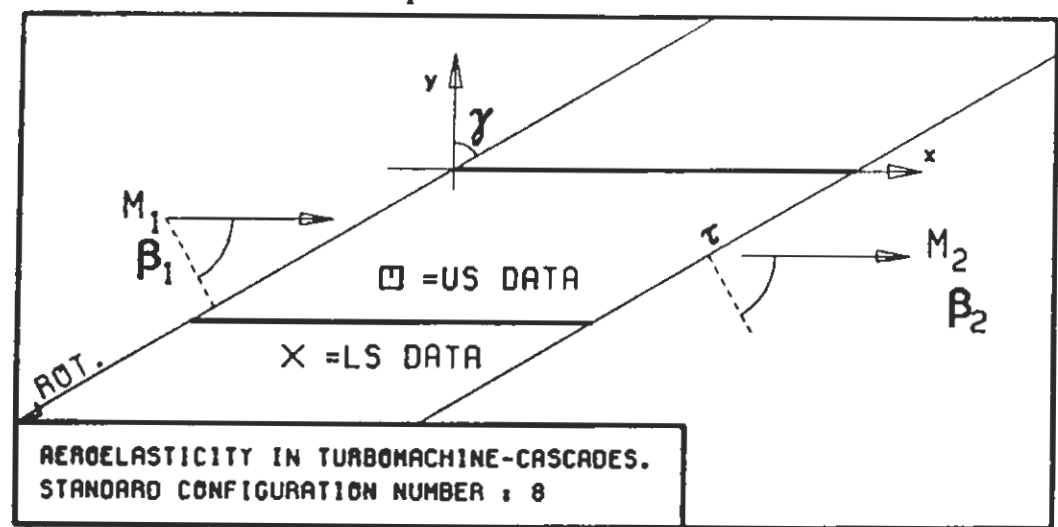
PLOT 7.8-3.33: EIGHTH STANDARD CONFIGURATION, CASE 33.
 MAGNITUDE AND PHASE LEAD OF UNSTEADY BLADE
 SURFACE PRESSURE DIFFERENCE DISTRIBUTION.
 (x: IN PITCH MODE, NOTATION VALID UPSTREAM OF PITCH AXIS)



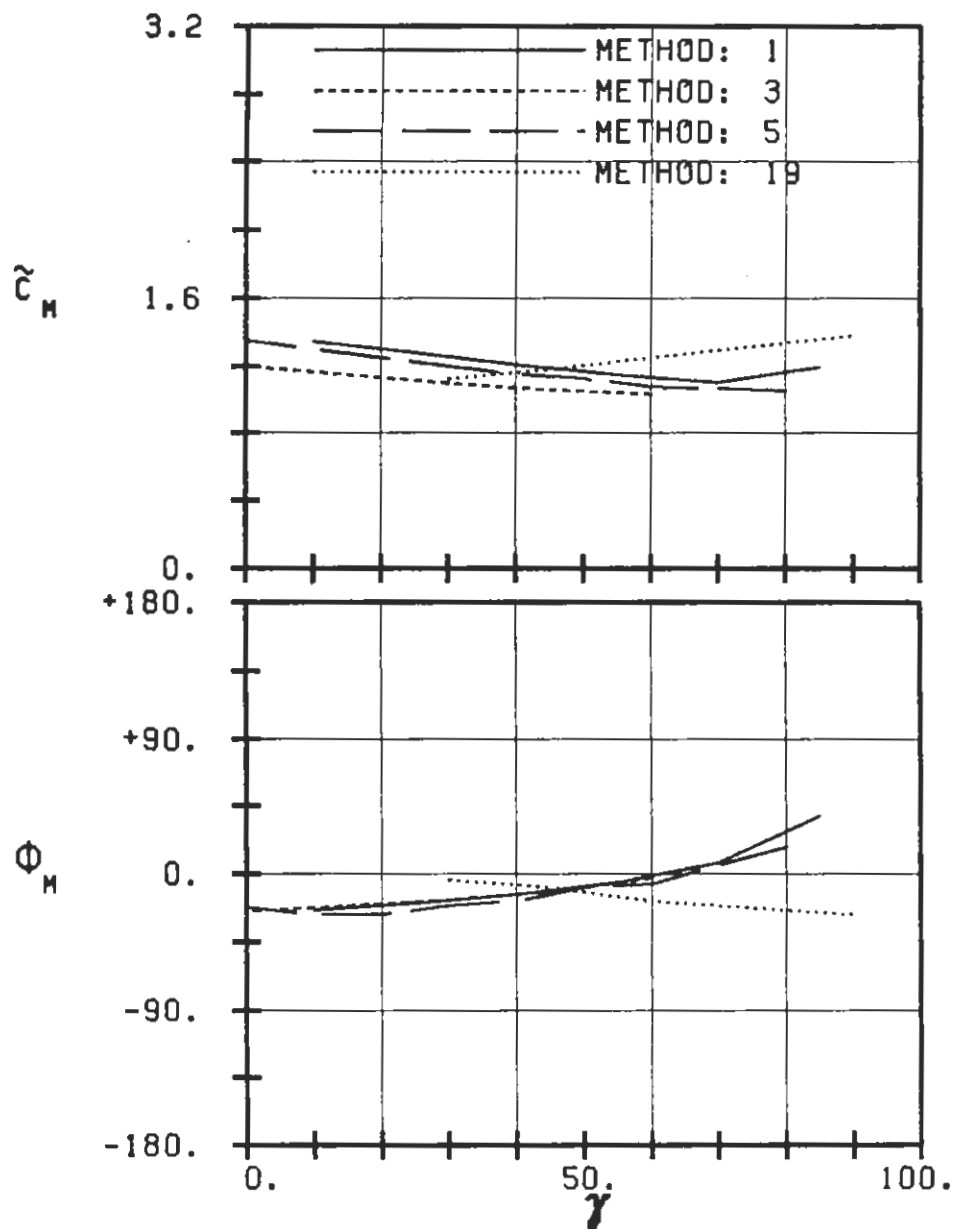
PLOT 7.8-3.34: EIGHTH STANDARD CONFIGURATION, CASE 34.
MAGNITUDE AND PHASE LEAD OF UNSTEADY BLADE
SURFACE PRESSURE DIFFERENCE DISTRIBUTION.
(\times : IN PITCH MODE, NOTATION VALID UPSTREAM OF PITCH AXIS)



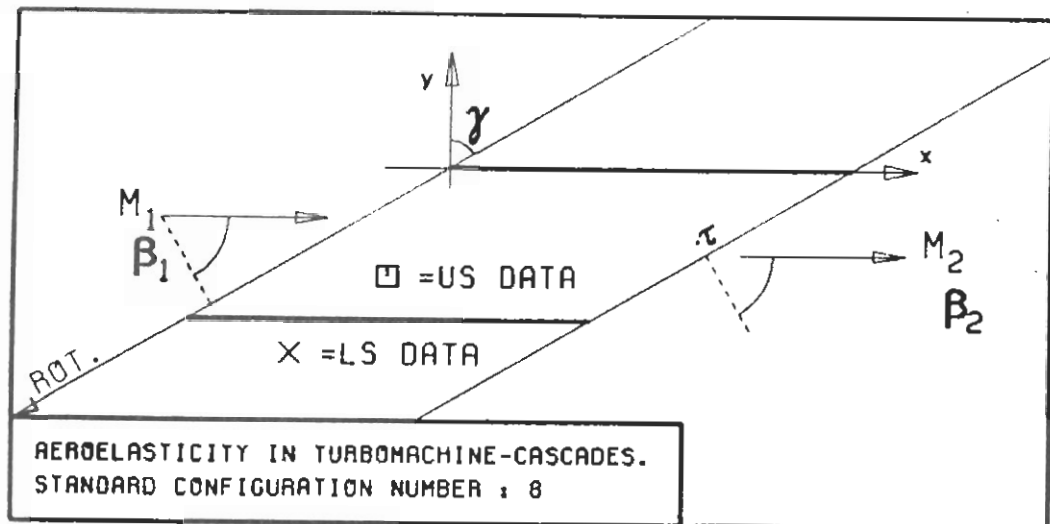
PLT 7.8-3.35: EIGHTH STANDARD CONFIGURATION, CASE 35.
MAGNITUDE AND PHASE LEAD OF UNSTEADY BLADE
SURFACE PRESSURE DIFFERENCE DISTRIBUTION.
(*: IN PITCH MODE, NOTATION VALID UPSTREAM OF PITCH AXIS)



c : 0.1M
 τ : 0.75
 γ :
 x_∞ : 0.5
 y_∞ : 0.
 M_1 : 0.
 β_1 :
 i : 0.
 M_2 : 0.
 β_2 :
 h_X : -
 h_Y : -
 α : .0349
 ω : -
 k : 1.0
 δ : -
 σ : 90.
 d : -

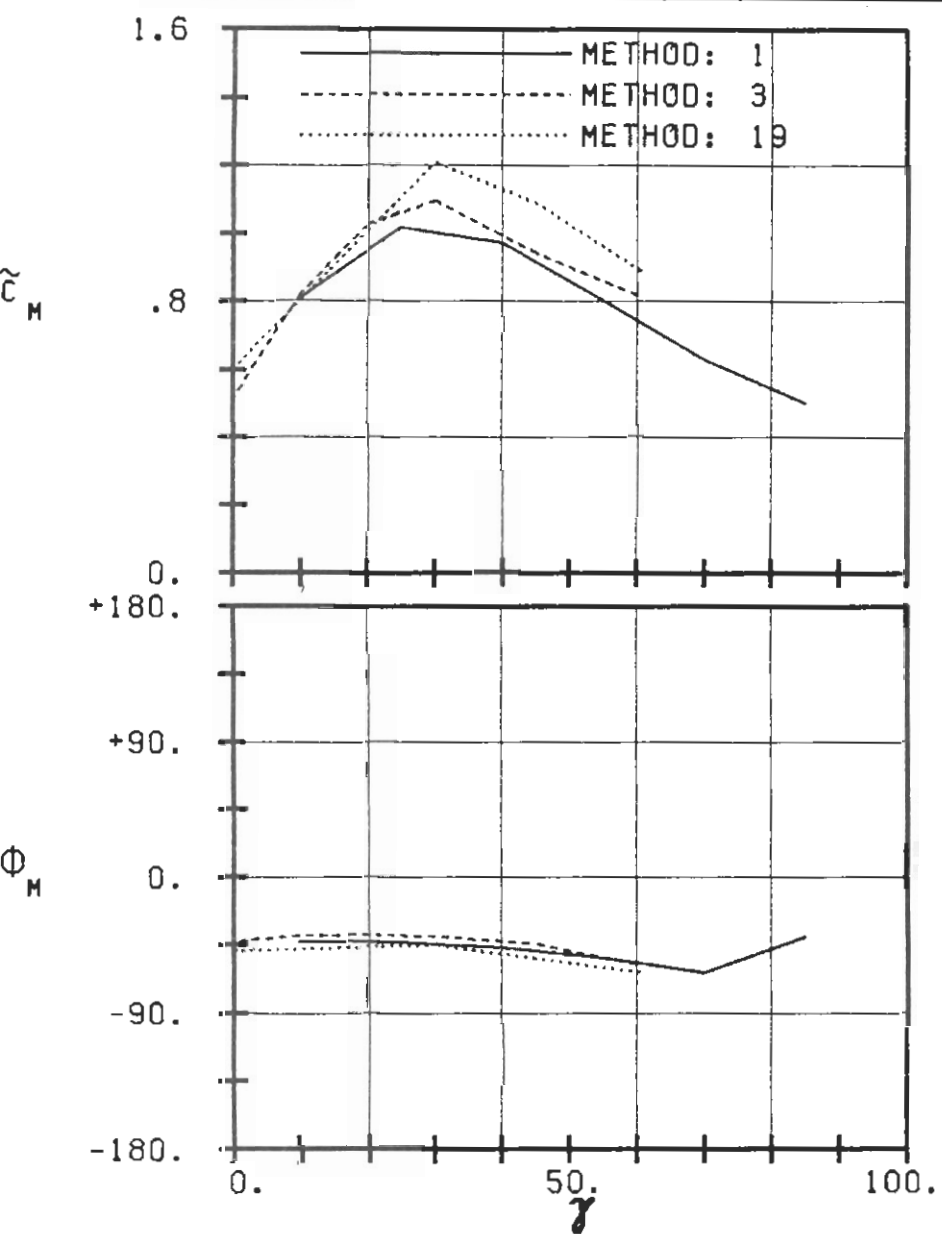


**PLOT 7.8-5.1: EIGHTH STANDARD CONFIGURATION, CASES 1-4.
AERODYNAMIC MOMENT COEFFICIENT AND PHASE LEAD
IN DEPENDANCE OF STAGGER ANGLE.**



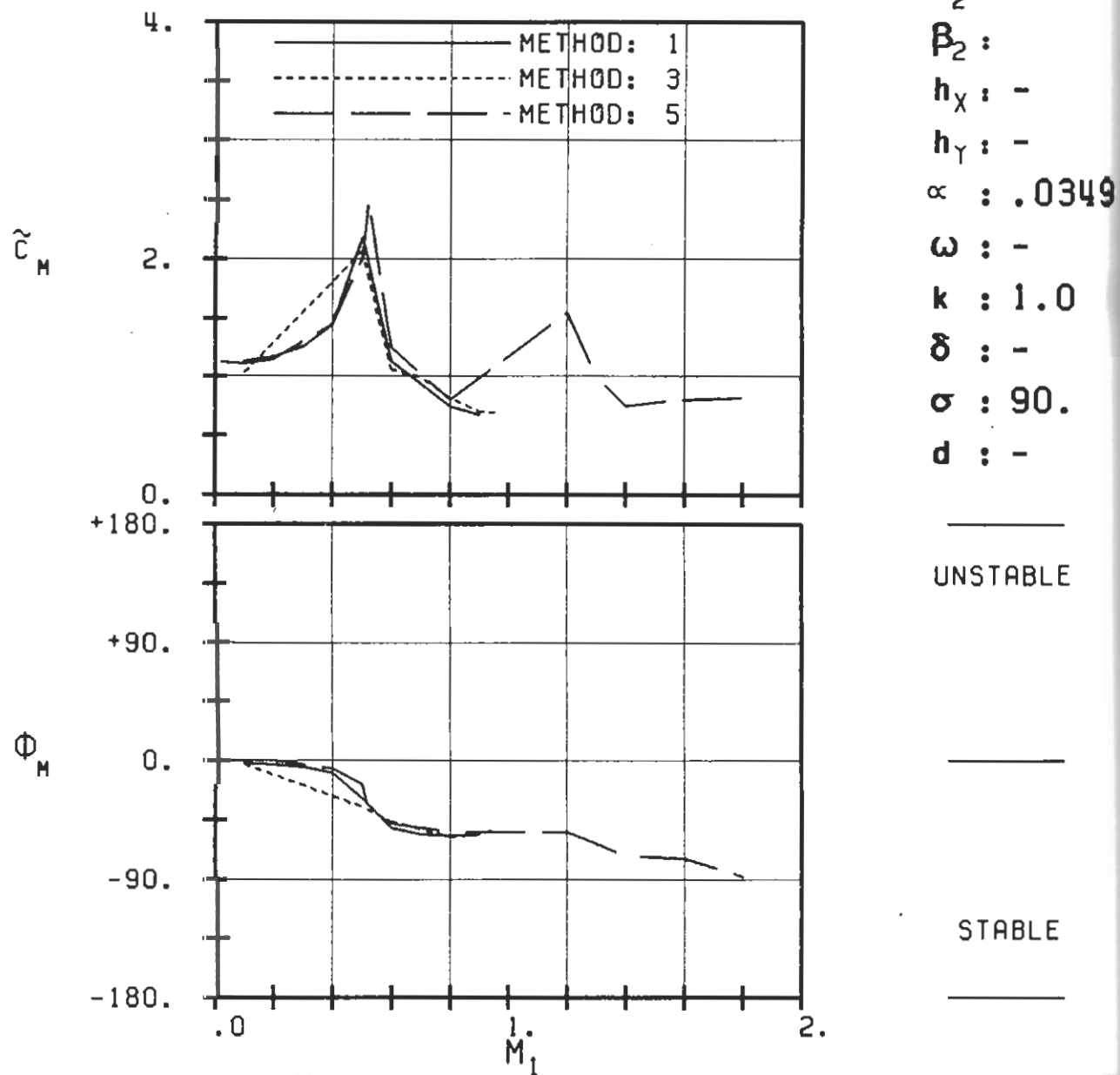
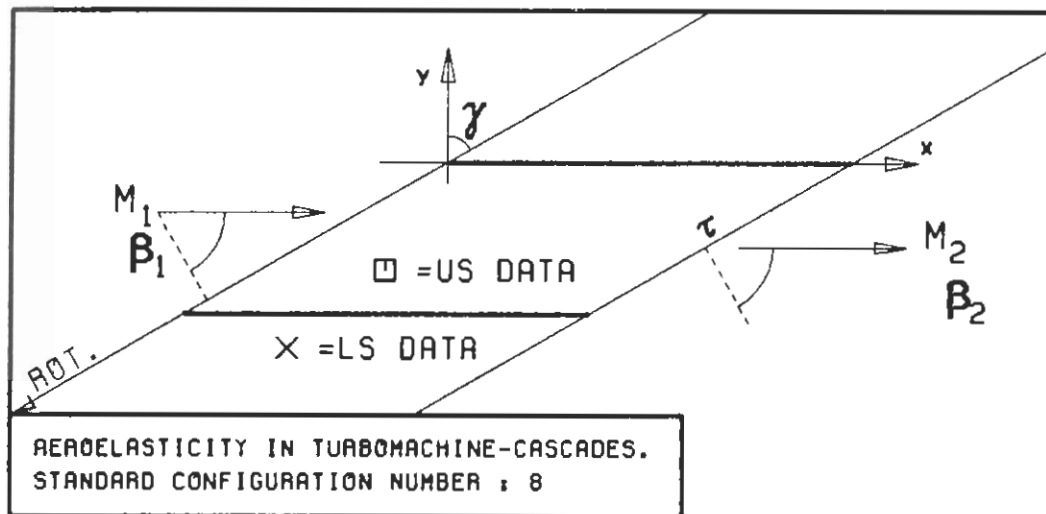
c : 0.1M
 τ : 0.75
 γ :
 x_α : 0.5
 y_α : 0.
 M_1 : 0.8
 β_1 :
 i : 0.
 M_2 : 0.8
 β_2 :
 h_x : -
 h_y : -
 α : .0349
 ω : -
 k : 1.0
 δ : -
 σ : 90.
 d : -

UNSTABLE

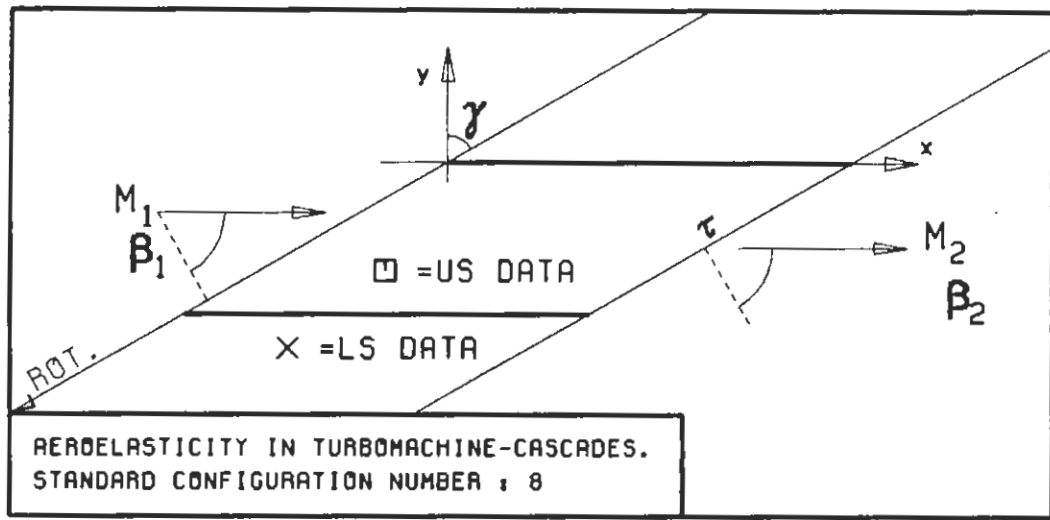


STABLE

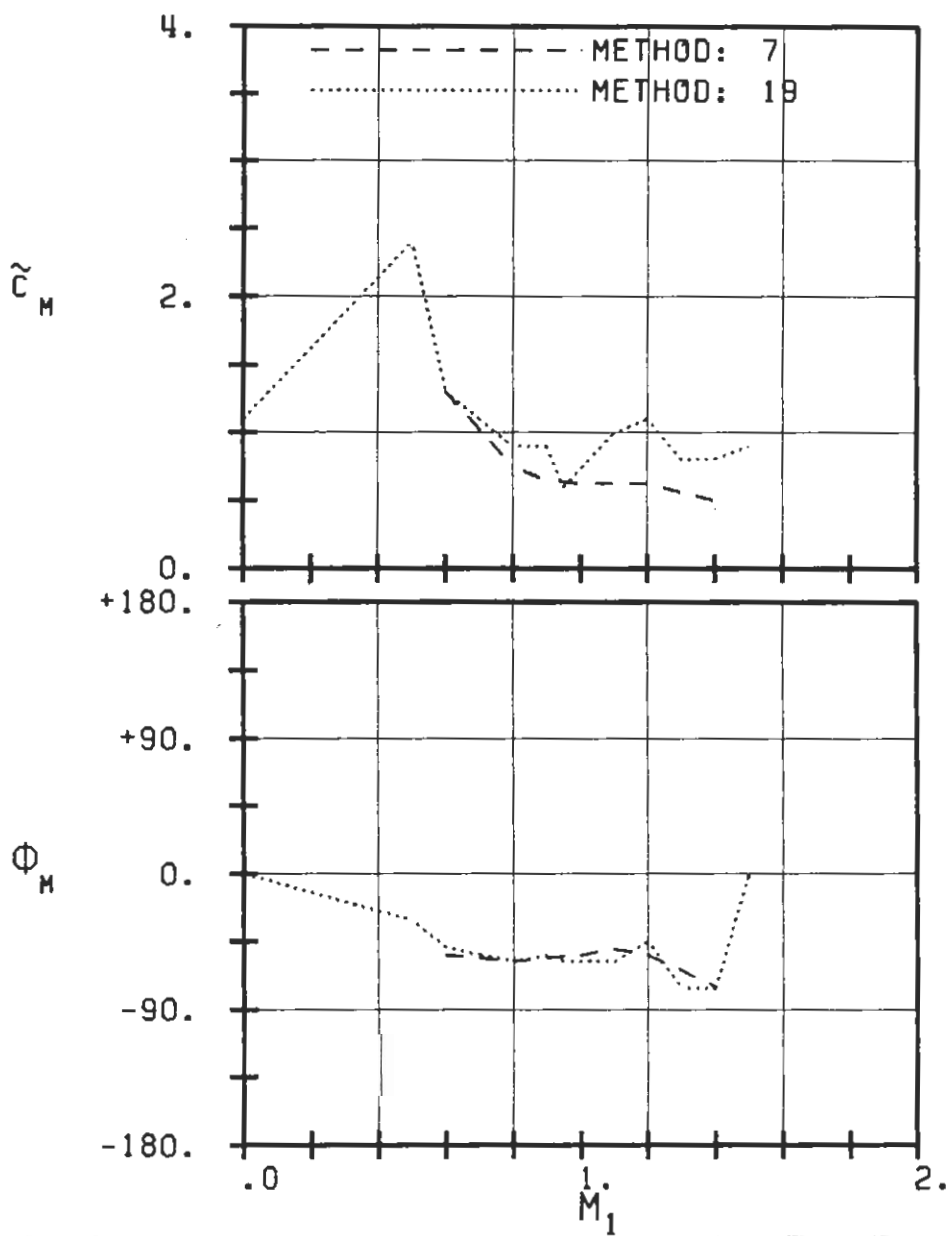
PLOT 7.8-5.2: EIGHTH STANDARD CONFIGURATION, CASES 8,11-13.
AERODYNAMIC MOMENT COEFFICIENT AND PHASE LEAD
IN DEPENDANCE OF STAGGER ANGLE.



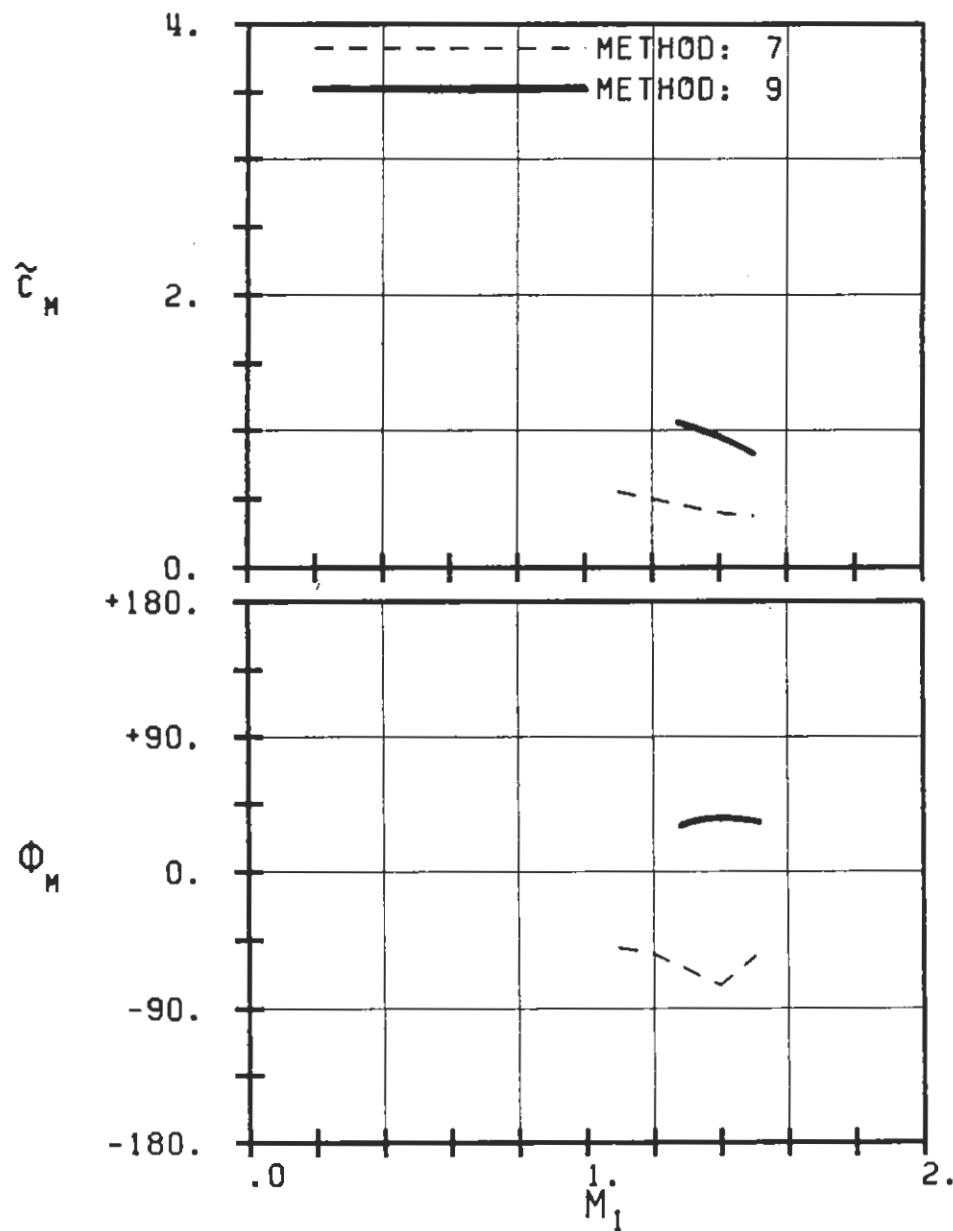
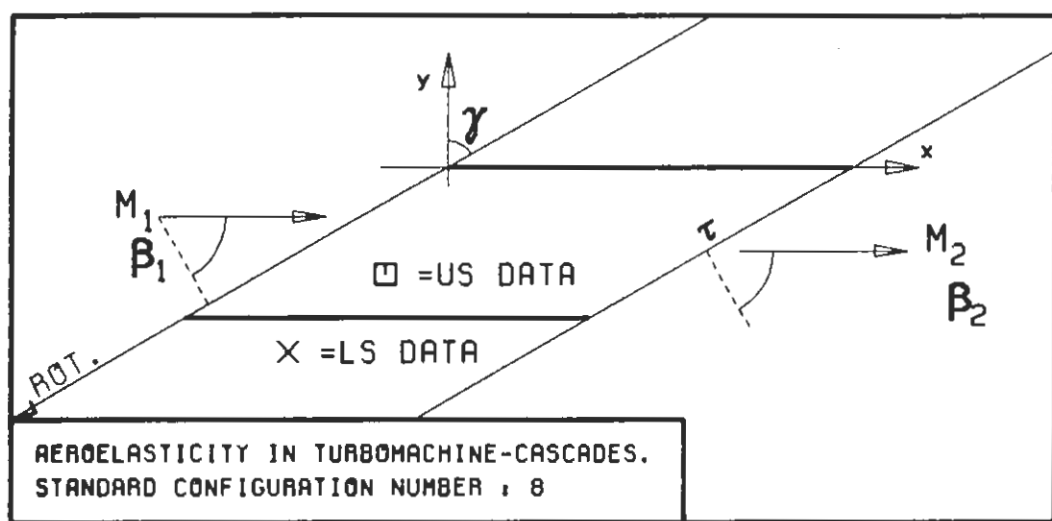
PLOT 7.8-5.3A: EIGHTH STANDARD CONFIGURATION, CASES 1,5-10.
AERODYNAMIC MOMENT COEFFICIENT AND PHASE LEAD
IN DEPENDANCE OF INLET MACH NUMBER (NO SHOCK).



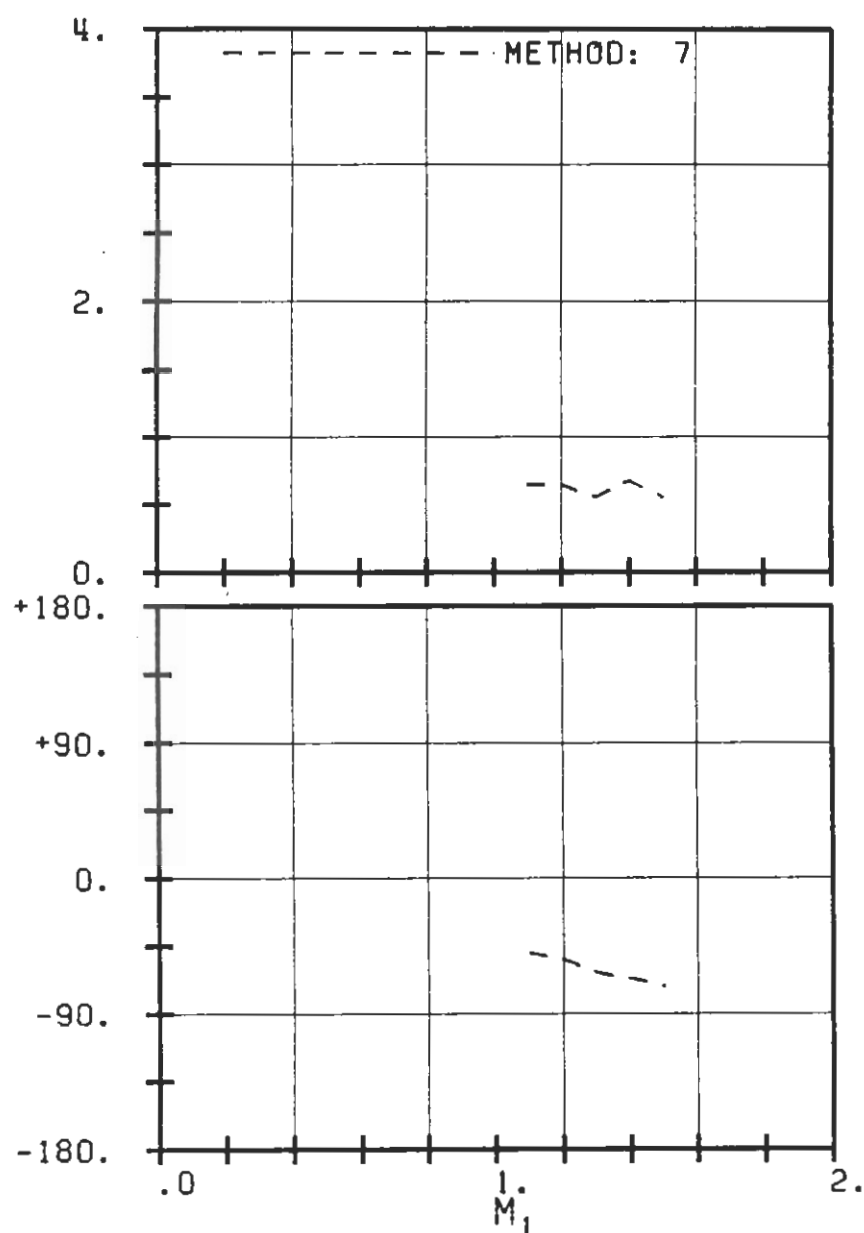
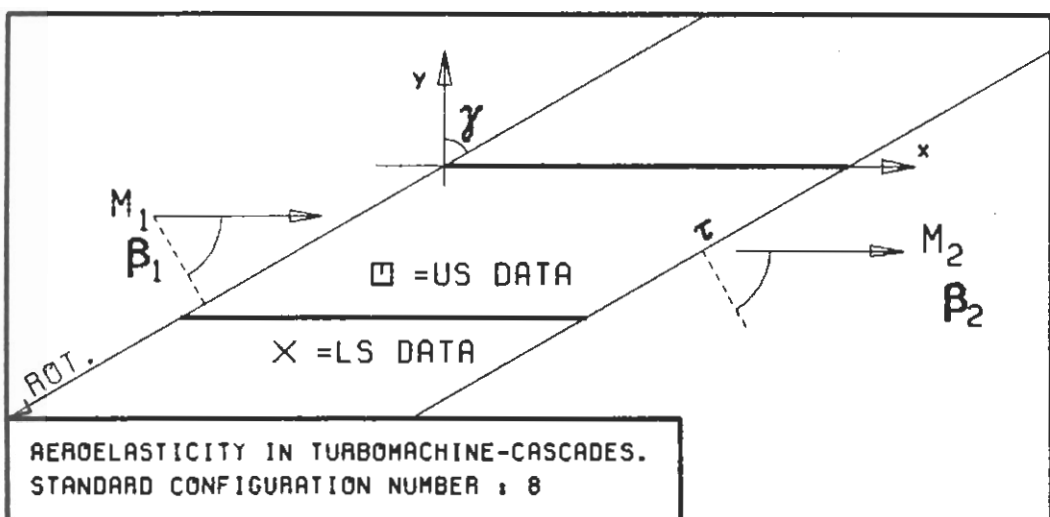
c : 0.1M
 τ : 0.75
 γ : 60.
 x_α : 0.5
 y_α : 0.
 M_1 : -
 β_1 : -60.
 i : 0.
 M_2 : -
 β_2 : -
 h_x : -
 h_y : -
 α : .0349
 ω : -
 k : 1.0
 δ : -
 σ : 90.
 d : -



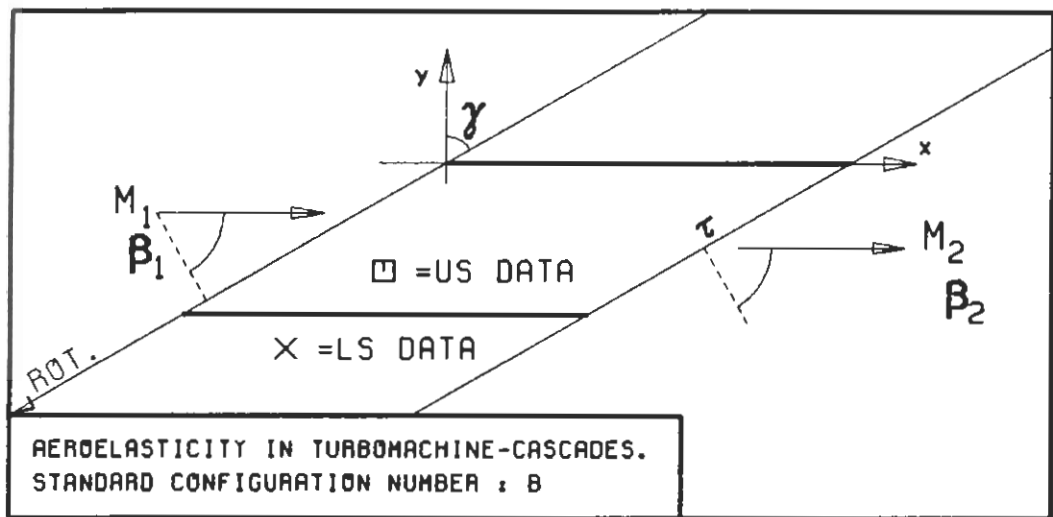
PLOT 7.8-5.3B: EIGHTH STANDARD CONFIGURATION, CASES 1,5-10.
AERODYNAMIC MOMENT COEFFICIENT AND PHASE LEAD
IN DEPENDANCE OF INLET MACH NUMBER (NO SHOCK).



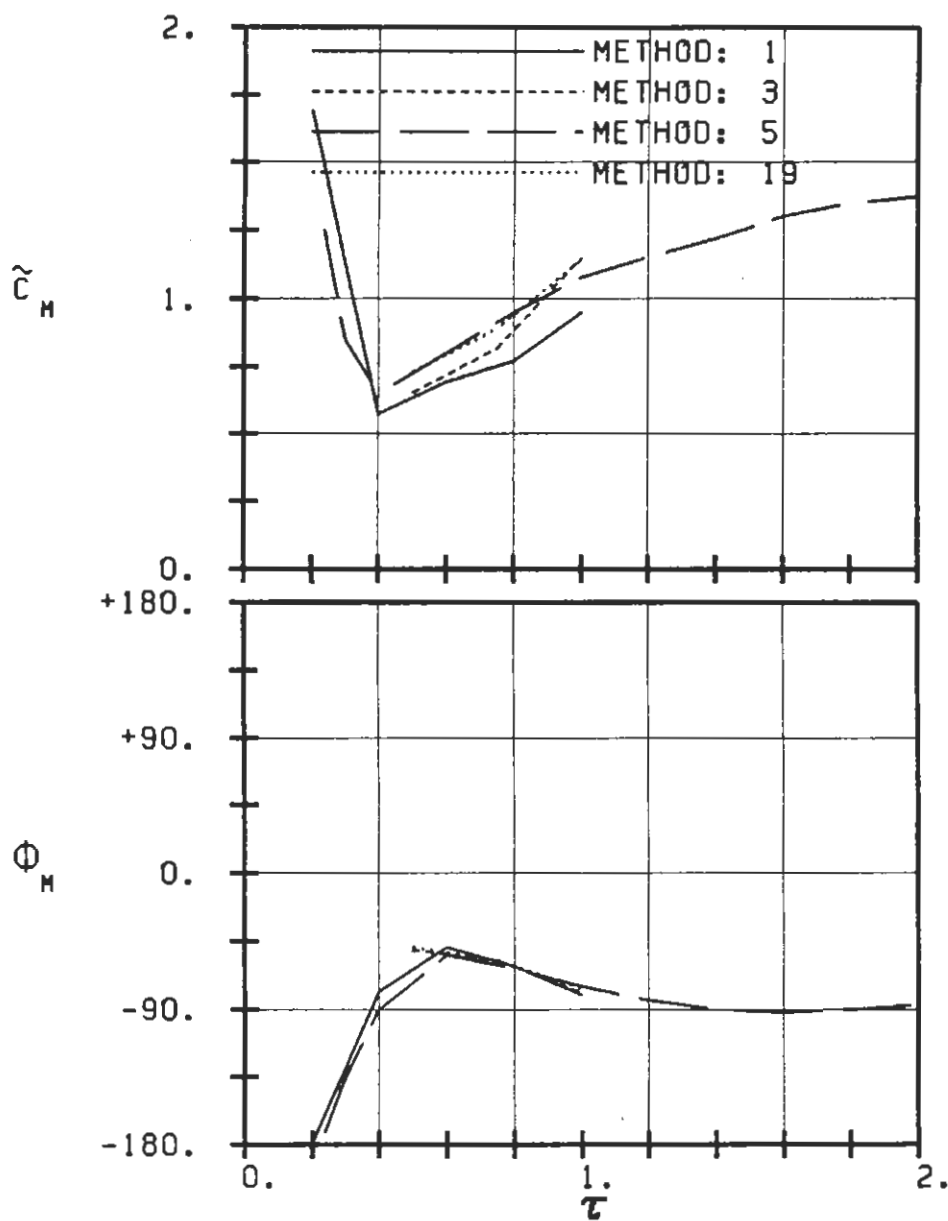
PLOT 7.8-5.4A: EIGHTH STANDARD CONFIGURATION.
AERODYNAMIC MOMENT COEFFICIENT AND PHASE LEAD
IN DEPENDANCE OF INLET MACH NUMBER, WITH LE SHOCK



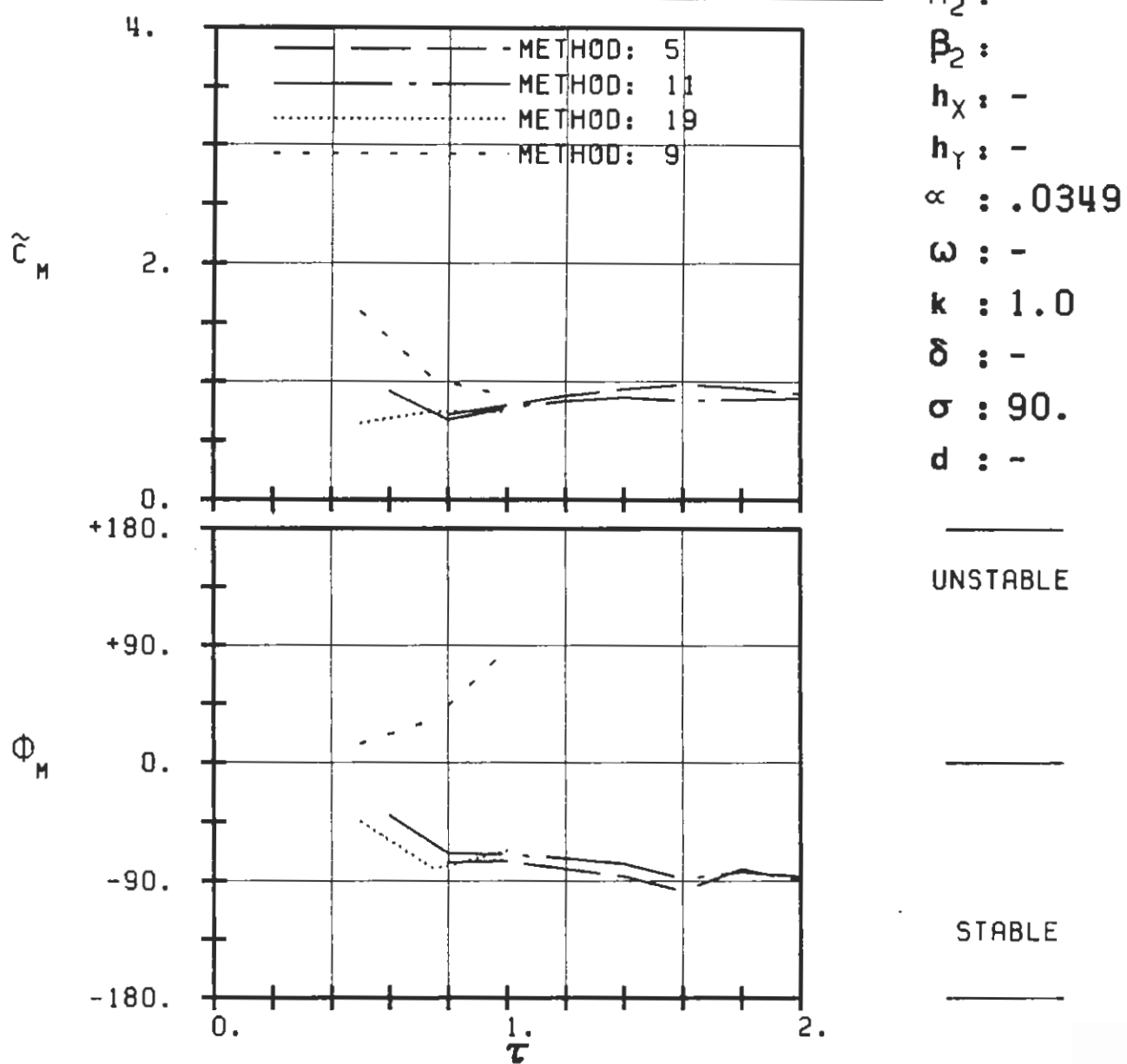
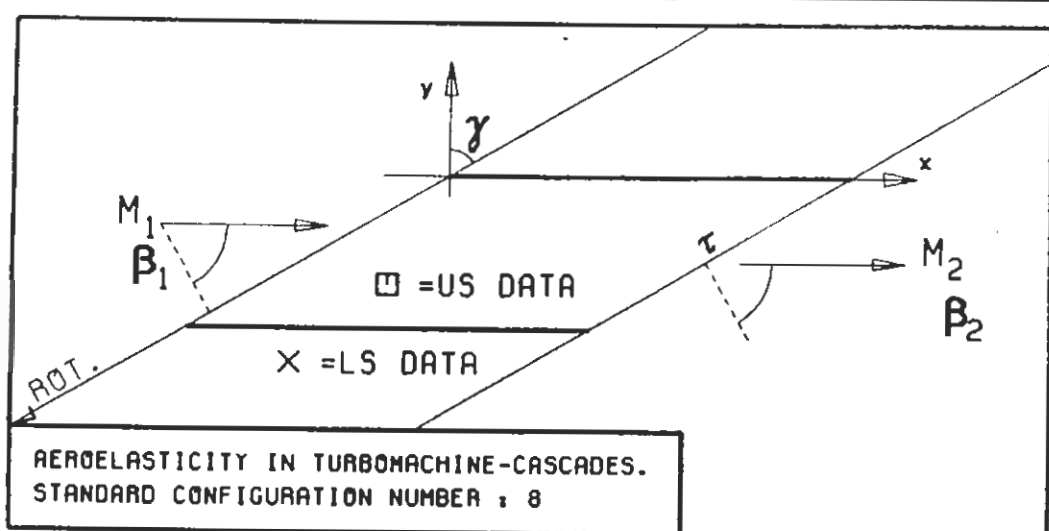
PLOT 7.8-5.5: EIGHTH STANDARD CONFIGURATION.
AERODYNAMIC MOMENT COEFFICIENT AND PHASE LEAD
IN DEPENDANCE OF INLET MACH NUMBER, WITH TE SHO



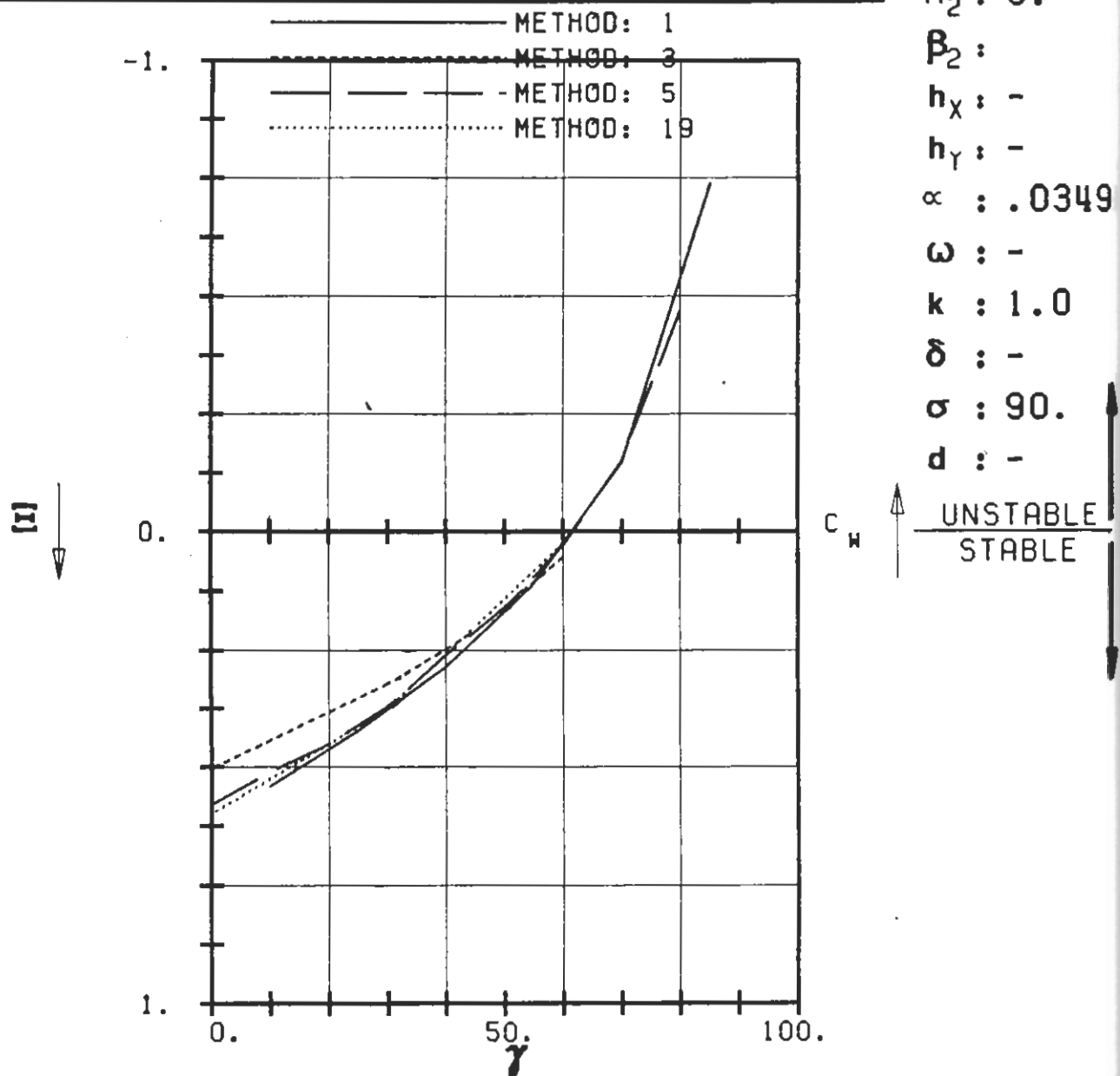
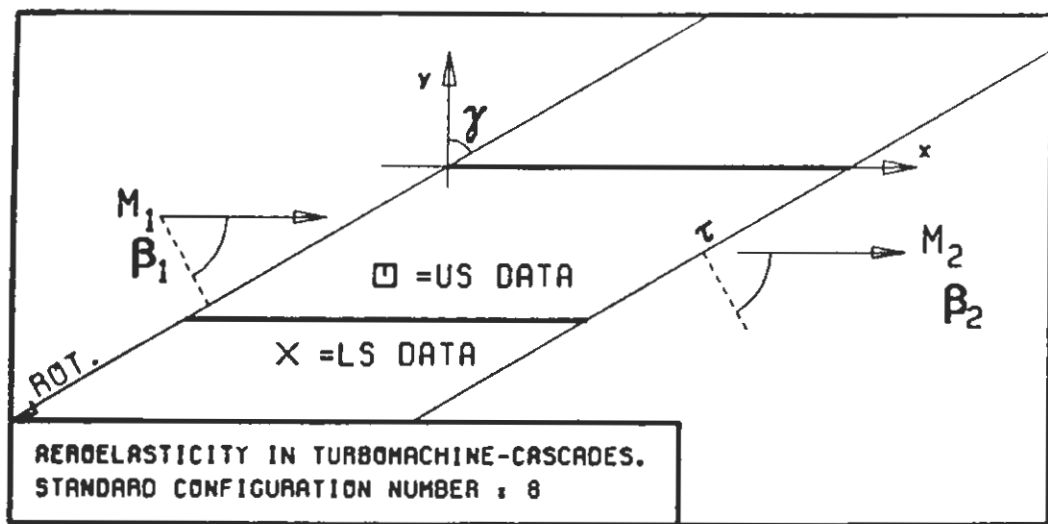
$c : 0.1M$
 $\tau : .75$
 $\gamma : 60.$
 $x_\infty : 0.5$
 $y_\infty : 0.$
 $M_1 : 0.8$
 $\beta_1 : -60.$
 $i : 0.$
 $M_2 : -$
 $\beta_2 : -$
 $h_x : -$
 $h_y : -$
 $\alpha : .0349$
 $\omega : -$
 $k : 1.0$
 $\delta : -$
 $\sigma : 90.$
 $d : -$



PLLOT 7.8-5.6: EIGHTH STANDARD CONFIGURATION, CASES 8,14-15.
AERODYNAMIC MOMENT COEFFICIENT AND PHASE LEAD
IN DEPENDANCE OF SOLIDITY.

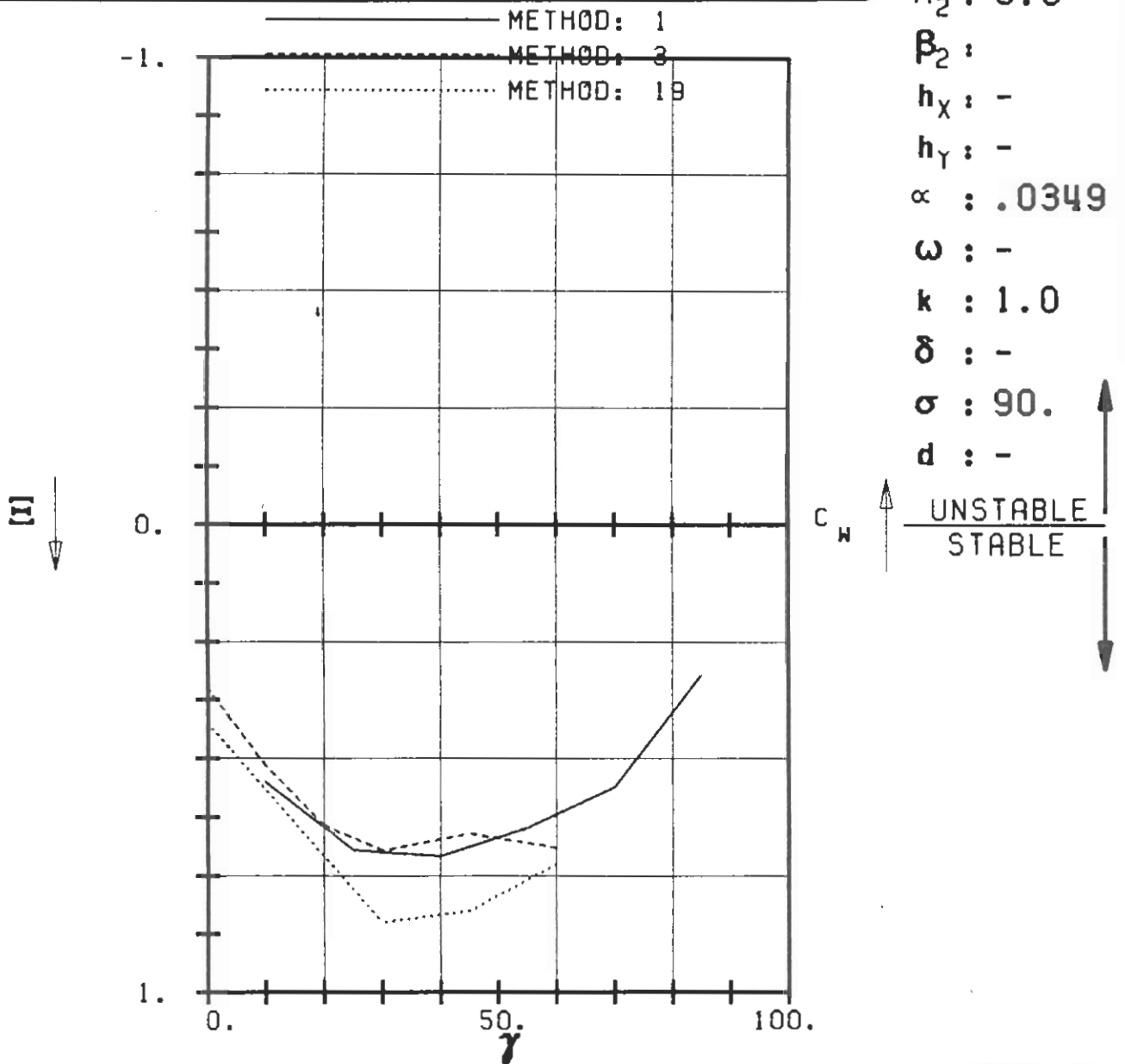
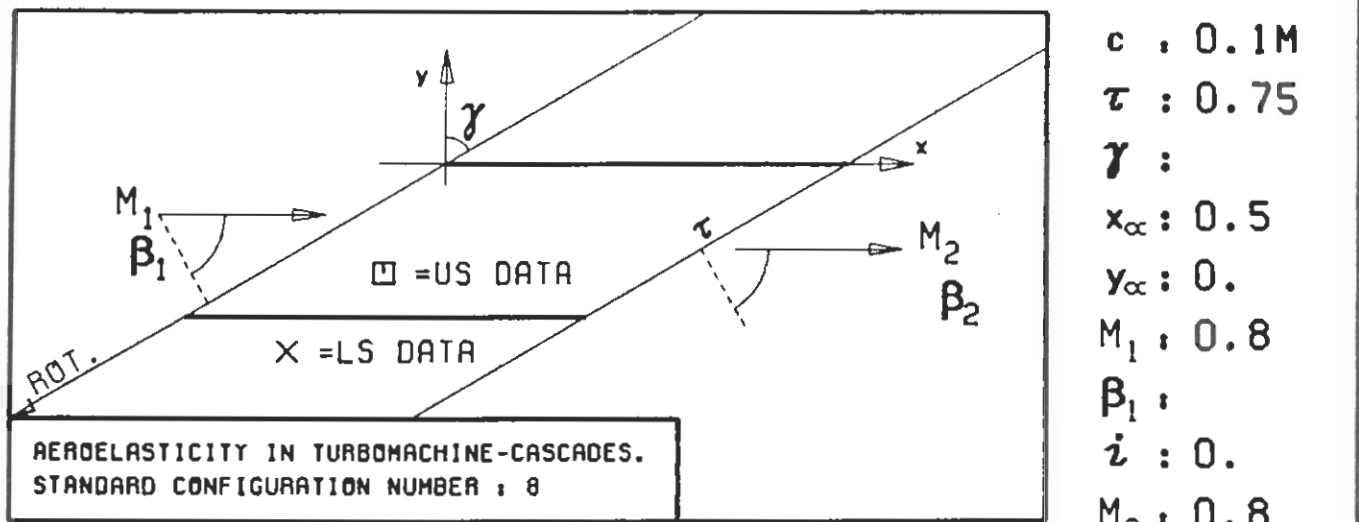


PLOT 7.8-5.7: EIGHTH STANDARD CONFIGURATION, CASES 22-23, 31-
AERODYNAMIC MOMENT COEFFICIENT AND PHASE LEAD
IN DEPENDANCE OF SOLIDITY.

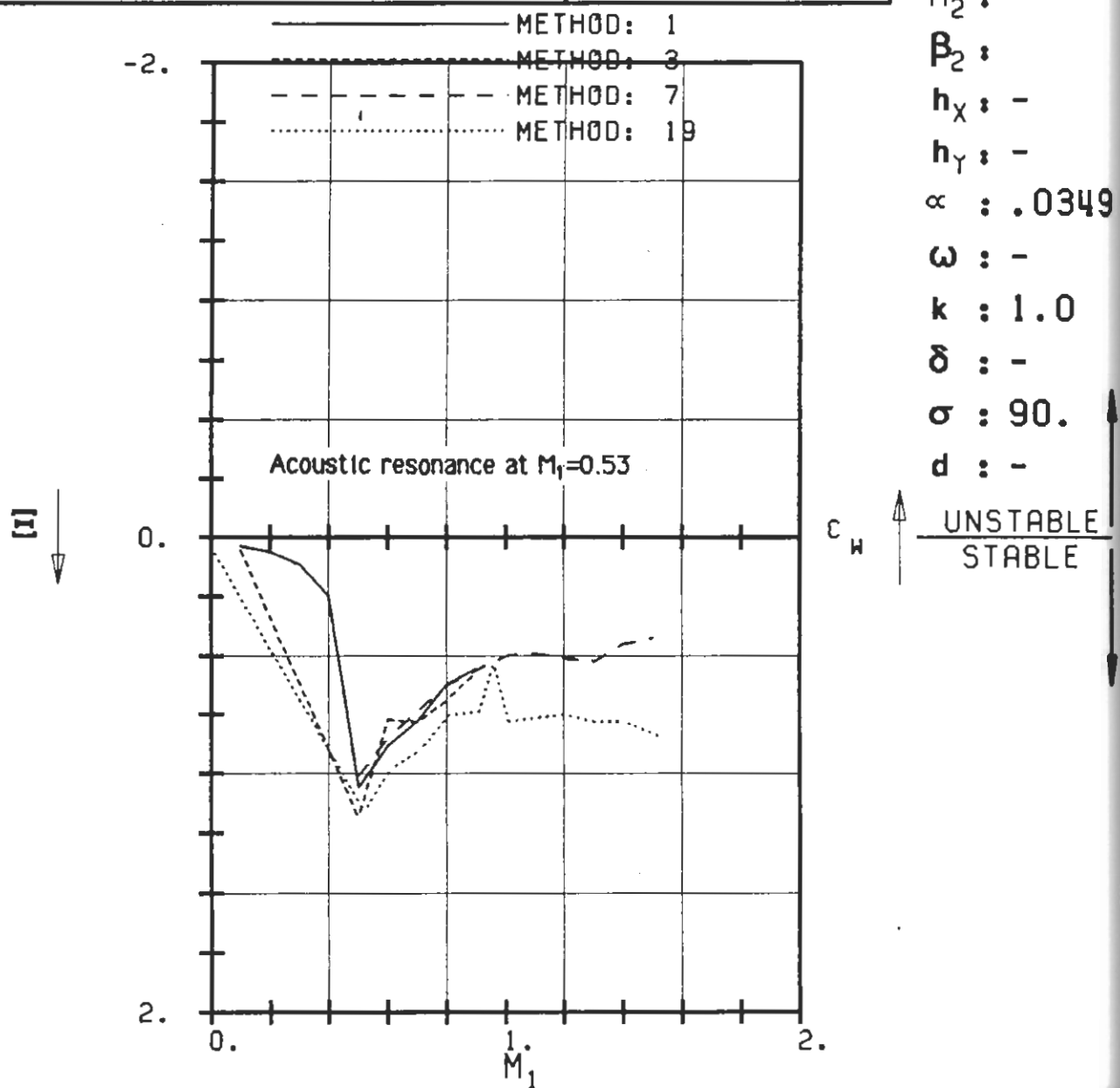
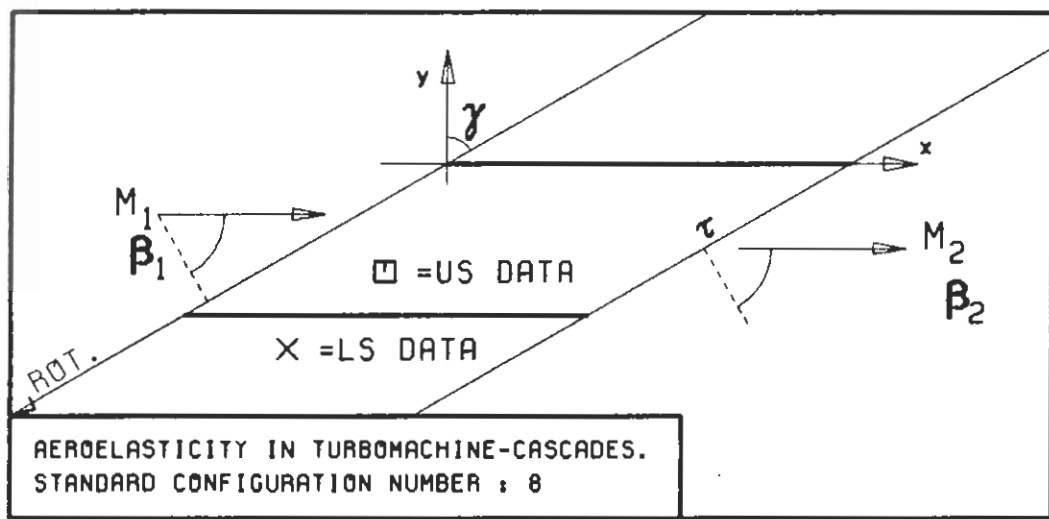


PLOT 7.8-6.1: EIGHTH STANDARD CONFIGURATION, CASES 1-4.
AERODYNAMIC WORK AND DAMPING COEFFICIENTS
IN DEPENDANCE OF STAGGER ANGLE.

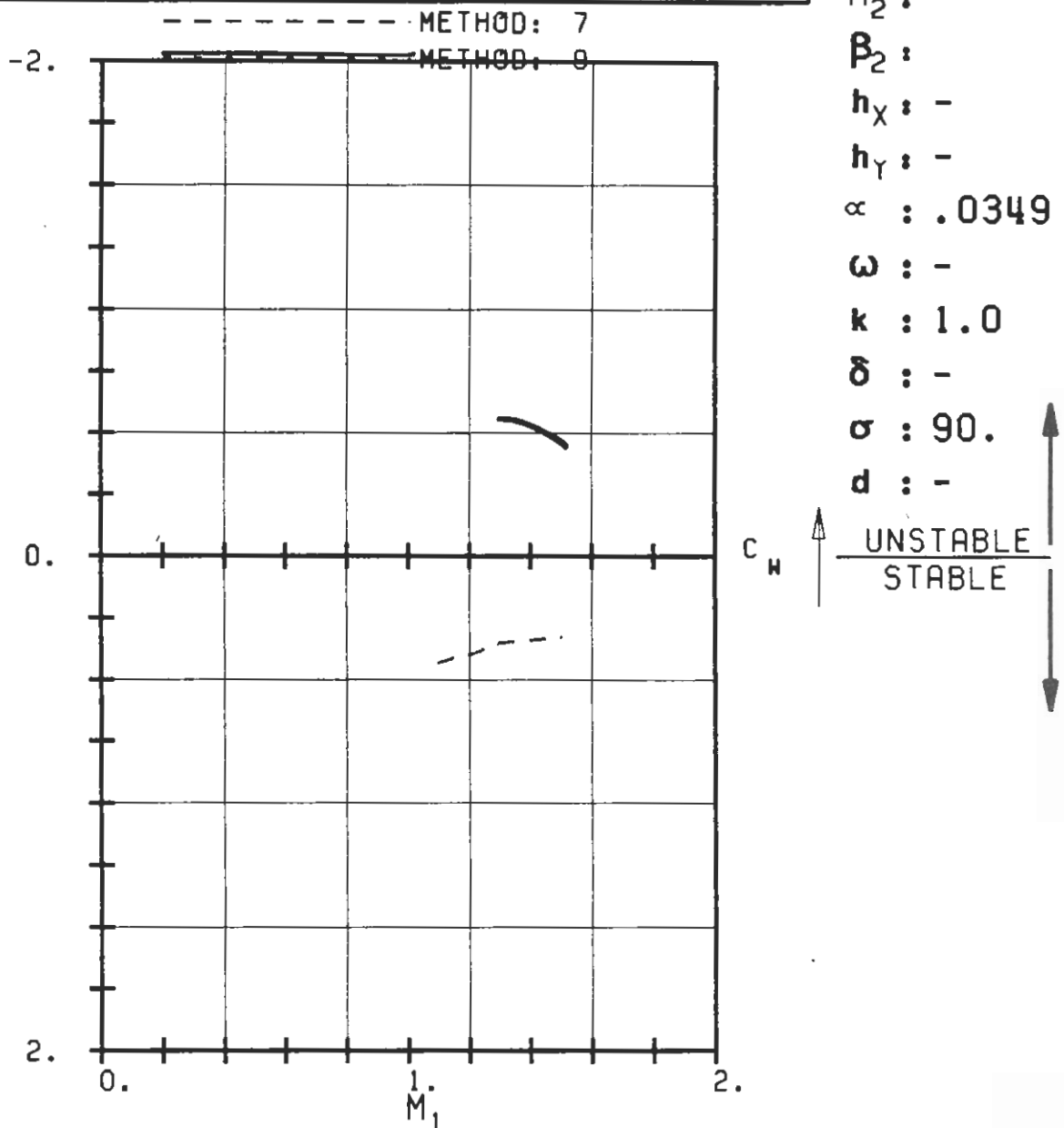
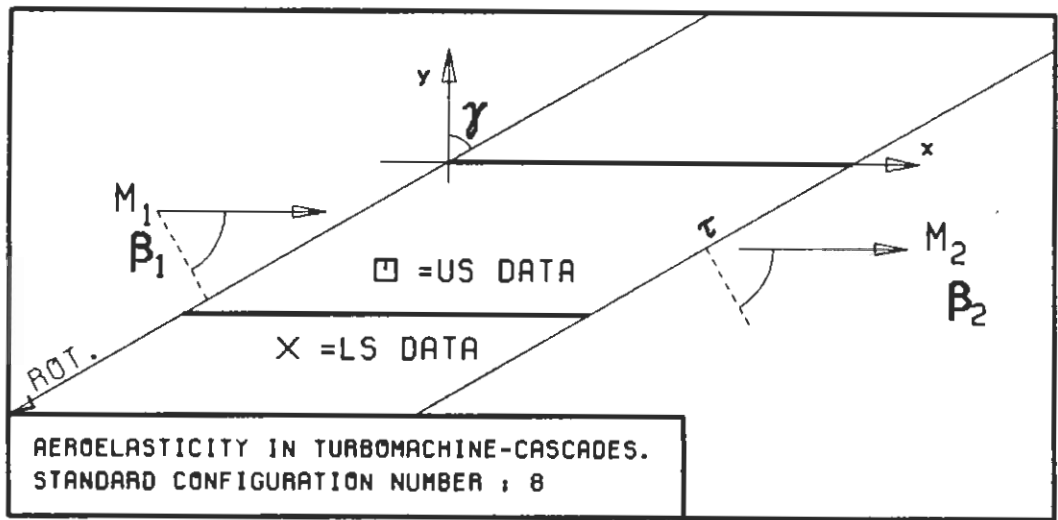
c : 0.1M
 τ : 0.75
 γ :
 x_∞ : 0.5
 y_∞ : 0.
 M_1 : 0.
 β_1 :
 i : 0.
 M_2 : 0.
 β_2 :
 h_x : -
 h_y : -
 α : .0349
 ω : -
 k : 1.0
 δ : -
 σ : 90.
 d : -



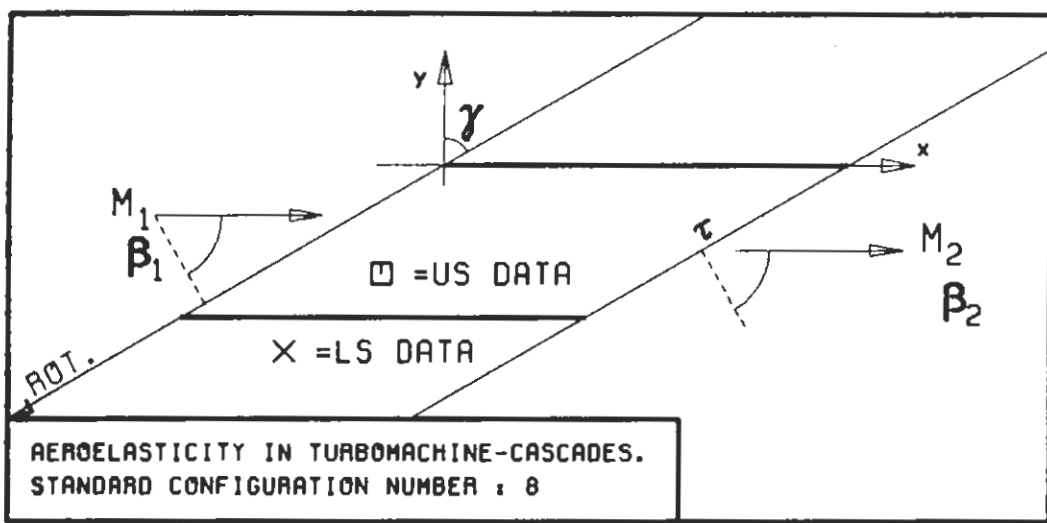
PLOT 7.8-6.2: EIGHTH STANDARD CONFIGURATION, CASES 8,11-13.
 AERODYNAMIC WORK AND DAMPING COEFFICIENTS
 IN DEPENDANCE OF STAGGER ANGLE.



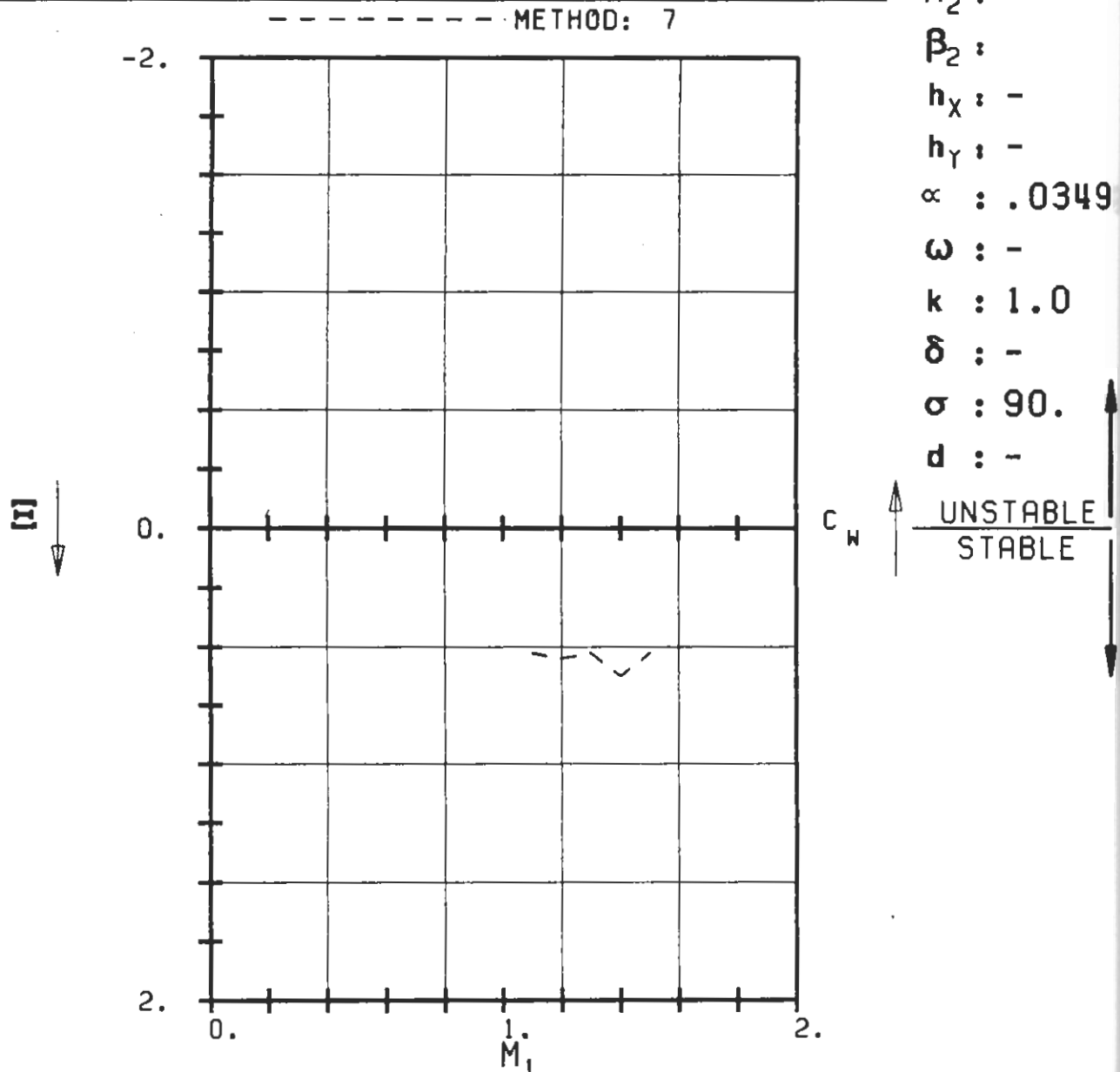
PLOT 7.8-6.3: EIGHTH STANDARD CONFIGURATION, CASES 1,5-10.
AERODYNAMIC WORK AND DAMPING COEFFICIENTS
IN DEPENDANCE OF INLET MACH NUMBER (NO SHOCK).



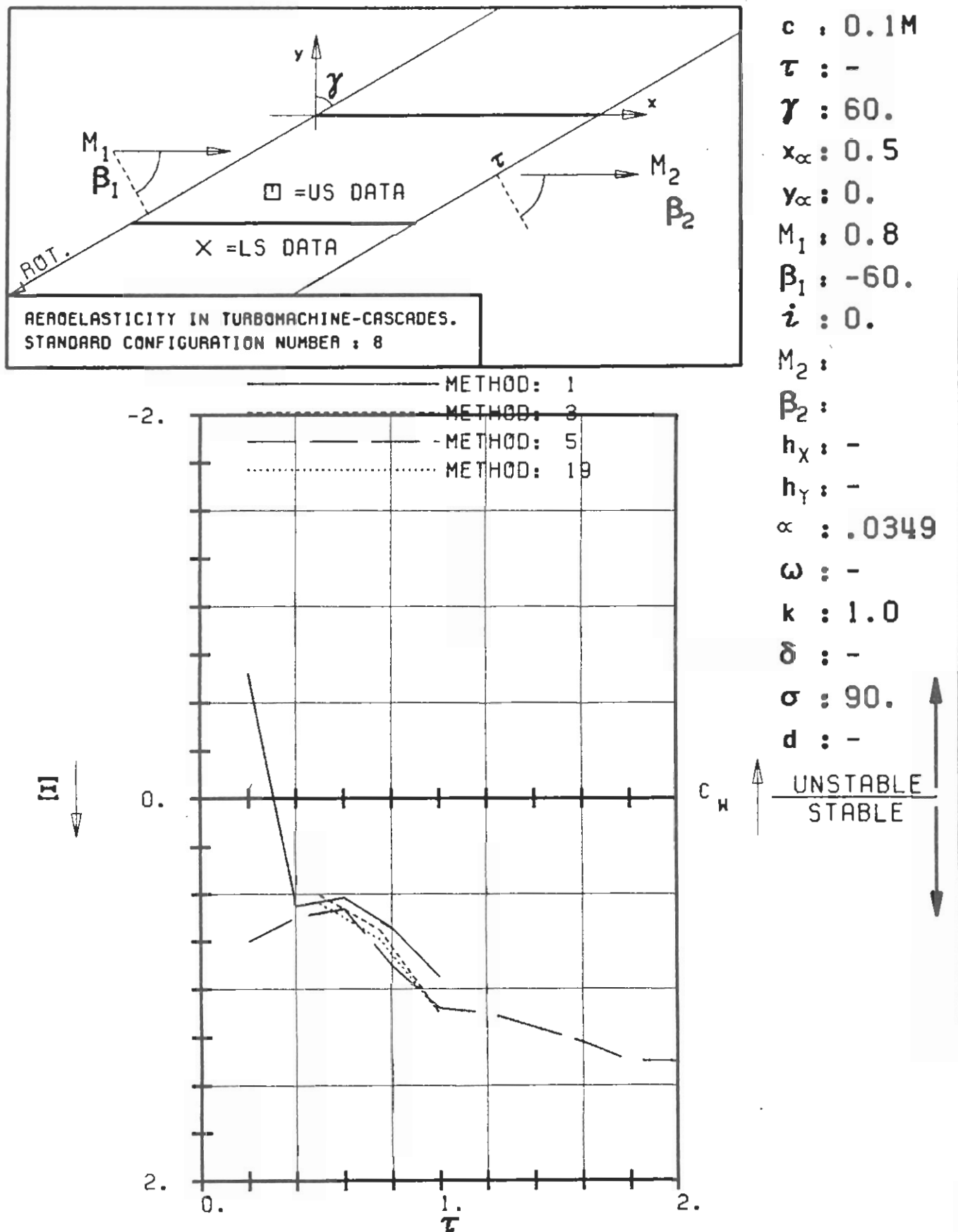
PLOT 7.8-6.4: EIGHTH STANDARD CONFIGURATION.
 AERODYNAMIC WORK AND DAMPING COEFFICIENTS
 IN DEPENDANCE OF INLET MACH NUMBER, WITH LE SHOCK



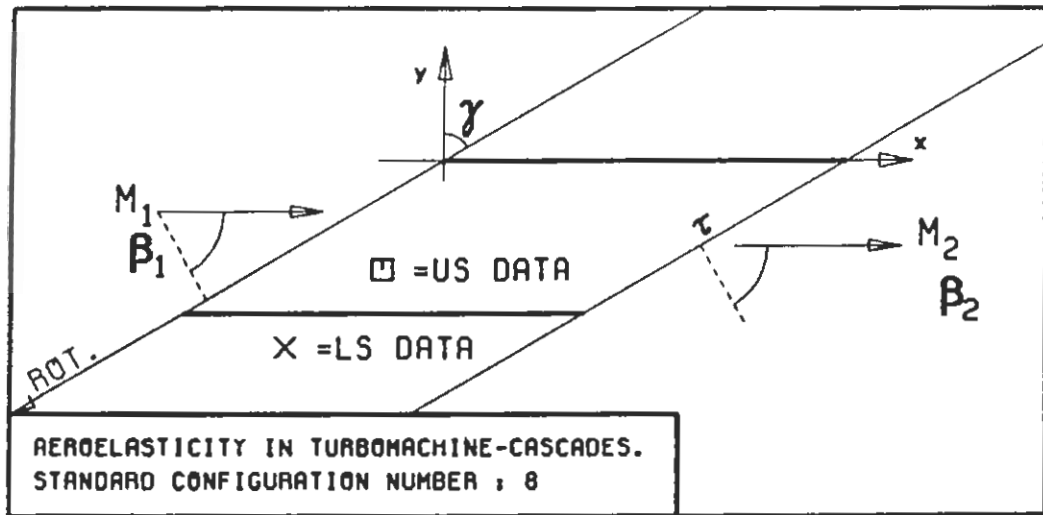
$c : 0.1M$
 $\tau : 0.75$
 $\gamma : 60.$
 $x_\alpha : 0.5$
 $y_\alpha : 0.$
 $M_1 : -$
 $\beta_1 : -60.$
 $i : 0.$
 $M_2 : -$
 $\beta_2 : -$
 $h_X : -$
 $h_Y : -$
 $\alpha : .0349$
 $\omega : -$
 $k : 1.0$
 $\delta : -$
 $\sigma : 90.$
 $d : -$



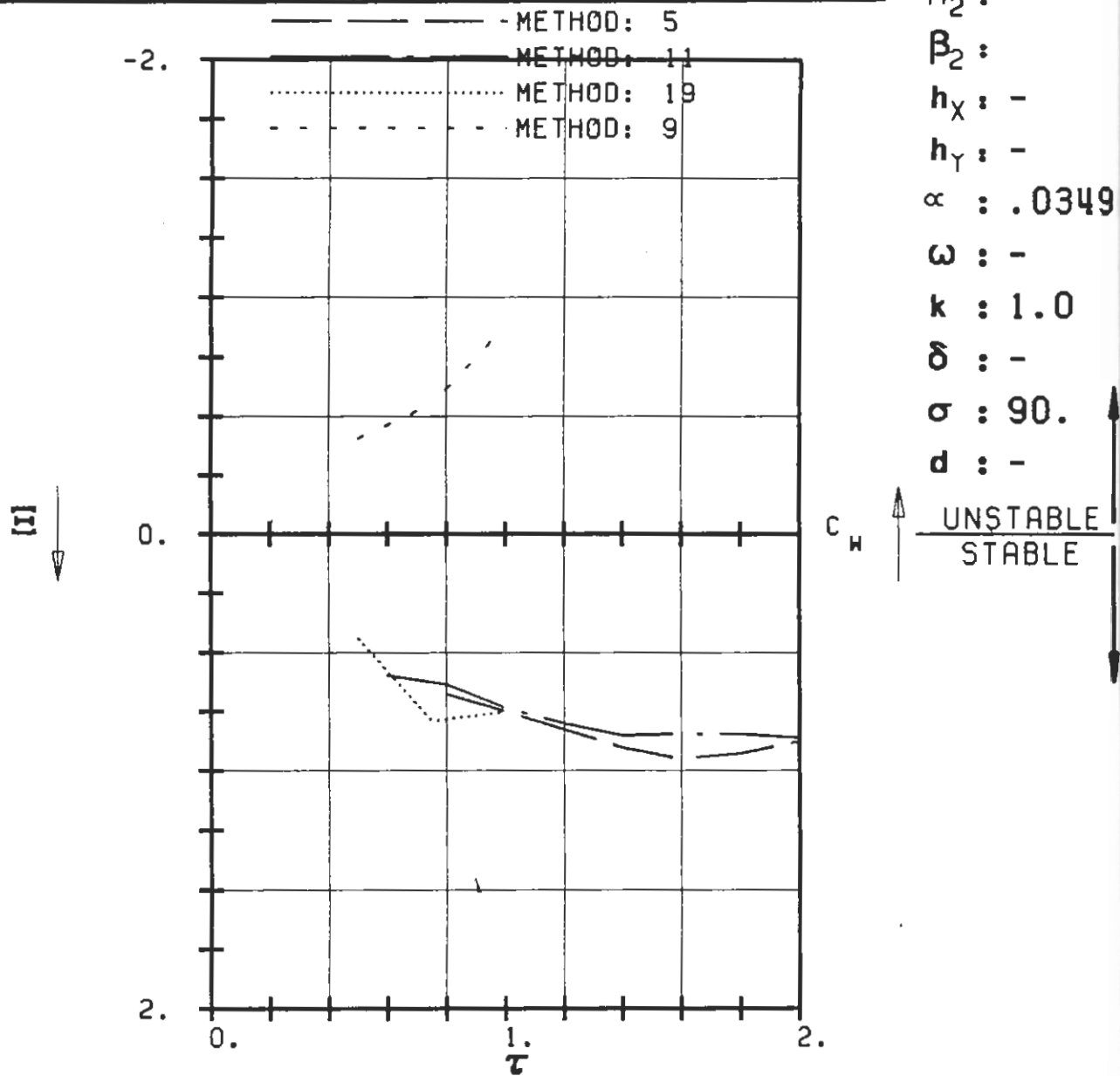
PLOT 7.8-6.5: EIGHTH STANDARD CONFIGURATION.
 AERODYNAMIC WORK AND DAMPING COEFFICIENTS
 IN DEPENDANCE OF INLET MACH NUMBER, WITH TE SHOCK



PLOT 7.8-6.6: EIGHTH STANDARD CONFIGURATION, CASES 8,14-15.
 AERODYNAMIC WORK AND DAMPING COEFFICIENTS
 IN DEPENDANCE OF SOLIDITY.



c : 0.1M
 τ : -
 γ : 60.
 x_α : 0.5
 y_α : 0.
 M_1 : 1.3
 β_1 : -60.
 i : 0.
 M_2 :
 β_2 :
 h_x : -
 h_y : -
 α : .0349



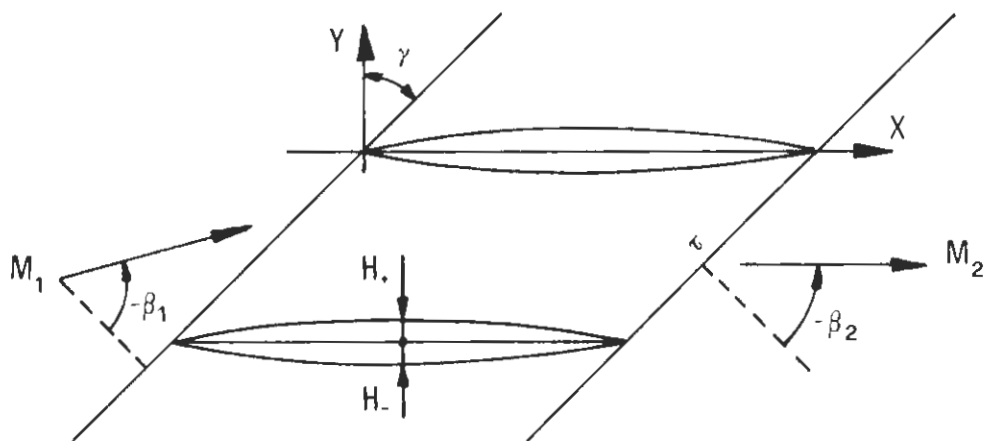
PLOT 7.8-6.7: EIGHTH STANDARD CONFIGURATION.
AERODYNAMIC WORK AND DAMPING COEFFICIENTS
IN DEPENDANCE OF SOLIDITY.

AEROELASTICITY IN TURBOMACHINE-CASCADES

NINTH STANDARD CONFIGURATION

Definition

Symmetric/Flat-Bottomed Circular Arc Profiles.



Equation:

$$y_{\pm}(x) = \begin{cases} \operatorname{sgn}(H_{\pm})[|H_{\pm}| - R_{\pm} + \{R_{\pm}^2 - (x-0.5)^2\}^{0.5}] & \text{if } H_{\pm} \neq 0, \\ 0 & \text{if } H_{\pm} = 0. \end{cases}$$

$$R = (H^2 + 0.5^2) / (2|H|)$$

$$\operatorname{sgn}(H) = \pm 1 \text{ for } H > < 0.$$

+ = upper surface

- = lower surface

Maximum thickness at $x = 0.5$

Vibration in pitch around $(x_{\alpha}, y_{\alpha}) = (0.5, \text{camber-line})$

$d = (\text{thickness/chord}) = 0.01 - 0.1$

$\alpha = 2.0^\circ (= 0.0349 \text{ rad}) \quad |\alpha| = 90^\circ$

$c = 0.1 \text{ m} \quad |i| = 0^\circ \text{ (for } M_1 < 1.)$

$\tau = 0.75 \quad \text{camber} = 0^\circ \text{ (for symmetric profiles)}$

$k = 1.0 \quad |\gamma| = 45^\circ, 60^\circ$

$M_1 = \text{variable (0.0-1.5)}$

Fig. 7.9-1. Ninth standard configuration: Cascade geometry

AEROELASTICITY IN TURBOMACHINE-CASCADES

NINTH STANDARD CONFIGURATION

Aeroelastic Test Cases

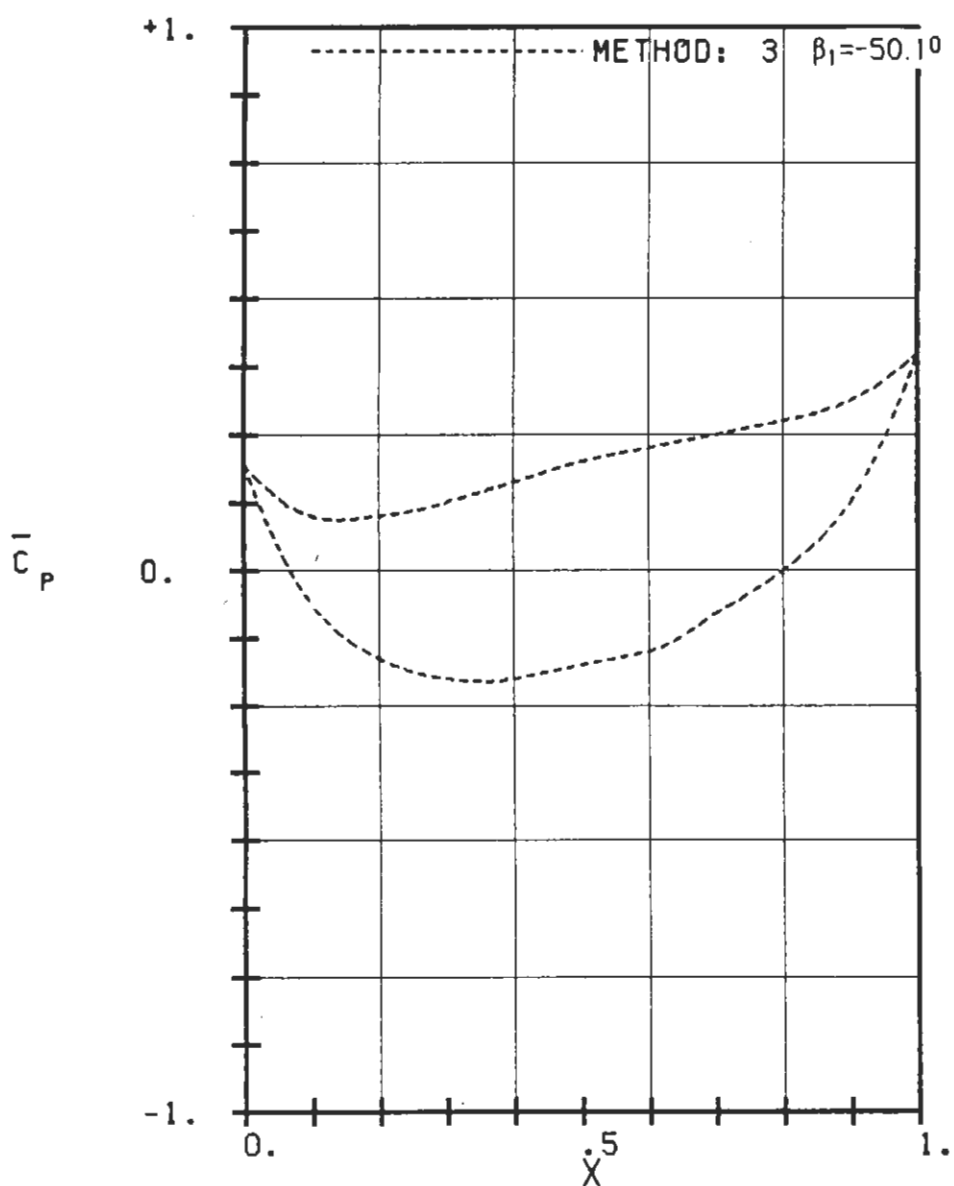
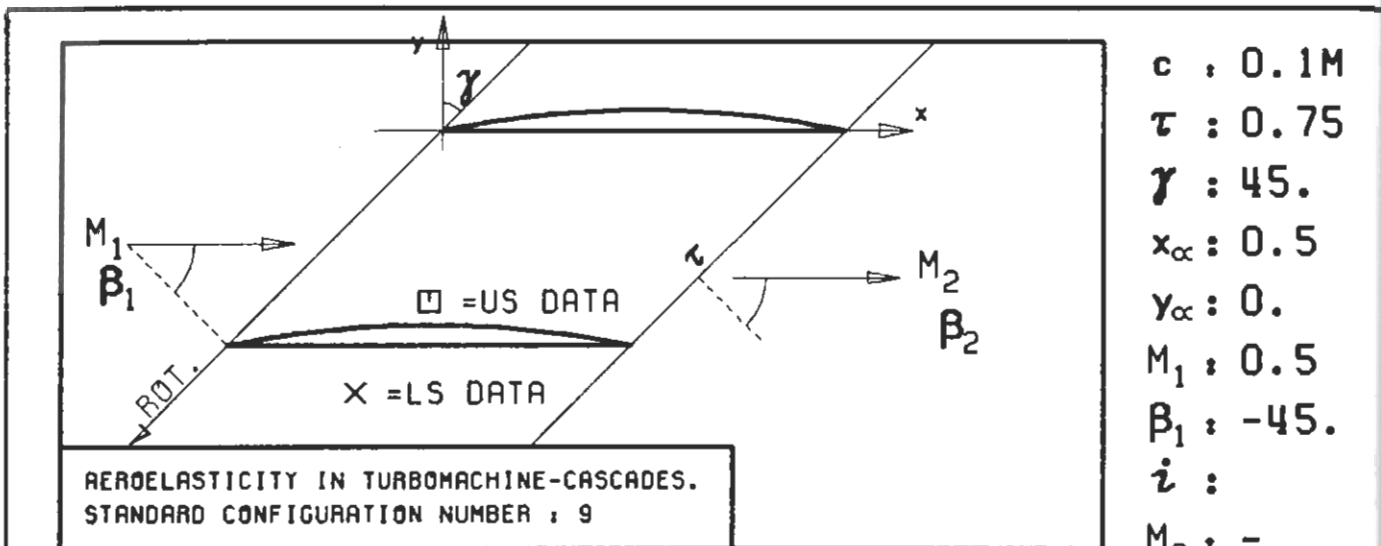
Aeroelastic Test Case No	Time-Averaged Parameters					
	M_1 (-)	γ (°)	β_1 (°)	H_+ (-)	H_- (-)	d (-)
1	0.0	60	- 60	0.01	0.01	0.02
2	"	"	"	0.02	0.02	0.04
3	"	"	"	0.03	0.03	0.06
4	"	"	"	0.05	0.05	0.10
5	0.5	"	"	0.01	0.01	0.02
6	0.7	"	"	0.005	0.005	0.01
7	"	"	"	0.01	0.01	0.02
8	"	"	"	0.0015	0.0015	0.03
9	"	"	"	0.02	0.02	0.04
10	0.8	"	"	0.01	0.01	0.02
11	1.3	"	"	"	"	"
12	1.4	"	"	"	"	"
13	1.5	"	"	"	"	"
14	0.0	45	- 45	"	"	"
15	0.5	"	"	"	"	"
16	0.7	"	"	"	"	"
17	0.8	"	"	"	"	"
18	0.5	"	"	0.05	0.0	0.05
19	0.7	"	"	"	"	"
20	0.8	"	"	"	"	"
21	0.9	"	"	"	"	"

Table 7.9-1 Ninth standard configuration. 21 aeroelastic test cases

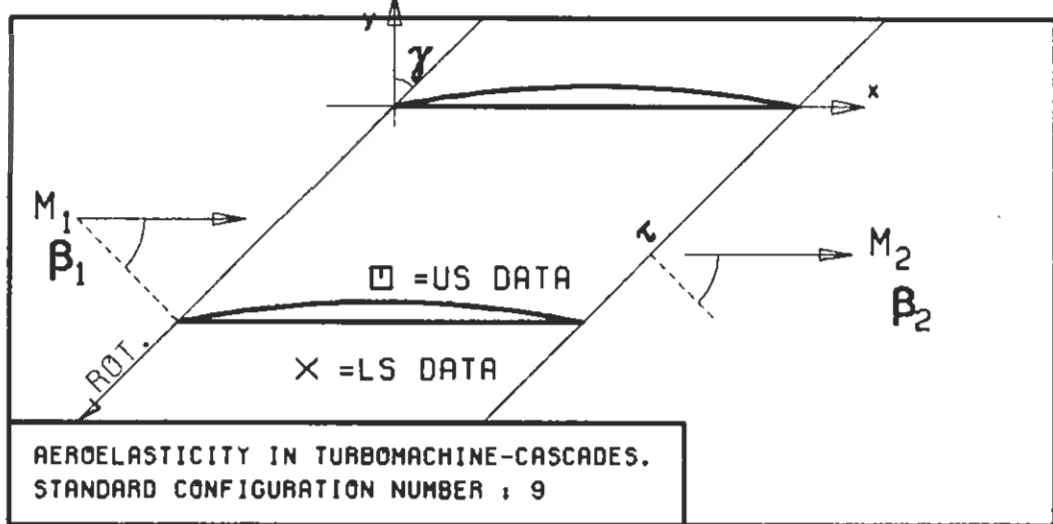
AEROELASTICITY IN TURBOMACHINE-CASCADES

NINTH STANDARD CONFIGURATION

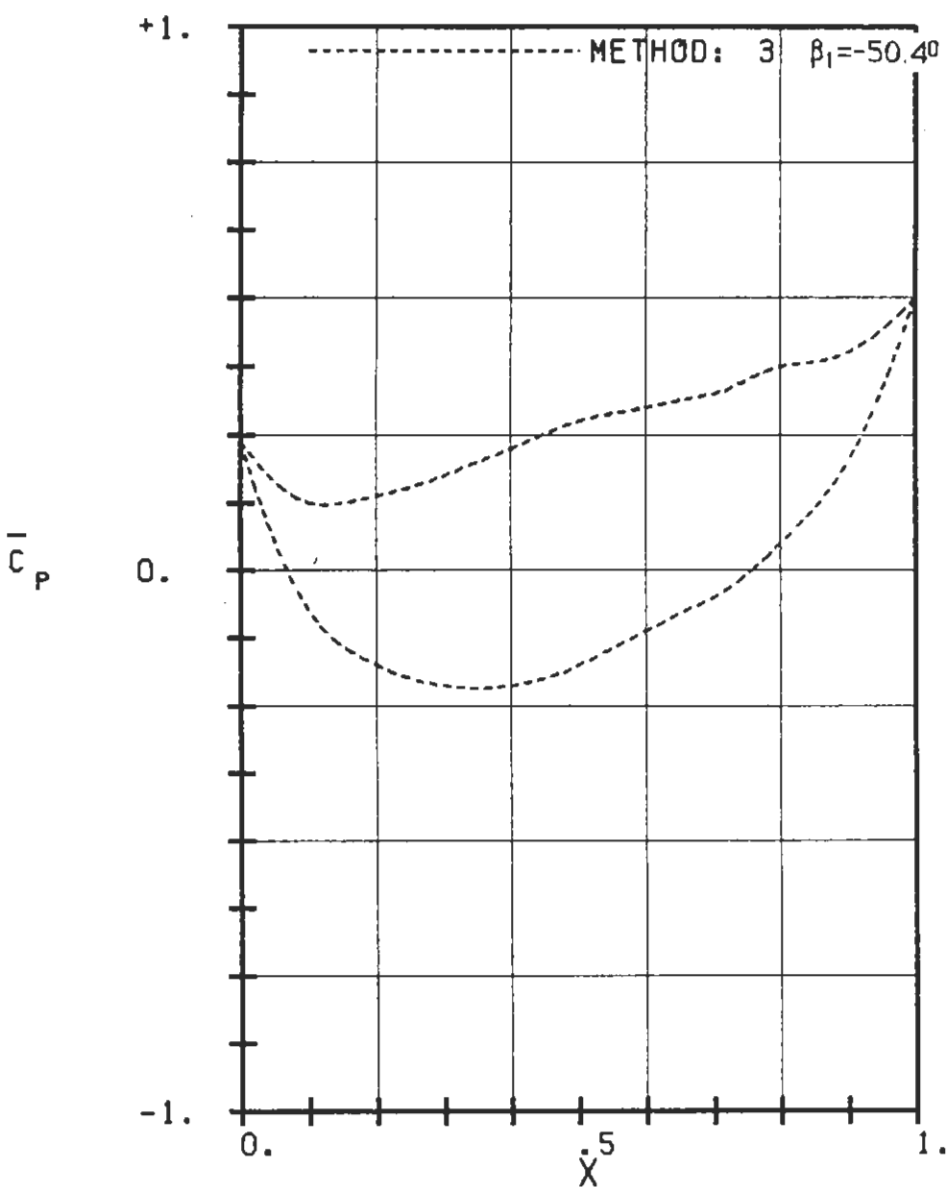
Experimental and Theoretical Results

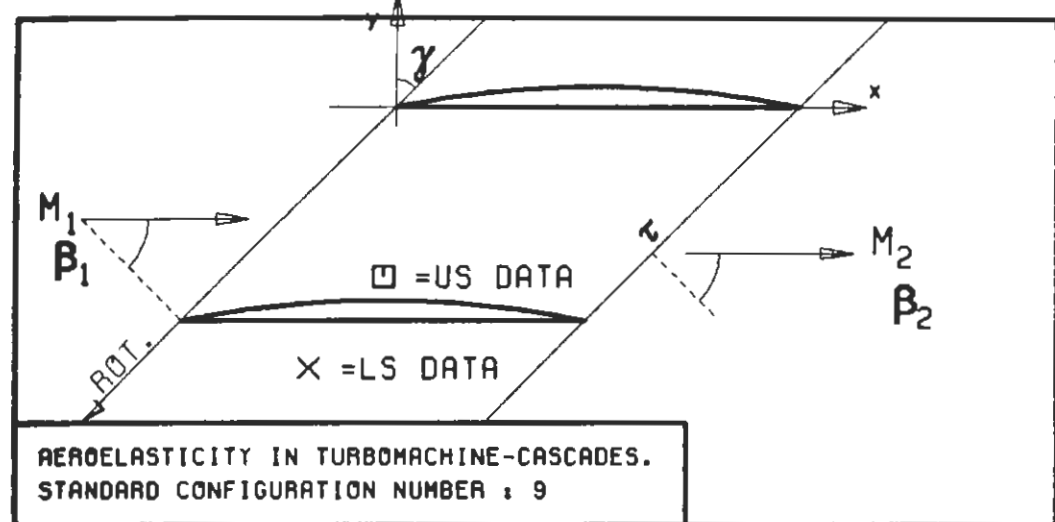


PLOT 7.9-1.1: NINTH STANDARD CONFIGURATION, CASE 18.
TIME AVERAGED BLADE SURFACE PRESSURE
DISTRIBUTION FOR $M_1=0.5$.

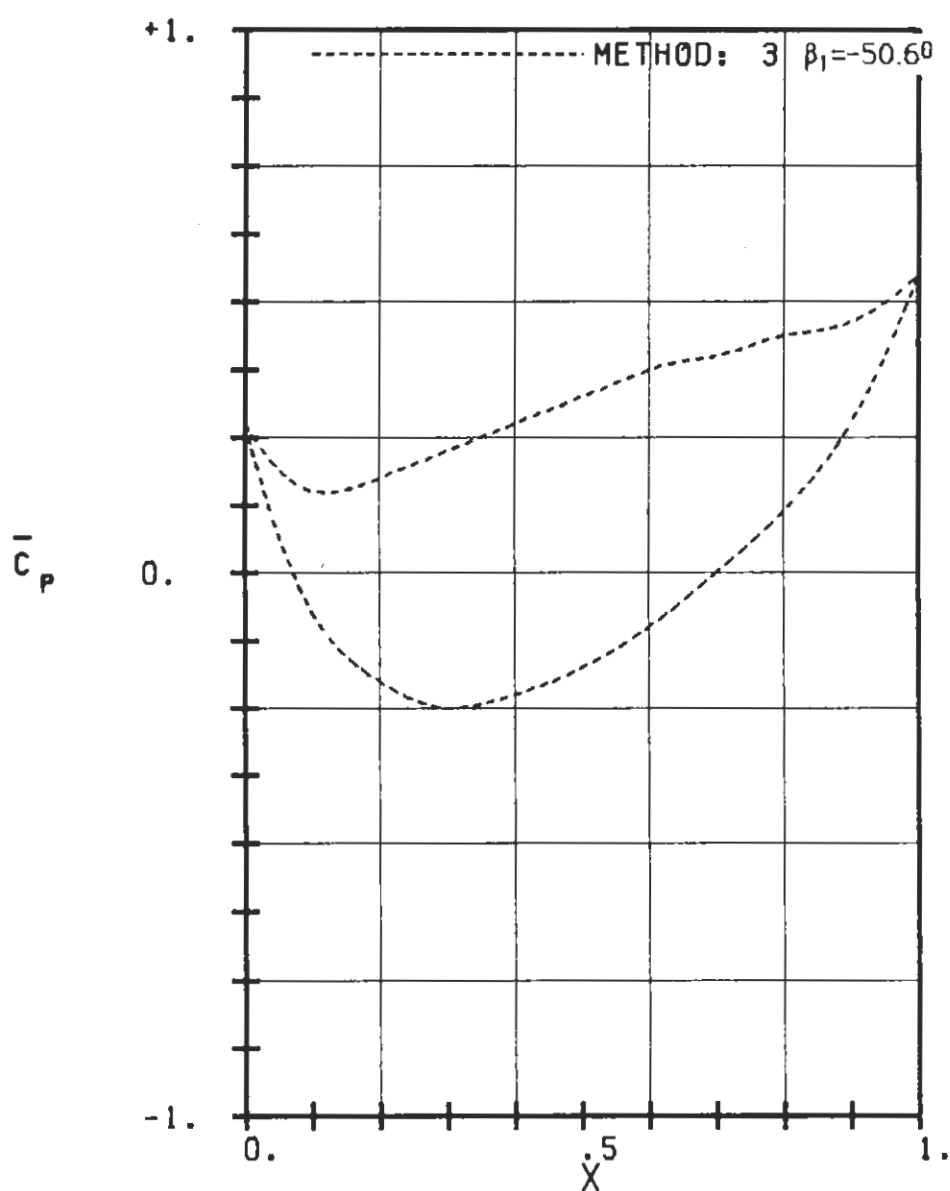


$c : 0.1M$
 $\tau : 0.75$
 $\gamma : 45.$
 $x_\alpha : 0.5$
 $y_\alpha : 0.$
 $M_1 : 0.7$
 $\beta_1 : -45.$
 $i :$
 $M_2 : -$
 $\beta_2 : -$
 $h_x : -$
 $h_y : -$
 $\alpha : .0349$
 $\omega : -$
 $k : 1.0$
 $\delta : -$
 $\sigma : 90.$
 $d : 0.05$

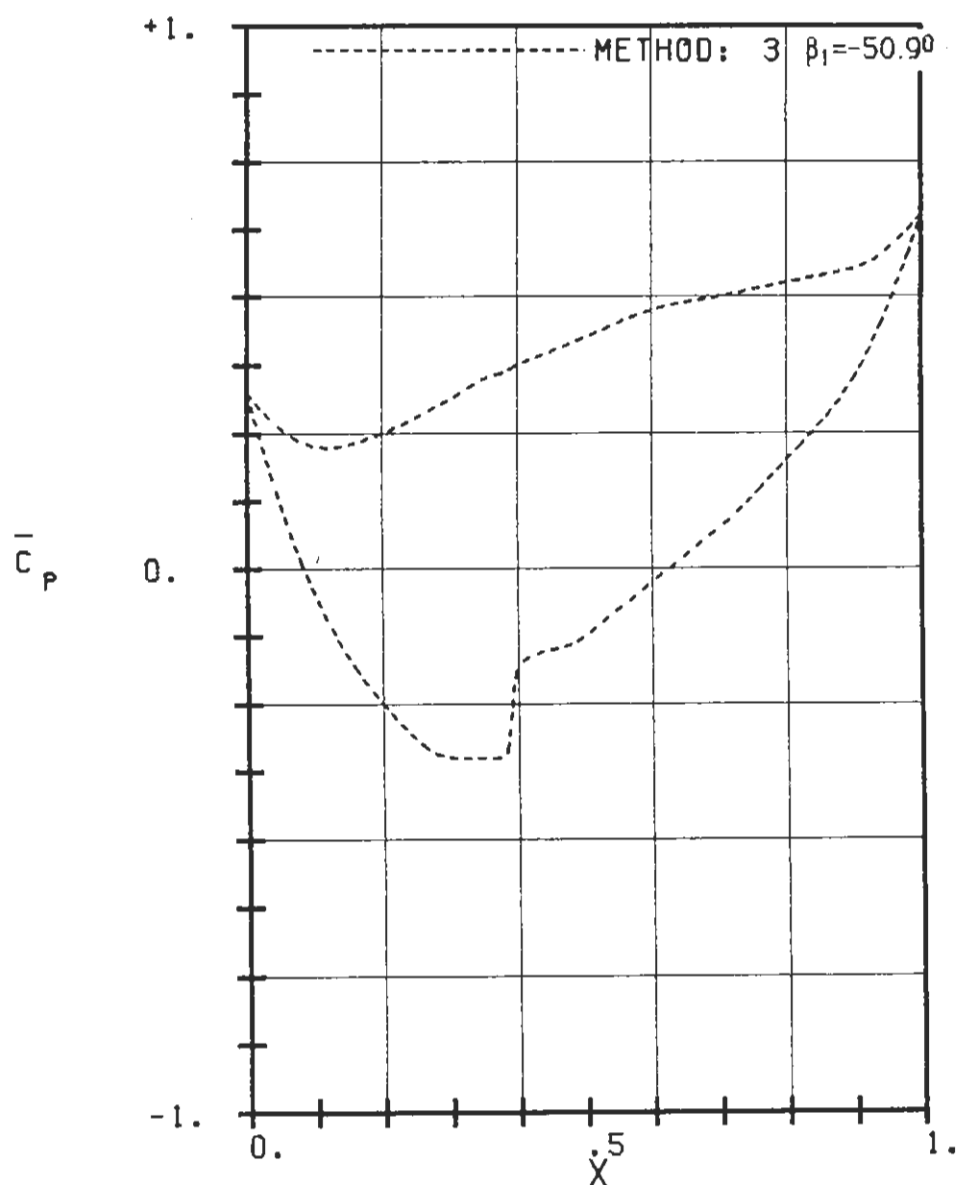
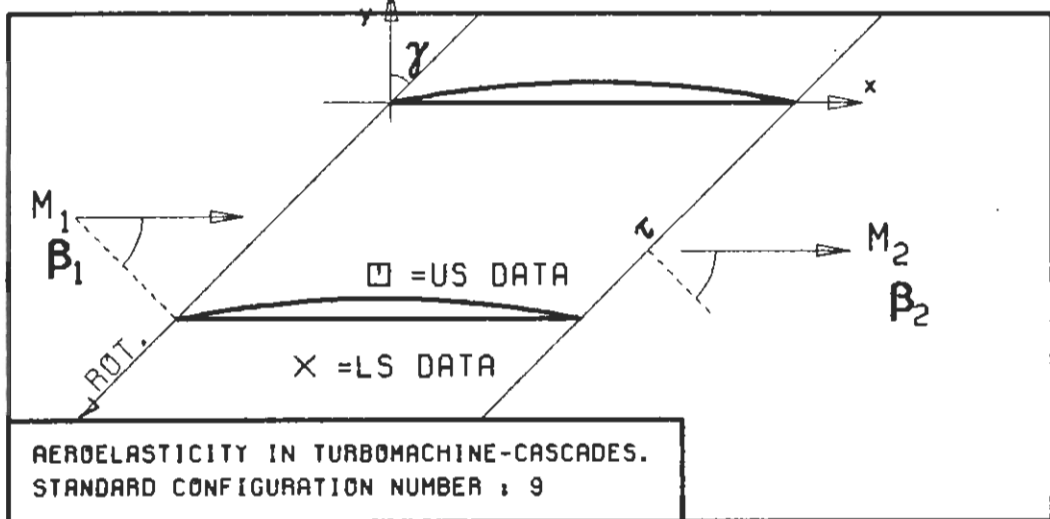




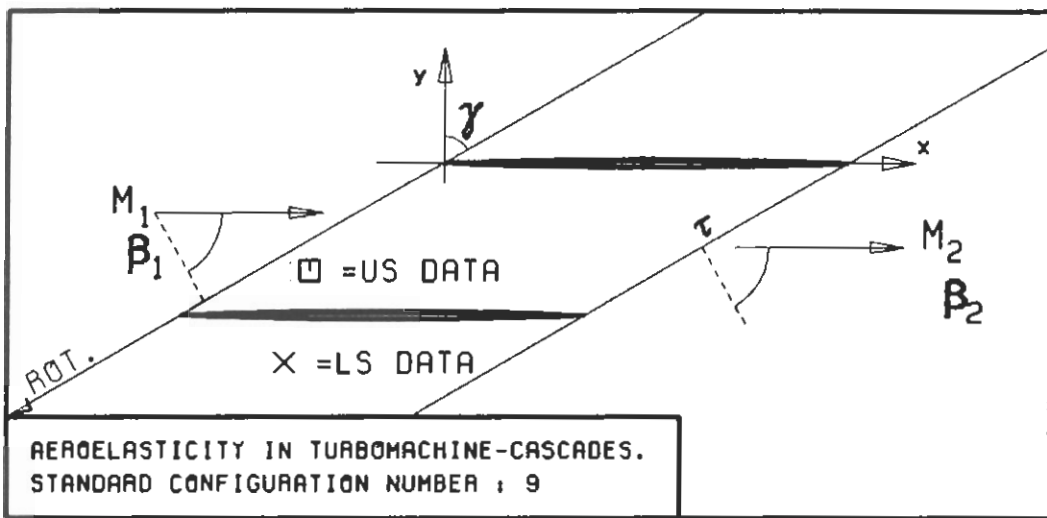
c : 0.1M
 τ : 0.75
 γ : 45.
 x_∞ : 0.5
 y_∞ : 0.
 M_1 : 0.8
 β_1 : -45.
 i :
 M_2 : -
 β_2 :
 h_x : -
 h_y : -
 α : .0349
 ω : -
 k : 1.0
 δ : -
 σ : 90.
 d : 0.05



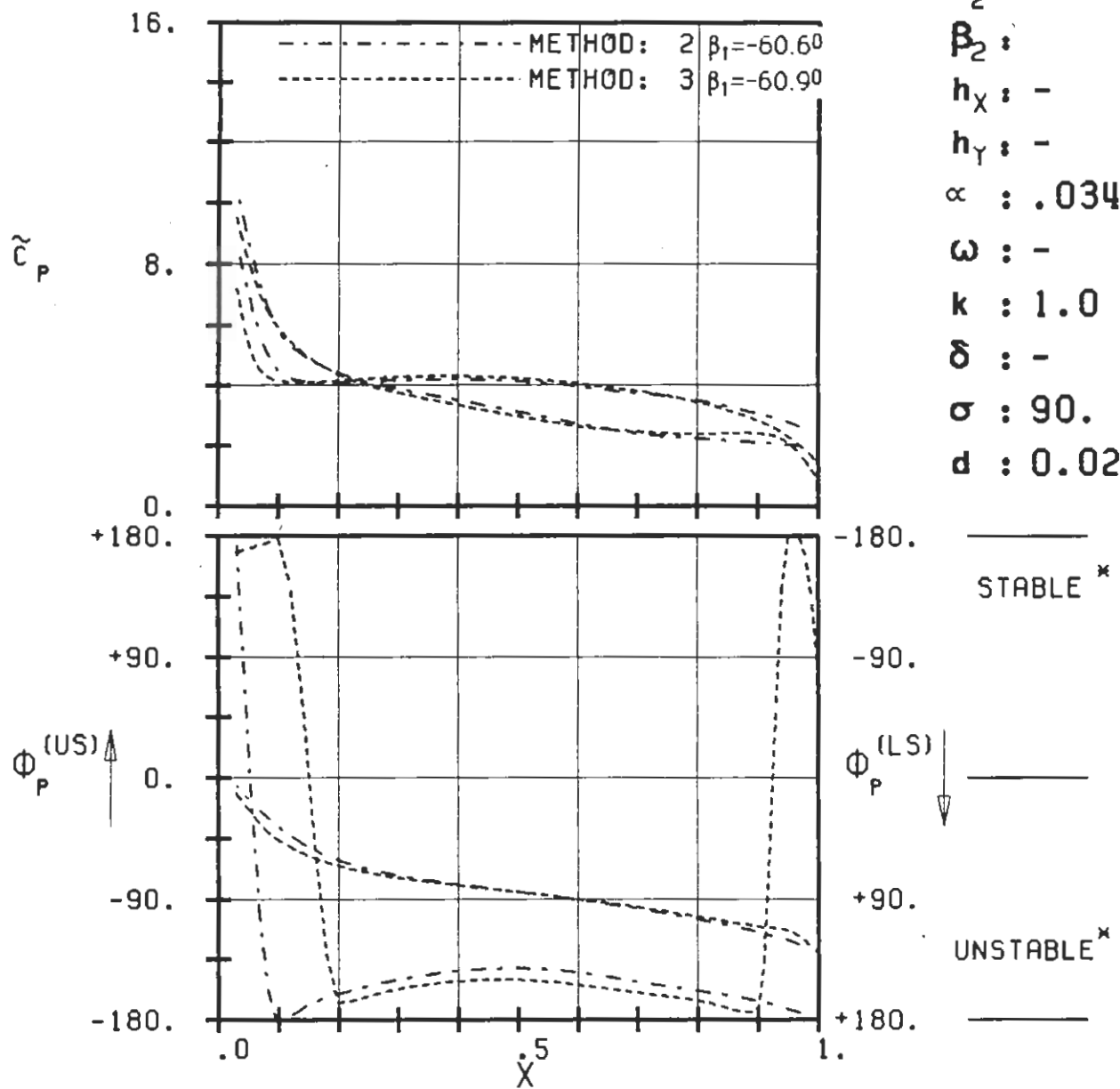
PLOT 7.9-1.3: NINTH STANDARD CONFIGURATION, CASE 20.
TIME AVERAGED BLADE SURFACE PRESSURE
DISTRIBUTION FOR $M_1=0.8$.



PLT 7.9-1.4: NINTH STANDARD CONFIGURATION, CASE 21.
TIME AVERAGED BLADE SURFACE PRESSURE
DISTRIBUTION FOR $M_1=0.9$.

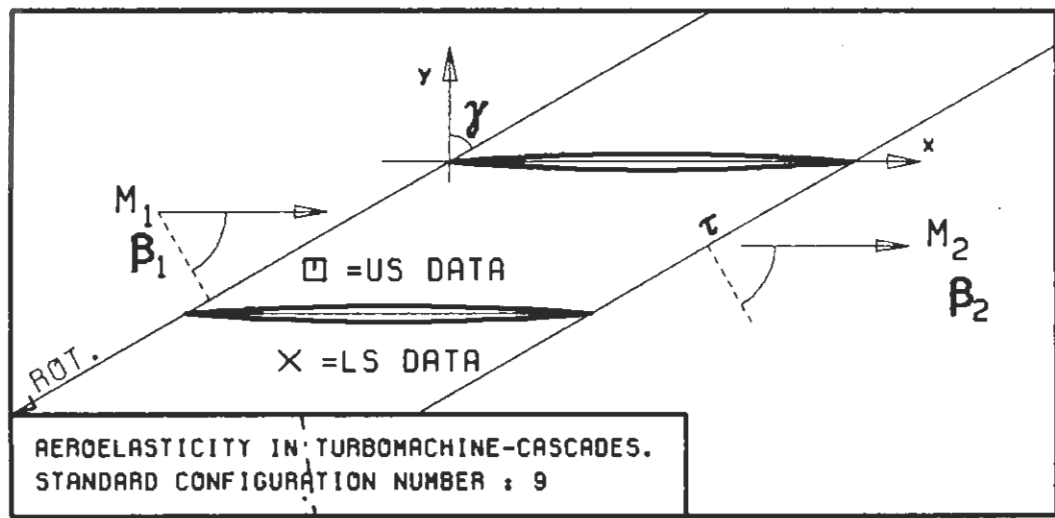


c : 0.1M
 τ : 0.75
 γ : 60.
 x_∞ : 0.5
 y_∞ : 0.
 M_1 : 0.
 β_1 : -60.
 i :
 M_2 : -
 β_2 :
 h_x : -
 h_y : -
 α : .0349
 ω : -
 k : 1.0
 δ : -
 σ : 90.
 d : 0.02

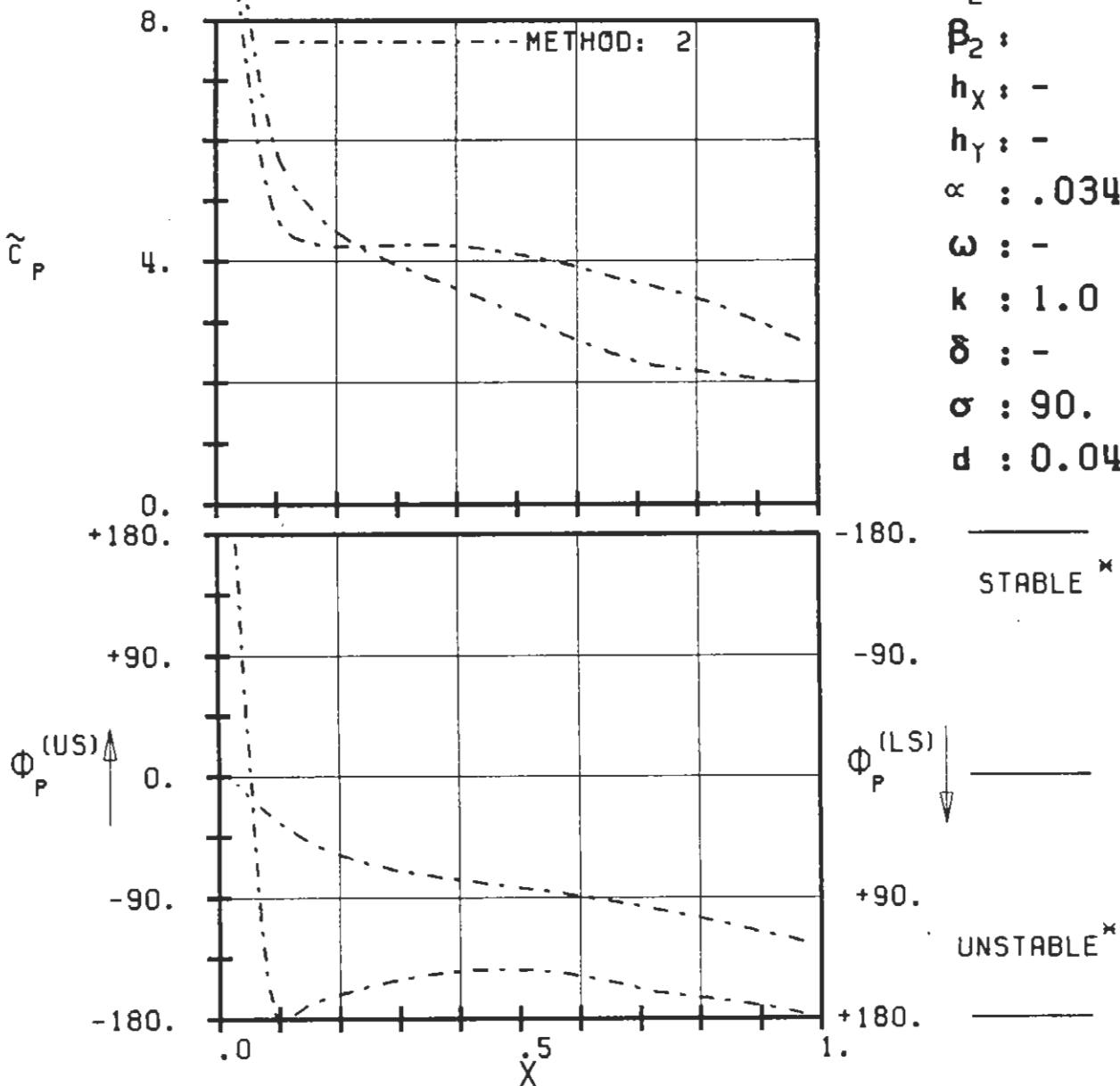


PLOT 7.9-2.1: NINTH STANDARD CONFIGURATION, CASE 1.
MAGNITUDE AND PHASE LEAD OF UNSTEADY BLADE
SURFACE PRESSURE DISTRIBUTION.

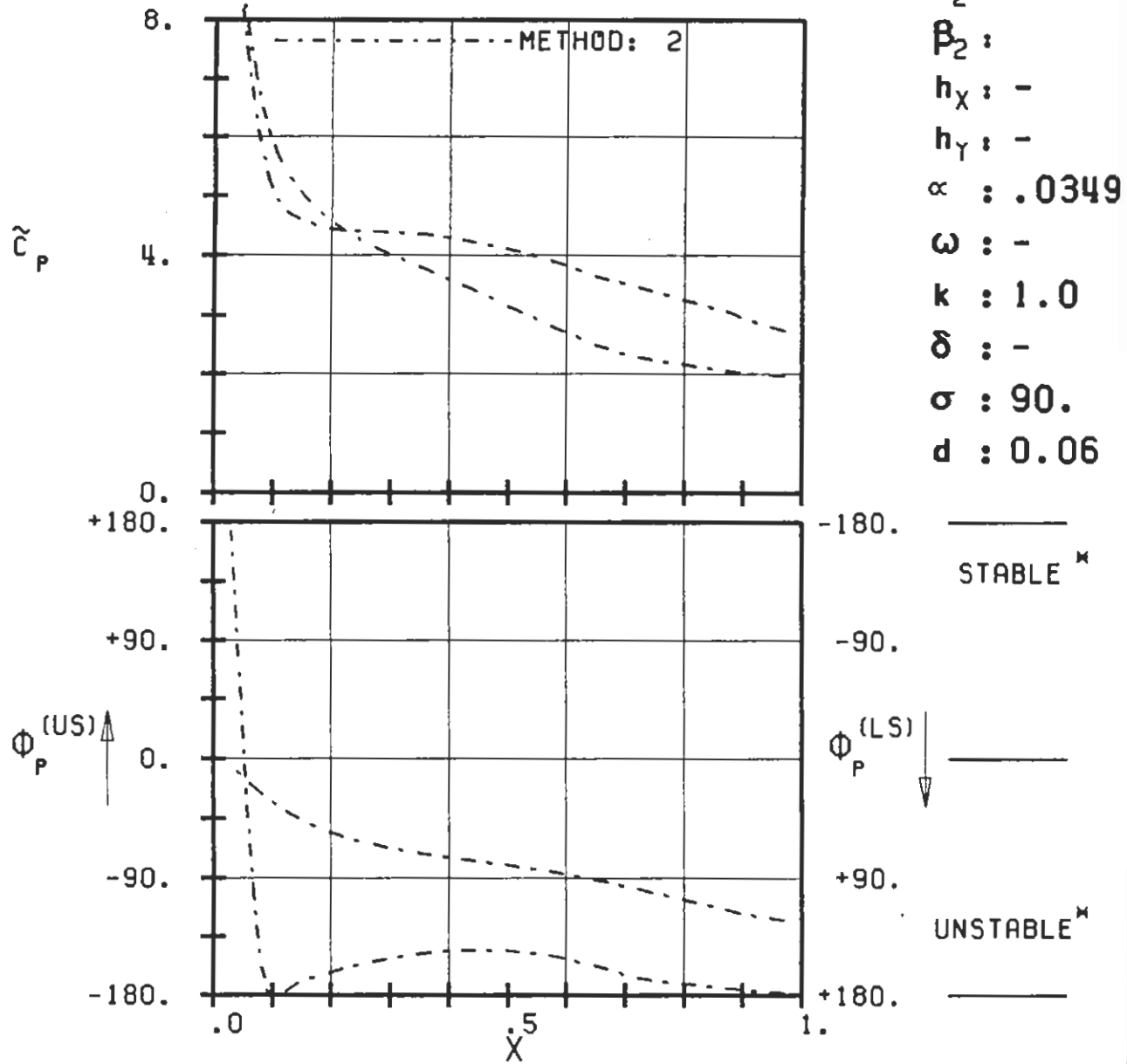
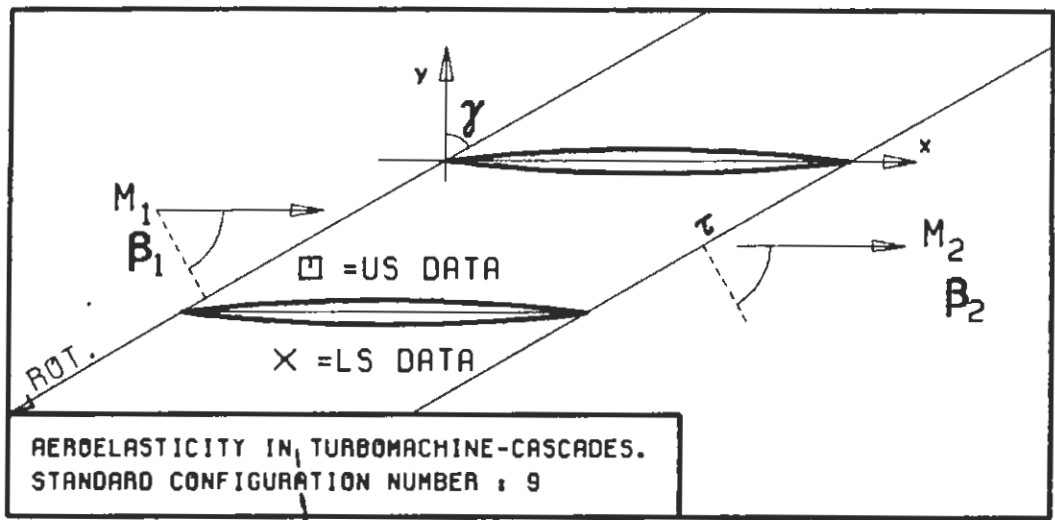
(*: IN PITCH MODE, NOTATION VALID UPSTREAM OF PITCH AXIS)



c : 0.1M
 τ : 0.75
 γ : 60.
 x_∞ : 0.5
 y_∞ : 0.
 M_1 : 0.
 B_1 : -60.
 i :
 M_2 : -
 B_2 :
 h_x : -
 h_y : -
 α : .0349
 ω : -
 k : 1.0
 δ : -
 σ : 90.
 d : 0.04

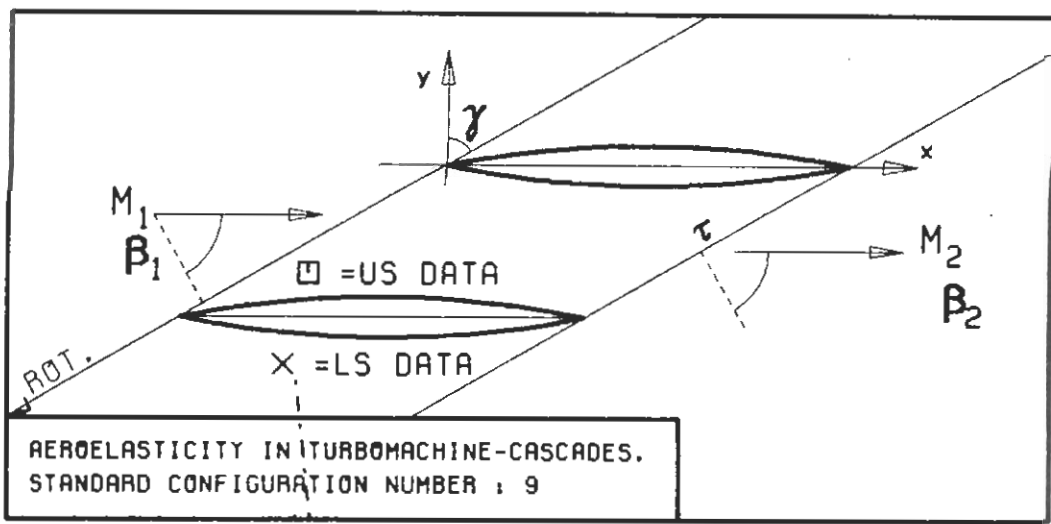


PLOT 7.9-2.2: NINTH STANDARD CONFIGURATION, CASE 2.
MAGNITUDE AND PHASE LEAD OF UNSTEADY BLADE
SURFACE PRESSURE DISTRIBUTION.
(X: IN PITCH MODE, NOTATION VALID UPSTREAM OF PITCH AXIS)

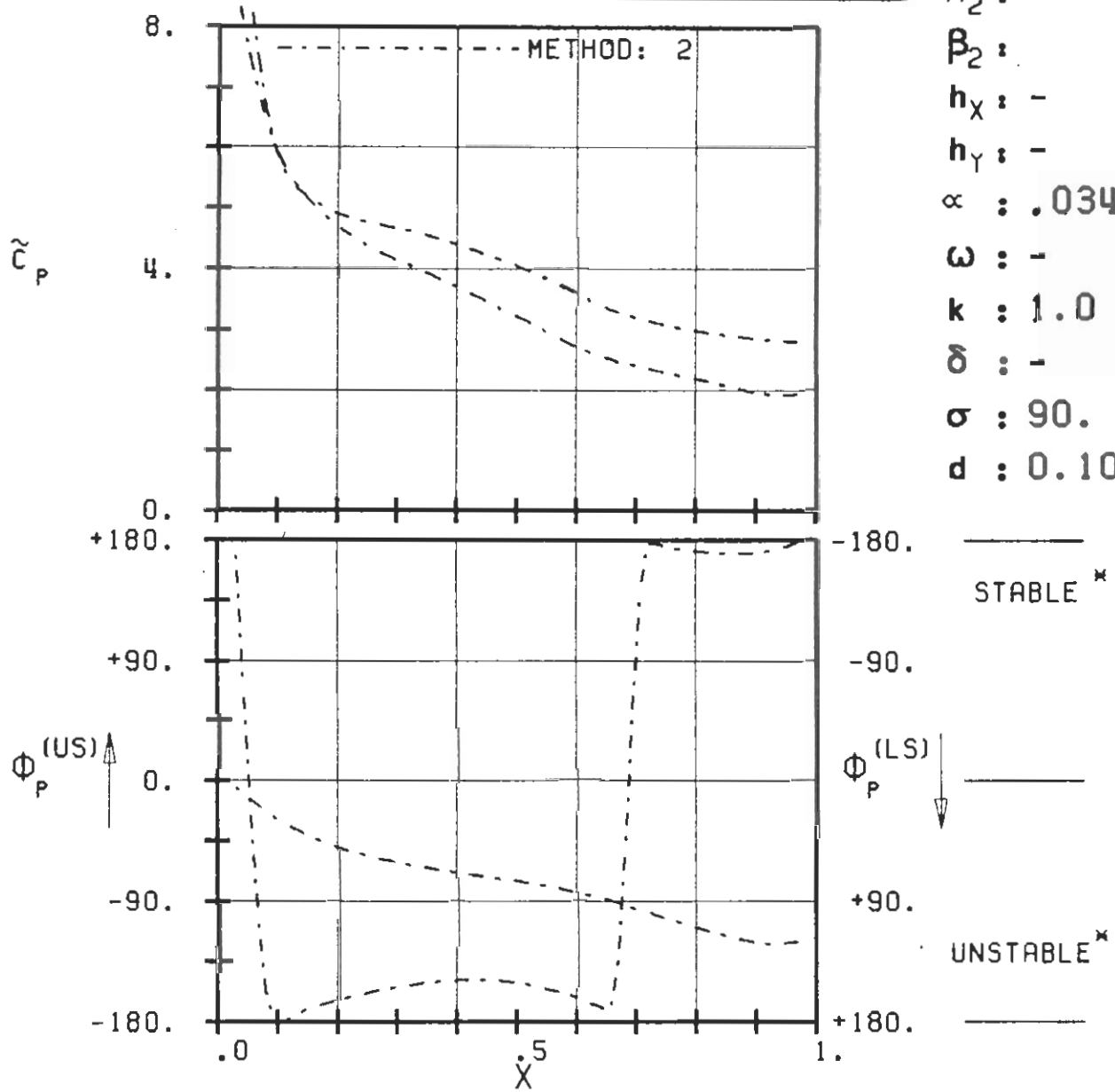


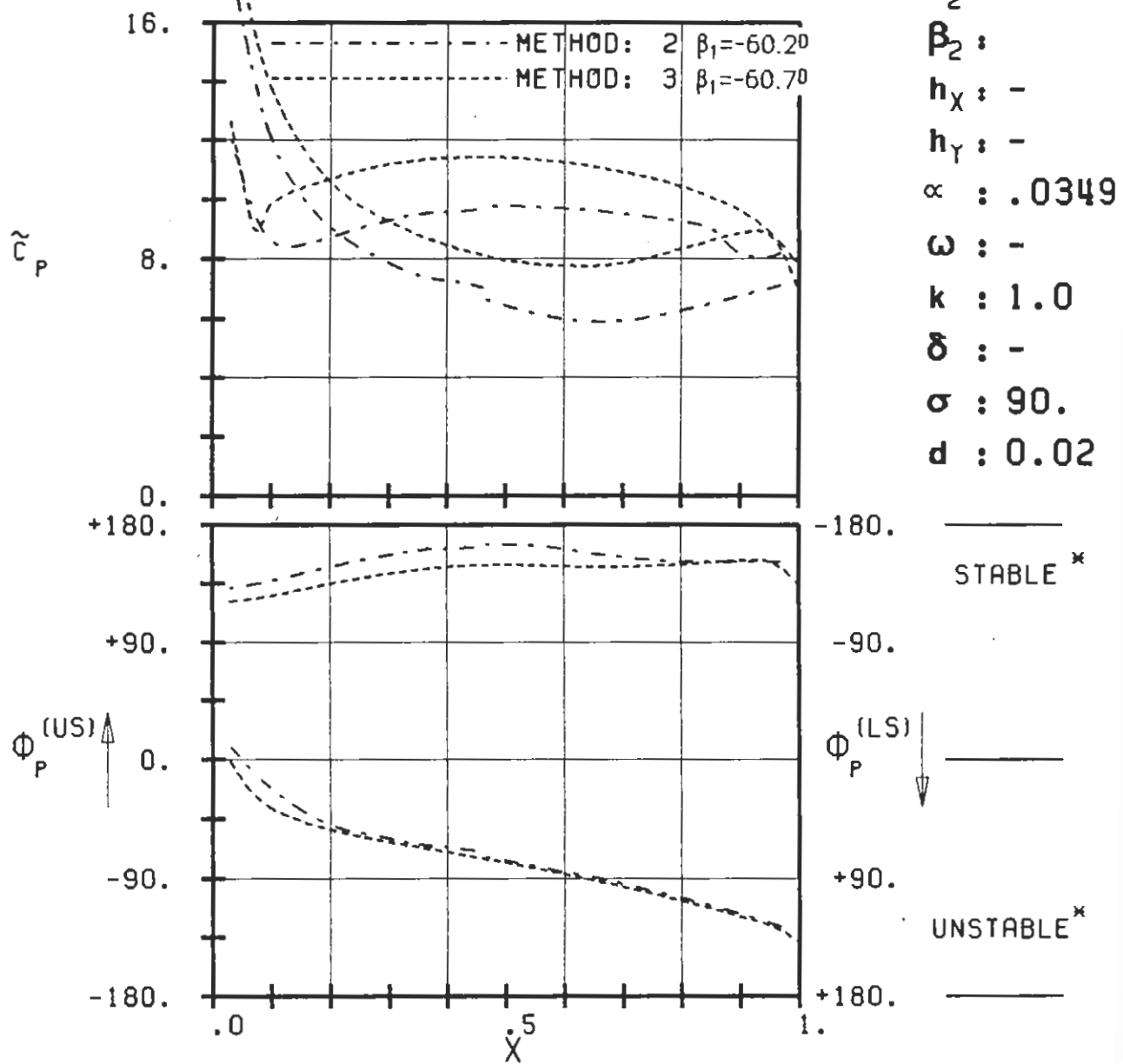
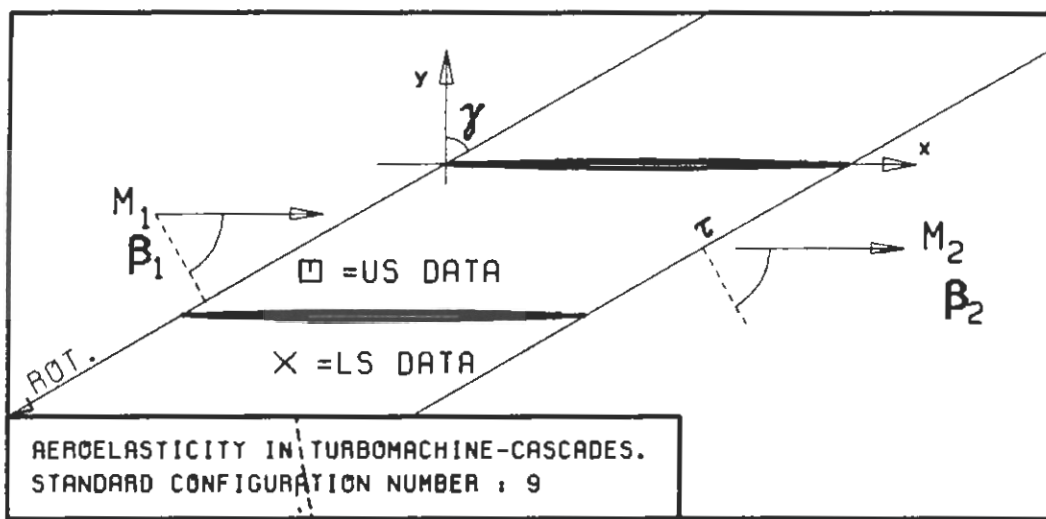
PLOT 7.9-2.3: NINTH STANDARD CONFIGURATION, CASE 3.
MAGNITUDE AND PHASE LEAD OF UNSTEADY BLADE
SURFACE PRESSURE DISTRIBUTION.

(*: IN PITCH MODE, NOTATION VALID UPSTREAM OF PITCH AXIS)



$c = 0.1M$
 $\tau = 0.75$
 $\gamma = 60.$
 $x_\infty = 0.5$
 $y_\infty = 0.$
 $M_1 = 0.$
 $\beta_1 = -60.$
 $i :$
 $M_2 :$
 $\beta_2 :$
 $h_X :$
 $h_Y :$
 $\alpha = .0349$
 $\omega :$
 $k = 1.0$
 $\delta :$
 $\sigma = 90.$
 $d = 0.10$

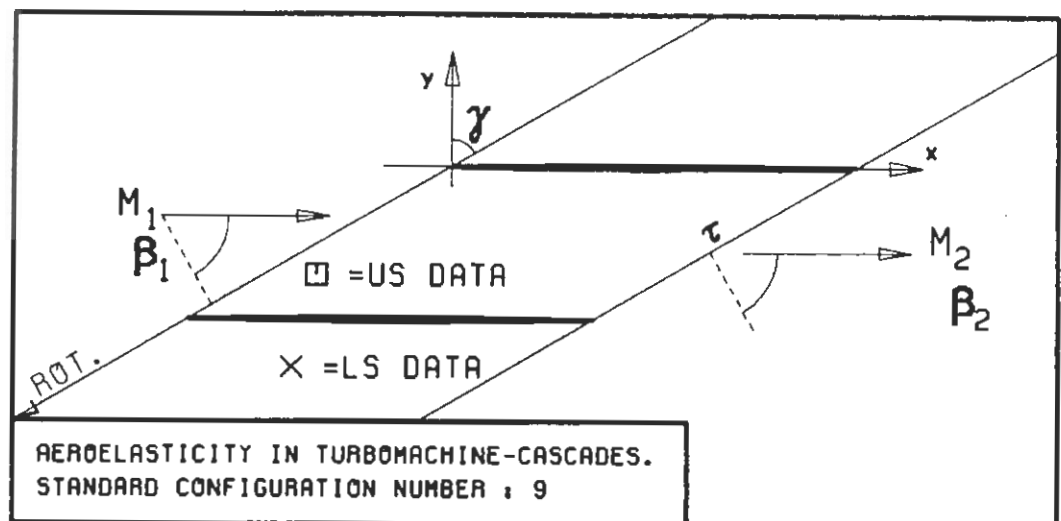




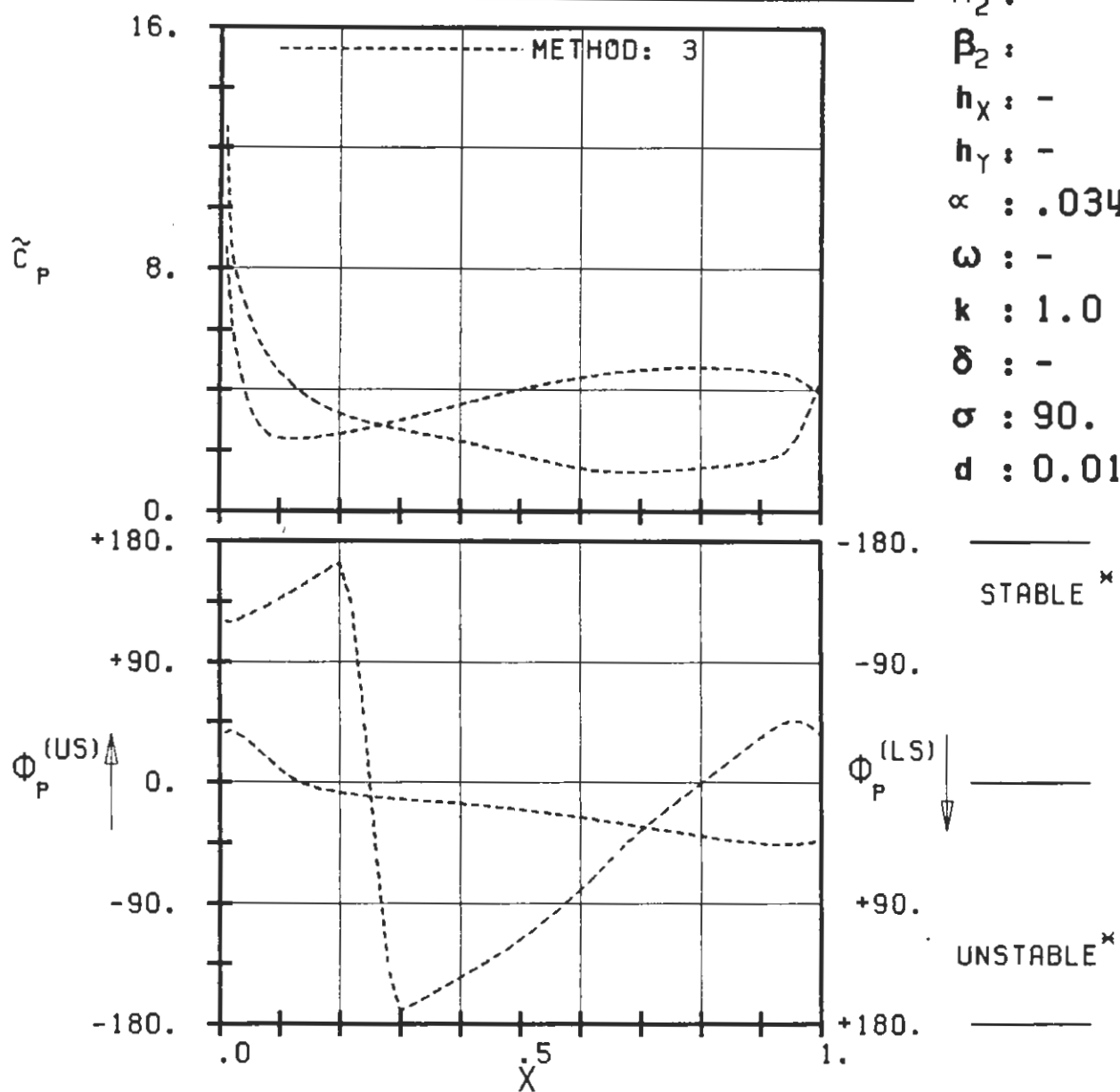
PLOT 7.9-2.5: NINTH STANDARD CONFIGURATION, CASE 5.
MAGNITUDE AND PHASE LEAD OF UNSTEADY BLADE
SURFACE PRESSURE DISTRIBUTION.

(X: IN PITCH MODE, NOTATION VALID UPSTREAM OF PITCH AXIS)

c : 0.1M
 τ : 0.75
 γ : 60.
 x_∞ : 0.5
 y_∞ : 0.
 M_1 : 0.5
 β_1 : -60.
i :
 M_2 : -
 β_2 :
 h_X : -
 h_Y : -
 α : .0349
 ω : -
 k : 1.0
 δ : -
 σ : 90.
 d : 0.02

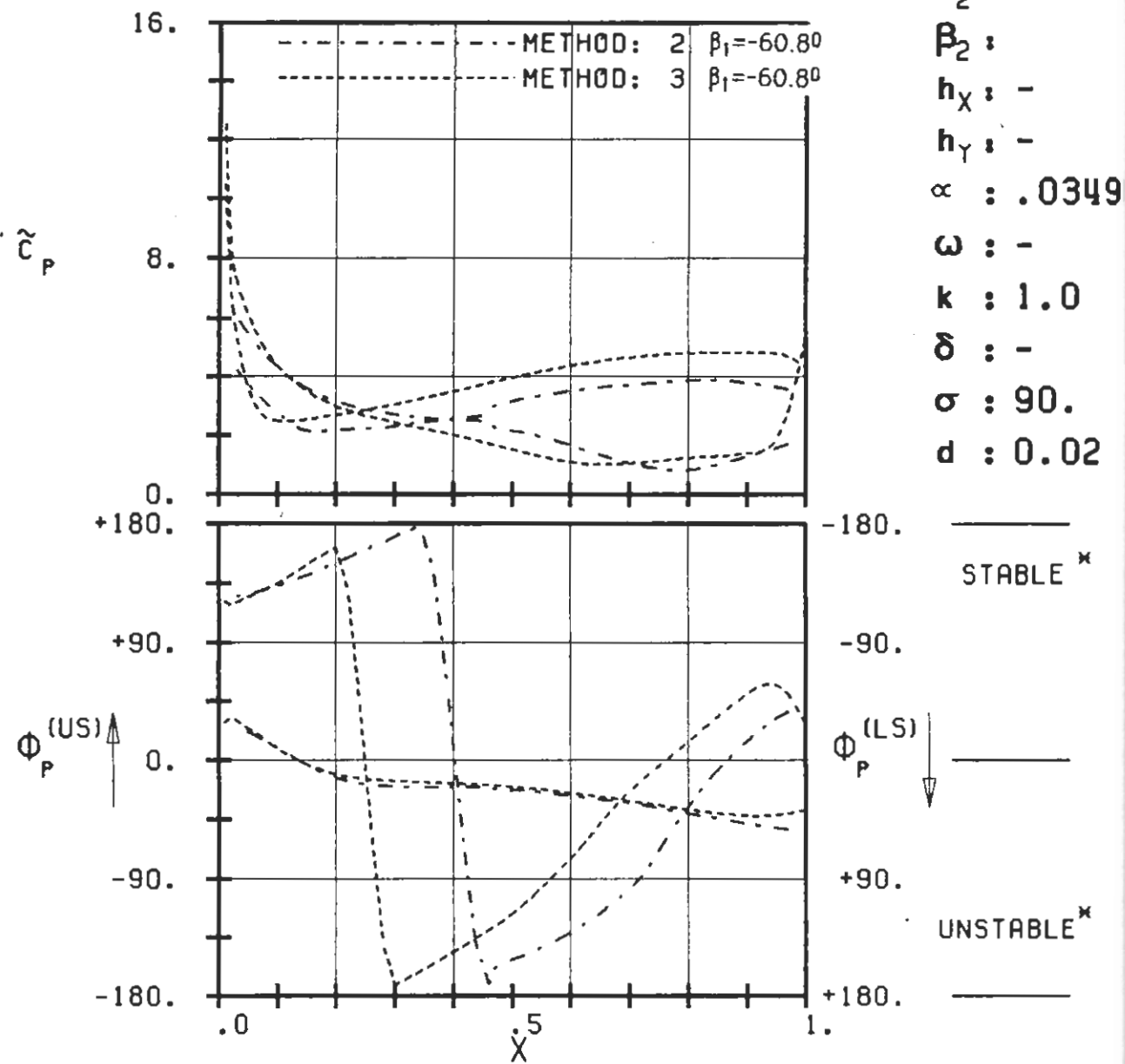
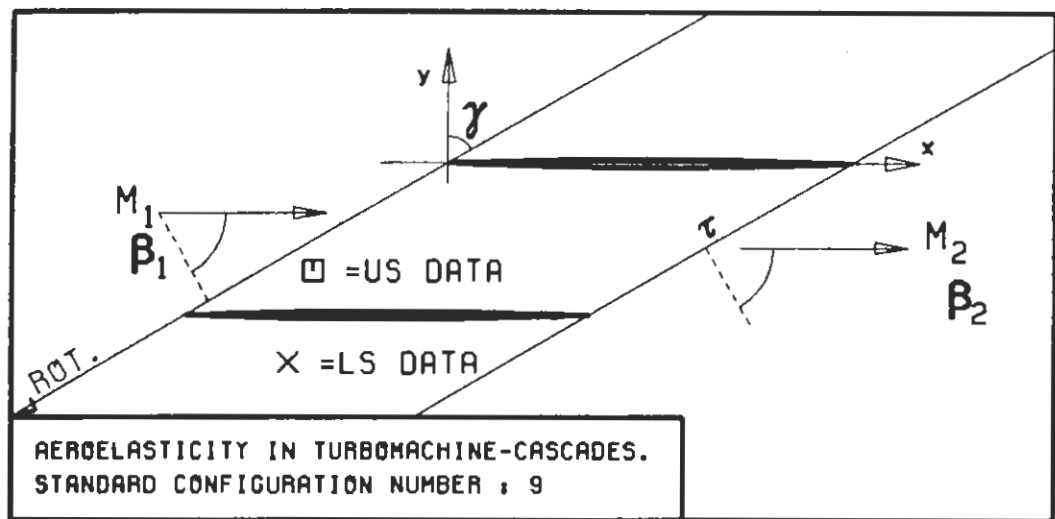


$c : 0.1M$
 $\tau : 0.75$
 $\gamma : 60.$
 $x_\infty : 0.5$
 $y_\infty : 0.$
 $M_1 : 0.7$
 $\beta_1 : -60.$
 $i :$
 $M_2 : -$
 $\beta_2 : -$
 $h_x : -$
 $h_y : -$
 $\alpha : .0349$
 $\omega : -$
 $k : 1.0$
 $\delta : -$
 $\sigma : 90.$
 $d : 0.01$

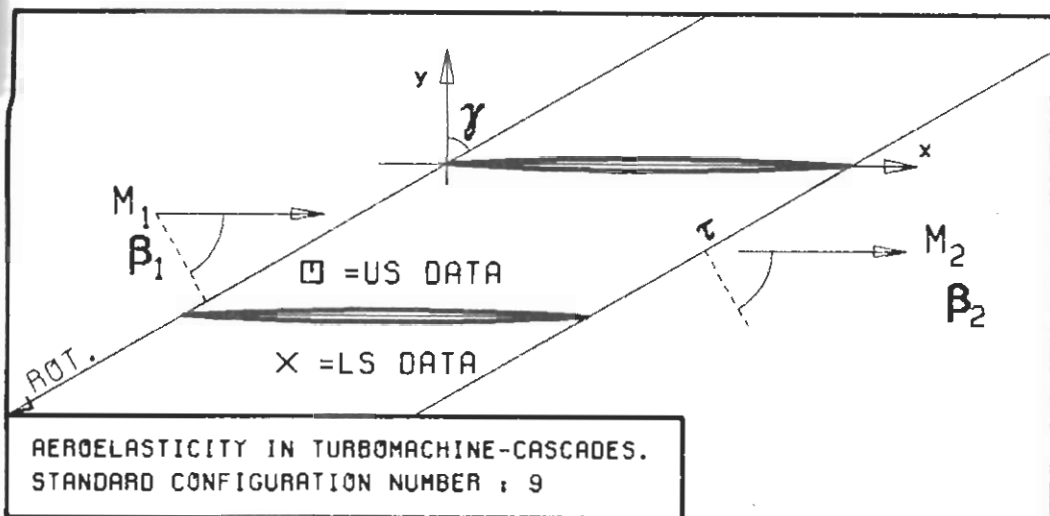


PLOT 7.9-2.6: NINTH STANDARD CONFIGURATION, CASE 6.
MAGNITUDE AND PHASE LEAD OF UNSTEADY BLADE
SURFACE PRESSURE DISTRIBUTION.

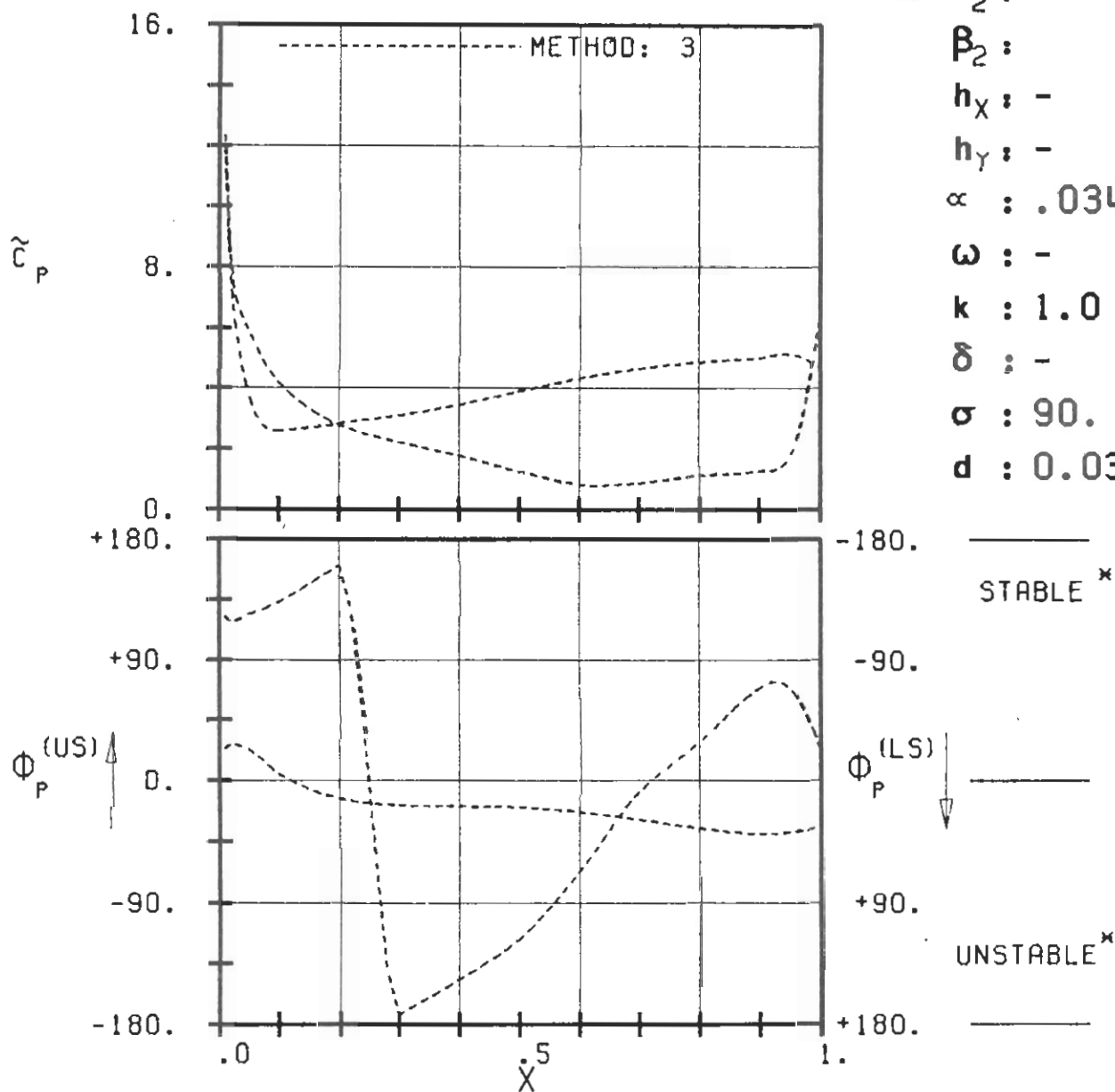
(*: IN PITCH MODE, NOTATION VALID UPSTREAM OF PITCH AXIS)



PLOT 7.9-2.7: NINTH STANDARD CONFIGURATION, CASE 7.
MAGNITUDE AND PHASE LEAD OF UNSTEADY BLADE
SURFACE PRESSURE DISTRIBUTION.
(\times : IN PITCH MODE, NOTATION VALID UPSTREAM OF PITCH AXIS)

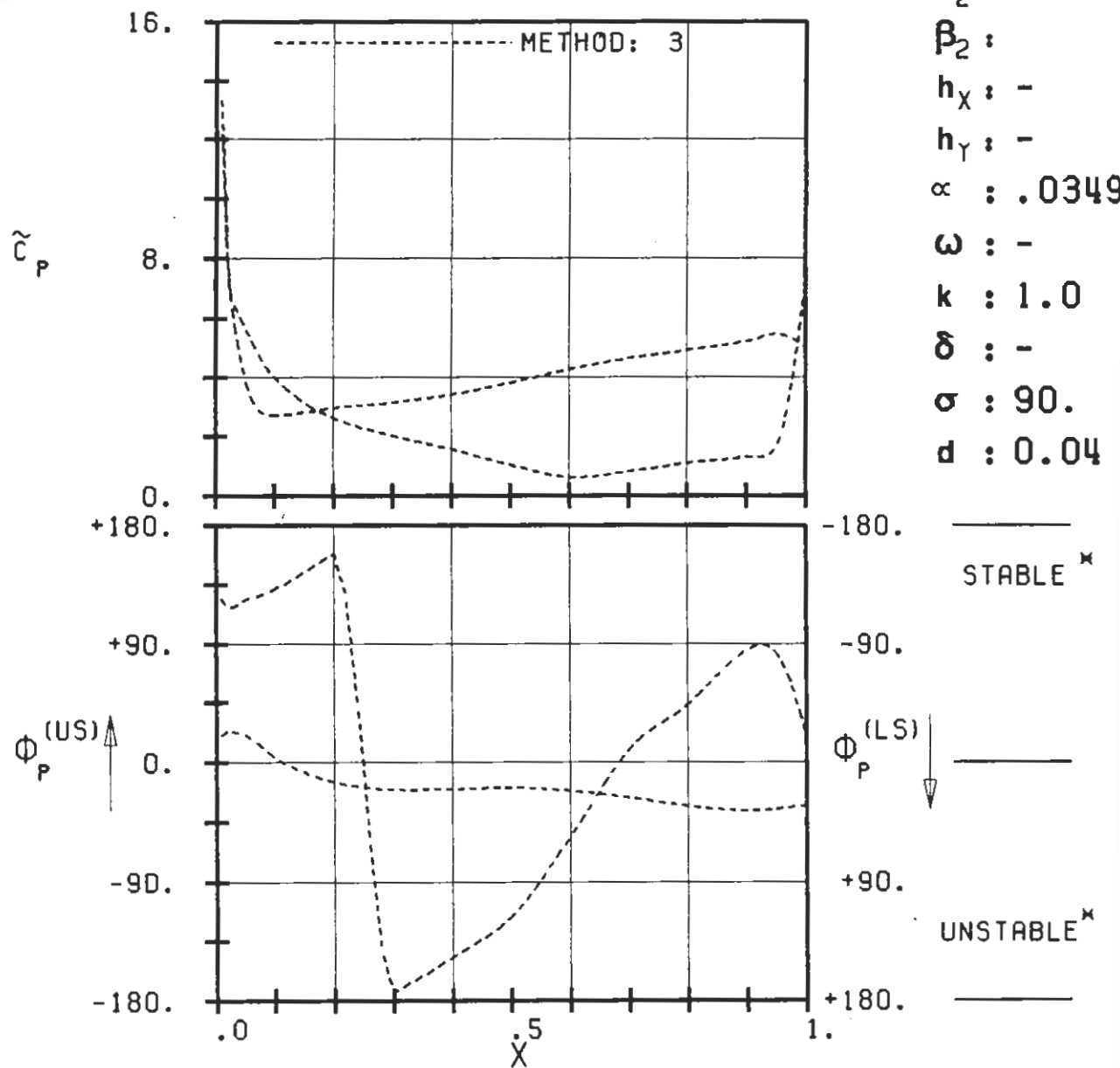
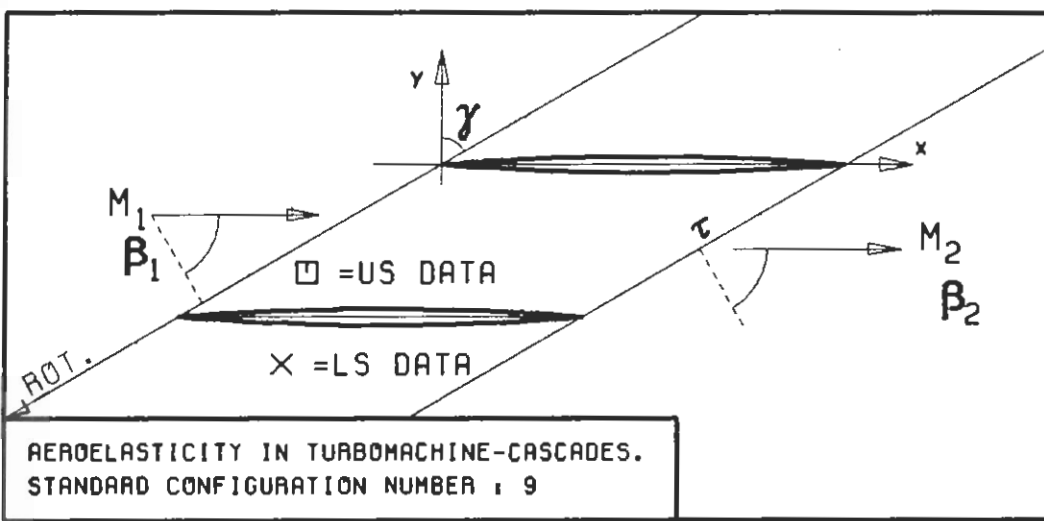


$c : 0.1M$
 $\tau : 0.75$
 $\gamma : 60.$
 $x_\alpha : 0.5$
 $y_\alpha : 0.$
 $M_1 : 0.7$
 $\beta_1 : -60.$
 $i :$
 $M_2 : -$
 $\beta_2 : -$
 $h_X : -$
 $h_Y : -$
 $\alpha : .0349$
 $\omega : -$
 $k : 1.0$
 $\delta : -$
 $\sigma : 90.$
 $d : 0.03$

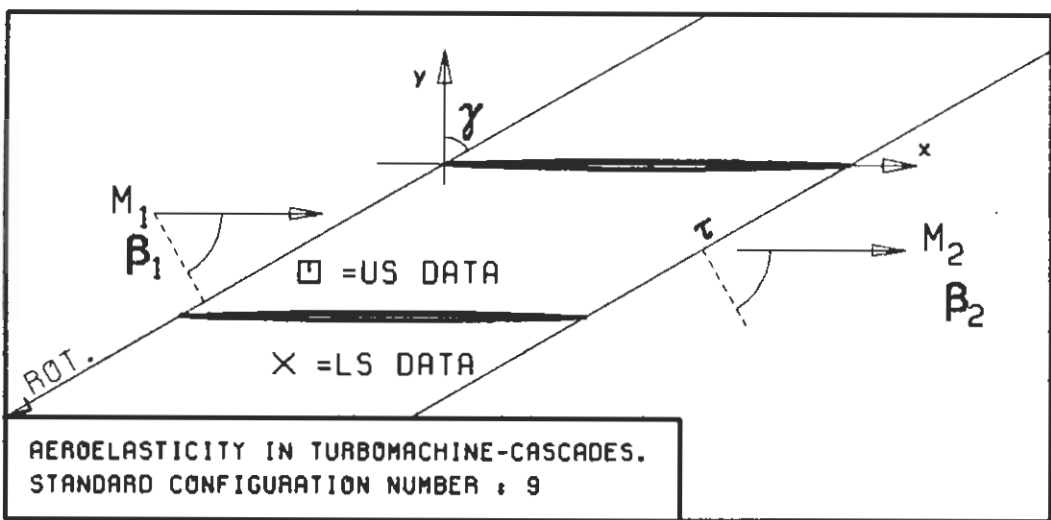


PLOT 7.9-2.8: NINTH STANDARD CONFIGURATION, CASE 8.
MAGNITUDE AND PHASE LEAD OF UNSTEADY BLADE SURFACE PRESSURE DISTRIBUTION.

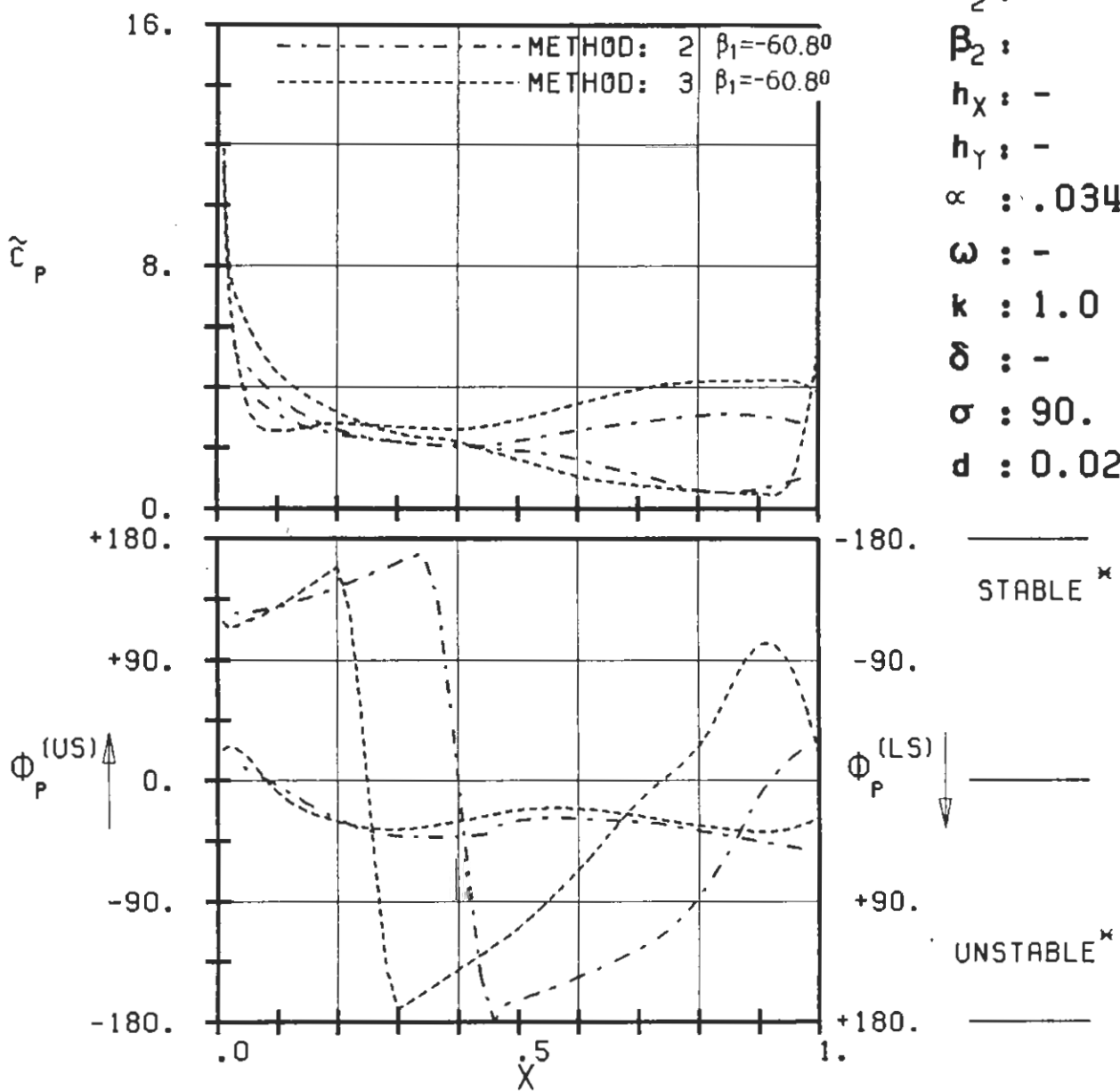
(*: IN PITCH MODE, NOTATION VALID UPSTREAM OF PITCH AXIS)



PLOT 7.9-2.9: NINTH STANDARD CONFIGURATION, CASE 9.
MAGNITUDE AND PHASE LEAD OF UNSTEADY BLADE
SURFACE PRESSURE DISTRIBUTION.
(*: IN PITCH MODE, NOTATION VALID UPSTREAM OF PITCH AXIS)

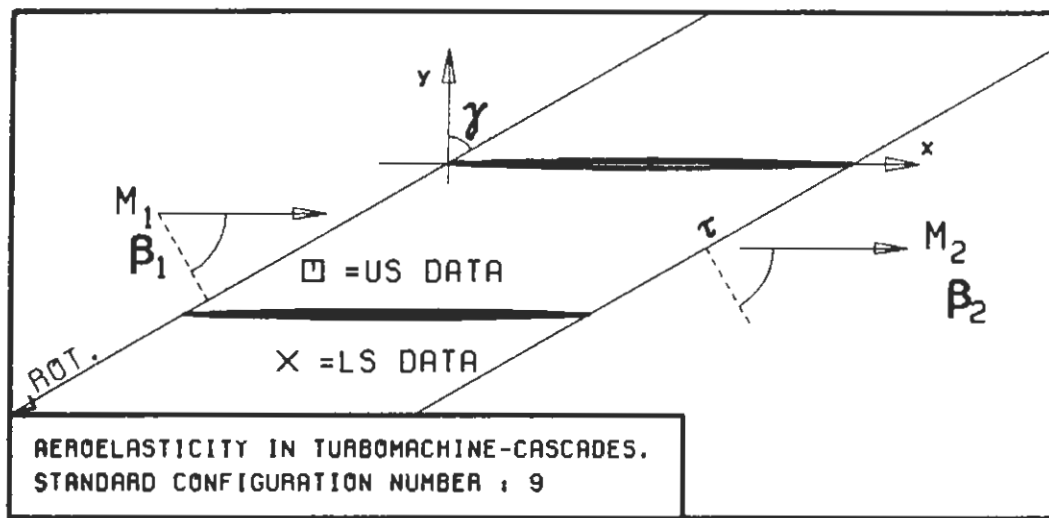


$c : 0.1M$
 $\tau : 0.75$
 $\gamma : 60.$
 $x_\infty : 0.5$
 $y_\infty : 0.$
 $M_1 : 0.8$
 $\beta_1 : -60.$
 $i :$
 $M_2 : -$
 $\beta_2 : -$
 $h_x : -$
 $h_y : -$
 $\alpha : .0349$
 $\omega : -$
 $k : 1.0$
 $\delta : -$
 $\sigma : 90.$
 $d : 0.02$

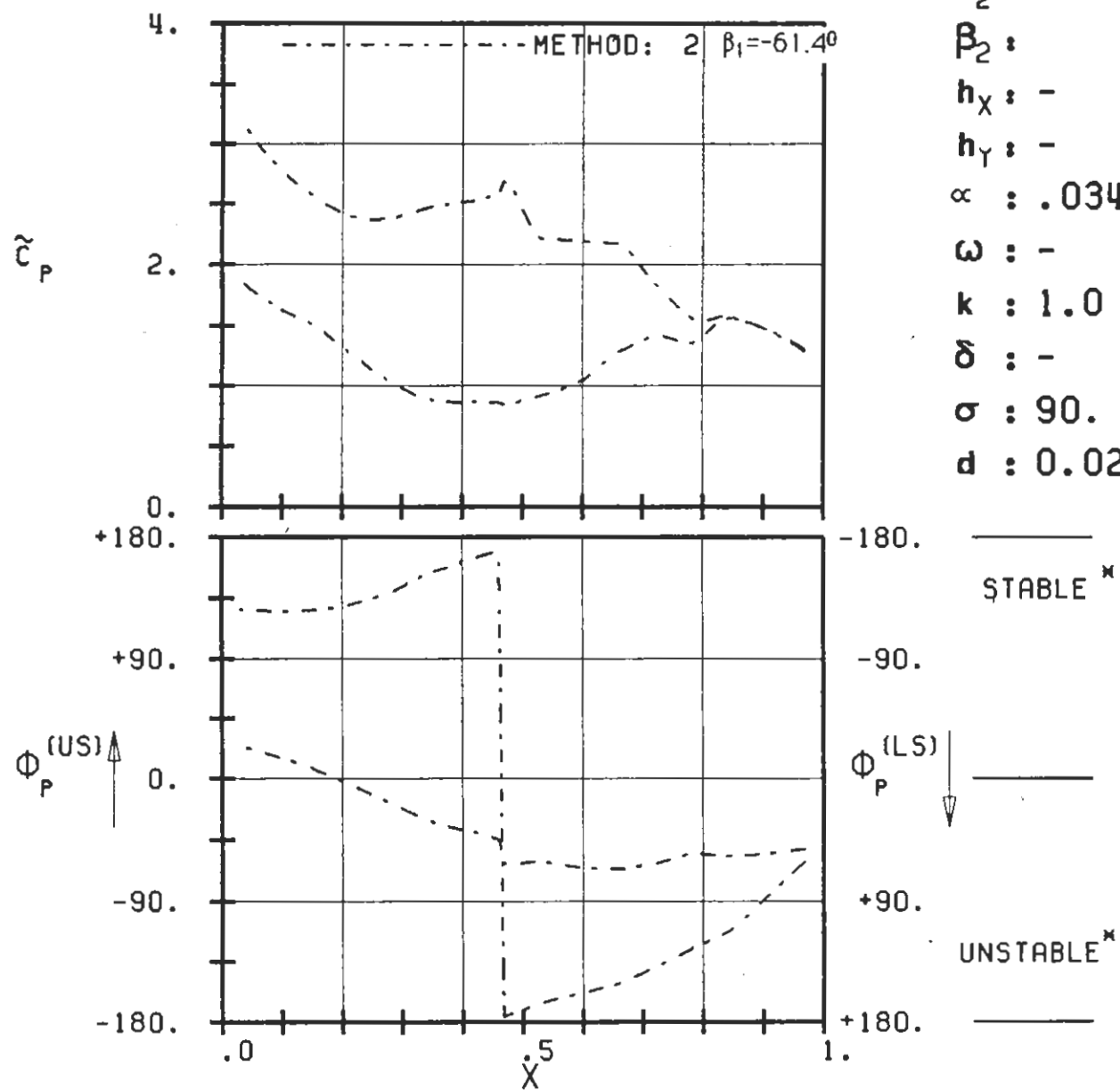


PLT 7.9-2.10: NINTH STANDARD CONFIGURATION, CASE 10.
MAGNITUDE AND PHASE LEAD OF UNSTEADY BLADE
SURFACE PRESSURE DISTRIBUTION.

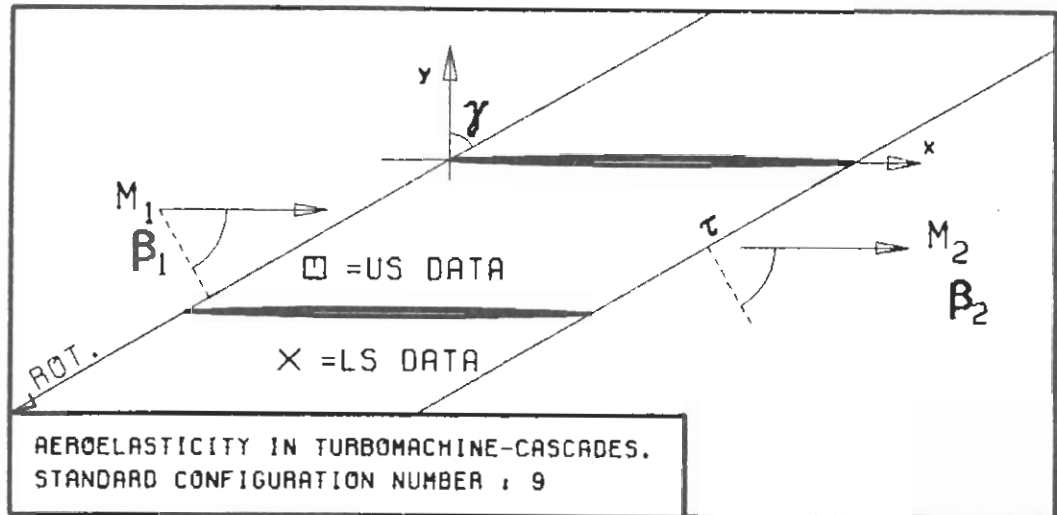
(*: IN PITCH MODE, NOTATION VALID UPSTREAM OF PITCH AXIS)



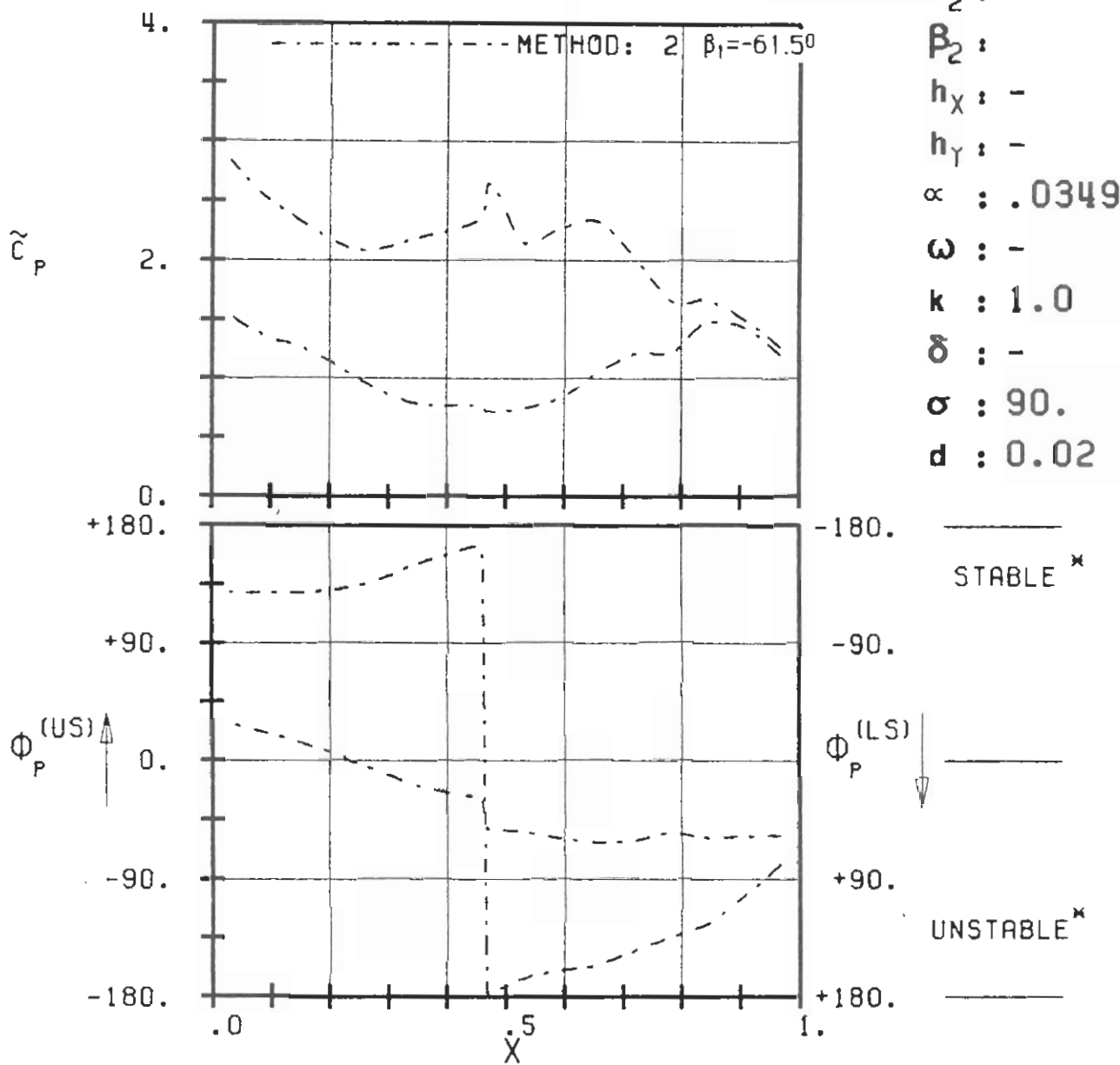
c : 0.1M
 τ : 0.75
 γ : 60.
 x_α : 0.5
 y_α : 0.
 M_1 : 1.3
 β_1 : -60.
 i :
 M_2 : -
 β_2 :
 h_x : -
 h_y : -
 α : .0349
 ω : -
 k : 1.0
 δ : -
 σ : 90.
 d : 0.02



PLOT 7.9-2.11: NINTH STANDARD CONFIGURATION, CASE 11.
 MAGNITUDE AND PHASE LEAD OF UNSTEADY BLADE
 SURFACE PRESSURE DISTRIBUTION.
 (*: IN PITCH MODE, NOTATION VALID UPSTREAM OF PITCH AXIS)

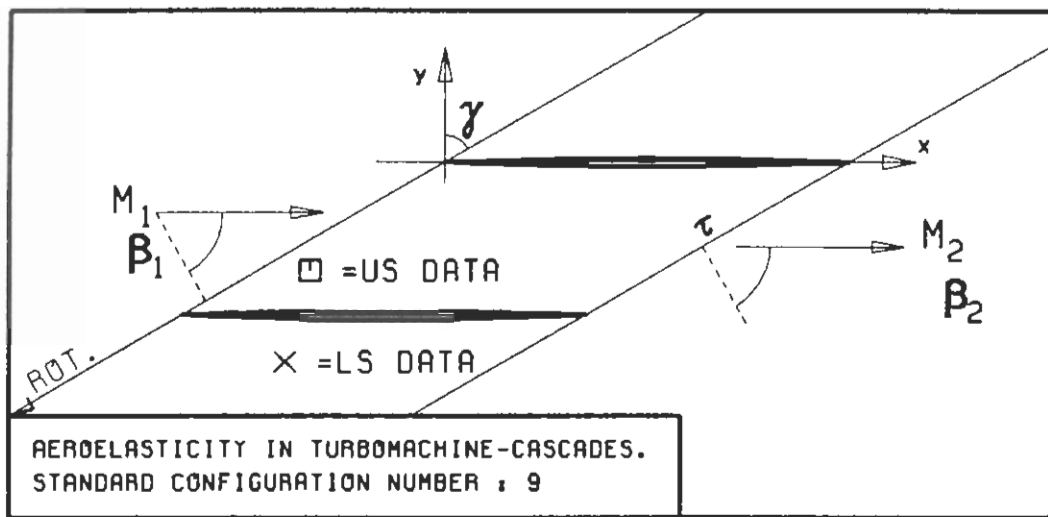


c : 0.1M
 τ : 0.75
 γ : 60.
 x_∞ : 0.5
 y_∞ : 0.
 M_1 : 1.4
 β_1 : -60.
 i :
 M_2 : -
 β_2 :
 h_x : -
 h_y : -
 α : .0349
 ω : -
 k : 1.0
 δ : -
 σ : 90.
 d : 0.02

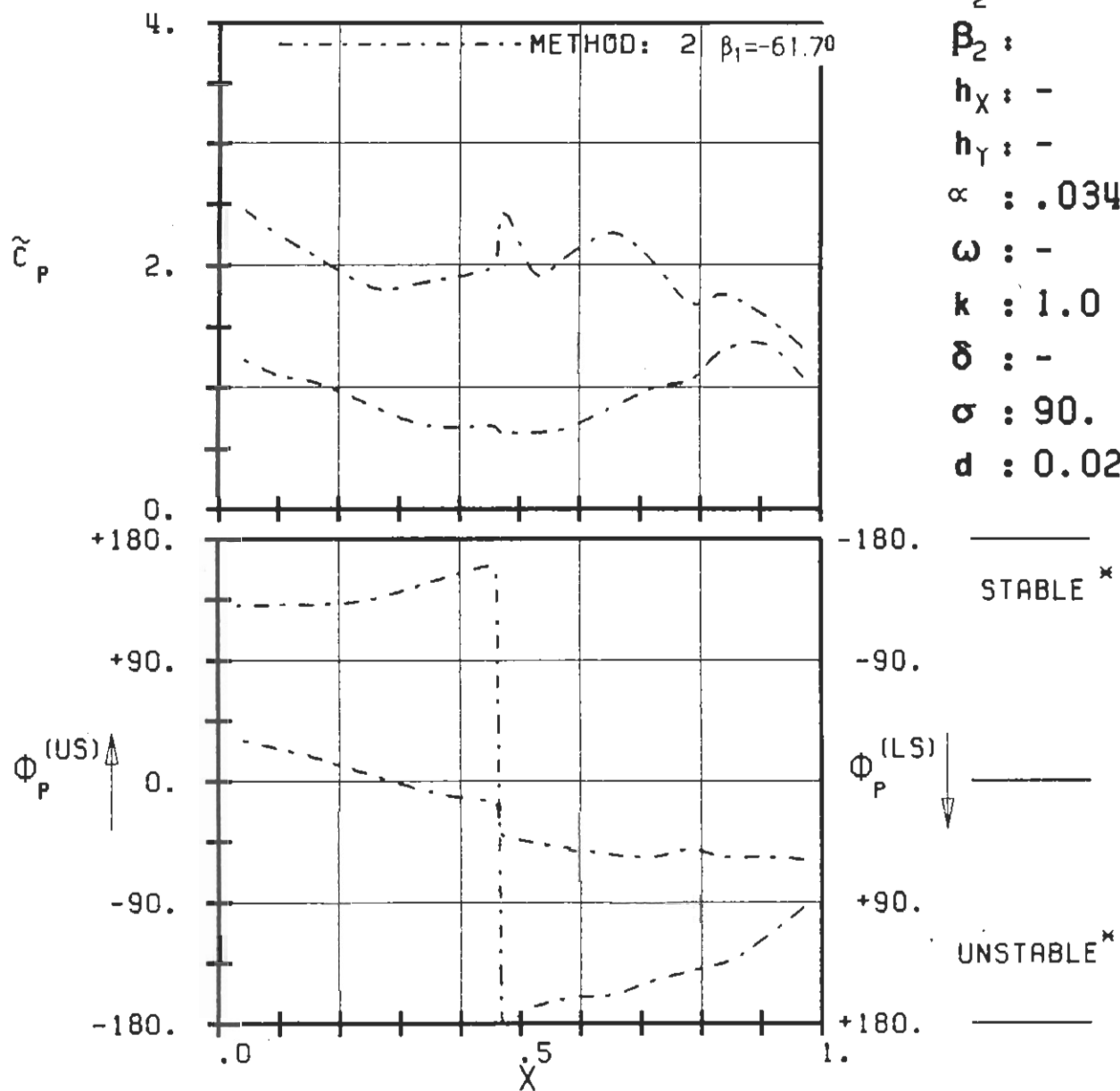


PLOT 7.9-2.12: NINTH STANDARD CONFIGURATION, CASE 12.
MAGNITUDE AND PHASE LEAD OF UNSTEADY BLADE
SURFACE PRESSURE DISTRIBUTION.

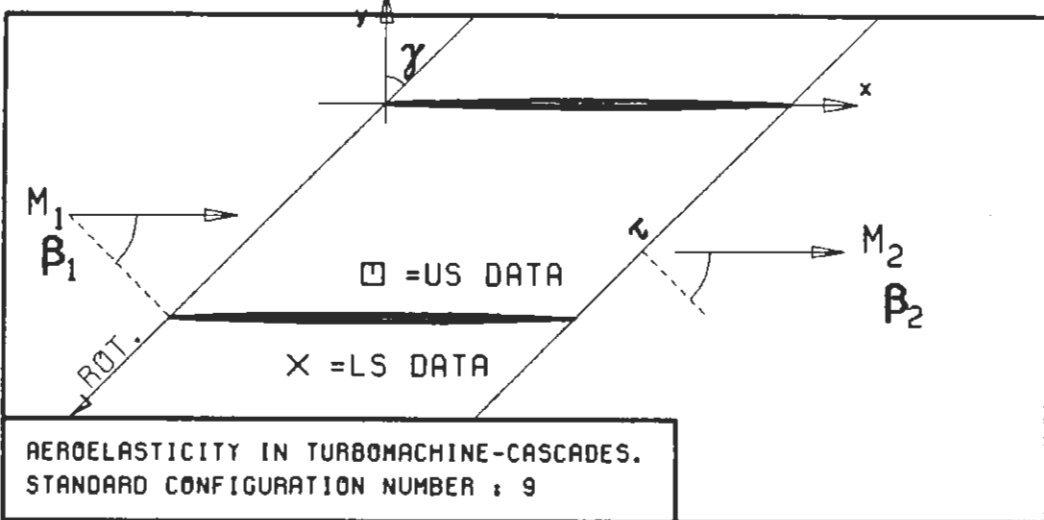
(*: IN PITCH MODE, NOTATION VALID UPSTREAM OF PITCH AXIS)



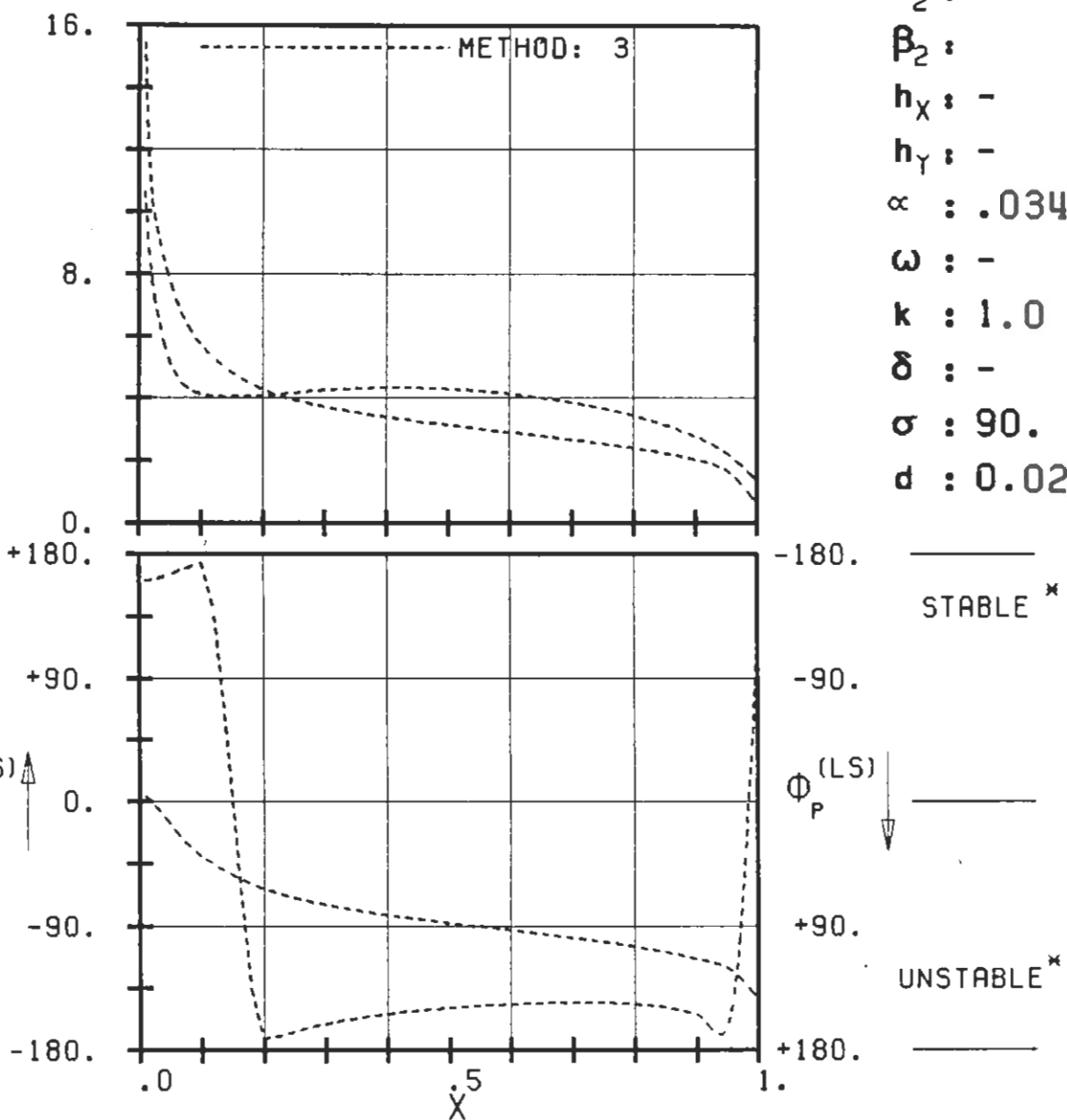
c : 0.1M
 τ : 0.75
 γ : 60.
 x_∞ : 0.5
 y_∞ : 0.
 M_1 : 1.5
 β_1 : -60.
 i :
 M_2 : -
 β_2 :
 h_X : -
 h_Y : -
 α : .0349
 ω : -
 k : 1.0
 δ : -
 σ : 90.
 d : 0.02



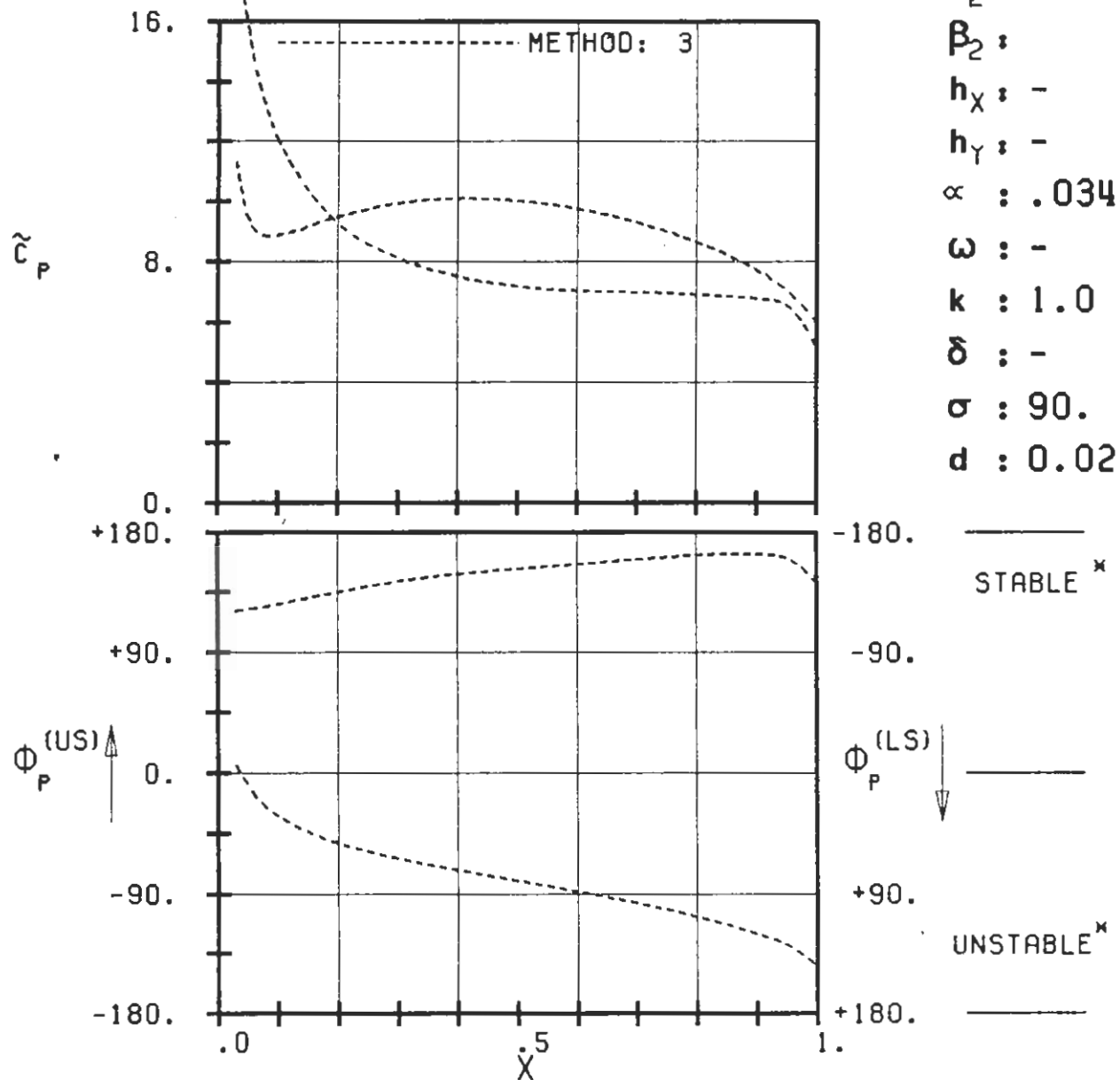
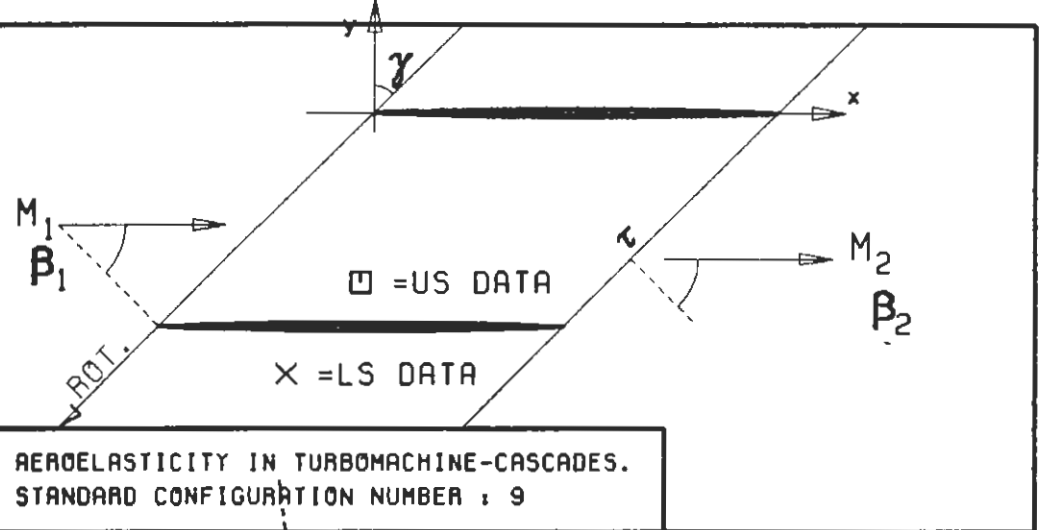
PLOT 7.9-2.13: NINTH STANDARD CONFIGURATION, CASE 13.
MAGNITUDE AND PHASE LEAD OF UNSTEADY BLADE
SURFACE PRESSURE DISTRIBUTION.
(X: IN PITCH MODE, NOTATION VALIO UPSTREAM OF PITCH AXIS)

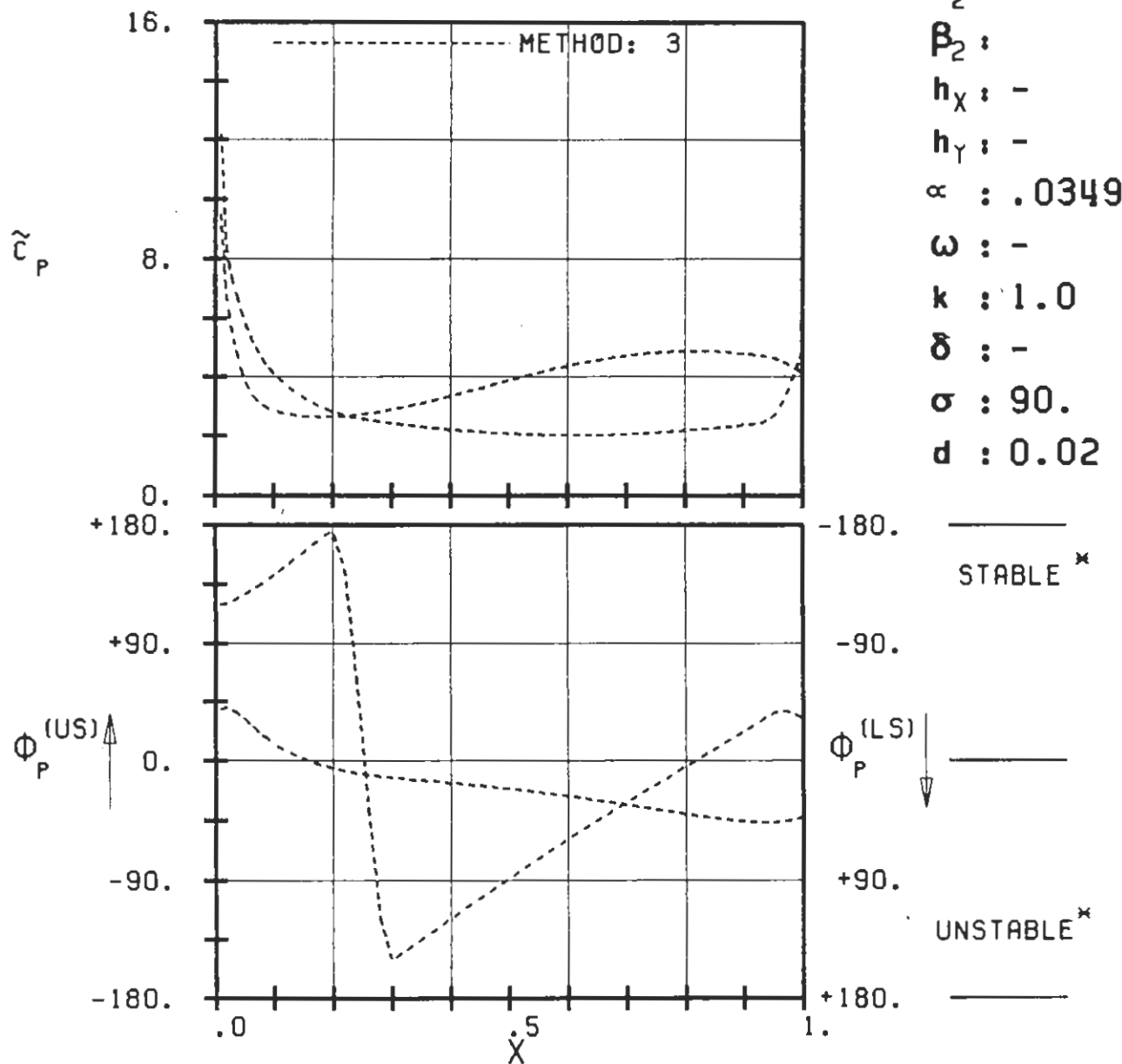
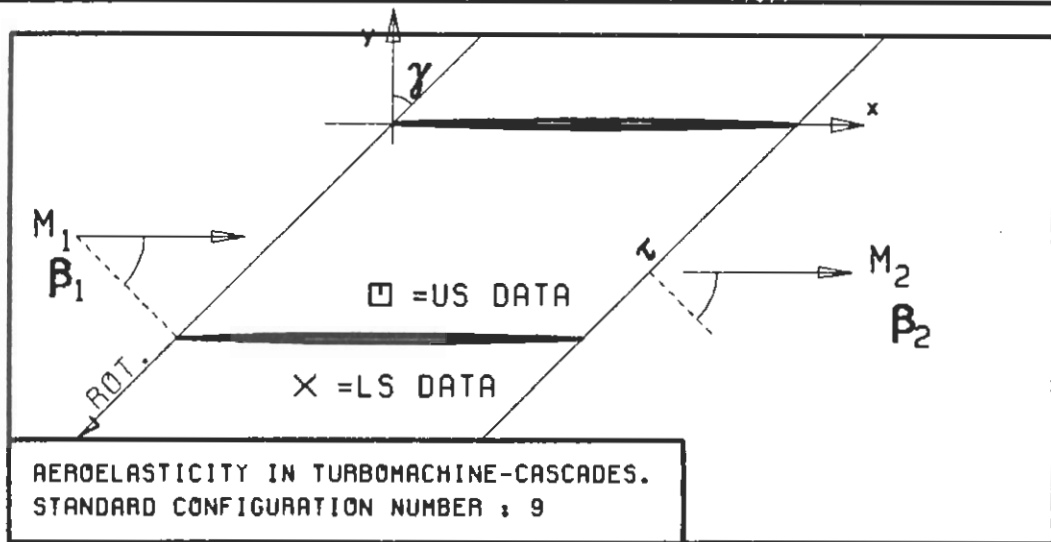


$c : 0.1M$
 $\tau : 0.75$
 $\gamma : 45.$
 $x_\alpha : 0.5$
 $y_\alpha : 0.$
 $M_1 : 0.$
 $\beta_1 : -45.$
 $i :$
 $M_2 : -$
 $\beta_2 : -$
 $h_X : -$
 $h_Y : -$
 $\alpha : .0349$
 $\omega : -$
 $k : 1.0$
 $\delta : -$
 $\sigma : 90.$
 $d : 0.02$

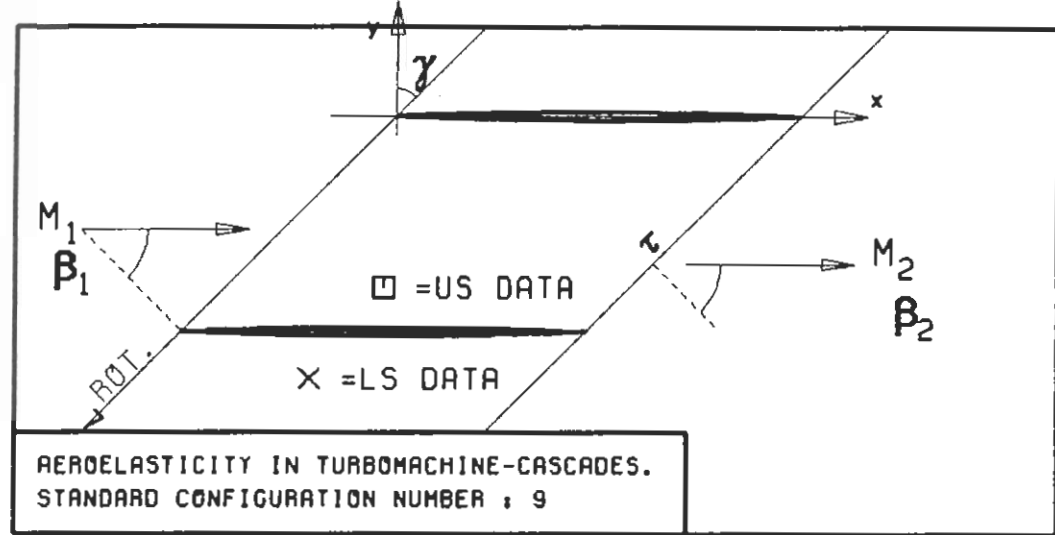


PLOT 7.9-2.14: NINTH STANDARD CONFIGURATION, CASE 14
MAGNITUDE AND PHASE LEAD OF UNSTEADY BLADE SURFACE PRESSURE DISTRIBUTION.
(*: IN PITCH MODE, NOTATION VALID UPSTREAM OF PITCH AXIS)

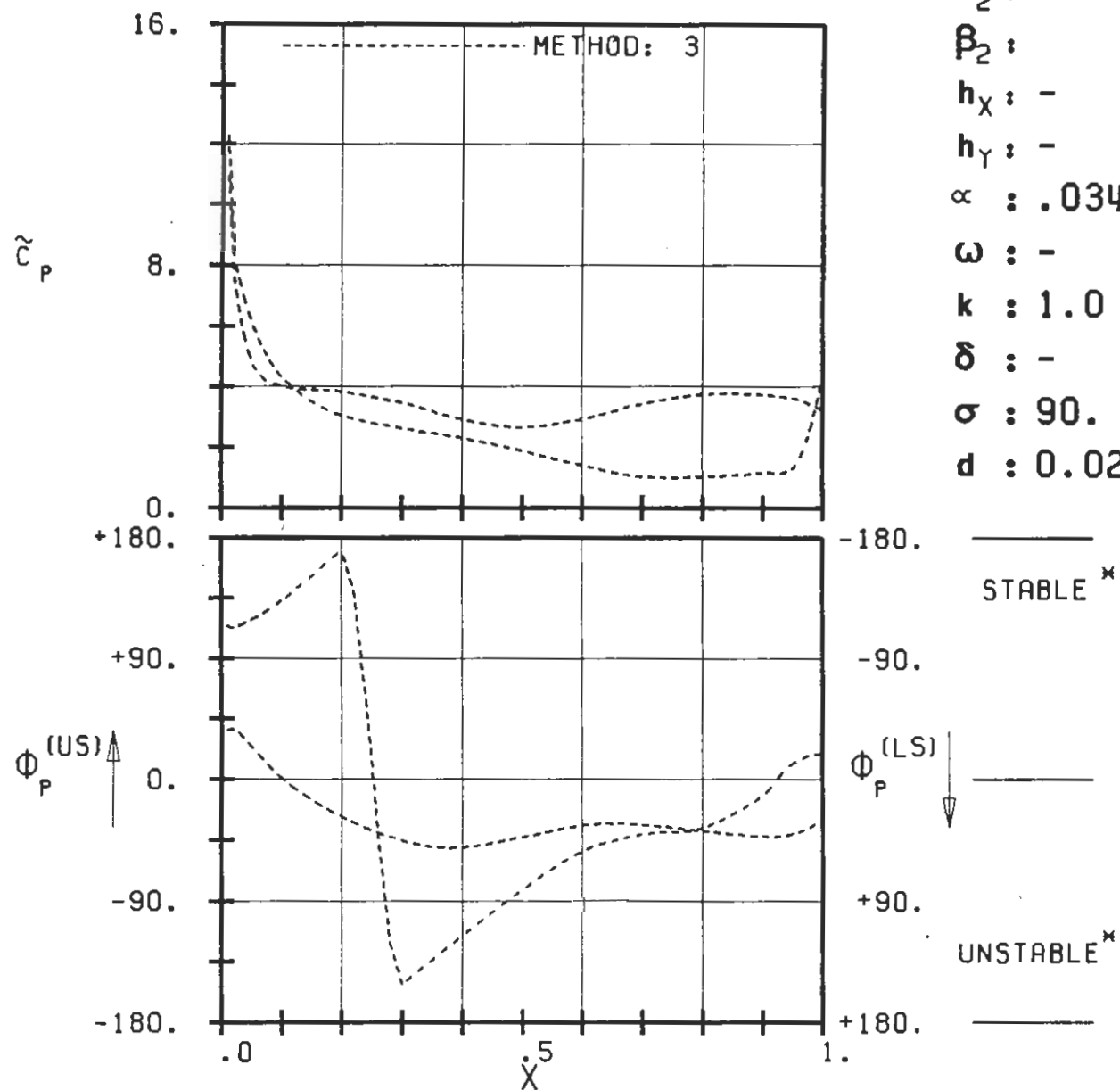


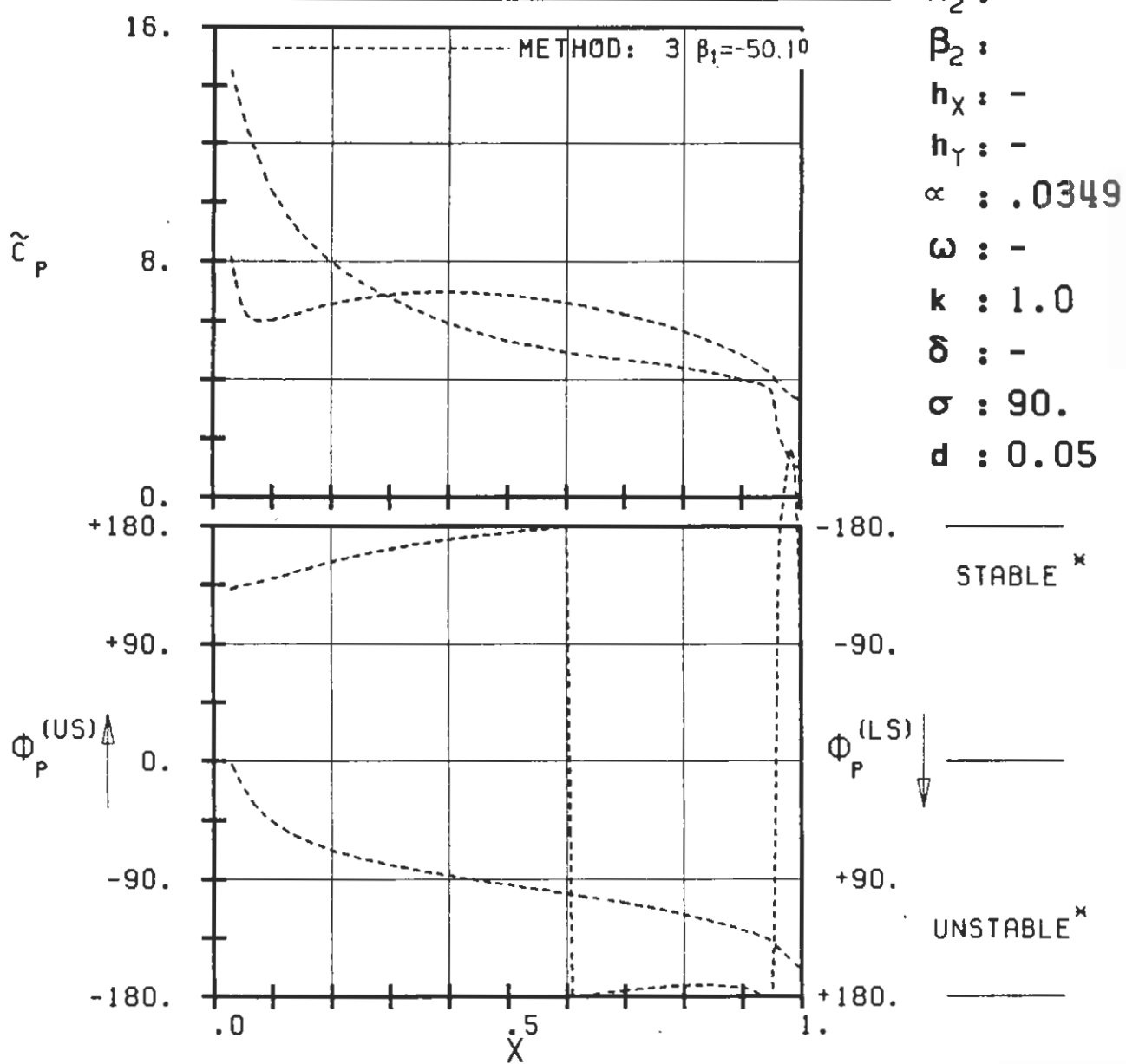
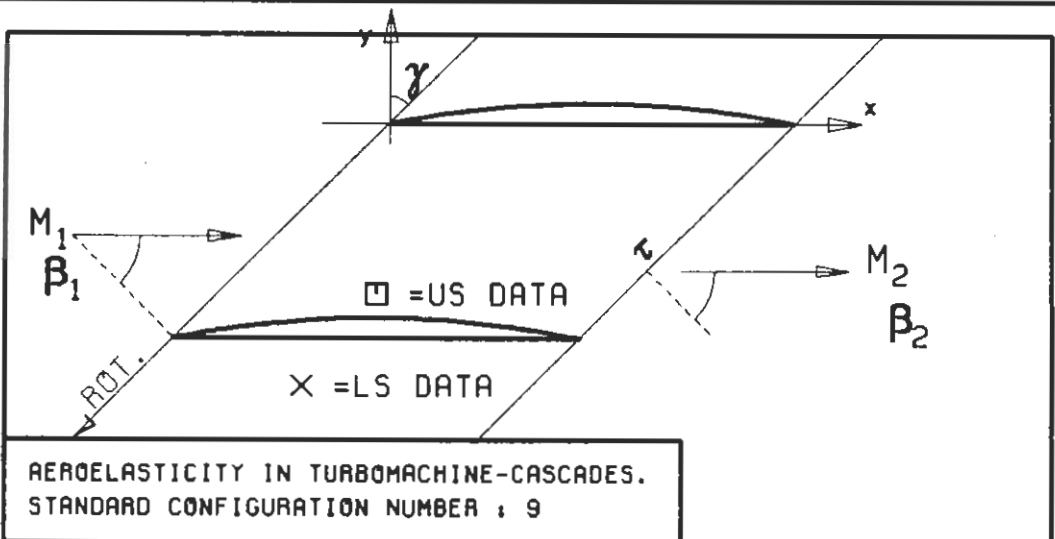


PLOT 7.9-2.16: NINTH STANDARD CONFIGURATION, CASE 16.
 MAGNITUDE AND PHASE LEAD OF UNSTEADY BLADE
 SURFACE PRESSURE DISTRIBUTION.
 (*: IN PITCH MODE, NOTATION VALID UPSTREAM OF PITCH AXIS)

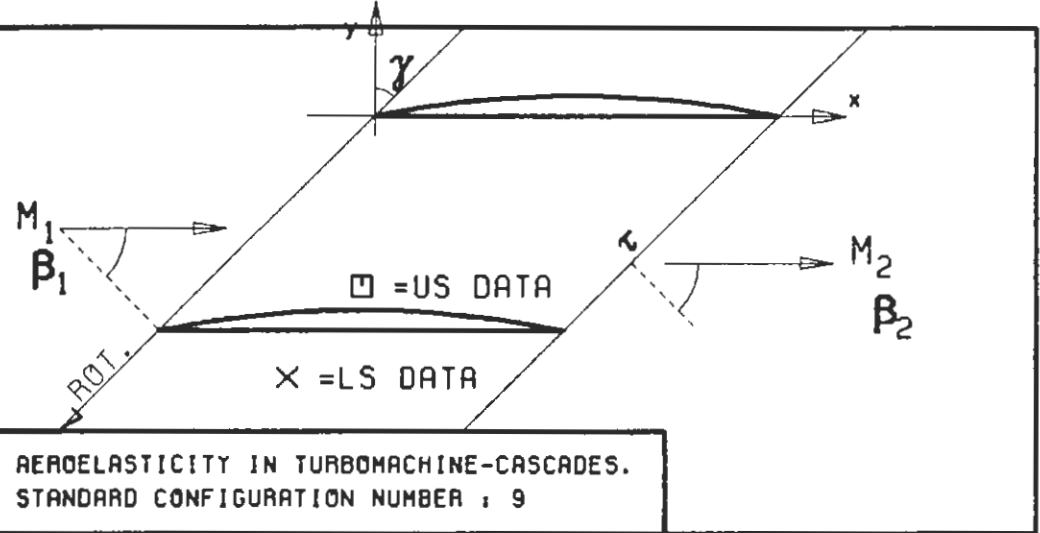


c : 0.1M
 τ : 0.75
 γ : 45.
 x_∞ : 0.5
 y_∞ : 0.
 M_1 : 0.8
 β_1 : -45.
 i :
 M_2 : -
 β_2 :
 h_x : -
 h_y : -
 α : .0349
 ω : -
 k : 1.0
 δ : -
 σ : 90.
 d : 0.02

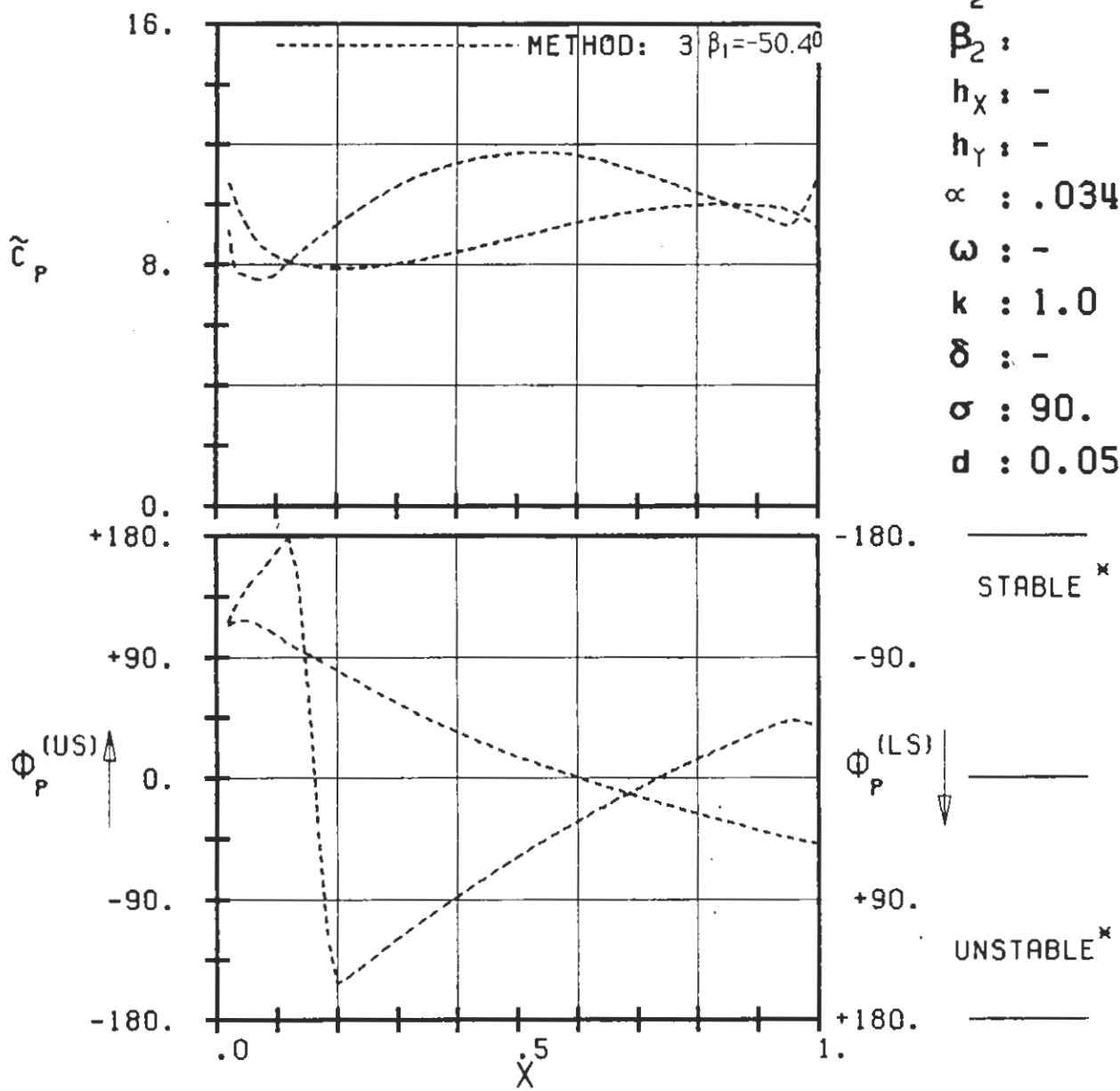




PLOT 7.9-2.18: NINTH STANDARD CONFIGURATION, CASE 18.
MAGNITUDE AND PHASE LEAD OF UNSTEADY BLADE
SURFACE PRESSURE DISTRIBUTION.
(*: IN PITCH MODE, NOTATION VALID UPSTREAM OF PITCH AXIS)

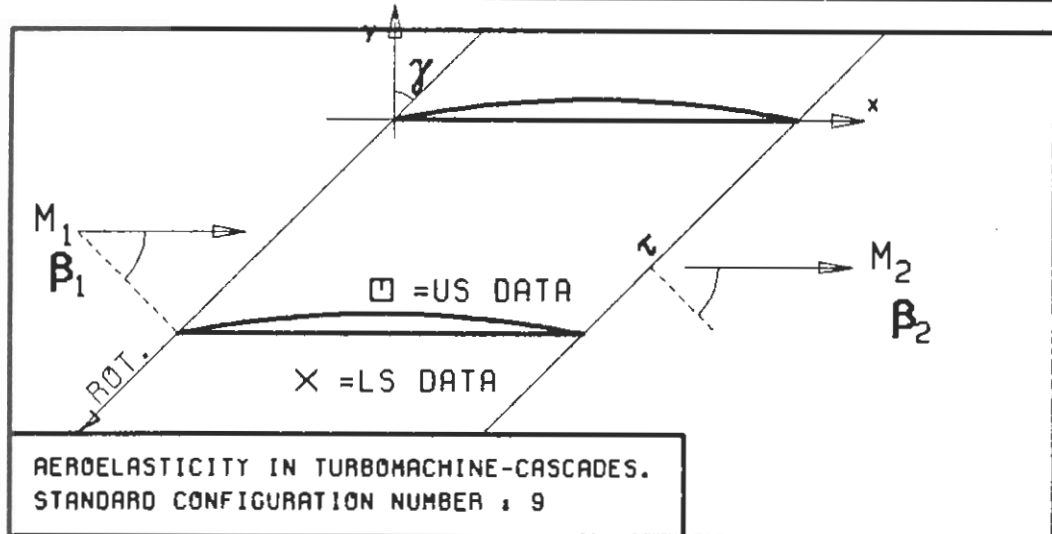


c : 0.1M
 τ : 0.75
 γ : 45.
 x_∞ : 0.5
 y_∞ : 0.
 M_1 : 0.7
 β_1 : -45.
 i :
 M_2 : -
 β_2 :
 h_x : -
 h_y : -
 α : .0349
 ω : -
 k : 1.0
 δ : -
 σ : 90.
 d : 0.05

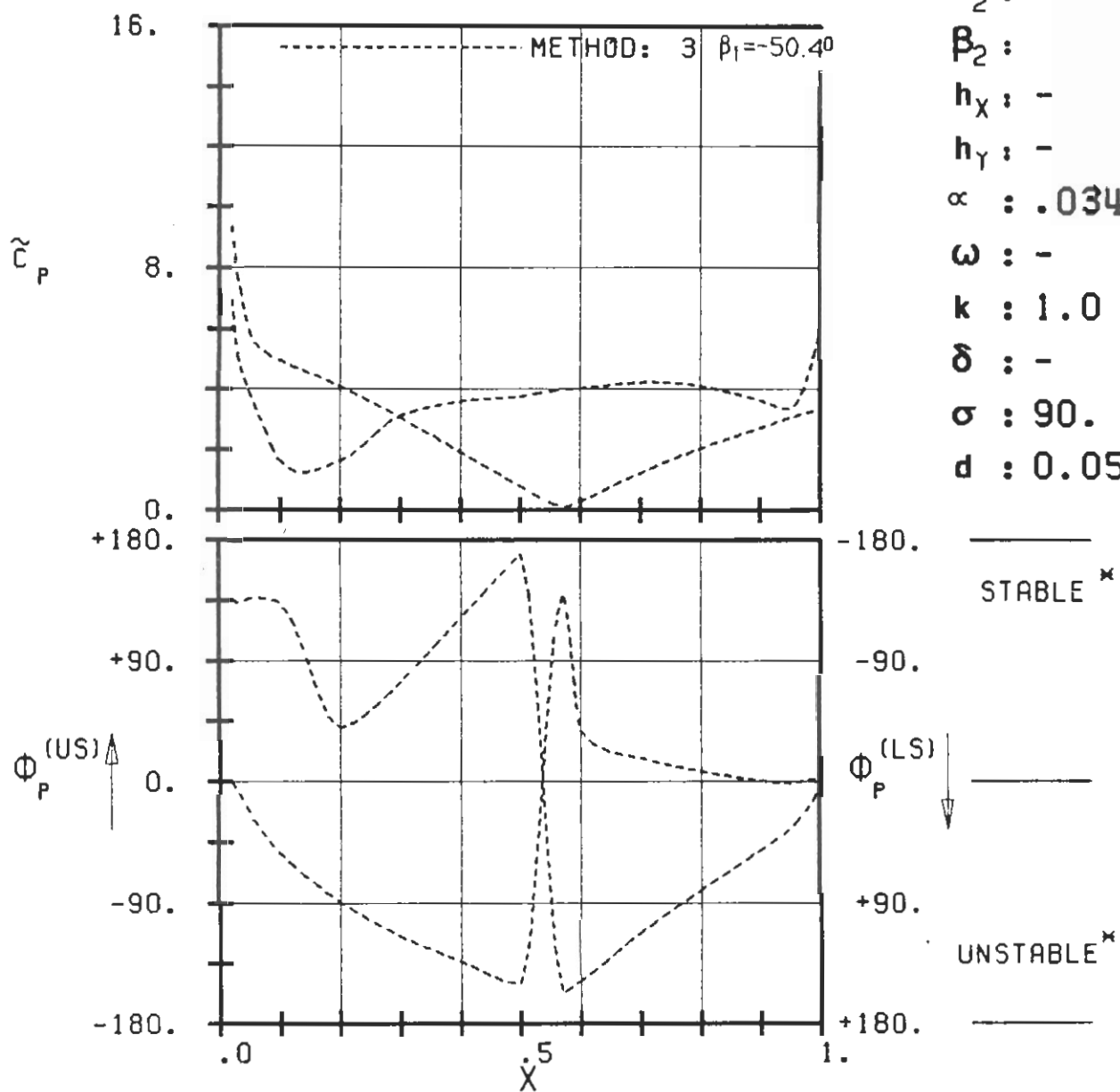


PLOT 7.9-2.19: NINTH STANDARD CONFIGURATION, CASE 19.
MAGNITUDE AND PHASE LEAD OF UNSTEADY BLADE SURFACE PRESSURE DISTRIBUTION.

(*: IN PITCH MODE, NOTATION VALID UPSTREAM OF PITCH AXIS)

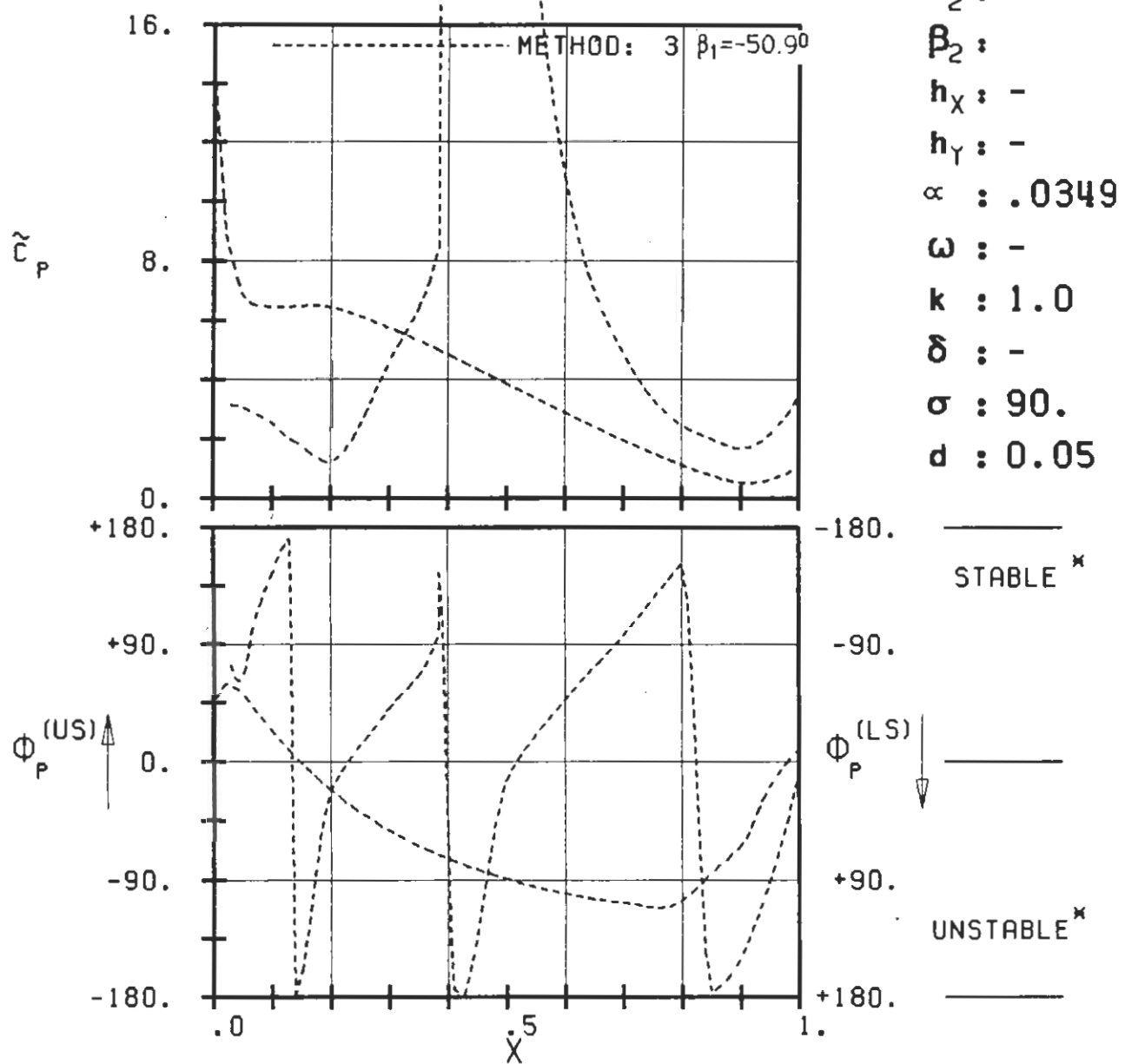
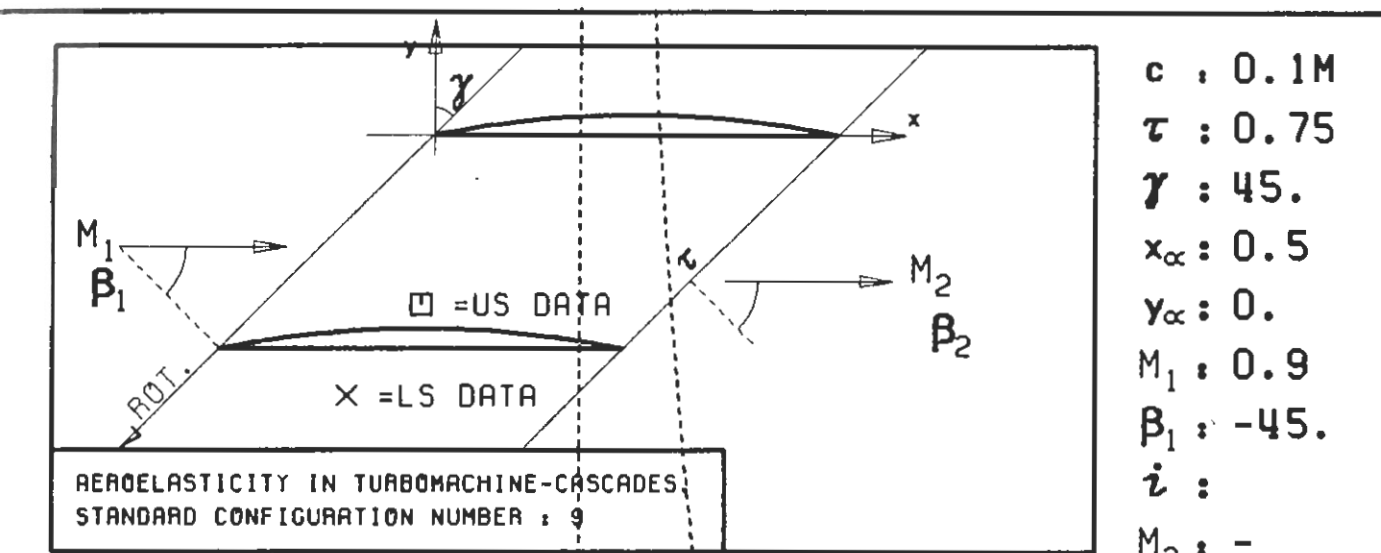


c : 0.1M
 τ : 0.75
 γ : 45.
 x_∞ : 0.5
 y_∞ : 0.
 M_1 : 0.8
 β_1 : -45.
 i :
 M_2 : -
 β_2 :
 h_x : -
 h_y : -
 α : .0349
 ω : -
 k : 1.0
 δ : -
 σ : 90.
 d : 0.05



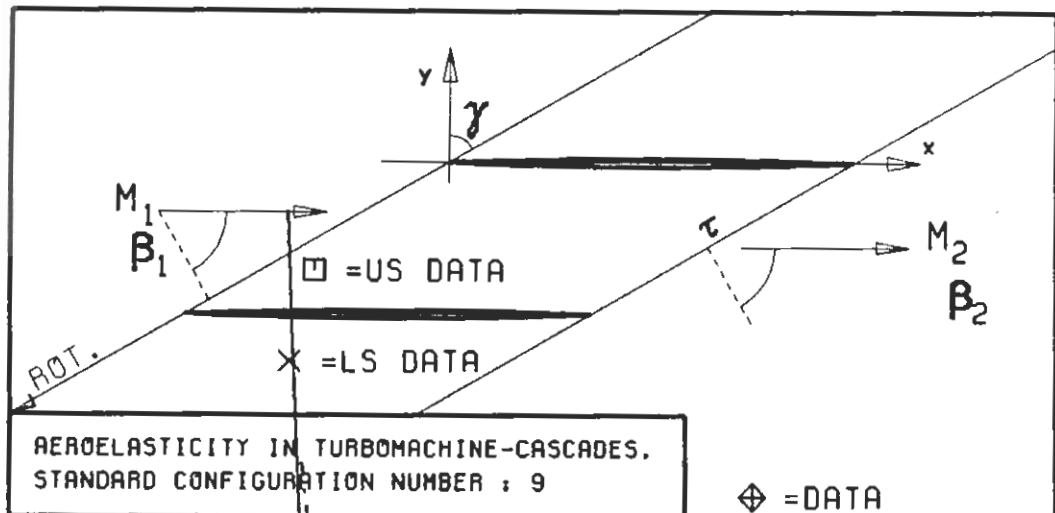
PLOT 7.9-2.20: NINTH STANDARD CONFIGURATION, CASE 20.
MAGNITUDE AND PHASE LEAD OF UNSTEADY BLADE SURFACE PRESSURE DISTRIBUTION.

(\times : IN PITCH MODE, NOTATION VALID UPSTREAM OF PITCH AXIS)

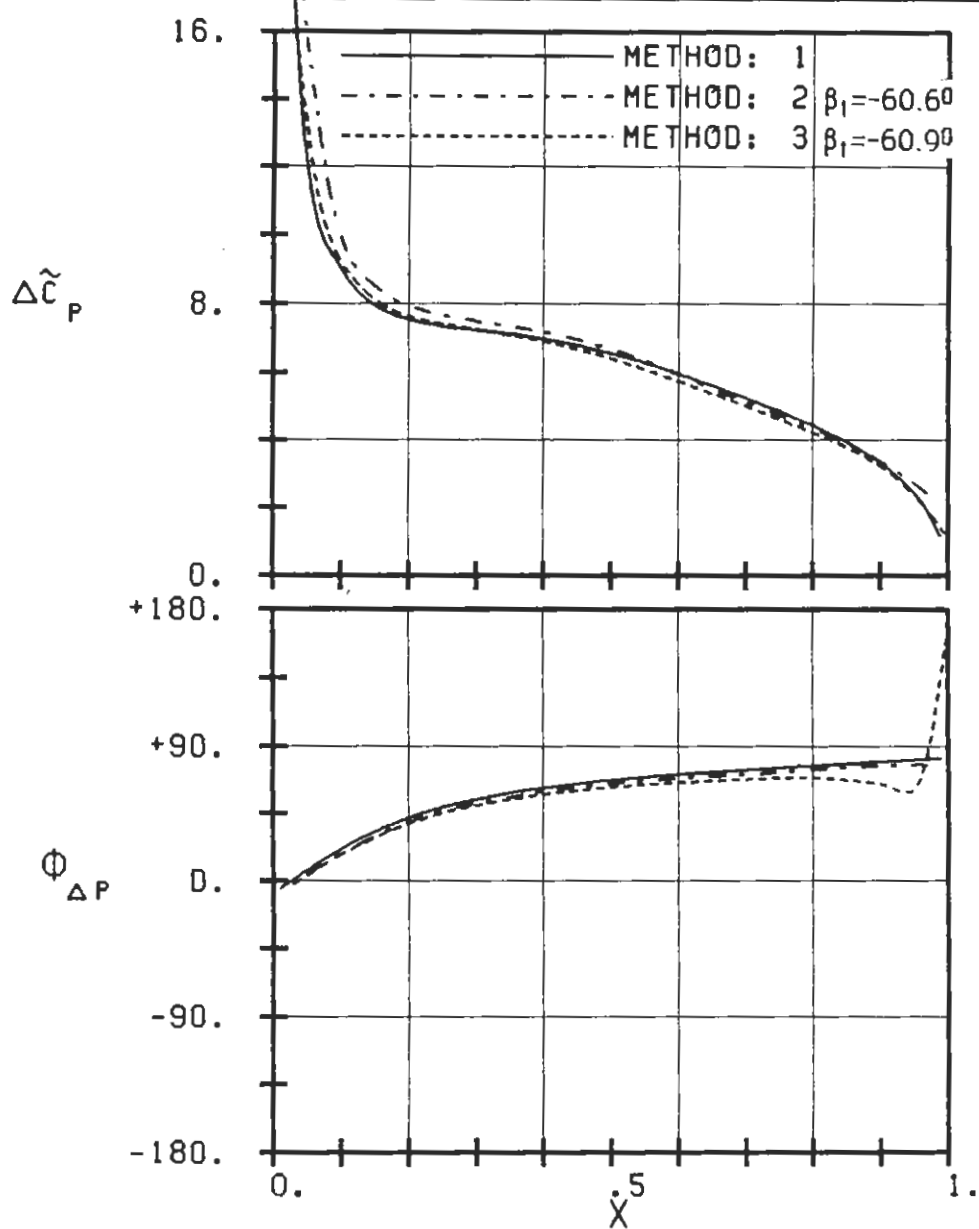


PLOT 7.9-2.21: NINTH STANDARD CONFIGURATION, CASE 21.
MAGNITUDE AND PHASE LEAD OF UNSTEADY BLADE SURFACE PRESSURE DISTRIBUTION.

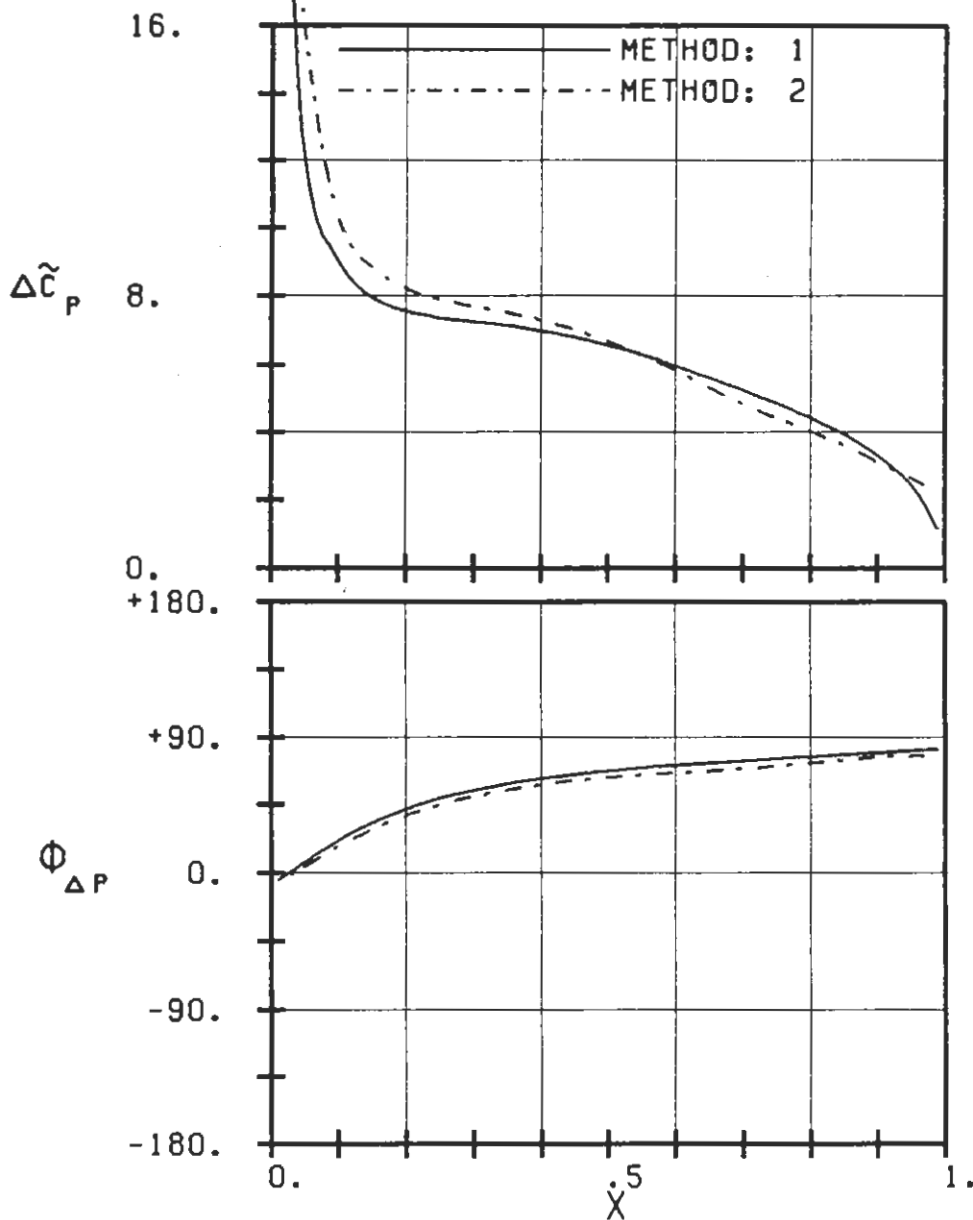
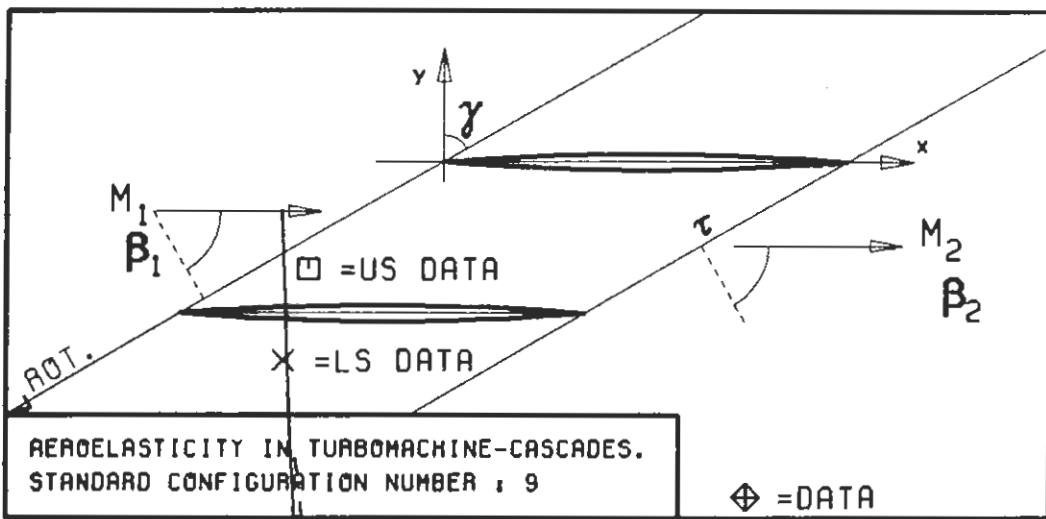
(\rightarrow : IN PITCH MODE, NOTATION VALID UPSTREAM OF PITCH AXIS)



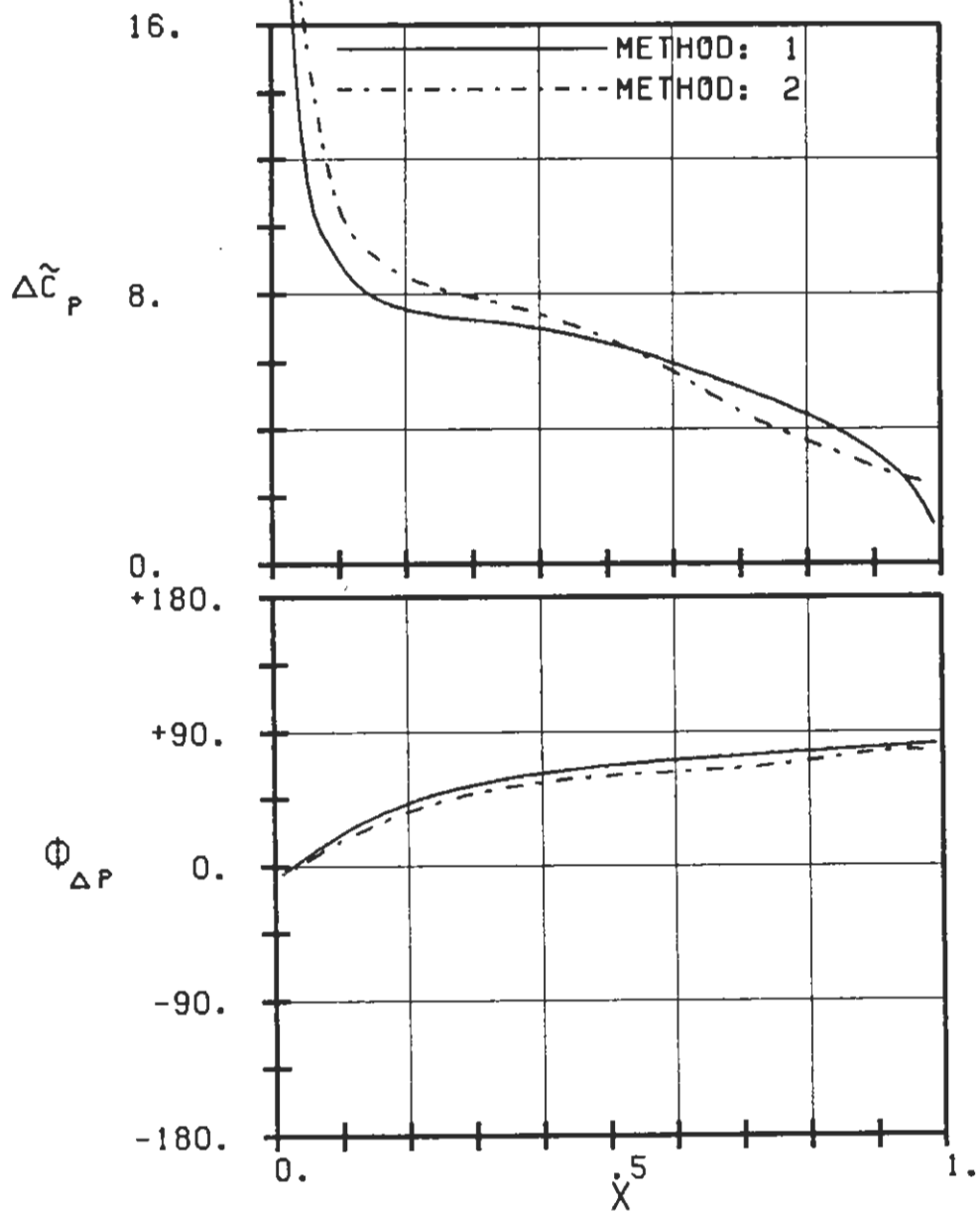
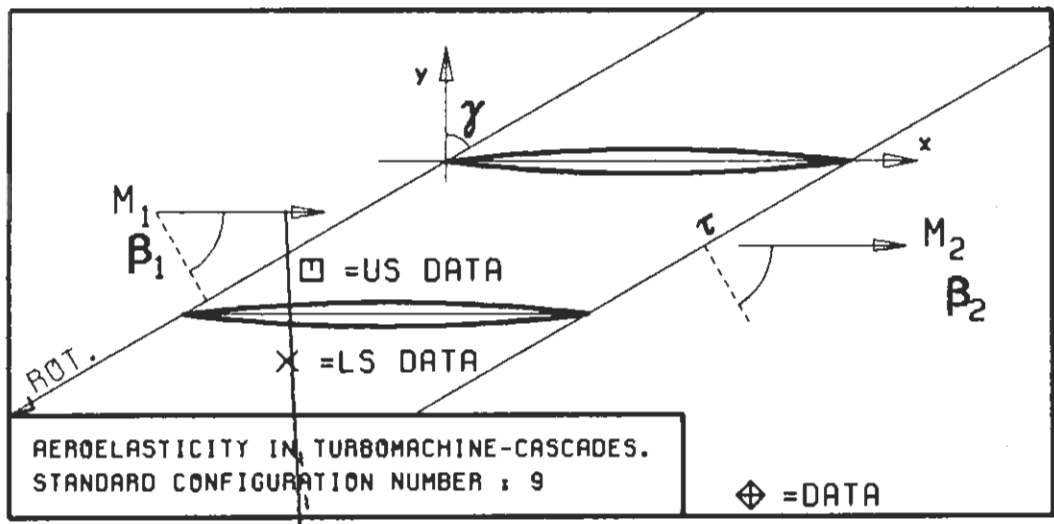
$c : 0.1M$
 $\tau : 0.75$
 $\gamma : 60.$
 $x_\infty : 0.5$
 $y_\infty : 0.$
 $M_1 : 0.$
 $B_1 : -60.$
 $i :$
 $M_2 : -$
 $B_2 :$
 $h_X : -$
 $h_Y : -$
 $\alpha : .0349$
 $\omega : -$
 $k : 1.0$
 $\delta : -$
 $\sigma : 90.$
 $d : 0.02$



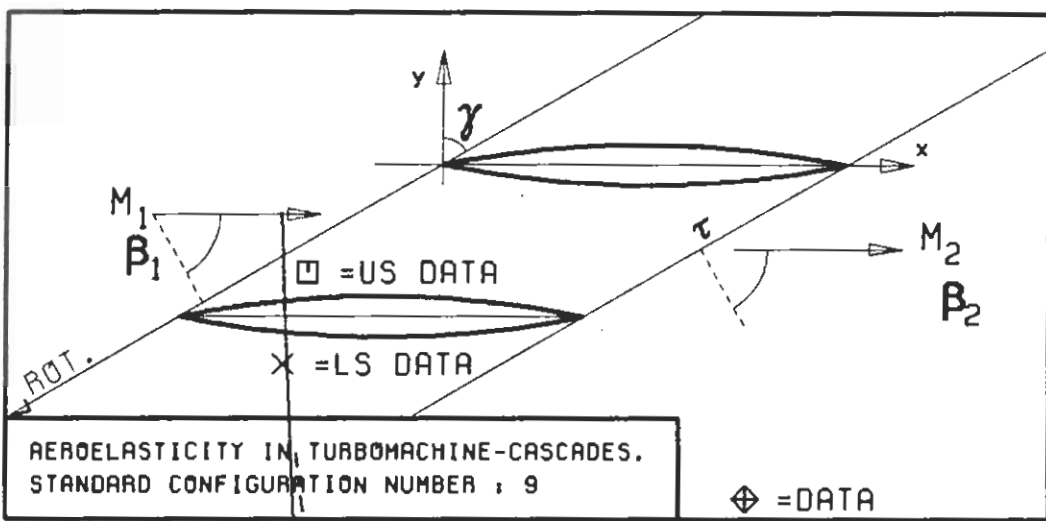
PLOT 7.9-3.1: NINTH STANDARD CONFIGURATION, CASE 1.
MAGNITUDE AND PHASE LEAD OF UNSTEADY BLADE
SURFACE PRESSURE DIFFERENCE DISTRIBUTION.
(X: IN PITCH MODE, NOTATION VALID UPSTREAM OF PITCH AXIS)



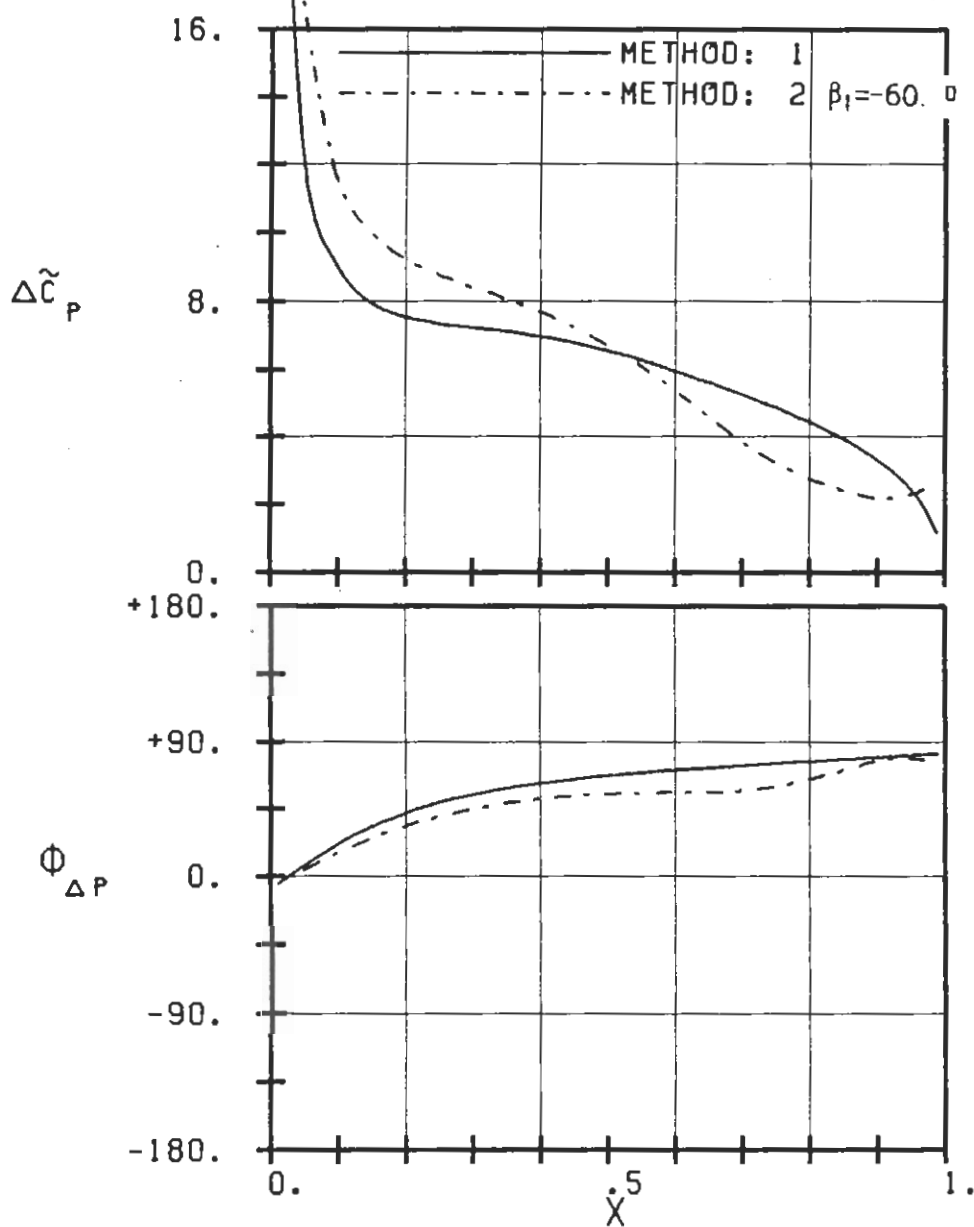
PLOT 7.9-3.2: NINTH STANDARD CONFIGURATION, CASE 2.
 MAGNITUDE AND PHASE LEAD OF UNSTEADY BLADE
 SURFACE PRESSURE DIFFERENCE DISTRIBUTION.
 (\times : IN PITCH MODE, NOTATION VALID UPSTREAM OF PITCH AXIS)



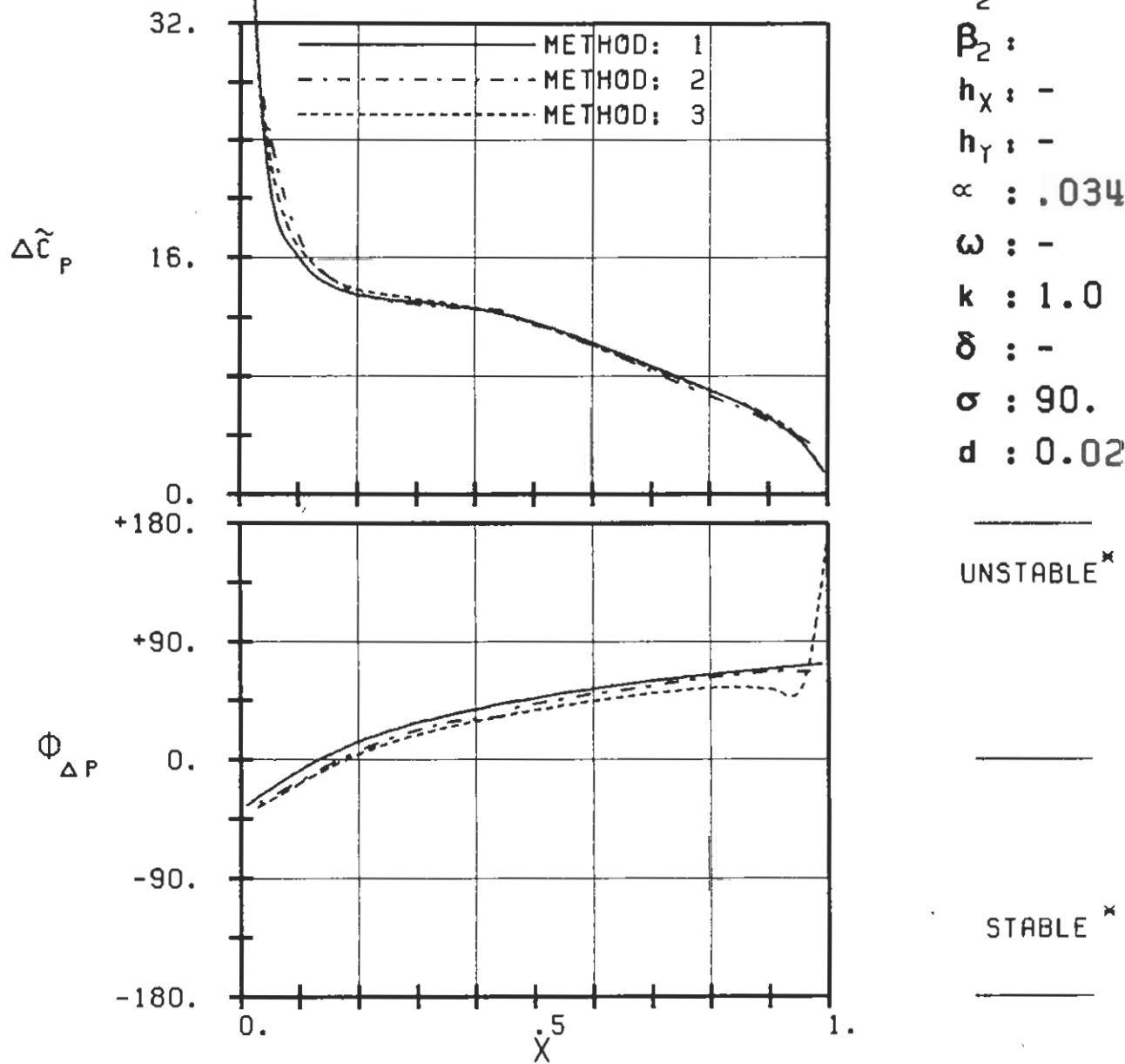
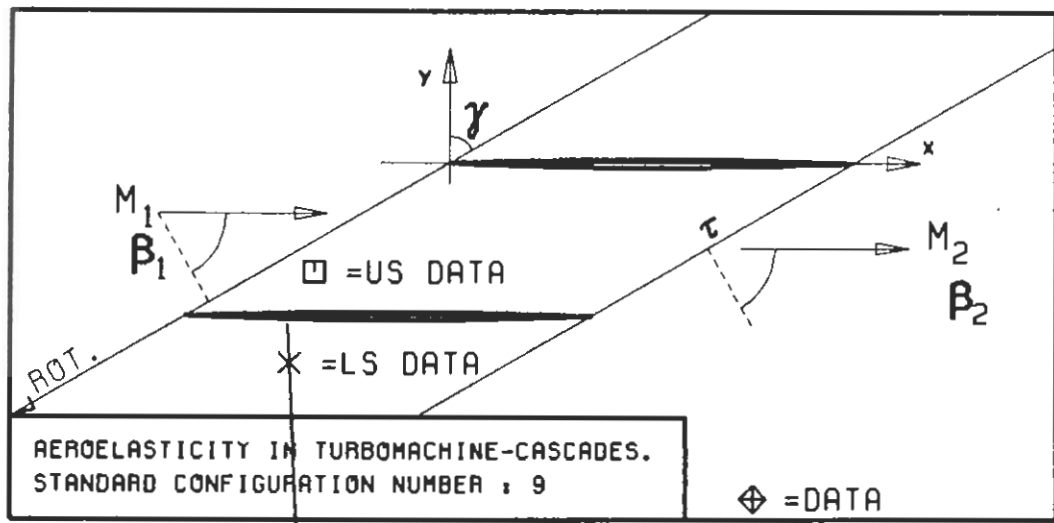
PLOT 7.9-3.3: NINTH STANDARD CONFIGURATION, CASE 3.
 MAGNITUDE AND PHASE LEAD OF UNSTEADY BLADE
 SURFACE PRESSURE DIFFERENCE DISTRIBUTION.
 (\times : IN PITCH MODE, NOTATION VALID UPSTREAM OF PITCH AXIS)



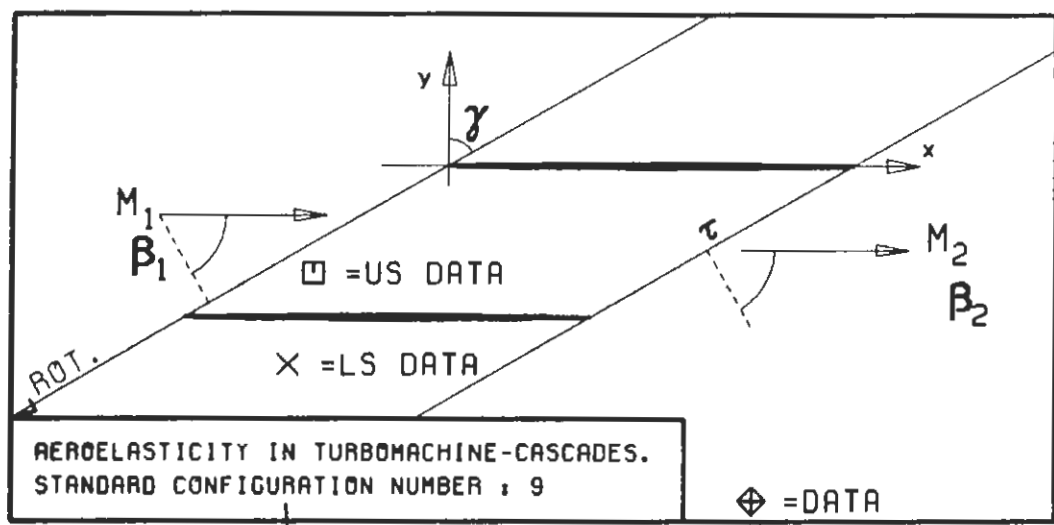
c : 0.1M
 τ : 0.75
 γ : 60.
 x_α : 0.5
 y_α : 0.
 M_1 : 0.
 β_1 : -60.
 i :
 M_2 : -
 β_2 : -
 h_x : -
 h_y : -
 α : .0349
 ω : -
 k : 1.0
 δ : -
 σ : 90.
 d : 0.10



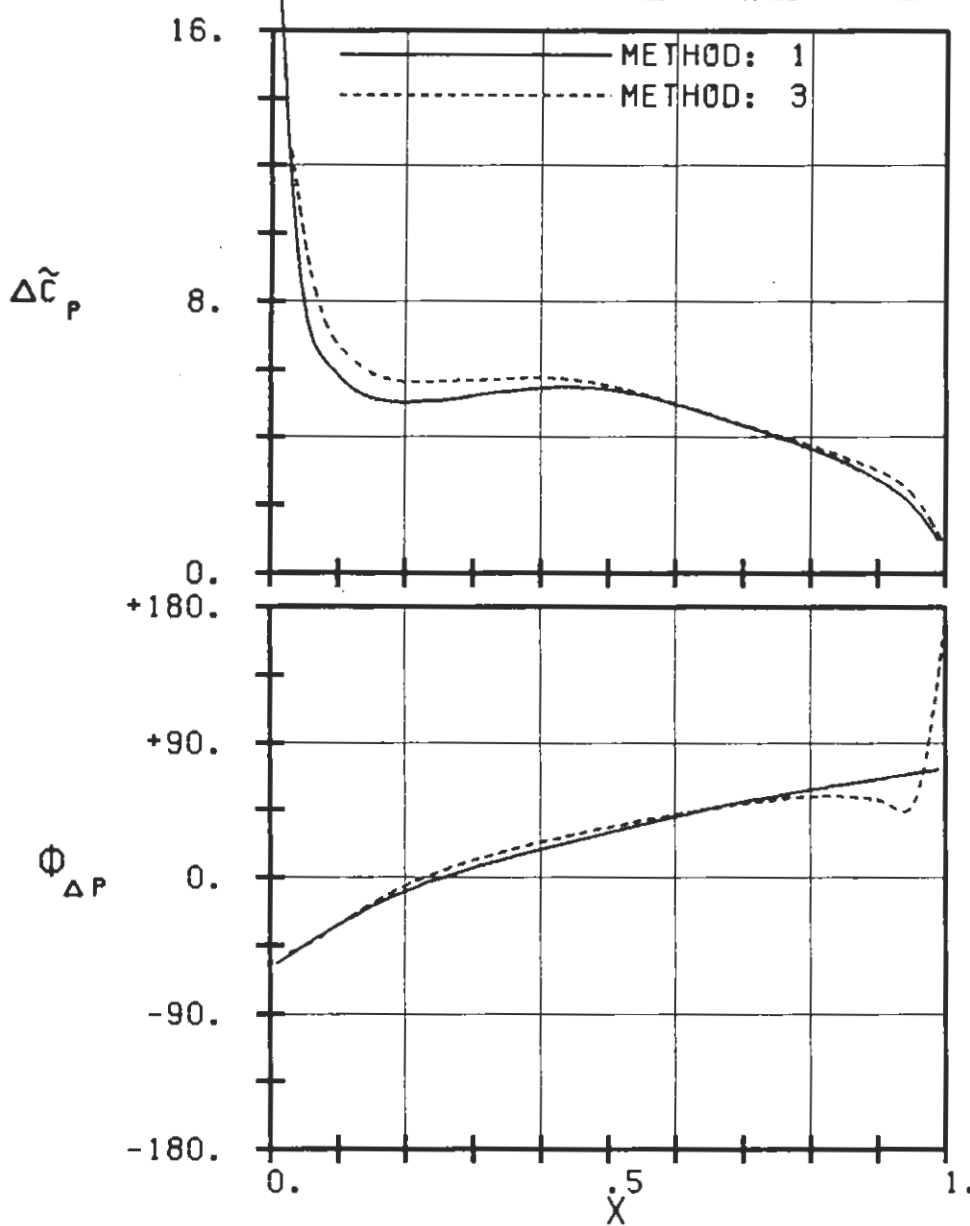
PLOT 7.9-3.4: NINTH STANDARD CONFIGURATION, CASE 4.
MAGNITUDE AND PHASE LEAD OF UNSTEADY BLADE SURFACE PRESSURE DIFFERENCE DISTRIBUTION.
(*: IN PITCH MODE, NOTATION VALID UPSTREAM OF PITCH AXIS)



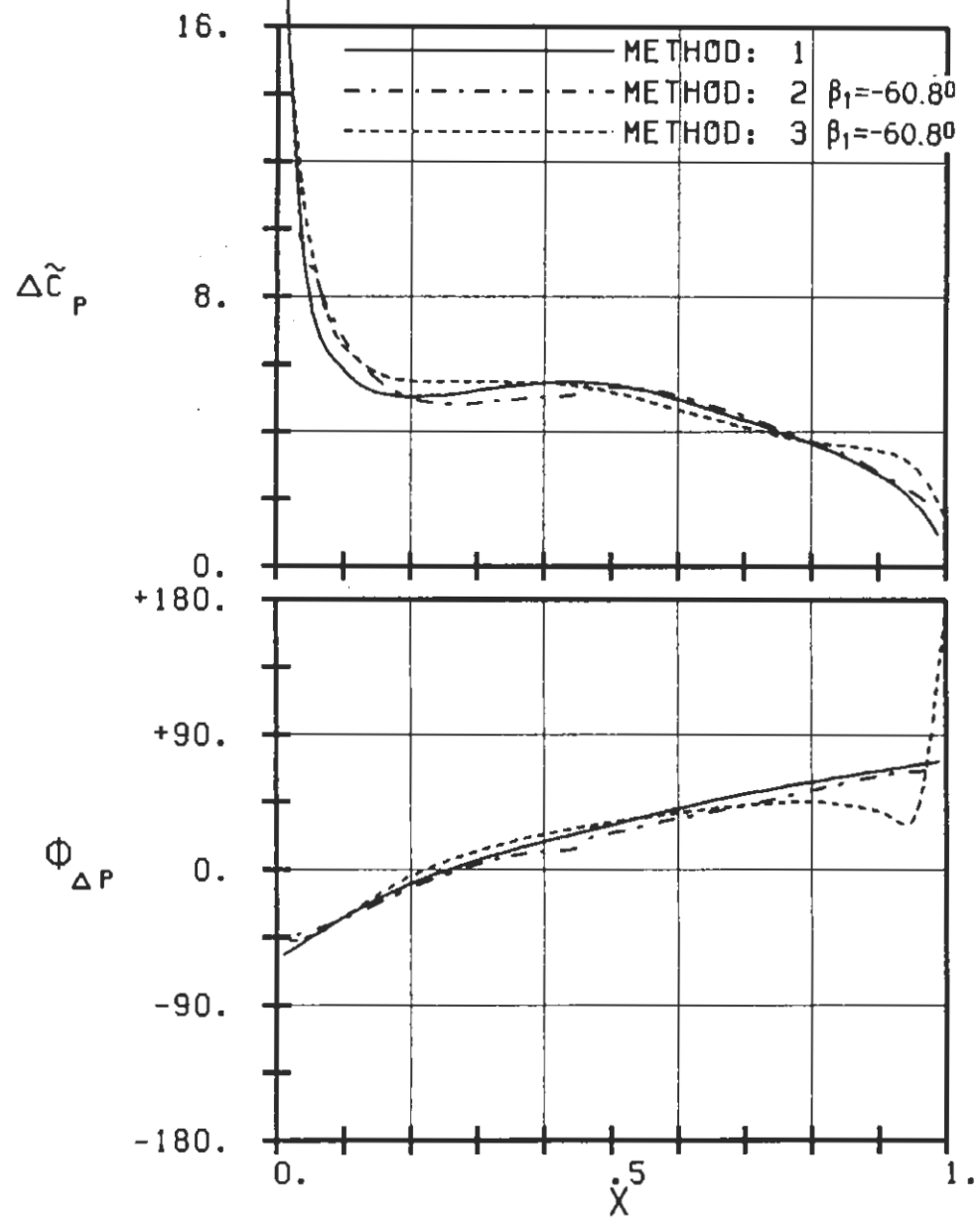
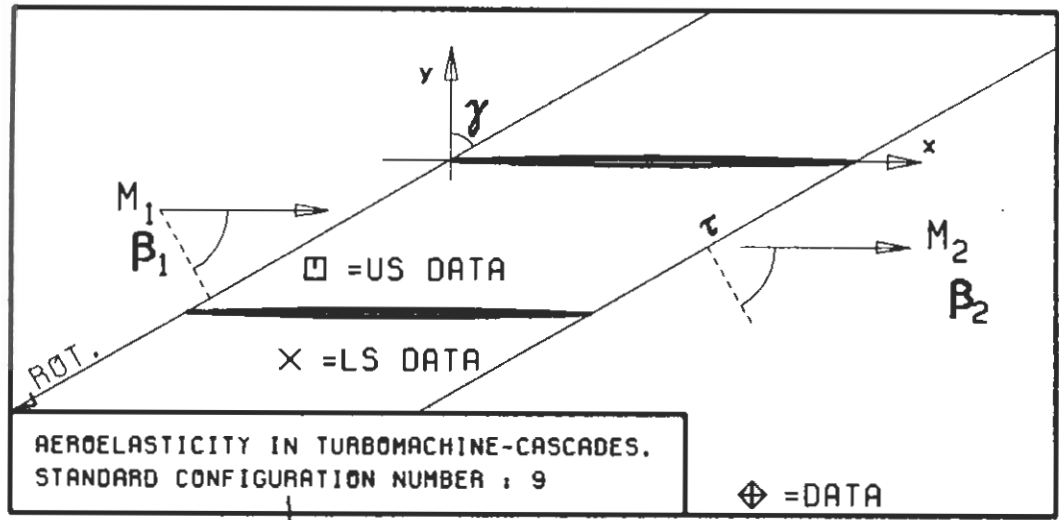
PLOT 7.9-3.5: NINTH STANDARD CONFIGURATION, CASE 5.
MAGNITUDE AND PHASE LEAD OF UNSTEADY BLADE
SURFACE PRESSURE DIFFERENCE DISTRIBUTION.
(*: IN PITCH MODE, NOTATION VALID UPSTREAM OF PITCH AXIS)



c : 0.1M
 τ : 0.75
 γ : 60.
 x_α : 0.5
 y_α : 0.
 M_1 : 0.7
 β_1 : -60.
 i :
 M_2 : -
 β_2 :
 h_x : -
 h_y : -
 α : .0349
 ω : -
 k : 1.0
 δ : -
 σ : 90.
 d : 0.01

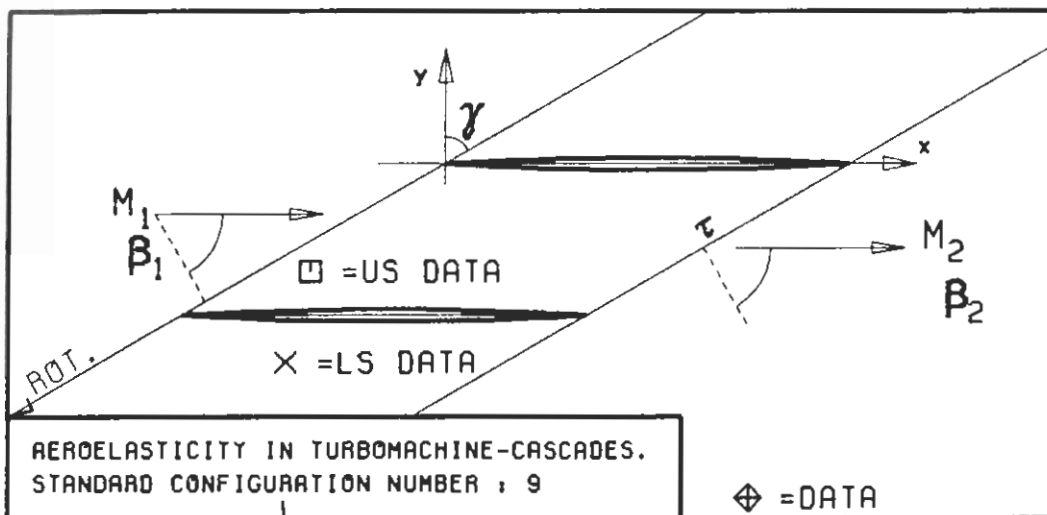


PLOT 7.9-3.6: NINTH STANDARD CONFIGURATION, CASE 6.
 MAGNITUDE AND PHASE LEAD OF UNSTEADY BLADE
 SURFACE PRESSURE DIFFERENCE DISTRIBUTION.
 (*: IN PITCH MODE, NOTATION VALID UPSTREAM OF PITCH AXIS)

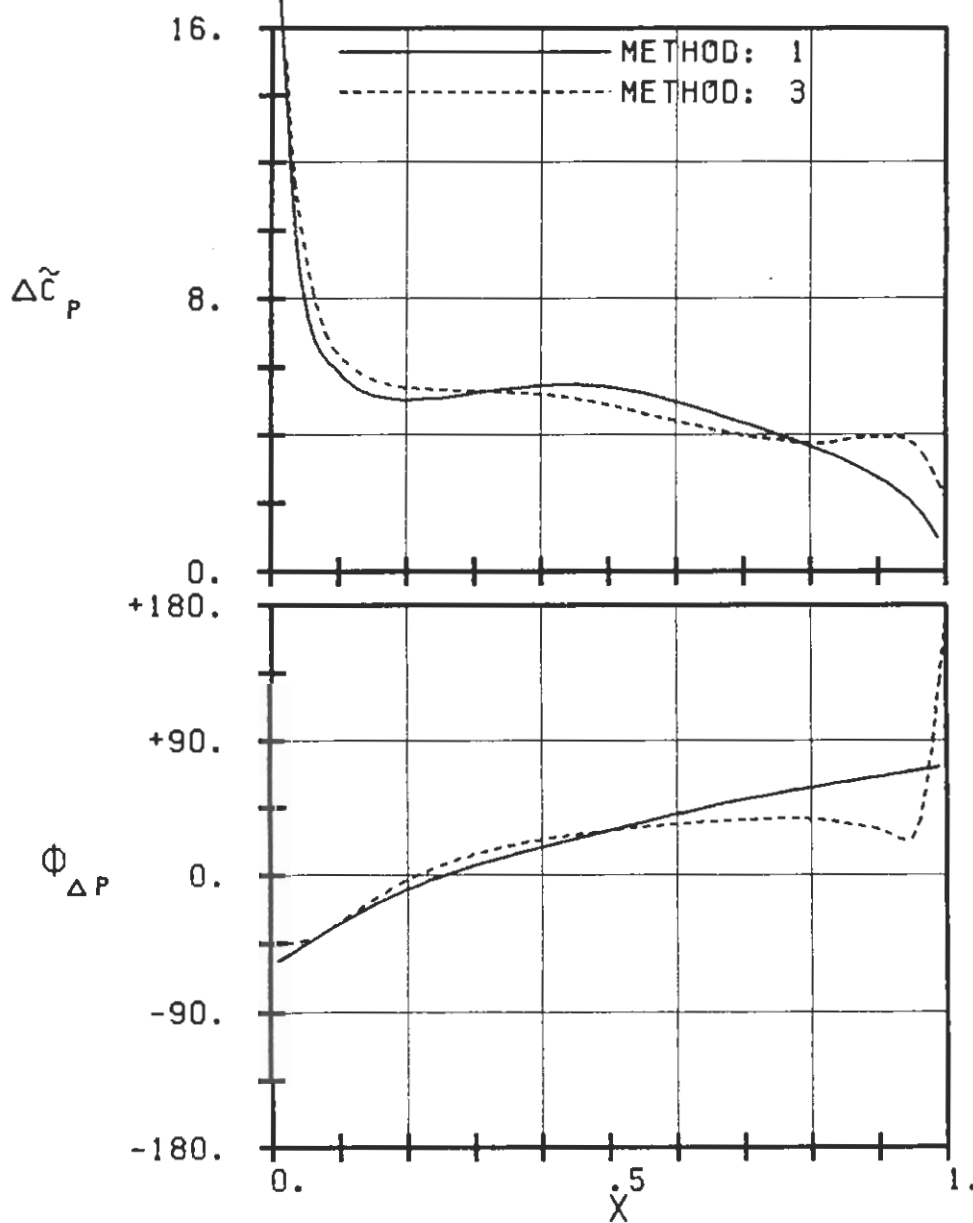


$c : 0.1M$
 $\tau : 0.75$
 $\gamma : 60.$
 $x_\alpha : 0.5$
 $y_\alpha : 0.$
 $M_1 : 0.7$
 $\beta_1 : -60.$
 $i :$
 $M_2 : -$
 $\beta_2 : -$
 $h_x : -$
 $h_y : -$
 $\alpha : .0349$
 $\omega : -$
 $k : 1.0$
 $\delta : -$
 $\sigma : 90.$
 $d : 0.02$

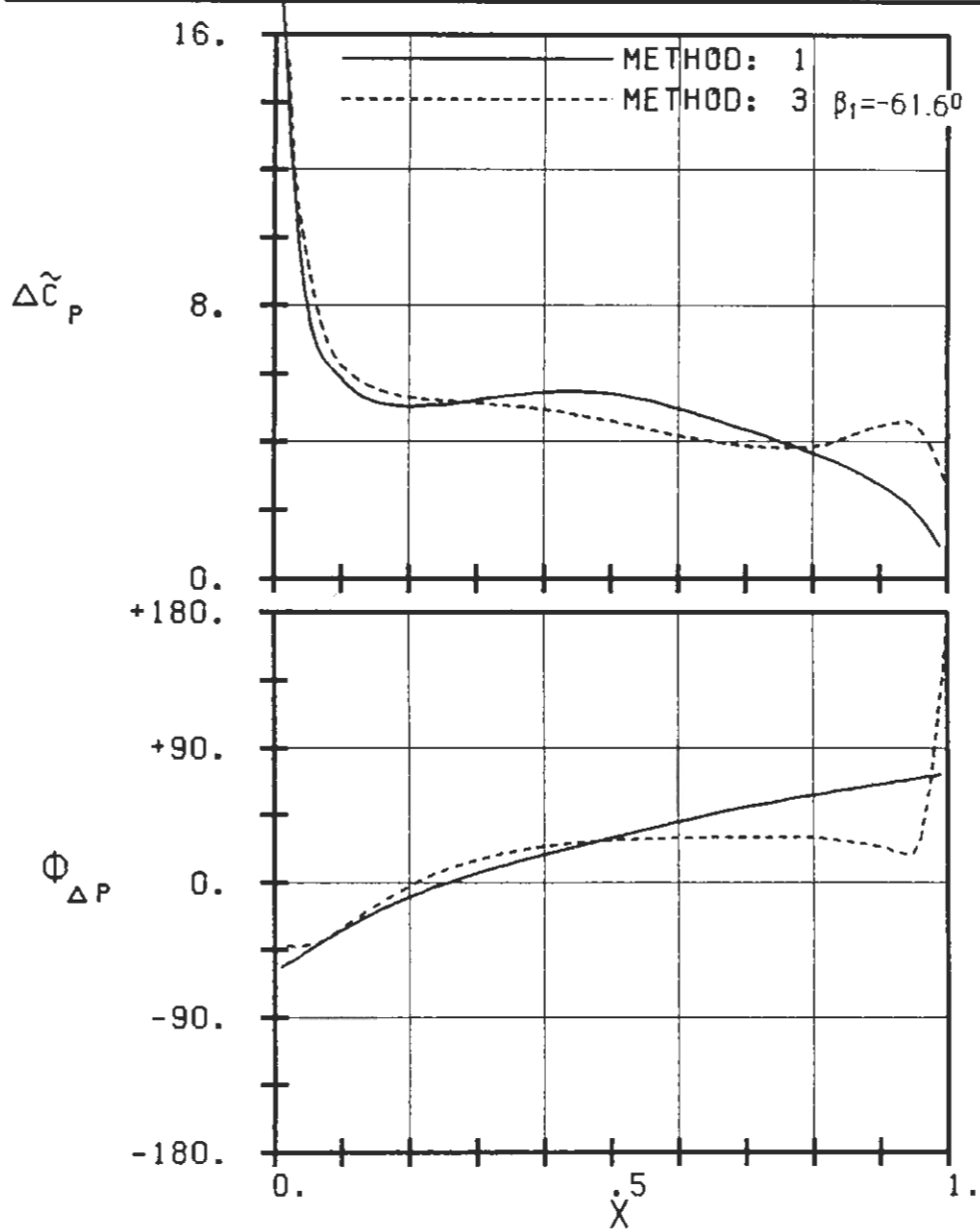
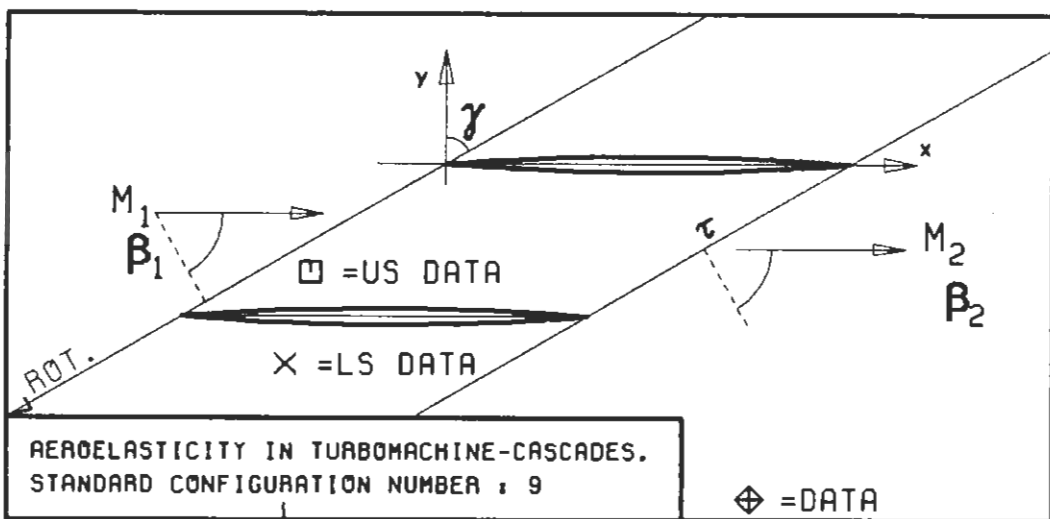
PLOT 7.9-3.7: NINTH STANDARD CONFIGURATION, CASE 7.
MAGNITUDE AND PHASE LEAD OF UNSTEADY BLADE
SURFACE PRESSURE DIFFERENCE DISTRIBUTION.
(\times : IN PITCH MODE, NOTATION VALID UPSTREAM OF PITCH AXIS)



$c : 0.1M$
 $\tau : 0.75$
 $\gamma : 60.$
 $x_\infty : 0.5$
 $y_\infty : 0.$
 $M_1 : 0.7$
 $\beta_1 : -60.$
 $i :$
 $M_2 : -$
 $\beta_2 : -$
 $h_x : -$
 $h_y : -$
 $\alpha : .0349$
 $\omega : -$
 $k : 1.0$
 $\delta : -$
 $\sigma : 90.$
 $d : 0.03$

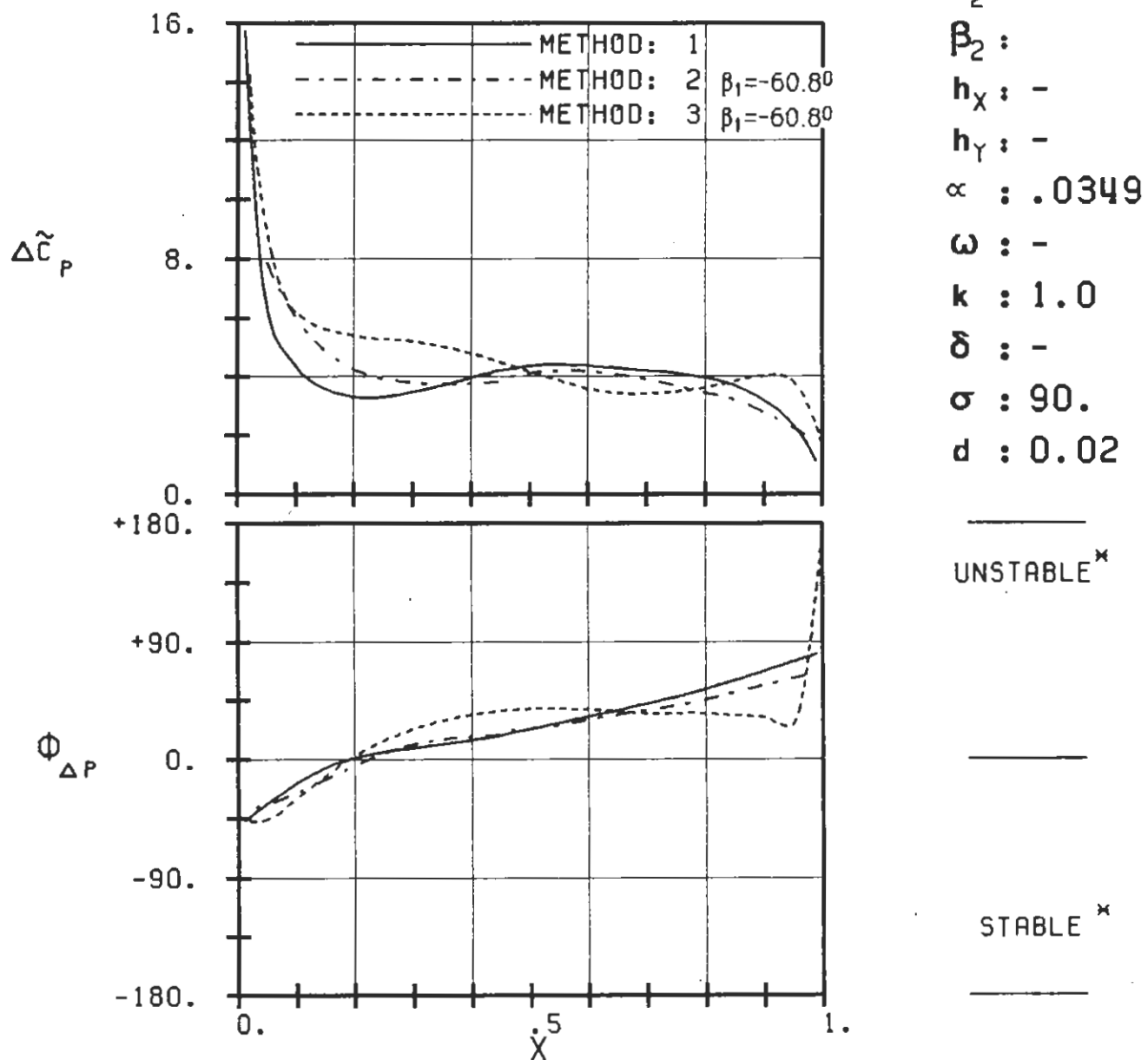
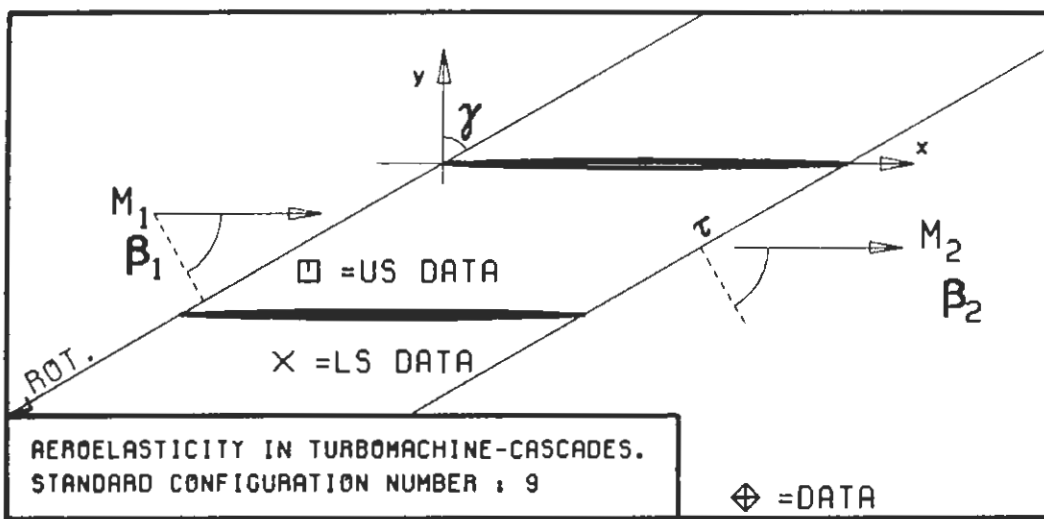


PLOT 7.9-3.8: NINTH STANDARD CONFIGURATION, CASE 8.
MAGNITUDE AND PHASE LEAD OF UNSTEADY BLADE
SURFACE PRESSURE DIFFERENCE DISTRIBUTION.
(*: IN PITCH MODE, NOTATION VALID UPSTREAM OF PITCH AXIS)



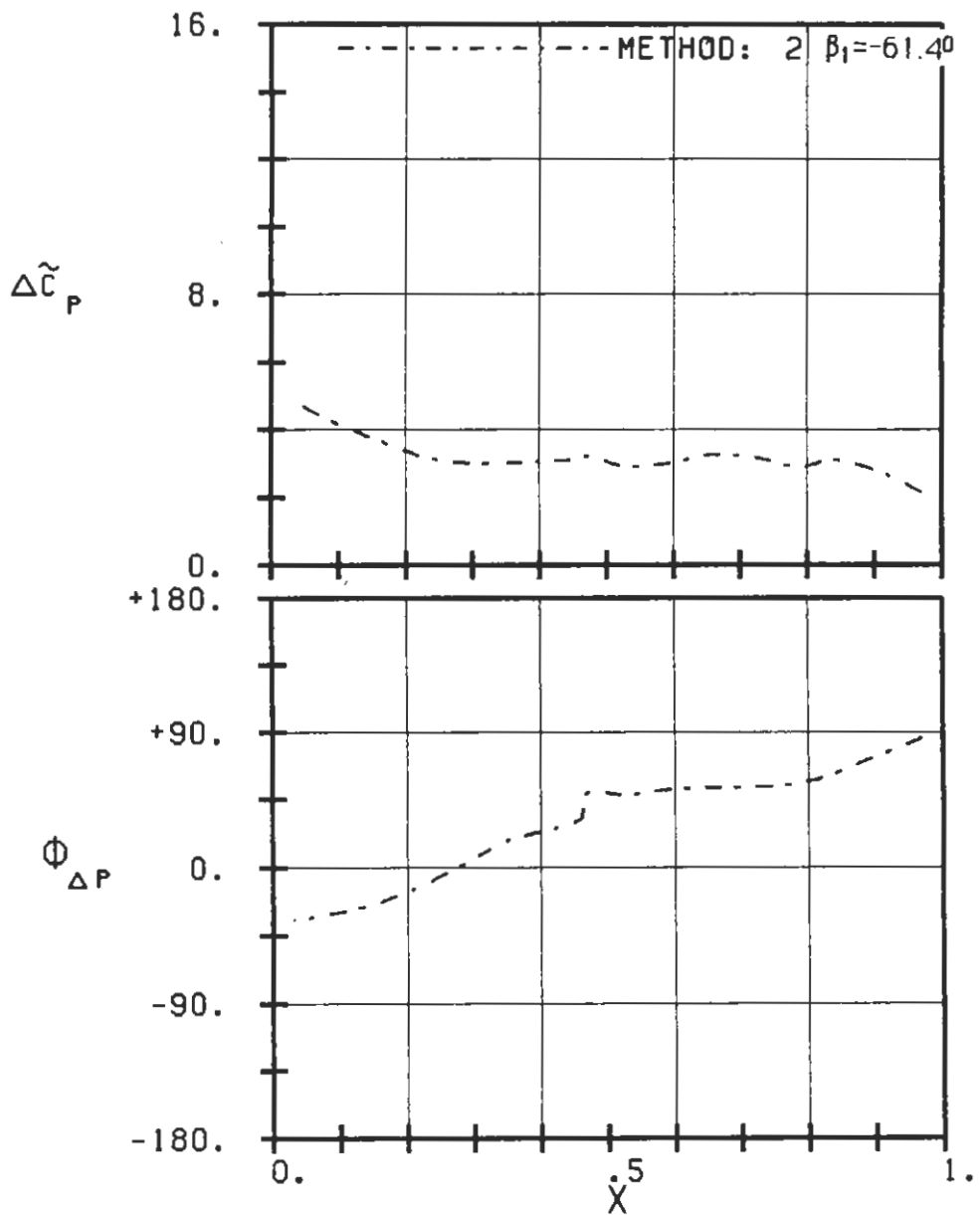
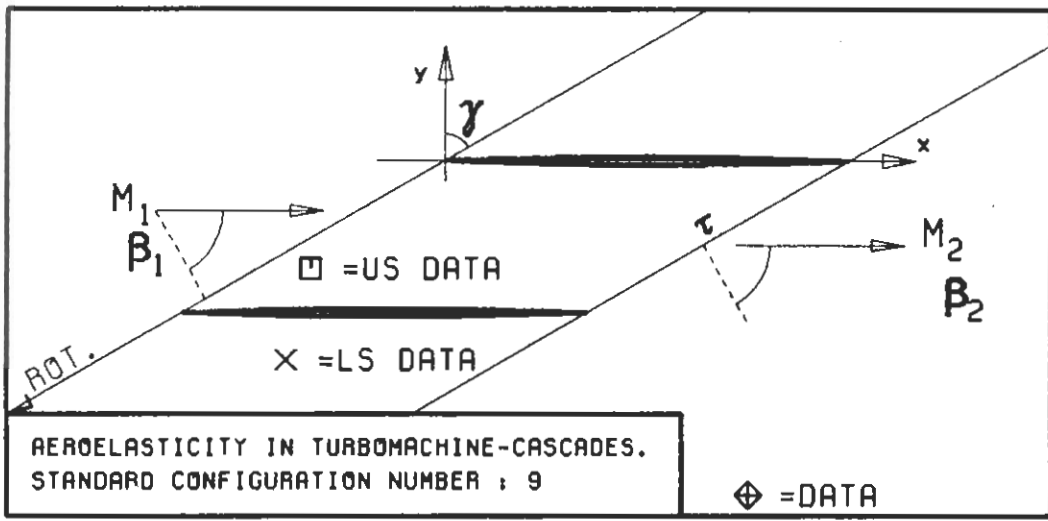
PLOT 7.9-3.9: NINTH STANDARD CONFIGURATION, CASE 9.
 MAGNITUDE AND PHASE LEAD OF UNSTEADY BLADE
 SURFACE PRESSURE DIFFERENCE DISTRIBUTION.
 (*: IN PITCH MODE, NOTATION VALID UPSTREAM OF PITCH AXES)

$c : 0.1M$
 $\tau : 0.75$
 $\gamma : 60.$
 $x_\infty : 0.5$
 $y_\infty : 0.$
 $M_1 : 0.7$
 $\beta_1 : -60.$
 $i :$
 $M_2 : -$
 $\beta_2 : -$
 $h_x : -$
 $h_y : -$
 $\alpha : .0349$
 $\omega : -$
 $k : 1.0$
 $\delta : -$
 $\sigma : 90.$
 $d : 0.04$

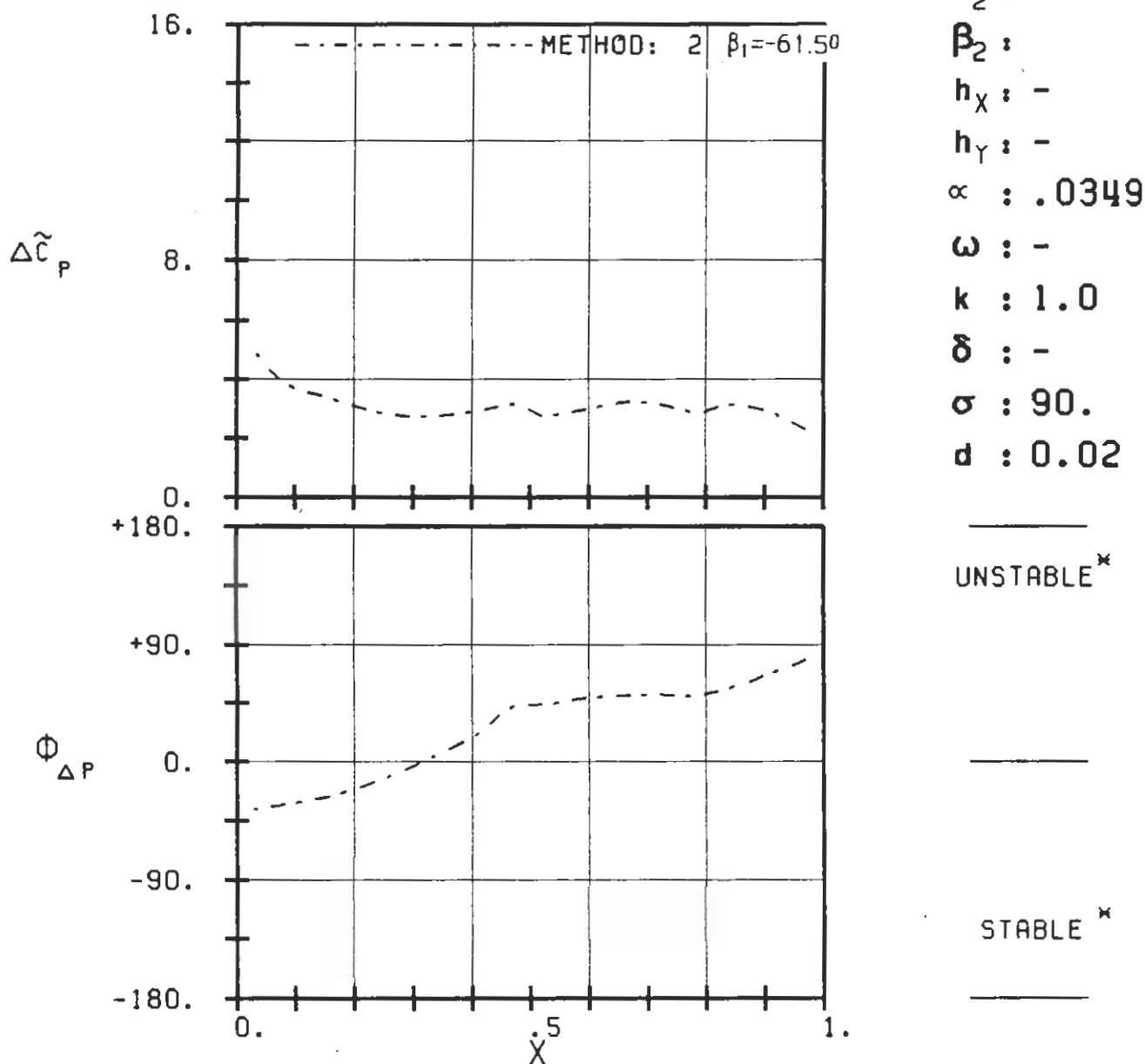
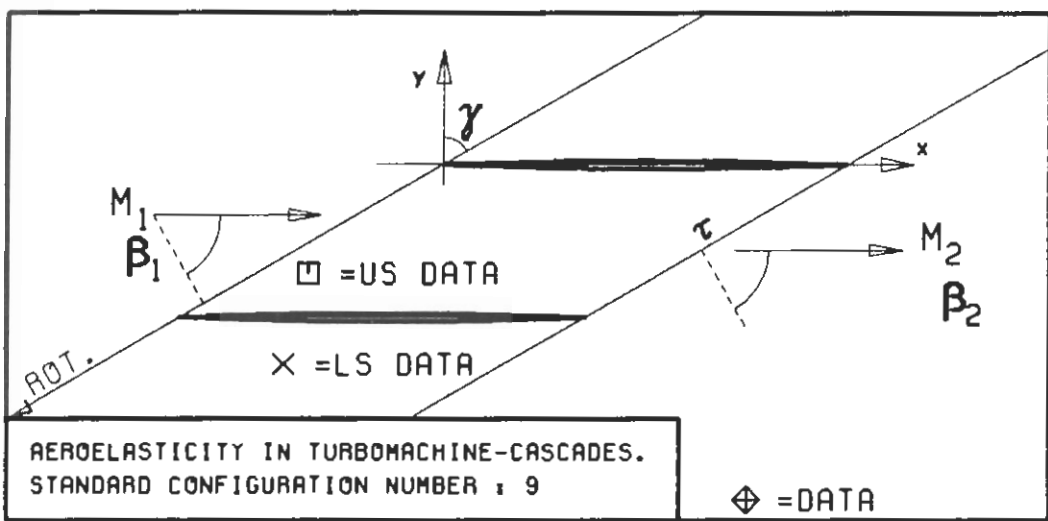


PLOT 7.9-3.10: NINTH STANDARD CONFIGURATION, CASE 10.
MAGNITUDE AND PHASE LEAD OF UNSTEADY BLADE SURFACE PRESSURE DIFFERENCE DISTRIBUTION.
(\times : IN PITCH MODE, NOTATION VALID UPSTREAM OF PITCH AXIS)

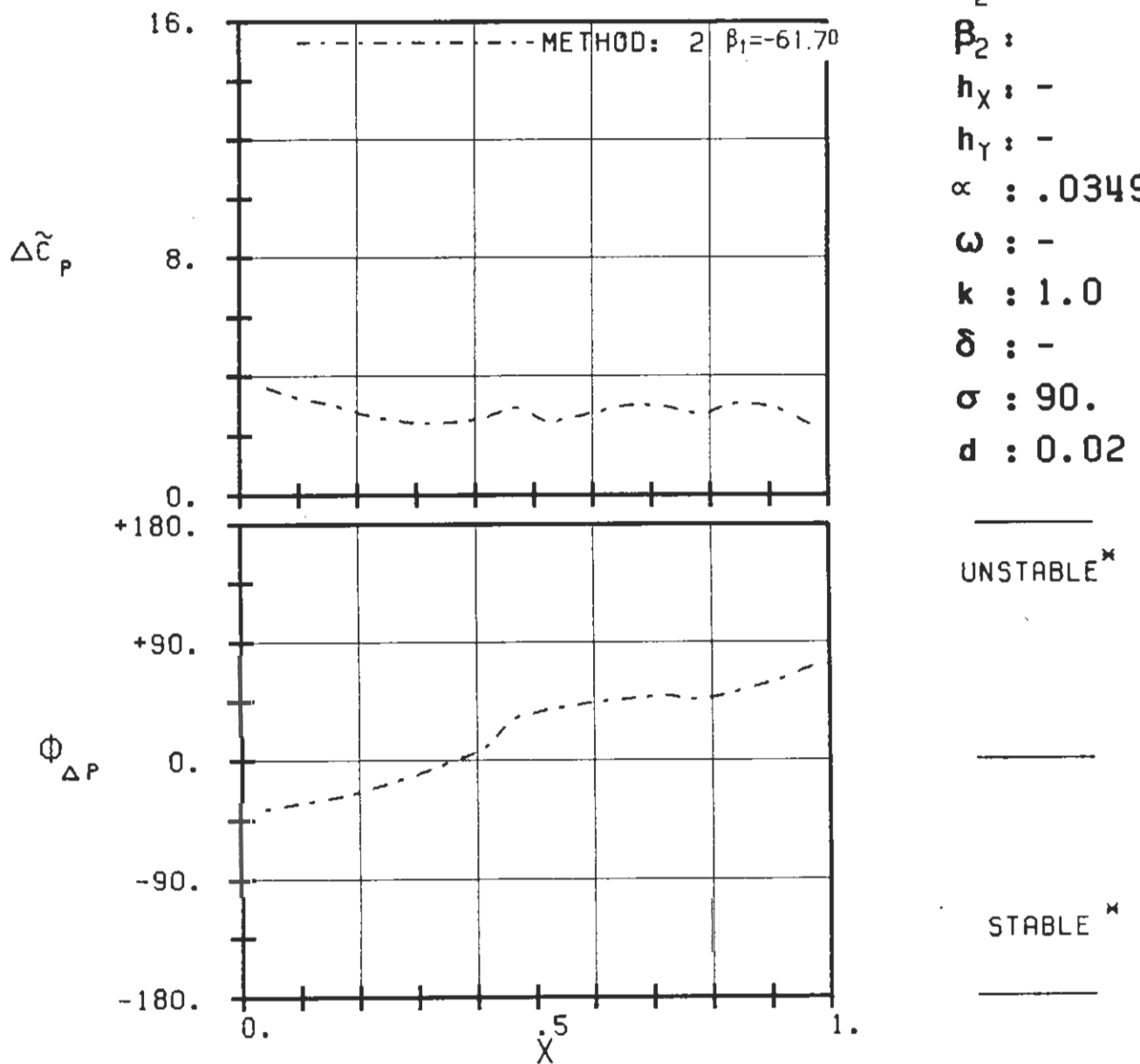
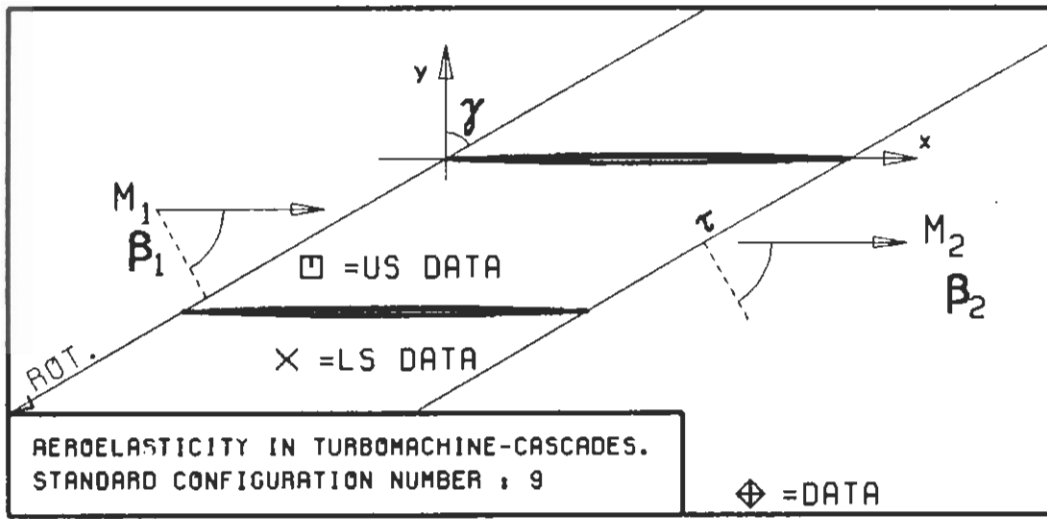
$c : 0.1M$
 $\tau : 0.75$
 $\gamma : 60.$
 $x_\infty : 0.5$
 $y_\infty : 0.$
 $M_1 : 0.8$
 $\beta_1 : -60.$
 $i :$
 $M_2 : -$
 $\beta_2 : -$
 $h_X : -$
 $h_Y : -$
 $\alpha : .0349$
 $\omega : -$
 $k : 1.0$
 $\delta : -$
 $\sigma : 90.$
 $d : 0.02$



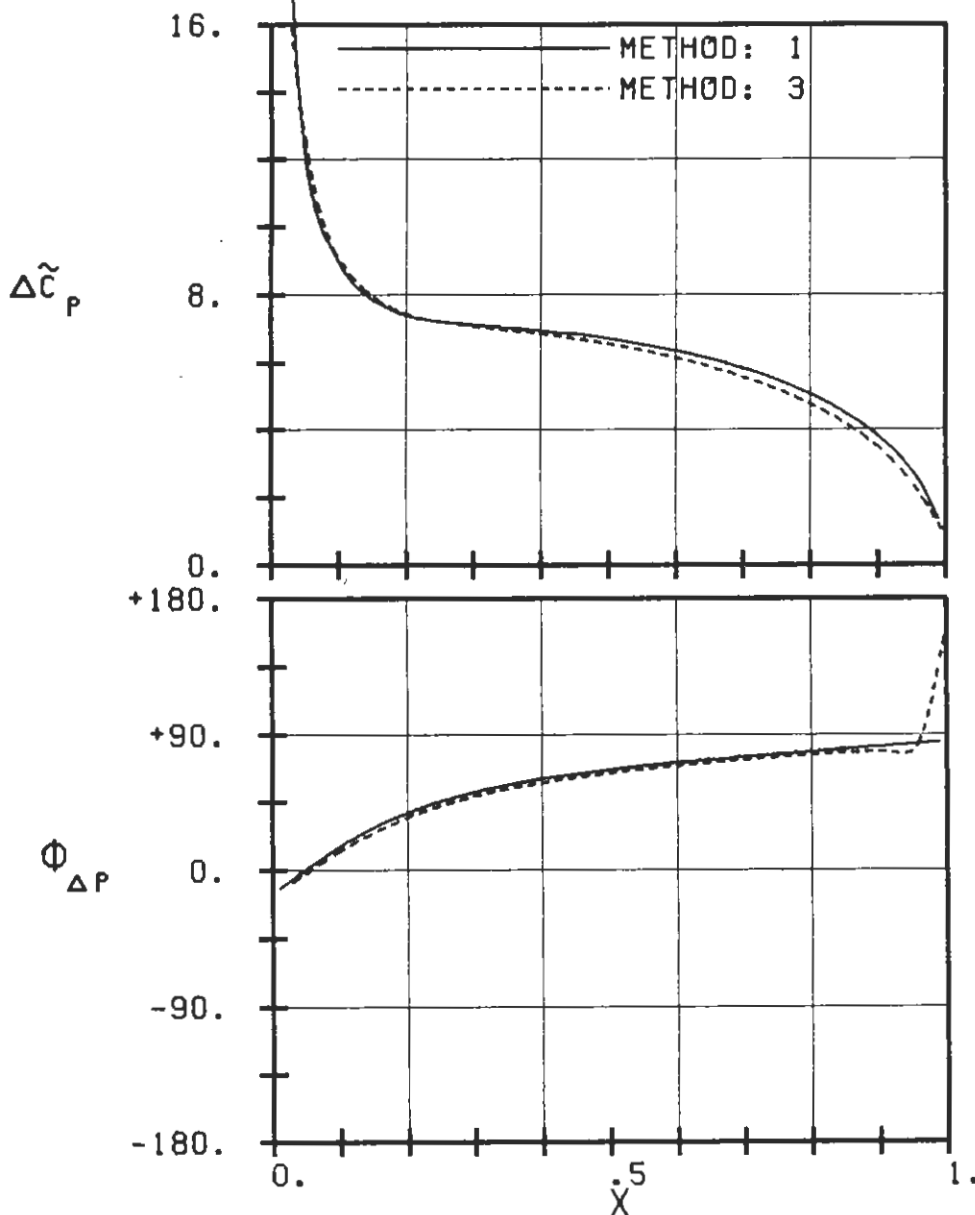
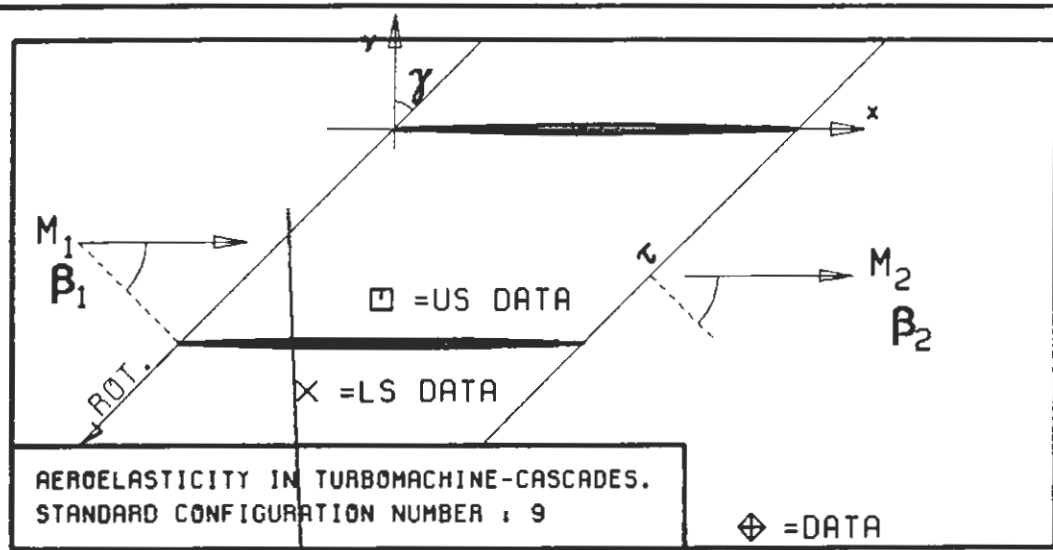
PLOT 7.9-3.11: NINTH STANDARD CONFIGURATION, CASE 11.
 MAGNITUDE AND PHASE LEAD OF UNSTEADY BLADE
 SURFACE PRESSURE DIFFERENCE DISTRIBUTION.
 (*: IN PITCH MODE, NOTATION VALID UPSTREAM OF PITCH AXIS)



PLOT 7.9-3.12: NINTH STANDARD CONFIGURATION, CASE 12.
MAGNITUDE AND PHASE LEAD OF UNSTEADY BLADE SURFACE PRESSURE DIFFERENCE DISTRIBUTION.
(X: IN PITCH MODE, NOTATION VALID UPSTREAM OF PITCH AXIS)

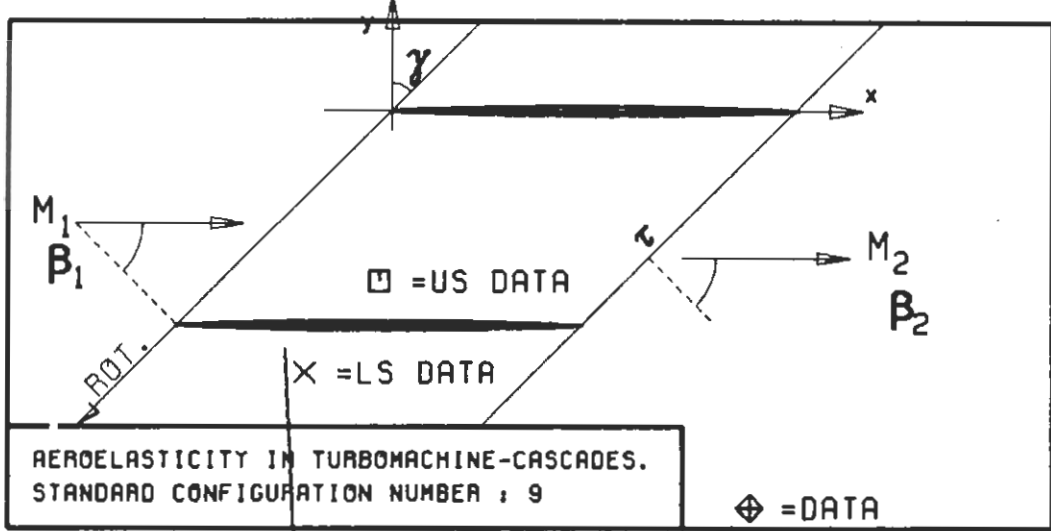


PLOT 7.9-3.13: NINTH STANDARD CONFIGURATION, CASE 13.
MAGNITUDE AND PHASE LEAD OF UNSTEADY BLADE
SURFACE PRESSURE DIFFERENCE DISTRIBUTION.
(*: IN PITCH MODE, NOTATION VALID UPSTREAM OF PITCH AXIS)

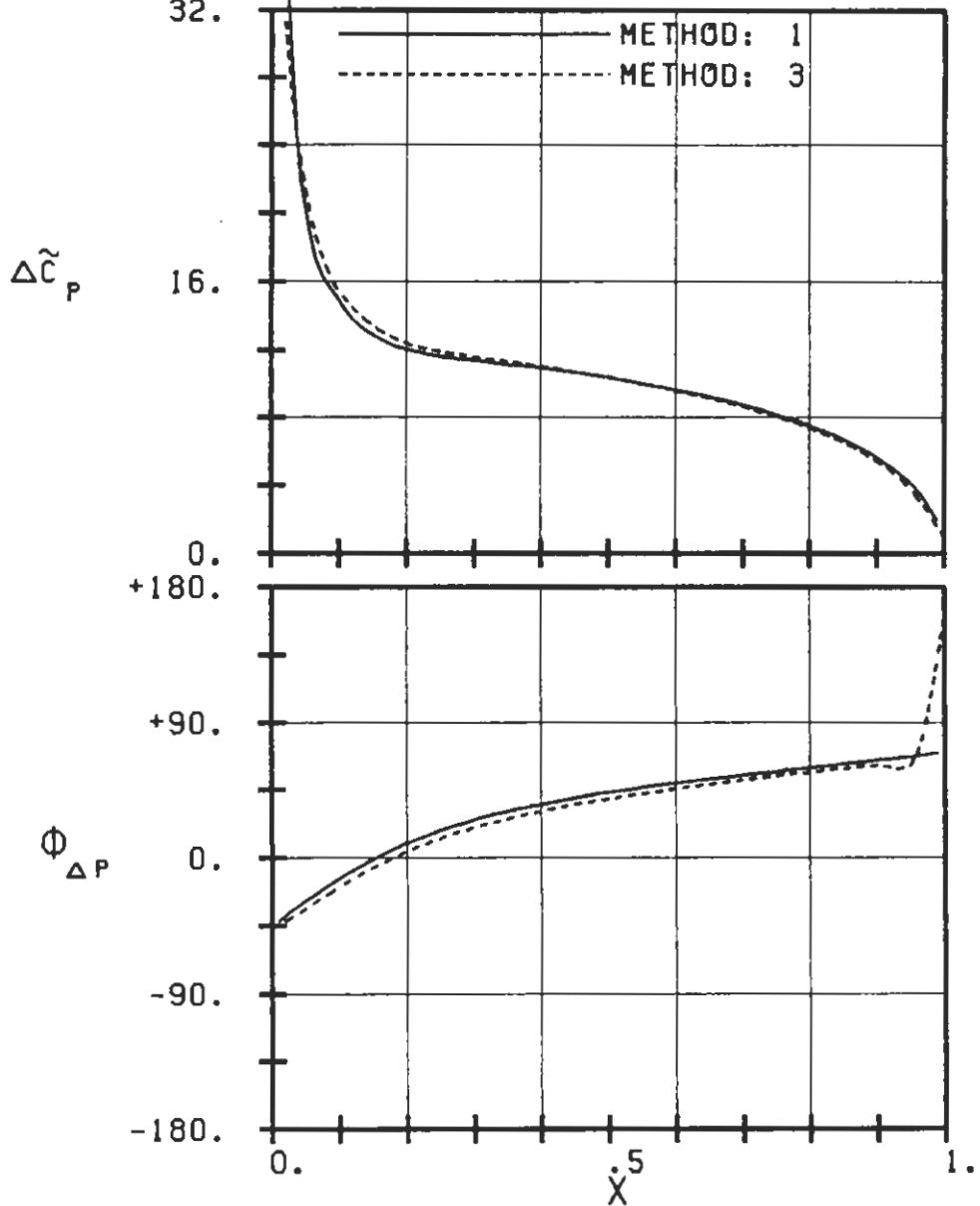


PLOT 7.9-3.14: NINTH STANDARD CONFIGURATION, CASE 14
MAGNITUDE AND PHASE LEAD OF UNSTEADY BLADE
SURFACE PRESSURE DIFFERENCE DISTRIBUTION.
(\times : IN PITCH MODE, NOTATION VALID UPSTREAM OF PITCH AXIS)

$c = 0.1M$
 $\tau = 0.75$
 $\gamma = 45.$
 $x_\alpha = 0.5$
 $y_\alpha = 0.$
 $M_1 = 0.$
 $B_1 = -45.$
 $i :$
 $M_2 = -$
 $B_2 = -$
 $h_x = -$
 $h_y = -$
 $\alpha = .0349$
 $\omega = -$
 $k = 1.0$
 $\delta = -$
 $\sigma = 90.$
 $d = 0.02$



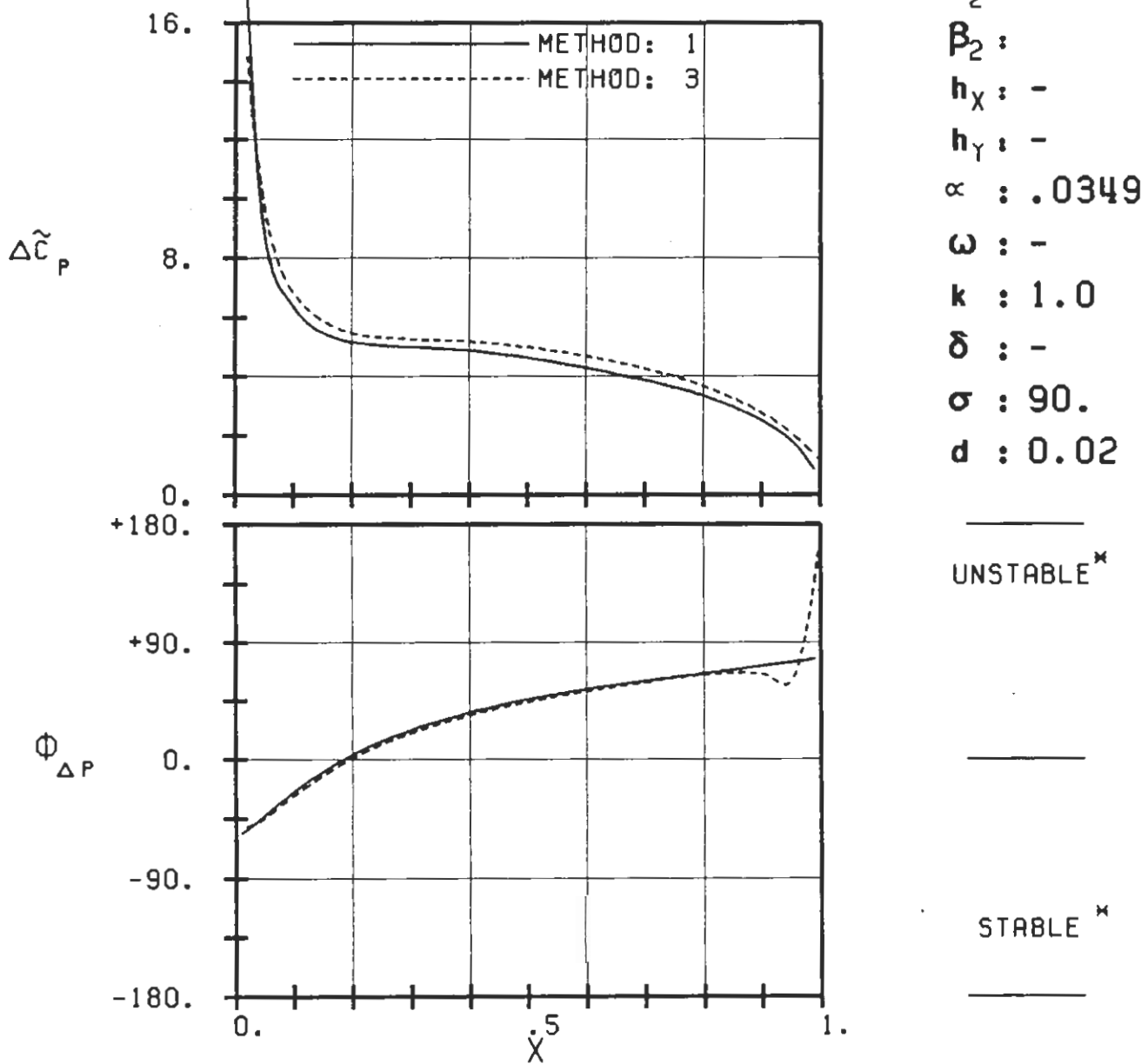
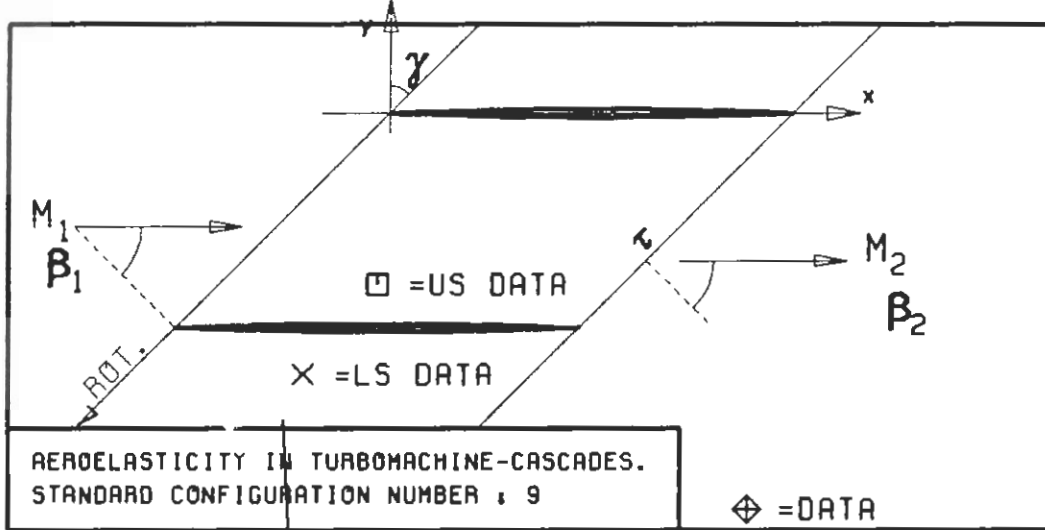
32.



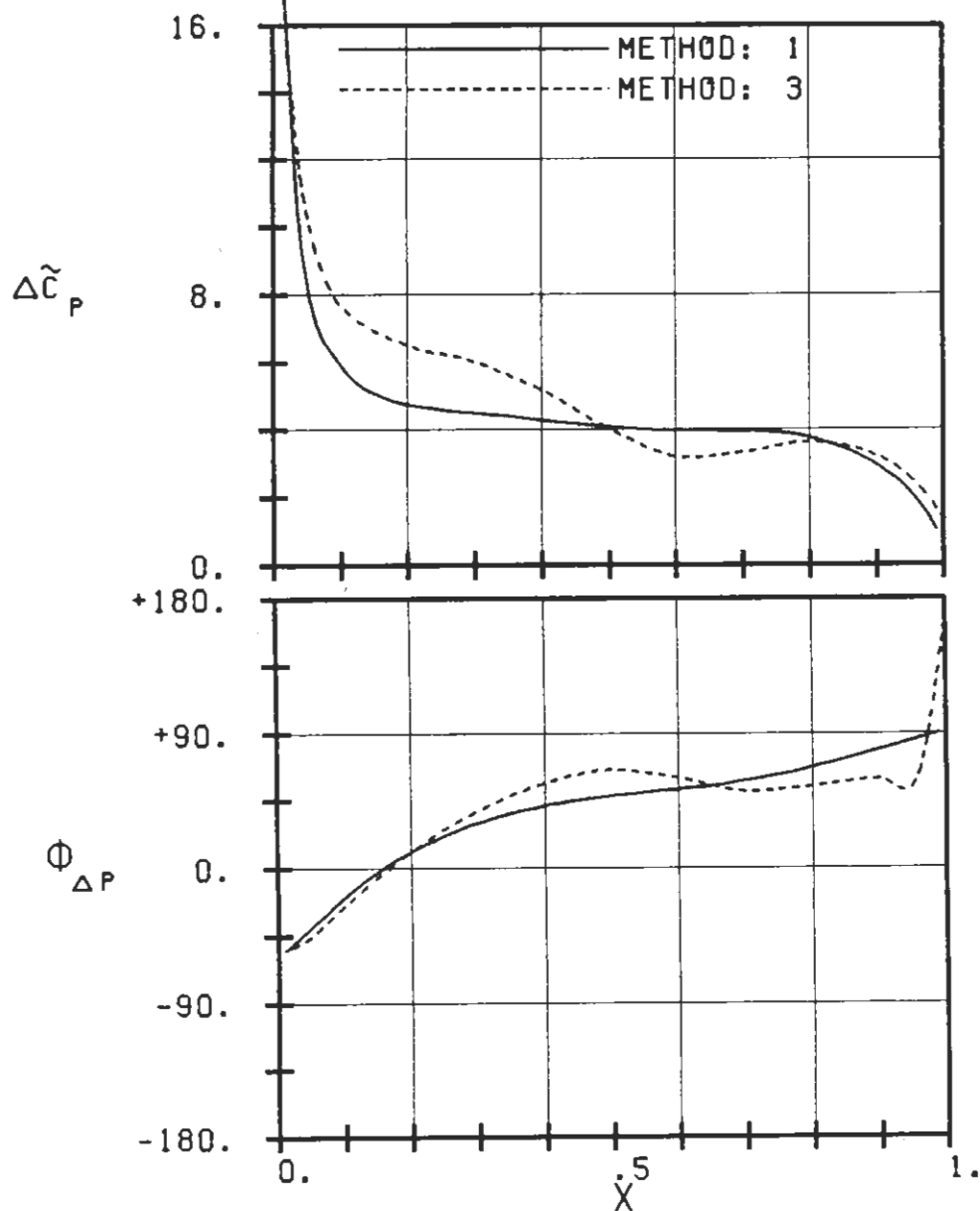
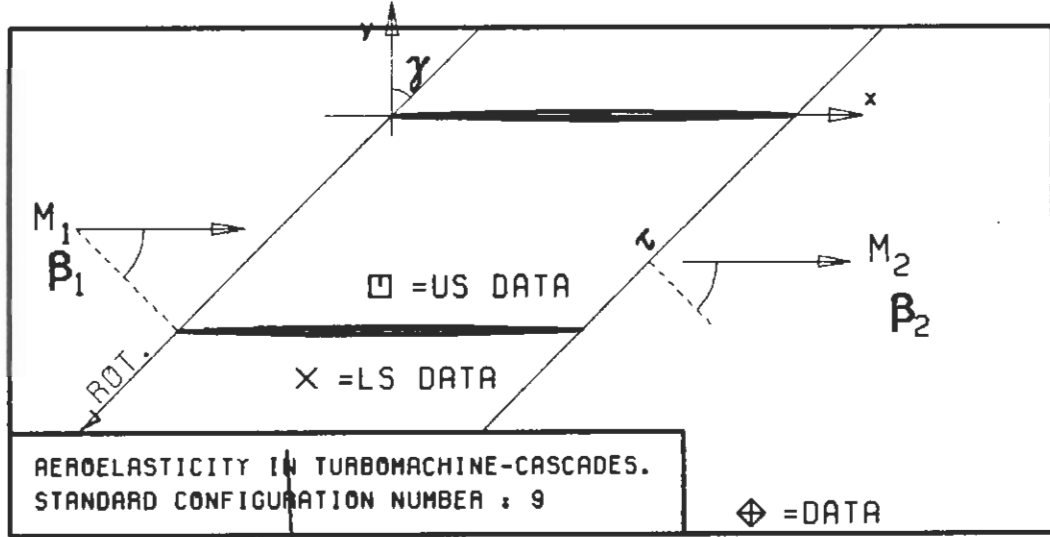
UNSTABLE *

STABLE *

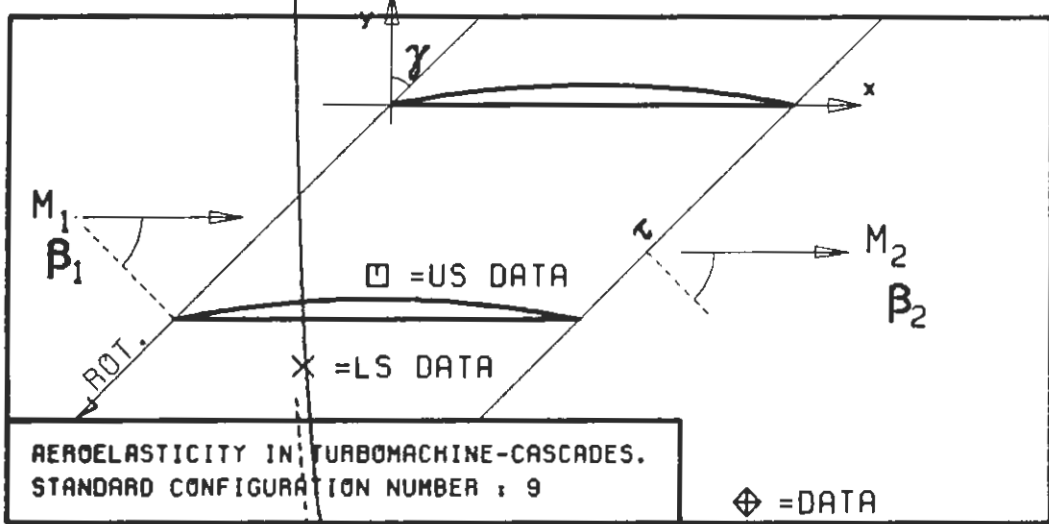
PLOT 7.9-3.15: NINTH STANDARD CONFIGURATION, CASE 15.
MAGNITUDE AND PHASE LEAD OF UNSTEADY BLADE
SURFACE PRESSURE DIFFERENCE DISTRIBUTION.
(*: IN PITCH MODE, NOTATION VALID UPSTREAM OF PITCH AXIS)



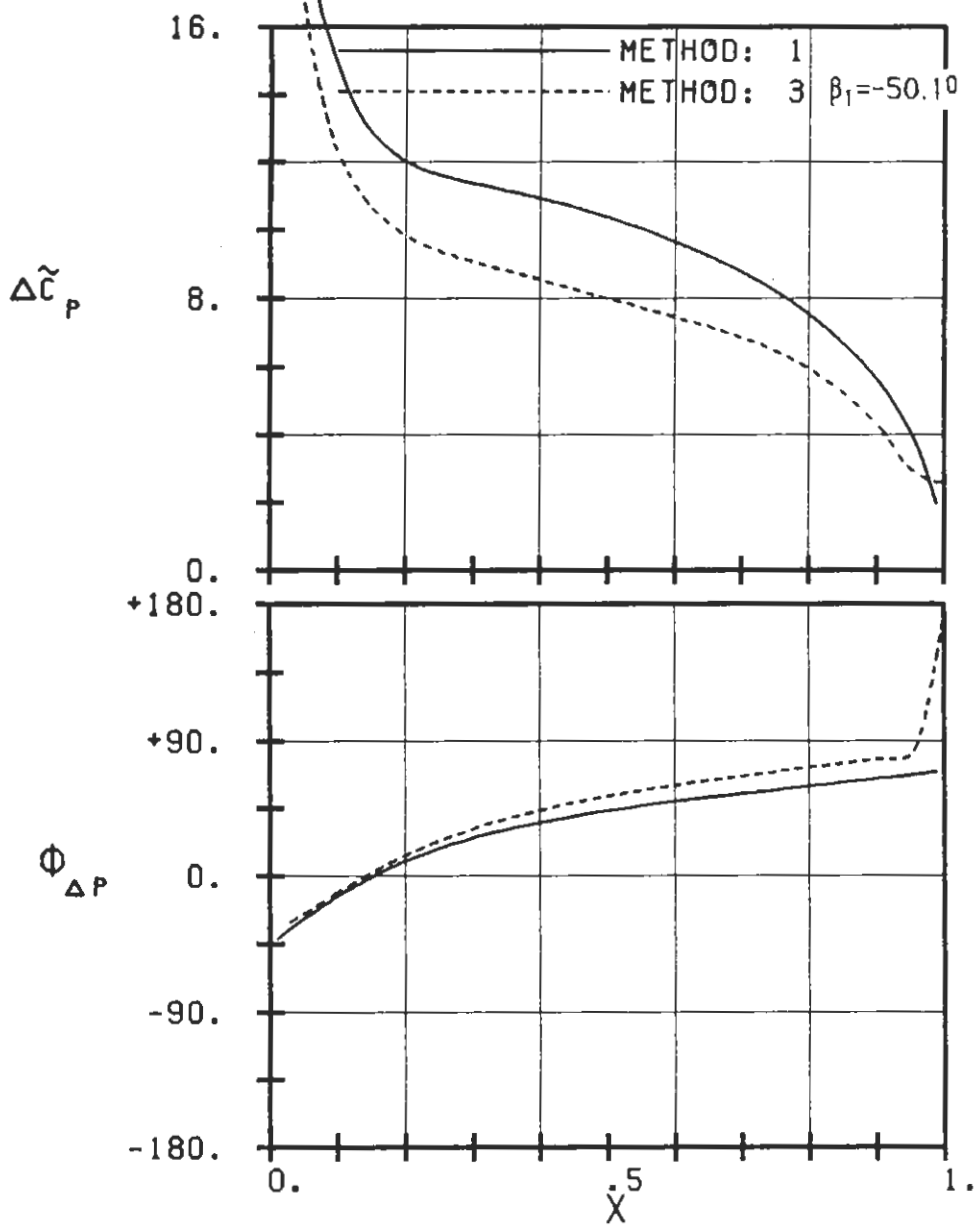
PLOT 7.9-3.16: NINTH STANDARD CONFIGURATION, CASE 16.
 MAGNITUDE AND PHASE LEAD OF UNSTEADY BLADE
 SURFACE PRESSURE DIFFERENCE DISTRIBUTION.
 (\times : IN PITCH MODE, NOTATION VALID UPSTREAM OF PITCH AXIS)



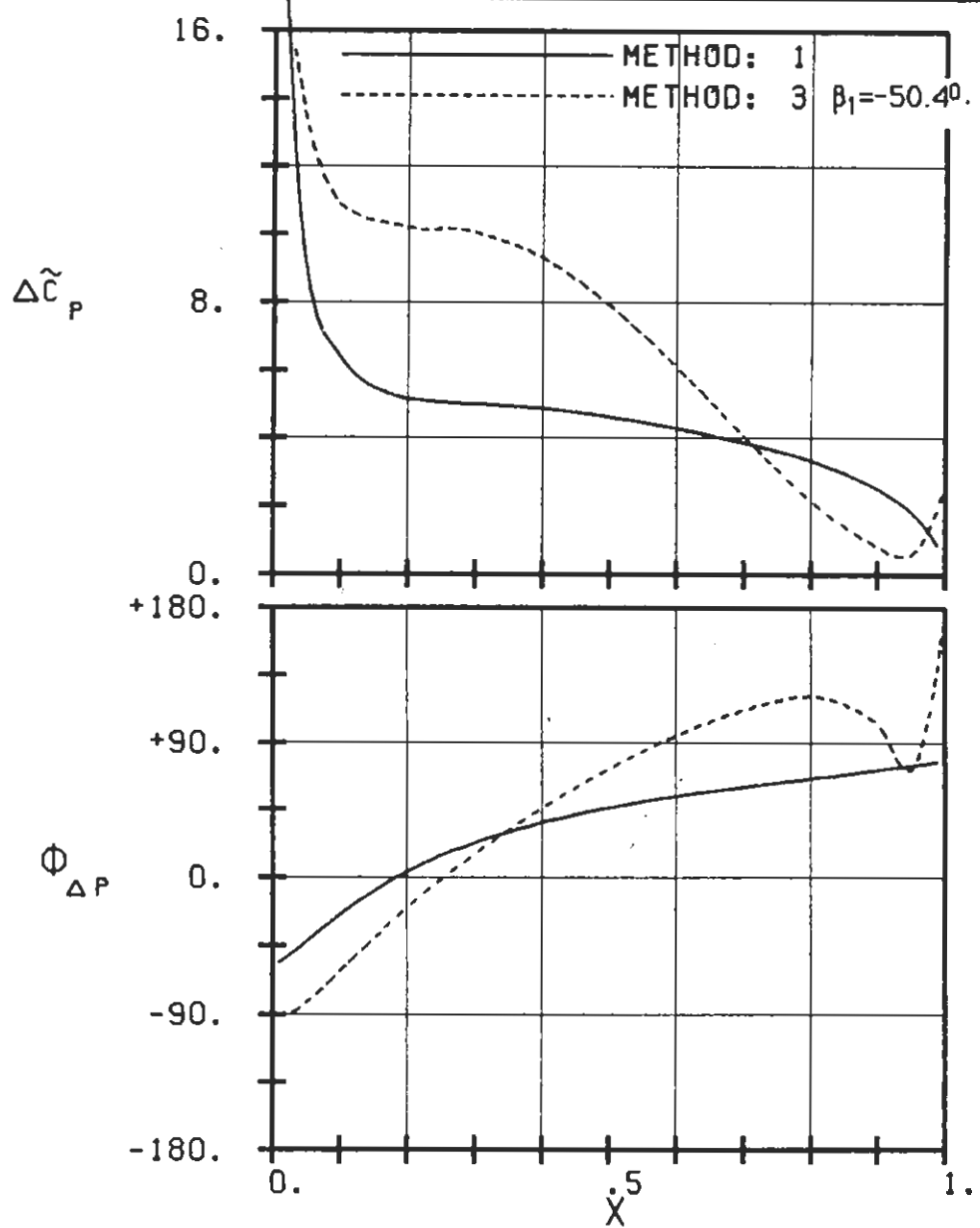
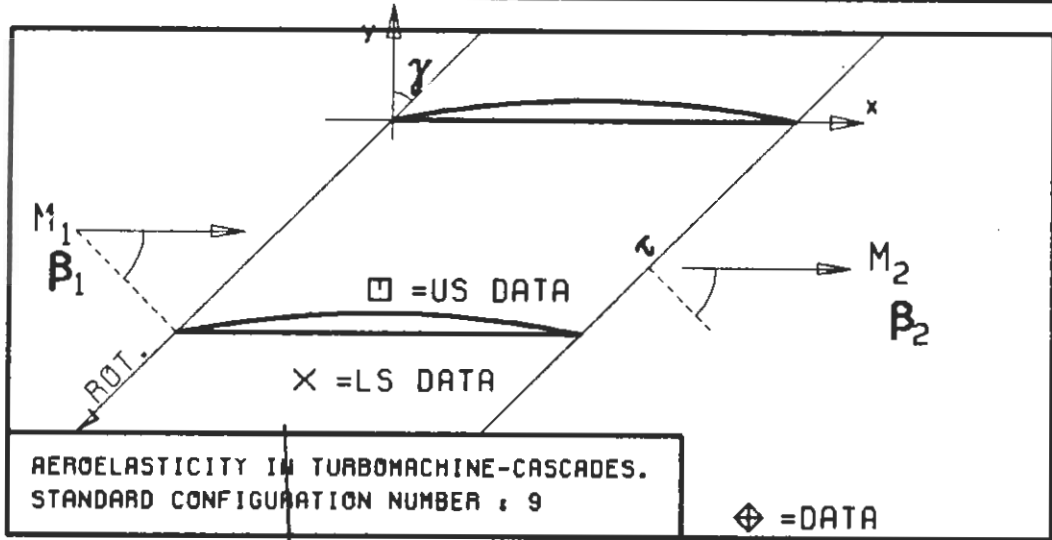
PLOT 7.9-3.17: NINTH STANDARD CONFIGURATION, CASE 17.
 MAGNITUDE AND PHASE LEAD OF UNSTEADY BLADE
 SURFACE PRESSURE DIFFERENCE DISTRIBUTION.
 (*: IN PITCH MODE, NOTATION VALID UPSTREAM OF PITCH AXIS)



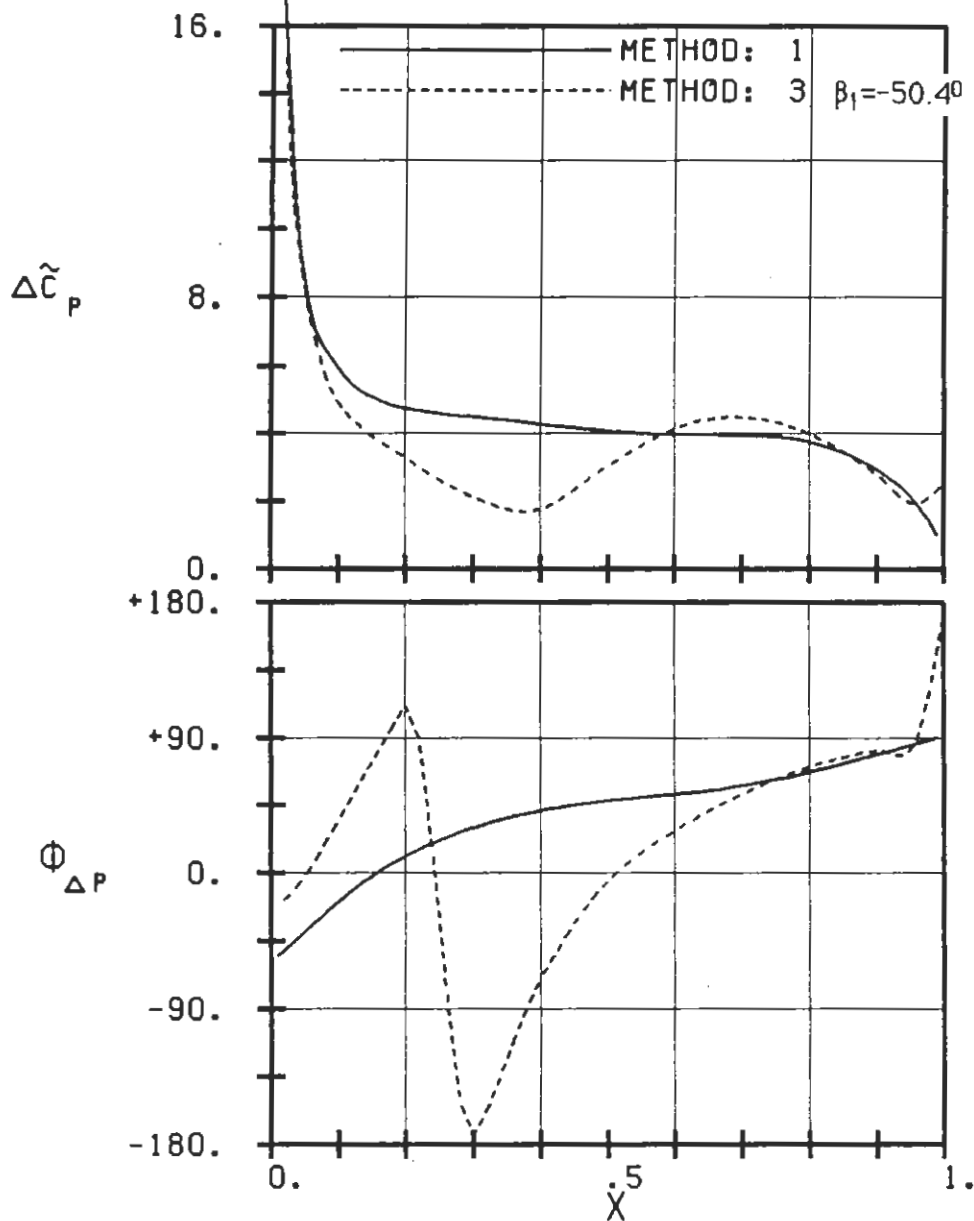
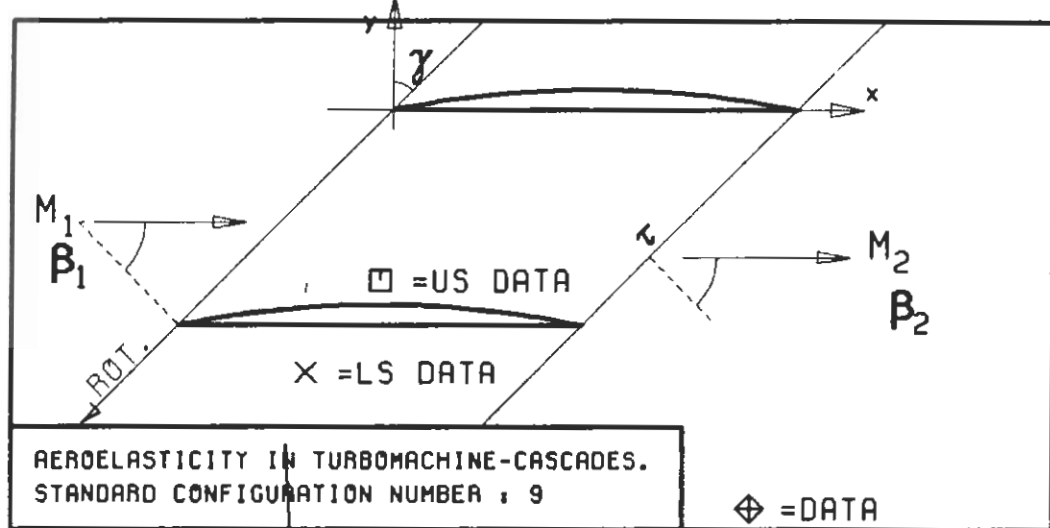
$c = 0.1M$
 $\tau = 0.75$
 $\gamma = 45.$
 $x_\alpha = 0.5$
 $y_\alpha = 0.$
 $M_1 = 0.5$
 $\beta_1 = -45.$
 $i :$
 $M_2 = -$
 $\beta_2 = -$
 $h_x = -$
 $h_y = -$
 $\alpha = .0349$
 $\omega = -$
 $k = 1.0$
 $\delta = -$
 $\sigma = 90.$
 $d = 0.05$



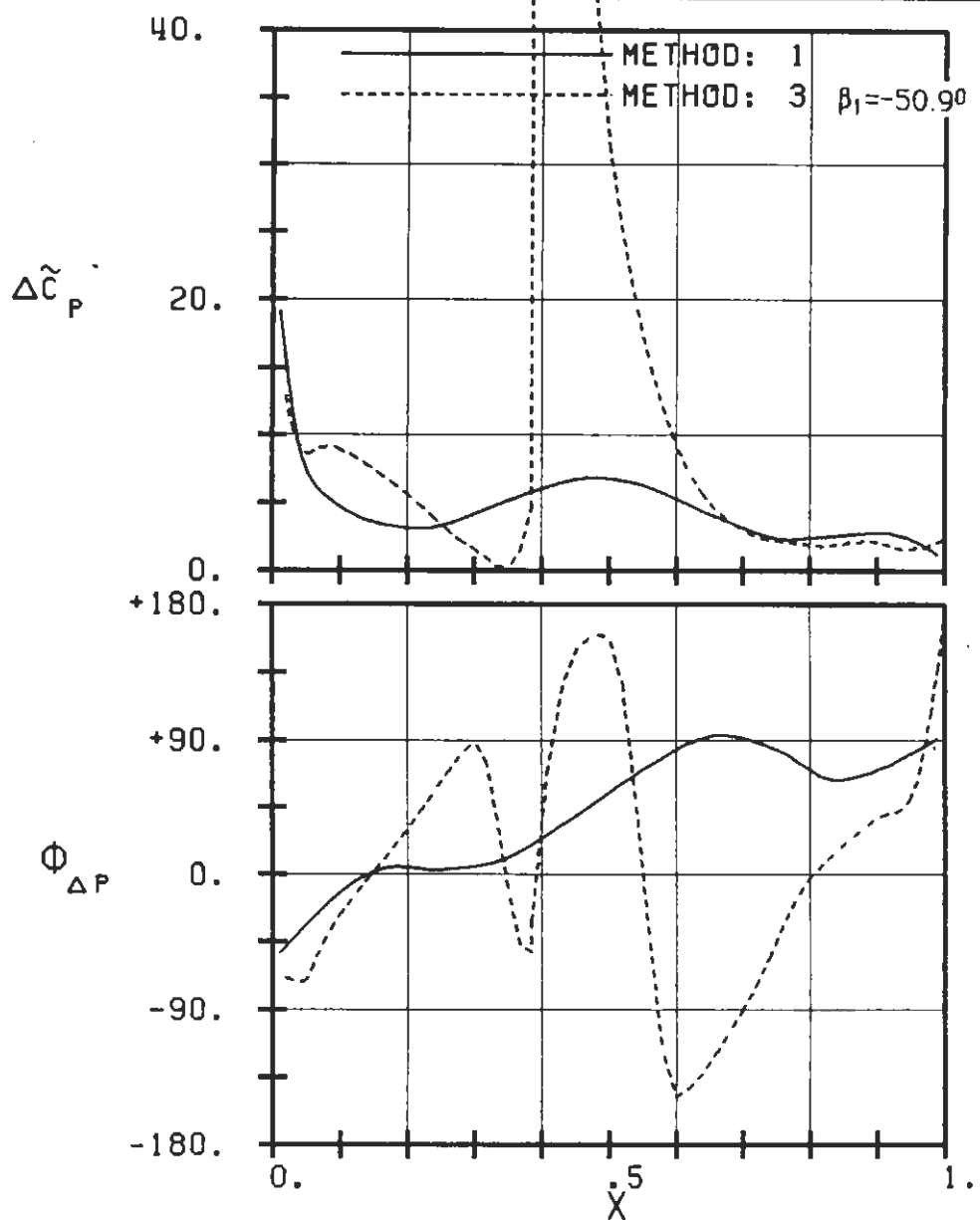
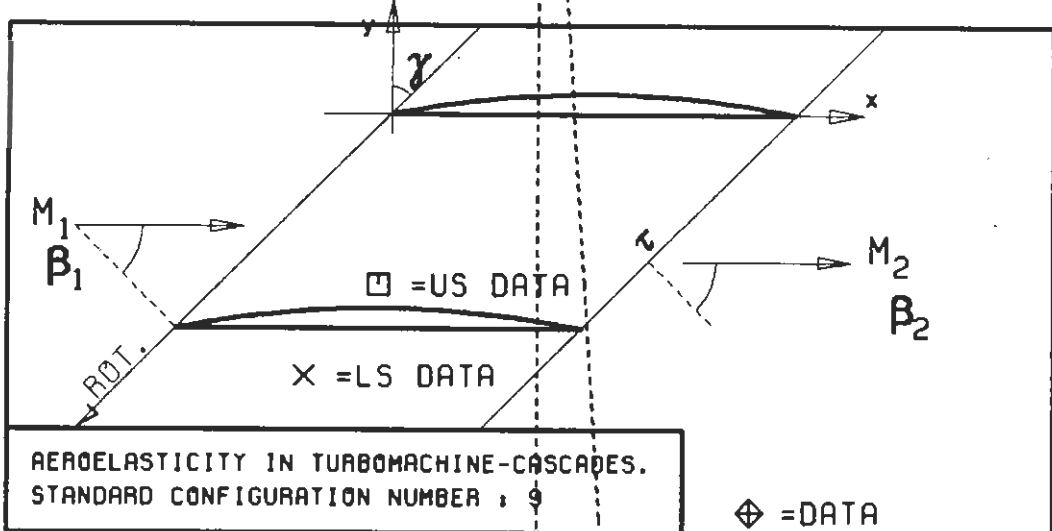
PLOT 7.9-3.18: NINTH STANDARD CONFIGURATION, CASE 18.
 MAGNITUDE AND PHASE LEAD OF UNSTEADY BLADE
 SURFACE PRESSURE DIFFERENCE DISTRIBUTION.
 (*: IN PITCH MODE, NOTATION VALID UPSTREAM OF PITCH AXIS)



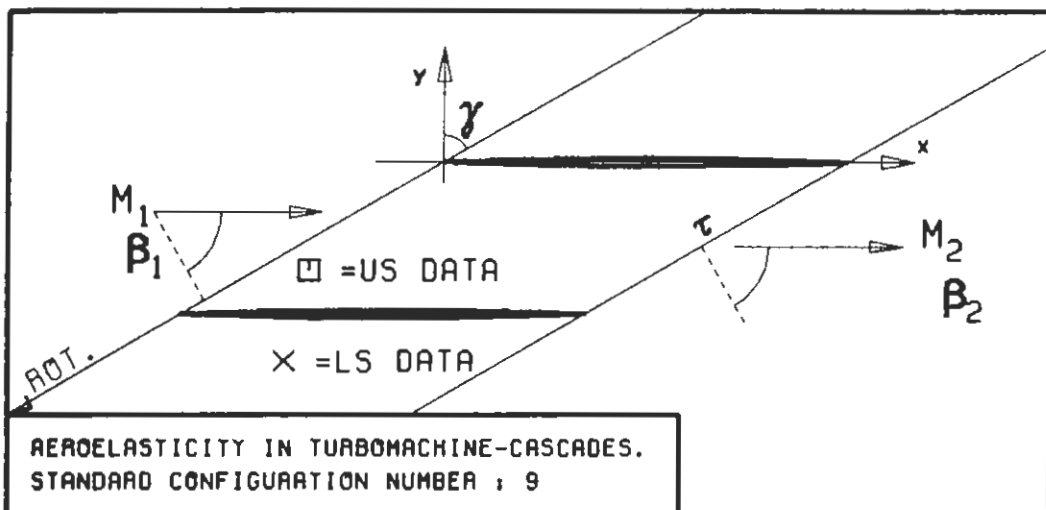
PLOT 7.9-3.19: NINTH STANDARD CONFIGURATION. CASE 19.
 MAGNITUDE AND PHASE LEAD OF UNSTEADY BLADE
 SURFACE PRESSURE DIFFERENCE DISTRIBUTION.
 (*: IN PITCH MODE, NOTATION VALID UPSTREAM OF PITCH AXIS)



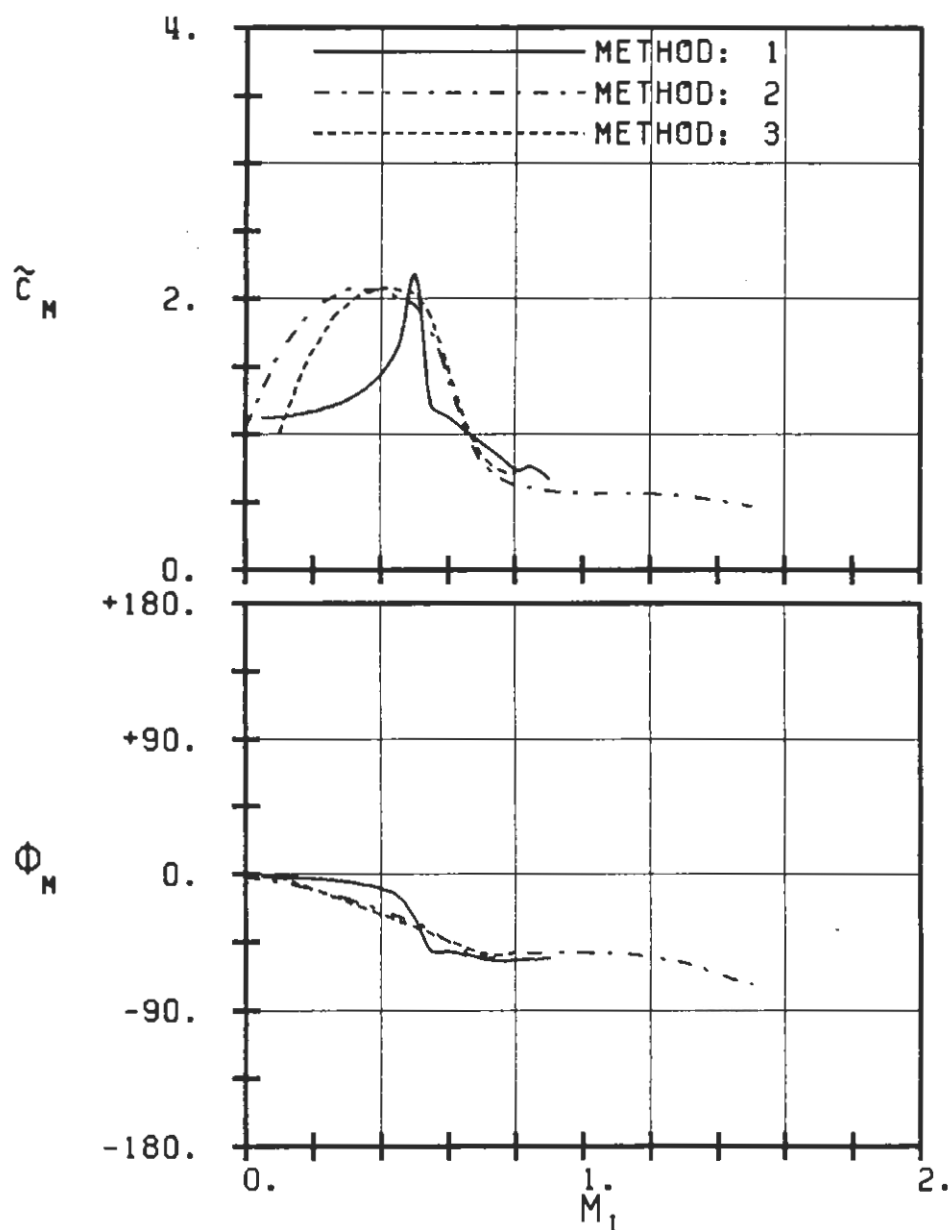
PLT 7.9-3.20: NINTH STANDARD CONFIGURATION, CASE 20.
 MAGNITUDE AND PHASE LEAD OF UNSTEADY BLADE
 SURFACE PRESSURE DIFFERENCE DISTRIBUTION.
 (X: IN PITCH MODE, NOTATION VALID UPSTREAM OF PITCH AXIS)



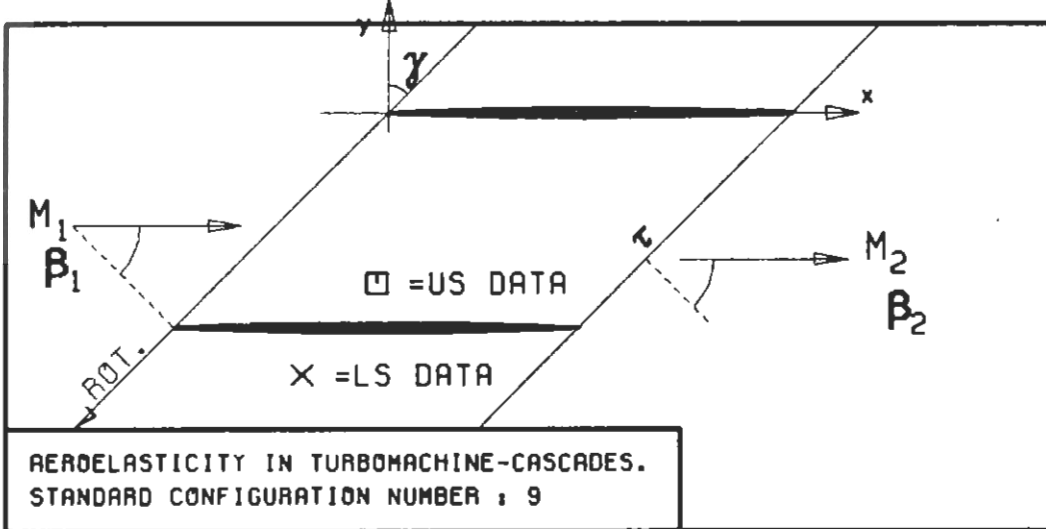
PLOT 7.9-3.21: NINTH STANDARD CONFIGURATION, CASE 21.
 MAGNITUDE AND PHASE LEAD OF UNSTEADY BLADE
 SURFACE PRESSURE DIFFERENCE DISTRIBUTION.
 (*: IN PITCH MODE, NOTATION VALID UPSTREAM OF PITCH AXIS)



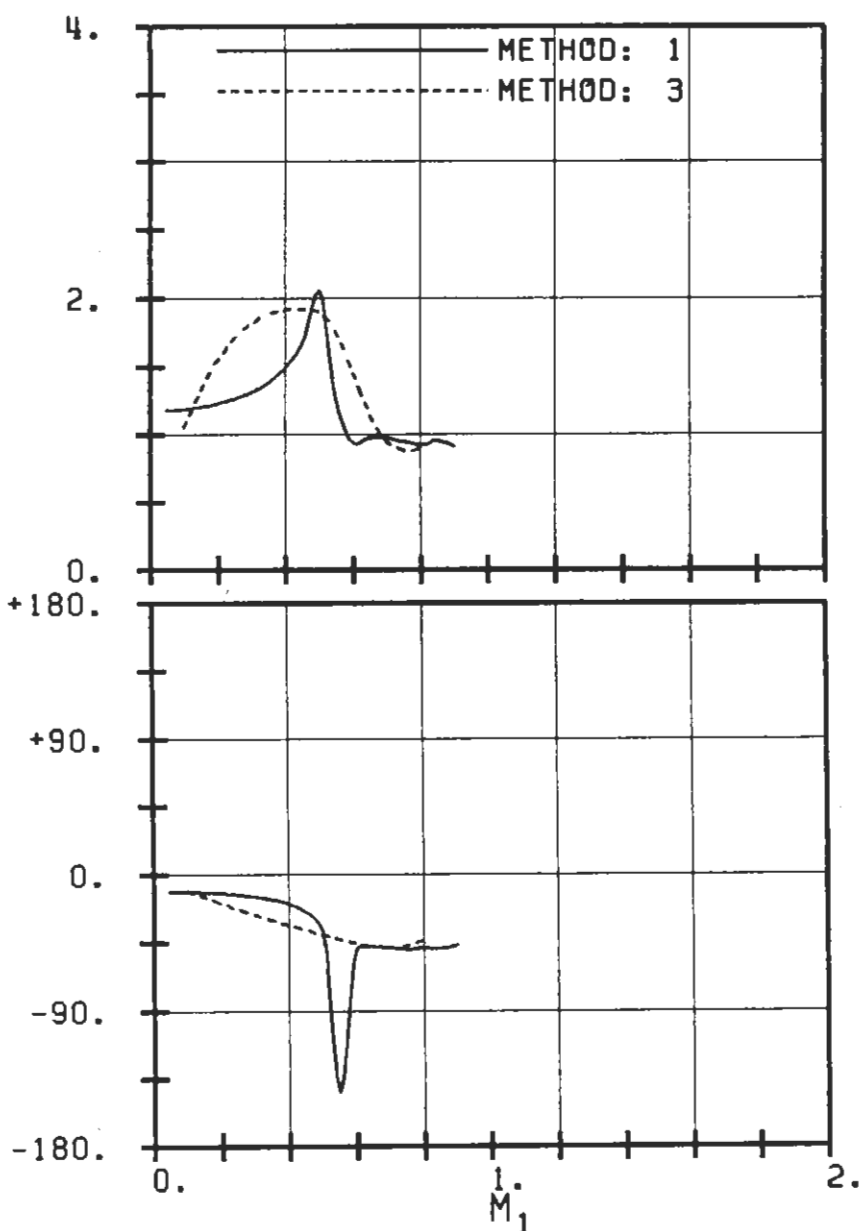
$c : 0.1M$
 $\tau : 0.75$
 $\gamma : 60.$
 $x_\alpha : 0.5$
 $y_\alpha : 0.$
 $M_1 : -$
 $\beta_1 : -60.$
 $i : 0.$
 $M_2 : -$
 $\beta_2 : -$
 $h_x : -$
 $h_y : -$
 $\alpha : .0349$
 $\omega : -$
 $k : 1.0$
 $\delta : -$
 $\sigma : 90.$
 $d : 0.02$



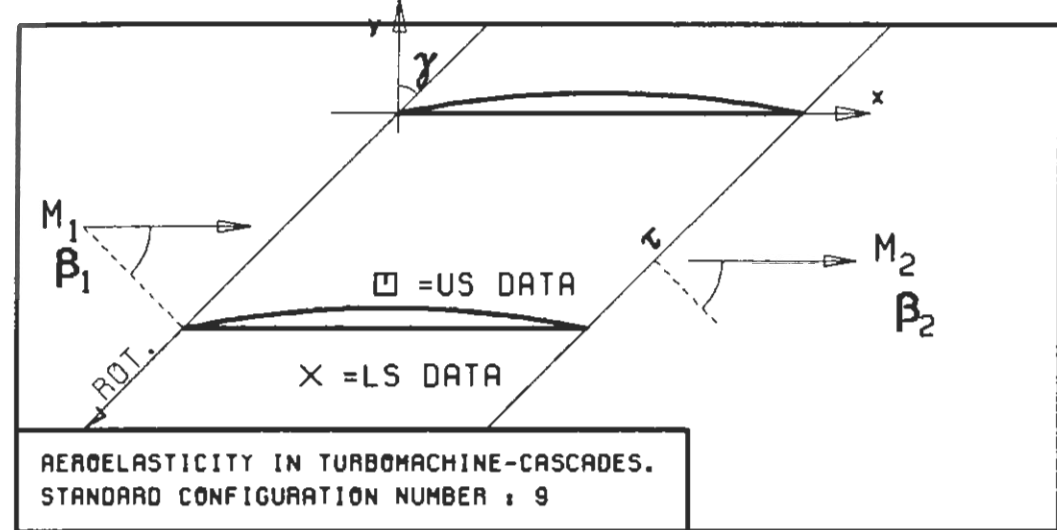
PLOT 7.9-5.1: NINTH STANDARD CONFIGURATION, CASES 1,5,7,10-13
AERODYNAMIC MOMENT COEFFICIENT AND PHASE LEAD
IN DEPENDANCE OF INLET MACH NUMBER.



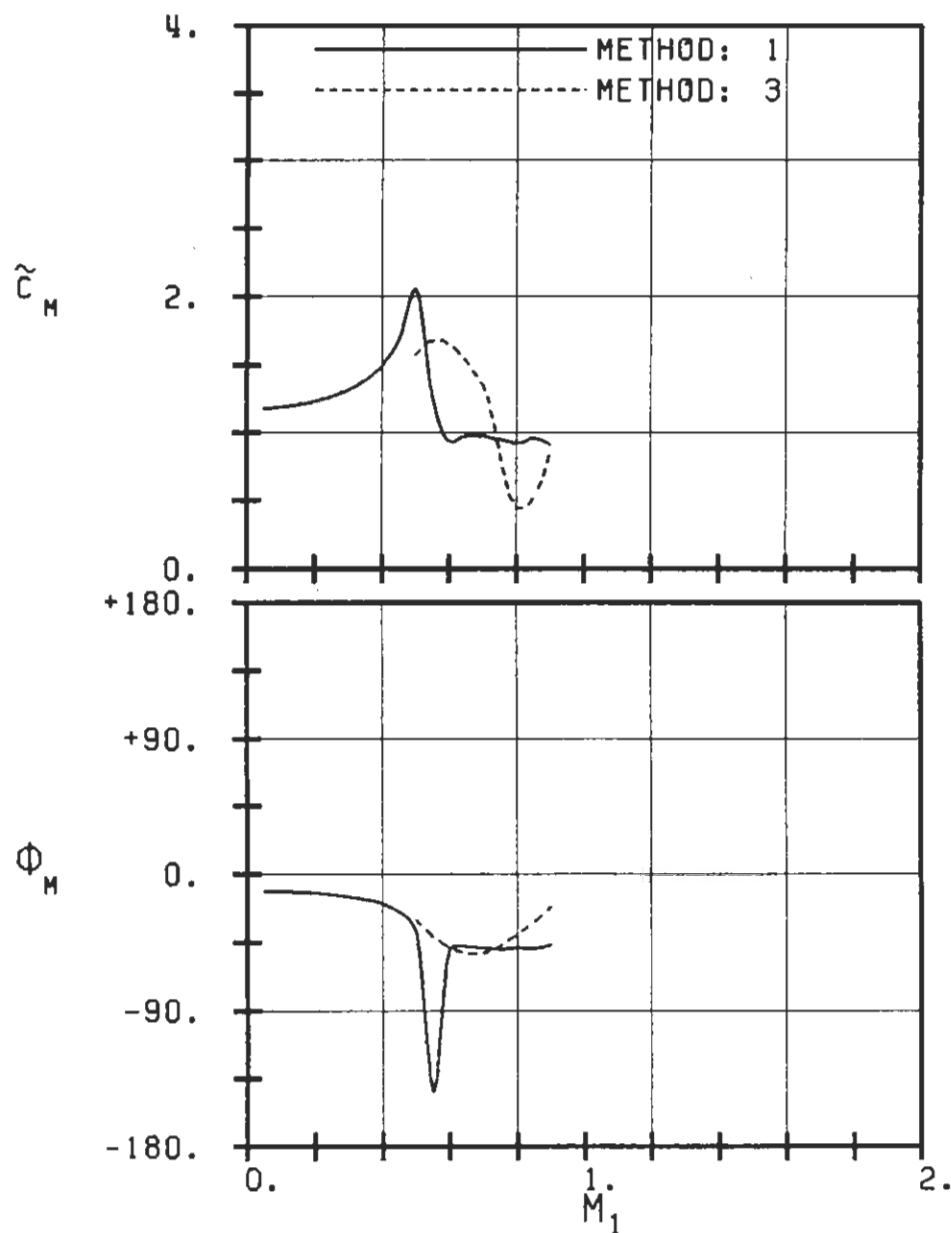
$c : 0.1M$
 $\tau : 0.75$
 $\gamma : 45.$
 $x_\alpha : 0.5$
 $y_\alpha : 0.$
 $M_1 : -$
 $B_1 : -45.$
 $i : 0.$
 $M_2 : -$
 $B_2 : -$
 $h_X : -$
 $h_Y : -$
 $\alpha : .0349$
 $\omega : -$
 $k : 1.0$
 $\delta : -$
 $\sigma : 90.$
 $d : 0.02$



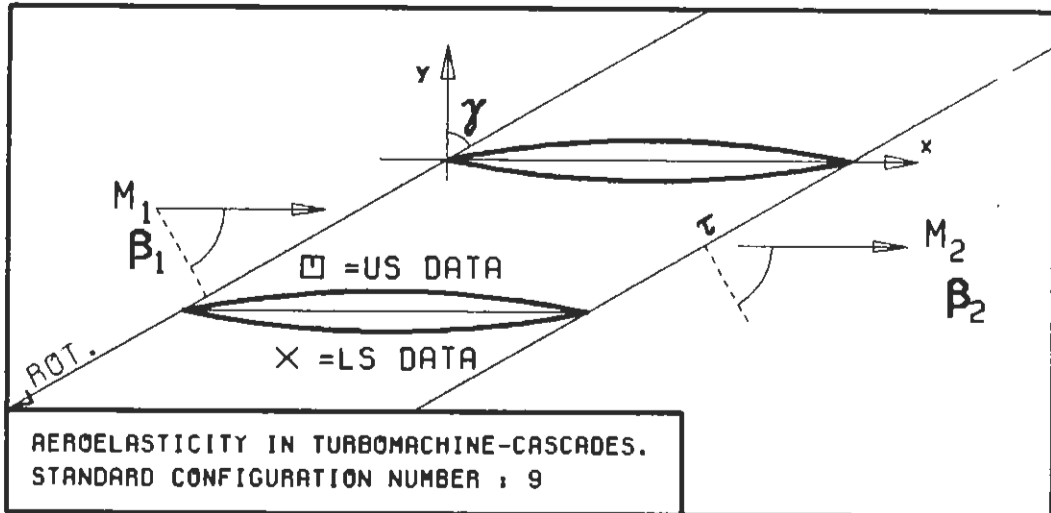
PLOT 7.9-5.2: NINTH STANDARD CONFIGURATION, CASES 14-17.
AERODYNAMIC MOMENT COEFFICIENT AND PHASE LEAD
IN DEPENDANCE OF INLET MACH NUMBER.



c : 0.1M
 τ : 0.75
 γ : 45.
 x_∞ : 0.5
 y_∞ : 0.
 M_1 : -
 β_1 : -45.
 i : 0.
 M_2 : -
 β_2 :
 h_x : -
 h_y : -
 α : .0349
 ω : -
 k : 1.0
 δ : -
 σ : 90.
 d : 0.05



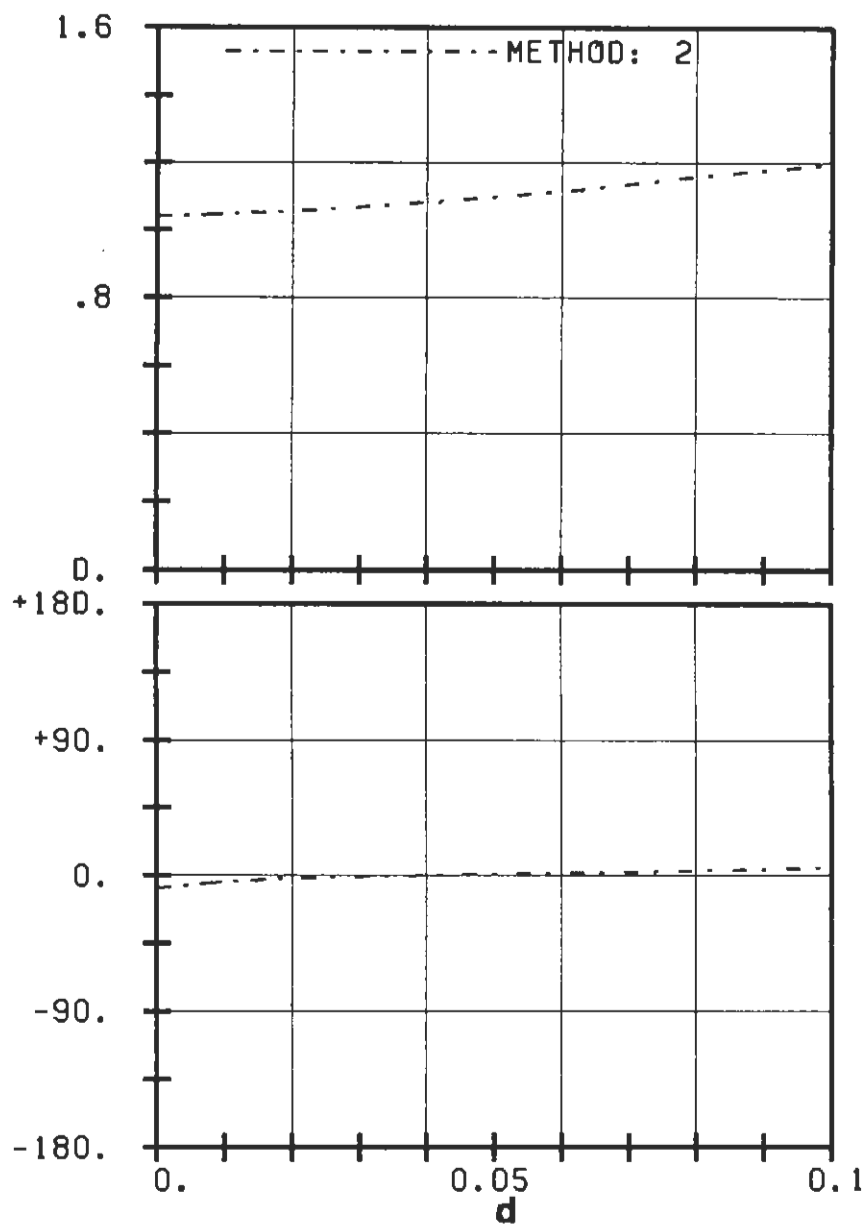
PLOT 7.9-5.3: NINTH STANDARD CONFIGURATION, CASES 18-21.
AERODYNAMIC MOMENT COEFFICIENT AND PHASE LEAD
IN DEPENDANCE OF INLET MACH NUMBER.

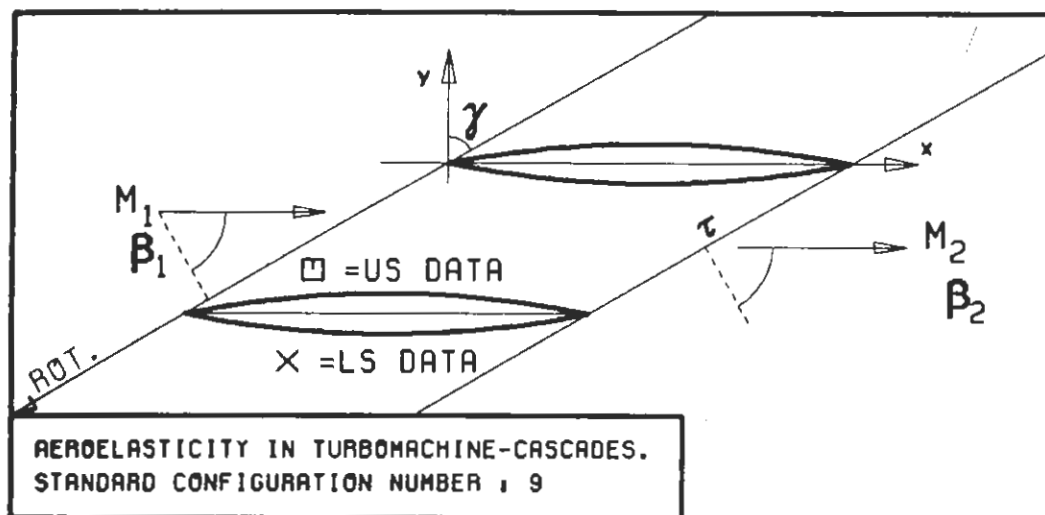


$c : 0.1M$
 $\tau : 0.75$
 $\gamma : 60.$
 $x_\alpha : 0.5$
 $y_\alpha : 0.$
 $M_1 : 0.$
 $\beta_1 : -60.$
 $i : 0.$
 $M_2 : -$
 $\beta_2 : -$
 $h_x : -$
 $h_y : -$
 $\alpha : .0349$
 $\omega : -$
 $k : 1.0$
 $\delta : -$
 $\sigma : 90.$
 $d : -$

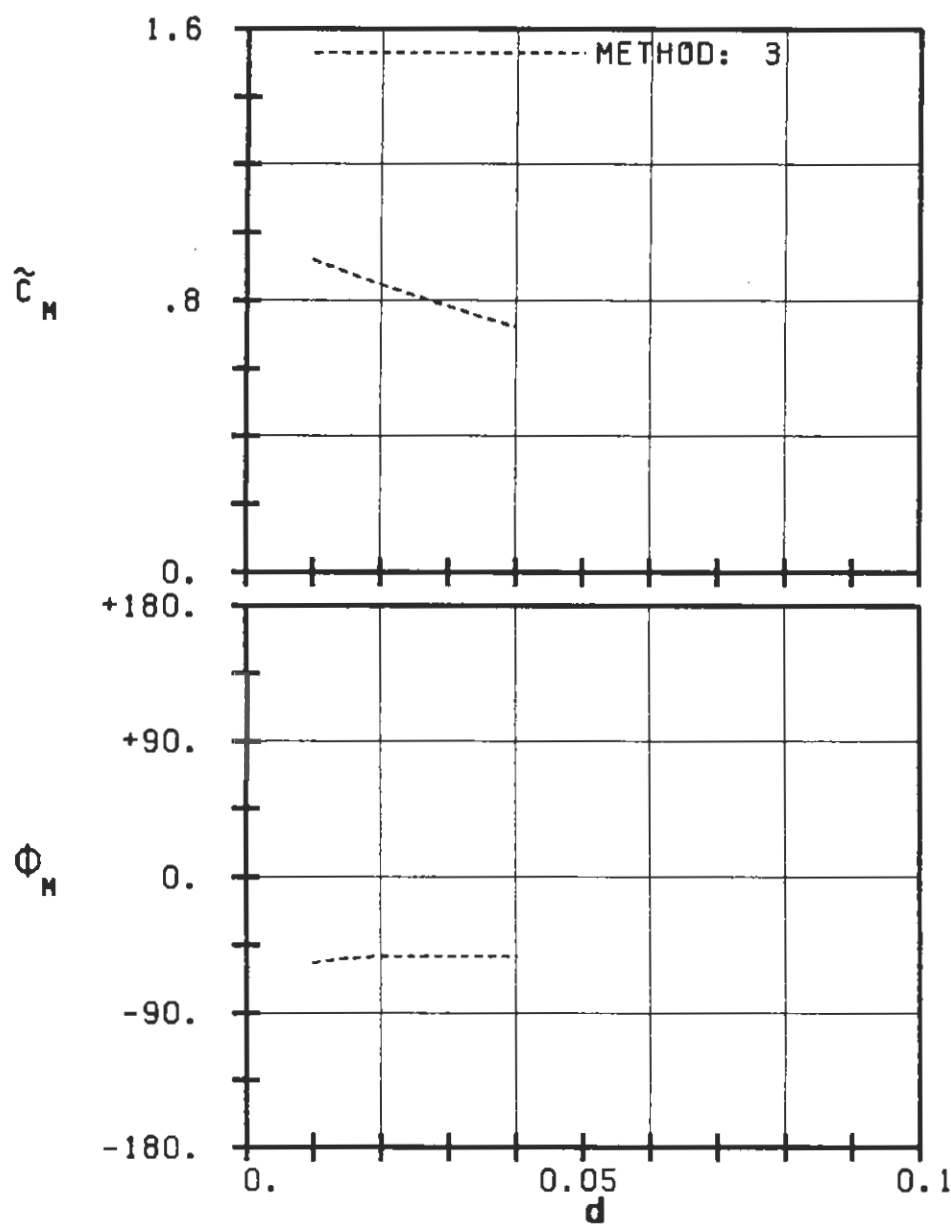
UNSTABLE

STABLE





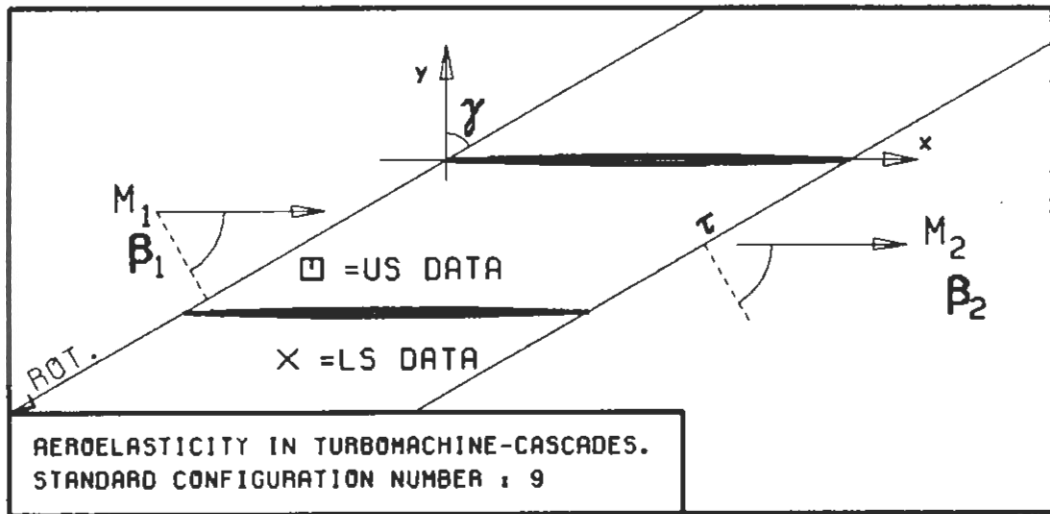
c : 0.1M
 τ : 0.75
 γ : 60.
 x_α : 0.5
 y_α : 0.
 M_1 : 0.7
 β_1 : -60.
 i : 0.
 M_2 : -
 β_2 : -
 h_X : -
 h_Y : -
 α : .0349
 ω : -
 k : 1.0
 δ : -
 σ : 90.
 d : -



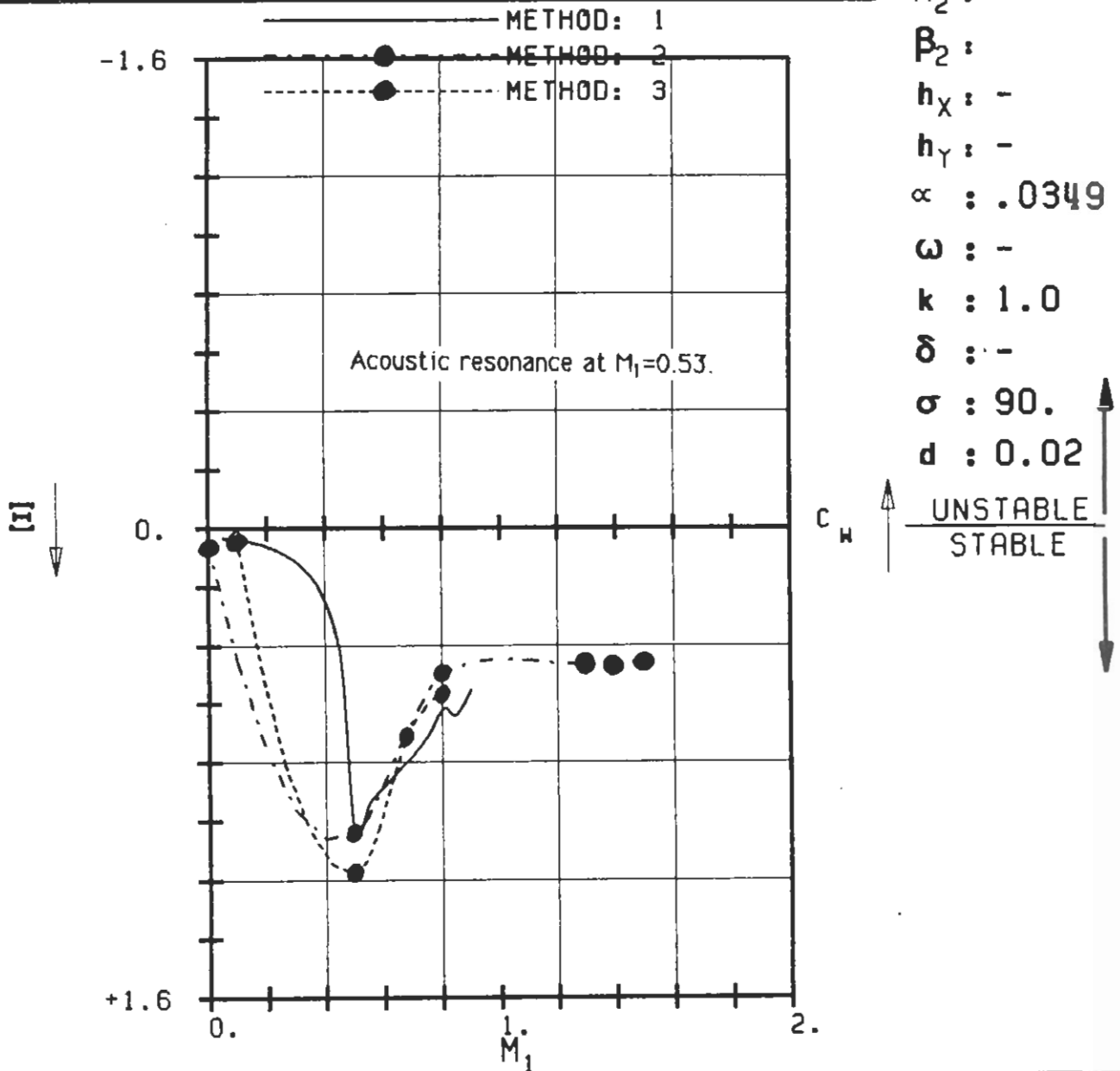
UNSTABLE

STABLE

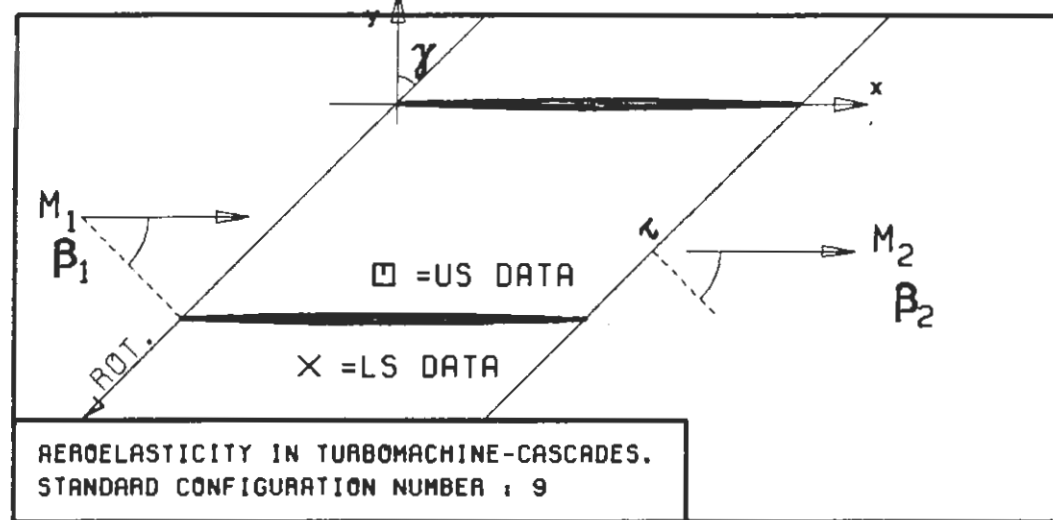
PLOT 7.9-5.5: NINTH STANDARD CONFIGURATION, CASES 6-9.
AERODYNAMIC MOMENT COEFFICIENT AND PHASE LEAD
IN DEPENDANCE OF BLADE THICKNESS.



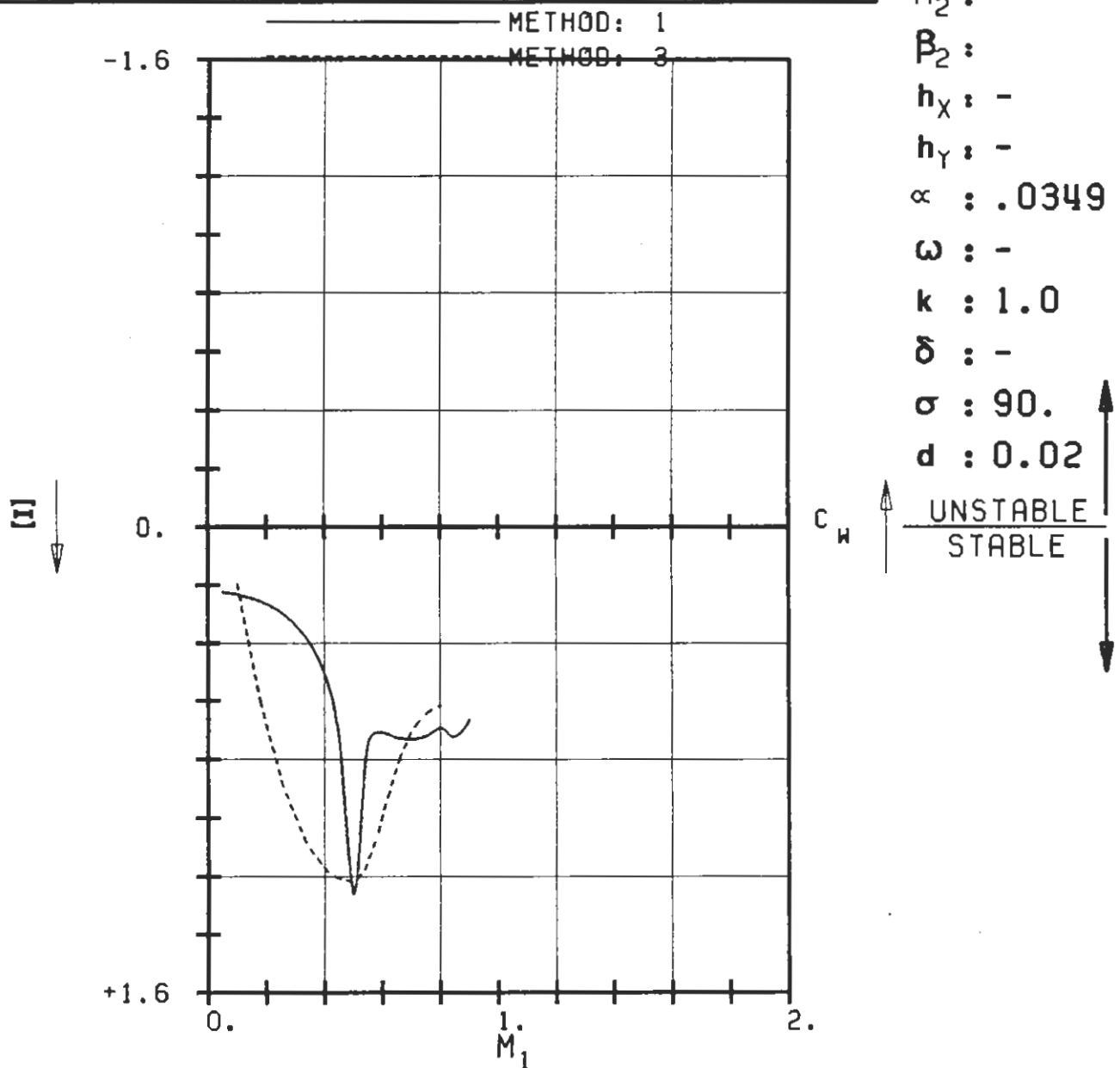
$c = 0.1M$
 $\tau = 0.75$
 $\gamma = 60.$
 $x_{\infty} = 0.5$
 $y_{\infty} = 0.$
 $M_1 = -$
 $\beta_1 = -60.$
 $i = 0.$
 $M_2 = -$
 $\beta_2 =$
 $h_x = -$
 $h_y = -$
 $\alpha = .0349$



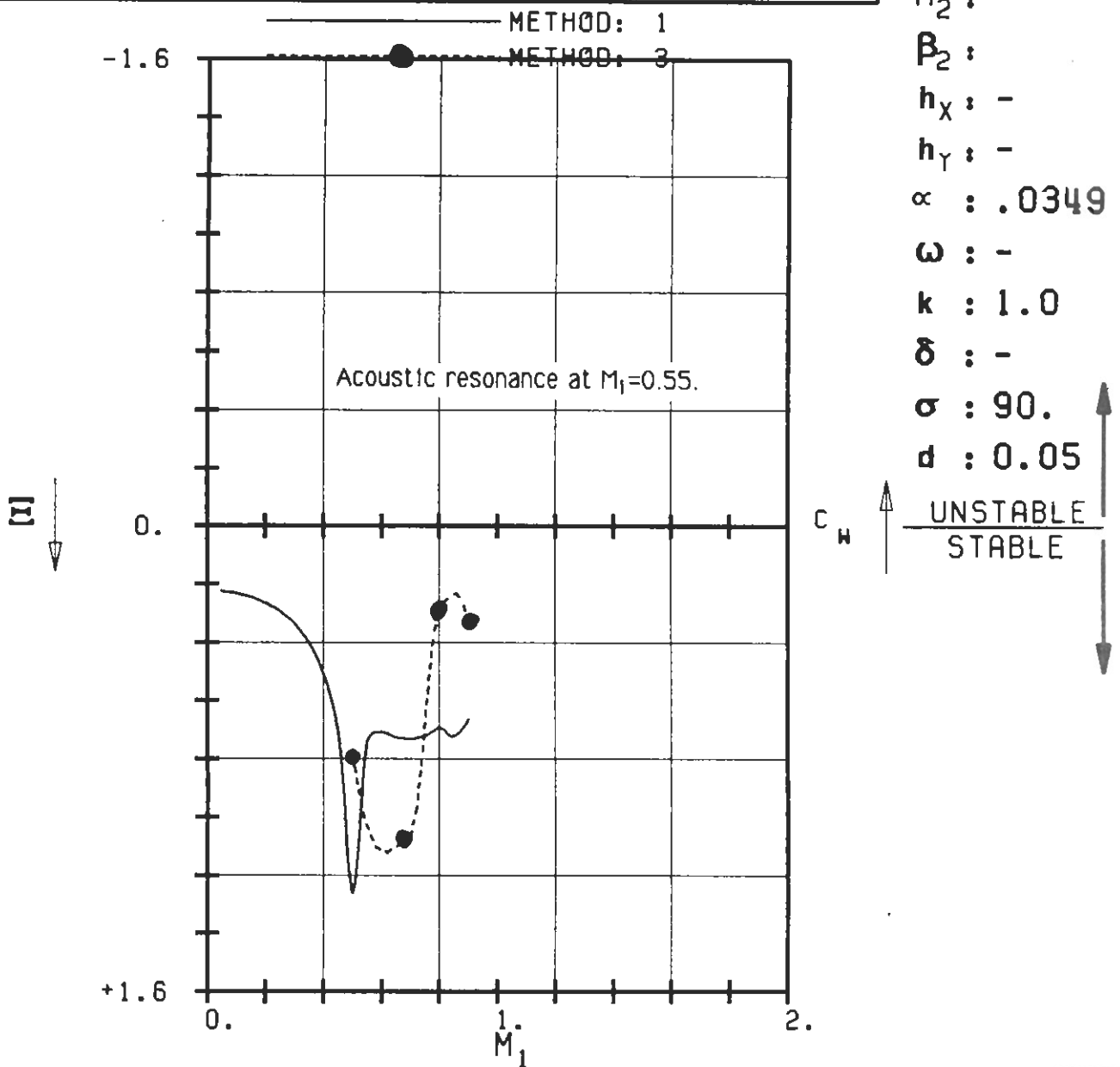
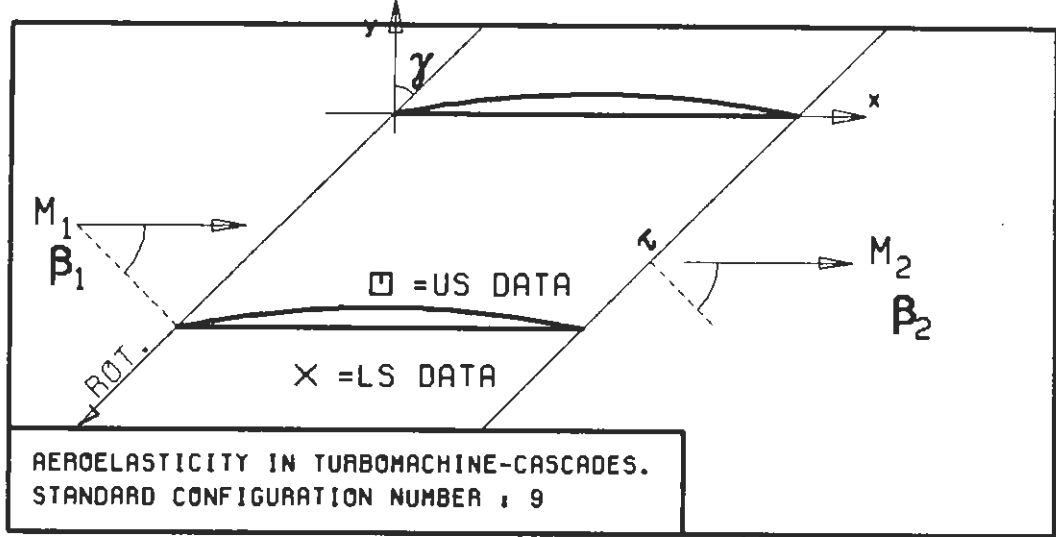
PLOT 7.9-6.1: NINTH STANDARD CONFIGURATION,CASES 1,5,7,10-13
AERODYNAMIC WORK AND DAMPING COEFFICIENTS
IN DEPENDANCE OF INLET MACH NUMBER.



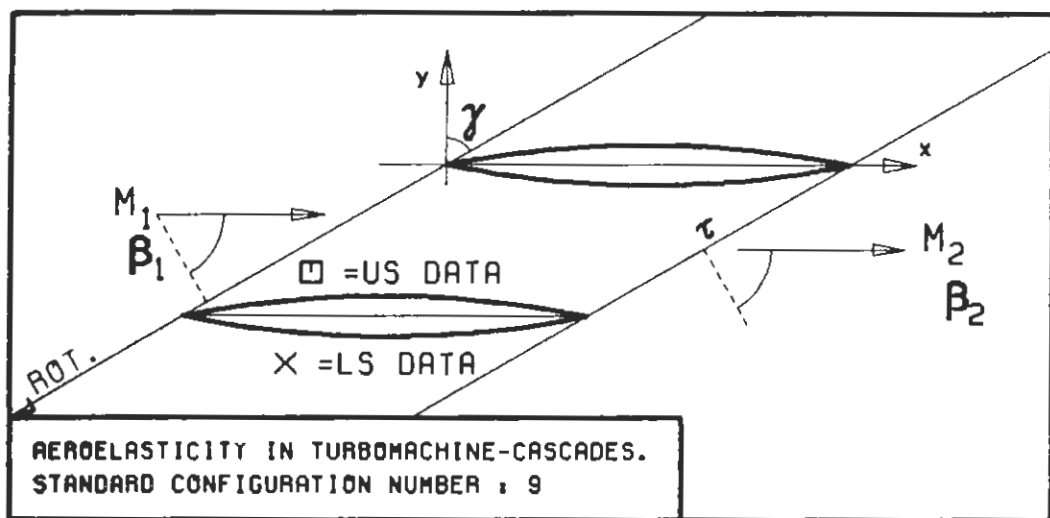
c : 0.1M
 τ : 0.75
 γ : 45.
 x_α : 0.5
 y_α : 0.
 M_1 : -
 β_1 : -45.
 i : 0.
 M_2 : -
 β_2 :
 h_x : -
 h_y : -
 α : .0349



PLOT 7.9-6.2: NINTH STANDARD CONFIGURATION, CASES 14-17.
AERODYNAMIC WORK AND DAMPING COEFFICIENTS
IN DEPENDANCE OF INLET MACH NUMBER.

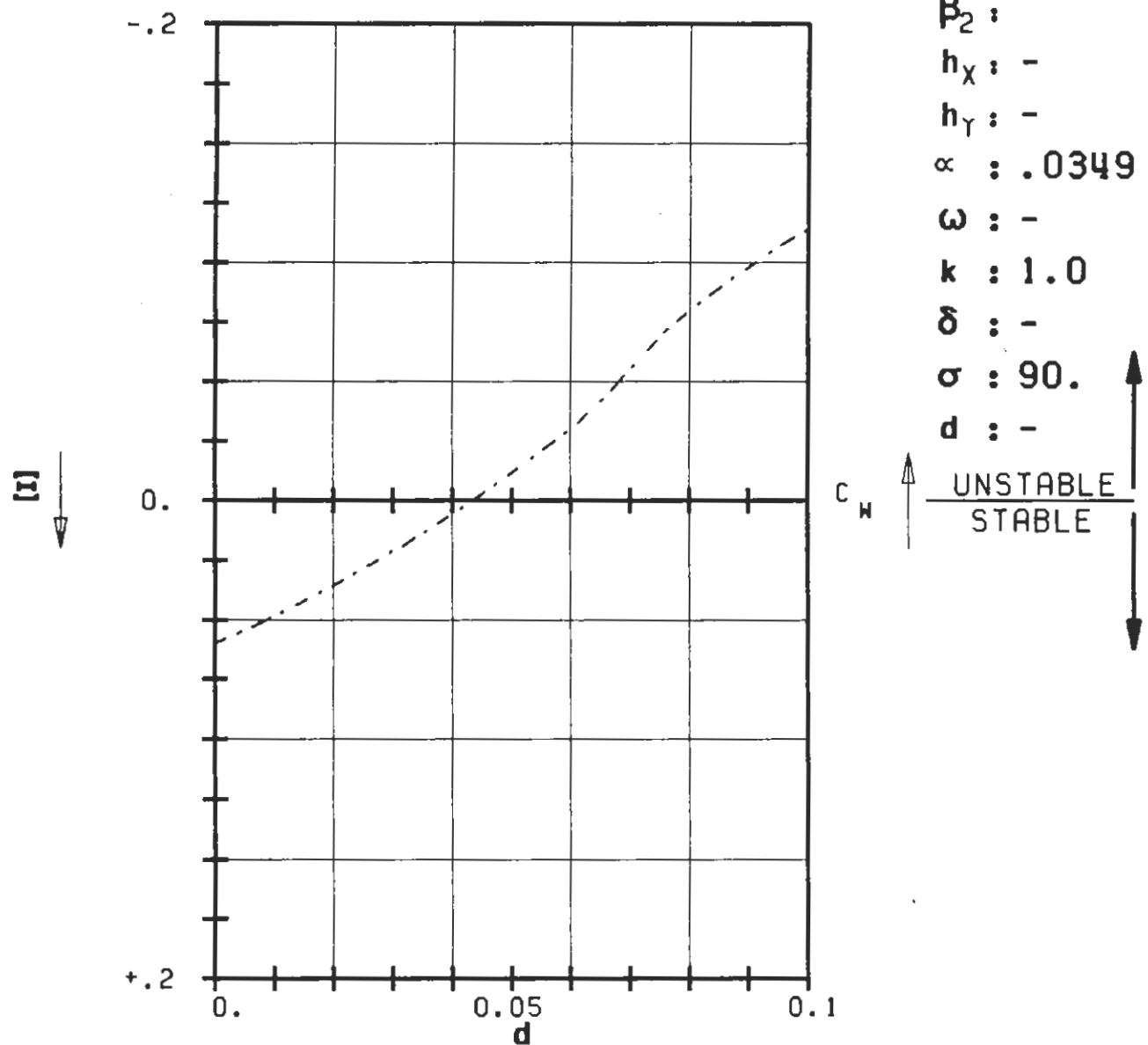


PLOT 7.9-6.3: NINTH STANDARD CONFIGURATION, CASES 18-21.
AERODYNAMIC WORK AND DAMPING COEFFICIENTS
IN DEPENDANCE OF INLET MACH NUMBER.

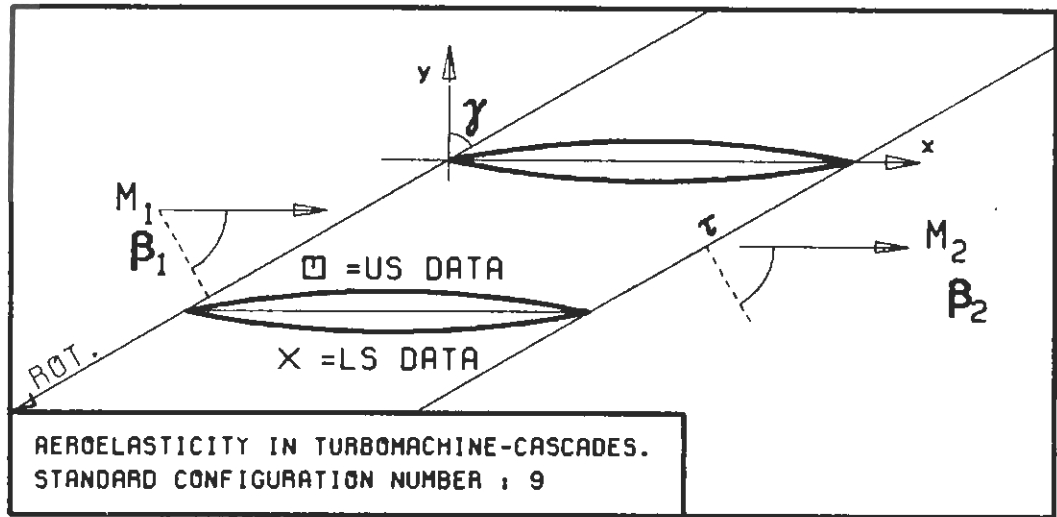


$c : 0.1M$
 $\tau : 0.75$
 $\gamma : 60.$
 $x_\infty : 0.5$
 $y_\infty : 0.$
 $M_1 : 0.$
 $\beta_1 : -60.$
 $i : 0.$
 $M_2 : -$
 $\beta_2 : -$
 $h_x : -$
 $h_y : -$
 $\alpha : .0349$
 $\omega : -$
 $k : 1.0$
 $\delta : -$
 $\sigma : 90.$
 $d : -$

-----METHOD: 2



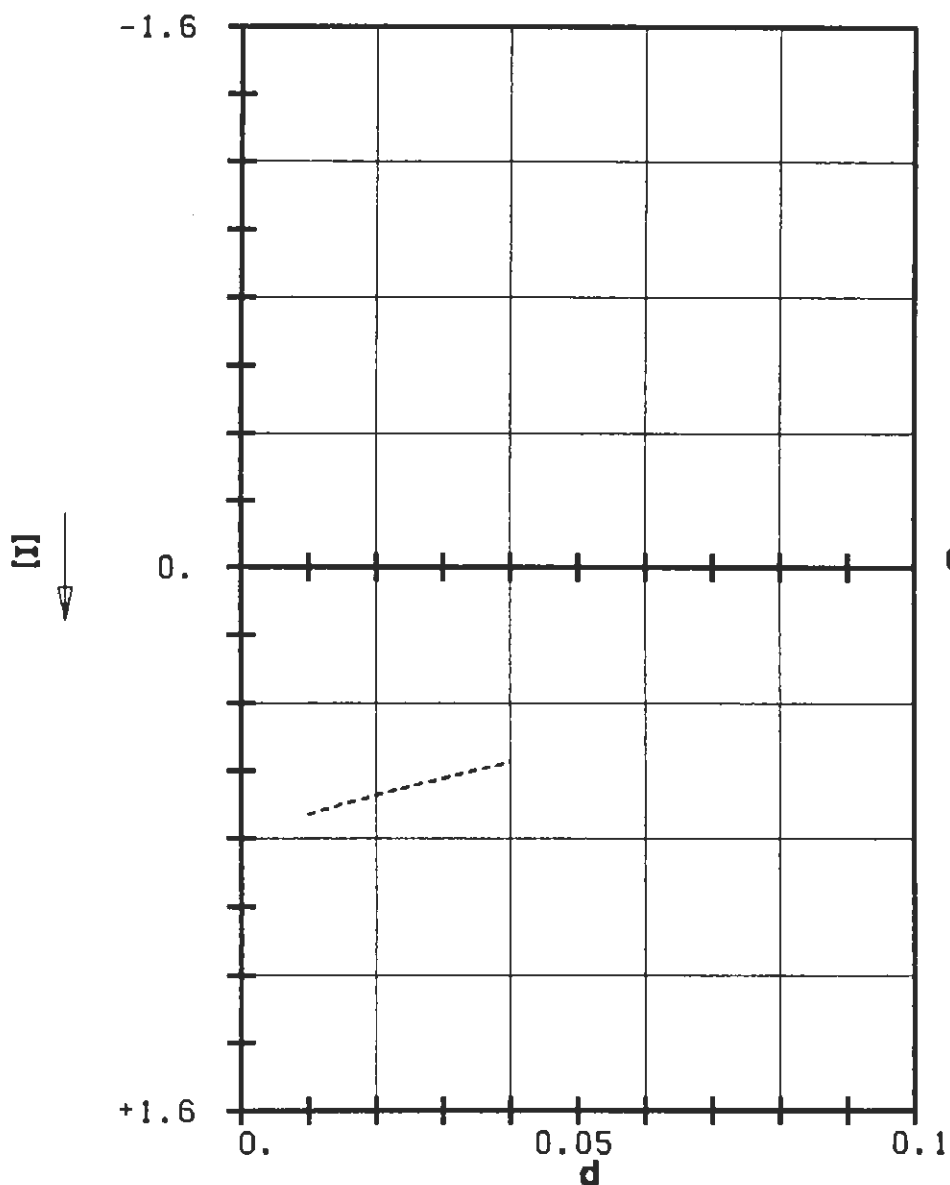
PLOT 7.9-6.4: NINTH STANDARD CONFIGURATION, CASES 1-4.
AERODYNAMIC WORK AND DAMPING COEFFICIENTS
IN DEPENDANCE OF BLADE THICKNESS.



c : 0.1M
 τ : 0.75
 γ : 60.
 x_α : 0.5
 y_α : 0.
 M_1 : 0.7
 B_1 : -60.
 i : 0.
 M_2 : -
 B_2 :
 h_X : -
 h_Y : -
 α : .0349

ω : -
 k : 1.0
 δ : -
 σ : 90.
 d : -

C_H ↑
UNSTABLE
STABLE



PLOT 7.9-6.5: NINTH STANDARD CONFIGURATION, CASES 6-9.
AERODYNAMIC WORK AND DAMPING COEFFICIENTS
IN DEPENDANCE OF BLADE THICKNESS.